

Cave and Karst Systems of the World

Philip J. Hobbs
Harrison Pienaar
Eddie van Wyk
Yongxin Xu *Editors*

Anatomy of a South African Karst Hydrosystem

The Hydrology and Hydrogeology of the Cradle
of Humankind World Heritage Site

Cave and Karst Systems of the World

Series Editor

James W. LaMoreaux, P. E. LaMoreaux and Associates, Tuscaloosa, AL, USA

This book series furthers the understanding of cave and karst related processes and facilitates the translation of current discipline-specific research to an interdisciplinary readership by dealing with specific cave or karst systems. Books in this series focus on a specific cave or karst system, on the cave or karst systems of a specific region, on a specific type of cave or karst system, or on any other perspective related to cave and karst systems of the world. The book series addresses a multidisciplinary audience involved in anthropology, archaeology, biology, chemistry, geography, geology, geomorphology, hydrogeology, paleontology, sedimentology, and all other disciplines related to speleology and karst terrains.

More information about this series at <https://link.springer.com/bookseries/11987>

Philip J. Hobbs · Harrison Pienaar ·
Eddie van Wyk · Yongxin Xu
Editors

Anatomy of a South African Karst Hydrosystem

The Hydrology and Hydrogeology
of the Cradle of Humankind World Heritage
Site

Editors

Philip J. Hobbs (deceased)
Pretoria, South Africa

Eddie van Wyk
Bloemfontein, South Africa

Harrison Pienaar
Smart Places—Water Centre
Council for Scientific and Industrial Research
Pretoria, South Africa

Hebei University of Engineering
Handan, China

Yongxin Xu
Department of Earth Sciences
University of the Western Cape
Bellville, South Africa

ISSN 2364-4591 ISSN 2364-4605 (electronic)
Cave and Karst Systems of the World
ISBN 978-3-030-95828-2 ISBN 978-3-030-95829-9 (eBook)
<https://doi.org/10.1007/978-3-030-95829-9>

© The Editor(s) (if applicable) and The Author(s), under exclusive license to Springer Nature
Switzerland AG 2022

This work is subject to copyright. All rights are solely and exclusively licensed by the Publisher, whether the whole or part of the material is concerned, specifically the rights of translation, reprinting, reuse of illustrations, recitation, broadcasting, reproduction on microfilms or in any other physical way, and transmission or information storage and retrieval, electronic adaptation, computer software, or by similar or dissimilar methodology now known or hereafter developed.

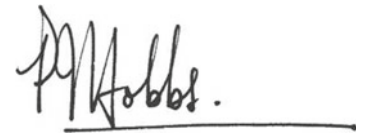
The use of general descriptive names, registered names, trademarks, service marks, etc. in this publication does not imply, even in the absence of a specific statement, that such names are exempt from the relevant protective laws and regulations and therefore free for general use.

The publisher, the authors, and the editors are safe to assume that the advice and information in this book are believed to be true and accurate at the date of publication. Neither the publisher nor the authors or the editors give a warranty, expressed or implied, with respect to the material contained herein or for any errors or omissions that may have been made. The publisher remains neutral with regard to jurisdictional claims in published maps and institutional affiliations.

This Springer imprint is published by the registered company Springer Nature Switzerland AG
The registered company address is: Gewerbestrasse 11, 6330 Cham, Switzerland

Declaration

I, **Philip J. Hobbs**, declare that this publication is my own work and has not previously been submitted by me for publishing at this or any other institution.

A handwritten signature in black ink, appearing to read "P. J. Hobbs.", is written above a horizontal line.



Panoramic view, looking south, of the COH WHS 'core' area in the John Nash Nature Reserve showing the valley carved by the Grootvlei Spruit from left (south-east) to right (north-west) across the landscape; also visible is the early winter smog layer over Johannesburg on the horizon (*Photo* P. Hobbs, date 19/05/2010)

Acknowledgements

It is with gratitude that I acknowledge Prof. Pat Eriksson, former Dean of the Faculty of Natural and Agricultural Sciences, and Prof. Louis van Rooy, Head of the Department of Geology, at the University of Pretoria. It is also fitting that the contributions of the Management Authority of the Cradle of Humankind World Heritage Site (COH WHS), and in particular Mr. Peter (Spike) Mills, Deputy Director Integrated Environment and Conservation Management for the COH WHS and Dinokeng Project, be acknowledged. The Management Authority is thanked for entrusting me with the task of improving the understanding of the water resources environment that contributes to the outstanding universal value of this globally treasured landscape. It is my hope that this publication will serve the Management Authority well in its task of managing and protecting also the water resources component of its UNESCO-entrusted mandate into the future. Peter Mills is thanked for his companionship and support on many excursions into the field.

The contribution of numerous other individuals to the work reflected in this dissertation is acknowledged separately at the end of the text. Many of these are landowners in the study area, and it is my hope that as stakeholders they will benefit from the material and knowledge presented in this dissertation. Others are professional colleagues in the employ of such organisations as the Department of Water and Sanitation (formerly the Department of Water Affairs), the Council for Geosciences and the Council for Scientific and Industrial Research. My thanks go to these individuals for the contribution of their time and effort.

In conclusion, I am thankful for the premeditated and fortuitous factors that a universal intelligence has considered fit to inform my professional career in a scientific discipline that offers so much unsolicited rich return. It is a privilege to contribute towards a better understanding of a complex and largely unseen hydrosystem such as underlies 'The Cradle'.

*"Entia non sunt multiplicanda praeter necessitatem."
(Entities must not be multiplied beyond necessity.)*

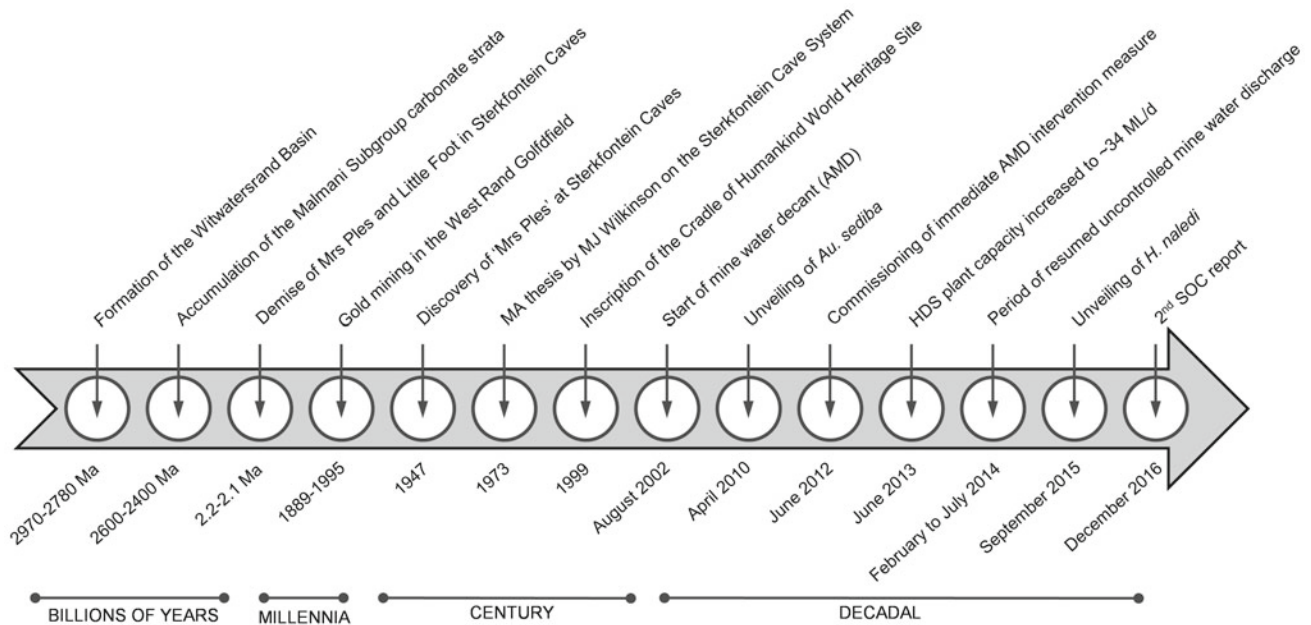
*John Punch
(Irish theologian 1603-1661)*

*aka
The law of parsimony (L. Lex parsimoniae)
as formulated by Occam's Razor*



View of surface flow and water quality monitoring station A2H049 at the lower end of the Bloubank Spruit at Zwartkop showing hut housing automated stage gauging instrumentation at left, and vertical stage gauge plates in middle and right foreground for visual observation; the blockage by vegetation and debris of the left flank of the weir (right of picture) is not ideal; the northern slope of the 1626 m amsl Zwartkop peak forms the backdrop to this view (*Photo* P. Hobbs, date 05/02/2010)

Historical Timeline of Key Events Relevant to this Dissertation

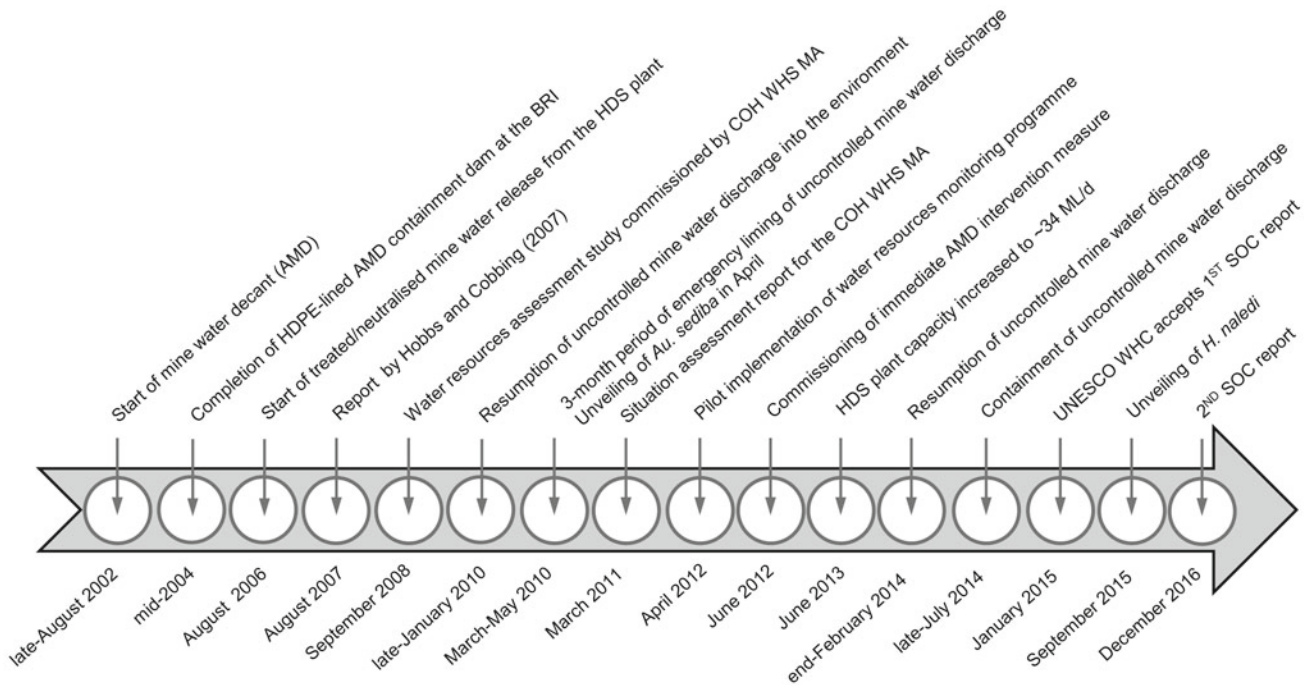


Timeline 1. Historical timeline of key events relevant to the study area. Acid mine drainage and its impact on receiving surface water and groundwater resources is a dynamic phenomenon that is continually evolving in response to both controlled (engineered) and uncontrolled (natural) circumstances. The immediate and short-term intervention measures implemented by the Department of Water and Sanitation (DWS) to control and manage acid mine drainage in the West Rand Goldfield (aka the Western Basin) were commissioned in June 2012. The impact of these measures on the receiving water resources is first manifested in August 2012. This marked the commencement of a new evolving dynamic in the study area, with the termination date for this study of September 2017 representing ~5 years of ‘new dynamic’ observation



Dolomite pinnacle protruding from a doline formed following flooding by stormwater of a soil borrow-pit alongside Dolomite Road (*Photo* P. Hobbs, date 04/11/2009)

Recent Timeline of Key Events Relevant to this Dissertation



Timeline 2. Recent timeline of key events relevant to the study area. August 2017 marks 15 years since the phenomenon of acid mine drainage first appeared in the Western Basin. The impact of the intervention measures implemented in mid-2010 by the DWS to control and manage AMD in the immediate and short-term started manifesting a positive impact on the downstream surface water resources in August 2012. This represents a key event in the evolving dynamic response of the receiving water resources environment. Under circumstances where much of the hydrological analyses set out in this dissertation use a hydrological and not a calendar year as base temporal unit, this combination of factors signify September 2017 (the most recent complete hydrological year) as an appropriate nominal termination date for the material presented and discussed in this work



Surface expression of the epikarst at the Swartkrans fossil site (*Photo P. Hobbs, date 18/05/2010*)

Extended Summary

Introduction

The fossil hominin sites of Sterkfontein, Swartkrans, Kromdraai and environs (the so-called Cradle of Humankind) were inscribed by UNESCO in 1999 for protection of their cultural heritage in terms of the World Heritage Convention Act (Act No 49, 1999). The Management Authority (MA) of the Cradle of Humankind World Heritage Site (COH WHS) property exercised its mandate to protect also the aquatic environment of the property by commissioning a study aimed at establishing a monitoring system for surface water and groundwater resources in its area of jurisdiction.

The implementation of an appropriate integrated hydrologic and hydrogeologic monitoring programme is crucial to the successful management of the water resources in the COH. An effective routine monitoring programme serves to measure and demonstrate the success or failure of management efforts by the MA to protect the aquatic environment of the property. Such protection is not only required for the preservation of the karst environment and its palaeo-anthropological wealth, but also for the water users who reside in the area and depend on local water resources (primarily groundwater) for their livelihood.

Surface Water Resources

Quantity

The Skeerpoort River system is in a nearly pristine condition. Its perennial nature is sustained mainly by the combined discharge ($>300 \text{ L/s} \approx 25.9 \text{ ML/d} \approx 9.6 \text{ Mm}^3/\text{a}$) of three high-yielding karst springs located in the John Nash Nature Reserve. The flow gauging record for the Skeerpoort River indicates a long-term median discharge of $\sim 9.57 \text{ Mm}^3/\text{a}$ to Hartbeespoort Dam via the Magalies River. This represents $\sim 5\%$ of the net capacity ($\sim 190 \text{ Mm}^3$) of the dam.

The flow record for the heavily impacted Bloubank Spruit system indicates a long-term median discharge of $\sim 22.7 \text{ Mm}^3/\text{a}$ to Hartbeespoort Dam via the Crocodile River. This represents $\sim 12\%$ of the net capacity of the dam. The Bloubank Spruit system experienced above average discharges in its upper reaches via the Tweelopie Spruit and the lower Riet Spruit following the resumption of uncontrolled raw mine water decant in late-January 2010. The combined discharge of raw and treated mine water realised quantified surface water losses of 20 to 32 ML/d to the karst aquifer from the lower Riet Spruit, equating to an infiltration rate of as much as $\sim 90 \text{ L/s/km}$. Together with the discharge from the Percy Stewart Wastewater Treatment Works (WWTW) via the Blougat Spruit, these circumstances resulted in an unprecedented volume of surface water flow in the Bloubank Spruit system through the 2010, 2011 and 2014 winter seasons. The median discharge of $\sim 4.7 \text{ Mm}^3/\text{a}$ ($\sim 13 \text{ ML/d}$) of treated

sewage effluent to the Blougat Spruit from the Percy Stewart WWTW equates to $\sim 21\%$ of the long-term median annual discharge of the Bloubank Spruit system.

The Crocodile River flow gauging record at the confluence with its Bloubank Spruit tributary indicates a long-term median discharge of $\sim 9.5 \text{ Mm}^3/\text{a}$ ($\sim 5\%$ of the Hartbeespoort Dam net capacity). As only 15% of this catchment falls within the COH, this discharge is excluded from the aggregate long-term contribution of $\sim 18\%$ ($\sim 34.7 \text{ Mm}^3/\text{a}$) delivered to Hartbeespoort Dam by the Skeerpoort River and Bloubank Spruit catchments. These catchments together represent $\sim 71\%$ of the study area.

Quality

The Skeerpoort River system delivers a CaMg-HCO_3 water composition of excellent quality. Up until mid-2010, the impact of the poor quality associated with the abnormal combined discharge of treated and raw mine water in the upper reaches of the Bloubank Spruit system was mitigated by the contribution of treated wastewater effluent discharged by the Percy Stewart WWTW and the above average surface water runoff associated with the extremely wet 2010 summer. Since mid-2010, the increase in specific electrical conductivity (SEC) of Bloubank Spruit water from ~ 50 to $>100 \text{ mS/m}$, together with a decrease in pH from 7.2 to 6.9 at the downstream end of the Zwartkrans Basin, reflects the increasing contribution of mine water to the middle reaches of the Bloubank Spruit.

The combination of long-term discharge and water chemistry records for the DWS gauging/sampling stations on the Skeerpoort River (A2H034), the Bloubank Spruit (A2H049) and the Crocodile River (A2H050) allow for an assessment of the total dissolved solids (TDS) loads associated with the respective drainages. This assessment indicates that the Skeerpoort River and (upper) Crocodile River deliver similar TDS loads of 2937 and 3249 t/a respectively, compared to the 10 173 t/a delivered by the Bloubank Spruit system. Again excluding the (upper) Crocodile River load, the values translate into contributions of 22% by the Skeerpoort River and 78% by the Bloubank Spruit system to the total TDS load of 13 110 t/a delivered to Hartbeespoort Dam by the COH drainages. In a regional context, this load constitutes only 13% of that entering the dam, being surpassed by the 51% (51 023 t/a) of the Jukskei River and the 28% (27 579 t/a) of the Hennops River. The balance of 8% (8085 t/a) is shared by the Crocodile River (3%) and the Magalies River (5%).

The quality of surface water resources in the Bloubank Spruit system is further compromised by bacterial contamination and associated elevated nitrate and phosphorus concentrations derived mainly from wastewater effluent. These circumstances also make it difficult to assess the agricultural impacts on the quality of surface water resources, as these are similarly associated with nutrient inputs. As a subset of the total salt load, the nutrient load entering Hartbeespoort Dam is of specific concern given the hypertrophic status of this impoundment. The sampling stations on the Bloubank Spruit system and the (upper) Crocodile River reflect median $\text{NO}_3\text{-N}$ and $\text{PO}_4\text{-P}$ loads of 129 and 2.9 t/a, respectively, to the dam in the period 1980 to 2013. A similar appraisal for the Jukskei and Hennops rivers indicates combined median $\text{NO}_3\text{-N}$ and $\text{PO}_4\text{-P}$ loads of 1245 and $\sim 104 \text{ t/a}$, respectively, for the same period. In summary, the Crocodile River and Bloubank Spruit systems together contribute $<10\%$ to the median long-term $\text{NO}_3\text{-N}$ load entering Hartbeespoort Dam, being overshadowed by the Jukskei River contribution of $\sim 70\%$ and the Hennops River contribution of $\sim 20\%$. The $\text{PO}_4\text{-P}$ load is dominated even more by the Jukskei and Hennops rivers, with the Crocodile River and Bloubank Spruit systems delivering $<3\%$ of this nutrient load to the dam annually.

A primary concern for the downstream environment is the impact of mine water, in particular the presence of trace/heavy metals, metalloids and radionuclides, on the quality of water in the Bloubank Spruit system. In the period of maximum likely impact, namely February 2010 to July 2012, median Fe and Mn levels of 0.013 mg Fe/L and 0.003 mg Mn/L in surface water at the lower end of the system on 33 sampling occasions, compare favourably

with levels of 163 mg Fe/L and 65 mg Mn/L in composite mine water discharge in the upper reaches of the system on 129 sampling occasions. Mercury levels in surface water typically do not exceed 0.002 mg/L. Arsenic levels similarly seldom exceed the detection limit of 0.002 mg/L. Nickel presents as the most persistent trace metal in upper (headwater) reaches, the median concentration of 0.1 mg Ni/L from 41 sampling occasions exceeding the SANS (2015a) limit of 0.07 mg/L. As with Fe and Mn, Ni levels in the lower reaches of the system do not test the 0.07 mg/L limit.

Uranium levels in surface water nowhere and on no sampling occasion exceeded the analytical detection limit of 0.001 mg/L for this analyte. Radon (^{222}Rn) activity levels representative of the headwater reach in the mine area fall within the minimum detectable activity (MDA) of ~ 0.5 Bq/L. This compares favourably with the maximum contaminant level (MCL) of 11.1 Bq/L set by the USAs Safe Drinking Water Act (SDWA). Similarly, radium (^{226}Ra) activity levels do not exceed the SDWAs MCL of 0.185 Bq/L for this radionuclide in the extremely sparse set of available data.

The persistence of poor bacteriological quality as reflected in alarmingly high faecal coliform and *E. coli* values associated with surface water in the Bloubank Spruit, continues to represent a significant threat to the ‘fitness for use’ of this resource. This situation reflects the poor score achieved by the Percy Stewart WWTW in both the 2009 and 2011 DWS ‘Green Drop’ reports, and in particular the non-compliance in regard to the effluent wastewater quality metric. A thorough evaluation of this threat is thwarted by the non-disclosure of pertinent monitoring data by the local authority.

Groundwater Resources

Quantity

Springs are widely recognised as the most appropriate gauging, sampling and monitoring points in a karst environment. The study has enumerated eleven springs (excluding the seven located in the Krugersdorp Game Reserve) in the subregion. The total number of such features in the subregion is almost certainly greater. Some of the features represent groups of springs (and seeps) located in close proximity to one another. Nine of these drain dolomitic strata, the ‘weakest’ delivering ~ 2 L/s and the ‘strongest’ ~ 307 L/s. The total yield of these sources amounts to ~ 827 L/s (~ 71.5 ML/d ≈ 26.1 Mm³/a). This equates to $\sim 14\%$ of the net capacity of Hartbeespoort Dam, and reflects the very important contribution of mainly good to excellent springwater to the water resources of the wider region. None of the enumerated springs are subject to regular and routine discharge measurements. Synoptic discharge measurements in this study have served to quantify the yield of many of these features for the first time.

Groundwater quantity is further represented by groundwater level data and information. The study has generated 117 groundwater level measurements from as many sources (18 springs and 99 boreholes). Each of these measurements has been translated into an absolute value representing a groundwater elevation above mean sea level. Together with the locations and elevations of the various springs, this information has led to an improved understanding of groundwater flow and movement especially in regard to the dolomitic strata. As a consequence, redefinition of the physical hydrogeologic environment recognises a degree of compartmentalisation that contributes significantly to a more informed understanding of the karst groundwater environment. A total of ten dolomitic compartments, two of which comprise subcompartments, are identified in the COH. Most of the compartments are drained by springs. Water budget calculations for the seven karst basins drained by springs with yields >20 L/s and factoring in their surface extent, indicates that $17 \pm 5\%$ of a mean annual precipitation of 710 mm provides a reasonable approximation of natural autogenic recharge from rainfall for the karst hydrosystem.

The behaviour of groundwater levels associated with the karst aquifer is reflected in the long-term water level records for 15 DWS monitoring boreholes dating back to 1985. In 11 of these instances, the record period extends to the present. An analysis of the data indicates a generally excellent agreement between the mean and median values. This reflects the large measure of constancy in this variable. Further, there is little correlation between the depth to groundwater rest level and the magnitude of water level variation; relatively small variations (<3 m) being associated with both 'deep' (>60 m bs) and comparatively 'shallow' (<30 m bs) water levels. The data set reveals a maximum water level variation value of ~ 12.2 m, with mean and median values of ~ 6.2 m and ~ 5.6 m, respectively. The slightly smaller differences associated with the 5%ile to 95%ile interval are characterised by a maximum value of 9.8 m, and mean and median values of 5.2 and 4.6 m respectively.

The very wet 2010, 2011 and 2014 summers precipitated an exceptional recharge of groundwater resources in the study area. A rise in groundwater rest levels by ~ 4.9 m on average testifies to these circumstances. Greater water level rises (by up to ~ 8 m) are attributed to artificial and allogenic recharge associated with the infiltration of surface water contributed from extraneous sources including mining and municipal wastewater effluent. This infiltration has amounted to as much as ~ 32 ML/d in the case of mine water, and ~ 7 ML/d in the case of municipal wastewater. The recent (since 2012) groundwater level (water table) elevations in the COH are the highest in the ~ 30 -year record of monitoring.

Quality

Groundwater quality in the COH is defined on the basis of chemical analyses carried out on water samples obtained from 51 sources (7 springs and 44 boreholes). The analytical suite include inorganic, organic and bacteriological variables, heavy/trace metals/metalloids and environmental isotopes as well as pesticide residue analyses employed selectively. In addition, numerous measurements of field variables (pH, EC, ORP/Eh and temperature) have been carried out on an ad hoc basis at a number of springs.

As might be expected, the hydrochemistry reflects a greater or lesser spatial variation depending on the position in the physical hydrogeologic environment. For instance, the subcompartments receiving water of compromised quality in terms of either trace/heavy metals/metalloids and elevated TDS loads associated with mine water, and/or elevated bacterial and nutrient loads associated with municipal wastewater (both representing allogenic recharge), reflect the poorest groundwater quality. Despite its location, however, the Lake water in Sterkfontein Cave continues to reflect an SEC of <70 mS/m as it did in June 2006. Karst basins receiving only autogenic recharge remain largely unaffected in terms of groundwater chemistry/quality.

Conclusions

The understanding of the surface water and groundwater environments in the COH, also in regard to the inter-relationship between these resources, is considerably expanded by this study. This understanding extends as much to the water chemistry aspect as it does to the water quantity aspect. The platform built from historical data, and its integration with a wide range of rigorous and defensible newly-generated and interpreted hydrologic and hydrogeologic data and information, convincingly underpins the situation assessment of the surface water and groundwater environments. This, in turn, has provided the means to objectively gauge the impact of varied and numerous threats on the water resources in the study area, and to develop a coordinated, appropriate and cost-effective water resources monitoring programme. Outcomes of the study that are considered especially significant are summarised as follows.

- The quantification of surface water flow losses, especially those dominated by a mine water character in the lower Riet Spruit valley.
- The quantification of spring discharges.
- The definition of basins/subcompartments and corresponding groundwater resource units (GRUs) associated mainly with the karst formations in the study area.
- The development of semi-quantitative resource water quality objectives (RWQOs) to inform surface and groundwater resource directed measures for the karst portions of the study area.
- The derivation of a fossil site risk assessment that informs the vulnerability of each recognised fossil site and associated cave system in the context of its hydrogeologic setting.

A cause for grave concern is the unprecedented abnormally high flow conditions experienced in the Bloubank Spruit system in the more recent hydrological years, as this discharge is the result of abnormally high mine water decant driven by copious recharge associated with above average rainfall. This has already manifested itself as historical maximum SEC and sulphate values at the lowest end of the Bloubank Spruit system.

Recommendations

The study has identified various concerns that give rise to the following general recommendations.

- The advisability of carrying out a gravimetric survey in the lower Riet Spruit valley extending from the confluence of the Tweelopie Spruit and the Riet Spruit down to the confluence of the Blougat Spruit and the Riet Spruit. The results of such a survey will indicate the measure of karst dissolution present in this important E–W corridor that hosts the N14 national road.
- The advisability of extending the hydrovulnerability assessment to other cave systems in the study area, together with a refinement of the applied assessment methodology.
- The establishment of a monitoring committee comprising a core of key stakeholder groupings, e.g. national, provincial and local government, environment and tourism, agriculture.
- The hosting (by the Management Authority) of a workshop or seminar to communicate the outcomes of the study to as wide an audience of stakeholders and interested and affected parties as are interested.
- The expansion of the mine water treatment capacity in the headwaters of the Tweelopie Spruit to accommodate a decant volume of ~ 60 ML/d, representing a 2-fold increase in the current treatment capacity.
- The establishment of additional mine water treatment facilities in the headwaters of the Tweelopie Spruit to further ‘polish’ the treated mine water that is generated by the expanded mine water treatment capacity and released into the environment.

Contents

| | |
|---|-----|
| Integrated Monitoring Approach | 1 |
| Harrison Pienaar and Philip J. Hobbs | |
| Introduction and Background | 5 |
| Harrison Pienaar and Philip J. Hobbs | |
| Description of the Physical Environment | 11 |
| Harrison Pienaar and Philip J. Hobbs | |
| Overview of Karst | 31 |
| Philip J. Hobbs and Harrison Pienaar | |
| Physical Hydrology | 43 |
| Harrison Pienaar and Philip J. Hobbs | |
| Chemical Hydrology | 83 |
| Harrison Pienaar, Philip J. Hobbs, Sebinasi Dzikiti, and Ranya Amer | |
| Physical Hydrogeology | 167 |
| Philip J. Hobbs, Harrison Pienaar, and Sebinasi Dzikiti | |
| Chemical Hydrogeology | 211 |
| Harrison Pienaar, Philip J. Hobbs, and Sebinasi Dzikiti | |
| Conclusions | 321 |
| Harrison Pienaar and Philip J. Hobbs | |
| Recommendations | 325 |
| Harrison Pienaar and Philip J. Hobbs | |
| Acknowledgements | 327 |
| Glossary | 335 |
| References | 339 |
| Bibliography | 353 |
| Index | 355 |

Symbols, Acronyms and Abbreviations

| | |
|-----------------|--|
| ~ | Approximately |
| ≡ | Equivalent |
| > | Greater than |
| >> | Much greater than |
| ≥ | Greater than or equal to |
| ≤ | Less than or equal to |
| < | Less than |
| # | Number |
| ± | Plus-minus |
| δ | Delta (notation) |
| Δ | Change in |
| Σ | The sum of |
| μg/g | Microgram(s) per gram |
| % | Per cent (parts per hundred) |
| ‰ | Per mil (parts per thousand) |
| %ile | Percentile |
| °C | Degree(s) Celsius (centigrade) |
| °C/m | Degree(s) Celsius per metre |
| °E | Degree(s) East (longitude) |
| °S | Degree(s) South (latitude) |
| ² H | Deuterium |
| ³ H | Tritium |
| ¹⁸ O | Oxygen-18 |
| a | Annum |
| a _h | Hydrological year |
| A. | Afrikaans |
| amsl | Above mean sea level |
| ABA | Acid base accounting |
| AET | Actual evapotranspiration |
| A.H. | Agricultural Holdings |
| aka | Also known as |
| Al | Aluminium |
| AMD | Acid mine drainage (or) decant (or) discharge |
| ARC | Agricultural Research Council |
| As | Arsenic |
| ASPT | Average score per taxon |
| ATSDR | Agency for Toxic Substances and Disease Registry |
| atm | Atmosphere(s) |
| Au. | Australopithecus |
| B | Boron |
| Ba | Barium |

| | |
|-----------------|--|
| bc | Below collar |
| BE | Built Environment (a business unit of the CSIR) |
| bgl | Below ground level |
| BP | Before present |
| Bq/g | Becquerel(s) per gram |
| Bq/L | Becquerel(s) per litre |
| bs | Below surface |
| BSR | Bacterial sulphate reduction |
| bwl | Below water level |
| C | Carbon |
| C_X | Concentration (C_U = upstream; C_D = downstream; C_F = furrow; C_S = spring; C_G = groundwater) |
| C_5 | Concentration exceeded 5% of the time (equivalent to 95%ile) |
| C_{50} | Concentration exceeded 50% of the time (equivalent to 50%ile) |
| C_{95} | Concentration exceeded 95% of the time (equivalent to 5%ile) |
| ca. | Circa (about) |
| Ca | Calcium |
| Cd | Cadmium |
| CD | Compact disc |
| CDSM | Chief Directorate: Surveys and Mapping (in the Department of Land Affairs) |
| cfu | Colony forming unit(s) |
| CGS | Council for Geoscience |
| Cl | Chloride |
| CMB | Chloride mass balance |
| CN | Cyanide |
| Co | Cobalt |
| CO ₂ | Carbon dioxide |
| COD | Chemical oxygen demand |
| COH WHS | Cradle of Humankind World Heritage Site |
| CoV | Coefficient of variation |
| CPOM | Coarse particulate organic matter |
| Cr | Chromium |
| CROSA | Cave Research Organisation of South Africa |
| CSIR | Council for Scientific and Industrial Research |
| CTR | Corrosion tendency ratio |
| Cu | Copper |
| d | Day(s) |
| dd.ddddd | Degrees latitude (or) longitude expressed to the 5th decimal |
| dd/mm/yyyy | Date format as day/month/year, e.g. 10/11/2012 \equiv 10 November 2012 |
| DEA | Department of Environmental Affairs (formerly Department of Environmental Affairs and Tourism) |
| DEAT | Department of Environmental Affairs and Tourism |
| DED | Department of Economic Development (Gauteng Province) |
| DL | Detection limit |
| DLA | Department of Land Affairs |
| dm | Decimetre |
| DME | Department of Minerals and Energy |
| DMR | Department of Mineral Resources (formerly Department of Minerals and Energy) |
| DMS | Dissolved mineral salts |
| DO | Dissolved oxygen |
| DOC | Dissolved organic carbon |

| | |
|----------------|--|
| DPLG | Department of Development, Planning and Local Government |
| D:RQS | Directorate: Resource Quality Services (a directorate in the DWS) |
| DWA | Department of Water Affairs (formerly Department of Water Affairs and Forestry) |
| DWAF | Department of Water Affairs and Forestry |
| DWS | Department of Water and Sanitation (formerly the Department of Water Affairs) |
| EB | Electrical balance (aka ion balance or charge balance) |
| EC | Electrical conductivity |
| ECL | Environmental critical level |
| <i>E. coli</i> | <i>Escherichia coli</i> bacteria |
| EDC | Endocrine disrupting chemical |
| Eh | Free electron (e^-) activity defined as $-\log_{10}[e^-]$; also assigned the abbreviation p_e |
| e.g. | <i>Exempli gratia</i> (for example) |
| EI&S | Ecological importance and sensitivity |
| EMF | Environmental management framework |
| EMS | Environmental management system |
| EoP | End-of-pipe |
| EPA | Environmental Protection Agency |
| Eq | Equation |
| eq | Equivalent |
| ERWAT | East Rand Water Care Company |
| ESE | East-south-east |
| ET | Evapotranspiration |
| EurepGAP | Euro-Retailer Produce Working Group Good Agricultural Practice |
| Fe | Iron |
| FFG | Functional feeding group |
| FIB | Faecal indicator bacteria |
| Fm. | Formation (geological term) |
| FPOM | Fine particulate organic matter |
| FSE | Federation for a Sustainable Environment |
| FSLTS | Feasibility study for a long-term solution (commissioned by the DWS) |
| G | Billion (10^9) |
| G1 | Gold1 (operating in conjunction with Rand Uranium) |
| g/t | Gram(s) per ton |
| Ga | Billion years |
| GC | Gas chromatograph |
| GDACE | Gauteng Department of Agriculture, Conservation and the Environment |
| GDARD | Gauteng Department of Agriculture and Rural Development (formerly GDACE) |
| Gg/a | Gigagram(s) per annum |
| GIS | Geographic information system |
| G.M. Co. | Gold Mining Company |
| GMU | Groundwater management unit |
| GNIP | Global network of isotopes in precipitation |
| Gp. | Group (geological term) |
| GPS | Global positioning system |
| GRA | Groundwater resource assessment |
| GRDM | Groundwater resource directed measures |
| GRU | Groundwater resource unit |
| h | Hour(s) |

| | |
|------------------------------------|---|
| H | Weighting value |
| <i>H.</i> | Homo |
| HCO ₃ | Bicarbonate |
| ha | Hectare(s) |
| HDS | High density sludge |
| HDPE | High density poly-ethylene |
| H _i | Hazard index |
| HPC | Heterotrophic plate count (also referred to as total plate count) |
| <i>i</i> | Hydraulic gradient |
| I&AP | Interested and affected party |
| ICOMOS | International Council on Monuments and Sites |
| ICP | Inductively coupled plasma |
| IDP | Integrated development plan |
| i.e. | <i>Id est</i> (that is to say) |
| IGTT | Inter-Governmental Task Team (on AMD) |
| IGU | International Geophysical Union |
| IHAS | Integrated Habitat Assessment System |
| IHIA | Integrated Habitat Integrity Assessment |
| IMC | Inter-Ministerial Committee (on AMD) |
| iro | In respect of |
| iTLABS | iThemba LABS (a National Research Foundation facility) |
| IUCN | International Union for Conservation of Nature |
| JFA | Johan Fourie and Associates (Environmental Consultancy) |
| JNNR | John Nash Nature Reserve |
| K | Potassium |
| K _X | Equilibrium constant for mineral X, where X = C = calcite, and X = D = dolomite |
| Ka | Thousand years |
| KFD | Koelenhof Farm Dam |
| kg/d | Kilogram(s) per day |
| kg/km ² /a | Kilogram(s) per square kilometre per annum |
| kg/m ³ | Kilogram(s) per cubic metre |
| KGR | Krugersdorp Game Reserve |
| km | Kilometre(s) |
| km ² | Square kilometre(s) |
| km/h | Kilometre(s) per second |
| kt | Kiloton(s) |
| <i>L.</i> | Latin |
| LC _x | Concentration causing x% lethality |
| L/kg/d | Litre(s) per kilogram per day |
| LMDC | Leadership and Management Development Centre (Nedbank's Olwazini Estate) |
| LoD | Locus of decant |
| L/s | Litre(s) per second |
| LSC | Liquid scintillation counting |
| L/s/km | Litre(s) per second per kilometre |
| m | Metre(s) |
| M | Million (10 ⁶) |
| m/Ma | Metre(s) per million years |
| m ² /d | Square metre(s) per day |
| m ³ /km ² /a | Cubic metre(s) per square kilometre per annum ≡ mm/Ka |
| m/s | Metre(s) per second |

| | |
|--------------------|--|
| m ³ /s | Cubic metre(s) per second (also referred to as 'cumec(s)') |
| MA | Management Authority |
| Ma | Million years |
| MAD | Mean annual discharge |
| MAP | Mean annual precipitation |
| MA _h P | Mean hydrological year precipitation |
| MAPE | Mean annual potential evaporation |
| MAR | Mean annual runoff |
| MAT | Mean annual temperature |
| max. | Maximum |
| MCL | Maximum contaminant level |
| MCLM | Mogale City Local Municipality |
| MDA | Minimum detectable activity |
| MDB | Municipal Demarcation Board |
| MEC | Member of the Executive Council |
| med. | Median |
| MG | Mogale Gold (operating in conjunction with Mintails SA) |
| Mg | Magnesium |
| mg/kg | Milligram(s) per kilogram |
| MG/MSA | Mogale Gold/Mintails SA |
| mg/L | Milligram(s) per litre |
| mg/s | Milligram(s) per second (1 mg/s \equiv 0.000084 t/d) |
| min. | Minimum |
| mL | Millilitre(s) |
| ML | Megalitre(s) (1 ML \equiv 1 million litres) |
| ML/d | Megalitre(s) per day |
| mm/a | Millimetre(s) per annum |
| mm/Ka | Millimetre(s) per thousand years |
| mm/yyyy | Month/year (e.g. 01/2010) |
| Mm ³ /a | Million cubic metre(s) per annum |
| Mm ³ /m | Million cubic metre(s) per month |
| Mn | Manganese |
| MNR | Motsetse Nature Reserve |
| Mo | Molybdenum |
| MP | Management plan |
| MPN | Most probable number |
| MRD | Mine residue deposit |
| mS/m | MilliSiemens per metre |
| MSM | Monitoring system manual |
| MSRF | Morphologic suite of rising flow |
| mV | MilliVolt(s) |
| n | Count (of sample population) |
| n.a. | Not analysed |
| n/a | Not applicable |
| Na | Sodium |
| n.d. | Not determined |
| NAEHMP | National Aquatic Ecosystem Health Monitoring Programme |
| NE | North-east |
| NFEPA | National Freshwater Ecosystem Priority Areas |
| NGO | Non-governmental organisation |
| NH ₃ | Ammonia nitrogen |
| NH ₄ | Ammonium nitrogen |

| | |
|-------------------|---|
| Ni | Nickel |
| n.m. | Not measured |
| nm | Nanometre(s) ($1 \text{ nm} = 1 \times 10^{-9} \text{ m}$) |
| No | Number |
| NO ₂ | Nitrite nitrogen |
| NO ₃ | Nitrate nitrogen |
| NOE | Nedbank Olwazini Estate |
| NRE | Natural Resources and the Environment (a business unit of the CSIR) |
| n/s | Not specified |
| NTU | Nephelometric turbidity unit(s) |
| O-PO ₄ | Ortho-phosphate |
| ORP | Oxidation reduction potential; also simply referred to as 'redox' potential |
| OUV | Outstanding universal value |
| p | Page |
| P | Phosphorus |
| Pb | Lead |
| pCi/L | PicoCurie(s) per liter |
| P_{CO_2} | Partial pressure (activity) of CO ₂ |
| $p\epsilon$ | Free electron (e^-) activity defined as $-\log_{10}[e^-]$; also assigned the abbreviation Eh |
| pH | Free hydrogen ion activity (α_{H^+}) defined as $-\log_{10}\alpha_{\text{H}^+}$ where $\alpha_{\text{H}^+} = f \times [\text{H}^+]$ with f the activity coefficient and $[\text{H}^+]$ the hydrogen ion concentration |
| PO ₄ | Phosphate |
| pp | Pages |
| Pt | Petaton |
| Pt | Platinum |
| Ptn | PORTION |
| Q_x | Flow or discharge (Q_U = upstream; Q_D = downstream; Q_F = furrow; Q_S = spring; Q_G = groundwater) |
| Q_{25} | Flow or discharge exceeded 75% of the time (equivalent to 25%ile) |
| Q_{50} | Flow or discharge exceeded 50% of the time (equivalent to 50%ile) |
| Q_{75} | Flow or discharge exceeded 25% of the time (equivalent to 75%ile) |
| Q^n | Ranking factor |
| Q_{min} | Minimum flow or discharge |
| Q_{max} | Maximum flow or discharge |
| R. | River |
| R^f | Reduction factor |
| RAIS | Risk Assessment Information System |
| REGM | Randfontein Estates Gold Mine |
| RET | Riparian evapotranspiration |
| RHP | River health programme |
| RI _i | Risk intensity index |
| RMW | Raw mine water |
| RSA | Republic of South Africa |
| RWQOs | Resource water quality objective(s) |
| RU | Rand Uranium (successor to Harmony Gold) |
| RU/G1 | Rand Uranium/Gold1 (successor first to Harmony Gold and then Uranium1) |
| RWL | Rest water level |
| S. | Spruit |
| SABS | South African Bureau of Standards |
| SAC | Satellite Applications Centre |
| SAFF | Submerged aeration fixed film |

| | |
|-----------------|---|
| SAIEEG | South African Institute of Engineering and Environmental Geology |
| SAKWG | South African Karst Working Group |
| SANAS | South African National Accreditation System |
| SANBI | South African National Biodiversity Institute |
| SANParks | South African National Parks |
| SANS | South African National Standard |
| SAR | Sodium adsorption ratio (a calculated chemical variable) |
| SASS | South African Scoring System |
| SAWS | South African Weather Service |
| Sbgp. | Subgroup (a geological term) |
| SC | Sterkfontein Cave |
| SD | Standard deviation |
| SDF | Spatial development framework |
| SDM | Synoptic discharge measurement |
| SDWA | Safe Drinking Water Act (administered and overseen by the US EPA) |
| Se | Selenium |
| SEC | Specific electrical conductivity (EC @ 25 °C) |
| SECL | Socio-economic critical level |
| SEM | Scanning electron microscopy |
| SHE | Standard hydrogen electrode |
| Si | Silicon |
| SI _C | Saturation index of calcite expressed as $\log\{[Ca^{2+}][CO_3^{2-}]/K_C\}$ |
| SI _D | Saturation index of dolomite expressed as $\log\{[Ca^{2+}][Mg^{2+}][CO_3^{2-}]^2/K_D\}$ |
| SMOW | Standard mean ocean water |
| SoC | State of conservation |
| SoE | State of the environment |
| SO ₄ | Sulphate |
| Sp. | Spring |
| Spgp. | Supergroup (a geological term) |
| Sr | Strontium |
| SRB | Sulphate reducing bacteria |
| SRK | Steffen, Robertson and Kirsten (Consulting Engineers and Scientists) |
| SS | Suspended solids |
| S-S | Sibanye-Stillwater (successor to Uranium1) |
| StatsSA | Statistics South Africa |
| SW | South-west |
| t | Ton(s) |
| <i>T</i> | Transmissivity |
| t/a | Ton(s) per annum |
| t/d | Ton(s) per day |
| t/m | Ton(s) per month |
| t/ML | Ton(s) per megalitre |
| T.Alk. | Total alkalinity (as CaCO ₃) |
| TC | Total carbon |
| TCLP | Toxicity characteristic leaching procedure |
| TCTA | Trans-Caledon Tunnel Authority |
| TDS | Total dissolved solids/salts |
| TIC | Total inorganic carbon |
| TMW | Treated/neutralised mine water |
| TOC | Total organic carbon |
| ToC | Table of Contents |
| TOL | Target operating level |

| | |
|-----------------|---|
| TON | Threshold odour number |
| ToR | Terms of reference |
| TR _i | Total risk index |
| TU | Tritium unit(s) (1 TU = 1 tritium in 10 ¹⁸ hydrogen atoms) |
| Turb. | Turbidity |
| TWQR | Target water quality range |
| U | Uranium |
| UIS | Union Internationale de Spéléologie (International Union of Speleology) |
| UNESCO | United Nations Educational, Scientific and Cultural Organisation |
| US(A) | United States (of America) |
| USACE | United States Army Corps of Engineers |
| USDA | United States Department of Agriculture |
| V | Vanadium |
| V _i | Vulnerability index |
| VCR | Ventersdorp Contact Reef |
| vs. | Versus |
| <i>w</i> | Width |
| WARMS | Water authorisation and registration management system (a DWS database] |
| WBTWG | Western Basin Technical Working Group |
| WCPA | World Commission on Protected Areas |
| WGC | Water Geosciences Consulting |
| WGS84 | World Geodetic System 1984 (reference ellipsoid for Hartebeesthoek94 Datum) |
| WHC | World Heritage Centre (could also denote World Heritage Committee) |
| WHO | World Health Organisation |
| WMA | Water management area |
| WNW | West-north-west |
| WRC | Water Research Commission |
| WRDM | West Rand District Municipality |
| WWTW | Wastewater treatment works |
| XRD | X-ray diffraction |
| XRF | X-ray fluorescence |
| <i>y</i> | Year(s) |
| Zn | Zinc |

List of Figures

Introduction and Background

| | | |
|--------|---|---|
| Fig. 1 | Location of the Cradle of Humankind World Heritage Site (COH WHS) in Gauteng Province (light shaded area), South Africa, and in relation to the distribution of ‘hard’ sedimentary carbonate deposits (darker shaded areas) of the Chuniespoort Group in the South African interior (adapted from Martini and Wilson, 1998) | 6 |
| Fig. 2 | Definition of the study area in regard to geographic localities, geology and hydrology | 8 |

Description of the Physical Environment

| | | |
|--------|--|----|
| Fig. 1 | Position of the study area within the national distribution of water management areas (WMAs; numbered and labelled) and the Limpopo WMA (#1) in particular | 12 |
| Fig. 2 | Definition of study area showing positions of rainfall, surface water flow and surface water quality gauging stations with hydrologic features superimposed on geology as backdrop | 13 |
| Fig. 3 | Composite annual and overlapping summer (wet season) rainfall record for stations PS and BRI; the mean summer precipitation of 632 mm is indicated by the dashed line labelled MSP | 14 |
| Fig. 4 | Correlation of monthly rainfall at Sterkfontein Cave with that at station HDS on the watershed for the period of common record June 2010 to September 2017; data set ($n = 71$) excludes months of no rainfall at both stations ($n = 17$) | 15 |
| Fig. 5 | Google Earth® image showing surface features relevant to the mining environment in the Western Basin | 23 |
| Fig. 6 | Diagram of mining-related features (e.g. geology, mine areas, shafts and pits) in the West Rand Goldfield. (Modified from Toens and Griffiths 1964; Tucker and Viljoen 1986) | 24 |
| Fig. 7 | Schematic profiles of geologic and mining-related features in the northern portion of the West Rand Goldfield (see Fig. 8 for profile transects) | 25 |
| Fig. 8 | Geologic map of the north-western portion of the Western Basin showing surface features of mining-related significance and the position of the profile transects illustrated in Fig. 9 (original geology from Mellor 1917) | 26 |
| Fig. 9 | Locality map of the UNESCO-inscribed fossil sites in the study area superimposed on a simplified geological, surface water drainage and road map | 27 |

Overview of Karst

| | | |
|--------|--|----|
| Fig. 1 | Distribution of karst regions worldwide, showing karst aquifers referenced in the text (sourced at http://www.circleofblue.org/waternews/ on 28/04/2012) | 32 |
| Fig. 2 | Schematic presentation of the components of an undisturbed karst hydro-ecosystem and its associated values and ecosystem services (modified after Goldscheider 2012). | 32 |
| Fig. 3 | Distribution of carbonate strata in South Africa, showing the main areas of karst development as A (Transvaal Supergroup dolomite), B (Cango Caves Group limestone) and C (Bredasdorp Group limestone) (from Martini 2006) | 35 |
| Fig. 4 | Map of the Sterkfontein Cave system showing the labyrinthic joint-controlled pattern of both the Sterkfontein and Lincoln cave sections (from Martini et al. 2003). | 38 |
| Fig. 5 | Sketch of ‘dome cavities’ in the Mound breccia of the Milner deposit beneath a protecting travertine layer in Sterkfontein Cave (from Wilkinson 1976) | 39 |

Physical Hydrology

| | | |
|---------|--|----|
| Fig. 1 | Schematic diagram of surface drainage and gauging network superimposed on the COH karst footprint; karst strata (not shown) extend to the west and east (see Fig. 1 in Chapter “Introduction and Background”). | 44 |
| Fig. 2 | Pattern and trend of Grootvlei Spruit mean annual (a_h) discharge gauged at station A2H033 in the period October 1964 to September 2015 | 45 |
| Fig. 3 | Long-term monthly hydrograph of the Grootvlei Spruit at station A2H033 for the period October 1964 to September 2015 | 45 |
| Fig. 4 | Long-term monthly discharge pattern of the Nouklip Spring, showing median values with 5%ile and 95%ile bounds and summer and winter trends as linear regression traces | 46 |
| Fig. 5 | Monthly discharge pattern of the Nouklip Spring in the period 1997–2015, showing median values with 5%ile and 95%ile bounds and summer and winter trends as linear regression traces | 47 |
| Fig. 6 | Pattern and trend of Skeerpoort River mean annual (a_h) discharge gauged at station A2H034 in the period October 1965 to September 2017 | 49 |
| Fig. 7 | Cumulative annual discharge at stations A2H033 and A2H034 illustrating the year-on-year constancy of flow in these springflow-driven drainages | 50 |
| Fig. 8 | Long-term monthly hydrograph of the Skeerpoort River at station A2H034 for the period October 1965 to September 2014. | 51 |
| Fig. 9 | Difference in long-term year-on-year discharge between stations A2H033 and A2H034 | 52 |
| Fig. 10 | Pattern and trend of Bloubank Spruit mean annual (a_h) discharge gauged at station A2H049 in the period October 1972 to September 2017 | 53 |
| Fig. 11 | Long-term monthly hydrograph of the Bloubank Spruit at station A2H049 for the period October 1972 to September 2017 | 54 |
| Fig. 12 | Pattern and trend of mine water discharge to the Tweelopie Spruit. | 55 |
| Fig. 13 | Pattern and trend of raw mine water discharge to the Tweelopie Spruit | 55 |
| Fig. 14 | Pattern and trend of RMW proportion in total mine water discharge | 56 |
| Fig. 15 | Pattern and trend of inflow to and effluent discharge from the Percy Stewart WWTW | 60 |

| | | |
|---------|---|----|
| Fig. 16 | Pattern and trend of (upper) Crocodile River annual (a_h) discharge at station A2H050 in the period October 1973 to September 2017 | 61 |
| Fig. 17 | Long-term monthly hydrograph of the upper reach of the Crocodile River at station A2H050 for the period October 1973 to September 2017 | 62 |
| Fig. 18 | Comparison of whole record (top), pre-2010 (left) and post-2009 (right) median annual (a_h) discharge contributions as Mm^3 and % ΣQ of the main rivers draining to Hartbeespoort Dam. | 63 |
| Fig. 19 | Pattern and trend of combined annual discharge (ΣQ) by main drainages in the Hartbeespoort Dam catchment in the period of common record, compared to the $\sim 190 Mm^3$ FSC of the dam (horizontal pecked line) that approximates the mean annual runoff to the dam; left to right legend order is stacked from bottom to top in bar graph | 64 |
| Fig. 20 | Pattern and trend of proportional contribution of karst basins to the total annual discharge (ΣQ) by main drainages in the Hartbeespoort Dam catchment in the period of common record | 65 |
| Fig. 21 | Flow reduction with distance along the middle reaches of the Bloubank Spruit system upstream of Sterkfontein Cave (data from Table 8, localities 1 to 4) | 66 |
| Fig. 22 | Manually gauged stream flow measurement sites employed in this study . . . | 71 |
| Fig. 23 | Pattern and trend of discharge and flow losses in the lower reach of the Riet Spruit (data from Table 12) | 72 |
| Fig. 24 | Correlation of SDMs at stations F11S12 and MRd in the Riet Spruit valley; error bars denote $\pm 10\%$ at F11S12 and $\pm 5\%$ at MRd (data from Table 12) | 74 |
| Fig. 25 | Historical Google Earth [®] images showing the development of ferrous hydroxide deposits in the channel of the Riet Spruit sometime between 22/05/2010 (top left) and 31/03/2011 (top right); stream section located between stations F11S12 and MRd as shown in Fig. 22 | 75 |
| Fig. 26 | Longitudinal profile along the course of the Tweelopie, Riet and Bloubank spruits from Kemp's Cave in the KGR to the south-eastern margin of the carbonate strata at the Nedbank Olwazini Estate | 78 |
| Fig. 27 | Schematic profile illustrating surface water gain/loss zones (A to D) and associated rates along the Tweelopie, Riet and Bloubank spruits from the Aviary Dam in the KGR to the Zwartkrans Spring | 80 |

Chemical Hydrology

| | | |
|--------|--|----|
| Fig. 1 | Variability of Skeerpoort River water major ion chemistry at station A2H034 in the period January 1976 to March 2017 (data from Table 1) . . . | 84 |
| Fig. 2 | Long-term pattern and trend of pH (top left), EC (top right), SO_4 (bottom left) and Fe (bottom right) associated with raw mine water produced by the BRI and #18 Winze point sources of AMD; significance of broken linking chevron lines and arrows explained in text | 86 |
| Fig. 3 | Variability of pH (top left), EC (top right), SO_4 (bottom left) and Fe (bottom right) associated with raw mine water produced by the BRI, #18 Winze and #17 Winze point sources of AMD, and the RMW mixture (MIX) drawn from the BRI Dam for treatment in the HDS Plant | 88 |
| Fig. 4 | Long-term pattern and trend of pH (top left), EC (top right), SO_4 (bottom left) and Fe and Mn (bottom right) associated with treated/neutralised mine water produced by the HDS mine water treatment plant and discharged into the Tweelopie Spruit at the end-of-pipe | 88 |
| Fig. 5 | Pattern and trend of pH of Tweelopie Spruit water from May 2004 to September 2014 | 89 |

| | | |
|---------|---|-----|
| Fig. 6 | Pattern and trend of SEC of Tweelopie Spruit water from September 2004 to September 2014 | 90 |
| Fig. 7 | Pattern and trend of SO ₄ levels in Tweelopie Spruit water from September 2004 to September 2014 | 91 |
| Fig. 8 | Pattern and trend of Fe levels in Tweelopie Spruit water from June 2009 to September 2014 | 92 |
| Fig. 9 | Pattern and trend of Mn levels in Tweelopie Spruit water from June 2009 to September 2014 | 93 |
| Fig. 10 | Period-specific surface water chemistry changes in the Tweelopie Spruit of the variables/analytes (from top to bottom) pH, SEC, SO ₄ , Fe and Mn at the Hippo Dam (left) and F11S12 (right) (data from Table 4) | 95 |
| Fig. 11 | Variability of Tweelopie Spruit water major ion chemistry at station F11S12 in the period November 2003 to September 2008, also showing mid-February 2010 values (X symbol) for comparison with more impacted conditions, and subsequent improvement in specific analytes/variables (text box) | 98 |
| Fig. 12 | Pattern and trend of SEC and pH at stations F11S12 and MRd in the Tweelopie/Riet Spruit system in the period February 2010 to September 2014 (data from Table 10) | 99 |
| Fig. 13 | Comparison of major ion chemistry at stations F11S12 and MRd in the Tweelopie/Riet Spruit system in mid-February 2010. | 101 |
| Fig. 14 | Comparison of some trace metals concentration at stations F11S12 and MRd in the Tweelopie/Riet Spruit system in mid-February 2010. | 101 |
| Fig. 15 | Variability of Blougat Spruit water major ion chemistry at station 188048 in the period June 2004 to September 2008, also showing more recent selected variable/analyte values (text box) for comparison | 103 |
| Fig. 16 | Comparison of inorganic quality of Blougat Spruit water upstream and downstream of the Percy Stewart WWTW (data from Tables 15 and 16). ... | 106 |
| Fig. 17 | Comparison of organic quality of Blougat Spruit water upstream and downstream of the Percy Stewart WWTW (data from Tables 15 and 16). ... | 106 |
| Fig. 18 | Comparison of bacteriological quality of Blougat Spruit water upstream and downstream of the Percy Stewart WWTW (data from Tables 15 and 16) | 107 |
| Fig. 19 | Variability of Tweefontein Spruit water major ion chemistry at station F14S15 in the period June 2004 to September 2008. | 108 |
| Fig. 20 | Recent electrical conductivity and pH pattern and trend in Bloubank Spruit water at station BB@M between Sterkfontein Cave and Zwartkrans Spring. | 109 |
| Fig. 21 | Variability of Bloubank Spruit water major ion chemistry at station A2H049 for the period May 1979 to August 2002 (top left), the period September 2002 to January 2010 (top right), the period February 2010 to July 2012 (bottom left), and the period August 2012 to September 2017 (bottom right) | 111 |
| Fig. 22 | Piper diagram of pre-2010 (long-term as per Fig. 29) and more recent Bloubank Spruit water chemistry at station A2H049. | 111 |
| Fig. 23 | Graphical comparison of surface water chemistry at various localities in the Bloubank Spruit system on 18/05/2010. | 113 |
| Fig. 24 | Comparison of the Bloubank Spruit water chemistry at the NOE property and station A2H049 in the period of common record November 2007 to September 2014 | 113 |

| | | |
|---------|--|-----|
| Fig. 25 | Comparison of bacterial concentrations in surface water at various locations in the Bloubank Spruit system on 18/05/2010; for comparison, note the earlier values at station BC1 as well as the $\sim 2\times$ difference in scale between the left and right vertical axes (data from Table 20) | 114 |
| Fig. 26 | Correlation of pH (top) and faecal coliform bacteria (bottom) levels in the Bloubank Spruit at the NOE property with monthly rainfall in the headwaters of the catchment | 115 |
| Fig. 27 | Variability of Crocodile River water major ion chemistry at station A2H050 in the period May 1979 to September 2014 (data from Table 3) | 117 |
| Fig. 28 | Piper diagram (top left) and Stiff diagrams (bottom and right) characterising pre-2010 surface water chemistry in the study area; note the different Stiff diagram horizontal scales | 119 |
| Fig. 29 | Schoeller diagrams characterising pre-2010 surface water chemistry in the study area; note the $10\times$ difference in scale between the left and right vertical axes | 120 |
| Fig. 30 | Comparison of the long-term (October 1976 to September 2014) median monthly TDS loads carried by the main drainages in the study area | 121 |
| Fig. 31 | Variance in the long-term (October 1976 to September 2014) monthly Skeerpoort River TDS load at station A2H034 | 123 |
| Fig. 32 | Variance in the long-term (October 1979 to September 2014) monthly Bloubank Spruit TDS load pattern at station A2H049 | 123 |
| Fig. 33 | Variance in the pre-2010 monthly Bloubank Spruit TDS load pattern at station A2H049 | 124 |
| Fig. 34 | Variance in the recent (2010 to 2014) monthly Bloubank Spruit TDS load pattern at station A2H049 | 124 |
| Fig. 35 | Variance in the long-term (October 1979 to September 2014) monthly Crocodile River TDS load pattern at station A2H050 | 125 |
| Fig. 36 | Long-term (June 1979 to September 2014) monthly TDS load pattern and trend in the Bloubank Spruit at station A2H049 | 125 |
| Fig. 37 | Long-term (May 1979 to September 2014) monthly TDS load pattern and trend in the upper reach of the Crocodile River at station A2H050 | 126 |
| Fig. 38 | Long-term (October 1979 to September 2014) monthly SO_4 load pattern and trend in the Bloubank Spruit at station A2H049 | 126 |
| Fig. 39 | Pattern and trend in the SO_4 concentration at station A2H049 since the start of mine water decant in the Western Basin | 127 |
| Fig. 40 | Long-term (June 1979 to September 2014) trend in the SO_4 :TDS ratio at station A2H049 | 128 |
| Fig. 41 | Pattern and trend in the SO_4 :TDS ratio at station A2H049 since the start of mine water decant in the Western Basin | 128 |
| Fig. 42 | Monthly TDS load pattern and trend at station A2H049 in each year of historical record | 129 |
| Fig. 43 | Pattern and trend of cumulative monthly TDS load delivered by the Bloubank Spruit system in the long-term | 129 |
| Fig. 44 | Pattern and trend of cumulative monthly SO_4 load delivered by the Bloubank Spruit system in the long-term | 130 |
| Fig. 45 | Cumulative long-term median monthly TDS loads discharged by the Bloubank Spruit and the upper reach of the Crocodile River | 131 |
| Fig. 46 | Comparison of cumulative median monthly Bloubank Spruit system TDS loads for three periods of record | 131 |
| Fig. 47 | Pattern and trend of daily SO_4 and TDS loads in mine water delivered to the Tweelopie Spruit | 132 |

| | | |
|---------|---|-----|
| Fig. 48 | Pattern and trend of TDS load losses in the lower reach of the Riet Spruit | 134 |
| Fig. 49 | Pattern and trend of SO_4 load losses in the lower reach of the Riet Spruit . . . | 136 |
| Fig. 50 | Pattern and trend of recent TDS load associated with treated municipal effluent discharge to the Blougat Spruit. | 138 |
| Fig. 51 | Comparison of annual TDS load contributions of the main drainages in the Hartbeespoort Dam catchment ($\Sigma\text{TDS} = 104\,943\text{ t/a}$) and the recent past (right) ($\Sigma\text{TDS} = 240\,089\text{ t/a}$) (data from Tables 32 and 33) | 139 |
| Fig. 52 | Pattern and trend of the N:P ratio for Bloubank Spruit water at the NOE and station A2H049 and for Crocodile River water at station A2H050 in the period January 2009 to September 2014 (note cut-off at 100:1 to magnify graphs at lower ratio values). | 140 |
| Fig. 53 | Pattern and trend of U_T in Tweelopie Spruit surface water. | 144 |
| Fig. 54 | Wilcox diagram illustrating the classification of surface water chemistry for irrigation purposes (data from Table 46); circle represents long-term median data and square single values | 148 |
| Fig. 55 | Magnitude of solubilisation of trace elements from streambed sediments in the Bloubank Spruit system | 163 |

Physical Hydrogeology

| | | |
|---------|---|-----|
| Fig. 1 | Potentiometric map of the south-western portion of the study area (modified after Hobbs and Cobbing 2007) | 169 |
| Fig. 2 | Previous definition of dolomitic basins/subcompartments as proposed by Holland (2007), and later modified by Holland (2009) and replicated by Meyer (2014). | 171 |
| Fig. 3 | Current understanding of dolomitic compartment/subcompartment distribution showing relationship to the spring outlets draining the hydrogeologic units. | 172 |
| Fig. 4 | Longitudinal surface and water table profile along the course of the Tweelopie, Riet and Bloubank Spruits from Kemp's Cave in the Krugersorp Game Reserve to beyond the Zwartkrans Spring | 175 |
| Fig. 5 | Graphic comparison of the statistical hydrographic response observed in DWS groundwater level monitoring stations in the period 1985–2014 (data from Table 6). | 183 |
| Fig. 6 | Long-term groundwater level response pattern in DWS monitoring boreholes. | 183 |
| Fig. 7 | Long-term groundwater level response pattern in Group A boreholes from Fig. 6 | 184 |
| Fig. 8 | Long-term groundwater level response pattern in Group B boreholes from Fig. 6 | 185 |
| Fig. 9 | Continuous groundwater level response pattern in Sterkfontein Cave over a period of 27 months (use of image courtesy of DWS). | 188 |
| Fig. 10 | Groundwater level response pattern and trend in borehole SF1 that serves as a proxy for the Lake water level in Sterkfontein Cave | 189 |
| Fig. 11 | Long-term potentiometric response in monitoring boreholes A2N0600 and A2N0602 compared to the response in borehole SF1 serving as a proxy for the cave water level. | 190 |
| Fig. 12 | Verification of the Kromdraai Spring discharge based on mass balance calculations | 195 |
| Fig. 13 | Hydrograph of the Nouklip Spring as gauged at station A2H033 on the Grootvlei Spruit ~ 525 m downstream of the spring | 197 |

| | | |
|---------|--|-----|
| Fig. 14 | Locality map of geosites in the mine area and Krugersdorp Game Reserve. | 201 |
| Fig. 15 | Schematic profile of hydrogeologic and mining-related features in the West Rand Goldfield (see Fig. 10 for profile positions) | 202 |
| Fig. 16 | Groundwater drainage map illustrating the conceptual flow patterns associated with the basins/sub-compartments that subdivide the karst aquifer in the study area; see Table 5 for statistical analysis of groundwater level data in the Bloubank Spruit system | 203 |
| Fig. 17 | Hydrogeological cross-section (top) through the karst aquifer from south-west to north-east (see Fig. 16) illustrating the differences in groundwater rest level between basins/subcompartments, and plan view (bottom) illustrating the corresponding conceptual groundwater drainage pattern as per conventional compass direction; note the autogenic recharge associated with the Danielsrust and Tweefontein springs | 204 |
| Fig. 18 | Elucidation of hydrological, geological and hydrogeological aspects along the southern boundary of the COH south-west of Sterkfontein Quarry; circled localities labelled 'a' to 'd' mark the position of significant grike features, and italicised values indicate the recent ambient groundwater elevation in each subcompartment as derived from individual borehole measurements (base image courtesy of Google Earth®). | 205 |
| Fig. 19 | Distribution of selected surface water and groundwater monitoring stations in the Zwartkrans Basin, also showing the groundwater flow paths followed by allogenic recharge (brown) and autogenic recharge (blue) | 206 |
| Fig. 20 | Oblique Google Earth® view of the Zwartkrans Basin illustrating the nexus of allogenic (municipal and mine wastewater) and autogenic groundwater fluxes | 208 |

Chemical Hydrogeology

| | | |
|--------|---|-----|
| Fig. 1 | Schoeller graphical comparison of natural hydrochemistry associated with the respective lithostratigraphic units represented in the study area (data from Table 1). | 212 |
| Fig. 2 | Piper diagram characterization of hydrochemistry associated with various surface water and groundwater sources in the study area (modified after Hobbs and Cobbing 2007) | 213 |
| Fig. 3 | Comparison of historical and more recent SO ₄ levels in groundwater from DWS monitoring boreholes in the Zwartkrans Basin | 214 |
| Fig. 4 | Comparison of the 'oldest' (open symbol ca. 1989) and most recent (solid symbol December 2014) groundwater chemical compositions at the longest-operating DWS monitoring stations. | 215 |
| Fig. 5 | Locality map of mine water and groundwater monitoring stations in the locus of decant and the Krugersdorp Game Reserve; borehole MGP4 located off southern edge of map below MGP5. | 216 |
| Fig. 6 | Pattern and trend of SEC monitored by MG/MSA in the mine area, compared to the true SEC values at depth in boreholes MGP1 and MGP3. | 218 |
| Fig. 7 | Observed SO ₄ trend at four groundwater quality monitoring stations along the losing reach of the Riet Spruit upstream of Oaktree | 219 |
| Fig. 8 | Graphic comparison of historical and current Sterkfontein Cave groundwater chemistry | 221 |

| | | |
|---------|---|-----|
| Fig. 9 | Piper diagram of historical and recent Sterkfontein Cave water chemistry compared to other karst groundwater and October 2012 and May 2014 Zwartkrans Spring (ZSp) water | 222 |
| Fig. 10 | Continuous electrical conductivity response pattern in Sterkfontein Cave water over a period of 27 months (use of image courtesy of DWS) | 222 |
| Fig. 11 | Pattern and trend of the SO_4 concentration and SO_4 :TDS ratio in Sterkfontein Cave Lake water since 2001 | 225 |
| Fig. 12 | Piper diagram of GRU water chemistry | 226 |
| Fig. 13 | Graphic comparison of groundwater chemistry associated with GRUs | 227 |
| Fig. 14 | Graphic comparison of groundwater chemistry associated with 'pristine' GRUs | 228 |
| Fig. 15 | Relationship of Pb isotopic ratios of water in the West Rand area to the Stacey–Kramers curve (dotted line); South African leaded petrol plots at Δ on this curve; different stages of crustal evolution shown by ages in Ga; arrow shows the direction of deviation of the Pb isotope signature associated with mine water impacts (modified from Coetzee and Rademeyer 2006) | 229 |
| Fig. 16 | Stable isotope composition of groundwater in the study area, also showing the characteristic fields associated with various sources (modified from Hobbs et al. 2010) | 231 |
| Fig. 17 | Graph of groundwater bacteriological quality in the study area; the $\sim 3\times$ difference in scale between the vertical axes explains those <i>E. coli</i> values that exceed total coliform counts. | 233 |
| Fig. 18 | Graphic comparison of ca. 2010 springwater chemistry (data from Table 5) | 235 |
| Fig. 19 | Piper diagram of ca. 2010 springwater chemistry (data from Table 5) compared to typical Malmani Subgroup karst groundwater. | 235 |
| Fig. 20 | Graphic comparison of ca. 2014 springwater chemistry (data from Table 6); compositions of DSP and JNNR2 are virtually identical | 236 |
| Fig. 21 | Saturation state of springwaters with respect to calcite (SI_C) and dolomite (SI_D) ca. 2010 and ca. 2014 (data from Tables 5 and 6) | 237 |
| Fig. 22 | Graphic comparison of Zwartkrans Spring water chemistry since 2006 | 238 |
| Fig. 23 | Pattern and trend of Zwartkrans Spring water salinity since mid-2013 | 239 |
| Fig. 24 | Pattern and trend of Zwartkrans Spring water electrical conductivity since mid-2010; the solid symbols mark the start and end values of Fig. 23 data record | 240 |
| Fig. 25 | Graphic comparison of Danielsrust Spring water chemistry between 2010 and 2014 | 241 |
| Fig. 26 | Graphic comparison of Plover's Lake springs water chemistry between 2006 and 2014 | 242 |
| Fig. 27 | Graphic of Kromdraai Spring water chemistry in 2014 | 243 |
| Fig. 28 | Schematic illustration of the hypothetical flow path (arrowed) taken by groundwater bearing a mine water impact into the Kromdraai Subcompartment toward the Kromdraai Spring | 244 |
| Fig. 29 | Graphic comparison of Tweefontein Spring water chemistry between 2006 and 2014 | 245 |
| Fig. 30 | Graphic comparison of Nouklip Spring water chemistry in 2010 and 2014 | 246 |
| Fig. 31 | Graphic comparison of Nash Spring water chemistry in 2010 and 2014 | 248 |
| Fig. 32 | Graphic comparison of median water chemistry associated with selected springs in the KGR in the period September 2009–September 2014 (data from Table 8) | 251 |

| | | |
|---------|---|-----|
| Fig. 33 | Salinity trend for water produced by springs SP1, SP2, and SP3 in the KGR in the period September 2009–September 2014. | 252 |
| Fig. 34 | Sulfate trend for water produced by springs SP1, SP2, and SP3 in the KGR in the period September 2009–September 2014; the Hippo Dam record provides a reference of contemporary surface water discharge quality. | 253 |
| Fig. 35 | Trend in pH for water produced by springs SP1, SP2, and SP3 in the KGR in the period September 2009–September 2014. | 254 |
| Fig. 36 | Piper diagram of KGR median springwater chemistry (data from Table 8) compared to pristine karst springwater chemistry | 255 |
| Fig. 37 | Locality map of pesticide residue sample sources CSIR8 and CFM1 | 256 |
| Fig. 38 | Comparison of surface water and groundwater chemistry in the vicinity of the historic Kromdraai Gold Mine | 257 |
| Fig. 39 | Definition of the principal flow path describing the passage of allogenic recharge through the Zwartkrans Basin to the Zwartkrans Spring based on late-2014 sulfate concentrations in groundwater. | 258 |
| Fig. 40 | Distribution of DWS monitoring boreholes with pH pattern and trend as bar graphs; arrow denotes principal direction of groundwater flow. | 259 |
| Fig. 41 | Distribution of DWS monitoring boreholes with SEC pattern and trend as bar graphs; arrow denotes principal direction of groundwater flow. | 260 |
| Fig. 42 | Distribution of DWS monitoring boreholes with SO ₄ pattern and trend as bar graphs; arrow denotes principal direction of groundwater flow. | 261 |
| Fig. 43 | Pattern and trend of SEC at flow gauging stations F11S12 and MRd on occasion of each synoptic discharge measurement (data from Table 10 in Chapter “Chemical Hydrology”). | 262 |
| Fig. 44 | Pattern and trend of pH at flow gauging stations F11S12 and MRd on occasion of each synoptic discharge measurement (data from Table 10 in Chapter “Chemical Hydrology”). | 263 |
| Fig. 45 | Saturation state of karst groundwaters in the Zwartkrans Basin with respect to calcite (SI _C) and dolomite (SI _D) | 264 |
| Fig. 46 | Long-term pattern and trend of SEC (at left) and SO ₄ (at right) in karst groundwater from DWS monitoring stations A2N0584/GP00302, A2N0586/GP00300, and A2N0600; note common time scales and postulated start of rise in concentrations (long vertical pecked line) | 265 |
| Fig. 47 | Piper diagram of recent groundwater chemistry defining the mine water impact on the karst groundwater of the Zwartkrans Basin. | 266 |
| Fig. 48 | Schematic profiles through the Bloubank Spruit valley and Sterkfontein Cave illustrating the relationship between the water table and lake elevations and the stream channel; lateral gradational shading reflects relative intensity of mine water impact on karst groundwater as shown by recent pH, SEC, and SO ₄ values; see Fig. 39 for location of the transects | 267 |
| Fig. 49 | Wilcox diagram illustrating the classification of groundwater chemistry in the study area for irrigation purposes | 268 |
| Fig. 50 | Wilcox diagram illustrating the classification of groundwater chemistry per GRU for irrigation purposes | 269 |
| Fig. 51 | Pattern and trend of mine water discharge into the karst environment (RMW = raw mine water; TMW = treated mine water). | 271 |
| Fig. 52 | Vertical profiles of field water chemistry variables in #18 Winze in October 2010 | 273 |

| | | |
|---------|---|-----|
| Fig. 53 | Vertical profiles of field water chemistry variables in the CPS borehole in February 2013. | 274 |
| Fig. 54 | Vertical profiles of field water chemistry variables in borehole RG1. | 275 |
| Fig. 55 | Vertical profiles of field water chemistry variables in borehole RG2 in December 2011. | 276 |
| Fig. 56 | Vertical profiles of field water chemistry variables in borehole RG3 in December 2011. | 277 |
| Fig. 57 | Vertical profiles of field water chemistry variables in borehole MGP1. | 278 |
| Fig. 58 | Vertical profiles of field water chemistry variables in borehole MGP2 in December 2011. | 279 |
| Fig. 59 | Vertical profiles of field water chemistry variables in borehole MGP3. | 280 |
| Fig. 60 | Comparison of contemporary field water chemistry variable profiles in boreholes RG1 and MGP3 on two occasions. | 281 |
| Fig. 61 | Vertical profiles of field water chemistry variables in borehole MGP4 in February 2013. | 282 |
| Fig. 62 | Pre- and post-sampling vertical profiles of field water chemistry variables in borehole GP00305. | 283 |
| Fig. 63 | Temporal variation in vertical profiles of field water chemistry variables in borehole GP00305. | 284 |
| Fig. 64 | Vertical profiles of field water chemistry variables in borehole GP00306 in November 2011. | 285 |
| Fig. 65 | Vertical profiles of field water chemistry variables in borehole GP00307 in November 2011. | 286 |
| Fig. 66 | Vertical profiles of field water chemistry variables in borehole GP00308 in November 2011. | 287 |
| Fig. 67 | Vertical profiles of field water chemistry variables in boreholes A2N0583 and GP00304 in November 2011. | 288 |
| Fig. 68 | Vertical profile of field water chemistry variables in boreholes A2N0584 and GP00302 in March 2014. | 289 |
| Fig. 69 | Temporal variation in vertical profiles of field water chemistry variables in borehole A2N0584. | 290 |
| Fig. 70 | Temporal variation in vertical profiles of field water chemistry variables in borehole GP00302. | 291 |
| Fig. 71 | Pre- and post-sampling vertical profiles of field water chemistry variables in borehole A2N0586. | 292 |
| Fig. 72 | Pre- and post-sampling vertical profiles of field water chemistry variables in borehole GP00300. | 293 |
| Fig. 73 | Temporal variation in vertical profiles of field water chemistry variables in borehole A2N0586. | 294 |
| Fig. 74 | Temporal variation in vertical profiles of field water chemistry variables in borehole GP00300. | 295 |
| Fig. 75 | Vertical profiles of field water chemistry variables in borehole GP00301 in October 2011. | 296 |
| Fig. 76 | Pre- and post-sampling vertical profiles of field water chemistry variables in borehole GP00309. | 297 |
| Fig. 77 | Temporal variation in vertical profiles of field water chemistry variables in borehole GP00309. | 298 |
| Fig. 78 | Vertical profiles of field water chemistry variables in borehole GP00311 in October 2011. | 299 |
| Fig. 79 | Vertical profiles of field water chemistry variables in borehole GP00312 in October 2011. | 300 |

| | | |
|---------|--|-----|
| Fig. 80 | Pre- and post-sampling vertical profiles of field water chemistry variables in borehole GP00313 | 301 |
| Fig. 81 | Temporal variation in vertical profiles of field water chemistry variables in borehole GP00313 | 302 |
| Fig. 82 | Vertical profiles of field water chemistry variables in borehole GP00314 in November 2011 | 303 |
| Fig. 83 | Pourbaix diagram showing the distribution of Eh–pH values in mine water and groundwater environments in the subregion in relation to limits in the natural environment (redrawn in green and blue from USDA 2012) as defined by Baas-Becking et al. (1960), Garrels and Christ (1965) and Langmuir (1996), and stability fields for solid and dissolved forms of Fe at 25 °C and 1 atm (redrawn in red from Hem 1985). | 304 |
| Fig. 84 | Comparison of trace metal and other variable concentrations in surface water and proximate groundwater sources (SEC as mS/m; SO ₄ as mg/L). . . | 305 |
| Fig. 85 | Correlation of empirically-derived and formula-derived karst denudation/dissolution rates | 308 |
| Fig. 86 | Denudation rate as a function of discharge for different P_{CO_2} values (insert diagram) at a temperature of 25 °C [redrawn from Ford and Williams (2007) and Kaufmann (2003)]; the shaded areas (main diagram) define the identical runoff ranges listed in Tables 16, 18 and 19, and the pecked arrows the mean discharge/runoff rate (113 mm/a) and associated theoretical denudation rates for a P_{CO_2} of $10^{-1.5}$ atm; see text for discussion of reverse (anti-clockwise) arrow | 309 |
| Fig. 87 | Pattern and trend of net alkalinity in groundwater from monitoring boreholes. | 313 |
| Fig. 88 | Enlarged view of pattern and trend of net alkalinity shown in Fig. 87 | 314 |
| Fig. 89 | Comparison of ‘diagnostic’ chemical variable values for raw mine water (BRI) and downstream surface water (F11S12) (data from Table 23). | 315 |

List of Tables

Description of the Physical Environment

| | | |
|---------|---|----|
| Table 1 | Geographic definition of quaternary catchments spanned by the study area. | 13 |
| Table 2 | Rainfall monitoring stations in the study area and surrounds | 15 |
| Table 3 | Comparison of mean precipitation for full calendar and hydrological years at four rainfall stations | 16 |
| Table 4 | Classification of the vegetation of the study area (after Mucina and Rutherford 2006). | 17 |
| Table 5 | Simplified lithostratigraphic subdivision of strata in the subregion. | 18 |
| Table 6 | Salient hydrologic and hydrogeologic aspects associated with the most well-known fossil sites in the study area | 19 |

Overview of Karst

| | | |
|---------|--|----|
| Table 1 | Geographic distribution of karst water level monitoring stations operated nationally by DWS (from Bertram 2008). | 34 |
|---------|--|----|

Physical Hydrology

| | | |
|----------|---|----|
| Table 1 | Statistical analysis of Grootvlei Spruit mean monthly discharge at station A2H033 in the period October 1964 to September 2015 (no data available since 13/12/2015) | 45 |
| Table 2 | Statistical analysis of Grootvlei Spruit mean monthly discharge at station A2H033 in the period October 1997 to September 2015 | 48 |
| Table 3 | Statistical analysis of Skeerpoort River mean monthly discharge at station A2H034 in the period October 1965 to September 2017 | 48 |
| Table 4 | Statistical analysis of Bloubank Spruit mean monthly discharge gauged at station A2H049 in the period October 1972 to September 2017 | 52 |
| Table 5 | Results of opportunistic flow measurements downstream of the Percy Stewart WWTW. | 60 |
| Table 6 | Statistical analysis of upper Crocodile River mean monthly discharge gauged at station A2H050 in the period October 1973 to September 2017. | 61 |
| Table 7 | Statistical analysis of the long-term annual (a_h) discharge contributions by the main rivers draining the Hartbeespoort Dam catchment | 62 |
| Table 8 | Flow gauging results ca. 1985 in the middle reaches of the Bloubank Spruit system (from Fig. 7.1 in Chapter “Physical Hydrogeology” of Bredenkamp et al. 1986) | 65 |
| Table 9 | Change in flow with distance downstream of the mine area on 05/02/2010 | 69 |
| Table 10 | Change in flow with distance downstream of the mine area on 01/04/2010 | 69 |

| | | |
|----------|---|----|
| Table 11 | Quantification of stream flow gains/losses in the lower reach of the Tweelopie Spruit | 69 |
| Table 12 | Quantification of stream flow losses in the lower reach of the Riet Spruit | 73 |
| Table 13 | Results of stream flow measurements in the Blougat Spruit on 18/05/2010 | 77 |
| Table 14 | Results of stream flow measurements in the Bloubank Spruit | 79 |
| Table 15 | Calculation of groundwater resurgence in the Bloubank Spruit upstream of Zwartkrans Spring on 15/01/2013 using measured flows and SEC-based TDS load values | 79 |

Chemical Hydrology

| | | |
|----------|---|-----|
| Table 1 | Statistical analysis of Skeerpoort River water chemistry at station A2H034 in the period January 1976 to March 2017 | 84 |
| Table 2 | Statistical analysis of raw mine water chemistry delivered by the BRI in the period January 2005 to September 2017 | 85 |
| Table 3 | Statistical analysis of treated/neutralised mine water chemistry discharge to the Tweelopie Spruit in the period April 2005 to September 2017 | 86 |
| Table 4 | Summary statistics of period-specific surface water chemistry changes in the Tweelopie Spruit associated with four distinct mine water discharge regimes | 94 |
| Table 5 | List of metal analytes monitored in treated/neutralised mine water discharged to the Tweelopie Spruit from the mine area per distinctive monitoring period | 96 |
| Table 6 | Statistical analysis of metal analyte concentrations in treated/neutralised mine water discharged to the Tweelopie Spruit from the mine area per distinctive monitoring period | 96 |
| Table 7 | Statistical analysis of metal analyte concentrations in treated/neutralised mine water discharged to the Tweelopie Spruit from the mine area per distinctive discharge period | 97 |
| Table 8 | Summary of SO ₄ : SEC ratio statistics for surface water in the Tweelopie Spruit and the Bloubank Spruit for the period September 2004 to September 2014 | 97 |
| Table 9 | Statistical analysis of Tweelopie Spruit water chemistry data associated with station F11S12 for the period November 2003 to September 2008 sourced from the DWS in November 2013 | 98 |
| Table 10 | Record of SEC and pH measurements at stations F11S12 and MRd on occasion of flow gauging measurements (SDMs), also showing derived SO ₄ and TDS concentrations | 100 |
| Table 11 | Statistical analysis of Blougat Spruit water chemistry at station 188048 for the period June 2004 to September 2008 (raw data sourced from the DWS in November 2013) | 102 |
| Table 12 | Concentration range of selected trace metals in Blougat Spruit water at three sites downstream of the Percy Stewart WWTW (from Awofolu et al., 2007) | 103 |
| Table 13 | Statistical analysis of Percy Stewart WWTW discharge chemistry data (from MCLM) for the period July 2007 to June 2009 | 104 |
| Table 14 | Statistical analysis of Percy Stewart WWTW effluent chemistry data associated with station PSFE for the period November 2002 to February 2010 sourced from the DWS November 2013 | 104 |

| | | |
|----------|---|-----|
| Table 15 | Statistical analysis of Blougat Spruit water chemistry at station BGS2 for the period November 2002 to July 2009 (raw data sourced from the DWS in November 2013) | 105 |
| Table 16 | Statistical analysis of Blougat Spruit water chemistry at station BGS1 for the period November 2002 to February 2010 sourced from the DWS in November 2013 | 105 |
| Table 17 | Water chemistry results for station BC1 on 06/03/2013 | 107 |
| Table 18 | Statistical analysis of Tweefontein Spruit water chemistry at station F14S15 for the period June 2004 to September 2008 sourced from the DWS in November 2013 | 108 |
| Table 19 | Statistical analysis of Bloubank Spruit water chemistry at station A2H049 for the period May 1979 to September 2017 | 110 |
| Table 20 | Comparison of mid-2010 surface water chemistry at various positions in the Bloubank Spruit system | 112 |
| Table 21 | Chemical characterisation of surface water drawn from the Bloubank Spruit at the NOE property in the period November 2007 to September 2014 | 114 |
| Table 22 | Analysis of Bloubank Spruit water nutrient and bacterial content at the NOE property in the period January 2009 to September 2014 | 116 |
| Table 23 | Statistical analysis of Crocodile River water chemistry at station A2H050 for the period May 1979 to September 2014 | 118 |
| Table 24 | Statistical analysis of Driefontein WWTW discharge water chemistry (at station DFE) for the period November 2002 to February 2010 sourced from the DWS in November 2013 | 119 |
| Table 25 | Annual long-term TDS load delivered by the main drainages in the study area | 122 |
| Table 26 | Median annual nutrient loads (as NO ₃ -N and PO ₄ -P) delivered by the Crocodile River system to Hartbeespoort Dam in the period 1979–'80 to 2013–'14 | 132 |
| Table 27 | Estimated TDS load contributed by various sources in the Bloubank Spruit system prior to the 2010 hydrological year | 133 |
| Table 28 | Statistical analysis of SO ₄ and TDS loads in composite mine water entering the Tweelopie Spruit in the period January 2006 to September 2013 | 134 |
| Table 29 | Assessment of TDS load losses to the karst aquifer between stations F11S12 and MRd | 135 |
| Table 30 | Assessment of SO ₄ load losses to the karst aquifer between stations F11S12 and MRd | 137 |
| Table 31 | Statistical analysis of TDS and SO ₄ load losses in the lower reach of the Riet Spruit | 138 |
| Table 32 | Median annual TDS load delivered by main drainages in the Hartbeespoort Dam catchment in the period of common hydrological and hydrochemical record (1980 to 2014) | 139 |
| Table 33 | Median annual TDS load delivered by main drainages in the Hartbeespoort Dam catchment in the hydrological and hydrochemical record period 2010 to 2014 | 139 |
| Table 34 | Comparison of the long-term (1980 to 2014) median TDS concentrations with those for the recent (2010 to 2014) hydrological years for the regional drainages | 140 |
| Table 35 | Comparison of the long-term (1980 to 2014) median discharges with those for the recent (2010 to 2014) hydrological years for the regional drainages | 141 |

| | | |
|----------|---|-----|
| Table 36 | Comparison of the long-term (1980 to 2014) median TDS load delivered to Hartbeespoort Dam with the median TDS load delivered in the 2010 to 2014 hydrological years | 142 |
| Table 37 | Statistical characterisation of the SO ₄ :Cl ratio for drainages in the study area for the full available record up to September 2014 and the common record period since June 2004 | 142 |
| Table 38 | Statistical values of the N:P ratio for drainages in the study area for various periods. | 143 |
| Table 39 | Statistical comparison of Fe and Mn concentrations in composite mine water discharge with Bloubank Spruit surface water at A2H049 in the period February 2010 to July 2012 | 145 |
| Table 40 | Summary of Hg values for mine and surface water sources in the study area | 146 |
| Table 41 | Summary of trace/heavy metal(loid) concentrations in Tweelopie Spruit water at the Hippo Dam and Brickworks Dam stations in the period December 2012 to September 2014 | 146 |
| Table 42 | Summary of trace/heavy metal concentrations in Bloubank Spruit water at the NOE in the period May 2011 to December 2014. | 147 |
| Table 43 | Net acidity and net alkalinity of various mine and surface waters in the study area. | 149 |
| Table 44 | Free acidity and metal acidity associated with the results presented in Table 43. | 150 |
| Table 45 | Summary of the acid load addition to the karst aquifer of the Zwartkrans Subcompartment in the period December 2012 to July 2014 | 151 |
| Table 46 | Range of representative SAR values for various surface water sources in the study area. | 153 |
| Table 47 | Evaluation of Bloubank Spruit system surface water quality for irrigation use | 154 |
| Table 48 | Change in surface water chemistry with distance downstream of the mine water source | 155 |
| Table 49 | Change in surface water chemistry with distance downstream of the mine water source | 155 |
| Table 50 | Surface water field chemistry variable values. | 160 |
| Table 51 | Chemical analysis laboratory report for surface water sample collected at station BB@M | 160 |
| Table 52 | Surface water and groundwater field chemistry variables on 14/01/2011 | 162 |
| Table 53 | Chemical analysis of pipe scaling precipitate as seen in Plate 1 in Chapter “Physical Hydrology” (data courtesy of Helmholtz Centre for Environmental Research—UFZ, 2007). | 164 |
| Table 54 | Ranking of analyte concentrations in sediment by maximum value (data from Venter et al., 2010). | 164 |
| Table 55 | Estimate of soluble mass of individual elements per length of stream reach | 165 |

Physical Hydrogeology

| | | |
|---------|--|-----|
| Table 1 | Groundwater data sources relevant to the COH obtained from the Bredenkamp et al. (1986) study. | 168 |
| Table 2 | DWS exploration boreholes with transmissivity values greater than ~ 1000 m ² /d (from Bredenkamp et al. 1986) | 170 |
| Table 3 | Enumeration of compartment and subcompartment definition from Fig. 2 | 173 |

| | | |
|----------|--|-----|
| Table 4 | Summary information of groundwater compartments in the COH | 177 |
| Table 5 | Definition of groundwater rest level variables for the Bloubank Spruit system | 182 |
| Table 6 | Salient statistics for long-term DWS groundwater level monitoring data . . . | 182 |
| Table 7 | Salient hydrogeologic attributes associated with selected DWS monitoring stations (from Bredenkamp et al. 1986) | 185 |
| Table 8 | Comparison of historical and more recent groundwater levels in the study area. | 186 |
| Table 9 | Salient information pertaining to enumerated springs in the COH | 191 |
| Table 10 | SDM and load-based calculation of the Zwartkrans Spring discharge on 27/07/2010 | 193 |
| Table 11 | SDM and load-based calculation of the Zwartkrans Spring discharge on 13/08/2010 | 193 |
| Table 12 | SDM and load-based calculation of the Zwartkrans Spring discharge on 16/05/2012 | 193 |
| Table 13 | SDM and load-based calculation of the Zwartkrans Spring discharge on 15/01/2013 | 194 |
| Table 14 | Verification of the Kromdraai Spring discharge using TDS load calculations | 195 |
| Table 15 | Description of springs enumerated in the Krugersdorp Game Reserve . . . | 200 |
| Table 16 | Interrogation of drill records of high-yielding DWS exploration boreholes located in the Zwartkrans Basin (from Bredenkamp et al. 1986) for mean conduit depth | 210 |
| Table 17 | Assessment framework for the closure/recommissioning of DWS water level monitoring stations | 210 |

Chemical Hydrogeology

| | | |
|----------|--|-----|
| Table 1 | Characterization of groundwater hydrochemistry per lithostratigraphic unit represented in the study area (data from Barnard 2000) | 212 |
| Table 2 | Median chemistry variable/analyte values for groundwater associated with MG/MSA monitoring boreholes in the mine area in the period January 2011–April 2012. | 217 |
| Table 3 | Historical and recent chemistry of Sterkfontein Cave groundwater. | 221 |
| Table 4 | Comparison of ca. mid-2009 isotope data for cave and springwater. | 230 |
| Table 5 | Springwater chemistry ca. mid-2010 | 234 |
| Table 6 | Springwater chemistry ca. mid-2014 | 236 |
| Table 7 | Field chemical variable values of springwater in the KGR. | 249 |
| Table 8 | Statistical analysis of groundwater chemistry delivered by springs SP1, SP2, and SP3 in the KGR in the period September 2009–September 2014. | 250 |
| Table 9 | Summary of mercury values for various water sources in the study area. | 267 |
| Table 10 | Range of SAR values for basins/subcompartments. | 268 |
| Table 11 | Summary of salient hydrophysical and hydrochemical data for monitoring boreholes subjected to vertical hydrochemical profiling in late-2011 | 270 |
| Table 12 | Summary of salient hydrophysical and hydrochemical data for monitoring boreholes subjected to vertical hydrochemical profiling in February 2013 | 271 |
| Table 13 | Summary of salient hydrophysical and hydrochemical data for monitoring boreholes subjected to vertical hydrochemical profiling in June 2013 | 272 |

| | | |
|----------|--|-----|
| Table 14 | Summary of salient hydrophysical and hydrochemical data for monitoring boreholes subjected to vertical hydrochemical profiling in September and October 2013. | 272 |
| Table 15 | Summary of salient hydrophysical and hydrochemical data for monitoring boreholes subjected to vertical hydrochemical profiling in March 2014. | 272 |
| Table 16 | Estimate of solutional denudation rate based on the Corbel formula (Eq. 3) for spring discharges and springwater chemistry in May 2010. | 306 |
| Table 17 | Estimate of solutional denudation rate based on the Corbel formula for spring discharges and springwater chemistry in August 2014. | 307 |
| Table 18 | Estimate of solutional denudation rate based on Eq. 4. | 307 |
| Table 19 | Empirically-derived estimate of dissolution rate based on the mass of CaCO_3 removed. | 307 |
| Table 20 | Comparison of formula-derived and empirically-derived solutional denudation rates per karst basin and associated fossil site(s) | 309 |
| Table 21 | Net acidity and net alkalinity of various groundwaters in the COH environment. | 311 |
| Table 22 | Free acidity and metal acidity associated with the results presented in Table 21. | 311 |
| Table 23 | Water chemistry data used in Fig. 89 to compare raw mine water from station BRI with Tweelopie Spruit surface water at station F11S12. | 316 |
| Table 24 | Summary of carbon flux and export rates associated with COH spring discharges ca. May 2010. | 319 |
| Table 25 | Summary of carbon flux and export rates associated with COH spring discharges ca. August 2014. | 319 |
| Table 26 | Comparison of carbon flux and export rates associated with COH spring discharges ca. May 2010 and ca. August 2014. | 320 |

List of Plates

Description of the Physical Environment

| | | |
|---------|--|----|
| Plate 1 | Epikarst exposed in the form of a pinnacle ~2.5 m high in the Eccles Formation, showing the preferential dissolution of dolomite interlayered with less soluble and therefore more prominent chert bands, the slanting aspect of which also defines the local ~15° dip of the strata to the north-west (at bottom left of picture), with a partially wad-filled and vegetated vertical joint ('slot') separating the pinnacle from the overgrown rock mass at right of picture | 21 |
| Plate 2 | Recovery of mine residue deposits on the northern side of Dump 20 (see Fig. 5 for location) destined for reworking in the Mogale Gold/Mintails SA plant; the excavated/eroded area in the foreground is the southern end of the Millsite Pit (photo W Bason, date 09/12/2009) | 22 |
| Plate 3 | Panoramic view of the HDPE-lined dam at the Black Reef Incline (under grid at front right-of-centre), showing the pump station at left-of-centre beyond the dam, from where the water is pumped to the HDS treatment plant located on the skyline (continental divide) at left of picture; the Tweelapie Spruit on the far side of the dam flows from left (south) to right (north) across this 'fish-eye' view (photo W Bason, date 09/12/2009). | 23 |

Overview of Karst

| | | |
|---------|--|----|
| Plate 1 | Examples of the epikarst in the COH showing a dolomite pillars intersected by cutters (dissolution 'slots') filled with soil and covered by a variable thickness of soil cover, b ~ 4-m thick epikarst horizon overlying the gently folded strata forming the vadose zone exposed in the southern sidewall of Sterkfontein Quarry, with detail of the exposed features illustrated in (Plate 2), c chert-rich dolomite outcrop in the form of a quasi-karren field, d chert-rich bedded and dipping dolomite outcrop, e dolomite outcrop with soil cover and infill at the Zwartkrans fossil site, and f exposed epikarst at the Gladysvale fossil site (all photos P Hobbs; date shown in upper right corner) | 40 |
| Plate 2 | Detail of epikarst and vadose zone features exposed in the southern sidewall of Sterkfontein Quarry; note that the lower image is contiguous with the right side of the upper image along the common chevron line . . . | 41 |

Physical Hydrology

| | | |
|---------|---|----|
| Plate 1 | View from the right bank of the combination V-notch/rectangular weir flow gauging station A2H033 on the Grootvlei Spruit, showing the stage recorder housing (top centre) on the opposite bank. | 46 |
|---------|---|----|

| | | |
|----------|--|----|
| Plate 2 | Damage to infrastructure caused in the upper reaches of the Skeerpoort River valley by a flash flood in October 2009; note flood stage height of ~2 m as indicated by the drift debris on pumphouse roof and in inset picture. | 51 |
| Plate 3 | Aerial view (looking north) of the HDPE-lined off-channel storage dam shortly after construction at the Black Reef Incline (circular structure at centre right) to contain mine water decanting from this structure; also visible are the pump station (centre left), the gravity-fed pipeline (45° diagonal from centre bottom) draining the upstream in-channel Portuguese Dam, and the course of the Tweelopie Spruit exiting picture at centre top (photo G Krige, 05/10/2004) | 54 |
| Plate 4 | Treated mine water EoP flow gauging weir | 56 |
| Plate 5 | Raw mine water flow gauging weir (original). | 57 |
| Plate 6 | Raw mine water flow gauging weir showing inadequacy at high flows despite modification of original; note extended superstructure relative to position of lower front 'lifting eye' (circled) in common with Plate 10 | 57 |
| Plate 7 | Additional flow measurement structure (at right) installed to better gauge uncontrolled high flows of raw mine water; compare with Plate 6 setup. | 57 |
| Plate 8 | View of synoptic discharge measurement with current meter in progress at site F11S12, showing both the relatively 'clean' cross-sectional area of flow (from bottom left to right foot of observer) and the laminar nature of flow over the crest of the weir. | 68 |
| Plate 9 | Original SDM flow gauging station MRd in separated pipe (below left, 05/02/2010) and one of two identical replacement culverts (below right, 05/10/2010) beneath the reconstructed gravel Malmani Road across the Riet Spruit at this location. | 70 |
| Plate 10 | View looking downstream of relic ferrous hydroxide deposits in the stream channel of the Riet Spruit (see Fig. 25 for photo location) | 76 |
| Plate 11 | Causeway across the Blougat Spruit on the Bergland Instant Lawn property downstream of the Percy Stewart WWTW, and site of station BC1 (photo P Hobbs; date 18/02/2010) | 76 |
| Plate 12 | Bridge culvert at the N14 national road crossing of the Blougat Spruit, and site of station BG@N14. | 77 |
| Plate 13 | View of the ~100-year old A-furrow at Ptn 8 of Kromdraai 520JQ, looking upstream; flow measured at ~154 L/s on date of photo | 81 |

Chemical Hydrology

| | | |
|---------|--|-----|
| Plate 1 | Corrosion of large-diameter pipe draining the Aviary Dam on the Tweelopie Spruit in the KGR; photo at left shows remnant (at bottom centre) tenuously attached to flange, and photo at right shows close-up view from opposite side | 152 |
| Plate 2 | View of station F11S12 showing concrete weir (dark linear shape below right hand of person) and object (circled) on causeway for common reference with Plate 3 (photo W Basson) | 154 |
| Plate 3 | View of station F11S12 showing concrete weir coated with freshly precipitated hydrous ferric oxide or ferrihydrite ($5\text{Fe}_2\text{O}_3 \cdot 9\text{H}_2\text{O}$) and object (circled) on causeway for common reference with Plate 2 | 156 |
| Plate 4 | Discharge at station F11S12 (Tweelopie Spruit) on 18/12/2010. Compare with Plate 13, Plates 2, 3 or Plate 41 to note the complete submergence of the causeway | 157 |
| Plate 5 | View looking north of the high discharge at BB@M (Bloubank Spruit) on 18/12/2010. | 157 |

| | | |
|---------|---|-----|
| Plate 6 | Examples of Fe-(orange) and Mn-oxide (black) precipitation as concentric scaling in pipe (left) and as ‘Yellow boy’ in ditch (right) (photo at left J Davies; photo at right W Basson). | 158 |
| Plate 7 | Excessive sludge deposition in the upper reaches of the Hippo Dam in the Krugersdorp Game Reserve as a result of emergency liming of raw mine water to raise its pH (photo S du Toit). | 159 |
| Plate 8 | View of the Tweelopie Spruit at its confluence with the Riet Spruit at Glen Almond showing the iron hydroxide and gypsum efflorescence on the flood plain at this juncture; the taller vegetation in the middle distance marks the stream channel | 162 |

Physical Hydrogeology

| | | |
|---------|--|-----|
| Plate 1 | View of the Zwartkrans Spring rising in basin at front right of picture, discharging into the Bloubank Spruit | 191 |
| Plate 2 | Discharge of the Grootvlei Spruit (centre right) into the Skeerpoort River (at left, looking downstream); flow in the Skeerpoort River before this confluence (in foreground) derives mainly from the ~ 130 L/s discharge of the Nash Spring | 196 |

Chemical Hydrogeology

| | | |
|----------|---|-----|
| Plate 1 | View looking south-west from #18 Winze over the locus of decant with Dump 39 (see Fig. 5 in Chapter “Description of the Physical Environment”) on the horizon (photo W. Basson). | 217 |
| Plate 2 | View from the Sterkfontein Cave Visitor Center looking north over the septic tank system soak-away area (circled) and the Bloubank Spruit valley (middle foreground) at the highest point in the COH WHS (arrowed). | 224 |
| Plate 3 | View of the biozone sewage treatment plant installed under the Sterkfontein Cave Visitor Center in mid-2011 | 224 |
| Plate 4 | Massive hummock tufa deposit (under cascading water) on the downstream side of gauging weir A2H033 ~525 m downstream of the spring | 246 |
| Plate 5 | Uppermost tufa terrace (barrage) extending across the channel of the Grootvlei Spruit ~600 m downstream of the spring. | 247 |
| Plate 6 | Waterfall tufa deposit at left of picture where the Grootvlei Spruit cascades ~4 m into the Skeerpoort River gorge ~650 m downstream of the spring | 247 |
| Plate 7 | View of an ‘illegal’ refuse disposal site in the channel of the Riet Spruit near its confluence with the Blougat Spruit. | 257 |
| Plate 8 | Data logger (length ~20 cm) from monitoring borehole GP00305 completely coated with black iron sulfide (FeS) precipitate on stainless steel instrument (photo N. de Meillon) | 306 |
| Plate 9 | Examples of a hard ferrihydrite crust effectively sealing the bottom of a stream channel, and b , c entombing/entombed in-stream vegetation. (Photo b , B Genthe) | 310 |
| Plate 10 | Waterfall over the quartzite ridge south of the Kruger Kloof Lodge in the KGR (photo H Weiss, date 13/05/2008) | 315 |
| Plate 11 | Outlet of the Charles Fourie Dam in the KGR | 315 |

- Plate 12 Overflow of the Aviary Dam (impounded by the earth embankment at rear of photo) at the northern end of the KGR; compare condition of outlet pipe at left with that of same pipe in Plate 1 in Chapter “Chemical Hydrology” 316
- Plate 13 Cascade and aeration of water over the causeway at station F11S12 (see Plate 8 in Chapter “Physical Hydrology” for scale of monitoring station) 316

List of Text Boxes

Integrated Monitoring Approach

| | | |
|-------------------|---|---|
| Text Box 1 | Excerpt from the World Heritage Centre draft decision 37 COM 7B.44 (WHC, 2013) presented at the 37th Session of the World Heritage Committee in Phnom Penh, Cambodia, 16 to 27 June 2013. . . . | 3 |
|-------------------|---|---|

Introduction and Background

| | | |
|-------------------|---|---|
| Text Box 1 | The IUCN-SA Karst Working Group | 7 |
|-------------------|---|---|

Overview of Karst

| | | |
|-------------------|-----------------------------------|----|
| Text Box 1 | Hypogenic speleogenesis | 40 |
|-------------------|-----------------------------------|----|

Physical Hydrology

| | | |
|-------------------|--|----|
| Text Box 1 | Mine water control and management in the Western Basin | 58 |
|-------------------|--|----|

| | | |
|-------------------|---|----|
| Text Box 2 | The permanence (insolubility) of iron (oxy)hydroxide precipitates | 70 |
|-------------------|---|----|

| | | |
|-------------------|--|----|
| Text Box 3 | The veracity of SDM-based surface water loss calculations. | 81 |
|-------------------|--|----|

Chemical Hydrology

| | | |
|-------------------|---|-----|
| Text Box 1 | TDS: Sec. and SO ₄ :TDS ratios for various water sources in the study area | 120 |
|-------------------|---|-----|

Physical Hydrogeology

| | | |
|-------------------|---|-----|
| Text Box 1 | The Kromdraai Spring/Plover's Lake Spring(s) conundrum. | 200 |
|-------------------|---|-----|

Chemical Hydrogeology

| | | |
|-------------------|---|-----|
| Text Box 1 | The veracity of ORP measurements. | 294 |
|-------------------|---|-----|

Précis

A poor understanding of the surface and groundwater resources of the Cradle of Humankind (COH) World Heritage Site (WHS) property has precipitated often alarmist reporting in the media regarding the negative impacts associated with various sources of poor quality water. The most notable of these is the acid mine drainage (AMD) threat to karst ecosystems and fossil sites across the property. These circumstances have generated wide and considerable concern for the preservation of the UNESCO-inscribed fossil sites and integrity of the water resources of the property. An assessment of the water resources environment has better informed this situation. It also formed the basis for the implementation of an integrated water resource monitoring programme in support of management efforts to protect the aquatic environment and assist in maintaining the outstanding universal value of the property. The combined results of these activities inform the multi-dimensional analysis set out in this work.

The surface water environment comprises the largely unspoilt Skeerpoort River catchment and the heavily impacted Bloubank Spruit system. These drain to the regionally important Hartbeespoort Dam via the Magalies River and the Crocodile River as respective main stems. The Skeerpoort River, with a long-term median discharge of $\sim 9.6 \text{ Mm}^3/\text{a}$, is fed by karst springs delivering a similar quantity of excellent quality karst groundwater. This contribution represents $\sim 5\%$ of the $\sim 190 \text{ Mm}^3$ full supply capacity (FSC) of Hartbeespoort Dam. The Bloubank Spruit system, with a long-term median discharge of $\sim 22.7 \text{ Mm}^3/\text{a}$ ($\sim 12\%$ of FSC), receives $>4.4 \text{ Mm}^3/\text{a}$ of poor quality raw and treated mine water and $>2.5 \text{ Mm}^3/\text{a}$ of treated municipal sewage effluent on average in its non-karst headwater reaches upstream of the karst environment. The balance is contributed by the karst aquifer delivering $>16.6 \text{ Mm}^3/\text{a}$ of good to excellent quality dolomitic groundwater. The Crocodile River median long-term discharge of $\sim 9.5 \text{ Mm}^3/\text{a}$ good quality surface water at the confluence with its Bloubank Spruit tributary, similarly represents $\sim 5\%$ of the dam's FSC. Expressed as a long-term (1980 to 2015) median annual salt load, these drainages contributed $\sim 2.9 \text{ kt}$ (Skeerpoort River), $\sim 10.6 \text{ kt}$ (Bloubank Spruit) and $\sim 3.8 \text{ kt}$ (Crocodile River) of total dissolved solids to the impoundment. The negative impact of a significant raw mine water discharge component for a large part of the 2010 to 2014 period on the Bloubank Spruit system, was partially mitigated by the commissioning in mid-2012 and further upgrades by mid-2013, of immediate and short-term mine water control and management interventions by the Department of Water and Sanitation. The persistence of poor to very poor bacteriological quality associated with surface water in the Bloubank Spruit represents a second significant and pernicious threat to the 'fitness for use' of the ambient water resources.

The karst hydrosystem is assessed as comprising eleven compartments (basins), two of which are subdivided into subcompartments. Most of the basins are drained by high-yielding ($>20 \text{ L/s}$) springs for which quantitative discharges and hydrochemical composition are known. The aggregate discharge of eleven enumerated karst springs amounts to $\sim 26.2 \text{ Mm}^3/\text{a}$ ($\sim 71.8 \text{ ML/d}$), or $\sim 13\%$ of the Hartbeespoort Dam FSC. Together with an additional $\sim 4.1 \text{ Mm}^3/\text{a}$ ($\sim 130 \text{ L/s}$) associated with groundwater resurgence along effluent stream sections traversing dolomite, the total groundwater yield of $\sim 30.3 \text{ Mm}^3/\text{a}$ ($\sim 83 \text{ ML/d}$) equals $\sim 16\%$ of the reservoir FSC. The combined long-term median discharge of the Skeerpoort River and

Bloubank Spruit amounts to $\sim 34.7 \text{ Mm}^3/\text{a}$ ($\sim 95.1 \text{ ML/d}$), a little over 18% of the dam's FSC. These circumstances reflect the important contribution of good to excellent quality karst groundwater rising mainly in the COH, to the water budget of the wider region.

Water budget calculations indicate that $17 \pm 5\%$ of a mean annual precipitation of 710 mm provides a reasonable approximation of natural (autogenic) recharge from rainfall for the karst hydrosystem. The very wet 2010, 2011 and 2014 summers resulted in exceptional recharge of groundwater resources in the study area. A rise in groundwater rest levels by $\sim 3 \text{ m}$ on average, also observed in the Sterkfontein Cave, reflects this. Water level rises of this magnitude and by as much as $\sim 5 \text{ m}$ are attributed jointly to allogenic recharge associated with the infiltration of surface water contributed in the form of mining and municipal wastewater effluent from upstream non-karst areas, and natural autogenic recharge. The allogenic recharge in the case of mine water has amounted to a minimum of $\sim 5.1 \text{ Mm}^3/\text{a}$ ($\sim 14 \text{ ML/d}$) rising to at least $\sim 11.7 \text{ Mm}^3/\text{a}$ ($\sim 32 \text{ ML/d}$), and from ~ 1.1 to $\sim 2.6 \text{ Mm}^3/\text{a}$ (~ 3 to 7 ML/d) in the case of municipal wastewater effluent. The mine water discharges have introduced a new set of drivers causing a resetting of the natural water resources environment. In the case of groundwater, this is immediately and most evident in potentiometric data. It is postulated that the impact on the physical hydrogeology will result in higher (by 10 to 15%) baseflows in the Bloubank Spruit system in the future.

A correlation between spring discharge, karst basin catchment area, springwater chemistry and rainfall recharge is demonstrated for most of the karst basins. This has provided an improved understanding of karst groundwater flow patterns in the study area that supports a plausible conceptual model of the hydrogeologic environment. Cognisant of the variation in climatological and physiographical factors that influence landscape development in the long-term, the mean solutional denudation rate of the COH karst landscape is placed at 9.5 mm/Ka within the range 5 to 14 mm/Ka . This represents a total rate of theoretical void development of $\sim 2100 \text{ m}^3/\text{a}$. The average total carbon loading in the karst springwaters is found to be 44 mg C/L in the range 31 to 65 mg C/L . The average total carbon flux carried in these waters is $\sim 442 \text{ kg/d}$ ($\sim 161 \text{ t/a}$), with eight high-yielding springs delivering a combined total C-flux of $\sim 3.1 \text{ t/d}$ ($\sim 1.1 \text{ t/a}$). The average C-export rate for seven karst basins is calculated at $\sim 4.6 \text{ t/km}^2/\text{a}$ in the range ~ 2.8 to $\sim 9.7 \text{ t/km}^2/\text{a}$. This is comparable to values reported in the literature for other karst terranes globally.

The analysis and interpretation of vertical hydrogeochemical profiles in the karst aquifer impacted by allogenic mine water recharge addresses an often neglected aspect and contributes materially to the multi-dimensional span of this work. Similar sentiments can be expressed in regard to the temporal assessment of net acidity of karst groundwaters, the environmental isotope characterisation of the water that characterises various sources, and the hydrovulnerability risk assessment of individual fossil sites.

The platform built from the integration of historical data with a wide range of newly-sourced and interpreted hydrologic and hydrogeologic data and information, convincingly supports a more robust understanding of the surface water and groundwater environments in the COH. This, in turn, has provided the means to objectively gauge the impact of varied and numerous threats to and on the water resources, and to develop an appropriate water resources monitoring programme. The unprecedented abnormally high flow conditions experienced in the 2010, 2011 and 2014 hydrological years in the Bloubank Spruit system precipitated adverse impacts attributable to abnormally high raw mine water discharges. Subsequent hydrologic and hydrogeologic observations have provided new insight into the response of the receiving karst groundwater resource. These circumstances have magnified the focus on the immediate and short-term intervention measures implemented in the Western Basin to manage and control mine water discharge. The impact of climate change on this situation in the long-term remains an unknown factor in quantitative terms.

Synoptic Information on Sterkfontein Cave

Sterkfontein Cave is the flagship fossil site on the Cradle of Humankind World Heritage Site property. It is synonymous with the property to the extent that a common and mistaken perception exists that the cave and its immediate surrounds represents the whole of the World Heritage Site, when in fact it occupies only a very small portion in the south-western corner of the property. The property has a maximum N–S extent of roughly 27 km, and an E–W extent of some 30 km. The cave is the quintessential archaeological and palaeoanthropological excavation on view to tourists, based as it is on a long and distinguished history as a ‘dig’ dating back to the 1930s. Yet a Google® search for such basic information as cave air temperature and humidity, cave water temperature and depth, and depth below surface reveals a surprising paucity of information. Synoptic information that characterises the physical surface and subsurface environment is tabulated below. This has proven useful to Sterkfontein Cave tour guides who are faced with questions about these aspects from tourists. The information contributes to broadening the general knowledge of the cave environment beyond merely the well documented archaeological and palaeoanthropological aspects.

| Parameter/aspect | Value as a range and unit |
|--|---|
| Surface elevation | 1440 m amsl (river) to 1487 m amsl (hilltop) |
| Rainfall (wet) season | Summer (October to March) |
| Mean annual precipitation | 684 mm |
| Mean summer precipitation | 588 mm |
| Mean daily temperature (surface) | 20 to 22 °C (summer) 10 to 12 °C (winter) |
| Mean annual evaporation (surface) | 2200 to 2400 mm |
| Mean daily relative humidity (surface) | 66 to 68% (summer) 58 to 60% (winter) |
| Mean in-cave air temperature | 17 to 19 °C (summer) 15 to 17 °C (winter) |
| Mean daily in-cave relative humidity | ?? to ??% (summer) ?? to ??% (winter) |
| Cave depth (known) below surface entrance | 50 to 55 m below hilltop (1487 m amsl) 42 to 47 m below entrance (1479 m amsl) |
| Cave water temperature | 15.5 to 18.5 °C |
| pH of the cave water (in situ) | 7.2 to 7.9 |
| TDS (total dissolved solids) of the cave water | 475 to 525 mg/L |
| Cave water saturation indices (calcite and dolomite) | SI _C –0.23; SI _D –0.72 (slightly under-saturated) |
| Cave water depth (known) | 3 m (below 1434 m amsl) 8 m (below 1439 m amsl) |

(continued)

| Parameter/aspect | Value as a range and unit |
|------------------------------------|--|
| Cave water level elevation | 1434 to 1439 m amsl (multi-year variation) |
| Cave water level fluctuation | 2 to 3 m (typical) over years 5 to 6 m (maximum) over decades and longer |
| Water table gradient and direction | 0.003 (30 cm per 100 m) to the ENE |
| Rainwater chemistry | pH = 5.1 to 6.5; TDS = 90 to 110 mg/L |
| Surface solutional denudation rate | 4.4 to 5.5 mm per 1000 years (local) 5.5 to 15.5 mm per 1000 years (regional) |
| Geological strata | Type: Dolomite of the Malmani Subgroup, Chuniespoort Group, Transvaal Supergroup Age: ~2600 million years Dip: ~20° to the NW (315°) |



Syenite boulders marking the position of the Plover's Lake Sill immediately downstream of the ~ 2 L/s Cradle Spring, discharging at back left of picture, in the Motsetse Nature Reserve (Photo P. Hobbs, date 21/12/2010)

We are to admit no more causes of natural things than such as are both true and sufficient to explain their appearances. Therefore, to the same natural effects we must, so far as possible, assign the same causes.

Sir Isaac Newton

(English physicist, mathematician, astronomer, natural philosopher, alchemist and theologian 1642-1727)

Integrated Monitoring Approach

Harrison Pienaar and Philip J. Hobbs

The Cradle of Humankind World Heritage Site (COH WHS) enjoys international significance for its palaeoanthropological and archaeological fossil finds. A review of international efforts has not located another UNESCO-protected property in the world [#35 on the World Heritage List with karst of outstanding universal value (Williams, 2008)] that experiences the impact of acid mine drainage (AMD). The mine water threat was first manifested in late-August 2002 (van Biljon, 2006) with the start of mine water decant from the West Rand Goldfield, aka the Western Basin. This situation has generated wide and considerable concern for the preservation of the UNESCO-inscribed fossil sites on the property. The Environmental Management Framework/Plan (EMF/P) Status Quo Report (Beater and Kilian, 2009) identified information in regard to sources, extent and affect of AMD in the COH as being deficient. It is therefore unfortunate but not surprising that the paucity of hydroscientific information in regard to the property precipitated the publication of largely unsubstantiated (and often alarmist) media reports regarding negative impacts on the fossil heritage sites (e.g. Béga, 2008a; 2008b; 2010; 2013; Seccombe, 2008; Masondo, 2010; Groenewald, 2010a). Regrettably, this perception is afforded credibility by Wells et al. (2009) in the respected publication *Environmental Management in South Africa* (Strydom and King, 2009), and also in generic scientific articles such as by Durand et al. (2010), Durand (2012) and, more recently, by Abiye (2014).

The COH property could clearly benefit from a comprehensive assessment of the water resources system(s) to

mediate an improved understanding of the integrated hydrologic (surface water) and hydrogeologic (groundwater) environments. In regard to the groundwater environment, this entails defining flow directions, boundary conditions and water chemistry (quality) aspects based on historical information, long-term monitoring data and new data and information. Similar considerations also apply to the surface water environment. The dynamics of interaction between surface water and groundwater resources in regard to both quantity (volumes) and quality (chemistry) is a crucial element of this understanding. This is especially important in the COH because of the risk to karst groundwater resources from threats such as over-abstraction associated with irrigated agriculture, mine dewatering and rewatering, and contamination/pollution from municipal wastewater, mine water discharge and on-site sanitation facilities on unserved properties, many of which are smallholdings.

Reporting on the conflict between different communities over water resources of the karst that hosts the Choranche Caves and forms the Coulmes Plateau in the Vercors Mountains, France, Gauchon et al. (2006) emphasise that ‘... water’s place in the system must be defined’. The material presented in this publication provides such definition for the COH by building on and extending the collective knowledge and understanding of the water resources environment. This finds support in a conceptual hydrophysical model of the integrated surface water and groundwater environments that accounts for observed congruencies between rainfall, groundwater recharge, groundwater drainage patterns, spring discharges, and the surface extent of groundwater basins. Characterisation of the hydrochemistry associated with the various water resource components lends further support and rigour to the conceptual model of the hydrophysical domain.

The water resources system assessment underpins the implementation of an appropriate integrated water resources monitoring programme for the COH. This is crucial to the successful management of water resources and the impact on these resources in the study area. A focussed routine

P. J. Hobbs: Deceased

H. Pienaar (✉)
Council for Scientific and Industrial Research, Smart Places,
Water Centre, Pretoria, South Africa
e-mail: hpienaar@csir.co.za

H. Pienaar
Hebei University of Engineering, Handan, China

P. J. Hobbs
Pretoria, South Africa

hydromonitoring programme provides the means to measure and demonstrate the success or failure of management efforts to protect the aquatic environment in the COH. The water resources system assessment and derived conceptual model also facilitate the evaluation of ancillary issues that include the following:

- the status quo of water resources monitoring activities;
- the state of conservation (SoC) of the water resources environment;
- the establishment of resource water quality objectives;
- solutional denudation as an agent in the evolution of the karst landscape;
- carbon flux associated with karst spring discharges; and

- the vulnerability of the fossil sites to impacts on the (hydro)environment.

The material provides a foil, as demonstrated by Béga (2012a), albeit fleetingly,¹ van Schie (2013) and Vermeulen (2013), for the many and widespread misperceptions founded on ignorance, sentiment and/or emotion that have driven the public awareness of this World Heritage property. Most importantly, however, it informs and supports sound management actions in regard to responsible and effective governance of the water resources environment to also protect this aspect of the outstanding universal value (OUV) of the property in the interest and on behalf of all nations and humankind (WHC, 2013 and Text Box 1, p. 3).



View from inside Sterkfontein Cave upward through an aven extending ~45 m to surface with a sheltering tree visible through the surface opening; the near-circular geometry of the feature reveals the

modification of a natural aven by early miners into a shaft for hoisting limestone to surface rather than via the steep and tortuous natural access route

¹ See the article published by the same journalist just two weeks later (Béga, 2012b).

Text Box 1 Excerpt from the World Heritage Centre draft decision 37 COM 7B.44 (WHC, 2013) presented at the 37th Session of the World Heritage Committee in Phnom Penh, Cambodia, 16 to 27 June 2013

In January 2011, the World Heritage Centre requested the State Party to undertake a study to address concerns that had been raised by various parties about a potential threat to the World Heritage property posed by effluent from abandoned and active mines in the vicinity. The study, commissioned by the Cradle of Humankind World Heritage Site Management Authority, Department of Economic Development, Gauteng Province, South Africa, was prepared in 2011 by the Council for Scientific and Industrial Research. On 14 March 2013, ICOMOS completed an assessment of this exhaustive study. This assessment is available online at the following Web address: <http://whc.unesco.org/en/list/915/documents>.

Over a number of years, concerns have been raised that acidic waters rich in iron and other minerals (Acid Mine Drainage, or AMD) from abandoned mines in the vicinity of the World Heritage property, plus the input of treated mine water (and, in recent years, the overflow of untreated and partly treated mine waters at times of heavy rainfall) from the workings of an active mine about 15 km distant into the hydrology system of the property, might have a harmful effect on the caves that underpin the Outstanding Universal Value (OUV) of the property. The 2011 study, "Situation assessment of the surface water and groundwater resource environments in the Cradle of Humankind World Heritage Site", attempts for the first time to give a comprehensive picture of the surface and sub-surface water regime across the property.

The World Heritage Centre and the Advisory Bodies suggest that the Committee congratulate the State Party for an excellent study. The work described appears to have been undertaken in accordance with best practice, and the results appear to reflect current scientific knowledge. The amount of field measurements to support the work is impressive. The study has successfully answered some of the uncertainties in knowledge about the hydrology and hydrogeology of the property.

The World Heritage Centre and the Advisory Bodies are of the view that the recommendations in the 2011 study should be acted upon. Cooperation with other agencies, especially the Department of Water Affairs, should be strongly encouraged, and there should be consultation and agreement on the proposed resource water quality objectives. Regular monitoring should be established, and a timeframe set to meet the agreed quality objectives.

The World Heritage Centre and the Advisory Bodies note that since the study was written, the Department of Water Affairs has initiated a "Feasibility study for a long-term solution to address the AMD associated with the East, Central and West Rand underground mining basins". A void assessment report was issued in draft form in March 2013, and a feasibility report proposes a system of active treatment of AMD and leachate from mine dumps for the West, Central and East Rand. If implemented in the West Rand, it should reduce the risks of AMD to the OUV of the property. They recommend that a joint World Heritage Centre/ICOMOS reactive monitoring mission be undertaken in order to assess the AMD impact to the property and propose recommendations to the State Party.



View of the southern sidewall of Sterkfontein Quarry (part of the Bolt's Farm fossil site) showing the barricaded portal to Alladin's/Quarry Cave at centre right, the ~ 4 m thick epikarst zone (above the

sub-horizontal dotted line) and the gentle boudinage-type folding of the carbonate strata exposed in the sidewall

Introduction and Background

Harrison Pienaar and Philip J. Hobbs

1 Legal and Physical Framework

The UNESCO Convention concerning the Protection of the World Cultural and Natural Heritage (1971), ratified by South Africa in 1997 and incorporated into South African law in terms of the World Heritage Convention Act (Act No 49 of 1999), in 1999 inscribed the fossil hominid sites of Sterkfontein, Swartkrans, Kromdraai and environs (known as the Cradle of Humankind) for protection in terms of their ‘collective’ cultural heritage (Strydom, 2009). The Cradle of Humankind (COH) is located on the north-western margin of Gauteng Province in the central north-eastern part of South Africa (Fig. 1). It is among some 50 karst sites globally that have been inscribed by UNESCO (Hamilton-Smith, 2006), many of these for other values (e.g. cultural) than purely their karst landforms.

The management of a protected area is undertaken by the State Party, in this instance the Department of Environmental Affairs (DEA), that is answerable to UNESCO’s World Heritage Committee (WHC). The DEA has delegated the management function to the Management Authority (MA) assigned administrative responsibility at a provincial level. The MA of the COH WHS is hosted by the Department of Economic Development, Gauteng Provincial Government, that is answerable to the DEA on issues such as the State of Conservation (SoC) of the property.

A little more than 1 billion people (~15% of the global population) live on karst (Kaufmann 2013), and karst

aquifers are estimated to provide ~ 1.5 billion people with potable water (Ford and Williams 2007; Bauer et al. 2008; Supper et al. 2008). Karst areas also count among the most vulnerable hydrogeologic environments to human impacts in the world. The distribution in South Africa of Neoproterozoic (~2.65 to 2.50 Ga) major ‘hard’ sedimentary carbonate deposits is shown in Fig. 1. These are the Malmani Subgroup and the Campbell Rand Subgroup located east and west of longitude 25°E, respectively. Together representing at least 98% of carbonate strata (dolomite, limestone, calccrete, dolocrete, travertine, etc.) in South Africa, these formations cover ~ 3% of the total surface area of the country (van Schalkwyk 1981). The CGS/SAIEEG (2003) guideline provides a concise description of the dolomite and limestone occurrences in South Africa. A more detailed description can be found in Martini and Wilson (1998) and Martini (2006). In regard to land and water resources issues, Vesper (2008) identifies the following characteristics unique to karst systems that require focussed study:

- close connections between surface and subsurface processes render karst systems highly vulnerable to impacts from surface activities;
- spatial heterogeneity hinders the ability to easily monitor and assess water quality and quantity;
- rates of physical processes are highly variable;
- subsidence may occur at an almost imperceptible rate or be nearly instantaneous;
- contaminants may be rapidly flushed through the system or trapped indefinitely; and
- water flow at springs may be consistent through time or change rapidly in response to storm events.

The International Union for Conservation of Nature and Natural Resources (IUCN) publication by Watson et al. (1997) lists some of the reasons for the protection of karst landscapes as their provision of the following ‘goods and services’:

P. J. Hobbs: Deceased

H. Pienaar (✉) · P. J. Hobbs
Smart Places, Council for Scientific and Industrial Research,
Pretoria, South Africa
e-mail: hpienaar@csir.co.za

H. Pienaar
Hebei University of Engineering, Handan, China

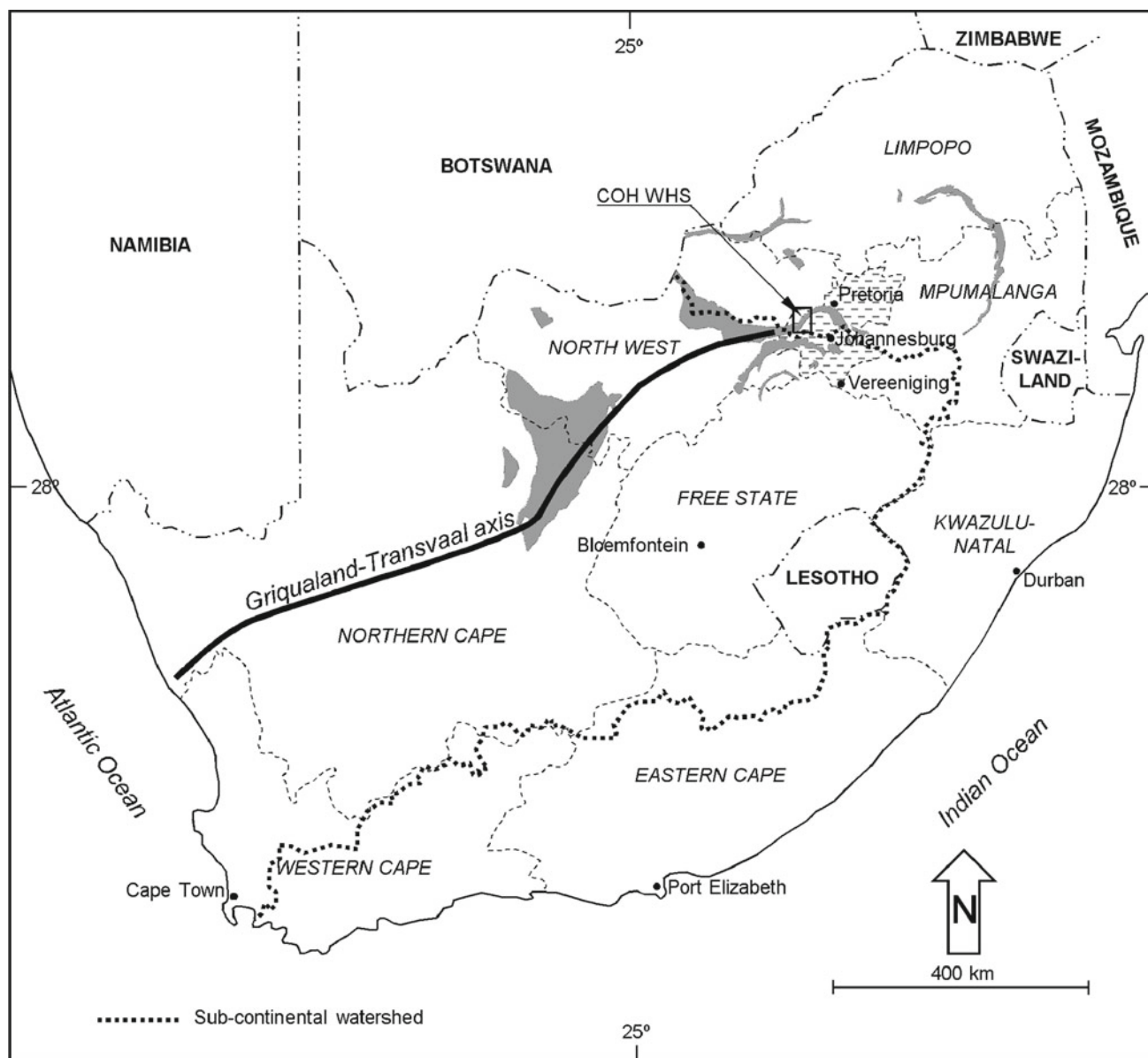


Fig. 1 Location of the Cradle of Humankind World Heritage Site (COH WHS) in Gauteng Province (light shaded area), South Africa, and in relation to the distribution of 'hard' sedimentary carbonate

deposits (darker shaded areas) of the Chuniespoort Group in the South African interior (adapted from Martini and Wilson, 1998)

- habitat for endangered species of flora and fauna;
- sites containing rare minerals or unique landforms;
- important sites for the study of geology, geomorphology, palaeontology and other disciplines;
- culturally important sites, both historic and prehistoric;
- spiritual or religious features;
- specialised agriculture and industries;
- 'windows' into understanding regional hydrology and karst hydrogeology;
- sources of economically important materials, especially groundwater;
- tourism and its associated economic benefits;

- purely recreational areas, both scenic and challenging; and
- *role as carbon source and sink in the context of the global carbon cycle¹.*

Although the COH was inscribed for its cultural heritage represented by the reasons shown as **bold text** in the above list, it is evident that the property also meets many of the other criteria (shown as underlined text) in the list. The

¹ Italicised text added by author.

earlier activities of the IUCN-SA² Karst Working Group (Fourie 2005) are described in Text Box 1, and in the WRC/IUCN/SAKWG (2010) publication titled *'The karst system of the Cradle of Humankind World Heritage Site'*.

Text Box 1 The IUCN-SA Karst Working Group

In May 2004, the South African country office of IUCN-The World Conservation Union, in collaboration with the Gauteng Department of Agriculture, Conservation and Environment (GDACE) and the Cave Research Organisation of South Africa (CROSA), established a Karst Working Group, made up of more than 30 individuals from diverse backgrounds and disciplines, including national, provincial and local government, industry, four national universities and a number of voluntary caving organisations. Their task is to develop a holistic monitoring and management system for karst systems in South Africa, and they have chosen the Cradle of Humankind World Heritage Site as a pilot study, in part to support the Cradle in meeting its reporting obligations to the World Heritage Authority. One of the group's main concerns is the threat of water pollution in the Cradle area, and the effect of such pollution on the karst ecosystems. The group is supported by the GDACE, the Water Research Commission and the IUCN World Commission on Protected Areas Cave and Karst Taskforce. It is also establishing partnerships with research institutions in Europe, as well as international NGOs Flora & Fauna International and Earthwatch.

From Fourie (2005).

The National Water Act (RSA 1998) posits the reminder that water resource protection is mandated in terms of Section 19 of the National Water Act (NWA), Act No 36 of 1998, with a particular focus on 'prevention and remedying effects of pollution'. Moreover, the NWA also provides mechanisms for promoting the sustainable use of inland waters (King and Pienaar 2011), as well as specific legal provisions to develop and implement groundwater protection measures, in particular the Resource Directed Measures (RDM) as described in Chap. 3 of the NWA (Pienaar et al. 2021). Section 19 of the NWA requires of a landowner, person in control of land or person occupying or using land to take all reasonable measures to prevent pollution of a water resource from occurring, continuing or recurring. It is perhaps even more pertinent to

recognise the need to query the popular perception of a large-scale 'tragedy of the commons', as formulated by Hardin (1968), playing itself out regarding water resource pollution and consequential loss of fossil site integrity in the COH and, ultimately, loss of World Heritage status. This situation represents a 'wicked problem' as described by Davidson and Wei (2012).

2 Hydrophysical Framework

Ford and Williams (2007) report that karst resources are coming under increasing pressure worldwide and have great need of sustainable management. This has no greater relevance than for a World Heritage property, where the successful execution of administrative responsibilities is not sufficient to ensure that desired results in terms of environmental management outcomes are or will be achieved. Kasum et al. (2019) also argue that water resources are indissolubly linked to a wide range of human-made activities defined by terms such as *underwater exploitation* and *human health* (among other), which necessitates the development and advancement of models for forensic hydrography. Successful achievement of environmental objectives such as appropriate water quality and adequate biodiversity, require specific and directed interventions informed by a sound understanding of the water resources environment. Parrish et al. (2003) recognise monitoring programmes as crucial elements of any protected area management programme.

Knowledge of the current situation, trends of change, likely source(s) of undesirable constituents, threat status, etc. underpins the implementation of sound management actions directed at responsible and effective governance on the part of a Management Authority. The implementation of an appropriate integrated hydrologic and hydrogeologic monitoring programme is crucial to the successful management of water resources and protection of the aquatic environment in the COH. Such protection is not only required for the preservation of karst features and palaeoanthropological finds, but also for resident water users who depend on local water resources (primarily groundwater) for their livelihood. The Environmental Management Framework/Management Plan (EMF/MP) developed for the COH (Brown 2009), presents a first but understandably superficial description of the water resources of the property. An earlier study by Holland (2007) focussed on groundwater resources only.

3 Aims and Objectives

The primary objective of this study is to develop a sound and integrated conceptual model of the hydrologic and hydrogeologic environments that comprise the COH. Regarding

² South African country office of the IUCN-The World Conservation Union.

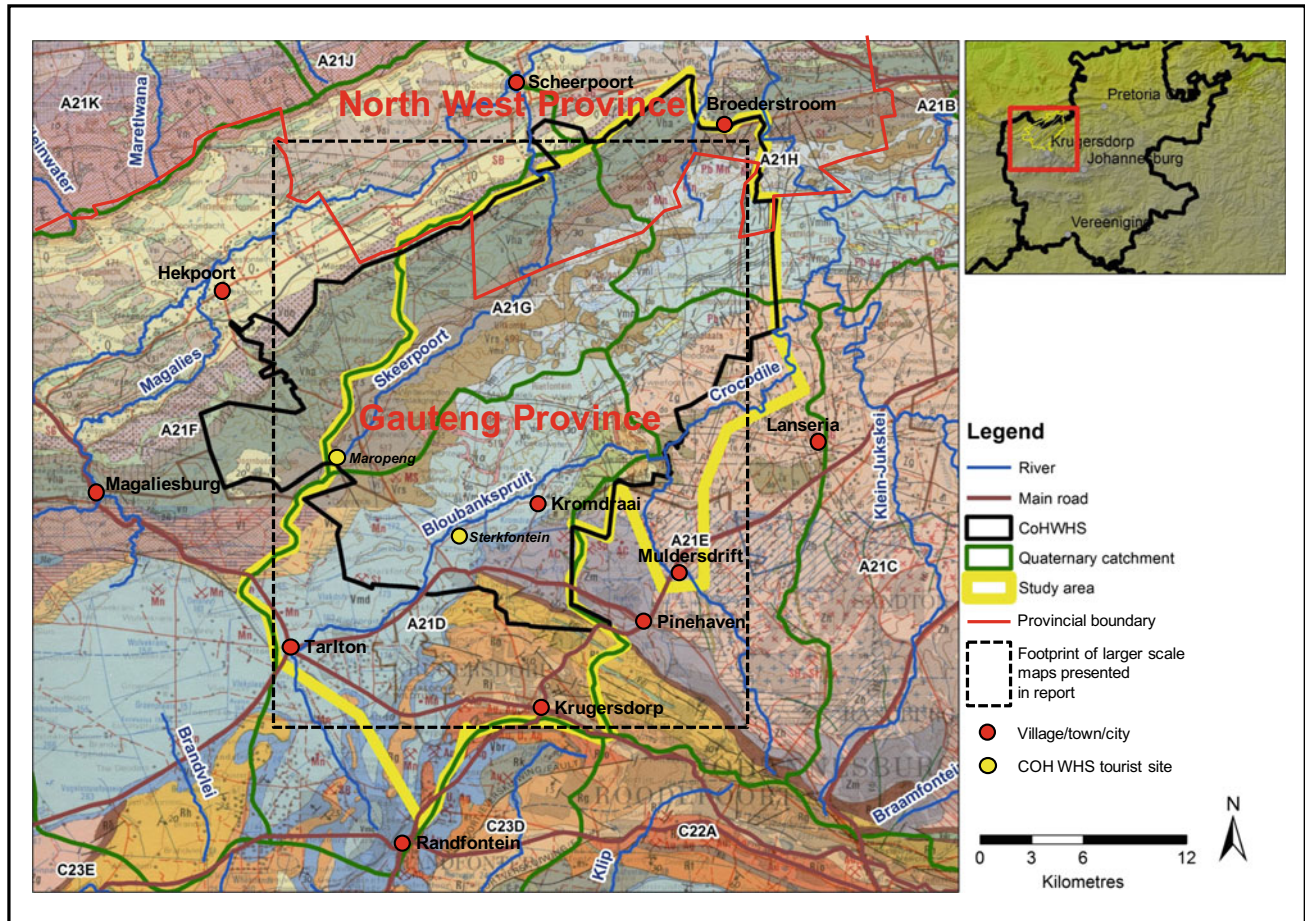


Fig. 2 Definition of the study area in regard to geographic localities, geology and hydrology

the groundwater environment, this entails defining flow directions, boundary conditions and water chemistry (quality) aspects based on historical information, long-term monitoring data and new data and information. Although similar considerations also apply to the surface water environment, the dynamics of the surface and subsurface hydrologic interaction (aka stream – aquifer interaction) is considered a key element of this understanding. The successful outcome will provide a basis for implementing measures aimed at ensuring the sustainable functioning of the karst ecohydrology of the COH in the face of rapidly growing pressure from a variety of anthropogenic impacts.

An assessment of the water resources system (s) that provides an improved and rigorous understanding of the integrated hydrologic and hydrogeologic environments, also provides a more informed reference framework against which to gauge the veracity of concerns for the heritage value of the property. The integrated conceptual model of the surface water and groundwater environments developed in this study meets this requirement, and also identifies data and information gaps in the water resources environment. Further, the outcome elucidates ancillary aspects such as the following:

- the status quo of water resources monitoring activities;
- the state of conservation of the water resources environment (e.g. DEA 2014a, 2016);
- the establishment of resource water quality objectives for the water resources;
- solutional denudation as an agent in the evolution of the karst landscape;
- carbon flux associated with karst spring discharges; and
- the vulnerability of the fossil sites from negative impacts on the water resources.

4 Definition of the Study Area

The area defined in Fig. 2 represents the most appropriate demarcation based primarily on the harmonisation of the COH property boundary (as promulgated) with aspects such as drainage basin footprints, the distribution of geological strata with emphasis on the vulnerable karst hydrosystem, and the location of known threats associated with mining, industrial, urban and agricultural land uses. The measure of

congruence between the study area boundary and the Quaternary surface water catchments is evident in Fig. 2.

The study area encompasses $\sim 64\,900$ ha, compared to the $\sim 52\,000^3$ ha of the COH property. The inclusion of the mining area in the extreme southern part of the study area between Krugersdorp and Randfontein (Fig. 2) recognises the importance of this activity and land use not only in terms of the mine water threat, but also the comparatively large amount of data and information related to this activity that already exists for this portion of the study area. The inclusion of a portion of the (upper) Crocodile River in Quaternary catchment A21E as far upstream as Muldersdrift in the south-eastern corner, incorporates the potential impact of the Driefontein Wastewater Treatment Works (WWTW) together with that of the Percy Stewart WWTW located in the upper reaches of Quaternary catchment A21D (Fig. 2), on the water resources environment.

Excluded from the study area is that portion of the property in Quaternary catchment A21F (the Magalies River catchment)

along the north-western margin. Much of this area is located on younger geological strata (Sect. 4 in Chapter “[Description of the Physical Environment](#)”), and it does not share to any significant degree the sensitive groundwater environment that forms the core of the COH. The carbonate strata extending to the west-southwest beyond the study area boundary defines the eastern portion of the adjoining Steenkoppies Basin. This basin is drained by Maloney’s ‘Eye’ (spring) (Sect. 1 in Chapter “[Physical Hydrology](#)”), the source of the Magalies River, and therefore also does not share the karst hydrosystem of the COH beyond purely geologic proximity/contiguity (Sect. 7 in Chapter “[Physical Hydrogeology](#)”).

The Steenkoppies Basin has recently been studied in some detail (Holland et al. 2009) with a view to managing the high demand placed on the karst water resource for intensive irrigated agriculture. This demand has impacted negatively on the yield of Maloney’s Eye, to the detriment of downstream water users in the fertile Magalies River Valley which supports intensive irrigated agriculture.



Irrigation of ‘instant’ (cultivated) lawn with treated municipal wastewater effluent (from the Percy Stewart WWTW) on dolomite in the south-western portion of the study area; compare the early spring

brown natural vegetation typical of the Transvaal Highveld in the background with the lush green foreground

³ The area of $\sim 47\,000$ ha commonly reported, refers to the core area (i.e. excluding the buffer zone).

Description of the Physical Environment

Harrison Pienaar and Philip J. Hobbs

1 Morphology and Drainage

The surface water drainage characteristics (physical hydrology) of the study area, including drainage pattern and mean annual runoff (MAR), are discussed in greater detail in Sect. 5.1 in Chapter “Physical Hydrology”. The following discussion provides a synoptic general overview of this aspect.

The watershed that forms the continental divide between the Vaal River system to the south (draining westward to the Atlantic Ocean) and the Limpopo River system to the north (draining eastward to the Indian Ocean) (see Fig. 1 in Chapter “Introduction and Background”), also occupies the highest natural elevation (~ 1720 m amsl) in the study area. Extending to the north of this divide is a diverse landscape that includes undulating terrain with low to moderate relief along an SW–NE strike roughly concordant with the main drainages. This terrain is flanked to the south-east by prominent ridges incised at right angles by mainly ephemeral tributaries, and to the north-west by sub-parallel ridges and valleys. The flanking landscapes mark a transition in the geology across the landscape, with dolomite sandwiched between older underlying sedimentary strata (quartzite) in the south-east and younger overlying sedimentary rocks (quartzite and shale) in the north-west.

At an elevation of 1664 m amsl, the peak of Spioenkop on the farm Danielsrust 518JQ is the highest point in the study area. This is followed by Zwartkop peak at 1626 m amsl on the farm Zwartkop 525JQ near the south-eastern margin of the property. The lowest elevation of ~ 1200 m

amsl occurs in the vicinity of Broederstroom (Fig. 2 in Chapter “Introduction and Background”), a hamlet at the north-eastern end of the property immediately south of the regionally important (Sect. 5.1 in Chapter “Physical Hydrology”) Hartbeespoort Dam storage reservoir (Fig. 1). This fits the description by Kruger (1983), who characterises the terrain morphology as undulating hills and lowlands with relief in the range 130 to 450 m, a drainage density of 0.5 to 2 km/km², a stream frequency of 0 to 6 per km², and 20–50% of the area having slopes of $<5\%$. The property spans portions of five Quaternary catchments (Fig. 2 in Chapter “Introduction and Background” and Table 1) located in the Limpopo Water Management Area (WMA #1) (Fig. 1). Table 1 shows that basins A21D (the Bloubank¹ Spruit system) and A21G (Skeerpoort River) together cover $\sim 70\%$ of the study area, followed in roughly equal proportions ($\sim 15\%$) by basins A21E (upper² Crocodile River) and A21H (lower Crocodile River).

2 Climate and Rainfall

The property falls within the warm temperate summer rainfall region that characterises the typical Highveld climate of the central north-eastern South African interior. The following synoptic information is sourced mainly from Schulze et al. (1997).

The mean annual temperature (MAT) falls in the range of 16 to 18 °C, with daily mean temperatures in the range of

P. J. Hobbs: Deceased

H. Pienaar (✉) · P. J. Hobbs
Smart Places, Council for Scientific and Industrial Research,
Pretoria, South Africa
e-mail: hpienaar@csir.co.za

H. Pienaar
Hebei University of Engineering, Handan, China

¹ The spelling ‘Bloubank’ subscribes to that used on the most recent edition of the published 1:50 000 scale topocadastral map 2527DD Broederstroom (5th ed., 2001), and not to that of ‘Blaauwbank’ used on earlier maps and in other reports (e.g. Holland et al., 2009; SRK, 2009).

² The terms ‘upper’ and ‘lower’ are used in the context of the reaches above and below the confluence with the Bloubank Spruit upstream of Hartbeespoort Dam, and not in the context of the entire reach of the Crocodile River down to its confluence with the Marico River to form the Limpopo River (Fig. 3).

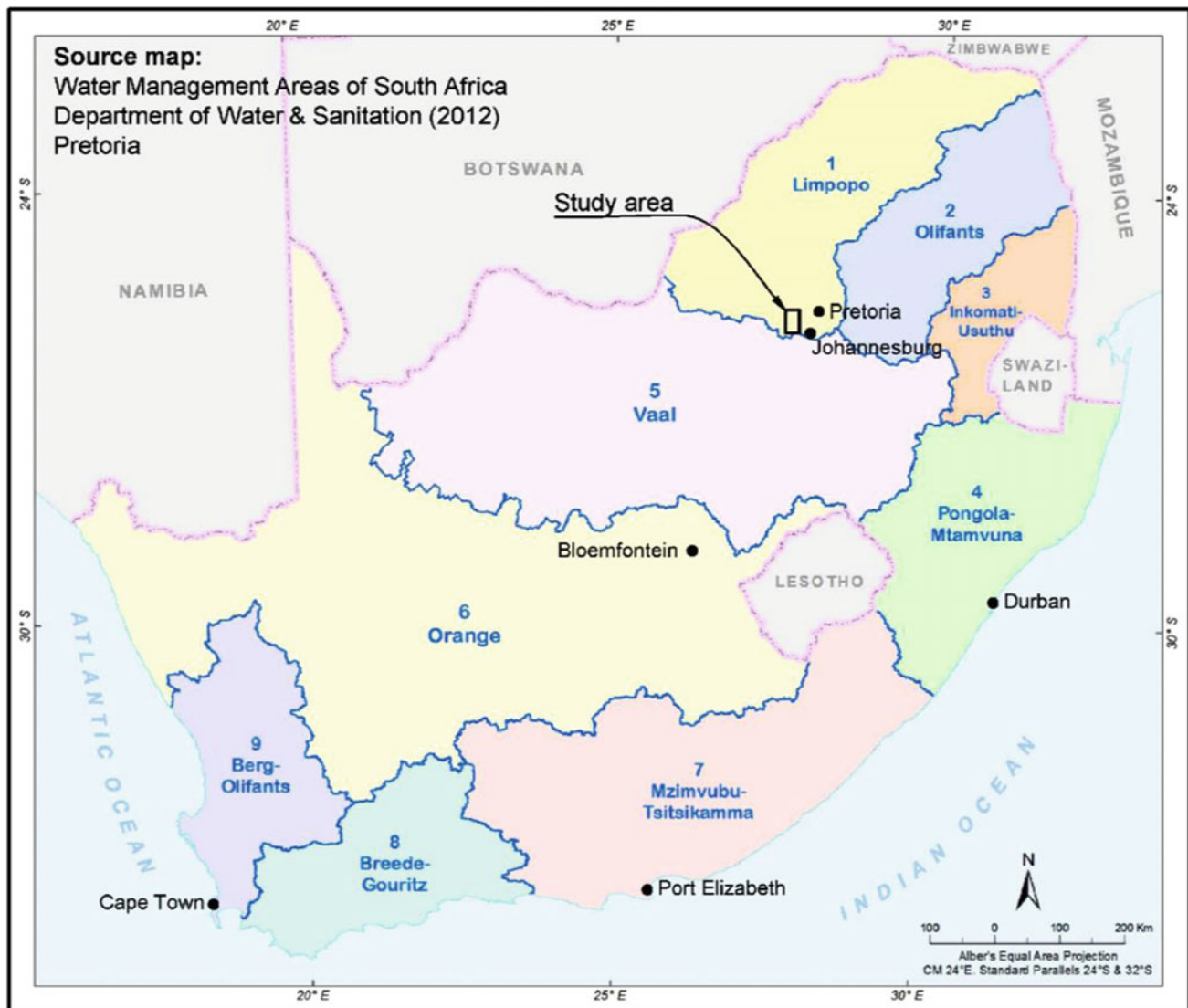


Fig. 1 Position of the study area within the national distribution of water management areas (WMAs; numbered and labelled) and the Limpopo WMA (#1) in particular

20–22 °C in summer (December/January) and 10 to 12 °C in winter (June/July). The daily mean relative humidity falls in the range 58–60% in winter and 66 to 68% in summer, with daily minima falling in the ranges 32–34% and 46–48% for these seasons, respectively. The A-pan equivalent mean annual potential evaporation (MAPE) falls in the range of 2200–2400 mm. The long-term A-pan evaporation recorded at OR Tambo International Airport located at 26.13°S—28.29°E, a distance of ~55 km east-southeast of the property, is 2160 mm/a. This study accepts the lower bound of 2200 mm/a as representative of the A-pan evaporation value for the study area, and a mean actual evapotranspiration of 1540 mm/a.

As the principal agent of groundwater recharge, rainfall is an integral component of the hydrological cycle, rendering knowledge of its magnitude and distribution an important

aspect of a study such as this. The distribution of rainfall gauging stations in the study area and surroundings is shown in Fig. 2. The mean annual precipitation (MAP) associated with each of the Quaternary basins in the study area (DWA 2006) is shown in Table 1 and indicates a mean value of 696 mm/a (excluding catchment A21F representing 1% of the area).

The rainfall stations reflect a skewed geographic distribution that favours the south-western portion of the subregion. They are operated by various entities identified as follows:

- South African Weather Service (SAWS), generally located at police stations and municipal offices;
- Sibanye-Stillwater (S-S), located at various sites on the mine property;
- Mogale City Local Municipality (MCLM), located at the Percy Stewart WWTW; and

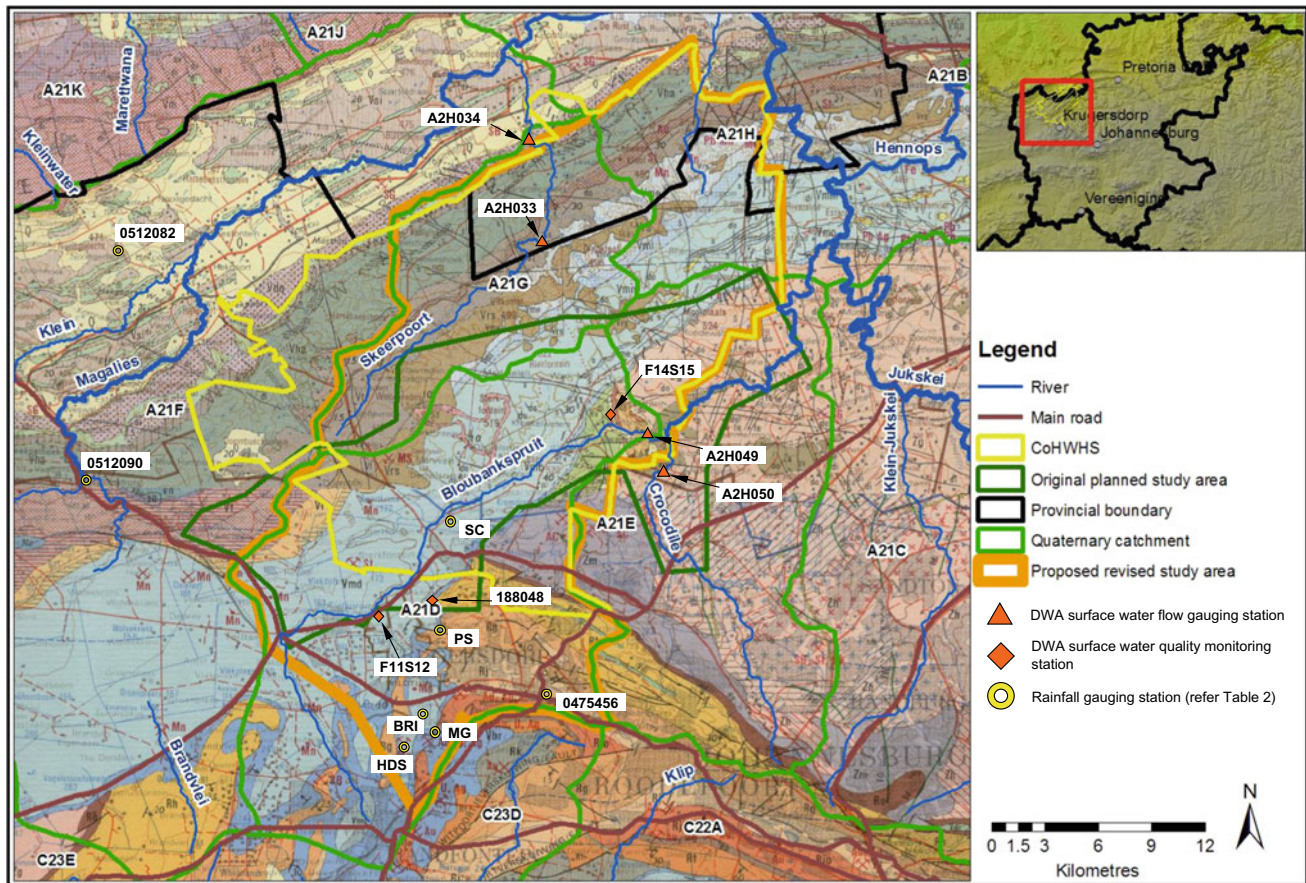


Fig. 2 Definition of study area showing positions of rainfall, surface water flow and surface water quality gauging stations with hydrologic features superimposed on geology as backdrop

Table 1 Geographic definition of quaternary catchments spanned by the study area

| Quaternary basin | Main drainage and relative latitude | MAP (mm) | Total area (km ²) | Proportion of basin in study area | |
|------------------|-------------------------------------|----------|-------------------------------|-----------------------------------|------|
| | | | | (km ²) | (%) |
| A21D | Bloubank spruit system south | 714 | 372 | 303 | 46.7 |
| A21E | Crocodile River (upper) south | 707 | 290 | 100 | 15.4 |
| A21F | Magalies river north | 677 | 1001 | 1 | 0.2 |
| A21G | Skeerpoort river central | 694 | 160 | 156 | 24.0 |
| A21H | Crocodile river (lower) north | 668 | 514 | 89 | 13.7 |
| Total | | | 2337 | 649 | 100 |

- Department of Water and Sanitation (DWS) located at Sterkfontein Cave and, since 2013, also on Ptn 36 of Vlakplaats 160IQ near Tarlton, Ptn 8/2 of Sterkfontein 173IQ north of the Krugersdorp Game Reserve, and at the HDS mine water treatment plant.

A daily precipitation record is maintained in most of the above-listed instances. The DWS stations comprise a cumulative (totalling) gauge developed by van Wyk (2010).

These gauges have a rainfall equivalent capacity of ~ 450 mm and are therefore emptied every 2–4 months depending on season. The length of record and other information associated with each station is given in Table 2. It shows that rainfall monitoring by S–S (and its predecessors) in the mine area is comparatively recent. This reflects the importance of rainfall and associated recharge on the hydrostatic head in the subsurface mine workings and the more recent periodic recurrence of excess mine water discharge (Sect. 5.3.1 in

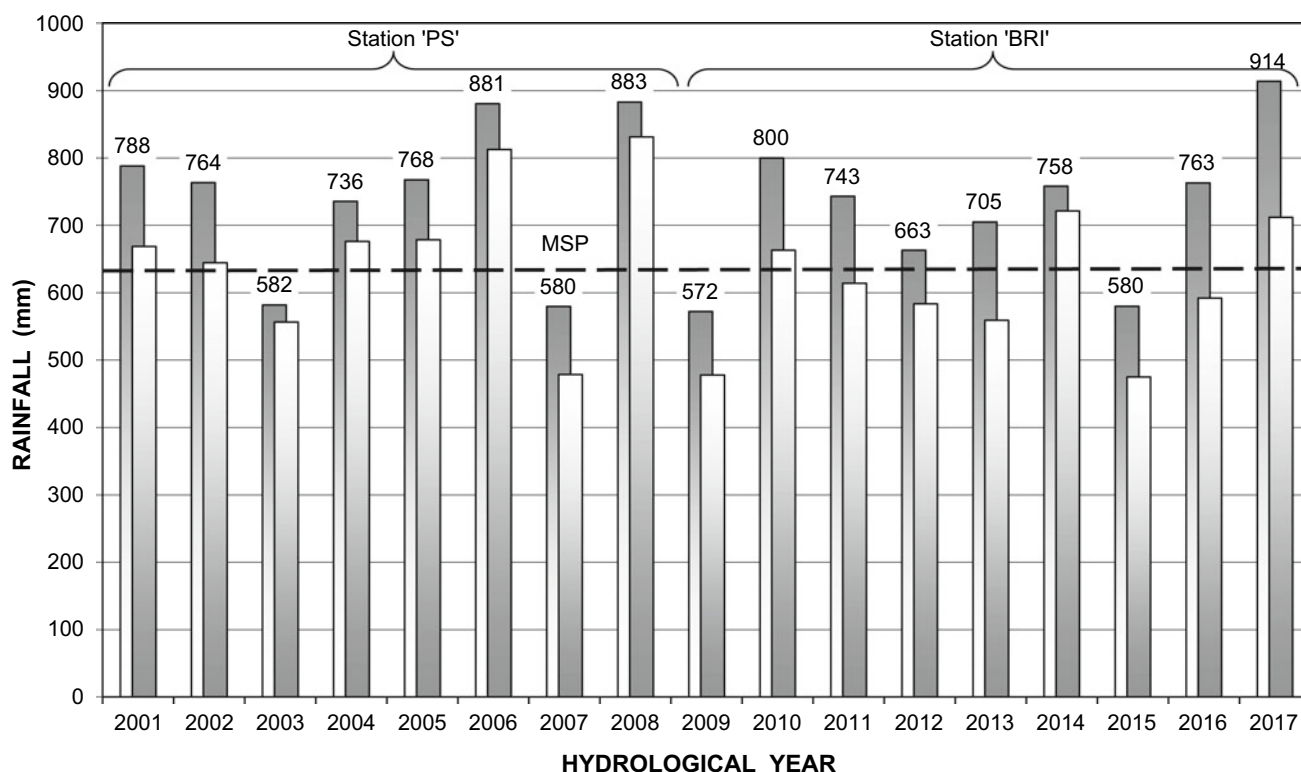


Fig. 3 Composite annual and overlapping summer (wet season) rainfall record for stations PS and BRI; the mean summer precipitation of 632 mm is indicated by the dashed line labelled MSP

Chapter “Physical Hydrology”). Nevertheless, an analysis of the available precipitation record indicates that rainfall is distributed approximately 80–20% between the wet summer and the dry winter seasons.

The composite precipitation record of rainfall stations PS [for the 2001 to 2008 hydrological years³ (a_h)] and BRI (for a_h 2009 to 2017) shows the ‘wetter’ 2006 (813 mm), 2008 (831 mm), 2010 (663 mm), 2014 (721 mm) and 2017 (712 mm) summer rainfall seasons (Fig. 3). Both these stations are located north of the watershed (Fig. 2).

A comparison of the HDS and Sterkfontein Cave (SC) monthly rainfall data for the period of common record June 2010 to September 2017 returns the correlation shown in Fig. 4. The data set excludes months of no rainfall at both stations in order to remove the false correlation created by common null values. This shows that station SC experiences ~22% less rainfall on a monthly basis than does station HDS on the watershed ~13 km to the south. Wet months at both stations represent ~80% of the annual (a_h) record, equating to 9.6 such months per year. The regional reduction in rainfall northward that is evident in Table 1 is therefore echoed at the subregional scale. In summary, the long-term MAP for the northern third of the study area falls

in the range 668–694 mm. The remaining ~67% comprising the central and south-western portion experiences ~710 mm (Table 1).

Considered of greater significance is the observation that ~52% of the 2014 summer rainfall at Sterkfontein Cave (396 out of 760 mm) and at station HDS (413 out of 799 mm) occurred in February and March 2014. These circumstances explain the resumption of uncontrolled mine water discharge from the mine area in late-February 2014 (Hobbs 2014a). This is similar to the situation that prevailed in the 2010 and 2011 wet seasons (Hobbs 2013a, b) that led to the severest mine water impact on the receiving water resources environment. The increased capacity of the mine water treatment plant to ~34 ML/d in June 2013 (Timeline 2 p. ii and Text Box 1 in Chapter “Physical Hydrology”, p. 61) remained insufficient to contain and treat the volume of mine water issuing from the flooded underground mine workings following recharge. Similarly, a_h 2017 experienced an anomalous rainfall pattern marked by the following:

- A wetter than average summer (864 mm at station HDS and 712 mm at station BRI) yet in both instances typically representing ~80% of the MA_hP of each station; and

³ See GLOSSARY.

Table 2 Rainfall monitoring stations in the study area and surrounds

| Station | Station name | Source | Coordinates ^a | | Elevation (m amsl) | Start date (mm/yyyy) |
|----------------------|-----------------------------|--------|--------------------------|------------|--------------------|----------------------|
| | | | Latitude | Longitude | | |
| 0475338 | Randfontein | SAWS | 26.13°S | 27.70°E | 1710 | 12/1954 ^b |
| 0475456 | Krugersdorp kroningspark | | 26.10°S | 27.77°E | 1699 | 07/1904 |
| 0475605 ^c | Wits botanical gardens | | 26.08°S | 27.85°E | — | 04/1988 |
| 0512082 | Hekpoort nooitgedacht | | 25.87°S | 27.55°E | 1463 | 01/1972 ^d |
| 0512090 | Magaliesburg police station | | 26.00°S | 27.55°E | 1480 | 01/1969 |
| 0512783 ^c | Pelindaba | | 25.80°S | 27.92°E | — | 01/1965 |
| PS ^c | Percy stewart WWTW | MCLM | 26.08°S | 27.73°E | 1590 | 01/2000 |
| BRI ^c | Black reef incline | S-S | 26.11566°S | 27.72319°E | 1662 | 10/2004 |
| HDS ^c | HDS plant | | 26.13384°S | 27.71579°E | 1714 | 10/2004 |
| SC ^{c, e} | Sterkfontein cave | DWS | 26.01566°S | 27.73413°E | 1480 | 07/2007 ^f |

^a Reported as decimal degrees in Hartebeesthoek94 Datum, WGS84 ellipsoid

^b Closed March 2009

^c Not used in WR 2005 (Middleton and Bailey 2008a, b)

^d Closed November 2009

^e Identified as STERK_RF by the DWS

^f Data only available from June 2010

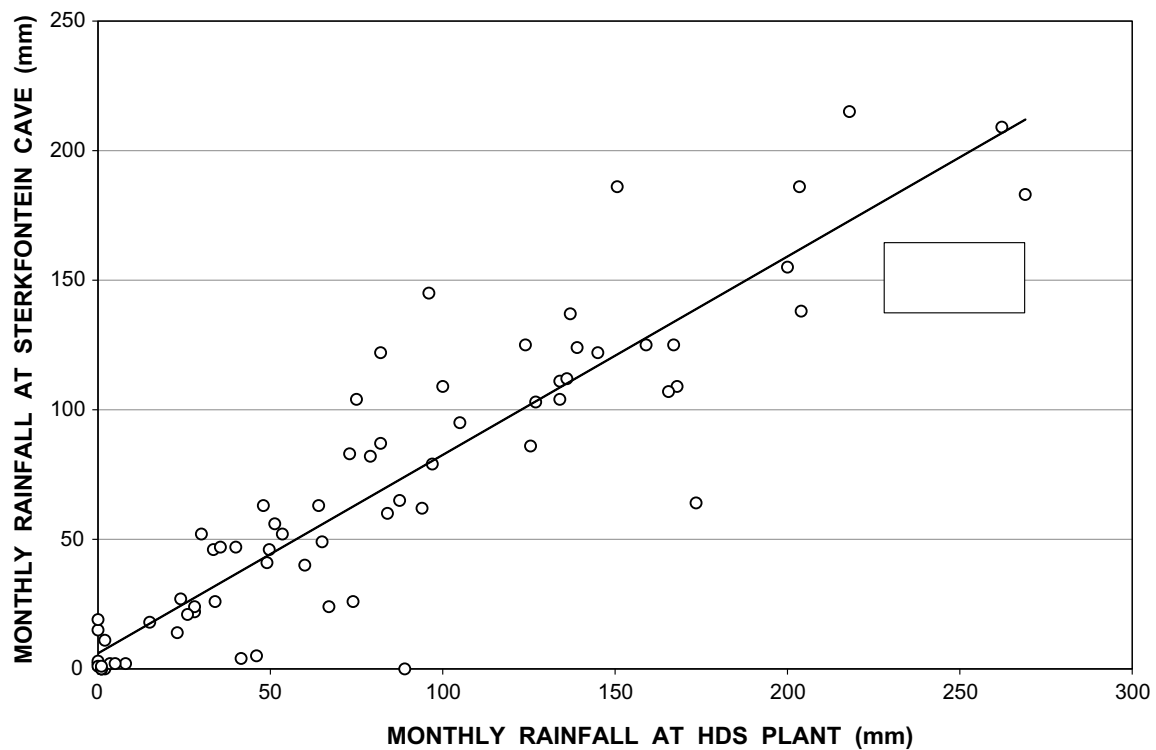


Fig. 4 Correlation of monthly rainfall at Sterkfontein Cave with that at station HDS on the watershed for the period of common record June 2010 to September 2017; data set ($n = 71$) excludes months of no rainfall at both stations ($n = 17$)

- A very wet early winter (~ 200 mm at both stations HDS and BRI) representing $\sim 20\%$ of the MA_{hP} , i.e. equivalent to the typical proportional full dry season contribution.

An aspect not revealed in the preceding discussion is the correlation between individual high rainfall periods and flooding. For example, the rainfall event recorded for 16/12/2010, when 90 mm was measured at the HDS station and 106 mm at Sterkfontein Cave, precipitated the flooding in the region that contributed to a fish mortality event (Sect. 6.5.2 in Chapter “[Chemical Hydrology](#)”) in January 2011 (Hobbs and Mills 2011).

A further aspect of precipitation that requires inspection for its potential relevance to groundwater recharge estimations, is the period considered for calculation of the annual mean. MAP values reported in the literature generally pertain to calendar years. In water resources assessments, however, it is the hydrological year that serves as base temporal unit, and it is, therefore, appropriate that a comparison be drawn between MAPs based on calendar and hydrological years. An inspection of the monthly data associated with the PS, HDS, BRI and SC stations aggregated to calendar and hydrological years, returns the results presented in Table 3. It is evident that the MAP values for calendar and hydrological years at each of the rainfall stations are similar, although the stations’ PS and SC indicate hydrological years to be marginally wetter (by $\sim 3\%$) than calendar years. The location of these two stations in more rugged terrain prone to orographic effects north of the watershed might explain this result.

Nevertheless, it is concluded that natural groundwater recharge estimations based either on calendar or hydrological year averages will return similar results.

Middleton and Bailey (2008a) report an A-pan evaporation rate for the study area in the range of 2200 to 2600 mm/a. In broad terms, the mean annual potential evaporation in the study area exceeds the MAP by a factor of three. The drainages in the COH, however, are not characterised by large expanses of open water that promote evaporation losses. The dense arboreal vegetation along substantial reaches of the drainage channels provides a canopy that further inhibits evaporation, but more than likely promotes riparian evapotranspiration (RET).

Evapotranspiration (ET) has been identified in various studies (e.g. Hail and Prudic 1998; Harlow et al. 2005; Martini and Kavalieris 1976; Prudic et al. 1995; Schaefer et al. 2005) as representing the most important water ‘loss’ component of the water resources budget in karst environments. Rutledge and Mesko (1996) draw attention to the particular contribution of riparian evapotranspiration (RET) in this regard. The potential significance of RET as a water loss component in the hydro(geo)logic budget of the study area is evaluated in Sect. 7.4.1 in Chapter “[Physical Hydrogeology](#)”.

Bredenkamp and van Staden (2009) report that the riparian tree zone is typically 10–20 m wide and the vegetation is dense and almost forest-like, dominated by indigenous trees and very dense forest-like bush on both banks of rivers, streams and creeks. Krige (2009) reports a calculated (R)ET value of 5 ML/d based on a total stream length of ~ 27.5 km on average 40 m wide, and subject to

Table 3 Comparison of mean precipitation for full calendar and hydrological years at four rainfall stations

| Calendar year | Station rainfall (mm) | | | | Hydrological year | Station rainfall (mm) | | | |
|---------------|-----------------------|------|-----|-----|-------------------|-----------------------|-----|-----|-----|
| | PS | HDS | BRI | SC | | PS | HDS | BRI | SC |
| 2002 | 702 | | | | 2002 | 764 | | | |
| 2003 | 482 | | | | 2003 | 582 | | | |
| 2004 | 780 | | | | 2004 | 736 | | | |
| 2005 | 776 | | | | 2005 | 768 | | | |
| 2006 | 962 | | | | 2006 | 881 | | | |
| 2007 | 567 | | | | 2007 | 580 | | | |
| 2008 | 772 | | | | 2008 | 883 | | | |
| 2009 | | 737 | 612 | | 2009 | | 679 | 572 | |
| 2010 | | 903 | 823 | | 2010 | | 870 | 800 | |
| 2011 | | 885 | 711 | 750 | 2011 | | 967 | 743 | 824 |
| 2012 | | 735 | 714 | 691 | 2012 | | 660 | 663 | 606 |
| 2013 | | 714 | 662 | 596 | 2013 | | 752 | 705 | 702 |
| 2014 | | 805 | 739 | 808 | 2014 | | 832 | 758 | 812 |
| 2015 | | 451 | 490 | 462 | 2015 | | 596 | 580 | 566 |
| 2016 | | 1043 | 863 | 709 | 2016 | | 822 | 763 | 592 |
| Average | 722 | 784 | 702 | 669 | Average | 742 | 772 | 698 | 684 |

Table 4 Classification of the vegetation of the study area (after Mucina and Rutherford 2006)

| Biome | Bioregion | Vegetation unit |
|---------------|-------------------------------|--|
| Grassland (G) | Dry Highveld Grassland (Gh) | Carletonville Dolomite Grassland (Gh15) |
| | Mesic Highveld Grassland (Gm) | Soweto Highveld Grassland (Gm8) |
| | | Egoli Granite Grassland (Gm10) |
| Savanna (SV) | Central Bushveld (SVcb) | Moot Plains Bushveld (SVcb8) |
| | | Gold Reef Mountain Bushveld (SVcb9) |
| | | Gauteng Shale Mountain Bushveld (SVcb10) |
| | | Andesite Mountain Bushveld (SVcb11) |

an ET rate of 1674⁴ mm/a. The significance of RET in the COH must, however, be tempered by the observed depth to groundwater level in and along stream reaches as discussed in Sect. 7.3 in Chapter “Physical Hydrogeology”, except in those instances where the potentiometric surface approaches and intersects the stream channel (Sect. 7.4.1 in Chapter “Physical Hydrogeology”). Compared to RET, the mean annual actual evapotranspiration (AET) in the study area amounts to 1540 mm (Schulze et al. 1997).

3 Vegetation and Soils

The study area encompasses two biomes, namely the Grassland Biome and the Savannah Biome (Mucina and Rutherford 2006). As shown in Table 4, the Grassland Biome is represented by two bioregions, and the Savanna Biome by a single bioregion. Further subdivision of the bioregions recognises the vegetation units listed in Table 4 as occurring in the study area. A more comprehensive discussion of the vegetation types in the subregion is provided by Bredenkamp and van Staden (2009).

As the name implies, the Carletonville Dolomite Grassland (Gh15) vegetation unit covers the area underlain by dolomitic strata of the Malmani Subgroup (Table 5). It therefore also covers the largest expanse (~50%) of study area characterised mostly by the shallow Mispah and Glenrosa soil forms, with deeper red to yellow apedal soils of the Hutton and Clovelly forms occurring sporadically. The vegetation is characterised by species-rich grasslands forming a complex mosaic pattern with many species dominant (Mucina and Rutherford 2006). A notable characteristic of this vegetation unit is the occupation of sheltered valleys and sinkholes by trees such as *Celtis Africana* (white stinkwood, *A. witstinkhout*), *Kiggelaria Africana* (wild peach, *A. wildeperske*) and *Leucosidea sericea* (old-wood, *A. ouhout*) that represent traces of temperate or transitional forest (Acocks 1988). The Soweto Highveld

Grassland (Gm8) vegetation unit occurs along the southern margin of the study area underlain by quartzitic strata of the Witwatersrand Supergroup. The deep, reddish soils on flat plains are absent in the presence of outcropping bedrock. The landscape supports short to medium-high, dense, tufted grassland dominated by *Themeda triandra* (red grass, *A. rooigras*).

The Egoli Granite Grassland (Gm10) vegetation unit occurs along the south-eastern margin of the study area where it is underlain by Halfway House Granite that builds the pluton known as the Johannesburg Dome. The landscape supports leached, shallow, coarsely grained, sandy and nutrient-poor soils of the Glenrosa form. Grassland vegetation is dominated by *Hyparrhenia hirta* (common thatchgrass, *A. dektamboekiegras*) with some woody species on outcropping bedrock.

The Savanna Biome is represented by the Gold Reef Mountain Bushveld (SVcb9) and Andesite Mountain Bushveld (SVcb11) vegetation units that occupy very small portions along the south-eastern margin of the study area, and the Moot Plains Bushveld (SVcb8) and Gauteng Shale Mountain Bushveld (SVcb10) vegetation units found along the north-western margin. The latter two units are readily defined by their association with the mainly sedimentary strata (quartzite and shale) of the Pretoria Group that overlie the Malmani Subgroup dolomite (Sect. 4). The soils vary from stony, colluvial, clay-loam, red-yellow freely drained forms to shallow Mispah soil forms. The low, broken ridges varying in steepness support shortly (3–6 m tall), semi-open thicket dominated by a variety of woody species including *Acacia caffra* (hook thorn, *A. haakdong*) and *Cussonia spicata* (common cabbage tree, *A. kiepersol*).

4 Geology and Geophysics

The geology of the broader region is described in numerous texts, e.g. Clendenin (1989), Eriksson and Reczko (1995), Eriksson et al. (2006), Obbes (2001) and Robb and Robb (1998a). The geology of the study area is dominated by carbonate strata (primarily dolomite) associated with the Malmani Subgroup of the Chuniespoort Group within the

⁴ Equal to 0.775 of the long-term A-pan equivalent of 2160 mm/a at OR Tambo International Airport.

Table 5 Simplified lithostratigraphic subdivision of strata in the subregion

| Basic lithology ^a | Lithostratigraphic unit | | | Era (Age) | |
|--|--------------------------------|--------------------|--------------------------|--------------------------------|---------|
| Alluvium | Quaternary sediments | | | Late Cenozoic (<10 000 y) | |
| Dolerite/diabase/syenite [Jd] | Dyke/sill intrusive structures | | | Early Mesozoic (150 to 190 Ma) | |
| Andesite, basalt, subordinate shale [Vh] | Hekpoort formation | Pretoria group | Transvaal supergroup | (~ 2224 Ma) (~ 2555 Ma) | Vaalian |
| Ferruginous shale and quartzite, hornfels [Vt] | Timeball hill formation | | | | |
| Quartzite, shale, chert breccia [Vrs] | Rooihoogte formation | | | | |
| Dolomite [Vmd] | Malmani subgroup | Chuniespoort group | | | |
| Quartzite, shale [Vbr] | Black reef formation | | | (~ 2650 Ma) | |
| Graywacke, conglomerate, volcanics [R-Vk] | Kameeldoorns formation | Platberg group | Ventersdorp supergroup | (~ 2650 Ma) (~ 2780 Ma) | Randian |
| Quartzite, conglomerate [Rjo] | Johannesburg subgroup | Central rand group | Witwatersrand supergroup | (~ 2780 Ma) (~ 2970 Ma) | |
| Shale, quartzite [Rj] | Jeppes town subgroup | West rand Group | | | |
| Quartzite, greywacke [Rg] | Government subgroup | | | | |
| Ferruginous shale, quartzite [Rh] | Hospital hill subgroup | | | | |
| Mafic and ultramafic rocks [Zm] and granite [Zg] | Undifferentiated | | | Swazian (>3100 Ma) | |

^a Lithology colours correlate broadly with those used in Fig. 2 in Chapter “[Introduction and Background](#)”

Ma = million years

Transvaal Supergroup succession of mainly sedimentary strata. The Malmani Subgroup is subdivided into four units identified as the Oaktree Formation at the base, overlain in turn by the Monte Christo, the Lyttelton and the Eccles formations. In a regional context, these strata dip to the north-west at an angle of between 15° and 30°, disappearing beneath younger Pretoria Group sedimentary rocks (quartzite and shale) roughly coincident with the SW–NE strike of the Skeerpoort River valley (Fig. 2 in Chapter “[Introduction and Background](#)” and Fig. 9).

The moderately rugged relief that occupies an elevation ranging between ~1400 and ~1600 m amsl between the Skeerpoort River draining the north-western portion of the property, and the Bloubank Spruit system draining the southern and south-eastern portions (Fig. 2 in Chapter “[Introduction and Background](#)” and Fig. 9), forms the escarpment-type karst morphology defined by Martini and Kavalieris (1976). These features reflect the degree of structural geologic influence on the landscape as recognised, amongst others, by Dirks and Berger (2013) as an agent in landscape dynamics in the Malapa and Gladysvale sections of the property (Table 6). The much flatter terrain occupying

an elevation between ~1560 and ~1660 m amsl that characterises the landscape of the Steenkoppies Basin west of Tarlton (Fig. 2 in Chapter “[Introduction and Background](#)”), represents the plateau-type karst morphology of Martini and Kavalieris (1976).

The outcrop of individual karst formations is only defined north of latitude 26°S on published geological maps (RSA 1973a, b). South of 26°S, only the composite Malmani Subgroup is defined to the west as far as longitude 27°15'E (RSA 1986), beyond which the formations are again individually mapped.

Along the southern and south-eastern margin, the Malmani Subgroup dolomite rests on older sedimentary rocks of the Witwatersrand Supergroup and even older intrusive granitic and gneissic rocks forming the Archaean basement exemplified by the Halfway House Granite pluton. The stratigraphic relationship of the various lithologies described above is shown in Table 5.

The significance of karst formations such as underlie ~26 860 ha (~52%) of the COH, and ~27 850 ha (~43%) of the study area, is summarised by Hamilton-Smith (2006) who states that karst often has ‘.....

Table 6 Salient hydrologic and hydrogeologic aspects associated with the most well-known fossil sites in the study area

| Fossil site | Coordinates ^a | Quaternary catchment | Main drainage | Groundwater basin | Synoptic cave morphology | SAAN ^b # with brief description and main significance |
|---------------|--------------------------|----------------------|------------------|-------------------|------------------------------|---|
| Bolt's farm | 26.03°S 27.72°E | A21D | Bloubank spruit | Zwartkrans | Near-surface and underground | SAAN—: comprises a complex of ~ 23 caves that include the oldest deposits in the Sterkfontein Valley on the basis of microfaunal dating; also the site of the recent <i>H. naledi</i> finds in the Rising Star Cave system |
| Swartkrans | 26.02°S 27.72°E | | | | Near-surface and underground | SAAN—0021: well-documented excavations and faunal analyses by CK Brain, hosts the largest collection of <i>Paranthropus robustus</i> fossils and evidence for the use of fire and bone and horn tools; has yielded >500 hominin fossils |
| Sterkfontein | 26.01566°S 27.73413°E | | | | Near-surface and underground | SAAN—0020: internationally recognised focus of the COH WHS and home of the <i>Au. africanus</i> specimens Mrs. Ples (Sts 5) and Little Foot (StW 573), has yielded >500 hominin fossils, and >25 000 identifiable fossils in total |
| Cooper's | 26.01°S 27.75°E | | | | Near-surface | SAAN—0023: specimens of <i>Paranthropus robustus</i> , including a face, uncovered; potential for more hominins and faunal dating |
| Kromdraai | 26.01°S 27.75°E | | | | Near-surface | SAAN—0022: one of the earliest sites studied, yielded the remains of at least three <i>Paranthropus robustus</i> individuals, and a few earlier Stone Age artefacts |
| Minnaar's | 26.01°S 27.74°E | | | | Near-surface and underground | SAAN—0004: known for the excavation of an extinct jackal skull, has the potential for the discovery of hominin fossils |
| Plover's lake | 25.98°S 27.78°E | | | Krombank | Near-surface and underground | SAAN—0025: hosting breccias <1 Ma old and revealing no hominin remains as yet, this site retains the potential for revealing the remains of early modern humans associated with Middle Stone Age artefacts |
| Wonder Cave | 25.97033°S 27.77143°E | | | | Underground | SAAN—0027: perhaps the best example of a tourist-centred (show) cave, as yet not known to host hominin fossils, but demonstrates the development of a recent talus cone containing semi-fossilised skeletal material |
| Drimolen | 25.97°S 27.76°E | A21G | Skeerpoort River | Danielsrust | Near-surface | SAAN—0024: has yielded ~ 75 <i>Paranthropus robustus</i> specimens and five <i>Homo sapiens</i> species, as well as bone and horn tools |
| Gladysvale | 25.90°S 27.77°E | | | Uitkomst | Near-surface and underground | SAAN—0001: has yielded several thousand Plio-Pleistocene mammalian remains including hominin (<i>Au. africanus</i>) teeth |
| Motsetse | 25.91°S 27.83°E | | | Diepkloof | Near-surface | SAAN—0030: although not renowned for any significant discoveries, has research potential coupled with an attractive setting and visitor access |
| Haasgat | 25.86°S 27.83°E | | | Diepkloof | Near-surface | SAAN—: has yielded 83 craniodental fossils of the Cercopithecidae Family (Old World monkeys) primate <i>Papio angusticeps</i> , extinct relative of <i>Papio ursinus</i> (Chacma Baboon) |

(continued)

Table 6 (continued)

| Fossil site | Coordinates ^a | Quaternary catchment | Main drainage | Groundwater basin | Synoptic cave morphology | SAAN ^b # with brief description and main significance |
|-------------|--------------------------|----------------------|------------------|-------------------|------------------------------|---|
| Gondolin | 25.83°S 27.86°E | A21H | Crocodile river | Broederstroom | Near-surface | SAAN—0031: has yielded <i>Paranthropus robustus</i> specimens |
| Malapa | 25.90°S 27.80°E | A21G | Skeerpoort river | Diepkloof | Near-surface and underground | SAAN—: host to <i>Au. sediba</i> , the recent anthropological find in the COH |

^a All coordinates except for Sterkfontein Cave and Wonder Cave truncated to the 2nd decimal in order to protect these sites from unwelcome visitation

^b Site number from Berger and Brink (undated), together with a substantial amount of ancillary descriptive information including a mixed assemblage list of fauna

- Invaluable geological data (particularly in the cave floors);
- Important geomorphic structures and processes;
- Characteristic surface and often significant landscapes;
- Important surface ecosystems and even more important subterranean ecosystems; and
- Fossils and cultural heritage (pre-historic, historic and living)’;

to which must be added.

- Significant quantities of fresh groundwater; and
- A capacity to function as a sink for carbon in the global carbon cycle.

The hydrogeologic significance of the chert-rich dolomitic strata of the Monte Christo and Eccles formations, versus that of the chert-poor Oaktree and Lyttelton formations, bears mention. The chert-rich formations are associated with significantly greater water-bearing properties than the chert-poor formations, due mainly to preferential dissolution of the dolomite that is interlayered with the chert bands (Martini and Kavalieris 1976). In outcrop, the insoluble chert bands protrude from the dolomite as is illustrated in Plate 1, Plate 1. Preferential dissolution is enhanced in the presence of fractures and joints that intersect the rock mass and facilitate the movement of infiltrating slightly acidic rainwater as primary speleogenetic agent, as observed by Wilkinson (1973) in Sterkfontein Cave.

The structural complexity of the geologic environment in the subregion presents a significant challenge. This challenge pertains, amongst others, to an understanding of the geologic control that structures such as faulting, folding and intrusions of dolerite, diabase or syenite in the form of sills (subhorizontal intrusions) and dykes (subvertical intrusions) exercise on the hydrogeologic regime. Staff and students of the Witwatersrand University (Wits) School of Geoscience and of the University of Johannesburg continue to carry out structural

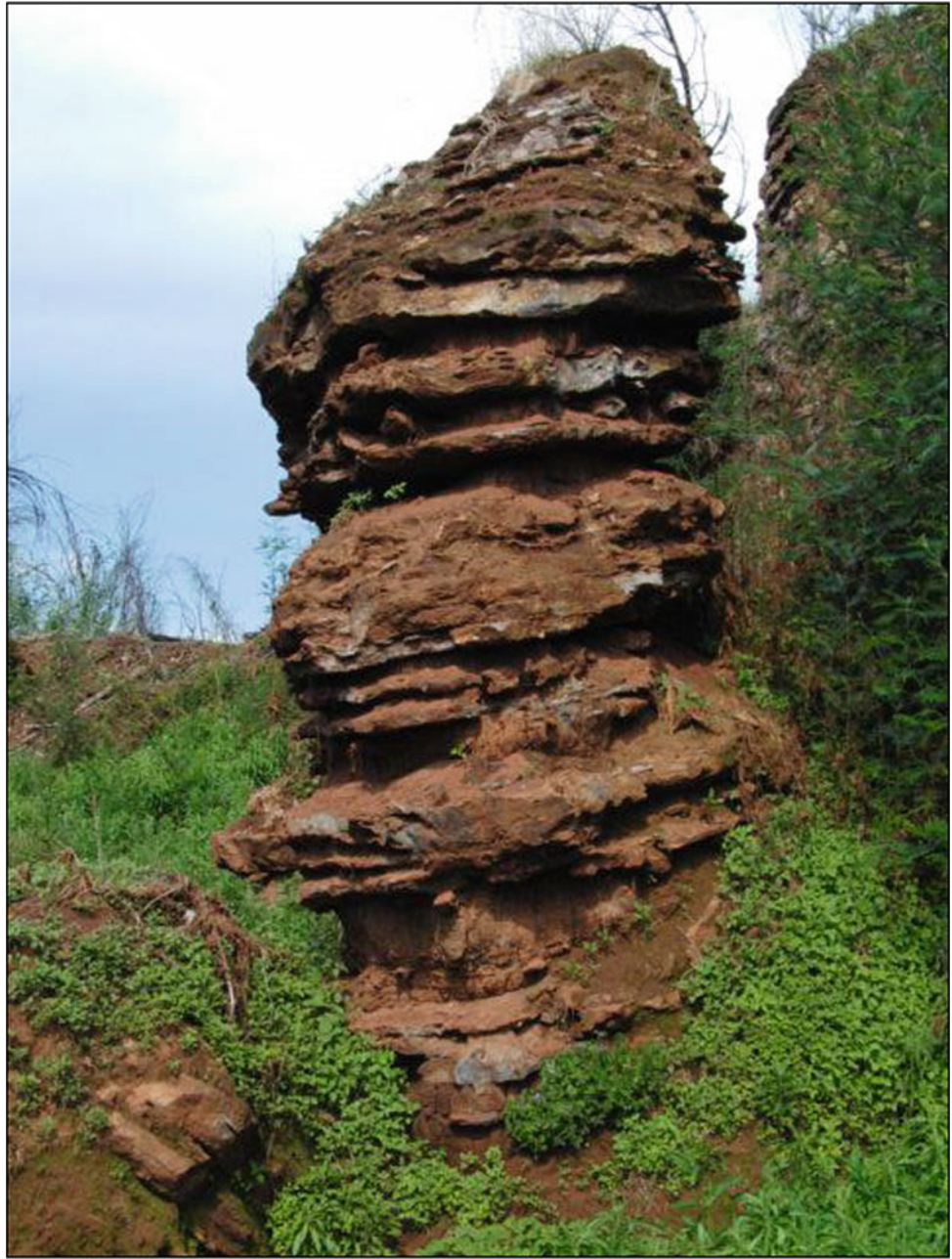
geologic mapping and other bio- and geo-environmental studies (including hydrogeology) in the area.

A number of geophysical surveys that help inform various aspects of the geological environment in the subregion and wider surroundings have been carried out in the past. The most significant of these is considered to be the gravimetric survey carried out by the then Department of Water Affairs and Forestry (DWAF) in the mid-1980s (Brendenkamp et al. 1986). This survey covered large tracts of the eastern portion of the Steenkoppies Basin and the western portion of the Zwartkrans Basin (refer to Sect. 7.2 in Chapter “Physical Hydrogeology” for compartment definition), spanning ~ 90 km² at a grid interval of 100 m between measurement stations.

The gravity survey was augmented with ground-based magnetic and electromagnetic surveys primarily to better define linear geological structures (mainly intrusive dolerite, diabase or syenite dykes) of possible hydrogeological significance. The magnetic surveys indicated that the dyke intrusions generally exhibit a negative magnetic signature, i.e. possess a magnetic field strength that is lower than that of the host rock intruded by these structures. The gravimetric data set has been converted to digital format (F Wiegman, personal communication) which facilitates its further application and use in a GIS environment.

More recently (ca. 2005), the then DWA commissioned the Council for Geoscience (CGS) to carry out a regional aeromagnetic (airborne magnetic) survey covering the West Rand and Far West Rand goldfields. The limited ground-based application of the magnetic, electromagnetic and resistivity tomography survey methods to identify potential subsurface conduits of mine water drainage in the Krugersdorp Game Reserve (KGR) is reported by Coetzee et al. (2009). The CGS has also recently (in mid-2010) carried out an airborne electromagnetic survey of the area covered by the earlier aeromagnetic survey. Funded by the Department of Mineral Resources (DMR), the data generated by this survey has yet to be published and made

Plate 1 Epikarst exposed in the form of a pinnacle ~2.5 m high in the Eccles Formation, showing the preferential dissolution of dolomite interlayered with less soluble and therefore more prominent chert bands, the slanting aspect of which also defines the local ~15° dip of the strata to the north-west (at bottom left of picture), with a partially wad-filled and vegetated vertical joint ('slot') separating the pinnacle from the overgrown rock mass at right of picture



available for wider application. It is imperative, however, that the additional information generated by this survey be applied to further inform the geologic and hydrogeologic understanding developed and presented in this manuscript.

A geophysical survey carried out as part of the water resources situation assessment for the MA (Hobbs et al. 2011a) has sought to better define features that inform the structural geologic setting of Sterkfontein Cave. This survey employed ground-based magnetic, electromagnetic and electrical resistivity surveys (Chirenje et al. 2010), and was successful in identifying several structures and their possible influence on the cave morphology.

5 Mining Geology

The threat posed to the COH by the legacy of mining in the West Rand Goldfield, in particular, that associated with mine water discharge, is an important aspect of the water resources environment in the study area. It is therefore pertinent that a discussion of this activity is included for the purpose of elucidating its position within this environment.

The mining geology of the West Rand Goldfield (aka the Western Basin) is described by Toens and Griffiths (1964)

and Tucker and Viljoen (1986), amongst numerous others. The history of mining is discussed by Handley (2004), from which it would appear that gold mining in this field commenced in ca. 1889 with the opening of Randfontein Estates Gold Mining Company (REGM). Another mining activity in the area has included uranium (together with gold), limestone from caves (e.g. Sterkfontein) and excavations (e.g. Sterkfontein Quarry). Although primary extraction of these mineral commodities is now history, secondary extraction of gold is associated with the reworking of the older mine surface residue deposits in the form of sand dumps (Plate 2 and Fig. 5). The tailings reclaimed by Mogale Gold/Mintails SA (MG/MSA) have reported grades in the range of 0.26 to 0.3 g/t (Louw 2012), compared to average in-situ ore grades in the range of 4 to 19 g/t for the auriferous reefs in the West Rand Goldfield (Handley 2004). Total gold production in the 114 years to 2002 amounted to ~ 2.4 kt at an average grade of 5.09 g/t (Handley 2004). In the period 1952 to 1995, this

goldfield also produced ~ 27.9 kt of uranium at an average grade of 370 g/t (Cole 1998), extracted primarily from the Main, White and Monarch reefs of the Johannesburg Subgroup. The REGM operations closed in 1999.

Surface features of mining-related significance in the Western Basin are identified in Figs. 5 and 6. The conceptual inter-relation of these features with the geologic environment in the subsurface is illustrated in Fig. 7. The illustrations show the association of the opencast mining activities (represented by the West Wits and Millsite pits) with the package of auriferous Kimberley Reefs, and the positions of the Black Reef Incline (BRI, Plate 3), #s 8, 9 and 9E Shafts, and #s 17 and 18 Winzes in the geologic environment. The position of the Main Reef in this environment, its exploitation by underground workings via shafts such as the ~ 450 m deep #8 Shaft, and its possible linkage to the Black Reef workings via the BRI and #17 and #18 Winzes, is also illustrated.



Plate 2 Recovery of mine residue deposits on the northern side of Dump 20 (see Fig. 5 for location) destined for reworking in the Mogale Gold/Mintails SA plant; the excavated/eroded area in the foreground is the southern end of the Millsite Pit (photo W Bason, date 09/12/2009)



Plate 3 Panoramic view of the HDPE-lined dam at the Black Reef Incline (under grid at front right-of-centre), showing the pump station at left-of-centre beyond the dam, from where the water is pumped to the HDS treatment plant located on the skyline (continental divide) at left

of picture; the Tweelapie Spruit on the far side of the dam flows from left (south) to right (north) across this 'fish-eye' view (photo W Bason, date 09/12/2009)

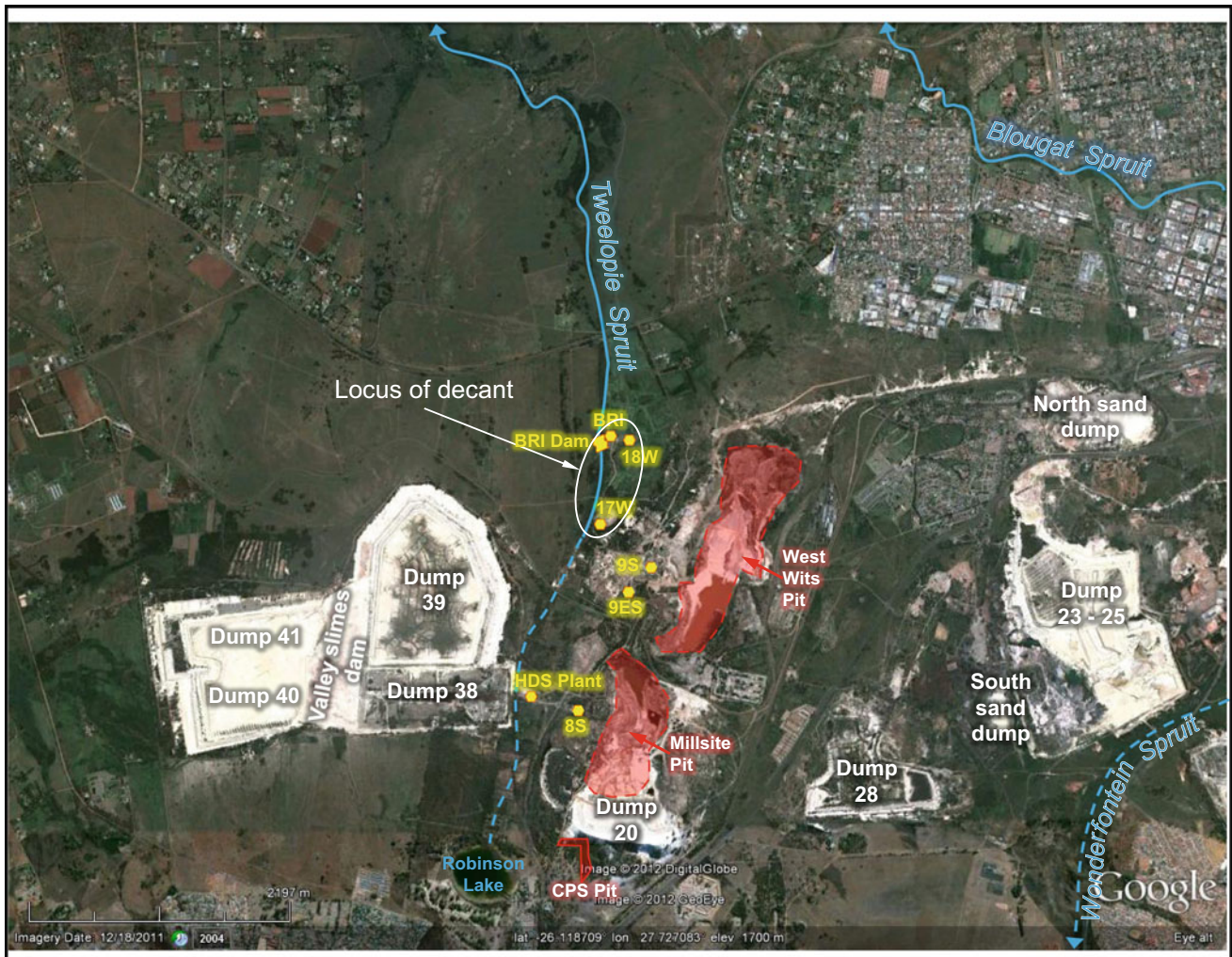


Fig. 5 Google Earth® image showing surface features relevant to the mining environment in the Western Basin

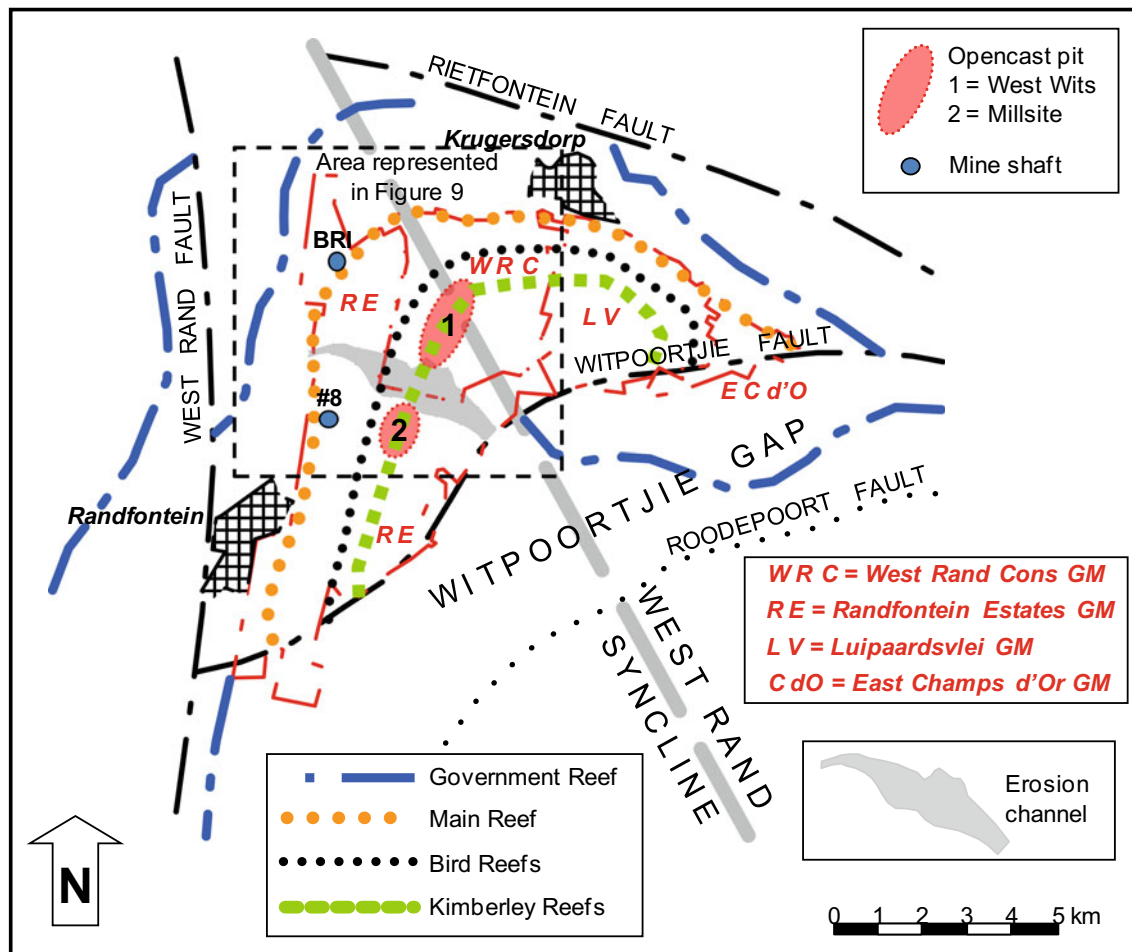


Fig. 6 Diagram of mining-related features (e.g. geology, mine areas, shafts and pits) in the West Rand Goldfield. (Modified from Toens and Griffiths 1964; Tucker and Viljoen 1986)

6 Palaeontology, Archaeology and Ecology

The palaeontology and archaeology of the study area are intimately associated with the karst terrane of the subregion. Fossil sites often represent the erosional remnants of ancient cave systems and their contents (Esterhuysen 2009) and, for this reason, are dynamic features that continue to evolve in response to natural (mainly geomorphological) processes and anthropogenic impacts. Whereas the natural processes such as weathering and erosion occur over extended periods of time (typically millennia), the anthropogenic impacts are often manifested in centuries or even decades. Partridge (1973) derived estimates for when the Sterkfontein and Swartkrans caves became drained of 3.26 and 2.57 Ma, respectively. The difference of ~ 0.7 Ma is surprising given the similar geomorphologic settings of these two cave systems located only ~ 1100 m apart in the same dolomitic subcompartment. The estimated base elevation of Swartkrans Cave (~ 1465 m amsl) places it ~ 25 m above the current

ambient groundwater rest level elevation of ~ 1439 m amsl (Sect. 7.3.2.2 in Chapter “Physical Hydrogeology”). Although this cave system is not accessible (at least as is known at present) to the same depth as that of the Sterkfontein system, it might be expected from the similar surface elevations occupied by both systems (1470–1487 m amsl) and from their shared hydrogeologic environment, that they would have drained contemporaneously.

The most well-known Australopithecine fossils associated with the Sterkfontein Cave site, namely the remains of ‘Little Foot’ (catalogue # StW 573) and of the *Australopithecus africanus* species ‘Mrs Ples’ (catalogue # Sts 5), have been assigned ages of ~ 2.2 and ~ 2.1 Ma, respectively (Pickering 2010; Pickering and Kramers 2010). The age of ‘Little Foot’ (*Au. prometheus*) was more recently set at ≥ 3 Ma (Bruxelles et al. 2014), and most recently at 3.67 Ma (Gardner 2015). The relevance of these ages in regard to landscape development in the region is examined in Sect. 8.12.1 in Chapter “Chemical Hydrogeology”.

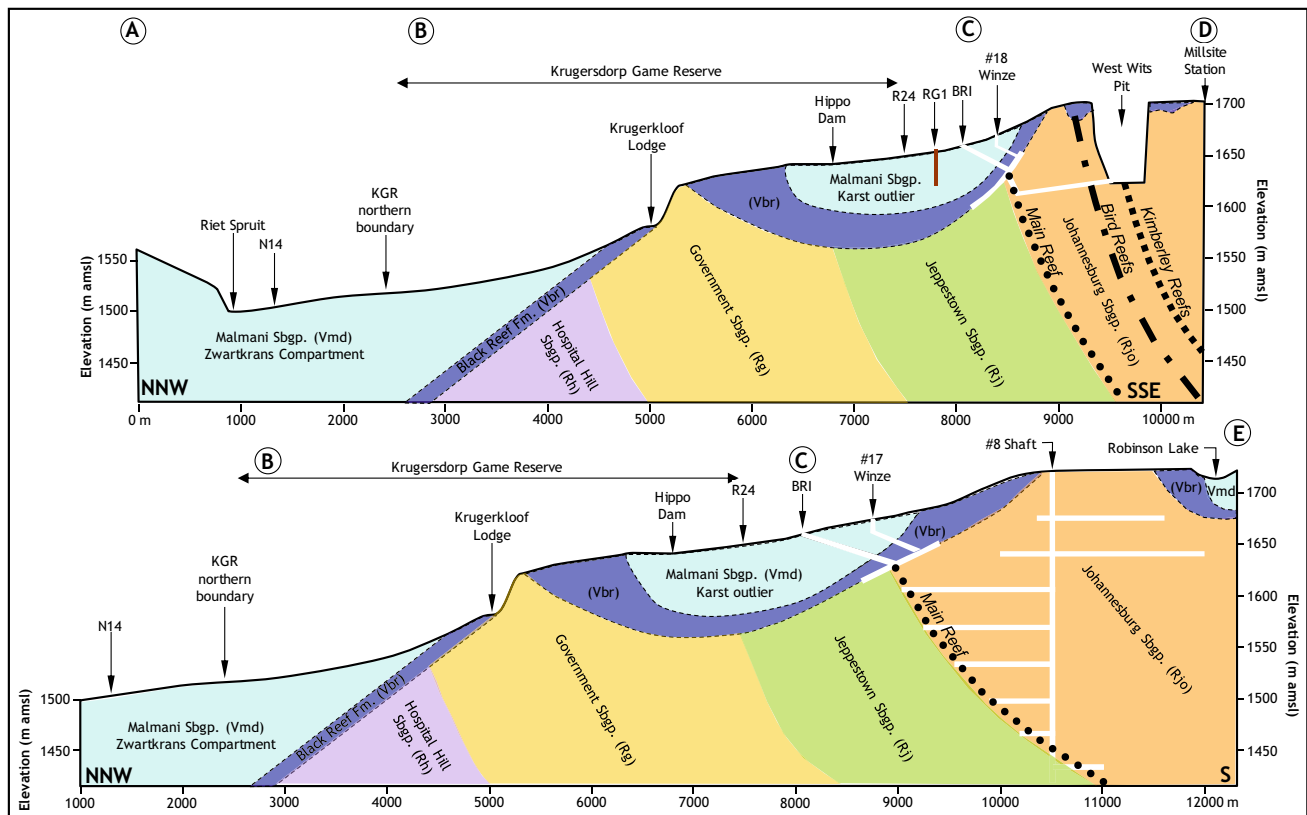


Fig. 7 Schematic profiles of geologic and mining-related features in the northern portion of the West Rand Goldfield (see Fig. 8 for profile transects)

The Sterkfontein Cave site has yielded >500 hominin⁵ fossils (Table 6) since the discovery of ‘Mrs. Ples’ in 1947 (Cooke 1969). Thirteen fossil sites in the COH (Fig. 9) have been declared National Heritage Sites in accordance with the National Heritage Resources Act (Act No 25 of 1999). Many fossil-bearing deposits and sites of palaeontological, archaeological, historical and cultural heritage importance (both categorised and uncategorised) are known to exist in the study area (Esterhuysen 2009). The COH has already yielded ~35% of the total record of human evolution in Africa (McCarthy and Rubidge 2005). The probable existence of yet undiscovered sites on the property that may yield material of palaeontological and archaeological value is substantial. This is exemplified by the unveiling on 08/04/2010 of the *Au. sediba* species fossils (Berger et al. 2010), dated at 1.977 ± 0.002 Ma (Pickering et al. 2011), found at the Malapa site in the north-eastern part of the COH (Dirks et al. 2010). An even more recent example is the unveiling on 09/09/2015 of the *Homo naledi* remains (a new species in the genus *Homo*) from the Dinaledi Chamber of

the Rising Star Cave in the Bolt’s Farm complex (Berger et al. 2015; Dirks et al. 2015) in the south-western portion of the property.

An important ecological aspect associated with the cave systems in the study area is their provision of a habitat for stygobitic fauna (Tasaki 2006). The aquatic cave-dwelling biota, typically blind amphipods, have been found in Sterkfontein Cave and two other caves in the study area (Koelenhof and Yom Tov) that intersect the water table. It is probable, therefore, that investigation of other more remote and less accessible caves in the area that intersect the water table might yield results of ecological significance also in this regard. This might alter the situation where no ‘hotspot’ of subterranean biodiversity is identified on the African continent (Culver and Sket 2000). Although it is beyond the scope of this study to comment on the suitability of the current subsurface habitat(s) that support this fauna, it does provide information (e.g. water chemistry data) that, in the hands of appropriate experts and applied with caution, might better inform this aspect. Some discussion on this topic is provided in Sect. 8.9.3 in Chapter “[Chemical Hydrogeology](#)”. Further ecological significance is afforded by Durand and Peinke (2010) to the many cave features in the subregion that provide a habitat and roost for bat colonies.

⁵ Use of the term hominin (as opposed to hominid) after Berger (2001).

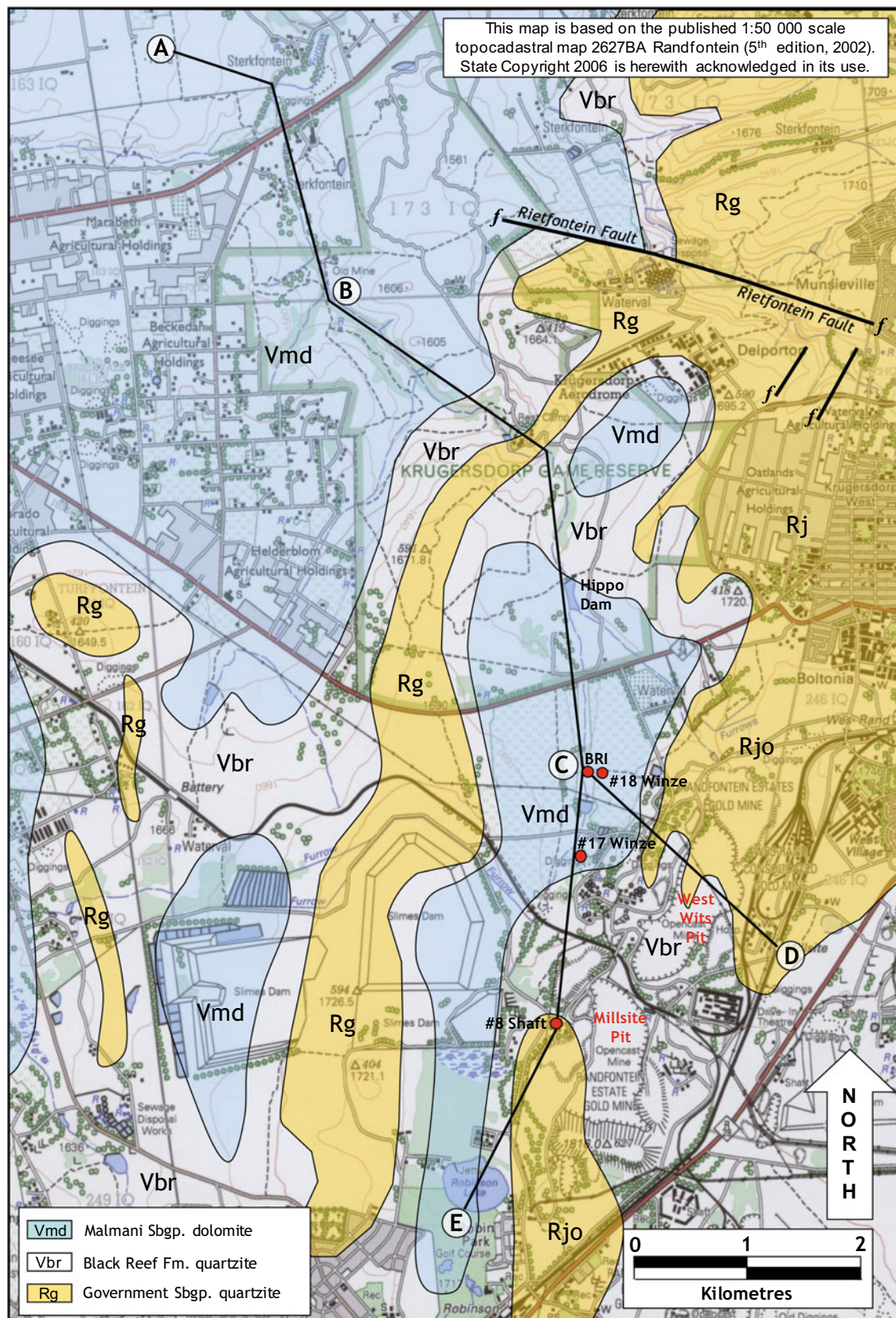


Fig. 8 Geologic map of the north-western portion of the Western Basin showing surface features of mining-related significance and the position of the profile transects illustrated in Fig. 9 (original geology from Mellor 1917)

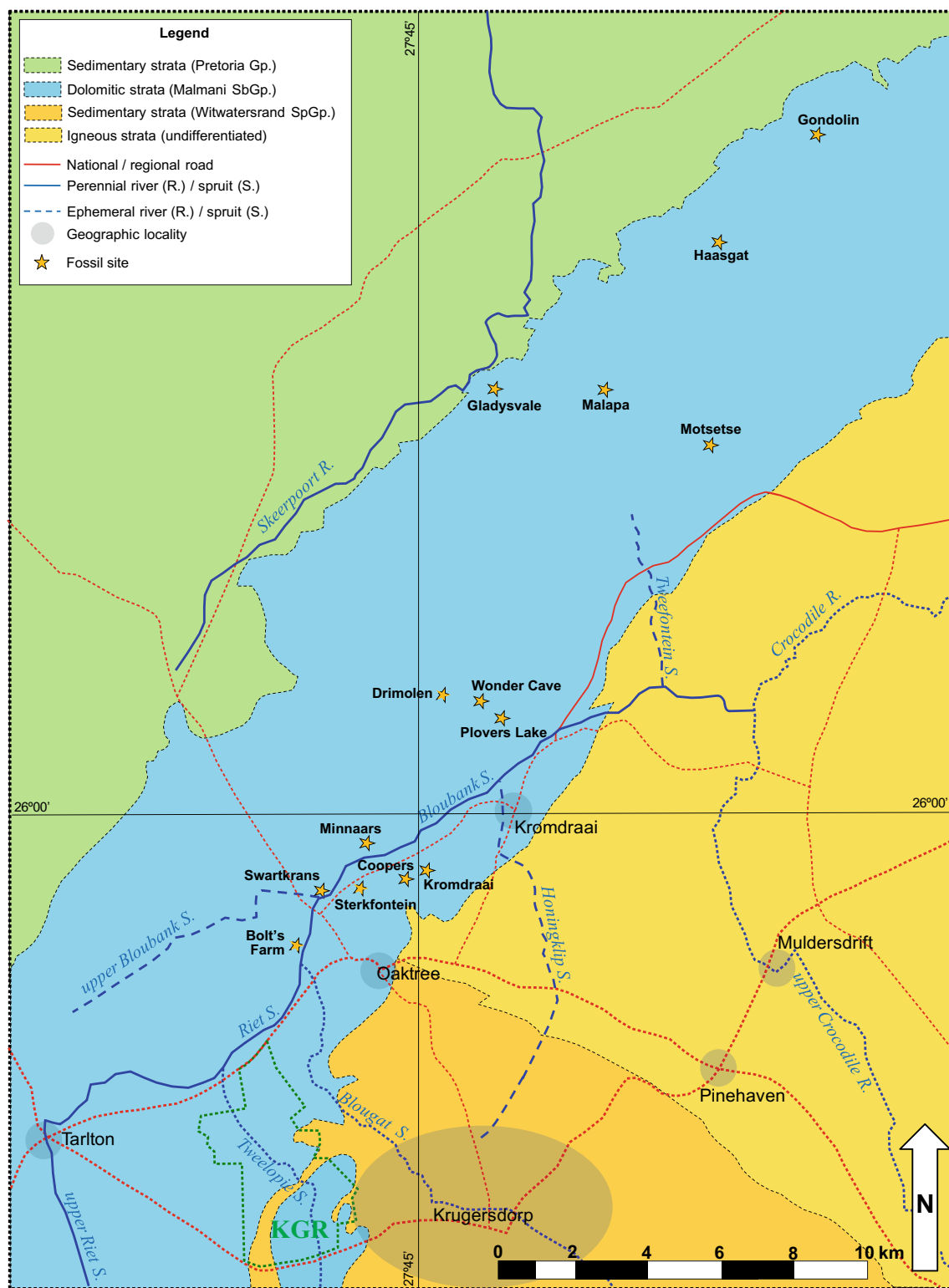


Fig. 9 Locality map of the UNESCO-inscribed fossil sites in the study area superimposed on a simplified geological, surface water drainage and road map

The hydrological and hydrogeological settings associated with the inscribed⁶ fossil sites in the COH are summarised in Table 6. Although some of the tabulated information (e.g. the groundwater compartment and groundwater rest level elevation information) is presented prematurely (i.e. without prior context in terms of this work), it is provided for completeness of this section of text. The observation that the geographic footprint of karst basins (e.g. the Diepkloof Basin, Table 6) spans adjacent (and hydrologically separate) surface drainage systems testifies to the hydraulic continuity that exists between surface water and groundwater systems in the COH karst terrane.

Included in Table 6 is a synoptic description of the cave morphology associated with each of the fossil sites. This description attempts to arbitrarily classify the morphology of a cave system in relation to its setting in the landscape. Simplistically, a near-surface morphology describes a cave system that does not extend more than ~5 m below surface, whereas an underground morphology describes a cave system with a substantial subsurface extension. The ultimate expression of the latter is intersection of the water table, e.g. Sterkfontein Cave. Caves of this nature are classified as water table caves (Ford and Williams 2007), and those that lie above the water table as vadose caves.

The CGS (undated) reports that in all instances in the COH, the important palaeontological finds are located within the upper 10 m of the host cave system. Whilst this may be

generally true, at least in the case of Sterkfontein Cave the ‘Little Foot’ find is located a greater depth (~25 m) below surface (Partridge et al. 2003). Given a (maximum) surface elevation of 1487 m amsl (Sect. 7.1 in Chapter “Physical Hydrogeology”), this places the ‘Little Foot’ site at an elevation of ~1462 m amsl, at least ~22 m above the contemporary maximum attainable cave water level of ~1440 m amsl (Sect. 7.3.2 in Chapter “Physical Hydrogeology”). These descriptions have specific relevance to the vulnerability of each of the fossil sites (and their associated cave systems) where these are examined and discussed in the context of their hydrogeologic setting.

The Malapa excavation understandably suffers from a relative paucity of hydrogeologic information. This site is in the process of being listed with UNESCO as the fourteenth site on the property to be inscribed. Recently published material associated with the hominin remains being excavated at this site (Henry et al. 2012) affords the site ever-increasing importance. These circumstances inform the concern of the MA for the protection of the pre-historic ‘treasures’ of the COH as much as its concern for the current and future ecological sustainability of the property. This dictates the need for support of all components of the environment (including human habitation and settlement) that inform the outstanding universal value (OUV) of the area (P Mills, personal communication).

⁶ Registered with UNESCO for protection in terms of their cultural heritage as part of the COH.



Accumulation of flood debris blocking the entrance to culverts of the N14 bridge over the Blougat Spruit near Oaktree; the hazard for potential flood damage to the national road is self-evident

Overview of Karst

Philip J. Hobbs and Harrison Pienaar

1 General Overview of Global Karst

Dolomite [$\text{CaMg}(\text{CO}_3)_2$] bears the name of the French naturalist/geologist/mineralogist Déodat Gratet de Dolomieu (1750–1801) who first described this rock in 1791 from outcrops in the Dolomite Alps of northern Italy. The Serbian geographer/geomorphologist Jovan Cvijić (1865–1927) studied this rock in the Dinaric Kras region of Slovenia in central Europe, where he established its association with rock dissolution giving rise to the diagnostic landscape characterised by features such as dolines, sinkholes, caves and solutional conduit networks. Since this region represents ‘classical’ karst, in geologic terms the type area globally for such a landscape, the term karst (Germanic translation of *kras*) has become the internationally recognised name for any similar landscape¹ worldwide. Gams (1991), however, suggests that the word *karst* derives from the pre-Indoeuropean word *karra/gara* meaning stone.

The surface extent of carbonate strata across the globe (Fig. 1) is placed at ~13% of the total ice-free land (continental) surface area (Kaufmann 2013).

P. J. Hobbs: Deceased

¹ The term karst is not limited to carbonate formations, since a similar landscape developed in other strata, e.g. the dissolution features formed in the Table Mountain Group sandstone, the quarzitic karst of South America, and the basalt lava fields that form the Pacific Northwest Pseudokarst Aquifer in the north-western United States, is typically referred to as pseudo-karst.

H. Pienaar (✉)
Council for Scientific and Industrial Research, Smart Places,
Pretoria, South Africa
e-mail: hpienaar@csir.co.za

H. Pienaar
Hebei University of Engineering, Handan, China

P. J. Hobbs
Pretoria, South Africa

It is well known that karst aquifers form some of the most productive of all groundwater resources globally. This alone is testimony to their importance and value as a sustainable natural resource and, as this literature review shows, is equally true of a number of South African karst formations (Sect. 2). There is also a growing awareness of the potential role of karst in the global carbon budget as a carbon ‘sink’ (e.g. Gombert 2002; Larson and Mylroie 2013; Martin et al. 2013; Veni 2013; White 2013) for its carbon sequestration properties. Finally, the value of ecosystem services delivered by karst terranes is an often forgotten benefit that similarly is gaining awareness in the literature (e.g. Bonacci et al. 2009; Goldscheider 2012; Kiss et al. 2011; Zhang et al. 2011). The schematic diagram presented in Fig. 2 provides an indication of the diversity of elements that contribute to a karst hydro-ecosystem.

1.1 Age and Distribution

The majority of the considerable number of karst formations on earth (Fig. 1) formed in the Mesozoic Era 250–65 Ma before present (BP). The European carbonate strata that include the classic Dinaric Karst and the Italian Dolomites² belong to this era. The limestone formations of the English Midlands in the United Kingdom formed in the Cretaceous Period (144–65 Ma). The spectacular landscape of the Fengcong (cone) and Fenglin (tower) karsts of the Libo Karst cluster in the South China Karst³ that covers large parts of the Yunnan, Guizhou and Guangxi provinces of southern China (Waltham 2008), date back to the Permian Period (298–250 Ma). The oldest of the numerous karst aquifers of North America are the Ozark Plateau Karst Aquifer in the east-central USA dating back to the Palaeozoic Era (542–251 Ma), and the Cambrian to Mississippian (542–318 Ma) karst of Alberta Province, Canada. It is evident, therefore, that these karst environments are not

² Declared a World Heritage Site in 2009.

³ Declared a World Heritage Site in 2007.

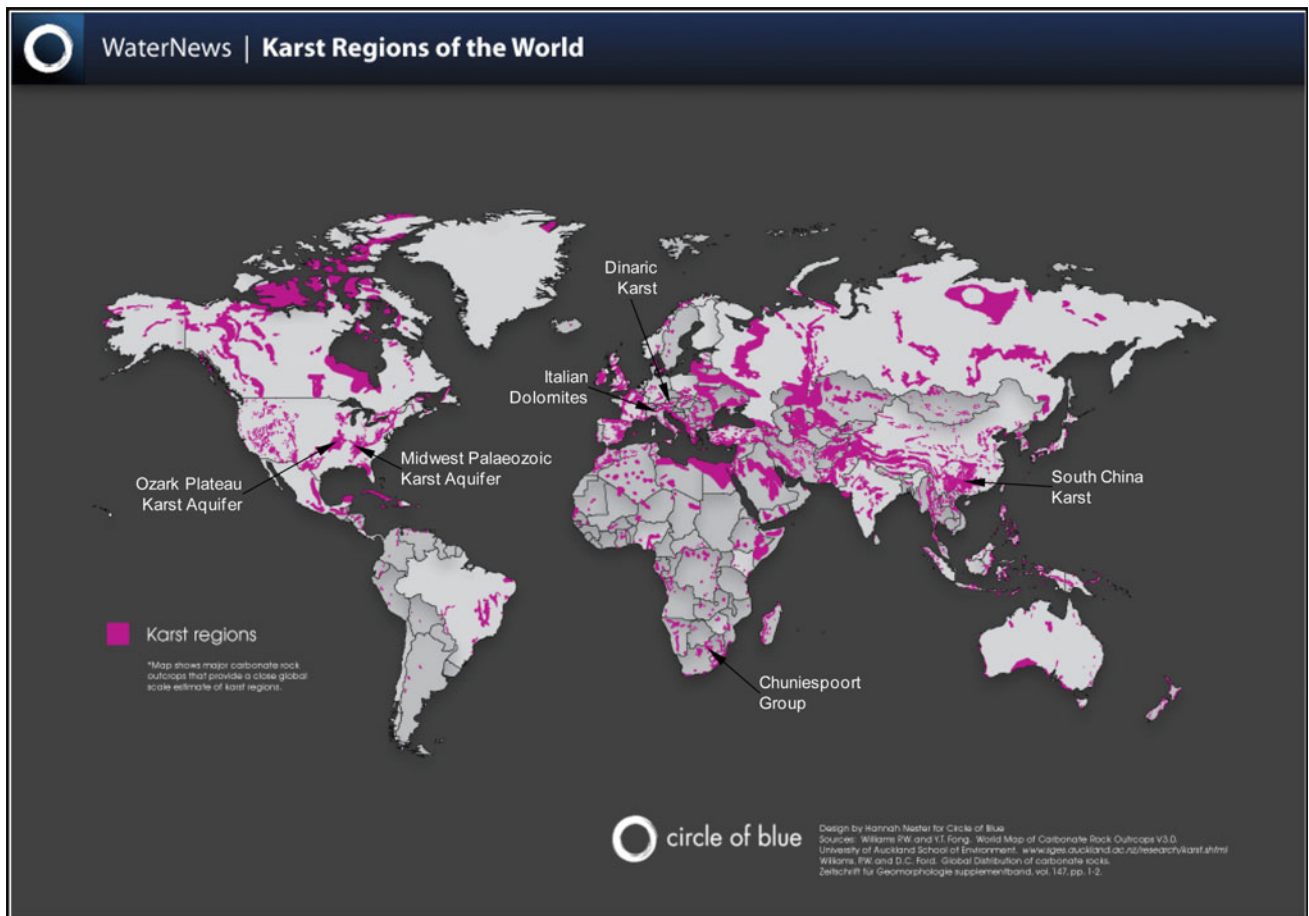
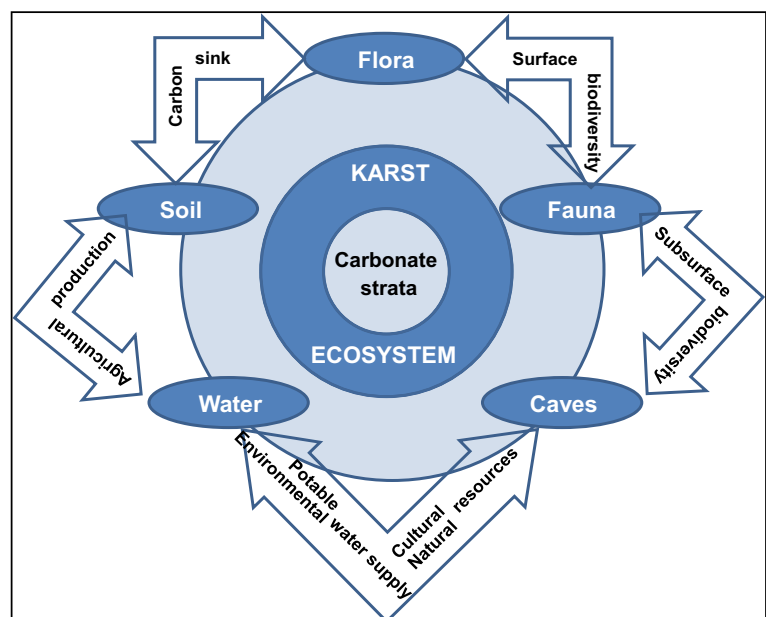


Fig. 1 Distribution of karst regions worldwide, showing karst aquifers referenced in the text (sourced at <http://www.circleofblue.org/waternews/> on 28/04/2012)

Fig. 2 Schematic presentation of the components of an undisturbed karst hydro-ecosystem and its associated values and ecosystem services (modified after Goldscheider 2012)



directly comparable to the local and regional ‘hard’ carbonate formations associated with the considerably older (by a factor of 5–10) Neoarchaeon Vaalian strata (~ 2.55 Ga) of the Chuniespoort Group (Table 5 in Chapter “[Description of the Physical Environment](#)”) that bracket the late Archaean and early Proterozoic. Apparent from Fig. 1 is the relative paucity of carbonate strata in South America, Australia and, indeed, the southern hemisphere. White and White (2009) do, however, describe the Bullita Cave system in the mid-Proterozoic (~ 1.6 Ga) dolomite that forms the Gregory Karst in the Northern Territory, Australia.

1.2 Karst and Acid Mine Drainage

There is comparatively little scientific material in the literature (at least in English publications) regarding karst resources that are impacted or threatened by acid mine drainage. The studies by Sasowsky and White (1993), Webb and Sasowsky (1994) and Sasowsky et al. (1995) describe the interaction between coal mine AMD and the Carboniferous Period karst formations (primarily limestone) of the Midwest Palaeozoic Carbonate Aquifer in the Obey River Basin in north-central Tennessee, USA. These studies reflect a situation where the acidity of mine water infiltrating a limestone aquifer survives a travel distance of ~ 8 km to where it exits the aquifer at a spring. The acid neutralisation results from dolomite dissolution and dissociation of carbonic acid (H_2CO_3) through CO_2 degassing (Sect. 8.12 in Chapter “[Chemical Hydrogeology](#)”).

Observations made in the COH, where mine water has been infiltrating a portion of the karst aquifer since late-2002, have the potential to significantly advance the understanding of the interaction between acidic mine water and a receiving karst hydrosystem. The circumstances that describe this impact are further complicated by the simultaneous contribution of municipal wastewater discharge (albeit of lesser magnitude) into the same karst hydrosystem. This portion of the COH karst environment therefore represents a natural laboratory where the interaction between metal- and metalloid-compromised mine water discharge and bacteriologically and nutrient-compromised municipal wastewater effluent has occurred naturally and ‘by default’ in the subsurface over the last 1½ decades.

2 Overview of South African Karst Water Resources

2.1 Water Supply Aspect

Springs (also known locally as ‘eyes’) are as much a characteristic of karst environments as are dissolution features

such as caves and sinkholes. In a country where the geology dictates that much of the hydrogeologic environment is characterised by generally low-yielding fractured and weathered-and-fractured secondary aquifers, it is no surprise that the high yielding cold springs drain karst aquifers.

Vegter (1995) lists 57 cold springs in South Africa yielding > 1 ML/d (> 11.6 L/s). Most of these drain karst aquifers. Perhaps the best known example is the Kuruman Eye in the Northern Cape Province delivering ~ 18 ML/d (~ 208 L/s) (Martin 2006). The Tshwane Metropole in Gauteng Province obtains $\sim 7\%$ (22.7 Mm^3) of its total bulk input of $305 \text{ Mm}^3/\text{a}$ (Lotter 2012) from dolomitic groundwater resources via springs and boreholes. Irrigated agriculture (excluding so-called ‘improved grassland’) in Gauteng Province alone covers 275 km^2 , of which 95 km^2 ($\sim 35\%$) is located on dolomite. This testifies to the fact that portions of the karst landscape are admirably suited to large-scale irrigated agriculture, with the attendant threats of groundwater over-abstraction (Hobbs 2008a), pesticide/insecticide/herbicide contamination and nutrient-enriched agricultural return flow. An example in this regard is the situation that has developed in the Steenkoppies Basin immediately to the west of the COH, where unbridled expansion of irrigated agriculture based on the abstraction of karst groundwater has impacted adversely on the discharge of Maloney’s Eye (Holland and Cobbing 2008; Holland et al. 2009), the source of the Magalies River.

It is not surprising, therefore, that karst aquifers have been the focus of detailed hydrogeologic studies aimed primarily at determining and utilising their water supply potential. This is exemplified by the groundwater investigations carried out in the 1980s by the then DWAF into the water supply potential of the carbonate strata in the Pretoria-Witwatersrand-Vereeniging (PWV or present-day Gauteng Province) area. These studies were precipitated by the prolonged drought experienced in the region from 1977 to 1986 (Roberts 1988), during which period the main source of water supply for the industrial heartland of the country, the Vaal Dam, emptied to only 7% of its capacity of $\sim 2610 \text{ Mm}^3$. The karst aquifers were identified as an emergency source of potable water (Vegter 1988), and their potential exploitation for this purpose explored and evaluated on a large-scale commencing in 1983. These studies are documented in reports by, amongst others, Kok et al. (1985), Bredenkamp et al. (1986), Kafri et al. (1986), Leskiewicz (1986), Reynders (1988), Hobbs (1988a) and Kuhn (1989). At the time, Roberts (1988) put the cost of these studies to the State at R18 million.

In the period late-1983 to mid-1987, some 400 large diameter (≥ 165 mm up to 381 mm) boreholes were sunk in the carbonate strata of the PWV area (Hobbs 1988b; Mulder 1988). Despite the successful establishment of numerous extremely high-yielding boreholes (many capable of

yielding >25 L/s, and some even >100 L/s) in the course of these studies (Hobbs 1988b), and with the exception of the Tshwane Metro use mentioned earlier, exploitation was limited to land owners who later capitalised on these facilities for irrigated agricultural use and, in at least one instance near Olifantsfontein south of Pretoria, for municipal water supply purposes. Nevertheless, the legacy of these studies is two-fold, namely:

- The unprecedented deepening of the knowledge and understanding of the hydrophysical and hydrochemical characteristics of these groundwater resources; and
- The incorporation of many of the boreholes (297 in Gauteng Province alone, Table 1) in a network of groundwater monitoring stations that continues to generate invaluable hydrogeologic data some three decades later.

Prior to the above-mentioned studies, the dolomitic aquifers of the Far West Rand first attracted attention in a geotechnical and engineering geologic context (Sect. 2.2). These aquifers later drew the attention of Fleisher (1981) in a study of their hydrogeologic characteristics against the backdrop of their substantial dewatering by the deep gold mines in the Carletonville Goldfield (aka the Far Western Basin) (Sect. 2.2).

Further to the west, the karst aquifer of the Campbell Rand Subgroup on the Ghaap Plateau in north-central South Africa (Fig. 1 in Chapter “Introduction and Background”) was mapped and described by Beukes (1978; 1987). Dewatering of this aquifer at Sishen Iron Ore Mine at ~36 ML/d on average (WS&E 2012) has resulted in water level drawdowns of >100 m in order to establish safe

opencast mining conditions at the mid-2012 depth of 260 m below surface (bs), but raising concerns for the impact on small-scale groundwater users and the environment (van Dyk et al. 2007; WS&E 2012). In general, however, this groundwater resource has not received the same measure of attention as that of its eastern equivalent, the Malmani Subgroup.

The considerably younger (16–5 Ma) karst formations occurring mostly along the South African coastline (Fig. 3), comprise mainly limestone and calcarenites (calcareous sandstone). These formations make up the remaining 2% of carbonate strata. Many coastal towns and villages augment their surface water supplies with groundwater drawn from these strata, yet documentation of these instances remains fragmented and poorly quantified.

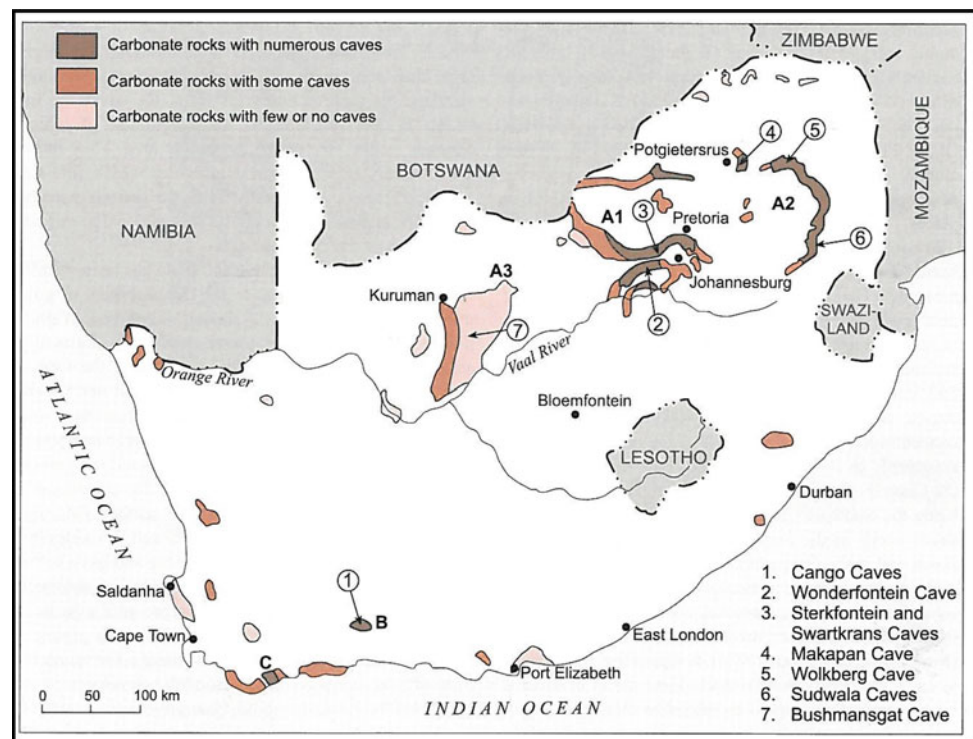
2.2 Geotechnical and Vulnerability Aspects

Studies of the geotechnical characteristics of the karst aquifers of the Far West Rand (Carletonville Goldfield) were precipitated by the severe and sometimes catastrophic sink-hole formation triggered by mine dewatering activities (Brink 1996). Most notable in this regard was the West Driefontein Mine sinkhole disaster of 12/12/1962. Drawdown in the Oberholzer Basin exceeded 300 m in the mid-1960s (Foosse 1967) in the endeavour of West Driefontein Mine to ‘make safe’ its mine workings. Prior to this, the Venterspost Basin had been dewatered by the early-1960s when pumping rates peaked at ~ 57 ML/d (Brink 1996), and for which Swart et al. (2003) report a drawdown of 118 m in early-1974. Similar impacts were manifested in the Bank Basin in the early-1970s following

Table 1 Geographic distribution of karst water level monitoring stations operated nationally by DWS (from Bertram 2008)

| Province | Geographic area | # of stations | | Karst hydrosystem |
|---------------|-----------------|---------------|-----|------------------------|
| Gauteng | Centurion | 13 | 297 | Malmani Subgroup |
| | East Rand | 84 | | |
| | Kempton Park | 13 | | |
| | Natal Spruit | 67 | | |
| | Pretoria | 5 | | |
| | Rietvlei | 20 | | |
| | Tarlton | 37 | | |
| | West Rand | 58 | | |
| North West | Bo-Molopo | 122 | 191 | |
| | Dinokana | 16 | | |
| | Lichtenburg | 5 | | |
| | Polfontein | 11 | | |
| | Ventersdorp | 37 | | |
| Northern Cape | Danielskuil | 14 | 14 | Campbell Rand Subgroup |
| Total | | 502 | | |

Fig. 3 Distribution of carbonate strata in South Africa, showing the main areas of karst development as A (Transvaal Supergroup dolomite), B (Cango Caves Group limestone) and C (Bredasdorp Group limestone) (from Martini 2006)



dewatering at rates of up to 340 ML/d (Brink 1996). These studies helped build a sound understanding of the hydrogeotechnical and hydrogeologic characteristics of the karst formations that overlie the Ventersdorp Supergroup and gold-bearing Witwatersrand Supergroup strata. The voluminous data and writings generated in the course of these activities, and secured for posterity in the collection of Prof. EJ (Leslie) Stoch (deceased), has facilitated studies such as those by Schrader et al. (2014).

The vulnerability of karst aquifers to contamination is described extensively in the literature, and has resulted in the development of numerous mapping methods⁴ to quantify their susceptibility to pollution, e.g. DRASTIC⁵ (Aller et al. 1985), EPIK (Doerflinger et al. 1999), COP (Vías et al. 2003), PI (Goldscheider 2003), VULK (Cornaton et al. 2003), Localised European Approach (Dunne 2003), Time-Input Method (Kralik and Keimel 2003) and VUKA (Leyland et al. 2008). The VUKA method was developed for South African karst environments, and its application demonstrated in the COH (Leyland et al. 2008; Witthüser et al. 2010) and the Blyde River Canyon dolomite in Mpumalanga Province (Witthüser et al. 2010). An improvement on the VUKA method that incorporates a risk assessment as applied to the COH, is presented by Leyland (2010).

⁴ Many as part of the COST Action 620 project (Zwahlen, 2003).

⁵ Developed for groundwater resources in general, and not karst aquifers in particular.

3 Speleogenesis of Karst Aquifers

Following the earlier work by Choquette and Pray (1970), it has been recognised in the international karst literature that the development of karst systems progresses from syngenetic (eogenetic) forms through hypogenic (mesogenetic) forms to hypergenic (epigenetic) forms (Ford 2006; Ford and Williams 2007; Gunn 2004; Klimchouk et al. 2000; Klimchouk and Ford 2009; Palmer 2007; Dublyansky 2014; Klimchouk 2014). This 'evolution' is described by Klimchouk and Ford (2009) as follows.

- Eogenetic forms associated with coastal and oceanic sediments (primarily limestone) occurring in young rocks (Cenozoic Era) with high matrix porosity and permeability where caves form in the zone of mixing of marine and meteoric water.
- Hypogenic forms mainly associated with confined systems formed by burial of the eogenetic forms normally for very long periods of time, and where aggressive water enters the soluble formation from below driven by either solute or thermal density differences, creating cross-formational hydraulic continuity between laterally transmissive beds in heterogeneous soluble strata across cave-forming zones.
- Hypergenic forms associated with unconfined systems formed by geologic processes such as tectonic uplift and erosion (giving rise to so-called telogenetic karst) that

result in the gradual exhumation of hypogenic karst forms, and characterised by gravity-driven flow systems wherein downward meteoric water (rainwater) recharge drives a process such as carbonic acid dissolution further.

The listed sequence of karst development is readily recognised as correlating to the normal geologic, diagenetic and hydrogeologic sequence that describes the evolution of geologic strata (Klimchouk and Ford 2009). Equally recognisable is the potential for a later form of speleogenesis to inherit some measure of dissolutional structure and geometry from a preceding form. Ford and Williams (2007) recognise that the development of flow paths in karst aquifers depends on the availability and distribution of energy derived from the following:

- Throughput of water;
- Hydraulic gradient between recharge and discharge areas;
- Spatial distribution and nature of recharge; and
- Aggressiveness of the recharge water(s).

Bakalowicz (2006) draws attention to the different schools of thought represented by European and North American karst scientists (karstologists), respectively. Whereas the European view emphasised tectonic features, fractures and faults as the principal agents in karst development, the North American view assigned greater significance to bedding planes. These differing views are rooted in the different geological environments that characterise the carbonate strata of the respective continents. Compared to the relatively undisturbed nature of the North American strata, that of south-central and south-eastern Europe reflects severe deformation as a result of tectonic uplift. Perhaps the Neoproterozoic karst strata of the South African interior represent a combination of the European and North American views on speleogenesis, varying from a bias toward the North American view in the plateau-type karst morphology, and toward the European view in the escarpment-type karst morphology (Sect. 3.4 in Chapter “[Description of the Physical Environment](#)”).

3.1 Speleogenesis of South African Karst

3.1.1 Overview

An extensive review of international efforts has not revealed the assignment of South African karst systems to the above-mentioned forms of speleogenesis (karst development). Local opinion has followed the historical international trend of accepting the concepts and theories developed for unconfined karst systems (Klimchouk 2011), namely epigenetic/hypogenic forms of speleogenesis, as characterising

karst hydrologic and associated geomorphologic processes locally. The efficacy of these processes in the COH is discussed in Sect. 8.12.1 in Chapter “[Chemical Hydrogeology](#)”. Klimchouk (2011) suggests, however, that Martini and Kavalieris (1976) and Martini et al. (2003) recognise a hypogenic form of speleogenesis in the so-called ‘Transvaal Basin’. The following discussion explores the admittedly sparse evidence that provides hypothetical exploration of this question in a South African context. Although South African karst systems are addressed in broad terms, specific attention is afforded the COH.

Martini and Kavalieris (1976) recognise four periods of karstification in the ~2.5 Ga history of the Chuniespoort Group dolomite. These are the following:

- Pre-Pretoria Group period (>2.2 Ga), defined by the Rooihooft Formation representing a palaeokarst residual breccia at the base of the Pretoria Group, and therefore developed on the weathered surface of the Chuniespoort Group carbonates;
- Pre-Waterberg Group period (>1.9 Ga), defined by dissolution cavities located at the unconformity with the overlying 1.9–1.5 Ga Waterberg Group;
- Pre-Karoo Supergroup period (>320 Ma), defined by palaeosinkholes filled with chert breccia, kaolinitic clay, carbonaceous sediments (including coal horizons) and, most tellingly, diamictite associated with the ~300 Ma Dwyka Group filling solution cavities in Transvaal Supergroup dolomite near Vereeniging in southern Gauteng Province (McCarthy and Rubidge 2005); and
- Tertiary to Recent Period (<65 Ma), defined by the present karst terrain formed after the removal of sufficient of the overlying Karoo Supergroup strata (following late Mesozoic uplift) allowed epigenetic speleogenesis to sculpt the landscape, the geometry of preferential dissolution being informed (at least in part) by the overprint of regional WNW–ESE striking structural lineaments in the COH that cut through the NW dipping stratigraphic sequence of carbonate strata (Sect. 3.4 in Chapter “[Description of the Physical Environment](#)” and Dirks and Berger 2013).

3.1.2 Discussion

The distribution of carbonate (limestone and dolomite) strata in South Africa is shown in Fig. 3. This provides a basis for interrogating the speleogenesis of local karst systems in light of the forms described earlier in this section.

The ‘young’ Cenozoic shallow marine De Hoopvlei Formation (Bredasdorp Group) limestone deposits of middle- to late-Miocene age (16–5 Ma) along the southern Cape coast described by Malan (1990) readily represent a syngenetic/eogenetic system. Whereas caves that developed

in the purer more indurated limestone are preserved, the softer more sandy limestone developed on marine platforms host only large depressions and shallow dolines (Martini 2006). Although currently of a terrestrial (land-based or continental) nature, their coastal setting accommodates a syngenetic form of speleogenesis associated with a coastline that in the last 120,000 years witnessed an ice-age related fall in sea level of ~ 130 m, recovering to its present position only in the last 10,000 years (McCarthy and Rubidge 2005; Roberts et al. 2006). Syngenetic/eogenetic speleogenesis in coastal settings, although created by unconfined circulation (i.e. epigenic karst speleogenesis), results in distinct porosity patterns because of the specific conditions associated with the mixing of different water chemistries at the halocline producing dissolution of porous, poorly indurated carbonates. It is for this reason that it is commonly distinguished as a separate category (Klimchouk 2011).

The much older ‘hard’ sedimentary carbonate deposits of Vaalian age (~ 2.5 Ga) in north-central and north-eastern South Africa undoubtedly host comparatively recent epigenic karst forms. Bearing in mind that the mapped distribution of carbonate strata represents their respective outcrop footprints, it is plausible that the much more extensive buried portions of these deposits might selectively host (even currently) the ‘intermediate’ hypogenic form of speleogenesis. There is therefore little reason to question the likelihood that the currently exposed and readily classified epigenic karst systems might earlier have represented a hypogenic form. The ramiform and spongework geometry that is a characteristic of hypogenic karst (Ford 2003; Klimchouk 2011) is evident in Sterkfontein Cave (Fig. 4), although Palmer (2011) has pointed out that maze caves may also result from hypergenic speleogenesis.

The hypogene mechanism of speleogenesis invokes the existence of a confined system within which the upward migration of ‘aggressive’ solutions results in selective dissolution of the carbonate strata and the formation of a significant secondary porosity. Klimchouk (2011) recognises thermal H_2S solutions as a prime candidate for dissolution agent, which requires that sufficient sources of dissolved sulphate exist for reduction to H_2S and, further, that the H_2S can escape from its reducing environment. When rising H_2S -rich waters mix with infiltrated oxygenated CO_2 -rich meteoric groundwaters at shallower depths, sulphuric acid dissolution manifests as a strong speleogenetic agent (Klimchouk 2011; Kirkland 2014).

The presence of palaeokarst features infilled with Karoo Supergroup sediments in the present karst landscape (and which defines the pre-Karoo period of karstification recognised by Martini and Kavalieris 1976) indicates the confining role played by the late-Palaeozoic Permian (298–250 Ma) and Mesozoic (250–65 Ma) strata prior to its removal by peneplanation following tectonic uplift,

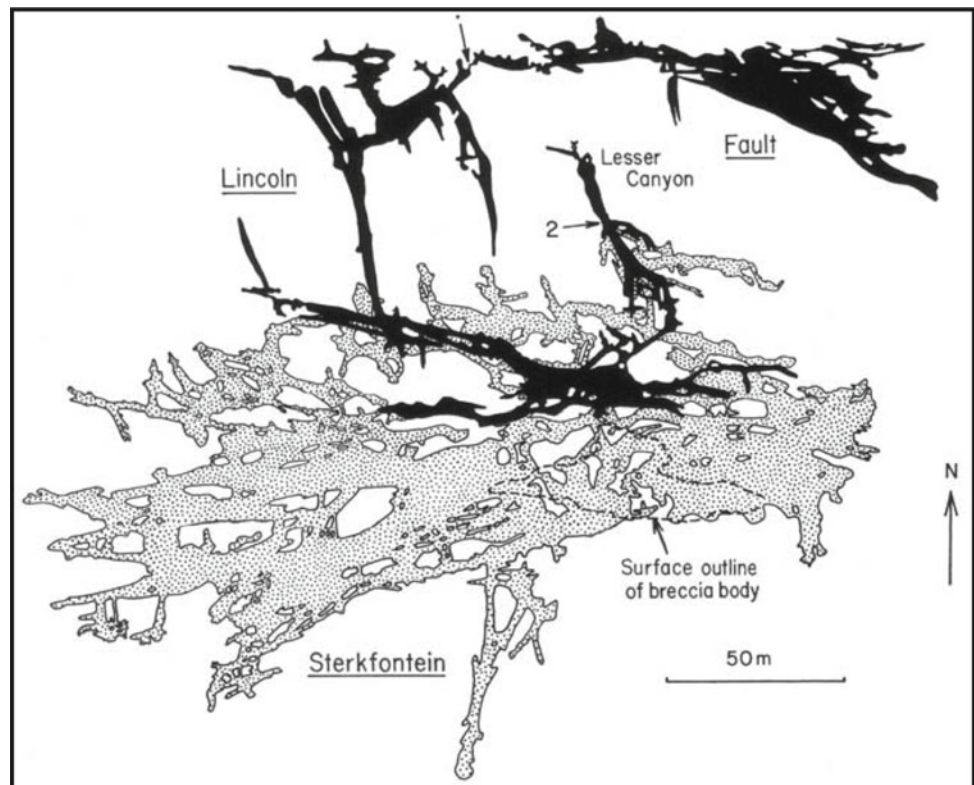
culminating by late-Mesozoic (Cretaceous) to early-Cenozoic (Tertiary) times (~ 65 Ma) in the African surface after the removal of >1200 m of material (Partridge and Maud 1987). Erosion in the post-African cycles subsequently exposed the pre-Karoo surface to the extent that it forms an important component of the present landscape in the southern and south-western portions of the Gauteng and North-West provinces. Dirks and Berger (2013) report a revised⁶ erosion rate of 5–6 m/Ma for the plateau representing the African Erosion Surface south of the Malapa fossil site, and a \sim tenfold greater rate of ~ 55 m/Ma in the Skeerpoort River valley to the WNW of this site. The discussion presented in Sect. 8.12.1 in Chapter “[Chemical Hydrogeology](#)” suggests that solutional denudation in the COH averages 9.5 m/Ma in the range 5–14 m/Ma (see also Hobbs and Smith 2018). Klimchouk (2011) suggests that the hypogene speleogenesis of the Sterkfontein Cave system might have commenced in the early Miocene (18 Ma BP), but does not offer a potential source of ‘aggressive’ solutions that might serve as speleogenetic agent. The following discussion explores the possibility that hypogene speleogenesis of the Malmani Subgroup dolomite might date much further back to the early palaeo-Proterozoic (~ 2 Ga BP). It also offers potential sources of aggressive solutions from older Randian and Vaalian formations.

The carbonate strata of the Chuniespoort Group in the north-central and north-eastern parts of the country were formed in a marine environment developed on the stable Kaapvaal Craton (Eriksson and Reczko 1995) already carrying the 2.97–2.78 Ga Witwatersrand Supergroup and 2.78–2.65 Ga Ventersdorp Supergroup strata. By 2.7 Ga, these strata had been subjected to regional faulting and fracturing associated with the emplacement of the basaltic lavas of the Klipriviersberg Group (McCarthy and Rubidge 2005). Subsequent to the complete development of the Transvaal Supergroup by ~ 2.05 Ga, further structural disturbance of the accumulated Randian and Vaalian strata on the Kaapvaal Craton came in the form of:

- The Bushveld Igneous Complex (BIC) intrusion at ~ 2.05 Ga (Cawthorn et al. 2006) coeval with;
- Deformation resulting from a north-east verging compressive event which reactivated basement structures that were propagated through the Black Reef–Malmani–Rooihooft succession (McCarthy et al. 1986; Obbes 2001); and
- The Vredefort meteorite impact event at ~ 2.02 Ga (Reimold 2006).

⁶ Dirks et al. (2010) report an erosion rate of 3 to 5 m/Ma for the same landscape (see Sect. 8.12.1 in Chapter “[Chemical Hydrogeology](#)”).

Fig. 4 Map of the Sterkfontein Cave system showing the labyrinthine joint-controlled pattern of both the Sterkfontein and Lincoln cave sections (from Martini et al. 2003)



The geological setting of the Witwatersrand Basin as repository for ‘the greatest of the world’s gold fields’ (John Hays Hammond as quoted in Pretorius 1986) has been intensively studied and hence well defined (see Robb and Robb 1998a and McCarthy 2006 and references therein). Duane et al. (1997) discuss the geochemistry of some deep gold mine waters (12 samples collected at a depth of 1050–3400 m bs in four mines⁷) from the Witwatersrand Basin, reporting the occasional encounter at depth of hot water (up to 40 °C). Zhao et al. (1994) note the enrichment of the Ventersdorp Contact Reef (VCR) with base metal sulphides such as pyrite (FeS₂), pyrrhotite [Fe_(1-x)S (x = 0 to 0.2), e.g. FeS = troilite], galena (PbS), sphalerite (ZnS) and chalcopyrite (CuFeS₂). In a study of lead (Pb) isotopes associated with chalcopyrite and pyrrhotite in the VCR, Zartman and Frimmel (1999) note temperatures of up to 300 °C corresponding to the peak regional metamorphic temperature associated with burial of the VCR beneath 6500 m of Ventersdorp and Transvaal Supergroup strata.

The VCR separates the Witwatersrand clastic sediments from the overlying Ventersdorp volcanics (lavas). The carbonate formations of the Malmani Subgroup, sandwiched between the underlying Witwatersrand and Ventersdorp strata and the overlying Pretoria Group sediments (Table 5), could therefore not have escaped the intrusion of hot

H₂S-rich connate groundwater rising from the still comparatively young buried bedrock strata. The invariable presence of carbon-rich material in the form of kerogen (bitumen) in association with the gold-bearing conglomerates (McCarthy and Rubidge 2005) is of further interest. Representing a form of hydrocarbon typically associated with CO₂-rich waters, this provides another source of thermal acidic fluid conducive to hypogene speleogenesis. Migration pathways for the hydrothermal brine might have taken the form of fractures, fissures and faults created by the afore-mentioned BIC intrusive and Vredefort impact events. Such circumstances clearly favour hypogenic speleogenesis of the carbonate formations by any of the mechanisms described in Text Box 1 (p. 45) long before their exhumation in the more recent geologic past. The mechanism of artesian transverse speleogenesis as identified by Klimchouk (2006) is therefore readily invoked in regard to a confined Malmani Subgroup karst hydrosystem both in the geologic past and, under specific conditions such as might be associated with the deeply buried dolomitic strata of the Chuniespoort Group basin, perhaps even at present. In this regard it is worth noting that numerous thermal springs in the southern Waterberg area of Limpopo Province, e.g. Warmbaths Spring at Bela-Bela (52 °C), and Die Oog (39 °C) and Rhemardo Spring (42 °C) at Mookophong (Olivier et al. 2008). These springs occur in the central part of the Bushveld Complex where sandstone of the Swaershoek

⁷ Western Deep Levels, Vaal Reefs, Freddie's and President Steyn.

Formation at the base of the Waterberg Group rests unconformably on felsites of the Rooiberg Group, and locally also on granites of the Lebowa Granite Suite (Bushveld Complex). Updomed fragments of Bushveld Complex floor rocks (dolomite) also occur in this area (Visser 1989) where structural disturbance is evidenced by regional faults and diabase dyke intrusions with which the springs are variously associated (Olivier et al. 2008).

Attention is also drawn to the recognition by Wilkinson (1973) of ‘dome cavities’ developed in breccia capped by a resistant travertine carapace (Fig. 5) in Sterkfontein Cave. Wilkinson (1973) attributes these features to current-induced erosion by water flowing through the cave system, the protrusion of fragile bones from the breccia surface suggesting gentle flow conditions. Palmer (2003) reports the enlargement of ceiling solution pockets by turbulent eddies (Slabe 1995 in Palmer 2003) or by elevated CO₂ partial pressure resulting from the compression of air by rising water (Lismonde 2000 in Palmer 2003). Such agents would occur in epiphreatic conditions during flooding of the cave system. Nevertheless, the Sterkfontein ‘dome cavities’ are reminiscent of the ceiling cupolas recognised by Klimchouk (2011) as a component in a suite of morphologic features created by transverse rising flow (aka ‘morphologic suite of rising flow’ or MSRF) associated with hypogene speleogenesis. The age (<3 Ma) of the breccia, however, is too young for the ‘dome cavities’ to represent ceiling cupolas formed by upward flow in a confined karst aquifer. Certainly closer inspection of the Sterkfontein Cave and other cave systems in the area for features such as described above is warranted.

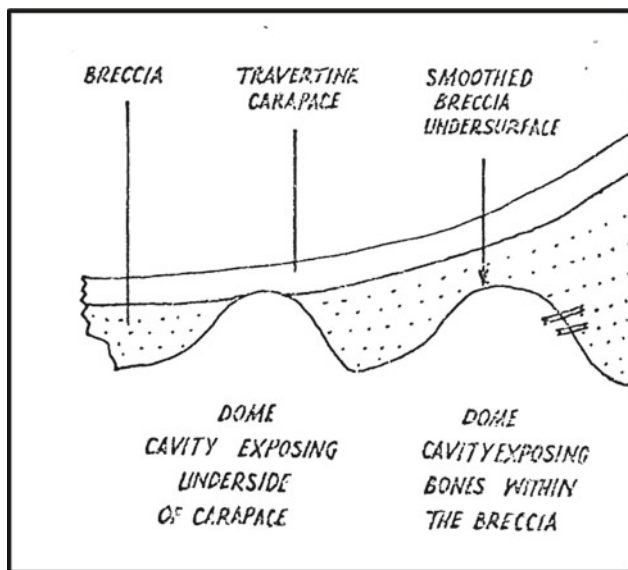


Fig. 5 Sketch of ‘dome cavities’ in the Mound breccia of the Milner deposit beneath a protecting travertine layer in Sterkfontein Cave (from Wilkinson 1976)

3.2 The Epikarst

3.2.1 General Discussion

Epikarst is recognised as an integral component of the karst landscape by Williams (1983), who referred to this zone as the subcutaneous layer or ‘skin’ that overlies karst formations at the surface. Its significance derives from specific functions together serving as a regulatory subsystem at the top of the unsaturated zone within which autogenic recharge is stored, segregated into several components and spatially distributed to preferential ingress paths developed in the underlying vadose zone. In classical terms, stress release and weathering are the principal agents of formation of the incipient epikarst zone, and dissolution plays only a minor role. The processes of stress release and weathering (both mechanical and chemical) are common to virtually all rock types (including insoluble) exposed at surface. The regolith (weathered mantle) is formed as a consequence of the extension and opening of existing joints and formation of new joints, the accentuation and opening of bedding planes and micro-fissures, and the enhancement of fissure frequency and connectivity of fissure networks. Chemical weathering penetrates deeper into the bedrock, the resulting mineralogical alteration of the parent strata producing fines that may ‘choke’ the regolith and decrease its permeability. Controlling factors in this regard are the composition and structure of host rocks, climate, rate of unloading informed by the competition between uplift and denudation rates, and topography (Klimchouk 2004).

Klimchouk (2004) distinguishes between ‘classical’ weathering as described above, and karstification represented by the dissolutational removal of material accumulated in the regolith developed over carbonate bedrock. A key element in karstification is the development of greater porosity and an increasingly organised permeability focused on vertical drains in the underlying vadose zone. The evolution of these properties progresses from an incipient epikarst on a freshly exposed carbonate surface, through a young epikarst to a mature soil-covered epikarst, and culminating in a barren old relict epikarst surface.

3.2.2 Epikarst of the COH

The epikarst of the COH represents primarily a soil-covered mature epikarst landscape characterised by dolines representing dispersed but evolving karstification favouring the concentration of autogenic recharge. This is illustrated in Plate 1, from which it is evident that denudation of the carbonate surface is an active process in the current landscape. The presence of soil enhances solutional enlargement of fissures in the epikarst by providing a ready source of CO₂. The landscape of the COH also hosts at least 412 sinkholes and dolines that have been classified as ‘swallow’

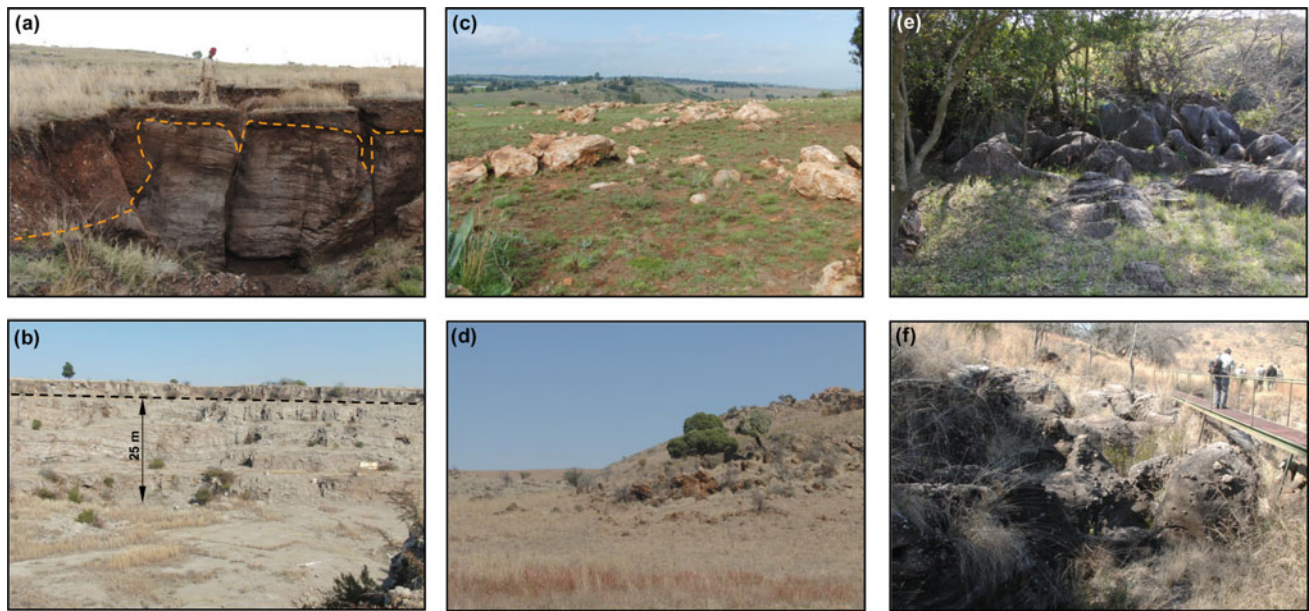


Plate 1 Examples of the epikarst in the COH showing **a** dolomite pillars intersected by cutters (dissolution ‘slots’) filled with soil and covered by a variable thickness of soil cover, **b** ~ 4-m thick epikarst horizon overlying the gently folded strata forming the vadose zone exposed in the southern sidewall of Sterkfontein Quarry, with detail of

the exposed features illustrated in (Plate 2), **c** chert-rich dolomite outcrop in the form of a quasi-karren field, **d** chert-rich bedded and dipping dolomite outcrop, **e** dolomite outcrop with soil cover and infill at the Zwartkrans fossil site, and **f** exposed epikarst at the Gladysvale fossil site (all photos P Hobbs; date shown in upper right corner)

features after field verification of 734 suspected such features (R Leyland, personal communication). The question arises whether these features are also associated with epikarst evolution and therefore form part of the epikarst, or not. Klimchouk (2004) suggests that features such as point recharge dolines and collapse sinkholes are unrelated to epikarst morphogenesis, and simply represent holes in the epikarst. The author is of the opinion that these features are an intrinsic component of epikarst evolution.

As recognised by Klimchouk (2004), the epikarst and vadose zone fulfills crucial hydrologic functions and roles also in the regional karst system in the COH. Principal of these is the retardation of throughflow and mixing of recharge in its often lengthy and tortuous pathway to the aquifer. These circumstances account for the relatively constant flows—Martini (2006) refers to ‘very regular discharges at resurgences’—that characterise springs draining the Neo-Proterozoic carbonate strata of the South African interior, compared to the ‘flashy’ nature of springs that drain the telogenetic and much younger European karst formations (Florea and Vacher 2006). It is posited that the local karst terrane, despite the absolute age of its carbonate strata, is in transition from a juvenile to a mature stage of evolution. The epikarst of the COH deserves considerably more study than it has received in the past. Unravelling the typology of this epikarst will contribute to the global understanding of karst morphogenesis and the transport of carbon through the vadose zone (Jones 2013).

Text Box 1 Hypogenic speleogenesis

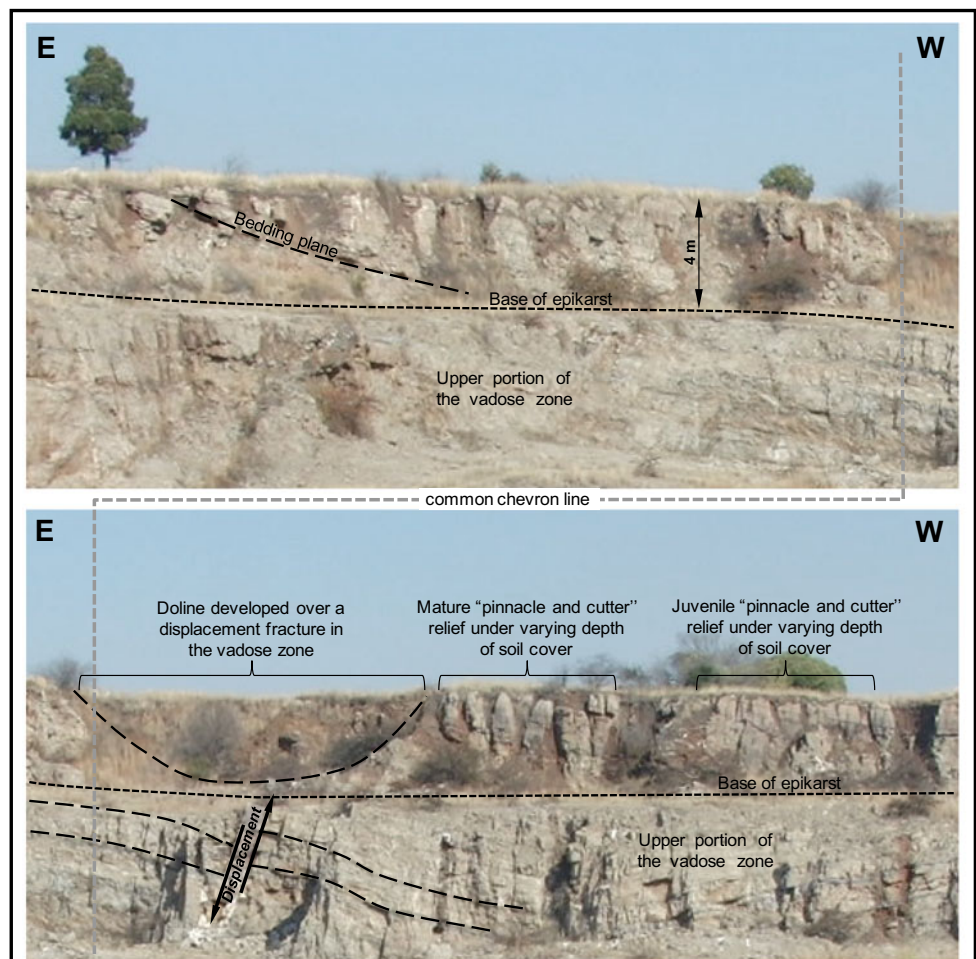
Carbonic acid dissolution, which dominates overwhelmingly in epigenic carbonate speleogenesis, also operates as a hypogenic agent, though the origin of the acidity is different. It can be related to CO₂ generated from igneous processes, by thermometamorphism of carbonates, or by thermal degradation and oxidation of deep-seated organic compounds by mineral oxidants. The latter is common in hydrocarbon fields, where waters characteristically contain high CO₂ concentrations (Kaveev 1963). Hydrogen sulfide is another common hypogenic source of acidity where there are sufficient sources of dissolved sulfate for reduction and where the H₂S generated can escape from the reducing zones. However, it is generally believed that creation of significant caves, where these acids provide the dissolution mechanism, depends mainly upon rejuvenation of aggressiveness by mixing or cooling. These conditions are commonly met in the ascending limbs of intermediate or regional flow systems, when they interact with shallower flow systems. Aggressiveness in hypogenic speleogenesis may also reflect acquisition of new sources of acid within the soluble formation itself, when groundwater flows transversely across it, or can be due to a number of

mechanisms that rejuvenate the dissolutive capacity of fluids, such as the cooling of water, mixing of groundwaters of contrasting chemistry, and sulfate reduction and dedolomitization as mentioned above. In shallower conditions, where H_2S -bearing waters rise to interact with oxygenated meteoric groundwaters, sulfuric acid dissolution can be a very strong speleogenetic agent. It is recognised as the main speleogenetic process for certain large caves (e.g. caves such as the Carlsbad Caverns in the Guadalupe reef complex in New Mexico, south-western USA, and Frasassi Cave in Italy) and many smaller caves. Based on this, some researchers distinguish sulfuric acid karst/speleogenesis as a peculiar type (Hill 1996; 2000a; 2003a). Substantial sulfuric acid dissolution can also be caused by oxidation of iron sulfides such as pyrite and marcasite, where it is localised in ore bodies (Bottrell et al. 2000). Lowe (1992) suggested that oxidation of pyrite along certain horizons or bedding planes in carbonates ("inception horizons") may create preferential flowpaths that later will be inherited by epigenetic speleogenesis. The increased

solubility of calcite in cooling waters can cause dissolution along ascending flowpaths. The latter mechanism is commonly labeled as hydrothermal speleogenesis, occurring in high-gradient zones where ascending flow is localised along some highly permeable paths (Malinin 1979; Dublyansky 1980; Dubljansky Ju 1990, 2000a; Ford and Williams 1989; Palmer 1991; Andre and Rajaram 2005). Solutional aggressiveness can be renewed or enhanced by mixing of waters of contrasting chemistry and dissolved gas content (Laptev 1939; Bogli 1964; Palmer 1991), the effect widely cited in the karst literature as "mixing corrosion".

There are an increasing number of arguments and evidence suggesting that more than one process could be involved in many cases, operating either in combination or sequentially. Cross-formation flow is the main mechanism for hypogenic speleogenesis, which can integrate and trigger many cave-generating processes. Either carbonic acid or H_2S dissolution can operate in hydrothermal systems, which are essentially ascending transverse phenomena common in many

Plate 2 Detail of epikarst and vadose zone features exposed in the southern sidewall of Sterkfontein Quarry; note that the lower image is contiguous with the right side of the upper image along the common chevron line



basins. Mixing of contrasting waters is also commonly involved in hypogenic speleogenesis, at least at some stages. This, again, suggests that labeling types of karst and speleogenesis by a single dissolutional mechanism is misleading and should be avoided.

From Klimchouk (2007).
See BIBLIOGRAPHY for references herein.



Tufa terraces across the channel of the Grootvlei Spruit ~600 m downstream of the Nouklip Spring

Physical Hydrology

Harrison Pienaar and Philip J. Hobbs

1 Surface Water Drainage

The study area encompasses the Quaternary catchments and drainages identified in Table 1 in Chapter “Description of the Physical Environment”, Sect. 3.1 in Chapter “Description of the Physical Environment”. The water resources of the subregion are sparsely described in the literature, their extent militating against the regional scale at which studies are typically carried out, i.e. the effort expended in analysing the runoff characteristics of subcatchments such as straddle the study area is often not warranted. It is most often sufficient to simply describe the hydrology in terms of mean annual runoff (MAR) and catchment size. The MAR is reported either as a volume typically with units Mm^3/a , or as an equivalent depth of precipitation in millimetres (mm) over the catchment footprint area.

The study area spans the south-western quadrant of the Hartbeespoort Dam catchment. The net capacity of the dam, equivalent to its full supply capacity (FSC), is slightly less than its gross capacity of 195.1 Mm^3 , which approximates the combined MAR of the contributing catchments. Middleton and Bailey (2008b) report an observed long-term MAR of 193.9 Mm^3 and a simulated MAR of 185.4 Mm^3 for Hartbeespoort Dam. Given this range of reservoir capacities, a nominal value of $\sim 190 \text{ Mm}^3$ is used in this study to represent the FSC of the dam. It is a regionally significant reservoir for various reasons, including the following (in no specific order of importance):

- the attenuation of floods generated by rainfall on the highly urbanised Witwatersrand ridge that forms the continental divide which defines the southern boundary of the catchment;
- the provision of water for municipal water supply to towns and villages located downstream of the dam;
- the provision of water for irrigated agriculture, historically via a canal system, to riparian properties downstream of the dam;
- the support of a burgeoning property industry that has seen the expansion of residential areas and the proliferation of up-market security estates on the shores of the dam; and
- leisure and tourist activities.

Runoff in the study area is gauged at the four stations labelled A2H033, A2H034, A2H049 and A2H050 in Fig. 2 in Chapter “Description of the Physical Environment”. A simplistic ‘stick’ diagram (Fig. 1) provides more readily identifiable components of the regional surface water drainage pattern and associated flow gauging stations.

Whereas the adjoining Steenkoppies Basin to the west-southwest is naturally drained by a single high-yielding spring,¹ the study area is drained by numerous and distributed such features. These feed either the Skeerpoort River or the Bloubank Spruit system. A more complete description of the discharge characteristics of these drainage systems is presented in the relevant sections that follow. Although the contribution of groundwater resources to the surface water hydrology of the study area is mentioned in the following sections (where relevant), the inseparable nature of the surface and subsurface environments that characterise the largely

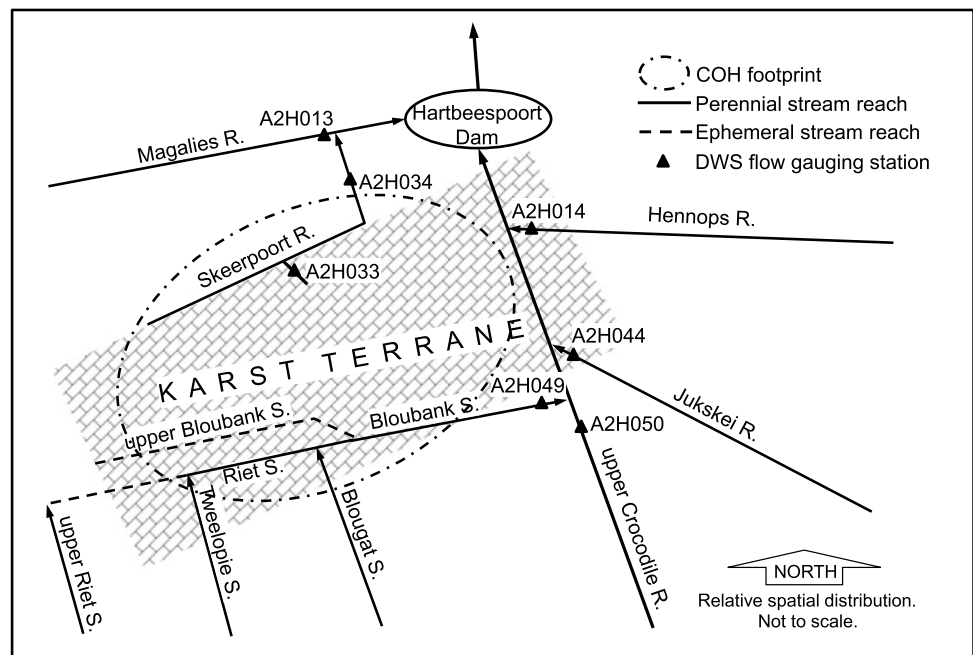
P. J. Hobbs: Deceased

H. Pienaar (✉) · P. J. Hobbs
Smart Places, Council for Scientific and Industrial Research,
Pretoria, South Africa
e-mail: hpienaar@csir.co.za

H. Pienaar
Hebei University of Engineering, Handan, China

¹ Maloney’s Eye, with a long-term mean annual discharge of $\sim 14.4 \text{ Mm}^3$ ($\sim 456 \text{ L/s}$), reduced to $\sim 9.8 \text{ Mm}^3/\text{a}$ ($\sim 311 \text{ L/s}$) in the first decade of the 21st Century (Holland et al., 2009).

Fig. 1 Schematic diagram of surface drainage and gauging network superimposed on the COH karst footprint; karst strata (not shown) extend to the west and east (see Fig. 1 in Chapter “Introduction and Background”).



karst terrane of the study area is described in greater detail in Sect. 7.2 in Chapter “Physical Hydrogeology”.

2 Skeerpoort River System

DWS flow gauging station A2H033 provides a ~50-year discharge record of the Grootvlei Spruit, a tributary of the Skeerpoort River, just before its confluence with the latter (Fig. 1). It yields the monthly discharge statistics presented in Table 1 and for which the annual discharge per hydrological year is shown in Fig. 2. The autumn month of March reflects the lowest coefficient of variation (CoV) of ~43%, and September the lowest monthly median discharge of 0.284 Mm^3 (~110 L/s).

Driven by the perennial Nouklip Spring discharge, the instantaneous flow pattern at station A2H033 up to September 2015 (the DWS record only extends up to November 2015) is shown in Fig. 3. This reveals a distinct step-like increase from ~0.05 to ~0.12 m^3/s (~50 to ~120 L/s) in the ‘base’ values ca. October 1996. This step is also observed in the A2H034 record (Fig. 8 in Chapter “Physical Hydrology”). Although approached for an explanation, the DWS has not resolved this anomaly. Also evident in Fig. 3 are distinct recession curves following peak discharge events, for example ca. February 1978 and May 2000. Hydrograph segments of 260 days in 1999 (spanning the 1999 winter season) and of 220 days in 2005 (also spanning the winter season) were analysed graphically by Holland (2007), from which total potential groundwater discharges of 5.09 and 5.0 Mm^3 , respectively, were

estimated. These results prompted Holland (2007) to estimate, by extrapolation, a groundwater contribution to base-flow in 2005 of 8.3 Mm^3 . This value significantly exceeds the 1997 to 2015 median discharge of ~5.4 Mm^3/a_h [~170 L/s (text box, Fig. 2)]. It also exceeds the maximum discharge value of ~7.5 Mm^3/a_h [~238 L/s (text box Fig. 2)] in the year 2000 of this period.

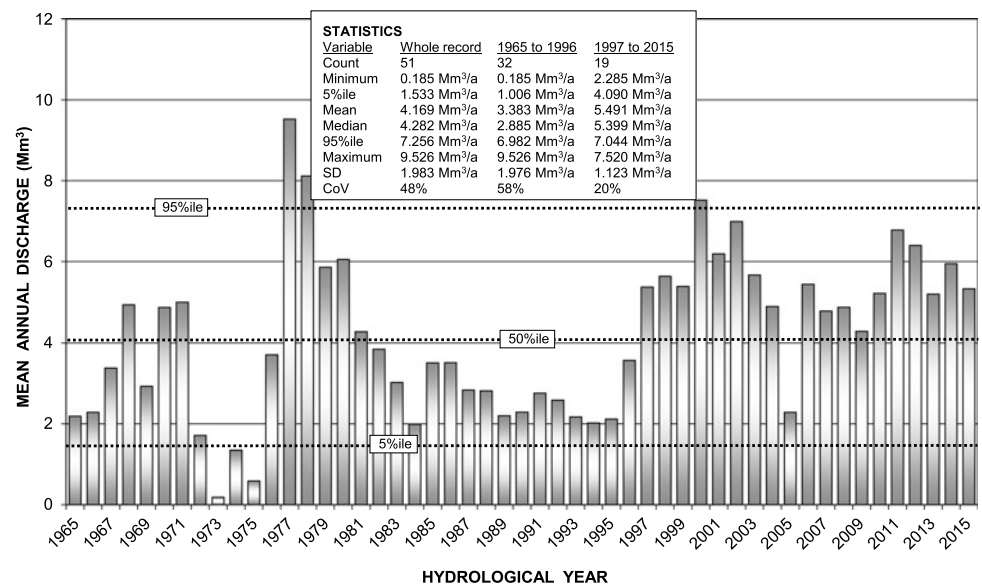
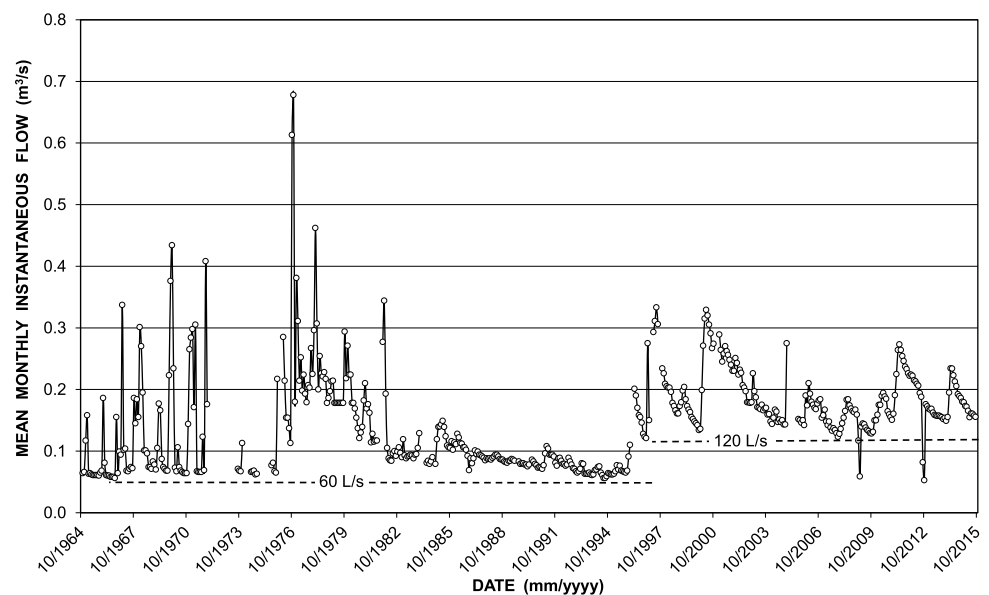
The Nouklip Spring synoptic discharge measurements (SDMs) of ~173 L/s in May 2010 and ~211 L/s in August 2014 following very wet summers (Fig. 3 in Chapter “Description of the Physical Environment”), equate to flows of ~5.4 and ~6.7 Mm^3/a_h respectively. The former is in good agreement with the median discharge in the period 1997–2015 reported above, and exceeds by <10% the shorter segment values obtained by Holland (2007). This suggests that aggregating segmental recession-based calculations of groundwater contributions to an annual value is invalid in this instance.

An inspection of the data presented in Table 1 provides further insight into the Nouklip Spring discharge. Station A2H033 (Plate 1) is located ~525 m downstream of the spring, and therefore provides a measure of the springflow regime when very high flows dominated by storm runoff from the catchment above the spring are neglected. It is one of only eight DWS gauging stations in the country that record the discharge of a karst spring up to as recently as 2017. High yielding municipal water supply sources such as the Tshwane Metro’s Pretoria Fountains, Grootfontein Spring and Sterkfontein Spring are gauged by the local authority. The long-term (whole record) median monthly flow ranges from 165 L/s in April (end of the wet summer

Table 1 Statistical analysis of Grootvlei Spruit mean monthly discharge at station A2H033 in the period October 1964 to September 2015 (no data available since 13/12/2015)

| Variable | Month | | | | | | | | | | | |
|----------|-------|-------|-------|-------|-------|-------|-------|-------|-------|-------|-------|-------|
| | Oct | Nov | Dec | Jan | Feb | Mar | Apr | May | Jun | Jul | Aug | Sep |
| n | 47 | 46 | 48 | 44 | 43 | 42 | 44 | 44 | 47 | 46 | 48 | 48 |
| Minimum | 0.160 | 0.159 | 0.165 | 0.166 | 0.142 | 0.162 | 0.155 | 0.160 | 0.150 | 0.151 | 0.150 | 0.145 |
| 5%ile | 0.170 | 0.166 | 0.178 | 0.185 | 0.162 | 0.179 | 0.194 | 0.176 | 0.161 | 0.165 | 0.166 | 0.160 |
| Mean | 0.382 | 0.400 | 0.409 | 0.431 | 0.410 | 0.411 | 0.411 | 0.404 | 0.366 | 0.372 | 0.358 | 0.321 |
| Median | 0.345 | 0.370 | 0.402 | 0.400 | 0.384 | 0.424 | 0.428 | 0.407 | 0.358 | 0.358 | 0.340 | 0.284 |
| 95%ile | 0.706 | 0.904 | 0.733 | 0.789 | 0.755 | 0.722 | 0.731 | 0.725 | 0.695 | 0.695 | 0.675 | 0.596 |
| Maximum | 1.642 | 1.756 | 1.162 | 1.02 | 1.118 | 0.822 | 0.816 | 0.881 | 0.829 | 0.891 | 0.821 | 0.692 |
| SD | 0.249 | 0.286 | 0.203 | 0.208 | 0.212 | 0.175 | 0.177 | 0.187 | 0.179 | 0.180 | 0.170 | 0.144 |
| CoV (%) | 65.1 | 71.6 | 49.5 | 48.2 | 51.7 | 42.6 | 43.0 | 46.2 | 49.0 | 48.4 | 47.6 | 44.8 |

All units are Mm^3 unless otherwise indicated. Analysis excludes months with missing and station rating exceedance data, but includes unaudited (recent) and estimated data

Fig. 2 Pattern and trend of Grootvlei Spruit mean annual (a_h) discharge gauged at station A2H033 in the period October 1964 to September 2015**Fig. 3** Long-term monthly hydrograph of the Grootvlei Spruit at station A2H033 for the period October 1964 to September 2015

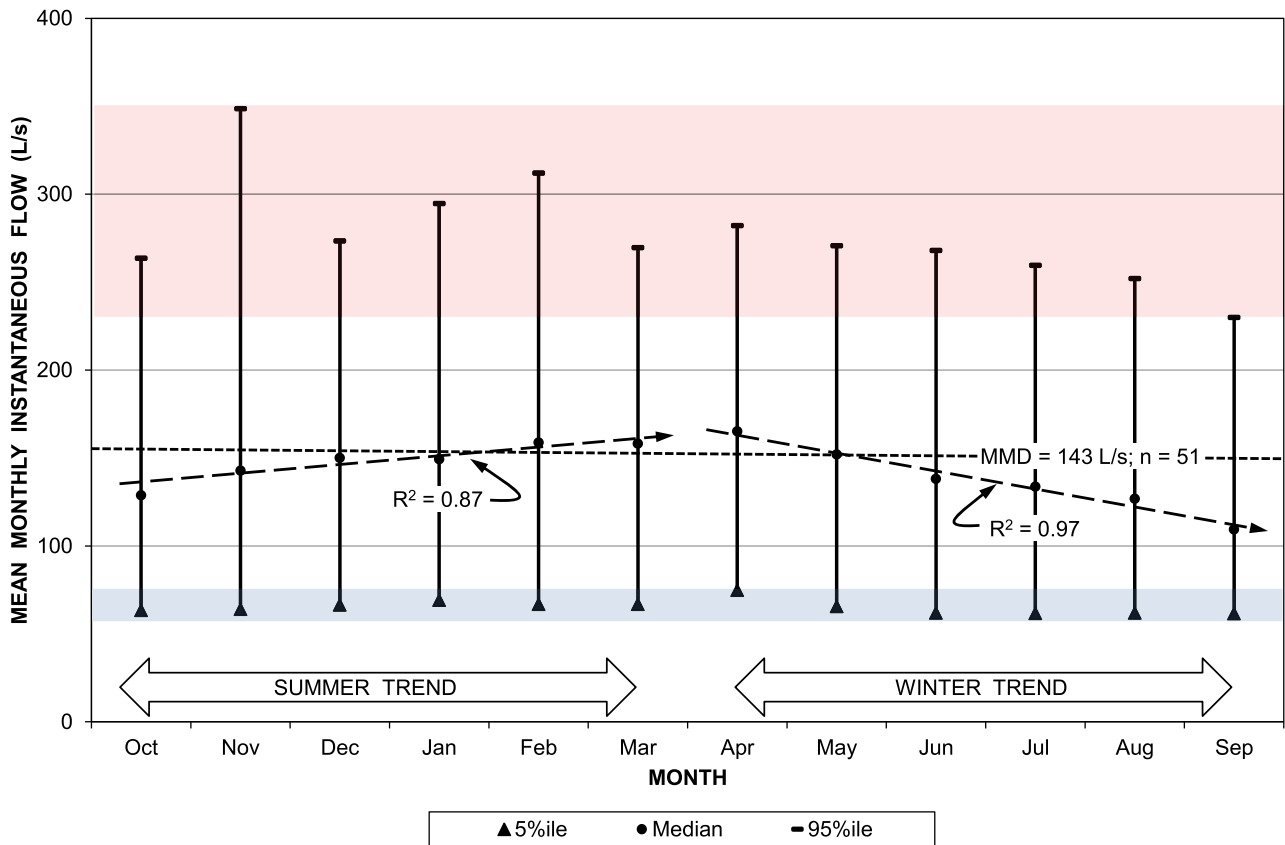


Fig. 4 Long-term monthly discharge pattern of the Nouklip Spring, showing median values with 5%ile and 95%ile bounds and summer and winter trends as linear regression traces

Plate 1 View from the right bank of the combination V-notch/rectangular weir flow gauging station A2H033 on the Grootvlei Spruit, showing the stage recorder housing (top centre) on the opposite bank



season) to 109 L/s at the end of winter in September (Fig. 4), bracketing mean and median annual values of 143 and 146 L/s, respectively. The 5%ile value occupies the comparatively narrow range 62–75 L/s, and the 95%ile value the broader range 230–349 L/s. The flow record indicates that a 2σ deviation at the 95%ile level exceeds the long-term mean monthly discharge (MMD) by $\sim 40\%$

to $\sim 111\%$. These circumstances illustrate the Martini (2006) statement regarding the ‘very regular discharges’ that characterise karst springs of the Malmani Subgroup.

A similar analysis for the period 1997–2015 yields a median monthly flow ranging from 159 L/s in November to 187 L/s in March and May (Fig. 5), bracketing mean and median monthly values of 171 L/s. The 5%ile values occupy

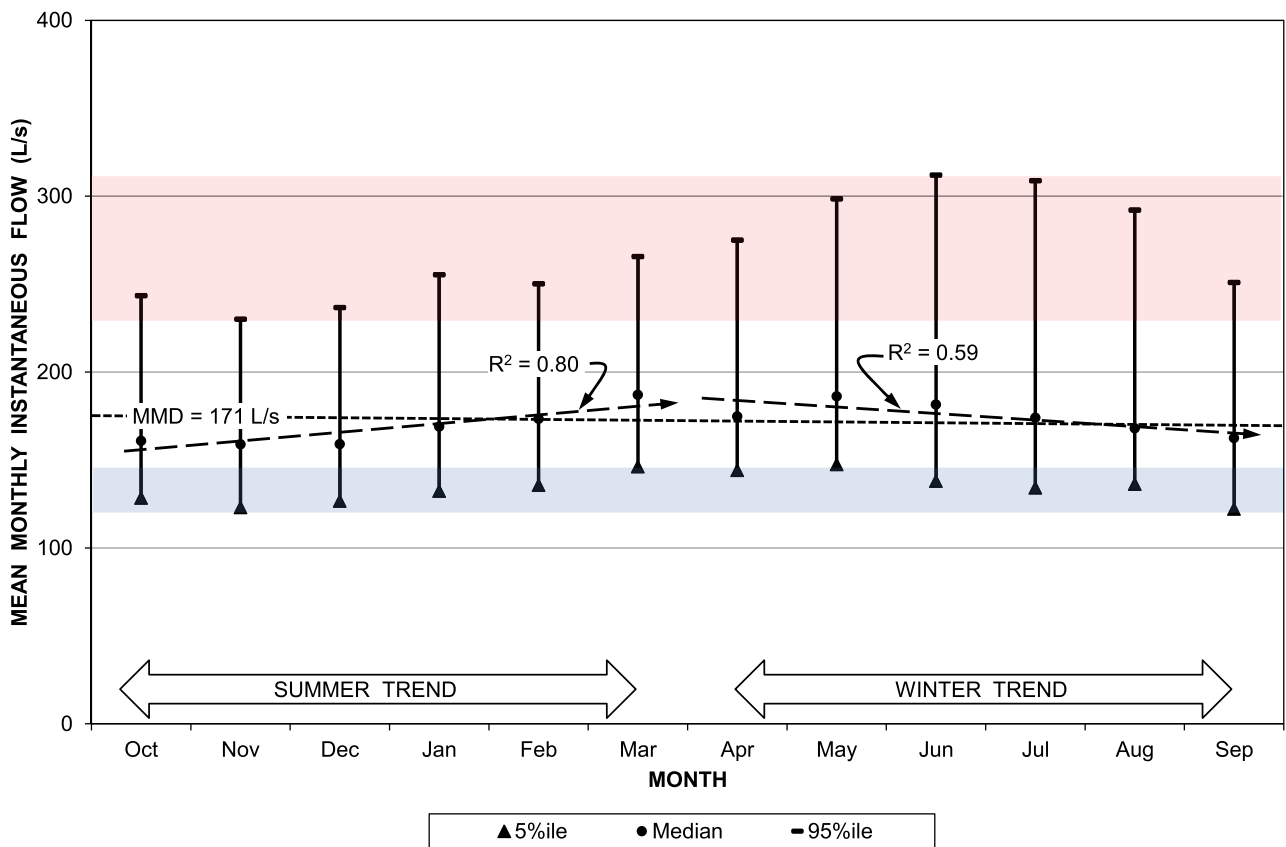


Fig. 5 Monthly discharge pattern of the Nouklip Spring in the period 1997–2015, showing median values with 5%ile and 95%ile bounds and summer and winter trends as linear regression traces

the narrow range 123–147 L/s, and the 95%ile values the range 230–309 L/s. The flow record indicates that a 2σ deviation at the 95%ile level exceeds the mean monthly discharge (MMD) by ~35% to ~81%. The differences with the whole record analysis are apparent. The most interesting of these is the difference in the 95%ile pattern which, in Fig. 5, shows increasingly greater excursions from late summer through to late winter, peaking in June and July. As this pattern cannot be due to flood-driven runoff from high rainfall, it must reflect the hydraulic response time of the Diepkloof Basin (Sect. 7.2.7 in Chapter “Physical Hydrogeology”) to groundwater recharge in the preceding wet season(s) (Table 2).

The 95%ile ‘peaks’ in June and July suggest a hydraulic response lag time of at least three months for the Diepkloof Basin karst aquifer. The mainly springflow-driven median values also reveal similar peaks of ~186 L/s in March and May. It is also evident that the decline in median discharge through the winter season continues into November and December with flows of 159 L/s. An aspect of the flow pattern that is not evident from the preceding discussion, is the fact that the spring discharge includes the autogenic recharge contribution of the hydrogeologically separated Tweefontein

Spring (Sect. 7.4.6 in Chapter “Physical Hydrogeology”). This was measured at ~30 L/s (~0.95 Mm³/a) in May 2010, and ~26 L/s (~0.82 Mm³/a) in August 2014. Clearly, this contribution would be included in the recession-based calculation of groundwater contribution to surface discharge as performed by Holland (2007), and would therefore not explicitly recognise the hydrogeologically separated Diepkloof and Tweefontein basins drained by the Nouklip and Tweefontein springs respectively. Against this background, the February 2018 SDM value of 105 L/s is inexplicably low, although Table 2 shows a minimum value of 0.142 Mm³ (59 L/s) for February. A more detailed analysis of the springflow characteristics is presented in Sect. 7.4.7 in Chapter “Physical Hydrogeology”.

It should also be noted that at its confluence with the Grootvlei Spruit, the Skeerpoort River already carries the discharge of the Nash Spring (Sect. 7.4.8 in Chapter “Physical Hydrogeology”). This spring is located a distance of ~4.9 km (measured along the sinuous river reach) upstream of this confluence. Its discharge was measured at ~130 L/s (~4.1 Mm³/a) in May 2010, and ~208 L/s (~6.6 Mm³/a) in August 2014. Together with the preceding discussion, these circumstances further inform the discharge

Table 2 Statistical analysis of Grootvlei Spruit mean monthly discharge at station A2H033 in the period October 1997 to September 2015

| Variable | Month | | | | | | | | | | | |
|----------|-------|-------|-------|-------|-------|-------|-------|-------|-------|-------|-------|-------|
| | Oct | Nov | Dec | Jan | Feb | Mar | Apr | May | Jun | Jul | Aug | Sep |
| n | 19 | 19 | 18 | 17 | 18 | 17 | 17 | 18 | 18 | 18 | 19 | 18 |
| Minimum | 0.342 | 0.318 | 0.324 | 0.313 | 0.142 | 0.374 | 0.368 | 0.384 | 0.357 | 0.356 | 0.355 | 0.212 |
| 5%ile | 0.344 | 0.319 | 0.339 | 0.355 | 0.328 | 0.392 | 0.374 | 0.395 | 0.358 | 0.359 | 0.365 | 0.317 |
| Mean | 0.459 | 0.434 | 0.463 | 0.485 | 0.438 | 0.518 | 0.513 | 0.547 | 0.519 | 0.525 | 0.504 | 0.441 |
| Median | 0.431 | 0.412 | 0.426 | 0.453 | 0.420 | 0.501 | 0.453 | 0.499 | 0.471 | 0.466 | 0.450 | 0.421 |
| 95%ile | 0.652 | 0.596 | 0.634 | 0.684 | 0.605 | 0.712 | 0.713 | 0.799 | 0.809 | 0.827 | 0.782 | 0.650 |
| Maximum | 0.733 | 0.607 | 0.736 | 0.736 | 0.698 | 0.726 | 0.816 | 0.881 | 0.829 | 0.891 | 0.821 | 0.692 |
| SD | 0.106 | 0.086 | 0.109 | 0.118 | 0.116 | 0.103 | 0.122 | 0.144 | 0.146 | 0.152 | 0.136 | 0.114 |
| CoV (%) | 23.1 | 19.9 | 23.6 | 24.3 | 26.4 | 19.8 | 23.7 | 26.4 | 28.1 | 29.0 | 27.0 | 25.9 |

All units are Mm^3 unless otherwise indicated. Analysis excludes months with missing and station rating exceedance data, but includes unaudited (recent) and estimated data

Table 3 Statistical analysis of Skeerpoort River mean monthly discharge at station A2H034 in the period October 1965 to September 2017

| Variable | Month | | | | | | | | | | | |
|----------|-------|-------|-------|-------|-------|-------|-------|-------|-------|-------|-------|-------|
| | Oct | Nov | Dec | Jan | Feb | Mar | Apr | May | Jun | Jul | Aug | Sep |
| n | 49 | 48 | 48 | 49 | 49 | 47 | 49 | 50 | 51 | 48 | 50 | 49 |
| Minimum | 0.266 | 0.349 | 0.353 | 0.397 | 0.333 | 0.334 | 0.321 | 0.362 | 0.405 | 0.452 | 0.401 | 0.334 |
| 5%ile | 0.399 | 0.393 | 0.491 | 0.448 | 0.381 | 0.388 | 0.374 | 0.383 | 0.465 | 0.462 | 0.447 | 0.364 |
| Mean | 0.782 | 0.867 | 1.011 | 1.206 | 1.239 | 1.348 | 1.091 | 1.050 | 0.939 | 0.865 | 0.847 | 0.770 |
| Median | 0.735 | 0.791 | 0.935 | 1.061 | 0.940 | 0.994 | 0.840 | 0.836 | 0.806 | 0.812 | 0.801 | 0.718 |
| 95%ile | 1.344 | 1.832 | 2.294 | 2.401 | 3.329 | 2.725 | 2.089 | 2.210 | 1.766 | 1.595 | 1.634 | 1.527 |
| Maximum | 2.078 | 2.25 | 3.498 | 3.16 | 6.625 | 8.55 | 5.581 | 6.231 | 4.396 | 1.972 | 1.902 | 1.843 |
| SD | 0.361 | 0.431 | 0.591 | 0.678 | 1.179 | 1.299 | 0.847 | 0.928 | 0.623 | 0.368 | 0.367 | 0.356 |
| CoV (%) | 46.1 | 49.8 | 58.4 | 56.2 | 95.1 | 96.3 | 77.6 | 88.4 | 66.4 | 42.6 | 43.3 | 46.2 |

All units are Mm^3 unless otherwise indicated. Analysis excludes months with missing and station rating exceedance data, but includes unaudited (recent) and estimated data

characteristics of the Skeerpoort River as gauged at station A2H034 located ~ 7 km downstream of station A2H033 (Fig. 1). At this location, the river has left the pristine environment of the John Nash Nature Reserve, traverses Pretoria Group sedimentary strata, and also supports agricultural activities in the vicinity of the confluence with the Witwatersrand Spruit.

The A2H034 flow record spans a period of 52 years. It provides the monthly discharge statistics presented in Table 3, and for which the annual discharge per hydrological year is shown in Fig. 6. The winter month of July reflects the lowest CoV value of $\sim 43\%$, and September the lowest median discharge value of 0.718 Mm^3 (277 L/s). The data again reflect the constancy and perennial nature of the spring-driven autogenic discharge at this location. The combined discharge ($>300 \text{ L/s}$) of the karst springs that sustain the Skeerpoort River (Sects. 7.4.6, 7.4.7 and 7.4.8 in Chapter “Physical Hydrogeology”) equates to a discharge of at least $9.5 \text{ Mm}^3/\text{a}_h$, similar to the long-term median value

of $\sim 10.2 \text{ Mm}^3/\text{a}_h$ (text box, Fig. 6). These values represent $\sim 5\%$ of the $\sim 190 \text{ Mm}^3$ FSC of Hartbeespoort Dam (Sect. 1), testifying the important groundwater contribution delivered by this portion of the COH to the regional water resources budget.

The truncated period statistics presented in Fig. 6 for station A2H034 mimic those of Fig. 2 for station A2H033 in order to provide a direct comparison under circumstances where the A2H034 record extends to September 2017, whereas that of A2H033 only extends to November 2015. This comparison is taken further in Fig. 6, which shows the cumulative discharge at stations A2H033 and A2H034 over the truncated period of common record.

The discharge pattern at station A2H034 for the complete record is shown in Fig. 8. Although less evident than in Fig. 3, distinct recession curves following peak discharge events, for example ca. October 1977 and October 2000, are also discernible in the hydrograph. Evident at the end of this record are the exceptional discharges (some of the highest on

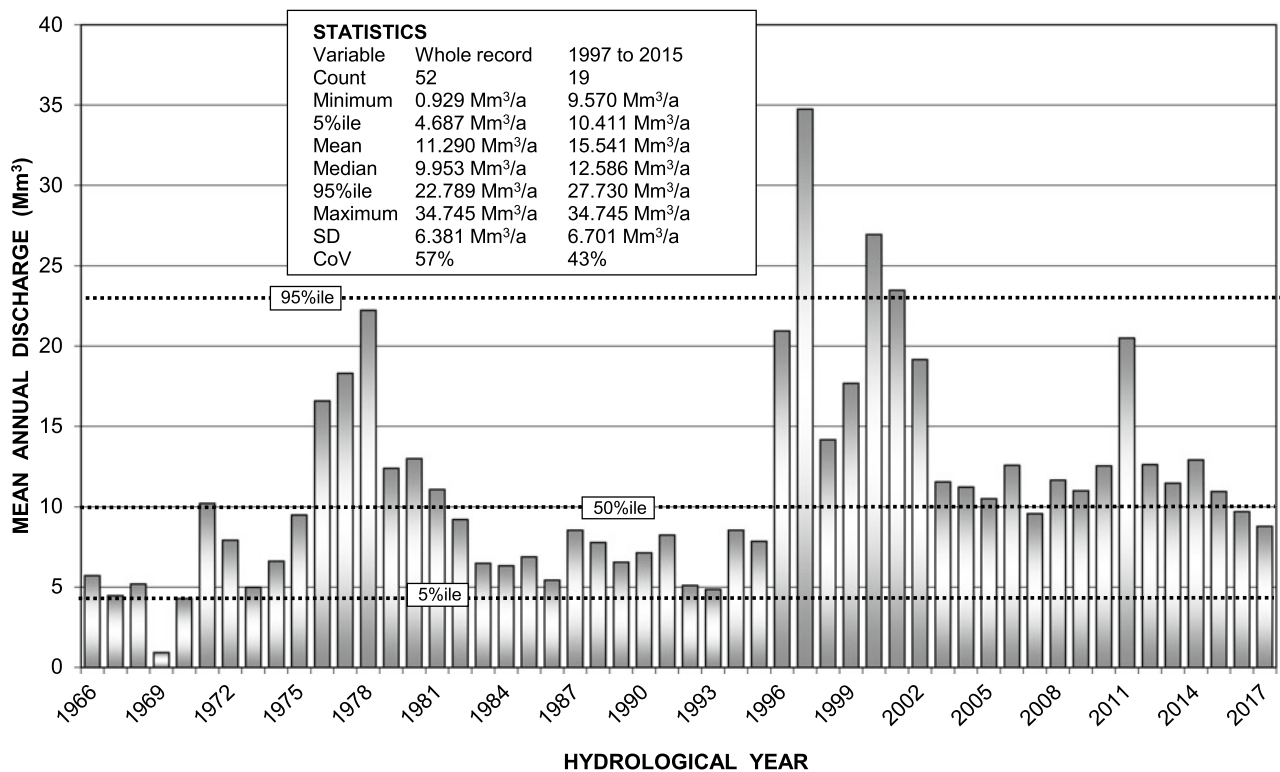


Fig. 6 Pattern and trend of Skeerpoort River mean annual (a_n) discharge gauged at station A2H034 in the period October 1965 to September 2017

record excluding the uncensored anomalous data) recorded in January and March 2011 and March 2014. The aftermath of such events is shown in Plate 2 taken on the farm Dwarsvlei 503JQ in the upper reaches of the Skeerpoort River valley following a flash flood event in October 2009. Notable, however, is the absence in Fig. 9 of a flow peak associated with this response in Fig. 9, illustrating the degree to which singular events are absorbed in monthly and annual values. As indicated previously, station A2H034 is located a substantial distance downstream of its principal perennial sources at a location where agricultural impacts in the form of abstraction for irrigation, as well as the contribution of the ephemeral Witwatersrand Spruit tributary entering from the east, are also likely manifested. These circumstances negate attempting a correlation between spring discharge and rainfall as has been attempted by Holland et al. (2009) for Maloney's Eye draining the Steenkoppies Basin (Sects. 3.1, 4, 5.1 and 7.1 in Chapter "Physical Hydrogeology") (Fig. 7).

An inspection of the whole record cumulative annual discharge of the Grootvlei Spruit (station A2H033) and the Skeerpoort River (station A2H034) indicates a year-on-year difference in median annual discharge between these stations of 6.2 Mm³ (~ 197 L/s) for $n = 50$ values (Fig. 9). This approaches the August 2014 SDM value of ~ 208 L/s (Sect. 7.4.8 in Chapter "Physical Hydrogeology"). The

inter-quartile range is defined by values of ~ 4.8 Mm³ (~ 152 L/s) and ~ 8.0 Mm³ (~ 253 L/s). The $>75\%$ ile excursions are unequivocally associated with the periods of surface runoff-driven flow (see also Fig. 7), and the $<25\%$ ile excursions with the pre-October 1996 period of lower baseflow values (Fig. 8). The year-on-year difference in median discharge places the long-term median discharge of the ungauged Nash Spring at ~ 200 L/s (~ 6.3 Mm³/a).

The agreement already demonstrated between the combined discharge of the karst springs (~ 9.5 Mm³/a) and the long-term median stream discharge (~ 10.2 Mm³/a) quantifies the baseflow component of the Skeerpoort River with sufficient rigour. As will be made evident in Sect. 8.7 in Chapter "Chemical Hydrogeology", it is not only the volumetric contribution of this component to Hartbeespoort Dam, but also the generally excellent quality of the karst groundwater, that is important to the severely compromised quality of that received by and impounded in this hypertrophic reservoir from other much larger tributaries (Hobbs 2017c).

3 Bloubank Spruit System

The Bloubank Spruit system comprises the following main drainages, described sequentially downstream from the headwater reaches (see Fig. 1 for reference).

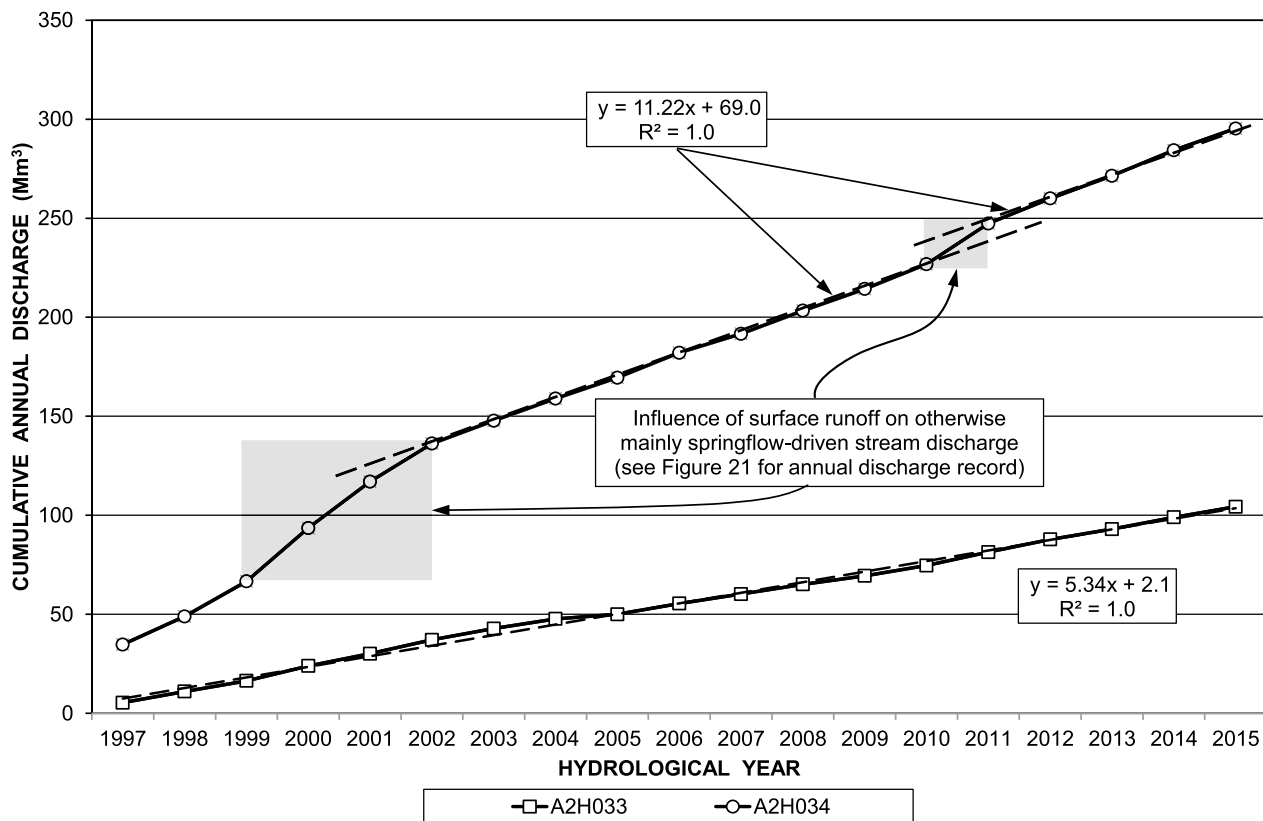


Fig. 7 Cumulative annual discharge at stations A2H033 and A2H034 illustrating the year-on-year constancy of flow in these springflow-driven drainages

- The Bloubank Spruit rises on the farm Reydal 165IQ north of Tarlton, and flows east-north-eastwards past Sterkfontein Cave and Kromdraai down to its confluence with the Crocodile River in the vicinity of Glenburn Lodge at Zwartkop. Its upper reaches traversing the Zwartkrans Basin (Sect. 7.2.1 in Chapter “[Physical Hydrogeology](#)”), are ephemeral.
- The north-westerly draining upper reach of the Riet Spruit, which rises in Riebeeck Lake in Randfontein and flows past the Randfontein WWTW toward Tarlton, where it swings 90° to the east-north-east. Its middle and lower reaches follow the N14 national road down to the confluence with the Bloubank Spruit near the Swartkrans fossil site.
- The Tweelopie Spruit, a tributary of the Riet Spruit, can be traced upstream to Robinson Lake² between Randfontein and Krugersdorp, and drains northward through the Krugersdorp Game Reserve, intersecting the N14 before its confluence with the Riet Spruit.
- The Blougat Spruit, another tributary of the Riet Spruit, rises in the Factoria industrial area of Mogale City and

first drains in a north-westerly direction through the city as a canal before flowing northward past the Munsieville township and Percy Stewart WWTW, intersecting the N14 before its confluence with the Riet Spruit.

Minor drainages are (a) the Honingklip Spruit,³ an ephemeral tributary of the Bloubank Spruit that rises on the northern margin of Mogale City in the Rant-en-Dal and Paardekraal areas, and flows northwards to join the Bloubank Spruit at Kromdraai, and (b) the Tweefontein Spruit⁴ that rises in the John Nash Nature Reserve, and drains southward across the farm Rietfontein 522JQ to join the Bloubank Spruit near Brookwood Trout Farm and the eastern boundary of the Nedbank Olwazini Estate.

The discharge of the Bloubank Spruit system is gauged at station A2H049 (Fig. 2 in Chapter “[Description of the Physical Environment](#)”) located ~12 km downstream from Sterkfontein Cave. The ~45-year record yields the monthly

² This does not imply that Robinson Lake (an endoreic feature) is the source of the Tweelopie Spruit.

³ Name assigned to a drainage that for most of its path traverses the farm Honingklip 178IQ, but is unnamed on the 1:50 000 scale topocadastral map 2627BB Roodepoort (RSA, 2002).

⁴ Name given to an unnamed drainage on the 1:50 000 scale topocadastral map 2527DD Broederstroom (RSA, 2001).

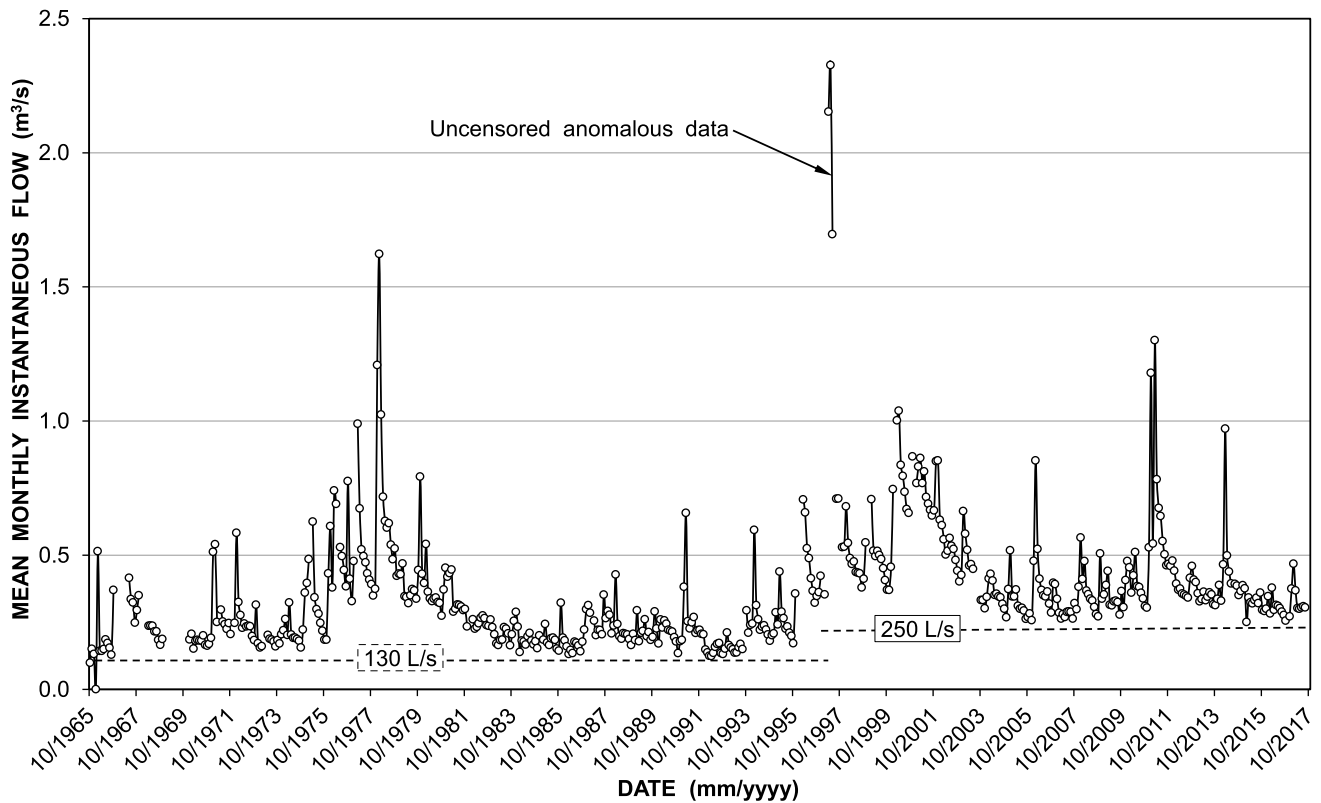


Fig. 8 Long-term monthly hydrograph of the Skeerpoort River at station A2H034 for the period October 1965 to September 2014



Plate 2 Damage to infrastructure caused in the upper reaches of the Skeerpoort River valley by a flash flood in October 2009; note flood stage height of ~ 2 m as indicated by the drift debris on pump house roof and in inset picture

discharge statistics presented in Table 4. This shows that the summer month of November has the lowest CoV value of $\sim 44\%$, September the lowest median discharge of 1.56 Mm^3 ($\sim 602 \text{ L/s} \approx 52.0 \text{ ML/d}$), and October the lowest minimum discharge of 0.68 Mm^3 ($\sim 254 \text{ L/s} \approx 21.9 \text{ ML/d}$).

The discharge per hydrological year is shown in Fig. 10. This indicates that four of the last eight hydrological years experienced the 2nd, 3rd, 4th and 5th highest runoff (59.1 , 54.5 , 47.0 and 44.9 Mm^3 after the 66.9 Mm^3 of 1978) in the historical record of this catchment. The significance hereof is evident in the impact on the long-term median discharge of the Bloubaank Spruit system, which reflects a median value of $\sim 19.3 \text{ Mm}^3/\text{a}$ for the 37-year period 1973 to 2009, and a $\sim 115\%$ greater value of $\sim 41.4 \text{ Mm}^3$ for the last eight years of the record (Fig. 10). These circumstances indicate that an analysis of hydrological data (both quantity and quality) must recognise the influence imposed on the long-term data set by the discharges of the last eight hydrological years. The pre-2010 and post-2009 median annual discharges represent 10 and 22% respectively of the FSC ($\sim 190 \text{ Mm}^3$) of Hartbeespoort Dam. Equally significant is the substantially smaller CoV value for the post-2009 record (23%) compared to that of the pre-2010 set (46%). This is irrefutable evidence of the perennial impact of the mine water discharge contribution on the flow regime of the Bloubaank Spruit in the recent past.

The instantaneous monthly flow pattern at station A2H049 for the complete record is shown in Fig. 11. This reveals a comparatively constant lowest value of $\sim 260 \text{ L/s}$

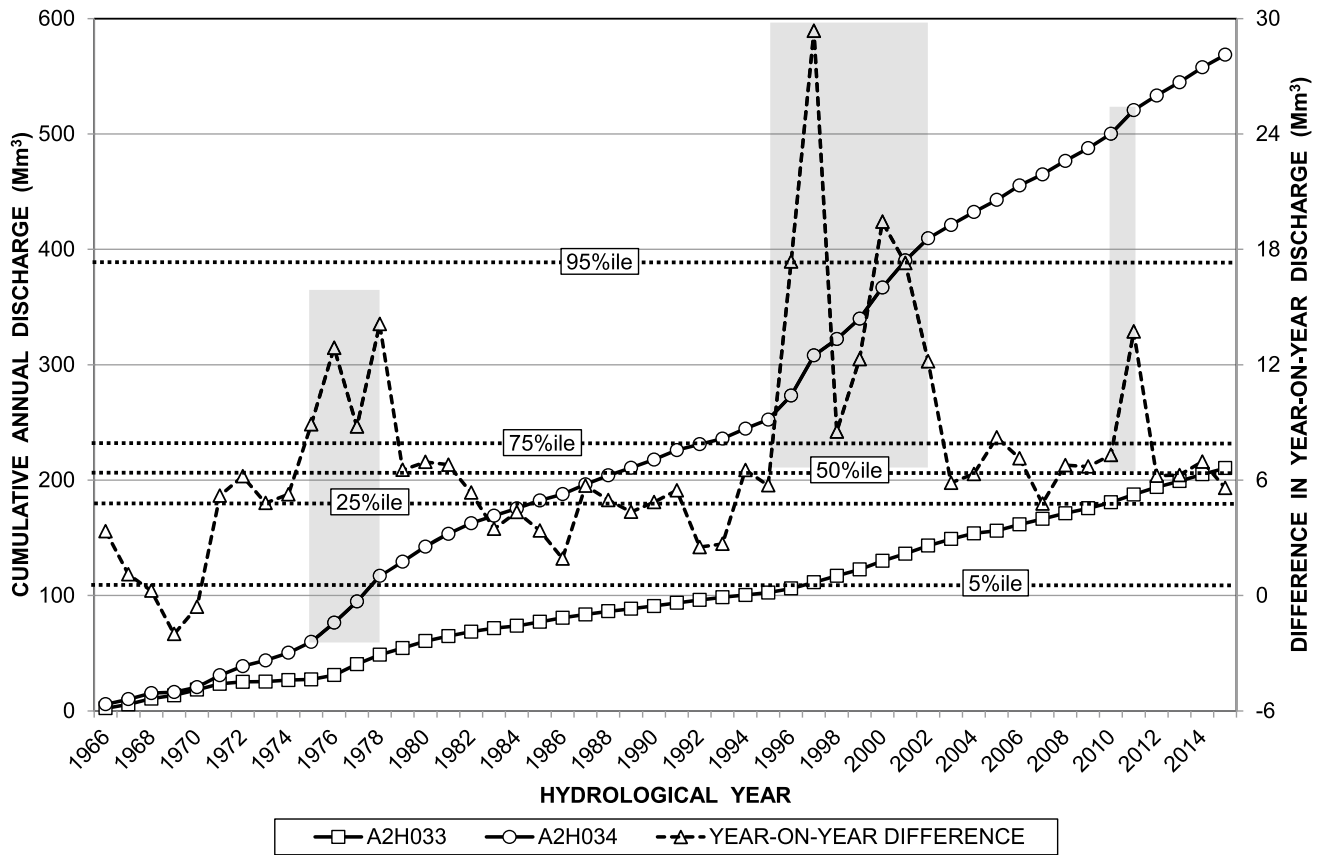


Fig. 9 Difference in long-term year-on-year discharge between stations A2H033 and A2H034

Table 4 Statistical analysis of Bloubank Spruit mean monthly discharge gauged at station A2H049 in the period October 1972 to September 2017

| Variable | Month | | | | | | | | | | | |
|-----------|-------|-------|-------|--------|--------|--------|-------|-------|-------|-------|-------|-------|
| | Oct | Nov | Dec | Jan | Feb | Mar | Apr | May | Jun | Jul | Aug | Sep |
| Count (n) | 43 | 43 | 44 | 44 | 45 | 45 | 45 | 44 | 45 | 45 | 44 | 43 |
| Minimum | 0.682 | 0.815 | 0.711 | 0.721 | 0.706 | 0.828 | 0.886 | 0.847 | 0.894 | 0.939 | 0.890 | 0.770 |
| 5%ile | 0.789 | 0.860 | 1.043 | 1.097 | 0.901 | 1.066 | 1.187 | 0.998 | 0.964 | 0.961 | 0.921 | 0.802 |
| Mean | 1.874 | 1.886 | 2.276 | 2.745 | 2.702 | 3.031 | 2.436 | 2.297 | 2.103 | 2.086 | 1.961 | 1.804 |
| Median | 1.676 | 1.743 | 2.066 | 2.471 | 2.222 | 2.534 | 1.987 | 1.925 | 1.797 | 1.695 | 1.676 | 1.561 |
| 95%ile | 3.824 | 2.952 | 4.501 | 5.355 | 6.328 | 7.863 | 5.355 | 4.882 | 4.115 | 4.058 | 3.658 | 3.509 |
| Maximum | 4.211 | 4.577 | 5.900 | 12.079 | 10.619 | 11.351 | 6.081 | 5.373 | 5.166 | 4.754 | 4.055 | 4.342 |
| SD | 0.921 | 0.830 | 1.094 | 1.931 | 1.932 | 2.208 | 1.301 | 1.197 | 0.976 | 0.944 | 0.876 | 0.883 |
| CoV (%) | 49.1 | 44.0 | 48.1 | 70.4 | 71.5 | 72.8 | 53.4 | 52.1 | 46.4 | 45.3 | 44.7 | 49.0 |

All units are Mm^3 unless otherwise indicated

Analysis excludes months with missing and station rating exceedance data, but includes unaudited (recent) and estimated data

up until early-2007. Again evident in the hydrograph are distinct recession curves following peak discharge events, for example ca. January 1978, March 1997 and February 2000. Station A2H049, however, is not only located a substantial distance (5–10 km) downstream of its primary perennial natural sources, the Zwartkrans and Kromdraai springs, but also receives the discharge of other ‘smaller’

springs (e.g. the Plover’s Lake and Aquamine springs) and ephemeral tributaries such as the Honingklip Spruit. These circumstances again negate a correlation between spring discharge and rainfall. The rising trend in lowest monthly mean instantaneous flow observed since October 2007 (Fig. 11) reflects the impact of mine water discharge mentioned earlier. A detailed interrogation of the discharge

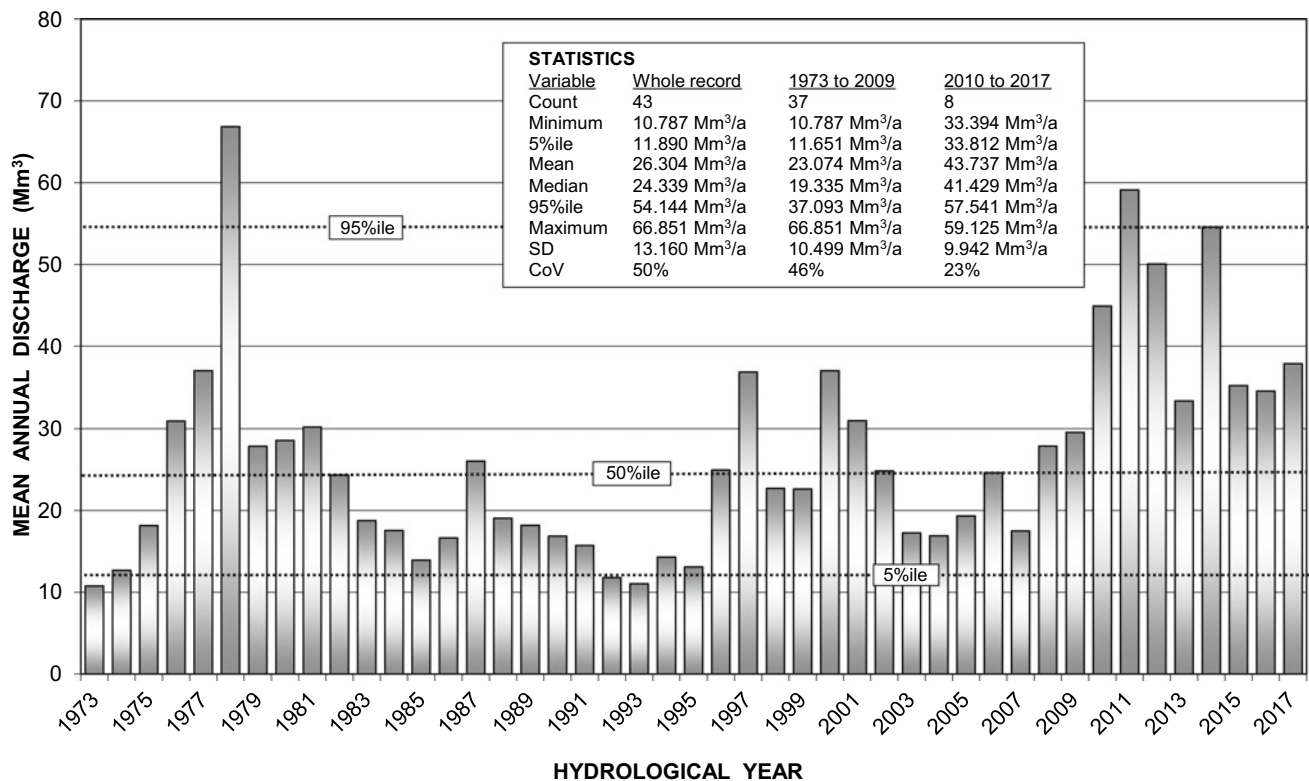


Fig. 10 Pattern and trend of Bloubank Spruit mean annual (a_n) discharge gauged at station A2H049 in the period October 1972 to September 2017

regime in the upper reaches of this system better informs the hydrological and hydrochemical response observed at station A2H049.

A discussion of the two most significant tributary drainages in the Bloubank Spruit system, namely the Tweelopie Spruit and the Blougat Spruit, is presented in the following sections. These two drainages attract attention for (a) the unnatural (anthropogenic) characteristics that dominate their flow regimes in terms of both water quantity and quality, and (b) the availability of historical flow and water quality data associated with the allogenic sources, in particular the mine water driven Tweelopie Spruit.

3.1 Tweelopie Spruit

The decant of mine water in the upper reaches of the Tweelopie Spruit commenced in August 2002 (JFA 2006). In 2004, Sibanye-Stillwater (then Harmony Gold) constructed an HDPE-lined dam (Plate 3) at the Black Reef Incline (BRI) shaft. The dam serves two main functions, namely (a) the collection, control and temporary storage of raw mine water from the various point and diffuse sources in the area, and (b) the prevention of raw mine water release into the downstream receiving environment. The raw mine

water (RMW) is pumped from here to the high density sludge (HDS) mine water treatment plant on the continental divide to the south for basic treatment (neutralisation).

The earliest record of routinely frequent mine water discharge and quality measurements is traced back to spreadsheet data commencing in January 2005. These early records reveal several periods of zero discharge (notably June 2005 to January 2006) separating periods of active discharge. The historical record of RMW and treated/neutralised mine water (TMW) discharge as gauged at the end-of-pipe (EoP) (Plate 4) is shown in Fig. 12. The TMW Parshall-type flume gauging structure was installed in the period prior to 2008 when very little RMW left the property, partly because the gradually increasing rate of decant remained within the early capacity (~ 15 ML/d) of the treatment plant. Fig. 12 indicates that these circumstances changed in early-2008, when discharges >15 ML/d became the norm, and the contribution of RMW to the total mine water discharge became significant. Fig. 12 suggests that total mine water discharges >20 ML/d were irregular and occasional. Nevertheless, these circumstances resulted in the installation of a second flume (Fig. 15) adjacent to the EoP flume to also gauge the RMW component leaving the mine property. Later proving inadequate (in the 2011 wet season) despite being extended (Fig. 16), a third RMW flume was

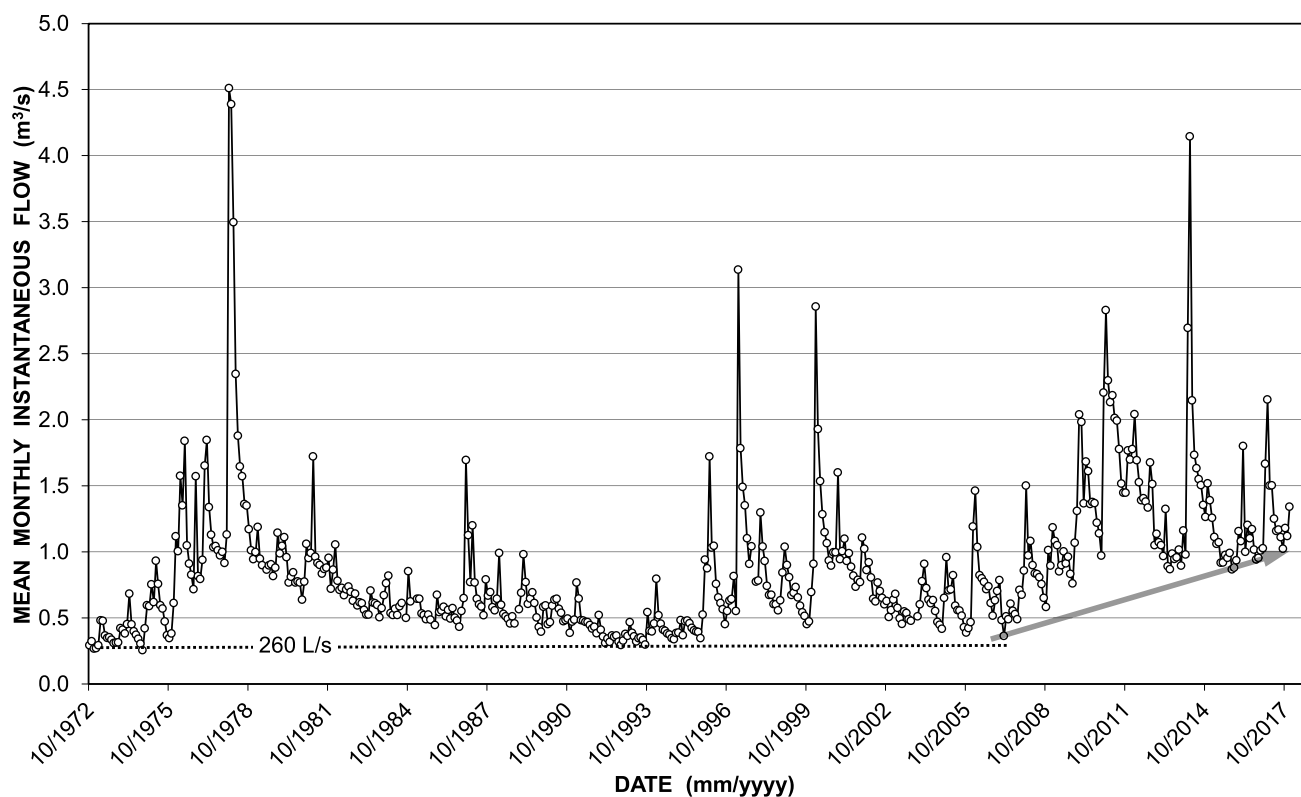


Fig. 11 Long-term monthly hydrograph of the Bloubank Spruit at station A2H049 for the period October 1972 to September 2017



Plate 3 Aerial view (looking north) of the HDPE-lined off-channel storage dam shortly after construction at the Black Reef Incline (circular structure at centre right) to contain mine water decanting from this structure; also visible are the pump station (centre left), the gravity-fed pipeline (45° diagonal from centre bottom) draining the upstream in-channel Portuguese Dam, and the course of the Tweelapie Spruit exiting picture at centre top (photo G Krige, 05/10/2004)

installed (Fig. 17). The accuracy of flow measurements associated with all of the flumes remains questionable, especially for high flows.

The circumstances illustrated in Fig. 12 describe the ‘tipping point’ for the Bloubank Spruit system, when RMW discharges started to consistently exceed 10 ML/d in February 2010. These exceedances are evident in Fig. 13, indicating their duration for extended periods (months). Together with their considerable magnitude (often $\gg 30$ ML/d), these circumstances manifested a marked impact on surface water chemistry (Sect. 6.1.2 in Chapter “[Chemical Hydrology](#)”) observed ~ 28 km downstream from the mine area at station A2H049 (Table 9 in Chapter “[Chemical Hydrology](#)”). Fig. 14 shows that for the first time since the advent of mine water treatment, the RMW component regularly equalled or exceeded the TMW component in the total discharge released into the Tweelapie Spruit and downstream receiving environment. The trigger of this ‘tipping point’, dated to 30/01/2010, rests with the chemistry associated with the contributing RMW and TMW sources, and the impact thereof on the hydrochemical composition of the combined discharge to the Tweelapie Spruit. This influence is interrogated in Sects. 6.1.2 and 6.2.2 in Chapter “[Chemical Hydrology](#)”.

The very high discharges in four of the last eight hydrological years (Fig. 10) reflect an abnormal mine water discharge regime which the immediate and short-term mine water interventions have sought to normalise. A closer inspection of the discharge statistics for station A2H049

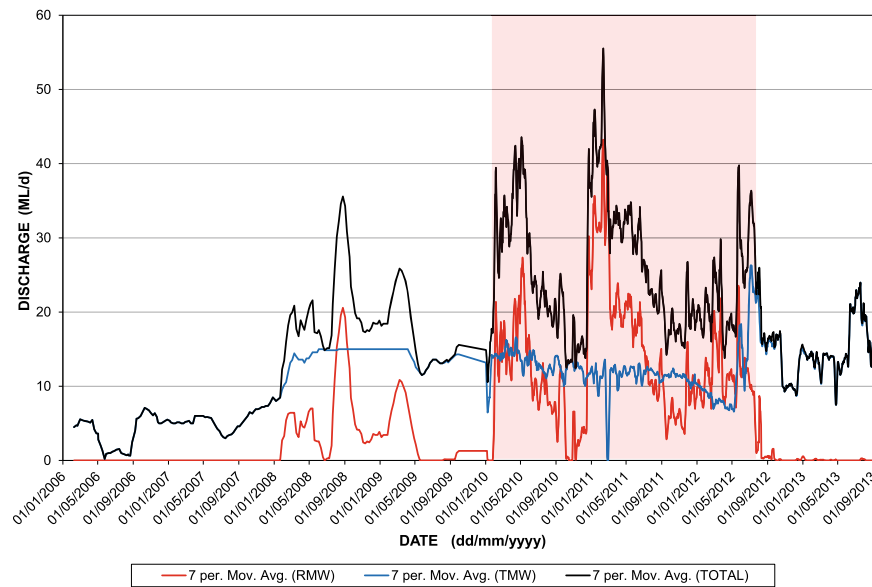


Fig. 12 Pattern and trend of mine water discharge to the Tweelopie Spruit

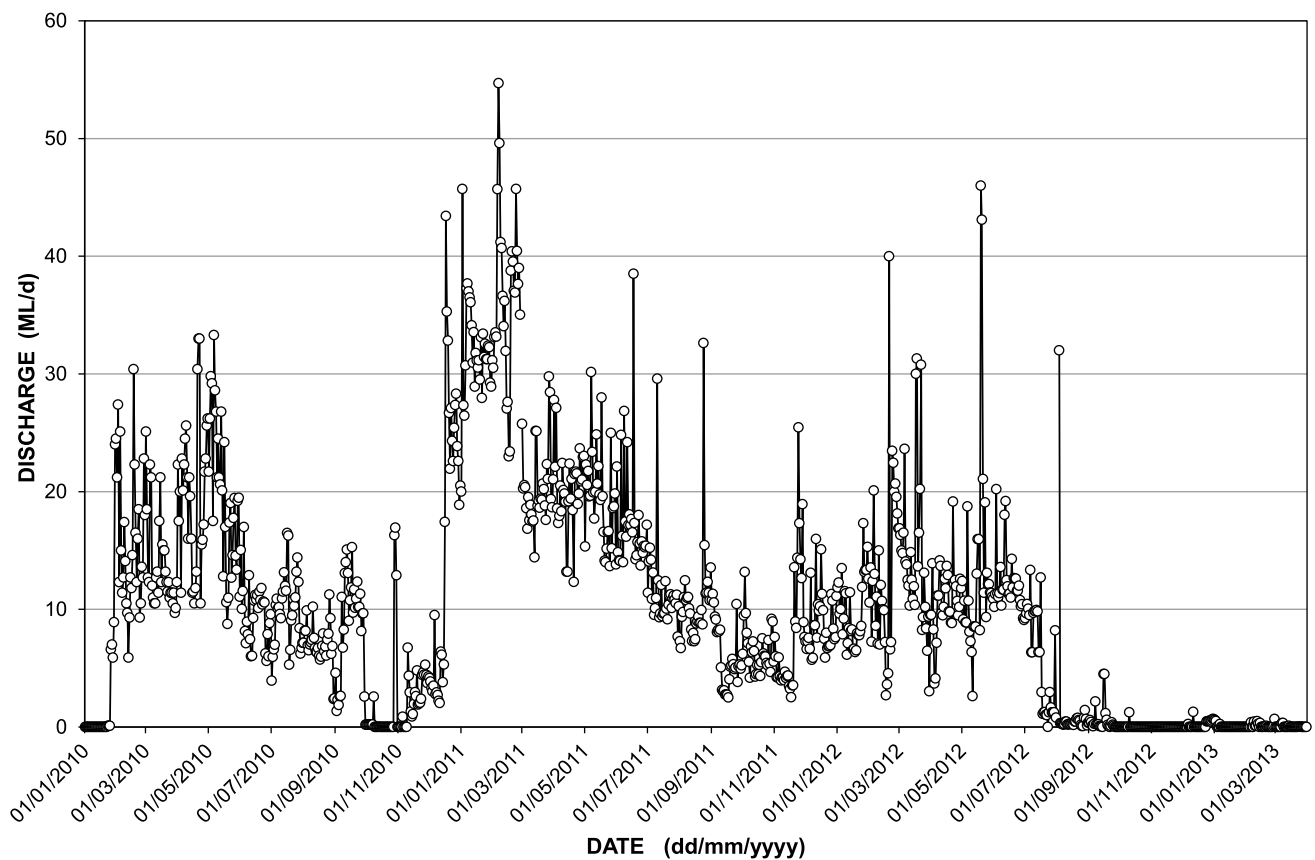


Fig. 13 Pattern and trend of raw mine water discharge to the Tweelopie Spruit

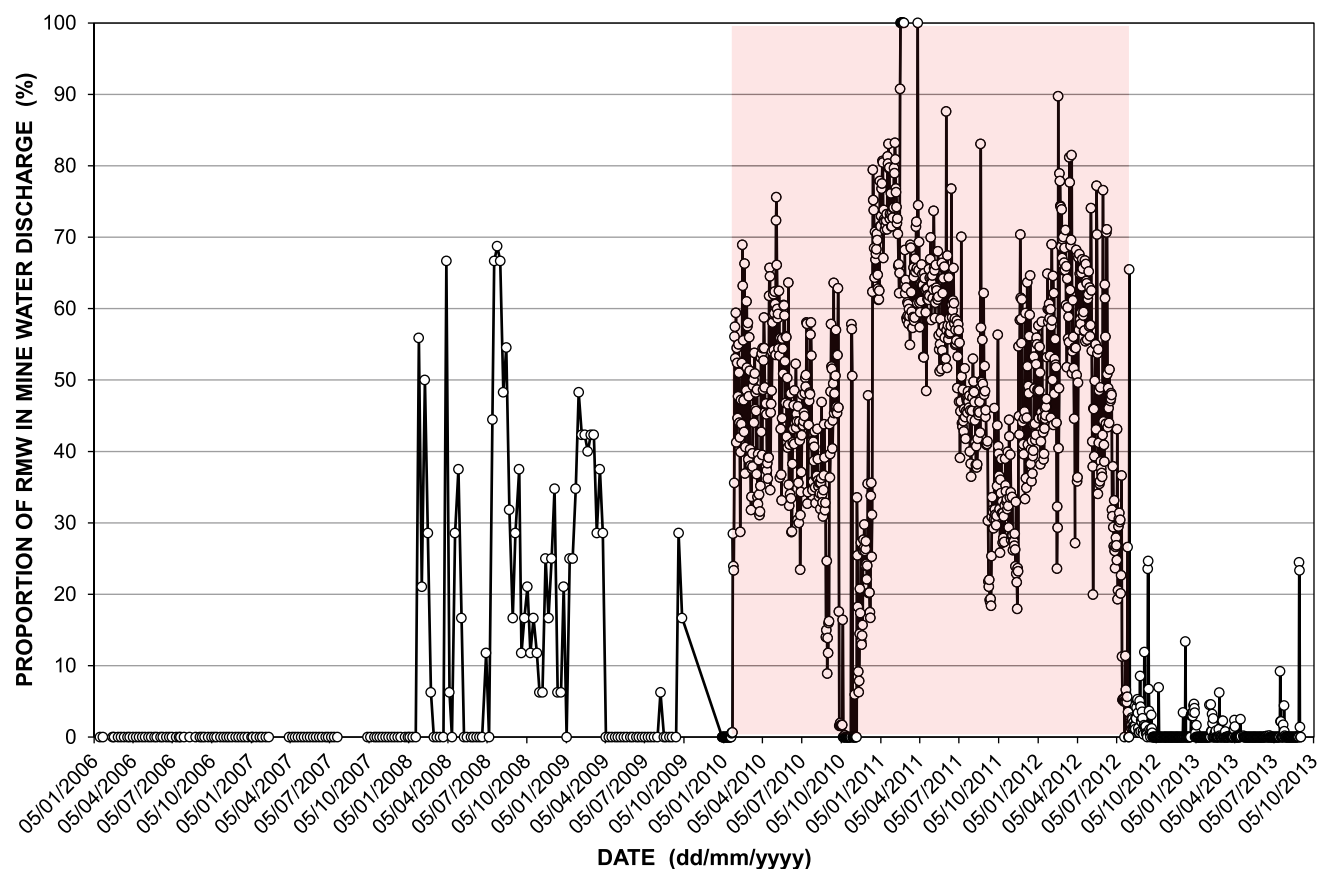


Fig. 14 Pattern and trend of RMW proportion in total mine water discharge

Plate 4 Treated mine water EoP flow gauging weir



presented in Fig. 10 reveals a difference in median discharge of $\sim 22.1 \text{ Mm}^3/\text{a}$ ($\sim 61 \text{ ML/d}$) between the pre-2010 and the post-2009 periods of record. The mine water treatment plant capacity of 34 ML/d since mid-2013 (Text Box 1) explains $\sim 56\%$ of the much greater median annual discharge of the post-2009 period. The remaining $\sim 9.9 \text{ Mm}^3/\text{a}$ ($\sim 27 \text{ ML/d}$) comprises raw mine water discharges via the

Tweelopie Spruit, municipal wastewater effluent via the Blougat Spruit (Sect. 3.2), and natural surface water runoff.

Alternative measures to mitigate the impact of adverse outcomes likely to be generated by the immediate and short-term mine water intervention measures include distributing the treated/neutralised mine water discharge between two or more drainages. Candidate drainages are the

Plate 5 Raw mine water flow gauging weir (original)



Plate 6 Raw mine water flow gauging weir showing inadequacy at high flows despite modification of original; note extended superstructure relative to position of lower front 'lifting eye' (circled) in common with Plate 10



Plate 7 Additional flow measurements structure (at right) installed to better gauge uncontrolled high flows of raw mine water; compare with Plate 6 setup



Blougat Spruit to the east of the Tweelopie Spruit, and the upper Riet Spruit to the west (Fig. 1). The latter drains into the Steenkoppies Basin which supports large-scale and intensive irrigation, and discharges via Maloney's Eye into

the Magalies River. In both cases, the target drainages receive treated municipal wastewater effluent, in the case of the Blougat Spruit from the Percy Stewart WWTW, and in that of the upper Riet Spruit from the Randfontein WWTW.

Text Box 1 Mine water control and management in the Western Basin

As was the case for all of the gold mines on the Witwatersrand in the first century of mining, mine water control and management in the West Rand Goldfield (aka the Western Basin) focussed on the removal of water ‘made’ in the underground workings to surface. This water was pumped out to keep the workings safe and productive (Handley 2004). The volumes involved were generally manageable, and it was only when mining descended beneath the productive karst aquifers of the overlying Malmani Subgroup dolomite that considerable and sometimes catastrophic volumes were encountered.

In the Western Basin, the pumping of mine water resulted in the drying up of a number of springs in the Krugersdorp Game Reserve. The water was released into the Tweelopie Spruit, from where it contributed to the discharge of the Bloubank Spruit and Crocodile River. The quality of this water was considered suitable for discharge without prior treatment beyond settling of suspended material and fines in a natural holding facility such as Robinson Lake. Nevertheless, the impact of this discharge on groundwater quality in the receiving karst environment of the Zwartkrans Basin was already evident in the data generated by the DWS emergency water supply study of the mid-1980s (Bredenkamp et al. 1986) (see Section 8.2.2 in Chapter “Chemical Hydrogeology” and Fig. 20 in Chapter “Physical Hydrogeology”).

In the late-1990s, geologists and environmental scientists in the employ of Randfontein Estates Gold Mine drew attention to the probability of acid mine drainage impacting on surface water resources following the cessation of mining. Calculations based on the observed rewatering rate and knowledge of the mine geometry predicted the ‘when’ and ‘where’ with remarkable accuracy. These predictions and cautions were ignored by the mining company and authorities. The recent effort to control and manage mine water decant in the Witwatersrand Basin is based on recommendations by Coetzee et al. (2010) to the Inter-Ministerial Committee on Acid Mine Drainage. Amongst other factors, the use of 1000 ML/d of high quality water from the Lesotho Highlands Water Scheme to maintain a TDS level of 600 mg/L in the Vaal River System drives the need for such control and management. The DWS tasked the Trans-Caledon Tunnel Authority (TCTA) with the implementation of

those recommendations required immediately and in the short-term, such as demanded by the active decant in the Western Basin. The scope and magnitude of these interventions in the Western Basin comprise the following activities (after TCTA 2012).

- *The immediate upgrading and retrofitting of the existing high density sludge (HDS) treatment plant to a capacity of ~24 ML/d. This was achieved and the plant commissioned in June 2012.*
- *The pumping of mine water from #8 Shaft to reduce the potentiometric head in the flooded underground mine workings and so eliminate active decant from mine structures such as #17 Winze, #18 Winze and the Black Reef Incline (BRI) Shaft in the locus of decant.*
- *The further upgrade of the HDS plant to a capacity of ~34 ML/d in the short-term. This was achieved in June 2013.*

The immediate and short-term intervention measures have been amended (DEA 2014b) to encompass pumping an average of 53 ML/d (peak of 60 ML/d) from #9 Shaft in order to reduce the potentiometric head in the flooded mine void to an elevation of ~1550 m amsl (~165 m below surface) from its current ~1670 m amsl. This will meet the obligation of maintaining an environmental critical level (ECL) at an elevation where the mine water potentiometric head has a negligible impact on the water resources environment. The treatment capacity in late-2017, however, was only some 40 ML/d.

The DWS embarked (mid-2017) on the implementation of a long-term solution (LTS) formulated in a multi-disciplinary study (DWA 2013a) completed in mid-2013 for all three basins in the Witwatersrand Goldfield. Strydom et al. (2016) provide a synopsis of the complex inter-relationships that describe the Witwatersrand AMD conundrum.

The potential benefits of mixing mine water with municipal wastewater effluent are discussed in Sect. 8.11 in Chapter “Chemical Hydrogeology”. An obvious advantage for the Steenkoppies Basin is the enhanced recharge of a karst aquifer that already suffers from over-abstraction for irrigated agriculture. The magnitude of this impact has resulted in a drastic reduction in the discharge of Maloney’s Eye (Holland et al. 2009), as well as the implementation of regulatory measures by the DWS to control abstraction (RSA 2008).

3.2 Blougat Spruit

The Blougat Spruit receives the effluent discharge from the Percy Stewart WWTW. This has turned an ephemeral stream into a perennial drainage since the commissioning of the plant in the 1950s. Designed to treat domestic sewage at a rate of 25 ML/d based on a design norm chemical oxygen demand (COD) of 600 mg/L, the inclusion of low-cost housing and industrial wastewater increased the COD loading to 1000 mg/L, reducing the plant capacity to 15 ML/d. Other factors such as poor maintenance and failure of structures (the facility straddles the regional Rietfontein Fault) reduced this even further to 5 ML/d. Following refurbishment completed in 2010, the treatment capacity is currently 24 ML/d (DWA 2011). This compares favourably with the recent inflow of 16 to 18 ML/d, i.e. 67–75% of capacity.

The record of effluent discharge (Fig. 15) indicates a median value of ~ 13 ML/d (~ 4.7 Mm³/a) and a 95%ile value of ~ 17.4 ML/d (~ 6.4 Mm³/a) in the period July 2007 to June 2009.⁵ The median discharge equates to $\sim 21\%$ of the long-term median annual discharge of the Bloubank Spruit system at station A2H049 (Fig. 10). The 2008 summer discharge of 16 to 18 ML/d reflects the rainfall of 883 mm gauged at the WWTW in this season (Fig. 3 in Chapter “Description of the Physical Environment”), compared to the 584 mm gauged in the 2009 summer and the average MAP of 767 mm for the 14 hydrological years since 2001 (Sect. 3.2 in Chapter “Description of the Physical Environment”).

Fig. 18 also shows the pattern of median daily inflow received by the facility. A comparison of this volume with that discharged to the Blougat Spruit indicates that the latter represented 44% (on average) of the inflow in the period up to September 2008, and 77% (on average) in the subsequent period of lesser inflow. The Percy Stewart WWTW also discharges a portion of its treated effluent to the adjacent Bergland property for the irrigation of cultivated lawn (unnumbered Plate, p 10). This amounted to ~ 1.3 ML/d (on average) in the period July 2007 to June 2009, i.e. the equivalent of 4.5% of the inflow into the plant, and 10% of the median discharge to the Blougat Spruit.

The results of opportunistic SDMs carried out at the causeway across the Blougat Spruit downstream of the Percy Stewart WWTW are presented in Table 5. The 2012 results indicate good agreement with the July 2007 to June 2008 record (Fig. 18). A significant increase is evident in the 2013 results, although the December 2013 result is

probably biased by heavy rainfall experienced in the region earlier in the week of 09/12/2013. The receiving drainage, the Blougat Spruit, drains much of the central Mogale City business district and north-western suburbs, including the Munsieville township and Delperton industrial area. The ‘return’ in 2017 to pre-2013 levels is not readily explained, but confirms the most probable minimum discharge of the plant.

The provision of treated effluent to the KGR for game watering and the flood irrigation of kikuyu grass in the northern portion of the reserve amounted to ~ 0.97 ML/d (on average). This is equivalent of 3.3% of the inflow received, and 7% of the discharge released to the Blougat Spruit. This practice was curtailed on 08/08/2008 (Brink 2008). The primary reason for the curtailment of this transfer and use was concern expressed by the West Rand District Municipality (WRDM) for the bacteriological quality of groundwater in the dolomitic aquifer that underlies this portion of the study area. The primary driver for this concern was a complaint by the landowner of Ptn 2/7/Rem of the farm Sterkfontein 1731Q regarding the poor quality of groundwater produced by a water supply borehole on the property. These circumstances were investigated and reported on by Hobbs (2008b), who concluded that the deterioration in groundwater quality was attributable to the excessive discharge of treated and untreated mine water, exacerbated by impoundment of this water in the stream channel promoting allogenic recharge (Sect. 8.2.3.3 in Chapter “Chemical Hydrogeology” and Fig. 10 in Chapter “Chemical Hydrogeology”). The absence of any indication of bacteriological contamination that might reasonably be attributed to the municipal wastewater impact confounds the decision to curtail the supply to the KGR on these grounds. It also begs the question why the similar practice on the adjoining Bergland property continues to be sanctioned, despite evidence that the ambient groundwater quality in Month 200 already reflected elevated nitrate concentrations (Sect. 8.2.3.2 in Chapter “Chemical Hydrogeology” and Fig. 10 in Chapter “Chemical Hydrogeology”).

In light of the above, it is lamentable that the apparent impact of the Percy Stewart WWTW as a significant contributor of poor quality water in the study area, remains poorly defined. Fortunately, routine monitoring at the Nedbank Olwazini Estate (NOE) further downstream in the Bloubank Spruit system provides data on bacterial levels (Sect. 6.1.2.6 in Chapter “Chemical Hydrology”) and nutrient concentrations (Sect. 6.3.2 in Chapter “Chemical Hydrology”) that bridge this deficiency to some extent. The veracity of this monitoring is, of course, subject to the possible opportunistic high volume release of poorly treated effluent at unconventional times such as at night.

⁵ The Mogale City Local Municipality has not made any monitoring data available since the provision of that for the period July 2007 to June 2009. The contribution of this facility to the flow and quality of the Bloubank Spruit in the last decade is therefore largely inscrutable.

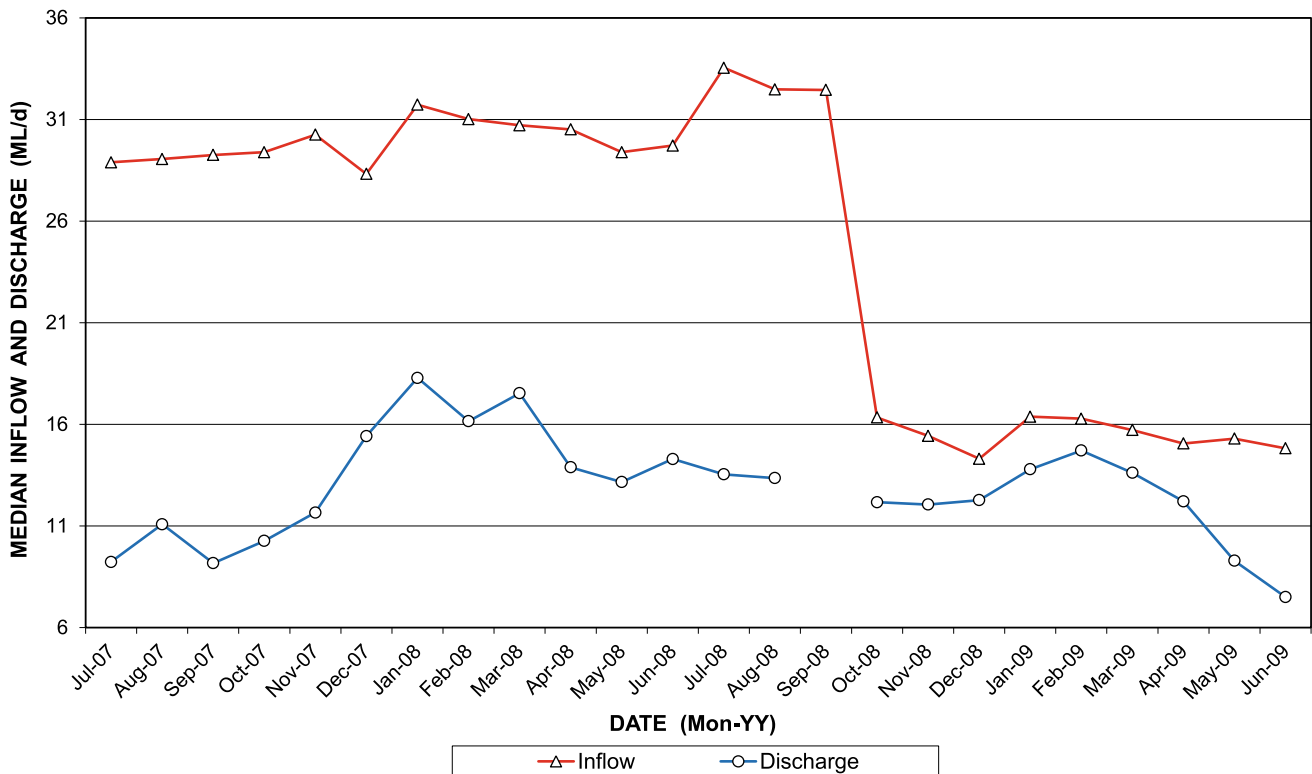


Fig. 15 Pattern and trend of inflow to and effluent discharge from the Percy Stewart WWTW

Table 5 Results of opportunistic flow measurements downstream of the Percy Stewart WWTW

| Date | 26/09/2012 | 24/10/2012 | 15/08/2013 | 12/12/2013 | 04/12/2017 |
|-------------------|------------|------------|------------|------------|------------|
| SDM Result (ML/d) | 15.9 ± 1.6 | 16.3 ± 1.6 | 24.0 ± 2.4 | 39.4 ± 5.9 | 14.8 ± 1.5 |

3.3 Crocodile River

The Crocodile River drains the north-western quadrant of the Johannesburg Metropole in Quaternary catchment A21E. This drainage flows northwards into Hartbeespoort Dam. Although it does not enter the COH (Fig. 2 in Chapter “Introduction and Background”), it is included in the study area because it traverses the COH buffer zone and receives the treated wastewater effluent discharged from the Driefontein WWTW operated and managed by the City of Johannesburg Metropolitan Municipality. The Driefontein WWTW collects and treats sewage from the northern areas of Roodepoort and Mogale City, has a treatment capacity of 35 ML/d (DWA 2011), and currently treats ~31 ML/d, or 88% of its capacity (DWA 2011). Gauging station A2H050 is located downstream of this facility (Fig. 2 in Chapter “Description of the Physical Environment”) before the confluence with the Bloubaank Spruit.

The DWS flow record for station A2H050 () spans a period of 44 years. It provides the monthly discharge statistics presented in Table 6. This shows that the month of

August reflects the lowest CoV value of ~76%, September the lowest median discharge value of 0.518 Mm³ (200 L/s), and October the lowest minimum discharge of 0.003 Mm³ (1.2 L/s).

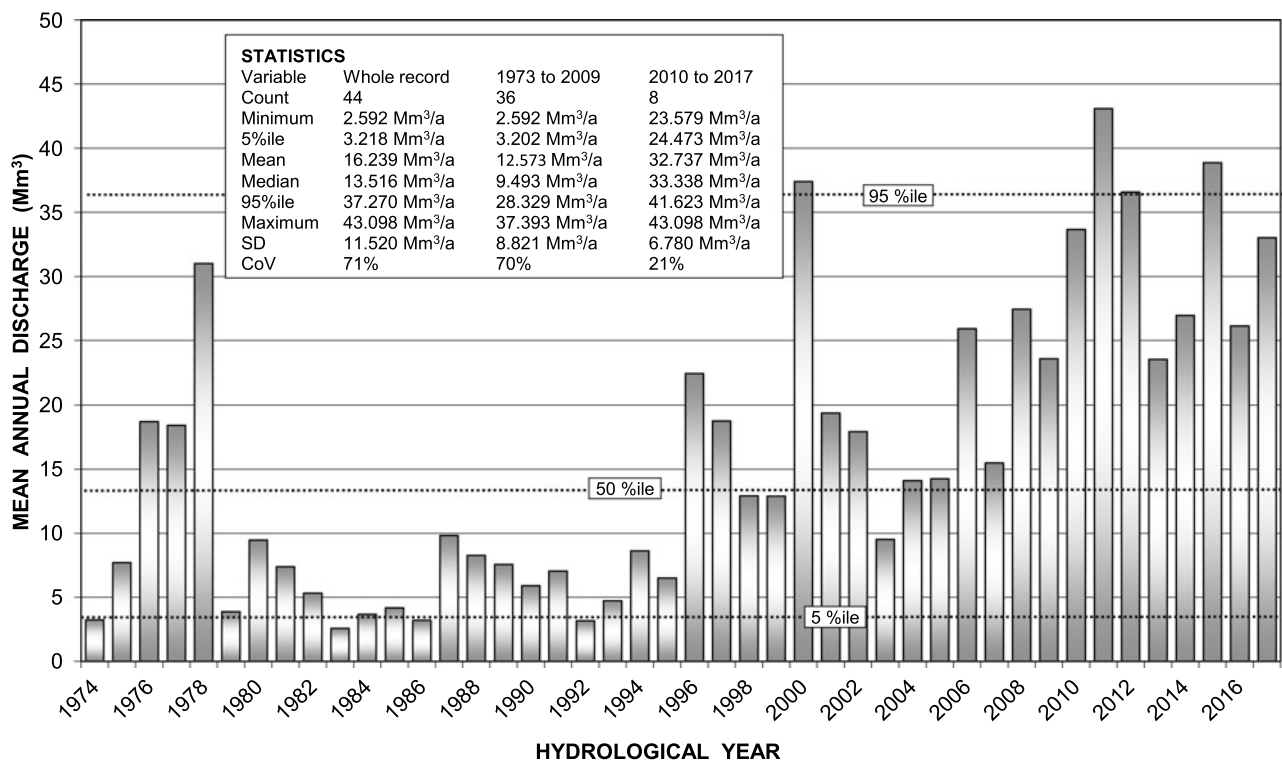
The long-term (whole record) median annual discharge of ~13.5 Mm³/a is ~56% that of the Bloubaank Spruit (Fig. 10), and represents ~7% of the Hartbeespoort Dam FSC. A more robust comparison with the Bloubaank Spruit discharge record must, however, consider separating the A2H050 hydrograph into two similar periods, namely a pre-2010 and a post-2009 period. The substantial difference in discharge statistics between these two periods and the whole record analysis is clearly evident (text box Fig. 16). The pre-2010 median contribution to Hartbeespoort Dam of 5% FSC more than trebles to ~17% FSC in the post-2009 period. Any number of reasons might account for an increase of this magnitude, but the expanding densely urbanised nature of the catchment is considered the major contributor.

The instantaneous monthly flow pattern at station A2H050 (Fig. 17) reveals a comparatively constant minimum value of <0.1 m³/s for the period up to at least October

Table 6 Statistical analysis of upper Crocodile River mean monthly discharge gauged at station A2H050 in the period October 1973 to September 2017

| Variable | Month | | | | | | | | | | | |
|----------|-------|-------|-------|--------|-------|-------|-------|-------|-------|-------|-------|-------|
| | Oct | Nov | Dec | Jan | Feb | Mar | Apr | May | Jun | Jul | Aug | Sep |
| n | 43 | 44 | 44 | 44 | 42 | 43 | 44 | 43 | 44 | 43 | 44 | 43 |
| Minimum | 0.003 | 0.107 | 0.196 | 0.262 | 0.151 | 0.157 | 0.131 | 0.141 | 0.153 | 0.130 | 0.081 | 0.039 |
| 5%ile | 0.104 | 0.188 | 0.329 | 0.339 | 0.224 | 0.205 | 0.191 | 0.172 | 0.181 | 0.183 | 0.164 | 0.137 |
| Mean | 0.860 | 1.073 | 1.527 | 2.304 | 2.440 | 2.152 | 1.527 | 1.240 | 1.018 | 0.871 | 0.762 | 0.709 |
| Median | 0.620 | 0.846 | 1.001 | 1.605 | 1.546 | 1.752 | 1.093 | 0.962 | 0.725 | 0.670 | 0.618 | 0.518 |
| 95%ile | 2.198 | 2.458 | 4.104 | 5.061 | 7.427 | 5.442 | 4.238 | 3.640 | 2.452 | 2.069 | 1.823 | 1.498 |
| Maximum | 2.612 | 2.696 | 6.715 | 10.084 | 9.583 | 7.350 | 5.097 | 4.203 | 3.574 | 2.478 | 2.290 | 3.200 |
| SD | 0.714 | 0.796 | 1.358 | 2.176 | 2.403 | 1.813 | 1.316 | 1.125 | 0.861 | 0.666 | 0.583 | 0.641 |
| CoV (%) | 83.1 | 74.2 | 88.9 | 94.4 | 98.5 | 84.2 | 86.2 | 90.7 | 84.6 | 76.5 | 76.4 | 90.4 |

All units are Mm^3 unless otherwise indicated. Analysis excludes months with missing and station rating exceedance data, but includes unaudited (recent) and estimated data

**Fig. 16** Pattern and trend of (upper) Crocodile River annual (a_h) discharge at station A2H050 in the period October 1973 to September 2017

1995, followed by a gradual increase since October 2002 to a value of $\sim 0.5 \text{ m}^3/\text{s}$ ($15.8 \text{ Mm}^3/\text{a}$) by August 2017. This pattern is attributed to discharge from the Driefontein WWTW where the treatment capacity of Unit 2, originally 15 ML/d when commissioned in 1988, was increased to 25 ML/d in 2002. The ‘base’ discharge of $15.8 \text{ Mm}^3/\text{a}$ is roughly half the volume currently treated by the plant.

4 Regional Context and Synthesis

The significance of the Bloubank Spruit system in the catchment of the regionally important Hartbeespoort Dam (Sect. 1) is evident in Table 7 and Fig. 18. Although the long-term normalised median discharge of the Bloubank Spruit, expressed as Mm^3/km^2 (mm) ranks only 5th out of

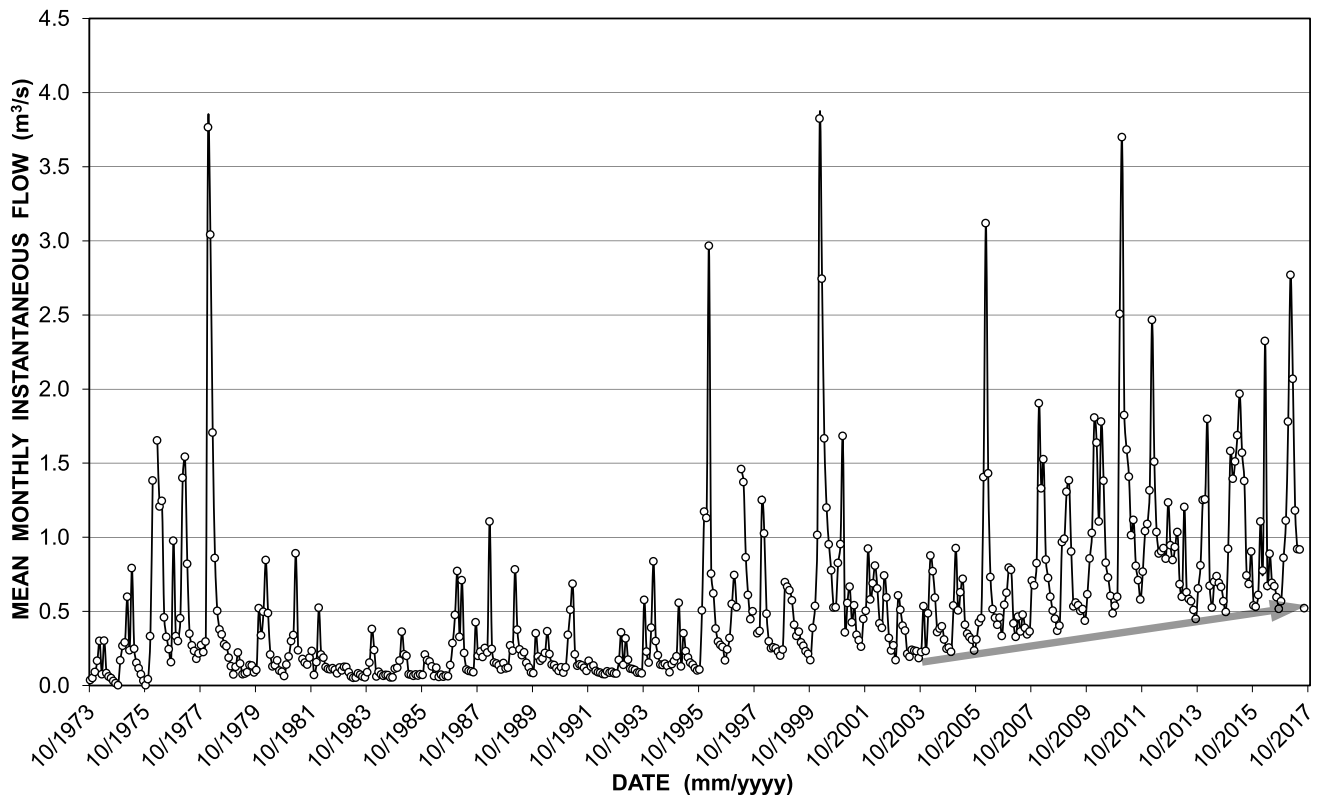


Fig. 17 Long-term monthly hydrograph of the upper reach of the Crocodile River at station A2H050 for the period October 1973 to September 2017

Table 7 Statistical analysis of the long-term annual (a_h) discharge contributions by the main rivers draining the Hartbeespoort Dam catchment

| Statistical parameter | Gauging station # and drainage | | | | | |
|--------------------------|--------------------------------|------------------|---------------------|------------------|--------------------|-----------------------|
| | A2H013 magalies R | A2H014 hennops R | A2H034 skeerpoort R | A2H044 jukskei R | A2H049 bloubank Sp | A2H050 crocodile R |
| Area (km ²) | 1171 | 1007 | 150 | 798 | 371 | 148 |
| Minimum | 0.799 | 11.422 | 4.858 | 66.027 | 11.051 | 2.592 |
| 5%ile | 1.179 | 16.259 | 5.478 | 70.729 | 12.688 | 3.215 |
| Mean | 30.607 | 70.373 | 12.497 | 155.710 | 26.674 | 15.604 |
| Median | 19.642 | 68.281 | 11.040 | 129.844 | 24.485 | 12.905 |
| 95%ile | 100.273 | 155.707 | 23.410 | 309.312 | 54.371 | 37.352 |
| Maximum | 127.094 | 187.304 | 34.745 | 326.546 | 66.851 | 43.098 |
| SD | 32.504 | 47.353 | 6.408 | 76.858 | 13.092 | 11.380 |
| CoV (%) | 106 | 67 | 51 | 49 | 49 | 73 |
| 50%ile MAR Ranking | 17 mm 6th | 68 mm 4th | 74 mm 3rd | 163 mm 1st | 66 mm 5th | 87 mm 2 nd |

All units are Mm³ unless otherwise indicated. Analysis excludes months with missing and station rating exceedance data, but includes unaudited (recent) and estimated data

The analysis period spans the 42 hydrological years 1974–2015 common to all six stations; A_h 2016 and 2017 not included because of periods of no record at the highest ranking station A2H044

The Crocodile River data exclude the ungauged discharge generated downstream of gauging stations A2H014, A2H044, A2H049 and A2H050

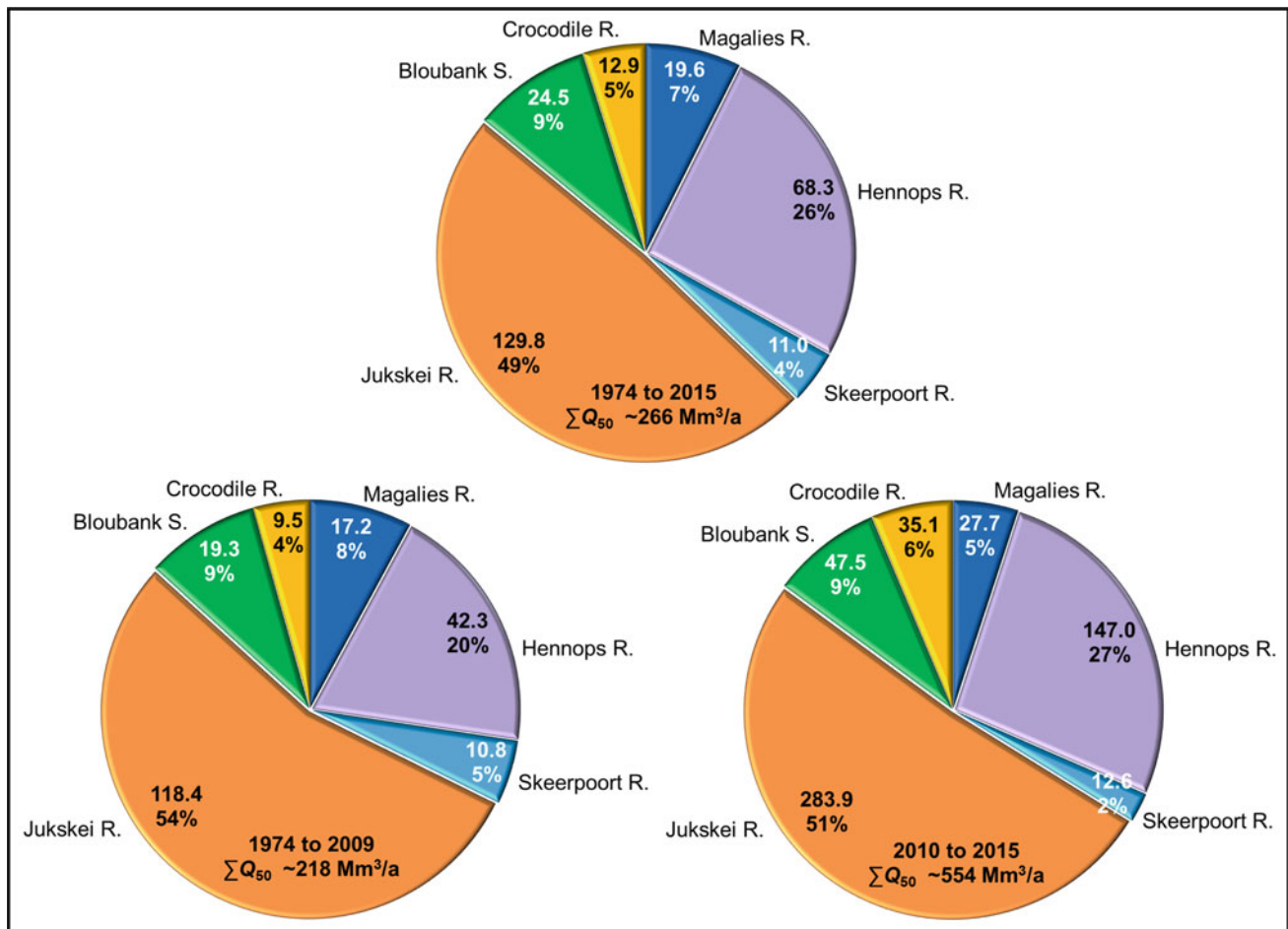


Fig. 18 Comparison of whole record (top), pre-2010 (left) and post-2009 (right) median annual (a_h) discharge contributions as Mm^3 and $\% \Sigma Q$ of the main rivers draining to Hartbeespoort Dam

six (Table 7), this system contributes the third highest discharge (9%) to the dam after the Jukskei River (48%) and Hennops River (26%) in the long-term (Fig. 18).

The long-term annual discharge contributions are also compared to those for the more recent 2010 to 2015 period⁶ (Fig. 18). This reveals the similar proportional contributions despite the $\sim 126\%$ greater aggregate discharge in the much shorter more recent period. The lowest CoV values reported in Table 7 are associated with those drainages that host sources of perennial discharge either in the form of an artificial contribution such as the Northern WWTW to the Jukskei River, or a natural contribution such as the karst springs of Quaternary basins A21D (Bloubank Spruit system) and A21G (Skeerpoort River). These ‘moderating’ contributions are reflected in CoV values of $\sim 50\%$ (Skeerpoort River, Jukskei River and Bloubank Spruit). The

poorest CoV value of 106% is associated with the Magalies River (Quaternary basin A21F), and reflects the two-fold impact of excessive groundwater abstraction in the Steenkoppies Basin on the discharge of Maloney’s Eye (the source of the river), and agricultural use in the intensively developed fertile valley. Proposed opencast gold mining in the Blaauwbank Spruit⁷ valley upstream (west) of the town of Magaliesburg (Fig. 2 in Chapter “Description of the Physical Environment”) poses a further threat to the water resources of the Magalies River.

Further inspection of the discharge data for the different drainages in the period 1974 to 2015 indicates that the $\sim 190 Mm^3$ FSC of Hartbeespoort Dam was equalled or exceeded in 30 of the 42 hydrological years on record (Fig. 19). The years of ‘deficit’ ($\Sigma Q < MAR$) all precede 1994. The sustained period of ‘below normal’ runoff

⁶ Hydrological years 2016 and 2017 excluded because of periods of no record at station A2H044.

⁷ Not to be confused with the Bloubank Spruit of the COH WHS.

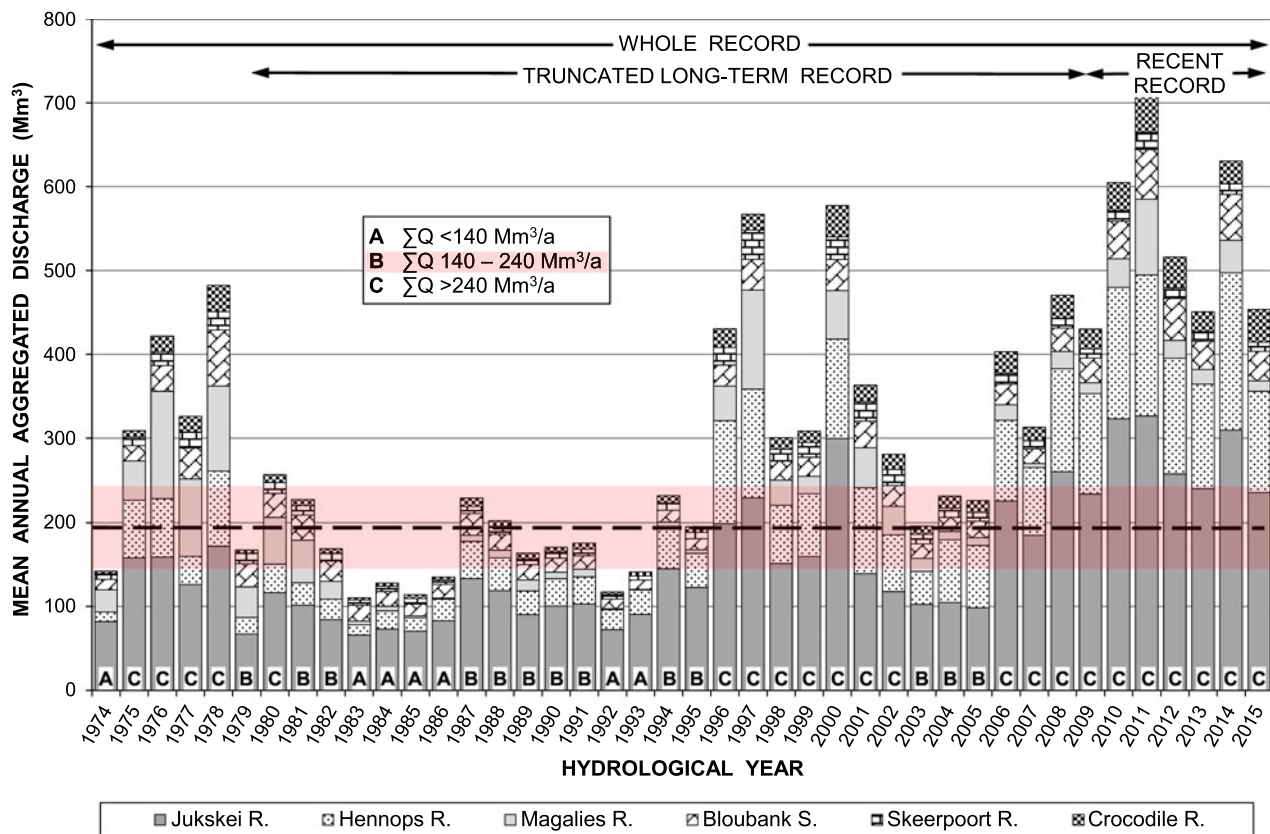


Fig. 19 Pattern and trend of combined annual discharge (ΣQ) by main drainages in the Hartbeespoort Dam catchment in the period of common record, compared to the $\sim 190 \text{ Mm}^3$ FSC of the dam

(horizontal pecked line) that approximates the mean annual runoff to the dam; left to right legend order is stacked from bottom to top in bar graph

commencing in 1979, terminated with $> \text{MAR}$ conditions in 1986. The relative constancy of the springflow-driven Bloubank Spruit and Skeerpoort River in the 'lean' runoff years is evident. Equally evident is the sustained period of above normal runoff commencing in 2006, and including the two highest runoff years (2011 and 2014) in the 42-year record.

As shown in Fig. 20, the proportional contribution of the karst basins to discharge in the Hartbeespoort Dam catchment is greater during periods when the aggregate runoff ($\Sigma Q/a$) is $< \text{FSC}$ of the dam. An analysis of the $\Sigma Q < 140 \text{ Mm}^3/a$ ($\text{FSC} - 25\%$) threshold returns a median contribution of 16.3%, and that for the $\Sigma Q > 240 \text{ Mm}^3/a$ ($\text{FSC} + 25\%$) threshold a median contribution of 11.8%. The $\Sigma Q/a = \text{FSC} \pm 25\%$ ($140\text{--}240 \text{ Mm}^3$) data bracket defines a median contribution of 14.1%. Expressed as a percentage of the FSC of the dam for the 36-year truncated long-term record, the two karst-dominated basins A21D and A21G together delivered a median annual contribution of $\sim 16\%$ ($\sim 32 \text{ Mm}^3$) in the range 8% (2008) to 24% (1979).

5 Surface Water Gains/Losses

5.1 Historical Information

In a regional DWS groundwater study in the mid-1980s (Brendenkamp et al. 1986), flow gaugings made at six locations in the Bloukat Spruit, the Riet Spruit and the Bloubank Spruit (Table 8) sought to quantify surface water losses to the karst aquifer. The results for the first four localities representing three water loss transects, are graphed in Fig. 21.

The results suggest that flow losses occur more or less uniformly at a rate of $\sim 23 \text{ L/s/km}$ along the reach of measurement. Immediately downstream of the Zwartkrans Spring (locality #5, Table 8), the gaugings reflect a surface flow of 258 L/s (22.3 ML/d) in the Bloubank Spruit. This value is replicated in the 2004 water balance for the Zwartkrans Basin presented by van Biljon (2006). Subtracting the 13 L/s of locality #4 from this value suggests a discharge of 245 L/s for the Zwartkrans Spring. The flow

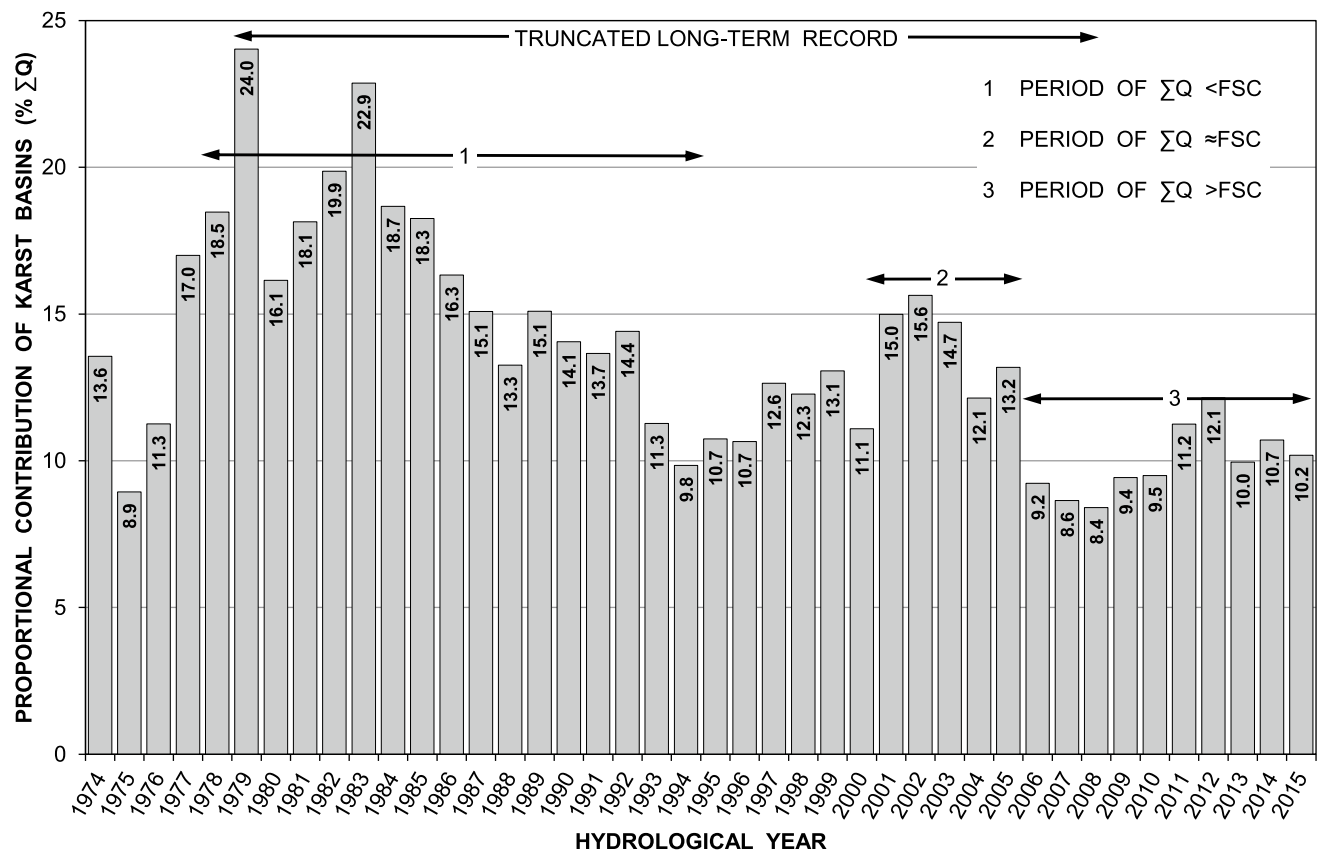


Fig. 20 Pattern and trend of proportional contribution of karst basins to the total annual discharge (ΣQ) by main drainages in the Hartbeespoort Dam catchment in the period of common record

Table 8 Flow gauging results ca. 1985 in the middle reaches of the Bloubank Spruit system (from Fig. 7.1 in Chapter “Physical Hydrogeology” of Bredenkamp et al. 1986)

| Locality # | Description | Distance (km) | Flow | | Gain/Loss Rate (L/s/km) | |
|------------|---|---------------|------|------|-------------------------|-------|
| | | | L/s | ML/d | | |
| 1 | Blougat Spruit downstream of Percy Stewart WWTW | 0 | 200 | 17.3 | -22.2 | - |
| 2 | Riet Spruit upstream of Oaktree agricultural holdings | 4.5 | 100 | 8.6 | | -40.7 |
| 3 | Riet Spruit upstream of Sterkfontein Cave | 6.0 | 39 | 3.4 | -21.7 | |
| 4 | Riet Spruit opposite Sterkfontein Cave | 7.2 | 13 | 1.1 | | +123 |
| 5 | Riet Spruit downstream of Zwartkrans Spring | 9.2 | 258 | 22.3 | +23.3 | |
| 6 | Bloubank Spruit downstream of Plover's Lake | 14.0 | 370 | 32.0 | | - |

then increases by 112 L/s (43%) between gauging localities #5 and #6, indicating a significant contribution from a source (or sources) not identified by Bredenkamp et al. (1986). The Kromdraai Spring, attributed a discharge of 30 L/s by Bredenkamp et al. (1986), is certainly a contributor, but leaves the balance of 82 L/s unaccounted for. An answer in this regard is provided in Sect. 7.4.3 in Chapter “Physical Hydrogeology”.

The results suggest that flow losses occur more or less uniformly at a rate of ~ 23 L/s/km along the reach of

measurement. Immediately downstream of the Zwartkrans Spring (locality #5, Table 8), the gaugings reflect a surface flow of 258 L/s (22.3 ML/d) in the Bloubank Spruit. This value is replicated in the 2004 water balance for the Zwartkrans Basin presented by van Biljon (2006). Subtracting the 13 L/s of locality #4 from this value suggests a discharge of 245 L/s for the Zwartkrans Spring. The flow then increases by 112 L/s (43%) between gauging localities #5 and #6, indicating a significant contribution from a source (or sources) not identified by Bredenkamp et al. (1986).

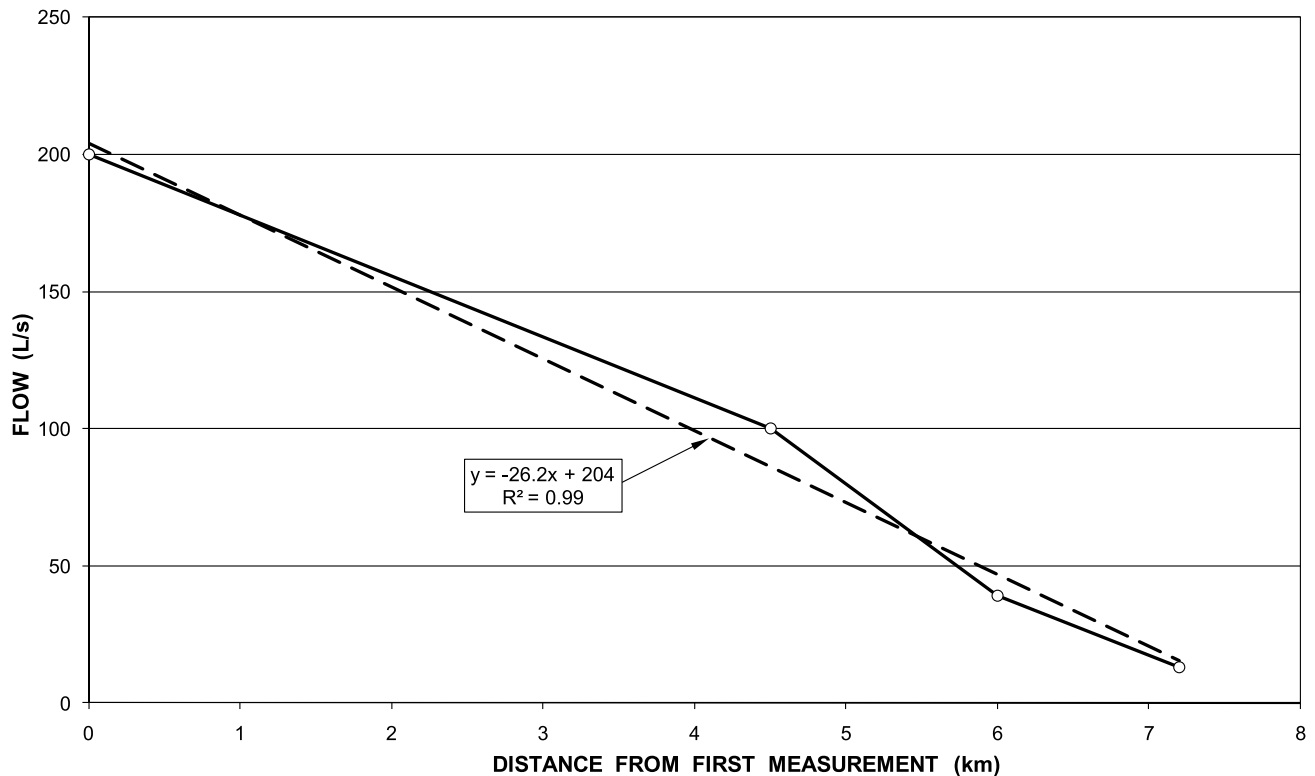


Fig. 21 Flow reduction with distance along the middle reaches of the Bloubank Spruit system upstream of Sterkfontein Cave (data from Table 8, localities 1 to 4)

The Kromdraai Spring, attributed a discharge of 30 L/s by Bredenkamp et al. (1986), is certainly a contributor, but leaves the balance of 82 L/s unaccounted for. An answer in this regard is provided in Sect. 7.4.3 in Chapter “Physical Hydrogeology”.

A more detailed ‘final’ water balance reported by JFA (2006) reflects a discharge of 208 L/s (18 ML/d) in the Bloubank Spruit (presumably in the vicinity of the Zwartkrans Spring). This comprised a 172 L/s component described as ‘Canal leaving stream at Danielsrust’ and a 36 L/s component described as ‘River flow leaving compartment’. The first (larger) component represents the A-furrow (Sect. 6.2) immediately downstream of the Zwartkrans Spring. Although the gain from locality #5 to locality #6 is also reported as a L/s/km value, it is more realistic to regard much (if not all) of this as concentrated point source input from the Plover’s Lake springs (Sect. 7.4.2 in Chapter “Physical Hydrogeology”) and the Kromdraai Spring (Sect. 7.4.3 in Chapter “Physical Hydrogeology”). Flow measurements generated in this study (Sect. 7.2.2.2 in Chapter “Physical Hydrogeology”) indicate no losses from the Bloubank Spruit in the reach between the Zwartkrans and Kromdraai springs.

Under normal flow conditions, the middle reach of the Riet Spruit between Tarlton and its confluence with the

Tweelopie Spruit is dry, having lost the flow from its upper reaches (sustained mainly by the treated effluent discharge from the Randfontein WWTW⁸) to the westerly Steenkoppies Basin by the time it reaches Tarlton (Barnard 1996; Holland et al. 2009). Whilst Hobbs and Cobbing (2007) verified only the former of these circumstances, Holland et al. (2009) present groundwater quality information that shows a WWTW effluent discharge signature in two samples, one sourced from a borehole located south of Tarlton in the Steenkoppies Basin, and the other north-east of Tarlton in the Zwartkrans Basin. The latter instance is provisionally considered to reflect the ingress of surface water bearing a WWTW effluent signature into the Zwartkrans Basin under abnormally high flow conditions. It is under such circumstances that the upper Riet Spruit carries water past Tarlton in a north-easterly direction across the hydrogeologic boundary between the Steenkoppies and Zwartkrans basins, after which it is lost through evaporation, evapotranspiration and infiltration in the river channel within a distance of ~3.4 km. Such circumstances were observed in early-2009 at the time the Holland et al. (2009) sample was

⁸ Data presented by Holland et al. (2009) indicate that the Randfontein WWTW discharged on average some 3.1 ML/d (36 L/s) to the upper Riet Spruit in the 5-year period 2004 to 2008.

collected in January 2009, and again in the first six months of 2010.

Flow rates measured in the 2005 winter at various locations on the Tweelopie Spruit as part of the then Harmony Gold (now Sibanye-Stillwater) Environmental Impact Assessment (EIA) (JFA 2006) represent a more recent attempt to quantify surface discharge in this portion of the study area. These measurements record an increase in discharge from 17 L/s (1.47 ML/d) designated as ‘..... originating from the mine void’ (i.e. in the mine area), to 29 L/s (2.51 ML/d) where the 4×4 trail crosses the Tweelopie Spruit at the Oukraal Lapa in the KGR, to 50 L/s (4.32 ML/d) where the tar road crosses the stream near the entrance to the lion enclosure in the KGR, to 59 L/s (5.10 ML/d) at the Aviary Dam outlet in the KGR, before declining to only 9 L/s (0.78 ML/d) immediately upstream of where the N14 national road crosses the stream. Discounting the possibility of surface water abstraction, these circumstances suggest that 50 L/s (4.32 ML/d) of stream flow was lost to the karst aquifer over a reach length of ~ 1.5 km. Although the loss rate of ~ 33 L/s/km is not too dissimilar to the ~ 23 L/s/km obtained from the Bredenkamp et al. (1986) data, it remains to be established whether groundwater resources (primarily springs) in the KGR contribute as much as 42 L/s (3.63 ML/d) to the flow in the Tweelopie Spruit upstream of the reach in question. Especially the almost doubling of flow between the 4×4 crossing and the entrance to the predator sanctuary (a distance of only ~ 730 m) seems extraordinary in the absence of a known source or sources. Admittedly outdated, especially against the background of known changes in the mine water discharge regime since 2005, these results are reported for the context they provide for similar measurements generated in this study.

Krige (2009) further illuminates the JFA (2006) set of historical flow measurements for the Blougat Spruit, from the point of discharge of Percy Stewart WWTW effluent to a position 5.86 km downstream on the Bloubank Spruit near the Sterkfontein Cave, reporting a loss rate of 26.6 L/s/km in late-winter 2005. This is again similar to the ~ 23 L/s/km obtained from the Bredenkamp et al. (1986) data, although the Percy Stewart WWTW contribution is represented by a mean annual discharge value of 19.3 ML/d rather than by a contemporaneous SDM. Nevertheless, this result is again reported for the context it provides to this study.

A re-assessment of the Krige (2009) reported loss rate of ~ 26.6 L/s/km suggests that this is an underestimate for the following reason. The distance of 5.86 km along which the loss rate is calculated, traverses 1.46 km of quartzitic bedrock followed by 4.4 km of dolomitic substrate, the reach ending in the vicinity of Sterkfontein Quarry. The loss rate should therefore be calculated only for the karst reach of 4.4 km, which yields a value of ~ 35 L/s/km. Even then, the

greater portion (2.84 km) of the 4.4 km karst reach traverses chert-poor dolomite of the Oaktree Formation over which losses to the aquifer might reasonably be expected to be minimal. If only the last 1.56 km of river reach traversing chert-rich Monte Christo Formation dolomite is considered, then the loss rate amounts to ~ 100 L/s/km. Of course, this loss rate is readily accomplished via a single point source infiltration feature such as an instream swallet.

The critical review of the JFA (2006) and Krige (2009) flow data is equally relevant to the Bredenkamp et al. (1986) data reported in Table 8. This is especially true for the flow loss of 100 L/s observed between localities 1 and 2 in Table 8. The last ~ 1 km of the 4.5 km reach between these localities traverses chert-rich dolomite of the Monte Christo Formation. The loss rate of ~ 100 L/s/km is similar to that re-calculated from the JFA (2006) and Krige (2009) observations for an overlapping reach.

It is also important to recognise that the results obtained by both Bredenkamp et al. (1986) and Krige (2009) pertain to the hydrodynamic conditions that existed in the relevant river/stream reaches ca. 1985 and 2005, respectively. To what extent these conditions have changed over time has not been investigated, although the similar results obtained in 1985 and 2005 suggest that any changes were negligible and probably absorbed by the unreported error margin(s) associated with the original flow measurements. Despite these qualifications, the historical discharge measurement and flow loss rate data provide an important reference for the similar assessment presented in Sect. 5.2.

5.2 Recent/Current Information

5.2.1 Tweelopie Spruit and Riet Spruit

Flow gauging at the inlet to the KGR and streamflow measurements at the Aviary Dam outlet in the KGR, as reported by DD Science Laboratory cc. at Western Basin Technical Working Group⁹ meetings, unfortunately reflect equivocal results. This is attributed to the lower confidence afforded the accuracy of gauged flow measurements at the downstream station (D Dorling, personal communication). The exceptionally wet 2010 and 2011 summer rainfall seasons again manifested excessive discharge in the Tweelopie Spruit. This was driven mainly by the resumption in late-January 2010 of uncontrolled mine water discharge in the mine area upstream of the KGR. The resulting discharge, comprising a mixture

⁹ The Western Basin Technical Working Group (WBTWG) was a forum convened by the Department of Water Affairs to consider the issue of AMD in the West Rand Goldfield. Its bi-annual meetings were attended by a wide range of stakeholders representing environmental lobby groups, mining houses, provincial and national government departments, local and district municipalities and research councils.

of treated/neutralised mine water from the HDS Plant and raw mine water subjected to emergency in-stream liming¹⁰ at the point of release, again peaked at ~ 50 ML/d as it did in early-2008.

Field (2006) and Walter et al. (2012) recognise estimations of leakage rate through a streambed by any means other than synoptic discharge measurements (Plate 8) as a poor substitute for in-stream flow gain–loss measurements between upstream and downstream gauging stations. Further, that the error will be unquantifiable and will range from insignificant to severe in all instances. The SDM data were obtained using a current meter¹¹ applied in two basic scenarios, namely (a) the classical cross-sectional flow section (width \times depth \times velocity) method (Plate 8) and (b) the cross-sectional pipe section (chord length¹² \times velocity) method. Computation of the data was facilitated through spreadsheet-based algorithms.

The results of SDMs carried out on two occasions at a number of localities (Fig. 22) in the downstream receiving drainages are presented in Tables 9 and 10. These indicate a general loss of water down to locality #6, followed sequentially by a water gain to locality #7 (Plate 8) and a substantial loss to locality #8 (Table 9). Whereas localities #1, #5, #6 and #7 reflect flow in the Tweelapie Spruit, locality #8 reflects flow in the lower reaches of the Riet Spruit immediately before its confluence with the Blougat Spruit tributary. SDMs carried out at localities #6 and #7 on 11 occasions returned equivocal results (Table 11). The comparatively small differences seldom exceed the error margin ($\pm 10\%$) of the measurements. Nevertheless, the results indicate a gain on six occasions, and a loss on five occasions. The gains fall in the range 9 to 46 L/s/km over the ~ 1.5 km distance between the sites, and the losses a similar range of 9 to 35 L/s/km. These findings contextualise reports by JFA (2006), Holland (2007) and Krige (2009) that the Tweelapie Spruit loses water¹³ to the karst via the Rietfontein Fault (Fig. 22 and Fig. 14 in Chapter “Physical Hydrogeology”) that intersects the stream between these two sites (Plate 9).



Plate 8 View of synoptic discharge measurement with current meter in progress at site F11S12, showing both the relatively ‘clean’ cross-sectional area of flow (from bottom left to right foot of observer) and the laminar nature of flow over the crest of the weir

The stream flow discharge and loss data are illustrated in Fig. 23. This shows that prior to the 2010 summer, site MRd witnessed surface flow only under exceptional discharge conditions,¹⁴ when under ‘normal’ circumstances all of the discharge entering the Riet Spruit at Glen Almond via the Tweelapie Spruit was lost primarily to recharge of the karst aquifer before reaching this station. This is exemplified in the measurements recorded on 09 and 22/09/2009 respectively (Table 12 and Fig. 23). These indicate an absorptive capacity defined by an ingress value of ~ 14 ML/d (~ 41 L/s/km). A similar situation is described by Katz et al. (1998) and Katz et al. (2004) for sinkhole lakes in the Suwannee and northern Leon counties, respectively, in northern Florida, USA. These lakes overflow when inflow exceeds ~ 200 L/s (~ 17 ML/d). Sasowsky and White (1993) describe similar circumstances for the East Fork of the Obey River in north-central Tennessee (USA), reporting that at discharges of <4.5 m³/s the entire flow of the river disappears into the subsurface. Bailly-Comte et al. (2009) relate the ‘swallow capacity’ of a cave in a karst watershed in southern France with a losing stream.

¹⁰ Carried out in the period mid-March to mid-May 2010 (Sect. 6.5.1 in Chapter “Chemical Hydrology” and Footnote 59).

¹¹ Flow velocity determined with an OTT C20 current meter and Z400 signal counter set using impeller # 1–239627 (diameter = 125 mm, pitch = 0.25 m) mounted on a 20 mm diameter rod.

¹² Height of water flow through circular pipe section of known diameter.

¹³ JFA (2006) report a single measurement (see Table 4 in Chapter “Description of the Physical Environment”, p 46) of a water loss of 4.3 ML/d in late-winter 2005, which translates to a loss of ~ 40 L/s/km over the 1.25 km distance between the JFA localities.

¹⁴ Caused by excessive and uncontrolled AMD overflow from the mine area together with excess surface runoff associated with very high rainfall events.

Table 9 Change in flow with distance downstream of the mine area on 05/02/2010

| Locality # and description | | Distance (m) | | Flow | |
|----------------------------|-----------------------------------|--------------|------------|------|-----------------------------|
| | | segmental | cumulative | ML/d | ΔQ (+ gain; – loss) |
| 1 | KGR inflow | 0 | 0 | 40 | |
| 6 | Aviary dam inlet in KGR | 4905 | 4905 | 32 | + 3 ML/d |
| 7 | KBW dam outlet at N14 (F11S12) | 1540 | 6445 | 35 | [+23 L/s/km] |
| 8 | Riet Spruit at Malmani road (MRd) | 3900 | 10 345 | 7 | –28 ML/d [–83 L/s/km] |

Table 10 Change in flow with distance downstream of the mine area on 01/04/2010

| Locality # and description | | Distance (m) | | Flow | |
|----------------------------|------------------------------------|--------------|------------|------|--|
| | | Segmental | cumulative | ML/d | ΔQ (+ gain; – loss) |
| 5 | 4 × 4 Track at Oukraal Lapa in KGR | 2815 | 2815 | 52 | |
| 6 | Aviary Dam inlet in KGR | 2090 | 4905 | 34 | + 6 ML/d [+46 L/s/km] |
| 7 | KBW Dam (F11S12) | 1540 | 6445 | 40 | |
| 8 | Riet Spruit at Malmani Road (MRd) | 3900 | 10,345 | 10 | –16 ML/d [–88 L/s/km] –30 ML/d [–89 L/s/km] |

Table 11 Quantification of stream flow gains/losses in the lower reach of the Tweelopie Spruit

| Date | Flow @ aviary dam inlet (ML/d) | Flow @ F11S12 (ML/d) | Flow difference (ML/d) | Flow gain/Loss rate ^a (L/s/km) |
|------------|--------------------------------|----------------------|------------------------|---|
| 22/09/2009 | 19.4 ± 1.9 | 14.9 ± 1.5 | –4.5 | –35 |
| 05/02/2010 | 32.1 ± 3.2 | 35.2 ± 3.5 | +3.1 | +24 |
| 01/04/2010 | 34.4 ± 3.4 | 40.4 ± 4.0 | +6.0 | +46 |
| 19/08/2010 | 22.0 ± 2.2 | 25.8 ± 2.6 | +3.8 | +44 |
| 19/11/2010 | 21.0 ± 2.1 | 22.2 ± 2.2 | +1.2 | +9 |
| 27/07/2011 | 30.2 ± 3.0 | 31.9 ± 3.2 | +1.7 | +13 |
| 14/08/2012 | 23.7 ± 2.4 | 22.5 ± 2.3 | –1.2 | –9 |
| 06/03/2013 | 22.7 ± 2.3 | 20.7 ± 2.1 | –2.0 | –15 |
| 15/08/2013 | 31.9 ± 3.2 | 30.1 ± 3.0 | –1.8 | –14 |
| 15/10/2013 | 31.4 ± 3.1 | 29.6 ± 3.0 | –1.8 | –14 |
| 12/12/2013 | 18.3 ± 1.8 | 22.2 ± 2.2 | +3.9 | +30 |

^a Based on a distance of ~1.5 km between localities
 Bold text denotes result exceeds the error margin of ±10%

Flow measurements made on 31 occasions at stations F11S12 and MRd (Table 12) further quantify and elucidate the magnitude of surface water loss to the karst aquifer. It is notable that eight of the 14 measured discharges at the downstream station MRd in Period 3 substantially exceed the previous highest measured value of 11.7 ML/d recorded on 06/05/2010 (Table 12). Further, that five of the 15 Period 3 surface flow losses between stations F11S12 and MRd represent the lowest in the record of measurements since flow at station MRd was first recorded. These circumstances suggest that the absorptive capacity of the karst aquifer underlying the losing ~3.9 km reach of the Riet Spruit reached a new equilibrium condition in the 2011 wet season that continued through to the end of a_h 2015.

It is recognised that not all of the water loss is to the karst aquifer of the Zwartkrans Subcompartment. A part thereof is lost through evaporation and riparian evapotranspiration (Sect. 7.4.1 in Chapter “Physical Hydrogeology”). Nevertheless, the measured flow losses reflect mean and median values of ~54 L/s/km (18.1 ML/d) and 51 L/s/km (17.3 ML/d), respectively (Table 12). Although the minimum value of ~20 L/s/km (Period 3) compares favourably with the typical leakage rate of ~25 L/s/km reported in earlier studies (Sect. 5.1), the maximum value of 95 L/s/km (period 2) approaches the re-calculated upper limit of ~100 L/s (Sect. 5.1). Fig. 23 suggests that a threshold flow value exists at station F11S12 below which all surface flow is lost to the karst aquifer, leaving the downstream



Plate 9 Original SDM flow gauging station MRd in separated pipe (below left, 05/02/2010) and one of two identical replacement culverts (below right, 05/10/2010) beneath the reconstructed gravel Malmani Road across the Riet Spruit at this location

station MRd dry. Conversely, flow that exceeds the threshold value at F11S12 results in surface water flow past station MRd. This observation is explored in Fig. 24. The linear regression equation for Period 2 yields a cut-off y-value of ~ 15 ML/d. The similar equation for Period 3 returns a cut-off value of ~ 14 ML/d. These flows define the 'threshold' value range.

The existence of two different regression equations associated with different time periods of a single data set supports the conclusion regarding a change in the hydraulic response that characterises the surface and subsurface hydrologic interaction along the subject stream reach. The set of 'before-and-after' historical Google Earth® images presented in Fig. 25 provide a possible explanation. These images (and Plate 10) show the formation of ferrous hydroxide $[\text{Fe}(\text{OH})_2]$ deposits in the stream channel that might reduce streambed permeability. In any event, it is concluded that the 'absorptive capacity' (and therefore also the 'transmissive capacity') of the epikarst along the ~ 3.9 km reach of the Riet Spruit between stations F11S12 and MRd, functions with 100% efficiency at surface discharges of up to ~ 15 ML/d (175 L/s). Above this threshold, the 'absorptive capacity' is exceeded, the per cent infiltration of surface flow reduces, and the volume of surface water discharge passing station MRd is greater.

Text Box 2 The permanence (insolubility) of iron (oxy)hydroxide precipitates

A key environmental concern regarding the impact of AMD on receiving watercourses is the permanence of the iron oxyhydroxide efflorescence (precipitate) that

coats/encrusts stream channels. This depends on a number of factors including pH, temperature, ionic strength and organic ligands, e.g. humic acid (Liu and Millero 1999), and microbial activity and specific surface area (Bonneville et al. 2009). These factors influence the solubility of the precipitate, which ranges from fairly soluble poorly crystalline forms such as freshly precipitated amorphous ferrihydrite and hydrous ferric oxide, to insoluble crystalline forms such as goethite and hematite. The former present as a slimy/gelatinous ferric hydroxide $[\text{Fe}(\text{OH})_3]$ coating that is quite easily rubbed off the surface on which it has formed. The latter form the hard ferrous hydroxide $[\text{Fe}(\text{OH})_2]$ crust that 'cements' the streambed and encapsulates stones and vegetation.

The solubility of a substance in a given solvent is measured as the Saturation concentration, where adding more solute does not increase the concentration of the solution. Solubility is commonly expressed as a concentration, e.g. mg/kg, mg/L, molarity, molality mole, function or similar. The maximum equilibrium amount of solute that can dissolve per amount of solvent is its solubility in that solvent under prevailing specific conditions, e.g. temperature and pressure. Solubility products of ferric oxyhydroxides reported in the literature span more than three orders of magnitude (Bonneville et al. 2009). The fairly soluble poorly crystalline forms pose a lesser risk in regard to permanency than do the insoluble crystalline forms. The solubility of the former are $\sim 10^{-14}$, and of the latter $\sim 10^{-36}$ (Gayer and Woontner 1956). Fox (1988) derived a solubility equation for aqueous ferric

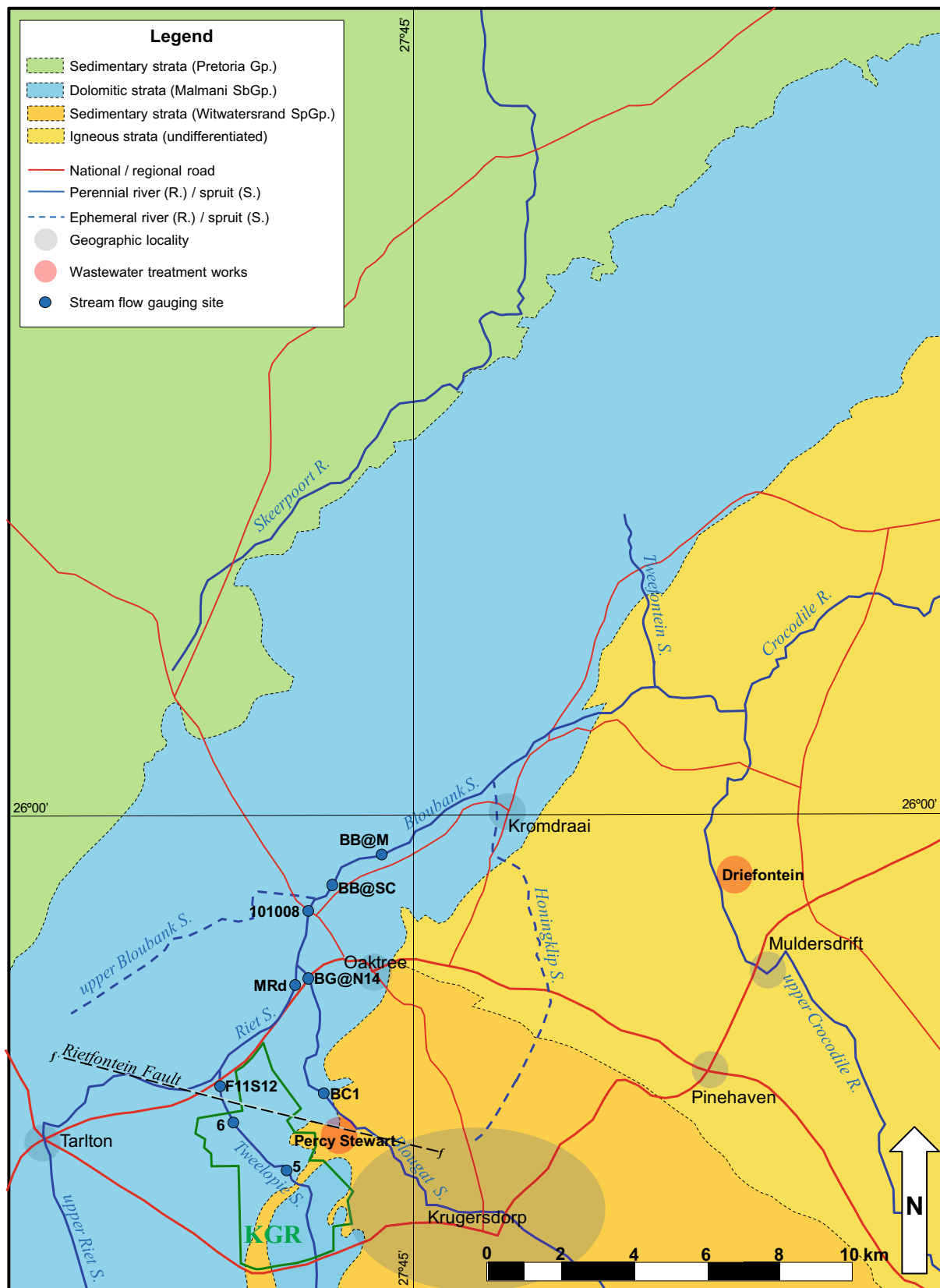


Fig. 22 Manually gauged stream flow measurement sites employed in this study

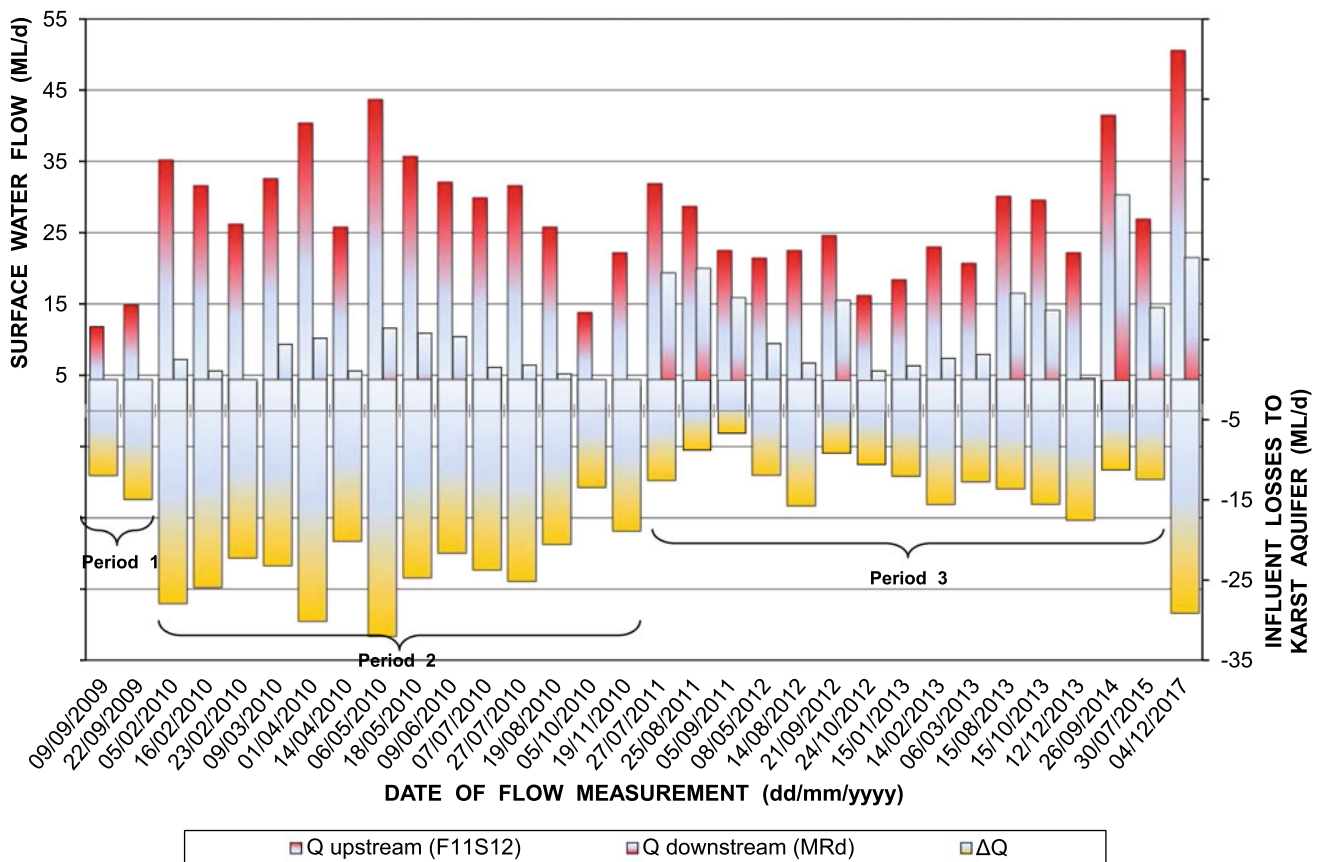


Fig. 23 Pattern and trend of discharge and flow losses in the lower reach of the Riet Spruit (data from Table 12)

hydroxide colloids that returned a solubility value of $10^{-31.7}$. Appelo and Postma (2009) report solubility product (K) values of common Fe-oxyhydroxides in the range 10^{-37} to 10^{-43} .

As with all solid material exposed to the environment, the insoluble crystalline forms are susceptible to weathering and decomposition. In this instance, this takes the form of erosion through in-stream mechanical abrasion by continuous flow and suspended matter that, with time, will remove the precipitate and transport it downstream. It will eventually erode to fine particulate matter visually indistinguishable from natural stream sediments.

5.2.2 Blougat Spruit

Flow measurements carried out at two stations on the Blougat Spruit on 18/05/2010 (Table 13) corroborate the figures reported by Bredenkamp et al. (1986) for flow losses downstream of the Percy Stewart WWTW. The upstream station BC1 (Fig. 26 and Plate 11) is a causeway across this

stream located ~ 1.1 km downstream of the WWTW effluent discharge point (EoP) into this drainage. The downstream station BG@N14 (Fig. 26 and Plate 12) is located at the intersection with the N14 national road. The apparent loss rate of ~ 23 L/s/km (Table 13) is similar to the ~ 22 L/s/km reported by Bredenkamp et al. (1986) between localities 1 and 2 (Table 8).

The result, however, is subject to a similar re-calculation as was applied to the Bredenkamp et al. (1986) data, returning a slightly higher loss rate of ~ 26 L/s/km across the 3.1 km reach that crosses over dolomite. Restricting the losing reach to <1 km over chert-rich dolomite of the Monte Christo Formation increases the loss rate to at least ~ 81 L/s/km. This again approaches the ~ 100 L/s/km obtained for the re-calculated historical data (Sect. 5.1). Nevertheless, the observations confirm the Blougat Spruit as a source of allogenic recharge to the karst system in the amount of ~ 7 ML/d.

5.2.3 Bloubank Spruit

This drainage rises on dolomite in the western portion of the Zwartkrans Basin, and traverses only dolomite in its easterly path to the confluence with the Riet Spruit at Oaktree.

Table 12 Quantification of stream flow losses in the lower reach of the Riet Spruit

| Date | Flow @ F11S12 (ML/d \pm 10%) | | Flow @ MRd (ML/d \pm 5%) | | Flow loss (ML/d) | | Flow loss rate (L/s/km) ^a | |
|------------|--------------------------------|----------------|----------------------------|----------------|------------------|----------|--------------------------------------|-----------------|
| 09/09/2009 | 11.9 \pm 1.2 | Period 1 | 0 | Period 1 | 11.9 | Period 1 | 35 | Period 1 |
| 22/09/2009 | 14.9 \pm 1.5 | | 0 | | 14.9 | | 44 | |
| 05/02/2010 | 35.2 \pm 3.5 | Period 2 | 7.3 \pm 0.4 | Period 2 | 27.9 | Period 2 | 83 | Period 2 |
| 16/02/2010 | 31.6 \pm 3.2 | | 5.7 \pm 0.3 | | 25.9 | | 77 | |
| 23/02/2010 | 26.2 \pm 2.6 | | 4.0 \pm 0.2 | | 22.2 | | 66 | |
| 09/03/2010 | 32.6 \pm 3.3 | | 9.4 \pm 0.5 | | 23.2 | | 69 | |
| 01/04/2010 | 40.4 \pm 4.0 | | 10.3 \pm 0.5 | | 30.1 | | 89 | |
| 14/04/2010 | 25.8 \pm 2.6 | | 5.7 \pm 0.3 | | 20.1 | | 60 | |
| 06/05/2010 | 43.7 \pm 4.4 | | 11.7 \pm 0.6 | | 32.0 | | 95 | |
| 18/05/2010 | 35.7 \pm 3.6 | | 11.0 \pm 0.6 | | 24.7 | | 73 | |
| 09/06/2010 | 32.1 \pm 3.2 | | 10.5 \pm 0.5 | | 21.6 | | 64 | |
| 07/07/2010 | 29.9 \pm 3.0 | | 6.2 \pm 0.3 | | 23.7 | | 70 | |
| 27/07/2010 | 31.6 \pm 3.2 | | 6.5 \pm 0.3 | | 25.1 | | 74 | |
| 19/08/2010 | 25.8 \pm 2.6 | | 5.3 \pm 0.3 | | 20.5 | | 61 | |
| 05/10/2010 | 13.8 \pm 1.4 | | 0.4 | | 13.4 | | 40 | |
| 19/11/2010 | 22.2 \pm 2.2 | | 3.4 \pm 0.2 | | 18.8 | | 56 | |
| 27/07/2011 | Period 3 | 31.9 \pm 3.2 | Period 3 | 19.4 \pm 1.0 | Period 3 | 12.5 | Period 3 | 37 |
| 25/08/2011 | | 28.7 \pm 2.9 | | 20.0 \pm 1.0 | | 8.7 | | 26 |
| 05/09/2011 | | 22.5 \pm 2.3 | | 15.9 \pm 0.8 | | 6.6 | | 20 |
| 08/05/2012 | | 21.4 \pm 2.1 | | 9.6 \pm 0.5 | | 11.9 | | 35 |
| 14/08/2012 | | 22.5 \pm 2.3 | | 6.8 \pm 0.3 | | 15.7 | | 47 |
| 21/09/2012 | | 24.6 \pm 2.5 | | 15.5 \pm 0.8 | | 9.1 | | 27 |
| 24/10/2012 | | 16.2 \pm 1.6 | | 5.7 \pm 0.3 | | 10.5 | | 31 |
| 15/01/2013 | | 18.4 \pm 1.8 | | 6.4 \pm 0.3 | | 12.0 | | 36 |
| 14/02/2013 | | 23.0 \pm 2.3 | | 7.5 \pm 0.4 | | 15.5 | | 46 |
| 06/03/2013 | | 20.7 \pm 2.1 | | 8.0 \pm 0.4 | | 12.7 | | 38 |
| 15/08/2013 | | 30.1 \pm 3.0 | | 16.5 \pm 0.8 | | 13.6 | | 40 |
| 15/10/2013 | | 29.6 \pm 3.0 | | 14.1 \pm 0.7 | | 15.5 | | 46 |
| 12/12/2013 | | 22.2 \pm 2.2 | | 4.7 \pm 0.2 | | 17.5 | | 52 |
| 26/09/2014 | | 41.5 \pm 4.2 | | 30.3 \pm 1.5 | | 11.2 | | 33 |
| 30/07/2015 | | 26.9 \pm 2.7 | | 14.5 \pm 0.7 | | 12.4 | | 37 |
| 04/12/2017 | 50.6 \pm 5.1 | | 21.5 \pm 1.1 | | 29.1 | | 86 | |
| n | 32 | | 32 | | 32 | | 14 ^b | 15 ^c |
| Minimum | 11.9 | | 0.0 | | 6.6 | | 39.8 | 19.6 |
| Mean | 27.6 | | 9.8 | | 17.5 | | 70.9 | 36.7 |
| Median | 26.6 | | 7.7 | | 15.5 | | 70.3 | 36.8 |
| Maximum | 50.6 | | 30.3 | | 32.0 | | 95.0 | 51.9 |

^a Based on a distance of \sim 3.9 km between localities^b Period 2 statistics^c Period 3 statistics

Although it is an ephemeral drainage upstream of this junction, these circumstances identify it as a source of autogenic recharge to the Zwartkrans Basin when it carries runoff.

Of greater importance are the Tweelopie and Riet spruit tributaries that deliver mine water from the Western Basin in the south-western portion of the study area. A 17.7 km long stream profile spanning an elevation difference of 150 m is

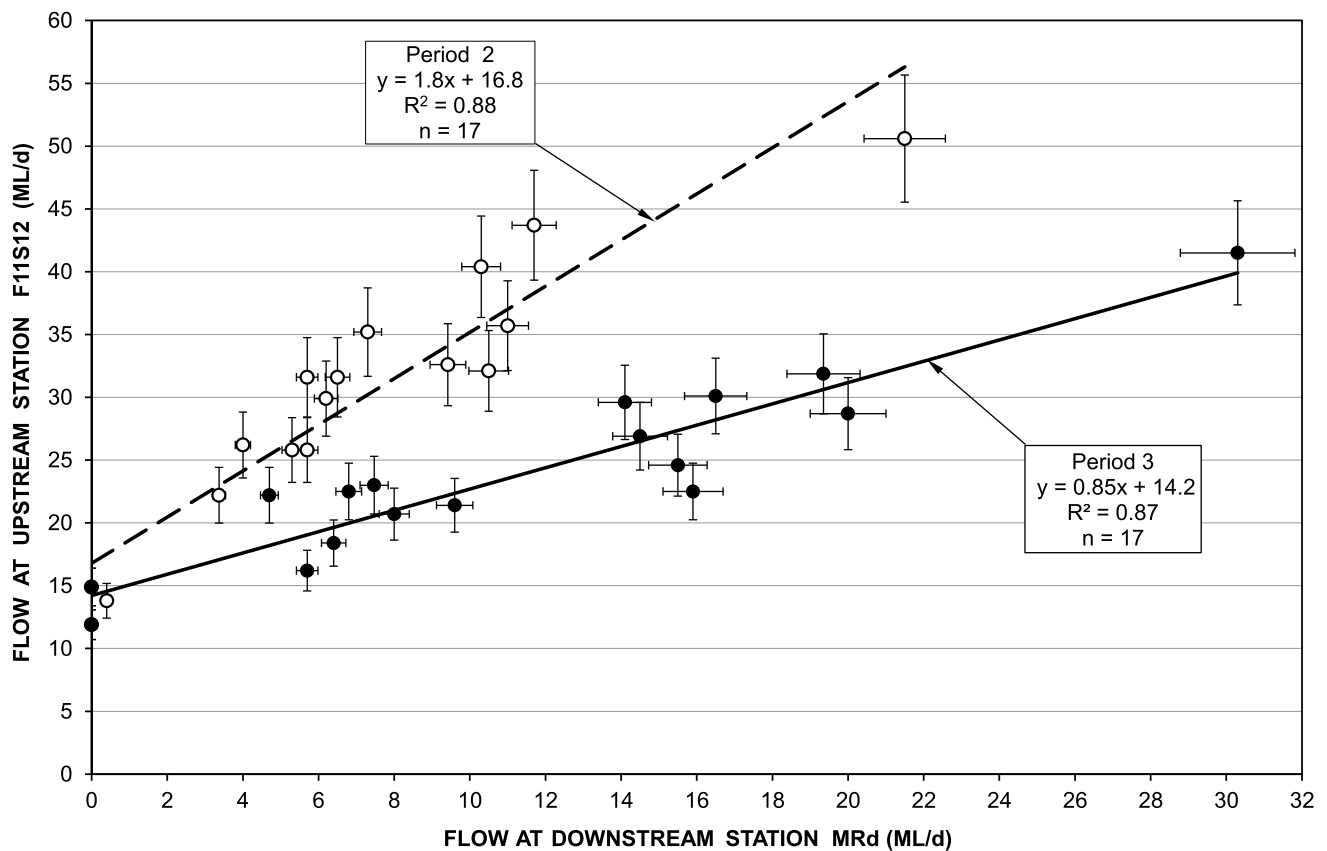


Fig. 24 Correlation of SDMs at stations F11S12 and MRd in the Riet Spruit valley; error bars denote $\pm 10\%$ at F11S12 and $\pm 5\%$ at MRd (data from Table 12)

presented in Fig. 26. The profile follows the Tweelopie Spruit from the vicinity of Kemp's Cave near the predator sanctuary entrance in the KGR, down the Riet Spruit and the Bloubank Spruit, ending on the south-eastern margin of the carbonate strata near the Nedbank Olwazini Estate (NOE) downstream of Kromdraai.

Traversing the karst terrane from end to end, the profile reveals two distinct gradients. As might be expected, the steeper gradient is associated with the Tweelopie Spruit in the upper 3 km section of the profile. This section cuts orthogonally across the regional strike of the karst strata (Fig. 22) with an average gradient of 0.0164 (1:61). The slope associated with the Riet and Bloubank spruits is $\sim 60\%$ shallower at 0.0068 (1:147) on average. This section of the profile, which is subparallel to the regional SW–NE strike of the strata, shows no marked deviation in slope at the locus of either the Zwartkrans or the Kromdraai springs. The relevance of the 'step' evident in the Bloubank Spruit opposite Sterkfontein Cave (Fig. 26) is discussed later in this section.

Flow measurements carried out in the Bloubank Spruit at localities bracketing (i.e. located upstream and downstream) the Sterkfontein Cave indicate an increase in surface water discharge rather than a loss as observed further upstream.

The outcome of two sets of measurements reflecting this are presented in Table 14. The September 2009 value of 260 L/s for the downstream station closely approximates the 258 L/s reported by Bredenkamp et al. (1986) for locality 5 (Table 8) located downstream of the Zwartkrans Spring. Given that the downstream station BB@M is located ~ 460 m upstream of the Zwartkrans Spring, these circumstances indicate that recent late-winter flow in the Bloubank Spruit upstream of the Zwartkrans Spring is considerably greater than the historical observation suggests. This is also evident in Fig. 11. The discharge of 258 L/s reported by Bredenkamp et al. (1986) is all the more impressive considering that the mid-1980s experienced one of the longer and more severe drought periods in the region, and which was broken only in 1987 (Sect. 4.2.1 in Chapter "Literature Review").

A set of flow measurements made on 16/05/2012 at the localities BB@M and BB@L bracketing the Zwartkrans Spring, returned values of ~ 306 and ~ 631 L/s respectively. The difference of ~ 325 L/s must represent a groundwater contribution that includes the Zwartkrans Spring discharge. The discharge of the spring has been set at ~ 136 L/s. If it is assumed that the yield of the spring is comparatively constant, then it would appear that ~ 190 L/s (~ 16.4 ML/d) represents

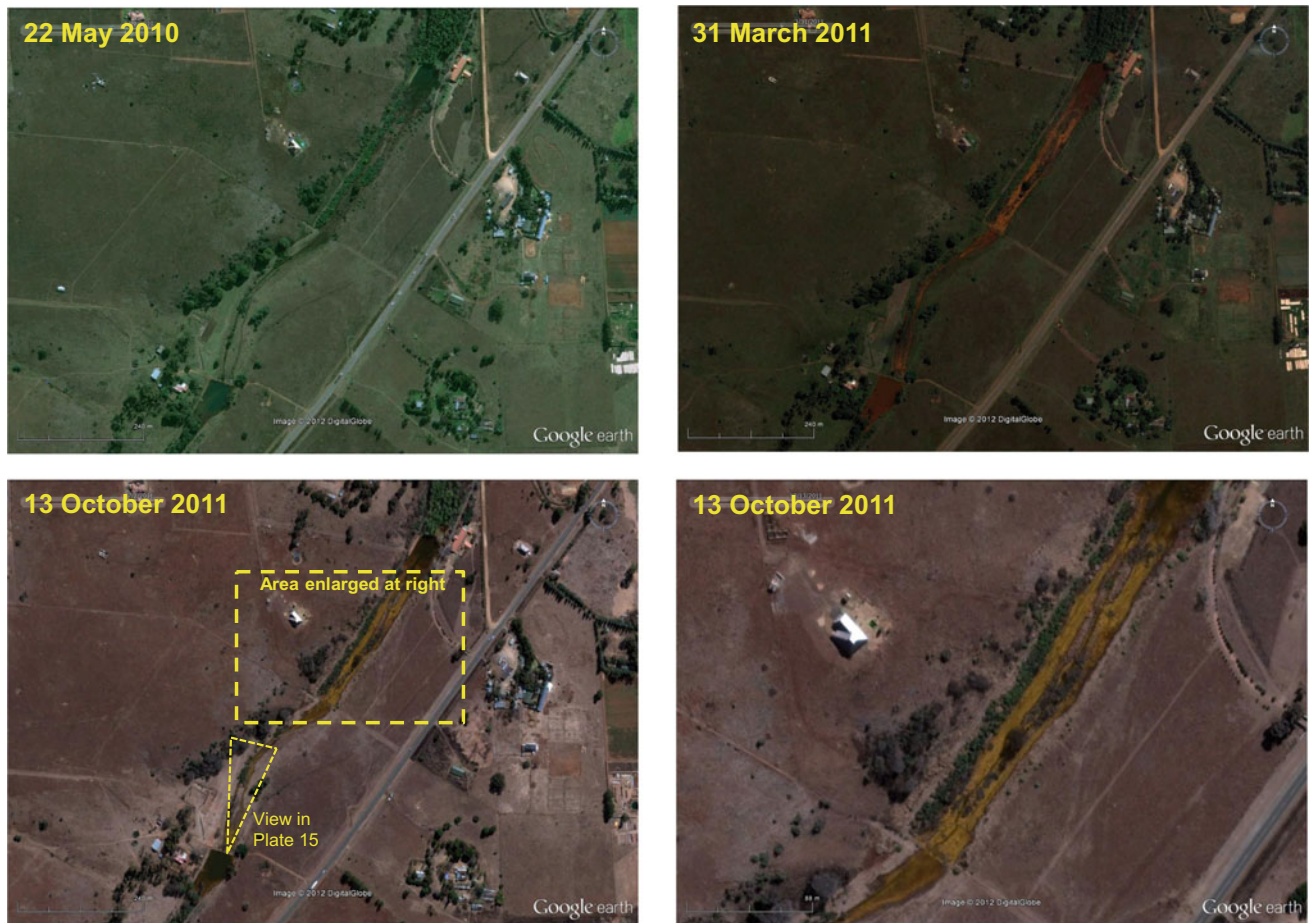


Fig. 25 Historical Google Earth® images showing the development of ferrous hydroxide deposits in the channel of the Riet Spruit sometime between 22/05/2010 (top left) and 31/03/2011 (top right); stream section located between stations F11S12 and MRd as shown in Fig. 22

groundwater entering the river channel in the ~ 460 m reach between station BB@M and the spring. This conclusion finds support in the similar electrical conductivity values of 92 and 99 mS/m recorded for the springwater and the river water at station BB@M, respectively, on 16/05/2012. The surface water ‘gain’ of ~ 16.4 ML/d is similar to the ~ 17 ML/d measured on 18/05/2010 for a 2.1 km reach upstream of station BB@M (Table 14). The flow and specific electrical conductivity (SEC) values measured on 16/05/2012 at stations BB@M, BB@L and Zwartkrans Spring provide data for a mass balance calculation (see Sect. 7.4.1 in Chapter “Physical Hydrogeology”) that supports the observed total groundwater contribution of ~ 325 L/s.

Synoptic discharge measurements carried out on 24/10/2012 at the three stations MRd, BG@N14 and BB@M returned flows of ~ 5.7 , ~ 16.2 and ~ 29.7 ML/d respectively. The stations MRd and BG@N14 contribute the only visible surface flow to the Bloubank Spruit. As reported earlier, the station BB@M is located ~ 460 m upstream of

the Zwartkrans Spring. The flow at this station should therefore represent the sum of that at stations MRd and BG@N14. The reported SDM values, however, indicate that the flow exceeds the sum of the upstream stations by ~ 7.8 ML/d. Further analysis of this value (~ 90 L/s) indicates that it represents a resurgence rate of ~ 56 L/s/km over the ~ 1600 m reach extending upstream from this station to opposite Sterkfontein Cave. This is in reasonable agreement with the mean and median loss rates (~ 70 L/s/km) calculated for the ~ 3.9 km reach of the Riet Spruit between stations F11S12 and MRd in Period 2 (Table 12). The only possible source of the additional flow is groundwater resurgence in the channel of the Bloubank Spruit.

Flow measurements carried out at station BB@M and ~ 20 m upstream of Zwartkrans Spring on 15/01/2013 provide additional data that further elucidate the postulated resurgence of groundwater in the stream channel upstream of the spring. The data presented in Table 15 describe the results obtained.



Plate 10 View looking downstream of relic ferrous hydroxide deposits in the stream channel of the Riet Spruit (see Fig. 25 for photo location)



Plate 11 Causeway across the Blougat Spruit on the Bergland Instant Lawn property downstream of the Percy Stewart WWTW, and site of station BC1 (photo P Hobbs; date 18/02/2010)

The veracity of the flow measurements presented in Table 15 is again interrogated on the basis of a mass balance calculation as follows:

$$Q_Q = [(Q_D C_D) - (Q_U C_U)] \div C_0 \\ = [301656 - 215600] \div 665 = 129 \text{ L/s}$$

The derived groundwater resurgence value of $\sim 125 \text{ L/s}$ (Q_G , Table 15) is similar to the mass balance calculated value of 129 L/s . These results indicate a surface water gain of $\sim 125 \text{ L/s}$ over a stream reach of $\sim 460 \text{ m}$, which equates to $\sim 270 \text{ L/s/km}$. This result offers further insight into the stream gain values reported in Table 14. It is likely that these circumstances are similar to the Pescara River ‘linear’ or ‘streambed’ springs described by Salvati (2002) as draining, together with the Giardino Spring, the Morrone Mount Ridge carbonate massif in the Central Apennines of west-central Italy.

The stream gain value of 77 L/s/km reported in Table 14 for the reach immediately upstream of station BB@M clearly falls well short of the $\sim 270 \text{ L/s/km}$ reported above for the $\sim 460 \text{ m}$ stream reach between station BB@M and the Zwartkrans Spring. This ‘discrepancy’ is explained by recognising the improbability of a constant ‘gain rate’ under hydraulic circumstances that describe a varying potentiometric head along a stream reach. These circumstances posit that the potentiometric head that drives groundwater resurgence in the stream channel is greatest at the spring, and decreases with distance upstream to extinction at the point where the potentiometric surface no longer intersects the stream channel. This position is postulated to lie to the north opposite Sterkfontein Cave, and could be marked by the ‘step’ evident in the channel gradient shown in Figs. 26 and 27.

Table 13 Results of stream flow measurements in the Blougat Spruit on 18/05/2010

| Station | Description | Flow ^a | | Loss Rate ^b (L/s/km) |
|---------------------|--|-------------------|------|---------------------------------|
| | | L/s | ML/d | |
| BC1 (upstream) | Causeway on the Bergland property downstream of the Percy Stewart WWTW | 655 | 56.6 | 23.1 |
| BG@N14 (downstream) | Intersection of the Blougat Spruit with the N14 national road | 574 | 49.6 | |

^a Flow measurement based on the cross-sectional flow method using the average of six measured surface velocities of styrofoam flotsam over known distances. The relatively shallow flow depth (80–150 mm) negates reduction of the calculated flow values by 25% to account for a mean velocity that is less than the surface velocity (Brassington 1998)

^b Based on a distance of ~3.5 km between the stations

**Plate 12** Bridge culvert at the N14 national road crossing of the Blougat Spruit, and site of station BG@N14

In light of the above, it is more realistic to increment groundwater resurgence in the stream channel over shorter reach lengths of say 100 m rather than 1 km. In the case of the Bloubank Spruit upstream of Zwartkrans Spring, this might amount to unit resurgences of up to 30 L/s per 100 m of stream reach. Assigning a uniform channel width of 5 m to each such reach gives a streambed area of 500 m² delivering a unit resurgence of up to 0.06 L/s/m² (6 L/s per 100 m²). This could be expected to gradually decrease in a headward (upstream) direction. Closer to Sterkfontein Cave, the unit resurgence might reduce to only ~0.01 L/s/m² (1 L/s per 100 m²) of stream channel area before reaching extinction.

On the basis of groundwater level and streambed elevation information, it is postulated that the water table and land surfaces intersect at an elevation of ~1439 to 1440 m amsl in the Sterkfontein Valley (Bloubank Spruit) opposite the caves. These circumstances drive the resurgence of groundwater in the stream at the downstream end of the Zwartkrans Basin between Sterkfontein Cave and the Zwartkrans Spring, and partly explain the observed decrease

in SEC values and increase in pH values observed at station BB@M since late-2011 (Fig. 23 in Chapter “Chemical Hydrology”, Sect. 6.1.2.6 in Chapter “Chemical Hydrology”). The surface water gain/loss data and associated stream reaches in the Zwartkrans Basin are illustrated schematically in Fig. 27.

An attempt to quantify the ‘not measured’ loss component (C in Fig. 27) in the upper portion of the Zwartkrans Subcompartment is based on the following simple water balances¹⁵:

[Minimum loss B] + [Loss C] = [Minimum gain D] + [Zwartkrans Spring]

$$7 + C = 3 + 11.7\text{ML/d, so that } C = 7.7\text{ML/d} = 89\text{L/s}$$

[Maximum loss B] + [Loss C] = [Maximum gain D] + [Zwartkrans Spring]

$$32 + C = 23 + 11.7\text{ML/d, so that } C = 2.7\text{ML/d} = 31\text{L/s}$$

The above results show the following encouraging agreement:

- the loss of 7.7 ML/d effectively balances the measured groundwater resurgence of 7.8 ML/d reported earlier in this section for component D (Fig. 27);
- the unit loss rates across the ~3.8 km reach of component C amount to 23 and 8 L/s/km, in keeping with values determined for other stream reaches in the study area (e.g. Sections 5.2.1 and 5.2.2); and
- the highest component C loss occurs when the component B loss (across a reach length of ~3.9 km) is least, and vice versa.

¹⁵ The discharge of the Zwartkrans Spring is assigned a ‘constant’ value of ~11.7 ML/d (~136 L/s) derived from an analysis of SDM data and TDS load calculations (Sect. 7.4.1).

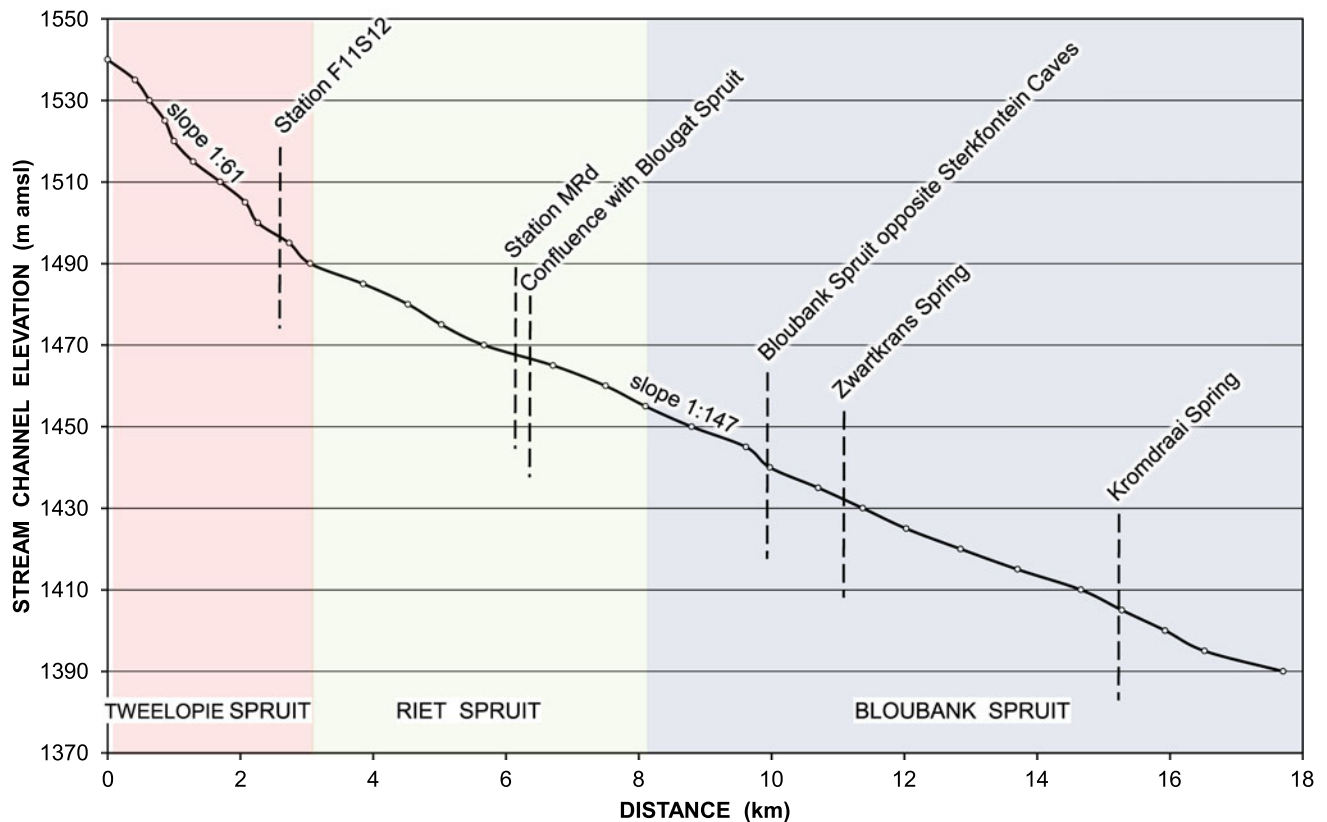


Fig. 26 Longitudinal profile along the course of the Tweeloopie, Riet and Bloubank spruits from Kemp's Cave in the KGR to the south-eastern margin of the carbonate strata at the Nedbank Olwazini Estate

6 Surface Water Use

6.1 WARMS Data

From an assessment of water use information sourced from the DWS Water Authorisation and Registration Management System (WARMS), Holland and Cobbing (2008) report a total surface water use of 3.5 Mm³/a as being registered for mainly agricultural purposes in the Zwartkrans Basin. Breckenkamp et al. (1986) and van Biljon (2006) reported values of 5.52 and 6.62 Mm³/a, respectively.

6.2 Canals

The Skeerpoort River feeds a canal that starts immediately upstream of where the R400 regional road crosses this

drainage on the farm Hartebeesthoek 498JQ. This canal, however, does not influence the flow regime of the Skeerpoort River in the study area, and is therefore not considered further. By comparison, the network of canals/furrows¹⁶ that distribute water to riparian users in the Bloubank Spruit system represent an important component of surface water use in the study area. The following canal systems are identified and described.

- The defunct canal that starts at Glen Almond on the farm Sterkfontein 173IQ and follows the right bank¹⁷ of the drainage for a distance of ~1.7 km, ending on Ptn 8/2 of Sterkfontein 173IQ.
- The so-called A-furrow (canal) managed by the Kromdraai Irrigation Board, as described by Mr M Gomes¹⁸ (personal communication). This canal starts immediately downstream of the Zwartkrans Spring on the farm Zwartkrans 172IQ, and follows the right bank for a distance of ~3.6 km, ending in the Honingklip Spruit

¹⁶ A canal is a properly designed, engineered and constructed water transfer structure over a substantial distance traversing numerous properties, and a furrow a simple (typically hand-dug) trench serving a similar local purpose over a considerably shorter distance typically limited to an individual property.

¹⁷ By convention, the bank to the right of an observer facing downstream.

¹⁸ Current Chairman of the Kromdraai Irrigation Board.

Table 14 Results of stream flow measurements in the Bloubank Spruit

| Date | Station | Description | Distance (km) | Flow ^a | | Gain Rate |
|------------|--------------------|---|---------------|-------------------|-------------------|---------------------------|
| | | | | L/s | ML/d | |
| 09/09/2009 | 101,008 (upstream) | R563 regional road crossing | 2.95 | 225 ^b | 19.5 ^b | + 3.0 ML/d + 12 L/s/km |
| | BB@M (downstream) | Crossing of Danielsrust road downstream of Sterkfontein Cave | | 260 ^c | 22.5 ^c | |
| 18/05/2010 | BB@SC (upstream) | Crossing of Swartkrans fossil site road upstream of Sterkfontein Cave | 2.1 | 311 ^c | 23.9 ^c | +16.9 ML/d +77 L/s/km |
| | BB@M (downstream) | Crossing of Danielsrust road downstream of Sterkfontein Cave | | 472 ^c | 40.8 ^c | |

^a Flow measurements carried out with the current meter described in Footnote 28 (Sect. 5.2.1)

^b Flow measurement based on the cross-sectional flow method (width x depth x velocity)

^c Flow measurements based on the cross-sectional pipe method (chord length x velocity)

Note Although damage to the outlets of two of the three culverts at the downstream locality (BB@M) influence the accuracy of the 18/05/2010 SDMs, the margin of error is not considered greater than the observed difference in flow. This damage had not yet occurred on 09/09/2010, generating greater confidence in these SDMs at station BB@M

Table 15 Calculation of groundwater resurgence in the Bloubank Spruit upstream of Zwartkrans Spring on 15/01/2013 using measured flows and SEC-based TDS load values

| Flow location | Field SEC (mS/m) | TDS [C] (mg/L) | Discharge [Q] | | TDS Load | |
|-----------------------------------|------------------|-------------------------------------|---------------------------------------|--------|--------------|------|
| | | | (L/s) | (ML/d) | mg/s [=QXCX] | t/d |
| Downstream ^a | 105 | 735 ^c [=C _D] | ~ 410 ^d [=Q _D] | 35.5 | 301,656 | 26.1 |
| Upstream ^b | 108 | 756 ^c [=C _U] | ~ 285 ^d [=Q _U] | 24.6 | 215,600 | 18.6 |
| Calculated difference in TDS load | | | | | 86,056 | 7.5 |
| Groundwater resurgence | 95 ^c | 665 ^c [=C _G] | ~ 125 ^f [=Q _G] | 10.8 | 83,125 | 7.2 |

^a Located ~ 20 m upstream of the Zwartkrans Spring

^b Located at station BB@M

^c SEC × 7.0 used as a proxy to derive a theoretical TDS value

^d Synoptic discharge measurement (SDM) value

^e Assumed similar to that of the Zwartkrans Spring (Table 13 in Chapter “Physical Hydrogeology”)

^f Derived value from the difference of the SDM values

immediately downstream of the R540 road crossing at the Kromdraai T-junction. This canal (Plate 13) serves 18 properties. The allocation of water from the canal is made on a rotational basis that at any one time provides three properties with 70 L/s each for two days per week,¹⁹ and two half-days every other week. Theoretically, therefore, it carries an absolute minimum permanent discharge of 210 L/s ostensibly fed by the Zwartkrans Spring.²⁰ The discharge measured at Ptn 8 of Kromdraai 520JQ on 27/07/2010 was ~ 154 L/s. A second measurement carried out further upstream at Ptn 5 on 13/08/2010 returned a slightly higher value of ~ 176 L/s. Both measurements are in reasonable agreement with the 172 L/s reported by JFA (2006) (Sect. 5.1). The very high flow conditions in

mid-December 2010 not only caused significant damage to this furrow, but also silted up the sluice gate at its entrance, cutting off flow in the furrow. These circumstances continued to prevail as at December 2017, and will remain so for as long as the entrance to the furrow remains obstructed.

- The so-called B-furrow, also managed by the Kromdraai Irrigation Board, which starts at the position where the A-furrow enters the Honingklip Spruit. A weir constructed in this spruit at this position provides the head that feeds water into the B-furrow, which follows the topographic contour along the right bank of the Bloubank Spruit for a distance of ~ 3.7 km before entering the Bloubank Spruit on the Nedbank Olwazini Estate property. Since the ephemeral Honingklip Spruit delivers an excellent quality surface water into the Bloubank Spruit system (Table 21 in Chapter “Chemical Hydrology”), the quality of water entering the B-furrow in the summer months must similarly reflect a better quality than that

¹⁹ Based on a 6-day week, respecting Sunday as the Christian Sabbath, day of rest.

²⁰ See Sect. 7.4.1 in Chapter “Physical Hydrogeology” for a discussion of groundwater discharge from the Zwartkrans Compartment.

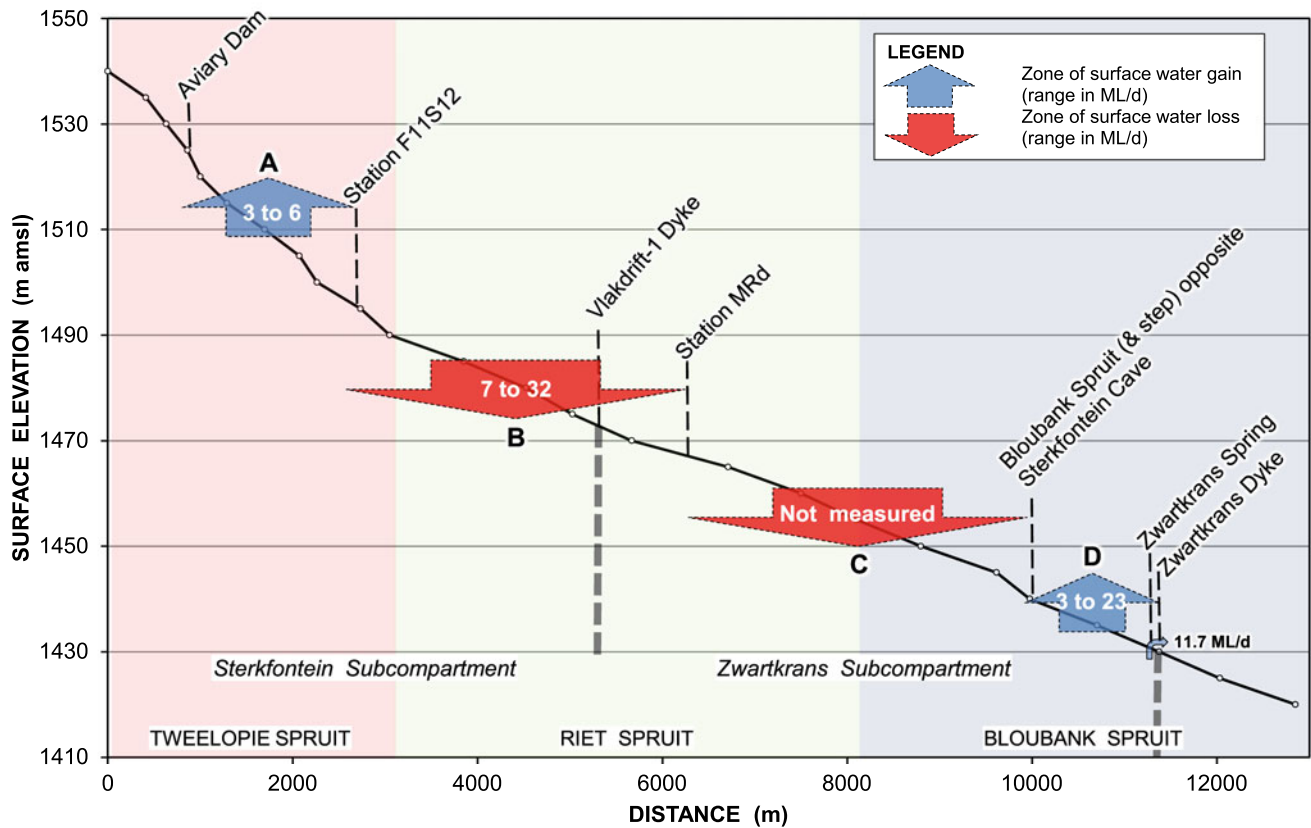


Fig. 27 Schematic profile illustrating surface water gain/loss zones (A to D) and associated rates along the Tweelapie, Riet and Bloubank spruits from the Aviary Dam in the KGR to the Zwartkrans Spring

delivered by the A-furrow at this location, representing as it does a blend of Bloubank Spruit and Honingklip Spruit water. In the winter months, flow in the B-furrow is sustained solely from the A-furrow. A site inspection of the B-furrow on 27/03/2012 in the presence of others²¹ confirmed that it was blocked where the furrow passes beneath the R540 road at the Nirox property. The blockage was caused by damage from trenching carried out in the road reserve in mid-2011, severing the culvert and cutting off flow to the downstream properties (including Kenjara Lodge) that used the water for landscape watering and the irrigation of fodder. The blockage remained in place as at December 2014.

- The furrow that draws water from the Bloubank Spruit immediately upstream of the Nedbank Olwazini Estate (NOE), and follows the right bank of this drainage for a distance of ~3.9 km before re-entering the spruit on the Kloofzicht Lodge Estate. The ‘management’ of this canal does not fall within the ambit of the Kromdraai Irrigation Board. The NOE draws water from this canal for on-site

treatment in a purification plant to potable quality for own use in the average amount of 40 m³/d (14,600 m³/a) (H Carpenter, personal communication). As this canal/furrow also passes through a number of dams, many of which are stocked with trout, it is evident that this water supply function probably represents the main purpose of this structure. The estate also operates its own wastewater treatment plant, using the treated wastewater effluent for landscape irrigation purposes. A water use licence application to the DWS for return of the treated wastewater to the Bloubank Spruit has been unsuccessful (H Carpenter, personal communication) on the basis of unacceptably high nitrate and phosphate levels produced by the treatment process.

6.3 Conclusion

Although surface water use on the property is poorly quantified, the ephemeral nature of the good quality streams and the poor water quality of the perennial streams are limiting factors in this regard (Plate 13).

²¹ Peter Mills of the COH WHS MA, and local residents/landowners Hannes Fourie and Belinda Cooper.



Plate 13 View of the ~100-year old A-furrow at Ptn 8 of Kromdraai 520JQ, looking upstream; flow measured at ~154 L/s on date of photo

Text Box 3 The veracity of SDM-based surface water loss calculations

The synoptic discharge measurements (SDMs) carried out at stations F11S12 and MRd are typically made within 30 minutes of each other. The flow velocity at the upstream station (F11S12) falls in the range 0.3–0.4 m/s (1.1–1.4 km/h), which translates into a travel time of ~5.6 to 4.4 hours between stations. This suggests that the equivalent representative flow at the downstream station will only be manifested ~5 hours after a measurement at the upstream station. As this does not include the retention time of water impounded in dams (e.g. that on Ptn 8/2 of Sterkfontein 173IQ) along the intervening stream reach, nor the lower velocities in wider, shallower and/or more vegetated sections of the river channel, a longer time interval might be considered more applicable. It must

also be recognised that flow losses introduced by other agents such as evaporation and evapotranspiration are not factored into the SDM-based inter-station water loss calculations. It is apparent, therefore, that the interval of ~0.5 hours between sequential SDMs does not accommodate changes in discharge that are mutually observable only over periods ≥ 5 hours. The p used by neglect of the above-mentioned factors must be gauged against the understanding that significant variations in discharge along the stream reach in question result from event-driven high runoff associated with rainfall or abnormal mine water discharges. Further, that the SDMs themselves incorporate an inaccuracy estimated to be in the ranges ± 5 and $\pm 10\%$. The lower value is associated with station MRd where the smaller volumes passing through culvert(s) provide for a more rigorous flow measurement than the weir at F11S12, which is assigned an

error margin of $\pm 10\%$ also because of the higher flows. Against this background, the short period between measurements is not considered to introduce a significant gauging error when carried out under 'normal' flow conditions. The calculated losses

therefore represent the worst case scenario in regard to the possible volume of poor quality water lost to the karst aquifer.

Chemical Hydrology

Harrison Pienaar, Philip J. Hobbs, Sebinasi Dzikiti, and Ranya Amer

1 Surface Water Chemistry

1.1 Skeerpoort River

Water quality in this drainage is monitored by the DWS at station A2H034 (Fig. 4 in “[Introduction and Background](#)”) shortly before its confluence with the Magalies River. Monthly water quality monitoring by the DWS at station A2H035Q01 located ~6 km upstream on the farm Hartebeesthoek 498JQ in the middle reaches of the Skeerpoort River, was discontinued in July 1982 after only ~2.5 years. This was followed by four opportunistic analyses, one each in late 1986, early 1996, late 1998 and early 1999. These data have not been evaluated in this study. The water quality delivered by the Nouklip Spring located ~7 km upstream in the John Nash Nature Reserve, is monitored at station A2H033 on the Grootvlei Spruit tributary of the Skeerpoort River. Representing mainly groundwater, these data are evaluated in Sect. 7.7 in Chapter “[Chemical Hydrogeology](#)”. An evaluation of the A2H034 water chemistry record, which

represents the integrated Skeerpoort River quality, yields the information presented in Table 1.

It is evident from Table 1 that the SANS (2015a) recommended limit for Class 1 drinking water is easily met in respect of the 95%ile value of each analyte reported. A high degree of confidence is afforded the analytical results on the basis that the median and mean electrical balance (EB) values fall well within the $\pm 5\%$ limit (i.e. 95–105%) that defines an acceptable error margin for freshwater (Hem, 1985). The mean and median TDS:SEC ratio value of 8.1 is a useful factor for calculating the TDS of this water from an SEC measurement. It is also evident that sulfate (SO_4) typically comprises only 3% of the TDS associated with this water. The small variability in the chemical composition of Skeerpoort River water evident in the narrow 2σ (5%ile to 95%ile) range shown for each analyte, with the possible exception of bicarbonate (HCO_3), in Fig. 1, is attributed to the karstic Tweefontein, Nouklip and Nash springs (Table 8 in Chapter [Physical Hydrogeology](#)) as main perennial source. The aggregate discharge of ~300 L/s (~9.5 Mm^3/a) approximates the long-term median discharge of the Skeerpoort River at station A2H034 (Sect. 2 in Chapter “[Physical Hydrology](#)”), which also explains the dominant MgCa-HCO_3 composition of the surface water at this station.

P. J. Hobbs: Deceased

H. Pienaar (✉) · P. J. Hobbs
Smart Places, Council for Scientific and Industrial Research,
Pretoria, South Africa
e-mail: hpienaar@csir.co.za

H. Pienaar
Hebei University of Engineering, Handan, China

S. Dzikiti
Department of Horticultural Science, Stellenbosch University,
Cape Town, South Africa
e-mail: sdzikiti@sun.ac.za

R. Amer
Genetic Engineering and Biotechnology Research Institute
(GEBRI), City of Scientific Research and Technological
Applications (SRTA-City), New Borg El Arab City,
Alexandria, Egypt
e-mail: ramer@srtacity.sci.eg

1.2 Bloubank Spruit System

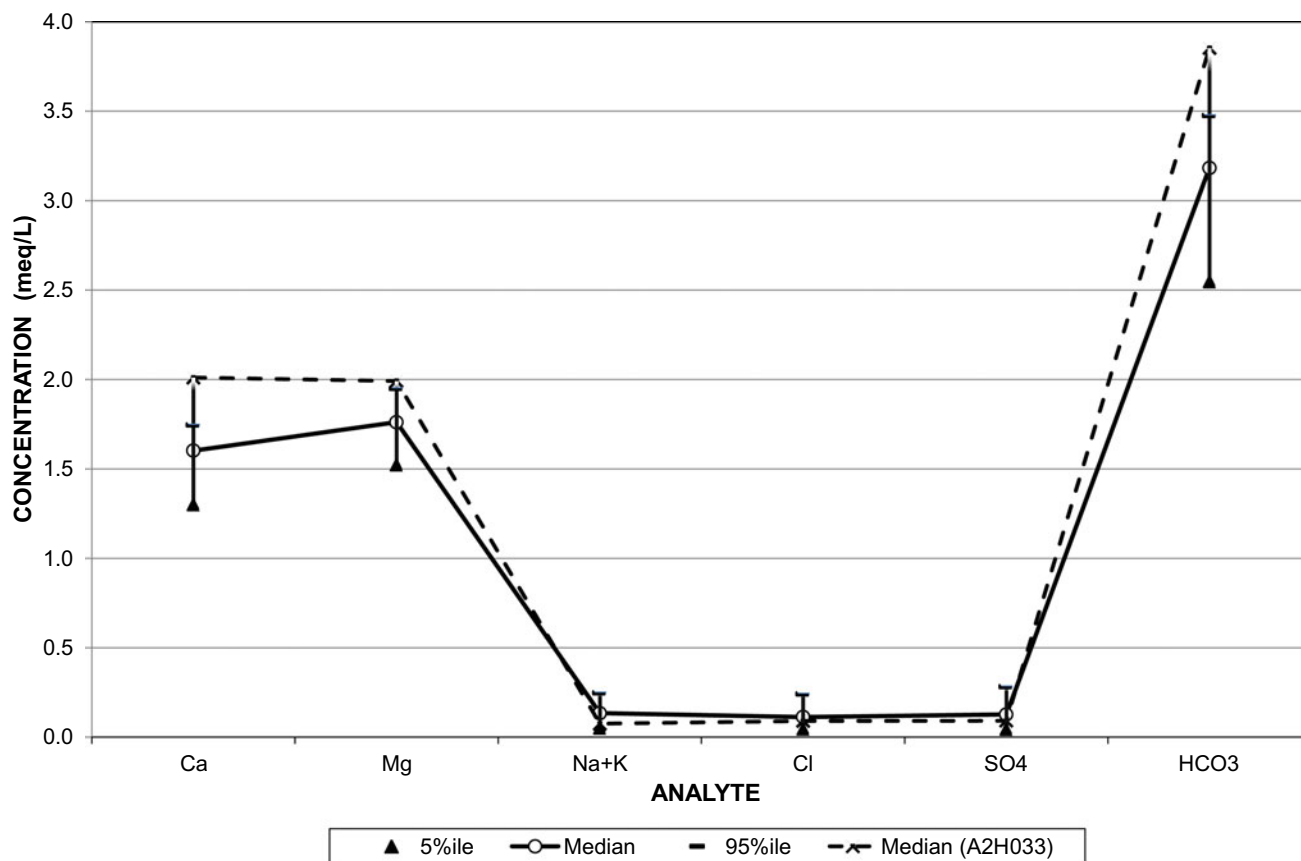
1.2.1 Locus of Mine Water Discharge (Decant)

The monitoring of surface water chemistry (quality) in the study area is heavily biased in favour of the headwaters of the Bloubank Spruit system. Especially the Tweelopie Spruit, which encompasses the locus of mine water discharge/decant (LoD) in its upper reaches, is intensively monitored by SS. Water quality monitoring in the mine area originally focussed on two sources. One of these was the composite chemistry represented by the raw mine water

Table 1 Statistical analysis of Skeerpoort River water chemistry at station A2H034 in the period January 1976 to March 2017

| Variable/Analyte | Statistical parameter | | | | | | | SANS (2015a) ¹ |
|--|-----------------------|-------|------|--------|--------|------|---------|---------------------------|
| | n | 5%ile | Mean | Median | 95%ile | SD | CoV (%) | |
| pH ($-\log_{10}a_{H^+}$) | 1631 | 7.5 | – | 8.2 | 8.6 | 0.4 | 4 | 5.0 – 9.7 |
| SEC (mS/m) | 1718 | 28.5 | 32.2 | 32.5 | 35.2 | 2.6 | 8 | ≤ 170 |
| TDS (mg/L) | 1407 | 229 | 262 | 265 | 284 | 20.3 | 8 | ≤ 1200 |
| Ca (mg/L) | 1512 | 26.1 | 31.6 | 32.1 | 35.0 | 3.2 | 10 | n.s |
| Mg (mg/L) | 1503 | 18.4 | 21.3 | 21.4 | 23.7 | 2.3 | 11 | n.s |
| Na (mg/L) | 1472 | 1.0 | 2.9 | 2.8 | 4.5 | 2.1 | 72 | ≤ 200 |
| K (mg/L) | 1480 | 0.15 | 0.72 | 0.49 | 0.72 | 0.93 | 129 | n.s |
| Cl (mg/L) | 1513 | 1.5 | 4.2 | 4.0 | 8.6 | 2.8 | 66 | ≤ 300 |
| SO ₄ (mg/L) | 1514 | 2.0 | 6.7 | 6.1 | 13.7 | 4.2 | 62 | ≤ 500 |
| HCO ₃ (mg/L) | 1522 | 156 | 191 | 194 | 212 | 18.3 | 10 | n.s |
| NO ₃ + NO ₂ (mg N/L) | 1577 | 0.09 | 0.65 | 0.60 | 1.27 | 0.53 | 81 | ≤ 11 |
| F (mg/L) | 1474 | 0.05 | 0.17 | 0.14 | 0.38 | 0.17 | 99 | 1.5 |
| Si (mg/L) | 1568 | 5.0 | 6.2 | 6.1 | 7.3 | 1.3 | 21 | n.s |
| EB (%) | – | 4.0 | 1.1 | 1.0 | –1.4 | – | – | ± 5 |
| TDS:SEC | – | 8.0 | 8.1 | 8.2 | 8.1 | – | – | n.s |
| SO ₄ :TDS (%) | – | 1 | 3 | 3 | 5 | – | – | n.s |

¹Standard health-related limit for consumption of 2 L/d over 70 years by a 60 kg person

**Fig. 1** Variability of Skeerpoort River water major ion chemistry at station A2H034 in the period January 1976 to March 2017 (data from Table 1)

(RMW) collected in the HDPE-lined dam (Plate 3 in Chapter “Physical Hydrology”) at the Black Reef Incline (BRI) from various point and diffuse sources. The other was at the point of discharge (end-of-pipe or EoP) (Plate 4 in Chapter “Physical Hydrology”) of treated/neutralised mine water (TMW) into the stream immediately upstream of the R24 regional road and the Krugersdorp Game Reserve. The main point sources of mine water discharge are the Black Reef Incline shaft, #17 Winze and #18 Winze. Individual monitoring of the RMW chemistry from these mine structures commenced in early to mid-2009.

Mine water discharge to the Tweelopie Spruit ideally comprises only a TMW component from the HDS treatment plant (Fig. 12 in Chapter “Physical Hydrology”). The RMW collected in the HDPE-lined dam at the BRI shaft (Plate 3 in Chapter “Description of the Physical Environment” and Plate 3 in Chapter “Physical Hydrology”) overflows from this dam in times of excessive discharge (Sect. 3.1 in Chapter “Physical Hydrology”), and leaves the mine property untreated. The chemistry of the two mine water components is summarised in Tables 2 and 3 respectively, and illustrated in Fig. 2 for the analytes pH, SEC, SO₄ and Fe. An important aspect of the data presented in Tables 2 and 3 is the recognition of detection limits (DLs) (see Table 6 for temporal variation of DLs) and the influence of non-detect values on the statistical results. For example, the metal

analytes Al, Cr, V and Pb reflect a particularly high proportion of non-detect values (conversely few > DL or ‘actual’ values), which contextualises the veracity of the associated statistical results. Also indicated is the extent to which the reported analytes exceed the SANS (2015a) standard health-related limit for drinking water.

Also shown in Tables 2 and 3 is the TDS:SEC ratio that for natural surface water in the region is typically 7.5 (Text Box 1 in Chapter “Study Framework”), but for RMW has a value of 12.9 (Table 2), and for TMW a value of 10.9 (Table 3). Sulfate typically comprises ~63% of the TDS (Tables 2 and 3) irrespective of whether it is RMW or TMW.

The pattern and trend associated with the RMW produced by the two most productive point sources of AMD, viz. the BRI and #18 Winze (#18 W), is illustrated in Fig. 2 for pH, SEC, SO₄ and Fe. The linear regression analyses applied to each of the variables reflect a general increase in pH and decrease in SEC, SO₄ and Fe levels. A further notable characteristic is the greater variability in Fe concentration in the first half of the BRI record (Fig. 2), compared to the later half of the record. This is associated with the apparent ‘levelling out’ of values evident in the latter portion of each record (to the right of each of the vertical chevron lines in Fig. 2), an explanation for which remains obscure. Perhaps a clue in this regard is the timing of the start of the ‘levelling out’ trend, which is similar for the interdependent variables

Table 2 Statistical analysis of raw mine water chemistry delivered by the BRI in the period January 2005 to September 2017

| Variable/Analyte | Statistical parameter | | | | | | | SANS (2015a) ² |
|--|---|-------------|--------------|-------------|--------------|-------|---------|---------------------------|
| | n _T (n _A) ¹ | 5%ile | Mean | Median | 95%ile | SD | CoV (%) | |
| pH (–log ₁₀ a _{H+}) | 501 | 3.2 | – | 4.3 | 6.2 | 1.0 | 21 | 5.0–9.7 |
| SEC (mS/m) | 500 | 361 | 471 | 476 | 571 | 74 | 16 | ≤ 170 |
| TDS (mg/L) | 263 ³ | 4434 | 5316 | 5240 | 6309 | 618 | 12 | ≤ 1200 |
| SO ₄ (mg/L) | 501 | 2860 | 3773 | 3700 | 4790 | 725 | 19 | ≤ 500 |
| Fe (mg/L) | 499 | 283 | 712 | 642 | 1271 | 345 | 49 | ≤ 2 |
| Mn (mg/L) | 272 (271) | 40 | 86 | 60 | 217 | 84 | 97 | ≤ 0.5 |
| Al (mg/L) | 262 (104) | 0.005 | 1.042 | 0.100 | 4.965 | 3.1 | 302 | ≤ 0.3 |
| Cr (mg/L) | 174 (120) | 0.001 | 0.031 | 0.001 | 0.013 | 0.276 | 892 | ≤ 0.05 |
| V (mg/L) | 174 (17) | 0.001 | 0.003 | 0.001 | 0.012 | 0.007 | 230 | ≤ 0.2 |
| Pb (mg/L) | 215 (129) | 0.001 | 0.008 | 0.004 | 0.030 | 0.011 | 147 | ≤ 0.01 |
| Co (mg/L) | 174 (173) | 0.07 | 1.27 | 1.05 | 2.80 | 0.84 | 66 | ≤ 0.5 |
| Ni (mg/L) | 262 (262) | 0.20 | 1.70 | 0.80 | 7.28 | 2.12 | 125 | ≤ 0.07 |
| U _T (µg/L) | 265 (244) | 7 | 61 | 55 | 135 | 46 | 76 | ≤ 15 ⁴ |
| TDS:SEC | 263 | 10.8 | 12.9 | 12.9 | 15.3 | 1.4 | 11 | n.s |
| SO ₄ :TDS (%) | 263 | 54 | 62 | 62 | 71 | 6 | 10 | n.s |

¹n_T denotes total number of analyses; n_A denotes number of analyses exceeding detection limit

²Standard health-related limit for consumption of 2 L/d over 70 years by a 60 kg person

³Monitoring of this variable commenced in August 2009

⁴The SANS (2015a) only recognises U; it uses the WHO (2011) *Guidelines for Drinking-water Quality* as reference, which sets a provisional value for U_T of 30 µg/L (Table 9.2, footnote c, p 211)

Bold text denotes value exceeds standard health-related limit as described in note 1

Table 3 Statistical analysis of treated/neutralised mine water chemistry discharge to the Tweelopie Spruit in the period April 2005 to September 2017

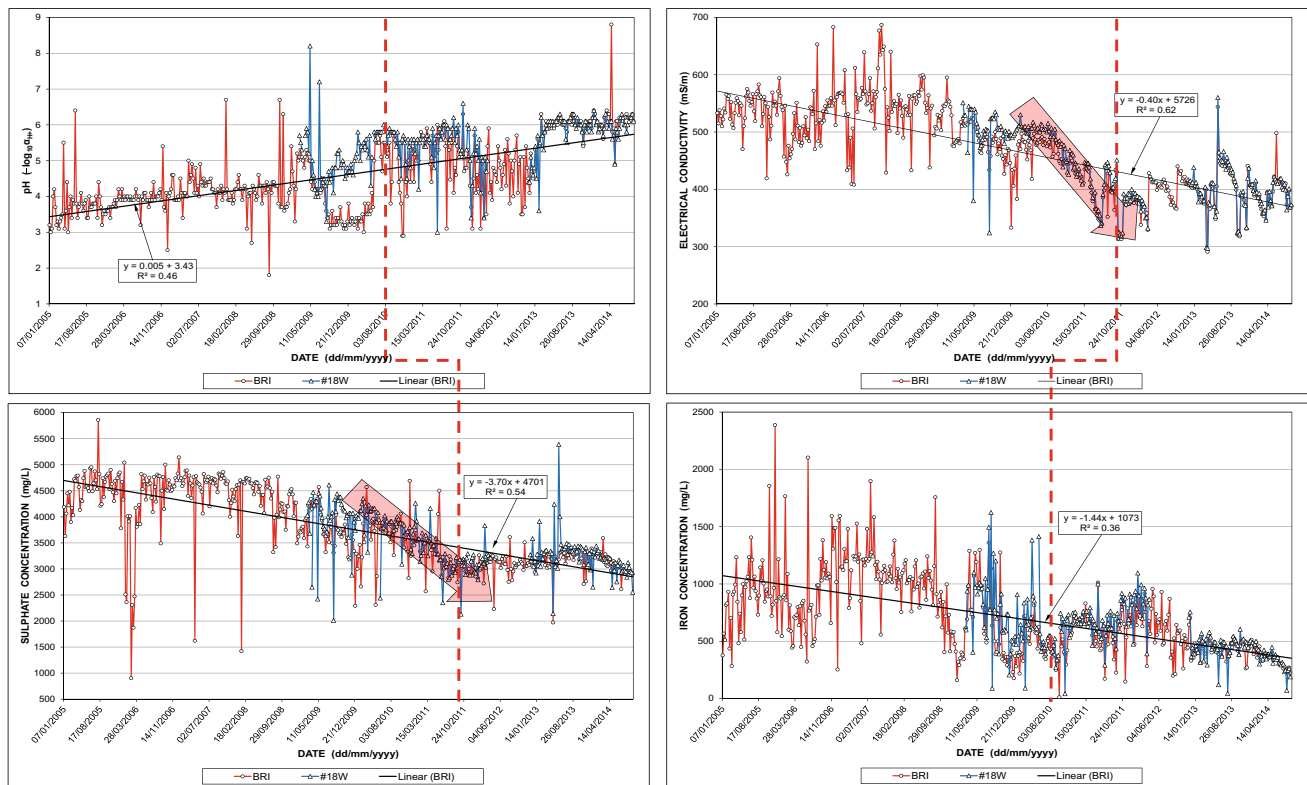
| Variable/Analyte | Statistical parameter | | | | | | | SANS(2015a) ¹ |
|----------------------------|--------------------------------|-------------|--------------|--------------|--------------|-------|---------|--------------------------|
| | n_T (n_A) ⁽²⁾ | 5%ile | Mean | Median | 95%ile | SD | CoV (%) | |
| pH ($-\log_{10}a_{H^+}$) | 458 | 3.0 | – | 7.0 | 9.9 | 1.8 | 26 | 5.0–9.7 |
| SEC (mS/m) | 458 | 305 | 382 | 381 | 459 | 56.5 | 15 | ≤ 170 |
| TDS (mg/L) | 458 | 3207 | 4168 | 4200 | 4982 | 582 | 14 | ≤ 1200 |
| SO ₄ (mg/L) | 458 | 2051 | 2647 | 2680 | 3102 | 379 | 14 | ≤ 500 |
| Fe (mg/L) | 457 (401) | 0.006 | 21.0 | 0.8 | 100.3 | 73.5 | 351 | ≤ 2 |
| Mn (mg/L) | 264 (260) | 0.9 | 15.6 | 9.5 | 60.1 | 19.5 | 125 | ≤ 0.5 |
| Al (mg/L) | 261 (87) | 0.002 | 0.154 | 0.010 | 0.100 | 0.871 | 567 | ≤ 0.3 |
| Cr (mg/L) | 174 (27) | 0.001 | 0.120 | 0.001 | 0.400 | 0.507 | 423 | ≤ 0.05 |
| V (mg/L) | 174 (6) | 0.001 | 0.001 | 0.001 | 0.002 | 0.000 | 44 | ≤ 0.2 |
| Pb (mg/L) | 262 (42) | 0.001 | 0.009 | 0.002 | 0.030 | 0.015 | 171 | ≤ 0.01 |
| Co (mg/L) | 174 (171) | 0.020 | 0.221 | 0.050 | 1.480 | 0.515 | 234 | ≤ 0.5 |
| Ni (mg/L) | 262 (256) | 0.022 | 0.348 | 0.100 | 1.625 | 0.899 | 259 | ≤ 0.07 |
| U _T (µg/L) | 174 (119) | 5.9 | 75.9 | 16.0 | 672.0 | 191.1 | 252 | ≤ 15 |
| U _D (µg/L) | 204 (88) | 5.1 | 15.1 | 9.9 | 42.3 | 18.4 | 122 | $\leq 15^{(3)}$ |
| TDS:SEC | 458 | 9.0 | 11.0 | 10.9 | 13.3 | 1.4 | 12 | n.s |
| SO ₄ :TDS (%) | 458 | 55 | 64 | 64 | 74 | 7.3 | 12 | n.s |

¹Standard health-related limit for consumption of 2 L/d over 70 years by a 60 kg person

² n_T denotes total number of analyses; n_A denotes number of analyses exceeding detection limit

³The SANS (2015a) only recognises U; it uses the WHO (2011) *Guidelines for Drinking-water Quality* as reference, which sets a provisional value for U_T of 30 µg/L (Table 9.2, footnote c, p. 211)

Bold text denotes value exceeds standard health-related limit as described in note 1.

**Fig. 2** Long-term pattern and trend of pH (top left), EC (top right), SO₄ (bottom left) and Fe (bottom right) associated with raw mine water produced by the BRI and #18 Winze point sources of AMD; significance of broken linking chevron lines and arrows explained in text

pH and Fe ca. mid-2010, and later (ca. mid-2011) for the interdependent variables EC and SO_4 . Neither of the ca. mid-2010 or mid-2011 timelines have any relevance in the timeframe of mine water management intervention measures¹ (Text Box 1 in Chapter “Physical Hydrology”). The mid-2010 timeline, however, occurs ~6 months after the onset of uncontrollable RMW decant (Sect. 3.1 in Chapter “Physical Hydrology”) precipitated by the very high rainfall in December 2009 and January 2010 (Sect. 2 in Chapter “Description of the Physical Environment”).

It is postulated within the framework of the above observations, that the pH and opposite concomitant Fe response patterns reflect the influence of ‘fresh’ and oxygenated recharge to the flooded mine void. The increase in pH might be driven by redox reactions in the mine water body, leading to the subaerial precipitation of iron hydroxide in the flooded mine workings. The reactions driving this response took a longer time to manifest steeply over a period of ~1 year (arrowed in Fig. 2) on the SEC (and less markedly on the SO_4) of the RMW discharge. Understanding the hydrogeochemistry behind these observed responses will advance the understanding of AMD evolution in the Western Basin and, by extrapolation, possibly elsewhere in the region and globally.

The variability associated with the RMW produced not only by the BRI and #18 Winze, but also that associated with #17 Winze and the mixture drawn from the BRI Dam for treatment in the HDS Plant, is illustrated in Fig. 3. The data set of $n = 91$ values spans the period of common record December 2012 to September 2014. The results present a striking reflection of the complexity that informs the hydrochemistry of AMD at source in the Western Basin revealing, amongst others, the following characteristics:

- BRI consistently produces the least variable RMW chemistry;
- BRI and #18 Winze consistently produce the most similar RMW chemistry;
- #17 Winze consistently produces RMW with the most variable pH and SEC; and
- the low median pH and Fe values associated with the RMW mixture compared to each of the sources are consistent with the production of free hydrogen ions and precipitation of iron associated with hydrolysis (Sect. 5.1) in the oxygenated BRI Dam.

Turning attention to the TMW produced by the HDS mine water treatment plant and discharged to the Tweelopie Spruit at the end-of-pipe, an inspection of the pH, SEC, SO_4 ,

Fe and Mn associated with this water is presented in Fig. 4. The patterns and trends are readily explained by various factors such as the onset of uncontrollable RMW discharge (Sect. 3.1 in Chapter “Physical Hydrology”) in February 2010, which explain the period of consistently low pH values (<4) and elevated Fe concentrations in the second half of the record. The marked difference in mean and median Fe values in this water (reflected in the CoV value of 356%, Table 3), is attributed to the bias introduced by the ca. May 2006, February 2010 to July 2012 and March to July 2014 concentrations illustrated in Figs. 4 and 8. The efficacy of the mine water treatment process especially since the commissioning of the immediate and short-term intervention measures in mid-2012 and expanded in mid-2013 (Text Box 4 in Chapter “Physical Hydrology”), is clearly reflected in the more acceptable pH, Fe and SO_4 levels during periods of controlled mine water discharge.

1.2.2 Tweelopie Spruit

The chemistry of Tweelopie Spruit water is monitored by SG at five localities from where it leaves the mine property down to the confluence with the Riet Spruit north of the KGR, a distance of ~6.4 km. These localities are identified as (a) the inlet to the KGR, (b) the Hippo Dam, (c) the Charles Fourie Dam, (d) the Aviary Dam and (e) the (Krugersdorp) Brickworks Dam (station F11S12). The monitoring therefore provides a record of the mine water quality discharge that eventually enters the karst terrane of the COH.

The weekly monitoring of the variables pH, EC and SO_4 dates back to May 2004. The results for the upstream Hippo Dam and the downstream F11S12 (Brickworks Dam) are presented in Fig. 5 (pH), Fig. 6 (SEC) and Fig. 7 (SO_4). The KGR inlet data are excluded due to their close proximity to the Hippo Dam, and consideration of the fact that the residence time of this water in the Hippo Dam renders the data for the latter location more representative of the mine water entering the Tweelopie Spruit. The Charles Fourie Dam and Aviary Dam data are excluded because of their congruence as intermediate compositions between those observed at the Hippo and Brickworks dams (Volume 2).

The patterns revealed in the graphs indicate the trend and variation in the respective variable concentrations through the KGR over time. De Villiers and Mkwelo (2009) have demonstrated the use of SO_4 as a measure of surface water deterioration in the Olifants River catchment similarly influenced by mine water impacts, using the long-term record of this analyte to assess the efficacy of the DWSs surface water quality monitoring.

It is clear from Fig. 5, and to a lesser extent from Figs. 6 and 7, that the severest and most sustained mine water impact on the receiving surface water environment of the Tweelopie Spruit commenced ca. February 2010. This is unequivocally shown in the somewhat shorter record of Fe (Fig. 8) and

¹ Which have no influence on the chemistry of the raw mine water produced by any AMD source.

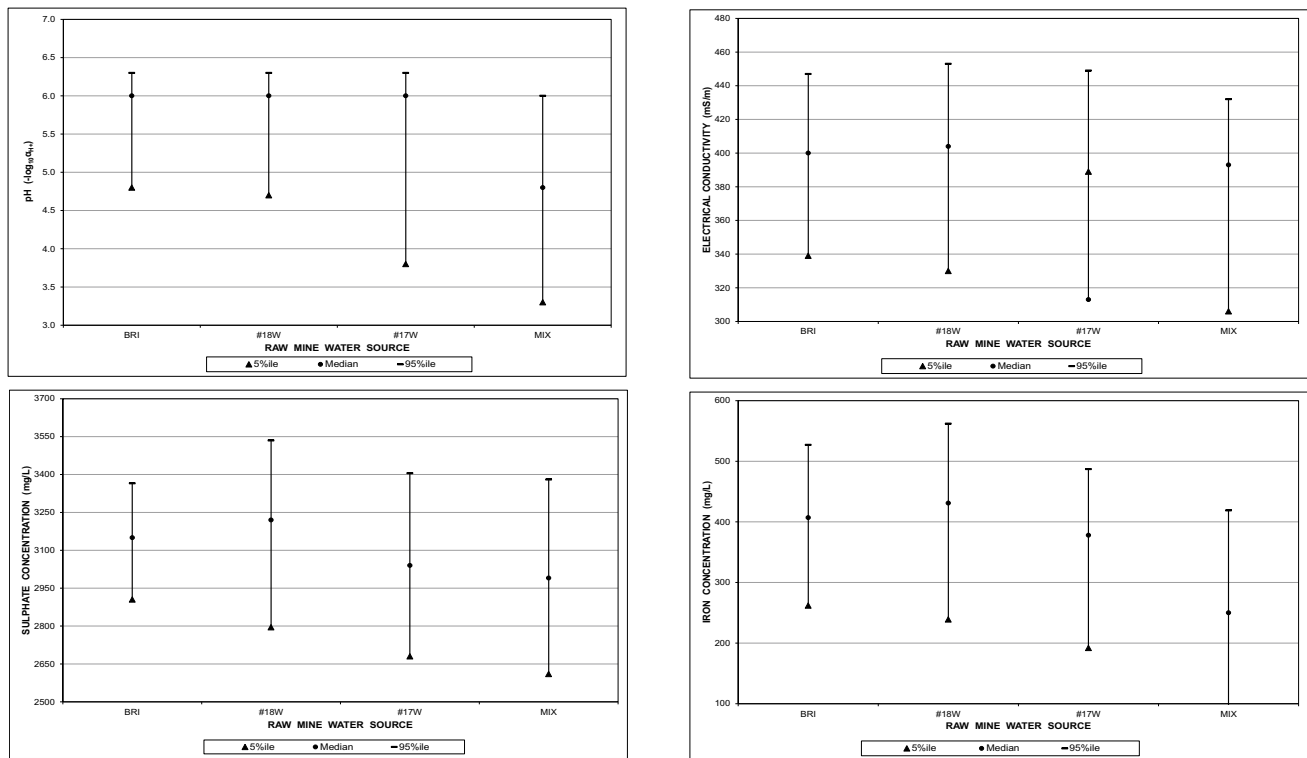


Fig. 3 Variability of pH (top left), EC (top right), SO_4 (bottom left) and Fe (bottom right) associated with raw mine water produced by the BRI, #18 Winze and #17 Winze point sources of AMD, and the RMW mixture (MIX) drawn from the BRI Dam for treatment in the HDS Plant

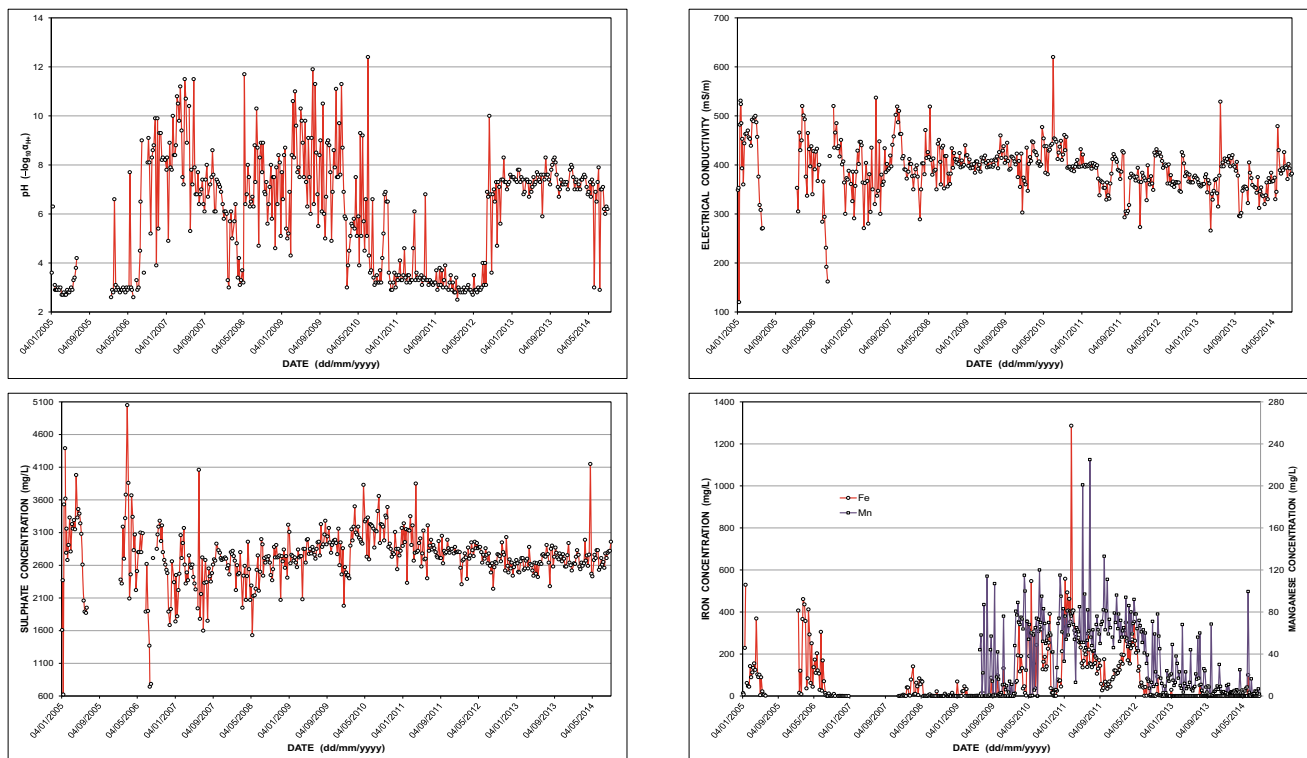


Fig. 4 Long-term pattern and trend of pH (top left), EC (top right), SO_4 (bottom left) and Fe and Mn (bottom right) associated with treated/neutralised mine water produced by the HDS mine water treatment plant and discharged into the Tweelopie Spruit at the end-of-pipe

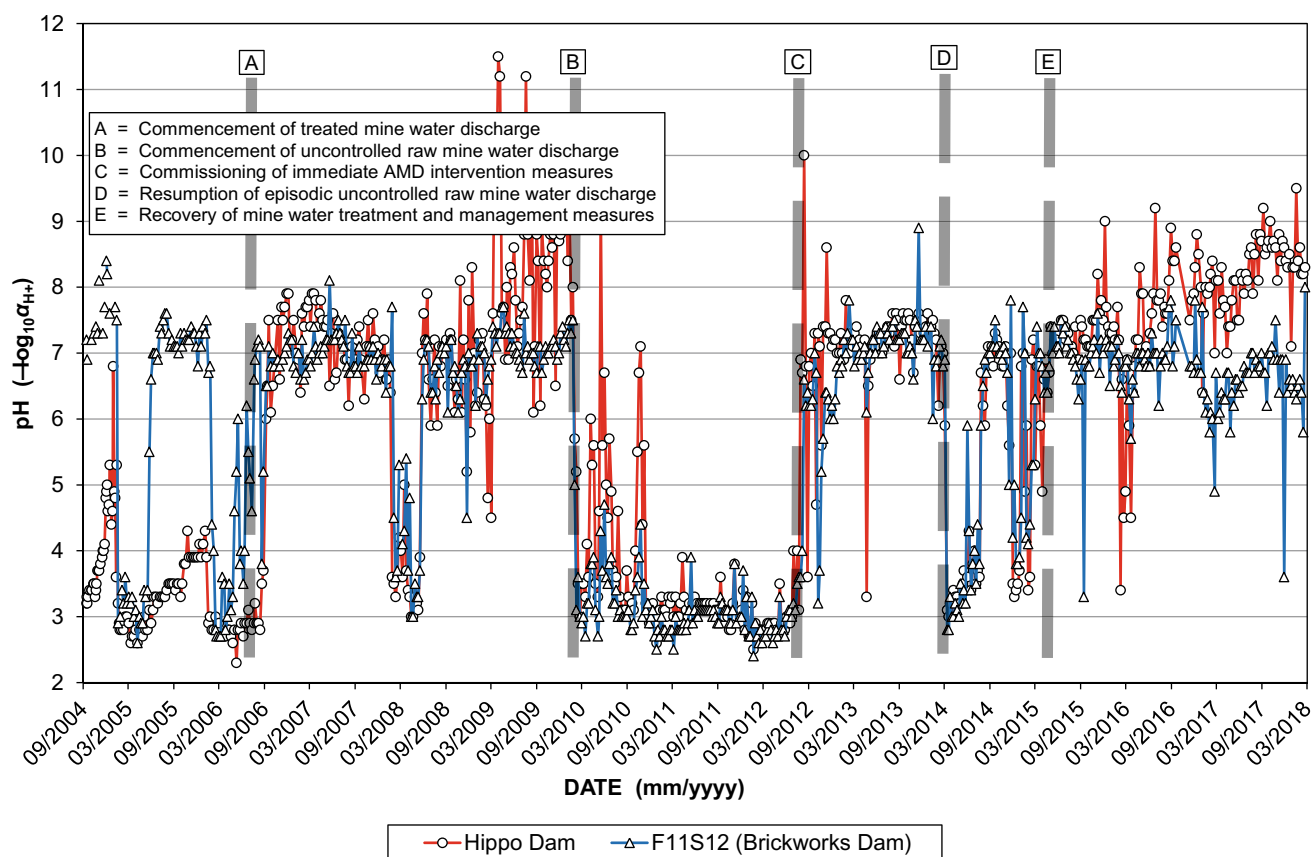


Fig. 5 Pattern and trend of pH of Tweelapie Spruit water from May 2004 to September 2014

especially the Mn values (Fig. 9). Prior to this, the gradual ‘increase’ in impact since 2004 is evidenced by the increasing SEC and SO_4 trends up to the persistent elevated levels in the second half of the record period (Figs. 6 and 7). The discharge regimes associated with these observations are discussed in Sect. 3.1 in Chapter “Physical Hydrology”.

A scrutiny of the differences between the three periods of record defined by the divisions recognised in Figs. 5, 6 and 7 returns the information presented in Table 4 and illustrated in Fig. 10. The graphs not only illustrate the differences, most notably the ‘poorer’ values in the B–C period of severest mine water impact, but also reveal other salient aspects such as the following.

- The generally greater variability in analyte/variable concentrations at the upstream Hippo Dam station compared to the F11S12 station.
- The typically lower analyte/variable concentrations (except pH) at the F11S12 station compared to the upstream Hippo Dam station.

The statistics for total uranium (U_T) indicate the need for caution when considering U concentrations under circumstances where significant differences between the ‘normal’

A–B and C–D periods and the ‘abnormal’ B–C period are evident. The mean and median values at both stations in the B–C period exceed the SANS (2015a) limit of 0.015 mg/L associated with a chronic health risk attributable to ingestion over an extended period. In contrast, the mean and median values for the other two periods meet the limit. A factor that is not considered, however, is the potential under-evaluation of U concentrations associated with a ‘biased’ sample collection regimen. For example, Winde et al. (2004) report differences in U concentrations between daytime and night-time samples, the latter typically returning higher concentrations. Reasons put forward for this include preferential groundwater exfiltration and lower pH values at night when biological decalcification and the associated U immobilisation is also at a minimum.

The association of mine water with the presence of other metals such as aluminium (Al), cadmium (Cd), copper (Cu), mercury (Hg), nickel (Ni), lead (Pb) and zinc (Zn) raises concern for the levels of these elements in the water discharged into the environment. The weekly surface water quality monitoring programme carried out by SG, and which forms the basis for the analysis presented in Sect. 1.2, has since January 2005 included the metal analytes listed in Table 5 for the periods indicated (Table 6). Interrogation of

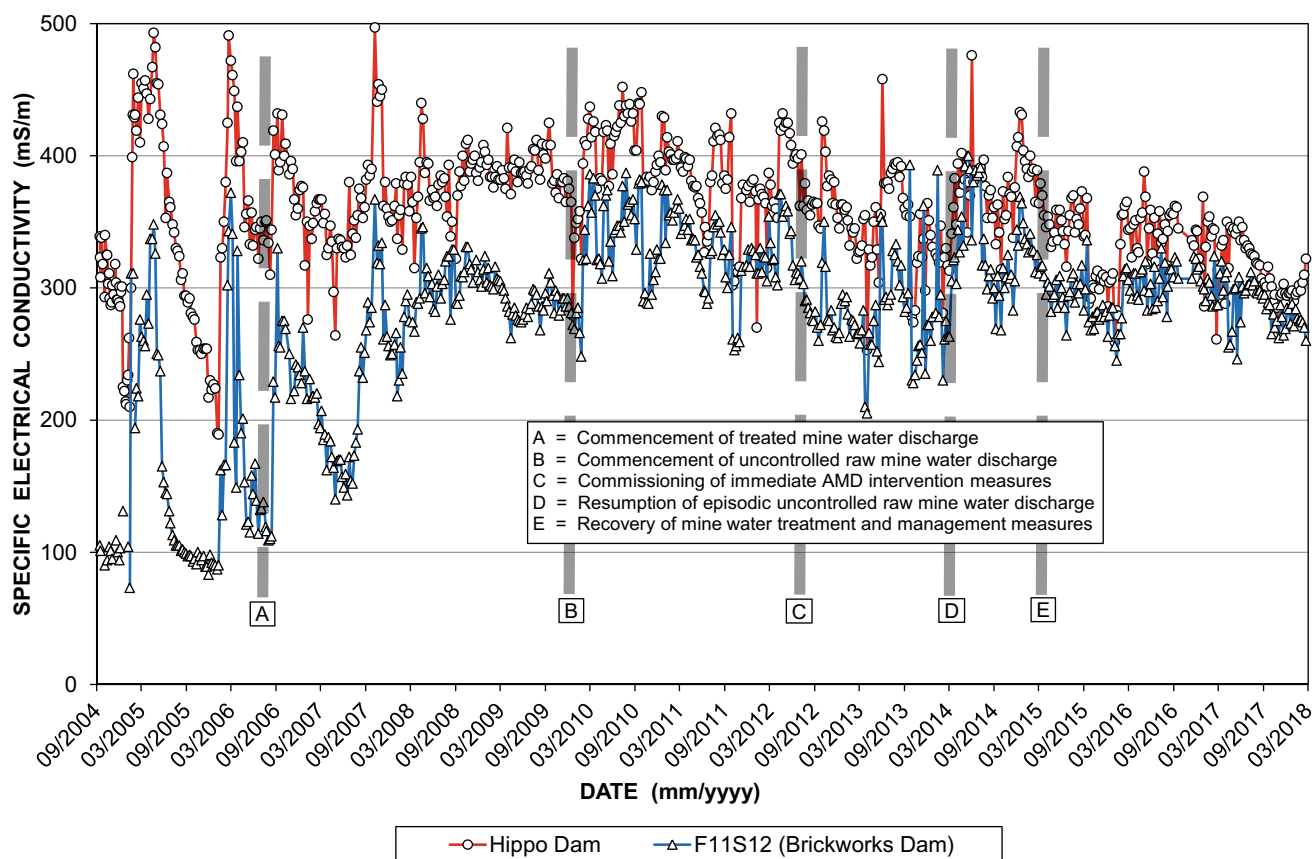


Fig. 6 Pattern and trend of SEC of Tweelopie Spruit water from September 2004 to September 2014

the data set presented in Table 5 returns the statistical results given in Table 6. The results reflect concern for the analytes Mn, Ni and Cd at the 50%ile level.

A slightly different picture emerges when an interrogation of the data set represented in Table 5 is carried out for the first three periods of distinctly different discharge chemistry recognised in Figs. 5, 6, 7 and 8 and 9 and Table 4. This is presented in Table 7, and despite the differences with Table 6, the results again reflect concern for the analytes Mn, Ni and Cd at the 50%ile level.

Although Heath et al. (2009) report a poor correlation between electrical conductivity and sulfate in the Lower Vet River Catchment, the congruence that is apparent between the SEC values and the SO_4 concentrations illustrated in Figs. 6 and 7 prompts an inspection of the correlation between these hydrochemical variables for the study area. In a study of AMD produced by the copper and sulfur mines at Avoca, South-East Ireland, Gray (1996) reports the use of EC to predict the SO_4 concentration in both AMD and contaminated surface waters using regression analysis. The correlation between these variables at three sites in the Tweelopie Spruit and at station A2H049 at the end of the Bloubank Spruit system, computed on the basis of the SO_4 :SEC ratio, is summarised in Table 8. Graphs of the correlations are

presented in Volume 2. The similarity of the linear regression expressions for the Tweelopie Spruit stations and that of Gray (1996) is apparent. Also evident is the improvement in the regression coefficient value (R^2) from 0.63 at the upstream Hippo Dam station to 0.92 at station A2H049.² This result is at odds with the finding by Gray (1996) that the strength of the correlation improves with increasing AMD contamination which, in this instance, would hold for the upstream Hippo Dam and Charles Fourie Dam stations.

Unlike other ions, SO_4 is unaffected by variations in pH and is not significantly removed by sorption or precipitation processes (Gray 1996). A provisional explanation for the improved correlation is therefore attributed to an initially less stable water chemistry which approaches chemical equilibrium with distance along the flow path. This might be associated with the continued precipitation of dissolved ferrous iron as ferric iron (oxy)hydroxide (FeOOH).

Whatever the reason for the improved correlation along the flow path, it is evident that the reasonable correlation

²It is shown in **Annexure B** that the A2H049 data support either an exponential trend or a bi-linear trend with an inflection point at 60 mS/m, where values <60 mS/m reflect the mitigating influence of the karst springs, and values ≥ 60 mS/m the mitigating influence of AMD.

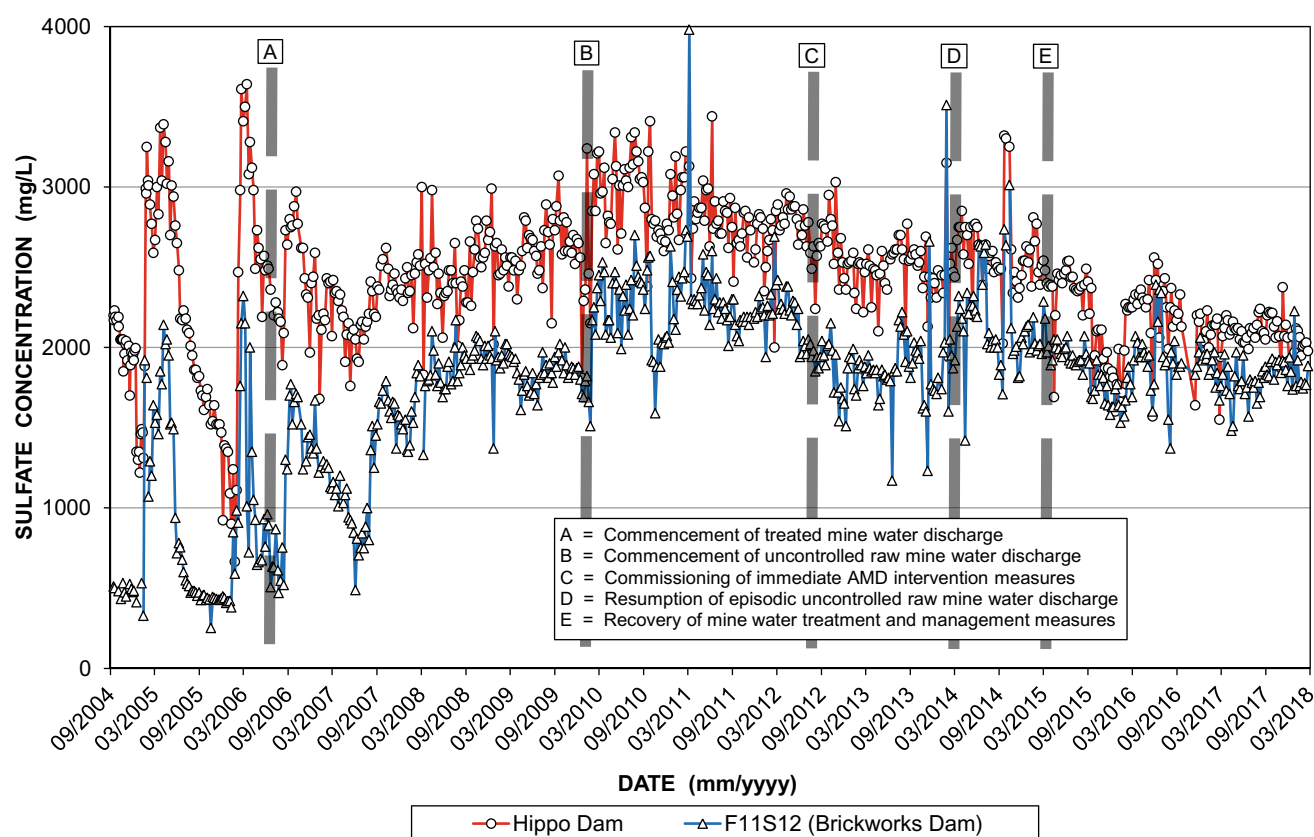


Fig. 7 Pattern and trend of SO_4 levels in Tweelopie Spruit water from September 2004 to September 2014

allows the readily determined SEC value to be used to calculate an approximate SO_4 concentration for AMD-impacted surface water in the study area. This is especially useful under circumstances where SO_4 analysis in the field is difficult due to a lack of ion-specific electrodes. As noted by Gray (1996), it also has application where the optimal measure of dilution of a water sample prior to analysis of SO_4 in a laboratory (e.g. by ICP) must be determined.

The data presented in Table 9 summarise the results of the DWS water quality monitoring³ at station F11S12. This period precedes the 2010, 2011 and 2014 hydrological years when the chemistry of water in the drainages receiving mine water experienced a much greater raw mine water influence (see discussion earlier in this section). Nevertheless, it is evident from Table 9 that the historical median SEC, TDS, SO_4 and Mn values exceed the SANS (2015a) limits for these analytes, and that this exceedance extends to Fe and Al at the 95%ile level. All these six variables/analytes show non-compliance in regard to their mean values. Despite these circumstances, the mean and median electrical balance values remain acceptable. Sulfate typically comprises ~65% of

the TDS, very similar to the ~64% that characterises RMW (Table 2) and TMW (Table 3). Together with the Ca- SO_4 composition (Fig. 11), the mine water dominance in the surface water at this location is again unequivocal, as is the significant variance associated with Ca and especially SO_4 .

1.2.3 Riet Spruit

Although the Riet Spruit rises in Riebeeck Lake in Randfontein (Sect. 3 in Chapter “Physical Hydrology”), it is only from its confluence with the Tweelopie Spruit tributary at Glen Almond north of the Krugersdorp Game Reserve that it gains relevance for the COH, and for the following reasons:

- the Riet Spruit receives the mine water discharge from the Western Basin via the Tweelopie Spruit;
- the confluence is located just outside the south-western boundary of the COH, and surface water drains into the WHS via both the surface and subsurface from this position; and
- the receiving reach of the Riet Spruit is a losing drainage contributing allogenic mine water recharge to the karst aquifer of the Zwartkrans Basin (Sect. 5.2.1 in Chapter “Physical Hydrology”).

³ Data sourced from the DWS in November 2013 indicates that the most recent analysis on record for station F11S12 is dated 29/09/2008.

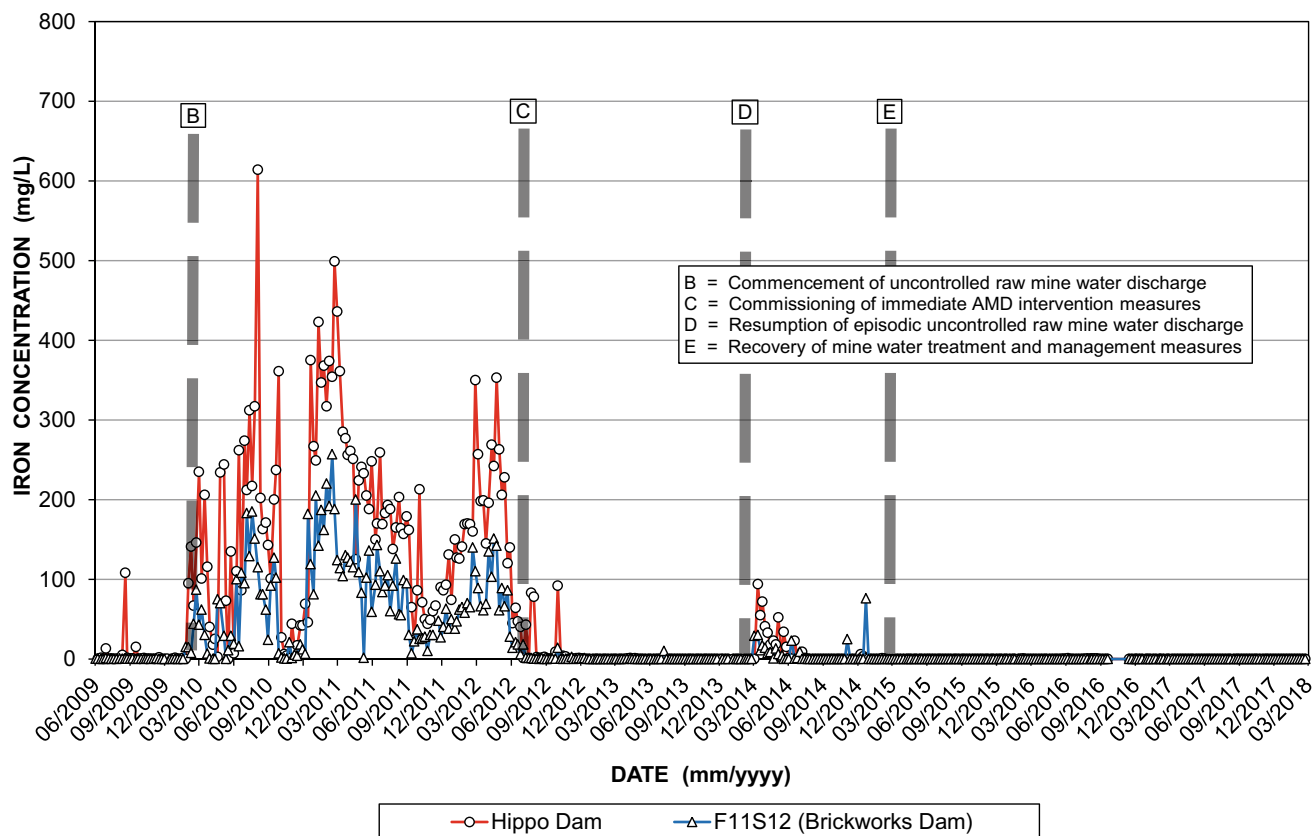


Fig. 8 Pattern and trend of Fe levels in Tweelopie Spruit water from June 2009 to September 2014

The temporal behaviour of SEC and pH at stations F11S12 and MRd over a period of four years is illustrated in Fig. 12. Based on the data presented in Table 10, the record starts after the resumption of uncontrolled raw mine water decant on 30/01/2010. These circumstances have been discussed in Sect. 3.1 in Chapter “Physical Hydrology” and illustrated in Fig. 13 in Chapter “Physical Hydrology” in regard to discharge rates, and earlier in this section in regard to hydrochemistry.

The record in Fig. 12 reflects already acidic conditions (pH 3.2–4.4) that worsen from August 2010 (pH < 3) until an improvement is manifested in late 2012. A similar response is observed in regard to the SEC values, which typically exceed 350 mS/m until late 2012, after which values reduce to <300 mS/m. It is also evident from Fig. 12 that the pH value at station MRd is generally lower than at station F11S12, especially in the latter part of the record. This response is readily explained as the result of hydrolysis (Sect. 5).

Although spanning a distance of only ~3.9 km, the chemistry of surface water passing stations F11S12 and MRd is revealing in itself. It reflects both the hydrochemistry of allogenic recharge to the karst aquifer and the evolution of water quality in this section of river reach. The close similarity of the major ion composition at the sampling stations

is reflected in Fig. 13. The concentrations of selected trace metals (Fig. 14), on the other hand, indicate increases in Mn and Al and a decrease in Fe concentration at the downstream station. The lower Fe concentration is readily explained on the basis of precipitation of this metal out of solution in the presence of oxygen. The low pH, in turn, might also explain the increase in Al and Mn levels (Fig. 14) because of mobilisation of these metals from streambed sediments (Beltrán et al., 2010). This aspect is discussed in Sect. 5.4. The reader is reminded of the significance of the sampling date in the timeframe of the mine water discharge regime (Sect. 3.1 in Chapter “Physical Hydrology”).

1.2.4 Blougat Spruit

The next tributary to the east of the Tweelopie Spruit, the Blougat Spruit is monitored by the DWS at station 188048 (Fig. 4) downstream of the Percy Stewart WWTW treated sewage effluent discharge point. This position is ~3.5 km above the confluence with the Riet Spruit. The data presented in Table 11 summarise the results of this monitoring.⁴ The median and mean electrical balance values only

⁴ Data obtained from the DWS in November 2013 for station 188048 indicated a most recent sample date of 30/09/2008.

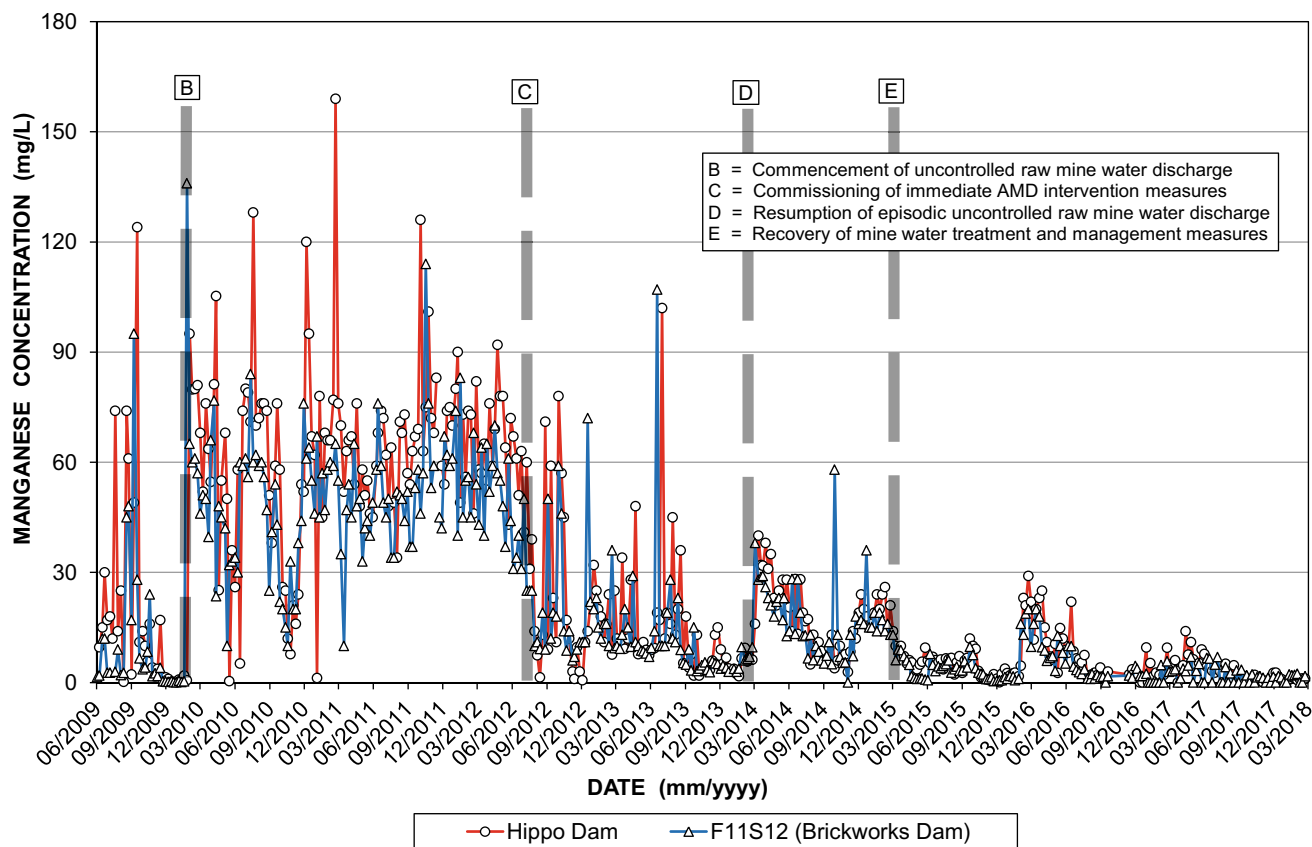


Fig. 9 Pattern and trend of Mn levels in Tweelapie Spruit water from June 2009 to September 2014

marginally exceed the acceptable error margin of $\pm 5\%$ and, considering the source of this water, render the veracity of the analytical results acceptable. The median values of $\text{NO}_3 + \text{NO}_2$ and Mn, and the 95%ile values of SEC, SO_4 , $\text{NO}_3 + \text{NO}_2$, Fe and Mn exceed the standard health related limits (SANS, 2015a). The treated wastewater origin of this discharge readily explains the SO_4 and $\text{NO}_3 + \text{NO}_2$ exceedances, as well as the high measure of variance in the SO_4 concentration (Fig. 15). Sulfate typically comprises $\sim 33\%$ of the TDS of this water (Table 11 and Text Box 1), whilst TDS typically represents 6.3 times the SEC of this water.

Awofolu et al. (2007) report the results (Table 12) of the trace metal analyses Cd, Pb, Mn, Zn, Ni and Cu in water samples collected on four occasions in late 2006 from three sites located downstream of the Percy Stewart WWTW. The sites coincide with the stations identified in this study as BG@N14 (Blougat Spruit at the N14), BB@M (Bloubank Spruit at Makiti) and BB@PL (Bloubank Spruit at Plover's Lake) (Fig. 24). The results are in agreement regarding an elevated Mn concentration, which raises concern for the presence of this metal in the municipal wastewater discharge. It is postulated that this result reflects the industrial wastewater component received by the WWTW, which was originally designed to receive only domestic wastewater.

The data presented in Table 13 summarise the chemistry of the treated wastewater effluent discharged by the Percy Stewart WWTW as monitored and reported by the MCLM. The analysis reveals compliance of all the inorganic and organic analytes (including $\text{NO}_3 + \text{NO}_2$) with the SANS (2015a) limits. This observation suggests that the $\text{NO}_3 + \text{NO}_2$ exceedances noted in Table 11 for station 188048 either pre-date July 2007 or derive from a source located upstream of the Percy Stewart WWTW. This disparity warrants interrogation in a separate study. The significant exceedances shown by the bacteriological variables in Table 13 are cause for considerable concern, as are the coliform counts reported in the text box in Fig. 15. Similarly, the mean and median PO_4 values of >4 mg P/L and the elevated chemical oxygen demand (COD) values generate concern for potential eutrophication in downstream receiving water bodies. A notable exclusion from the MCLM analytical suite is SO_4 .

The data presented in Table 14 summarise the chemistry of the treated wastewater effluent discharged by the Percy Stewart WWTW as reported to the DWS for station PSFE.

Table 14 data record goes back to late 2002, compared to the shorter MCLM record (Table 13). The data support the observed exceedances associated with the bacteriological

Table 4 Summary statistics of period-specific surface water chemistry changes in the Tweelopie Spruit associated with four distinct mine water discharge regimes

| Variable /Analyte | Statistical parameter | Hippo Dam | | | | F11S12/Brickworks Dam | | | |
|----------------------------|-----------------------|--------------------|--------------------|--------------------|-----------------|-----------------------|--------------------|--------------------|-----------------|
| | | A–B ¹ | B–C ² | C–D ³ | D– ⁴ | A–B ¹ | B–C ² | C–D ³ | D– ⁴ |
| pH ($-\log_{10}a_{H^+}$) | n | 176 | 129 | 83 | 20 | 173 | 128 | 83 | 20 |
| | 5%ile | 3.6 | 2.8 | 5.9 | 3.0 | 3.9 | 2.7 | 5.3 | 2.8 |
| | Mean | – | – | – | – | – | – | – | – |
| | Median | 7.2 | 3.2 | 7.2 | 3.4 | 6.9 | 3.0 | 7.0 | 3.4 |
| | 95%ile | 9.3 | 5.7 | 7.6 | 4.0 | 7.4 | 3.9 | 7.4 | 4.5 |
| | SD | 1.5 | 1.0 | 0.8 | 0.3 | 0.9 | 0.4 | 0.9 | 0.7 |
| | CoV | 22 | 30 | 11 | 10 | 14 | 14 | 13 | 20 |
| SEC (mS/m) | n | 175 | 129 | 83 | 20 | 172 | 128 | 83 | 20 |
| | 5%ile | 324 | 320 | 285 | 342 | 167 | 288 | 230 | 305 |
| | Mean | 374 | 391 | 350 | 382 | 268 | 332 | 281 | 356 |
| | Median | 379 | 393 | 354 | 383 | 283 | 330 | 276 | 349 |
| | 95%ile | 426 | 438 | 395 | 406 | 329 | 378 | 350 | 400 |
| | SD | 32 | 33 | 34 | 28 | 48 | 29 | 34 | 34 |
| | CoV | 9 | 8 | 10 | 7 | 18 | 9 | 12 | 10 |
| SO ₄ (mg/L) | n | 176 | 128 | 82 | 20 | 171 | 128 | 83 | 20 |
| | 5%ile | 2017 | 2511 | 2221 | 2381 | 893 | 1947 | 1600 | 1990 |
| | Mean | 2445 | 2846 | 2520 | 2638 | 1636 | 2264 | 1879 | 2260 |
| | Median | 2460 | 2815 | 2525 | 2655 | 1760 | 2240 | 1870 | 2250 |
| | 95%ile | 2810 | 3220 | 2770 | 2774 | 2015 | 2593 | 2148 | 2640 |
| | SD | 259 | 226 | 193 | 153 | 349 | 245 | 268 | 273 |
| | CoV | 11 | 8 | 8 | 6 | 21 | 11 | 14 | 12 |
| Fe (mg/L) | n | 33 | 129 | 83 | 20 | 33 | 128 | 82 | 20 |
| | 5%ile | 0.1 | 6.5 | 0.004 | 0.2 | 0.1 | 1.2 | 0.006 | 0.1 |
| | Mean | 4.7 | 168.4 | 2.490 | 24.6 | 0.3 | 72.9 | 0.466 | 8.8 |
| | Median | 0.4 | 163.0 | 0.030 | 18.0 | 0.2 | 64.0 | 0.075 | 6.7 |
| | 95%ile | 13.8 | 365.2 | 3.090 | 73.0 | 0.8 | 186.3 | 1.000 | 29.1 |
| | SD | 18.8 | 116.2 | 13.150 | 26.7 | 0.3 | 57.7 | 1.896 | 9.7 |
| | CoV | 399 | 69 | 528 | 109 | 94 | 79 | 407 | 110 |
| Mn (mg/L) | n | 34 | 129 | 83 | 20 | 33 | 128 | 83 | 20 |
| | 5%ile | 0.2 | 22.2 | 1.9 | 13.9 | 0.1 | 20.7 | 3.3 | 12.6 |
| | Mean | 18.1 | 62.7 | 16.5 | 25.5 | 10.3 | 50.3 | 14.4 | 21.9 |
| | Median | 9.8 | 65.0 | 11.0 | 26.5 | 2.7 | 50.0 | 10.0 | 22.5 |
| | 95%ile | 74.0 | 95.0 | 56.1 | 38.1 | 46.2 | 76.0 | 45.0 | 29.5 |
| | SD | 27.6 | 23.5 | 18.0 | 7.7 | 19.4 | 17.6 | 15.8 | 7.0 |
| | CoV | 153 | 38 | 109 | 30 | 188 | 35 | 110 | 32 |
| U _T (mg/L) | n | 56 | 129 | 61 | – | 56 | 128 | 61 | – |
| | 5%ile | 0.003 ⁵ | 0.003 ⁵ | 0.003 ⁵ | – | 0.003 ⁵ | 0.003 ⁵ | 0.003 ⁵ | – |
| | Mean | 0.013 | 0.049 | 0.009 | – | 0.008 | 0.035 | 0.004 | – |
| | Median | 0.010 | 0.043 | 0.006 | – | 0.003 ⁵ | 0.030 | 0.003 ⁵ | – |
| | 95%ile | 0.030 | 0.109 | 0.025 | – | 0.026 | 0.076 | 0.011 | – |
| | SD | 0.018 | 0.042 | 0.008 | – | 0.011 | 0.032 | 0.003 | – |
| | CoV | 135 | 85 | 98 | – | 147 | 91 | 95 | – |

¹September 2006–January 2010²February 2010–July 2012³August 2012–February 2014⁴March 2014–September 2017⁵Value biased by the detection limit (DL) of 0.005 mg/L, analysed as 50% DL (0.0025 mg/L) if < DL

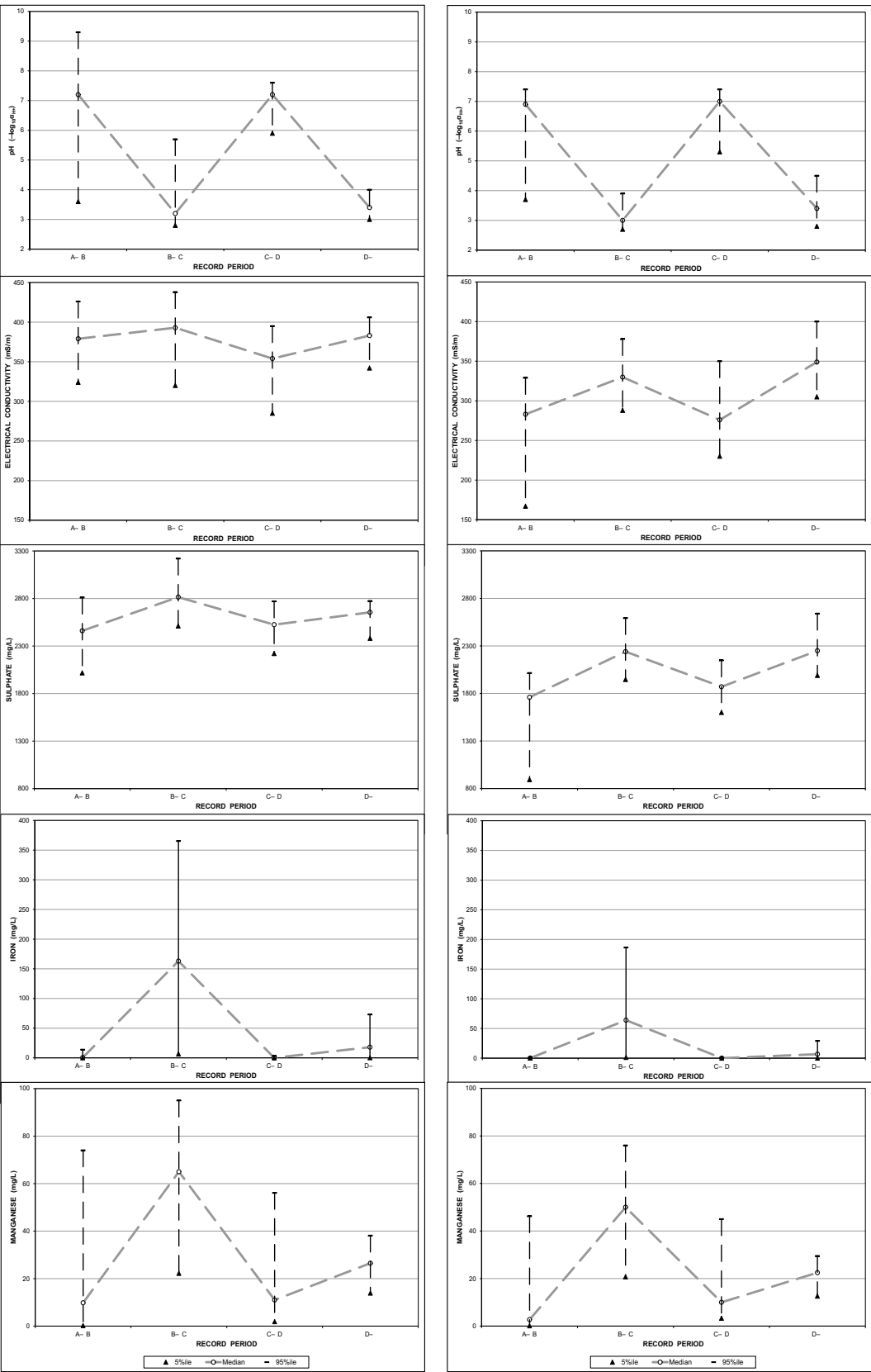


Fig. 10 Period-specific surface water chemistry changes in the Tweeloping Spruit of the variables/analytes (from top to bottom) pH, SEC, SO_4 , Fe and Mn at the Hippo Dam (left) and F11S12 (right) (data from Table 4)

Table 5 List of metal analytes monitored in treated/neutralised mine water discharged to the Tweelapie Spruit from the mine area per distinctive monitoring period

| Analyte | Monitoring period | | | | SANS (2015a) ¹ |
|-----------------------|-------------------|-----------------|-----------------|-----------------|---------------------------|
| | 01/2005–07/2009 | 08/2009–09/2010 | 10/2010–11/2012 | 12/2012–05/2014 | |
| Fe (mg/L) | 0.1 | 0.1 | 0.1 | 0.001 | ≤ 2 |
| Al (mg/L) | | 1.0 | 1.0 | 0.001 | ≤ 0.3 |
| Mn (mg/L) | | 0.1 | 0.1 | 0.1 | ≤ 0.5 |
| U _T (µg/L) | | 5.0 | 5.0 | | ≤ 15 |
| Cr (mg/L) | | 0.001 | 0.001 | | ≤ 0.05 |
| V (mg/L) | | 0.001 | 0.001 | | ≤ 0.2 |
| Pb (mg/L) | | 0.001 | 0.001 | 0.001 | ≤ 0.01 |
| Co (mg/L) | | 0.001 | 0.001 | | ≤ 0.5 |
| Ni (mg/L) | | 0.001 | 0.001 | 0.001 | ≤ 0.07 |
| U _D (µg/L) | | | 5.0 | 5.0 | ≤ 15 |
| Cd (mg/L) | | | | 0.001 | ≤ 0.003 |
| Cu (mg/L) | | | | 0.001 | ≤ 2 |
| Zn (mg/L) | | | | 0.001 | ≤ 5 |

¹Standard health-related limit for consumption of 2 L/d over 70 years by a 60 kg person

U_T denotes total uranium, and U_D denotes dissolved uranium

Bold cells denote analyte monitoring period and associated detection limit

Blank cells denote absence/discontinuance of analyte monitoring

Table 6 Statistical analysis of metal analyte concentrations in treated/neutralised mine water discharged to the Tweelapie Spruit from the mine area per distinctive monitoring period

| Analyte | Monitoring period | | | | | | | | | | | |
|-------------------------------|-------------------|-----|--------------|--------------|-----------------|-----|--------------|---------------|--------------------------------|-----|--------------|--------------|
| | 08/2009–09/2010 | | | | 10/2010–11/2012 | | | | 12/2012–05/2014 ⁽²⁾ | | | |
| | Σn | >DL | 50%ile | 95%ile | Σn | >DL | 50%ile | 95%ile | Σn | >DL | 50%ile | 95%ile |
| Fe ⁽¹⁾ | 254 | 246 | 0.7 | 162 | 113 | 108 | 1.0 | 31.5 | 77 | 77 | 0.025 | 0.336 |
| Al | 61 | 0 | – | – | 113 | 0 | – | – | 74 | 74 | 0.009 | 0.061 |
| Mn | 61 | 58 | 8.65 | 66.35 | 113 | 112 | 11.00 | 60.90 | 77 | 77 | 8.600 | 50.40 |
| U _T | 61 | 30 | 14.00 | 73.25 | 113 | 89 | 16.00 | 700.20 | | | | |
| Cr | 61 | 9 | 0.001 | 0.019 | 113 | 18 | 0.001 | 0.866 | | | | |
| V | 61 | 4 | 0.001 | 0.002 | 113 | 2 | 0.001 | 0.001 | | | | |
| Pb | 61 | 16 | 0.002 | 0.033 | 113 | 22 | 0.005 | 0.030 | 75 | 2 | 0.002 | 0.002 |
| Co | 61 | 60 | 0.070 | 2.005 | 113 | 111 | 0.050 | 0.350 | | | | |
| Ni | 61 | 56 | 0.150 | 3.725 | 113 | 113 | 0.170 | 0.940 | 75 | 75 | 0.100 | 0.118 |
| U _D ⁽²⁾ | | | | | 113 | 51 | 9.9 | 35.0 | 77 | 32 | 7.850 | 26.35 |
| Cd | | | | | | | | | 75 | 2 | 0.007 | 0.010 |
| Cu | | | | | | | | | 75 | 55 | 0.002 | 0.010 |
| Zn | | | | | | | | | 75 | 75 | 0.017 | 0.100 |

¹Values for period 08/2009–09/2010 calculated from 01/2005 as per Table 5

²Detection limit for U_D raised from 5 µg/L to 20 µg/L as from June 2014

Analyte units (and symbols) as per Table 5

>DL denotes number of analyte values that exceed the detection limit as per Table 5

Bold text denotes value exceeds standard limit as described in Table 5 (note 1)

Table 7 Statistical analysis of metal analyte concentrations in treated/neutralised mine water discharged to the Tweelopie Spruit from the mine area per distinctive discharge period

| Analyte | Discharge period | | | | | | | | | | | |
|----------------|------------------|-----|------------|--------------|------------------|-----|--------------|--------------|------------------|-----|--------------|--------------|
| | A–B ¹ | | | | B–C ² | | | | C–D ³ | | | |
| | n | >DL | 50%ile | 95%ile | n | >DL | 50%ile | 95%ile | n | >DL | 50%ile | 95%ile |
| Fe | 116 | 103 | 0.5 | 77.4 | 130 | 121 | 1.200 | 29.0 | 82 | 80 | 0.033 | 4.07 |
| Al | 26 | 0 | – | – | 130 | 0 | – | – | 79 | 61 | 0.009 | 0.100 |
| Mn | 26 | 24 | 6.5 | 72.7 | 130 | 128 | 10.5 | 46.95 | 82 | 82 | 9.450 | 59.85 |
| U _T | 26 | 13 | 12.0 | 66.2 | 130 | 90 | 16.5 | 700 | 18 | 16 | 15.5 | 79.0 |
| Cr | 26 | 3 | 0.010 | 0.024 | 130 | 19 | 0.001 | 0.764 | 18 | 5 | 0.001 | 0.003 |
| V | 26 | 2 | 0.002 | 0.002 | 130 | 4 | 0.001 | 0.001 | 18 | 0 | – | – |
| Pb | 26 | 6 | 0.002 | 0.023 | 130 | 27 | 0.005 | 0.037 | 80 | 7 | 0.002 | 0.003 |
| Co | 26 | 25 | 0.039 | 2.900 | 130 | 130 | 0.050 | 1.063 | 18 | 16 | 0.023 | 0.523 |
| Ni | 26 | 22 | 0.069 | 7.995 | 130 | 129 | 0.180 | 1.820 | 80 | 80 | 0.100 | 0.210 |
| U _D | | | | | 95 | 43 | 9.8 | 22.9 | 82 | 35 | 7.550 | 40.50 |
| Cd | | | | | | | | | 62 | 2 | 0.007 | 0.010 |
| Cu | | | | | | | | | 62 | 46 | 0.002 | 0.010 |
| Zn | | | | | | | | | 62 | 62 | 0.020 | 0.100 |

¹September 2006–January 2010²February 2010–July 2012³August 2012–February 2014

Analyte units (and symbols) as per Table 5

>DL denotes number of analyte values that exceed the detection limit as per Table 5

Bold text denotes value exceeds standard limit as described in Table 5 (note 1)

Table 8 Summary of SO₄: SEC ratio statistics for surface water in the Tweelopie Spruit and the Bloubank Spruit for the period September 2004 to September 2014

| Statistical parameter | Drainage and monitoring station | | | |
|-----------------------|--|--------------------|-----------------------|------------------------------|
| | Tweelopie Spruit | | | Bloubank Spruit |
| | Hippo Dam | Charles Fourie Dam | F11S12/Brickworks Dam | A2H049 |
| n | 535 | 476 | 509 | 159 |
| 5%ile | 5.64 | 5.11 | 4.60 | 1.20 |
| Mean | 6.80 | 6.39 | 6.19 | 1.79 |
| Median | 6.82 | 6.41 | 6.33 | 1.48 |
| 95%ile | 7.89 | 7.70 | 7.46 | 3.52 |
| SD | 0.92 | 0.88 | 1.02 | 0.71 |
| CoV (%) | 13.5 | 13.8 | 16.5 | 39.4 |
| Regression Eq. (1) | y = 6.89x – 17 y = 7.7x – 69.5 ³ | y = 7.31x – 243 | y = 7.19x – 223 | y = 6.39x – 315 ² |
| R ² | 0.63 | 0.85 | 0.88 | 0.92 |
| Distance from LoD (m) | 935 | 2820 | 6390 | 28 160 |

¹y = SO₄ as mg/Lx = SEC as mS/m²For SEC ≥ 60 mS/m³Relationship reported by Gray (1996) for AMD-impacted surface waters

variables. Similarly, the even higher mean and median PO₄ values of > 5 mg P/L again generate concern for potential eutrophication in downstream receiving impoundments.

Encouragingly, the longer term mean and median COD values are significantly lower (~50%) than reported in Table 13. The water quality situation in regard to the Blougat

Table 9 Statistical analysis of Tweelopie Spruit water chemistry data associated with station F11S12 for the period November 2003 to September 2008 sourced from the DWS in November 2013

| Variable/Analyte | Statistical parameter | | | | | | | SANS (2015a) ¹ |
|--|-----------------------|-------|--------------|-------------|--------------|-------|---------|---------------------------|
| | n | 5%ile | Mean | Median | 95%ile | SD | CoV (%) | |
| pH ($-\log_{10}a_{H^+}$) | 54 | 3.3 | – | 7.2 | 8.0 | 1.4 | 21 | 5.0–9.7 |
| SEC (mS/m) | 52 | 86 | 172 | 158 | 296 | 76.3 | 44 | ≤ 170 |
| TDS (mg/L) | 44 | 583 | 1262 | 1150 | 2300 | 602.8 | 48 | ≤ 1200 |
| Ca (mg/L) | 53 | 108.0 | 243.2 | 210.7 | 482.1 | 123.3 | 51 | n.s |
| Mg (mg/L) | 52 | 32.1 | 60.7 | 55.9 | 109.2 | 22.8 | 38 | n.s |
| Na (mg/L) | 53 | 21.4 | 70.0 | 44.0 | 141.7 | 45.1 | 64 | ≤ 200 |
| K (mg/L) | 52 | 1.3 | 4.1 | 3.8 | 7.1 | 2.3 | 56 | n.s |
| Cl (mg/L) | 53 | 13.7 | 23.2 | 20.8 | 36.1 | 7.9 | 34 | ≤ 300 |
| SO ₄ (mg/L) | 52 | 295 | 916 | 811 | 1848 | 527 | 58 | ≤ 500 |
| HCO ₃ (mg/L) | 47 | 11.8 | 39.2 | 36.5 | 77.2 | 19.7 | 50 | n.s |
| NO ₃ + NO ₂ (mg N/L) | 47 | 0.60 | 1.15 | 0.98 | 2.04 | 0.6 | 50 | ≤ 11 |
| Si (mg/L) | 48 | 3.32 | 4.99 | 4.88 | 7.07 | 1.2 | 24 | n.s |
| Fe (mg/L) | 52 | 0.01 | 2.68 | 0.01 | 10.11 | 11.8 | 439 | ≤ 2 |
| Mn (mg/L) | 52 | 0.01 | 14.30 | 7.99 | 60.37 | 19.3 | 135 | ≤ 0.5 |
| Al (mg/L) | 53 | 0.01 | 1.38 | 0.09 | 8.57 | 3.0 | 217 | ≤ 0.3 |
| EB (%) | 46 | –8.2 | 1.1 | 0.8 | 12.8 | 8.5 | 737 | ± 5 |
| TDS:SEC | 44 | 6.7 | 7.8 | 7.7 | 9.3 | 0.9 | 11 | n.s |
| SO ₄ :TDS (%) | 42 | 53 | 64 | 66 | 69 | 1 | 9 | n.s |

¹Standard health-related limit for consumption of 2 L/d over 70 years by a 60 kg person

Bold text denotes value exceeds standard limit as described in note 1

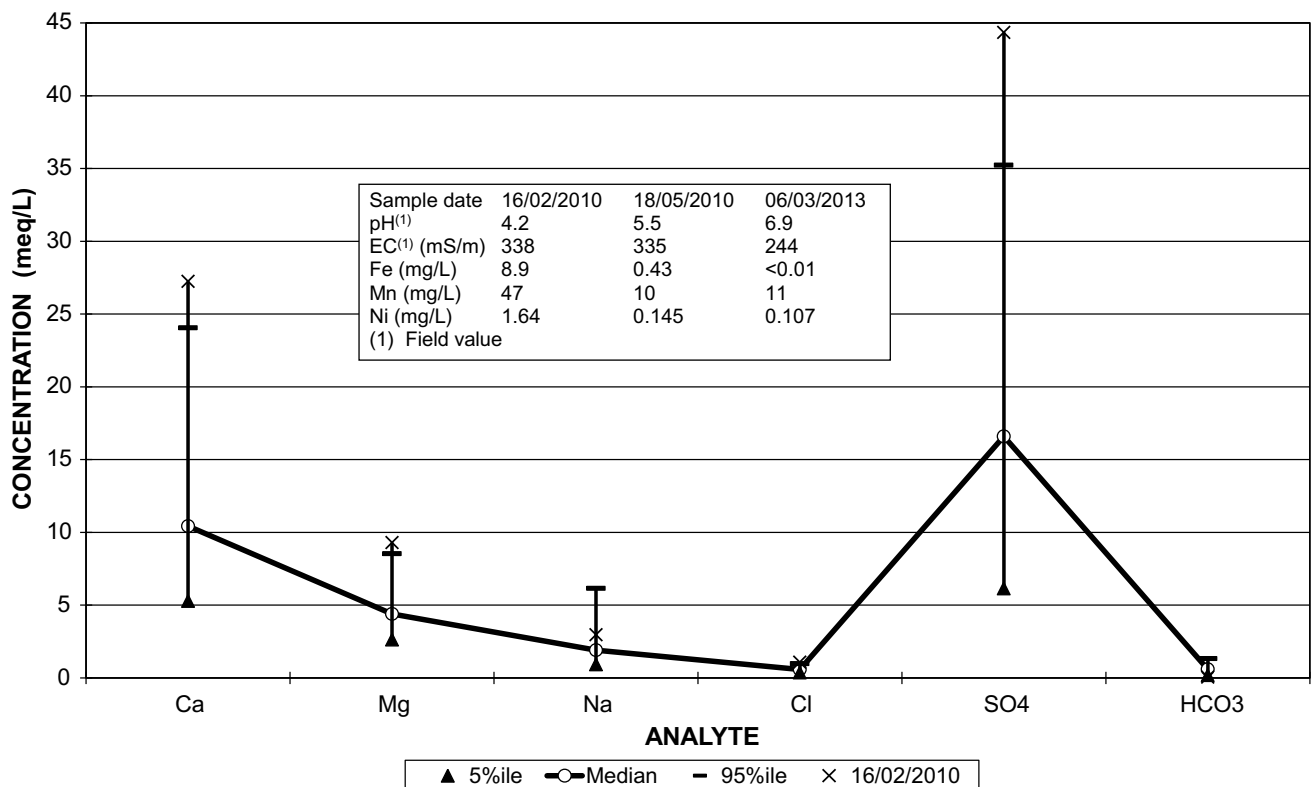


Fig. 11 Variability of Tweelopie Spruit water major ion chemistry at station F11S12 in the period November 2003 to September 2008, also showing mid-February 2010 values (X symbol) for comparison with

more impacted conditions, and subsequent improvement in specific analytes/variables (text box)

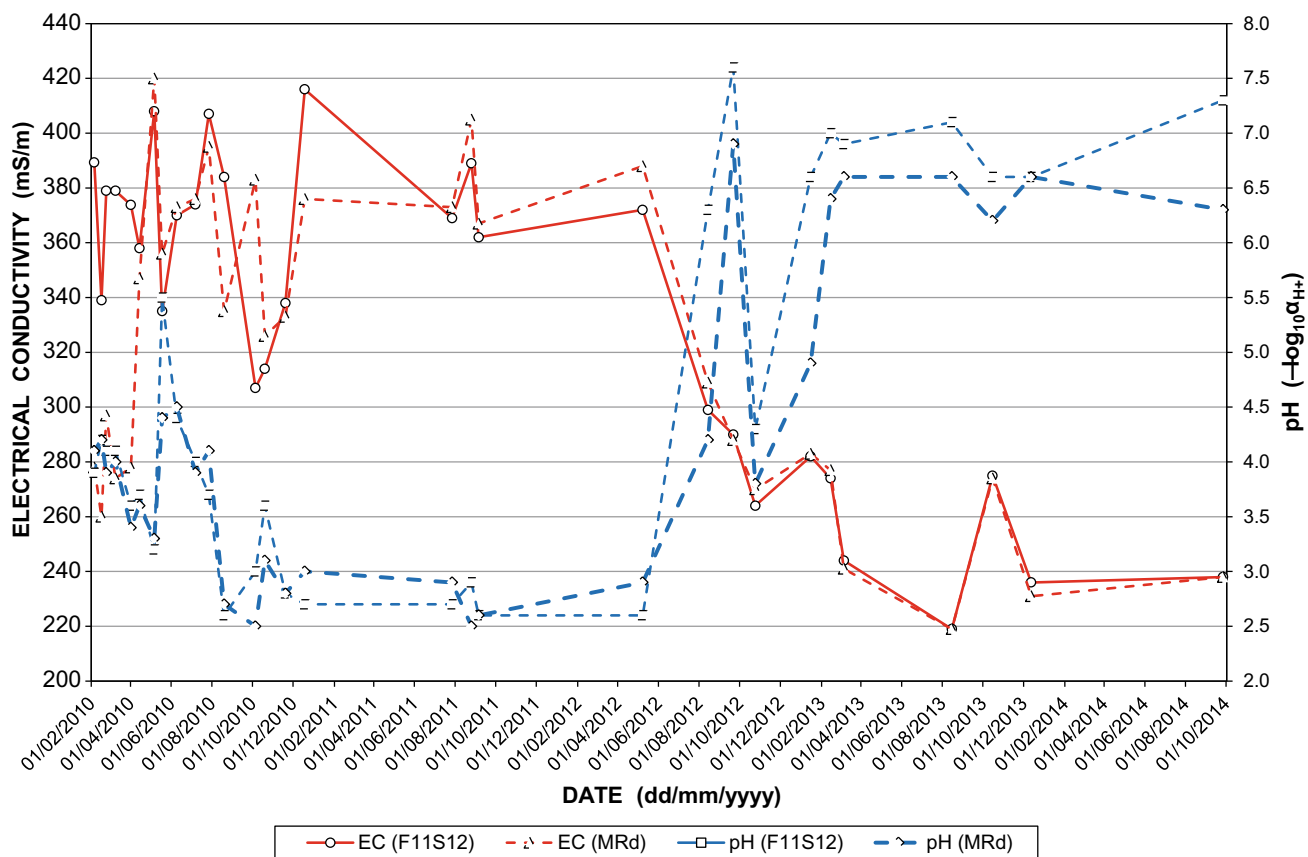


Fig. 12 Pattern and trend of SEC and pH at stations F11S12 and MRd in the Tweelopie/Riet Spruit system in the period February 2010 to September 2014 (data from Table 10)

Spruit is further informed by the DWS monitoring records for stations located upstream (station BGS2) and downstream (BGS1) of the Percy Stewart WWTW. These data are presented in Tables 15 and 16, respectively.

The results for SEC and the inorganic analytes Cl , SO_4 and HCO_3 are shown in Fig. 16, and for the organic analytes $\text{NO}_3 + \text{NO}_2$, NH_4 and PO_4 in Fig. 17. The bacteriological variables faecal coliforms and *E. coli* are compared in Fig. 18. The comparison of the upstream and downstream water quality data indicates that the Percy Stewart WWTW discharge leads to a doubling of the inorganic analyte concentration values in the downstream water (Fig. 16). Further, that the NH_4 and PO_4 nutrient concentrations similarly reflect substantial increases (Fig. 17). Most notable, however, are the orders of magnitude increase in the bacteriological variables (Fig. 18).

The lower $\text{NO}_3 + \text{NO}_2$ concentration at the downstream station BGS1 (Fig. 17) is the single exception to the trend shown by the other variables. A possible explanation lies in a combination of factors such as the relatively large difference in discharge at the two stations and a comparatively

small difference in concentration to begin with. The WWTW discharges at least 16 ML/d ($5.8 \text{ Mm}^3/\text{a}$) to the Blougat Spruit, although SDMs downstream of the plant suggest values closer to the current 24 ML/d capacity of the facility (Sect. 3.2 in Chapter “Physical Hydrology”). The headwater contribution is unknown, but is almost certainly much less under ‘normal’ flow conditions.

An inspection of the surface water quality results associated with monitoring station BC1 provides an indication of the chemical composition of the surface water discharged from the WWTW. Although the results are related to opportunistic sampling activities rather than to regular and routine monitoring activities, they nevertheless provide a rigorous snapshot of the surface water quality in the Blougat Spruit downstream of the WWTW at the time of sampling. The analytical results of a water sample collected at station BC1 on 06/03/2013 are presented in Table 17. The results show similar values for ammonia ($\text{NH}_3\text{-N}$) and ortho-phosphate ($\text{PO}_4\text{-P}$) as are reflected for station BGS1 in Fig. 17. The dissolved organic carbon (DOC) concentration of 10 mg/L matches the standard limit for total organic

Table 10 Record of SEC and pH measurements at stations F11S12 and MRd on occasion of flow gauging measurements (SDMs), also showing derived SO_4 and TDS concentrations

| Date | Station F11S12 | | | | Station MRd | | | |
|------------|----------------|-------------------------------|----------------------------|------------------------------------|---------------|-------------------------------|------------------------------|------------------------------------|
| | SEC (mS/m) | $\text{SO}_4^{(1)}$ (mg/L) | TDS ² (mg/L) | pH ($-\log_{10} a_{\text{H}^+}$) | SEC (mS/m) | $\text{SO}_4^{(1)}$ (mg/L) | TDS ⁽²⁾ (mg/L) | pH ($-\log_{10} a_{\text{H}^+}$) |
| 22/09/2009 | 322 | 2092 | 2479 | 6.7 | – | – | – | – |
| 05/02/2010 | 389 | 2574 | 2997 | 3.9 | 358 | 2351 | 2759 | 4.1 |
| 16/02/2010 | 339 | 2214 | 2610 | 4.2 | 335 | 2186 | 2581 | 4.2 |
| 23/02/2010 | 379 | 2502 | 2918 | 4.1 | 383 | 2531 | 2948 | 3.9 |
| 09/03/2010 | 379 | 2502 | 2918 | 4.1 | 353 | 2315 | 2720 | 4.0 |
| 01/04/2010 | 374 | 2466 | 2878 | 3.6 | 358 | 2351 | 2759 | 3.4 |
| 14/04/2010 | 358 | 2351 | 2757 | 3.7 | 347 | 2272 | 2672 | 3.6 |
| 06/05/2010 | 408 | 2711 | 3142 | 3.2 | 420 | 2797 | 3234 | 3.3 |
| 18/05/2010 | 335 | 2186 | 2580 | 5.5 | 356 | 2337 | 2741 | 4.4 |
| 09/06/2010 | 370 | 2437 | 2 849 | 4.4 | 373 | 2459 | 2872 | 4.5 |
| 07/07/2010 | 374 | 2466 | 2880 | 4.0 | 376 | 2480 | 2895 | 3.9 |
| 27/07/2010 | 407 | 2703 | 3134 | 3.7 | 395 | 2617 | 3042 | 4.1 |
| 19/08/2010 | 384 | 2538 | 2957 | 2.6 | 335 | 2186 | 2580 | 2.7 |
| 05/10/2010 | 307 | 1984 | 2364 | 3.0 | 383 | 2531 | 2949 | 2.5 |
| 19/10/2010 | 314 | 2035 | 2418 | 3.6 | 326 | 2121 | 2510 | 3.1 |
| 19/11/2010 | 338 | 2207 | 2603 | 2.8 | 333 | 2171 | 2564 | 2.8 |
| 18/12/2010 | 416 | 2768 | 3203 | 2.7 | 376 | 2480 | 2895 | 3.0 |
| 27/07/2011 | 369 | 2430 | 2841 | 2.7 | 373 | 2459 | 2872 | 2.9 |
| 25/08/2011 | 389 | 2574 | 2995 | 2.9 | 405 | 2689 | 3119 | 2.5 |
| 05/09/2011 | 362 | 2380 | 2787 | 2.6 | 367 | 2416 | 2826 | 2.6 |
| 08/05/2012 | 372 | 2452 | 2864 | 2.6 | 388 | 2567 | 2988 | 2.9 |
| 14/08/2012 | 299 | 1927 | 2302 | 6.3 | 309 | 1999 | 2379 | 4.2 |
| 21/09/2012 | 290 | 1862 | 2233 | 7.6 | 288 | 1848 | 2218 | 6.9 |
| 24/10/2012 | 264 | 1675 | 2033 | 4.3 | 270 | 1718 | 2079 | 3.8 |
| 15/01/2013 | 282 | 1805 | 2171 | 6.6 | 283 | 1812 | 2179 | 4.9 |
| 14/02/2013 | 274 | 1747 | 2110 | 7.0 | 277 | 1769 | 2133 | 6.4 |
| 06/03/2013 | 244 | 1531 | 1879 | 6.9 | 241 | 1510 | 1856 | 6.6 |
| 15/08/2013 | 219 | 1352 | 1686 | 7.1 | 219 | 1352 | 1686 | 6.6 |
| 15/10/2013 | 275 | 1754 | 2118 | 6.6 | 274 | 1747 | 2110 | 6.2 |
| 12/12/2013 | 236 | 1474 | 1817 | 6.6 | 231 | 1438 | 1779 | 6.6 |
| 26/09/2014 | 238 | 1488 | 1833 | 7.3 | 238 | 1488 | 1833 | 6.3 |
| 30/07/2015 | | | | | | | | |
| 04/12/2017 | | | | | | | | |
| n | 31 | 31 | 31 | 31 | 30 | 30 | 30 | 30 |
| Minimum | 219 | 1352 | 1686 | 2.6 | 219 | 1352 | 1686 | 2.5 |
| Mean | 333 | 2167 | 2563 | – | 332 | 2166 | 26,559 | – |
| Median | 349 | 2214 | 2683 | 4.1 | 350 | 2294 | 2696 | 4.0 |
| Maximum | 416 | 2768 | 3203 | 7.6 | 420 | 2797 | 3234 | 6.9 |
| SD | 58 | 411 | 447 | 1.7 | 56 | 404 | 433 | 1.4 |
| CoV (%) | 17 | 19 | 17 | 38 | 17 | 19 | 17 | 34 |

¹ $\text{SO}_4 = 7.19 \times \text{SEC} - 223$ ($R^2 = 0.88$) from Table 8 for station F11S12² $\text{SEC} \times 7.7$ to derive a theoretical representative TDS value (from Text Box 1)

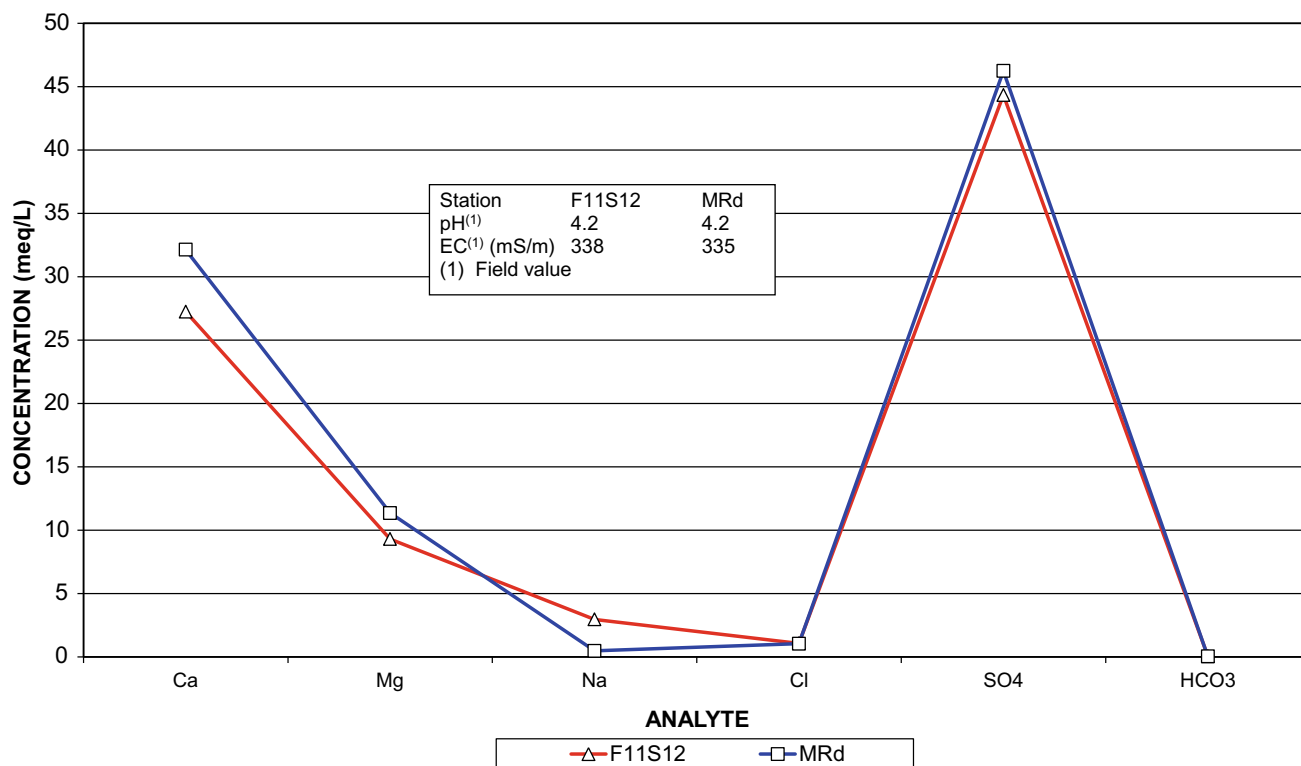


Fig. 13 Comparison of major ion chemistry at stations F11S12 and MRd in the Tweelopie/Riet Spruit system in mid-February 2010

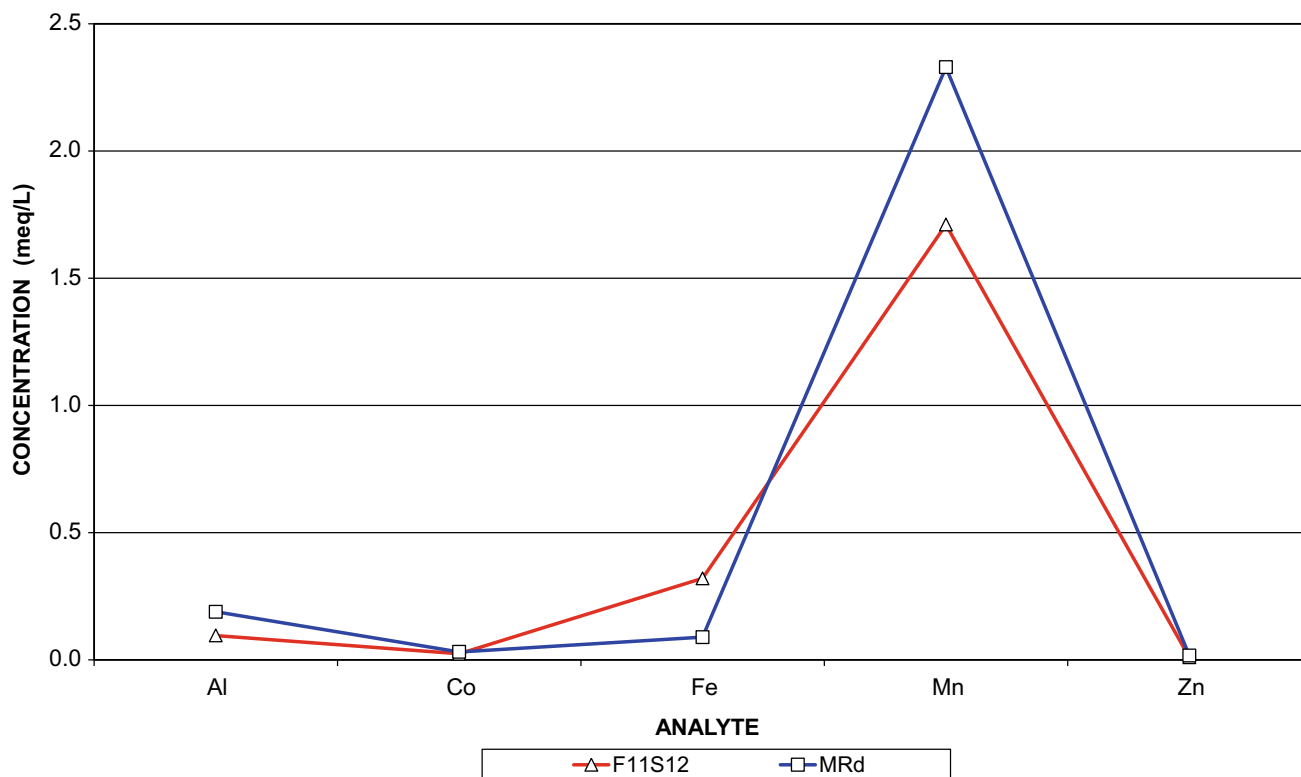


Fig. 14 Comparison of some trace metals concentration at stations F11S12 and MRd in the Tweelopie/Riet Spruit system in mid-February 2010

Table 11 Statistical analysis of Blougat Spruit water chemistry at station 188048 for the period June 2004 to September 2008 (raw data sourced from the DWS in November 2013)

| Variable/Analyte | Statistical parameter | | | | | | | SANS (2015a) ¹ |
|--|-----------------------|--------------|--------------|------------|--------------|-------|---------|---------------------------|
| | n | 5%ile | Mean | Median | 95%ile | SD | CoV (%) | |
| pH ($-\log_{10}a_{H^+}$) | 48 | 4.2 | – | 6.7 | 7.8 | 1.0 | 16 | 5.0–9.7 |
| SEC (mS/m) | 48 | 58 | 89 | 82 | 156 | 27.3 | 31 | ≤ 170 |
| TDS (mg/L) | 43 | 384 | 551 | 502 | 927 | 172.3 | 31 | ≤ 1200 |
| Ca (mg/L) | 46 | 34.8 | 56.5 | 54.0 | 77.1 | 15.6 | 28 | n.s |
| Mg (mg/L) | 46 | 6.6 | 9.4 | 9.5 | 12.6 | 1.9 | 21 | n.s |
| Na (mg/L) | 46 | 52.1 | 86.0 | 85.2 | 119.4 | 21.1 | 25 | ≤ 200 |
| K (mg/L) | 45 | 8.4 | 13.2 | 13.1 | 19.8 | 3.7 | 28 | n.s |
| Cl (mg/L) | 48 | 45.3 | 65.3 | 64.3 | 79.5 | 12.9 | 20 | ≤ 300 |
| SO ₄ (mg/L) | 48 | 71 | 187 | 151 | 430 | 120 | 64 | ≤ 500 |
| HCO ₃ (mg/L) | 45 | 12 | 59 | 48 | 158 | 47 | 79 | n.s |
| NO ₃ + NO ₂ (mg N/L) | 45 | 0.27 | 12.63 | 10.63 | 30.52 | 10.0 | 79 | ≤ 11 |
| PO ₄ (mg P/L) | 47 | 0.72 | 3.79 | 2.68 | 11.19 | 3.2 | 85 | n.s |
| Si (mg/L) | 47 | 3.59 | 6.41 | 6.32 | 9.37 | 2.3 | 37 | n.s |
| Fe (mg/L) | 48 | 0.006 | 0.678 | 0.068 | 4.116 | 2.0 | 290 | ≤ 2 |
| Mn (mg/L) | 48 | 0.004 | 0.903 | 0.267 | 2.011 | 3.5 | 392 | ≤ 0.5 |
| Al (mg/L) | 46 | 0.008 | 0.156 | 0.035 | 0.280 | 0.7 | 428 | ≤ 0.3 |
| EB (%) | 46 | –13.8 | 5.7 | 5.3 | 20.7 | 10.1 | 178 | ± 5 |
| TDS:SEC | 43 | 5.0 | 6.2 | 6.3 | 7.3 | 0.7 | 12 | n.s |
| SO ₄ :TDS (%) | 43 | 16 | 32 | 33 | 51 | 11 | 33 | n.s |

¹Standard health-related limit for consumption of 2 L/d over 70 years by a 60 kg person

Bold text denotes value exceeds standard limit as described in note 1

carbon (TOC) specified in SANS 241-1 (SANS, 2015a). These analytes represent nutrient contaminants that hold severe repercussions for the eutrophic status of the receiving surface water resources.

1.2.5 Tweefontein Spruit

Still further downstream, the Tweefontein Spruit draining southwards from the ~7300 ha (H Visser, personal communication) John Nash Nature Reserve area is monitored for water quality at DWS station F14S15 (Fig. 4). Although rising on dolomite, this drainage for much of its flow path follows the contact between older Witwatersrand Supergroup and Ventersdorp Supergroup strata that outcrop along the south-eastern margin of the study area. The Witwatersrand Supergroup strata are represented primarily by quartzite of the Hospital Hill Subgroup, and the Ventersdorp Supergroup by shaly sandstone (Table 5).

The generally good quality water (Table 18) delivered by this drainage exhibits a distinct CaMg–HCO₃ composition (Fig. 19). This suggests that the principal source feeding this drainage is the karst system that forms the headwaters of this catchment. The slightly elevated 95%ile Fe and Mn values are attributed to the ferruginous nature of strata such as the

Hospital Hill Subgroup quartzite (Table 5) that underlie part of this catchment.

The acceptable mean and median electrical balance values again testify to the veracity of the analytical results. It is a little surprising, however, that the SO₄:TDS ratio is as high as 18%. Although this is similar to the 19% of its main stem the Bloubank Spruit at station A2H049 (Text Box 1), it is an order of magnitude greater than the 2% associated with pristine karst springwater.

1.2.6 Bloubank Spruit

The significant loss of poor quality water⁵ from the Riet Spruit into the karst aquifer upstream of Sterkfontein Cave and the Oaktree area has been discussed in Sect. 5.2.1 in Chapter “Physical Hydrology” and illustrated in Fig. 23. In the middle reaches of the Bloubank Spruit downstream of the confluence⁶ with the Riet Spruit in the vicinity of Sterkfontein Cave and down to the Zwartkrans Spring, groundwater

⁵ Mainly water that originates in the mine area located in the upper reaches of the Tweelapie Spruit.

⁶ Located immediately downstream of the R540 road crossing over the Riet Spruit near the Swartkrans fossil site.

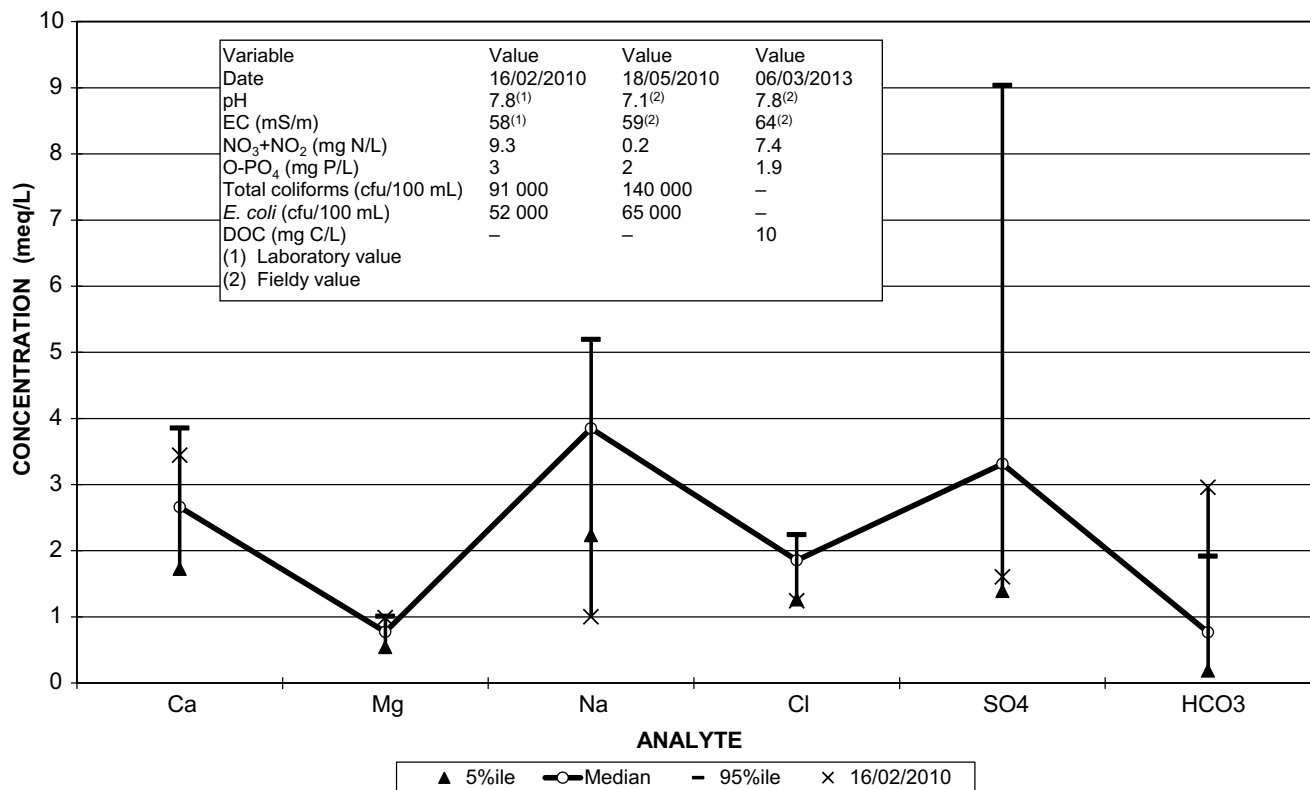


Fig. 15 Variability of Blougat Spruit water major ion chemistry at station 188048 in the period June 2004 to September 2008, also showing more recent selected variable/analyte values (text box) for comparison

Table 12 Concentration range of selected trace metals in Blougat Spruit water at three sites downstream of the Percy Stewart WWTW (from Awofolu et al., 2007)

| Trace metal | Concentration range | | SANS (2015a) ⁽¹⁾ |
|-------------|---------------------|---------------------|-----------------------------|
| | Minimum (mg/L) | Maximum (mg/L) | |
| Cd | Trace (<0.002) | 0.05 | ≤ 0.003 |
| Pb | Trace (<0.004) | 0.13 ± 0.03 | ≤ 0.01 |
| Mn | 4.35 ± 0.004 | 942 ± 7.26 | ≤ 0.5 |
| Zn | 0.10 ± 0.002 | 0.41 ± 0.001 | ≤ 5.0 |
| Ni | 0.08 ± 0.004 | 0.88 ± 0.002 | ≤ 0.07 |
| Cu | 0.15 ± 0.003 | 0.742 ± 0.001 | ≤ 2.0 |

¹Standard health-related limit for consumption of 2 L/d over 70 years by a 60 kg person
Bold text denotes value exceeds standard limit as described in note 1

resurgence in the streambed partly explains the observed decrease in SEC values and increase in pH values observed at station BB@M since late 2011 (Fig. 20). Average SEC and pH values of 107 mS/m and 7.5, respectively, are similar to the contemporary Zwartkrans Spring values of 95 mS/m and 7.5 (Sect. 7.1 in Chapter “Chemical Hydrogeology”).

The elevated SEC (mean of 159 mS/m) and depressed pH values in the period after mid-December 2010 (Fig. 20) are attributed to the increasing contribution of mine water⁷

⁷The fate of mine water in the receiving drainages is discussed in greater detail in Sect. 5.

entering the system as surface flow via the Riet Spruit (Sect. 5.2.1 in Chapter “Physical Hydrology”). This also applies to the impacts associated with the very high flow conditions experienced in mid-December 2010 (Plate 5). As is evident in Fig. 20, the mid-December 2010 flood event⁸ precipitated the second highest SEC and second lowest pH

⁸The DWS flow gauging station A2H049 at the lower end of the Bloubank Spruit recorded a second highest daily average flow rate of 18.6 m³/s on 16/12/2010. The maximum (highest) historical daily average flow rate gauged at this station is 34.3 m³/s recorded on 28/01/1978.

Table 13 Statistical analysis of Percy Stewart WWTW discharge chemistry data (from MCLM) for the period July 2007 to June 2009

| Variable/Analyte | Statistical parameter | | | | | | | SANS (2015a) ¹ |
|--|-----------------------|----------------|----------------|----------------|----------------|----------------|---------|---------------------------|
| | n | 5%ile | Mean | Median | 95%ile | SD | CoV (%) | |
| pH ($-\log_{10}a_{H^+}$) | 24 | 7.5 | – | 7.8 | 8.2 | 0.3 | 4 | 5.0–9.7 |
| SEC (mS/m) | 24 | 83 | 100 | 101 | 120 | 11.7 | 40 | ≤ 170 |
| TDS ⁽²⁾ (mg/L) | 16 | 699 | 783 | 781 | 883 | 72 | 9 | ≤ 1200 |
| Na (mg/L) | 19 | 62.1 | 81.6 | 84.5 | 102.4 | 12.9 | 16 | ≤ 200 |
| Cl (mg/L) | 24 | 63.3 | 72.3 | 73.9 | 80.2 | 5.7 | 8 | ≤ 300 |
| HCO ₃ (mg/L) | 16 | 251 | 312 | 315 | 367 | 34.0 | 13 | n.s |
| NO ₃ + NO ₂ (mg N/L) | 24 | 0.8 | 2.4 | 1.4 | 7.4 | 2.3 | 94 | ≤ 11 |
| NH ₃ (mg N/L) | 24 | 14.2 | 30.7 | 31.5 | 42.0 | 8.1 | 26 | ≤ 1.5 |
| PO ₄ (mg P/L) | 24 | 2.05 | 4.55 | 4.10 | 7.42 | 1.85 | 41 | n.s |
| COD (mg/L) | 24 | 112 | 202 | 197 | 288 | 58.3 | 29 | n.s |
| Faecal coliforms (cfu/100 mL) | 22 | 69 150 | 359 075 | 244 834 | 801 883 | 371 560 | 104 | ≤ 10 in 1% of samples |
| <i>E. coli</i> (cfu/100 mL) | 6 | 151 417 | 264 333 | 241 167 | 408 000 | 109 408 | 41 | ≤ 1 in 1% of samples |
| TDS:SEC | 16 | 6.3 | 7.4 | 7.5 | 8.1 | 0.6 | 8 | n.s |

¹Standard health-related limit for consumption of 2 L/d over 70 years by a 60 kg person²TDS calculated as the sum of the reported TDS value (determined @ 180 °C) and HCO₃

Bold text denotes value exceeds standard limit as described in note 1

Table 14 Statistical analysis of Percy Stewart WWTW effluent chemistry data associated with station PSFE for the period November 2002 to February 2010 sourced from the DWS November 2013

| Variable/Analyte | Statistical parameter | | | | | | | SANS (2015a) ¹ |
|--|-----------------------|-------------|----------------|----------------|------------------|-----------|---------|---------------------------|
| | n | 5%ile | Mean | Median | 95%ile | SD | CoV (%) | |
| pH ($-\log_{10}a_{H^+}$) | 31 | 6.2 | – | 7.2 | 7.9 | 0.6 | 8 | 5.0–9.7 |
| SEC (mS/m) | 30 | 46 | 99 | 103 | 136 | 29.1 | 29 | ≤ 170 |
| Cl (mg/L) | 19 | 61.6 | 81.5 | 82.0 | 102.9 | 20.6 | 25 | ≤ 300 |
| HCO ₃ (mg/L) | 20 | 23 | 194 | 180 | 401 | 158.1 | 81 | n.s |
| SO ₄ (mg/L) | 24 | 103 | 235 | 199 | 579 | 151.6 | 64 | ≤ 500 |
| NO ₃ + NO ₂ (mg N/L) | 28 | 0.05 | 6.20 | 3.00 | 18.50 | 8.21 | 132 | ≤ 11 |
| NH ₃ (mg N/L) | 29 | 0.01 | 0.55 | 0.17 | 2.83 | 0.99 | 180 | ≤ 1.5 |
| NH ₄ (mg N/L) | 29 | 5.38 | 26.23 | 21.90 | 55.08 | 16.85 | 64 | n.s |
| PO ₄ (mg P/L) | 31 | 1.30 | 5.01 | 3.70 | 10.00 | 3.06 | 61 | n.s |
| COD (mg/L) | 30 | 5 | 118 | 68 | 336 | 149.3 | 126 | n.s |
| Total coliforms (count/100 mL) | 11 | 6885 | 814 750 | 155 000 | 4 140 000 | 1 330 961 | 163 | n.s |
| Faecal coliforms (cfu/100 mL) | 33 | 218 | 763 983 | 131 000 | 4 500 000 | 1 676 161 | 219 | ≤ 10 in 1% of samples |
| <i>E. coli</i> (cfu/100 mL) | 22 | 830 | 231 705 | 30 000 | 1 150 000 | 480 840 | 208 | ≤ 1 in 1% of samples |

¹Standard health-related limit for consumption of 2 L/d over 70 years by a 60 kg person

Bold text denotes value exceeds standard limit as described in note 1

values recorded at station BB@M in the course of the monitoring record.

The elevated SEC is also manifested in the lower reaches of the Bloubank Spruit as revealed by the DWS surface

water quality record for station A2H049. Both the long-term mean and median SEC values of ~60 mS/m and the 95%ile value of 70 mS/m (Table 19) have consistently been exceeded since mid-2010 (Volume 2). A historical

Table 15 Statistical analysis of Blougat Spruit water chemistry at station BGS2 for the period November 2002 to July 2009 (raw data sourced from the DWS in November 2013)

| Variable/Analyte | Statistical parameter | | | | | | | SANS (2015a) ¹ |
|--|-----------------------|-------|-------------|-------------|---------------|--------|---------|---------------------------|
| | n | 5%ile | Mean | Median | 95%ile | SD | CoV (%) | |
| pH ($-\log_{10}a_{H^+}$) | 27 | 6.3 | – | 7.5 | 8.5 | 0.8 | 10 | 5.0–9.7 |
| SEC (mS/m) | 27 | 25 | 53 | 32 | 124 | 36.9 | 70 | ≤ 170 |
| Cl (mg/L) | 22 | 19.3 | 44.6 | 31.5 | 84.9 | 24.1 | 54 | ≤ 300 |
| HCO ₃ (mg/L) | 22 | 26.9 | 72.4 | 73.2 | 115.8 | 32.4 | 45 | n.s |
| SO ₄ (mg/L) | 26 | 24 | 120 | 36 | 379 | 149.5 | 124 | ≤ 500 |
| NO ₃ + NO ₂ (mg N/L) | 26 | 0.43 | 5.10 | 4.15 | 13.20 | 4.00 | 79 | ≤ 11 |
| NH ₃ (mg N/L) | 26 | 0.000 | 0.068 | 0.041 | 0.191 | 0.09 | 136 | ≤ 1.5 |
| NH ₄ (mg N/L) | 26 | 0.05 | 8.47 | 1.50 | 39.25 | 14.61 | 172 | n.s |
| PO ₄ (mg P/L) | 27 | 0.05 | 2.04 | 0.05 | 9.04 | 3.43 | 169 | n.s |
| COD (mg/L) | 27 | 5 | 38 | 17 | 143 | 48.7 | 128 | n.s |
| Total coliforms (count/100 mL) | 11 | 310 | 48 029 | 19 000 | 165 000 | 65 369 | 136 | n.s |
| Faecal coliforms (cfu/100 mL) | 25 | 1 | 6984 | 980 | 29 200 | 11 851 | 170 | ≤ 10 in 1% of samples |
| <i>E. coli</i> (cfu/100 mL) | 14 | 1 | 1610 | 245 | 8100 | 3388 | 211 | ≤ 1 in 1% of samples |

¹Standard health-related limit for consumption of 2 L/d over 70 years by a 60 kg person

Bold text denotes value exceeds standard limit as described in note 1

Table 16 Statistical analysis of Blougat Spruit water chemistry at station BGS1 for the period November 2002 to February 2010 sourced from the DWS in November 2013

| Variable/Analyte | Statistical parameter | | | | | | | SANS (2015a) ¹ |
|--|-----------------------|--------------|----------------|---------------|----------------|---------|---------|---------------------------|
| | n | 5%ile | Mean | Median | 95%ile | SD | CoV (%) | |
| pH ($-\log_{10}a_{H^+}$) | 33 | 6.9 | – | 7.4 | 8.2 | 0.4 | 6 | 5.0–9.7 |
| SEC (mS/m) | 33 | 24 | 68 | 78 | 105 | 27.1 | 40 | ≤ 170 |
| Cl (mg/L) | 22 | 28.1 | 56.0 | 61.5 | 80.8 | 22.0 | 39 | ≤ 300 |
| HCO ₃ (mg/L) | 22 | 37 | 165 | 138 | 314 | 111.5 | 67 | n.s |
| SO ₄ (mg/L) | 26 | 21 | 109 | 110 | 199 | 64.0 | 59 | ≤ 500 |
| NO ₃ + NO ₂ (mg N/L) | 32 | 0.35 | 5.26 | 2.65 | 17.58 | 6.23 | 116 | ≤ 11 |
| NH ₃ (mg N/L) | 32 | 0.002 | 0.432 | 0.105 | 2.049 | 0.77 | 179 | ≤ 1.5 |
| NH ₄ (mg N/L) | 32 | 0.05 | 13.40 | 9.25 | 34.68 | 12.38 | 92 | n.s |
| PO ₄ (mg P/L) | 33 | 0.05 | 1.87 | 1.90 | 4.56 | 1.55 | 83 | n.s |
| COD (mg/L) | 33 | 5 | 59 | 50 | 143 | 44.8 | 75 | n.s |
| Total coliforms (count/100 mL) | 11 | 25 | 8 652 | 740 | 41 000 | 20 659 | 239 | n.s |
| Faecal coliforms (cfu/100 mL) | 32 | 52 | 169,396 | 18,000 | 989,000 | 354,833 | 210 | ≤ 10 in 1% of samples |
| <i>E. coli</i> (cfu/100 mL) | 21 | 1 900 | 179,433 | 76,000 | 700,000 | 258,409 | 144 | ≤ 1 in 1% of samples |

¹Standard health-related limit for consumption of 2 L/d over 70 years by a 60 kg person

Bold text denotes value exceeds standard limit as described in note 1

Fig. 16 Comparison of inorganic quality of Blougat Spruit water upstream and downstream of the Percy Stewart WWTW (data from Tables 15 and 16)

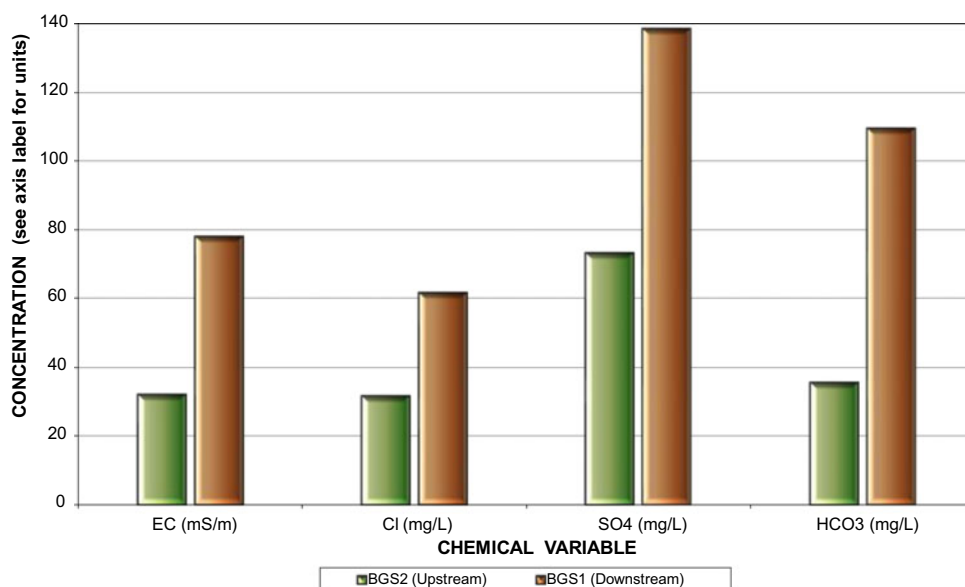
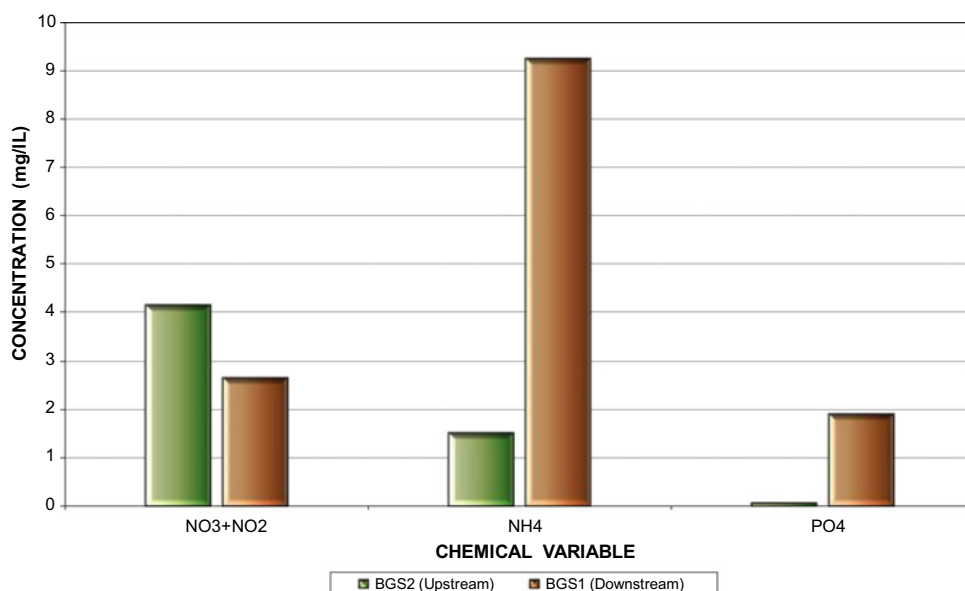


Fig. 17 Comparison of organic quality of Blougat Spruit water upstream and downstream of the Percy Stewart WWTW (data from Tables 15 and 16)



maximum value of ~ 122 mS/m was recorded as recently as May 2014. The latter part of the record shown in Fig. 20 indicates the recovery to pre-2010 conditions in regard to pH values, with SEC values that are lower but still almost double those of the pre-2010 period. This ‘reversal’ occurred in the 2012 winter following the commissioning of the refurbished and upgraded HDS mine water treatment facility (Text Box 4 in Chapter “Physical Hydrology”).

The contribution of surface water losses in the Blougat Spruit (Sect. 5.2.2 in Chapter “Physical Hydrology”) adds another dimension to the quantity and quality of the groundwater resources in this portion of the Zwartkrans Basin. A particular concern relates to the performance of the Percy Stewart WWTW, in particular the unacceptable

bacteriological quality of the treated effluent discharged to the Blougat Spruit by this facility (Sect. 1.2.4). These circumstances have resulted in bacterially contaminated surface water entering the karst aquifer along the lower reaches of the Blougat Spruit at a rate of up to ~ 7 ML/d (Sect. 5.2.2 in Chapter “Physical Hydrology”). The presence of this contamination in surface water is reflected in *E. coli* concentrations of $>50,000$ cfu/100 mL (Fig. 18).

Whilst the introduction of bacterial contamination into a groundwater resource is normally regarded an environmental tragedy, it is also possible that such contamination might in fact provide an energy (carbon) source that promotes the natural chemical process of bacterial sulfate reduction (BSR). As discussed in Sect. 11 in Chapter “Chemical

Fig. 18 Comparison of bacteriological quality of Blougat Spruit water upstream and downstream of the Percy Stewart WWTW (data from Tables 15 and 16)

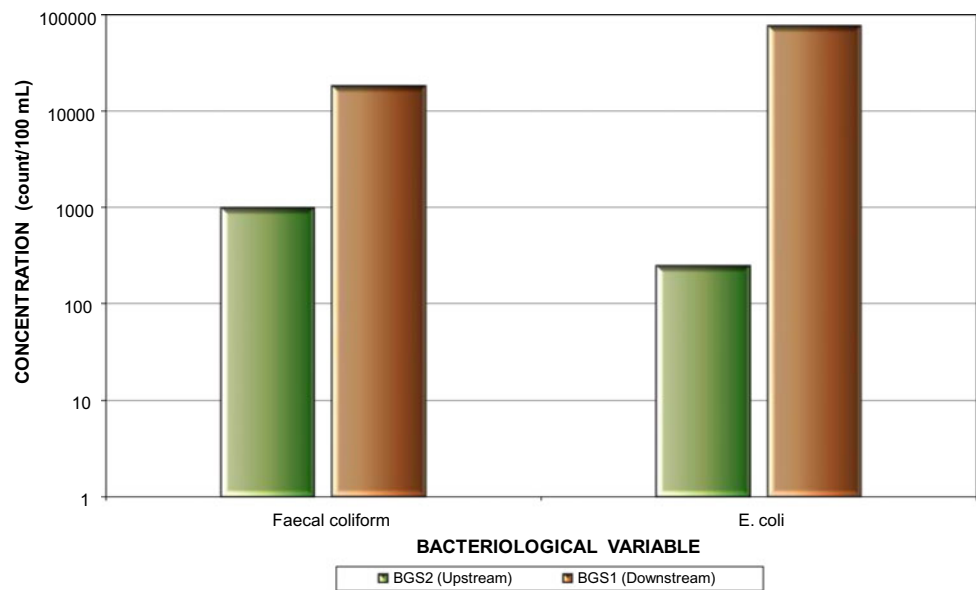


Table 17 Water chemistry results for station BC1 on 06/03/2013

| Variable/Analyte | Value | SANS (2011a) ¹ | Variable/Analyte | Value | SANS (2015a) ¹ |
|--|-----------|---------------------------|------------------|--------------|---------------------------|
| pH ($-\log_{10} \text{H}^+$) | 7.6 | 5.0–9.7 | Sr (mg/L) | 0.113 | n.s |
| SEC (mS/m) | 70 | ≤ 170 | Se (mg/L) | 0.011 | ≤ 0.01 |
| Ca (mg/L) | 39 | n.s | Zn (mg/L) | 0.015 | ≤ 5 |
| Mg (mg/L) | 9.7 | n.s | Al (mg/L) | <0.010 | ≤ 0.3 |
| Na (mg/L) | 70 | ≤ 200 | As (mg/L) | <0.010 | ≤ 0.01 |
| K (mg/L) | 11 | n.s | Be (mg/L) | <0.010 | n.s |
| Cl (mg/L) | 57 | ≤ 300 | Cd (mg/L) | <0.010 | ≤ 0.003 |
| SO ₄ (mg/L) | 84 | ≤ 500 | Co (mg/L) | <0.010 | ≤ 0.5 |
| HCO ₃ (mg/L) | 171 | n.s | Cr (mg/L) | <0.010 | ≤ 0.05 |
| NO ₃ + NO ₂ (mg N/L) | 7.4 | ≤ 11 | Cu (mg/L) | <0.010 | ≤ 2.0 |
| NH ₃ (mg N/L) | 11 | ≤ 1.5 | Fe (mg/L) | <0.010 | ≤ 2.0 |
| F (mg/L) | 0.2 | ≤ 1.5 | Hg (mg/L) | <0.001 | ≤ 0.006 |
| PO ₄ (mg P/L) | 1.9 | n.s | Mn (mg/L) | <0.010 | ≤ 0.5 |
| DOC (mg C/L) | 10 | n.s | Pb (mg/L) | <0.010 | ≤ 0.01 |
| Ba (mg/L) | 0.022 | n.s | Sb (mg/L) | <0.010 | ≤ 0.02 |
| B (mg/L) | 0.109 | n.s | Ti (mg/L) | <0.010 | n.s |
| Mo (mg/L) | 0.079 | n.s | U (mg/L) | <0.001 | ≤ 0.015 |
| Ni (mg/L) | 0.044 | ≤ 0.07 | V (mg/L) | <0.010 | ≤ 0.2 |

¹Standard health-related limit for consumption of 2 L/d over 70 years by a 60 kg person
 Bold text denotes value exceeds standard limit as described in note 1

Hydrogeology”, this process has relevance for the potentially ameliorative influence it might have on the mine water impact in the karst aquifer in the zone of wastewater convergence.

At the bottom end of the Bloubank Spruit system, surface water quality is monitored at flow gauging station A2H049 (Fig. 4 in Chapter 2) located ~700 m before the confluence with the Crocodile River. A summary of the statistics that

characterise this water quality record is presented in Table 19. Again, the median (and mean) electrical balance values afford the analytical results a high degree of confidence. The 95%ile EB value of 9.5% suggests the increasing inaccuracy of analyses at higher SO₄ concentrations. None of the analytes recorded in Table 19 exceed the respective SANS (2015a) health-related limit where specified. The distinct CaMg–HCO₃ composition of the water (Fig. 21)

Table 18 Statistical analysis of Tweefontein Spruit water chemistry at station F14S15 for the period June 2004 to September 2008 sourced from the DWS in November 2013

| Variable/Analyte | Statistical parameter | | | | | | | SANS (2015a) ¹ |
|--|-----------------------|-------|-------|--------|------------|------|---------|---------------------------|
| | n | 5%ile | Mean | Median | 95%ile | SD | CoV (%) | |
| pH ($-\log_{10}a_{H^+}$) | 46 | 7.6 | — | 8.2 | 8.5 | 0.7 | 8 | 5.0–9.7 |
| SEC (mS/m) | 46 | 51 | 59 | 60 | 66 | 4.8 | 8 | ≤ 170 |
| TDS (mg/L) | 42 | 383 | 439 | 448 | 485 | 34.8 | 8 | ≤ 1200 |
| Ca (mg/L) | 45 | 43.9 | 50.7 | 51.3 | 58.3 | 4.9 | 10 | n.s |
| Mg (mg/L) | 45 | 25.8 | 30.6 | 30.9 | 34.2 | 2.6 | 8 | n.s |
| Na (mg/L) | 45 | 11.1 | 24.2 | 26.3 | 32.4 | 7.4 | 30 | ≤ 200 |
| K (mg/L) | 43 | 0.3 | 0.3 | 0.3 | 0.3 | 0.0 | 0 | n.s |
| Cl (mg/L) | 46 | 19.5 | 33.6 | 35.8 | 42.5 | 7.5 | 22 | ≤ 300 |
| SO ₄ (mg/L) | 46 | 39.9 | 77.9 | 81.6 | 107.9 | 22.1 | 29 | ≤ 500 |
| HCO ₃ (mg/L) | 44 | 167 | 203 | 199 | 246 | 24.5 | 12 | n.s |
| NO ₃ + NO ₂ (mg N/L) | 44 | 0.97 | 4.22 | 3.97 | 6.91 | 2.5 | 59 | ≤ 11 |
| PO ₄ (mg/L) | 45 | 0.02 | 0.18 | 0.13 | 0.48 | 0.2 | 91 | n.s |
| Si (mg/L) | 45 | 5.26 | 6.22 | 6.11 | 7.33 | 0.7 | 12 | n.s |
| Fe (mg/L) | 49 | 0.006 | 0.066 | 0.014 | 0.370 | 0.2 | 254 | ≤ 2 |
| Mn (mg/L) | 49 | 0.001 | 0.031 | 0.006 | 0.172 | 0.1 | 182 | ≤ 0.5 |
| Al (mg/L) | 47 | 0.006 | 0.049 | 0.026 | 0.091 | 0.1 | 286 | ≤ 0.3 |
| EB (%) | 42 | -2.1 | 1.7 | 2.5 | 5.2 | 2.8 | 162 | ± 5 |
| TDS:SEC | 42 | 7.0 | 7.4 | 7.4 | 8.0 | 0.3 | 5 | n.s |
| SO ₄ :TDS (%) | 42 | 10 | 17 | 18 | 23 | 4 | 25 | n.s |

¹Standard health-related limit for consumption of 2 L/d over 70 years by a 60 kg person

Bold text denotes value exceeds standard limit as described in note 1

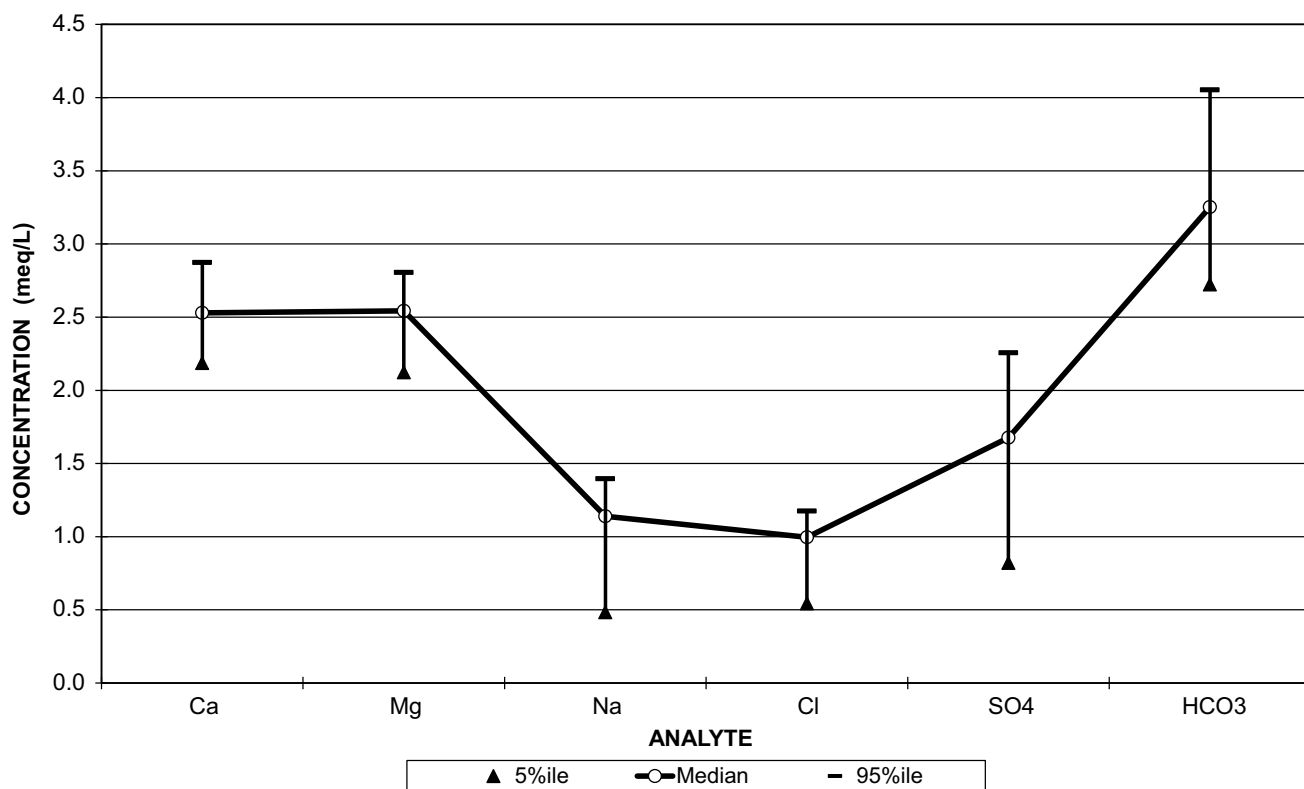


Fig. 19 Variability of Tweefontein Spruit water major ion chemistry at station F14S15 in the period June 2004 to September 2008

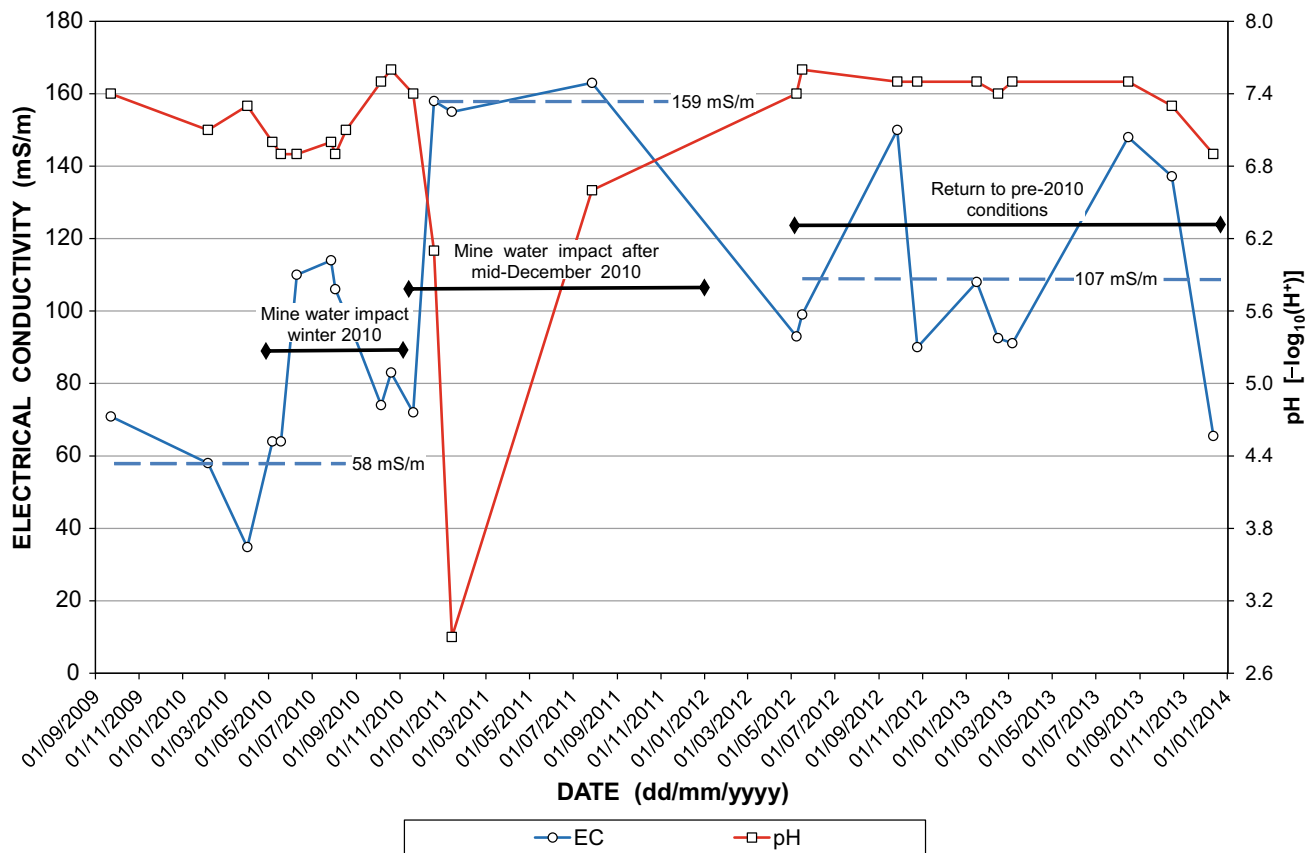


Fig. 20 Recent electrical conductivity and pH pattern and trend in Bloubank Spruit water at station BB@M between Sterkfontein Cave and Zwartkrans Spring

again reflects the significant contribution of dolomitic groundwater discharged from the karst aquifer in this catchment (Sect. 4.16 in Chapter “Physical Hydrogeology”).

Further inspection of the long-term water quality record is premised on four periods of observation, namely May 1979 to August 2002, September 2002 to January 2010, February 2010 to July 2012 and August 2012 to February 2014. These timeframes bracket the pre-decant period, the period of ‘normal’ mine water discharge up to the commencement of abnormally high decant volumes, the period of abnormally high mine water discharge and, finally, the period following the commissioning of the immediate and short-term mine water control and management measures (Text Box 1 in “Physical Hydrology”). The latter resulted in some recovery of the situation before the resumption of high mine water discharge in the period March to July 2014.

The data reveal little difference in the CaMg–HCO₃ chemical composition between the pre-decant period and first period of ‘normal’ decant. The slight but notable increases in the median Na and Cl concentrations in the decant period are considered to reflect the municipal wastewater influence on surface water quality. Evident in Fig. 21, however, is the change to a Ca–SO₄HCO₃ chemical

composition in the subsequent two periods. The change is further characterised by a significantly greater variability in the concentrations of Ca, Mg, SO₄ and HCO₃ as reflected in the range of 5–95%ile values. In the case of Ca, Mg and SO₄, the variability is biased in favour of the 95%ile values, and in the case of HCO₃ in favour of the 5%ile value. These circumstances together reflect the impact of mine water on the chemical composition of the water discharged by the Bloubank Spruit system since February 2010. A more insightful understanding of the hydrochemical ‘evolution’ of surface water at station A2H049 over three decades is presented in Volume 2. The results are synthesised as follows.

The recorded SEC and SO₄ pattern and trend clearly reflect the manifestation of a strong mine water component in the recent discharge hydrochemistry of the Bloubank Spruit system. This finds support in the equivalent Ca:SO₄ ratios that reflect a declining trend indicative of a greater proportion of SO₄ relative to Ca in the latter part of the record. Both Na and Cl exhibit an increasing trend over the historical record. Attributing the increasing Cl trend to a municipal wastewater influence finds support in the PO₄-P (phosphorus) pattern and trend. A similar trend is not as evident in the NO₃-N (nitrate) values, possibly for reasons

Table 19 Statistical analysis of Bloubank Spruit water chemistry at station A2H049 for the period May 1979 to September 2017

| Variable/Analyte | Statistical parameter | | | | | | | SANS (2015a) ¹ |
|--|-----------------------|-------|-------|--------|------------|-------|---------|---------------------------|
| | n | 5%ile | Mean | Median | 95%ile | SD | CoV (%) | |
| pH ($-\log_{10}a_{H^+}$) | 966 | 7.4 | – | 8.2 | 8.5 | 0.3 | 4 | 5.0–9.7 |
| SEC (mS/m) | 1071 | 51 | 60 | 61 | 70 | 8.4 | 14 | ≤ 170 |
| TDS (mg/L) | 1071 | 356 | 438 | 444 | 496 | 62 | 14 | ≤ 1200 |
| Ca (mg/L) | 888 | 42.9 | 54.2 | 53.6 | 63.5 | 11.5 | 21 | n.s |
| Mg (mg/L) | 886 | 25.1 | 32.5 | 32.4 | 37.9 | 5.0 | 15 | n.s |
| Na (mg/L) | 882 | 10.0 | 21.9 | 21.8 | 33.4 | 7.1 | 32 | ≤ 200 |
| K (mg/L) | 880 | 0.7 | 1.9 | 1.8 | 3.5 | 0.9 | 47 | n.s |
| Cl (mg/L) | 892 | 20.0 | 31.8 | 32.1 | 40.8 | 6.0 | 19 | ≤ 300 |
| SO ₄ (mg/L) | 889 | 65.1 | 91.3 | 83.6 | 134.1 | 43.9 | 48 | ≤ 500 |
| HCO ₃ (mg/L) | 883 | 146 | 192 | 197 | 219 | 24.6 | 13 | n.s |
| NO ₃ + NO ₂ (mg N/L) | 923 | 3.00 | 4.55 | 4.36 | 6.41 | 1.74 | 38 | ≤ 11 |
| PO ₄ (mg P/L) | 962 | 0.005 | 0.093 | 0.054 | 0.317 | 0.106 | 115 | n.s |
| Si (mg/L) | 962 | 5.08 | 5.98 | 5.98 | 6.82 | 0.81 | 14 | n.s |
| Fe (mg/L) | 116 | 0.004 | 0.029 | 0.014 | 0.118 | 0.097 | 338 | ≤ 2 |
| Mn (mg/L) | 116 | 0.001 | 0.113 | 0.002 | 0.145 | 0.645 | 571 | ≤ 0.5 |
| Al (mg/L) | 111 | 0.003 | 0.044 | 0.011 | 0.091 | 0.218 | 493 | ≤ 0.3 |
| EB (%) | 840 | –1.2 | 3.6 | 3.6 | 9.5 | 3.9 | 109 | ± 5 |
| TDS:SEC | 1070 | 6.7 | 7.3 | 7.2 | 8.1 | 0.5 | 7 | n.s |
| SO ₄ :TDS (%) | 889 | 16 | 20 | 19 | 27 | 7 | 36 | n.s |

¹Standard health-related limit for consumption of 2 L/d over 70 years by a 60 kg person

Bold text denotes value exceeds standard limit as described in note 1

such as denitrification and uptake of this nutrient by aquatic vegetation and sequestration in eutrophic systems along the ~23-km reach between the Percy Stewart WWTW and station A2H049.

Perhaps the clearest indication of a mine water impact on the chemistry of water discharged by the Bloubank Spruit at station A2H049 is provided by the Piper diagram presented in Fig. 22. The shift towards the apex of the central diamond field that characterises the Ca–SO₄ composition of the February 2011 chemistry is reversed in the return to a more ‘normal’ pre-2009–’10 chemistry in January 2012.

A suite of surface water samples collected on 18/05/2010 at seven stations in the Bloubank Spruit system provide a ‘snapshot in time’ of the water chemistry in this system. A graphical comparison of the major ion results presented in Table 20 is made in Fig. 23. The sampling positions are shown in Fig. 24.

The graphical comparison (Fig. 23) reveals the extremely dominant Ca–SO₄ composition of the water at the Riet Spruit station MRd influenced by the mine water received via the Tweelopie Spruit. It also reveals the similar Na–HCO₃ composition at the Blougat Spruit stations BC1 and BG@N14, and further downstream at BB@M on the

Bloubank Spruit. The manifestation of Na as the dominant cation matches the long-term record at station 188048 (Fig. 15). The ranking of HCO₃ as the dominant anion in the May 2010 analysis (compared to SO₄ in the long-term record) is attributed to the greater contribution of rainwater runoff compared to effluent discharge from the Percy Stewart WWTW in early to mid-2010.

The Ca–HCO₃ composition of the water at station BB@PL further downstream on the Bloubank Spruit at Kromdraai reflects the contribution of karst groundwater upstream of this station. The principal sources of this water are the Kromdraai, Zwartkrans and Plover’s Lake springs (Sect. 4 in Chapter “Physical Hydrogeology”). The Mg–HCO₃ composition of the Honingklip Spruit water (HS1) at Kromdraai contrasts sharply with that of the Bloubank Spruit at this location, and reflects the different geology of the contributing catchment.

With the exception of the ephemeral Honingklip Spruit tributary, it is apparent from Table 20 that Fe, Mn and Ni are persistent trace metals in the other Bloubank Spruit system surface waters. This is also apparent for the persistence of poor bacteriological quality as reflected in the *E. coli* values (see also Fig. 15). Encouragingly, the Honingklip Spruit

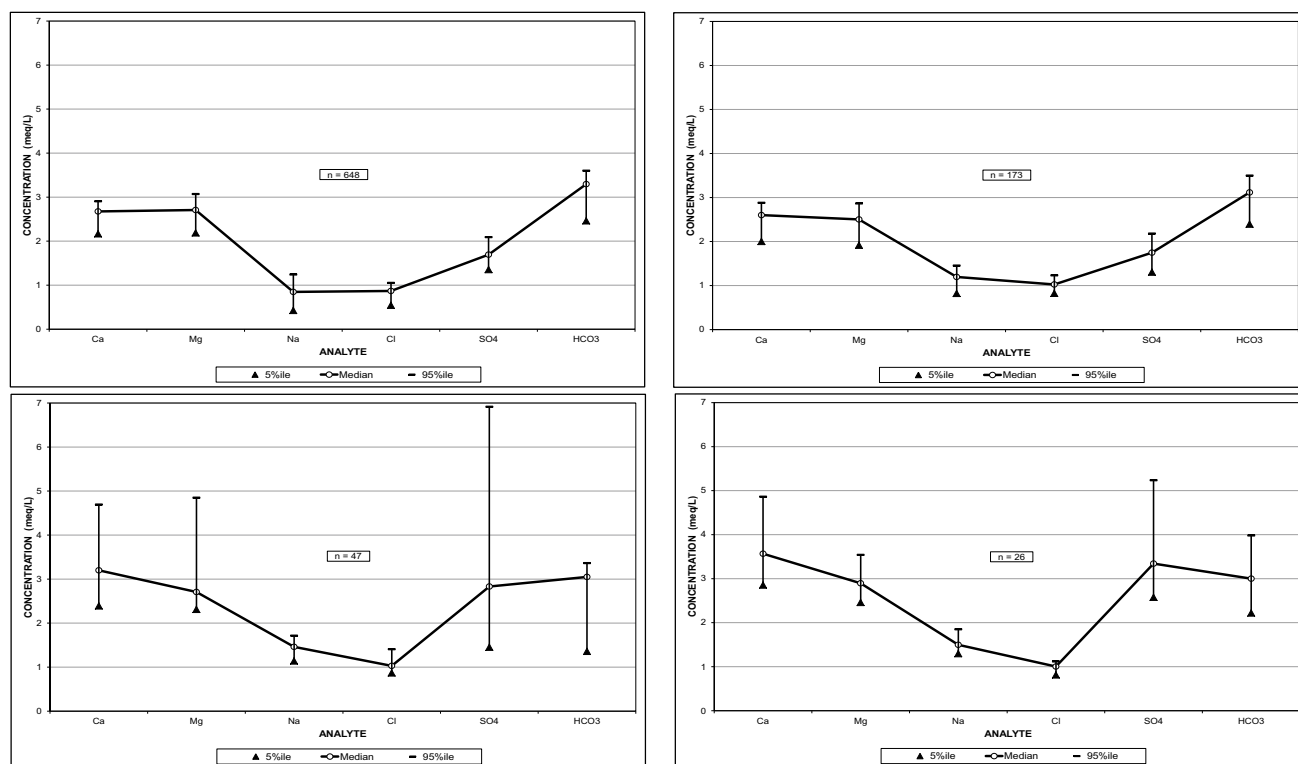


Fig. 21 Variability of Bloubank Spruit water major ion chemistry at station A2H049 for the period May 1979 to August 2002 (top left), the period September 2002 to January 2010 (top right), the period February

2010 to July 2012 (bottom left), and the period August 2012 to September 2017 (bottom right)

Fig. 22 Piper diagram of pre-2010 (long-term as per Fig. 29) and more recent Bloubank Spruit water chemistry at station A2H049

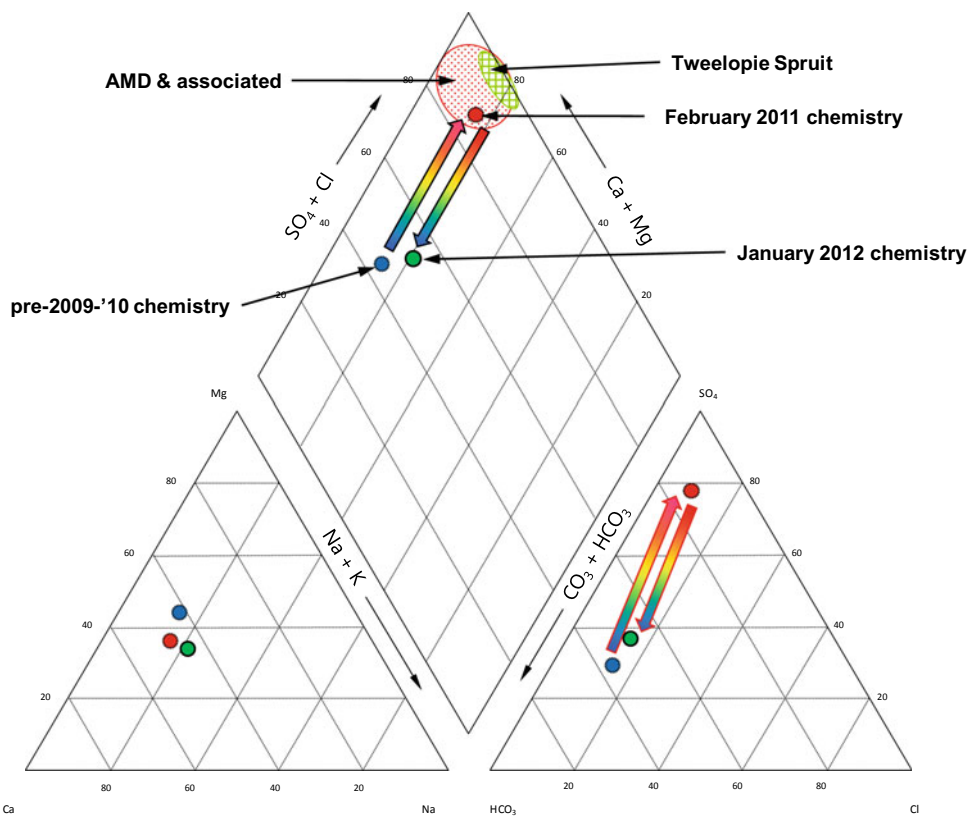


Table 20 Comparison of mid-2010 surface water chemistry at various positions in the Bloubank Spruit system

| Variable/Analyte | Sampling station | | | | | | | SANS (2015a) ¹ |
|--|------------------|--------------|---------------|---------------|--------------|---------|------------|---------------------------|
| | F11S12 | MRd | BC1 | BG@N14 | BB@M | HS1 | BB@PL | |
| Date | 18/05/2010 | | | | | | | |
| pH ($-\log_{10}a_{H^+}$) (field) | 5.5 | 4.4 | 7.1 | 6.9 | 6.9 | 6.9 | 7.0 | 5.0–9.7 |
| SEC (mS/m) (field) | 355 | 356 | 59 | 51 | 64 | 22 | 60 | ≤ 170 |
| TDS (mg/L) | 2700 | 2751 | 384 | 338 | 400 | 164 | 409 | ≤ 1200 |
| Ca (mg/L) | 662 | 689 | 41 | 38 | 45 | 15 | 54 | n.s |
| Mg (mg/L) | 70 | 81 | 10 | 11 | 15 | 18 | 29 | n.s |
| Na (mg/L) | 115 | 103 | 55 | 48 | 52 | 5 | 34 | ≤ 200 |
| K (mg/L) | 10.4 | 9.4 | 8.6 | 8.0 | 8.1 | 1.1 | 3.0 | n.s |
| Cl (mg/L) | 43 | 44 | 52 | 45 | 50 | 12 | 40 | ≤ 300 |
| SO ₄ (mg/L) | 1794 | 1819 | 56 | 42 | 74 | 15 | 78 | ≤ 500 |
| HCO ₃ (mg/L) | <6 | <6 | 161 | 146 | 156 | 98 | 171 | n.s |
| NO ₃ + NO ₂ (mg N/L) | 0.6 | 0.6 | 0.2 | 0.5 | 3.2 | 1.9 | 6.0 | ≤ 11 |
| F (mg/L) | <0.2 | <0.2 | 0.2 | 0.2 | <0.2 | <0.2 | <0.2 | ≤ 1.5 |
| PO ₄ (mg P/L) | <0.2 | <0.2 | 2.0 | 2.5 | 2.4 | <0.2 | 0.5 | n.s |
| Total coliforms (cfu/100 mL) | n.d | n.d | 140,000 | 34,000 | 3500 | 0 | 720 | n.s |
| <i>E. coli</i> (cfu/100 mL) | n.d | n.d | 65,000 | 26,000 | 3000 | 0 | 470 | ≤ 1 in 1% of samples |
| Si (mg/L) | 0.8 | 1.7 | 5.2 | 4.9 | 5.4 | 5.3 | 5.3 | n.s |
| Fe (mg/L) | 0.431 | 0.934 | 0.528 | 0.682 | 0.906 | 0.073 | 0.358 | ≤ 2 |
| Mn (mg/L) | 10 | 18 | 0.279 | 0.470 | 0.665 | 0.087 | 0.293 | ≤ 0.5 |
| Al (mg/L) | < 0.1 | 0.121 | 0.118 | < 0.1 | 0.134 | < 0.1 | 0.137 | ≤ 0.3 |
| Hg (mg/L) | < 0.001 | < 0.001 | < 0.001 | < 0.001 | < 0.001 | < 0.001 | < 0.001 | ≤ 0.001 |
| U (mg/L) | < 0.001 | < 0.001 | < 0.001 | < 0.001 | < 0.001 | < 0.001 | < 0.001 | ≤ 0.015 |
| Ni (mg/L) | 0.145 | 0.117 | 0.049 | 0.035 | 0.029 | < 0.025 | < 0.025 | ≤ 0.07 |
| Sn (mg/L) | 0.097 | < 0.025 | 0.153 | 0.138 | 0.167 | < 0.025 | 0.091 | n.s |
| Sr (mg/L) | 0.500 | 0.395 | 0.123 | 0.117 | 0.096 | 0.036 | 0.054 | n.s |
| Zn (mg/L) | 0.048 | 0.379 | 0.043 | 0.025 | < 0.025 | < 0.025 | < 0.025 | ≤ 5.0 |
| EB (%) | 6.6 | 7.8 | 1.9 | 5.6 | 3.4 | 4.1 | 8.1 | ± 5 |
| TDS:SEC | 7.6 | 7.7 | 6.5 | 6.6 | 6.3 | 7.5 | 6.8 | n.s |
| SO ₄ :TDS (%) | 66 | 66 | 15 | 12 | 19 | 9 | 19 | n.s |

¹Standard health-related limit for consumption of 2 L/d over 70 years by a 60 kg person

Bold text denotes value exceeds standard limit as described in note 1

displayed no bacteriological contamination on the date sampled. Perhaps even more encouraging is the observation that the *E. coli* value at the most downstream station BB@PL is two orders of magnitude less than at the most upstream station BC1 on the day of sampling. This situation by no means suggests that a value of 470 cfu/100 mL is acceptable, merely that a measure of natural amelioration of bacteriological contamination in the drainage system is apparent.

The results of water chemistry monitoring carried out at the NOE (Nedbank Olwazini Estate) property downstream of station BB@PL substantiate the above observations.

The NOE monitoring programme provides a valuable additional measure of water quality in the lower reaches of the Bloubank Spruit. This is particularly relevant under circumstances where discharge quality data since mid-2009 for the Percy Stewart WWTW and the DWSs water quality data for upstream monitoring stations are unavailable. The monitoring has further significance for its location in proximity to where the Bloubank Spruit drainage leaves the karst environment and traverses older strata down to its confluence with the Crocodile River. Unlike the A2H049 water chemistry record, therefore, the NOE record represents almost exclusively the water which drains the karst portion

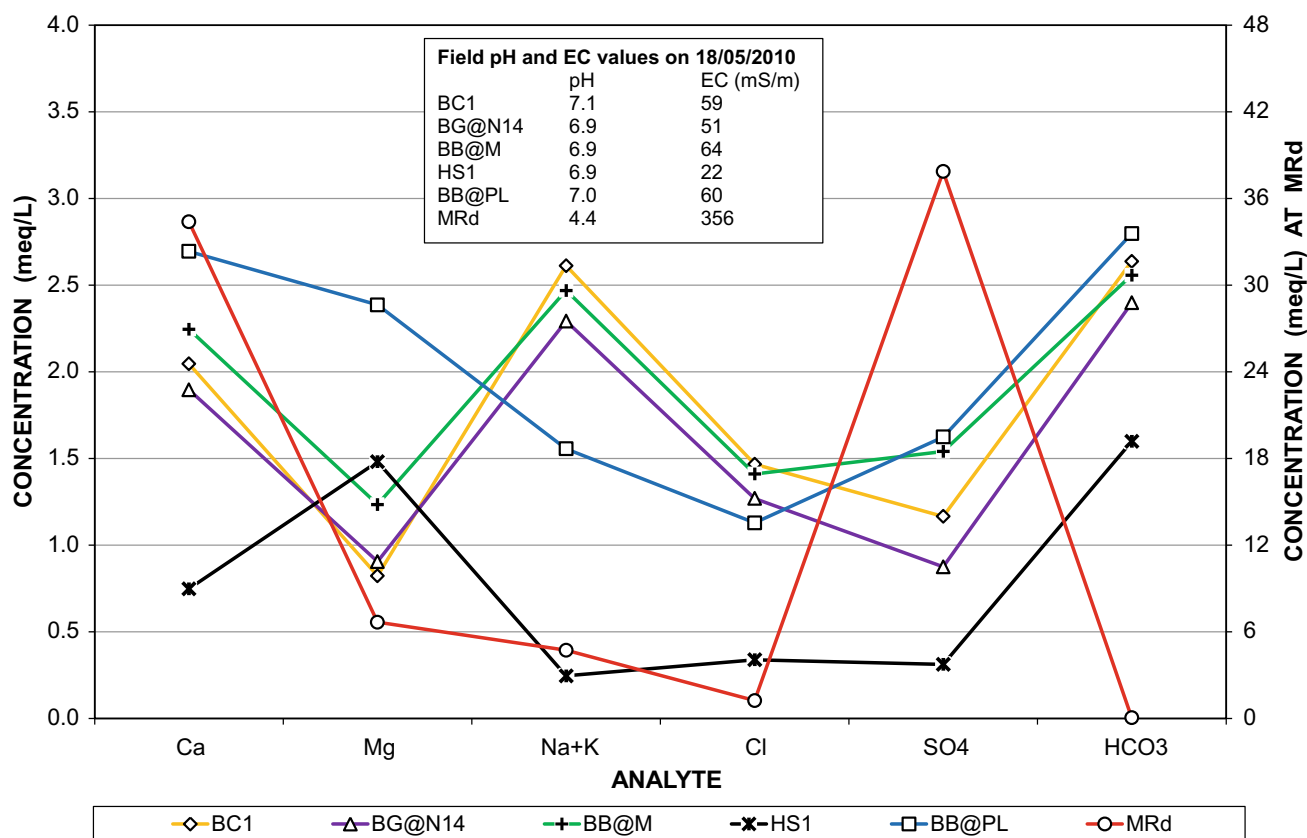


Fig. 23 Graphical comparison of surface water chemistry at various localities in the Bloubank Spruit system on 18/05/2010

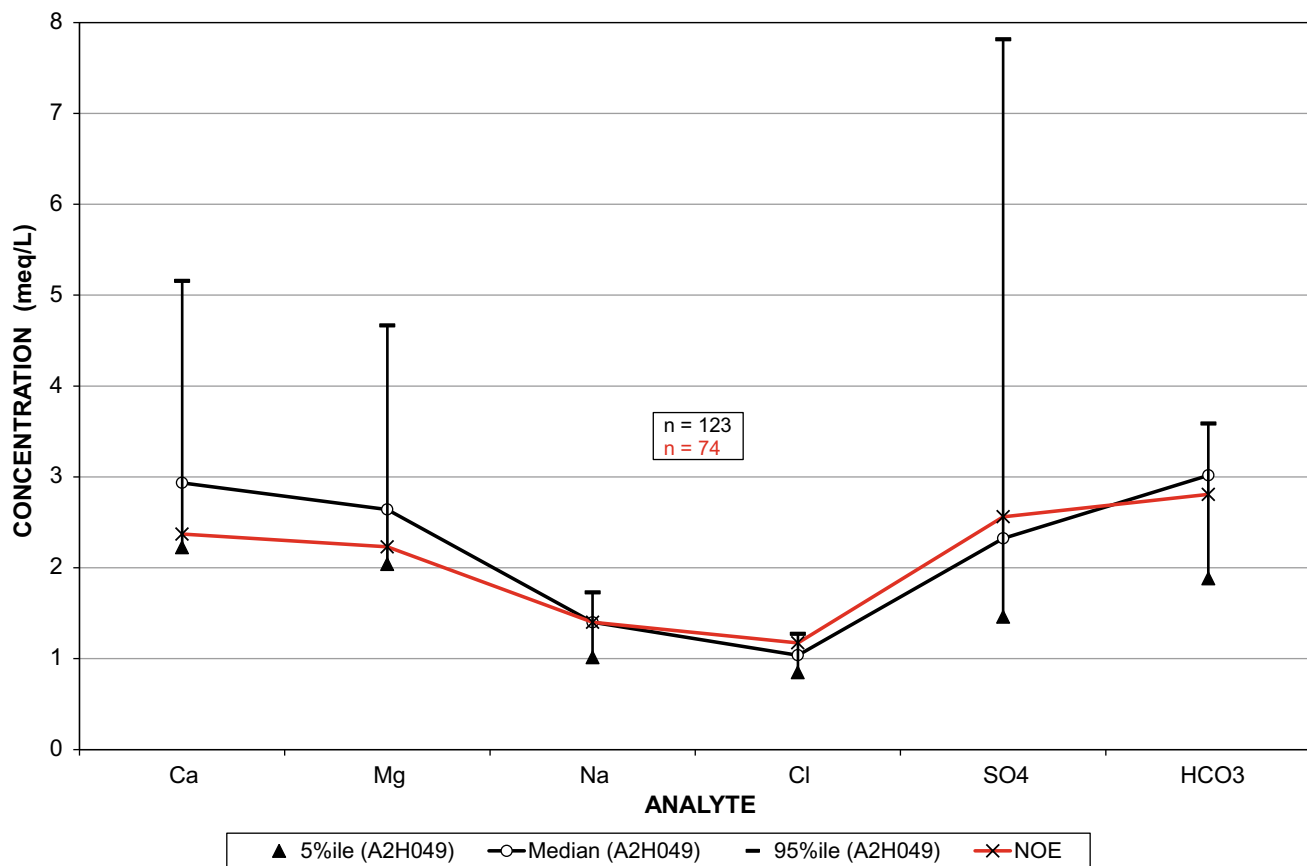


Fig. 24 Comparison of the Bloubank Spruit water chemistry at the NOE property and station A2H049 in the period of common record November 2007 to September 2014

Table 21 Chemical characterisation of surface water drawn from the Bloubank Spruit at the NOE property in the period November 2007 to September 2014

| Variable/Analyte | Statistical parameter | | | | | | | SANS (2015a) ¹ |
|----------------------------|-----------------------|--------------|-------------|-------------|-------------|-------|---------|---------------------------|
| | n | 5%ile | Mean | Median | 95%ile | SD | CoV (%) | |
| pH ($-\log_{10}a_{H^+}$) | 74 | 7.0 | – | 7.7 | 8.3 | 0.4 | 5 | 5.0–9.7 |
| SEC (mS/m) | 74 | 52 | 73 | 68 | 117 | 20 | 27 | ≤ 170 |
| TDS (mg/L) | 74 | 325 | 490 | 427 | 866 | 176 | 36 | ≤ 1200 |
| Ca (mg/L) | 74 | 26.0 | 48.1 | 47.5 | 77.9 | 15.4 | 32 | n.s |
| Mg (mg/L) | 72 | 13.4 | 29.2 | 27.1 | 44.4 | 15.5 | 53 | n.s |
| Na (mg/L) | 72 | 16.7 | 33.0 | 32.2 | 44.9 | 11.9 | 36 | ≤ 200 |
| K (mg/L) | 72 | 2.3 | 3.4 | 3.0 | 4.5 | 2.4 | 72 | n.s |
| Cl (mg/L) | 74 | 34.0 | 44.8 | 41.6 | 63.6 | 9.7 | 21 | ≤ 300 |
| SO ₄ (mg/L) | 73 | 22.4 | 164.6 | 123.0 | 357.0 | 116.3 | 71 | ≤ 500 |
| HCO ₃ (mg/L) | 74 | 65.6 | 161.8 | 171.3 | 212.9 | 41.5 | 26 | n.s |
| NO ₃ (mg N/L) | 70 | 2.6 | 6.5 | 6.4 | 10.2 | 3.3 | 51 | ≤ 11 |
| Fe (mg/L) | 41 | 0.00 | 0.05 | 0.03 | 0.12 | 0.08 | 150 | ≤ 2 |
| Mn (mg/L) | 54 | 0.00 | 0.49 | 0.06 | 3.04 | 1.01 | 206 | ≤ 0.5 |
| Al (mg/L) | 35 | 0.015 | 0.061 | 0.050 | 0.146 | 0.044 | 73 | ≤ 0.3 |
| EB (%) | 74 | –49.3 | –8.3 | –5.2 | 22.4 | 20.7 | –250 | ± 5 |
| TDS:SEC | 74 | 5.2 | 7.7 | 6.3 | 9.6 | 8.3 | 108 | n.s |
| SO ₄ :TDS (%) | 73 | 6 | 33 | 31 | 59 | 19 | 59 | n.s |

¹Standard health-related limit for consumption of 2 L/d over 70 years by a 60 kg person

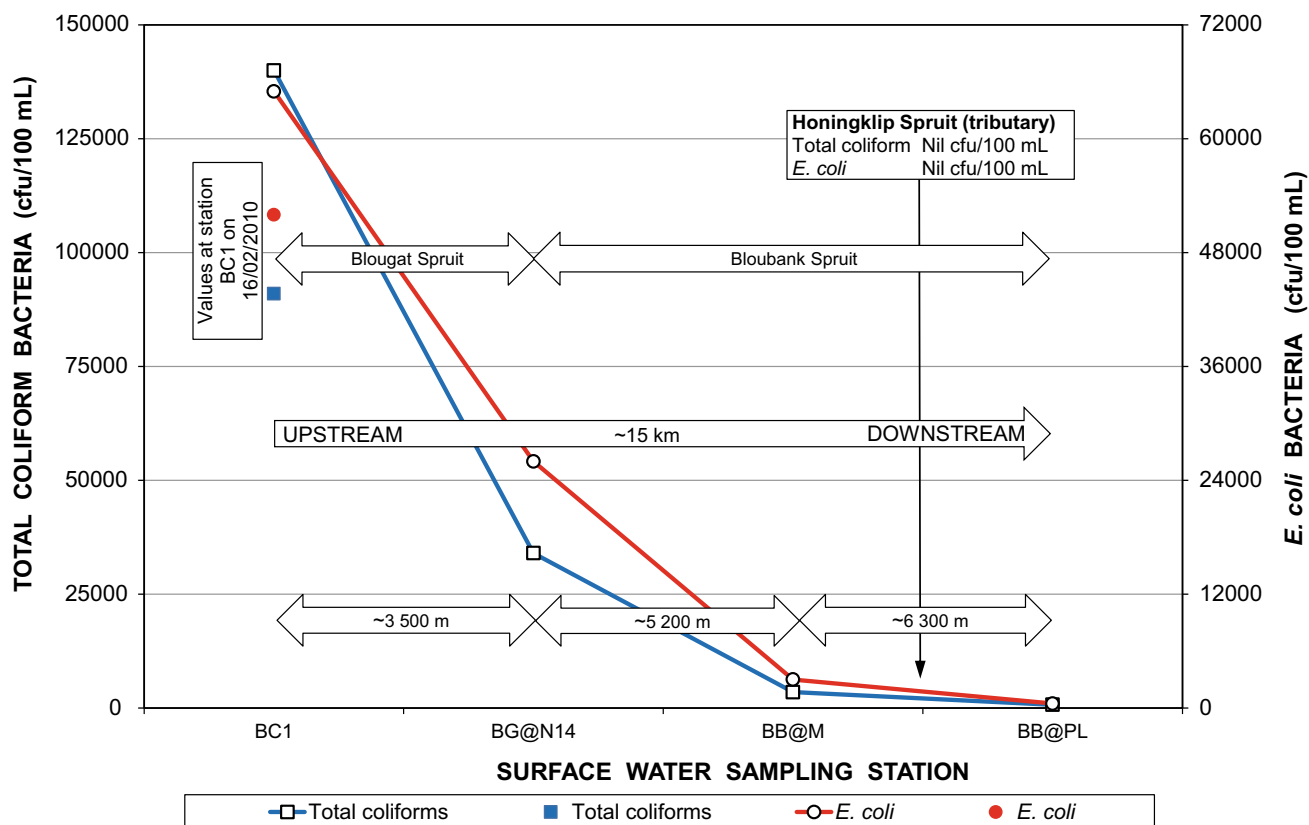


Fig. 25 Comparison of bacterial concentrations in surface water at various locations in the Bloubank Spruit system on 18/05/2010; for comparison, note the earlier values at station BC1 as well as the ~2×

difference in scale between the left and right vertical axes (data from Table 20)

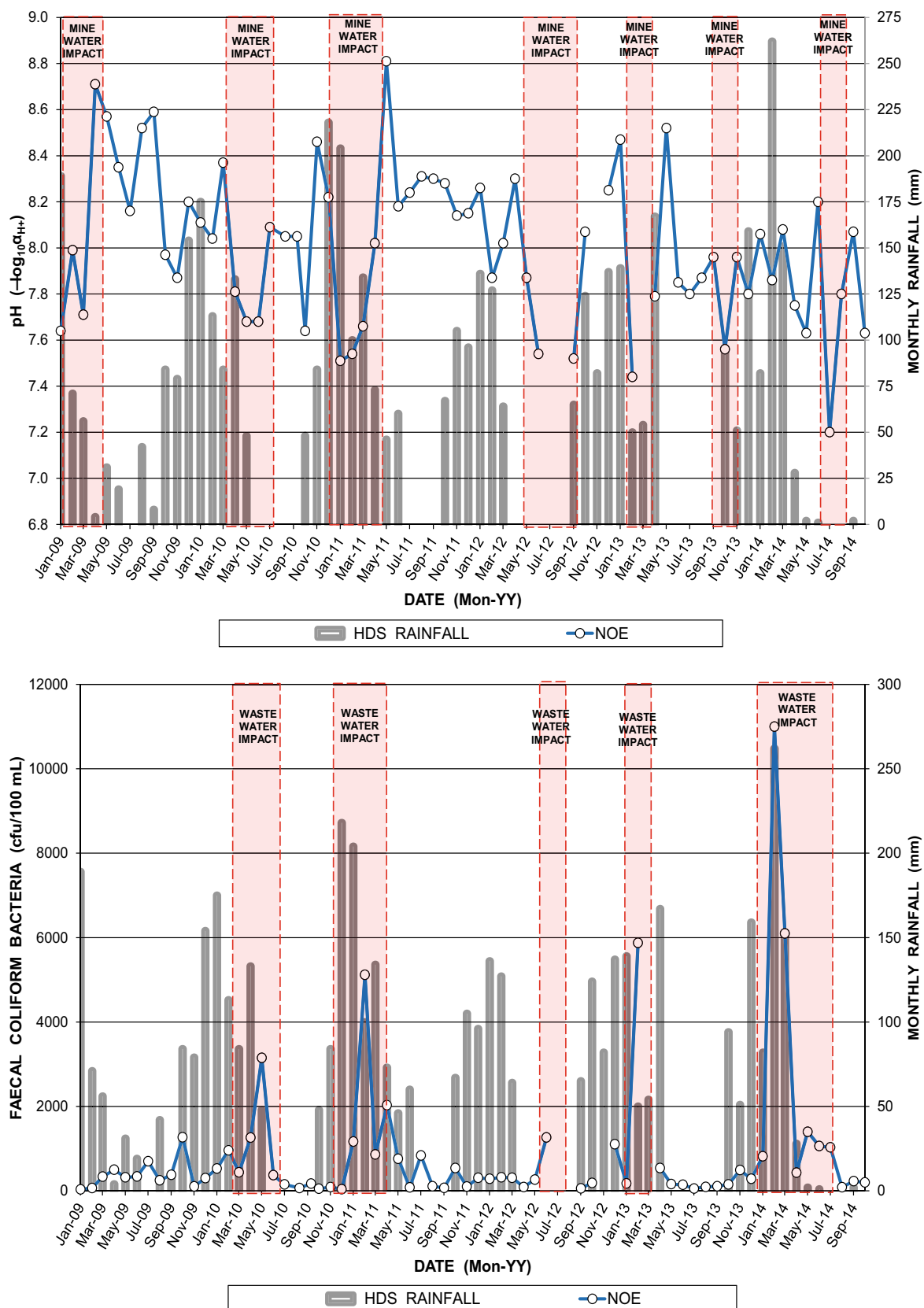


Fig. 26 Correlation of pH (top) and faecal coliform bacteria (bottom) levels in the Bloubank Spruit at the NOE property with monthly rainfall in the headwaters of the catchment

of the catchment. These circumstances are explored in the following text.

The NOE complex draws its water from the Bloubank Spruit, subjects the raw water to on-site purification for potable and general domestic use, and treats the wastewater generated by the complex for garden irrigation and landscaping use. These circumstances inform the sophistication of the purification plant, which must deal with both bacteriological and trace metal impacts on the feed water. The complex has been granted authority by the DWS to dispose of its treated wastewater effluent to land via irrigation (H Carpenter, personal communication). The chemistry of Bloubank Spruit water prior to purification for on-site potable and 'domestic' use at the NOE complex is described in Table 21. The graphical comparison made in Fig. 24 further reveals the similar chemical composition of surface water at NOE and A2H049. The congruence between the respective chemical compositions indicates that the NOE water quality data record serves as a suitable proxy for that generated at A2H049.

The trend in bacterial concentrations in surface water at various locations in the Bloubank Spruit system on 18/05/2010 is shown in Fig. 25. This reveals a marked decrease in concentrations with distance downstream of the principal source.

The pH values and NO₃-N, PO₄-P, COD and bacterial concentrations in Bloubank Spruit water at the upstream end of the NOE complex in the period January 2009 to September 2014 (~6 years) are presented in Table 22. This record covers the period for which the MCLMs Percy Stewart WWTW data and the DWSs water quality data for the upstream stations 188048, PSFE, BGS1 and BGS2 (Sect. 1.2.4) are unavailable.

The temporal patterns of the pH and bacterial variables are compared to rainfall in Fig. 26. The congruence between

lower pH values (associated with mine water impacts) and elevated faecal coliform levels (associated with municipal wastewater impacts) is evident. Congruence of the variable response patterns with the monthly rainfall is more obscure.

It is concerning that the faecal coliform count as far downstream as the NOE property reflects elevated levels (~4× the limit) at the 1%ile level. The mean and median values of 882 and 315 cfu/100 mL respectively (Table 22), are compared to August 2014 *E. coli* levels of > 2419 MPN/100 mL obtained at the upstream stations BC1, BB@M and BB@PL. The lower NOE values are commensurate with the decreasing pattern associated with 'distance from source' that is illustrated in Fig. 26. Nevertheless, the results indicate a severe non-conformance of faecal coliforms (and therefore almost certainly of *E. coli*) in regard to potable, animal and recreational use in the Bloubank Spruit system. There is no doubt that the principal source of this contamination is the Percy Stewart WWTW (Sect. 1.2.4).

1.3 Crocodile River

Water quality in this drainage is monitored at the DWS station A2H050 (Fig. 4 in Chapter "Introduction and Background") shortly before its confluence with the Bloubank Spruit. The data (Table 23) show that the SANS (2015a) drinking water limit is not exceeded in regard to any variable/analyte. The electrical balance mean and median values again indicate the comparative reliability and accuracy of the chemical analyses in the data record. The water exhibits a distinct Na-HCO₃ composition (Fig. 27) that is representative of the predominantly granitic nature of this catchment. The alkali-rich granitic rocks comprise sodium feldspars (NaAlSi₃O₈), e.g. the sodium-plagioclase albite

Table 22 Analysis of Bloubank Spruit water nutrient and bacterial content at the NOE property in the period January 2009 to September 2014

| Variable/Analyte | Statistical parameter | | | | | | | | SANS (2015a) ¹ | TWQR ² TWQR ³ |
|--|-----------------------|-----------|-----------|------------|------------|-------------|------|---------|---------------------------|--|
| | n | 1%ile | 5%ile | Mean | Median | 95%ile | SD | CoV (%) | | |
| pH (-log ₁₀ a _{H+}) | 66 | – | 7.5 | – | 8.0 | 8.6 | 0.3 | 4 | 5.0–9.7 | – |
| NO ₃ (mg N/L) | 57 | – | 2.7 | 7.5 | 7.1 | 14.9 | 3.6 | 48 | < 11 | – |
| O-PO ₄ (mg P/L) | 66 | – | 0.02 | 0.4 | 0.3 | 1.1 | 0.4 | 94 | n.s | – |
| COD (mg/L) | 48 | – | 6.4 | 54.6 | 43.0 | 158.3 | 51.3 | 93 | n.s | – |
| N:P (ratio) ⁽⁴⁾ | 54 | – | 6.8 | 37.1 | 28.8 | 116.5 | 35.5 | 96 | – | – |
| Faecal coliforms (cfu/100 mL) | 66 | 36 | 57 | 882 | 315 | 4627 | 1757 | 199 | ≤ 10 in 1% of samples | ≤ 200 ² ≤ 130 ³ |

¹Standard health-related limit for consumption of 2 L/d over 70 years by a 60 kg person

²Target Water Quality Range for livestock watering as per DWAF (1996b)

³Target Water Quality Range for recreational water use as per DWAF (1996d)

⁴Derived from NO₃-N and PO₄-P values

Bold text denotes value exceeds standard limit as described in note 1

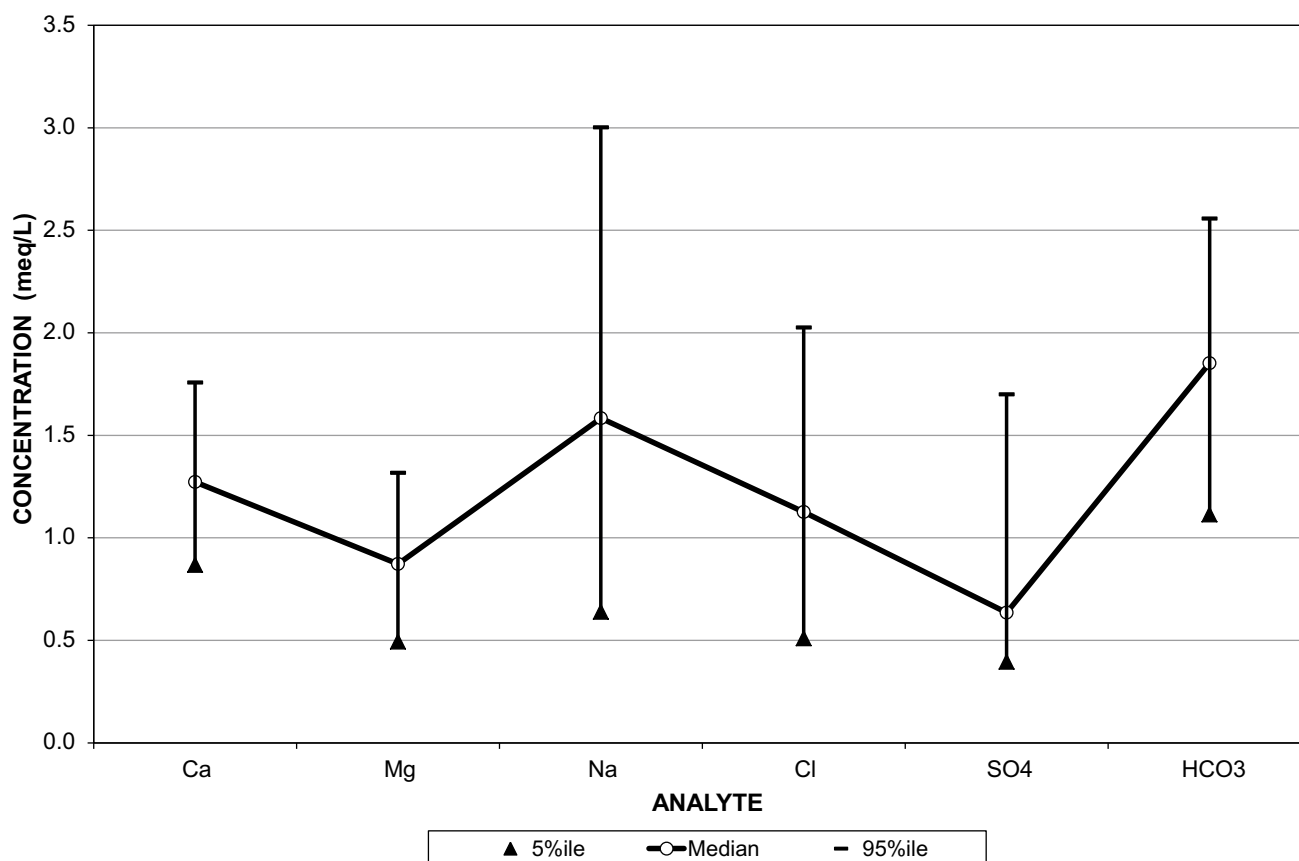


Fig. 27 Variability of Crocodile River water major ion chemistry at station A2H050 in the period May 1979 to September 2014 (data from Table 3)

that contributes Na as a silicate weathering product. The higher Cl concentration (also the second most abundant anion) compared to that of the Skeerpoort River and Bloubank Spruit water most likely reflects the influence of municipal wastewater discharge from the Driefontein WWTW, which also explains the greater variability evident in the analytes Na and Cl.

The data presented in Table 24 summarise the chemistry of the treated wastewater effluent discharged by the Driefontein WWTW as reported for station DFE by the DWS. Although this record only goes back to late 2002 compared to the much longer record of station A2H050 (Table 23), it provides an assessment of the effluent chemistry more recently discharged from this facility.

The statistics indicate that the Driefontein WWTW meets the SANS (2015a) limit in regard to all of the inorganic and organic variables adjudicated with the exception of ammonium (NH_4) at the mean and 95%ile levels. The exceedances in regard to the bacteriological variables, whilst a concern, are orders of magnitude smaller than those associated with the Percy Stewart WWTW (Table 14). Similarly, the mean and median PO_4 values are an order of magnitude smaller than those for the Percy Stewart WWTW.

1.4 Synthesis of Surface Water Chemistry

The Piper and Stiff diagrams presented in Fig. 28, and the Schoeller diagrams in Fig. 28, characterise the hydrochemistry of the respective sources. They are based on the median long-term major ion chemistry of surface water monitored in the Skeerpoort River, the Bloubank Spruit system and the upper Crocodile River. A comparison of the Piper diagram characterisation with that of groundwater sources in the south-western portion of the study area (Fig. 2 in Chap. “Chemical Hydrogeology”) shows a marked similarity reflecting the large measure of hydraulic continuity between surface water and groundwater resources.

- The Skeerpoort River water (A2H034) with its MgCa-HCO_3 composition characterises pristine dolomitic (karst) groundwater. As observed by Huizenga (2004), this drainage does not show any sign of pollution. Its water quality can therefore serve as a benchmark against which to gauge the level of degradation experienced by other karst-fed rivers in the study area.
- The Bloubank Spruit system water chemistry varies with the main source as follows:

Table 23 Statistical analysis of Crocodile River water chemistry at station A2H050 for the period May 1979 to September 2014

| Variable/Analyte | Statistical parameter | | | | | | | SANS (2015a) ¹ |
|--|-----------------------|-------------|-------|--------|-------------|-------|---------|---------------------------|
| | n | 5%ile | Mean | Median | 95%ile | SD | CoV (%) | |
| pH ($-\log_{10}a_{H^+}$) | 1007 | 7.0 | – | 7.9 | 8.2 | 0.4 | 5 | 5.0–9.7 |
| SEC (mS/m) | 1113 | 27 | 45 | 44 | 63 | 17.6 | 39 | ≤ 170 |
| TDS (mg/L) | 872 | 177 | 289 | 286 | 412 | 71.3 | 25 | ≤ 1200 |
| Ca (mg/L) | 933 | 17.54 | 25.9 | 25.5 | 35.2 | 5.3 | 21 | n.s |
| Mg (mg/L) | 934 | 6.0 | 10.8 | 10.6 | 16.0 | 3.2 | 30 | n.s |
| Na (mg/L) | 915 | 14.9 | 38.0 | 36.5 | 68.9 | 16.8 | 44 | ≤ 200 |
| K (mg/L) | 922 | 4.0 | 7.7 | 7.4 | 13.1 | 2.8 | 37 | n.s |
| Cl (mg/L) | 934 | 18.2 | 42.1 | 39.8 | 71.6 | 16.6 | 39 | ≤ 300 |
| SO ₄ (mg/L) | 933 | 19.1 | 36.7 | 30.6 | 81.1 | 20.5 | 56 | ≤ 500 |
| HCO ₃ (mg/L) | 927 | 68 | 112 | 113 | 156 | 26.9 | 24 | n.s |
| NO ₃ + NO ₂ (mg N/L) | 977 | 0.584 | 3.067 | 2.710 | 6.569 | 2.1 | 68 | ≤ 11 |
| PO ₄ (mg P/L) | 1006 | 0.026 | 0.531 | 0.145 | 2.909 | 1.251 | 236 | n.s |
| Si (mg/L) | 1006 | 4.7 | 6.6 | 6.6 | 8.6 | 1.2 | 18 | n.s |
| F (mg/L) | 896 | 0.13 | 0.24 | 0.21 | 0.43 | 0.10 | 44 | ≤ 1.5 |
| Fe (mg/L) | 116 | 0.004 | 0.066 | 0.022 | 0.300 | 0.114 | 172 | ≤ 2 |
| Mn (mg/L) | 116 | 0.001 | 0.029 | 0.004 | 0.150 | 0.063 | 219 | ≤ 0.5 |
| Al (mg/L) | 111 | 0.002 | 0.025 | 0.012 | 0.091 | 0.038 | 154 | ≤ 0.3 |
| EB (%) | 804 | –5.1 | 2.5 | 2.5 | 10.1 | 5.0 | 199 | ± 5 |
| TDS:SEC | 772 | 6.0 | 6.7 | 6.7 | 7.6 | 0.5 | 7 | n.s |
| SO ₄ :TDS (%) | 773 | 8 | 13 | 11 | 22 | 5 | 40 | n.s |

¹Standard health-related limit for consumption of 2 L/d over 70 years by a 60 kg person

Bold text denotes value exceeds standard limit as described in note 1

- the Ca–SO₄ composition of the Tweelopie Spruit (F11S12) and Riet Spruit waters characterises both raw and treated mine water;
- the Blougat Spruit water (188048) reflects a Na–SO₄ composition when treated municipal wastewater contributes the bulk of flow in this drainage, and a Na–HCO₃ composition when rainfall runoff provides a significant contribution;
- the Honingklip Spruit⁹ delivers a good quality Mg–HCO₃ type water; and
- the Bloubank Spruit downstream of its tributaries (A2H049) exhibits a CaMg–HCO₃ composition that reflects the significant contribution of karst springwater draining from the carbonate strata that dominate this catchment; the elevated SO₄ and Cl concentrations from the influence of mine water (F11S12) and municipal wastewater (188048) sources respectively, explain the shift in the Piper diagram plotting position relative to the Skeerpoort River water (A2H034).
- The Crocodile River water (A2H050) exhibits a distinctly different Na–HCO₃ composition representative of the predominantly granitic nature of this catchment. This water also shows an elevated Cl concentration compared to that of the Skeerpoort River and Bloubank Spruit water that most likely reflects the municipal wastewater influence on the chemical composition of this water.

2 Salt Load Assessment

2.1 Catchment Scale

A second aspect of water quality is the salt load associated with the water chemistry of the main drainages in the study area. Calculated as the product of concentration [*C*] and discharge [*Q*], yielding a load value typically expressed as tons per day (t/d), the calculation might target individual analytes such as SO₄ or NO₃ + NO₂, or it may target a composite variable such as TDS. The latter approach has been taken to compare the annual TDS load that is discharged at each of the sampling stations A2H034, A2H049

⁹Not shown in Fig. 28 because of the lack of a long-term water chemistry record for this drainage.

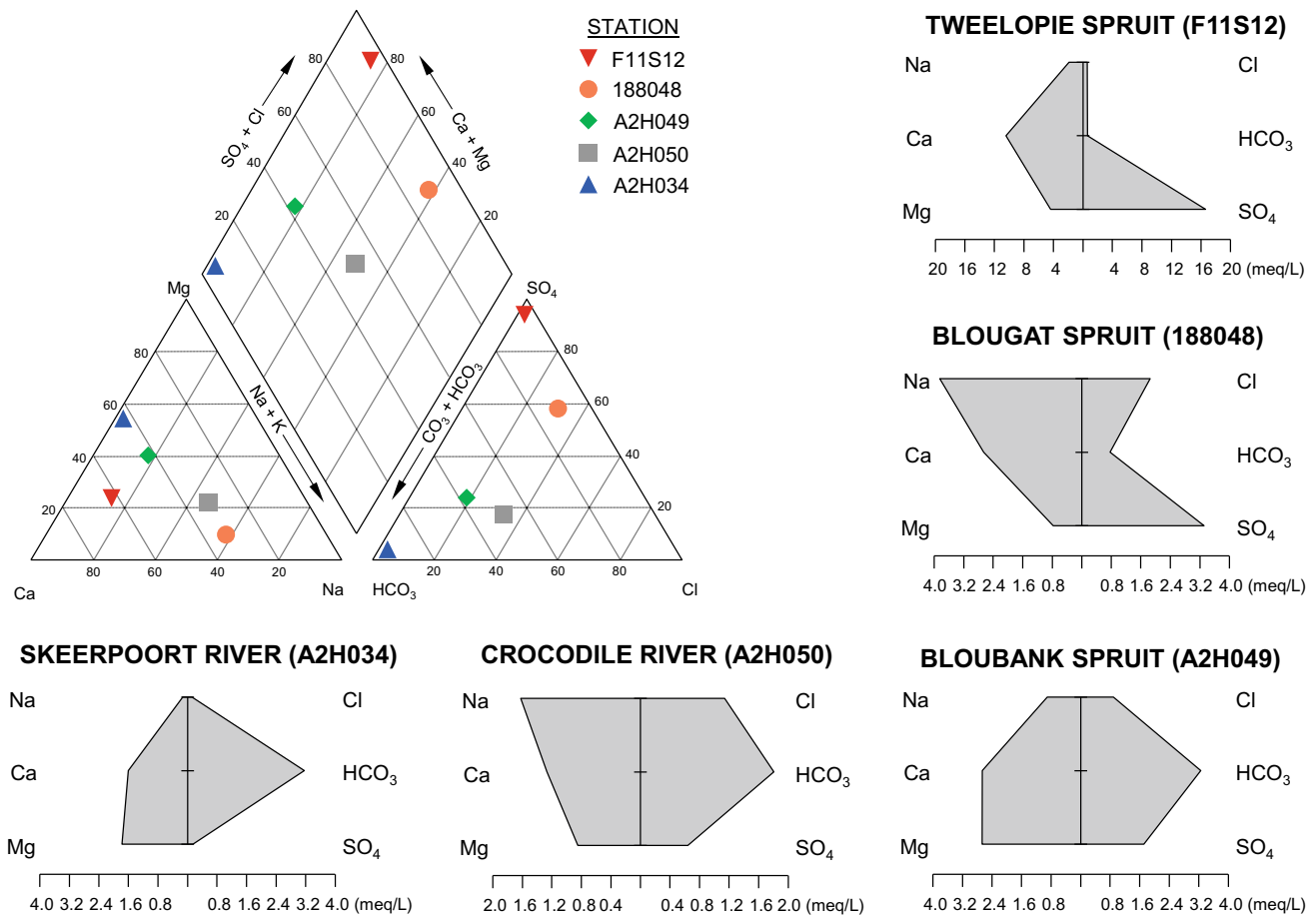


Fig. 28 Piper diagram (top left) and Stiff diagrams (bottom and right) characterising pre-2010 surface water chemistry in the study area; note the different Stiff diagram horizontal scales

Table 24 Statistical analysis of Driefontein WWTW discharge water chemistry (at station DFE) for the period November 2002 to February 2010 sourced from the DWS in November 2013

| Variable/Analyte | Statistical parameter | | | | | | | SANS (2015a) ¹ |
|--|-----------------------|----------|-------------|-----------|-------------|-------|---------|----------------------------|
| | n | 5%ile | Mean | Median | 95%ile | SD | CoV (%) | |
| pH ($-\log_{10}a_{H^+}$) | 31 | 6.9 | – | 7.3 | 7.9 | 0.5 | 7 | 5.0–9.7 |
| SEC (mS/m) | 31 | 50 | 56 | 56 | 67 | 7.7 | 14 | ≤ 170 |
| Cl (mg/L) | 21 | 55.0 | 74.5 | 73.0 | 125.0 | 26.0 | 35 | ≤ 300 |
| HCO ₃ (mg/L) | 21 | 89 | 141 | 132 | 198 | 60.0 | 43 | n.s |
| SO ₄ (mg/L) | 25 | 34.4 | 49.2 | 46.0 | 58.8 | 24.5 | 50 | ≤ 500 |
| NO ₃ + NO ₂ (mg N/L) | 30 | 0.35 | 3.92 | 3.50 | 8.00 | 3.54 | 90 | ≤ 11 |
| NH ₃ (mg N/L) | 30 | 0.000 | 0.020 | 0.005 | 0.102 | 0.04 | 206 | ≤ 1 |
| NH ₄ (mg N/L) | 30 | 0.05 | 1.10 | 0.30 | 4.20 | 2.51 | 229 | ≤ 1 |
| PO ₄ (mg P/L) | 31 | 0.05 | 1.31 | 0.20 | 1.60 | 5.56 | 425 | n.s |
| COD (mg/L) | 31 | 5.0 | 25.7 | 25.0 | 45.5 | 15.5 | 60 | n.s |
| Total coliforms (cfu/100 mL) | 10 | 16 | 578 | 59 | 2880 | 1 556 | 269 | n.s |
| Faecal coliforms (cfu/100 mL) | 30 | 2 | 212 | 25 | 1400 | 439 | 208 | ≤ 10 in 1% of samples |
| <i>E. coli</i> (cfu/100 mL) | 20 | 4 | 469 | 46 | 2160 | 1206 | 257 | ≤ 1 in 1% of samples |

¹Standard health-related limit for consumption of 2 L/d over 70 years by a 60 kg person.

Bold text denotes value exceeds standard limit as described in note 1

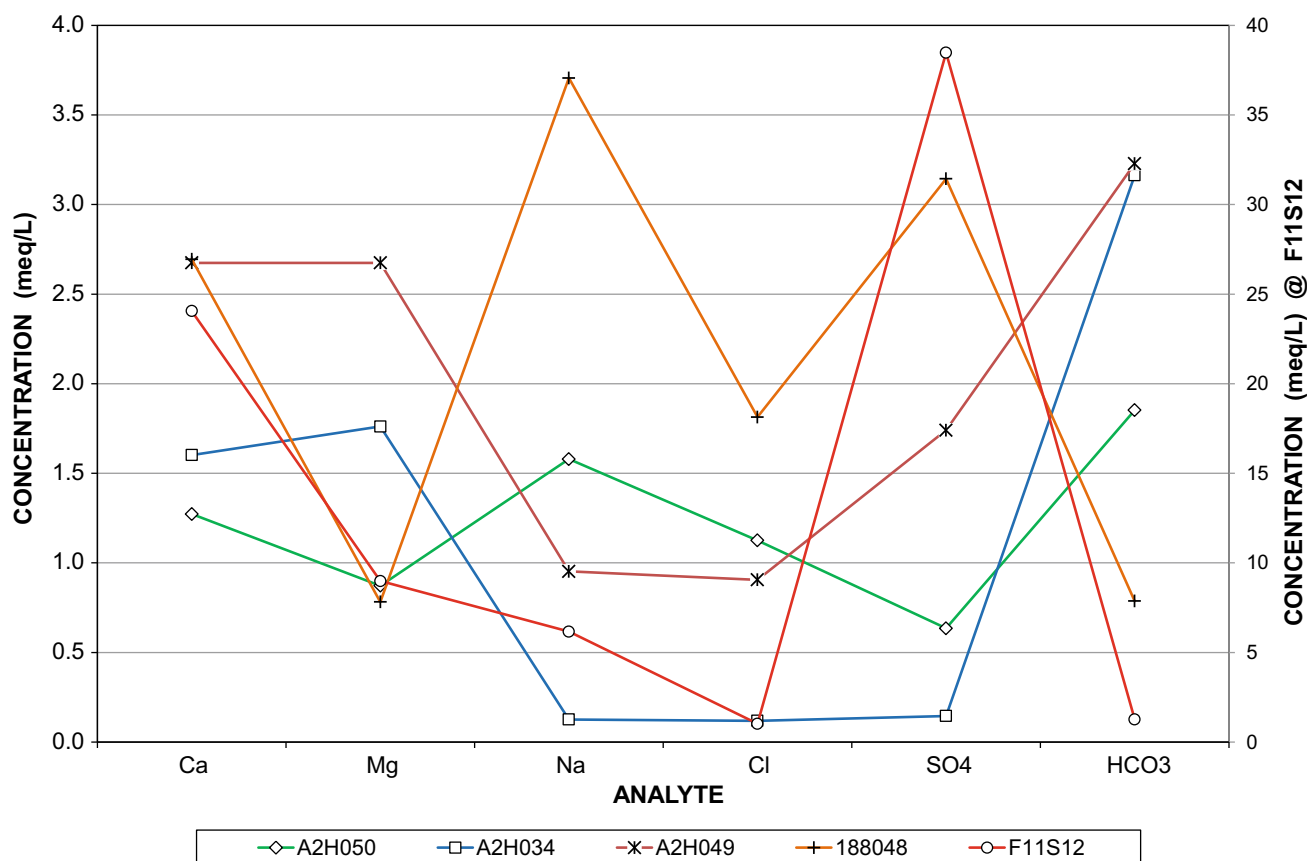


Fig. 29 Schoeller diagrams characterising pre-2010 surface water chemistry in the study area; note the 10× difference in scale between the left and right vertical axes

and A2H050 (Table 25). The comparison is made on the basis of the median long-term discharge and TDS values previously reported for each station. It would appear that the upper reach of the Crocodile River contributes only a slightly greater TDS load than does the pristine Skeerpoort River.

A more detailed comparison is made on the basis of the median long-term TDS concentration calculated for each month of mutual flow and water quality record (Fig. 30). This shows that the Skeerpoort and (upper) Crocodile rivers carry similar TDS loads that are typically 3–4 times less than that carried by the Bloubank Spruit system.

Text Box 1 TDS: Sec. and SO₄:TDS ratios for various water sources in the study area

The ratio of total dissolved solids (TDS) to electrical conductivity (SEC) provides a useful factor to estimate the TDS (in mg/L) from an easily obtained SEC measurement. The value of this ratio for natural water typically falls in the range 5.5–7.5 (Hem, 1985) for SEC in mS/m. An average value of 6.5 is generally taken as the most applicable empirical factor. More

acidic, poorly buffered and/or more saline water will differ from this empirical norm, with higher values generally being associated with water containing higher SO₄ concentrations (Hem 1985). The dominance of SO₄ in the chemical composition of mine water facilitates the recognition of a mine water impact in other water sources. In this regard, the SO₄:TDS ratio provides a useful measure to identify sources impacted by AMD. The appropriate data sourced by this study facilitates exploration of the above relationships in greater detail for the various water sources in the study area. The following analysis is based on median values reported in the referenced sections.

The long-term monthly TDS load data are interrogated further in Figs. 31, 32, 33, 34 and 35 to determine the variance associated with this variable at stations A2H034, A2H049 (for three periods of record) and A2H050.

All the graphs reveal the significant variance in TDS load associated with the summer months (especially February and March). Also evident in all five figures, although muted in

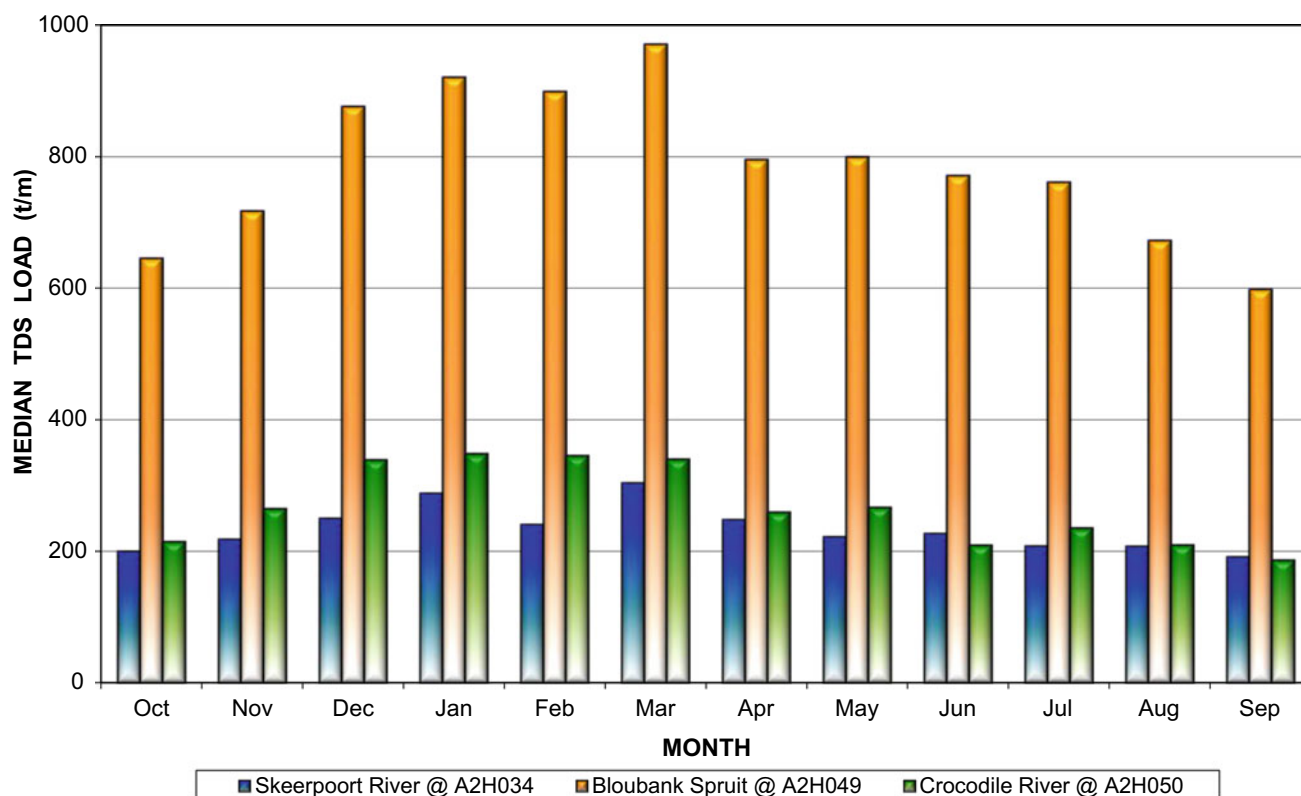


Fig. 30 Comparison of the long-term (October 1976 to September 2014) median monthly TDS loads carried by the main drainages in the study area

Fig. 33, is the bimodal nature of discharge in the respective drainages. The peaks associated with largely natural discharge regimes occur in January and March (Figs. 31, 33 and 35). Those associated with an anthropogenically modified discharge regime occur in February and May (Fig. 34). The pattern reflected in Fig. 34 reveals the extent to which mine water discharges in the last five hydrological years have altered the flow regime of the Bloubank Spruit system.

The modification of the Bloubank Spruit system flow regime is also reflected in the hydrochemistry. The median TDS load pattern (as a measure of water quality) associated with a largely natural water quality regime exhibits a unimodal shape peaking in summer (Figs. 31, 33 and 35). By comparison, that associated with an anthropogenically modified water quality regime exhibits peaks in February, May and August (Fig. 34). Further, the bias of variance at the 95%ile level evident in January, March and June (Fig. 34) again reflects the recent influence of mine water discharge in the Bloubank Spruit system. This is substantiated by comparison with the graph for the pre-2009–'10 period of the A2H049 record (Fig. 33).

The long-term constancy of the monthly median TDS load in the Skeerpoort River (Fig. 31) again reflects the dominant contribution of the perennial karst springs to the water quality in this drainage. The discharge from the

Driefontein WWTW on the Crocodile River upstream of station A2H050 explains the similar circumstances describing the monthly median TDS load in this drainage (Fig. 35).

The long-term monthly pattern and trend in the TDS loads delivered by the Bloubank Spruit and upper reach of the Crocodile River are shown in Figs. 36 and 37, respectively. Inspection of the graphs shows that both stations reflect an increasing TDS load (as indicated by the visually inserted arrows) since the early to mid-2000s. In the case of station A2H050, the commissioning of Unit 2 of the Driefontein WWTW might explain this observation (refer Sect. 3.3 in Chapter “Physical Hydrology”).

The text box in Fig. 36 lists the median and 95%ile values associated with different periods of the record. The post-January 2010 period reveals the greatest difference with the long-term record. This is readily attributable to the contemporary very high mine water discharges (Sect. 3.1 in Chapter “Physical Hydrology”). Less obvious are the following comparisons:

- the similar median and 95%ile values of the pre-August 2002 and post-July 2002 periods—this indicates little change in the water chemistry following the commencement of decant from the Western Basin in August 2002; and

Table 25 Annual long-term TDS load delivered by the main drainages in the study area

| Drainage | Station | Median TDS (mg/L) | Median discharge (Mm ³ /a) | TDS Load | | |
|------------------|---------|---------------------|--|----------|--------|------------|
| | | | | t/d | t/a | % of total |
| Skeerpoort River | A2H034 | 265 (from Table 22) | 10.21 (from Fig. 6 in Chapter “Physical Hydrology”) | 7.4 | 2703 | 16.1 |
| Bloubank Spruit | A2H049 | 444 (from Table 19) | 23.52 (from Fig. 11 in Chapter “Physical Hydrology”) | 28.6 | 10 443 | 62.0 |
| Crocodile River | A2H050 | 286 (from Table 23) | 12.89 (from Fig. 22 in Chapter “Physical Hydrology”) | 10.1 | 3687 | 21.9 |
| Total | | | | 46.1 | 16 833 | 100 |

- the similar 95%ile values but doubled median value of the post-July 2012 period compared to the whole record period—this indicates an increase in the TDS load in the most recent past without manifesting excursions at the 95%ile level. Figure 36 suggests that this increase amounts to ~100% (from 750 to 1500 t/m).

| Surface water (Station) | Section | TDS (mg/L) | SEC (mS/m) | TDS:SEC | SO ₄ :TDS (%) |
|--|--|--------------------|------------|---------|--------------------------|
| Skeerpoort River (A2H034) | 1.1 | | | | |
| Tweelopie Spruit (F11S12) ¹ | 1.2.2 | 2890 | 283 | 10.2 | 63 |
| Tweelopie Spruit (F11S12) ² | 1.2.2 | 3500 | 330 | 10.5 | 64 |
| Tweelopie Spruit (F11S12) ³ | 1.2.2 | 3030 | 295 | 10.3 | 63 |
| Blougat Spruit (188,048) | 1.2.4 | 502 | 82 | 6.1 | 33 |
| Tweefontein Spruit (F14S15) | 1.2.5 | 448 | 60 | 7.5 | 18 |
| Bloubank Spruit (A2H049) | 1.2.6 | 451 | 61 | 7.4 | 19 |
| Honingklip Spruit | 1.2.6 | 164 | 22 | 7.5 | 9 |
| Crocodile River (A2H050) | 1.3 | 290 | 44 | 6.6 | 11 |
| <i>Groundwater</i> | | | | | |
| Pristine karst springwater | 7 in Chapter “Chemical Hydrogeology” | 310 | 36 | 8.6 | 2 |
| Impacted karst groundwater | 8.4 in chapter “Chemical Hydrogeology” | 1699 | 192 | 8.5 | 62 |
| Quartzitic strata ⁴ | — | 40 | 9 | 4.6 | 11 |
| <i>Wastewater</i> | | | | | |
| Raw mine water ⁵ | 1.2.1 | | | | |
| Treated mine water | 1.2.1 | | | | |
| <i>Municipal sewage effluent</i> | | | | | |
| Percy Stewart WWTW | 1.2.4 | 649 ⁽⁶⁾ | 103 | (6.3) | 31 ⁽⁶⁾ |
| Driefontein WWTW | 1.3 | 358 ⁽⁶⁾ | 56 | (6.4) | 13 ⁽⁶⁾ |

¹Associated with the pre-February 2010 period of record

²Associated with the February 2010 to July 2012 period of record

³Associated with the August 2012 to September 2017 2014 period of record

⁴Derived from data presented by Hobbs and Cobbing (2007) and Hobbs (2011a)

⁵Associated with the Black Reef Incline discharge

⁶Value based on the TDS:SEC ratio shown in brackets

Notes

(a) The similar SO₄:TDS values reported for the Blougat Spruit / Percy Stewart WWTW (33%/31%), the Crocodile River/Driefontein WWTW (11%/13%) and the Tweelopie Spruit/mine water (66%/64%) sources indicate the veracity of the assessments for these sources

(b) The similar SO₄:TDS values reported for Honingklip Spruit and Crocodile River surface water on the one hand, and groundwater sourced from quartzitic strata on the other, reflects the similar geologic environments common to the provenance areas of these water sources

(c) The similar SO₄:TDS values reported for Tweelopie Spruit surface water, raw and treated mine water and impacted karst groundwater similarly reflects the common influence of AMD

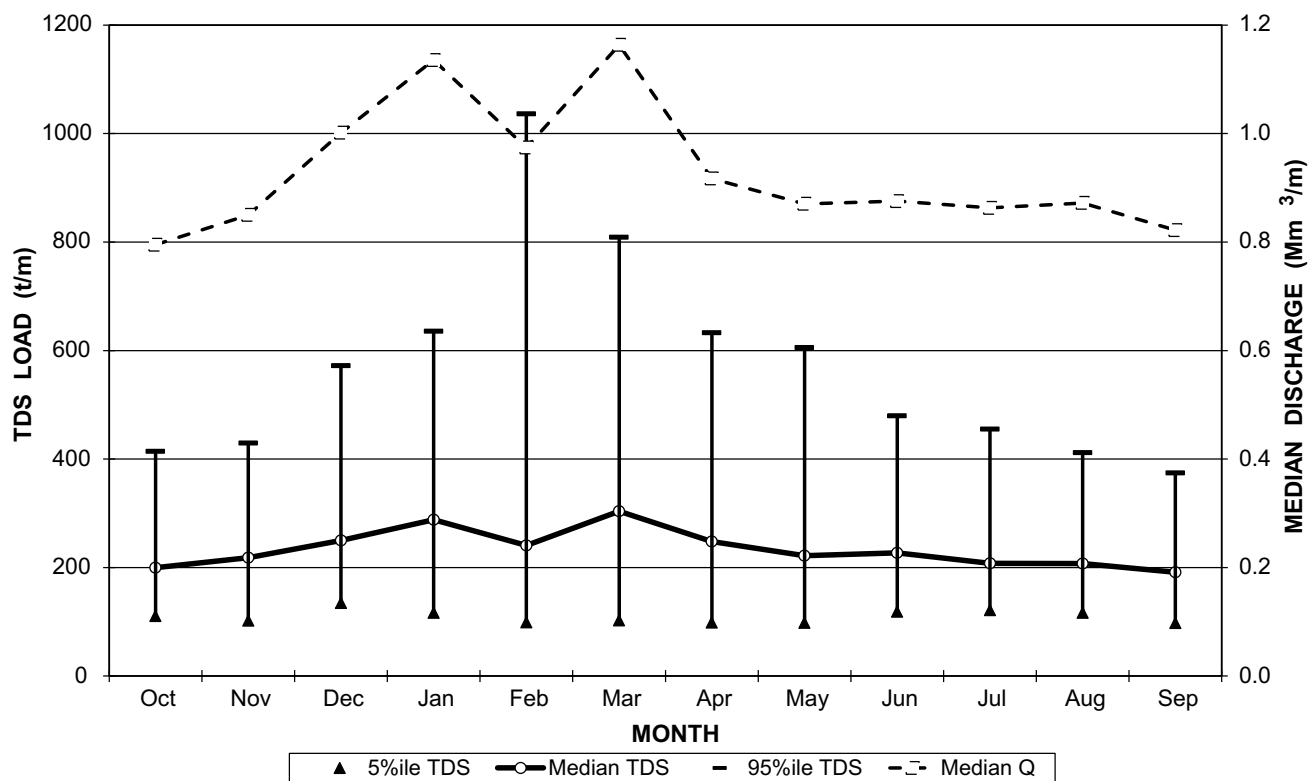


Fig. 31 Variance in the long-term (October 1976 to September 2014) monthly Skeerpoort River TDS load at station A2H034

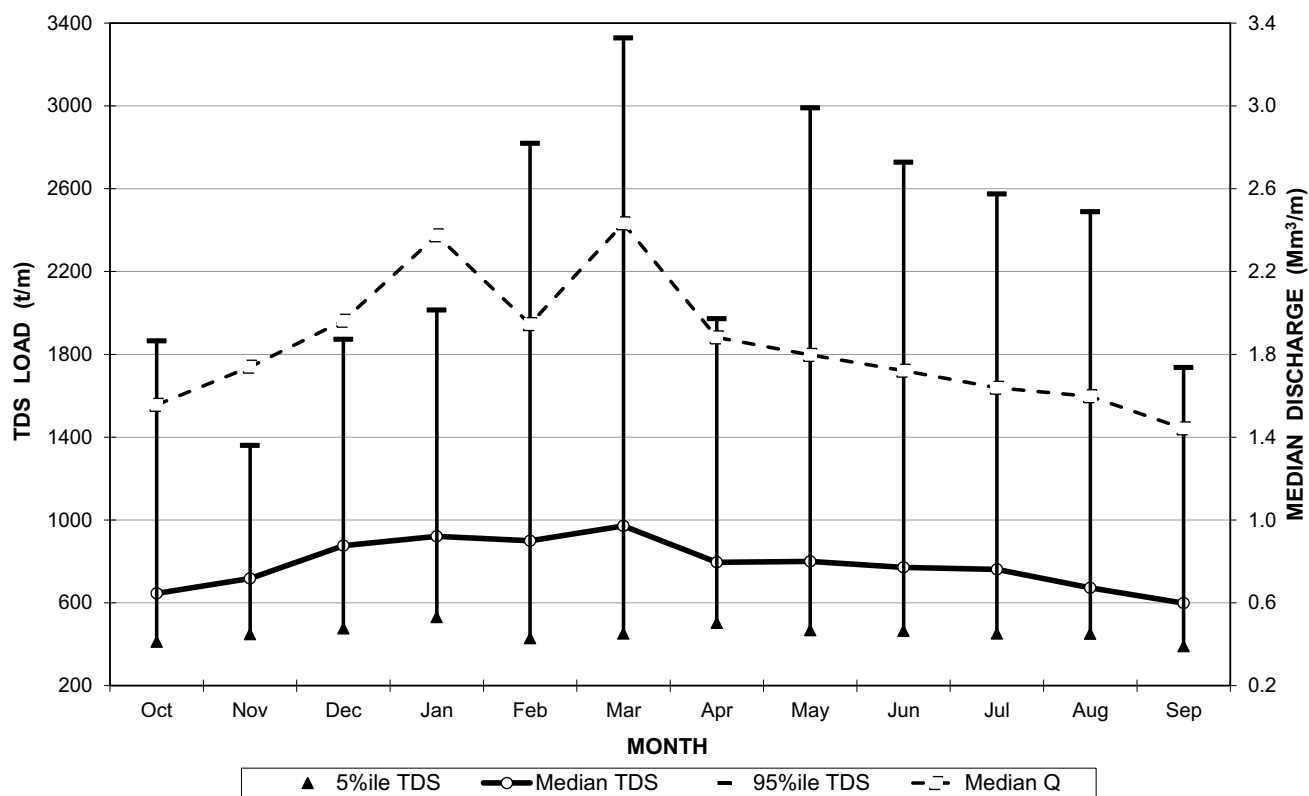


Fig. 32 Variance in the long-term (October 1979 to September 2014) monthly Bloubank Spruit TDS load pattern at station A2H049

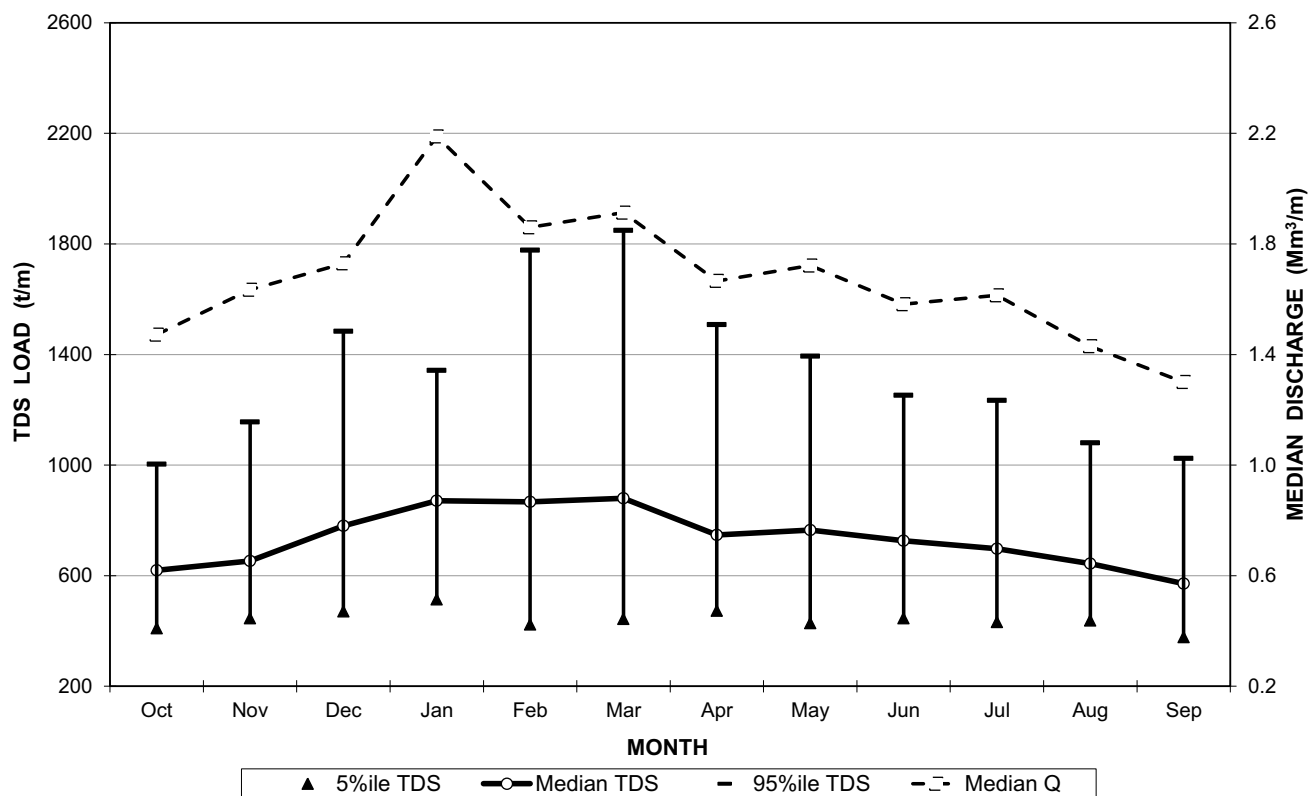


Fig. 33 Variance in the pre-2010 monthly Bloubank Spruit TDS load pattern at station A2H049

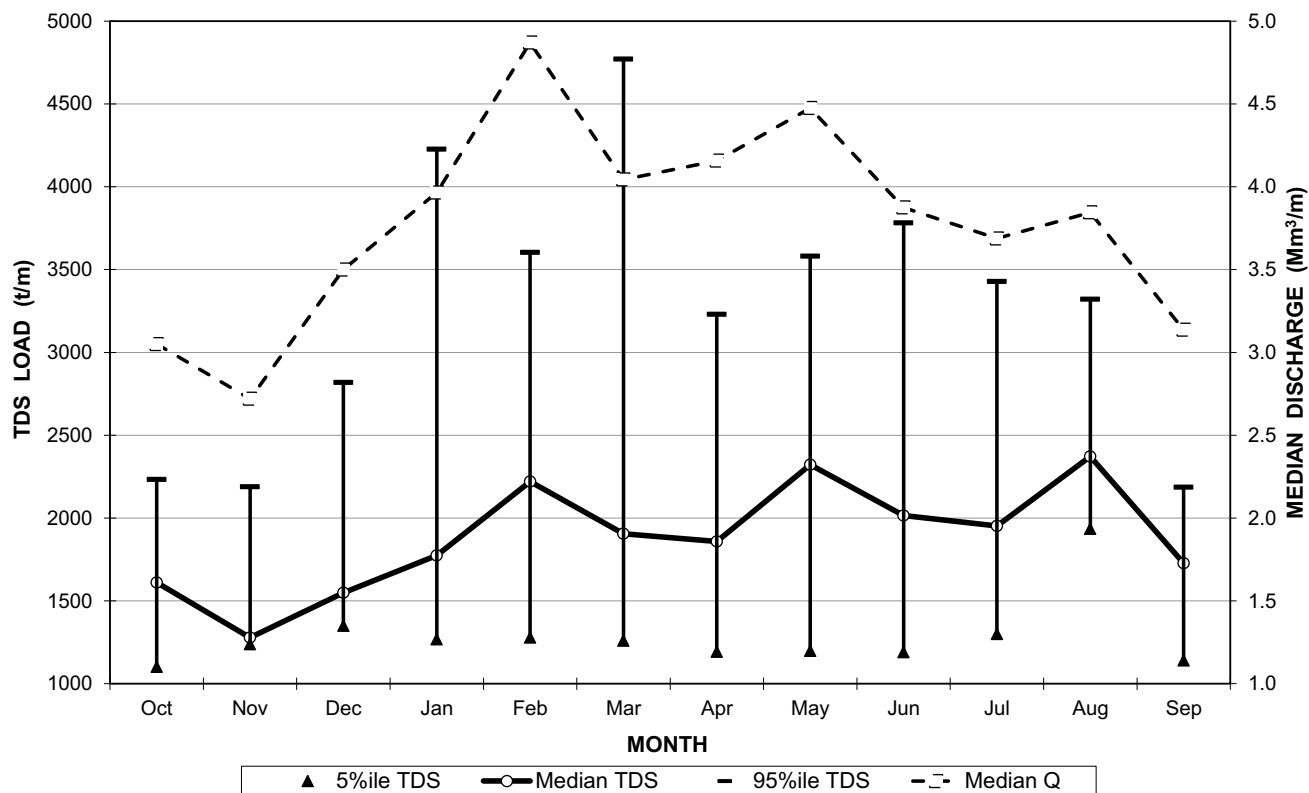


Fig. 34 Variance in the recent (2010 to 2014) monthly Bloubank Spruit TDS load pattern at station A2H049

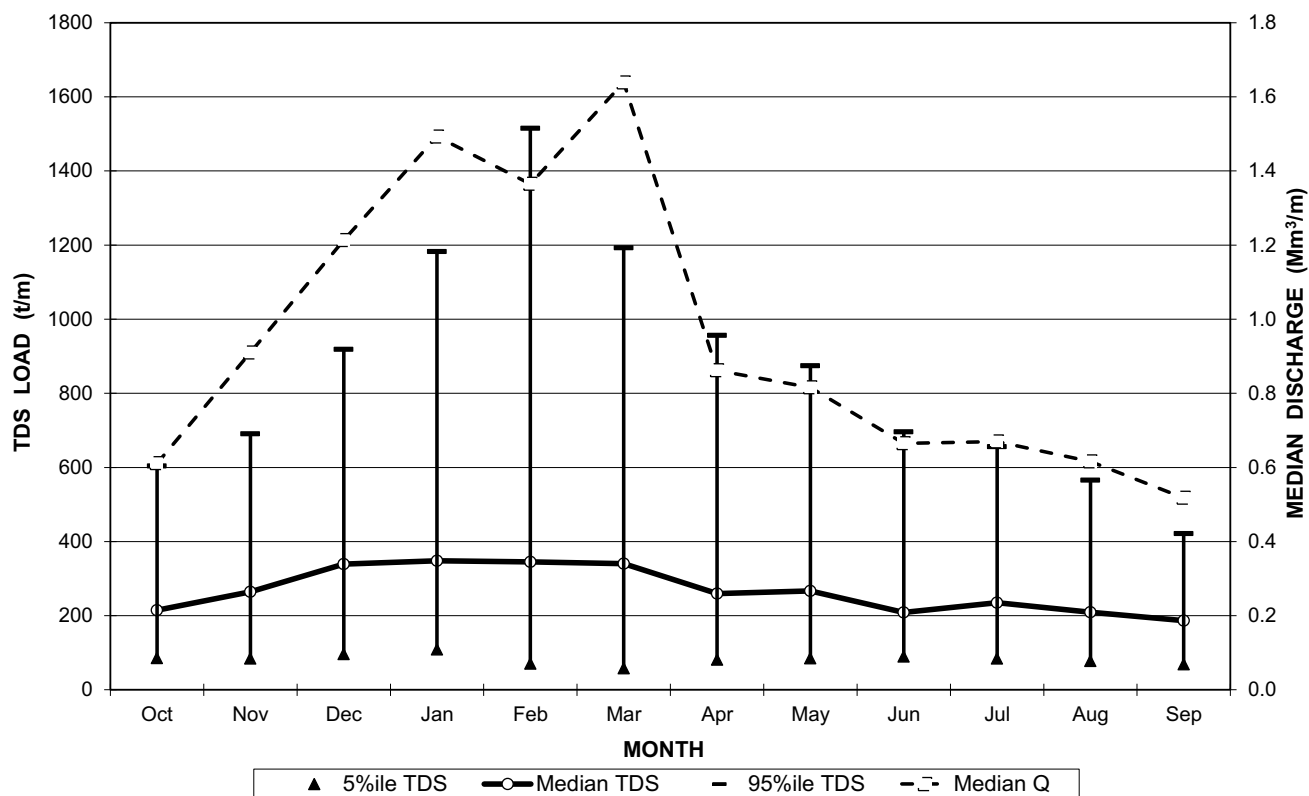


Fig. 35 Variance in the long-term (October 1979 to September 2014) monthly Crocodile River TDS load pattern at station A2H050

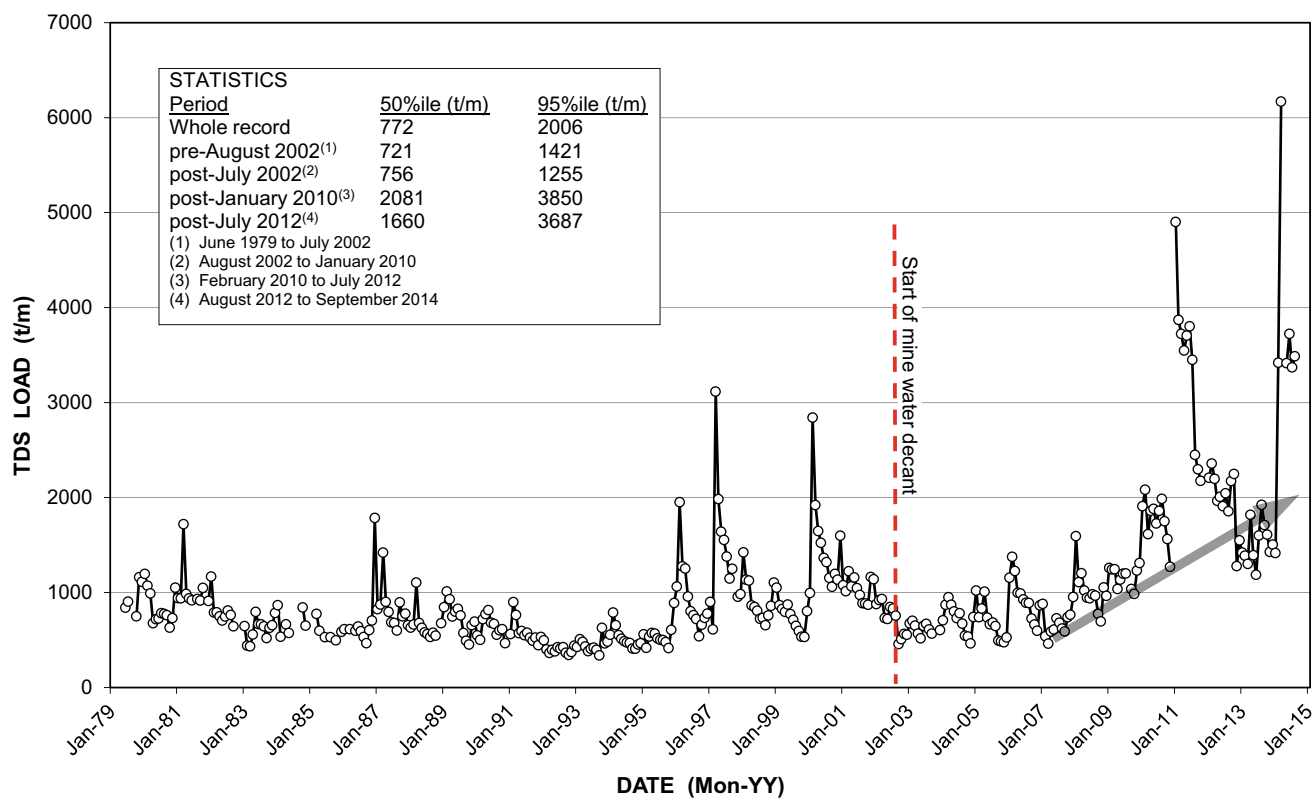


Fig. 36 Long-term (June 1979 to September 2014) monthly TDS load pattern and trend in the Bloubank Spruit at station A2H049

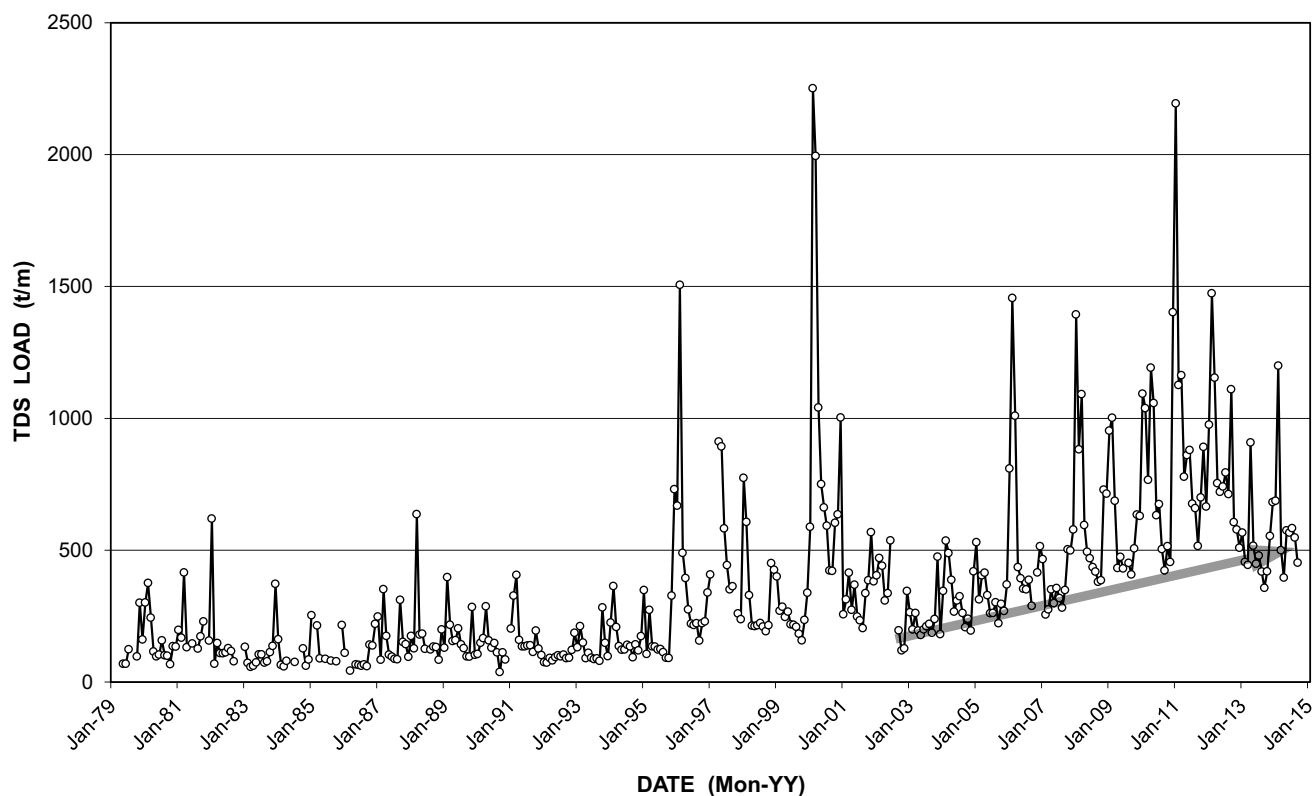


Fig. 37 Long-term (May 1979 to September 2014) monthly TDS load pattern and trend in the upper reach of the Crocodile River at station A2H050

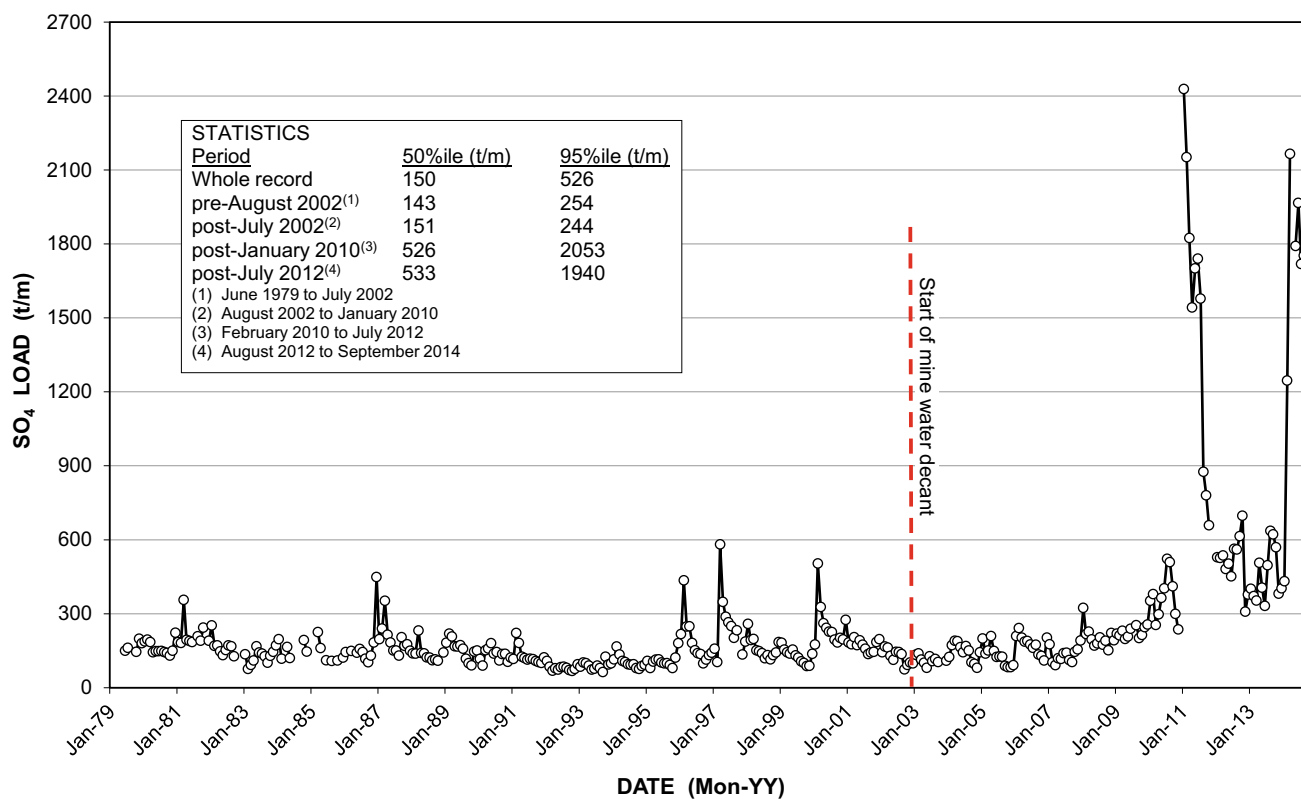


Fig. 38 Long-term (October 1979 to September 2014) monthly SO₄ load pattern and trend in the Bloubank Spruit at station A2H049

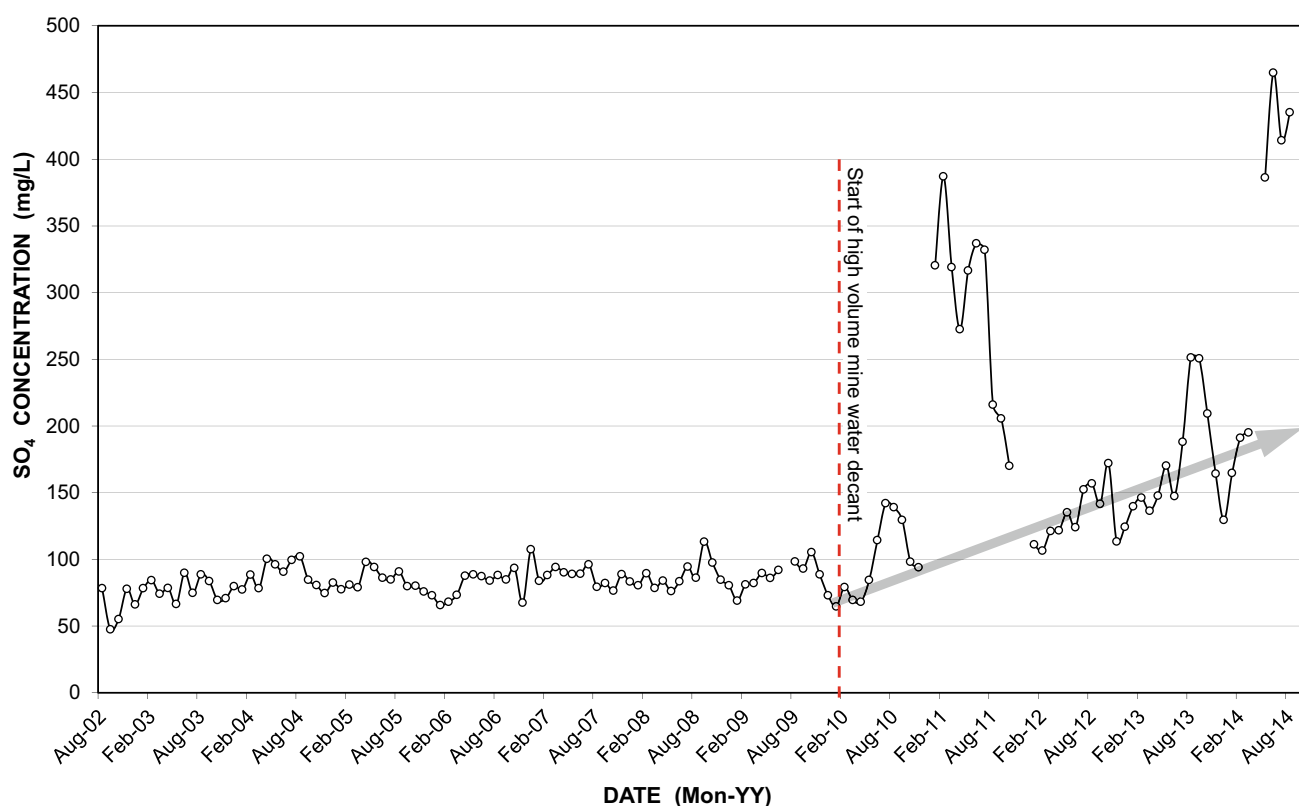


Fig. 39 Pattern and trend in the SO_4 concentration at station A2H049 since the start of mine water decant in the Western Basin

The long-term monthly trend in the SO_4 load delivered by the Bloubank Spruit is shown in Fig. 38, and since the start of decant in Fig. 39. Unsurprising under circumstances where SO_4 comprises $\sim 63\%$ of the major ion concentration in mine water (Text Box 1), the most recent period of record mimics the TDS load pattern and trend (Fig. 36 and 38).

The SO_4 :TDS ratio provides a further measure of the mine water impact on the chemistry of surface water at the downstream end of the Bloubank Spruit system. This is illustrated in Fig. 40 for the long-term record, and in Fig. 41 for the period since the start of decant.

The rising trends (arrowed) indicate that SO_4 contributes an increasing proportion of the TDS concentration in the more recent past. Quantification of this ratio for various sources of water in the study area is presented in Text Box 1. Clearly the 19% value reported in Text Box 1 for the Bloubank Spruit at A2H049 more recently approaches 30 to 35% (ignoring the greater short-term exceedances in mid-2011 and mid-2014). This trend is in contrast to the pre-decant trend revealed in Fig. 40, which reflects a distinct decline in the SO_4 :TDS ratio in the period 1986 to 2001.

A possible explanation for the 1986 to 2001 trend is the greater contribution of karst groundwater, typically with a very low SO_4 concentration, draining from the Zwartkrans and Krombank compartments following the breaking of the

drought that characterised the early 1980s (Sect. 2.1 in Chapter 4). The preceding (1979 to 1985) rising SO_4 trend (Fig. 40) possibly reflects the increasing impact of contemporary mine water releases from still active mining operations in the Western Basin, exacerbated by a concurrent drought-related decrease in spring discharges. These observations are considered to provide the clearest indication that mine water originating in the Western Basin has had both an historical and a recent impact on the quality of surface water (and groundwater) resources in the south-western portion of the study area. Further discussion of this impact is presented in Sect. 2.3.3 in Chapter “[Chemical Hydrogeology](#)”.

The magnitude of the large mine water discharges in 2011 and 2014 is also illustrated in Fig. 42, which depicts the monthly TDS load in each year of record. The high loads observed in 1997 and 2000 (concentrated in the months February, March and April in both instances) are surpassed by the 2011 and 2014 loads.

The data presented in Fig. 42 further indicate that the month of March has produced the highest monthly TDS load on seven occasions (1981, 1985, 1987, 1988, 1997, 2004 and 2014) in the 36-year record period. The most recent is also the highest monthly load on record. March has also produced the 2nd highest load on a further seven occasions (1989, 1991, 1994, 1996, 2000, 2006 and 2008). These

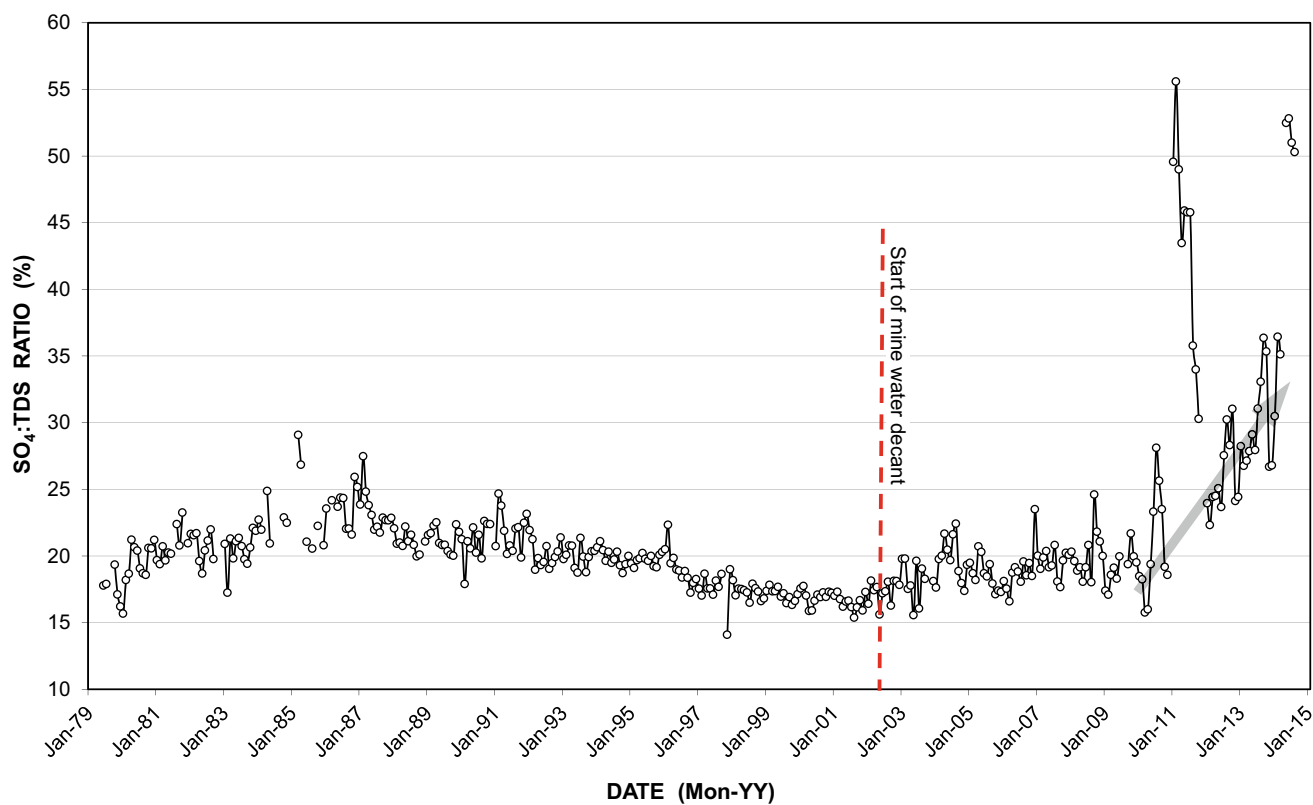


Fig. 40 Long-term (June 1979 to September 2014) trend in the SO_4 :TDS ratio at station A2H049

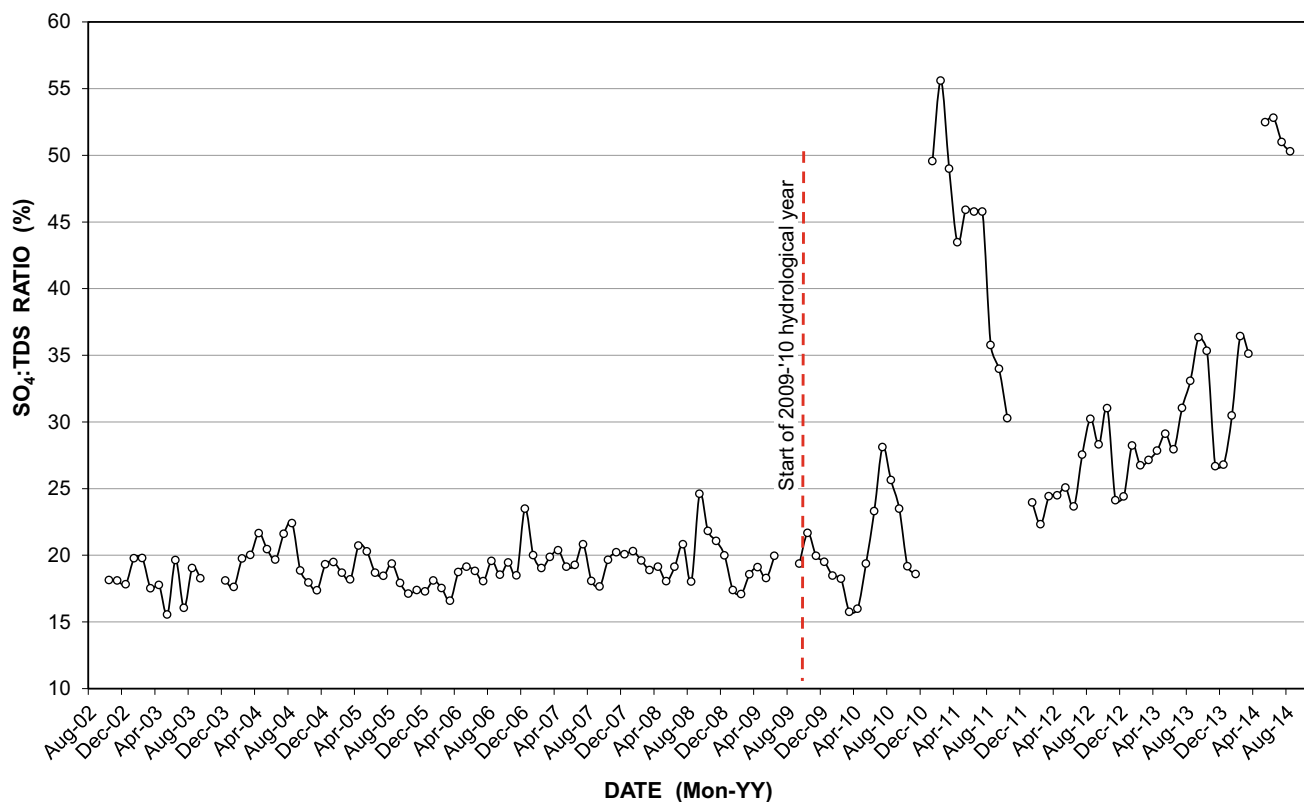


Fig. 41 Pattern and trend in the SO_4 :TDS ratio at station A2H049 since the start of mine water decant in the Western Basin

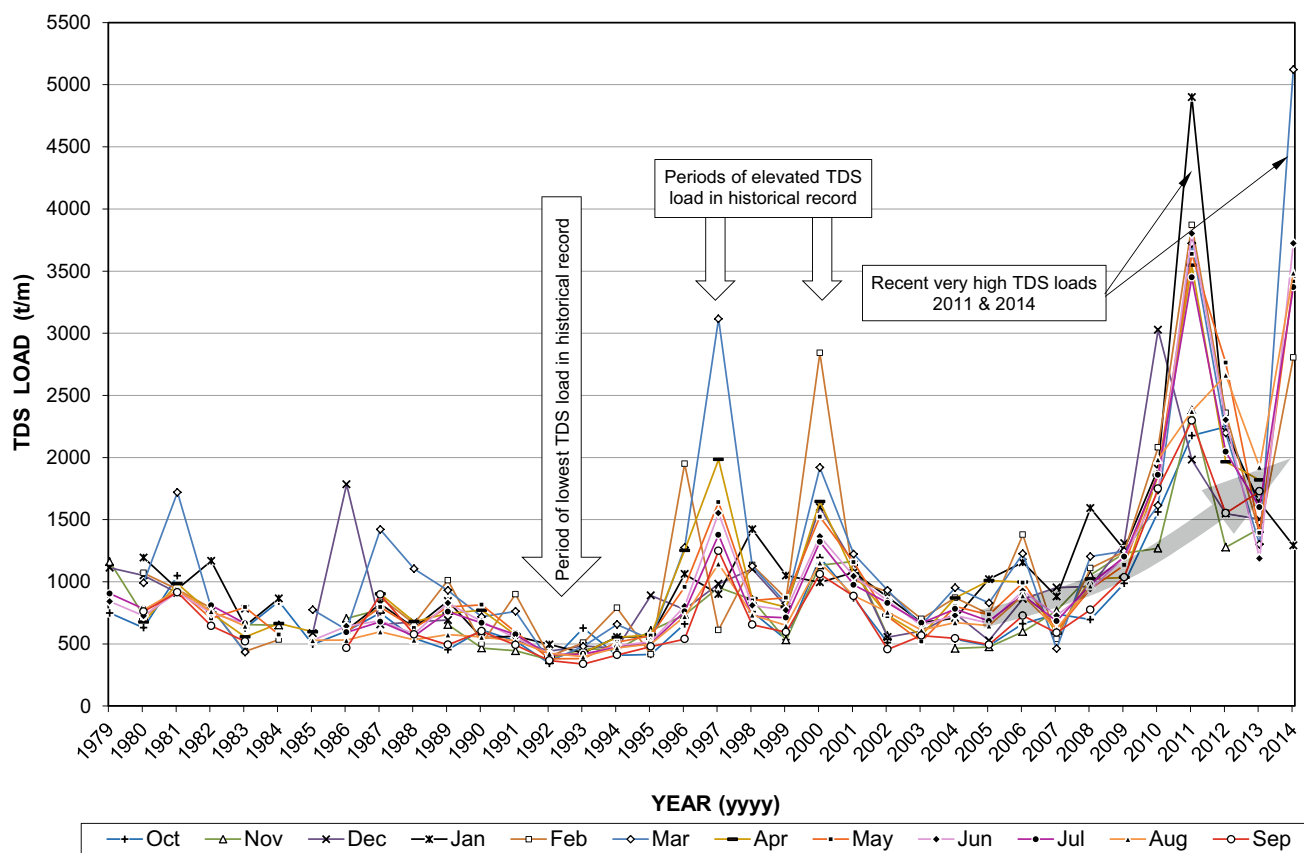


Fig. 42 Monthly TDS load pattern and trend at station A2H049 in each year of historical record

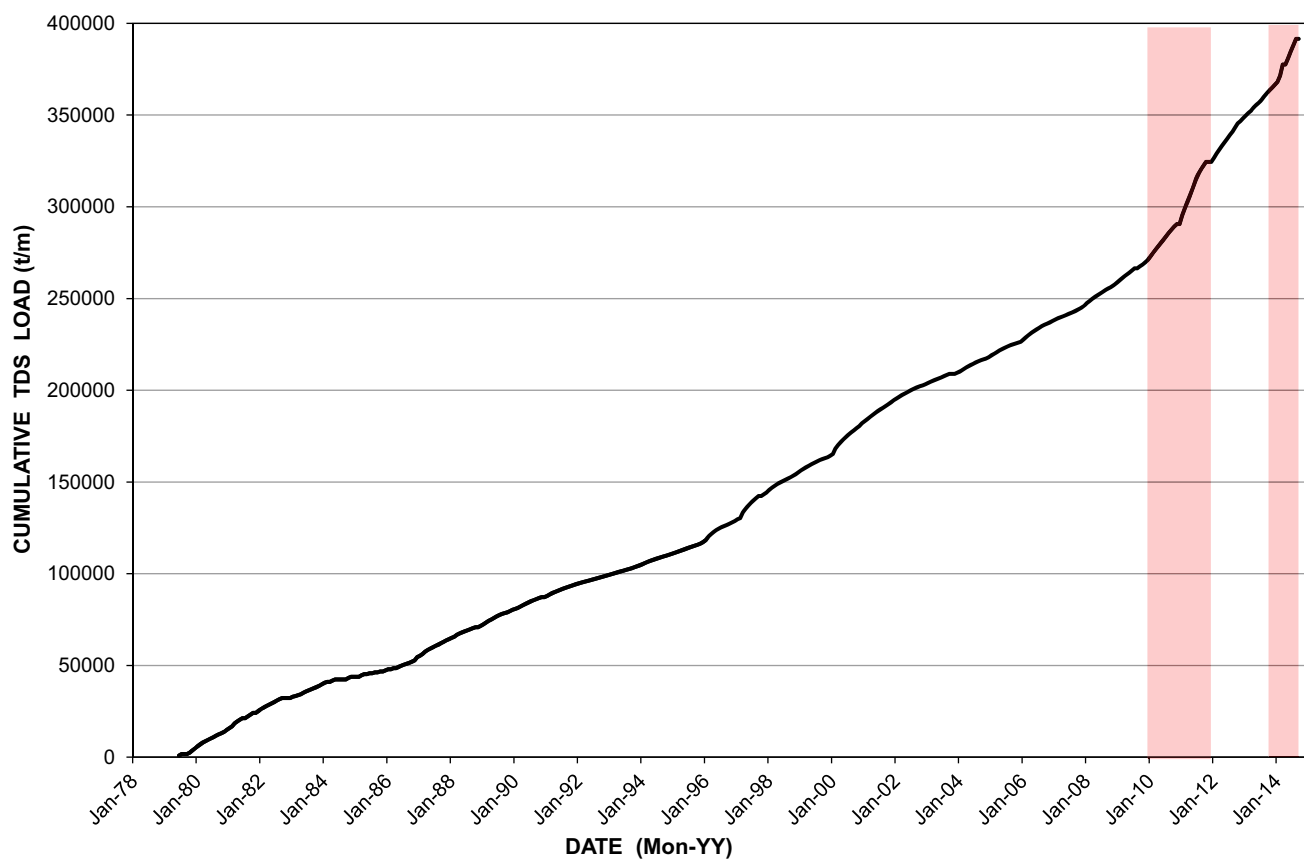


Fig. 43 Pattern and trend of cumulative monthly TDS load delivered by the Bloubank Spruit system in the long-term

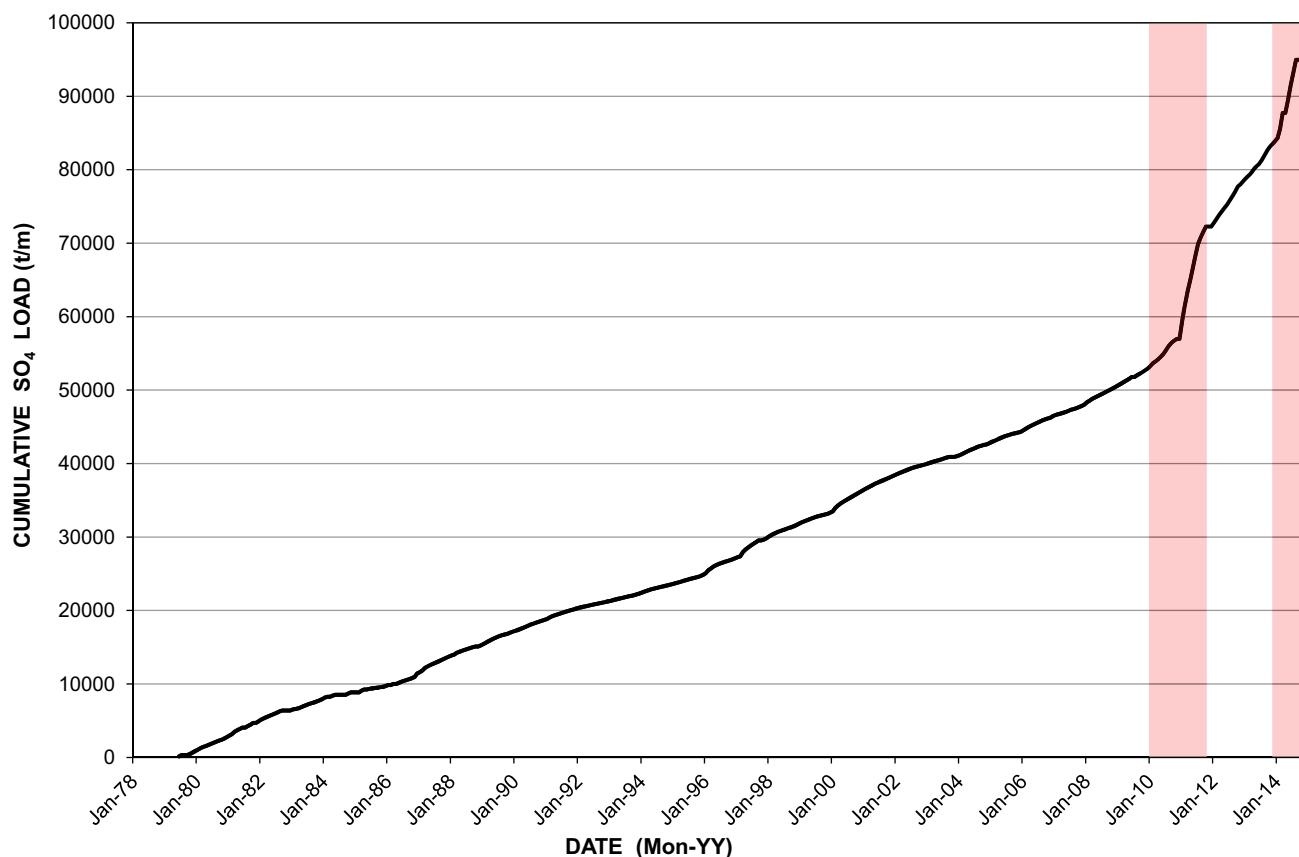


Fig. 44 Pattern and trend of cumulative monthly SO_4 load delivered by the Bloubank Spruit system in the long-term

occurrences together represent 39% of the record period, suggesting that March is the most ‘prolific’ load-bearing month of a hydrological year in the Bloubank Spruit drainage system.

It is since mid-2010 that the large mine water discharges resulted in a significant change in the chemical composition of surface water leaving the Bloubank Spruit system at station A2H049. This serves as confirmation that a significantly greater mine water component, and in particular raw mine water, characterised the surface water chemistry in the middle and lower reaches of the Bloubank Spruit system than before mid-2010.

The reduction in monthly TDS loads through 2012 into 2013 was reversed by the excessive mine water discharge in the period March to July 2014. It is therefore worth exploring the effects of the large mine water discharges during the 2010, 2011 and 2014 rainfall seasons in the context of the long-term TDS and SO_4 loads delivered by the Bloubank Spruit system. This is attempted in Figs. 43 and 44, which show the respective cumulative monthly TDS and SO_4 loads at station A2H049 in the long-term.

The cumulative TDS and SO_4 loads in the pre-January 2010 period suggest a slight change in slope ca. January 1996. This change, although interesting, is not considered

significant enough to warrant more detailed inspection in this study. More significant is the sharper change in slope commencing January 2010 and expressed most dramatically (especially in the case of SO_4) ca. January 2011. Similar circumstances are again evident in early 2014. These are unequivocal manifestations of the impact of mine water on the surface water chemistry delivered by the Bloubank Spruit system.

The cumulative long-term median contribution to the TDS load delivered by each of the Bloubank Spruit and the (upper) Crocodile River is shown in Fig. 45. The analysis, based on the hydrological years 1980 to 2014, reflects the ~ 3 times greater contribution of the Bloubank Spruit system.

A similar inspection of the TDS load data for only the Bloubank Spruit system over the period of record 1980 to 2014 is presented in Fig. 46. The similarity of the pre-2010 and whole record data contrasts markedly with the pattern and trend associated with the period 2010 to 2014. The analysis reveals the $\sim 140\%$ greater load discharged since the 2009 hydrological year, compared to the preceding ~ 30 years. These circumstances further illustrate the impact of mine water discharges on the recent water chemistry of the Bloubank Spruit system. This analysis also provides the

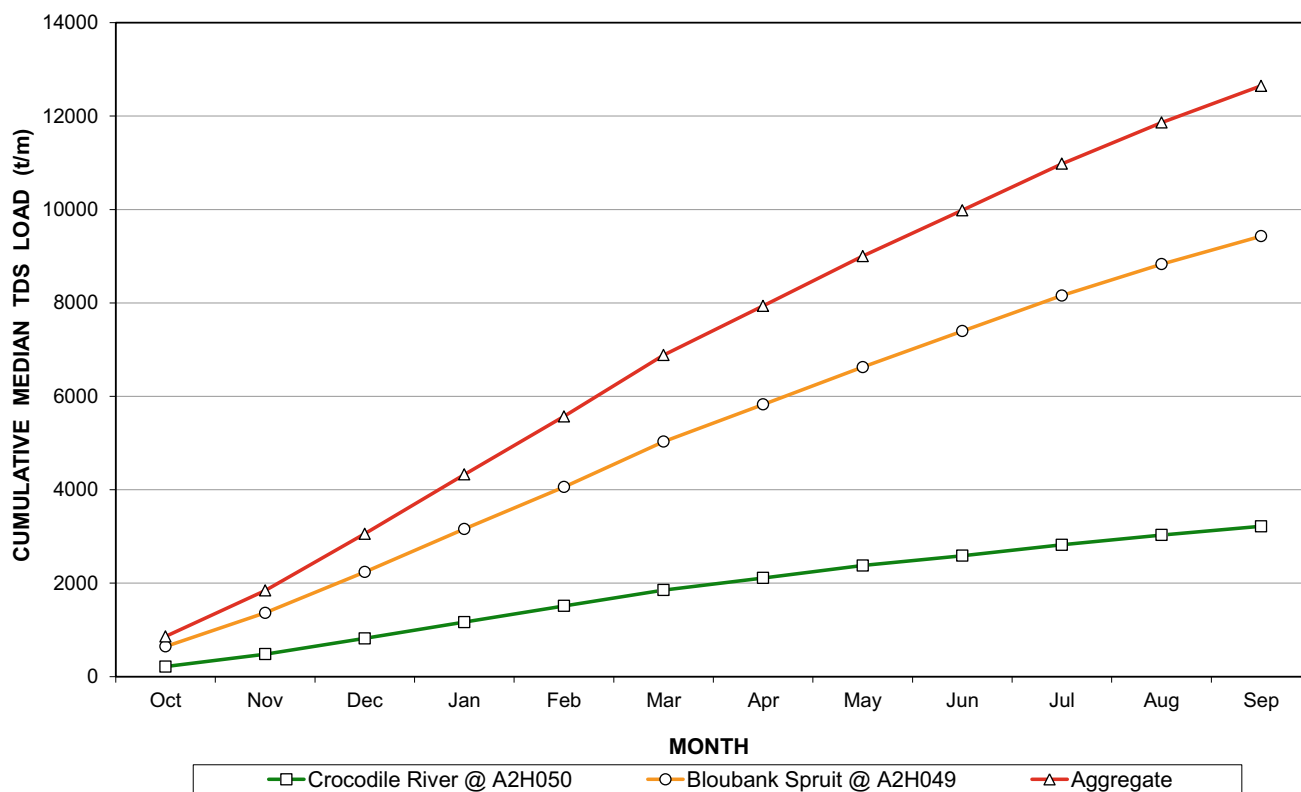


Fig. 45 Cumulative long-term median monthly TDS loads discharged by the Bloubank Spruit and the upper reach of the Crocodile River

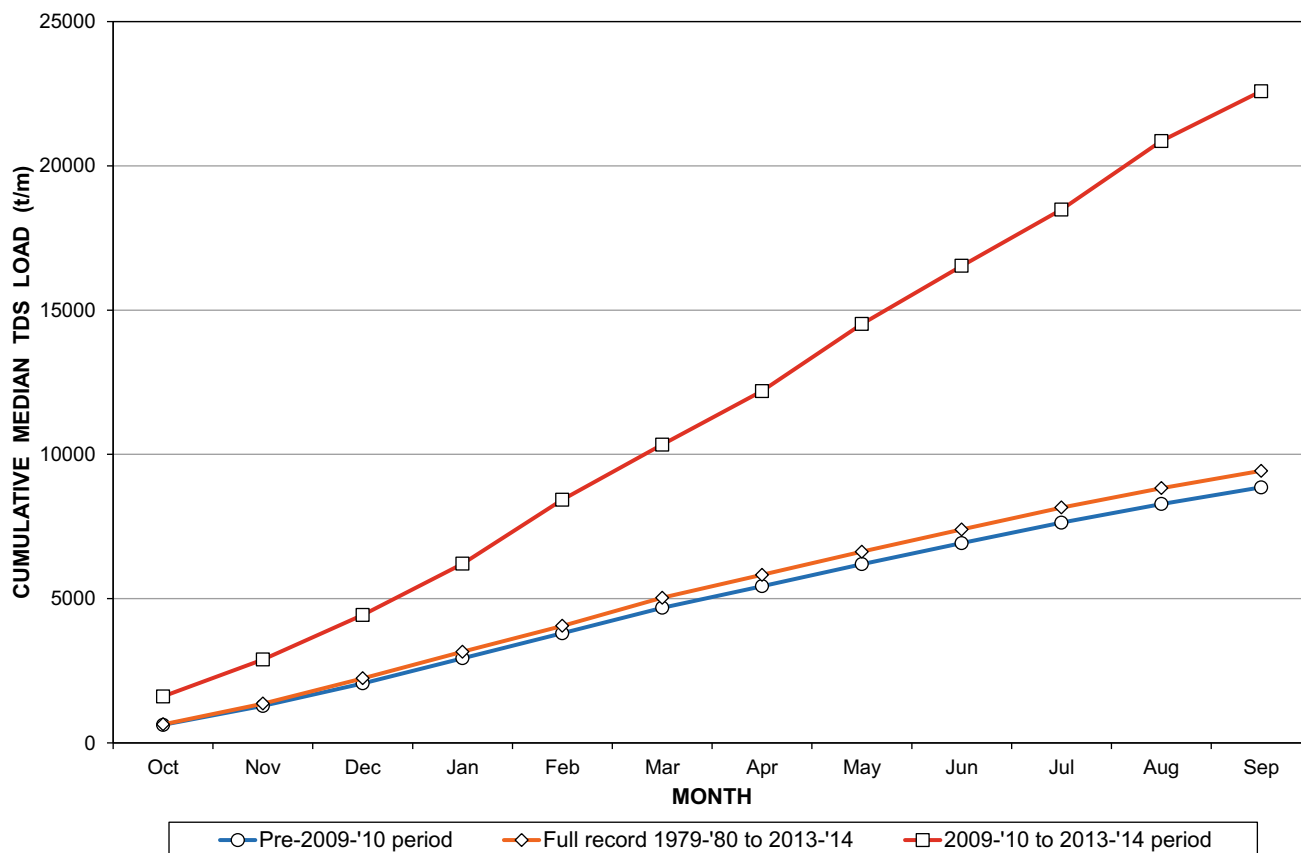


Fig. 46 Comparison of cumulative median monthly Bloubank Spruit system TDS loads for three periods of record

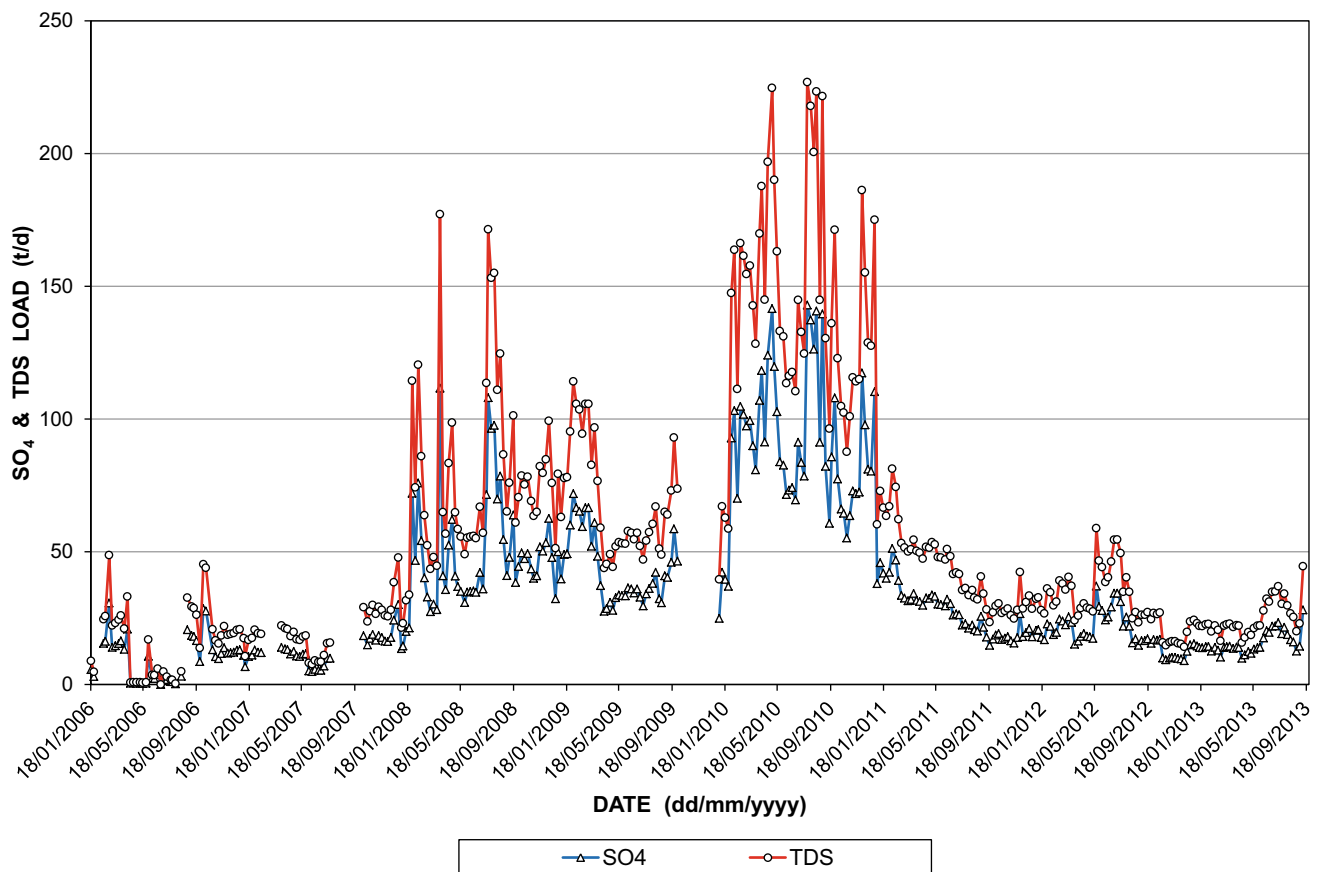


Fig. 47 Pattern and trend of daily SO₄ and TDS loads in mine water delivered to the Tweelopie Spruit

background for the interrogation of the mine water impacts in a regional context as set out in Sect. 2.3. The relevance of specific timeframes in such an exercise is evident.

Perhaps of greater consequence for the downstream environment that includes the Hartbeespoort Dam, is the nutrient load delivered by the Bloubank Spruit and the (upper) Crocodile River catchments. The evaluation of nutrients such as NO₃-N and PO₄-P as indicators of pollution is presented in greater detail in Sect. 3.2 in Chapter 6.

The Percy Stewart WWTW on the Blougat Spruit in the Bloubank Spruit system is reported to have delivered a

median orthophosphate (PO₄ as mg P/L) load of ~19.3 t/a to this catchment in the period July 2007 to June 2009 (Hobbs, 2011a). This is calculated from a median PO₄ concentration of 4.1 mg P/L (Table 13) and a median plant discharge of ~4.7 Mm³/a (Sect. 3.2 in Chapter “Physical Hydrology”). An inspection of the average monthly concentrations and flows recorded at stations A2H049 (0.25 mg P/L at 27 Mm³/a) and A2H050 (0.18 mg P/L at 25.3 Mm³/a) in a similar period (mid-2007 to mid-2008) indicates loads of ~6.7 and ~4.6 t/a passing these stations, respectively.

Table 26 Median annual nutrient loads (as NO₃-N and PO₄-P) delivered by the Crocodile River system to Hartbeespoort Dam in the period 1979–’80 to 2013–’14

| Drainage (station #) | Median discharge (Mm ³ /a) | Median NO ₃ -N (mg/L) | Median PO ₄ -P (mg/L) | Median Load | | % of Total | |
|--------------------------|---------------------------------------|----------------------------------|----------------------------------|--------------------------|--------------------------|--------------------|--------------------|
| | | | | NO ₃ -N (t/a) | PO ₄ -P (t/a) | NO ₃ -N | PO ₄ -P |
| Hennnops River (A2H014) | 67.570 | 4.72 | 0.617 | 319 | 41.2 | 22.4 | 36.6 |
| Jukskei River (A2H044) | 122.845 | 7.88 | 0.557 | 968 | 68.4 | 68.2 | 60.7 |
| Bloubank Spruit (A2H049) | 22.701 | 4.36 | 0.054 | 99 | 1.2 | 7.0 | 1.1 |
| Crocodile River (A2H050) | 12.892 | 2.66 | 0.139 | 34 | 1.8 | 2.4 | 1.6 |
| Total | | | | 1 420 | 112.6 | 100 | 100 |

The median phosphorus load of ~ 19.3 t/a delivered by the Percy Stewart WWTW contrasts markedly with the much smaller median load of ~ 6.7 t/a passing station A2H049 located further downstream. This discordance remains valid even if the comparative coarseness of the calculations is considered, and prompts the following discussion.

It is shown in Table 20 that PO_4 concentrations of ~ 2.4 mg P/L were observed at stations BB@N14 and BB@M on 18/05/2010, whilst at station BB@PL further downstream it amounted to only 0.5 mg P/L on the same day. The reduction is readily attributed to the dilution provided by the Kromdraai Spring, and might account for the smaller downstream PO_4 -P load. It is also possible, however, that immobilisation processes involving phosphorus and heavy metals such as aluminium and iron (see for example Johnson and Younger, 2006; Omoike and Vanloon, 1999; Strosnider and Nairn, 2010) might account for this. This possibility is explored in Sect. 11 in Chapter “Chemical Hydrogeology”. It is worth noting that even the most severely impacted karst groundwater source (Sect. 4 in Chapter “Chemical Hydrogeology”) returned an orthophosphate concentration of <0.2 mg P/L, i.e. below the analytical detection limit.

It is shown in Table 26 that the Bloubank Spruit and Crocodile River drainages together contributed median NO_3 -N and PO_4 -P loads of 133 and 3 t/a, respectively, to Hartbeespoort Dam in the period 1980 to 2014. By comparison, an appraisal of similar DWS data for this period shows that the Jukskei and Hennops river catchments contributed combined median NO_3 -N and PO_4 -P loads of 1287 and ~ 110 t/a, respectively.

Seen in context, therefore, the southern and south-western catchments represented by the (upper) Crocodile River and Bloubank Spruit systems respectively, contribute $<10\%$ to the median NO_3 -N load entering Hartbeespoort Dam. This contribution is substantially exceeded by those of the Jukskei River ($\sim 68\%$) and the Hennops River ($\sim 22\%$). The situation in regard to the PO_4 -P load is even more weighted towards the Jukskei and Hennops rivers, with the Crocodile

River and Bloubank Spruit systems delivering $< 3\%$ of the PO_4 -P load (Table 26). These results find support in an evaluation presented by Roux (2010) and Oelofse et al. (2012). They are also in agreement with an earlier finding by Harding et al. (2004), who report a total phosphorus (TP) load of ~ 166 t/a (within a range of 80 to 300 t/a) entering the dam, $>99\%$ of which is via the Crocodile River including the contributions of all its tributaries.

2.2 Subcatchment Scale

The information in Table 27 provides an estimate of the TDS load contributed by various sources in the Bloubank Spruit system compared to that leaving this system at station A2H049. The data are applicable to the prevailing conditions preceding the 2010 hydrological year since when, as has been shown, mine water discharges have substantially modified the water chemistry delivered by this drainage.

Table 27 shows that the historical TDS load at station A2H049 (8560 t/a) is within 3% of the sum (8827 t/a) of the contributions from the upstream sources represented by the Zwartkrans, Kromdraai and Plover’s Lake springs, the Blougat Spruit and groundwater resurgence in the Bloubank Spruit upstream of the Zwartkrans Spring. It has been shown that the Tweelopie and Blougat spruits represent the two most impacted contributing sources within the Bloubank Spruit system. The contribution of the Tweelopie Spruit is not explicitly accounted for in this estimate, because a significant proportion of the discharge in this drainage into the Riet Spruit is lost as allogenic recharge to the karst aquifer. This contribution is reflected in the groundwater resurgence upstream of the Zwartkrans Spring. In summary, the Blougat Spruit reflects a $\sim 27\%$ contribution to the load at station A2H049 compared to the $\sim 53\%$ of the combined spring-water sources. The contribution of groundwater resurgence accounts for the balance of 20%. As discussed in Sect. 1.2.6, however, the very wet 2010, 2011 and 2014 summer rainfall seasons (Sect. 2 in Chapter “Description of the Physical Environment”) precipitated a significant change in these

Table 27 Estimated TDS load contributed by various sources in the Bloubank Spruit system prior to the 2010 hydrological year

| Source (station #) | Description | TDS (mg/L) | Discharge (Mm ³ /a) | | TDS load (t/a) | |
|-------------------------------------|-------------------------|------------|--------------------------------|-------|----------------|-------|
| Blougat Spruit (188,048) | Treated sewage effluent | 502 | 4.75 | 23.00 | 2385 | 8 827 |
| Groundwater resurgence ¹ | Surface water | 665 | 2.63 | | 1749 | |
| Zwartkrans Sp. | Groundwater | 244 | 4.27 | | 1042 | |
| Plover’s Lake Sp. | Groundwater | 110 | 1.89 | | 208 | |
| Kromdraai Sp. | Groundwater | 364 | 9.46 | | 3443 | |
| Bloubank Spruit (A2H049) | Surface water | 444 | 22.70 | | 8560 | |

¹Refer Sect. 5.2.3 in Chapter “Physical Hydrology” for a comprehensive discussion of this component

Table 28 Statistical analysis of SO₄ and TDS loads in composite mine water entering the Tweelopie Spruit in the period January 2006 to September 2013

| Load variable /Analyte | Statistical parameter | | | | | | |
|------------------------|-----------------------|-------|-------|--------|--------|-------|---------|
| | n | 5%ile | Mean | Median | 95%ile | SD | CoV (%) |
| Sulfate (t/d) | 365 | 5.36 | 35.23 | 25.47 | 102.52 | 34.19 | 97 |
| TDS (t/d) | | 8.51 | 55.92 | 40.43 | 162.73 | 49.59 | 89 |

circumstances. Drainage-specific TDS loads that reflect the latter are discussed in more detail in the following subsections.

2.2.1 Tweelopie Spruit

A TDS load assessment for this drainage must be based on the blended raw mine water and treated/neutralised mine water components leaving the mine property (Fig. 13 in Chapter “Physical Hydrology”). The outflow from the Hippo Dam provides a measure of this variable with due cognisance of the following. The Hippo Dam data represents a poorer condition than that of station F11S12 located much closer to where the allogenic recharge of the karst aquifer occurs (Sect. 5.2.1 in Chapter “Physical Hydrology”).

Both the Hippo Dam and F11S12 stations suffer the drawback that their water quality record is not matched by a similarly abundant set of discharge data. The Hippo Dam station, however, benefits from its proximity to the end-of-pipe (EoP) stations where the mine water discharge (both raw and treated/neutralised) is gauged (Fig. 13 in Chapter “Physical Hydrology”). Accepting that evaporation and evapotranspiration losses do not significantly reduce the outflow from the dam compared to that entering the dam from the mine area, it is possible to derive a SO₄ load for the Tweelopie Spruit in its upper reaches below the mine area.

Although TDS is not a monitoring variable downstream of the mine area, a theoretical TDS load can be derived

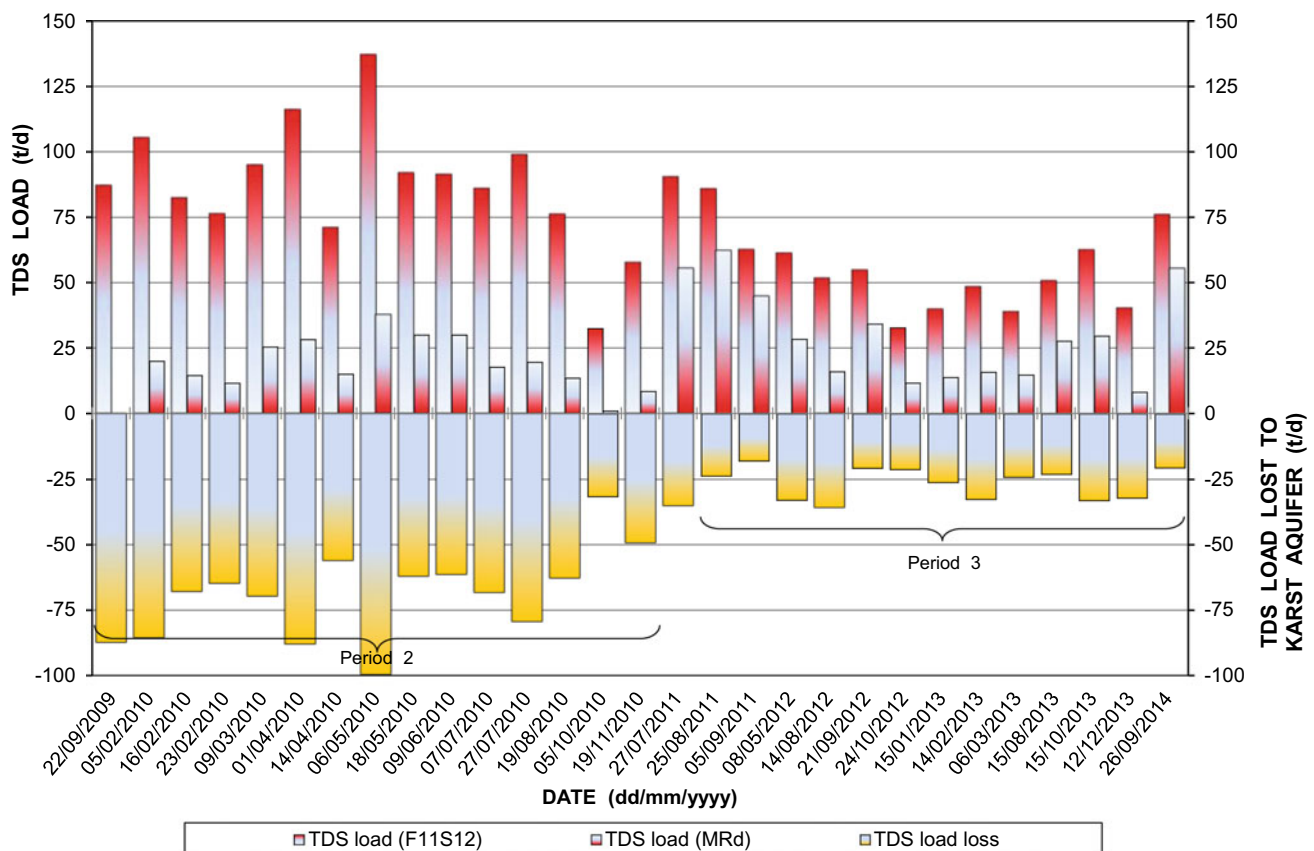


Fig. 48 Pattern and trend of TDS load losses in the lower reach of the Riet Spruit

from the empirical observation that SO_4 typically represents ~63% of the TDS concentration in mine water (Text Box 1). This ratio also applies at station F11S12. Salient statistics that describe this information are

presented in Table 28, and the relationships used to compile the record of SO_4 and TDS loads associated with composite mine water entering the Tweelopie Spruit illustrated in Fig. 47.

Table 29 Assessment of TDS load losses to the karst aquifer between stations F11S12 and MRd

| Date | Station F11S12 | | | | Station MRd | | | | Δ TDS Load (t/d) |
|------------|-------------------------|---------------------------|-------------|------------|-------------------------|-------------------------|-------------|------------|-------------------------|
| | SEC ¹ (mS/m) | TDS ⁽¹⁾ (mg/L) | Flow (ML/d) | Load (t/d) | SEC ¹ (mS/m) | TDS ¹ (mg/L) | Flow (ML/d) | Load (t/d) | |
| 22/09/2009 | 322 | 2479 | 14.9 | 36.9 | – | – | 0.0 | – | –36.9 |
| 05/02/2010 | 389 | 2997 | 35.2 | 105.5 | 358 | 2759 | 7.3 | 20.1 | –85.4 |
| 16/02/2010 | 339 | 2610 | 31.6 | 82.5 | 335 | 2581 | 5.7 | 14.7 | –67.8 |
| 23/02/2010 | 379 | 2918 | 26.2 | 76.5 | 383 | 2948 | 4.0 | 11.8 | –64.7 |
| 09/03/2010 | 379 | 2918 | 32.6 | 95.1 | 353 | 2720 | 9.4 | 25.6 | –69.5 |
| 01/04/2010 | 374 | 2878 | 40.4 | 116.3 | 358 | 2759 | 10.3 | 28.4 | –87.9 |
| 14/04/2010 | 358 | 2757 | 25.8 | 71.1 | 347 | 2672 | 5.7 | 15.2 | –55.9 |
| 06/05/2010 | 408 | 3142 | 43.7 | 137.3 | 420 | 3234 | 11.7 | 37.8 | –99.5 |
| 18/05/2010 | 335 | 2580 | 35.7 | 92.1 | 356 | 2741 | 11.0 | 30.2 | –61.9 |
| 09/06/2010 | 370 | 2849 | 32.1 | 91.5 | 373 | 2872 | 10.5 | 30.2 | –61.3 |
| 07/07/2010 | 374 | 2880 | 29.9 | 86.1 | 376 | 2895 | 6.2 | 17.9 | –68.2 |
| 27/07/2010 | 407 | 3134 | 31.6 | 99.0 | 395 | 3042 | 6.5 | 19.8 | –79.3 |
| 19/08/2010 | 384 | 2957 | 25.8 | 76.3 | 335 | 2580 | 5.3 | 13.7 | –62.6 |
| 05/10/2010 | 307 | 2364 | 13.8 | 32.6 | 383 | 2949 | 0.4 | 1.2 | –31.4 |
| 19/11/2010 | 338 | 2603 | 22.2 | 57.8 | 333 | 2564 | 3.4 | 8.7 | –49.1 |
| 27/07/2011 | 369 | 2841 | 31.9 | 90.6 | 373 | 2872 | 19.4 | 55.7 | –35.0 |
| 25/08/2011 | 389 | 2995 | 28.7 | 86.0 | 405 | 3119 | 20.0 | 62.4 | –23.6 |
| 05/09/2011 | 362 | 2787 | 22.5 | 62.7 | 367 | 2826 | 15.9 | 44.9 | –17.8 |
| 08/05/2012 | 372 | 2864 | 21.4 | 61.3 | 388 | 2988 | 9.6 | 28.7 | –32.9 |
| 14/08/2012 | 299 | 2302 | 22.5 | 51.8 | 309 | 2379 | 6.8 | 16.2 | –35.6 |
| 21/09/2012 | 290 | 2233 | 24.6 | 54.9 | 288 | 2218 | 15.5 | 34.4 | –20.6 |
| 24/10/2012 | 264 | 2033 | 16.2 | 32.9 | 270 | 2079 | 5.7 | 11.9 | –21.1 |
| 15/01/2013 | 282 | 2171 | 18.4 | 39.9 | 283 | 2179 | 6.4 | 13.9 | –26.0 |
| 14/02/2013 | 274 | 2110 | 23.0 | 48.5 | 277 | 2133 | 7.5 | 16.0 | –32.5 |
| 06/03/2013 | 244 | 1879 | 20.7 | 38.9 | 241 | 1856 | 8.0 | 14.8 | –24.0 |
| 15/08/2013 | 219 | 1686 | 30.1 | 50.7 | 219 | 1686 | 16.5 | 27.8 | –22.9 |
| 15/10/2013 | 275 | 2118 | 29.6 | 62.7 | 274 | 2110 | 14.1 | 29.8 | –32.9 |
| 12/12/2013 | 236 | 1817 | 22.2 | 40.3 | 231 | 1779 | 4.7 | 8.4 | –32.0 |
| 26/09/2014 | 238 | 1833 | 41.5 | 76.1 | 238 | 1833 | 30.3 | 55.5 | –20.5 |
| 30/07/2015 | | | | | | | | | |
| 04/12/2017 | | | | | | | | | |
| n | 29 | 29 | 29 | 29 | 28 | 28 | 29 | 28 | 29 |
| Minimum | 219 | 1686 | 13.8 | 32.6 | 219 | 1686 | 0.0 | 1.2 | –17.8 |
| Mean | 330 | 2543 | 27.4 | 70.8 | 331 | 2549 | 9.6 | 24.8 | –46.8 |
| Median | 339 | 2610 | 26.2 | 71.1 | 350 | 2696 | 7.5 | 20.0 | –35.6 |
| Maximum | 408 | 3142 | 43.7 | 137.3 | 420 | 3234 | 30.3 | 62.4 | –99.5 |
| SD | 57 | 438 | 7.7 | 26.6 | 58 | 444 | 6.5 | 15.3 | 23.8 |
| CoV (%) | 17 | 17 | 28 | 38 | 17 | 17 | 67 | 61 | –51 |

¹From Table 10

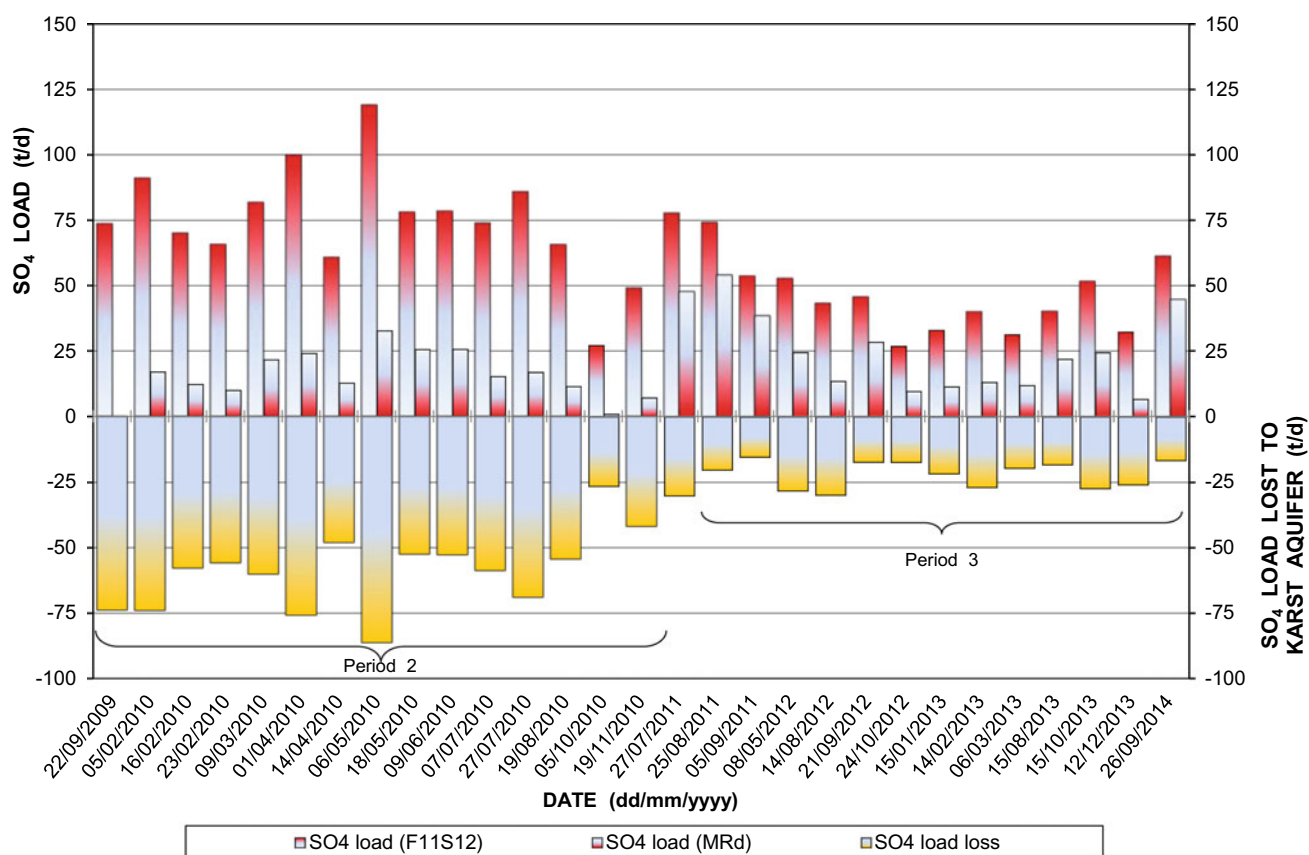


Fig. 49 Pattern and trend of SO_4 load losses in the lower reach of the Riet Spruit

The information presented in Fig. 47 clearly reveals the exceptionally high loads delivered to the Bloubaank Spruit system from the Western Basin throughout 2010. It also reveals that elevated loads prior to 2010 were common since early 2008. It is evident from Table 28 that median SO_4 and TDS loads of ~ 5 and ~ 40 t/d, respectively, have entered the Tweelopie Spruit from the mine area since January 2006. The 95%ile values of ~ 103 t SO_4 /d and ~ 163 t TDS/d provide an indication of the upper limits associated with these loads.

The SO_4 and TDS loads since mid-2011 are noticeably lower than the long-term median values (Fig. 47). Against the historic record, this reduction is a positive development for the receiving downstream environment, and once again demonstrates the value of the immediate and short-term mine water control and management interventions (Text Box 4 in Chapter “Physical Hydrology”).

2.2.2 Riet Spruit

The record of surface water losses between stations F11S12 and MRd documented in Table 18, together with the contemporary SEC measurements documented in Table 10, provide material for an assessment of the TDS load lost to the karst aquifer between these two stations. This assessment

is set out in Table 29 and illustrated in Fig. 48. A similar assessment for SO_4 , also based on data presented in Table 10, is set out in Table 30 and illustrated in Fig. 49.

The concern previously expressed for the quality of the allogenic recharge entering the karst aquifer (Sect. 1.2.6), is echoed in the median TDS and SO_4 load losses of ~ 36 and ~ 30 t/d, respectively (Table 29 and Table 30). In recognition of the two distinct periods¹⁰ identified in each of Figs. 48 and 49, however, it is warranted to explore the respective loads (and load losses) associated with each of these periods. The respective load losses are summarised in Table 31, the information reflecting the smaller losses associated with Period 3 compared to Period 2. These circumstances mimic the change in flow regime shown in Fig. 31 in Chapter “Physical Hydrology”, and also span the period of positive impact following the start of the immediate mine water intervention measures in mid-2012 (Text Box 4).

¹⁰ The periods are numbered ‘2’ and ‘3’ in accordance with those labeled in Fig. 35.

Table 30 Assessment of SO₄ load losses to the karst aquifer between stations F11S12 and MRd

| Date | Station F11S12 | | | | Station MRd | | | | Δ SO ₄ Load (t/d) |
|------------|-------------------------|------------------------|-------------|------------|-------------------------|-------------------------------------|-------------|------------|------------------------------|
| | SEC ¹ (mS/m) | SO ₄ (mg/L) | Flow (ML/d) | Load (t/d) | SEC ¹ (mS/m) | SO ₄ ¹ (mg/L) | Flow (ML/d) | Load (t/d) | |
| 22/09/2009 | 322 | 2092 | 14.9 | 73.6 | – | – | 0.0 | – | –73.7 |
| 05/02/2010 | 389 | 2574 | 35.2 | 90.6 | 358 | 2351 | 7.3 | 17.2 | –73.9 |
| 16/02/2010 | 339 | 2214 | 31.6 | 70.0 | 335 | 2186 | 5.7 | 12.5 | –57.9 |
| 23/02/2010 | 379 | 2502 | 26.2 | 65.6 | 383 | 2531 | 4.0 | 10.1 | –55.7 |
| 09/03/2010 | 379 | 2502 | 32.6 | 81.6 | 353 | 2315 | 9.4 | 21.8 | –60.0 |
| 01/04/2010 | 374 | 2466 | 40.4 | 99.6 | 358 | 2351 | 10.3 | 24.2 | –75.7 |
| 14/04/2010 | 358 | 2351 | 25.8 | 60.7 | 347 | 2272 | 5.7 | 13.0 | –47.9 |
| 06/05/2010 | 408 | 2711 | 43.7 | 118.4 | 420 | 2797 | 11.7 | 32.7 | –86.2 |
| 18/05/2010 | 335 | 2186 | 35.7 | 78.0 | 356 | 2337 | 11.0 | 25.7 | –52.4 |
| 09/06/2010 | 370 | 2437 | 32.1 | 78.2 | 373 | 2459 | 10.5 | 25.8 | –52.6 |
| 07/07/2010 | 374 | 2466 | 29.9 | 73.7 | 376 | 2480 | 6.2 | 15.4 | –58.6 |
| 27/07/2010 | 407 | 2703 | 31.6 | 85.4 | 395 | 2617 | 6.5 | 17.0 | –68.8 |
| 19/08/2010 | 384 | 2538 | 25.8 | 65.5 | 335 | 2186 | 5.3 | 11.6 | –54.2 |
| 05/10/2010 | 307 | 1984 | 13.8 | 27.4 | 383 | 2531 | 0.4 | 1.0 | –26.4 |
| 19/11/2010 | 338 | 2207 | 22.2 | 49.0 | 333 | 2171 | 3.4 | 7.4 | –41.8 |
| 27/07/2011 | 369 | 2430 | 31.9 | 77.5 | 373 | 2459 | 19.4 | 47.7 | –30.0 |
| 25/08/2011 | 389 | 2574 | 28.7 | 73.9 | 405 | 2689 | 20.0 | 53.8 | –20.1 |
| 05/09/2011 | 362 | 2380 | 22.5 | 53.5 | 367 | 2416 | 15.9 | 38.4 | –15.2 |
| 08/05/2012 | 372 | 2452 | 21.4 | 52.5 | 388 | 2567 | 9.6 | 24.6 | –28.1 |
| 14/08/2012 | 299 | 1927 | 22.5 | 43.4 | 309 | 1999 | 6.8 | 13.6 | –29.7 |
| 21/09/2012 | 290 | 1862 | 24.6 | 45.8 | 288 | 1848 | 15.5 | 28.6 | –17.1 |
| 24/10/2012 | 264 | 1675 | 16.2 | 27.1 | 270 | 1718 | 5.7 | 9.8 | –17.3 |
| 15/01/2013 | 282 | 1805 | 18.4 | 33.2 | 283 | 1812 | 6.4 | 11.6 | –21.5 |
| 14/02/2013 | 274 | 1747 | 23.0 | 40.2 | 277 | 1769 | 7.5 | 13.3 | –26.8 |
| 06/03/2013 | 244 | 1531 | 20.7 | 31.7 | 241 | 1510 | 8.0 | 12.1 | –19.5 |
| 15/08/2013 | 219 | 1352 | 30.1 | 40.7 | 219 | 1352 | 16.5 | 22.3 | –18.2 |
| 15/10/2013 | 275 | 1754 | 29.6 | 51.9 | 274 | 1747 | 14.1 | 24.6 | –27.2 |
| 12/12/2013 | 236 | 1474 | 22.2 | 32.7 | 231 | 1438 | 4.7 | 6.8 | –25.8 |
| 26/09/2014 | 238 | 1488 | 41.5 | 61.8 | 238 | 1488 | 30.3 | 45.1 | –16.5 |
| 30/07/2015 | | | | | | | | | |
| 04/12/2017 | | | | | | | | | |
| n | 29 | 29 | 29 | 29 | 28 | 28 | 29 | 28 | 29 |
| Minimum | 219 | 1352 | 13.8 | 27.1 | 219 | 1352 | 0.0 | 1.0 | –15.1 |
| Mean | 330 | 2151 | 27.4 | 60.0 | 331 | 2157 | 9.6 | 21.0 | –39.8 |
| Median | 339 | 2214 | 26.2 | 60.7 | 350 | 2294 | 7.5 | 17.1 | –29.8 |
| Maximum | 408 | 2711 | 43.7 | 118.4 | 420 | 2797 | 30.3 | 53.8 | –85.7 |
| SD | 57 | 409 | 7.7 | 23.4 | 58 | 414 | 6.5 | 13.0 | –20.8 |
| CoV (%) | 17 | 19 | 28 | 39 | 17 | 19 | 67 | 62 | –52 |

¹From Table 10.

2.2.3 Blougat Spruit

The pattern of TDS load associated with treated effluent released into the Blougat Spruit from the Percy Stewart WWTW (Fig. 50) resembles the discharge pattern

(Fig. 17 in Chapter “Physical Hydrology”, Sect. 3.2 in Chapter “Physical Hydrology”). The median value of 9.4 t/d is significantly less than the ~ 61 t/d delivered by the Tweelopie Spruit in the same period (Fig. 47). Although the

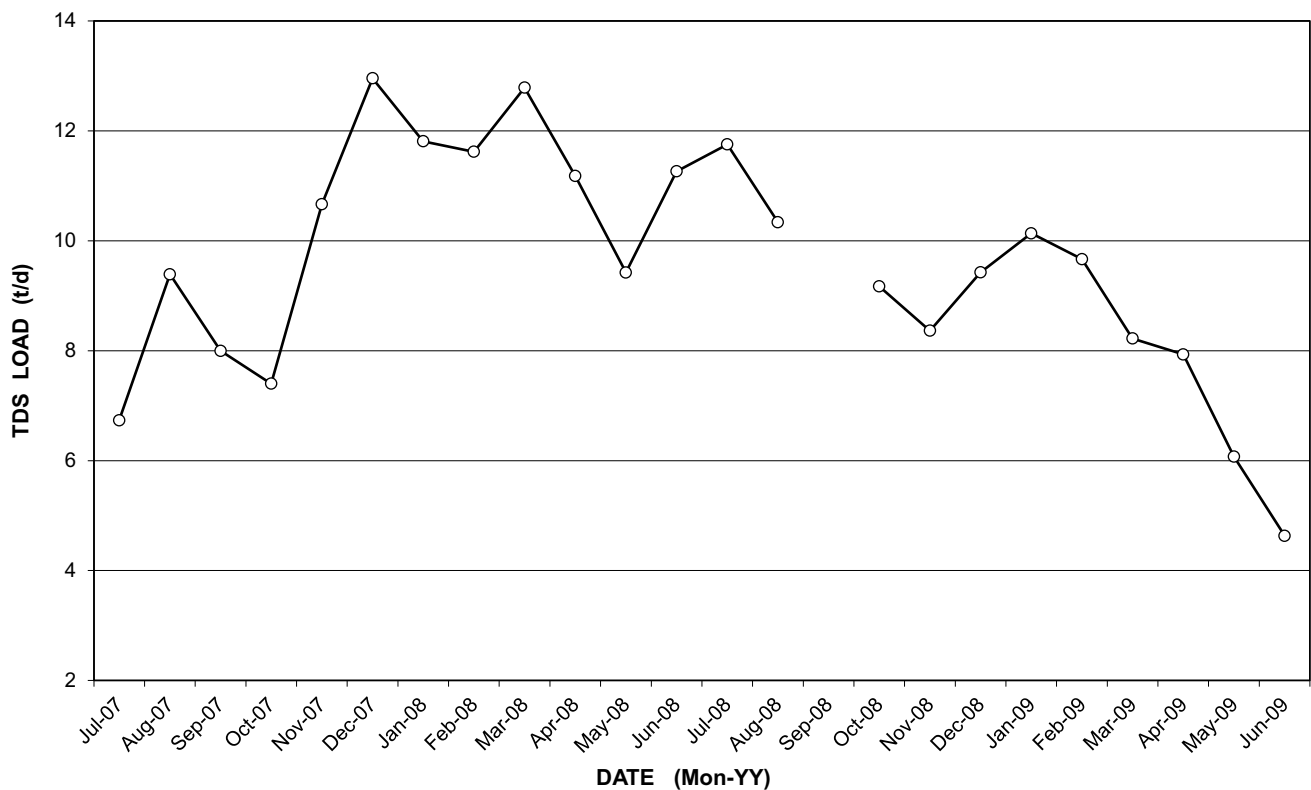


Fig. 50 Pattern and trend of recent TDS load associated with treated municipal effluent discharge to the Blougat Spruit

Table 31 Statistical analysis of TDS and SO₄ load losses in the lower reach of the Riet Spruit

| Statistical parameter | TDS load loss (t/d) | | SO ₄ load loss (t/d) | | % Loss | |
|-----------------------|---------------------|----------|---------------------------------|----------|----------|----------|
| | Period 2 | Period 3 | Period 2 | Period 3 | Period 2 | Period 3 |
| n | 15 | 14 | 15 | 14 | 15 | 14 |
| Minimum | 31.4 | 17.8 | 26.4 | 15.2 | 67 | 27 |
| Mean | 68.8 | 27.0 | 59.0 | 22.4 | 80 | 51 |
| Median | 67.8 | 25.0 | 57.6 | 20.8 | 80 | 53 |
| Maximum | 99.5 | 35.6 | 86.2 | 30.0 | 100 | 79 |
| SD | 17.2 | 6.3 | 15.0 | 5.3 | 9.2 | 17.3 |
| CoV | 25 | 23 | 25 | 23 | 11 | 34 |

DWS reports the effluent chemistry at station PSFE dating back to November 2002, the exclusion of TDS from this data set (Table 14) limits a longer term load assessment for this variable.

2.3 Regional Context and Synthesis

Given the regional importance of Hartbeespoort Dam as a storage reservoir (Sect. 1 in Chapter “Physical Hydrology”), an assessment of the TDS load must include that delivered

by all of the contributing main drainages (Table 32). The assessment spans the complete hydrological and hydrochemical record common to all six drainages. It provides a regional context for the TDS load delivered by the Bloubank Spruit system.

The assessment shows that although the Bloubank Spruit contributed the third highest TDS load to Hartbeespoort Dam (after the combined ~79% of the Jukskei and Hennops rivers) in the period 1980 to 2014, this represented only ~10% of the total load. It is shown in Sect. 3 in Chapter “Physical Hydrology”, however, that the quality of

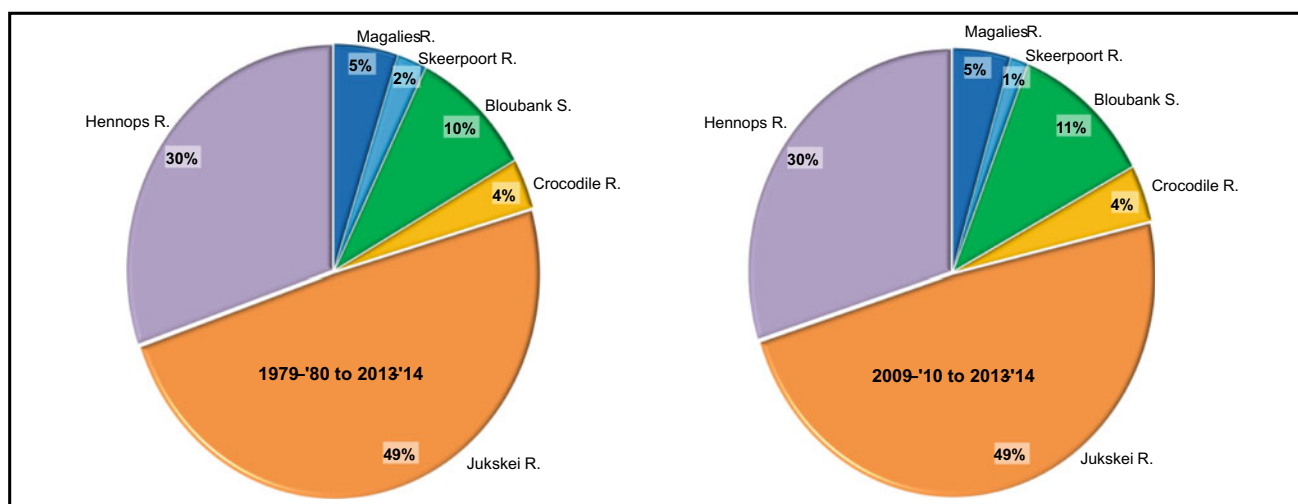


Fig. 51 Comparison of annual TDS load contributions of the main drainages in the Hartbeespoort Dam catchment in the long-term (left) ($\Sigma\text{TDS} = 104\,943\text{ t/a}$) and the recent past (right) ($\Sigma\text{TDS} = 240\,089\text{ t/a}$) (data from Tables 32 and 33)

Table 32 Median annual TDS load delivered by main drainages in the Hartbeespoort Dam catchment in the period of common hydrological and hydrochemical record (1980 to 2014)

| Drainage | Station | Median TDS (mg/L) | Median Discharge ⁽¹⁾ (Mm ³ /a) | Median TDS Load | | |
|------------------|---------|-------------------|--|-----------------|----------------|------------|
| | | | | t/d | t/a | % of Total |
| Magalies River | A2H013 | 336 | 15.689 | 14.4 | 5272 | 5.0 |
| Hennops River | A2H014 | 470 | 67.570 | 87.0 | 31 758 | 30.3 |
| Skeerpoort River | A2H034 | 218 | 11.083 | 6.6 | 2416 | 2.3 |
| Jukskei River | A2H044 | 420 | 122.845 | 141.4 | 51 595 | 49.2 |
| Bloubank Spruit | A2H049 | 446 | 22.701 | 27.7 | 10 125 | 9.6 |
| Crocodile River | A2H050 | 293 | 12.892 | 10.3 | 3777 | 3.6 |
| TOTAL | | | | 287.4 | 104 943 | 100 |

Table 33 Median annual TDS load delivered by main drainages in the Hartbeespoort Dam catchment in the hydrological and hydrochemical record period 2010 to 2014

| Drainage | Station | Median TDS (mg/L) | Median Discharge (Mm ³ /a) | Median TDS Load | | |
|------------------|---------|-------------------|---------------------------------------|-----------------|----------------|------------|
| | | | | t/d | t/a | % of Total |
| Magalies River | A2H013 | 323 | 34.026 | 30.1 | 10 990 | 4.6 |
| Hennops River | A2H014 | 458 | 156.672 | 196.6 | 71 756 | 29.9 |
| Skeerpoort River | A2H034 | 274 | 12.626 | 9.5 | 3460 | 1.4 |
| Jukskei River | A2H044 | 378 | 309.817 | 320.9 | 117 111 | 48.8 |
| Bloubank Spruit | A2H049 | 539 | 50.054 | 73.9 | 26 979 | 11.2 |
| Crocodile River | A2H050 | 291 | 33.655 | 26.8 | 9794 | 4.1 |
| TOTAL | | | | 657.8 | 240 089 | 100 |

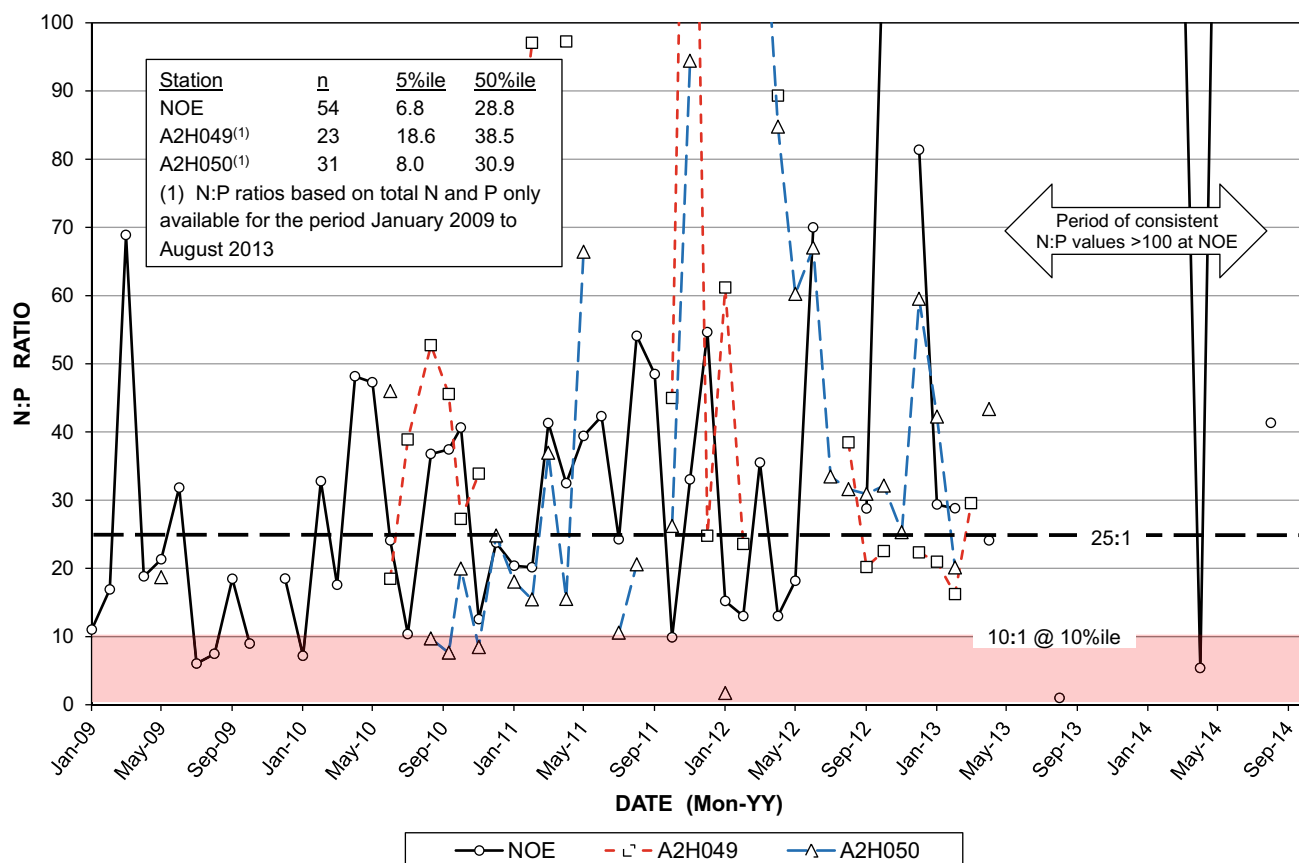


Fig. 52 Pattern and trend of the N:P ratio for Bloubank Spruit water at the NOE and station A2H049 and for Crocodile River water at station A2H050 in the period January 2009 to September 2014 (note cut-off at 100:1 to magnify graphs at lower ratio values)

Table 34 Comparison of the long-term (1980 to 2014) median TDS concentrations with those for the recent (2010 to 2014) hydrological years for the regional drainages

| Drainage | Station | Long-term Median TDS (mg/L) | Recent Median TDS (mg/L) | Change in TDS | |
|------------------|---------|-----------------------------|--------------------------|---------------|----------|
| | | | | mg/L | % Change |
| Magalies River | A2H013 | 336 | 323 | −13 | −3.9 |
| Hennops River | A2H014 | 470 | 458 | −12 | −2.6 |
| Skeerpoort River | A2H034 | 218 | 274 | 56 | 25.7 |
| Jukskei River | A2H044 | 420 | 378 | −42 | −10.0 |
| Bloubank Spruit | A2H049 | 446 | 539 | 93 | 20.9 |
| Crocodile River | A2H050 | 293 | 291 | −2 | −0.7 |

surface water discharged by the Bloubank Spruit deteriorated since the 2008–'09 hydrological year, and especially so in the 2010, 2011 and 2014 hydrological years (Fig. 39). To examine the relative impact of this change in both a regional and historical context, a similar assessment as above but spanning only the 2010 to 2014 period is presented in Table 33.

This assessment shows an overall increase in total TDS load of ~129% in the more recent period. The contribution of the Bloubank Spruit system to this increase is negligible,

increasing from ~10% to only ~11% at the cost of the Skeerpoort River. As in the long-term, the Jukskei and Hennops rivers again share the bulk (~79%) of the recent total TDS load also in similar proportions, viz. ~3:2, as in the long-term. These circumstances are illustrated and compared in Fig. 51.

Closer examination of the data presented in Tables 32 and 33 indicates that the changes in TDS concentration between the two periods of analysis are comparatively small (Table 34). In four instances (the Magalies, Hennops,

Table 35 Comparison of the long-term (1980 to 2014) median discharges with those for the recent (2010 to 2014) hydrological years for the regional drainages

| Drainage | Station | Long-term median discharge (Mm ³) | Recent median discharge (Mm ³) | Change in discharge | |
|------------------|---------|---|--|---------------------|----------|
| | | | | Mm ³ | % Change |
| Magalies River | A2H013 | 15.689 | 34.026 | 18.337 | 117 |
| Hennops River | A2H014 | 67.570 | 156.672 | 89.102 | 132 |
| Skeerpoort River | A2H034 | 11.083 | 12.626 | 1.543 | 14 |
| Jukskei River | A2H044 | 122.845 | 309.817 | 186.972 | 152 |
| Bloubank Spruit | A2H049 | 22.701 | 50.054 | 27.353 | 120 |
| Crocodile River | A2H050 | 12.892 | 33.655 | 20.763 | 161 |

Jukskei and Crocodile rivers), the TDS levels reduced. This is attributed to dilution by greater volumes of ‘fresh’ surface water runoff. Surprisingly, the pristine Skeerpoort River reflects a greater increase (~26%) than the Bloubank Spruit (~21%). This is partly attributed to an increase in CaCO₃ delivered by the perennial karst springs that feed the Skeerpoort River¹¹ in the median amount of ~9.5 Mm³/a (Sect. 2 in Chapter “Physical Hydrology”).

Significantly greater changes, without exception increases, are reflected in the comparison of discharges (Table 35). The Crocodile River leads in this regard with 161%. The Bloubank Spruit reflects the third lowest increase (120%).

Further analysis of the TDS load delivered to Hartbeespoort Dam in the 2010 to 2014 period compared to the long-term median load, is summarised in Table 36. This indicates that the Bloubank Spruit delivered the second lowest percentage increase (69%) after the Skeerpoort River (44%). The increase in the other drainages exceeded 100%, headed by the Crocodile River with 160%.

The Jukskei and Hennops rivers share the 2nd greatest percentage increase of ~127%. The present mean discharge of 380 ML/d (~139 Mm³/a) of the 450 ML/d (~164 Mm³/a) capacity Northern WWTW represents ~45% of the median annual discharge (~310 Mm³) of the Jukskei River (Table 33). A contribution of this magnitude provides a quite plausible explanation for the relative ‘insensitivity’ of the Jukskei River water quality to the higher natural discharges, compared to that experienced by the other drainages (with the exception of the Skeerpoort River) in the Hartbeespoort Dam catchment in the 2010 to 2014 period. As might be expected, the spring flow dominated Skeerpoort River also exhibits an ‘insensitivity’ to the contemporary higher discharges, the increase in TDS load amounting to 44% (Table 36).

¹¹ The median total alkalinity concentration at stations A2H033 and A2H034 increased from 190 to 202 mg CaCO₃/L, and from 158 to 167 mg CaCO₃/L respectively, in the two periods of analysis.

3 Pollution Indicators and Pollutants

3.1 Sulfate-to-Chloride Ratio

A further perspective on surface water quality is provided by the SO₄:Cl ratio. This ratio (based on milliequivalent values) is an indicator of potential mining and/or industrial impact on water quality. Its median value for the near-pristine Skeerpoort River water is ~ 1.1:1, with a 95%ile value of 3.5:1 (Table 37). Against this local ‘natural’ benchmark, the median ratio value of ~45–48:1 associated with raw mine water and slightly ‘better’ value of ~ 28:1 associated with surface water discharge in the Tweelopie Spruit at the downstream station F11S12, provides further unequivocal proof of a mine water impact. Encouragingly, the median values further downstream and elsewhere in the Bloubank Spruit system are only marginally greater than that for the Skeerpoort River. This reflects the comparatively unimpacted inorganic chemistry of the surface water in these drainages.

The Crocodile River reflects a median SO₄:Cl value of 0.6:1, indicating the dominance of Cl over SO₄ in this surface water. This is most reasonably attributable to the influence of treated effluent discharge from the Driefontein WWTW (Sect. 1.3).

3.2 Nitrate-to-Phosphorus Ratio

Any assessment of the impact of inorganic nitrogen concentrations should be coupled to an evaluation of the inorganic nitrogen to inorganic phosphorus ratio (DWAF 1996a). This also applies to inorganic phosphorus concentrations. The N:P ratio for unimpacted (oligotrophic) systems typically is >25:1, reducing to <10:1 for impacted (eutrophic or hypertrophic) systems. The median N:P ratio values for selected drainages in the study area for various timeframes are presented in Table 38. The information

Table 36 Comparison of the long-term (1980 to 2014) median TDS load delivered to Hartbeespoort Dam with the median TDS load delivered in the 2010 to 2014 hydrological years

| Drainage | Station | Long-term median TDS Load (t/d) | Recent median TDS Load (t/d) | Increase in TDS load | |
|--------------------|---------|---------------------------------|------------------------------|----------------------|------------|
| | | | | t/d | % Increase |
| Magalies River | A2H013 | 14.4 | 30.1 | 15.7 | 109 |
| Hennops River | A2H014 | 87.0 | 196.6 | 109.6 | 126 |
| Skeerpoort River | A2H034 | 6.6 | 9.5 | 2.9 | 44 |
| Jukskei River | A2H044 | 141.4 | 320.9 | 179.5 | 127 |
| Bloubank Spruit | A2H049 | 27.7 | 74.6 | 46.9 | 69 |
| Crocodile River | A2H050 | 10.3 | 26.8 | 16.5 | 160 |
| COMPOSITE ANALYSIS | | 287.4 | 658.5 | 371.1 | 129 |

Table 37 Statistical characterisation of the $\text{SO}_4\text{:Cl}$ ratio for drainages in the study area for the full available record up to September 2014 and the common record period since June 2004

| Drainage | Station | Statistical Parameter | | | | | | |
|--------------------|--------------------------|-----------------------|-------|------|--------|--------|------|---------|
| | | n | 5%ile | Mean | Median | 95%ile | SD | CoV (%) |
| Skeerpoort River | A2H034 | 1447 ⁽¹⁾ | 0.3 | 1.5 | 1.1 | 3.5 | 1.9 | 129 |
| | | 247 | 0.4 | 1.8 | 1.2 | 3.8 | 1.9 | 105 |
| Tweelapie Spruit | BRI ⁽²⁾ | 88 | 19.2 | 47.1 | 47.4 | 78.3 | 17.5 | 37 |
| | #17 Winze ⁽²⁾ | 88 | 17.5 | 45.0 | 44.5 | 71.2 | 17.0 | 38 |
| | #18 Winze ⁽²⁾ | 88 | 20.5 | 50.8 | 48.2 | 87.3 | 19.6 | 39 |
| | F11S12 ⁽³⁾ | 138 | 14.2 | 29.0 | 28.3 | 48.0 | 13.5 | 47 |
| Blougat Spruit | 188,048 ⁽⁴⁾ | 42 | 1.1 | 2.1 | 1.9 | 4.4 | 1.1 | 53 |
| Tweefontein Spruit | F14S15 ⁽⁴⁾ | 42 | 1.4 | 1.7 | 1.7 | 2.3 | 0.3 | 19 |
| Bloubank Spruit | A2H049 | 889 ⁽⁵⁾ | 1.5 | 2.1 | 2.0 | 3.0 | 0.8 | 40 |
| | | 209 | 1.4 | 2.5 | 1.8 | 6.6 | 1.6 | 64 |
| Crocodile River | A2H050 | 833 ⁽⁵⁾ | 0.3 | 0.7 | 0.6 | 1.5 | 0.4 | 51 |
| | | 238 | 0.4 | 0.6 | 0.6 | 0.8 | 0.1 | 22 |

¹Since January 1976²Raw mine water since December 2012³Since November 2003⁴Record period terminates in September 2008 as per Table 11 (188048) and Table 18 (F14S15)⁵Since May 1979

presented indicates the measure of impact associated with the Percy Stewart WWTW effluent discharge into the Blougat Spruit compared to the Bloubank Spruit and Crocodile River.

Given that Zohary et al. (1988) already reported an N:P ratio of $\leq 7:1$ for Hartbeespoort Dam more than two decades ago, the longer records of stations A2H049 (Bloubank Spruit) and A2H050 (Crocodile River) prompt an inspection of the variability of this parameter over time. This shows a smaller variability when only the last ten years of record is considered, whilst still reflecting a largely unimpacted character. Accepting that much of the nutrient loads in the Bloubank Spruit and Crocodile River derive from the Percy

Stewart and Driefontein WWTWs, respectively, then closer scrutiny of the data in Table 38 reveals the following circumstances:

- the smaller mean and median $\text{NO}_3\text{-N:PO}_4\text{-P}$ ratio values for the last ten years compared to the long-term values suggest that the performance of the Percy Stewart WWTW has deteriorated; and
- the greater mean and median $\text{NO}_3\text{-N:PO}_4\text{-P}$ ratio values for the last ten years compared to the long-term values suggest that the performance of the Driefontein WWTW has improved.

Table 38 Statistical values of the N:P ratio for drainages in the study area for various periods

| Drainage (station) | Period | Statistical Parameter | | | | | | |
|-------------------------------------|-----------------|-----------------------|-------------|-------------|-------------|-------------|--------------|------------|
| | | n | 5%ile | Mean | Median | 95%ile | SD | CoV (%) |
| Blougat Spruit (Percy Stewart WWTW) | 07/2007–06/2009 | 24 | 3.8 | 9.0 | 7.5 | 18.4 | 5.2 | 58 |
| Blougat Spruit (188048) | 06/2004–03/2008 | 41 | 0.03 | 6.3 | 3.3 | 26.0 | 9.6 | 152 |
| Bloubank Spruit (A2H049) | 06/2004–03/2008 | 99 | 11.1 | 32.6 | 28.7 | 68.2 | 19.1 | 59 |
| | | 46 | <i>11.1</i> | <i>24.5</i> | <i>22.1</i> | <i>45.7</i> | <i>11.12</i> | 45 |
| | 05/1979–09/2014 | 920 | 16.0 | 219.7 | 83.5 | 820.7 | 477.6 | 227 |
| | | 76 | <i>11.6</i> | <i>39.1</i> | <i>25.0</i> | <i>97.1</i> | <i>49.9</i> | <i>128</i> |
| | 10/2003–09/2014 | 199 | 11.6 | 140.4 | 32.7 | 876.7 | 325.4 | 232 |
| | | 75 | <i>11.6</i> | <i>37.6</i> | <i>24.8</i> | <i>91.6</i> | <i>48.6</i> | <i>129</i> |
| Crocodile River (A2H050) | 06/2004–03/2008 | 99 | 3.7 | 27.3 | 25.9 | 57.8 | 18.2 | 67 |
| | | 47 | 4.1 | <i>17.3</i> | <i>17.4</i> | <i>31.9</i> | 9.7 | 56 |
| | 05/1979–09/2014 | 795 | 0.3 | 42.3 | 18.3 | 162.2 | 92.7 | 219 |
| | | 89 | 4.1 | 25.0 | 20.1 | 63.9 | 20.5 | 82 |
| | 10/2003–09/2014 | 219 | 5.3 | 83.3 | 38.1 | 335.1 | 148.9 | 179 |
| | | 89 | 4.1 | 25.0 | 20.1 | 63.9 | 20.5 | 82 |

Notes Bold text indicates ratio values < 10:1 indicative of eutrophic or hypertrophic systems

Italicised text (highlighted rows) indicates N:P ratio derived from total N and P values, compared to NO₃–N and PO₄–P derived values reported in preceding row

The above circumstances provide further substance to the results reported in the ‘Green Drop’ report (DWA, 2011) in regard to the Percy Stewart WWTW (Sect. 1.2.4). By comparison, the Driefontein WWTW recorded a 100% score for the wastewater quality compliance performance area (DWA 2011).

Further indictment of the poor performance of the Percy Stewart WWTW is provided by the following observations. Station A2H049 is located much further (~22 km) downstream from the Percy Stewart WWTW than station A2H050 is (~2 km) from the Driefontein WWTW. In addition, the quality at station A2H049 benefits from the significant volumes of good quality karst groundwater contributed to the river (Sect. 4.16 in Chapter 7), which benefit is absent in the case of A2H050. Finally, the discharge of the Percy Stewart WWTW is significantly less than that of the Driefontein facility. These circumstances suggest that the water quality at station A2H049 should be considerably less sensitive to poor quality municipal wastewater discharges than that at station A2H050.

A concern in regard to PO₄–P is the concentrations observed at several surface water sampling stations in the Bloubank Spruit system (see for example Table 20). The values of 0.5 mg P/L and 6 mg N/L observed at station BB@PL (Table 20) return a N:P ratio of 12:1. This compares unfavourably with the median value of 41:1 observed for the shorter record at station A2H049 (Table 38). It also explains the degree of eutrophication observed in the defunct trout dams at the Nirox Estate at Kromdraai.

The routine water quality monitoring carried out at the Nedbank Olwazini Estate (NOE) provides an additional source of NO₃–N and PO₄–P data. This data set has already been interrogated in regard to its nutrient and bacterial content (Table 22), which returns a median N:P ratio value of ~29:1 and a 5%ile value of ~7:1 in the period January 2009 to September 2014. The pattern and trend described by the N:P ratio at the NOE and stations A2H049 and A2H050 in this period is compared in Fig. 52. This reveals a generally acceptable N:P ratio, where the limit of 10:1 below which eutrophic or hypertrophic systems are identified is exceeded in 47 of the 54 values (Table 22 and text box Fig. 52).

3.3 Trace/Heavy Metals and Metalloids

The presence of trace/heavy metal(loid)s provides a further indication of especially mine water pollution. These analytes therefore represent a concern for their impact on the quality of surface water in the Bloubank Spruit system. The metals iron (Fe) and manganese (Mn) arguably receive most attention,¹² the former for its very high concentrations in raw mine water and the latter for its persistence in solution at higher pH levels. In addition to these analytes, this section

¹² Refer to Tables 2, 3, 4, 7, 9, 11, 12, 18, 19, 21 and 23.

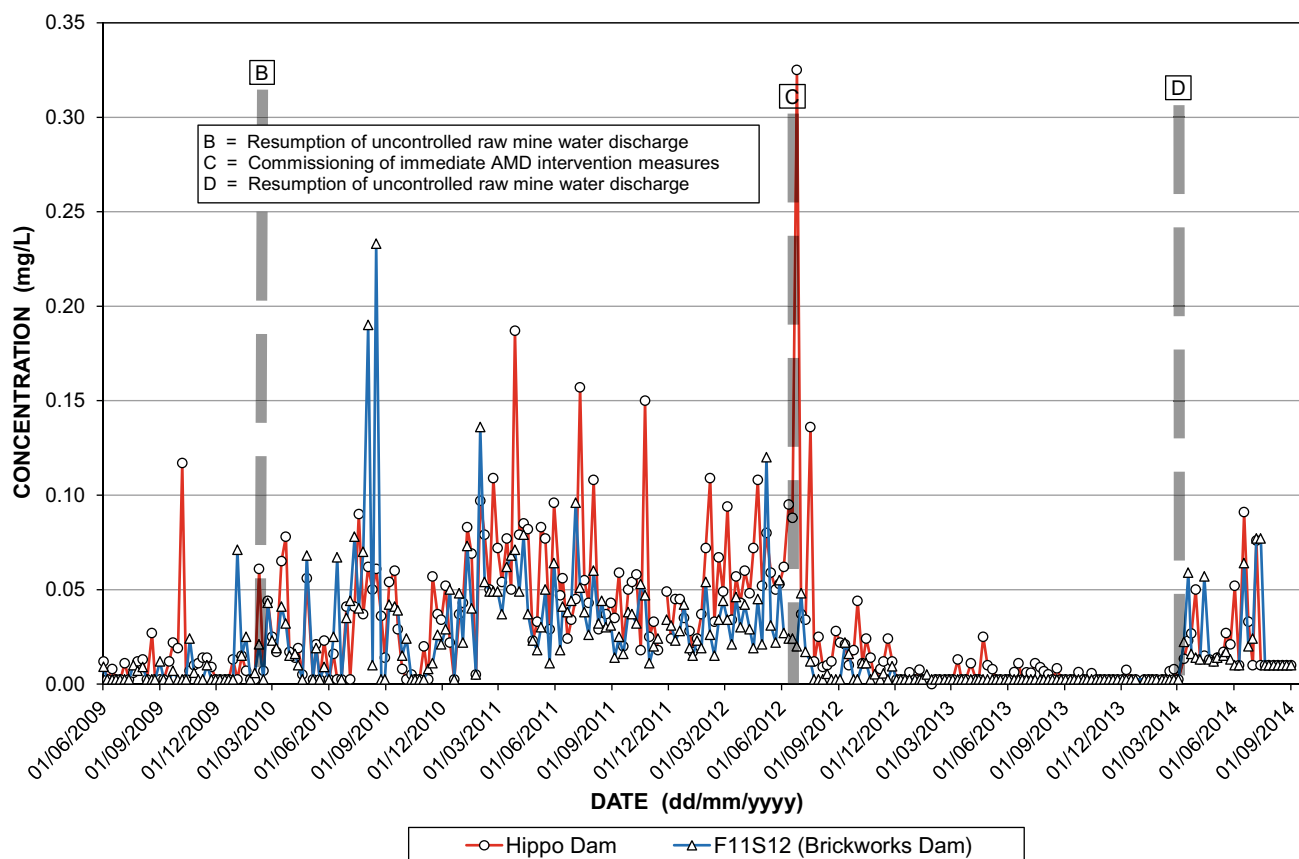


Fig. 53 Pattern and trend of U_T in Tweelopiespruit surface water

reports on a much broader suite of analytes that are not often afforded attention under circumstances such as occur in the study area.

3.3.1 Iron (Fe) and Manganese (Mn)

A surface water sample collected in May 2010 near Sterkfontein Cave returned Fe and Mn values of 0.91 and 0.67 mg/L, respectively (station BB@M, Table 20). A sample collected at Plover's Lake further downstream on the same day (station BB@PL, Table 20) returned Fe and Mn values of 0.36 and 0.29 mg/L, respectively. Although both sets of values significantly exceed the long-term median values of 0.014 and 0.003 mg/L determined for these analytes at station A2H049 (Table 19), the significant differences between the 'upstream' and 'downstream' samples caution against a direct comparison with the long-term values at A2H049. A more appropriate comparison is considered to be with the values reported for mine water discharged from the mine area (Table 7) for which median values of 1.2 mg Fe/L and 10.5 mg Mn/L characterise these analytes in the period B–C (February 2010 to July 2012).

It has been shown that the period February 2010 to July 2012 experienced the most serious impact from mine water

discharges (Sects. 3.1 in Chapter "Physical Hydrology" and 1.2 in Chapter 6). It is therefore appropriate to interrogate the contemporary A2H049 water chemistry record for at least Fe and Mn for comparison with these analyte values in the composite ¹³mine water discharge in this timeframe. This comparison is presented in Table 39. The reduction in concentrations at A2H049 even in the period of most likely greatest impact is self-evident, questioning reports (Allison et al., 2011) that the AMD impact on the quality of surface water entering Hartbeespoort Dam has compromised the quality of water impounded in this ~190 Mm³ reservoir.

3.3.2 Mercury (Hg)

Mercury (Hg), a heavy metal known for its propensity for bioaccumulation in the food chain (particularly predatory fish species) and impact on human health (Holmes et al. 2009), reveals equivocal levels in mine water in the study area, and generally very low levels (<0.002 mg/L) in surface water and groundwater sources. SANS (2015a) sets a

¹³ It is shown in Sect. 1.2.2 that the raw mine water component greatly exceeded the treated/neutralised mine water component for much of this period (Fig. 16 in "Physical Hydrology").

Table 39 Statistical comparison of Fe and Mn concentrations in composite mine water discharge with Bloubank Spruit surface water at A2H049 in the period February 2010 to July 2012

| Statistical parameter | Analyte and source | | | |
|---------------------------|--------------------|--------|-------------|--------------|
| | Fe | | Mn | |
| | Hippo Dam | A2H049 | Hippo Dam | A2H049 |
| n | 129 | 33 | 129 | 33 |
| 5%ile (mg/L) | 6.5 | 0.001 | 22.2 | 0.001 |
| Mean (mg/L) | 168.4 | 0.020 | 62.7 | 0.292 |
| Median (mg/L) | 163.0 | 0.013 | 65.0 | 0.003 |
| 95%ile (mg/L) | 365.2 | 0.086 | 95.0 | 1.692 |
| SD (mg/L) | 116.2 | 0.025 | 23.5 | 1.136 |
| CoV (%) | 69 | 1 | 38 | 4 |
| SANS (2015a) ¹ | ≤ 2.0 | | ≤ 0.5 | |

¹Standard health-related limit for consumption of 2 L/d over 70 years by a 60 kg person

Bold text denotes value exceeds standard limit as described in note 1

standard health-related limit of ≤ 0.006 mg/L for this element, and the USAs Safe Drinking Water Act (SDWA) a maximum contaminant level (MCL) of 0.002 mg/L.

Although a single mine water sample reported by Hobbs and Cobbing (2007) returned a value below a detection limit of 0.0001 mg/L (Table 40), a larger population ($n = 6$) reported by Hobbs et al. (2010) returned values in the range 0.398 mg/L (for treated/neutralised mine water) to 3.61 mg/L (for raw mine water sourced from mine shafts). Actively decanting shafts such as the Black Reef Incline and #17 and #18 winzes exhibited the highest levels (2.07 to 3.61 mg/L), compared to #8 Shaft mine water (0.634 mg/L). By comparison, Hg levels in surface water typically do not exceed the strictest analytical detection limit of 0.001 mg/L (Table 40), and are therefore not considered a threat in this resource.

The higher levels in raw mine water will only become a concern if circumstances similar to those experienced in the period February 2010 to July 2012 are manifested (Sect. 3.1 in Chapter “Physical Hydrology”, Figs. 13 and 16). More analyses, and especially of the composite well-mixed raw and treated/neutralised mine water discharge, would be required to better inform such concern.

3.3.3 Aluminium (Al)

Aluminium (Al) is set a standard health-related limit of ≤ 0.3 mg/L (SANS 2015a). Its threat to human health especially via the consumption of water remains largely unknown, as is borne out by its SANS (2015a) association with an operational risk rather than a chronic health risk. The level in treated/neutralised mine water since November 2012¹⁴ (to September 2013) exhibits a median value of 0.009 mg/L and a 95%ile value of 0.12 mg/L (Table 7).

¹⁴ The detection limit for Al was lowered from 1 mg/L to 0.001 mg/L in December 2012 (Table 5).

These values are similar to the 0.007 and 0.105 mg/L ($n = 40$) for the mixed raw and treated/neutralised mine water leaving the Hippo Dam. The level in raw mine water since November 2012 reflects a median value of 0.1 mg/L and a 95%ile value of 0.88 mg/L ($n = 41$). It has also been recorded on two occasions, however, that the Al concentration in raw mine water returned conflicting values of 3.9 mg/L (in May 2012) and <0.01 mg/L (in March 2013).

By comparison, the level in surface water at the lower end of the Tweelopie Spruit (Brickworks Dam/F11S12) since November 2012 reflects median and 95%ile values of 0.007 and 0.03 mg/L, respectively. The activity of aluminium in water is strongly dependent on pH (Appelo and Postma, 2009). It is least soluble at a pH in the range 6 to 7, and increasingly soluble at pH <4.5 and >7 . The pH of the surface water at the Brickworks Dam/F11S12 since November 2012 ranged from 6.2 (5%ile value) to 7.4 (95%ile value) with a median of 7.2, i.e. favouring aluminium insolubility circumstances. Unfortunately a similar evaluation for the pre-December 2012 period, and in particular the period February 2010 to July 2012 when pH values ranged from 2.7 (5%ile) to 3.9 (95%ile) at the Brickworks Dam/F11S12 (Table 4), is thwarted by the paucity of data due to non-exceedance of the coarse detection limit of 1 mg/L.

Nevertheless, the higher levels in raw mine water might only become a concern if circumstances similar to those experienced in the period February 2010 to July 2012 are manifested (Sect. 3.1 in Chapter “Physical Hydrology”, Figs. 13 and 16). More analyses, and especially of the composite well-mixed raw and treated/neutralised mine water discharge, would be required to better inform such concern.

3.3.4 Arsenic (As)

The metalloid arsenic (As), another element of concern for human health, is set a standard health-related limit of

Table 40 Summary of Hg values for mine and surface water sources in the study area

| Detection limit (DL) | Mine Water ¹ | | Surface water | | Σn | Data source |
|----------------------|-------------------------|-----|---------------|-----|------------|--------------------------|
| | n | >DL | n | >DL | | |
| 0.0001 mg/L | 1 | 0 | 1 | 0 | 2 | Hobbs and Cobbing (2007) |
| Value(s) > DL | – | – | – | – | – | – |
| 0.002 mg/L | 6 | 6 | 2 | 0 | 8 | Hobbs et al. (2010) |
| Value(s) > DL | 0.398 to 3.61 mg/L | – | – | – | – | – |
| 0.001 mg/L | 3 | 0 | 17 | 0 | 20 | This study |
| Value(s) > DL | – | – | – | – | – | – |

¹Comprises both raw and treated/neutralised mine water

≤ 0.01 mg/L (SANS, 2015a). Hobbs and Cobbing (2007) report values of 0.159 and 0.214 mg/L for the actively decanting Black Reef Incline and #18 Winze, respectively. In all but one of the seven surface water sources sampled (including a treated/neutralised mine water sample), the detection limit of 0.002 mg/L was not exceeded. This pattern has subsequently been replicated on four further sampling campaigns targeting surface water in the Tweelopie, Riet, Blougat and Bloubank spruits.

The higher levels in raw mine water will only become a concern if circumstances similar to those experienced in the period February 2010 to July 2012 are manifested (Sect. 3.1 in Chapter “Physical Hydrology”, Figs. 13 and 16). More analyses, and especially of the composite well-mixed raw and treated/neutralised mine water discharge, would be required to better inform such concern.

3.3.5 Other Metals

The activity of other metals/metalloids in Tweelopie Spruit surface water is reported in Table 41. Of the listed analytes, only nickel (Ni) poses a threat on the basis of its concentration even at the 5%ile level. The threat from exposure to Ni or Ni compounds to human health is primarily via dermal (skin) and respiratory (inhalation) exposure (ATSDR 2011; RAIS 1995).

The results for cadmium (Cd) and lead (Pb) are not afforded much significance because of the very small number of analyses that exceed the detection limit(s), militating against meaningful interpretation. What is considered significant is that >90% of the analyses do not exceed the detection limit(s).

The routine water quality monitoring carried out at NOE also provides an additional source of data for the trace/heavy

Table 41 Summary of trace/heavy metal(loid) concentrations in Tweelopie Spruit water at the Hippo Dam and Brickworks Dam stations in the period December 2012 to September 2014

| Statistical parameter | Analyte and source | | | | | | | | | | | |
|---------------------------|--------------------|-----------------|-----------------|-----------------|-----------------|-----------------|-----------------|-----------------|-----------------|-----------------|-----------------|-----------------|
| | B | | Cd | | Cu | | Ni | | Pb | | Zn | |
| | HD ¹ | BD ² | HD ¹ | BD ² | HD ¹ | BD ² | HD ¹ | BD ² | HD ¹ | BD ² | HD ¹ | BD ² |
| n | 88 | 88 | 88 | 88 | 88 | 88 | 88 | 4188 | 88 | 88 | 88 | 88 |
| $n > DL^3$ | 88 | 88 | 6 | 5 | 76 | 75 | 88 | 87 | 24 | 26 | 86 | 88 |
| 5%ile (mg/L) | 0.20 | 0.20 | 0.001 | 0.001 | 0.001 | 0.001 | 0.04 | 0.10 | 0.001 | 0.001 | 0.01 | 0.02 |
| Mean (mg/L) | 0.56 | 0.49 | 0.031 | 0.002 | 0.006 | 0.005 | 0.17 | 0.16 | 0.011 | 0.006 | 0.07 | 0.09 |
| Median (mg/L) | 0.40 | 0.30 | 0.001 | 0.001 | 0.003 | 0.002 | 0.10 | 0.10 | 0.008 | 0.005 | 0.03 | 0.10 |
| 95%ile (mg/L) | 1.38 | 1.31 | 0.130 | 0.006 | 0.019 | 0.021 | 0.40 | 0.34 | 0.046 | 0.010 | 0.17 | 0.18 |
| SD (mg/L) | 0.59 | 0.52 | 0.068 | 0.003 | 0.007 | 0.008 | 0.13 | 0.11 | 0.014 | 0.003 | 0.07 | 0.05 |
| CoV (%) | 107 | 107 | 222 | 143 | 125 | 138 | 75 | 73 | 134 | 60 | 104 | 58 |
| SANS (2015a) ⁴ | n.s | | ≤ 0.003 | | ≤ 2.0 | | ≤ 0.07 | | ≤ 0.01 | | ≤ 5.0 | |

¹Hippo Dam

²Brickworks Dam (station F11S12)

³See Table 5 for analyte detection limits

⁴Standard health-related limit for consumption of 2 L/d over 70 years by a 60 kg person

Bold text denotes value exceeds standard limit as described in note 4

Table 42 Summary of trace/heavy metal concentrations in Bloubank Spruit water at the NOE in the period May 2011 to December 2014

| Statistical parameter | Analyte | | | | | | | | |
|-----------------------------|---------|--------|-------|-------|-------|--------|--------------|--------|-------|
| | Cd | Cr | Co | Cu | Fe | Pb | Mn | Ni | Zn |
| N | 11 | 11 | 12 | 12 | 12 | 11 | 12 | 12 | 12 |
| 5%ile (mg/L) | 0.000 | 0.000 | 0.000 | 0.000 | 0.000 | 0.000 | 0.000 | 0.000 | 0.000 |
| Mean (mg/L) | 0.000 | 0.000 | 0.003 | 0.006 | 0.023 | 0.000 | 0.345 | 0.009 | 0.023 |
| Median (mg/L) | 0.000 | 0.000 | 0.000 | 0.000 | 0.010 | 0.000 | 0.008 | 0.000 | 0.020 |
| 95%ile (mg/L) | 0.000 | 0.000 | 0.019 | 0.033 | 0.089 | 0.000 | 1.832 | 0.044 | 0.054 |
| SD (mg/L) | 0.000 | 0.000 | 0.009 | 0.017 | 0.042 | 0.000 | 1.139 | 0.018 | 0.021 |
| CoV (%) | – | – | 266 | 297 | 188 | – | 330 | 200 | 93 |
| SANS (2015a) ⁽¹⁾ | ≤ 0.003 | ≤ 0.05 | ≤ 0.5 | ≤ 2.0 | ≤ 2.0 | ≤ 0.01 | ≤ 0.5 | ≤ 0.07 | ≤ 5.0 |

¹Standard health-related limit for consumption of 2 L/d over 70 years by a 60 kg person

Bold text denotes value exceeds standard limit as described in note 1

metals listed in Table 42. The analyses reflect a nominal sampling frequency of three months.

The information presented in Table 42 largely corroborates the analysis presented in Table 39 for Fe and Mn (the latter again at the 95%ile level). The results similarly reflect non-detect activities at 50%ile levels for all but Fe, Mn and Zn, and generally do not raise concern for the listed analytes at this locality.

Reference to Table 12 suggests that a greater concern should be given to the metal concentrations in municipal wastewater discharged from the Percy Stewart WWTW. This is at least relevant for Cd, Mn, Pb and Ni.

3.4 Radionuclides

3.4.1 Uranium (²³⁸U and ²³⁴U)

Both SANS (2015a) and the WHO (2011) set a drinking water limit of 15 µg/L for uranium (U). The USAs SDWA proposes a MCL value of 30 µg/L. The comparatively recent inclusion of U (both total U (U_T) and dissolved U (U_D) as per Table 5) as an analyte in the weekly surface water monitoring programme carried out by SG in the Tweelopie Spruit, provides a more detailed record of the pattern and trend of this element in the receiving aquatic environment. Table 7 indicates that median U_T¹⁵ and U_D levels of 16.5 and 9.8 µg/L, respectively, were observed in treated/neutralised mine water discharged to the Tweelopie Spruit in the period B–C (February 2010 to July 2012) of maximum mine water impact. Raw mine water in the same period carried a median U_T concentration of 61 µg/L (n = 131), quadruple both the treated/neutralised mine water median U_T

value and the SANS (2015a) limit, and a 95%ile value of twice that (122 µg/L).

The pattern and trend of U_T at the upper and lower ends of the Tweelopie Spruit is illustrated in Fig. 53. Importantly, the water represents a mixture of raw and treated/neutralised mine water. Salient statistics presented in Table 4 (Sect. 1.2.2) more clearly reveal the differences between the two stations in each distinctive period of mine water discharge.

The statistics show that in the period of maximum mine water impact (B–C), the U_T level at the distal Brickworks Dam (F11S12) station exhibited median and 95%ile values of 30 and 76 µg/L, respectively. The 95%ile values of 26 and 11 µg/L in the preceding and subsequent periods at this station (Table 4) do not represent levels of undue concern if it is considered that Roychoudury and Starke (2006) report a median ²³⁸U¹⁶ value of 26 µg/L in surface water of the East Rand Basin.

The results in Table 4 indicate a 70% reduction in U_T concentration between the two stations located ~5.4 km apart under ‘normal’ discharge conditions. Uranium in its most soluble oxidation state of U(VI), takes the form of the uranyl ion (UO₂²⁺) which, in oxidising water/systems, is both stable and strongly adsorbed onto Fe oxides (Wanty and Nordstrom, 1993 and references therein). Adsorption is stronger at circum-neutral pH, and weaker at higher and lower values. This behaviour readily explains the observed reduction in U_T.

Although the Hobbs et al. (2010) study targeted ²²²Rn as a hydrological tracer in natural and polluted environments, other radionuclides such as ²³⁸U, ²³⁴U and ²²⁶Ra were also investigated. The Western Basin (amongst other areas) was identified as a suitable candidate for testing this hypothesis,

¹⁵ SANS (2015a) requires that the method used to analyse metal analytes be capable of determining the acid soluble (pH < 2) metal present, i.e. the total concentration and not the dissolved fraction only.

¹⁶ Elemental U comprises ~99.3% ²³⁸U, rendering ²³⁸U concentrations practically equivalent to U_T.

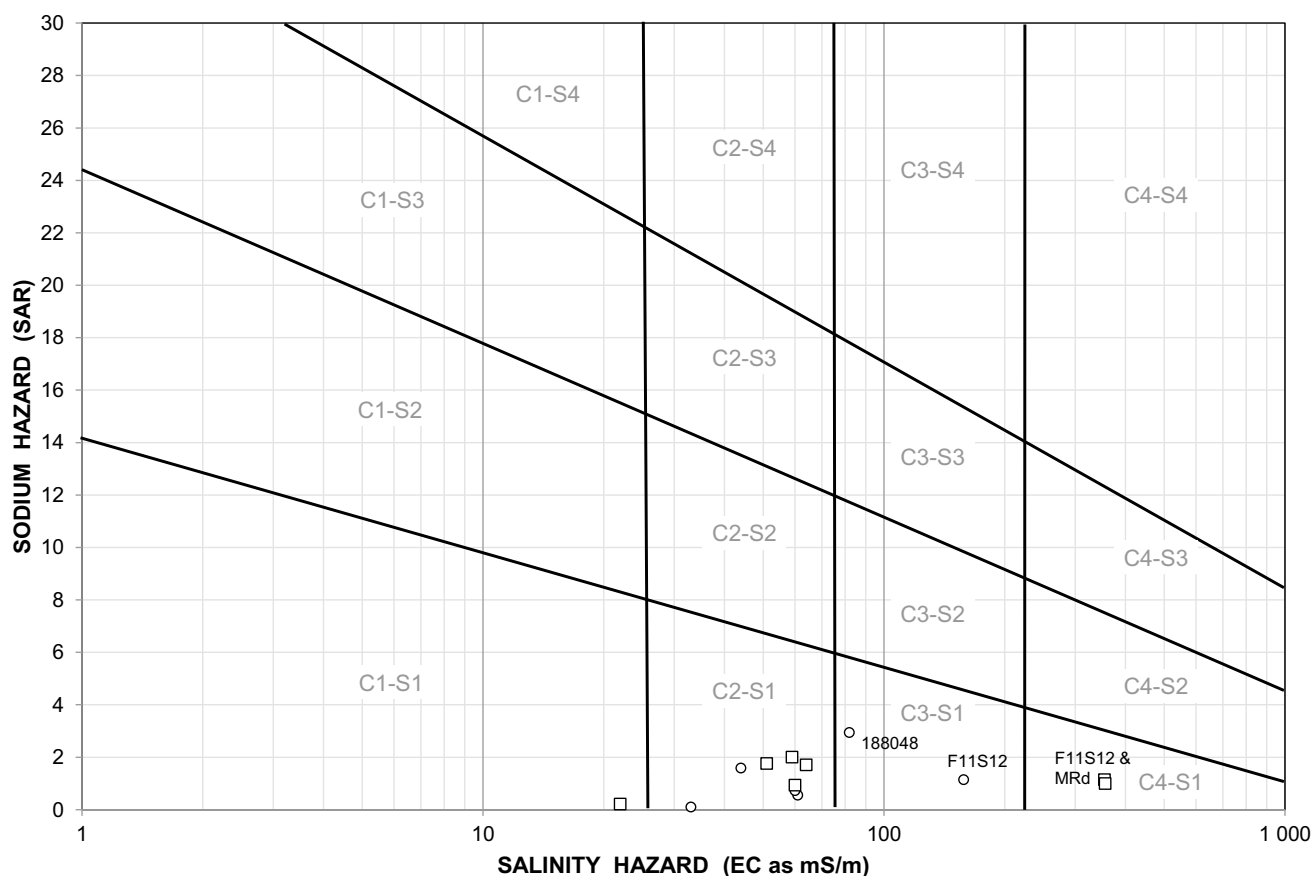


Fig. 54 Wilcox diagram illustrating the classification of surface water chemistry for irrigation purposes (data from Table 46); circle represents long-term median data and square single values

and various sources of water were targeted for radionuclide sampling. A treated/neutralised mine water sample returned a similar value of 0.02 ± 0.005 Bq/L for both ^{238}U and ^{234}U . The equivalent U_T level of $1 \mu\text{g/L}$ compares favourably with the results reported for the periods A–B and C– in Table 7.

Of potentially greater concern is the level of ^{238}U activity in raw mine water in the study area. Five mine water samples analysed by Hobbs et al. (2010) returned levels in the range 0.82 to 2.47 Bq/l (147 to 200 $\mu\text{g/L}$). These are an order of magnitude greater than the U_T limit of $15 \mu\text{g/L}$ set by SANS (2011a) for drinking water, and 5 to 6 times greater than the median U_T level observed in surface water at the lower end of the Tweelopie Spruit.

3.4.2 Radon (^{222}Rn)

The USAs SDWA proposes a MCL of 300 pCi/L ($11.1 \text{ Bq/L} \equiv 1.953 \cdot 10^{-12} \text{ mg/L}$) for radon (^{222}Rn) in drinking water. Results reported by Hobbs (2010) indicate

^{222}Rn activity levels in the range $0.06 \pm 0.16 \text{ Bq/L}$ ($\text{MDA}^{17} = 0.54 \text{ Bq/L}$) to $0.15 \pm 0.12 \text{ Bq/L}$ ($\text{MDA} = 0.39 \text{ Bq/L}$) for surface water in the Tweelopie Spruit. It is evident that the very low ^{222}Rn concentrations do not exceed the minimum detectable activity (MDA) levels associated with the analytical accuracy. These circumstances reflect both the comparatively short half-life (3.82 d) of this radionuclide, and the ready degassing in the turbulent flow regime that characterises the Tweelopie Spruit drainage through the KGR.

In light of the above, the radionuclide ^{222}Rn is not considered to present a threat to the surface water resources in the study area. Concerns for its airborne threat from mine shafts and residues (FSE, 2013) through inhalation in a confined environment would be justified for activity levels $> 100 \text{ Bq/m}^3$ (2.7 pCi/L), the WHO (2009) recommended reference level.

3.4.3 Radium (^{226}Ra and ^{228}Ra)

The USAs SDWA proposes a MCL of 5 pCi/L (0.185 Bq/L) for the aggregate of ^{226}Ra and ^{228}Ra in drinking water. Values for ^{226}Ra reported by Hobbs et al. (2010) provide a

¹⁷ Minimum detectable activity associated with NECSA liquid scintillation counting (LSC) analysis method.

Table 43 Net acidity and net alkalinity of various mine and surface waters in the study area

| Water source | Water type ¹ | Acidity calculation analytes | | | | | | | |
|---------------------|-------------------------|--|-----------------|-----------|-----------|-----------|---|----------------|-------------|
| | | Total alkalinity (mg CaCO ₃ /L) | pH ² | Fe (mg/L) | Mn (mg/L) | Al (mg/L) | Total acidity (mg CaCO ₃ /L) | Net alkalinity | Net acidity |
| BRI | 1 | <5 | 4.0 | 1153 | 69 | n.a | 2197 | −2192 | 2192 |
| #18 Winze | 1 | <5 | 4.2 | 1306 | 47 | n.a | 2429 | −2424 | 2424 |
| #8 Shaft | 1 | <5 | 3.6 | 725 | 148 | 25 | 1743 | −1738 | 1738 |
| CSIR26 | 1 | <5 | 2.6 | 190 | 477 | n.a | 1335 | −1330 | 1330 |
| End-of-pipe | 2 | 36 | 8.5 | 82 | 51 | n.a | 153 | −117 | 117 |
| F11S12 ³ | 3 | <5 | 4.2 | 8.94 | 47 | 0.86 | 109.56 | −105 | 105 |
| F11S12 ⁴ | 3 | <5 | 5.5 | 0.431 | 10 | 0.1 | 19.70 | −15 | 15 |
| F11S12 ⁶ | 3 | <5 | 3.0 | 33 | 29 | n.a | 163 | −158 | 158 |
| MRd ³ | 3 | <5 | 4.2 | 2.49 | 64 | 1.7 | 133.64 | −129 | 129 |
| MRd ⁴ | 3 | <5 | 4.4 | 0.934 | 18 | 0.121 | 37.12 | −32 | 32 |
| MRd ⁶ | 3 | <5 | 3.0 | 18 | 28 | n.a | 134 | −129 | 129 |
| BB@M ⁴ | 4 | 128 | 6.9 | 0.906 | 0.665 | 0.134 | 3.6 | 124 | −124 |
| BB@M ⁵ | 3 | 5 | 2.9 | 44 | 16 | 0.78 | 175 | −170 | 170 |
| BB@M ⁶ | 4 | 66 | 7.1 | 8.1 | 11 | n.a | 36 | 30 | −30 |

¹ 1 = raw mine water; 2 = treated mine water; 3 = impacted surface water; 4 = slightly impacted surface water

² −log₁₀a_{H+}

³ Sample date 16/02/2010

⁴ Sample date 18/05/2010

⁵ Sample date 12/01/2011

⁶ Sample date 16/05/2014

measure of its presence in various sources of mine water and groundwater. The two values available for surface water indicated a ²²⁶Ra level of 0.008 ± 0.002 Bq/L for treated/neutralised mine water, and 0.002 ± 0.001 Bq/L for water from the toe of a slimes dam. These levels compare favourably with those for five mine water sources which ranged from 0.12 to 1.38 Bq/L with a mean of 0.65 Bq/L. The results support the following observations by de Jesus (1985):

- that mine waters obtained at source in various underground mines sporadically showed ²²⁶Ra values > 0.37 Bq/L (10 pCi/L), and
- that tailings dams do not represent a significant threat as a source of ²²⁶Ra in the receiving surface and groundwater environments.

The extreme sparseness of ²²⁶Ra values for surface water in the study area cautions against conclusive observations regarding the threat of this radionuclide in rivers and streams downstream of the mine area. Nevertheless, the very low level of ²²⁶Ra in treated/neutralised mine water suggests that this source does not pose a threat in this regard. The higher levels in raw mine water will only become a concern if circumstances similar to those experienced in the period

February 2010 to July 2012 are manifested (Sect. 3.1 in Chapter “Physical Hydrology”, Figs. 13 and 16). More analyses, and especially of the composite well-mixed raw and treated/neutralised mine water discharge, would be required to better inform such concern.

3.5 Net Alkalinity and Net Acidity

It has been shown by Wirries and McDonnell (1983) that pH is a relatively poor measure of the acidity of AMD. This strengthens the need to understand the chemical characteristic of mine water defined by its net alkalinity, or more importantly the converse, net acidity. The latter variable presents as an indicator of AMD in a water resource, and an evaluation of this characteristic further informs an assessment of mine water impact in the receiving hydrologic environment.

The concepts of net alkalinity and net acidity are discussed at length by Kirby and Cravotta (2005a; 2005b). The term net alkalinity describes a water that is suitable for discharge into a stream after treatment (typically neutralisation by the addition of alkaline material) to remove metals to concentrations low enough to avoid negative impact on aquatic life or human health. As alkalinity is equal to zero at

Table 44 Free acidity and metal acidity associated with the results presented in Table 43

| Water source | Water type ¹ | Free acidity (mg CaCO ₃ /L) | Metal acidity (mg CaCO ₃ /L) | Total (calculated) Acidity (mg CaCO ₃ /L) | Free: total Acidity ratio (%) |
|--------------|-------------------------|---|--|---|----------------------------------|
| BRI | 1 | 5 | 2192 | 2197 | 0.23 |
| #18 Winze | 1 | 3 | 2426 | 2429 | 0.12 |
| #8 Shaft | 1 | 13 | 1730 | 1743 | 0.75 |
| CSIR26 | 1 | 126 | 1209 | 1335 | 9.4 |
| End-of-pipe | 2 | 0 | 153 | 153 | 0 |
| F11S12 | 3 | 3 | 106 | 109 | 2.75 |
| | | 0.2 | 19.5 | 19.7 | 1.02 |
| | | 50 | 113 | 163 | 30.7 |
| MRd | 3 | 3.2 | 130.5 | 133.7 | 2.39 |
| | | 2 | 35 | 37 | 5.41 |
| | | 50 | 84 | 134 | 37.2 |
| BB@M | 64 | 0.01 | 3.58 | 3.59 | 0.2 |
| BB@M | 3 | 63 | 112 | 175 | 36.0 |
| BB@M | 4 | 0 | 36 | 36 | 0 |

¹ 1 = raw mine water; 2 = treated mine water; 3 = impacted surface water; 4 = slightly impacted surface water

a pH of 6.4, a net alkaline water ideally has a pH ≥ 6.4 . This also applies to complex metal-rich solutions that have been allowed to react to reach equilibrium. Water that is net acidic would have a pH < 6.4 after hydrolysis and precipitation of metals.

The (total) acidity is calculated from the pH and dissolved metals concentrations (C_{Metal} in mg/L) as follows (from Kirby and Cravotta, 2005a):

$$\text{Acidity}_{\text{calc}} (\text{mg CaCO}_3/\text{L}) = 50 \left(10^{(3-\text{pH})} + 2C_{\text{Fe}}/55.8 + 2C_{\text{Mn}}/54.9 + 3C_{\text{Al}}/27.0 \right) \quad (1)$$

where the term $50(10^{(3-\text{pH})})$ represents the free acidity contributed by HSO_4^- and hydrogen ion (H^+) activity (pH), and the term $50(2C_{\text{Fe}}/55.8 + 2C_{\text{Mn}}/54.9 + 3C_{\text{Al}}/27.0)$ represents the metal acidity (acidity contributed by metals). The difference between the Total Alkalinity and the $\text{Acidity}_{\text{calc}}$ values gives the Net Alkalinity value (all as mg CaCO_3/L). Net Acidity is simply the negative of the Net Alkalinity, i.e.

$$\text{Net Alkalinity (mg CaCO}_3/\text{L)} = \text{Alkalinity (mgCaCO}_3/\text{L)} - \text{Acidity}_{\text{calc}} = - \text{Net Acidity or}$$

$$\text{Net Acidity (mg CaCO}_3/\text{L)} = \text{Acidity}_{\text{calc}} - \text{Alkalinity (mgCaCO}_3/\text{L)} = - \text{Net Alkalinity}$$

Applying these concepts to raw mine water, treated mine water and various surface waters in the study area gives an indication of the hydrochemical suitability (or otherwise) of these waters in the environment. The outcome is presented in Table 43. A comprehensive discussion of net alkalinity and net acidity in regard to groundwater is provided in Sect. 13.2 in Chapter “Chemical Hydrogeology”.

The results reveal the extremely high net acidity (~ 1700 to 2400 mg/L) associated with the raw mine water. The single treated mine water sample similarly reflects a positive net acidity (negative net alkalinity), albeit typically $\leq 5\%$ of that of raw mine water. The marginally positive net acidity in the range 15 to 158 mg CaCO_3/L (Table 43) associated with the surface water collected at stations F11S12 and MRd confirms the very strong mine water presence in this water on the sampling dates. This contrasts with the -124 mg/L net acidity value of the surface water at station BB@M on 18/05/2010 attributed to the municipal wastewater effluent contribution. The latter contribution is negated by mine water at station BB@M on 12/01/2011 (net acidity = 170 mg CaCO_3/L), a characteristic that violates the positive net alkalinity requirement for surface water suitability. It also helps explain the role of mine water in precipitating the Koelenhof Farm fish mortality event (Hobbs and Mills 2011).

The free (H^+ activity) and metal (mineral) acidity components associated with the various waters listed in Table 43 yields the information presented in Table 44. This shows that

the free acidity contribution to total acidity ranges from 0 to ~37%. Without exception, the greater contributions (30–37%) are associated with surface water at stations located >6 km downstream of the mine area. These circumstances support the influence of hydrolysis (Sects. 3.5 in Chapter 6 and 5.1 in Chapter 6) on the chemistry of mine water impacted surface water in its passage downstream from the mine area.

The net acidity of Tweelopie Spruit water at station F11S12 (Brickworks Dam) is of particular interest for the reason that this station is located shortly before the losing reach of the Riet Spruit that straddles the south-western boundary of the COH. The magnitude of influent losses to the karst aquifer has previously been quantified in Sect. 5.2.1 in Chapter “Physical Hydrology”. Coupling this loss with the net acidity of the influent surface water provides an indication of the acid load that enters the karst aquifer as a component of the allogenic recharge. A coupling of the surface water losses in the period mid-December 2012 to late July 2014 with the two periods of distinctively different net acidity concentrations, namely:

- mid-December 2012 to early March 2014 (coinciding with the period C–D in Sect. 1.2.2); and
- early March 2014 to late July 2014 (coinciding with the period D– in Sect. 1.2.2),

yields the acid loads presented in Table 45. These are calculated as the product of the 5%ile, median and 95%ile flow losses and the 5%ile, median and 95%ile net acidity concentrations (as mg CaCO₃/L).

It is shown that the aquifer received a net alkalinity load equivalent to 36.5 t CaCO₃/a at the 5%ile level in the mid-December 2012 to early March 2014 period only. An acid load equivalent to ≥ 15.7 t CaCO₃/a otherwise characterises this addition to the karst aquifer in both periods,

attaining a value of 1042 t CaCO₃/a at the 95%ile level in the period spanning both a ‘moderate’ and a ‘severe’ mine water impact. The impact of the acid load on the receiving karst groundwater resources is discussed in Sect. 13.2 in Chapter “Chemical Hydrogeology”.

4 Surface Water Fitness

4.1 Potable Use

The fitness of water for human consumption is gauged against the SANS (2015a) standard for drinking water quality. The extent to which the water quality analytes associated with the various surface water sources in the study area meet the limits of the SANS (2015a) standard in the long-term is already reflected in various tables (e.g. Tables 2, 9, 11, 18, 19, 22 and 23). It is evident that drainages such as the Skeerpoort River (Table 22) and the Tweefontein Spruit (Table 18) experience an excellent quality water in all respects. It is equally evident, however, that the drainages receiving mine water (Tweelopie and Riet spruits) and treated municipal wastewater (Blougat Spruit) experience exceedances in regard to SEC, Ca, SO₄, Fe, Mn and Al.

The information in Tables 13 and 14 indicates that the Blougat Spruit additionally experiences severe exceedances in regard to the bacteriological quality as represented by the faecal coliform and *E. coli* counts. These circumstances seriously compromise the use of the surface water in these drainages for human consumption. However, Table 20 and Fig. 26 indicate that the situation improves significantly in the main stem, the Bloubank Spruit. Nevertheless, the persistent presence of bacteriological contamination in surface water of the Bloubank Spruit system cautions strongly against its unqualified use for human consumption without treatment.

Table 45 Summary of the acid load addition to the karst aquifer of the Zwartkrans Subcompartment in the period December 2012 to July 2014

| Period | Variable/Analyte | Statistical Parameter Value | | |
|---------------------------------------|------------------------------------|-----------------------------|--------|--------|
| | | 5%ile | Median | 95%ile |
| Mid-December 2012 to early March 2014 | n | 63 | 63 | 63 |
| | pH | 6.6 | 7.1 | 7.5 |
| | Discharge (ML/d) | 8.0 | 12.3 | 16.3 |
| | Acid load (t CaCO ₃ /a) | –36.5 | 15.7 | 224.9 |
| Early March 2014 to late July 2014 | n | 20 | 20 | 20 |
| | pH | 2.8 | 3.4 | 4.5 |
| | Discharge (ML/d) | 8.0 | 12.3 | 16.3 |
| | Acid load (t CaCO ₃ /a) | 61.3 | 357.8 | 1042.4 |

4.2 Agricultural Use

4.2.1 Livestock Watering

Guidelines in this regard are provided in the DWAF (1996b) publication. The target water quality range (TWQR) limits for the major inorganic analytes are typically less strict than for human consumption. For example, the TWQR for SO_4 (an analyte that, together with TDS and Cl, effects the palatability of water also for livestock) is 1000 mg/L compared to the 400 mg/L for humans. This is also true for trace/heavy metals, e.g. Mn and Fe with a TWQR of ≤ 10 mg/L for livestock compared to ≤ 0.1 mg Mn/L and ≤ 0.2 mg Fe/L for humans. Even the observed presence of bacteriological contamination in surface water of the Bloubank Spruit system is rendered more acceptable for livestock by the faecal coliforms TWQR of ≤ 1000 c/100 mL in 20% of samples, compared to the ≤ 10 c/100 mL in 1% of samples for humans.

The chemical analysis results for surface water in the study area cautions against the unqualified use thereof for livestock watering. Water of the Tweelopie/Riet Spruit subsystem is characterised by an elevated salt load reflecting a dominant Ca-SO_4 composition that accounts for 84% of the TDS load in this water (Sect. 8.4 in Chapter “[Chemical Hydrogeology](#)”). This water is not, however, compromised in regard to its trace/heavy metals or bacteriological composition for livestock watering. Water of the Blougat Spruit, on the other hand, exhibits a suitable inorganic and trace/heavy metals composition, but is compromised by unacceptable levels of bacteriological contamination. Although these circumstances improve markedly in the Bloubank Spruit downstream of Sterkfontein Cave

(Sect. 1.2.6 and Fig. 25), caution is still advised against its unqualified use for livestock watering.

4.2.2 Irrigation

The fitness of water for irrigation use is assessed on the basis of the sodium adsorption ratio (SAR) and salinity (expressed as electrical conductivity) of the water. The SAR is calculated as the ratio between the Na concentration and the combined Ca and Mg concentrations using the formula

$$\text{SAR} = \text{Na} \div [(\text{Ca} + \text{Mg}) \div 2]^{0.5} \quad (\text{concentrations as meq/L}) \quad (2)$$

to derive the sodium hazard (designated S) associated with the water. This value is graphed against the electrical conductivity value, which represents the salinity hazard (designated C), to derive an alpha-numeric classification (e.g. C#-S#) defined by the Wilcox diagram (Fig. 54), and where the numeric component ranks as follows: 1 = low, 2 = medium, 3 = high and 4 = very high.

The range of SAR values that represent the various surface water sources in the study area is presented in Table 46. The results (also shown graphically in Fig. 54) indicate that the sodium hazard in no instance exceeds a low (S1) classification. However, the salinity hazard associated with the drainage impacted by mine water (stations F11S12 and MRd) reflects a very high (C4) ranking. This limits the use of this water to the irrigation of crops with a very good salt tolerance on well-drained permeable soils.

Other aspects of the water chemistry that have relevance to the irrigation use of the water are the N:P ratio and the corrosion tendency ratio (CTR) values. The N:P ratio is



Plate 1 Corrosion of large-diameter pipe draining the Aviary Dam on the Tweelopie Spruit in the KGR; photo at left shows remnant (at bottom centre) tenuously attached to flange, and photo at right shows close-up view from opposite side

Table 46 Range of representative SAR values for various surface water sources in the study area

| Station | Range of representative SAR values | | | | | Classification per median ¹ |
|---------|------------------------------------|---------------------|------|--------|--------|--|
| | Source | 5%ile | Mean | Median | 95%ile | |
| A2H034 | Table 22 | 0.07 | 0.10 | 0.10 | 0.15 | C2–S1 |
| A2H049 | Table 19 | 0.30 | 0.59 | 0.58 | 0.83 | C2–S1 |
| A2H050 | Table 23 | 0.77 | 1.58 | 1.53 | 2.42 | C2–S1 |
| F11S12 | Table 9 | 0.46 | 1.04 | 0.70 | 1.52 | C3–S1 |
| | Table 20 | 1.14 ⁽²⁾ | | | | C4–S1 |
| MRd | Table 20 | 0.99 ⁽²⁾ | | | | C4–S1 |
| 188,048 | Table 11 | 2.12 | 2.79 | 2.81 | 3.32 | C3–S1 |
| BC1 | Table 20 | 2.00 ⁽²⁾ | | | | C2–S1 |
| BG@N14 | Table 20 | 1.76 ⁽²⁾ | | | | C2–S1 |
| F14S15 | Table 18 | 0.33 | 0.66 | 0.72 | 0.83 | C1–S1 |
| BB@M | Table 20 | 1.71 ⁽²⁾ | | | | C2–S1 |
| BB@PL | Table 20 | 0.93 ⁽²⁾ | | | | C2–S1 |
| HS1 | Table 20 | 0.21 ⁽²⁾ | | | | C1–S1 |

¹Where applicable (refer source tables for sample population sizes)

²Single value as per source table

discussed in greater detail in Sect. 6.3.2, where concern is expressed in regard to N:P ratio values as low as 12 recently observed at several stations in the Bloubank Spruit system.

The CTR is calculated as the ratio between the sum of the Cl and SO₄ concentrations and the Total Alkalinity (CaCO₃) concentration using the formula

$$\text{CTR} = [\text{Cl} + \text{SO}_4] \div \text{TAlk} \quad (\text{concentrations as mg/L}) \quad (3)$$

It is used to estimate the corrosive tendency of Cl and SO₄ ions. A ratio of ≤ 0.1 indicates general freedom from corrosion in neutral to slightly alkaline (pH 7–8) oxygenated waters (DWAF 1996c), and increasingly higher ratios a tendency towards greater corrosivity.

The CTR values associated with the surface water samples collected at seven stations in the Bloubank Spruit system in May 2010 are presented in Table 47, together with other analytes for which the DWAF (1996c) provides a target water quality range (TWQR) for irrigation use. The information presented in regard to stations F11S12 and MRd, and to a lesser extent stations BB@M and BB@PL, reflects the severest impact of mine water on the Bloubank Spruit system as a result of the discharge conditions discussed in Sect. 5.3.1.

The corrosivity of Tweelopie Spruit surface water is evident in Plate 1, although the severity of corrosive attack in this instance is most probably exacerbated by the high degree of aeration and the high flow velocity of the water through the pipe.

A chemical analysis of surface water collected at station BB@M in mid-January 2011 yielded a CTR value of 338 which, together with a pH of ~ 3 , indicated the water to be extremely corrosive. This is commensurate with the manifestation of a greater mine water component in the middle to lower reaches of the Bloubank Spruit system especially during the 2011 rainfall season (Figs. 13 and 15). However, corrosion of pipelines and fittings is only likely to manifest as a problem through continued medium- to long-term use of water with this chemical characteristic. The likelihood of this occurring depends on the success (or otherwise) of mine water treatment interventions in the Western Basin proposed by the Inter-Ministerial Committee (IMC) on AMD (Coetzee et al. 2010).

4.3 Recreational Use

Guidelines in this regard are provided in the DWAF (1996d) publication. The need to assess the fitness of surface water for recreational use is indicated by businesses that provide adventure activities in the area. Of concern is that the target group for such activities is mainly schoolchildren, and that some of the activities also involve full-body water contact activities. This is especially problematic where the surface water environment is strongly impacted by acid mine water and/or bacteriological contamination.

An inspection of the TWQR for recreational use (DWAF 1996d) reveals limits that are much less rigorously defined than for other uses. In many instances, the criteria are

Table 47 Evaluation of Bloubank Spruit system surface water quality for irrigation use

| Variable/Analyte | Sampling station | | | | | | | DWAF TWQR ¹ |
|--|------------------|--------------|---------------|---------------|--------------|--------------|--------------|---------------------------------------|
| | F11S12 | MRd | BC1 | BG@N14 | BB@M | HS1 | BB@PL | |
| Date | 18/05/2010 | | | | | | | |
| pH ($-\log_{10}a_{H^+}$) (field) | 5.5 | 4.4 | 7.1 | 6.9 | 6.9 | 6.9 | 7.0 | 6.5–8.4 |
| SEC (mS/m) (field) | 355 | 356 | 59 | 51 | 64 | 22 | 60 | ≤ 40 |
| Na (mg/L) | 115 | 103 | 55 | 48 | 52 | 5 | 34 | ≤ 70 |
| Cl (mg/L) | 43 | 44 | 52 | 45 | 50 | 12 | 40 | ≤ 100 |
| NO ₃ + NO ₂ (mg N/L) | 0.6 | 0.6 | 0.2 | 0.5 | 3.2 | 1.9 | 6.0 | $\leq 5.0^{(2)}$ $\leq 0.5^{(3)}$ |
| F (mg/L) | < 0.2 | < 0.2 | 0.2 | 0.2 | < 0.2 | < 0.2 | < 0.2 | ≤ 2.0 |
| <i>E. coli</i> (count/100 mL) | n.a | n.a | 65 000 | 26 000 | 3000 | 0 | 470 | ≤ 1 in 1% of samples |
| Fe (mg/L) | 0.431 | 0.934 | 0.528 | 0.682 | 0.906 | 0.073 | 0.358 | $\leq 5.0^{(2)}$ $\leq 0.2^{(3)}$ |
| Mn (mg/L) | 10 | 18 | 0.279 | 0.470 | 0.665 | 0.087 | 0.293 | $\leq 0.02^{(2)}$ $\leq 0.2^{(3)}$ |
| Al (mg/L) | < 0.1 | 0.121 | 0.118 | < 0.1 | 0.134 | < 0.1 | 0.137 | ≤ 5.0 |
| U (mg/L) | < 0.001 | < 0.001 | < 0.001 | < 0.001 | < 0.001 | < 0.001 | < 0.001 | ≤ 0.01 |
| Ni (mg/L) | 0.145 | 0.117 | 0.049 | 0.035 | 0.029 | < 0.025 | < 0.025 | ≤ 0.2 |
| Zn (mg/L) | 0.048 | 0.379 | 0.043 | 0.025 | < 0.025 | < 0.025 | < 0.025 | ≤ 1.0 |
| N:P value | 6 | 6 | 0.1 | 0.2 | 1.3 | 19 | 12 | n.s |
| SAR value | 1.14 | 0.99 | 2.00 | 1.76 | 1.71 | 0.21 | 0.93 | ≤ 2.0 |
| CTR value | 772 | 783 | 1.0 | 0.9 | 1.2 | 0.4 | 1.0 | n.s |

¹Recommended target water quality range (TWQR) limit for irrigation use (from DWAF, 1996c)²Effect on crop yield and quality³Effect on irrigation equipment (mainly drip irrigation systems)

Bold text denotes values that exceed the TWQR recommended limit for irrigation use

Plate 2 View of station F11S12 showing concrete weir (dark linear shape below right hand of person) and object (circled) on causeway for common reference with Plate 3 (photo W Basson)

Table 48 Change in surface water chemistry with distance downstream of the mine water source

| Locality | | Distance (m) | | SEC (mS/m) | pH ⁽¹⁾ | Flow (ML/d) |
|----------|---|--------------|-----------------------|------------|-------------------|-----------------------|
| | | Segmental | Cumulative | | | |
| 1 | KGR Inflow (raw mine water) | 0 | 0 | 354 | 4.5 | 21.0 |
| 2 | KGR Inflow (treated mine water) | | | 306 | 6.3 | 19.0 |
| 3 | Hippo Dam outlet in KGR | 950 | 950 | 332 | 5.6 | n.m |
| 5 | Poplar Grove in KGR | 850 | 1800 | 324 | 4.3 | n.m |
| 6 | Aviary Dam inlet in KGR | 3105 | 4905 | 302 | 4.0 | 32.1 |
| 7 | KBW Dam outlet at N14 (F11S12) | 1540 | 6445 | 302 | 3.9 | 35.2 |
| 8 | Riet Spruit at Malmani Road (MRd) | 3900 | 10 345 | 278 | 4.1 | 7.3 |
| 9 | Bloubank Spruit downstream of Makiti (BB@M) | 5050 | 15 395 | 45 | 7.1 | 43.2 |
| 10 | Bloubank Spruit at A2H049 | 12 000 | 27 255 | 44 | 7.2 | n.m |
| 11 | Blougat Spruit tributary of the Riet Spruit at N14 (BB@N14) | n/a | 10 835 ⁽²⁾ | 51 | 6.9 | ~ 36.0 ⁽³⁾ |
| 12 | Honingklip Spruit tributary of the Bloubank Spruit at Kromdraai (HS1) | n/a | 18 905 ⁽²⁾ | 19 | 7.2 | n.m |

¹(-log₁₀α_{H+})²Distance of confluence with main stem downstream from the mine water source³Difference between flow measured at localities 8 and 9

n.m. denotes not measured

Table 49 Change in surface water chemistry with distance downstream of the mine water source

| Locality | | Distance (m) | | SEC (mS/m) | pH (-log ₁₀ α _{H+}) | Flow (ML/d) |
|----------|---|--------------|---------------------|------------|--|--------------------|
| | | Segmental | Cumulative | | | |
| 3 | Hippo Dam outlet in KGR | 950 | 950 | 406 | 5.5 | n.m |
| 4 | Poplar Grove in KGR | 850 | 1800 | 322 | 3.6 | n.m |
| 5 | 4 × 4 Track at Oukraal Lapa in KGR | 1015 | 2815 | 302 | 3.5 | 52.3 |
| 6 | Aviary Dam inlet in KGR | 2090 | 4905 | 293 | 3.4 | 34.4 |
| 7 | Brickworks Dam outlet / F11S12 | 1540 | 6445 | 290 | 3.6 | 40.4 |
| 8 | Riet Spruit at Malmani Road (MRd) | 3900 | 10,345 | 278 | 3.4 | 10.3 |
| 9 | Bloubank Spruit downstream of Makiti (BB@M) | 5050 | 15,395 | 27 | 7.3 | 128.7 |
| 11 | Blougat Spruit tributary of the Riet Spruit at N14 (BB@N14) | n/a | 10,835 ¹ | 28 | 7.5 | ~ 118 ² |
| 12 | Honingklip Spruit tributary of the Bloubank Spruit at Kromdraai (HS1) | n/a | 18 905 ¹ | 14 | 7.4 | n.m |

¹Distance of confluence with main stem downstream from the mine water source²Difference between flow measured at localities 8 and 9

n.m. denotes not measured

qualitative and adherence to general principles is advocated. The greater part of the guidelines pertains to indicator organisms, e.g. faecal coliforms, *E. coli*, faecal streptococci, coliphages, enteric viruses and schistosoma/bilharzia. The limits for these are necessarily less stringent than the TWQR limits for drinking water (Sect. 6.4.1), e.g. faecal coliforms ≤ 30 c/100 mL for full-contact recreation (swimming and diving) and ≤ 1000 c/100 mL for intermediate contact recreation (waterskiing, canoeing, angling, paddling and wading) versus ≤ 10 c/100 mL for drinking water.

5 Mine Water Chemistry in the Receiving Drainages

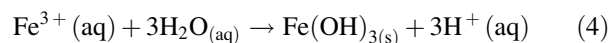
5.1 Ad Hoc Observations

The ad hoc measurement of field pH and SEC values triggered by the advent of excessive mine water decant in late January 2010 provided the opportunity to gather valuable information on the chemistry of surface water in the

receiving environment. Comprising a mixture of treated/neutralised mine water from the HDS Plant and raw mine water, the pH and SEC of this water was measured at various localities in the downstream receiving drainages. The data presented in Tables 48 and 49 reflect the degree of change recorded on 05/02/2010 and 01/04/2010, respectively, in the analytes pH and SEC with distance downstream from where the mine water leaves the mine property. The latter data set occurs in the period mid-March to mid-May 2010 when the raw mine water discharge was subjected to in-stream liming (as a DWS-funded emergency treatment measure) at the point of concentrated release into the environment (refer Footnote 59).

The measurements reveal the following hydrochemical responses.

- The decrease in the pH of the water with distance downstream of the mine water source area, from a value of ~ 5.6 at the Hippo Dam outlet to a value of ≤ 4.1 at the Brickworks Dam/F11S12 outlet on the Tweelopie Spruit and at the Malmani Road crossing on the Riet Spruit. This response is readily accounted for by hydrolysis reactions (Hem, 1985), in this instance the precipitation of iron out of the water producing free hydrogen ions, with the increase in hydrogen ion activity lowering the pH as illustrated in the following reaction (amongst many similar such reactions)



Hydrolysis of the ferric iron (Fe^{3+}) by water forms an amorphous ferric hydroxide $[\text{Fe}(\text{OH})_3]$ efflorescence, a residue also called ‘ochre’ or ‘Yellow boy’. The production of free hydrogen ions generates acidity which maintains the solubility of the Fe(III) (Banks, 2004). The rapidity of this process is illustrated in Plate 2 and 3, which show the appearance of the concrete weir at the outlet of station F11S12 on 28/01/2010 and 08/02/2010, a period of only 10 days apart. At this stage, the ferrihydrite efflorescence visible in Plate 3 merely formed a thin (<1 mm thick) slick film coating the concrete and that could be rubbed off with a finger. Through aggregation and ageing of the ferrihydrite (Webb and Sasowsky, 1994), it had formed a hard goethite ($\text{FeO} \cdot \text{OH}$) crust $\sim 1\text{--}2$ cm thick by ca. mid-2012. This crust gradually eroded away following the improvement in mine water quality discharge in mid-2012.

The situation illustrated in Plate 2 and 3 marks the transition from a surface water chemistry characterised by the discharge of mainly treated/neutralised mine water in which there is very little iron, to a situation where raw mine water comprises $\geq 50\%$ of the mine water waste stream discharged from the mine area (Sect. 3.1 in Chapter “Physical Hydrology” and Fig. 16). The very

Plate 3 View of station F11S12 showing concrete weir coated with freshly precipitated hydrous ferric oxide or ferrihydrite ($5\text{Fe}_2\text{O}_3 \cdot 9\text{H}_2\text{O}$) and object (circled) on causeway for common reference with Plate 2



Plate 4 Discharge at station F11S12 (Tweelopie Spruit) on 18/12/2010. Compare with Plate 13, Plates 2, 3 or Plate 41 to note the complete submergence of the causeway



Plate 5 View looking north of the high discharge at BB@M (Bloubank Spruit) on 18/12/2010



high concentrations of iron (5% ile = 322 mg/L, 50% ile = 687 mg/L) dissolved in the raw mine water (Table 2) lead to the rapid precipitation of ferrihydrite much further downstream (as observed at station F11S12, Plate 3) than was observed previously (Plate 2). Figure 16 indicates that 30/01/2010 marks the setting of the surface water chemical regime in the drainage system to a lower or 'poorer' state, which monitoring data indicates returned to 'normal' ca. mid-2012.

- The significant improvement in surface water quality downstream of the Riet Spruit/Blougat Spruit confluence, as indicated by the SEC values of 45 and 27 mS/m and the pH values of 7.1 and 7.3 measured in the Bloubank Spruit downstream of the Makiti Wedding and Conference Centre, compared to the 278 mS/m and pH of ≤ 4.1 measured in the Riet Spruit at the Malmani Road crossing (station MRd). This is attributed to the mitigating influence of the significant discharges (estimated at ~ 36 and ~ 118 ML/d, respectively) contributed by the better inorganic quality of Blougat Spruit water characterised by an SEC in the range 30–50 mS/m and a pH in the range 6.9–7.3. It is evident from the information presented and discussed in Sect. 1.2.4, however, that the microbiological quality of this water is a grave concern.

5.2 Opportunistic Observations

Peak flow (flood) conditions were experienced in the Tweelopie Spruit, the lower Riet Spruit and the Bloubank Spruit following the high rainfall experienced in

mid-December 2010 (Sect. 3.2). Various localities in the area reported precipitation in the order of 130 to 140 mm in a period of some 24 h ca. 16/12/2010. The rainfall gauging station operated by SG at the Black Reef Incline in the LoD in the upper reaches of the Tweelopie Spruit recorded 90 mm (B van der Walt, personal communication) between 07h00 on 16 and 17/12/2010. The DWS flow gauging station A2H049 at the lower end of the Bloubank Spruit recorded a second highest recorded daily average flow rate of 18.6 m³/s on 16/12/2010, followed by rates of 6.9 and 2.9 m³/s on the following two days. The maximum (highest) historical daily average flow rate gauged at this station is 34.3 m³/s recorded on 28/01/1978.

The aftermath of the mid-December 2010 flood event was still visible on 18/12/2010 (Plates 3 and 4) when a series of opportunistic surface water field chemistry measurements were made at the 'key' locations along the effected drainages shown in Fig. 55. The results, obtained roughly a month before the fish mortality event that occurred in the study area in mid-January 2011 (Hobbs and Mills, 2011), are presented in Table 50.

Perhaps the most significant impact of the flood was the disruption of flow into the A-furrow (Sect. 5.6.2). Flow into this furrow was only restored, albeit partially, on 10/01/2011 (M Gomes, personal communication), i.e. a day before the fish mortality event. At this time, Mr. Gomes (Chairman of the Kromdraai Irrigation Board) expressed concern for the yellow appearance of the furrow water and its suitability for various uses including stock watering and irrigation. Unaware of the fish mortality event, this communication precipitated another round of field water quality monitoring on 12/01/2011, the results of which are also reported in Table 50.



Plate 6 Examples of Fe-(orange) and Mn-oxide (black) precipitation as concentric scaling in pipe (left) and as 'Yellow boy' in ditch (right) (photo at left J Davies; photo at right W Basson).

A closer inspection of the 12/01/2011 data (Table 50) reveals the following hydrochemical characteristics:

- The very low pH values and elevated SEC values of ~ 400 mS/m at the uppermost two stations F11S12 and MRd indicating a strong mine water signature at these localities.
- The generally good inorganic quality associated with the Percy Stewart WWTW discharge via the Blougat Spruit (station BG@N14) into the Bloubank Spruit system as shown by the high pH value and low SEC value; this by no means implies an acceptable bacteriological quality.
- The very low pH and elevated SEC of the surface water at station BB@M, again indicative of a mine water impact on the quality of the surface water at this locality. Whereas the pH value represents the most extreme value observed at this station in the project period, the SEC value is only exceeded by that observed on 18/12/2010 (Table 50). Significantly, the ORP value of 221 mV (indicative of an oxidising environment) approximates those observed at the upstream stations F11S12 and MRd.
- The improvement in quality at the downstream station BB@PL, as reflected in a higher pH and lower SEC compared to that at station BB@M, is attributed to the mitigatory influence contributed by the ~ 307 L/s Kromdraai and ~ 60 L/s Plover's Lake springs.
- The still quite 'acceptable' pH and SEC values at station A2H049 at the bottom end of the Bloubank Spruit system at Glenburn Lodge near Zwartkop, although the pH value approaches the long-term 5%ile value of 7.4, and the SEC value of 87 mS/m exceed the long-term 95%ile value of 67 mS/m (Table 19) recorded at this DWS gauging station. Even so, the observed SEC value does not exceed the maximum value of ~ 122 mS/m recorded in the 36-year period May 1979 to September 2014 that represents the historical record of water chemistry data available for this station from the DWS.

The SEC values of 158 and 155 mS/m (Table 50) recorded at station BB@M approach the highest recorded at this station in the course of the study, and the pH value of 2.9 similarly the lowest observed. A surface water sample collected for more complete laboratory chemical analysis¹⁸ returned the results presented in Table 51. These circumstances reflect the dominant contribution of raw mine water discharge to the chemistry of surface water at this locality on this occasion. Of specific relevance to the fish mortality



Plate 7 Excessive sludge deposition in the upper reaches of the Hippo Dam in the Krugersdorp Game Reserve as a result of emergency liming of raw mine water to raise its pH (photo S du Toit)

event is the very low field pH value of 2.9 observed on 12/01/2011 (Plate 5).

The author was notified on 13/01/2011 of fish mortalities that had occurred on Koelenhof Farm upstream of the Kromdraai T-junction (M Liefferink, personal communication). The mortalities occurred in an off-channel irrigation water storage dam fed by the A-furrow, and not in the natural stream course of the Bloubank Spruit. It is therefore probable that the restored flow of A-furrow water into this dam resulted in oxygen depletion associated with the precipitation of iron hydroxides in this low energy impounding environment. It is also probable that the slow rate of iron precipitation resulted in the accumulation of this efflorescence in the gills of fish, compounding the suffocating effect of a depleted oxygen supply and contributing to the observed fish mortalities in this impoundment.

The above circumstances are also likely to have similar consequences for crustaceans and macroinvertebrates resident in these dams. Enquiries further established that above average fish mortalities had also been experienced at the Brookwood Trout Farm located downstream of station BB@PL (Table 50) (H Carpenter, personal communication). The Koelenhof Farm fish mortality event precipitated further field studies on 14/01/2011 by the author and P Mills of the MA (Hobbs and Mills, 2011). The results are summarised in Table 52.

The nature of the event that precipitated the 14/01/2011 studies necessitated the inclusion of dissolved oxygen (DO) as a field water chemistry variable. An inspection of the data presented in Table 52 reveals the following hydrochemical characteristics:

- In regard to the station BB@M;
 - the low pH value indicative of, amongst other sources, a combination of very low pH mine water and low pH

¹⁸ The oxidation of dissolved Fe^{2+} in the water sample resulted in the precipitation of an iron oxide in the sample bottle during transport and laboratory storage. This was not seen in the acidified sample bottle.

Table 50 Surface water field chemistry variable values

| Station | Field chemical variable | | | | | | | |
|---------|-----------------------------|------------|------------|------------|------------|------------|------------|------------|
| | pH ($-\log_{10} a_{H^+}$) | | SEC (mS/m) | | ORP (mV) | | Temp. (°C) | |
| | 18/12/2010 | 12/01/2011 | 18/12/2010 | 12/01/2011 | 18/12/2010 | 12/01/2011 | 18/12/2010 | 12/01/2011 |
| F11S12 | 2.7 | 2.5 | 416 | 397 | 230 | 243 | 21.3 | 21.1 |
| MRd | 3.0 | 2.3 | 276 | 410 | 217 | 254 | 24.1 | 25.0 |
| BG@N14 | n.m | 8.2 | n.m | 53 | n.m | −65 | n.m | 26.1 |
| BB@M | 6.1 | 2.9 | 158 | 155 | 51 | 221 | 24.8 | 23.9 |
| BB@PL | n.m | 6.8 | n.m | 94 | n.m | 12 | n.m | 21.3 |
| A2H049 | n.m | 7.7 | n.m | 87 | n.m | −37 | n.m | 22.3 |

Table 51 Chemical analysis laboratory report for surface water sample collected at station BB@M

| Variable/Analyte | Value | Source Indicator Analyte | | SANS (2011a) ¹ |
|--|-------------------|--------------------------|-------------------|---------------------------|
| | | Mine water | Sewage wastewater | |
| Laboratory | CSIR (Pretoria) | n/a | | n.a |
| Laboratory report # | 9156 | n/a | | n.a |
| Laboratory sample # | 82,235 | n/a | | n.a |
| Report date (dd/mm/yyyy) | 19/01/2011 | n/a | | n.a |
| Sample date (dd/mm/yyyy) | 12/01/2011 | n/a | | n.a |
| pH ($-\log_{10} a_{H^+}$) (field) | 2.9 | Yes | No | 5.0–9.5 |
| pH ($-\log_{10} a_{H^+}$) (lab value) | 3.2 | Yes | No | 5.0–9.5 |
| SEC (mS/m) (field) | 155 | Yes | No | ≤ 170 |
| SEC (mS/m) (lab) | 122 | Yes | No | ≤ 170 |
| Ca (mg/L) | 149 | Yes | No | ≤ 150 |
| Mg (mg/L) | 49 | Dual | | ≤ 70 |
| Na (mg/L) | 50 | Dual | | ≤ 200 |
| K (mg/L) | 9 | Dual | | ≤ 50 |
| Cl (mg/L) | 40 | No | Yes | ≤ 200 |
| SO ₄ (mg/L) | 758 | Yes | No | ≤ 400 |
| HCO ₃ (mg/L) | < 6 | Dual | | n/s |
| NO ₂ + NO ₃ (mg N/L) | 4.8 | No | Yes | ≤ 11 |
| NH ₃ + NH ₄ (mg N/L) | 2 | No | Yes | n/s |
| PO ₄ (mg P/L) | <0.2 | No | Yes | n/s |
| Fe (mg/L) | 44 | Yes | Subordinate | ≤ 0.2 |
| Mn (mg/L) | 16 | Yes | Subordinate | ≤ 0.1 |
| Al (mg/L) | 0.78 | Yes | Yes | ≤ 0.3 |
| Ni (mg/L) | 0.35 | Yes | Yes | ≤ 0.15 |
| CN (mg/L) | <0.01 | | | n/s |
| EB (%) | −3.0 ² | n/a | | ± 5 |
| Chemical character | CaSO ₄ | Yes | No | |

¹Standard health-related limit for consumption of 2 L/d over 70 years by a 60 kg person²Includes Fe and Mn in the calculation; value deteriorates to −10% without these cations.

Bold text denotes value exceeds standard limit as described in note 1

rainwater runoff in the discharge at this position in the Bloubank Spruit;

- the very low SEC value of ~ 22 mS/m compared to the value of 155 mS/m measured two days earlier on 12/01/2011 (Table 50), which similarly reflects the significant contribution of fresh water in the river on 14/01/2011; and
- the high level of oxygen saturation reflected by the DO value of 106%, which is readily explained by the degree of turbulence exhibited in the strong-flowing river and natural diffusion of gaseous oxygen (O_2) from the atmosphere into the water (DWAF, 1996a); the supersaturated oxygen state is possibly indicative of eutrophication associated with a high nutrient load attributable to the presence of sewage wastewater effluent
- The similar analyte values observed at the station A-furrow @ Lotz as were observed at station BB@M, which establishes the direct hydraulic link between the Bloubank Spruit surface water and that flowing in the A-furrow.
- The very low pH and DO¹⁹ values, and the elevated SEC and temperature²⁰ values of the Koelenhof Farm dam water, which likely represent an artefact of the water quality conditions that gave rise to the fish mortality event.
- The saturated oxygen content of the furrow water downstream of the Koelenhof Farm dam compared to the 60% DO concentration of the dam water.
- The similar analyte values (except for temperature) associated with the Zwartkrans Spring and Sterkfontein Cave Lake water, which establishes the hydraulic connection between these two groundwater sources. [Note: The cave water level response is discussed in greater detail in Sect. 7.3.2] Whereas the Zwartkrans springwater field SEC of ~ 74 mS/m is similar to its more recent 'historical' value, the cave water field SEC of ~ 56 mS/m is slightly lower than the typical 59–62 mS/m range that characterises this water quality variable. The fresher nature of the cave water is attributed to the influence of considerably fresher rainwater directly infiltrating the cave environment from above. For comparison, the DWS reports an SEC value²¹ of 74 mS/m in April 2001.

¹⁹ The Target Water Quality Range (TWQR) for the DO level in aquatic ecosystems brackets the range 80–120% of saturation, and a DO level below the Minimum Allowable Value (MAV) defined by a 7-day mean minimum value of $>60\%$ (sub-lethal) in combination with a 1-day minimum value of $>40\%$ (lethal), is likely to cause acute toxic effects on aquatic biota (DWAF, 1996).

²⁰ High water temperatures combined with low DO levels can compound stress effects on aquatic organisms (DWAF, 1996).

²¹ It is not indicated whether this is a field- or laboratory-based value.

5.3 Visual Observations

Perhaps the most striking behaviour of mine water in the receiving drainages is the visual impact in the form of efflorescence. These take a variety of forms ranging from pipe scaling (Plate 6) to sludge deposits (Plate 7) and surface encrustation (Plate 8).

A chemical analysis of the pipe scaling precipitate shown in Plate 6 is presented in Table 53. The excessive sludge build-up in the Hippo Dam (Plate 7) was the result of in-stream liming²² of the raw mine water where it leaves the mine property. The dam is located ~ 700 m downstream of this position.

Plate 8 shows the dual precipitation of iron hydroxides and gypsum on the floodplain of the Tweelopie Spruit at its confluence with the Riet Spruit on the Glen Almond property. This position is located a distance of ~ 6.3 km downstream (north) of the Hippo Dam. The permanence of these precipitates is a function of the solubility of Fe(III) oxyhydroxides which, as is evident from the discussion in Text Box 5, depends on numerous factors.

5.4 Sediment Chemistry

Although *sensu stricto* not a mine water chemistry issue, the uptake/immobilisation of trace metals and metalloids in streambed sediments and the possible release/remobilisation of these through acidification, is a topical subject. This is informed by the outcome of a streambed sediment chemistry investigation carried out in the south-western portion of the study area originally reported by Venter et al. (2010) and augmented by Hobbs and Venter (2010). The study included an assessment of remobilisation (solubilisation) of metals with exposure of the sediment through laboratory batch leach (BL), toxicity characterising leaching procedure (TCLP) and acid rain (AR) leaching tests.

5.4.1 Chemical Composition

The sediment chemistry results determined from XRF analysis are presented in Venter et al. (2010). The elements are ranked in order of decreasing maximum detected value in Table 54 for each of the sites and samples. Site 1 (the Hippo Dam) supports the maximum concentration in 18 of the 32 analytes listed,²³ sharing arsenic with site 2. This site is located closest to the mine area. Site 2 (the Lion Camp dam) supports a further six of the elements. Site 6 (the Riet Spruit

²² In-stream liming funded by the DWS at a cost of R6.9 million was employed as an emergency water treatment measure in the period mid-March to mid-May 2010.

²³ Counting only analytes where the detection limit is exceeded in at least one instance.

Table 52 Surface water and groundwater field chemistry variables on 14/01/2011

| Station | Field Chemical Variable | | | | |
|---|---------------------------------|------------|----------|--------|-----------------------------|
| | pH ($-\log_{10}[\text{H}^+]$) | SEC (mS/m) | ORP (mV) | DO (%) | Temp ($^{\circ}\text{C}$) |
| Bloubank Spruit at Makiti (BB@M) | 6.0 | 21.9 | 48 | 106 | 21.1 |
| Zwartkrans Spring (ZSp) | 7.3 | 73.6 | -19 | 66 | 19.1 |
| A-furrow @ Lotz (upstream of KFD) | 6.2 | 24.0 | 44 | 101 | 21.1 |
| Koelenhof Farm dam (KFD) | 3.6 | 128.7 | 178 | 60 | 24.0 |
| Koelenhof Farm furrow downstream of KFD | 5.6 | 126.8 | 72 | 103 | 21.5 |
| Sterkfontein Cave (Main Lake) | 7.8 | 55.8 | -49 | 66 | 16.7 |

immediately before its confluence with the Bloubank Spruit supports five of the remaining six elements, notably including Fe and Mn. Site 3 supports the highest hafnium (Hf) concentration of the eight sites.

The high Fe and Mn levels at site 6 are not readily explained on the basis of proximity to the mine area, given the distance of ~ 12.5 km from the latter. It is possible that these circumstances reflect the historical impact of Percy Stewart WWTW effluent, which also contains elevated Fe and Mn concentrations (Table 11), discharged via the Blougat Spruit. Whether this also explains the elevated levels of Ba, Rb and Mo observed at this locality is unclear.

The maximum values range from $\sim 66\,000$ mg Al/kg (66 kg Al/t) to 1.6 mg Ge/kg (0.002 kg Ge/t) of sediment. A similar perspective on elements such as Cr, U, As and Pb yields values of 0.6 kg Cr/t, 0.1 kg U/t, 0.08 kg As/t and 0.05 kg Pb/t. The USACE (reported in O'Bourke et al., 2008) indicates an average in situ density for mud (clay) and silt in the range 1200 to 1400 g/L. Taking the higher value, then a cubic metre of this material covering an area of 4 m^2 to a uniform depth of 0.25 m contains up to ~ 800 g Cr, 140 g U, ~ 110 g As and 70 g Pb. These values reduce to ~ 330 g Cr, 36 g U, 34 g As and 25 g Pb for mean element values. Each 100 m of stream reach 2 m wide would therefore contain 16.5 kg Cr, 1.8 kg U, 1.7 kg As and 1.25 kg Pb in elemental terms. The measure to which complexation and other geochemical (e.g. redox) and biogeochemical (e.g. BSR) reactions will modify these values has not been considered.

Table 12 indicates that Awofolu et al. (2007) recorded maximum Zn, Ni and Cu values at site S2, the same locality as site 7 in Table 54. A comparison of the S2/site7 results reveals significant differences, primarily the order of magnitude lower values reported for all analytes by Awofolu et al. (2007). It is possible that a similar difference might apply to the other results. An explanation for the observed differences has not been sought.



Plate 8 View of the Tweelopie Spruit at its confluence with the Riet Spruit at Glen Almond showing the iron hydroxide and gypsum efflorescence on the flood plain at this juncture; the taller vegetation in the middle distance marks the stream channel

5.4.2 Solubility and Remobilisation

The leach tests sought to quantify the extractable (mobile) fraction of the total concentration of analytes (primarily metals/metalloids) by ICP-MS (inductively coupled plasma—mass spectrometry). The results are discussed by Venter et al. (2010) and Hobbs and Venter (2010). Their significance warrants a little further interrogation in this work. Except in the case of aluminium, the TCLP method generally mobilised the greatest fraction, followed by the AR and the BL methods. The BL test manifested an equal or greater Al solubilisation result.

The trace elements that showed the greatest propensity for solubilisation/remobilisation (mobility) are Al, Ba, Co, Cu, Mn, Ni, Sr and Zn (in simply alphabetic order). The magnitude of solubilisation of these analytes at each of the eight sampling sites is shown in Fig. 55. The apparently random pattern of the localities where elements are mobilised in greatest concentrations (Fig. 55) is in keeping with observations by Sahuquillo et al. (2002) that:



Fig. 55 Magnitude of solubilisation of trace elements from streambed sediments in the Bloubank Spruit system

Table 53 Chemical analysis of pipe scaling precipitate as seen in Plate 1 in Chapter “Physical Hydrology” (data courtesy of Helmholtz Centre for Environmental Research—UFZ, 2007)

| Analyte | Value | Analyte | Value | Analyte | Value |
|--------------------------------|--------------|-------------------------------|-----------|---------|---------|
| MgO | 0.50% | Cr | 200 mg/L | Br | <2 mg/L |
| Al ₂ O ₃ | 0.13% | P ₂ O ₅ | <200 mg/L | Rb | <2 mg/L |
| SiO ₂ | 0.55% | Sr | 79 mg/L | Pb | <2 mg/L |
| K ₂ O | <0.01% | Co | 59 mg/L | U | <2 mg/L |
| CaO | 29.00% | Zn | 37 mg/L | Th | <2 mg/L |
| TiO ₂ | 0.005% | V | <10 mg/L | Mo | <2 mg/L |
| Fe ₂ O ₃ | 2.30% | Y | 6 mg/L | Ag | <2 mg/L |
| S | 160 000 mg/L | As | 4 mg/L | Cd | <2 mg/L |
| Mn | 1540 mg/L | Cu | 3 mg/L | Hg | <2 mg/L |
| Ni | 213 mg/L | Zr | 3 mg/L | Sb | <2 mg/L |

Table 54 Ranking of analyte concentrations in sediment by maximum value (data from Venter et al., 2010)

| Analyte | Site and sample # | | | | | | | | | | Max value (mg/kg) |
|-----------------|-------------------|---------------|------------|------------|------|--------|--------|---------------|--------|------|-------------------|
| | 1 | | | 2 | 3 | 4 | 5 | 6 | 7 | 8 | |
| | 001 | 002 | 003 | 005 | 007 | 008 | 010 | 012 | 014 | 016 | |
| Al ¹ | 48 314 | 66,014 | 38,001 | 56,290 | 5897 | 41,198 | 13,037 | 50,322 | 17,144 | 5897 | 66,014 |
| Fe ² | 50 579 | 9658 | 53,900 | 60,900 | 4276 | 36,934 | 18,783 | 62,916 | 34,821 | 4276 | 62,916 |
| Mn ³ | 4565 | 213 | 77 | 7850 | 120 | 4349 | 1057 | 8747 | 8498 | 120 | 8747 |
| Zn | 216 | 72 | 460 | 943 | 430 | 261 | 53 | 56 | 81 | 12 | 943 |
| Ba | 531 | 120 | 122 | 173 | 549 | 307 | 101 | 751 | 446 | 21 | 751 |
| Ni | 313 | 134 | 720 | 497 | 607 | 196 | 38 | 111 | 68 | 6.7 | 720 |
| Cr | 603 | 425 | 290 | 401 | 367 | 339 | 223 | 413 | 214 | 95 | 603 |
| Co | 119 | 17 | 202 | 154 | 149 | 72 | 11 | 28 | 25 | 1.7 | 227 |
| Zr | 227 | 213 | 143 | 197 | 154 | 164 | 61 | 177 | 50 | 21 | 227 |
| Cu | 105 | 60 | 135 | 174 | 49 | 57 | 15 | 46 | 35 | 4.2 | 174 |
| V | 126 | 137 | 100 | 116 | 99 | 84 | 30 | 97 | 51 | 9.6 | 137 |
| Ce | 100 | 126 | 130 | 83 | 100 | 48 | <10 | 48 | 31 | <10 | 130 |
| U | 41 | 35 | 107 | 50 | 6.3 | 9.9 | <2 | 3.6 | <2 | <2 | 107 |
| As | 83 | 9.3 | 65 | 83 | 18 | 14 | 6.4 | 15 | 7.8 | <4 | 83 |
| Nd | 30 | 61 | 73 | 61 | 46 | 29 | 10 | 27 | 10 | <10 | 73 |
| La | 37 | 57 | 62 | 66 | 64 | 37 | <10 | 33 | 18 | <10 | 66 |
| Pb | 52 | 25 | 31 | 32 | 29 | 37 | 9.4 | 13 | 17 | 2.9 | 52 |
| Sr | 30 | 11 | 39 | 27 | 38 | 16 | 14 | 17 | 19 | 2.1 | 49 |
| Rb | 28 | 35 | 23 | 43 | 37 | 42 | 9.4 | 47 | 17 | 7.5 | 47 |
| Y | 18 | 31 | 36 | 41 | 26 | 18 | 4.8 | 18 | 7.6 | 1.9 | 41 |
| Sc | 16 | 19 | 17 | 17 | 16 | 14 | 5.1 | 16 | 7.4 | <3 | 19 |
| Ga | 13 | 16 | 11 | 14 | 13 | 11 | 3.7 | 12 | 4.9 | 2 | 16 |
| Sm | <10 | 12 | 15 | <10 | <10 | <10 | <10 | <10 | <10 | <10 | 15 |
| Nb | 10 | 13 | 8.9 | 10 | 9.4 | 9 | 3.6 | 9.6 | 4 | 2.5 | 13 |
| Th | 10 | 8.6 | 8.7 | 8.4 | 7 | 6.3 | <3 | 7.2 | 3.7 | <3 | 10 |
| Br | <2 | 3.4 | 8.4 | 11 | 4.3 | 3.7 | <2 | 4.8 | <2 | <2 | 8.4 |

(continued)

Table 54 (continued)

| Analyte | Site and sample # | | | | | | | | | | Max value (mg/kg) |
|---------|-------------------|------------|------------|------------|------------|-----|-----|------------|-----|-----|-------------------|
| | 1 | | | 2 | 3 | 4 | 5 | 6 | 7 | 8 | |
| | 001 | 002 | 003 | 005 | 007 | 008 | 010 | 012 | 014 | 016 | |
| Cs | 6.3 | <5 | 8.2 | <5 | <5 | 5.5 | <5 | <5 | <5 | <5 | 8.2 |
| Hf | 5.4 | 5.4 | 4 | 4.1 | 6.2 | 4.2 | <3 | 5.6 | <3 | <3 | 6.2 |
| Yb | <3 | 3.8 | 5.0 | 4.3 | <3 | <3 | <3 | <3 | <3 | <3 | 5.0 |
| Mo | 2 | <2 | <2 | <2 | <2 | <2 | <2 | 2.3 | <2 | <2 | 2.3 |
| Se | 1.2 | 1.2 | 2 | 1.8 | <1 | <1 | <1 | <1 | <1 | <1 | 1.8 |
| Ge | <1 | 1.6 | <1 | 1 | 1.5 | 1 | <1 | 1.5 | <1 | 1.3 | 1.6 |
| Bi | <3 | <3 | <3 | <3 | <3 | <3 | <3 | <3 | <3 | <3 | – |
| Tl | <3 | <3 | <3 | <3 | <3 | <3 | <3 | <3 | <3 | <3 | – |
| W | <3 | <3 | <3 | <3 | <3 | <3 | <3 | <3 | <3 | <3 | – |
| Ta | <2 | <2 | <2 | <2 | <2 | <2 | <2 | <2 | <2 | <2 | – |
| Maxima | 5 | 6 | 7 | 6 | 1 | 0 | 0 | 5 | 0 | 0 | |

¹Calculated from weight% concentration of Al₂O₃²Calculated from weight% concentration of Fe₂O₃³Calculated from weight% concentration of MnO

All values are as mg/kg

Bold text denotes location of analyte maximum value

Table 55 Estimate of soluble mass of individual elements per length of stream reach

| Analyte | Mean concentration in sediment (mg/kg) | Mass per Unit volume of sediment (kg/m ³) | Mass per unit length of stream reach (kg/m) | Mean solubility (%) | Soluble Mass per length of stream reach | |
|---------|--|---|---|---------------------|---|---------|
| | | | | | (kg/m) | (kg/km) |
| Al | 29 762 | 41.667 | 20.83 | 0.02 | 0.4167 | 417 |
| Mn | 4413 | 6.179 | 3.090 | 1.39 | 4.2944 | 4294 |
| Zn | 257 | 0.359 | 0.180 | 1.01 | 0.1813 | 181 |
| Ba | 360 | 0.504 | 0.252 | 0.22 | 0.0554 | 55.4 |
| Ni | 230 | 0.321 | 0.161 | 0.80 | 0.1284 | 128 |
| Cr | 332 | 0.465 | 0.233 | 0.01 | 0.0023 | 2.33 |
| Co | 70 | 0.098 | 0.049 | 1.26 | 0.0617 | 61.7 |
| Cu | 61 | 0.085 | 0.043 | 0.10 | 0.0043 | 4.25 |
| U | 22 | 0.031 | 0.016 | 0.12 | 0.0019 | 1.86 |
| Sr | 20 | 0.029 | 0.014 | 0.63 | 0.0090 | 8.99 |

- extractability is not proportional to the total metal content; and
- samples with similar metal concentrations can exhibit very different metal extractability.

The magnitude of resolubility evident in Fig. 55 varies according to total concentration and element. For example, Mn typically produces > 10 mg/L; Ni and Zn > 1 mg/L; Al, Ba and Co < 1 mg/L; and Cu and Sr < 0.1 mg/L. The

results provide context for concerns in regard to the remobilisation of trace/heavy metals by acidic mine water discharges in the receiving drainages, and the resulting impact on the aquatic ecosystem(s).

The information presented in Table 55 attempts to quantify (a) the individual element mass per cubic metre of sediment, (b) the mass per metre length of stream reach and (c) mass of element potentially solubilised from streambed sediments per unit stream reach. The element mass per unit



Sediment sampling in the Tweelopie Spruit

length of stream reach is based on the product of the mean concentration (mg/kg) of the seven sampling sites and a sediment density of 1400 kg/m^3 over a streambed area of 4 m^2 ($2 \times 2 \text{ m}$) to a uniform depth of 0.25 m .

5.5 Historical Observations

It is worth noting that the SO_4 concentrations in DWS monitoring boreholes²⁴ (Sect. 7.1) in the area were substantially higher in 1986 than in 2006. This is discussed in greater detail in Sect. 8.2.2. These circumstances, however, illustrate the fact that a mine water impact on the water resources of the area is not a recent or new phenomenon. It also illustrates the fact that under suitable conditions, a karst aquifer is a resilient and self-cleansing system in the medium to long term.

²⁴ These boreholes were originally established as potential emergency water supply production boreholes (Bredenkamp et al., 1986).

Physical Hydrogeology

Philip J. Hobbs, Harrison Pienaar, and Sebinasi Dzikiti

1 Introduction

An early reference to the hydrogeology of the study area is found in Cooke (1969) who states simply that “The water table is regional and the underground lake is 186 feet below the crest of the hill with the ape-man quarry.” The ape-man quarry is the location of the *Australopithecine* find ‘Mrs Ples’ at Sterkfontein Cave. The depth of 186 feet (56.7 m) places the ‘water table’ at an elevation of ~ 1430 m amsl for a crest elevation of ~ 1487 m amsl as interpolated from the 1:10,000 scale orthophoto map 2627BA5 Sterkfontein (2nd ed., 1987). Wilkinson places the top of the “hillock” at 1485 m amsl, and Martini et al. (2003) the top of the ‘small hill’ at 1491 m amsl. Recent information places the current (since ca. January 2011) elevation of the free water surface in Sterkfontein Cave at ~ 1439 m amsl (Sect. 3.2.1 and Fig. 10). The interpolated elevation of the Zwartkrans Spring located ~ 1300 m down-gradient/downstream (north-east) of the caves is ~ 1433 m amsl.

The most comprehensive regional groundwater study is considered to be that carried out in the mid-1980s by the then DWAF (Bredenkamp et al. 1986), primarily for the reason that it saw the execution of a regional gravimetric survey and the establishment of 38 large-diameter boreholes directed at evaluating the groundwater supply potential of portions of the dolomitic aquifers represented by the Steenkoppies and

Zwartkrans compartments. A test pumping programme found 18 of the exploration boreholes to be high-yielding (≥ 25 L/s), with a maximum recommended long-term yield of 100 L/s in three instances. The boreholes were sited primarily on the basis of gravimetric survey data (Sect. 4 in Chapter “Description of the Physical Environment”). From Table 1 it is evident that the Bredenkamp et al. (1986) study enumerated 326 private water supply boreholes that produced 131 groundwater level measurements (a conversion ratio of sites enumerated to water level measurements of only $\sim 40\%$), and 29 groundwater chemistry analyses. The poor conversion ratio of the latter ($\sim 9\%$ of the number of boreholes enumerated) is attributed to the volumetric focus of this and similar contemporary studies, with groundwater quality attracting only secondary consideration.

Bredenkamp et al. (1986) state that “Ground-water in the Zwartkrans compartment drains north-east to the Danielspruit and Kromdraai springs.” It is presumed that reference to the Danielspruit Spring should, in fact, read Danielsrust Spring. Although not mentioned, it must also be presumed that the much stronger Zwartkrans Spring reportedly delivering 258 L/s (Bredenkamp et al. 1986), also drains this compartment under circumstances where the Danielsrust and Kromdraai springs¹ reportedly delivered only 3 and 28 L/s respectively (Bredenkamp et al. 1986). A later

P. J. Hobbs: Deceased

P. J. Hobbs · H. Pienaar (✉)
Smart Places, Council for Scientific and Industrial Research,
Pretoria, South Africa
e-mail: hpienaar@csir.co.za

H. Pienaar
Hebei University of Engineering, Handan, China

S. Dzikiti
Department of Horticultural Science, Stellenbosch University,
Stellenbosch, South Africa
e-mail: sdzikiti@sun.ac.za

¹ Field data and information sourced in this study indicates that the Kromdraai Spring(s) referred to by Bredenkamp et al. (1986) and Holland (2009) are in fact the Plover’s Lake springs referred to in this report. This study identifies the Kromdraai Spring as a single groundwater source quite separate from the Plover’s Lake springs; the plural in regard to the latter denotes a grouping of springs and seeps, as opposed to a single source. The Kromdraai Spring discharge of ~ 307 L/s is considerably greater than the ~ 60 L/s of the Plover’s Lake springs. It is presumed, therefore, that the Kromdraai Springs referred to by Bredenkamp et al. (1986) and more recently by Holland (2008), Holland and Cobbing (2008) and Holland et al. (2009), in fact represent the Plover’s Lake springs. Both Bredenkamp et al. (1986) and Holland and Cobbing (2008) show the position of the Kromdraai Spring(s) to be coincident with the Plover’s Lake springs location. Further discussion of this ‘discrepancy’ is presented in Text Box 1.

Table 1 Groundwater data sources relevant to the COH obtained from the Bredenkamp et al. (1986) study

| Topocadastral farm | # Of private boreholes enumerated ^a | # Of water levels determined | # Of water quality determinations | # Of state boreholes drilled |
|--------------------------------|--|------------------------------|-----------------------------------|------------------------------|
| Vlakplaats 160IQ | 141 | 75 | 5 | 12 |
| Vlakdrift 163IQ | 86 | 21 | 1 | 3 |
| Sterkfontein 173IQ | 49 | 22 | 4 | 15 |
| Zwartkrans 172IQ | 7 | 3 | 1 | 0 |
| Reydlal 165IQ | 41 | 10 | 0 | 3 |
| Eljeesee agricultural holdings | 2 | 0 | 0 | 0 |
| Danielsrust 518JQ | 0 | 0 | 3 | 0 |
| Elandsvlei 249IQ | 0 | 0 | 3 | 0 |
| Kromdraai 520JQ | 0 | 0 | 8 | 0 |
| Rietfontein 522JQ | 0 | 0 | 4 | 0 |
| TOTAL | 326 | 131 | 29 | 33 |

^aData pertain only to the Zwartkrans Basin

study by Holland et al. (2009) reports discharges of 260, 3.2 and 371 L/s for the Zwartkrans, Danielsrust and Kromdraai springs, respectively. The order of magnitude discrepancy in regard to the Kromdraai Spring discharge is a confirmed typing error (K Withüser, personal communication). In an earlier issue paper compiled for the IUCN Karst Working Group, Holland et al. (2005) discuss the geology, surface water and groundwater aspects of the COH in very broad and qualitative terms. A revision of this paper subsequently appeared in print in the WRC/IUCN/SAKWG (2010) report.

The portion of the Riet Spruit upstream of the Oaktree area, including its tributary the Tweelapie Spruit, has recently been the subject of hydrogeological studies (Hobbs and Cobbing 2007; Hobbs 2008b) that have helped define the impact of acid mine drainage on the groundwater resources in the LoD in the upper reaches of this drainage, as well as downstream of its confluence with the Riet Spruit at Glen Almond. The study by Hobbs and Cobbing (2007) enumerated 54 geosites (6 springs, 7 mine shafts and 41 boreholes), the latter two providing 48 potentiometric measurements. These data facilitated the construction of a potentiometric contour map for the south-western portion of the study area (Fig. 1). The data also informed a critique of the Bredenkamp et al. (1986) description of compartments (and subcompartments) and groundwater drainage patterns (Hobbs and Cobbing 2007).

An inspection of aquifer transmissivity (T) data generated by the Bredenkamp et al. (1986) study from pumping tests performed on exploration boreholes in the Zwartkrans Basin indicates a zone of higher transmissivity as defined in Fig. 3. The zone is demarcated by 13 exploration boreholes that returned T-values greater than $\sim 1000 \text{ m}^2/\text{d}$ (Table 2). The geometry of this zone (Fig. 3), notably its width, slightly

more northerly position and SW–NE orientation, suggests that it coincides with the position of the chert-rich Monte Christo Formation and the generally greater water-bearing potential associated with this formation (Sect. 4 in Chapter “Description of the Physical Environment”). The Bredenkamp et al. (1986) study, however, also reports T-values as low as $1 \text{ m}^2/\text{d}$. This corroborates the substantial heterogeneity and anisotropy that characterises the karst aquifers of the region as found by numerous contemporary studies (e.g. Kafri et al. 1986; Leskiewicz 1986; Hobbs 1988a; Kuhn 1989) and synthesised by Hobbs (1988b). Transmissivity values ranging through five orders of magnitude ($< 10^1$ to $> 10^4 \text{ m}^2/\text{d}$) are common to these aquifers.

A study by Leyland et al. (2008) applied the concept of vulnerability mapping to the COH. This study built on various internationally recognised methods and approaches to develop a South African version that takes account of local conditions. An improvement on this approach, including the results of its application to the COH, is presented by Leyland (2010). An investigation by Holland (2007) applied the concept of groundwater resource directed measures (GRDM) to the COH.

The Holland (op. cit.) study reports estimated average annual groundwater recharge volumes of 16.8 mm^3 (from Bredenkamp et al. 1986) and 14.3 mm^3 (from Krige 2006) for the Zwartkrans Basin. The Holland (op. cit.) study puts forward its own estimates of $16.6 \text{ mm}^3/\text{a}$ for the Zwartkrans Basin and $13.4 \text{ mm}^3/\text{a}$ for the Tweefontein Basin. The veracity of these estimates is explored in the discussion on groundwater recharge in Sect. 2.12. In addition to the 26 geosites provided by the Hobbs and Cobbing (2007) study, Holland (2007) enumerated a further 41 geosites (boreholes) in the COH (including 16 DWS boreholes) for which potentiometric measurements are given.

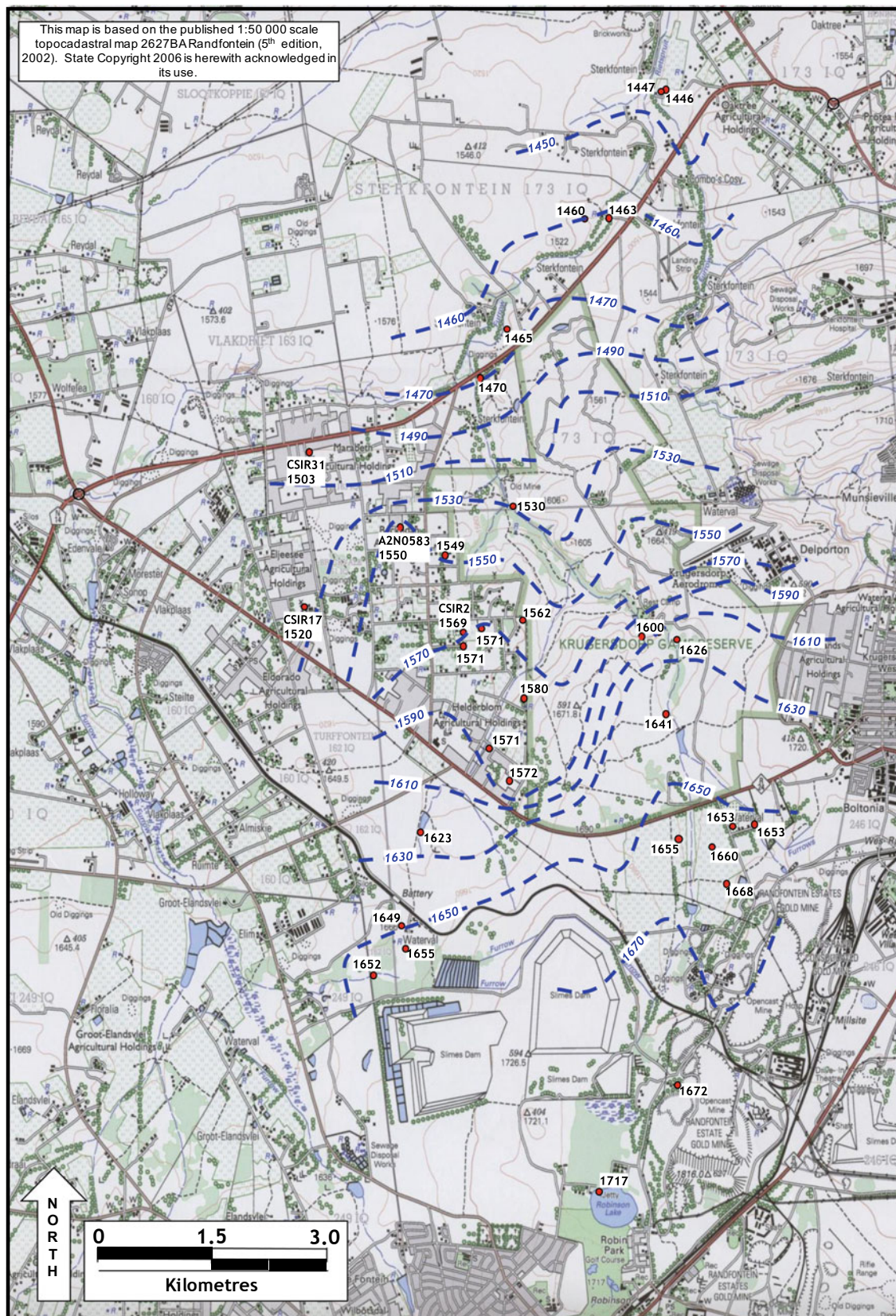


Fig. 1 Potentiometric map of the south-western portion of the study area (modified after Hobbs and Cobbing 2007)

Table 2 DWS exploration boreholes with transmissivity values greater than $\sim 1000 \text{ m}^2/\text{d}$ (from Bredenkamp et al. 1986)

| DWS exploration borehole # | DWS Geosite # | Coordinates | | Transmissivity (m^2/d) |
|----------------------------|---------------|-----------------------|------------------------|--|
| | | Latitude (dd. dddd°S) | Longitude (dd. dddd°E) | |
| G36320 | A2N0589 | <i>26.01632</i> | <i>27.70823</i> | 3000 |
| G36321 | A2N0593 | <i>26.02319</i> | <i>27.68882</i> | 13,900 |
| G36323 | A2N0590 | <i>26.02441</i> | <i>27.71527</i> | 20,500 |
| G36324 | A2N0592 | <i>26.03134</i> | <i>27.69753</i> | 11,200 |
| G36326 | A2N0588 | <i>26.03766</i> | <i>27.70903</i> | 3700 |
| G36327 | A2N0587 | <i>26.03668</i> | <i>27.71534</i> | 900 |
| G36328 | A2N0595 | <i>26.04684</i> | <i>27.67811</i> | 13,600 |
| G36329 | A2N0596 | <i>26.05139</i> | <i>27.67215</i> | 2400 |
| G36330 | A2N0597 | <i>26.05403</i> | <i>27.68415</i> | 5400 |
| G36331 | A2N0586 | <i>26.04761</i> | <i>27.70903</i> | 2100 |
| G36332 | A2N0598 | <i>26.06581</i> | <i>27.66622</i> | 4300 |
| G36335 | A2N0599 | <i>26.06585</i> | <i>27.66623</i> | 1500 |
| G36336 | A2N0581 | <i>26.07942</i> | <i>27.66628</i> | 1200 |

Note Italicised coordinate values denote DWS coordinates not verified in this study

2 Basin (Compartment) Definition

The phenomenon of compartmentalisation in the South African Neo-Proterozoic (2.64–2.50 Ga) telogenetic karst aquifers developed in diagenetically mature, well-compacted carbonate rocks, is well known (Martini and Kavalieris 1976). Osborne (2003) reports a similar phenomenon for the Palaeozoic (545–250 Ma) karst of eastern Australia. The phenomenon transforms a heterogeneous and anisotropic aquifer of considerable regional extent into smaller portions, allowing for more meaningful subregional analysis and understanding of the hydrogeologic environment. White (1993) uses the term ‘karstic ground-water basins’, recognition of which in the COH reveals a degree of compartmentalisation that contributes significantly to a more informed understanding of the groundwater environment.

The GRDM focus of the Holland (2007) study (Sect. 1) necessarily included the recognition of groundwater resource units (GRUs). These were identified as the Zwartkrans and Tweefontein compartments (Fig. 2). Both Holland (2007) and Holland and Cobbing (2008) accepted the subdivision of the Zwartkrans Basin into subunits defined by dykes originally put forward by Bredenkamp et al. (1986), and later adopted by JFA (2006), van Biljon (2006) and Krige (2009). Holland (2007) also presents a potentiometric map for the Zwartkrans Basin, which map identifies dykes (including sections of dykes) as variously representing actual or perceived impermeable or permeable hydrogeologic boundaries.

A later evaluation of the “West Rand Dolomite Compartments” by Holland (2009) for the DWS presents a more elaborate recognition of compartmentalisation of the karst

formations in the region (Fig. 2). The revised rendition still identifies three compartments represented by the Steenkoppies Basin in the south-west, the Zwartkrans Basin in the centre and the Tweefontein Basin in the north-east, each of these being defined as groundwater management areas (GMAs). The GMAs are subdivided into groundwater management units (GMUs), each of which is further subdivided into GRUs. The scope of this subdivision, which is based simply on the geographic distribution of mapped geological structures (i.e. not considering groundwater potentiometry, spring locations and discharges, groundwater chemistry, etc. to any significant degree), is reflected in Table 3.

The tenuous and arguably over-complicated (consider the 51 karst GRUs as per Table 3) definition of the karst environment in the study area in terms of compartmentalisation (both compartments and subcompartments) by Holland (2009), and replicated by Meyer (2014), precipitated closer inspection. Another factor prompting such review is the seemingly different interpretation of the term compartment by Holland (2009). The review focusses on the karst environment that supports the COH property, and therefore excludes the Steenkoppies Basin. The latter has been the subject of a study by Holland et al. (2009) which has adequately elucidated the karst environment of this compartment. The outcome in regard to the karst environment of the less studied and more poorly understood WHS property, presented in Fig. 3, recognises a total of eleven compartments,² two of which comprise subcompartments. The revised physical hydrogeologic layout is informed by a

² Distributed between the Zwartkrans and Tweefontein compartments of Holland (2009), and excluding the Steenkoppies Compartment.

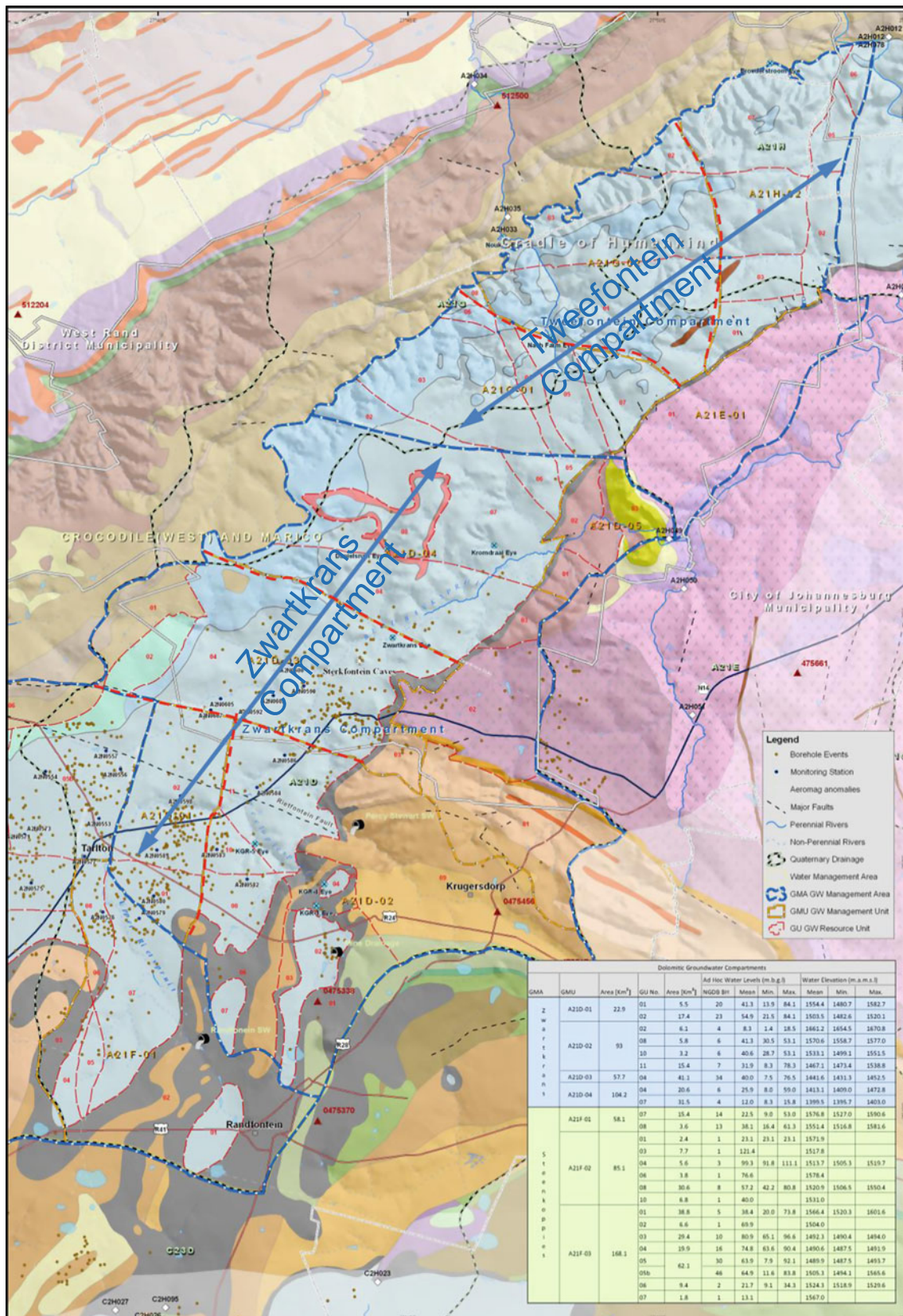


Fig. 2 Previous definition of dolomitic basins/subcompartments as proposed by Holland (2007), and later modified by Holland (2009) and replicated by Meyer (2014)

Table 3 Enumeration of compartment and subcompartment definition from Fig. 2

| Groundwater management area | Number of subdivisions | Groundwater resource unit | |
|-----------------------------|------------------------|--|-----------|
| | | Groundwater management unit (undifferentiated ^a) | |
| | | Karst | Non-karst |
| Steenkoppies Basin | 3 | 20 | 7 |
| Zwartkrans Basin | 5 | 15 | 11 |
| Tweefontein Basin | 4 | 16 | 1 |
| Total | 12 | 51 | 15 |

^a Undifferentiated in regard to ‘karst’ or ‘non-karst’ environment implies a ‘mixed’ hydrogeologic regime, i.e. management units straddle lithologic boundaries to encompass different geologic strata

combination of groundwater level data, spring locations and discharges, groundwater chemistry and geological structures. It is described and discussed in greater detail in the following sections, with the schematic layout (Fig. 3) providing a visual reference for this discussion.

2.1 Zwartkrans Basin

The Zwartkrans Basin is drained by the Zwartkrans Spring located ~ 1.4 km north-east (downstream) of Sterkfontein Cave on the farm Zwartkrans 172IQ. The compartment spans an area of ~ 9800 ha bounded in the south-west by the Tarlton Dyke system, in the north-east by the Zwartkrans Dyke, and along the south-eastern boundary by the geological contact between the Malmani Subgroup and Witwatersrand Supergroup quartzitic strata. To the north-west, the contact between the Malmani Subgroup dolomite and the overlying Pretoria Group sedimentary strata represents a pseudo-boundary under circumstances where the dolomite continues at depth beneath the latter.

The Zwartkrans Basin was subdivided by Bredenkamp et al. (1986) into nine subcompartments. The subdivision was based mainly on sharp transitions in water level over short distances, with partial verification of bounding dyke structures using ground and airborne geophysical information. This reasoning rests on the premise of very weak/flat hydraulic gradients in each subcompartment. These were also put forward by Bredenkamp et al. (1986) as the reason for not compiling a water level contour (potentiometric) map. It is notable, however, that the difference in ‘representative water level’ between five contiguous subcompartments is ~ 70 m over a distance of only ~ 8 km. This is considered to be an artefact of the comparatively sparse set of water level data used to define the subcompartments, and which raises doubt over the recognition of an overly disrupted groundwater flow pattern informed by perceived and unverified barrier boundaries (Hobbs and Cobbing 2007). For example, one of the Bredenkamp et al. (1986) subcompartments is recognised in this study as a separate compartment, namely the Krombank Basin (Sect. 2.2).

A simplified subdivision of the Zwartkrans Basin is proposed. This comprises only three subcompartments as described in the following sections.

2.1.1 Vlakdrift Subcompartment

The Vlakdrift Subcompartment (~ 2360 ha) forms the upper reaches of the Zwartkrans Basin. Its western margin is the Tarlton East Dyke that marks the boundary with the Steenkoppies Basin to the west (Holland et al. 2009). The eastern boundary is represented by the roughly N–S striking Sterkfontein Dyke, the northern boundary by the E–W striking Vlakdrift-1 Dyke, and the southern margin by the lithological contact with the older Witwatersrand Supergroup. Both the Sterkfontein Dyke³ and the Vlakdrift-1 Dyke are recognised by Holland et al. (2009) as hydrogeological boundaries. An upward step in water level elevation of 45–50 m from west to east across the Sterkfontein Dyke characterises the influence of this boundary on the potentiometric surface in the southern portion of the Vlakdrift Subcompartment (1a) and the adjoining Sterkfontein Subcompartment (1b). This is reflected in the groundwater elevations in boreholes CSIR17 (1520 m amsl) and CSIR2 (1569 m amsl), and CSIR31 (1503 m amsl) and A2N0583 (1550 m amsl) as shown in Fig. 1.

The main recharge to this subcompartment is from rainfall, although the anthropogenic (and allogenic) contribution from excess surface flow via the upper Riet Spruit past Tarlton, as is described in Sect. 5.2.1 in Chapter “Physical Hydrology”, represents a significant secondary input. The outflow from this subcompartment northwards into the Zwartkrans Subcompartment is a postulated subsurface drainage that coincides with a zone of higher transmissivity as described in Sect. 1 and illustrated in Fig. 3, as well as

³ Note that Holland et al. (2009) assigned the name Beckedan Barrier to the Vlakdrift-1 Dyke, whereas the names as applied in this study (Fig. 63 in Chapter “Chemical Hydrology”) conform to those assigned by Bredenkamp et al. (1986). It also seems probable that the western extension of the Vlakdrift-1 Dyke might form part of the Maloney’s Eye Dyke recognised by Bredenkamp et al. (1986).

significant grike features that intersect the Vlakdrift-1 Dyke (Sect. 6 and Fig. 18).

2.1.2 Sterkfontein Subcompartment

The Sterkfontein Subcompartment (~ 2450 ha) forms the south-central portion of the Zwartkrans Basin. It receives primarily allogenic recharge in the form of mine water delivered via the Tweelopie Spruit. The boundaries of this subcompartment are defined by the Sterkfontein Dyke in the west, the Vlakdrift-1 Dyke to the north, and the lithologic contact with the older Witwatersrand Supergroup strata to the south-east. The discontinuity in the potentiometric surface (water table) in the Oaktree area created by the Vlakdrift-1 Dyke is revealed by the following:

- potentiometric elevation differences of 15–20 m between boreholes AM1 and ME1 (at 1467 m amsl) to the south, and boreholes PD1 and CSIR9 (at 1450 m amsl) to the north; and
- the apparent northerly displacement of the mine water impact on karst groundwater quality (as revealed by elevated SEC and SO_4 levels) in the Oaktree area.

The outflow of this subcompartment over/through the Vlakdrift-1 Dyke into the Zwartkrans Subcompartment is similar to that of the adjoining Vlakdrift Subcompartment, namely subsurface flow via a zone of higher transmissivity that intersects the structure (Fig. 3). The principal groundwater flow vector at this position is north-northeast, and is considered to be partly driven by an artificial groundwater ‘mounding’ effect created by a combination of (a) the accumulation of infiltrating mine water lost from the Riet Spruit as described in Sect. 5.2.1 in Chapter “Physical Hydrology” and (b) this water damming up behind the Vlakdrift-1 Dyke (Fig. 4). The latter forms the boundary between the Sterkfontein and Zwartkrans subcompartments (see also Fig. 3 and Fig. 18), and influences the elevation of the water table either side of this feature as is shown for the years 2007 and 2011. The ~ 12 m step in water level from west to east across the Zwartkrans Dyke is also illustrated.

The profile further shows the intersection of the potentiometric surface with the land surface (represented by the riverbed of the Bloubank Spruit) at the downstream end of the Zwartkrans Subcompartment. This supports the observation (Sect. 2.1.3) that the Zwartkrans Subcompartment is drained not only by the Zwartkrans Spring, but also by groundwater losses to the effluent section of the Bloubank Spruit stream channel for some distance upstream of the spring. These circumstances also explain the difficulty in accurately gauging the discharge of the Zwartkrans Spring, and therefore also the wide range of values obtained for this feature (Sect. 4.1).

2.1.3 Zwartkrans Subcompartment

The Zwartkrans Subcompartment covers $\sim 51\%$ (~ 4990 ha) of the Zwartkrans Basin. Its boundaries are defined by the Vlakdrift-1 Dyke to the south, the lithologic contact with the younger Pretoria Group strata to the north-west, the lithologic contact with the older Witwatersrand Supergroup strata to the south-east, and the Zwartkrans Dyke to the north-east. The latter gives rise to the Zwartkrans Spring. It also gives rise to diffuse (and difficult to quantify) seepage in an area on the opposite (left) bank that is collected and channelled into trout dams on the Boland Farm property on Danielsrust 518JQ.

Groundwater rest levels measured in three boreholes that straddle the dyke structure reveal that it marks a step down in groundwater level, from west to east across the structure, of ~ 13 m. The potentiometric surface in the Zwartkrans Basin immediately upstream of the dyke occupies an elevation of ~ 1433 m amsl (the approximate elevation of the Zwartkrans Spring), and an elevation of ~ 1420 m amsl in the Krombank Basin (Sect. 2.2) immediately downstream of the dyke. It is postulated that the zone of higher transmissivity (Fig. 3) might extend in a north-easterly direction to intersect the Zwartkrans Dyke, thus also providing a subsurface outflow component into the Krombank Basin.

An equally over-looked discharge component is represented by the intersection of the water table with the streambed of the Bloubank Spruit for some distance (~ 2 km) upstream of the Zwartkrans Spring. Flow measurements described in Sects. 5.2.1 and 5.2.3 in Chapter “Physical Hydrology” indicate a surface water ‘gain’ of as much as 23 ML/d (266 L/s) in this reach of the Bloubank Spruit. This ‘gain’ is considered to be provided by diffuse in-channel (streambed) groundwater resurgence, in contrast to the ‘point-source’ off-channel Zwartkrans Spring. Note in this regard that monitoring borehole GP00314 sunk within 50 m of the Bloubank Spruit ~ 700 m upstream of the Zwartkrans Spring revealed unconsolidated sedimentary material down to 14 m bs, with a water table at ~ 2 m bs, i.e. a saturated thickness of ~ 12 m. Together with the ~ 136 L/s discharge of the Zwartkrans Spring (Sect. 4.1 and Table 13), the aggregate groundwater discharge from the Zwartkrans Subcompartment exceeds 300 L/s, and on occasion possibly even 400 L/s. Given the hydraulic continuity with the ‘upstream’ Sterkfontein and Vlakdrift subcompartments, this discharge represents that of the Zwartkrans Basin as a whole. For this reason, it necessarily excludes the potential contribution ‘lost’ to groundwater abstraction, e.g. for agriculture, in this compartment. Estimates of this use range from ~ 9 to $26 \text{ mm}^3/\text{a}$ (Sect. 9), which equate to values of ~ 285 to 824 L/s.

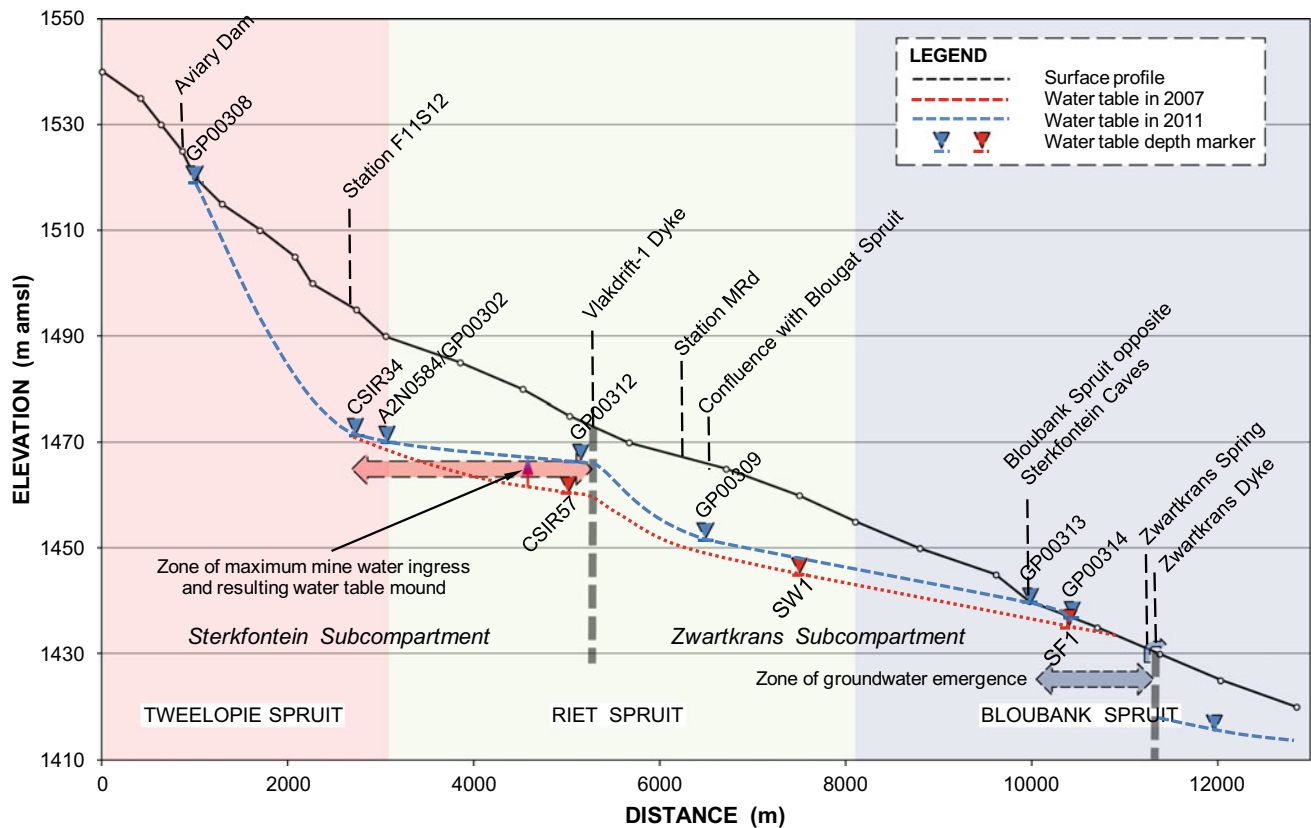


Fig. 4 Longitudinal surface and water table profile along the course of the Tweelopie, Riet and Bloubank Spruits from Kemp's Cave in the Krugersorp Game Reserve to beyond the Zwartkrans Spring

Although the Zwartkrans Subcompartment hosts the Sterkfontein Cave fossil site, the latter is located along the south-eastern margin of this subcompartment. It is postulated that this places the Sterkfontein fossil site to the south and outside the main groundwater flow vector that collects the subsurface discharge of both the Vlakdrift and Sterkfontein subcompartments, and directs these towards the Zwartkrans Spring along the trace of the 'dry' Bloubank Spruit upstream of its confluence with the Riet Spruit. These circumstances recognise the possible existence of a subsurface 'thalweg'⁴ associated with the relict surface expression of the ephemeral upper reaches of the Bloubank Spruit. The most visual discharge feature of this subcompartment and its contributing upstream subcompartments remains the Zwartkrans Spring (Sect. 4.1).

⁴ See GLOSSARY. Used here to describe a preferential subsurface flowpath such as a large channel (or network of channels) that might develop and occur in a karst aquifer and act as a "subsurface groundwater stream" (from Martini, 2006, p 664) or a "master drain" (after White, 1993).

2.2 Krombank Basin

This compartment (total area ~ 5080 ha) comprises two subcompartments identified as the Kromdraai Subcompartment drained by the Plover's Lake springs and the Kromdraai Spring located on the farm Kromdraai 520 JQ, and the Bloubank Subcompartment that straddles the Bloubank Spruit. The name 'Krombank' (a combination of the names Kromdraai and Bloubank) used to describe this compartment denotes the degree of hydraulic continuity considered to exist between these subcompartments.

2.2.1 Kromdraai Subcompartment

The Kromdraai Subcompartment covers an area of ~ 3470 ha (excluding the footprint of the separate superimposed barré associated with the Danielsrust Basin) bounded to the south-west by the Zwartkrans Dyke, to the north-west by the geological contact between the Malmani Subgroup dolomite and the overlying Pretoria Group sedimentary strata, to the north-east by the Twin Dyke structure, and along the south-eastern boundary by the Plover's Lake Sill, a north-westerly dipping syenite intrusion in the dolomite. This sill marks the common boundary with the Bloubank Subcompartment.

The potentiometric surface intersects the land surface at an elevation of ~ 1419 m amsl at the Plover's Lake Spring (s). The discharge of these springs (~ 60 L/s) is, however, too small to account for the postulated surface extent of this subcompartment. It is considered probable that structural discontinuities along the trace of the Plover's Lake Sill form additional flow paths for groundwater discharge from this subcompartment into the Bloubank Subcompartment. The fault zone on which the ~ 307 L/s Kromdraai Spring (Sect. 4.3) is located, almost certainly represents one such outlet. It is likely that this subcompartment receives a proportion of its recharge from the Zwartkrans Basin. This is explored in Sect. 2.12

2.2.2 Bloubank Subcompartment

The Bloubank Subcompartment straddles the course of the Bloubank Spruit for a distance of some 8 km from the Zwartkrans Dyke to where this drainage leaves the karst environment in the vicinity of Brookwood Trout Farm. Encompassing an area of ~ 1610 ha, its south-eastern boundary is formed by the contact between the Malmani Subgroup dolomite and the older Witwatersrand Supergroup quartzitic strata. The north-western margin is formed by the Plover's Lake Sill intrusion that follows a trace which runs subparallel to that of the south-eastern boundary. This subcompartment receives:

- the overflow from the Zwartkrans Basin via the Zwartkrans Spring and groundwater resurgence in the Bloubank Spruit upstream of the Zwartkrans Spring (Sect. 5.2.3 in Chapter "Physical Hydrology", Sect. 7.4.1, and Fig. 32 in Chapter "Physical Hydrology");
- discharge from the Kromdraai Subcompartment along its north-western margin via structural discontinuities in the bounding Plover's Lake Sill (Sect. 2.2.1); and
- infiltrating river water from losing sections of the Bloubank Spruit between the Zwartkrans and Kromdraai springs.

As shown in Table 4, the combined discharge of the Kromdraai and Plover's Lake springs (339 L/s excluding the Danielsrust Spring contribution), returns an unrealistically high equivalent recharge of $\sim 30\%$ of MAP as representing the 'recharge input' on the Krombank Basin footprint of 5080 ha. Circumstances that explain this anomaly are discussed in Sect. 2.12.

Anomalous groundwater rest level elevations in the extreme north-eastern corner of the subcompartment (e.g. boreholes VW1 and PvW1) are attributed to further sub-compartmentalisation formed by the NW–SE striking diabase Rietfontein Dyke at this location (Fig. 3). The small area (~ 30 ha) encompassed by this subcompartment,

however, negates recognition thereof as an important part of the hydrogeologic regime in the COH, and it has been aggregated with the Bloubank Subcompartment.

2.3 Danielsrust Basin

Located on the farm Danielsrust 518JQ, the Danielsrust Basin defines a perched karst aquifer (barré⁵) that supports a groundwater rest level located at an elevation of > 1490 m amsl, i.e. 50–70 m above the 1420–1440 m amsl elevation in the regional karst aquifer defined by the Kromdraai Basin. The cross-section in Fig. 17 illustrates the postulated hydrogeological relationship that describes the position of this groundwater system in the regional hydrogeological framework. The footprint of this compartment is defined by the dolerite outcrop (not recognised by Obbes 2001) which forms a quasi 'ring' structure (Fig. 3), and straddles the boundary between the farms Danielsrust 518JQ (west) and Sterkfontein 519JQ (east). This structure, measured around its outer perimeter to accommodate its entire footprint on the Kromdraai Subcompartment, encompasses an area of ~ 740 ha. It is postulated that the dolerite forms an impermeable basin that serves to contain groundwater which decants naturally at the Danielsrust Spring with an elevation of ~ 1490 m amsl. According to the landowner, the long-term discharge of this spring is 100,000 L/h (28 L/s) (P van der Merwe, personal communication). The establishment of three water supply boreholes within this compartment has added an artificial loss component to the water balance of this aquifer.

In order for the ~ 740 ha extent of the Danielsrust Basin to support a spring discharge of 28 L/s, it would be required that rainfall recharge amounts to $\sim 17\%$ of a mean annual precipitation (MAP) of 710 mm. This value compares favourably with the results of four different calculation methods used in the earlier study by Bredenkamp et al. (1986). These yielded recharge values in the range 15–21% of an MAP of 630 mm. Further support for recognition of the Danielsrust Basin as a distinctly separate hydrosystem is found in water chemistry data. Firstly, the SEC field values of 23–26 mS/m associated with the Danielsrust Spring water is notably lower than the 40–46 mS/m associated with the dolomitic groundwater in the wider area. Secondly, the stable isotope results (Holland 2007 and this study as reported in Sect. 5 in Chapter "Physical Hydrology") compare favourably with those of 'pristine' karst groundwater in the study area.

The above circumstances place all of the responsibility for the protection of this groundwater resource on those landowners of property located within the Danielsrust Basin. The greatest threat to this resource is considered to be that

⁵ See GLOSSARY.

Table 4 Summary information of groundwater compartments in the COH

| Basin | Sub-compartment | Extent (ha) | | Outflow feature | Discharge | | Recharge | | |
|-----------------|-----------------|-------------|------|-------------------------|-----------|------------------|--------------------|-------------------|------|
| | | | | | (L/s) | (ML/d) | mm | %MAP ^a | |
| Zwartkrans | | | 9800 | Zwartkrans Sp. | | 136 | 11.75 | 130 | ~ 18 |
| | | | | Resurgence ^b | | 270 | 23.33 | | |
| Krombank | Kromdraai | 3470 | 5080 | Plover's Lake Sp. | 60 | 339 ^c | 29.23 ^c | 210 | ~ 30 |
| | Bloubank | 1610 | | Kromdraai Sp. | 279 | | | | |
| Danielsrust | | | 740 | Danielsrust Sp. | | 28 | 2.42 | 119 | ~ 17 |
| Uitkomst | | | 2860 | Nash Sp. | | 130 | 11.23 | 143 | ~ 20 |
| Twefontein | | | 1160 | Twefontein Sp. | | 30 | 2.59 | 81 | ~ 11 |
| Rietfontein | | | 540 | Aquamine Sp. | | < 2 | < 0.17 | 11 | ~ 2 |
| Diepkloof | | | 3800 | Nouklip Sp. | | 143 ^d | 12.36 ^d | 119 | ~ 17 |
| Motsetse | | | 270 | Cradle Sp. | | 2 | 0.17 | 23 | ~ 3 |
| Rhenosterspruit | | | 850 | Not established | | – | – | – | – |
| Kalkheuvel | | | 720 | Barlow Sp. | | 2 | 0.17 | 48 | ~ 1 |
| Broederstroom | | | 1810 | Broederstroom Sp. | | 21 | 1.81 | 49 | ~ 7 |
| | | | | Lesedi Sp. | | 2 | 0.17 | | |
| | | | | Anderson Sp. | | 5 | 0.43 | | |
| (see Fig. 3) | | | 450 | Not established | | – | – | – | – |
| TOTAL AVERAGE | | 28,080 | | | 1110 | | 95.83 | 93 | 12.6 |

^a Mean annual precipitation = 710 mm

^b See discussion in Sect. 4.1 regarding groundwater resurgence upstream of the spring

^c The Plover's Lake and Kromdraai springs are combined to represent the theoretical groundwater discharge of the Krombank Basin excluding the autogenic recharge of 28 L/s contributed by the Danielsrust Spring

^d Excludes the autogenic recharge of 30 L/s contributed by the Twefontein Spring

associated with on-site sanitation facilities, particularly those which carry a potentially elevated load. The greatest part of the compartment supports game farming, which affords most of this resource an excellent measure of protection from pollution. However, the adjacent commercial tourist lodge and camp facility on the farm Sterkfontein 519JQ represents a concern that needs to be considered.

The location of the lodge near the 'downstream' end of the compartment means that much of this resource (i.e. the area located upstream of the camp) is 'immune' to contamination from this source. This does not apply to the spring located only ~ 500 m down-gradient of the lodge. Furthermore, abstraction from the lodge water supply borehole located immediately upstream of the spring exacerbates this threat by drawing groundwater closer. Although the spring does not currently serve a water supply function for any purpose, protection of its quality is mandated by Sect. 19 of the NWA (Act No 36, 1998), "Prevention and remedying effects of pollution.", which requires of a landowner, person in control of land or person occupying or using land to take all reasonable measures to prevent pollution of a water resource from occurring, continuing or recurring. These circumstances identify the Danielsrust Basin as a candidate groundwater management unit (GMU).

Although recognition of the Danielsrust Basin as a 'stand-alone' groundwater resource unit is fully justified, it could also be aggregated with the Krombank Basin in regard to both extent and yield/recharge. This is possible because the full discharge of the Danielsrust Spring drains into the Kromdraai Subcompartment of the Krombank Basin, manifesting an autogenic recharge component that contributes to the discharge of this karst basin. The Krombank and Danielsrust compartments are listed as separate basins in Table 4.

2.4 Uitkomst Basin

This compartment encompasses the southern portion of the ~ 7300 ha John Nash Nature Reserve. The Nash Spring (JNNR3), located at an elevation of ~ 1360 m amsl, represents the most logical outlet of this compartment. The ~ 130 L/s discharge of this spring suggests a substantial catchment area. A provisional assessment recognises the triangular footprint defined in Fig. 3 as a suitable description of this compartment spanning ~ 2860 ha (Table 4). It is named the Uitkomst Basin, as ~ 55% of its postulated extent is located on the farm Uitkomst 499 JQ. The spring

discharge of ~ 130 L/s represents 21% of an MAP of 710 mm. The compartment boundaries are defined by the Twin Dyke structure in the south, the geological contact between the Malmani Subgroup dolomite and the overlying Pretoria Group sedimentary strata along the north-western margin, and the NW–SE striking Rietfontein Dyke to the north-east.

The Nash Spring elevation of ~ 1360 m amsl (Table 9) ties in with the groundwater elevation of 1365 m amsl reported for the borehole MVR1 on the Moon Valley Ranch property (Ptn 38 of Rietfontein 522JQ) in the upper reaches of this compartment. Although these geosites are located at distance of ~ 3.8 km apart, they are both located in the Skeerpoort River catchment (A21G). Data sourced from station MVR1 and station RLGR5 on the Rhino and Lion Game Reserve property in the Kromdraai Subcompartment to the south, reveals a difference in groundwater level elevation of ~ 55 m across the Twin Dyke structure that separates these two stations and compartments (Figs. 3 and 17). This is an abnormally large difference between contiguous karst compartments, and indicates as complete a hydraulic separation as might reasonably be conceived in practical terms.

2.5 Tweefontein Basin

The enumeration of the Tweefontein and Nash springs in the John Nash Nature Reserve (Sects. 4.6 and 4.8) and the Cradle Spring in the Motsetse Nature Reserve (Sect. 4.10) provide a better definition of groundwater elevations (and associated compartmentalisation) in the central north-eastern portion of the COH. This area is characterised by a paucity of hydrogeological information, the scarcity of boreholes in this largely pristine natural landscape contributing to the poor definition of groundwater rest level elevations in this portion of the study area. This limitation is countered by the lack of groundwater abstraction via boreholes, so that the spring discharges approximate the full delivery of such karst systems.

It is postulated that the Tweefontein Basin encompasses a much smaller area than suggested by previous studies. For example, Holland (2007) and Holland and Witthüser (2009) indicate this compartment to extend from the Twin Dyke system north-eastwards all the way to almost 27.9°E , a longitude that coincides with the eastern extremity of Hartbeespoort Dam north of the village of Broederstroom, and encompassing an area of $\sim 12,750$ ha. New information such as quantified spring discharges and spring surface elevations (that serve as a proxy for the lowest potentiometric surface elevation of the contributing compartment), together with springwater chemistry (including isotope data) and likely recharge rates, support a redefinition of this compartment as shown in Fig. 3.

The Tweefontein Spring elevation of ~ 1450 m amsl is some 30 m above the potentiometric surface in the Krombank Basin to the south-west. It is hypothesised on the basis of the relatively small discharge (~ 30 L/s) of the Tweefontein Spring (Sect. 4.6), that it drains a shallow aquifer of limited surface extent described by the ~ 1160 ha triangular footprint shown in Fig. 3. Under these circumstances, the spring discharge of ~ 30 L/s represents 12% of an MAP of 710 mm. It is proposed, therefore, that the boundaries of this compartment are defined by the NW–SE striking Rietfontein Dyke to the west, the Tweefontein Dyke to the north-east, and the northern extension of the syenitic Plover's Lake Sill along the south-eastern margin. The tritium concentration of $\sim 3 \pm 0.3$ TU in the springwater (Sect. 7.5 in "Chapter Chemical Hydrogeology") suggests that this compartment is also characterised by comparatively recent and rapid rainfall recharge and a 'shallow' subsurface circulation regime (see Footnote 8 in Chapter "Chemical Hydrogeology").

In light of the above, it is postulated that the Tweefontein Basin located to the north-east of the Krombank Basin constitutes a shallow aquifer of comparatively limited extent. It is similar to the Danielsrust Basin in that its discharge via the Tweefontein Spring also provides autogenic recharge, in this instance northwards into the Diepkloof Basin (Sect. 2.7) drained by the Nouklip Spring.

2.6 Rietfontein Basin

The Rietfontein Basin (~ 540 ha) comprises a rectangular footprint adjoining the south-eastern margin of the Tweefontein Basin. It therefore shares the northern extension of the Plover's Lake Sill as the common boundary with the Tweefontein Basin to the north-west. Although the Aquamine Spring represents the most logical discharge (outflow) of groundwater from this compartment, the springflow of < 2 L/s does not adequately reflect the extent of the contributing karst aquifer. Not considered to be of consequence to the broader aims and objectives of this study, these circumstances nevertheless might attract further investigation in future hydrogeologic studies.

2.7 Diepkloof Basin

This compartment represents the comparatively poorly defined karst environment in the north-eastern portion of the COH. The north-westerly groundwater flow pattern in the Diepkloof Basin is based mainly on the surface drainage pattern that is characterised by deeply incised streams such as the Snake Stream and the Grootvlei Spruit. The elevation of the Nouklip Spring (~ 1330 m amsl) in the lower reaches of the Grootvlei Spruit supports this hypothesis. The

substantial yield of this spring (Sect. 4.7) again reflects a highly transmissive aquifer of substantial surface extent.

A provisional assessment recognises the rectangular footprint defined in Fig. 3 as a suitable geometric description of this compartment spanning ~ 3800 ha. This recognises the Tweefontein Dyke as the southern boundary, the E–W striking Hartbeesthoek Dyke as the northern boundary, the N–S striking Krokodilberg Dyke as the eastern boundary, and the geological contact between the Malmani Subgroup dolomite and the overlying Pretoria Group sedimentary strata the western margin. The mean spring discharge of 143 L/s^6 (Sect. 4.7) represents 17% of an MAP of 710 mm.

2.8 Motsetse Basin

The Motsetse Basin (name coined in this study) forms a small catchment (Fig. 3) located in the Motsetse Nature Reserve. It encompasses only ~ 270 ha, and is drained by the Cradle Spring at a rate of $\sim 2 \text{ L/s}$. This discharge represents $\sim 3\%$ of an MAP of 710 mm. Circumstances that might explain this anomalously low recharge value are discussed in Sect. 4.10. As this compartment is largely enclosed within a proclaimed nature reserve, its preservation in a natural state is reasonably well ensured.

2.9 Rhenosterspruit Basin

This compartment of ~ 850 ha is located in the north-eastern portion of the COH (Fig. 3) where the karst environment is poorly defined in terms of its hydrogeology. This is attributable to the more populated nature of this landscape, where numerous properties support residences mainly reliant on their own borehole water supplies for general domestic use. Abstraction for this use impacts negatively on the yield of springs that would drain this karst basin naturally. Not considered to be of consequence to the broader aims and objectives of this study, these circumstances nevertheless might attract further investigation in future hydrogeologic studies.

The north-western boundary of this compartment is associated with a set of SW–NE striking diabase sill intrusions, its western boundary with the Krokodilberg Dyke, its eastern boundary with the Rhenosterspruit Dyke, and its south-eastern boundary with the contact between the Malmani Subgroup dolomite and the older undifferentiated igneous strata.

2.10 Kalkheuwel Basin

Encompassing an area of ~ 720 ha, this compartment is drained by the Barlow Spring ($\sim 2 \text{ L/s}$) located in the north-eastern corner of this compartment (Fig. 3). The E–W striking Hartbeesthoek Dyke that separates the Barlow Spring from the Anderson Spring to the north, forms the northern boundary of this compartment. Its western boundary is formed by the Krokodilberg Dyke, its eastern boundary by the Rhenosterspruit Dyke, and its south-eastern boundary by the set of SW–NE striking diabase sill intrusions that forms the north-western boundary of the Rhenosterspruit Basin (Sect. 2.9).

The compartment hosts numerous residential properties (mainly associated with the Kalkheuwel West Estate) reliant to a large extent on own borehole water supplies for potable and general domestic water use. The impact of this use on natural spring discharge is seen in the observation that the flow of the Barlow Spring falls significantly short of the natural yield ($\sim 20\text{--}35 \text{ L/s}$) that might be expected for a recharge of $17 \pm 5\%$ of 710 mm MAP on the basin footprint area.

2.11 Broederstroom Basin

This compartment is located in the extreme north-eastern portion of the COH (Fig. 3) where the karst environment is comparatively poorly defined in terms of its hydrogeology. It encompasses an area of ~ 1810 ha. The $\sim 21 \text{ L/s}$ Broederstroom Spring (Sect. 4.14) on the Glen Afric Country Lodge property south of Broederstroom represents one of the more prominent natural features draining this compartment. Others include the $\sim 5 \text{ L/s}$ Anderson Spring and the $\sim 2 \text{ L/s}$ Lesedi Spring. Further, numerous boreholes abstract groundwater for potable and general domestic use. This use, when added to the aggregate $\sim 28 \text{ L/s}$ of the enumerated spring discharges, might well double the groundwater loss from this compartment and approach a natural rainfall recharge contribution of $17 \pm 5\%$, compared to the $\sim 7\%$ represented by the currently known natural discharges (Table 9).

2.12 Discussion of Basin Definition and Groundwater Recharge

The information presented in Table 4 summarises the definition of groundwater compartments in the COH as has been established from available information and data. The estimated size of each compartment and subcompartment is derived from planimetric measurements of its footprint. Where possible, the veracity of these values is gauged

⁶ Mean flow of 163 L/s minus the 14% mean contribution of the Tweefontein Spring (Sect. 4.6).

against the natural discharge (as represented by measured spring flows and other quantified groundwater discharge), converted to an equivalent depth of rainfall. This approach encapsulates the groundwater basin concept described, amongst others, by White (1993; 2007a).

It was reported in Sect. 1 that the Holland (2007) study reports estimated average annual groundwater recharge volumes of 16.8 mm³ (from Bredenkamp et al. 1986) and 14.3 mm³ (from Krige 2006) for the Zwartkrans Basin based on water budget calculations. The Holland (op. cit.) study puts forward its own estimates of 16.6 mm³/a for the Zwartkrans Basin and 13.4 mm³/a for the Tweefontein Basin based on chloride mass balance (CMB) calculations. In regard to the Zwartkrans Basin with a surface extent of ~ 9800 ha, the recharge estimates represent ~ 24% (~ 170 mm) of an MAP of 710 mm. The Holland (op. cit.) estimate for the 12,230 ha Tweefontein Basin represents 15.4% (~ 110 mm) of 710 mm MAP, and which would increase marginally to 16.4% for a slightly lower MAP of 668 mm (from Table 1 in Chapter “Description of the Physical Environment”) as characterises the north-eastern portions of the property.

The ‘basinal’ rainfall recharge values reported in Table 4 range from ~ 1 to ~ 30% of MAP, but if the anomalously high and low values are excluded, more typically fall in the range ~ 11 to ~ 20%. This is in reasonable agreement with the range of ~ 9 to ~ 18% of MAP (excluding the extremes of ~ 3 to ~ 23% that defines the full range) reported by Kok (1992) for 12 dolomitic springs in South Africa. It is also in reasonable agreement with the range 15–21% of an MAP of 630 mm cited by Bredenkamp et al. (1986).

It is posited that recharge in the range 17 ± 5% of MAP, where MAP ranges from ~ 670 to ~ 710 mm (Table 1 in Chapter “Description of the Physical Environment”), represents a typical value for the karst terrane of the COH. Gondwe (2010) reports a similar range (17 ± 3%) for the karst system of the Sian Ka’an Biosphere Reserve, Yucatan Peninsula, Mexico.

The approach described above fails in those areas where groundwater abstraction from boreholes is significant, and reduces the natural discharge via springs. This is particularly relevant in the north-eastern portion of the property that encompasses the Broederstroom, Kalkheuwel West and Rhenosterspruit rural communities. This failing is evidenced in Table 4, which reflects significantly lower annual recharge percentages than the 17 ± 5% of MAP posited above. Although the water demand on an individual borehole in such a setting is low (because of the lack of high-demand uses such as irrigated agriculture and the low-density estate character of the land development), annual groundwater use will be significant.

An indication of this significance is provided by the results of a hydrocensus carried out by Maidment (2015), who enumerated 43 boreholes and three springs distributed over 38 properties in the Kalkheuwel West and Broederstroom basins. Water use data for 14 boreholes returned a mean rate of ~ 1450 L/d (~ 0.5 ML/a) per installation. Aggregated for 44 equipped boreholes, this amounts to a groundwater use of ~ 0.022 mm³/a. The Broederstroom Basin also supports the Lesedi African Lodge and Cultural Village, a facility with a restaurant and overnight visitor accommodation, staffed by ~ 70 permanent residents. The borehole serving this facility produces ~ 12 m³/d (~ 0.004 mm³/a).

As shown in Table 4, the combined discharge of the Kromdraai and Plover’s Lake springs (339 L/s excluding the Danielsrust Spring autogenic contribution), returns an unrealistically high equivalent recharge of ~ 30% of MAP as representing the ‘recharge input’ on the Krombank Basin footprint of 5080 ha. An explanation for the anomalously high recharge associated with the Krombank Basin is sought in the following possibilities:

- that surface water is lost from an influent Bloubank Spruit downstream of the Zwartkrans Dyke; and
- that groundwater is gained from the Zwartkrans Basin via a subsurface route over/through the Zwartkrans Dyke.

A surface water contribution of 140 L/s would reduce the groundwater component of discharge from the Krombank Basin to 200 L/s, equivalent to a recharge of 17.5%. SDMs at localities BB@Lotz and ~ 450 m upstream of the Kromdraai Spring on 13/08/2010, however, returned similar values of 459 and 466 L/s respectively. This result eliminates a significant surface water contribution from a losing Bloubank Spruit as possible explanation. The SEC of 56 mS/m associated with the Kromdraai Spring water (Table 14), compared to the 38 mS/m of the Plover’s Lake springwater (Fig. 32 “Chapter Chemical Hydrogeology”), rather suggests some measure of allogenic impact. The autogenic recharge contributed by the ~ 28 L/s Danielsrust Spring introduces a further complication that needs to be accounted for in this regard. It is appropriate to again employ a mass balance approach in an attempt to resolve this conundrum.

Let

$$(Q_{DS}C_{DS}) + (Q_G C_G) + (Q_R C_R) \\ = (Q_{KS}C_{KS}) + (Q_{PLSP}C_{PLSP})$$

then

$$(28 \times 182) + (140 \times C_G) + (137 \times 35) \\ = (307 \times 392) + (60 \times 266)$$

And

$$C_G = 126413 \div 140 = 903 \text{ mg} \frac{\text{TDS}}{\text{L}} = 129 \frac{\text{mS}}{\text{m}} \text{Sec}$$

where

- Q_{DSp} is the discharge (L/s) of the Danielsrust Spring;
- C_{DSp} is the SEC (mS/m) of the Danielsrust Spring water converted to TDS by the multiplier factor 7;
- Q_G is the subsurface input (L/s) of groundwater from the Zwartkrans Basin;
- C_G is the SEC of the Zwartkrans Basin groundwater water converted to TDS as above;
- Q_R is the recharge (L/s) to the Krombank Basin at $\sim 17\%$ of an MAP of 710 mm;
- C_R is the SEC of the rainwater recharge converted to TDS as above;
- Q_{KS} is the discharge (L/s) of the Kromdraai Spring;
- C_{KS} is the SEC of the Kromdraai Spring water converted to TDS as above;
- Q_{PLS} is the discharge (L/s) of the Plover's Lake Spring(s); and
- C_{PLS} is the SEC of the Plover's Lake Spring(s) water converted to TDS as above.

The mass balance result suggests that ~ 140 L/s of groundwater with an SEC of 129 mS/m would explain and account for the 'missing' water budget component of the Krombank Basin. It is encouraging, therefore, that the SEC of groundwater sampled from monitoring borehole GP00313 (Fig. 21) on eight occasions between July 2012 and September 2014 return an average value of ~ 129 mS/m in the range 120–136 mS/m.

The slightly elevated recharge value reported for the Uitkomst Basin is attributed to the more rugged nature of the terrain that characterises this compartment. These circumstances promote runoff in the incised drainages which, owing to their geologic setting, are controlled by geologic structures (fracture and fault zones), and typically represent losing streams contributing autogenic recharge to the karst aquifer. This has been observed in the Grootvlei Spruit draining the Diepkloof Basin.

Whilst it is acknowledged that an assessment such as provided above is hypothetical and necessarily coarse, it does provide plausible order of magnitude volumes that offer a 'reality check'. A second 'reality check' of specifically the subcompartment definition in the south-western portion of the study area, based on a statistical analysis of groundwater rest level data, is presented in Table 5. Salient results of this analysis are summarised as follows:

- The difference in groundwater rest level depth and elevation between subcompartments 1a and 1b. Especially

the difference of 35–40 m in terms of the mean and median elevation (absolute) values supports the observations documented in Sect. 2.1.1 regarding the difference in groundwater rest level between these two subcompartments. Note that it is shown in Sect. 6 and Fig. 18 that this difference reduces at the contiguous northern ends of these two subcompartments.

- The difference in groundwater rest level depth and elevation between subcompartments 2a and 2b. Although the difference in mean and median elevation values is comparatively small (~ 3 m), the much shallower values that characterise subcompartment 2b reflect the association of this subcompartment with the Bloubank Spruit valley between the Zwartkrans Spring and Plover's Lake.

3 Groundwater Level Behaviour

3.1 Zwartkrans Basin

The behaviour of groundwater levels (the hydrostatic response) associated with the karst aquifer is reflected in the long-term water level records for the 15 oldest DWS monitoring boreholes in the study area. An assessment of these data returns the statistics presented in Table 6. A graphical representation of the information is shown in Fig. 5. An analysis of the %ile Δh data yields a 25%ile value of 3.86 m, a mean value of 5.35 m, a median value of 4.93 m, and a 75%ile value of 6.98 m. The information presented in Table 6 and Fig. 5 indicates that there is little correlation between the depth to groundwater rest level and the magnitude of variation evident in this hydrologic variable.

A selection of the hydrographs is compared in Fig. 6, which indicates two distinct groupings of hydrograph, namely Group A occupying an elevation of > 1530 m amsl, and Group B occupying an elevation < 1490 m amsl. The elevation difference of > 40 m reflects the location of these groupings in two different basins/subcompartments. It is evident from Table 6 that the maximum difference in groundwater rest level amounts to ~ 12.2 m (station A2N0598), with a mean of ~ 6.2 m and a median of ~ 5.6 m. The slightly smaller differences between the 5%ile and 95%ile limits are characterised by a maximum value of ~ 9.8 m (station A2N0598), and mean and median values of ~ 5.2 and ~ 4.6 m respectively. These results are in agreement with similar results obtained for the karst aquifer elsewhere in Gauteng Province, e.g. for the karst aquifer extending from south of Pretoria to Kempton Park, and from Rietvlei Dam in a south-easterly direction to Bapsfontein (Hobbs 2004). Previous analyses of these data (Hobbs and Cobbing 2007) indicate natural fluctuations in the order of

Table 5 Definition of groundwater rest level variables for the Bloubank Spruit system

| Basin/subcompartment | | Groundwater rest level variable | Statistical parameter | | | | | |
|----------------------|-------------------|------------------------------------|-----------------------|------------|------------|------------|------------|--------------------------|
| | | | n | 25%ile | Mean | Median | 75%ile | Inter-quartile Range (m) |
| Zwartkrans | Vlakdrift (1a) | Depth (m bs) Elevation (m amsl) | 11 | 48 1461 | 63 1502 | 62 1503 | 75 1535 | 27 74 |
| | Sterkfontein (1b) | Depth (m bs) Elevation (m amsl) | 16 | 20 1471 | 31 1536 | 28 1540 | 44 1570 | 24 99 |
| | Zwartkrans (1c) | Depth (m bs) Elevation (m amsl) | 25 | 17 1439 | 28 1446 | 22 1444 | 30 1450 | 13 11 |
| Krombank | Kromdraai (2a) | Depth (m bs) Elevation (m amsl) | 12 | 44 1418 | 60 1422 | 59 1420 | 74 1424 | 30 6 |
| | Bloubank (2b) | Depth (m bs) Elevation (m amsl) | 14 | 6 1410 | 12 1419 | 11 1417 | 18 1420 | 12 10 |
| | TOTAL | | 78 | – | – | – | – | – |

Table 6 Salient statistics for long-term DWS groundwater level monitoring data

| Station | Groundwater rest level (m bc) | | | | | Variability | | Record period ^a |
|---------|-------------------------------|-------|-------|--------|--------|------------------|-------------------|----------------------------|
| | n | 5%ile | Mean | Median | 95%ile | Max Δh^b | %ile Δh^c | |
| A2N0580 | 274 | 51.01 | 54.55 | 54.32 | 59.95 | 11.13 | 8.94 | 05/1985–09/2014 |
| A2N0582 | 210 | 35.77 | 40.11 | 40.15 | 42.91 | 8.53 | 7.14 | 05/1985–12/2010 |
| A2N0583 | 234 | 44.40 | 44.95 | 44.90 | 45.54 | 1.84 | 1.14 | 05/1985–10/2014 |
| A2N0584 | 268 | 21.82 | 25.52 | 26.26 | 28.09 | 8.19 | 6.81 | 05/1985–09/2014 |
| A2N0586 | 289 | 21.34 | 26.23 | 27.14 | 28.67 | 8.54 | 7.33 | 05/1985–10/2014 |
| A2N0589 | 169 | 27.92 | 28.89 | 28.97 | 29.90 | 3.85 | 1.98 | 05/1985–06/2010 |
| A2N0590 | 188 | 31.50 | 34.62 | 35.14 | 36.46 | 6.11 | 4.96 | 05/1985–10/2014 |
| A2N0592 | 278 | 73.62 | 76.92 | 77.33 | 78.53 | 6.33 | 4.91 | 06/1985–10/2014 |
| A2N0594 | 183 | 70.86 | 72.79 | 72.80 | 74.41 | 4.91 | 3.55 | 01/1985–09/2008 |
| A2N0598 | 89 | 53.53 | 58.76 | 58.84 | 63.32 | 12.17 | 9.79 | 07/1985–05/2010 |
| A2N0600 | 208 | 21.22 | 23.92 | 24.39 | 25.38 | 5.07 | 4.16 | 04/1989–10/2014 |
| A2N0602 | 233 | 51.02 | 54.30 | 54.85 | 55.95 | 6.44 | 4.93 | 06/1987–10/2014 |
| A2N0605 | 202 | 60.18 | 62.49 | 62.74 | 63.65 | 4.16 | 3.47 | 04/1989–09/2014 |
| A2N0606 | 72 | 64.83 | 67.07 | 67.06 | 69.51 | 5.11 | 4.68 | 08/1989–10/2014 |
| A2N0607 | 169 | 64.20 | 67.00 | 66.97 | 70.68 | 7.95 | 6.48 | 10/1993–10/2014 |

^a From month of first measurement to month of most recent available measurement as at November 2014 update from DWS; shaded rows denote stations no longer in service

^b Difference between minimum and maximum values (not shown in this table)

^c Difference between the 5%ile and 95%ile values

5–8 m manifested over a period of 2–5 years, i.e. not from season to season. In regard to the Sterkfontein Cave system, Martini et al. (2003) report a gradual water level fluctuation in response to the preceding precipitation pattern in the range ~ 2 m. The CGS (undated) also reports that the water level in the cave in 1983 was 2–3 m higher than its current (Presumably 2004) level.

The groupings shown in Fig. 6 are produced separately in Fig. 7 (Group A) and Fig. 8 (Group B). The large measure of similarity in the hydrostatic response of the Group B

stations is evident. By comparison, the Group A stations exhibit a poor correlation that is particularly evident in station A2N0583. An inspection of the original borehole drilling and test pumping records reported by Bredenkamp et al. (1986) provides a possible explanation for the observed response patterns.

The data in Table 7 identify station A2N0580 as intersecting an unproductive aquifer (also reflected in the very low transmissivity value of $1 \text{ m}^2/\text{d}$), which explains the more ‘ragged’ trace of this graph compared to the ‘smoother’

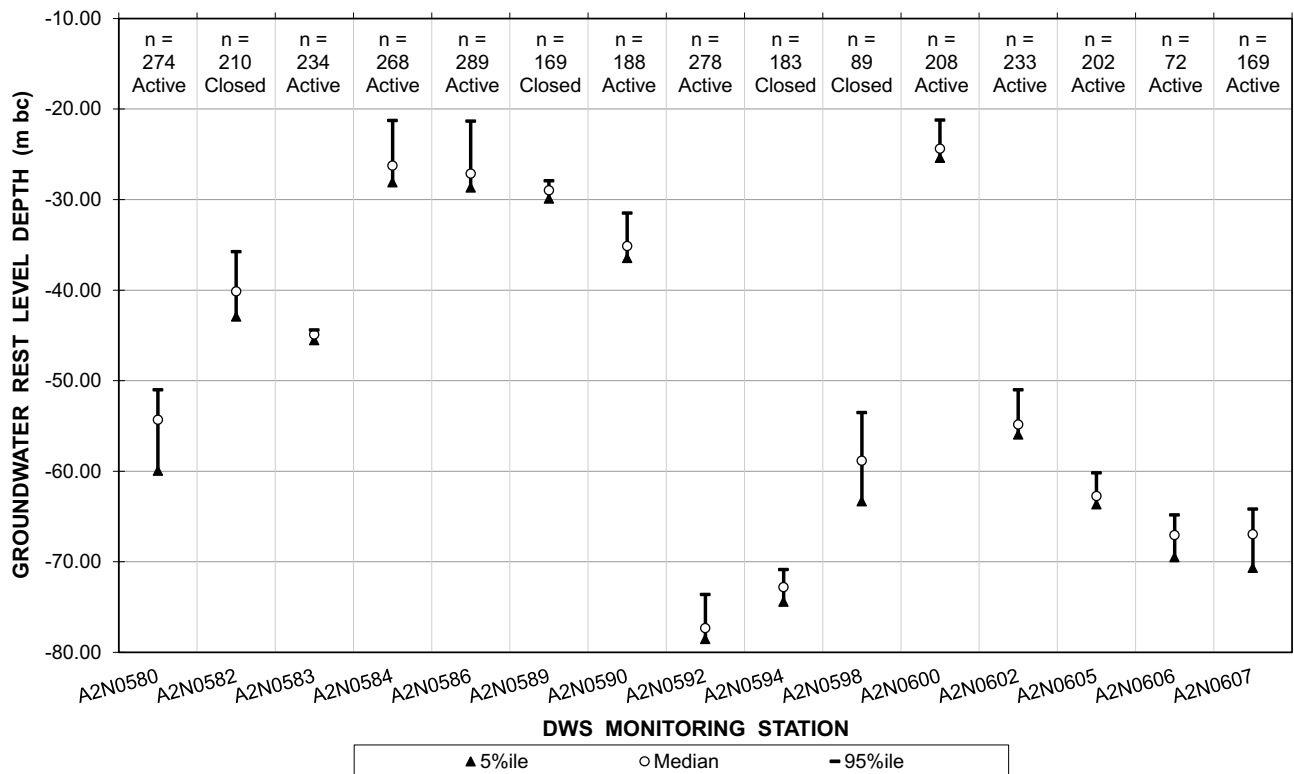


Fig. 5 Graphic comparison of the statistical hydrographic response observed in DWS groundwater level monitoring stations in the period 1985–2014 (data from Table 6)

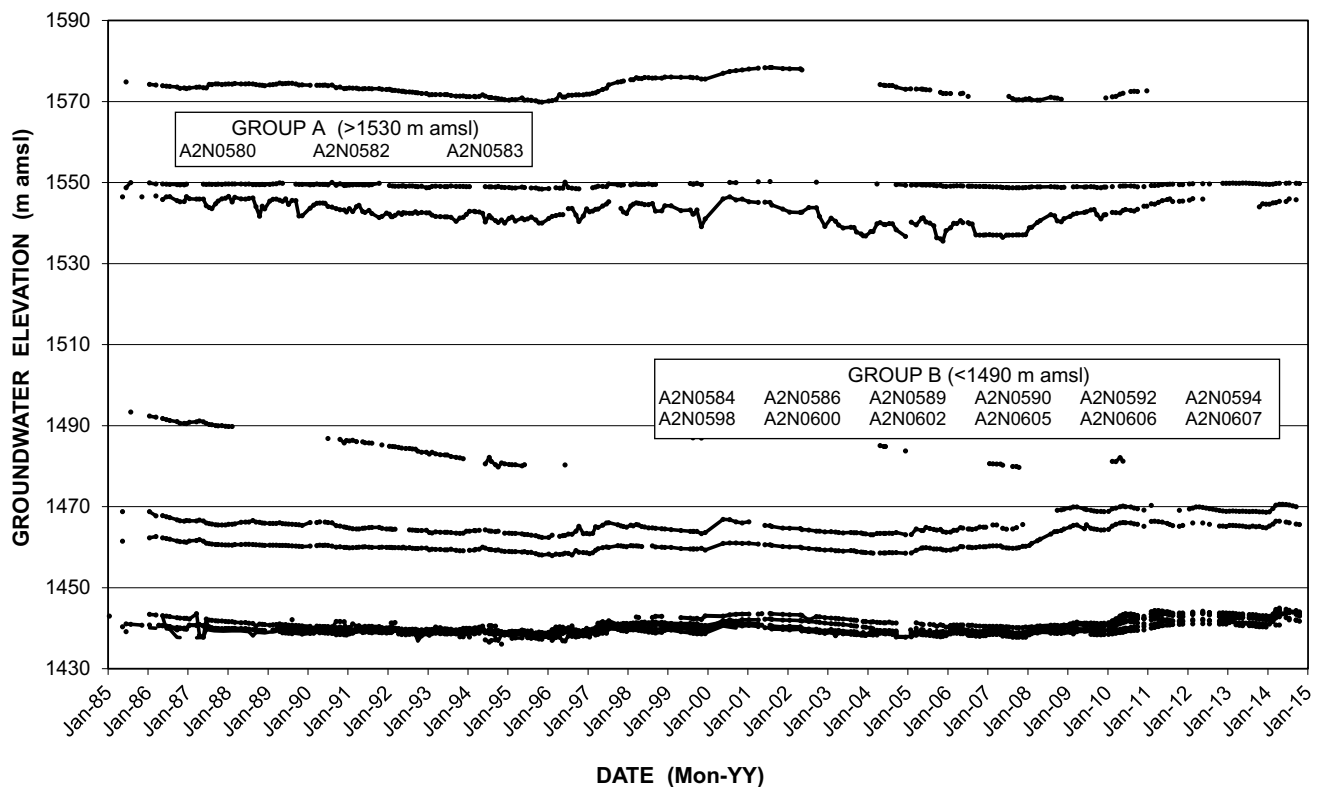


Fig. 6 Long-term groundwater level response pattern in DWS monitoring boreholes

graphs of stations A2N0582 and A2N0583 (Fig. 7). Especially the flat graph of station A2N0583 illustrates the capacity of the intersected groundwater resource to ‘absorb’ and ‘cushion’ the impact of recharge- or abstraction-induced stresses in the aquifer. This capacity derives from high transmissivity and/or storativity characteristics (Table 7).

The very productive aquifer(s) that support stations A2N0584 and A2N0586 (Fig. 8) similarly explain the relative ‘smoothness’ of these hydrographs. It is probable that the other stations reflected in Fig. 8 also penetrate productive groundwater systems.

The unprecedented rise in the groundwater level observed in stations A2N0584 and A2N0586 since late-2007 (Fig. 8) reflects the impact of exceptional recharge associated with raw and/or treated mine water being lost from the lower reaches of the Tweelopie Spruit and its receiving main stem, the Riet Spruit (Sect. 5.2.1 in Chapter “Physical Hydrology” and Sect. 2.1.2). Both these stations are located in proximity to the Riet Spruit. These circumstances were precipitated by the abnormally wet summers experienced in the region starting with the 2008 hydrological year, and resulting in treated mine water discharges > 25 ML/d to the Tweelopie Spruit (see Fig. 15 in Chapter “Physical Hydrology”). The additional contribution of raw mine water to this discharge in

the much wetter 2010, 2011 and 2014 rainy seasons has, on occasion, increased the flow in this drainage to > 60 ML/d (Sect. 5.2 in Chapter “Physical Hydrology”).

A comparison of ca. 2006 and ca. 2010 water level data for the same sites is provided in Table 8. This reveals an unequivocal rise in water level. The greatest rises (> 3 m) associated with boreholes located in the Riet Spruit valley upstream of Oaktree (CSIR57 and GB1) are again readily attributed to the ingress of surface water contributed primarily by the Tweelopie Spruit from the mining area. Further away from the Riet Spruit, the rise amounts to 0.5–1.5 m. Although the rise of ~ 0.6 m in the Danielsrust Basin (sites DRGF1 and DRGF2) is similar to the 0.4–0.8 m observed nearby in the main karst aquifer (sites BolandB1, SF1 and MB1), these compartments are not in hydraulic continuity with each other.

The resumption of uncontrolled mine water discharge in late-January 2010, combined with the exceptionally high rainfall experienced in the 2010, 2011 and 2014 summers, precipitated exceptional recharge conditions in the receiving Zwartkrans Basin. These conditions manifest as a rise in groundwater level of ~ 1 m within the space of only a few months in boreholes located next to the Riet Spruit, e.g. ≥ 0.86 m and ≥ 1.27 m in boreholes CSIR57 and

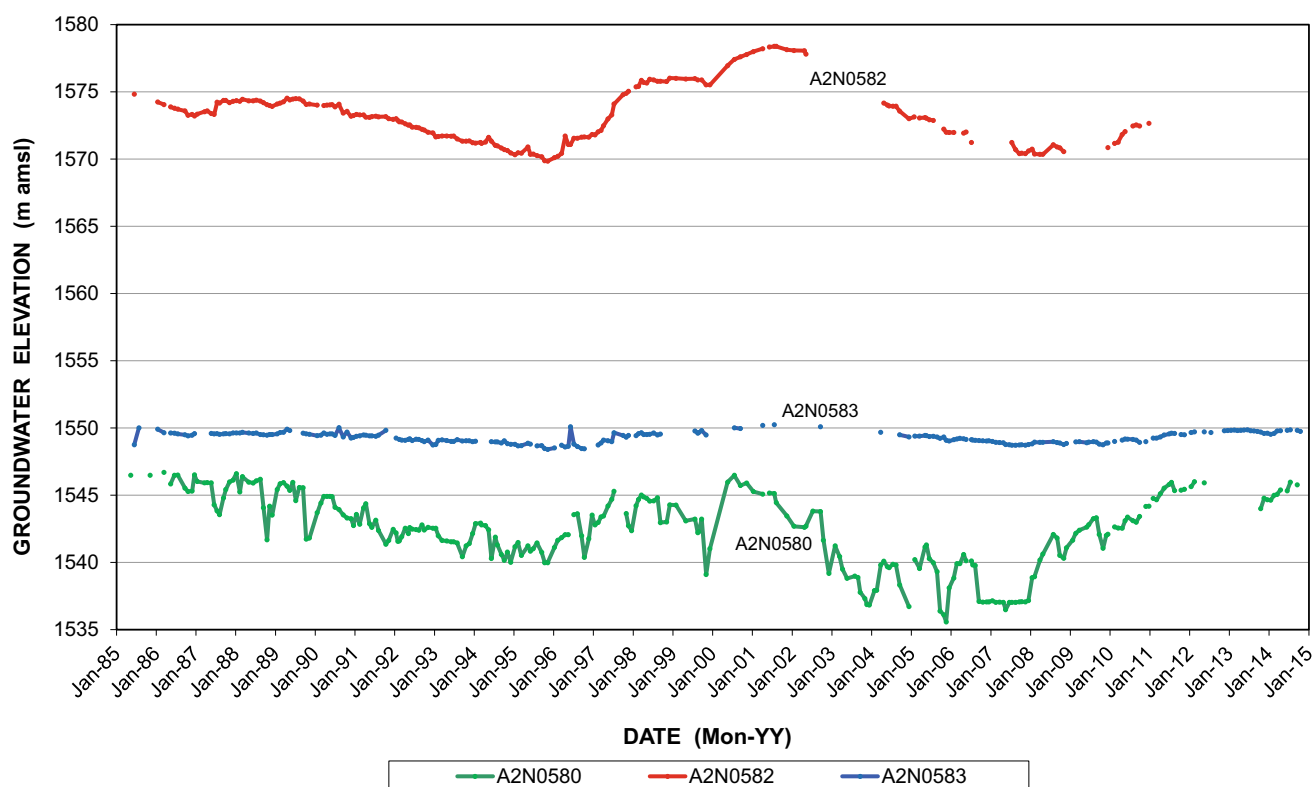
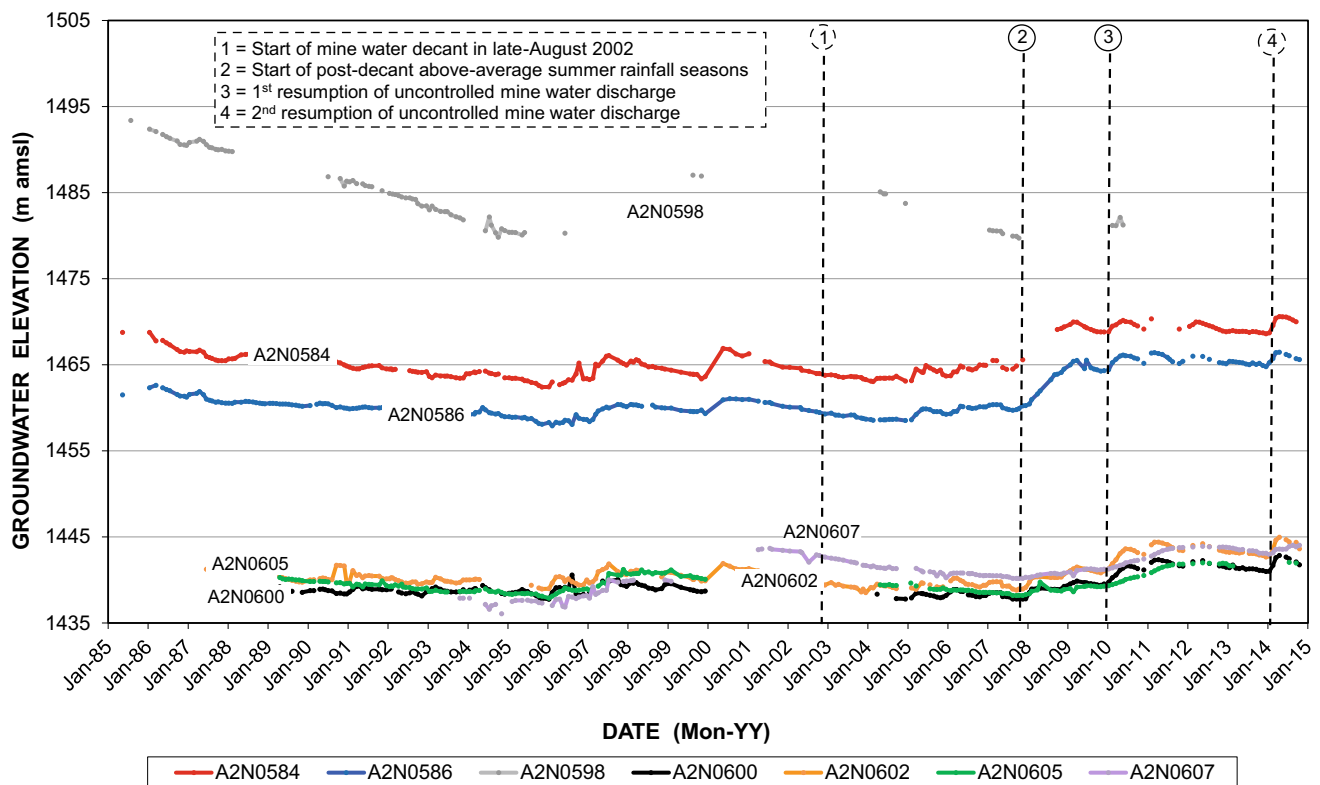


Fig. 7 Long-term groundwater level response pattern in Group A boreholes from Fig. 6

Table 7 Salient hydrogeologic attributes associated with selected DWS monitoring stations (from Bredenkamp et al. 1986)

| Station | Blowout yield (L/s) | Maximum tested yield (L/s) | Maximum drawdown (m) | Transmissivity (m ² /d) | Comment |
|---------|---------------------|----------------------------|----------------------|------------------------------------|-------------------------------|
| A2N0580 | 0 | 0.6 | 38.5 | 1 | Unproductive aquifer |
| A2N0582 | 15 | 25.2 | 4.52 | 1600 | Highly productive aquifer |
| A2N0583 | > 40 | 94.7 | 4.15 | 750 | Extremely productive aquifer |
| A2N0584 | > 40 | 18 | 13.17 | 34 | Moderately productive aquifer |
| A2N0586 | > 40 | 106.9 | 3.18 | 2100 | Extremely productive aquifer |

**Fig. 8** Long-term groundwater level response pattern in Group B boreholes from Fig. 6

GB1, respectively. Groundwater elevations are currently the highest (e.g. stations A2N0584, A2N0586 and A2N0600) in the ~ 30-year record of measurements.

3.2 Sterkfontein Cave System Water Level

3.2.1 General Discussion

It is common cause that the water level in the Sterkfontein Cave system has been the subject of considerable debate and at least some confusion. The water level in question is that

associated with what Martini et al. (2003) refer to as the 'Main Lake', which is the most readily accessible water body in the cave system. Wilkinson (1973) refers to this water body simply as the 'Lake', a convention followed in this manuscript. A recent substantial rise (~ 3 m) in the Lake water level has caused Maropeng aAfrica (the authority responsible for managing the tourist component of the site) to reroute the tourist path through the caves to successively higher elevations on three occasions since early-2010. The circumstances warrant separate and specific discussion.

Table 8 Comparison of historical and more recent groundwater levels in the study area

| Station | Historic water level | | | More recent water level | | | Difference (m bc) |
|--|----------------------|--------------|--------------------|-------------------------|---------------|--------------------|-------------------|
| | Date | Depth (m bc) | Elevation (m amsl) | Date | Depth (m bc) | Elevation (m amsl) | |
| SW1 | 09/12/2005 | 18.00 | 1441 | 11/02/2010 | 11.36 | 1448 | + 6.64 |
| A2N0594 | 25/01/2006 | 74.00 | 1439 | 08/02/2010 | 73.43 | 1440 | + 0.57 |
| DRP15 | 30/07/2006 | 59.00 | 1416 | 02/12/2009 | 58.63 | 1417 | + 0.37 |
| ZW1 | 30/07/2006 | 29.64 | 1438 | 17/02/2010 | 27.64 | 1440 | + 2.00 |
| A2N0600 | 30/07/2006 | 25.06 | 1438 | 17/02/2010 | 23.03 | 1440 | + 2.03 |
| DRGF1 | 30/07/2006 | 11.00 | 1486 | 11/02/2010 | 10.45 | 1487 | + 0.55 |
| DRGF2 | 30/07/2006 | 26.93 | 1486 | 11/02/2010 | 26.30 | 1487 | + 0.63 |
| BolandB1 | 30/07/2006 | 22.15 | 1438 | 17/02/2010 | 21.77 | 1438 | + 0.38 |
| SF1 | 01/10/2007 | 17.43 | 1437 | 17/02/2010 | 16.13 | 1438 | + 1.30 |
| | | | | 09/06/2010 | 15.54 | 1438 | + 1.89 |
| GB1 | 30/07/2006 | 20.36 | 1444 | 11/02/2010 | 17.64 | 1447 | + 2.72 |
| MB1 | 30/07/2006 | 15.07 | 1435 | 13/05/2010 | 13.79 | 1436 | + 1.28 |
| VW1 | 30/07/2006 | 13.94 | 1445 | 06/05/2010 | 9.71 | 1449 | + 4.23 |
| HW1 | 30/07/2006 | 8.00 | 1410 | 13/05/2010 | 6.09 | 1412 | + 2.09 |
| SWBH1 | 30/07/2006 | 28.00 | 1417 | 13/05/2010 | 27.30 | 1418 | + 0.70 |
| SBH1 | 30/07/2006 | 22.26 | 1415 | 13/05/2010 | 21.18 | 1416 | + 1.08 |
| A2N0584 | 08/02/2007 | 25.71 | 1466 | 16/02/2010 | 21.78 | 1469 | + 3.93 |
| CSIR34 | 13/02/2007 | 35.10 | 1470 | 14/04/2010 | 33.99 | 1471 | + 1.11 |
| CSIR8 | 13/02/2007 | 28.42 | 1447 | 14/04/2010 | 24.28 | 1451 | + 4.14 |
| A2N0586 | 08/03/2007 | 26.96 | 1460 | 16/02/2010 | 21.98 | 1465 | + 4.98 |
| CSIR57 | 08/03/2007 | 12.32 | 1461 | 16/02/2010 | 7.06 | 1466 | + 5.26 |
| A2N0598 | 16/05/2007 | 63.22 | 1480 | 09/06/2010 | 61.14 | 1482 | + 2.08 |
| Statistical analysis (excluding stations DRGF1 and DRGF2) | | | | | n | | 19 |
| | | | | | Minimum value | | 0.37 |
| | | | | | 5%ile value | | 0.38 |
| | | | | | Mean value | | 2.42 |
| | | | | | Median value | | 2.03 |
| | | | | | 95%ile value | | 5.40 |
| | | | | | Maximum value | | 6.64 |

The elevation of the Lake water level was reported as 1450.88 m amsl by JFA (2006). The discrepancy with the groundwater level elevation of 1437.5 m amsl in the nearby borehole SF1 (op. cit.) was attributed to perched aquifer conditions associated with the cave environment. A Western Basin Void Technical Group (WBVTG) meeting held on 28/02/2007 at the Rand Uranium Office Complex in Randfontein was informed that the Zwartkrans Spring was dry, and that any flow in this vicinity represented surface runoff. This was in response to a query regarding the potentiometric level of water in Sterkfontein Cave (reportedly 1436 m amsl) versus the elevation of the spring (reportedly 1439 m amsl). These circumstances were quite logically put forward as evidence that the water level in cave could not rise more than 3 m, i.e. up to the level at which the dolomitic Basin would overflow via the spring.

This information clearly contradicted the JFA (2006) Lake water level elevation. Besides, it was determined that the Zwartkrans Spring had not dried up in the ~ 31 years that the owner of the property had resided there (H Roos, personal communication).

A re-survey on 12/12/2007 of the benchmark in the cave from which the Lake water level is derived, placed it an elevation of 1437.94 m amsl compared to its previous elevation of 1452.37 as reported by JFA (2006). The difference of 14.43 m, when applied to the cave water level of 1450.88 reported by JFA (2006), returns a cave water level of 1436.5 m amsl, i.e. in agreement with that reported to the WBVTG. This compares favourably with both the reported groundwater level elevation of 1437.5 m amsl (JFA 2006) in the nearby monitoring borehole SF1, and the elevation of the

Zwartkrans Spring which is placed at ~ 1433 m amsl (this study).

A rest water level measurement in borehole SF1 on 01 October 2007 returned a value of 17.4 m bc which, for an interpolated surface elevation of 1454 m amsl, gives a potentiometric level of 1436.6 m amsl. This closely resembled that of the cave water level, suggesting that the groundwater rest level in SF1 and the caves represents a single potentiometric surface. This observation found support from Krige (2009, 2010) following a revision of an earlier report by Krige and van Biljon (2006). In practical terms, this indicates that the caves share the same aquifer as the nearby borehole SF1, and which is drained by the Zwartkrans Spring. Martini et al. (2003) report earlier similar discrepancies in elevation (up to 9 m) between various water bodies (up to 30 reported ‘static’ pools) inside the caves, but conclude that more recent measurements suggest elevation differences in the order of decimetres (tens of centimetres) rather than metres.

The above circumstances bring into question the relationship with the channel of the Bloubank Spruit north of (opposite) the cave system, which is placed at ~ 1440 m amsl (this study) compared to the 1445 m amsl attributed it by JFA (2006). The elevation difference of ~ 3 m between the surface drainage and the October 2007 groundwater level is not uncommon in the study area. It has been shown by Hobbs and Cobbing (2007) that the potentiometric surface in the Riet Spruit upstream of the Oaktree area (and therefore the caves) was separated from the overlying surface drainage by 12–30 m (Fig. 4). This difference has subsequently decreased significantly as a consequence of surface water inflow into the karst aquifer (see Sect. 5.2 in Chapter “Physical Hydrology” and Fig. 4). For example, by 09/06/2010 the water table in borehole SF1 had risen ~ 1.9 m from its October 2007 depth of ~ 17.4 m bc (Table 8). This places the water table elevation in June 2010 at ~ 1438 m amsl, which is only some 2 m below the ~ 1440 m amsl of the Bloubank Spruit channel. The difference can be expected to reduce even more as the streambed elevation approaches that of the Zwartkrans Spring, these surfaces coinciding in proximity to the spring. Under these circumstances, it is probable that groundwater also ‘resurfaces’ in the channel of the Bloubank Spruit upstream of the Zwartkrans Spring. Observations that support such resurgence are presented and discussed in Sect. 5.2.3 in Chapter “Physical Hydrology”.

Further informative aspects of the cave water level reported by Martini et al. (2003) are the following.

- The indication that the cave has dewatered from 20 to 25 m above the present water level, in the past 3.3 Ma

ago. The water level decline was irregular, being punctuated by temporary rises as indicated by re-solution of calcified deposits ~ 12 m above the current water level, and speleothems corroded up to 6 m above this level. The dewatering interval extends to an upper bounding elevation of 1456–1461 m amsl which, in terms of the present landscape, implies that the valley to the north of the caves would have been under water to a depth of 15–20 m (see Sect. 12 “Chapter Chemical Hydrogeology” for a perspective on this likelihood).

- The observation that the ca. 2003 cave lake water level fluctuation was within a range of ~ 2 m, and varied gradually in response to a prior rainfall pattern. Further, that speleothems (flowstone and stalactites) were corroded in the interval of roughly 3–6 m above the current (ca. 2003) water level, and that no speleothems occur below 2–3 m above this level in the vicinity of the lake. The latter observation indicates that this interval is the most aggressive in terms of carbonate re-solution, at least in the more recent speleogenesis of the cave system. This observation also accords with the evaluation of the ambient potentiometric response pattern (Sect. 3.2.2).

3.2.2 Potentiometric Response Pattern

The installation of a continuous water level monitoring device in the cave lake by the DWS in May 2005 yields information on the cave water level response pattern to July 2007. The recorded pattern is shown in Fig. 9. It reveals three periods of steady decline at a rate of between 0.08 and 0.06 m/month, the latter occurring after an upward ‘adjustment’ of ~ 0.5 m in the 2007 summer.

Also shown in Fig. 9 is the SF1 groundwater level elevation on 30/07/2006. This derives from a value of 17.00 m bc reported by Holland (2007), and which indicates a < 1 m discrepancy with that of the contemporary Lake water level elevation. The datum for the latter is a surveyed elevation (Krige 2009), and must therefore be regarded as accurate to < 0.1 m. By comparison, the SF1 datum is a surface elevation interpolated from the 1:10,000 scale orthophoto map 2627BA5 Sterkfontein (RSA 1987). With a contour interval of 5 m, an interpolation accuracy of < 2 m is feasible with knowledge of the landscape.

In sympathy with the observed rise in water levels in the study area in the 2010 and 2011 hydrological years (Sect. 3 and Table 8), a similar response is observed in the cave. In mid-May 2010, cave guide K Mangole (personal communication) estimated a rise of ~ 1 –2 feet (0.3–0.6 m) since late-2009. This is in good agreement with the ~ 0.6 m rise observed in the nearby borehole SF1 between February 2010 and June 2010 (Table 8), and the ~ 0.4 m rise in borehole MB1 between February 2010 and May 2010. A water level

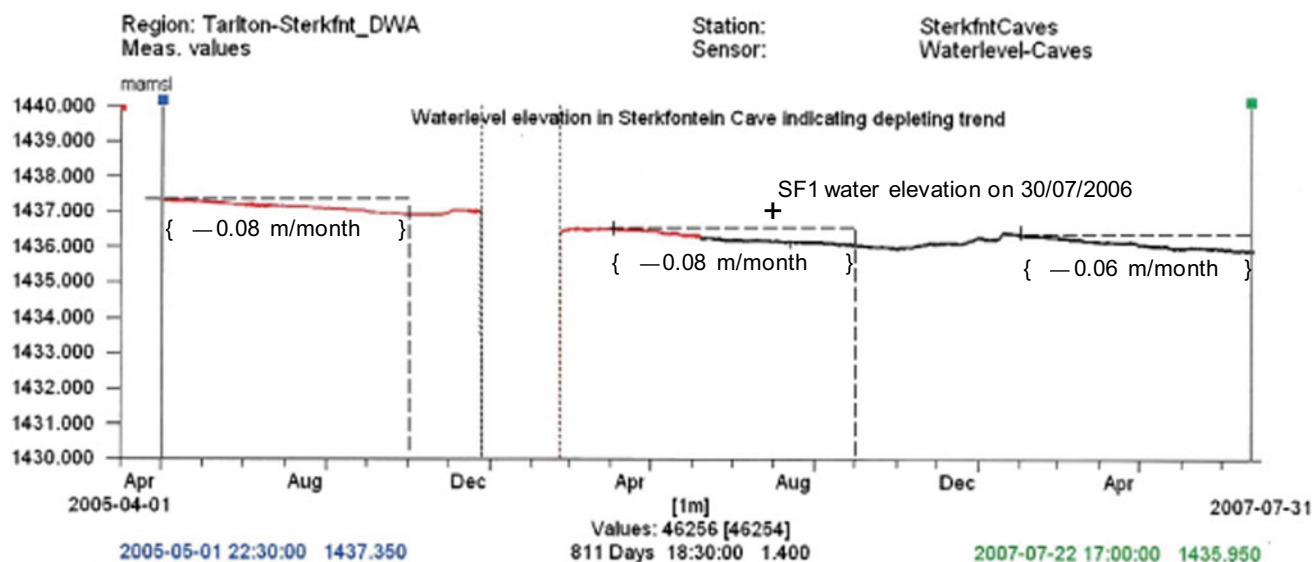


Fig. 9 Continuous groundwater level response pattern in Sterkfontein Cave over a period of 27 months (use of image courtesy of DWS)

measurement in borehole SF1 on 14/01/2011 indicated a further rise of ~ 0.7 m since June 2010, for a total rise of ~ 2.6 m between October 2007 and January 2011, increasing to ~ 2.8 m with a further rise of ~ 0.2 m being manifested in the 5-month period January 2011 to June 2011. The rates of rise in the three periods February 2010 to June 2011, June 2010 to January 2011, and January 2011 to June 2011 amount to ~ 0.15 , ~ 0.09 and ~ 0.04 m/month respectively. The latest measurements reflect a decline in the Lake water level.

The cave water level trend is shown in Fig. 10, and suggests that the water level might have started rising in mid-2009. This followed a decline (the early part of the SF1 record shown in Fig. 10) at a rate of ~ 0.03 m/month, i.e. roughly half the rate of 0.06–0.08 m/month reflected in the three earlier periods marked in Fig. 9.

The ‘maximum’ elevation of ~ 1439.5 m amsl (Fig. 10) approaches the ~ 1440 m amsl assigned to the Bloubank Spruit channel to the north of the caves. This suggests that the cave water level reaches equilibrium at an elevation of ~ 1440 m amsl when the karst water table intersects the stream channel of the Bloubank Spruit opposite the caves. If so, then the maximum possible rise of ~ 3 m agrees well with the zone of perceived most aggressive carbonate re-solution that defines the more recent speleogenetic evolution of the cave system as observed by Martini et al. (2003) (Sect. 3.2.1). Groundwater level measurements ca. mid- to late-2010 in boreholes indicate that the hydraulic gradient in the valley of the Bloubank Spruit to the north of Sterkfontein Cave amounted to 0.003 in an ENE direction. This is equal to a barely discernible fall of 0.3 m per 100 m in an ENE direction, which provides the context for the

‘apparently static’ nature of pools in the cave system observed by Martini et al. (2003).

The decline in water level in borehole SF1 in the period May 2012 to November 2013 indicates a rate of decline of ~ 0.03 m/month (Fig. 10). This is similar to the ~ 0.03 m/month reported for the earlier (pre-rise) portion of the SF1 record shown in Fig. 10. It is postulated that the Lake will maintain a high water level into the future because of sustained above-normal discharge in the upper tributaries of the Bloubank Spruit, provided that abnormal precipitation does not trigger excessive recharge resulting in a rise in groundwater levels in the Zwartkrans Basin. As is evident in Fig. 10, the high rainfall in February and March 2014 precipitated a rapid rise in the contemporary cave water level. It is highly unlikely, however, that the cave water level will rise above the elevation of ~ 1440 m amsl.

Martini et al. (2003) also report the observation of cave divers that the depth of the Lake does not exceed 4 m. Unfortunately, the authors do not provide a datum for this measurement. Wilkinson (1973), however, reports a similar depth for the Lake, and a depth of 6 m for water body W5 in Lincoln’s Cave. Although there is some doubt over the Wilkinson (1973) datum, the reported depth of 48 m below the top of the ‘hillock’ places the Lake water level at an elevation of ~ 1437 m amsl. This is in agreement with recent measurements, and places the deepest point of the Lake at ~ 1433 m amsl, similar to that of the Zwartkrans Spring (Table 9). The 6 m depth reported for water body W5 therefore occupies a base elevation of ~ 1431 m amsl. These circumstances prompt an assessment of the conduit flow depth associated with the karst aquifer as attempted in Sect. 8.

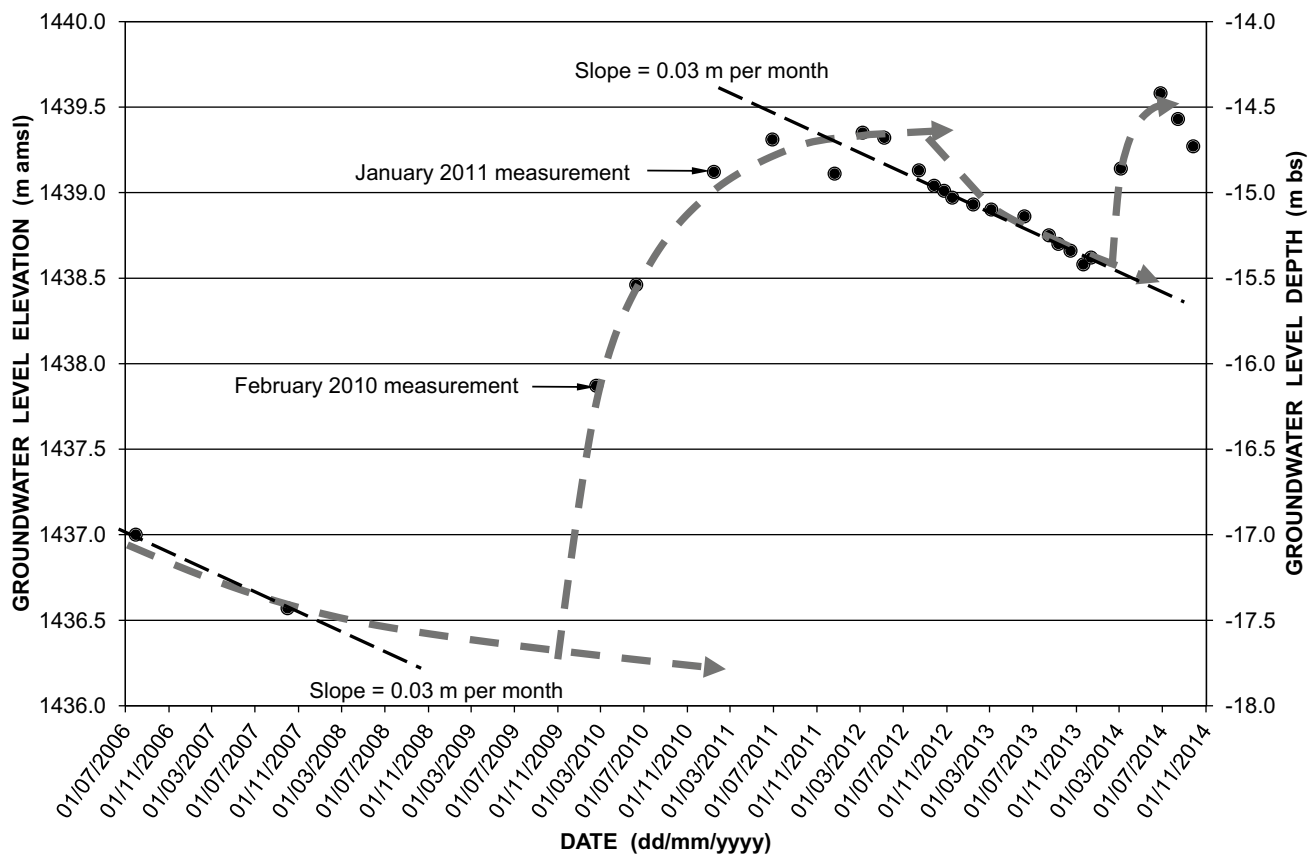


Fig. 10 Groundwater level response pattern and trend in borehole SF1 that serves as a proxy for the Lake water level in Sterkfontein Cave

Wilkinson (1973) suggested that resurgence occurred as underflow on the buried contact between the alluvial valley fill deposit and the underlying dolomitic bedrock located 12 m below the streambed (op cit., Fig. 7.5). Further, that the resurgence was driven by a vector directed normal to the stream channel rather than by an upstream migration driven by a rising water table. The hydraulic gradient of 0.1 (6°) reported by Wilkinson (1973) contrasts markedly with the much shallower slope of 0.003–0.005 (0.2–0.3°) established from recent information, and which is more typical of highly transmissive karst strata of the South African interior.

Exploration borehole information suggests that the main flowpath (thalweg) of groundwater discharge through the Zwartkrans Basin toward the spring lies ~ 600–700 m to the north-west of the caves coincident with the Bloubank Spruit drainage. It is postulated, therefore, that the location of the cave system on the south-eastern periphery of the main flowpath offers an explanation for the muted mine water impact on the cave water chemistry. These circumstances are discussed in greater detail in Sect. 8.4 “Chapter Chemical Hydrogeology”. It is also worth noting that the caves straddle the contact between the chert-poor Oaktree Formation that forms the south-eastern (and oldest) lithostratigraphic margin of the Malmani Subgroup, and the

overlying chert-rich strata of the Monte Christo Formation. The latter is generally associated with a more ‘productive’ aquifer, in contrast to the typically more ‘barren’ character of the Oaktree Formation. Nevertheless, the potentiometric response exhibits a spatially more uniform behaviour (Fig. 11) as might be expected in a highly transmissive karst aquifer.

4 Springs

Springs (or ‘eyes’) are hydrogeologic features that typically mark the intersection of the potentiometric surface with the land surface.⁷ For this reason, they represent the lowest point in a groundwater basin to which flow converges (Quinlan and Ewers 1986), and their flow behaviour, turbidity and

⁷The position of springs in the landscape is determined by numerous geologic factors including structural features such as intrusive dykes and sills and lithological contact zones between strata. These factors are used to describe each of the enumerated springs as either (1) a barrier dyke, (2) a barrier sill or (3) a lithologic contact type, respectively (see Table 8). Ford and Williams (2007) simply refer to such springs by the collective term ‘dammed springs’.

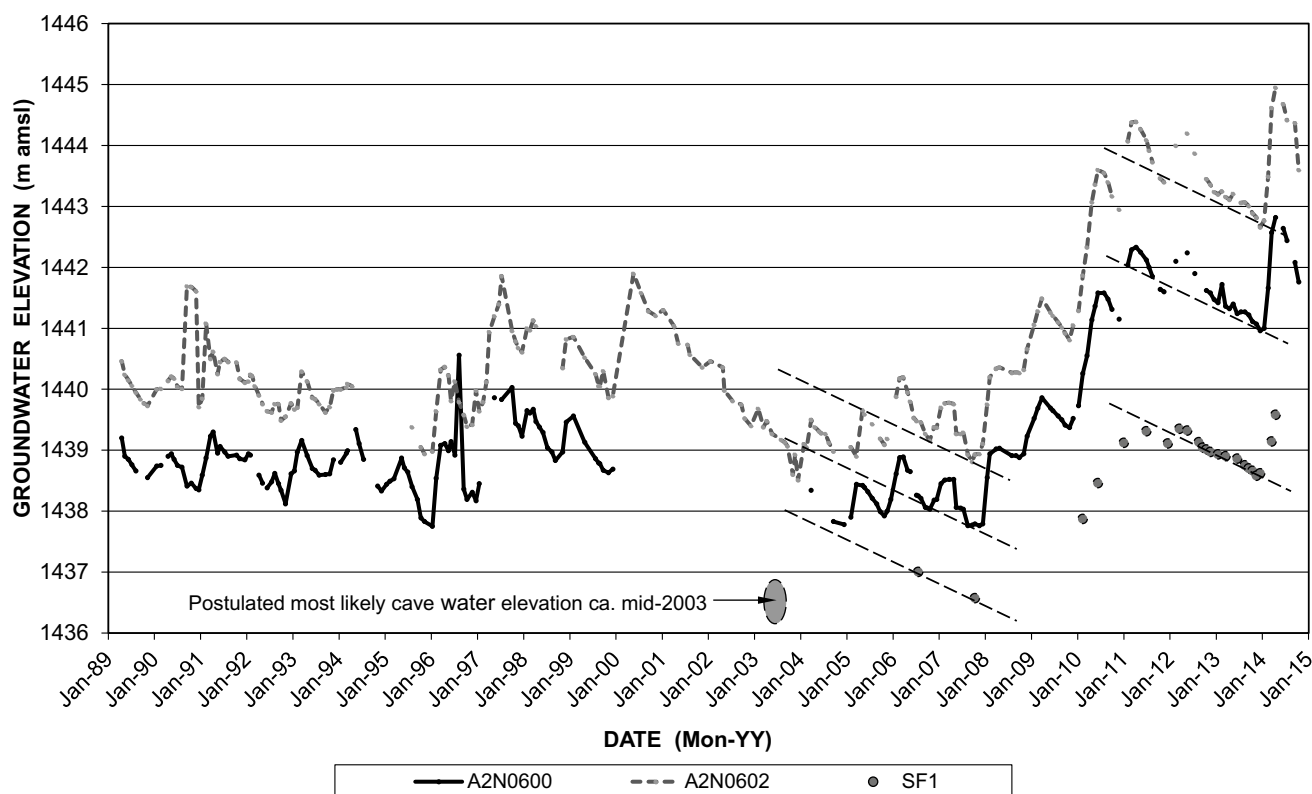


Fig. 11 Long-term potentiometric response in monitoring boreholes A2N0600 and A2N0602 compared to the response in borehole SF1 serving as a proxy for the cave water level

chemistry reflect a composite of everything that has happened upstream (White 2002). It is for this reason that Quinlan and Ewers (1985) stress that reliable monitoring in karst must involve springs, and not just boreholes. Bakalowicz (2005) goes as far as to state “The spring is the only place where one can obtain information on the functioning of the whole system, ...” and “Consequently, if the main spring cannot be monitored, ... the system cannot be simulated nor managed properly”. These circumstances define the recognition of springs as the most appropriate gauging, sampling and monitoring points also, and probably more particularly so, in a karst environment (Williams 2008).

Vegter (1995) lists 57 cold springs in South Africa yielding $> 1000 \text{ m}^3/\text{d}$ ($\sim 11.6 \text{ L/s}$). An inspection of this list and its accompanying map suggests that only one of these springs, namely #13 on Kromdraai 520JO (25.969°S – 27.788°E), might form part of those enumerated in the COH. It must be noted, however, that the Kromdraai Spring(s) reported by Bredenkamp et al. (1986), and echoed by Holland (2008) and Holland and Cobbing (2008) as representing #13 of Vegter (1995), cannot be associated with the Kromdraai Spring enumerated in this study for the reasons set out in Text Box 1.

Salient information pertaining to the 14 springs (Fig. 2) enumerated in the COH, is presented in Table 9. Some of these represent groups of springs (and seeps) located in close proximity to one another.

4.1 Zwartkrans Spring

Located $\sim 1.4 \text{ km}$ north-east (downstream) of Sterkfontein Cave, this spring drains the Zwartkrans Basin spanning the south-western dolomitic portion of Quaternary basin A21D. It represents a typical barrier contact spring formed by the Zwartkrans Dyke at this position, which also explains a seepage area located on the opposite (north) bank of the Bloubank Spruit on the farm Boland. The spring occupies a position immediately adjacent to the Bloubank Spruit at an elevation that is similar to that of the streambed (Plate 1). Discharging directly into the stream, these features share a common elevation of $\sim 1433 \text{ m amsl}$ at this location.

Flow measurements carried out on 27/07/2010 at locations $\sim 460 \text{ m}$ upstream and $\sim 2.5 \text{ km}$ downstream of the Zwartkrans Spring provided an early estimate of the spring discharge. The upstream measurement yielded a discharge of $\sim 426 \text{ L/s}$. The downstream discharge comprised the

Table 9 Salient information pertaining to enumerated springs in the COH

| Spring | Basin | Coordinates (dd.dddd) ^a | Elevation (m amsl) | Discharge ^b | | Type and Source Aquifer |
|---------------|---------------|---------------------------------------|-----------------------|------------------------|--------|--|
| | | | | (L/s) | (ML/d) | |
| Zwartkrans | Zwartkrans | 26.01°S 27.75°E | ~ 1433 | ~ 136 | ~ 11.7 | Barrier dyke contact: Dolomite (Malmani Sbgp.) |
| Plover's Lake | Krombank | 25.99°S 27.78°E | ~ 1419 | ~ 60 | ~ 5.2 | Barrier sill contact: Dolomite (Malmani Sbgp.) |
| Kromdraai | | 25.98°S 27.78°E | ~ 1406 | ~ 279 ^c | ~ 24.1 | Structural lineament: Dolomite (Malmani Sbgp.) |
| Danielsrust | Danielsrust | 25.98°S 27.74°E | ~ 1486 | ~ 28 | ~ 2.4 | Barrier sill contact: Dolomite (Malmani Sbgp.) |
| Aquamine | Rietfontein | 25.95°S 27.81°E | ~ 1436 | < 2 | < 0.2 | Lithologic contact: Shaly sandstone (Ventersdorp Spgp.) |
| Twefontein | Twefontein | 25.91°S 27.80°E | ~ 1450 | ~ 30 | ~ 2.6 | Barrier dyke contact: Dolomite (Malmani Sbgp.) |
| Nouklip | Diepkloof | 25.88°S 27.79°E | ~ 1330 | ~ 143 ^d | ~ 12.4 | Lithologic contact: Dolomite (Malmani Sbgp.) |
| Nash | Uitkomst | 25.89°S 27.77°E | ~ 1360 | ~ 130 | ~ 11.2 | Lithologic contact: Dolomite (Malmani Sbgp.) |
| Barlow | Kalkheuvel | 25.85°S 27.88°E | ~ 1363 | ~ 2 | ~ 0.2 | Lithologic contact: Dolomite (Malmani Sbgp.) |
| Uitkomst | (non-karst) | 25.91°S 27.74°E | ~ 1410 | ~ 2 | ~ 0.2 | Lithologic contact: Shale (Timeball Hill Fm.) |
| Cradle | Motsetse | 25.91°S 27.85°E | ~ 1405 | ~ 2 | ~ 0.2 | Barrier sill contact: Dolomite (Malmani Sbgp.) |
| Broederstroom | Broederstroom | 25.82°S 27.87°E | ~ 1281 | ~ 21 | ~ 1.8 | Lithologic contact: Dolomite (Malmani Sbgp.) |
| Anderson | | 25.85°S 27.88°E | ~ 1365 | ~ 5 | ~ 0.4 | Lithologic contact: Dolomite (Malmani Sbgp.) |
| Lesedi | | 25.84°S 27.88°E | ~ 1337 | ~ 2 | ~ 0.2 | Lithologic contact: Dolomite (Malmani Sbgp.) |
| | | | TOTAL | 842 | 72.7 | |

^a Coordinates truncated to two decimals to prevent unwelcome visitation of these features

^b Measured by the author using an OTT C20 current meter as described in Footnote 28

^c Excludes the autogenic recharge produced by the Danielsrust Spring

^d Excludes the autogenic recharge produced by the Twefontein Spring

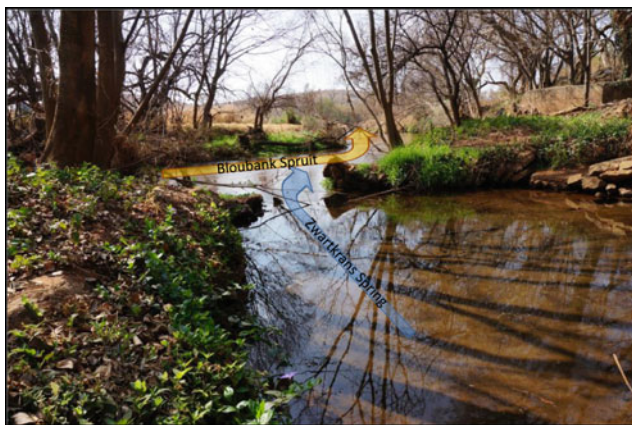


Plate 1 View of the Zwartkrans Spring rising in basin at front right of picture, discharging into the Bloubank Spruit

sum of the A-furrow discharge (~ 154 L/s) and the Bloubank Spruit discharge (~ 477 L/s) for a total of ~ 631 L/s. The difference of ~ 205 L/s (17.7 ML/d) might represent the discharge of the Zwartkrans Spring. However, the flow conditions and setting of the upstream and downstream SDM stations indicated that the calculated spring discharge value should be regarded as a relatively coarse approximation for the following reasons (amongst others):

- the distance (~ 2450 m) of the river measurement station downstream of the spring;
- the shallow and turbulent flow conditions that characterised the culvert settings of the downstream river measurement station;
- the possibility of unaccounted-for abstraction from the A-furrow upstream of the canal measurement station; and

- the unaccounted flow through streambed vegetation at the upstream gauging site.

As a consequence, a second set of measurements was carried out closer to the spring on 13/08/2010. These returned a discharge of ~ 535 L/s (46.2 ML/d) at the upstream station, and a total downstream discharge of ~ 635 L/s (54.8 ML/d) comprising the sum of the A-furrow discharge (~ 176 L/s) and the Bloubank Spruit discharge (~ 459 L/s). It is encouraging that the downstream river and A-furrow discharges on the two measurement dates are similar, viz. ~ 477 versus ~ 459 L/s and ~ 154 versus ~ 176 L/s, respectively. The total downstream discharges of ~ 631 and ~ 635 L/s on the two measurement dates differs by $< 1\%$. The 13/08/2010 set of measurements return a significantly lower discharge of ~ 100 L/s (8.64 ML/d) for the spring. These circumstances indicated the need to more accurately determine the discharge of the spring, perhaps focussing especially on the upstream measurement. The veracity of both sets of flow measurements is interrogated in Tables 10 and 11 on the basis of mass balance calculations as follows:

$$Q_s = [(Q_D C_D) - (Q_U C_U)] \div C_s = [416\,171 - 339\,948] \div 595 = 128 \text{ L/s}$$

$$Q_s = [(Q_D C_D) - (Q_U C_U)] \div C_s = [440\,055 - 396\,970] \div 595 = 72 \text{ L/s}$$

The mass balance results are in better agreement with each other than the SDM-based results. Further, the average of the mass balance results (~ 100 L/s) is similar to the SDM-based result of 13/08/2010. This finding suggests that the discharge of the Zwartkrans Spring on the gauging occasions is more likely in the order of 100 L/s than 200 L/s or greater.

The SDMs carried out at stations BB@M and BB@L on 16/05/2012 (Sect. 5.2.3 in Chapter “Physical Hydrology”) provided a third opportunity to establish the flow of the Zwartkrans Spring. The data presented in Table 12 describe the results obtained. The veracity of the flow measurements given in Table 12 is again interrogated on the basis of a mass balance calculation as follows:

$$Q_s = [(Q_D C_D) - (Q_U C_U)] \div C_s$$

$$= [415\,198 - 212\,058] \div 644 = 315 \text{ L/s}$$

The derived spring discharge value of 325 L/s (Q_s , Table 12) is encouragingly close to the mass balance calculated value of ~ 315 L/s. The difference of 10 L/s is readily accounted for by the negligible flow in the A-furrow (Q_F) which, if added to the downstream flow (Q_D) and assuming an SEC value (C_F) of 94 mS/m, returns a mass balance calculated value of ~ 327 L/s for the Zwartkrans Spring. The result, however, is clearly significantly greater than obtained in either of the previous attempts (Tables 10 and 11).

As postulated in Sect. 5.2.3 in Chapter “Physical Hydrology”, it is questionable whether the Zwartkrans Spring represents the only outlet of the Zwartkrans Basin, i.e. that it is the sole source of groundwater discharge. There is sufficient evidence to indicate that a significant proportion of the observed groundwater contribution to surface flow derives from effluent conditions in the stream channel upstream of the spring. It is quite plausible that the magnitude of this contribution (~ 90 L/s/km of stream reach) exceeds that of the spring itself. Given a stream reach length of ~ 460 m between the upstream BB@M SDM position and the spring, groundwater resurgence could amount to at least ~ 40 L/s. Subtracting this from the spring discharge of 325 L/s yields a value of 285 L/s. Although this is in reasonable agreement with historical reported spring flow values (Bredenkamp et al. 1986), it still far exceeds the results reported in Tables 10 and 11. Unfortunately these circumstances do not resolve the ambiguity that still exists in regard to more accurate quantification of the Zwartkrans Spring discharge.

A fourth set of SDMs carried out on 15/01/2013 provided an opportunity to resolve the existing ambiguity regarding the Zwartkrans Spring discharge. The difference on this occasion was the much tighter bracketing of the Zwartkrans Spring by the in-stream SDM positions. The upstream position was located ~ 20 m ‘above’ the spring, and the downstream position ~ 15 m ‘below’ the spring. Additional rigour was secured by having the irrigation water supply pumps installed at the spring switched off prior to the SDMs, a measure that was not implemented with any of the previous SDMs. The data presented in Table 13 describe the results obtained.

The veracity of the flow measurements given in Table 13 is again interrogated on the basis of a mass balance calculation as follows:

$$Q_s = [(Q_D C_D) - (Q_U C_U)] \div C_s$$

$$= [393\,713 - 301\,656] \div 665 = 138 \text{ L/s}$$

The derived spring discharge value of ~ 136 L/s (Q_s , Table 13) is very close to the mass balance calculated value of ~ 138 L/s. These results are in reasonable agreement with those obtained from the 13/08/2010 (Table 11) SDMs, as well as the mass balance derived discharges associated with the 27/07/2010 and 13/08/2010 measurements, which yielded a spring discharge in the range 72–128 L/s. These findings indicate that a discharge of ~ 136 L/s in mid-January 2013 may confidently be assigned to the Zwartkrans Spring.

A groundwater loss factor that is not accounted for in the preceding discussion, and which is additional to the groundwater resurgence, is that of riparian evapotranspiration (RET) (Sect. 2 in Chapter “Description of the Physical

Table 10 SDM and load-based calculation of the Zwartkrans Spring discharge on 27/07/2010

| Flow location | | Field SEC (mS/m) | TDS [C] (mg/L) | Discharge [Q] | | TDS load | |
|------------------------------------|----------|------------------|-------------------------------------|---------------------------------------|--------|--|------|
| | | | | (L/s) | (ML/d) | mg/s [=Q _x C _x] | t/d |
| Downstream | Stream | 93 | 651 ^a [=C _D] | ~ 477 ^b [=Q _D] | 41.2 | 310,527 | 26.8 |
| | A-furrow | 98 | 686 ^a [=C _F] | ~ 154 ^b [=Q _F] | 13.3 | 105,644 | 9.1 |
| Upstream | | 114 | 798 ^a [=C _U] | ~ 426 ^b [=Q _U] | 36.8 | 339,948 | 29.4 |
| Calculated difference in salt load | | | | | | 76,223 | 6.5 |
| Zwartkrans Spring | | 85 | 595 ^a [=C _S] | ~ 205 ^c [=Q _S] | 17.7 | 121,975 | 10.5 |

^a SEC · 7 used as a proxy to derive a theoretical TDS value^b Synoptic discharge measurement (SDM) value^c Derived value from the difference of the SDM values**Table 11** SDM and load-based calculation of the Zwartkrans Spring discharge on 13/08/2010

| Flow location | | Field SEC (mS/m) | TDS [C] (mg/L) | Discharge [Q] | | TDS load | |
|------------------------------------|----------|------------------|-------------------------------------|---------------------------------------|--------|--|------|
| | | | | (L/s) | (ML/d) | mg/s [=Q _x C _x] | t/d |
| Downstream | Stream | 99 | 693 ^a [=C _D] | ~ 459 ^b [=Q _D] | 39.7 | 318,087 | 27.5 |
| | A-furrow | 99 | 693 ^a [=C _F] | ~ 176 ^b [=Q _F] | 15.2 | 121,968 | 10.5 |
| Upstream | | 106 | 742 ^a [=C _U] | ~ 535 ^b [=Q _U] | 46.2 | 396,970 | 34.3 |
| Calculated difference in salt load | | | | | | 43,085 | 3.7 |
| Zwartkrans Spring | | 85 | 595 ^a [=C _S] | ~ 100 ^c [=Q _S] | 8.6 | 59,500 | 5.1 |

^a SEC · 7 used as a proxy to derive a theoretical TDS value^b Synoptic discharge measurement (SDM) value^c Derived value from the difference of the SDM values**Table 12** SDM and load-based calculation of the Zwartkrans Spring discharge on 16/05/2012

| Flow location | | Field SEC (mS/m) | TDS [C] (mg/L) | Discharge [Q] | | TDS load | |
|------------------------------------|----------|------------------|-------------------------------------|---------------------------------------|--------|--|------|
| | | | | (L/s) | (ML/d) | mg/s [=Q _x C _x] | t/d |
| Downstream | Stream | 94 | 658 ^a [=C _D] | ~ 631 ^b [=Q _D] | 54.5 | 415,198 | 35.9 |
| | A-furrow | 94 | 658 ^a [=C _F] | Negligible [=Q _F] | | | |
| Upstream | | 99 | 693 ^a [=C _U] | ~ 306 ^b [=Q _U] | 26.4 | 212,058 | 18.3 |
| Calculated difference in salt load | | | | | | 203,140 | 17.6 |
| Zwartkrans Spring | | 92 | 644 ^a [=C _S] | ~ 325 ^c [=Q _S] | 28.1 | 209,300 | 18.1 |

^a SEC · 7 used as a proxy to derive a theoretical TDS value^b Synoptic discharge measurement (SDM) value^c Derived value from the difference of the SDM values

Environment”). The magnitude of such loss has been estimated at 25–50 mm/a in the Valley and Ridge, Blue Ridge and Piedmont physiographic provinces in the eastern USA (Rutledge and Mesko 1996; Swain et al. 2004). These values equate to losses of 1250–2500 m³/a/km (0.04–0.08 L/s/km) for a 50-m wide zone⁸ spanning the Bloubank Spruit. It is

evident that even if the width of this zone was an order of magnitude greater, groundwater losses attributable to RET in the study area would still not approach those of groundwater resurgence along stream reaches where conditions favoured both these processes.

In conclusion, it is worth noting that the combined discharge of at least ~ 260 L/s represented by the Zwartkrans Spring and groundwater resurgence as set out in Table 13 and Table 5.15 respectively, agrees remarkably well with the 258 L/s reported by Bredenkamp et al. (1986) (Sect. 1) for the Zwartkrans Spring alone. To this must be added the

⁸ Bredenkamp and van Staden (2009) report that the riparian tree zone is typically 10–20 m wide and the vegetation is dense and almost forest-like, dominated by indigenous trees and very dense forest-like bush on both banks of rivers, streams and creeks (Sect. 3.2).

Table 13 SDM and load-based calculation of the Zwartkrans Spring discharge on 15/01/2013

| Flow location | Field SEC (mS/m) | TDS [C] (mg/L) | Discharge [Q] | | TDS load | |
|------------------------------------|------------------|-------------------------------------|---------------------------------------|--------|--|------|
| | | | (L/s) | (ML/d) | mg/s [=Q _x C _x] | t/d |
| Downstream | 103 | 721 ^a [=C _D] | ~ 546 ^b [=Q _D] | 47.2 | 393,713 | 34.0 |
| Upstream | 105 | 735 ^a [=C _U] | ~ 410 ^b [=Q _U] | 35.5 | 301,656 | 26.1 |
| Calculated difference in salt load | | | | | 92,057 | 7.9 |
| Zwartkrans Spring | 95 | 665 ^a [=C _S] | ~ 136 ^c [=Q _S] | 11.7 | 90,206 | 7.8 |

^a SEC · 7 used as a proxy to derive a theoretical TDS value

^b Synoptic discharge measurement (SDM) value

^c Derived value from the difference of the SDM values

groundwater resurgence that occurs upstream of station BB@M, which has been measured at between 90 and 190 L/s (Sect. 5.2.3 in Chapter “Physical Hydrology”), for a total groundwater discharge from the Zwartkrans Basin in the range 350–450 L/s. These discharges equate to recharge values of ~ 16 and ~ 20%, respectively, for the Zwartkrans Basin.

4.2 Plover’s Lake Springs

Located on the Crab Farm and Plover’s Lake estates in the Kromdraai area of Quaternary A21D, the features that comprise the group of springs and seeps collectively referred to as the Plover’s Lake springs⁹ produced a combined yield of ~ 60 L/s (5.2 ML/d) in both September 2009 and May 2010, and ~ 64 L/s (5.5 ML/d) in August 2014. The excellent quality karst groundwater (Sect. 7.3 “Chapter Chemical Hydrogeology”) is channelled into a landscaped central drainage feature with canals and furrows on either side that deliver water to various downstream properties on the Plover’s Lake and Crab Farm estates before discharging into the Bloubank Spruit. These springs also provide a basis for the extrapolated elevation of the potentiometric surface associated with the Plover’s Lake fossil site (Fig. 9 and Table 6 in Chapter “Description of the Physical Environment”) located ~ 200 m upgradient (west) of these features.

4.3 Kromdraai Spring

Also located in Quaternary catchment A21D, the Kromdraai Spring discharges directly into the Bloubank Spruit on the left bank of this drainage on Ptn 35 (Ekuthuleni Estate) of the farm Kromdraai 520 JQ. Its submerged discharge is distinguishable from that of the passing flow in the Bloubank Spruit on the basis of the following observations:

- displacement towards the opposite bank of floating particulate matter from upstream;
- a distinctive body of much clearer water in the river, together with a perceptibly perturbed flow environment directed at right-angles to the passing surface flow;
- a typical groundwater temperature of 19.4 °C at the discharge point in late winter,¹⁰ compared to the 13.3 °C of upstream river water (difference of 6.1 °C) at this time; and
- an SEC value of ~ 55 mS/m (Fig. 33 “Chapter Chemical Hydrogeology”) at the discharge point into the river, compared to an SEC of 84 mS/m for the river water upstream of the spring.

An assessment of the spring discharge obtained from the difference between flow measurements made immediately upstream and downstream of the site (Table 14) on 13/08/2010 returned a value of ~ 307 L/s (26.5 ML/d). This is by far the highest discharge of the eleven springs enumerated in the study area (Table 9). Understandably, this observation raised concern for the veracity of the SDMs. As applied in the Zwartkrans Spring discharge assessment (Sect. 4.1), a mass balance comparison of the upstream and downstream springwater TDS loads offers a means to verify the result. Using the values in Table 14, the mass balance calculation yields the following result.

$$Q_S = [(Q_D C_D) - (Q_U C_U)] \div C_S \\ = [400\,414 - 274\,008] \div 392 = 322\text{ L/s}$$

Accepting the margin of error associated with the flow measurements (possibly as much as ± 15%), the result indicates that the Kromdraai Spring TDS load closely approximates the difference between the upstream and downstream SDM values as illustrated in Fig. 12. A spring discharge of 322 L/s would account exactly for the calculated difference in TDS load of 10.9 t/d (Table 14). Although this result breeds confidence in the spring discharge value derived from the SDMs, it does not explain the anomalously large recharge estimation of ~ 30% which this result

⁹ Referred to as the Kromdraai Springs in previous studies, e.g. Bredenkamp et al. (1986) (see Text Box 1).

¹⁰ The measurements were made on 13/08/2010.

Table 14 Verification of the Kromdraai Spring discharge using TDS load calculations

| Flow location | Temp. (°C) | SEC (mS/m) | TDS [C] (mg/L) | Discharge [Q] | | TDS load | |
|------------------------------------|------------|------------|-------------------------------------|---------------------------------------|--------|--|------|
| | | | | (L/s) | (ML/d) | mg/s [=Q _x C _x] | t/d |
| Downstream | 14.8 | 74 | 518 ^a [=C _D] | ~ 773 ^b [=Q _D] | 66.8 | 400,414 | 34.6 |
| Upstream | 13.3 | 84 | 588 ^a [=C _U] | ~ 466 ^b [=Q _U] | 40.3 | 274,008 | 23.7 |
| Calculated difference in salt load | | | | | | 126,406 | 10.9 |
| Kromdraai Spring | 19.4 | 56 | 392 ^a [=C _S] | ~ 307 ^c [=Q _S] | 26.5 | 120,344 | 10.4 |

^a SEC · 7 used as a proxy to derive a theoretical TDS value

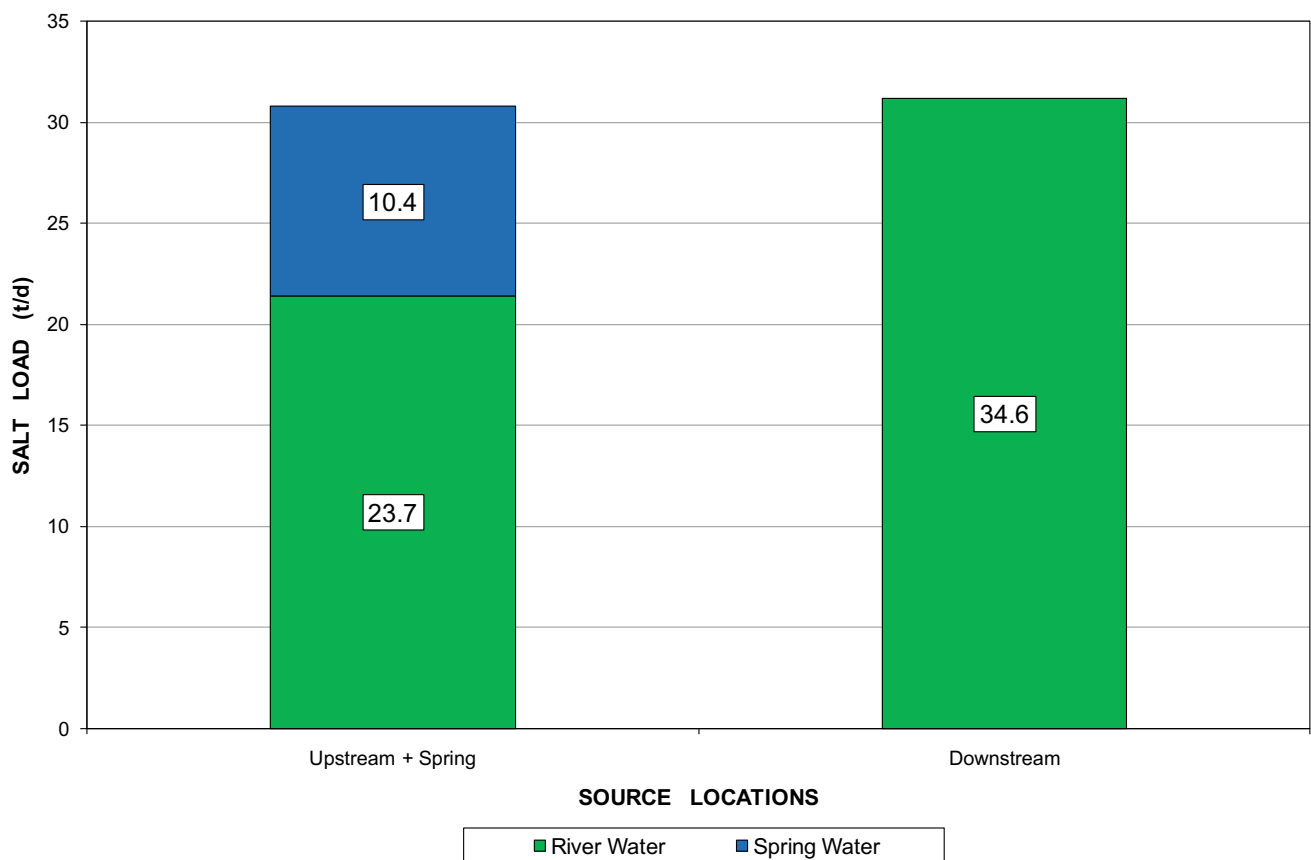
^b Synoptic discharge measurement (SDM) value

^c Derived value from the difference of the SDM values

attributes to the basin footprint area (Table 4). This circumstance is discussed in Sect. 2.12.

The discharge values suggest that the Kromdraai Spring contributed ~ 40% of the flow in the Bloubank Spruit at this location on the day of measurement. The downstream discharge of 66.8 ML/d equates to 24.4 mm³/a, which is slightly greater than the long-term median MAR value of 22.6 mm³/a recorded at gauging station A2H049 (Fig. 10 in Chapter “Physical Hydrology”). Accepting the extreme coarseness of

such a comparison, these circumstances reflect the abnormally high flow conditions experienced in the inter-connected surface water and groundwater components of the Bloubank Spruit system during the 2010 and 2011 winters. More significantly, however, the Kromdraai Spring discharge of 26.5 ML/d (9.7 mm³/a) represents ~ 43% of the long-term median MAR at station A2H049. This contribution from karst groundwater increases to ~ 53% with the inclusion of the Plover’s Lake springs discharge of ~ 60 L/s (5.2 ML/d).

**Fig. 12** Verification of the Kromdraai Spring discharge based on mass balance calculations

4.4 Danielsrust Spring

The Danielsrust Spring drains the Danielsrust Basin, a ‘perched’ karst aquifer ~ 740 ha in extent located within the Krombank Basin, and which clearly exhibits hydraulic separation from the latter (Sect. 2.3). The long-term discharge of 28 L/s (2.4 ML/d) is not used at present, and is lost to a combination of evaporation, evapotranspiration and infiltration into the Krombank Basin. These circumstances simultaneously describe autogenic discharge of the Danielsrust Basin and autogenic recharge of the Krombank Basin, both located in Quaternary catchment A21D.

4.5 Aquamine Spring

The Aquamine Spring rises in the upper reaches of the Tweefontein Spruit on the contact between Ventersdorp Supergroup and Dominion Group strata, but is provisionally considered to include the ~ 725 ha Rietfontein Basin in its catchment. The yield of the spring (< 2 L/s), however, is notably less than that of the karst springs draining karst basins of similar size, e.g. the 28 L/s Danielsrust Spring draining the ~ 740 ha Danielsrust Basin. These circumstances might attract further investigation in future hydrogeologic studies.

4.6 Tweefontein Spring

Of the 11 karst springs surveyed, the Tweefontein Spring (aka JNNR1) in the JNNR occupies the second highest elevation after the Danielsrust Spring (Table 9). It also exhibits a similar flow to that of the latter, namely ~ 30 L/s (SDM on 19/05/2010). SDMs on 12/08/2014 and 27/02/2018 returned flows of ~ 26 and ~ 12 L/s respectively. Although the spring is located in Quaternary basin A21G, its catchment of ~ 1160 ha includes dolomitic portions of Quaternary basins A21D and A21E. Rising in the Tweefontein Basin at an elevation of ~ 1450 m amsl, its discharge contributes autogenic recharge to the Diepkloof Basin to the north drained by the Grootvlei Spruit and Nouklip Spring. Contemporary SDM values indicate an average contribution of 14% to the discharge of the Nouklip Spring.

4.7 Nouklip Spring

The Nouklip Spring (aka JNNR2) rises in the lower reach of the Grootvlei Spruit and is impounded in the so-called ‘swimming pool’ dam in the north-western portion of the JNNR. This impoundment also collects the discharges (< 2

L/s each) of at least 11 other seepages in the vicinity (T Abiye, personal communication), and releases the aggregate flow (measured at ~ 173 L/s on 19/05/2010, ~ 211 L/s on 12/08/2014 and ~ 12 L/s on 27/02/2018) via the Grootvlei Spruit into the Skeerpoort River (Plate 2). Rising at an elevation of ~ 1330 m amsl at the contact between the Rooihooigte Formation and the overlying ferruginous shales of the Timeball Hill Formation (Pretoria Group), it drains the ~ 4125 ha Diepkloof Basin. This basin includes part of the dolomitic portions of Quaternary basins A21G and A21H.

The SDM flows of ~ 173 , ~ 211 and ~ 105 L/s translate into discharges of ~ 5.5 , ~ 6.7 and ~ 3.3 mm³/a. The mean discharge of 163 L/s (5.1 mm³/a) is in fair agreement with the median discharge per hydrological year of ~ 5.4 mm³ reported for gauging station A2H033 (Fig. 2 in Chapter “Physical Hydrology”) in the period 1997–2015. Subtracting the autogenic recharge delivered by the Tweefontein Spring returns ‘stand-alone’ flows for the Nouklip Spring in the range ~ 93 to ~ 183 L/s. On 19/05/2010, the losing reach downstream of the Tweefontein Spring extended for ~ 700 m. On 19/01/2012 it had increased to ~ 1450 m, and on 12/08/2014 to ~ 1550 m. By 27/02/2018, however, the losing reach had shrunk to < 600 m. This is considered to reflect the coeval lower SDM yield of ~ 12 L/s for the Tweefontein Spring (Sect. 4.6).

A closer inspection of the A2H033 hydrograph for the last seven hydrological years returns the information presented in Fig. 13. The median discharge of 170 L/s (~ 5.4 L/s) is similar to that for the longer period going back to 1997. The relative accuracy of the May 2010 and August



Plate 2 Discharge of the Grootvlei Spruit (centre right) into the Skeerpoort River (at left, looking downstream); flow in the Skeerpoort River before this confluence (in foreground) derives mainly from the ~ 130 L/s discharge of the Nash Spring

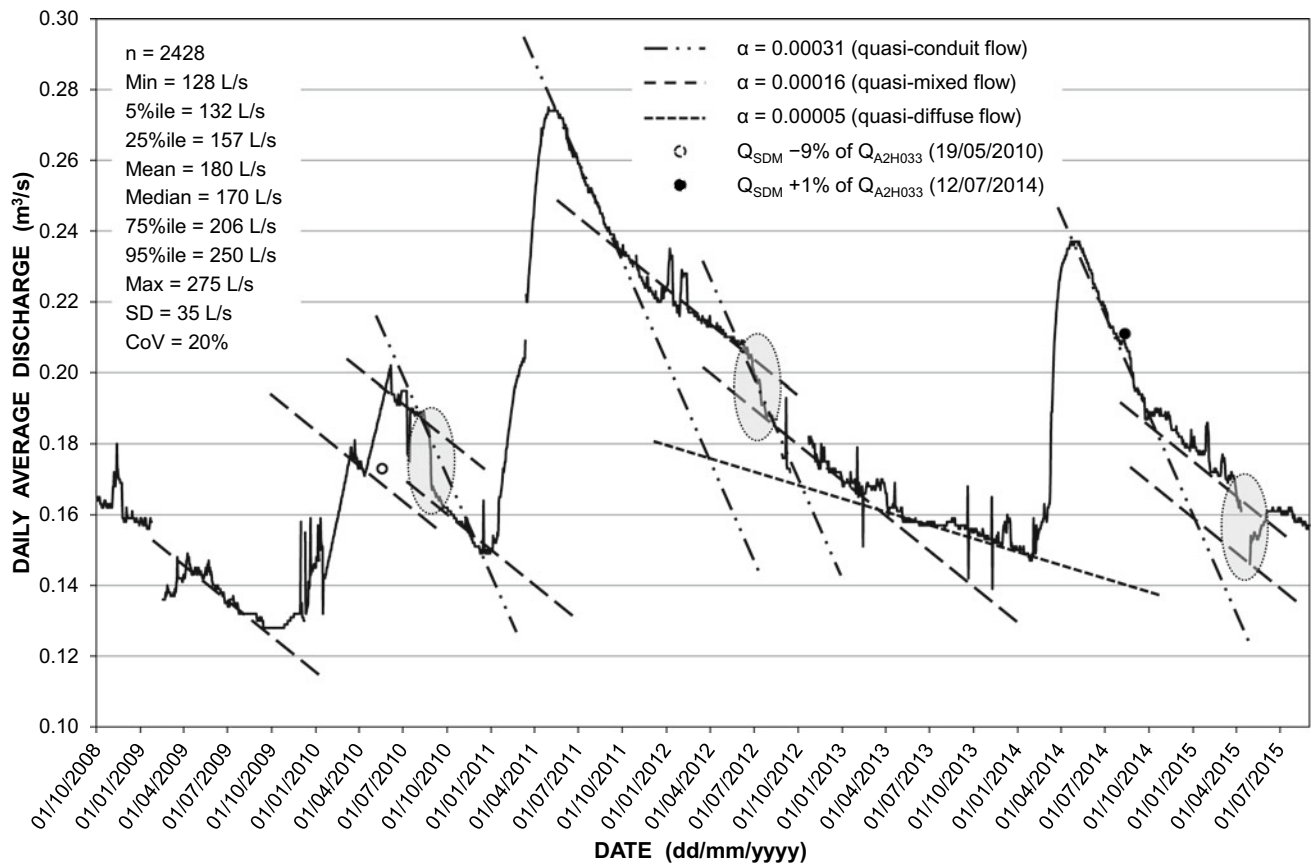


Fig. 13 Hydrograph of the Nouklip Spring as gauged at station A2H033 on the Grootvlei Spruit ~ 525 m downstream of the spring

2014 SDM values to the gauged values are shown to be $\pm 10\%$. The hydrograph reveals a complex recession comprising three distinct limbs defined by α -values (slopes) of 0.00031, 0.00016 and 0.00005 respectively. Taylor and Greene (2008) show that slopes of this magnitude describe the diffuse flow or slow flow components of karst drainage systems. This is somewhat misleading, as the steepest recession segments typically represent the conduit flow component, and the intermediate segments the mixed flow component of such systems.

A further characteristic of the hydrograph is the periods (shaded oval areas) of quasi-conduit (α_{q-c}) flow that ‘interrupt’ the periods of quasi-mixed (α_{q-m}) flow. These suggest that the discharge characteristics of the Diepsloot karst basin reflect a multi-layered karst system comprising a hydraulic continuum between three sets of hydrogeologic units where the porosity and permeability of $\alpha_{q-c} > \alpha_{q-m} > \alpha_{q-d}$ (quasi-diffuse flow) all within the domain of classic diffuse flow. The volume of water in storage in the saturated zone above the elevation of the spring, known as the dynamic

volume V^{11} (Ford and Williams 2007), is calculated at 530 mm^3 , being the sum of the component volumes V_{R0} (328 mm^3), V_{R1} (124 mm^3) and V_{R2} (78 mm^3). The sum of V_{R1} and V_{R2} (202 mm^3) represents the flood-water volume. The V_{RT} of 530 mm^3 is $\sim 280\%$ greater than the nominal FSC (190 mm^3) of Hartbeespoort Dam, equivalent to a uniform water depth of $\sim 14 \text{ m}$ over the 3800 ha extent of the Diepkloof Basin, or else a uniform depth of $\sim 70 \text{ m}$ for a storativity of 20% . Readers conversant in French are referred to the articles by A. Mangin, as reported in Ford and Williams (2007), for further literature on this topic.

It is postulated that the discharge characteristics of the Nouklip Spring are representative of the other high-yielding springs in the COH and, for that matter, in the wider distribution of Malmani Subgroup strata. The relative constancy and low variability (\sim twofold difference between Q_{\min} and Q_{\max}) of these features supports the Martini (2006) observation regarding the ‘very regular discharges at resurgences’ that characterise karst springs of the South African interior.

¹¹ $V = cQ_0/\alpha$, where the constant $c = 86\,400$ for baseflow Q_0 in m^3/s and slope α in days.

4.8 Nash Spring

The location of the Nash Spring (aka JNNR3) close to the contact between the dolomitic (Malmani Subgroup) and sedimentary (Timeball Hill Formation) strata in the north-western portion of the JNNR, together with the substantial discharge (~ 130 L/s on 19/05/2010, ~ 208 L/s on 12/08/2014 and > 100 L/s on 27/02/2018), indicates that this feature represents the main outflow of the ~ 2750 ha Uitkomst Basin north-westwards into the Skeerpoort River catchment (Quaternary basin A21G). The catchment of this spring also includes a small dolomitic portion of Quaternary catchment A21D.

4.9 Uitkomst Spring

This spring (aka JNNR4) issues from shale of the Timeball Hill Formation (Pretoria Group) in close proximity to the contact with the underlying older dolomite of the Eccles Formation, or possibly the Rooihooft Formation, in the north-western portion of the JNNR. The discharge of ~ 2 L/s is similar to that of the Aquamine Spring which also issues from non-dolomitic strata (Sect. 4.5). These circumstances again reflect the poorer water-bearing potential of the sedimentary rocks of the younger (overlying) Pretoria Group in Quaternary basin A21G compared to the dolomitic formations.

4.10 Cradle Spring

Located in the Motsetse Nature Reserve (MNR), the Cradle Spring is another example of a barrier sill contact spring in the COH. It drains the comparatively small (270 ha) Motsetse Basin in Quaternary basin A21E at an elevation of ~ 1405 m amsl. The groundwater level elevation of ~ 1432 m amsl determined for geosite MNR1, a borehole located ~ 1100 m upgradient of the spring, indicates a hydraulic gradient of 0.0245 between these two sources. This is 'normal' for a karst environment, and it is therefore surprising that the Cradle Spring delivers only ~ 2 L/s. This flow equates to a natural recharge of only $\sim 3\%$ of an MAP of 710 mm on the Motsetse Basin (Table 4). This presumes, of course, that the spring is the only outlet for this compartment. Other water 'loss' components that might factor into this equation, in order of decreasing likelihood, are:

- groundwater abstraction for water supply to the Cradle Boutique Hotel and Cradle Restaurant on the property;
- unaccounted for subsurface losses through the barrier sill; and

- evapotranspiration under circumstances of a comparatively shallow depth to groundwater level (~ 12 m bs) as observed in borehole MNR1 located upstream of the spring.

These components together need only amount to ~ 5 L/s to produce a natural recharge that is equivalent to $\sim 12\%$ of an MAP of 710 mm for this compartment. It is also possible, of course, that the spring drains mainly chert-poor strata of the Lyttelton Formation.

4.11 Anderson Spring

The Anderson Spring occupies an elevation of ~ 1365 m amsl in an easterly draining valley on the Kalkheuvel West Estate. It is located in the south-eastern corner of the Broederstroom Basin defined by the E–W striking Hartbeesthoek Dyke and the N–S striking Rhenosterspruit Dyke (Fig. 3). Its yield was measured at ~ 5 L/s on 27/11/2014.

4.12 Barlow Spring

The Barlow Spring is located ~ 1600 m south-southeast of the Anderson Spring, which places it in the north-eastern corner of the Kalkheuvel Basin at a similar elevation (~ 1365 m amsl) as the Anderson Spring. It comprises a number of seeps that individually are difficult to quantify, but which drain from the receiving dam at a rate of < 2 L/s.

4.13 Lesedi Spring

The Lesedi Spring is located at an elevation of ~ 1337 m amsl on the property of the Lesedi African Lodge and Cultural Village. This locates it in the Broederstroom Basin. It is a protected feature encased in a caisson-like structure which drains via a buried 100 mm uPVC pipe to a collection chamber. The collection chamber is fitted with a centrifugal pump to distribute water to residences located on the high ground (> 1450 m amsl) in the western portion of the Kalkheuvel West Estate.

4.14 Broederstroom Spring

Located on the Glen Afric Country Lodge property south of Broederstroom, this spring occupies an elevation of ~ 1281 m amsl in a northerly draining valley in Quaternary basin A21H. It is another example of a lithologic contact spring in the COH. Its measured yield of ~ 21 L/s

compares favourably with a reported maximum yield of 25 L/s (J Brooker, personal communication). Nevertheless, this equates to a natural recharge of only $\sim 5\%$ of an MAP of 710 mm on the 1810 ha Broederstroom Basin (Table 4), which supports the finding that other ‘drains’ (e.g. the Anderson Spring, Lesedi Spring and borehole abstractions) impact on the Broederstroom Basin groundwater store.

4.15 Krugersdorp Game Reserve Springs

The Krugersdorp Game Reserve hosts at least eight springs. As shown in Table 15, seven of these are associated with dolomite and one with quartzitic strata. The spring SP3 represents a group of distributed seeps rather than a single recognisable ‘eye’. In this instance, the discharge represents the aggregate flow of the contributing seeps as measured at a position downstream of the topographically lowest seep in the group.

Five of the seven karst springs drain the karst outlier that extends from the mine area located to the south, into the southern portion of the KGR (Fig. 14). The other two karst springs are located in the Zwartkrans Basin to the north of the quartzite ridge that strikes NE–SW diagonally through the centre of the KGR.

The springs typically support discharges < 5 L/s, although at least three (SP2, SP3 and Buffalo Sp.) yield > 5 L/s. The yield of Spring 2 (CSIR30) has not been measured, but JFA (2006) reported a yield of 12 L/s. SP3 delivers ~ 10 L/s on average, its catchment defined by the Tweelopie Spruit on the east and the Sterkfontein Dyke on the west (Fig. 3). It is doubtful whether the combined yield of all these features exceeds 30 L/s (2.6 ML/d).

4.16 Spring Discharge Context and Significance

The total number of springs in the study area is probably an order of magnitude greater than the eleven enumerated in this study (Table 9). Substantially greater investigative effort relying largely on the contribution of local residents is required to properly evaluate this aspect of the hydrogeologic environment. Nevertheless, the springs enumerated in the study area form two groups, namely those draining the Skeerpoort River catchment (Quaternary basin A21G) and those draining the Bloubank Spruit system (A21D).

The A21G springs together deliver ~ 305 L/s ($9.62 \text{ mm}^3/\text{a}$), the equivalent of $\sim 5\%$ of the MAR of Hartbeespoort Dam. The A21D springs together deliver ~ 504 L/s ($15.89 \text{ mm}^3/\text{a}$), to which must be added groundwater resurgence in the stream channel of at least ~ 130 L/s, delivering the equivalent of $\sim 10.5\%$ of the Hartbeespoort Dam MAR. Although certainly not all of the

spring discharge reaches the dam, the combined flow of $29.6 \text{ mm}^3/\text{a}$ still represents $\sim 16\%$ of the full supply capacity of the reservoir. More significantly, the collective groundwater discharge in the A21D catchment represents $\sim 88\%$ of the long-term median annual discharge (22.7 mm^3) of this basin. The value of this generally good to excellent quality groundwater in mitigating the negative impact of the mine and municipal wastewater cannot be over-emphasised.

It is evident, therefore, that the COH is not only one of the most productive palaeo-anthropological terranes in southern Africa, but also one of the most productive karst terranes from a groundwater yield perspective. Calculating the financial value of the ‘goods and services’ delivered by this karst terrane¹² in mitigating the negative impact of the mine and municipal wastewater components on downstream water resources presents a further challenging exercise that is beyond the scope of this study.

5 Water in the Mining Environment

It is common cause that the underground void created by gold mining in the West Rand Goldfield is flooded and actively decanting acid mine drainage (AMD). The import hereof for the study area is woven into the fabric of the water resource environment (Sect. 5 in Chapter “Description of the Physical Environment”). The conceptual model of the mine water relationship to the natural hydrogeologic setting is illustrated in Fig. 15 using the geologic profile presented in Fig. 7 in Chapter “Description of the Physical Environment” as basis. The hydraulic link between the subsurface Main Reef mine workings and the LoD via the Black Reef Incline (BRI), #17 and #18 winzes is evident. Also shown in Fig. 15 is the position of monitoring boreholes RG1 and MGP2 that aid in elucidating the occurrence of mine water in the hydrogeologic environment of the Western Basin. The need to lower the hydrostatic head in the flooded mine void if active decant is to be curtailed, is also evident from Fig. 15. This might be achieved with a reduction in head of as little as ~ 25 m, i.e. from ~ 1675 to ~ 1650 m amsl.

It has also been recognised, however, that sufficient freeboard needs to be created in the mine void to serve as buffer for excessive recharge during wetter than normal summer rainfall seasons. It is partly for this reason that a reduction in head of ~ 150 m (equivalent to an elevation of ~ 1525 m amsl) has been proposed (Coetzee et al. 2010). This has, however, already been revised upward

¹² The reader is referred to a discussion piece by Blackeagle (2014) on the distinction between ‘terrane’ and ‘terrain’, on the basis of which use of the term ‘terrane’ in this context is explicit.

Table 15 Description of springs enumerated in the Krugersdorp Game Reserve

| Spring | Alternative ID | Latitude ^a (dd.ddddd°S) | Longitude ^a (dd.ddddd°E) | Elevation (m amsl) | Source Aquifer | |
|------------|---------------------|---------------------------------------|--|--------------------|-------------------------|---|
| CSIR30 | Spring 2 @ cemetery | 26.09808 | 27.71892 | 1641 | Karst outlier | Also referred to as the cemetery group of springs |
| CSIR63 | Spring 1 @ cemetery | 26.09814 | 27.71958 | 1638 | | |
| SP1 | F6S7 (Cemetery) | 26.09694 | 27.71898 | 1637 | | |
| SP2 | F8S9 (Poplar Grove) | 26.09092 | 27.72011 | 1626 | Karst outlier | |
| Buffalo Sp | – | 26.09073 | 27.72230 | 1627 | Karst outlier ‘toe’ | |
| Lodge Sp | CSIR20 | 26.09044 | 27.71625 | 1600 | Witwatersrand quartzite | |
| Aviary Sp | CSIR55 | 26.07753 | 27.70092 | 1530 | Zwartkrans Basin | |
| SP3 | Flip-se-Gat stream | 26.08149 ^b | 27.69589 ^b | 1553 | Zwartkrans Basin | |

^a For a discussion of spring coordinates and disparity resolution, see Sect. 3.5 in Hobbs (2011)

^b Coordinates of the most westerly (highest) seepage contributing to the aggregate discharge measured and sampled at coordinates 26.07692°S–27.69928°E

to ~ 1550 m amsl (BKS 2011; DEA 2014), and might even be relaxed further to ~ 1575 m amsl if circumstances allow (DWA 2013a).

Text Box 1 The Kromdraai Spring/Plover’s Lake Spring(s) conundrum

The spring listed as #13 by Vegter (1995), and located on the farm Kromdraai 520JO¹³ located at 25.969°S–27.788°E¹⁴, has historically been regarded as the Kromdraai Spring. For example, Bredenkamp et al. (1986) refer to the Kromdraai Spring(s), as do Holland (2008) and Holland and Cobbing (2008). The Kromdraai Spring enumerated in this study, however, is located at coordinates 25.990°S–27.776°E (Table 85 and Fig. 5.27). This equates to a linear geometric disparity of ~ 2600 m compared to the Vegter (1995) coordinates, and cautions against a direct correlation based simply on the spring and topocadastral farm names.

Under circumstances where none of Bredenkamp et al. (1986), Holland (2008) and Holland and Cobbing (2008) report coordinates for the Kromdraai Spring, it is difficult to unravel the geographic uncertainty between this feature and the Plover’s Lake Spring(s). Further to the discussion presented in Footnote 62, an inspection of Fig. 7.1 in Bredenkamp et al. (1986), Figs. 2.1 and 2.2 in Holland and Cobbing (2008) and Fig.100 (from Holland, 2009) clearly

show the position of the Kromdraai Spring at the head of a short (~ 1000 m) left bank tributary of the Bloubank Spruit. As described in Sect. 4.3, the Kromdraai Spring enumerated in this study discharges directly into the Bloubank Spruit.

The coordinates of the Kromdraai “Eye” taken off Fig. 7.1 (scale 1:50,000) of Bredenkamp et al. (1986) are X 2,874,550 m and Y –77,870 m (Cape Datum), which translate to X 2,874,850 m and Y –77,835 m (Hartebeesthoek94 Datum). The latter coordinates are within 205 m of one of the group of springs that comprise the Plover’s Lake Spring(s) enumerated in this study. It is therefore reasonable to presume that the Kromdraai Spring referred to in earlier studies (e.g. Bredenkamp et al. 1986; Holland 2008; Holland and Cobbing 2008) are the Plover’s Lake Spring(s) of this study.

The preceding discussion does not, however, resolve the disparity in reported yield values for the Plover’s Lake Spring(s). This is given as ~ 30 L/s (0.946 mm³/a) by Bredenkamp et al. (1986) and ~ 60 L/s by this study (Sect. 4.2). Likely explanations for the disparity are that (a) the Plover’s Lake springs comprise two groups of springs and seeps delivering ~ 45 and ~ 15 L/s respectively, and (b) the mid-1980s was characterised by a drought period when spring yields in the region might reasonably be expected to have been lower than at present.

¹³ The topocadastral property is identified as Kromdraai 520JQ on the 1:50 000 scale topocadastral map sheet 2527DD Broederstroom (RSA, 2001).

¹⁴ Converted from the Cape Datum to the Hartebeesthoek94 Datum; the accuracy of the conversion is limited by the coarse resolution of the Vegter (1995) coordinates reported to only three decimals.

The reduction in mine water head pertains to the so-called environmental critical level (ECL) that defines the elevation above which AMD will not impact on the environment (Coetzee et al. 2010). In most instances, securing and/or maintaining the ECL requires pumping of the mine water at

significant cost. The latter varies according to the pumping volume (typically 10's of ML/d) and the head (typically > 100 m) against which this must be achieved, which is a direct function of the specified ECL. It is therefore imperative that an ECL be selected which accommodates both the environmental and economic concerns. The feasibility study commissioned by the DWS to investigate the long-term solution to control and manage acid mine drainage

in the Witwatersrand underground mining basins, has sought to refine aspects of this imperative also in regard to the Western Basin. These have been discussed in Text Box 1 in Chapter “Physical Hydrology”. This study, referred to as the AMD FSLTS study, introduced the additional terms socio-economic critical level (SECL) and target operating level (TOL) (DWA 2013b) into the discourse on mine water management.

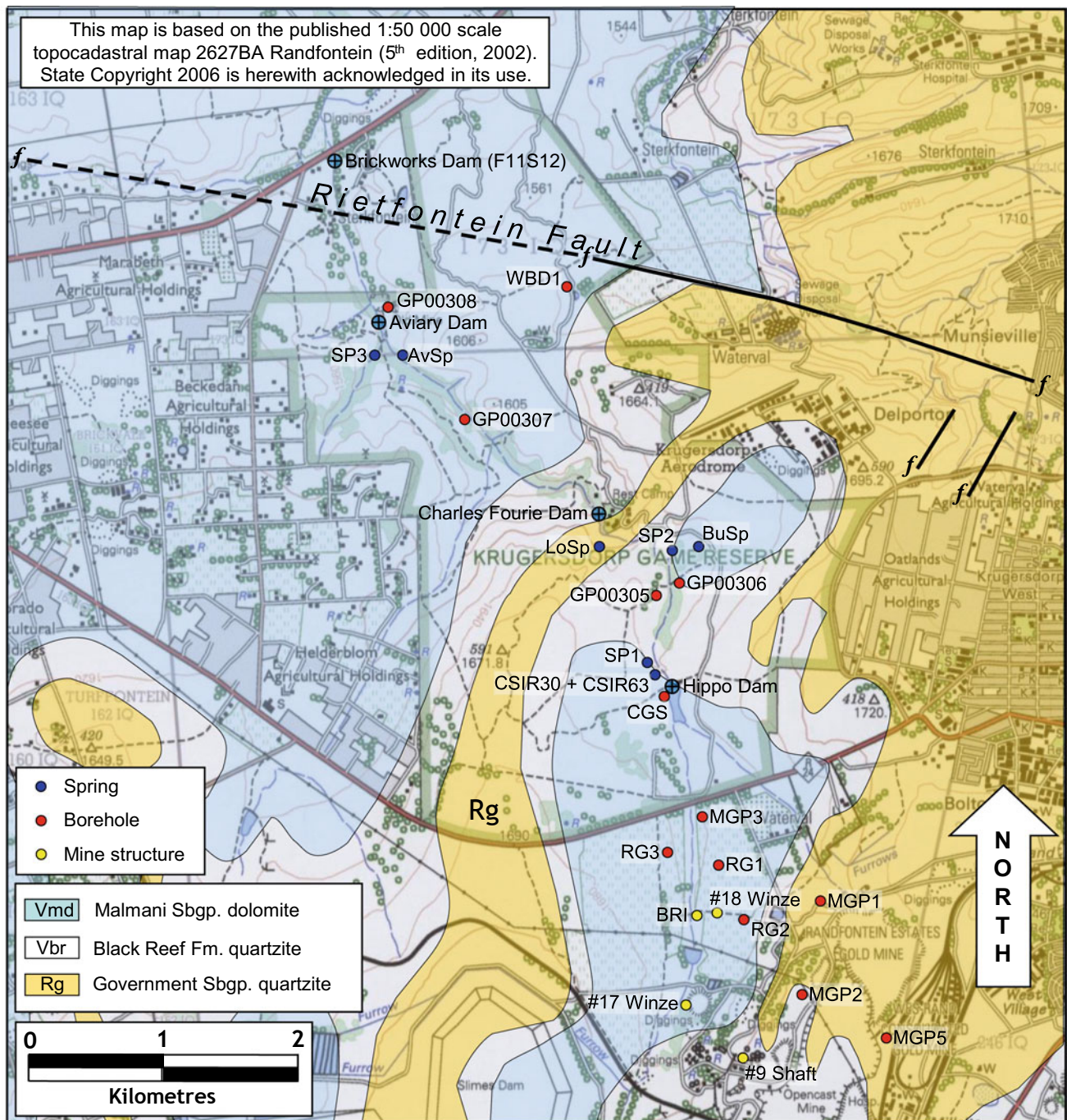


Fig. 14 Locality map of geosites in the mine area and Krugersdorp Game Reserve

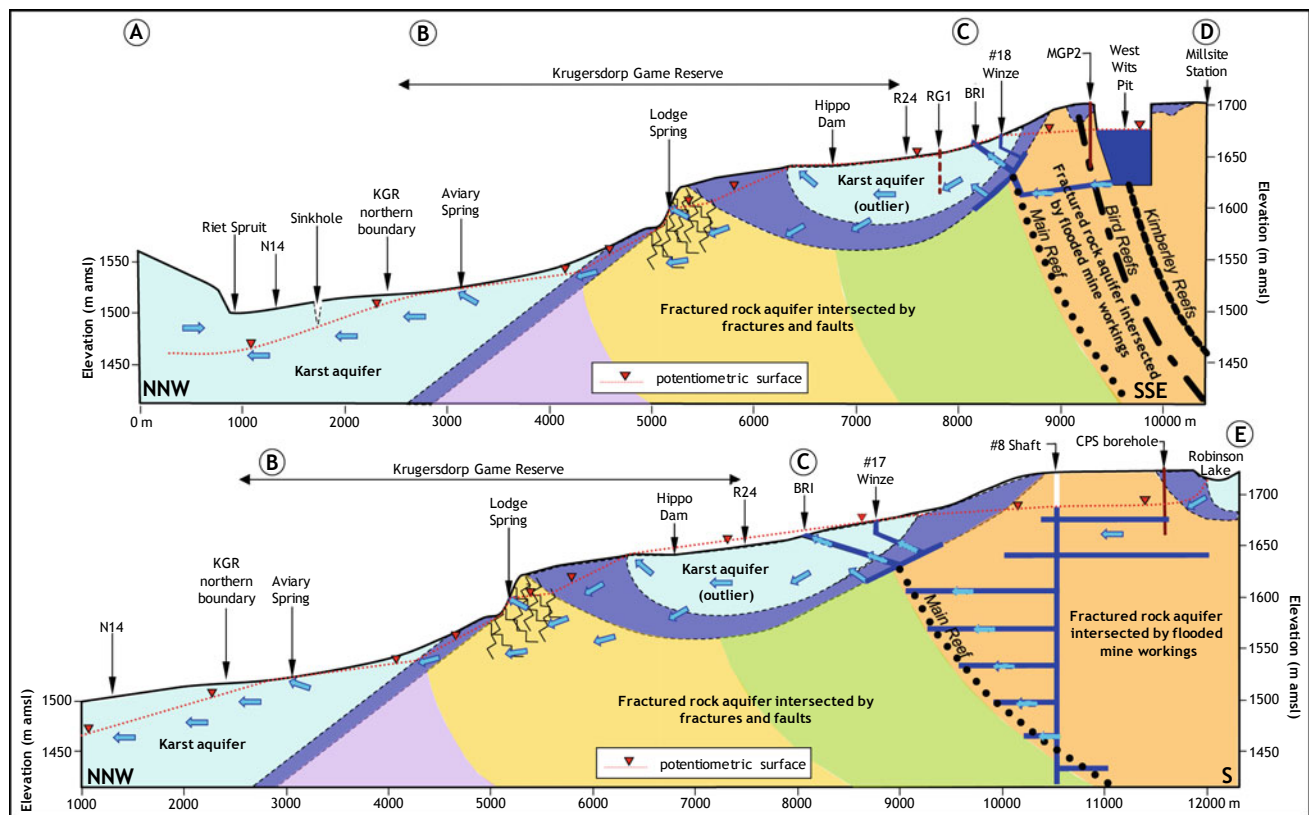


Fig. 15 Schematic profile of hydrogeologic and mining-related features in the West Rand Goldfield (see Fig. 10 for profile positions)

6 Groundwater Drainage Pattern

The groundwater drainage pattern in the karst of the WHS property has undoubtedly been one of the poorer understood hydrogeologic aspects of the study area. Hobbs and Cobbing (2007) criticise the Bredenkamp et al. (1986) subdivision of the Zwartkrans Basin into nine subunits that, together with a comparatively sparse set of water level data, raises doubt over the recognition of an overly disrupted groundwater flow pattern due to barrier boundaries and associated sub-compartmentalisation. Hobbs and Cobbing (2007) employed 48 potentiometric measurements and six spring elevations to develop a potentiometric map for the south-western portion of the study area (Fig. 1). Holland (2007) and Holland and Cobbing (2008) provide groundwater drainage maps for the Zwartkrans Basin that suffer a lack of rigorous discussion of their derivation. Nevertheless, groundwater drainage patterns in the south-western portion of the property have historically enjoyed a much better understanding than in the north-eastern portion.

Data sourced for the situation assessment study (Hobbs 2011a) forms the basis for an improved understanding of

groundwater drainage patterns throughout most of the study area. The drainage patterns rendered in Fig. 16 are based on potentiometric measurements associated with 160 geosites (mine shafts, boreholes, wells and springs) distributed across the WHS property. The information presented in Table 5 reflects the distribution of these sources in the Zwartkrans and Krombank basins, the total of 78 reflecting the relative abundance of geosites in this part of the property compared to the more remote and pristine north-eastern part dominated by the John Nash Nature Reserve. The relative density of enumerated geosites amounts to 0.006 per ha, or ~ 1.2 per 2 km^2 .

The groundwater drainage patterns are represented by the conceptual principal flow vectors associated with each of the basins/subcompartments, and recognise the 'drain' function served by the enumerated springs. This is further illustrated in Fig. 17, which presents a hydrogeologic profile along the section line A–B–C–D in Fig. 16. The surface profile is based on the 20-m contour interval of the published 1:50,000 scale topocadastral maps RSA (1996), RSA (2001) and RSA (2002). The potentiometric surfaces derive from groundwater rest level data sourced in boreholes or representing spring surface elevations as listed in Table 9. The horizontal

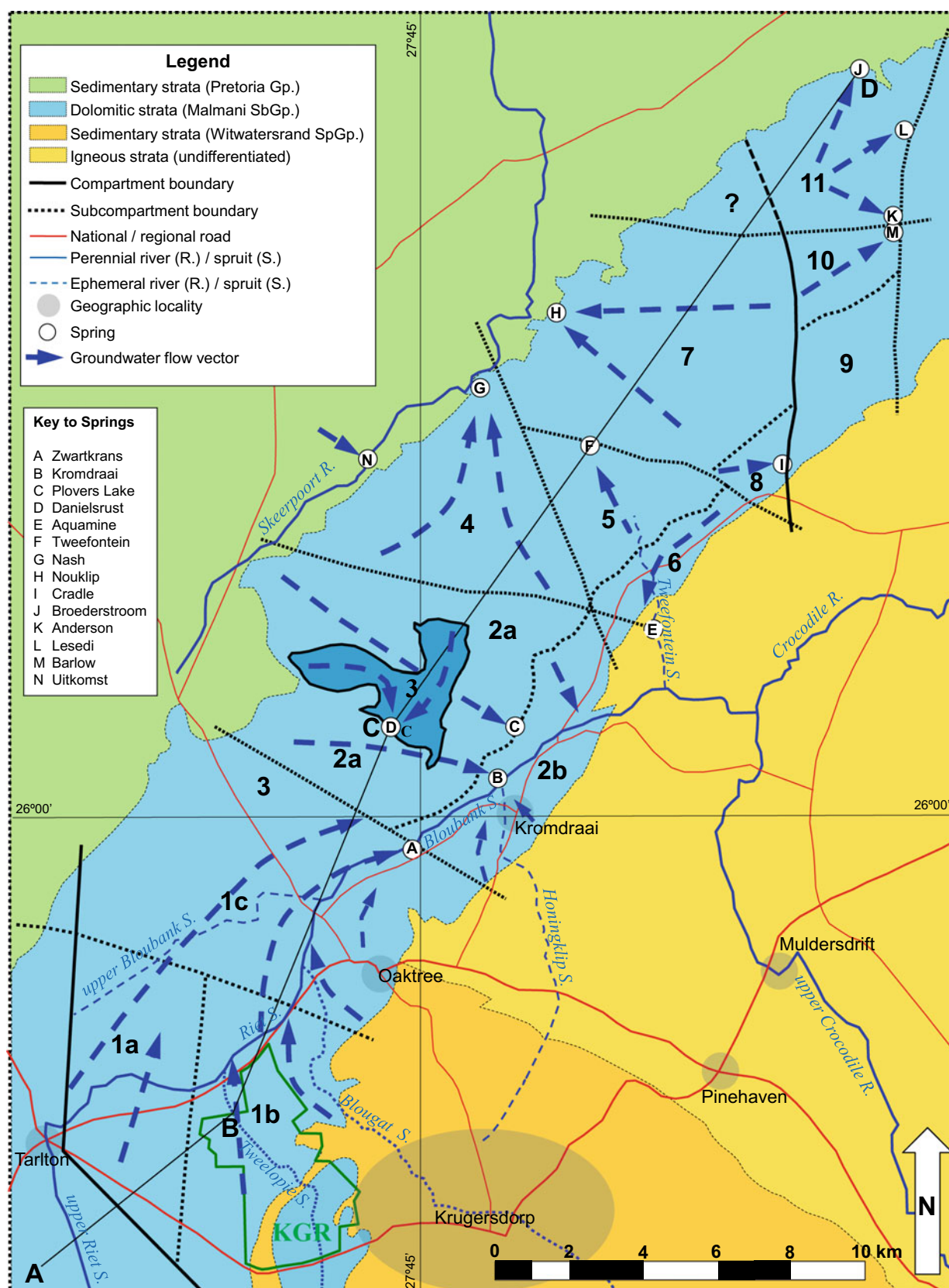


Fig. 16 Groundwater drainage map illustrating the conceptual flow patterns associated with the basins/sub-compartments that subdivide the karst aquifer in the study area; see Table 5 for statistical analysis of groundwater level data in the Bloubaank Spruit system

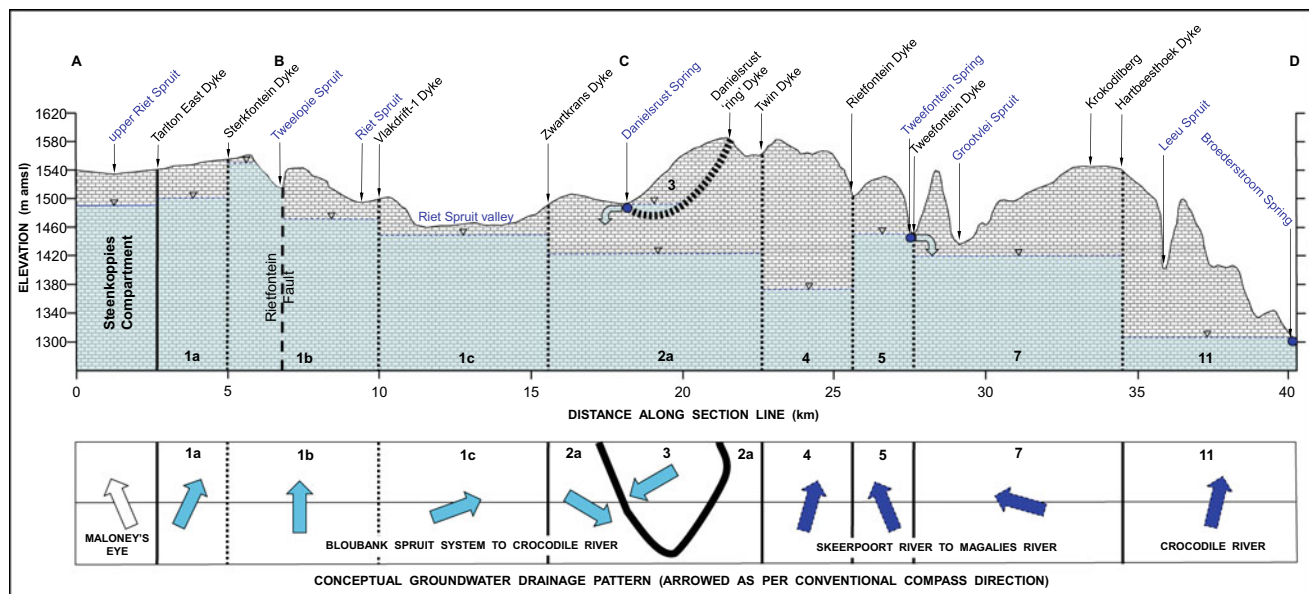


Fig. 17 Hydrogeological cross-section (top) through the karst aquifer from south-west to north-east (see Fig. 16) illustrating the differences in groundwater rest level between basins/subcompartments, and plan view

(bottom) illustrating the corresponding conceptual groundwater drainage pattern as per conventional compass direction; note the autogenic recharge associated with the Danielsrust and Tweefontein springs

attitude of these surfaces is accounted for mainly by their coincidence with equipotential drainage contours, i.e. orthogonal to the drainage vectors.

Perhaps the most salient aspect revealed by the drainage pattern is the complete hydrogeologic separation of the groundwater systems either side of the Twin Dyke. This contradicts previous contentions (e.g. Krige 2010) that the Zwartkrans Basin drains north-eastwards into the Tweefontein Basin¹⁵ and towards Broederstroom. In a revised rendition of compartments by Holland and Cobbing (2008) and Holland (2009), the Twin Dyke is recognised as the north-eastern boundary of the Zwartkrans Basin (Fig. 2). This is in keeping with the Bredenkamp et al. (1986) definition (in Fig. 7.1 op. cit.) of the Zwartkrans Basin. No indication is given, however, of the nature of the boundary formed by this structure, i.e. whether it constitutes an impervious barrier boundary or a semi-pervious leaky boundary.

It would appear that groundwater drainage from the Zwartkrans Basin as identified in the Bredenkamp et al. (1986) study, is focussed on the Zwartkrans and Kromdraai¹⁶ springs. The Holland (2007) and Holland and Cobbing (2008) studies echo this definition.

The movement of groundwater northwards from the Sterkfontein Subcompartment into the Zwartkrans Subcompartment through/over/across the Vlakt-drift-1 Dyke is a particularly vexing question given the observed ~ 20 m step in groundwater rest level elevation that exists from south (~ 1465 m amsl) to north (~ 1445 m amsl) across this 'barrier' (Fig. 18). Field observations at the four localities identified as 'a', 'b', 'c' and 'd' in this part of the study area (Fig. 18) reveal the existence of grikes¹⁷ with a distinct NW-SE orientation. These features are accessible to humans (a measure of their size), and features 'c' and 'd' extend many tens of metres into the subsurface. Some of these also demonstrate a significant visible linear length amounting to 10's of metres, most notably the feature identified as 'b', which extends ~ 60 m north-westwards from the valley of the Riet Spruit near its confluence with the Blougat Spruit.

It is reasonable to presume that the grike features represent an expression of similar sympathetic features that occur at depth, i.e. that intersect the water table of the karst aquifer. For this reason, they represent adequate conduits to establish a subsurface hydraulic connection through the Vlakt-drift-1 Dyke 'barrier', linking the Sterkfontein and Zwartkrans subcompartments. These circumstances, together with those set out in Sect. 5.2.1 in Chapter "Physical Hydrology", inform the observed escalation of a mine water impact on the karst groundwater in this portion of the COH (Hobbs 2013a, b, c; 2014a, b).

¹⁵ Term used in earlier studies (e.g. Holland, 2007; Holland and Cobbing, 2008; Holland et al., 2010) for the north-eastern expanse of karst strata extending from the Twin Dyke to Broederstroom at the north-eastern end of the COH (Fig. 2); also referred to as the North Compartment by Krige (2009; 2010).

¹⁶ The (mis)naming of this spring is discussed in Text Box 1.

¹⁷ See GLOSSARY.



Fig. 18 Elucidation of hydrological, geological and hydrogeological aspects along the southern boundary of the COH south-west of Sterkfontein Quarry; circled localities labelled 'a' to 'd' mark the position of significant grike features, and italicised values indicate the

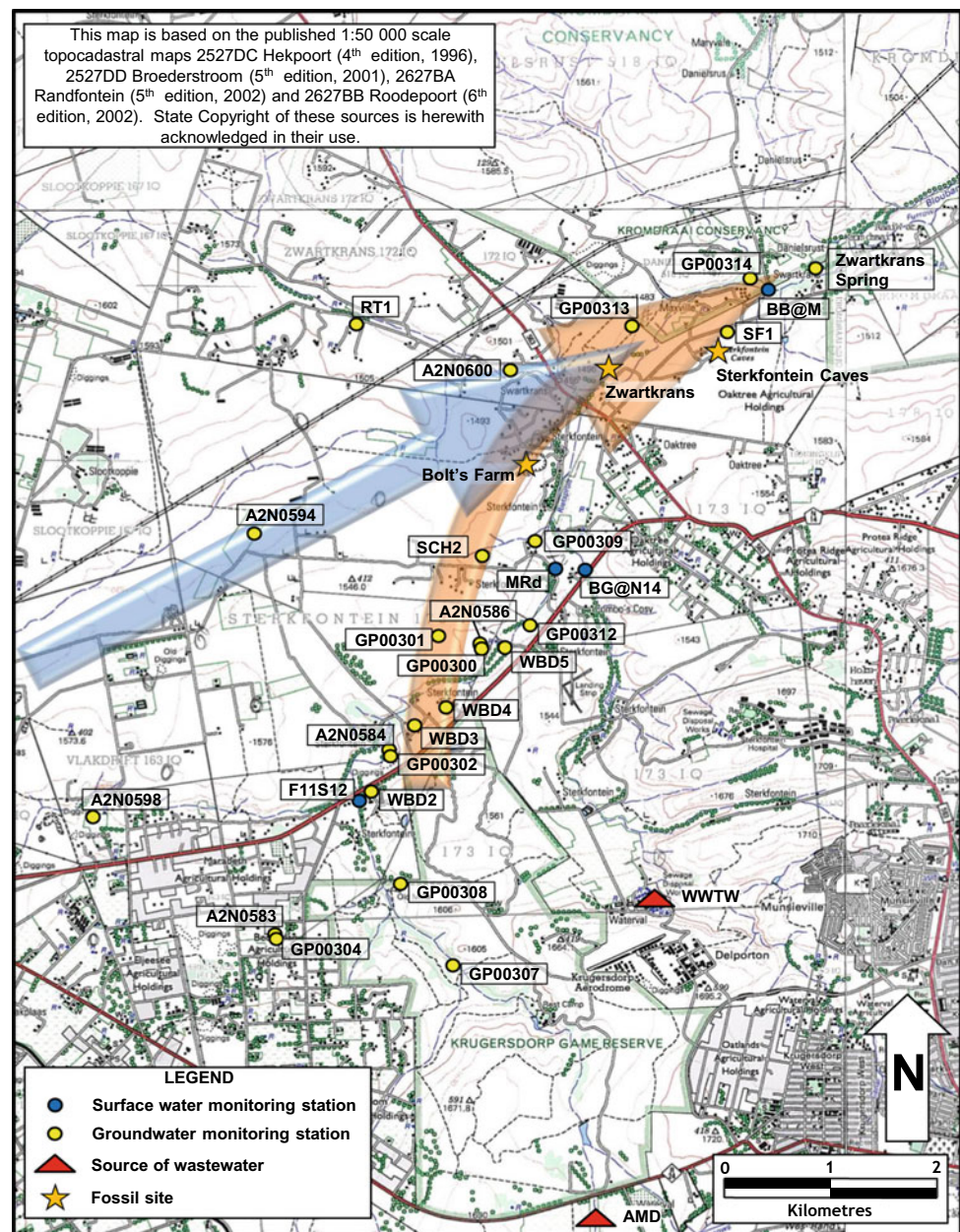
recent ambient groundwater elevation in each subcompartment as derived from individual borehole measurements (base image courtesy of Google Earth®)

The rendition of the groundwater drainage pattern in the extreme north-eastern portion of the property is obscured by the extremely rugged nature of the terrain. Centred on the high ground defined by Krokodilberg (Fig. 17) at an elevation of 1526 m amsl in the Broederstroom Basin, this terrain is drained to the west by the Witwatersrand Spruit, to the north-west by the Leeu Spruit (Fig. 17), and to the east by the Jukskei Spruit. The Broederstroom, Lesedi and Anderson springs (Fig. 16) represent the few natural outlets enumerated in this basin. It is probable that numerous other groundwater emergences occur in the valleys and ravines that dissect this terrain, and which contribute to the groundwater loss component of a basinal water budget. It is further apparent from Fig. 16 that the western boundary of the Broederstroom Basin is poorly understood in regard to the following aspects:

- the hydraulic characteristics of the possible northerly extension of the Krokodilberg Dyke indicated by the pecked line in Fig. 16; and
- the existence of natural groundwater emergences in the valley of the westerly draining Witwatersrand Spruit located in the triangular compartment/subcompartment designated '?' in Fig. 16.

| Key to basins/subcompartments | | | |
|-------------------------------|--------------------------|----|-----------------------------|
| 1a | Vlakdrift Subcompartment | 1b | Sterkfontein Subcompartment |
| 2a | Kromdraai Subcompartment | 3 | Danielsrust Basin |
| 5 | Tweffontein Basin | 7 | Diepkloof Basin |
| | | 11 | Broederstroom Basin |
| | | 4 | Uitkomst Basin |
| | | 1c | Zwartkrans Subcompartment |

Fig. 19 Distribution of selected surface water and groundwater monitoring stations in the Zwartkrans Basin, also showing the groundwater flow paths followed by allogenic recharge (brown) and autogenic recharge (blue)



7 Groundwater Fluxes

The surface water fluxes (gains and losses) discussed in Sect. 5 in Chapter “Physical Hydrology” necessarily impact on the groundwater environment. This is manifested as groundwater resurgence at springs and in stream channels in the discharge reaches of groundwater basins. It is most pertinent in regard to the Zwartkrans Basin, where allogenic recharge associated with the mine water and wastewater sources caused an unprecedented volumetric addition to the quantity of water in this aquifer. The fluxes associated with

the spring and groundwater resurgence in the stream channel upstream thereof are discussed in Sect. 4.1.

The magnitude of allogenic recharge of mine water to the karst aquifer along the Riet Spruit between stations F11S12 and MRd amounted to a median value of 17.3 ML/d in the last four years (Table 12 in Chapter “Physical Hydrology”). The path followed by this recharge is shown in Fig. 19 as encompassing monitoring stations A2N0584 and A2N0586 at the influent (upstream) end, and station A2N0600 further north midway to its discharge at the Zwartkrans Spring. The coarse dimensions of the flowpath from the upstream end to station A2N0600 are 4500 m (length) by 2200 m (width),

with a potentiometric difference of ~ 30 m. These values define a hydraulic gradient (i) of 0.0067. Applying Darcy's law and assuming an aquifer transmissivity (T) value of $\sim 1000 \text{ m}^2/\text{d}$ (roughly 50% of the T-value determined for the aquifer intersected in borehole G36331/A2N0586 as per Table 2), yields the following calculated flow estimate:

$$Q = T_{i,w} = 1000 \times 0.0067 \times 2200 \\ = 14,740 \frac{\text{m}^3}{\text{d}} (\sim 14.7 \frac{\text{ML}}{\text{d}})$$

This value is similar to the minimum of 14–15 ML/d associated with allogenic mine water recharge as per Fig. 24 in Chapter “5” (Sect. 5.2.1 in Chapter “Physical Hydrology”). It also finds support in semi-quantified fluxes such as those of the Zwartkrans Spring and related groundwater resurgence in the Bloubank Spruit at the discharge end of the Zwartkrans Basin. These have been estimated at between 11.6 and 25.6 ML/d (Sect. 5.2.1 in Chapter “Physical Hydrology”), with an average of 16.4 ML/d. The values are not in conflict with one another, and are considered to represent the pre-2010 hydrodynamic situation. A different picture emerges, however, from a mass balance calculation that considers the volume and concentration of the allogenic recharge at the influent end of the flow path, compared to that at station A2N0600. Using the relationship:

$$Q_U C_U = Q_D C_D$$

previously employed in Sect. 4.1, and where

| | |
|---------------------------------------|--|
| $Q_U = 17,300 \text{ m}^3/\text{d}$ | [median influent flow volume from Table 12 in Chapter “Physical Hydrology”] |
| $C_U = 2170 \text{ mg SO}_4/\text{L}$ | [SO ₄ concentration at influent end (station GP00312) ¹⁸] |
| $Q_D = \text{m}^3/\text{d}$ | [flow volume] |
| $C_D = 720 \text{ mg SO}_4/\text{L}$ | [SO ₄ concentration at downstream end (station A2N0600)] |

yields a Q_D value of ~ 52.1 ML/d. This represents an additional contribution of ~ 34.8 ML/d, of which 3–7 ML/d derives from municipal wastewater recharge (Sect. 5.2.2 in Chapter “Physical Hydrology”). The most probable source of the balance (~ 31.8 – 27.8 ML/d) is autogenic recharge (Fig. 19 and Fig. 20) from rainfall (Table 4). These volumes represent a water depth of 118–104 mm (16.6–14.6% of an MAP of 710 mm), well within the recharge rate of $17 \pm 5\%$ of MAP that generally applies in the COH (Sect. 2.12). The substantial agreement and congruence evident between the various figures derived, generates cautious confidence in the groundwater fluxes that

broadly characterise the Zwartkrans Basin since January 2010, when the mine water impact has been greatest. The caution derives from the use of SO₄ as an anionic tracer because of its propensity to participate in any number of bio (geo)chemical reactions, e.g. bacterial sulfate reduction as discussed in Sect. 11 “Chapter Chemical Hydrogeology”. In their discussion on the application of ‘conservative’ anionic tracers, Korom and Seaman (2012) elaborate on the properties of Br and Cl, and make no mention of SO₄ in this regard. Further caution is indicated by non-recognition of factors such as longitudinal dispersion in the aquifer and 3-component mixing.

The groundwater flux values presented in Fig. 19 provide a means to derive an approximate groundwater balance for the Zwartkrans Basin. Input and output values for such a calculation are known to varying degrees of accuracy. For example, readily quantifiable parameters such as recharge and spring discharge present more accurate values than groundwater use. The basic input values to a groundwater balance calculation for the Zwartkrans Basin are autogenic recharge of ~ 30 ML/d and allogenic recharge of ~ 22 ML/d (as derived earlier in this section) for a total of ~ 52 ML/d. Basic output values are groundwater discharge of ~ 30 ML/d (as determined in Sect. 4.1) and groundwater use of ~ 22 ML/d to balance the inputs. The reported values are considered to be in error by $< 10\%$. The veracity of the calculation is demonstrated by the plausibility of the groundwater use value, which compares favourably with the values reported in Sect. 9.

Bredenkamp et al. (1986) report a flux of $\sim 11.7 \text{ mm}^3/\text{a}$ leaving the karst environment of the Bloubank Spruit system downstream of Kromdraai. Being representative of discharge in the mid-1980s, this provides a historical perspective on this aspect. An inspection of the A2H049 hydrograph (Fig. 5.12) indicates that mean discharge in the 1985 and 1986 hydrological years amounted to ~ 13.9 and $\sim 16.6 \text{ mm}^3/\text{a}$, respectively. The discharge of $\sim 11.7 \text{ mm}^3/\text{a}$ approximates the 5%ile value of the long-term annual flow at A2H049. These observations support the comparatively low value reported by Bredenkamp et al. (1986). Under circumstances where the mid-1980s were a dry period, it is presumed that the flow of $\sim 11.7 \text{ mm}^3/\text{a}$ must represent mainly the groundwater contribution from the karst aquifer to discharge in the Bloubank Spruit system. This flow necessarily included the $\sim 0.9 \text{ mm}^3/\text{a}$ ($\sim 30 \text{ L/s}$) contribution of the Kromdraai ‘Eye’ as identified by Bredenkamp et al. (1986).

Further interrogation of the Bredenkamp et al. (1986) flow data indicates an upstream contribution of $\sim 8.1 \text{ mm}^3/\text{a}$ ($\sim 257 \text{ L/s}$) immediately below the Zwartkrans Spring. The difference of $3.6 \text{ mm}^3/\text{a}$ ($\sim 114 \text{ L/s}$) must therefore represent the combined contribution of the Plover's Lake and Kromdraai springs identified and enumerated in

¹⁸ See also borehole WBD5 in Fig. 7 in Chapter “Chemical Hydrogeology”

The main relationships developed by Worthington (2004) are defined by the following equations:

$$D = 0.18(L \times \theta)^{0.81} \quad [R^2 = 0.79] \quad (1)$$

$$D = 0.061 \times L^{0.91} \times \theta^{0.72} \quad [R^2 = 0.90] \quad (2)$$

$$D = 0.047 \times L^{0.85} \times \theta^{0.64} \times E^{0.11} \quad [R^2 = 0.90] \quad (3)$$

where

- D* mean conduit depth (m) below the water table;
- L* flow path length (m) from farthest input to spring;
- θ* dimensionless stratal dip (equal to the sine of the dip in degrees); and
- E* elevation difference (m) between the lowest spring and the highest point of recharge.

The two variables of stratal dip (*θ*) and flow path length (*L*) explain most of the variability in conduit flow depth. More recently, Boudinet (2012) has produced similar results using statistical modelling in an analysis of karstic flow conduits. In the case of Sterkfontein Cave with a stratal dip of $\sim 30^\circ$ (Martini et al. 2003), the farthest input to the Zwartkrans Spring falls in the range 5000–9000 m. These limits define the distance along strike²¹ to the Vlakfontein-1 Dyke and the Tarlton East Dyke, respectively.

The application of the above values in Eqs. 1 and 2 places the mean conduit depth at between 118 and 164 m bwl (Eq. 1), and between 86 and 147 m bwl (Eq. 2). These values appear unlikely in proximity to the caves, especially when gauged against the drilling information provided by DWS monitoring borehole GP00313. Located ~ 800 m to the north-west across the valley of the Bloubank Spruit from the cave (Fig. 19), this borehole intersected very weathered to decomposed and cavernous dolomite down to its completion depth of 37 m bs (~ 1423 m amsl), i.e. 17 m below the water table depth of ~ 20 m bs (~ 1440 m amsl). The most substantial cavity was encountered in the interval 17–32 m bs, i.e. 12 m bwl. Applied in Eq. 1, values for *D* in the range 12–17 m return *L*-values of only 180–280 m, which appear equally unlikely. It is possible that borehole GP00313 was terminated above the deepest conduit in this area.

It is informative to note that applying the distance of ~ 1400 m between the caves and the Zwartkrans Spring in Eqs. 1 and 2 returns *D*-values of 36 and 27 m bwl, respectively. It is also instructive to interrogate the Bredenkamp

et al. (1986) drilling records within the context of Eqs. 1, 2 and 3.

The results for the 13 high-yielding boreholes listed in Table 2 are presented in Table 16. The outcome indicates that Eq. 1 returns the greatest values which in each instance far exceed the empirical value derived from the drill record. Equation 3 returns the smallest values, which therefore also show the least difference with the empirical values.

9 Groundwater Use

From an assessment of water use information sourced from the DWS Water Authorisation and Registration Management System (WARMS), Holland and Cobbing (2008) report a total groundwater use of 8.7 mm³/a as being registered for mainly agricultural use in the Zwartkrans Basin. This figure contrasts sharply with those estimated by Schoeman and Associates (2006) of 14.1 mm³/a based on an interpretation of satellite imagery, and of 25.7 mm³/a estimated by JFA (2006) from a water budget calculation. The latter quantity is accepted by Krige (2009). A further measure of the variance in groundwater uses figures for the Zwartkrans Basin is provided by those of 15 and 18 mm³/a reported earlier by Bredenkamp et al. (1986) and van Biljon (2006), respectively.

The Rhino and Lion Game Reserve maintains an excellent record of the abstraction from borehole RLGR4 which serves the chalets and Wonder Cave. An inspection of this record indicates that an average daily abstraction of 17 m³/d (~ 6200 m³/a) is made from this borehole. Further to the north-east, developments such as the Kalkheuwel West Estate support numerous properties that are dependent on own borehole water supplies for potable and general domestic water use.

The occasional business opportunity where groundwater is bottled for wholesale distribution as ‘mineral water’ is also manifested in the study area. The number of such businesses and their combined annual abstraction is difficult to quantify. It is unlikely, however, that their combined groundwater use is sufficiently great to significantly impact on the groundwater resource supply potential of the karst aquifer(s) in the study area.

10 Closure of DWS Monitoring Stations

The comparatively recent closure of the DWS monitoring stations A2N0589, A2N0594, A2N0598 and A2N0606 is reported in Table 6. This circumstance was informed by the factors listed in Table 17.

It is envisaged by the DWS (E Bertram, personal communication) that in those instances where the stations have

²¹ According to Worthington (2001), this relationship is applicable irrespective of whether flow is along, oblique or normal to the strike of the strata.

Table 16 Interrogation of drill records of high-yielding DWS exploration boreholes located in the Zwartkrans Basin (from Breidenkamp et al. 1986) for mean conduit depth

| DWS Geosite # | Deepest Karst Horizon (m bs) ^a | Water level depth (m bs) | Depth of Karst Horizon (m bwl) ^b | Elevation difference (m) ^c | Mean conduit depth (m bwl) | | | Distance to ZSp (m) |
|---------------|---|--------------------------|---|---------------------------------------|----------------------------|-----|-----|---------------------|
| | | | | | 7-1 | 7-2 | 7-3 | |
| A2N0589 | 80 | 28 | 52 | 35 | 80 | 66 | 49 | 3742 |
| A2N0593 | 103 | 74 | 29 | 81 | 114 | 98 | 77 | 5773 |
| A2N0590 | 87 | 34 | 53 | 42 | 76 | 62 | 47 | 3496 |
| A2N0592 | 85 | 76 | 9 | 83 | 108 | 92 | 73 | 5406 |
| A2N0588 | 50 | 48 | 2 | 59 | 100 | 85 | 65 | 4915 |
| A2N0587 | 89 | 19 | 70 | 34 | 93 | 78 | 56 | 4463 |
| A2N0595 | 150 | 58 | 92 | 110 | 147 | 130 | 104 | 7881 |
| A2N0596 | 110 | 55 | 55 | 113 | 159 | 142 | 113 | 8681 |
| A2N0597 | 150 | 80 | 70 | 113 | 148 | 131 | 104 | 7911 |
| A2N0586 | 130 | 24 | 106 | 55 | 114 | 98 | 74 | 5748 |
| A2N0598 | 120 | 73 | 47 | 131 | 181 | 164 | 132 | 10,189 |
| A2N0599 | 130 | 51 | 79 | 110 | 180 | 163 | 128 | 10,124 |
| A2N0581 | 95 | 56 | 39 | 141 | 195 | 178 | 143 | 11,149 |

^a Intersected by drilling; in some instances onerous drilling conditions prevented further advance

^b Empirical value derived from the drill record

^c Difference between geosite surface elevation and Zwartkrans Spring elevation of ~ 1433 m amsl

Table 17 Assessment framework for the closure/recommissioning of DWS water level monitoring stations

| Station | Record length (months) | # Of records | Record frequency (per month) | Reason for closure ^a | Additional information (provided by author) |
|---------|------------------------|--------------|------------------------------|---------------------------------|--|
| A2N0589 | 285 | 170 | 0.60 | Borehole collapsed | Redundant and expendable due to proximity to A2N0600 with record frequency of 0.66 |
| A2N0594 | 288 | 187 | 0.65 | Borehole equipped | Should be reopened due to strategic position in upper reaches of the Zwartkrans Basin |
| A2N0598 | 283 | 93 | 0.33 | Borehole equipped | Should be reopened due to strategic position adjacent to the losing middle reaches of the Riet Spruit; record frequency is easily improved |
| A2N0606 | 243 | 36 | 0.15 | Borehole collapsed | Redundant and expendable due to proximity to A2N0594 with record frequency 0.65 |

^a E Bertram (personal communication)

been equipped with pumps and serve an active water supply function, the landowners will be required to provide alternative monitoring stations. This implies that the landowner (s) will establish a unique monitoring station that replaces the function of the original station. In both instances where this applies (stations A2N0594 and A2N0598, Table 17), such an approach is considered to be unrealistic and therefore not workable. Further, if deemed necessary for reasons such as long record or strategic location, the collapsed boreholes stations A2N0589 and A2N0606 (Table 17) will

be rehabilitated and returned to duty (E Bertram, personal communication).

A review of the situation within the framework of the additional information presented in Table 17, suggested that the closure of only two of the four stations was warranted and justifiable. A recommendation to the DWS that the decision in regard to stations A2N0594 and A2N0598 be rescinded has been acknowledged by the return of these stations to service.

Chemical Hydrogeology

Harrison Pienaar, Philip J. Hobbs, and Sebinasi Dzikiti

1 Regional Groundwater Chemistry

The main lithostratigraphic units in the study area are identified as the younger units of the Witwatersrand Supergroup and the older units of the overlying Transvaal Supergroup (Table 5, Sect. 4 in Chapter “[Description of the Physical Environment](#)”). Barnard (2000) provides information regarding the chemistry of groundwater regionally (and typically) associated with each of the relevant rock units.¹ This information is summarized in Table 1 and illustrated in Fig. 1.

Figure 1 reflects the similarity in chemical composition (MgCa-HCO_3) of groundwater associated with the Timeball Hill Formation, Black Reef Formation, and, to a lesser extent, Central Rand Group strata. This is attributed to the similar rock type (mainly quartzite) that builds these formations. Although the volcanic rocks (lava) of the Hekpoort Formation also exhibit a CaMg-HCO_3 composition, they can be distinguished on the basis of generally higher analyte concentrations, especially SO_4 and Na, as well as higher SEC and TDS values (Table 1). The Malmani Subgroup dolomitic strata exhibit the most dominant MgCa-HCO_3 composition

of all the formations represented. The higher Cl, SO_4 , and N concentrations (Table 1) in the karst groundwater are, however, indicative of contamination (Barnard 2000) which is uncharacteristic of pristine karst groundwater that still occurs in much of the study area. The Piper diagram presented in Fig. 2 provides further and possibly more distinct characterization of the water chemistry associated with the various surface and subsurface water resource environments.

2 Subregional Groundwater Chemistry

2.1 Background

Hobbs and Cobbing (2007) report groundwater (including raw and treated mine water) chemistry information for 42 sources enumerated in the southwestern portion of the study area. Surface water chemistry was determined for a further seven sites mostly located on the Tweelopie Spruit, but including one Blougat Spruit sample. This information has enabled the characterization of the hydrochemistry associated with the various water sources shown in Fig. 2. A similar characterization was also reported by Holland and Witthüser (2009).

2.1.1 West Rand Group (Witwatersrand Supergroup)

Groundwater from these strata is typically very weakly mineralized, as reflected in SEC values <20 mS/m and TDS values <120 mg/L, and exhibits a low pH (in the range 5.4–6.0). The latter is attributed to the very low alkalinity of this groundwater, with total alkalinity typically <10 mg CaCO_3/L (Hobbs and Cobbing 2007). This water is therefore also corrosive with a typical corrosion tendency ratio (CTR) of >1 .² An example from this study is the water from station

P. J. Hobbs: Deceased

¹ No groundwater chemistry data are available for the Rooihoogete Formation sandwiched between the Timeball Hill Formation and the Malmani Subgroup strata (Table 5, Sect. 4 in Chapter “[Description of the Physical Environment](#)”).

H. Pienaar (✉) · P. J. Hobbs
Council for Scientific and Industrial, Research, Smart Places,
Water Centre, Pretoria, South Africa
e-mail: hpienaar@csir.co.za

H. Pienaar
Hebei University of Engineering, Handan, China

S. Dzikiti
Department of Horticultural Science, Stellenbosch University,
Stellenbosch, South Africa
e-mail: sdzikiti@sun.ac.za

² For pH values in the range 7–8 and in the presence of dissolved oxygen, CTR values ≤ 0.1 indicate general freedom from corrosion, whereas higher values are indicative of more corrosive waters.

Table 1 Characterization of groundwater hydrochemistry per lithostratigraphic unit represented in the study area (data from Barnard 2000)

| Variable/analyte | Lithostratigraphic unit | | | | | SANS (2011a) ^a |
|----------------------------|-------------------------|-----------------------|-----------------------|-----------------------|-----------------------|---------------------------|
| | Hekpoort Fm. | Timeball Hill Fm. | Malmani Sbgp. | Black Reef Fm. | Central Rand Gp. | |
| pH ($-\log_{10}a_{H^+}$) | 7.5 | 7.2 | 7.6 | 7.0 | 7.3 | 5.0–9.7 |
| SEC (mS/m) | 52 | 34 | 63 | 34 | 29 | ≤ 170 |
| TDS (mg/L) | 398 | 278 | 444 | 238 | 207 | ≤ 1200 |
| Ca (mg/L) | 44.0 | 29.0 | 52.7 | 28.0 | 17.6 | n.s. |
| Mg (mg/L) | 26.0 | 19.0 | 35.4 | 18.0 | 13.7 | n.s. |
| Na (mg/L) | 30.0 | 15.0 | 24.1 | 14.0 | 20.0 | ≤ 200 |
| K (mg/L) | 2.0 | 1.6 | 2.3 | 1.7 | 2.6 | n.s. |
| Cl (mg/L) | 23.5 | 15.0 | 37.7 | 15.0 | 17.9 | ≤ 300 |
| SO ₄ (mg/L) | 79.0 | 26.0 | 70.5 | 36.0 | 33.5 | ≤ 500 |
| HCO ₃ (mg/L) | 190 | 152 | 216 | 120 | 104 | n.s. |
| NO ₃ (mg N/L) | 3.5 | 2.9 | 5.6 | 2.8 | 2.0 | ≤ 11 |
| F (mg/L) | 0.3 | 0.3 | 0.3 | 0.2 | 0.3 | ≤ 1.5 |
| TDS:SEC | 7.7 | 8.2 | 7.1 | 6.9 | 7.1 | n.s. |
| SO ₄ :TDS (%) | 20 | 9 | 16 | 15 | 16 | n.s. |
| Chemical character | CaMg–HCO ₃ | MgCa–HCO ₃ | MgCa–HCO ₃ | MgCa–HCO ₃ | MgCa–HCO ₃ | – |
| <i>n</i> | 41 | 81 | 223 | 52 | 18 | |

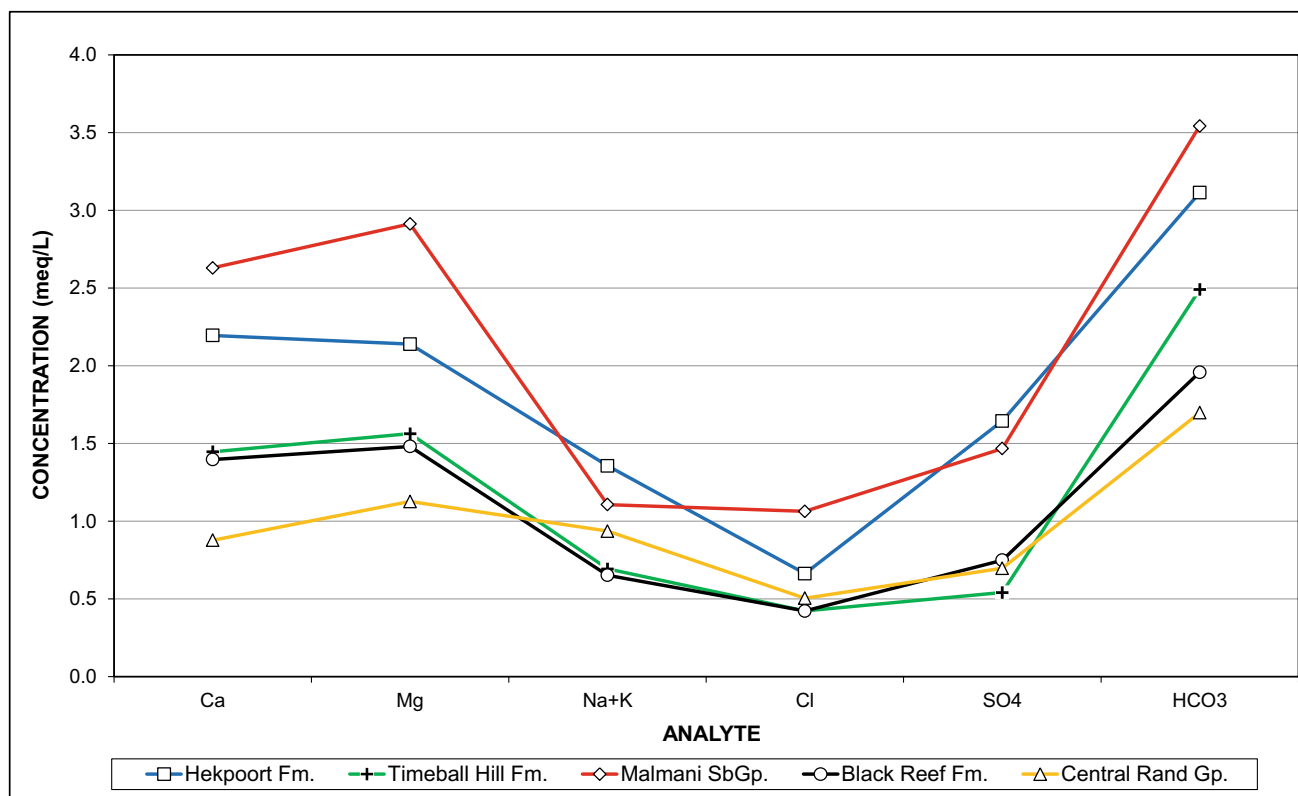
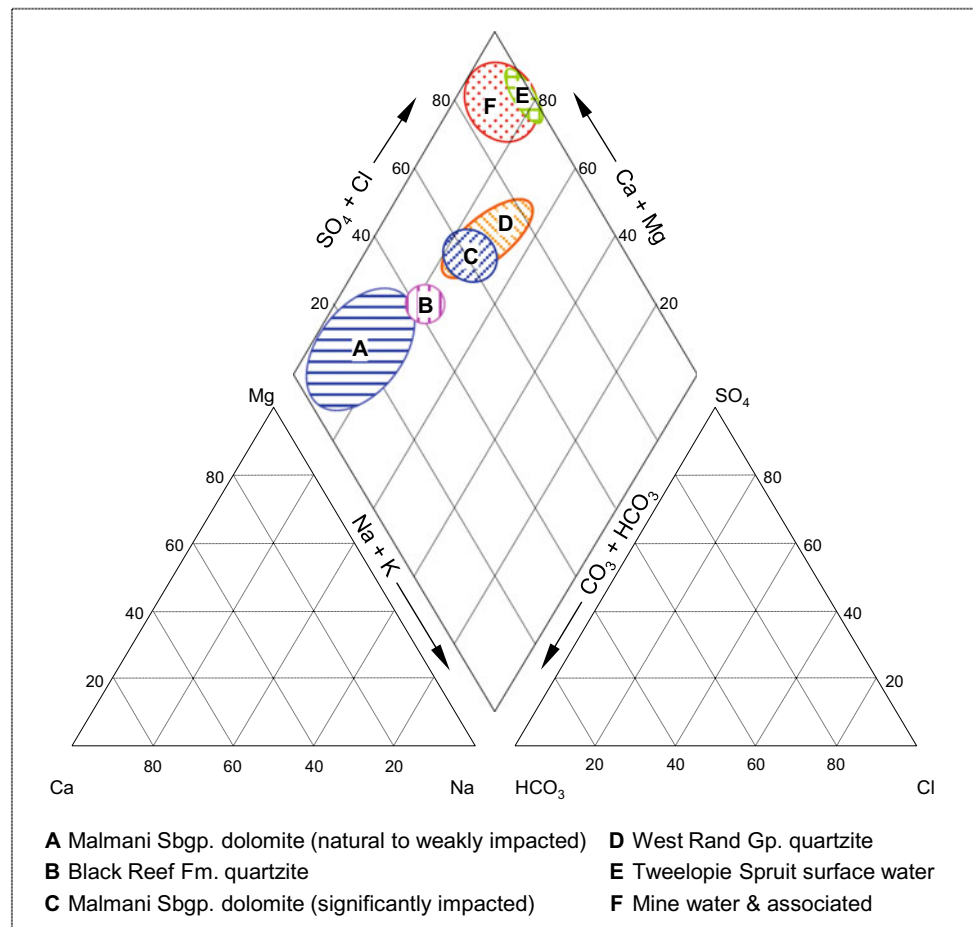
**Fig. 1** Schoeller graphical comparison of natural hydrochemistry associated with the respective lithostratigraphic units represented in the study area (data from Table 1)

Fig. 2 Piper diagram characterization of hydrochemistry associated with various surface water and groundwater sources in the study area (modified after Hobbs and Cobbing 2007)



PS3, a borehole located on the quartzite ridge to the east of the Blougat Spruit, which reflects an Mg–HCO₃ composition and the following variable-specific values:

$$\text{pH} = 6.0 \text{ (field); } \text{SEC} = 4 \frac{\text{mS}}{\text{m}} \text{ (field);}$$

$$\text{Total alkalinity} = \frac{8 \text{ mg CaCO}_3}{\text{L}} \text{ (lab)}$$

2.1.2 Malmani Subgroup (Chuniespoort Group)

Dolomitic groundwater is characterized by a CaMg–HCO₃ composition which, in its pristine state, also exhibits very low concentrations of Cl and SO₄ (generally <5 mg/L), a low SEC (in the range 20–40 mS/m), and a typically alkaline (basic) pH of 7.5–8.0. The water delivered by the Danielsrust, Nouklip, and Nash springs exemplify this observation. Anthropogenic impacts on this water quality are recognized on the basis of elevated Cl and SO₄ concentrations, higher SEC values (>60 mS/m), and lower pH values (<7.2).

2.1.3 Pretoria Group (Transvaal Supergroup)

The composition of groundwater associated with these strata is similar to that described for the Witwatersrand Supergroup

strata (Sect. 2.1.1). An example from this study is the analysis for the Uitkomst Spring (Fig. 16 in Chapter “Physical Hydrogeology”) draining interlayered shales and quartzites of the Timeball Hill Formation in the Skeerpoort River Valley, which reflects an Mg–HCO₃ composition together with the following variable-specific values:

$$\text{pH} = 7.0 \text{ (field); } \text{SEC} = 1.0 \frac{\text{mS}}{\text{m}} \text{ (field);}$$

$$\text{Total alkalinity} = \frac{16 \text{ mg CaCO}_3}{\text{L}} \text{ (lab)}$$

This groundwater is generally distinguishable from that of the West Rand Group strata (Sect. 2.1.1) on the basis of a more neutral pH, a slightly greater salinity, and detectable Fe and Mn concentrations which, in the case of the Uitkomst Spring, amounted to ~0.3 mg Fe/L and ~0.5 mg Mn/L in May 2010 (Table 5).

2.2 Temporal Groundwater Chemistry Assessment

The geographic extent of a mine water impact on the karst groundwater resources of the Zwartkrans Basin is postulated

in the EIA for Harmony Gold Mine (JFA 2006). The EIA report also, however, records SO_4 levels in DWS monitoring boreholes in the area that were substantially higher, in some instances by a factor of 4–6, in 1986 than in 2006. These circumstances are illustrated in Fig. 3, revealing an SO_4 reduction in the range of 30–83% (average 57%) from 1986 to 2006. The mine water impact on the groundwater resources of the area is therefore not a recent or new phenomenon. The improvement between 1986 and 2006 illustrates the resilience and self-cleansing nature of karst groundwater systems in the long-term, given conditions that are conducive to this.

Further illustration of the long-term pattern and trend observed in the groundwater chemistry recorded at the DWS groundwater quality monitoring stations A2N0583, A2N0584, A2N0586, and A2N0600. The position of these stations is shown in Fig. 19 in Chapter “Physical Hydrogeology”. The information shown in Fig. 4 compares the ‘oldest’ (first) and the latest groundwater chemical compositions at the longest-operating DWS monitoring stations. Apart from the discussion of SEC and SO_4 patterns and trends accompanying Fig. 46 in Sect. 8.4, the Volume 2 and Fig. 4 results are summarized as follows.

- Station A2N0583 reveals a gradual but persistent increase in the SO_4 concentration since June 2004 to produce a MgCa-SO_4 composition compared to the historical (ca. 1985) CaMg-HCO_3 composition. This is both surprising

and a concern is given the position of this borehole to the west of the Krugersdorp Game Reserve ostensibly outside the path of mine water impact.

- Station A2N0584 reflects a sharp increase in Ca and SO_4 concentrations since 2008, imparting a Ca-SO_4 character to this groundwater. It is also evident, however, that this chemistry is not too dissimilar to the historical chemistry as observed in July 1985 and March 1989, when SO_4 concentrations of 368 and 420 mg/L, respectively were recorded. Both the historical and current compositions indicate mine water infiltration into the karst aquifer at this locality.
- Station A2N0586 reflects a sharp increase in Ca and SO_4 concentrations since 2008, again imparting a Ca-SO_4 character to this groundwater. These circumstances are again indicative of mine water infiltration into the karst aquifer at this locality.
- Station A2N0600 reflects a less sharp increase in Ca, Mg, and SO_4 concentrations that is manifested over a longer period of time since 2008. The current Ca-SO_4 composition of the groundwater is much more pronounced than the similar historical composition. The ‘prominence’ of SO_4 throughout the observational record is out of character for karst groundwater, and not readily explained on the basis of available data. It may be postulated, however, that the earlier presence of notable but muted SO_4 levels (~ 170 mg/L) in the groundwater at this position again reflects a historical mine water impact.

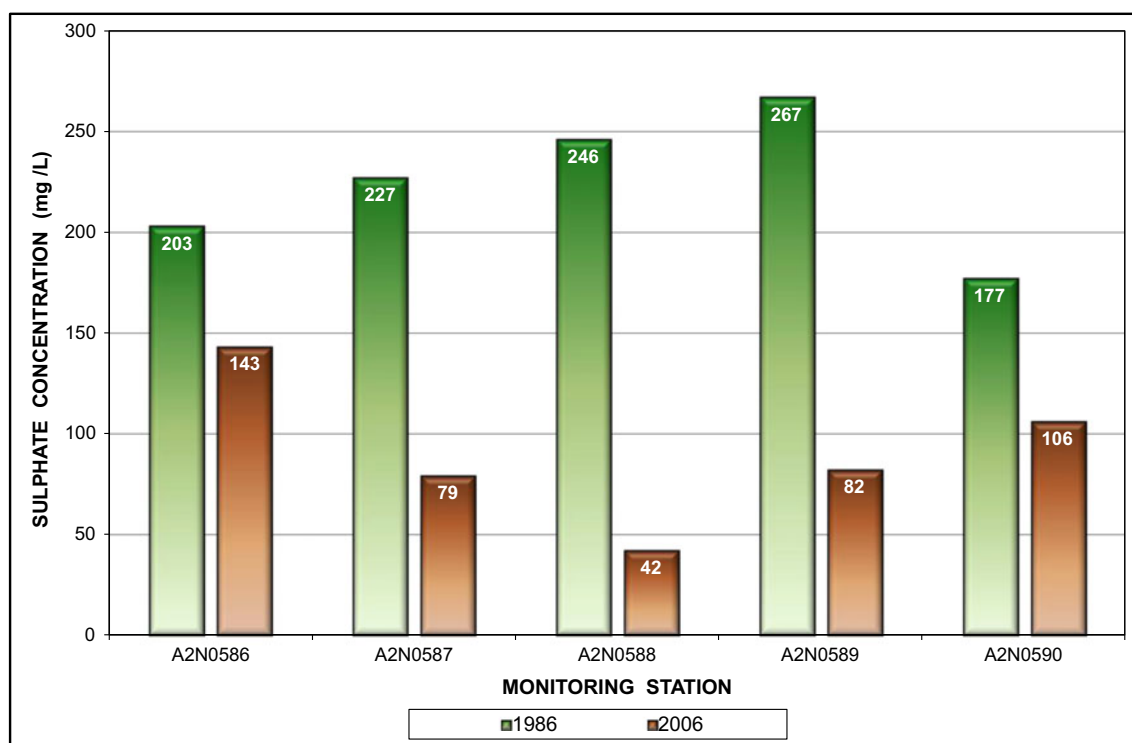


Fig. 3 Comparison of historical and more recent SO_4 levels in groundwater from DWS monitoring boreholes in the Zwartkrans Basin

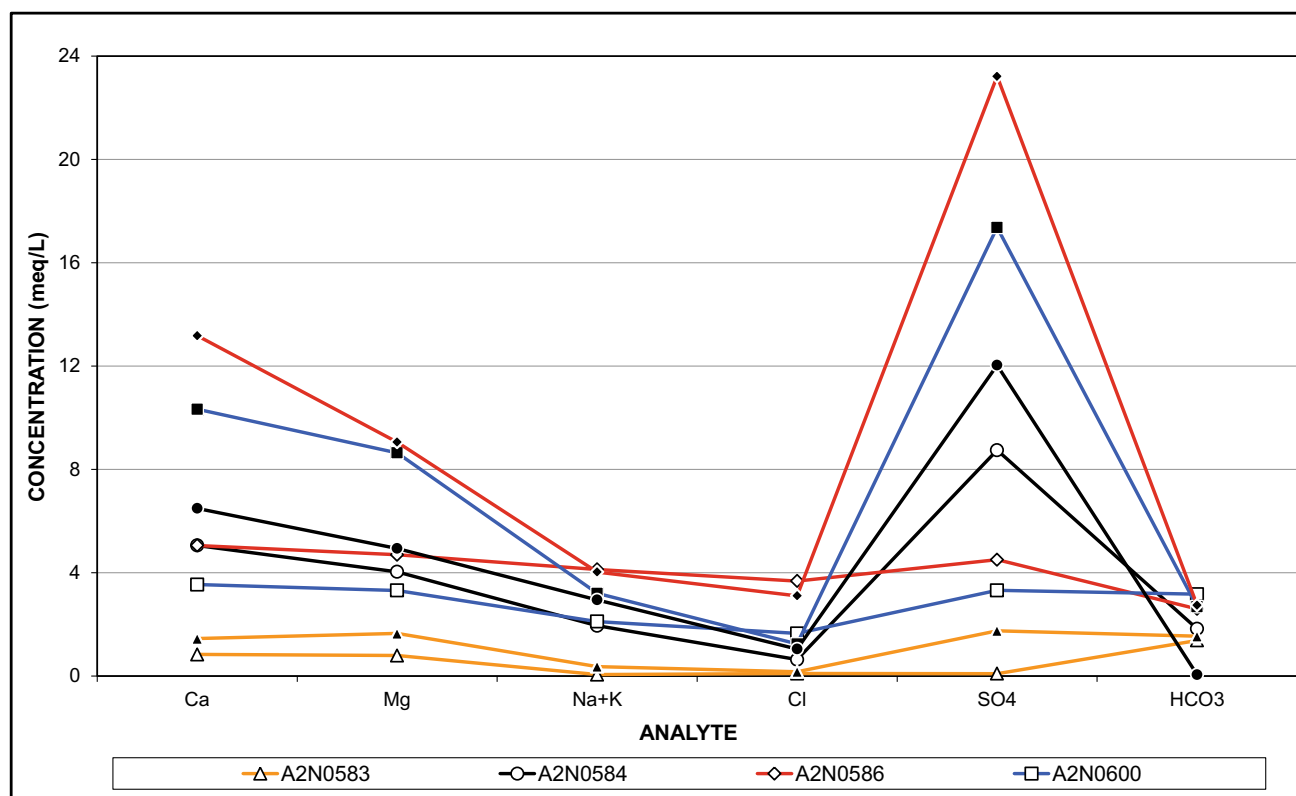


Fig. 4 Comparison of the ‘oldest’ (open symbol ca. 1989) and most recent (solid symbol December 2014) groundwater chemical compositions at the longest-operating DWS monitoring stations

2.3 Source-Specific Temporal Assessment

2.3.1 Mine Area (Locus of Decant)

The groundwater quality monitoring programs carried out by the mining houses (SG and MG/MSA) and the DWS historically focused on the area of mine water decant. The footprint of this monitoring gradually expanded to include areas adjacent to and further downstream of the mine area (S. du Toit, personal communication) as described in Sect. 2.3.3.

The groundwater chemistry monitoring in the area of mine water decant provides insight into the geochemical characterization of AMD in its host receiving environment that includes dolomite.³ Eight boreholes and three mine structures in this area (Fig. 5) provide information of varying relevance in this regard, as shown in the following discussion. Visualization of the geologic and hydrogeologic regimes that elucidate this discussion is provided in Figs. 7

in Chapter “Description of the Physical Environment” and 15 in Chapter “Physical Hydrogeology”, respectively.

Key to an understanding of the mine water relationship with the karst outlier is recognition of the situation that the Black Reef Incline (BRI), together with #17 and #18 Winzes (Fig. 5), allowed for mining of the Black Reef at comparatively shallow depth (<100 m) below surface in this area (Fig. 15 in Chapter “Physical Hydrogeology”). The Main Reef was accessed at greater depths via vertical shafts such as #8 and #9 shafts and inclines driven from the base of opencast mine workings such as the West Wits Pit. Although the opencast workings exploited the auriferous package comprising the Kimberley Reefs, inclines driven from the base of these pits targeted the Main Reef at shallower depth than the vertical shafts. This geometry explains the hydraulic continuity between the Black Reef Incline and #17 and #18 winzes, and the deeper-seated mine workings on the Main Reef.

The BRI and #17 and #18 winzes represent the most prolific point sources of mine water discharge (Plate 1). Whereas the BRI and #17 Winze were the more productive sources of mine water discharge in the earlier period of decant because of their lower surface elevations, #18 Winze gained prominence in this role (Plate 1) ca. early-2010 as the other two sources, which had gradually become blocked

³ Most, if not all, of the locus of mine water decant area is underlain by Malmani Subgroup dolomite forming an elongated basin-like outlier contained within Black Reef Formation and West Rand Group (Witwatersrand Supergroup) strata. This is illustrated in Figs. 7 in Chapter “Description of the Physical Environment” and 15 in Chapter “Physical Hydrogeology”.

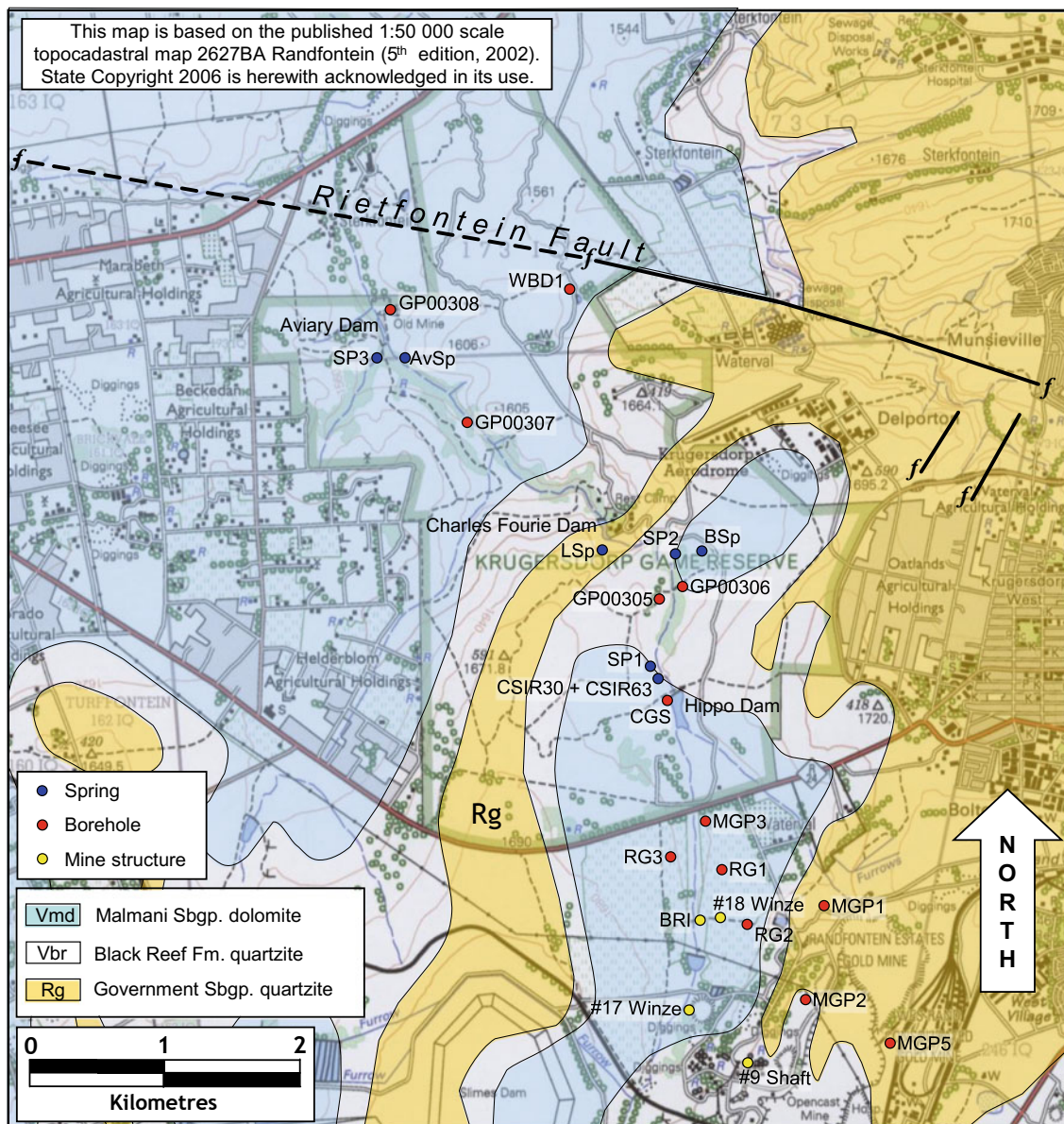


Fig. 5 Locality map of mine water and groundwater monitoring stations in the locus of decant and the Krugersdorp Game Reserve; borehole MGP4 located off southern edge of map below MGP5

with gypsiferous precipitate, could not cope with the substantial increase in discharge (Sect. 3.1 in Chapter “[Physical Hydrology](#)”) driven by the increasing potentiometric head associated with the flooded mine void. The presence of numerous surface seeps in the area is a further manifestation of the potentiometric head in the mine void.

The chemistry of the mine water produced by the BRI is characterized in Table 2 in Chapter “[Chemical Hydrology](#)” and discussed in detail in Sect. 1.2.1 in Chapter “[Chemical Hydrology](#)”. Familiarity with this material will promote a better grasp of the following discussion.

In addition to routine monitoring of the point source mine water discharges, the mines also serve a number of

monitoring boreholes. The SG boreholes RG1, RG2, and RG3, and the MG/MSA monitoring borehole MGP3, intersect the karst outlier in the mine area (Fig. 5). The MG/MSA monitoring boreholes MGP1, MGP2, MGP4, and MGP5 surround the West Wits Pit located on the water divide in the mine area. Borehole MGP3 lies at the northern end of the mine area. The results of monthly water chemistry monitoring associated with these boreholes yield the information presented in Table 2. The results for boreholes MGP1, MGP2, and MGP3 are graphed in Fig. 6. Although the monitoring results indicate that borehole MGP1 reflects SEC and pH values that represent natural quartzitic groundwater (Sect. 2.1.1), profiles of the water column in this borehole

Plate 1 View looking south-west from #18 Winze over the locus of decant with Dump 39 (see Fig. 5 in Chapter “Description of the Physical Environment”) on the horizon (photo W. Basson)



reveal a very different situation (Sect. 10.3.6). The median SEC and pH values of 9 mS/m and 5.4, respectively (Table 2), mask values of 100 mS/m and 4.0 for these water chemistry variables at a depth >15 m below water level in this borehole (Fig. 57). This phenomenon also applies to borehole MGP2 (Fig. 58) and MGP3 (Fig. 59), although it is much less pronounced in borehole MGP2.

2.3.2 Krugersdorp Game Reserve

The establishment of four monitoring boreholes in the KGR by the DWS in late-2010 has provided hydrogeological information for an area that previously suffered from a dearth

of such information. The boreholes GP00305, GP00306, GP00307, and GP00308 (Fig. 5) each target a specific aspect of the groundwater environment in the KGR. Borehole GP00305 targets the faulted, fractured, and jointed quartzitic strata that form the escarpment which separates the KGR into an elevated southern plateau and more incised lower northern portion. Borehole GP00306 targets the northern margin of the karst outlier in close proximity to the Tweelopie Spruit. Borehole GP00307 targets the karst aquifer of the Zwartkrans Basin at a position next to the Tweelopie Spruit very near the Kemp's Cave fossil site at the entrance to the predator sanctuary. Borehole GP00308 targets the

Table 2 Median chemistry variable/analyte values for groundwater associated with MG/MSA monitoring boreholes in the mine area in the period January 2011–April 2012

| Variable/analyte | Detection limit | Monitoring borehole # and median value | | | | | | | | | | SANS (2011a) ^a |
|--|-----------------|--|----|------|----|------|----|------|----|------|----|---------------------------|
| | | MGP1 | | MGP2 | | MGP3 | | MGP4 | | MGP5 | | |
| <i>n</i> | | | 16 | | 15 | | 16 | | 16 | | 16 | |
| pH (−log ₁₀ α _{H+}) | | 5.4 | 16 | 5.5 | 15 | 8.8 | 16 | 6.1 | 16 | 4.9 | 16 | 5.0–9.7 |
| SEC (mS/m) | | 9.0 | 16 | 6.1 | 15 | 183 | 16 | 8.5 | 16 | 25.0 | 16 | ≤ 170 |
| Ca (mg/L) | | 6.2 | 16 | 3.8 | 14 | 234 | 16 | 7.0 | 16 | 8.5 | 16 | n.s. |
| Mg (mg/L) | | 4.2 | 16 | 2.0 | 15 | 105 | 16 | 1.6 | 16 | 5.2 | 16 | n.s. |
| Na (mg/L) | 10 | 7.2 | | 8.2 | | 73.0 | | 8.2 | | 28.0 | | ≤ 200 |
| Cl (mg/L) | 5.0 | 13.5 | 12 | 10.0 | 9 | 42.0 | 16 | 10.5 | 12 | 36.5 | 16 | ≤ 300 |
| SO ₄ (mg/L) | 50 | <50 | 0 | <50 | 0 | 1105 | 16 | <50 | 0 | 58.0 | 1 | ≤ 500 |
| HCO ₃ (mg/L) | 2.4 | 4.3 | 14 | 6.7 | 14 | 9.8 | 14 | 9.8 | 16 | 6.1 | 12 | n.s. |
| Fe (mg/L) | 0.1 | 0.1 | 3 | 0.2 | 4 | 0.2 | 4 | 1.5 | 14 | 0.1 | 7 | ≤ 2 |
| Mn (mg/L) | 0.1 | 0.3 | 15 | 0.2 | 6 | 0.2 | 7 | 0.5 | 15 | 0.2 | 13 | ≤ 0.5 |
| U (μg/L) | 5.0 | 7.0 | 7 | 12.5 | 6 | 7.1 | 8 | 8.6 | 8 | 10.5 | 12 | ≤ 15 |

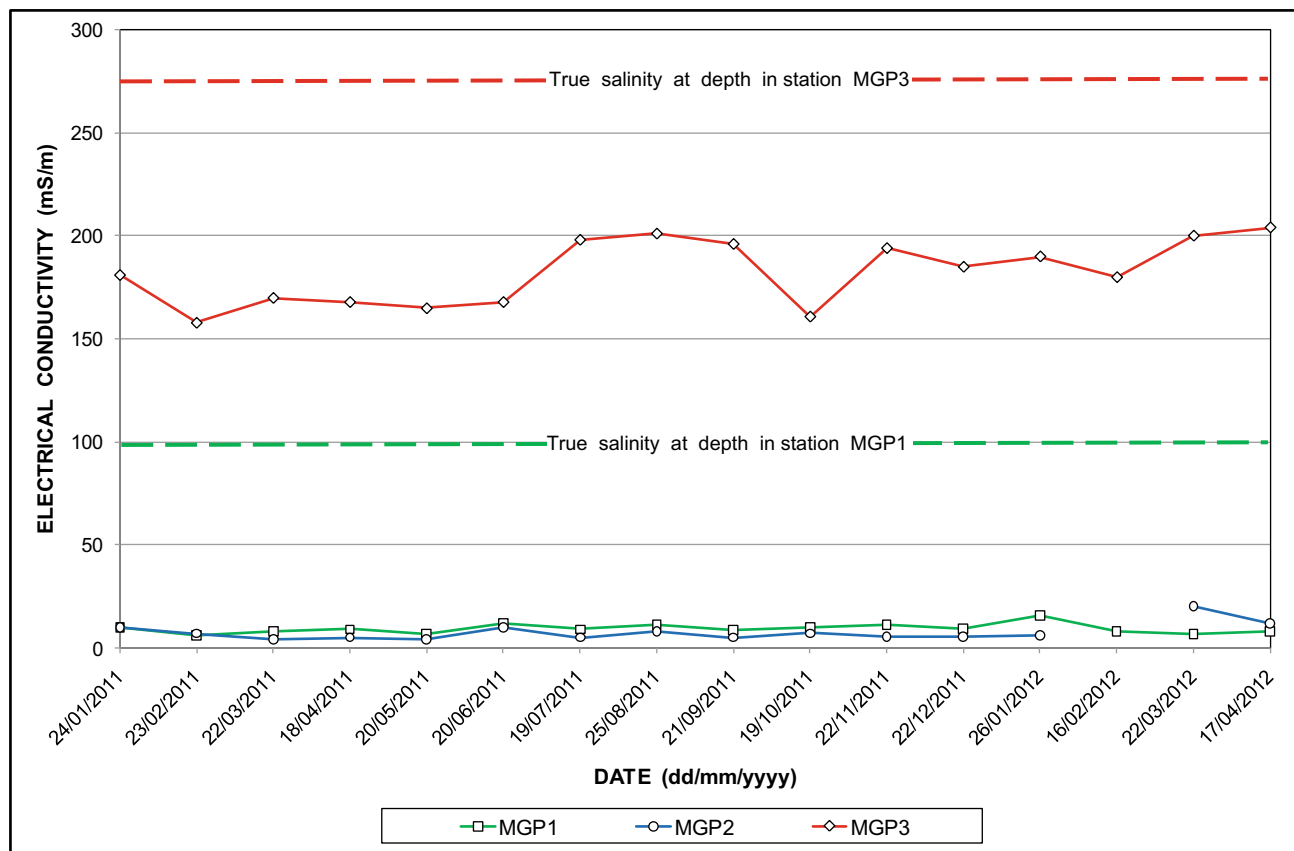


Fig. 6 Pattern and trend of SEC monitored by MG/MSA in the mine area, compared to the true SEC values at depth in boreholes MGP1 and MGP3

chert-poor dolomite of the Oaktree Formation near the Aviary Dam close to the northern boundary of the KGR.

Together with six springs and an earlier borehole (WBD1), the four recently established monitoring boreholes provide a deeper perspective on the hydrogeologic environment downstream of the mine area. This perspective includes the following hydrogeologic observations:

- a subsurface mine water impact manifested in the karst outlier;
- a surface water driven mine water impact in the south-eastern portion of the Zwartkrans Basin;
- a municipal wastewater impact in the south-eastern portion of the Zwartkrans Basin;
- a natural radiogenic impact associated with quartzitic groundwater; and
- the natural discharge of nearly pristine karst groundwater along the north-western margin of the KGR.

2.3.3 Lower Riet Spruit

This discussion considers those groundwater monitoring activities carried out to the north of the KGR, a distance of >6000 m from the area of mine water decant and its

immediate downstream receiving environment. This is informed by the need to better understand the impact of mine water discharge on groundwater quality in closer proximity to the COH, as the upstream impacts already receive considerable attention (Sect. 2.3.1). Routine sampling by SG of the four stations WBD2, WBD3, WBD4, and WBD5 (Fig. 19 in Chapter “Physical Hydrogeology”) reflect the SO_4 trends (and recent pH and SEC values) shown in Fig. 7. These are described as follows.

WBD2: The most upstream station, located on Ptn 106 of Sterkfontein 173IQ (the old Krugersdorp Brickworks property) where the water table occupies a depth of ~ 25 m below that of the nearby Tweelopie Spruit streambed, displays a gradual but comparatively linear increase through to February 2010.⁴ The SO_4 concentration doubled in this 3-year period when the borehole was in frequent production, thereby inducing flow from the Tweelopie Spruit located <50 m to the west of the borehole. After a hiatus of $\sim 2\frac{1}{2}$

⁴ Access to this property and station was curtailed in March 2010 when the business closed down and borehole use terminated. Access resumed in November 2012 following discussions with the new owner.

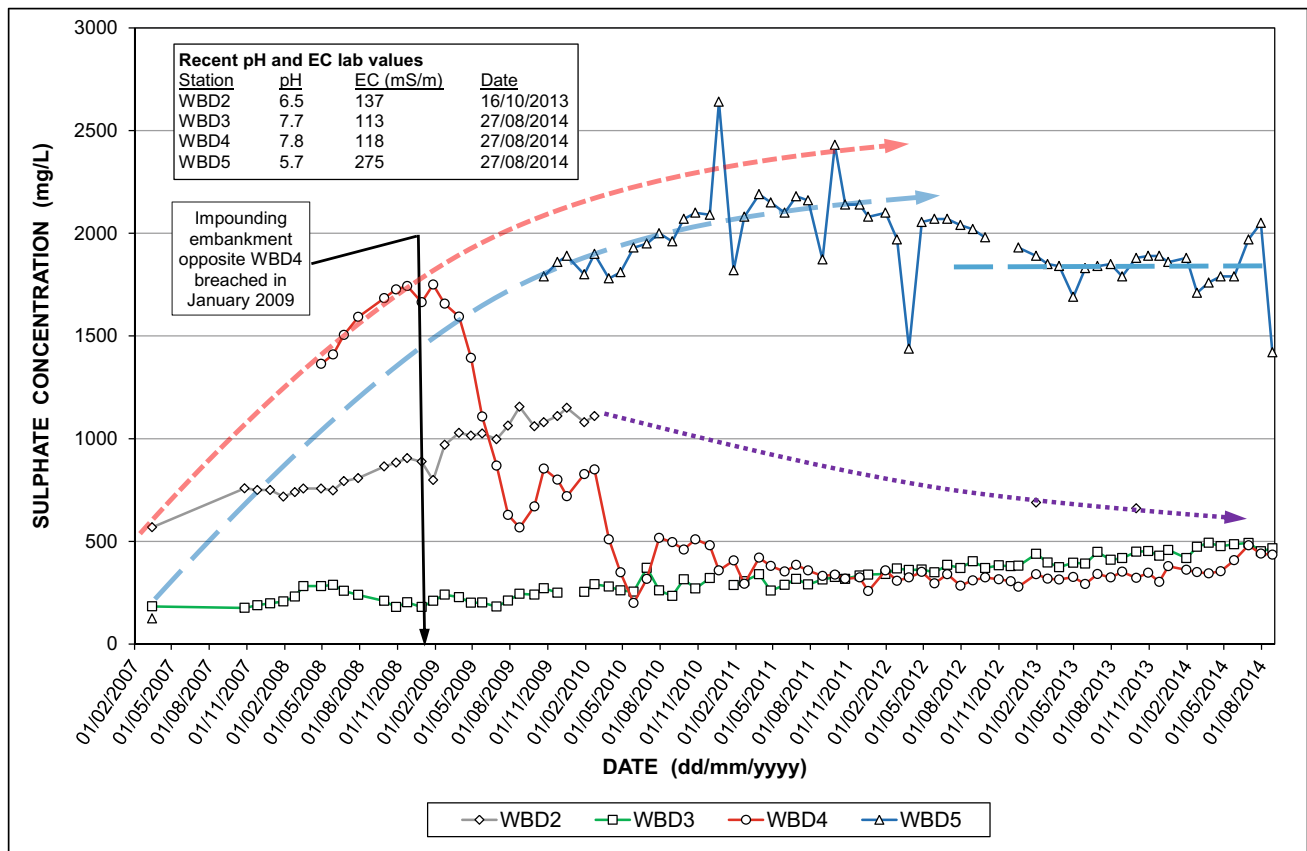


Fig. 7 Observed SO_4 trend at four groundwater quality monitoring stations along the losing reach of the Riet Spruit upstream of Oaktree

years (Footnote 4), the borehole was re-commissioned by the new owner in late-2012. The SO_4 concentrations of 689 and 661 mg/L for samples collected in January and October 2013, respectively are shown in Fig. 7. These indicate a significant decrease from the 1110 mg/L of the next earliest 2010 analysis, the October 2013 concentration of 661 mg SO_4 /L comparing favorably with the earliest value of 568 mg SO_4 /L.

WBD3: The next station downstream, a distance of ~880 m on the Ptn 96/7 of Sterkfontein 173IQ (the Mōrester property), displays a gradually increasing SO_4 concentration from ~200 to ~450 mg/L in the period of record. This is a somewhat anomalous trend compared to that observed at the other stations. A water level measurement in 2007 placed the groundwater rest level in this borehole at a depth of ~21 m below that of the nearby streambed (Hobbs and Cobbing 2007). The potentiometric response observed in the DWS monitoring borehole A2N0584 (Fig. 8 in Chapter “Physical Hydrogeology”) indicates that the water level in WBD3 has almost certainly also risen since the 2007 measurement was made.

WBD4: Located ~550 m downstream of WBD3 on the Remainder Ptn 7/2 of Sterkfontein 173IQ (the Royal Engineering property), a mid-2008 water level measurement in this

borehole placed the groundwater rest level at a depth of ~12 m below that of the nearby streambed (Hobbs 2008b). The groundwater chemistry shows an increase in SO_4 to a maximum of ~1750 mg/L in February 2009, followed by a rapid decline to a level of 322 mg/L in September 2013. The initial response is attributed to the damming up of the Riet Spruit on this property in early-2008, resulting in the enhanced infiltration of surface water comprising mainly treated/neutralized mine water into the karst aquifer at this location. Breaching of the impoundment in January 2009, following recommendations by Hobbs (2008b) to mitigate the adverse groundwater quality impact, produced the decrease in SO_4 concentrations observed since February 2009.

WBD5: This borehole is located ~950 m downstream of WBD4 on Ptn 8/2 of Sterkfontein 173IQ (the Chrisué property) on the left bank of the Riet Spruit adjacent to a dam. Having risen by ~5 m to an elevation of ~1466 m amsl by February 2010 (Table 8 in Chapter “Physical Hydrogeology”, station CSIR57), the water level in this borehole remains ~5 m⁵ below that of the Riet Spruit streambed at this

⁵ A groundwater rest level measurement on 01/09/2014 returned a value of 6.69 m bs.

position. The station displays an elevated and rising SO_4 concentration leveling out at ~ 2200 mg/L in late-2011. The extrapolation of the upward trend from the early-2007 value mimics that of the WBD4 data up to January 2009 (Fig. 7). A decrease in SO_4 concentration from ~ 2200 to ~ 1800 mg/L from late-2011 to September 2013 is also evident. The measure of water quality deterioration as represented by the increase from the earliest SO_4 concentration of 125 mg/L in March 2007 to ~ 2200 mg/L in late-2011, is again attributed to the damming up of surface water at this location. It is likely that a similar intervention as was applied in the case of WBD4, namely breaching of the impoundment to establish the free flow of surface water past this station, will most probably produce a similar result as observed at WBD4. The landowner, however, is not amenable to such an intervention.

The establishment in 2010 of additional monitoring boreholes in the lower Riet Spruit Valley by the DWS provides greater insight into the impact of mine water on the receiving groundwater resources of the Zwartkrans Basin. These stations are identified as GP00300, GP00301, GP00302, GP00309, GP00312, GP00313 and GP00314 in Fig. 19 in Chapter “Physical Hydrogeology”.

2.3.4 Sterkfontein Cave System

Holland et al. (2009) report SO_4 and Cl concentrations of 154 and 55 mg/L, respectively for groundwater sourced from a borehole (presumably SF1) near the Sterkfontein Cave. This is put forward as “... undoubtedly indicating anthropogenic impacts.” These values agree with the averages of 147 mg SO_4 /L and 66 mg Cl/L for three boreholes (CSIR7, CSIR8, and CSIR9) in the upstream Oaktree area reported by Hobbs and Cobbing (2007), and raise concern for the quality of the cave water.

A more complete comparison of earlier cave water chemistry with the present is provided by the analyses of April 2001 (from SG records), March 2005 (from DWS records), February 2006 (from Harmony Gold records), May 2010, January 2011, and May 2014 (this study), and August 2012 from Maropeng aAfrica. The data are presented in Table 3, and the graphical comparison is made in Fig. 8, which also shows the October 2013 and May 2014 results for Zwartkrans Spring water. The Piper diagram (Fig. 9) provides a synoptic picture of the respective groundwater chemistries. The similar chemical composition of the pre-2014 cave waters is readily apparent in Fig. 8. Also notable and significant is the increase in SO_4 in the latest cave water sample, and the very different Ca– SO_4 chemical composition of the Zwartkrans Spring water, which reflects an unequivocal mine water impact.

A comparison of the Sterkfontein Cave water chemistry with that of ‘pristine’ karst springs in the COH is shown in Fig. 9. The Piper diagram indicates that the difference is primarily associated with the anionic composition (Cl and SO_4) of the cave water.

The installation of a continuous EC monitoring device in the Lake by the DWS in May 2005 yields data on the cave water salinity response pattern in the 27 months to July 2007. This pattern (Fig. 10) reveals an initial SEC value of ~ 47 mS/m, followed after a hiatus of ~ 32 weeks by a notably higher value of ~ 60 mS/m. An analysis of the cave water sampled on 29/04/2005 (sourced from the DWS records), i.e., within a month of installation of the monitoring device, returned an SEC value of 59 mS/m (Fig. 8). As shown in Fig. 10, this suggests that the early salinity record might be in error by an ‘under-reading’ of ~ 12 mS/m. Later field SEC values of 62, 56, 63, and 69 mS/m (in May 2010, January 2011, May 2012, and May 2014, respectively) for the cave water confirm the constancy reflected in the continuous DWS record (Fig. 10). The observation that the SEC of the cave water has not changed much in the decade since mid-2005 must be welcomed under the circumstances described by acid mine drainage. This observation finds support in the PHREEQC-derived calcite (SI_C) and dolomite (SI_D) saturation index values (Table 3), which show a saturated to supersaturated state.

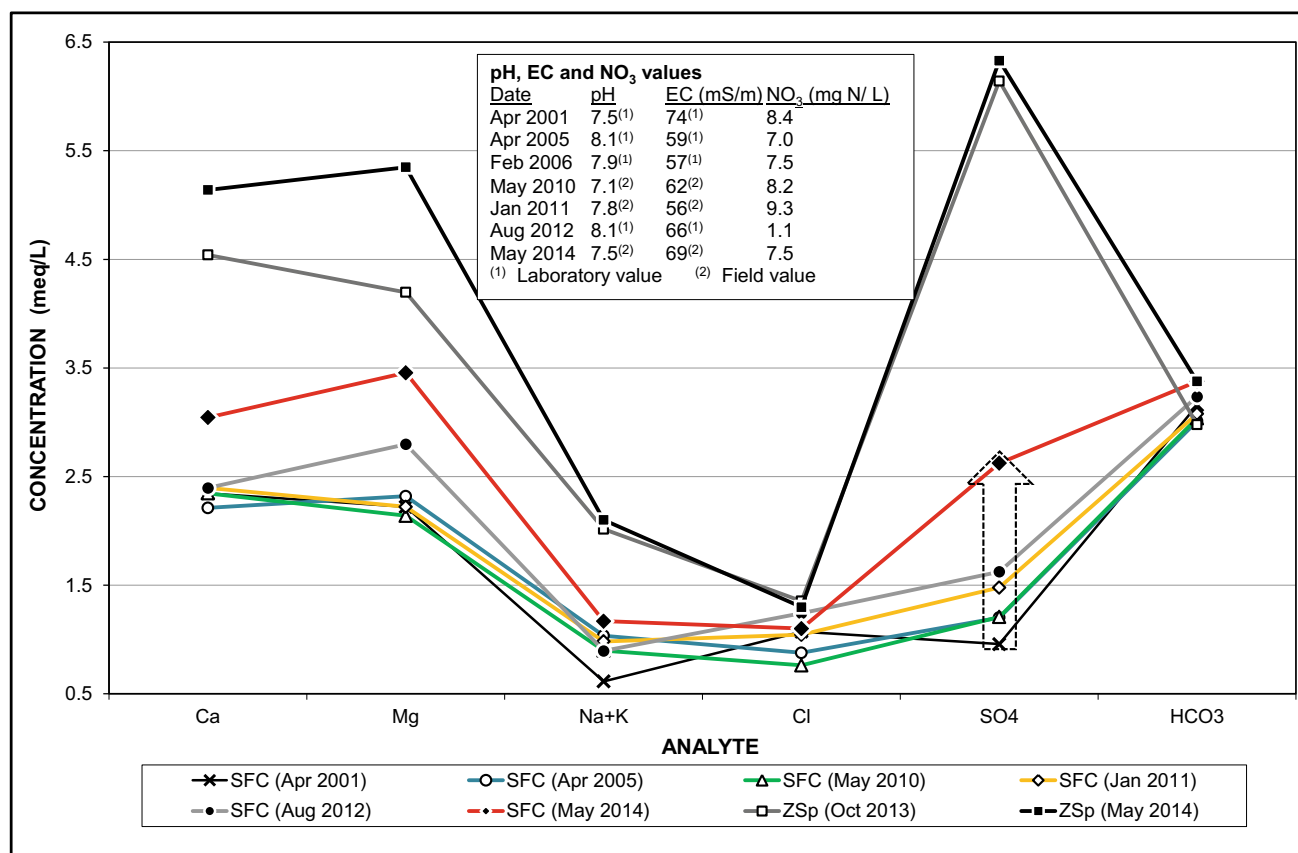
The similar chemical composition of Sterkfontein Cave water reflected in Figs. 8 and 9, despite the difference of some ten years between analyses, mimics the situation sketched by the near-continuous SEC record (Fig. 10). This is encouraging against the background of recent groundwater quality trends observed elsewhere in the Zwartkrans Basin (Sects. 2.3.3 and 4). Equally encouraging are the results of stable isotope analyses carried out on cave water in 2009 and 2010. The comparative data tabulated below indicate very little difference in the span of one year between analyses.

| Date | $\delta^2\text{H}$ (‰) | $\delta^{18}\text{O}$ (‰) | ^3H |
|------------|------------------------|---------------------------|------------------|
| 28/05/2009 | –19.8 | –3.53 | 1.3 ± 0.3 TU |
| 13/05/2010 | –20.3 | –3.55 | n.a. |

A comparison of the May 2009 cave water tritium value with that obtained in July 2009 for the Zwartkrans Spring (Sect. 7.1) reflects a significant difference of 1.1 ± 0.3 TU. The higher value associated with the springwater indicates that this feature delivers a younger groundwater than that which is represented by the cave water. The most plausible explanation for this situation is that the cave system does not lie in the main flow path of groundwater discharge toward the Zwartkrans Spring. Similarly, Groenewald (2010b) refers

Table 3 Historical and recent chemistry of Sterkfontein Cave groundwater

| Variable/analyte | Sample date | | | | | | | SANS (2011a) ^a |
|----------------------------|-------------|---------|---------|---------|---------|---------|---------|---------------------------|
| | 04/2001 | 04/2005 | 02/2006 | 05/2010 | 01/2011 | 08/2012 | 05/2014 | |
| pH ($-\log_{10}a_{H^+}$) | 7.5 | 8.1 | 7.9 | 7.9 | 7.6 | 8.1 | 7.5 | 5.0–9.7 |
| SEC (mS/m) | 74 | 59 | 57 | 59 | 46 | 66 | 69 | ≤ 170 |
| Ca (mg/L) | 47 | 44 | 46 | 47 | 48 | 48 | 61 | n.s. |
| Mg (mg/L) | 27 | 28 | 37 | 26 | 27 | 34 | 42 | n.s. |
| Na (mg/L) | 14 | 23 | 20 | 20 | 22 | 20 | 26 | ≤ 200 |
| K (mg/L) | 0.2 | 1.0 | <0.1 | 1.1 | 1.0 | 1.0 | 1.5 | n.s. |
| Cl (mg/L) | 38 | 31 | 46 | 27 | 37 | 44 | 39 | ≤ 300 |
| SO ₄ (mg/L) | 46 | 58 | 61 | 58 | 71 | 78 | 126 | ≤ 500 |
| HCO ₃ (mg/L) | 193 | 184 | 196 | 185 | 188 | 198 | 206 | n.s. |
| NO ₃ (mg N/L) | 8.4 | 7.0 | 7.5 | 8.2 | 9.3 | 1.0 | 7.5 | ≤ 11 |
| SI _C | −0.10 | 0.44 | 0.28 | 0.27 | −0.01 | 0.49 | −0.01 | n.s. |
| SI _D | −0.17 | 0.94 | 0.73 | 0.56 | −0.01 | 1.10 | 0.09 | n.s. |
| EB (%) | −1.3 | 3.4 | 2.5 | 2.3 | −1.3 | −0.3 | 3.0 | n.s. |

**Fig. 8** Graphic comparison of historical and current Sterkfontein Cave groundwater chemistry

to the cave as occupying a low energy groundwater system, and Martini et al. (2003) refer to the "... apparently static ..." pools in the cave system. These circumstances are discussed in greater detail in Sect. 4.

Attention must also be drawn to the NO₃ concentrations of 8.2 and 9.3 mg N/L recorded for the 13/05/2010 and 14/01/2011 samples of cave water (Table 3 and text box Fig. 8). This level of NO₃ is uncharacteristic of mine water

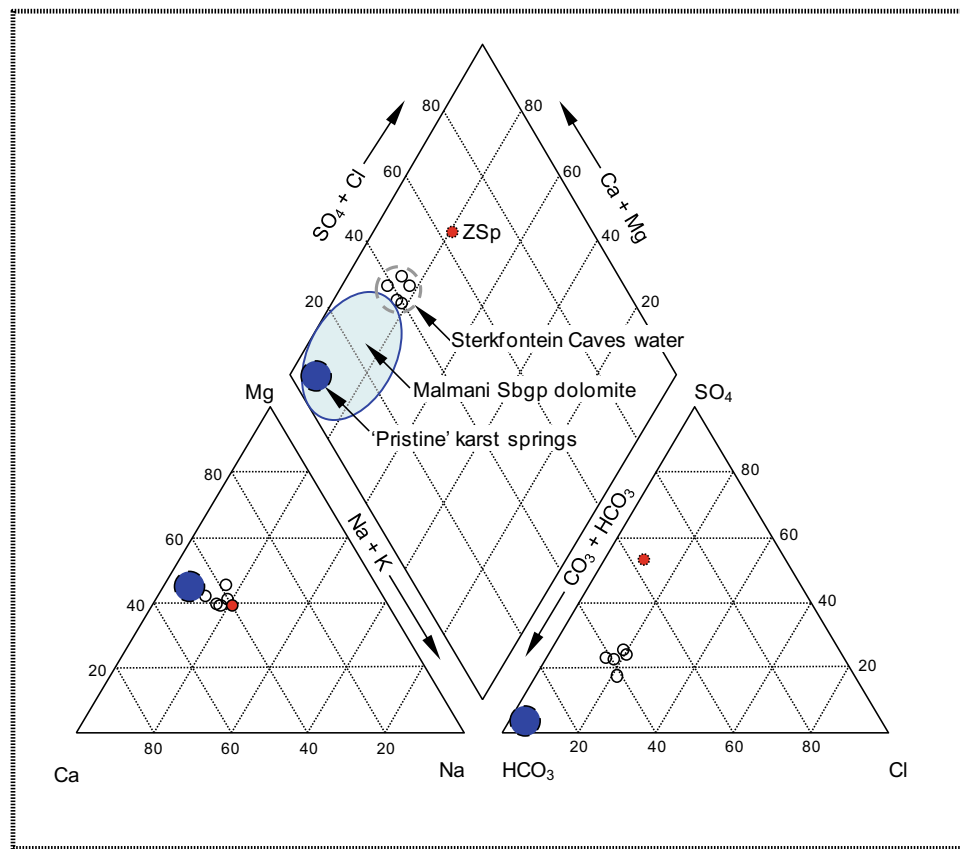


Fig. 9 Piper diagram of historical and recent Sterkfontein Cave water chemistry compared to other karst groundwater and October 2012 and May 2014 Zwartkrans Spring (ZSp) water

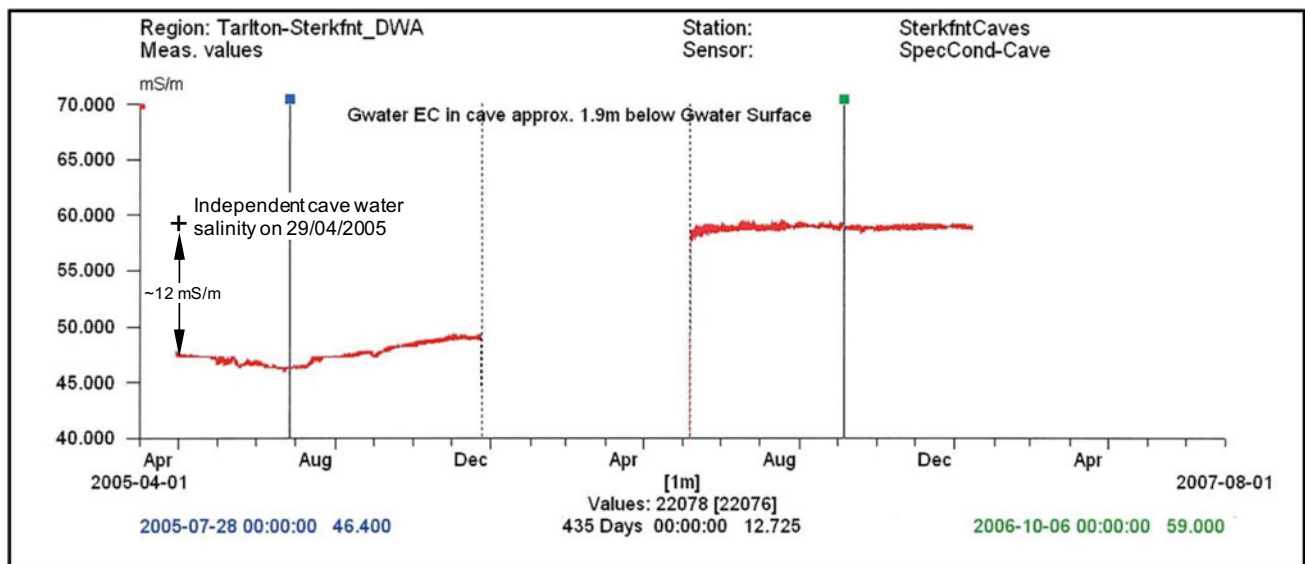


Fig. 10 Continuous electrical conductivity response pattern in Sterkfontein Cave water over a period of 27 months (use of image courtesy of DWS)

and indicates another source (or sources) of water contamination possibly reflecting a historical legacy. Nevertheless, the nitrate concentration suggests a measure of contamination by nutrient-rich water. Possible sources of such water include the following:

- upstream agricultural land-use practices—the Oaktree area supports extensive irrigated agriculture that includes maize, vegetables, and tunnel farming (of cut-flowers) using groundwater drawn locally from the karst aquifer;
- municipal wastewater effluent—the discharge from Percy Stewart WWTW imposes a median SO_4 concentration of ~ 160 mg/L in the receiving Blougat Spruit (Hobbs 2011a), an upper tributary of the Bloubank Spruit;
- on-site sanitation facilities on the numerous smallholdings in the Oaktree area—this area is not served by the Mogale City Local Municipality sewerage system;
- a piggery⁶ that used to be operated ~ 1150 m upstream (south-west) of Sterkfontein Cave on the right bank of the Bloubank Spruit—anecdotal evidence suggests that this facility routinely washed its surface accumulation of piggery waste into the adjacent stream as a means of disposal; and
- the sanitation facility serving the Sterkfontein Cave Visitors Center which, until mid-2011, comprised a septic tank system that was replaced with an environment-friendly self-contained bioreactor system (Sect. 4).

The source of the NO_3 contamination, i.e., whether from agriculture or municipal wastewater effluent, has not been established because of a paucity of historical groundwater chemistry information for this portion of the study area. In addition to the possibilities raised above, it might be speculated that the circumstances which precipitated the study by Barnard (1996) possibly could account for the elevated nitrate levels in the cave water. The possible impact of on-site sanitation facilities serving the visitor center at the caves also cannot be disregarded, especially in light of the following observations.

The septic tank and wetland sanitation system that previously served the visitor complex (Plate 2) was replaced with an environment-friendly self-contained bioreactor system in mid-2011 (I. Wright, personal communication). The $20 \text{ m}^3/\text{d}$ design capacity of the SAFF (submerged aeration fixed film) technology biozone system (Plate 3) is indicative of the sanitation load generated by the visitor center. This

center typically receives 110,000 people per annum (300 per day on average), with a peak of ~ 400 per day experienced during the 2010 soccer World Cup (T. Rubin, personal communication).

Replacement of the septic tank sanitation system has eliminated this as a possible/probable source of nutrient contamination and provides the most reasonable explanation for the 1 mg N/L concentration (i.e., an order of magnitude reduction) observed in the August 2012 cave water analysis (Table 3). The low PO_4 concentration (<0.2 mg P/L) and the absence of sunlight suggest that the trophic status of the Sterkfontein Cave water system is unlikely to change provided the current hydrochemical conditions prevail. Assurance in this regard can be obtained from a regular biomonitoring program (as described by Culver and Sket 2002) that targets stygobitic fauna.

Closer inspection of the data presented in Table 3 indicates that the SO_4 concentration in the cave water has increased by $\sim 174\%$ from 46 mg/L in April 2001 to 126 mg/L in May 2014 (Fig. 11). It has been shown (Sect. 1.4 in Chapter “Chemical Hydrology” and Text Box 1 in Chapter “Chemical Hydrology”) that SO_4 comprises $\sim 63\%$ of the TDS concentration associated with Western Basin mine water, $\sim 19\%$ of the TDS typical of surface water, and $\sim 2\%$ in the case of pristine karst groundwater. The SO_4 :TDS ratio value, therefore, serves as an indicator of mine water in receiving water resources. The SO_4 :TDS ratio associated with the cave water chemistry over time is shown in Fig. 11. The latest value ($\sim 25\%$) represents an increase of $\sim 92\%$ over the ca. 2001 value ($\sim 13\%$), and of $\sim 56\%$ over the ca. 2010 value (16%). This provides a clear indication of a surface water influence on the cave water chemistry. Given the previously demonstrated evidence of a mine water impact on the surface water chemistry of the Bloubank Spruit system, the corollary transposes a muted mine water impact also on the cave water environment. The reasons for a muted mine water impact as opposed to a more prominent impact are explored in Sect. 8.4 and illustrated in Fig. 48.

3 Groundwater Chemistry Assessment by GRU

Chemical analyses representing a combination of inorganic, organic, bacteriological, and stable isotope results for groundwater sourced from boreholes and springs provide information on the spatial distribution of groundwater chemistry (quality) in the COH. A representative sample was ensured by obtaining water only from equipped and active borehole installations, and as close to the installed headworks as possible.

⁶ Located in the north-eastern quadrant of the Kromdraai Road/R563 junction opposite the Cradle Food Market, this property now hosts the Sterkfontein Public Storage Facility.

Plate 2 View from the Sterkfontein Cave Visitor Center looking north over the septic tank system soak-away area (circled) and the Bloubank Spruit valley (middle foreground) at the highest point in the COH WHS (arrowed)

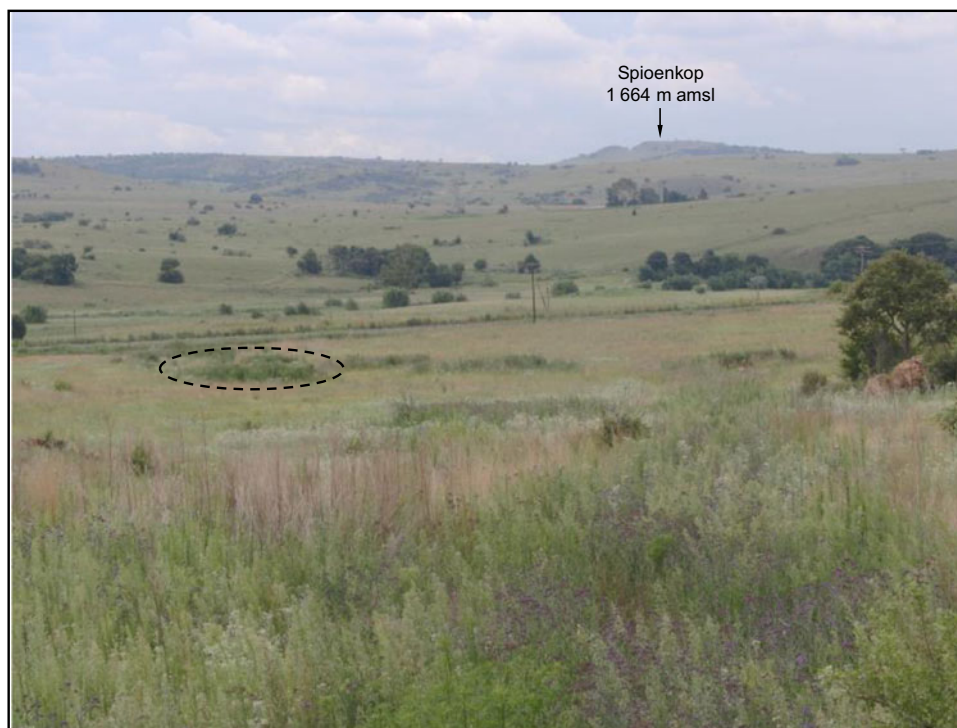


Plate 3 View of the biozone sewage treatment plant installed under the Sterkfontein Cave Visitor Center in mid-2011



The results of 48 analyses of water sourced from 39 boreholes and nine springs (excluding the KGR springs, which are discussed separately in Sect. 7.15) are grouped geographically according to the basins/subcompartments identified in Sect. 2 in Chapter “Physical Hydrogeology”,

and which are recognized as groundwater resource units⁷ (GRUs). The grouping of analyses on this basis, and

⁷ See Glossary.

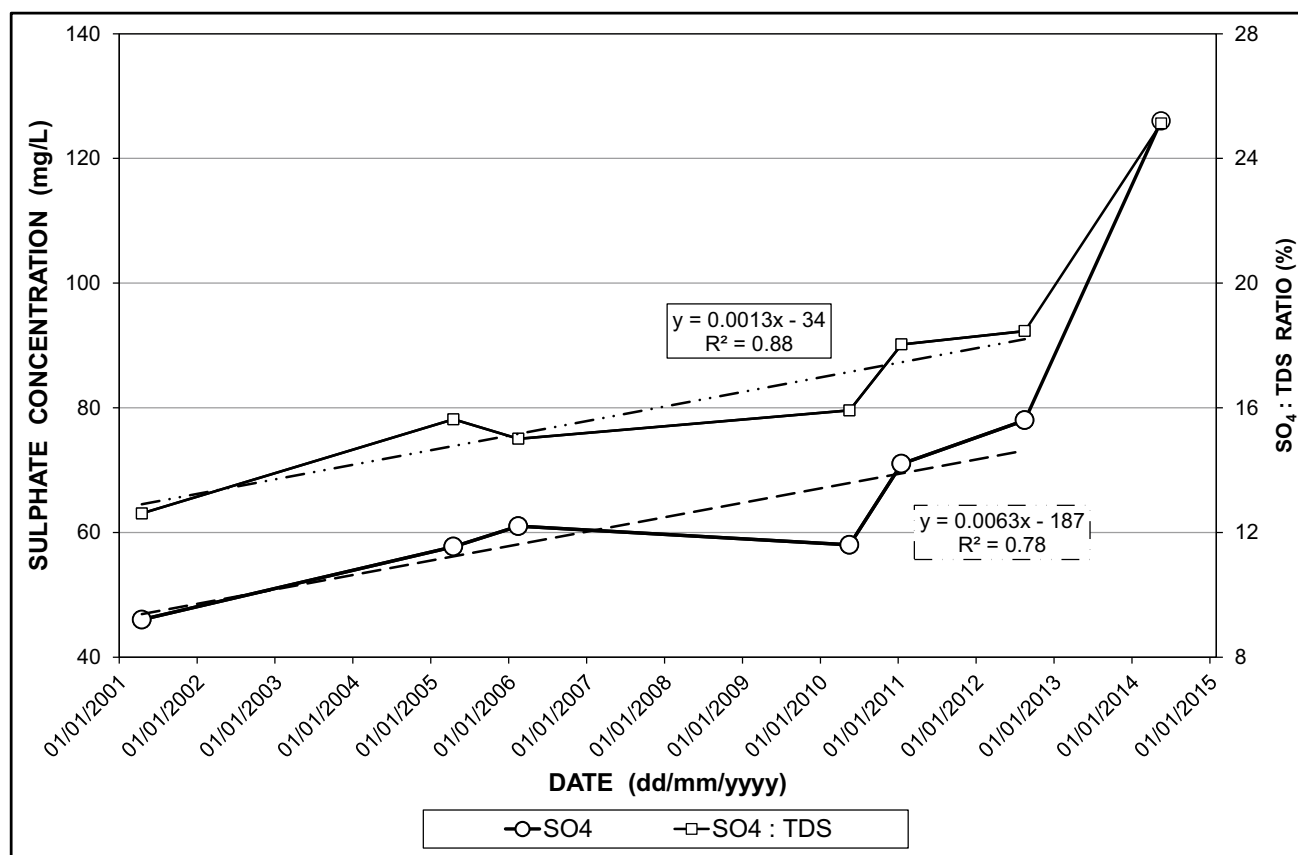


Fig. 11 Pattern and trend of the SO_4 concentration and SO_4 :TDS ratio in Sterkfontein Cave Lake water since 2001

considering the mean concentration of analytes per group, provides a measure of the current groundwater chemistry associated with these hydrogeologic units. This information is presented in Figs. 12, 13 and 14 and discussed in the following sections.

3.1 Zwartkrans Basin

3.1.1 Vlakdrift Subcompartment

It is evident from Figs. 12 and 13 that the groundwater chemistry associated with subcompartment GRU1a approaches that of a 'pristine' karst aquifer. The only concern is the indication of bacteriological contamination in the upper reaches of the subcompartment where it receives allogenic recharge via the upper Riet Spruit (Sects. 5.1 in Chapter "Physical Hydrology" and 6).

3.1.2 Sterkfontein Subcompartment

Figure 12 and 13 show the extent to which the groundwater chemistry in this subcompartment (GRU1b) differs from that in the other GRUs. The Ca- SO_4 groundwater character and

mean SEC value of 133 mS/m reflect the impact of mine water on the karst groundwater associated with this GRU.

3.1.3 Zwartkrans Subcompartment

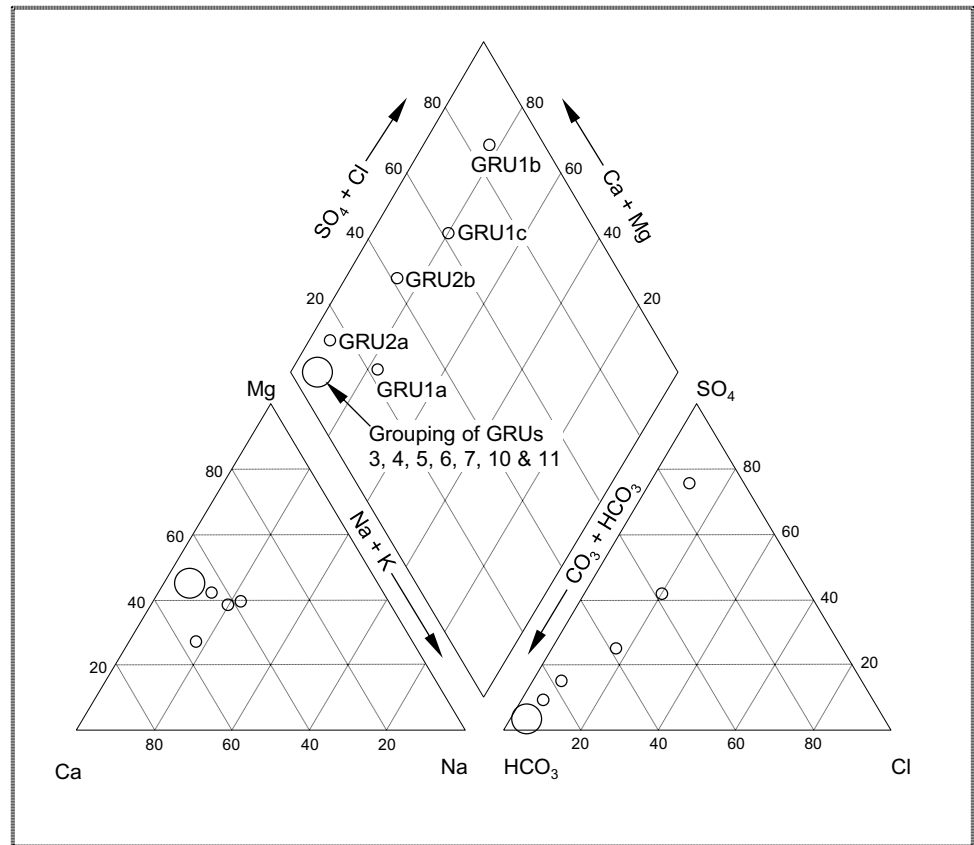
Albeit less pronounced compared to that of GRU1b, the Ca- SO_4 composition of the GRU1c groundwater (Figs. 12 and 13) still reflects the impact of mine water on the karst groundwater. Figure 13 also shows that this subcompartment supports the highest mean Cl concentration, which reflects the additional impact associated with the ingress of municipal wastewater effluent discharged from the Percy Stewart WWTW via the Blougat Spruit.

3.2 Krombank Basin

3.2.1 Kromdraai Subcompartment

Figure 14 indicates that the groundwater chemistry in this subcompartment (GRU2a) is similar to that in the other 'pristine' dolomite compartments (e.g., GRUs 3, 4, 5, and 7). However, station RLGR5 located at the Kiosk/Camp Site in the Rhino and Lion Game Reserve (RLGR) in this

Fig. 12 Piper diagram of GRU water chemistry



subcompartment indicates slight bacteriological contamination (Sect. 6 and Fig. 17). The *E. coli* concentration of 4 cfu/100 mL is cause for concern in the medium- to long-term, although routine monitoring of groundwater quality by the RLGR provides an appropriate management measure in this regard.

3.2.2 Bloubank Subcompartment

The similarity in mean groundwater chemical composition between GRU2b and GRU1c is evident in Figs. 12 and 13. The more muted composition associated with GRU2b groundwater reflects the situation where this unit is the main receiving groundwater resource for the discharge from GRU1c. It is therefore also not surprising that Fig. 14 indicates that groundwater quality in the Bloubank Subcompartment (GRU2b) is the ‘poorest’ of the ‘pristine’ dolomite compartments. This is also reflected in the mean SEC value of 49 mS/m that characterizes this groundwater.

3.3 Danielsrust Basin

Figure 14 shows that the groundwater chemistry in this compartment (GRU3) reflects a composition that is typical

of a ‘pristine’ dolomite aquifer. Again the only concern is the indication of bacteriological contamination, albeit slight, in the water produced by the Danielsrust Spring (Sect. 6 and Fig. 17). A more complete discussion on the springwater chemistry is presented in Sect. 7.2.

3.4 Uitkomst Basin

The Uitkomst Basin (GRU4) supports a pristine karst groundwater environment that is reflected in the chemical composition of the groundwater discharged from this compartment via the Nash Spring. The quality of this groundwater is described and discussed in Sect. 7.8.

3.5 Tweefontein Basin

The groundwater chemistry in GRU5 conforms to that associated with the more ‘pristine’ karst environments. Figure 14 indicates that the composition of this groundwater is virtually indistinguishable from that associated with GRU7 (the Diepkloof Basin drained by the Nouk-lip Spring). These circumstances support the postulated

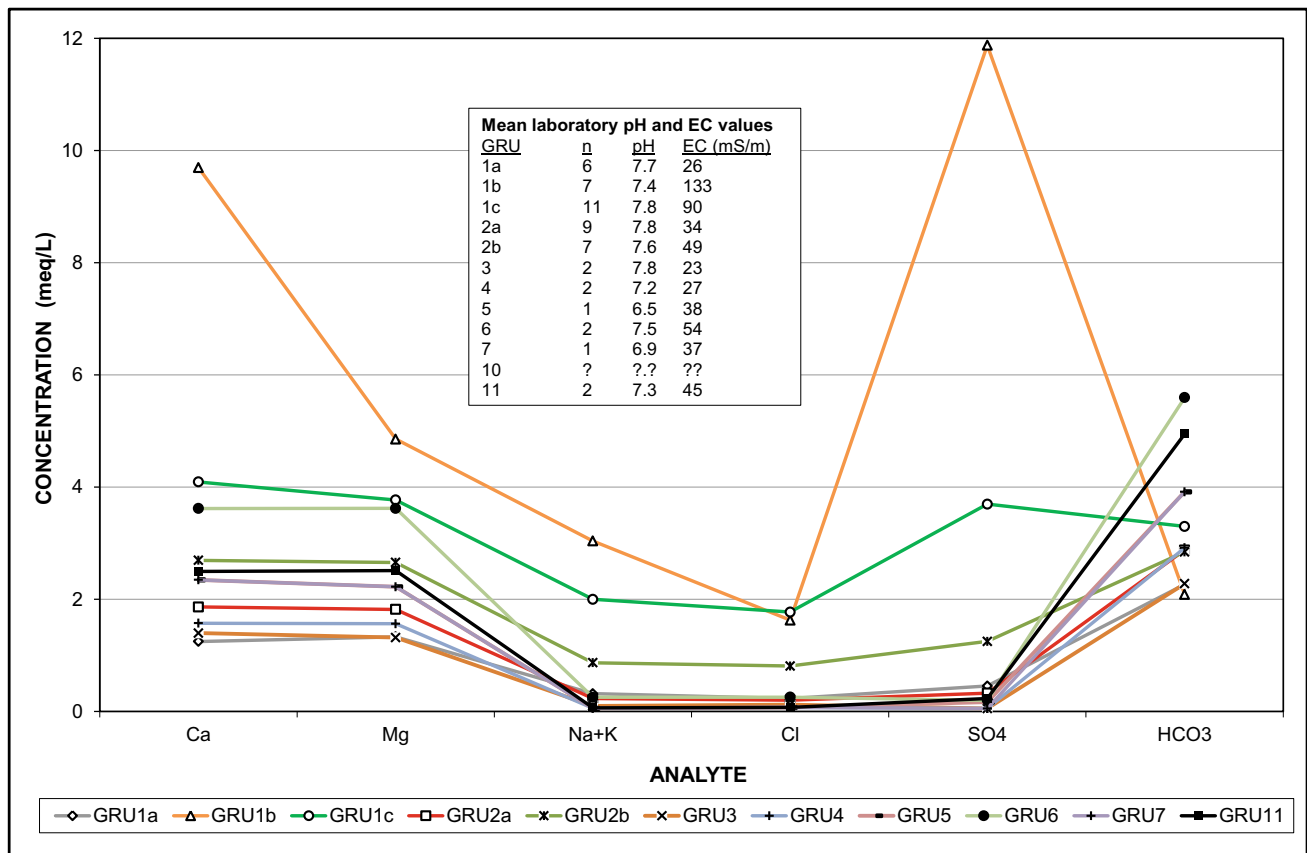


Fig. 13 Graphic comparison of groundwater chemistry associated with GRUs

autogenic recharge of GRU7 via the Tweefontein Spring discharge. Further information on the chemistry of this groundwater is provided in Sect. 7.5.

3.6 Rietfontein Basin

The Rietfontein Basin (GRU6) produces a good quality groundwater (Sect. 7.6) which reflects the different rock types (dolomite and undifferentiated igneous strata) that comprise this hydrogeologic unit. The influence of the non-karst groundwater on the mixture of karst and non-karst groundwater produced by GRU6 is evident in detectable concentrations of metals such as Fe (~2.6 mg/L) and Mn (~0.4 mg/L) (Table 5).

3.7 Diepkloof Basin

The Diepkloof Basin (GRU7) reflects a similar groundwater chemistry to that of GRU5, the Tweefontein Basin (Sect. 3.5). For this reason, it reflects a ‘pristine’ karst environment that produces good quality groundwater (see Sect. 7.7).

3.8 Motsetse Basin

The groundwater chemistry associated with GRU8 is represented by the field variables listed in Sect. 7.10. The SEC value of 64 mS/m is indicative of a slightly impacted karst groundwater chemistry.

3.9 Rhenosterspruit Basin

There are no groundwater chemistry data available for this hydrogeologic unit (GRU9).

3.10 Kalkheuvel Basin

Represented by the Barlow Spring and GF1 borehole groundwater (GRU10).

3.11 Broederstroom Basin

The groundwater chemistry of this compartment (GRU11) is represented by that of the Broederstroom, Anderson, and

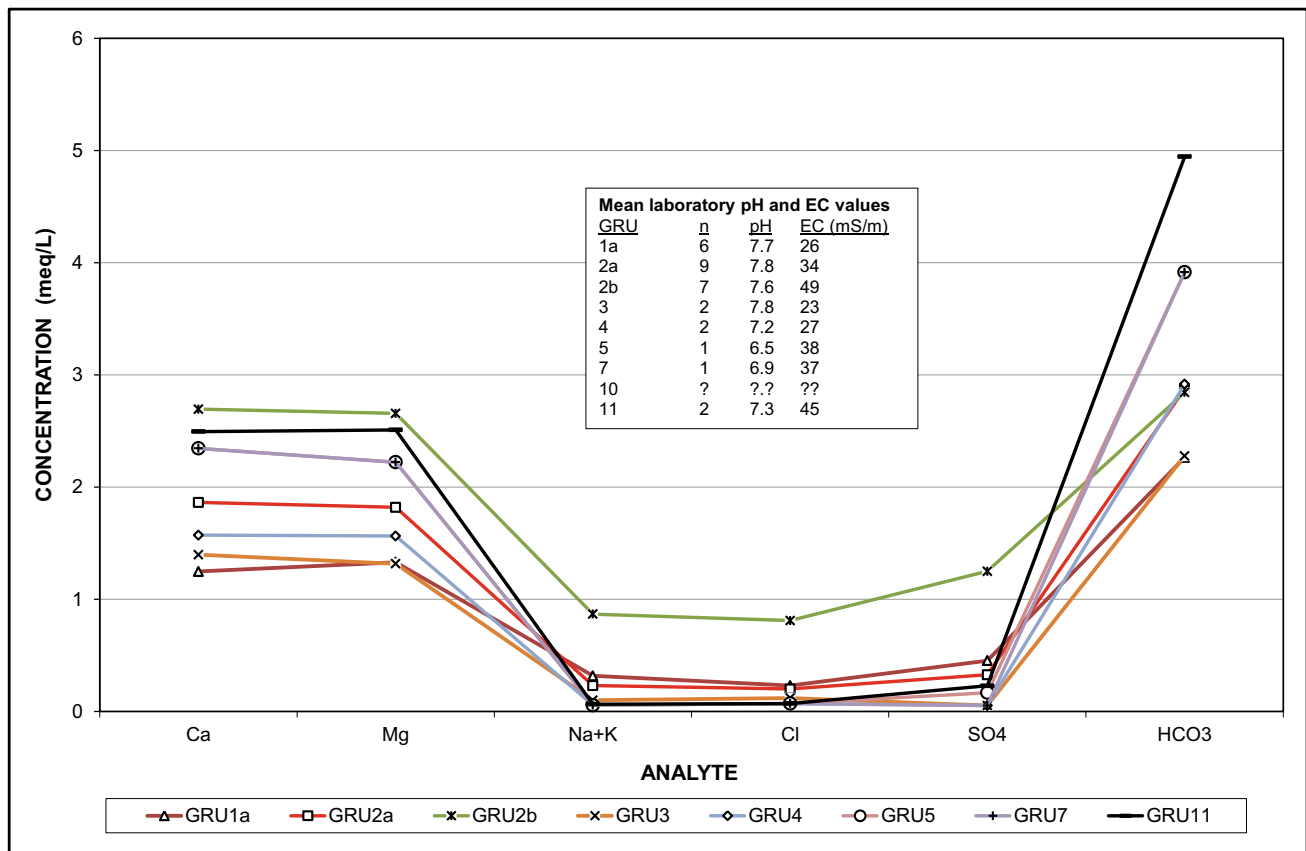


Fig. 14 Graphic comparison of groundwater chemistry associated with ‘pristine’ GRUs

Lesedi springs. The composition of the Anderson and Broederstroom springwaters (Sects. 7.12 and 7.14, respectively) again reflect that which characterizes the more ‘pristine’ karst environments (Fig. 14). Concern regarding the Lesedi springwater quality is discussed in Sect. 7.13.

4 Local Groundwater Chemistry Assessment

A real and present concern is the result returned by a chemical analysis carried out on the groundwater produced by geosite WBD1, the water supply borehole in the KGR established in 2009 to mitigate the termination of the wastewater supply from the Percy Stewart WWTW (see hereunder). This analysis yielded a nitrate concentration of 51 mg N/L, a Cl value of 103 mg/L, an SO_4 value of 110 mg/L, a Na concentration of 82 mg/L, and a laboratory SEC value of 103 mS/m. All of these concentrations are anomalous for karst groundwater and point to a significant impact on the karst groundwater delivered by this borehole. The most likely source of this impact is the irrigation of ~65 ha of instant lawn with treated wastewater effluent obtained from the Percy Stewart WWTW as discussed in

Sect. 3.2 in Chapter “Physical Hydrology” and shown in the unnumbered Plate on p. 10.

These circumstances are not new, as a similar situation precipitated the study by Barnard (1996). The Barnard (1996) study found that the practice of flood irrigation in the KGR using wastewater effluent from the Percy Stewart WWTW was the most likely cause of elevated NO_3 , SO_4 , and Cl concentrations in the groundwater produced by the borehole WBD4 (Sect. 2.3.3), as well as the source of bacteriological contamination of this groundwater.

The provision of wastewater to the KGR was terminated in September 2008 (Sect. 3.2 in Chapter “Physical Hydrology”) on the presumption that wastewater irrigation of kikuyu in the KGR was again the cause for the observed deterioration in mid-2008 of the groundwater quality produced by borehole WBD4 (Fig. 7). The more probable cause, however, was the ingress of a mixture of raw and treated mine water into the karst aquifer from the Riet Spruit (Sect. 2.3.3) as discussed by Hobbs (2008b). Other factors that inform this probability are the following:

- the borehole WBD4 is located ~180 m from the losing Riet Spruit drainage;

- the depth to groundwater rest level in the northern portion of the KGR where irrigation was practiced, exceeds 40 m from surface;
- the method of irrigation practiced in the KGR followed best practice for irrigation on dolomitic terrains such as ensuring no ponding of water (S. du Toit, personal communication) in dolines and other surface depressions; and most convincingly;
- the chemistry of the groundwater produced by borehole WBD4 in early- to mid-2008.

It remains a travesty, therefore, that the same practice that precipitated termination of the provision of ~ 0.97 ML/d wastewater to the KGR was conveniently overlooked in regard to the similar supply of ~ 1.3 ML/d to irrigate the 65 ha of instant lawn on the adjoining property to the east. Some of the wastewater provided to the KGR was also used for game watering.

5 Isotope Chemistry

The use of isotope chemistry is well established in both surface water and groundwater investigations (Cecil and Green 2000; Osmond and Cowart 2000; Wanty and Nordstrom 1993). Ford and Williams (2007), however, caution that the use of stable isotopes in hydrogeology merely provides information on the general source of waters, and does not identify the exact source. This is seen as a significant limitation. The principal isotopes are those of hydrogen (protium ^1H and deuterium ^2H) and oxygen (^{18}O and ^{16}O). These are not subjected to nuclear transformation, and therefore also known as stable isotopes. Radioactive isotopes, e.g., tritium (^3H), are subject to decay over time, which explains their use for dating.

It is standard practice to report stable isotope results as the ratio of the least abundant (heaviest) isotope to the most abundant (lightest) isotope (Kendall and Caldwell 1998). For oxygen, the ratio is $^{18}\text{O}/^{16}\text{O}$, and for hydrogen $^2\text{H}/^1\text{H}$. As variations in the isotopic ratios are small, the δ (delta) notation is used to express the deviation of the isotopic ratio in the sample with respect to the ratio in the standard (e.g., $\delta^{18}\text{O}$) in units of parts per thousand (‰) relative to a standard of known composition represented by that of Standard Mean Ocean Water (SMOW).

5.1 Previous Studies

The use of isotopes in the study of water chemistry in the project area (primarily the area of mine water decant) has been documented, among others, by CGS (undated), Holland (2007), Hobbs, and Cobbing (2007), and Hobbs et al.

(2010). The CGS (undated) employed a variety of isotopes ($^2\text{H}/^1\text{H}$, $^{18}\text{O}/^{16}\text{O}$, $^{87}\text{Sr}/^{86}\text{Sr}$, $^{34}\text{S}/^{32}\text{S}$, $^{206}\text{Pb}/^{207}\text{Pb}$, and $^{208}\text{Pb}/^{207}\text{Pb}$) to investigate the chemical (isotopic) relationship between various water sources in the area of mine water decant and immediate downstream environment. In regard to the $\delta^{34}\text{S}$ data, this study reported interpretation difficulties associated with the available information, due mainly to a lack of background reference values. Nevertheless, the observed $\delta^{34}\text{S}$ values are ascribed to natural oxidative weathering of pyritic Witwatersrand strata interacting with and leached by the water.

The $^{87}\text{Sr}/^{86}\text{Sr}$ data, viewed in conjunction with the $\delta^{34}\text{S}$ data, suggest the gradual mixing between waters of probably dolomitic provenance and mine effluents. The Pb isotope results, on the other hand, clearly reflect the difference between raw mine water and surface water and groundwater sources that exhibit a mine water impact (Fig. 15).

Both Holland (2007) and Hobbs and Cobbing (2007) used the stable isotope ratios $\delta^2\text{H}$ and $\delta^{18}\text{O}$ to distinguish between various natural and impacted water sources in the area (see Sect. 5.2). In addition, Holland (2007) reports the results of 21 tritium (^3H) analyses for groundwater and springwater samples in the study area. Hobbs et al. (2010) report on the additional application of the radio-isotopes ^{222}Rn (radon), ^{226}Ra (radium), and ^{238}U as possible hydrological tracers in a natural and polluted environment (Sect. 5.2.2). In a much wider geographic

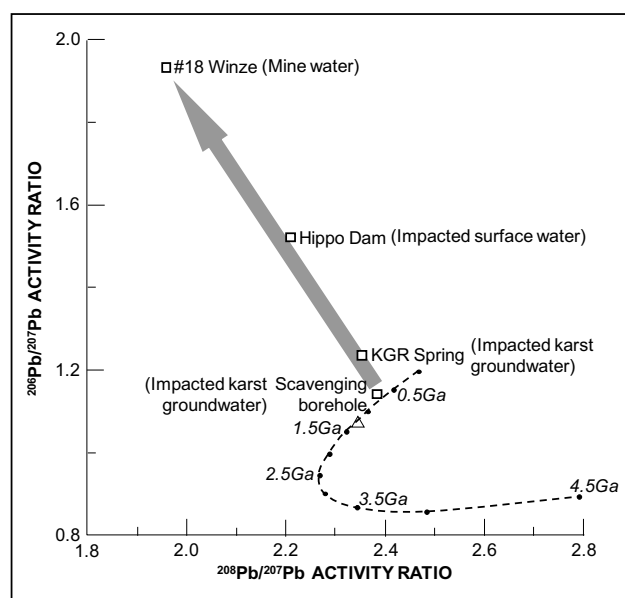


Fig. 15 Relationship of Pb isotopic ratios of water in the West Rand area to the Stacey–Kramers curve (dotted line); South African leaded petrol plots at Δ on this curve; different stages of crustal evolution shown by ages in Ga; arrow shows the direction of deviation of the Pb isotope signature associated with mine water impacts (modified from Coetzee and Rademeyer 2006)

Table 4 Comparison of ca. mid-2009 isotope data for cave and springwater

| Variable/analyte | Sterkfontein Cave | Zwartkrans Spring | Plover's Lake springs |
|----------------------------------|-------------------|-------------------|-----------------------|
| Date | 28/05/2009 | 17/07/2009 | 17/07/2009 |
| $\delta^2\text{H}$ (‰ SMOW) | −19.8 | −16.8 | −28.9 |
| $\delta^{18}\text{O}$ (‰ SMOW) | −3.53 | −3.17 | −5.01 |
| ^3H (TU $\pm 1\sigma$) | 1.3 ± 0.3 | 2.4 ± 0.3 | 1.6 ± 0.3 |
| ^{222}Rn (Bq/L) | n.a. | 8.8 | 10.5 |

context, Bredenkamp et al. (2007) report on the use of ^{14}C , ^3H , and CFCs in providing new insights into recharge and circulation processes in the karst aquifers of the South African interior. These insights extend to a derivation of mean residence (turnover) periods for groundwater in these hydrogeologic systems. For the Pretoria Springs, identified by Bredenkamp et al. (2007) as the Erasmus, Grootfontein, Pretoria Upper, Pretoria Lower, and Sterkfontein springs, these authors report residence periods in the range of 12.7–20.3 years.

5.2 Isotopic Information

5.2.1 Stable Isotopes

Isotope analyses performed on Sterkfontein Cave and Zwartkrans and Plover's Lake springs groundwaters in mid-2009 are presented in Table 4. The more similar $\delta^2\text{H}$ and $\delta^{18}\text{O}$ values of the Sterkfontein Cave and Zwartkrans Spring groundwaters support the water level (Sect. 3.2.1 in Chapter “Physical Hydrogeology”) and inorganic chemistry (Sect. 7.1) data that indicates that the cave system penetrates and shares the karst aquifer drained by the spring (Hobbs and De Meillon 2017). This observation also supports the use of these isotopes to distinguish between various water sources (and mixture of sources) in the study area.

Perhaps more significantly, however, is the difference in ^3H levels between the Sterkfontein Cave and Zwartkrans Spring groundwater. These values indicate that the springwater represents a younger water than that of the cave water. This observation supports the hypothesis (Sect. 2.1.3 in Chapter “Physical Hydrogeology”) that the Sterkfontein Cave does not lie in the main flow path of groundwater discharging to the Zwartkrans Spring.

The tritium value of the cave water is closer to that of the pristine Plover's Lake springs groundwater. The value of 1.3 ± 0.3 TU is representative of groundwater that is several decades old,⁸ compared to the ostensibly ‘younger’ Zwartkrans Spring water with a tritium value of 2.4 ± 0.3

TU. The circumstances that give rise to these differences are important in evaluating the risk posed to the Sterkfontein Cave system by poor quality groundwater in the Zwartkrans Basin that originates from anthropogenic impacts. For example, Martini et al. (2003) report the development of a dolerite sill immediately below Sterkfontein, but which has not been observed in the cave. It is possible that the resistivity surveys reported by Chirenje et al. (2010) might have recognized this structure.

Although the chemistry of springwater (including environmental isotope data) is discussed in more detail in Sect. 7, it is appropriate to note here that the relative age of the groundwater as indicated by the environmental tracers principally reflects the much slower flow paths through the matrix and narrow fractures in the rock (Worthington and Gunn 2009). These circumstances contribute to the apparently large difference in relative groundwater age (from <10 years to several decades) between different karst springs in the study area.

The stable isotope results generated by this study are illustrated in Fig. 16. The comparatively close grouping of six of the springwater samples in the ‘pristine’ karst groundwater field is apparent. Further up the theoretical ‘local’ evaporation line is the Sterkfontein Cave water sample, and beyond that the impacted Zwartkrans Spring groundwater. The elongated shape of the marginally impacted karst groundwater field reflects the wider mixture of isotopic composition associated with this groundwater, ranging from nearly pristine at the lower-left (‘heavier’) end to moderately impacted at the upper right (‘lighter’) end as the evaporative water signature increases. Covering, among others, the same area investigated by Hobbs and Cobbing (2007), a Water Research Commission (WRC) study (Hobbs et al. 2010) that included $\delta^{18}\text{O}$ and $\delta^2\text{H}$ analyses associated with groundwater, mine water, and surface water sources, further established the use of these analytes to distinguish between the various water sources as reflected in Fig. 16.

5.3 Radioactive Isotopes

The study by Hobbs et al. (2010) investigated the use of ^{222}Rn as a hydrological tracer in natural and polluted environments and added radioactive isotope data to the water

⁸ Tritium values <2 TU are generally associated with groundwater residence times in the order of several decades, whereas higher values are indicative of more recent recharge and faster circulation (see for e.g., Hershey et al. 2010).

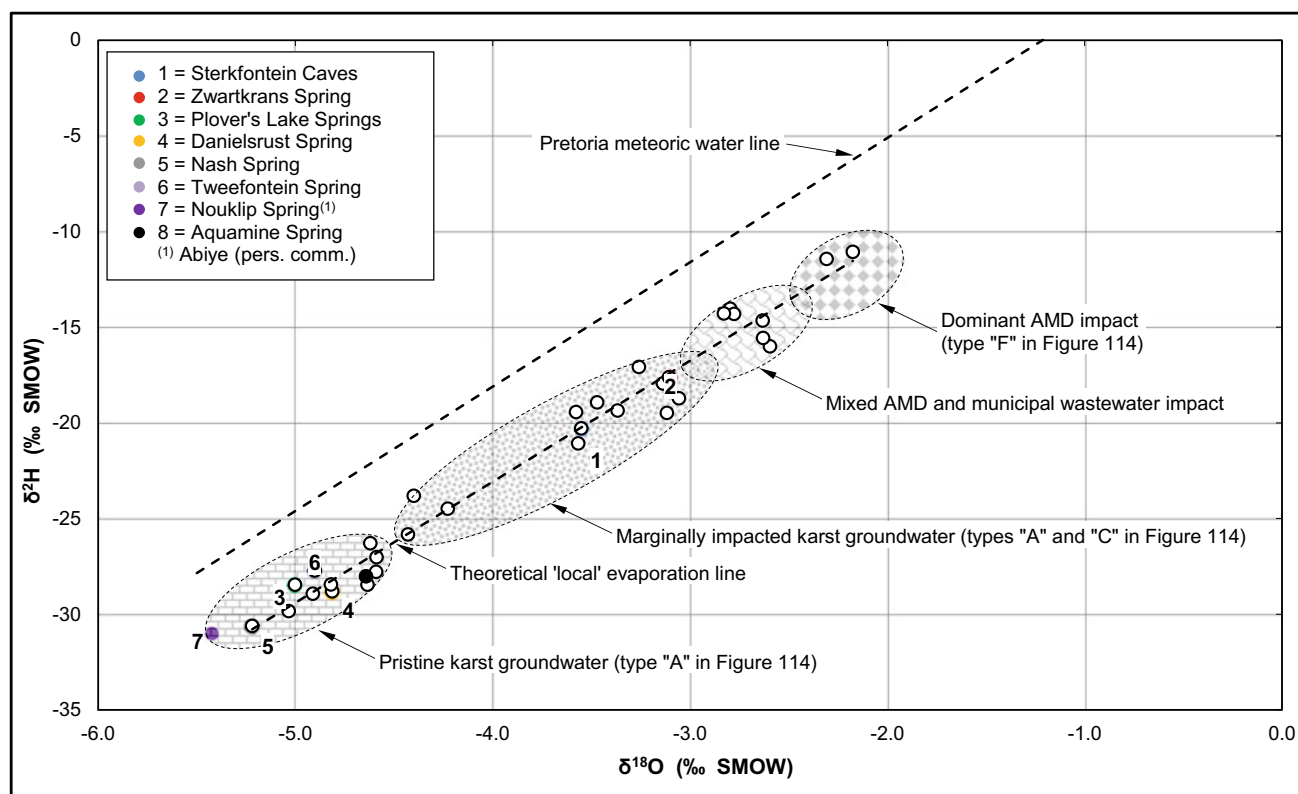


Fig. 16 Stable isotope composition of groundwater in the study area, also showing the characteristic fields associated with various sources (modified from Hobbs et al. 2010)

quality data set generated by the Hobbs and Cobbing (2007) study. The data included ^{222}Rn (radon), ^{226}Ra (radium), and ^{238}U (uranium) analyses associated with groundwater, mine water, and surface water sources collected on two occasions, once in early-2007 and again in early-2008. The radio-isotope data (^{222}Rn , ^{226}Ra , and ^{238}U) proved less successful as hydrological tracers than $\delta^{18}\text{O}$ and $\delta^2\text{H}$. For example, ^{222}Rn activity levels (concentrations) as high as 65 Bq/L were found in otherwise pristine groundwater issuing from quartzitic strata of the Witwatersrand Supergroup, whereas the median ^{222}Rn concentration associated with mine water sources was ~ 27 Bq/L. 'Pristine' karst groundwater yielded a median ^{222}Rn concentration of ~ 7 Bq/L, in good agreement with the values reported in Table 4 for the Zwartkrans and Plover's Lake springs.

The ^{226}Ra concentrations in mine water sources ranged from 0.12 to 1.38 Bq/L, the mean of 0.65 Bq/L exceeding the DWS (1999) target water quality range for domestic water use of 0.42 Bq/L. The comparatively low ^{226}Ra values of 0.029 and 0.002 Bq/L associated with a tailings dam source support findings by de Jesus (1985) that tailings dams do not represent a significant threat as a source of this radionuclide in the receiving surface and groundwater environments.

It should be considered that radium shows an affinity for manganese oxide, for example as represented by MnO and MnO_2 in manganese-impregnated fiber (Moore and Reid 1976). In this regard, the substantial presence of wad in the Malmani Subgroup dolomite is especially significant. Wad (manganiferous earth) is a weathering/decomposition product of dolomite. It comprises of manganese- and iron-oxides that exhibit insoluble and highly compressible properties (Brink 1996). The chemical composition of wad associated with the Oaktree Formation reflects an MnO_2 content of $\sim 42\%$ (and an Fe_2O_3 content of $\sim 20\%$). Its association with more leached dolomite and therefore preferential water-bearing horizons suggests that this material may selectively scavenge radium from any mine water that may recharge the karst aquifer. The median ^{238}U concentration of 1.82 Bq/L (0.15 mg/L) associated with mine water is an order of magnitude greater than the SANS (2011a) limit of 0.015 mg/L for this analyte.

The chemical analyses carried out as part of the current study in most instances included the determination of uranium (U) concentrations. Values in excess of the 0.001 mg/L detection limit were only observed in two surface water samples associated with mine water discharge in the Tweelapie/Riet Spruit system in mid-February 2010

when 0.026 mg U/L was recorded at stations F11S12 and MRd. Strachan et al. (2008) report that the Klip River Radioactivity Monitoring Program found a good linear correlation between the U concentration in water and the total radiation dose from all radionuclides. This prompted these authors to suggest that the U concentration might serve as an indirect measure of the total radiation dose from all radionuclides for screening and routine monitoring purposes in a catchment.

6 Bacteriological Quality

The bacteriological quality of groundwater in terms of the microbiological variables total coliform bacteria and *E. coli* has been determined for 16 sources (boreholes and springs) in the study area. Total coliforms and *E. coli* have traditionally been considered as the best fecal indicator bacteria (FIB) tracers of surface water and human fecal contamination in groundwater, respectively (Kozuskanich et al. 2010). Payment and Locus (2010) suggest that simple ‘presence-absence’ methods detecting both total coliforms and *E. coli* provide a reasonable approach when combined with an appropriate sampling frequency, to establish the measure of risk from enteric pathogens in water. The presence of total coliforms in groundwater indicates that microorganisms in surface water have entered the aquifer, and a more rigorous monitoring should begin for pathogens that might also reach the aquifer (Payment and Locus 2010).

Groundwater samples were collected from sources where the likelihood of bacteriological contamination was considered significant. The results are presented in Fig. 17, and indicate the presence of bacteriological contamination at station A2N0598 in the upper reaches of the Zwartkrans Basin, in the Oaktree area (stations CFM1, CSIR8, CSIR9, and NR1) and further downstream (stations MB1, BolandA, BolandC, ZSp, and OB1). Especially the presence of *E. coli* in some of the samples, notably the Zwartkrans Spring (ZSp) and station OB1, is a concern.

Station OB1, located the furthest downstream at Kromdraai, exhibits a surprising result given the following circumstances:

- the distance of ~870 m from the Bloubank Spruit with its elevated bacterial load (Table 20 in Chapter “Chemical Hydrology”); and
- the groundwater rest elevation of ~1420 m amsl compared to the ~1410 m amsl of the Bloubank Spruit, which indicates a hydraulic gradient toward the river at this locality.

Although the above circumstances suggest the Bloubank Spruit is an unlikely source of this contamination, the use of

the borehole for large-scale agricultural water supply might cause a reversal of the hydraulic gradient and draw in water from this source. In common with stations MB1 and ZSp each producing groundwater with an NO₃ concentration of 12 mg N/L, station OB1 similarly yields groundwater with an elevated nitrate level of 8 mg N/L. Another possible source of both the bacteriological and the nitrate ‘contamination’ in the aquifer supporting borehole OB1 is the presence of livestock (cattle) in the area. A cattle feedlot located ~600 m to the northwest of the borehole was decommissioned ca. 2002, although the surface infrastructure was only completely demolished sometime between July 2008 and November 2009.⁹

Also anomalous is the bacteriological impact is seen in the Danielsrust Spring (DSp) water, which otherwise reflects a pristine dolomitic groundwater quality. The exposed and unprotected setting of the spring likely attracts a greater risk of bacteriological contamination from game such as Eland (*Taurotragus oryx*) that roam freely in this setting. Such instances of bacteriological contamination might attract further investigation in future hydrogeologic studies.

7 Springwater Chemistry

The importance of springs in the study area warrants a comprehensive discussion of the chemical composition of the water produced by each of the enumerated features (Sect. 4 in Chapter “Physical Hydrogeology”). The discussion is informed by the data in Table 5, which also form the basis for the graphed stable isotope data (Fig. 16), the Schoeller graphs (Fig. 18), and the Piper diagram (Fig. 19) representation. It is also important to read this discussion on the springwater chemistry in conjunction with the description of the hydrophysical environment that defines each of the spring features (Sect. 4 in Chapter “Physical Hydrogeology”). Both Figs. 18 and 19 reveal the deviation (for reasons discussed in Sect. 7.1) of the dolomitic Zwartkrans Spring water chemistry from that of the other dolomitic sources. The deviation of the Uitkomst Spring (JNNR4) water chemistry with its Mg–HCO₃ composition and extremely low SEC is readily attributed to the non-dolomitic source, namely shale of the Pretoria Group, drained by this spring (Sect. 7.9). The circumstances that inform the exaggerated Ca–HCO₃ character of the Aquamine Spring (AqSp) water are discussed in Sect. 7.6.

The calcite (SI_C) and dolomite (SI_D) saturation index values reported in Table 5 reveal the typically undersaturated nature of the pristine springwaters in regard to these

⁹ Based on an inspection of historical Google Earth® imagery that brackets this time interval.

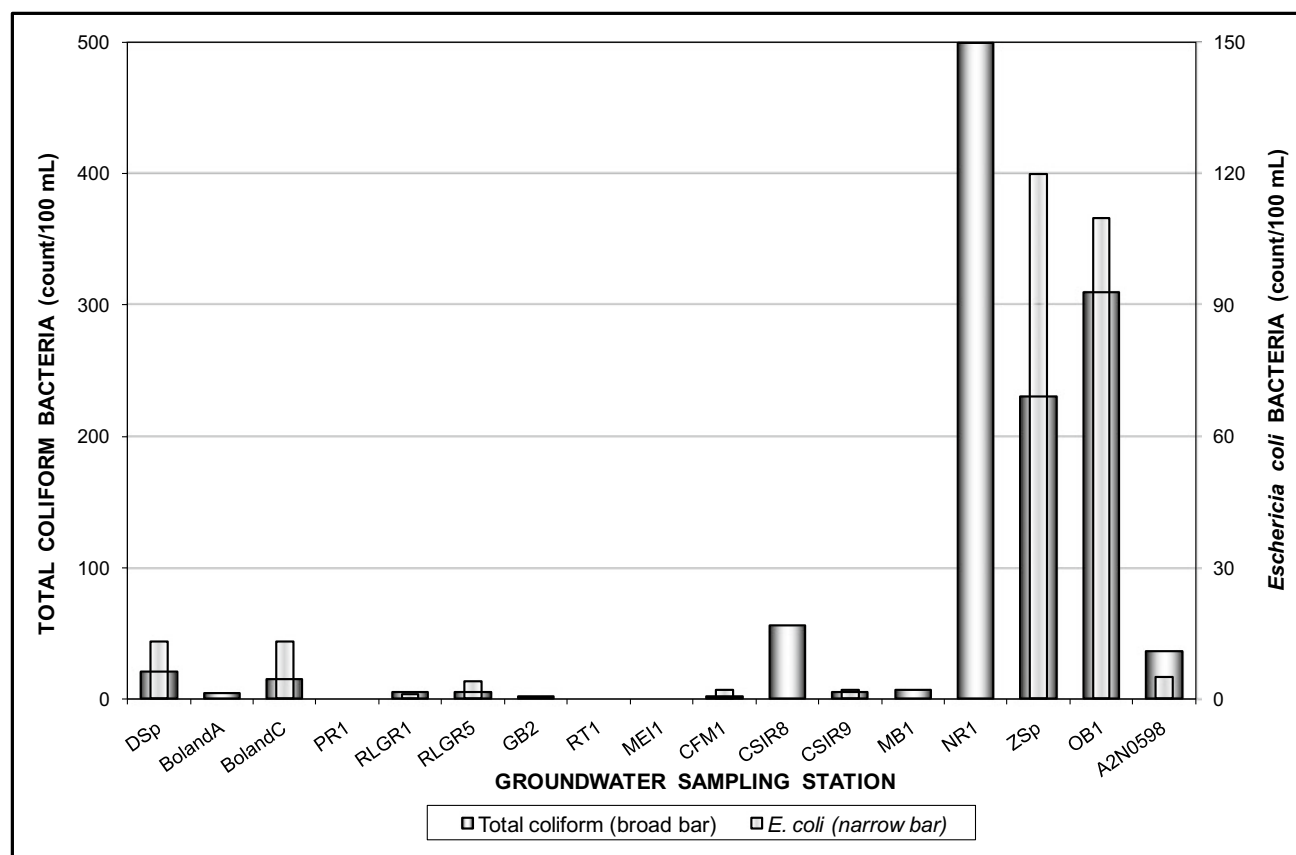


Fig. 17 Graph of groundwater bacteriological quality in the study area; the $\sim 3\times$ difference in scale between the vertical axes explains those *E. coli* values that exceed total coliform counts

minerals. The Zwartkrans (ZSp) and Broederstroom (BSp) springs reflect saturated¹⁰ (equilibrium) conditions for these minerals.

More recent (ca. 2014) springwater chemistry data (Table 6) provides a measure of the change in chemical composition of most of the springwaters represented in Table 5 and Fig. 18. The changes are discussed and illustrated individually in the following sections, and the grouped data are presented in Figs. 19 and 20 for comparative purposes.

The trend described by the SI_C and SI_D values associated with the various springwaters sampled in 2010 (Table 5) and 2014 (Table 6) is illustrated in Fig. 21. The comparison reveals that some of the springwaters (e.g., ZSp, PLSp, and DSP) reflect a change toward greater undersaturation, whereas others (e.g., JNNR1, JNNR2, and JNNR3) reflect a change toward lesser undersaturation.

7.1 Zwartkrans Spring

Bredenkamp et al. (1986) report an SEC value of 94 mS/m for the Zwartkrans Spring water. Figure 22 indicates that the chemical composition of the springwater has changed significantly since May 2006. The principal change is the increase in SO_4 concentration from 123 to 304 mg/L in May 2014. Compared to that of the other karst springs, the Ca- SO_4 composition of this water reflects the impact of poorer water quality sources (mainly mine water) on the karst groundwater draining the Zwartkrans Basin (Sect. 3.1). The springwater chemistry represents the composition of the groundwater aggregated upstream thereof. The SI_C and SI_D values (text box in Fig. 22) indicate equilibrium to slightly undersaturated conditions in regard to calcite and dolomite, respectively. It has previously been shown (Sects. 3 in Chapter “Physical Hydrology” and 1.2 in Chapter “Chemical Hydrology”) that the contributing sources include Ca- SO_4 dominated mine water, and Na- SO_4 dominated treated municipal wastewater effluent with its elevated Cl levels, all of which are evident in this springwater. The stable isotope chemistry of this springwater is reflected in analyses dated July 2009 (Table 4) and May

¹⁰ Adopting the Langmuir (1971) procedure where $-0.1 \leq SI \leq 0.1$ (SI expressed in logarithmic form) denotes saturated (equilibrium) conditions.

Table 5 Springwater chemistry ca. mid-2010

| Variable/analyte | Spring | | | | | | | | |
|------------------------------------|-----------|-----------|-----------|-----------|------------------------|-----------|--------|-----------|--------|
| | ZSp | PLSp | DSp | JNNR1 | JNNR2 | JNNR3 | JNNR4 | AqSp | BSp |
| Date (dd/mm) ^a | 13/05 | 13/05 | 10/02 | 19/05 | 19/05 | 19/05 | 19/05 | 10/02 | 21/12 |
| pH ($-\log_{10}a_{H^+}$) (field) | 7.5 | 7.7 | 6.9 | 6.5 | 6.9 | 7.0 | 7.0 | 6.8 | 7.3 |
| SEC (mS/m) (field) | 84 | 38 | 26 | 39 | 39 | 25 | 1 | 63 | 49 |
| Ca (mg/L) | 66 | 51 | 33 | 47 | 47 | 30 | <2 | 87 | 54 |
| Mg (mg/L) | 37 | 29 | 18 | 27 | 27 | 18 | 3 | 48 | 34 |
| Na (mg/L) | 36 | 2 | <2 | <2 | <2 | <2 | 2 | 4 | <2 |
| K (mg/L) | 1.5 | <1 | <1 | <1 | <1 | <1 | <1 | <1 | <1 |
| Cl (mg/L) | 57 | <5 | <5 | <5 | <5 | <5 | <5 | 10 | <5 |
| SO ₄ (mg/L) | 154 | 5 | <5 | 8 | <5 | <5 | <5 | 7 | 11 |
| HCO ₃ (mg/L) | 195 | 234 | 156 | 239 | 239 | 161 | 20 | 390 | 332 |
| NO ₃ (mg N/L) | 12 | 0.9 | 0.7 | 0.8 | 0.6 | 0.5 | 0.4 | <0.2 | 0.4 |
| Si (mg/L) | 6.0 | 5.9 | 5.9 | 5.0 | 5.2 | 5.5 | 4.1 | 7.5 | 6.5 |
| Fe (mg/L) | <0.025 | <0.025 | <0.025 | <0.025 | <0.025 | <0.025 | 0.315 | 2.57 | <0.02 |
| Mn (mg/L) | <0.025 | <0.025 | <0.025 | <0.025 | <0.025 | <0.025 | 0.466 | 0.38 | <0.005 |
| Al (mg/L) | 0.116 | <0.1 | <0.1 | <0.1 | <0.1 | <0.1 | <0.1 | 0.128 | <0.04 |
| Sr (mg/L) | 0.036 | <0.025 | <0.025 | <0.025 | <0.025 | <0.025 | <0.025 | 0.043 | 0.01 |
| V (mg/L) | 0.034 | 0.039 | 0.029 | <0.025 | <0.025 | <0.025 | <0.025 | 0.035 | <0.005 |
| Hg (mg/L) | <0.001 | <0.001 | <0.001 | n.a. | n.a. | n.a. | n.a. | 0.001 | n.a. |
| U (mg/L) | <0.001 | <0.001 | <0.001 | n.a. | n.a. | n.a. | n.a. | <0.001 | n.a. |
| δ^2H (‰) | -17.6 | -28.5 | -28.8 | -27.7 | -31.0 ^b | -30.6 | n.a. | -28.0 | n.a. |
| $\delta^{18}O$ (‰) | -3.11 | -5.00 | -4.81 | -4.90 | -5.42 ^b | -5.22 | n.a. | -4.64 | n.a. |
| ³ H (TU) | 2.1 ± 0.3 | 1.4 ± 0.3 | 1.3 ± 0.2 | 3.1 ± 0.3 | 0.6 ± 0.2 ^b | 0.1 ± 0.2 | n.a. | 3.4 ± 0.3 | n.a. |
| SI _C | -0.01 | 0.24 | -0.88 | -0.98 | -0.58 | -0.81 | -3.09 | -0.26 | 0.00 |
| SI _D | 0.00 | 0.50 | -1.76 | -1.93 | -1.12 | -1.57 | -5.43 | -0.50 | 0.06 |
| EB (%) | -1.6 | 11.1 | 8.4 | 5.2 | 6.6 | 4.6 | -11.9 | 10.8 | -1.6 |

^aAll dates are dd/mm/2010^bca. 2009 data from Abiye (see Footnote 17)

See text box in Fig. 18 for association of spring identifiers with spring names

2010 (Table 5). The results are compared below and reflect ostensibly small differences.

| Date | δ^2H (‰) | $\delta^{18}O$ (‰) | ³ H |
|------------|-----------------|--------------------|----------------|
| 17/07/2009 | -16.8 | -3.17 | 2.4 ± 0.3 TU |
| 13/05/2010 | -17.6 | -3.11 | 2.1 ± 0.3 TU |

A data logger installed in a stilling well at the spring in mid-2013 was set to record SEC and temperature at 30-min intervals. The SEC data captured by the logger are presented in Fig. 23. The near-continuous SEC record reveals a gradual and steady increase at a rate of 0.8 mS/m per month from ca. August 2013 to ca. March 2014, followed by a decrease of similar proportions (0.7 mS/m per month) to mid-2014, before reverting to an increase (again at 0.8 mS/m per month) to the end of record in September 2014. The peak

reached ca. March 2014 is interpreted as the passage through the spring of mine water impacted groundwater with a maximum SEC of ~103 mS/m, triggered by the ingress of poorer quality mine water in the period February 2010–June 2012. Hobbs (2013c) forecast that the worst of this water would pass through the spring by the end of 2013. The subsequent declining trend indicates a gradual and consistent (albeit slight) improvement in the quality of the springwater. The reversal of this trend in mid-2014 is interpreted to reflect the impact of poor quality mine water input in the period March–July 2014 into the karst system following the resumption of uncontrolled mine water discharge into the environment at end-February 2014 (Sect. 2 in Chapter “Description of the Physical Environment”). This triggered a second flush of more saline water through the aquifer toward the spring. These circumstances find support in the

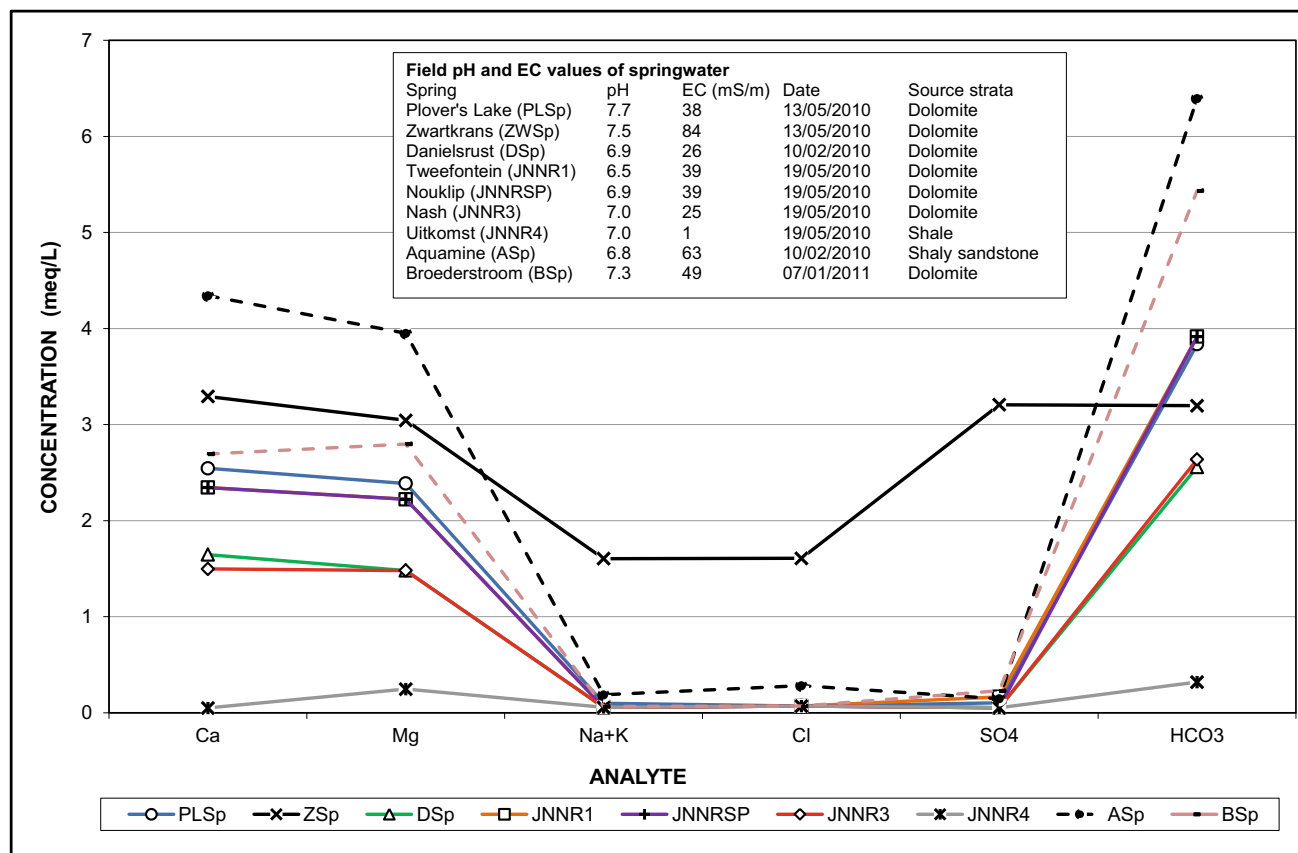
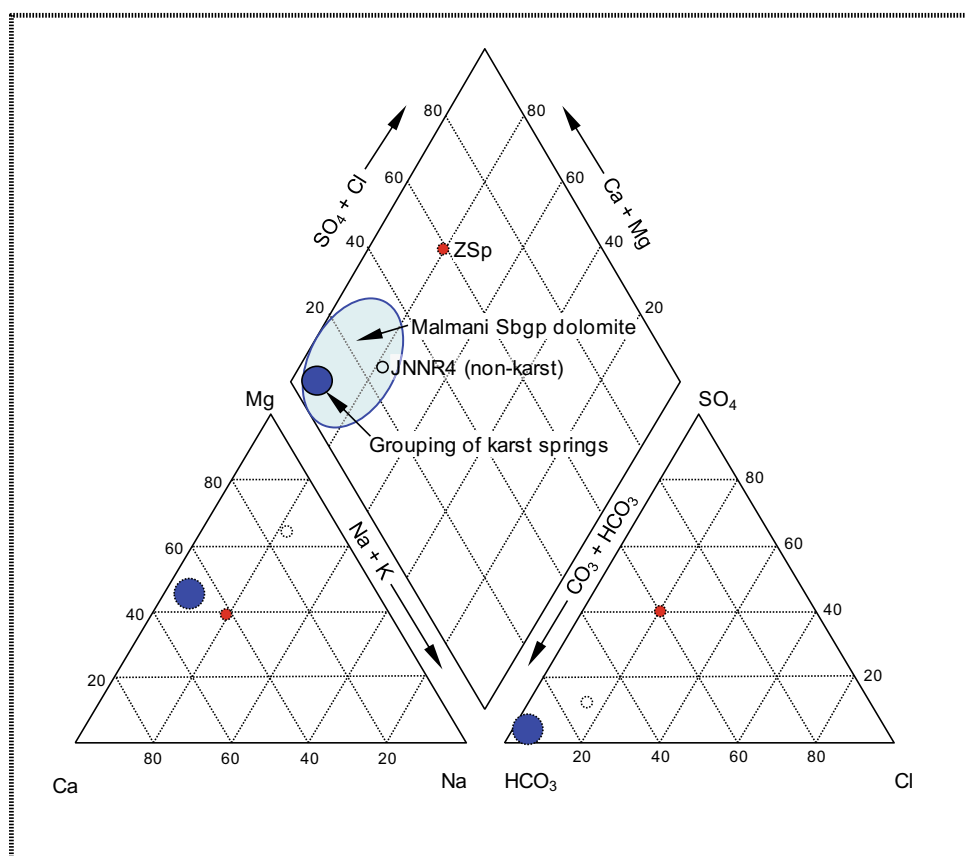


Fig. 18 Graphic comparison of ca. 2010 springwater chemistry (data from Table 5)

Fig. 19 Piper diagram of ca. 2010 springwater chemistry (data from Table 5) compared to typical Malmani Subgroup karst groundwater



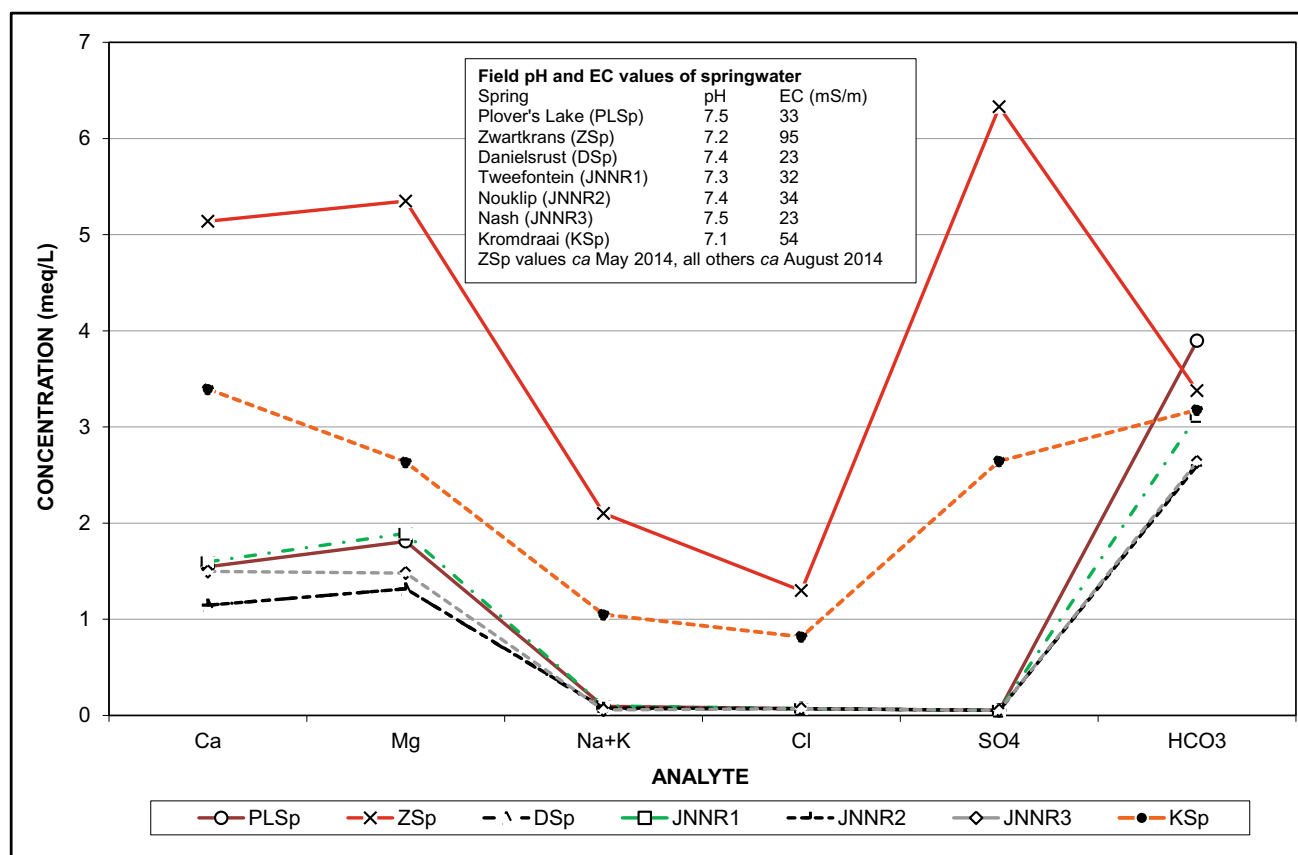


Fig. 20 Graphic comparison of ca. 2014 springwater chemistry (data from Table 6); compositions of DSsp and JNNR2 are virtually identical

Table 6 Springwater chemistry ca. mid-2014

| Variable/analyte | Spring | | | | | | |
|-------------------------------------|--------|--------|--------|-------|--------|--------|-------|
| | ZSp | PLSp | DSp | JNNR1 | JNNR2 | JNNR3 | KSp |
| Date (dd/mm) ^a | 16/05 | 14/08 | 14/08 | 14/08 | 14/08 | 14/08 | 20/08 |
| pH ($-\log_{10} a_{H^+}$) (field) | 7.2 | 7.5 | 7.4 | 7.3 | 7.4 | 7.5 | 7.1 |
| SEC (mS/m) (field) | 95 | 33 | 23 | 32 | 34 | 23 | 54 |
| Ca (mg/L) | 103 | 31 | 23 | 32 | 43 | 23 | 68 |
| Mg (mg/L) | 65 | 22 | 16 | 23 | 24 | 16 | 32 |
| Na (mg/L) | 47 | 1.9 | 1.3 | 1.6 | 1.4 | 1.5 | 23 |
| K (mg/L) | 2.2 | <1 | <1 | 1.2 | <1 | <1 | 1.9 |
| Cl (mg/L) | 46 | <5 | <5 | <5 | <5 | <5 | 29 |
| SO ₄ (mg/L) | 304 | <5 | <5 | <5 | 7.8 | <5 | 127 |
| HCO ₃ (mg/L) | 206 | 238 | 160 | 190 | 240 | 158 | 194 |
| NO ₃ (mg N/L) | 9.1 | 0.3 | 0.3 | 7.4 | 5.6 | 0.4 | 3.9 |
| Si (mg/L) | 6.2 | 5.8 | 5.2 | 54.8 | 4.9 | 5.0 | 5.7 |
| Fe (mg/L) | 0.04 | <0.02 | <0.02 | <0.02 | 0.022 | <0.02 | 0.049 |
| Mn (mg/L) | <0.005 | <0.005 | <0.005 | 0.006 | <0.005 | <0.005 | 0.16 |
| Hg (mg/L) | <0.001 | | n.a. | n.a. | n.a. | n.a. | n.a. |
| SI _C | -0.25 | -0.15 | -1.02 | -0.42 | -0.11 | -0.42 | -0.46 |
| SI _D | -0.44 | -0.17 | -1.92 | -0.72 | -0.21 | -0.74 | -0.98 |
| EB (%) | 6.1 | -7.6 | -4.0 | 3.3 | -0.8 | -3.5 | 2.7 |

^aAll dates are dd/mm/2014

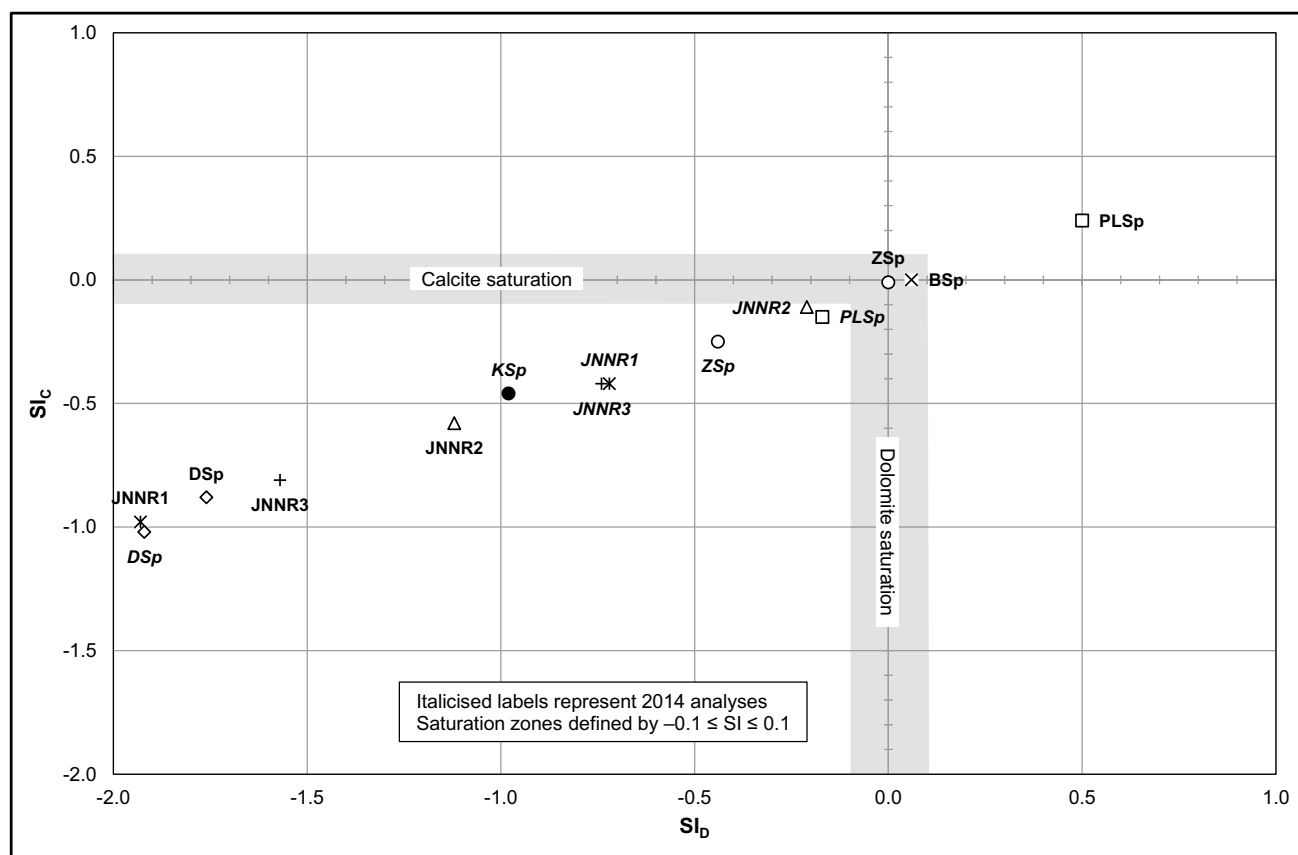


Fig. 21 Saturation state of springwaters with respect to calcite (SI_C) and dolomite (SI_D) ca. 2010 and ca. 2014 (data from Tables 5 and 6)

excursion of the SI_C and SI_D values from equilibrium to slightly undersaturated conditions (text box in Fig. 22) in 2012 and 2014.

The anomalies evident in the record are associated with two flood events (on 31/01/2014 and 03/02/2014, respectively), on which occasions the spring was completely submerged under fresher surface floodwater to a depth approaching 2 m. These are quite common occurrences given the location of the spring next to the Bloubank Spruit (Plate 1 in Chapter “Physical Hydrogeology”), and undoubtedly reflect the circumstances that prevailed during the 16/12/2010 flood event discussed in Sect. 5.1 in Chapter “Chemical Hydrology”. If nothing else, then the digital record captures and reflects the rapid recovery to ‘normal’ conditions following such flood events.

A slightly longer-term picture of the SEC trend of the Zwartkrans Spring water is shown in Fig. 24. Based on field measurements dating back to mid-2010, the gradually increasing trend supports the observation provided by Fig. 23. The rate of increase of 0.9 mS/m per month of the longer Fig. 24 record, is similar to the 0.8 mS/m per month of the much shorter rising limb segments of Fig. 23 record.

7.2 Danielsrust Spring

Together with that of the Nash Spring (JNNR3), the inorganic quality of the water delivered by this spring (DSp) is the best of any karst groundwater sourced by this study. The spring drains the Danielsrust Basin (Sect. 2.3 in Chapter “Physical Hydrogeology”). The water composition (Fig. 25) is virtually identical to that of the Nash Spring (JNNR3) (Fig. 18). The isotope hydrochemistry of the water (see comparison hereunder) similarly reflects a ca. 2010 composition that differs only marginally from an earlier analysis. The observed difference of +0.38‰ in $\delta^{18}O$ (ignoring possible analytical error margins) reflects a shift toward a marginally heavier isotopic composition. This suggests either a slightly greater evaporative component in this groundwater or a greater component of rainwater. Although the wetter than average past two summer rainfall seasons favor the rainfall influence, a possible anthropogenic influence from immediate upstream land-use practices in the form of a commercial tourist lodge facility (Sect. 2.3 in Chapter “Physical Hydrogeology”) cannot be ruled out. The SI_C and SI_D values (text box in Fig. 25) indicate

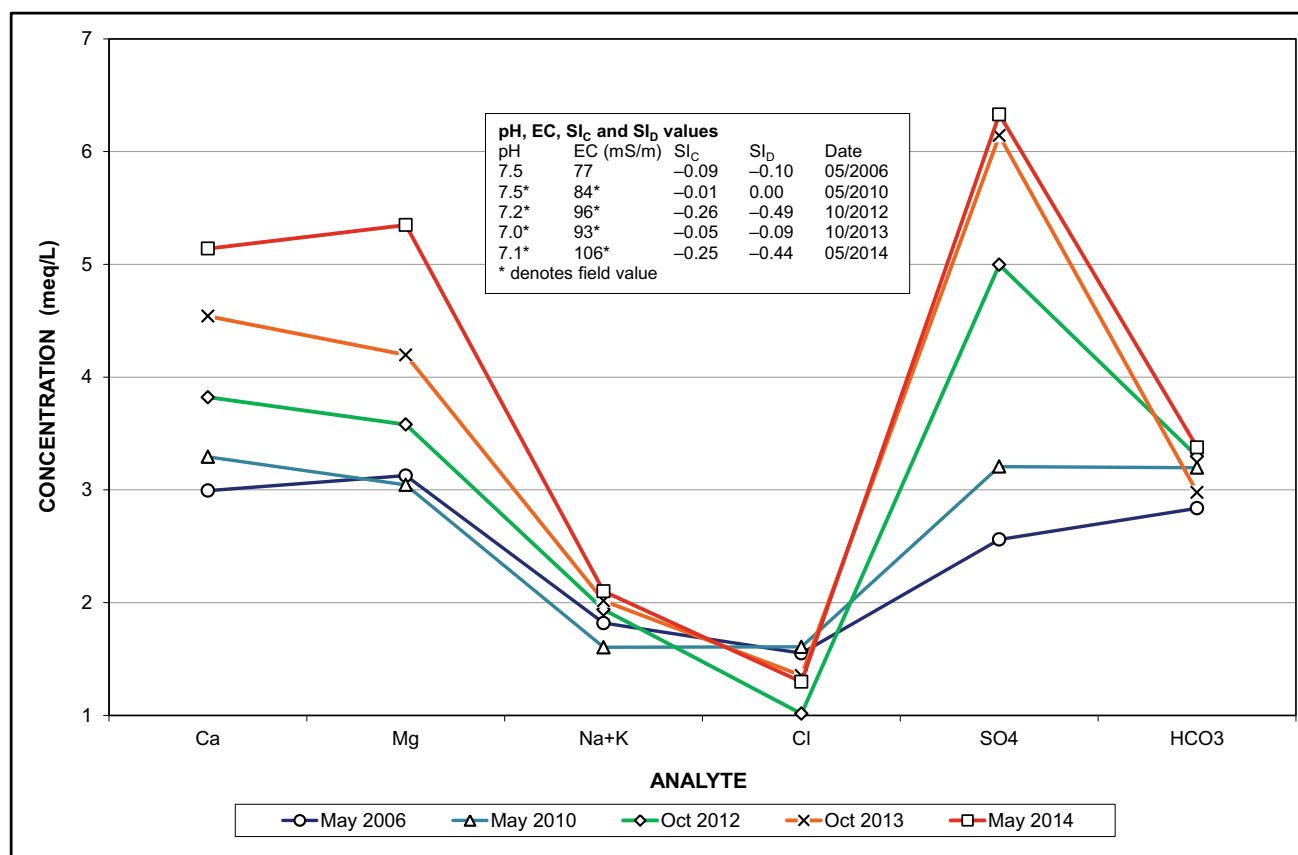


Fig. 22 Graphic comparison of Zwartkrans Spring water chemistry since 2006

undersaturation of the water with respect to calcite and dolomite, respectively, indicating the continued dissolution of these minerals in the Danielsrust Basin.

| Date | $\delta^2\text{H}$ (‰) | $\delta^{18}\text{O}$ (‰) | ^3H |
|------------------------|------------------------|---------------------------|----------------------|
| ca. 2006 ¹¹ | -28.4 | -5.19 | 1.2 ¹² TU |
| 10/02/2010 | -28.9 | -4.81 | 1.3 ± 0.2 TU |

7.3 Plover's Lake Springs

Figure 26 shows that the chemical composition of the springwater has changed very little since May 2006. The chemical composition also shows a close resemblance (virtually superimposed in Fig. 18) to that produced by the Tweefontein (JNNR1) and Nouklip (JNNR2) springs. All of these springs are representative of natural dolomitic groundwater with its typical CaMg-HCO_3 composition.

The Plover's Lake springs (PLSp) drain the Kromdraai Subcompartment of the Krombank Basin (Sect. 2.2 in Chapter "Physical Hydrogeology"). The stable isotope values of this springwater (compared hereunder) show very little difference between the two more recent sampling dates, but a significant difference compared to the earliest date. The heavier isotopic values of the two later analyses suggest that a greater component of comparatively recent recharge is manifested in these samples compared to the earlier sample. The SI_c and SI_D values (text box in Fig. 26) indicate near-equilibrium of the water with respect to calcite and dolomite, respectively.

| Date | $\delta^2\text{H}$ (‰) | $\delta^{18}\text{O}$ (‰) | ^3H |
|------------------------|------------------------|---------------------------|----------------------|
| ca. 2006 ¹³ | -30.3 | -5.62 | 0.7 ¹⁴ TU |
| 17/07/2009 | -28.9 | -5.01 | 1.6 ± 0.3 TU |
| 13/05/2010 | -28.5 | -5.00 | 1.4 ± 0.3 TU |

¹¹ Data from Holland (2007); no exact date of sampling readily discernible from source.

¹² Data from Holland (2007); no error margin reported.

¹³ See Footnote 11.

¹⁴ See Footnote 12.

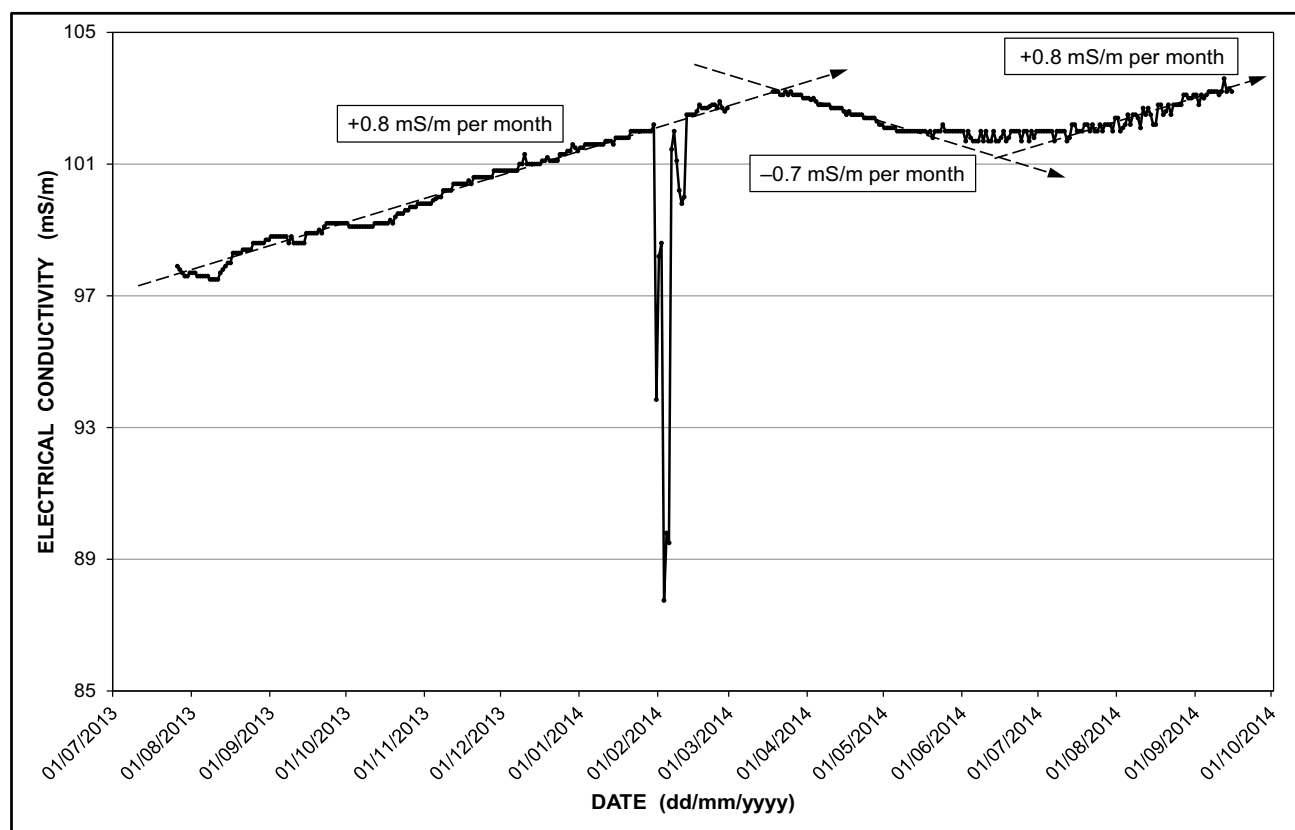


Fig. 23 Pattern and trend of Zwartkrans Spring water salinity since mid-2013

7.4 Kromdraai Spring

The location of this source complicates the collection of a representative sample. In situ measurements carried out from the riverbank at the locus of discharge gave an SEC value of 56 mS/m, a pH value of 7.2, and a temperature of 19.4 °C on 13/08/2010. These values are compared with those of river water upstream and downstream of the spring in Table 14 in Chapter “Physical Hydrogeology”. A water sample collected on 20/08/2014 returned the more definitive chemical composition reflected in Fig. 27. The Schoeller graph indicates a distinctive Ca–HCO₃ composition which is at variance with a typical pristine dolomitic water composition in regard to the following:

- the slight imbalance in the Ca:Mg ratio with a value of ~1.3 compared to the ~1 of pristine dolomitic groundwater; and
- the significantly elevated SO₄ level and elevated Na and Cl levels, all of which are minor constituents in pristine dolomitic groundwater.

It is evident that the Kromdraai Spring catchment receives water of a compromised quality. The SO₄:TDS ratio of ~27% points to mine water as the most likely source. The

circumstances sketched in Fig. 28 provide a conceptual model of the pathway taken by this contamination. Representing allogenic recharge of the Kromdraai Subcompartment, these circumstances also explain the anomalously high recharge rate of ~30% of MAP (Table 80) attributed to this karst basin. The import of these circumstances for the elucidation of water budget calculations is explored in Sect. 2.12 in Chapter “Physical Hydrogeology”. Nevertheless, SI_C and SI_D values of –0.46 and –0.98 (Fig. 27) associated with this water indicate undersaturation in regard to calcite and dolomite, respectively.

7.5 Tweefontein Spring

This spring (JNNR1) drains the Tweefontein Basin (Sect. 2.5 in Chapter “Physical Hydrogeology”). Its water chemistry is virtually identical in inorganic composition to that of the Nouklip Spring (JNNR2) (Fig. 18), and very similar to that produced by the Plover’s Lake springs. The chemical composition of the springwater has remained largely unchanged since May 2006 (Fig. 29). The stable isotope composition of this water, as sampled on various dates reported hereunder, reflects a shift from a lighter to a heavier δ²H and δ¹⁸O isotopic ratio. The shift in ³H values supports

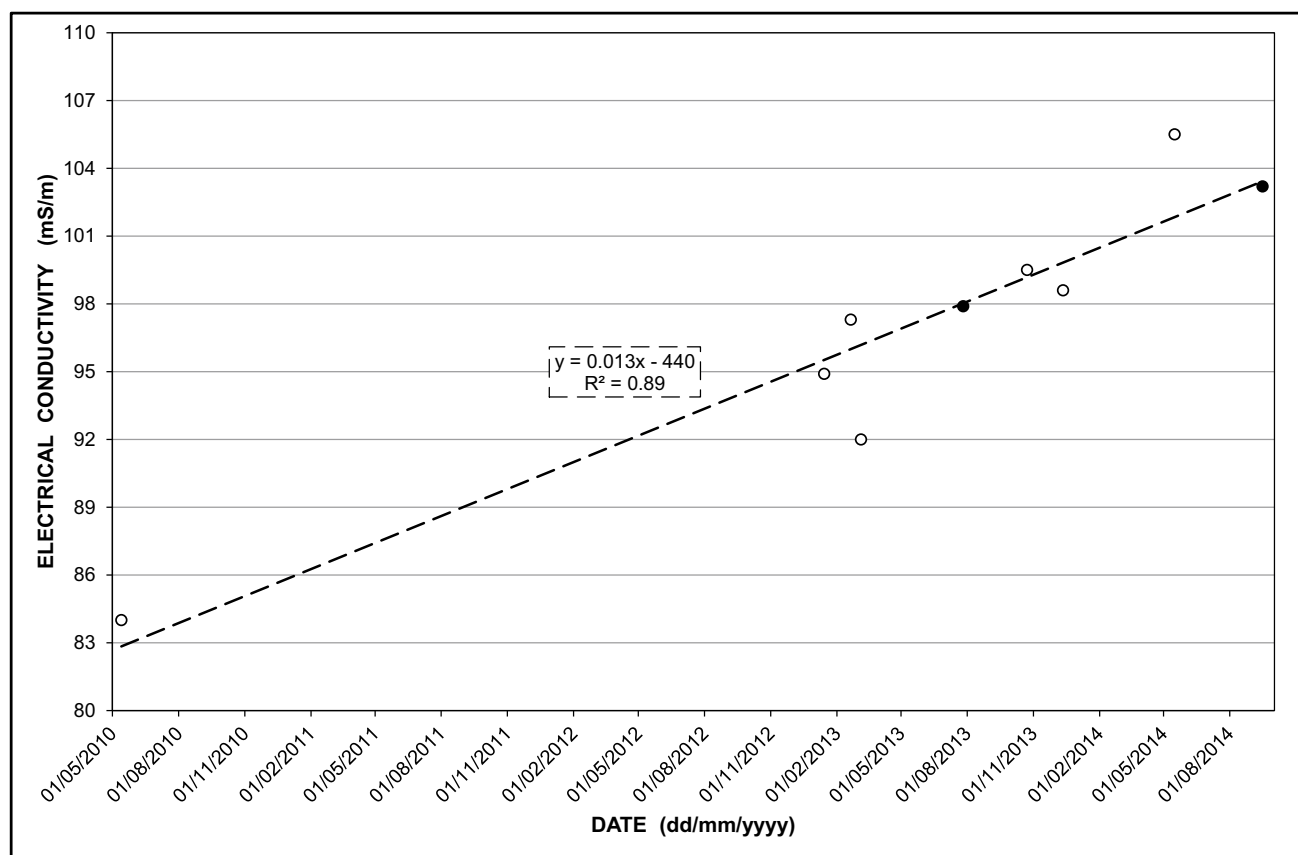


Fig. 24 Pattern and trend of Zwartkrans Spring water electrical conductivity since mid-2010; the solid symbols mark the start and end values of Fig. 23 data record

an interpretation that attributes this to a greater proportion of younger rainwater recharge in the 2010 spring discharge. The SI_C and SI_D values of (text box in Fig. 29) indicate undersaturation of the water with respect to calcite and dolomite, respectively.

| Date | δ^2H (‰) | $\delta^{18}O$ (‰) | 3H |
|------------------------|-----------------|--------------------|----------------------|
| ca. 2006 ¹⁵ | -29.2 | -5.52 | 2.1 ¹⁶ TU |
| ca. 2009 ¹⁷ | -29.0 | -5.17 | 2.9 ± 0.3 TU |
| 19/05/2010 | -27.7 | -4.90 | 3.1 ± 0.3 TU |

7.6 Aquamine Spring

The chemistry of the Aquamine Spring (AqSp) water, although also reflecting a $Ca-HCO_3$ character, is clearly different from that of the karst groundwater. It is postulated

that the upper reaches of the spring catchment comprise the dolomitic strata of the Rietfontein Basin (Sect. 2.6 in Chapter “Physical Hydrogeology”). The difference in chemistry is also evident in the detectable trace metal concentrations in this water (Table 5), compared to the generally undetectable levels in many respects in a number of the other springwaters. A further difference is the elevated 3H level in the Aquamine Spring water (Table 5) compared to that of some of the karst springwaters. This indicates the comparatively ‘young’ age, possibly coupled with a shallow circulation pattern, associated with this groundwater system. The SI_C and SI_D values of -0.26 and -0.50 (Table 5) indicate undersaturation of the water with respect to calcite and dolomite, respectively.

7.7 Nouklip Spring

This water is of excellent quality in respect of all the elements included in the analytical suite. The Nouklip Spring (JNNR2) drains the Diepkloof Basin (Sect. 2.7 in Chapter “Physical Hydrogeology”) and, as shown in Fig. 30, produces water that is virtually identical in composition to

¹⁵ See Footnote 11.

¹⁶ See Footnote 12.

¹⁷ Data from T. Abiye (personal communication).

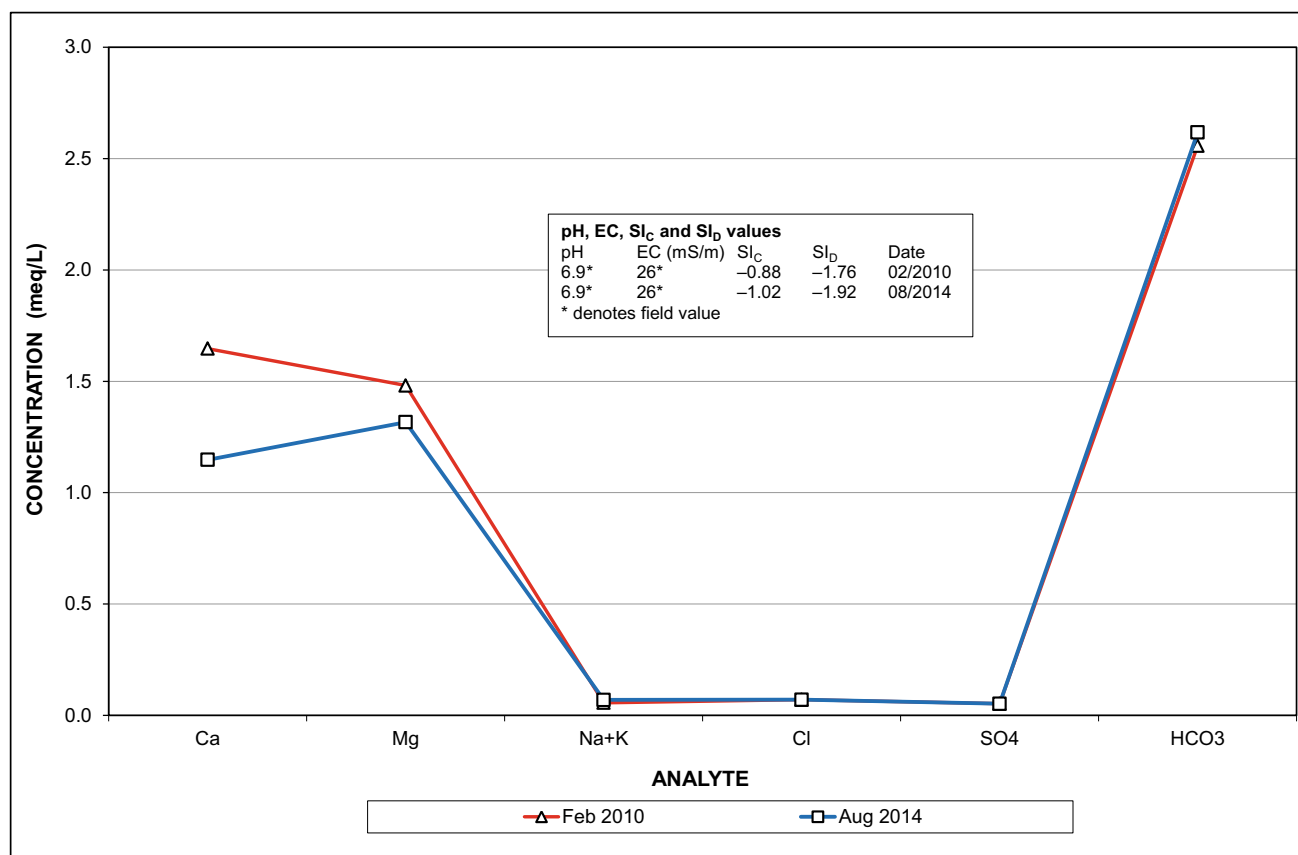


Fig. 25 Graphic comparison of Danielsrust Spring water chemistry between 2010 and 2014

that produced by the Tweefontein Spring (Fig. 18). It is, therefore, reasonable to presume that the May 2006 composition of the Tweefontein Spring water (Fig. 29) also reflects that of the Nouklip Spring at the time. The similarity, however, is not reflected in the isotope results as shown hereunder. These results, and in particular the ^3H values, indicate a large proportion of substantially older groundwater in the discharge of the Nouklip Spring compared to the Tweefontein Spring. The SI_C and SI_D values (text box in Fig. 30) indicate undersaturation of the water with respect to calcite and dolomite, respectively.

| Date | $\delta^2\text{H}$ (‰) | $\delta^{18}\text{O}$ (‰) | ^3H |
|------------------------|------------------------|---------------------------|----------------------|
| ca. 2006 ¹⁸ | -32.1 | -5.78 | 0.6 ¹⁹ TU |
| ca. 2009 ²⁰ | -31.0 | -5.42 | 0.6 ± 0.2 TU |

A notable aspect associated with the Nouklip Spring is the formation of tufa deposits in the lower reach of the Grootvlei Spruit near its confluence with the Skeerpoort

River. The deposits have formed in three environments identified (after Ford and Pedley 1996) as follows:

- a massive hummock type deposit in the high energy (turbulent) environment on the downstream side of a gauging weir where degassing of mainly CO_2 occurs (Plate 4);
- as arcuate terraces (barrages) spanning the 5–8 m wide stream channel further downstream of the gauging weir (Plate 5); and
- as a waterfall deposit where the stream cascades ~4 m into the Skeerpoort River (Plate 6).

7.8 Nash Spring

The quality of the typically CaMg-HCO_3 karst groundwater produced by this spring (JNNR3) reflects a pristine condition. This is unlikely to deteriorate for as long as the largely ‘wilderness’ character of the Uitkomst Basin (Sect. 2.4 in Chapter “Physical Hydrogeology”) is maintained. The isotope results presented hereunder reflect similar circumstances to those associated with the Nouklip Spring

¹⁸ See Footnote 11.

¹⁹ See Footnote 12.

²⁰ See Footnote 17.

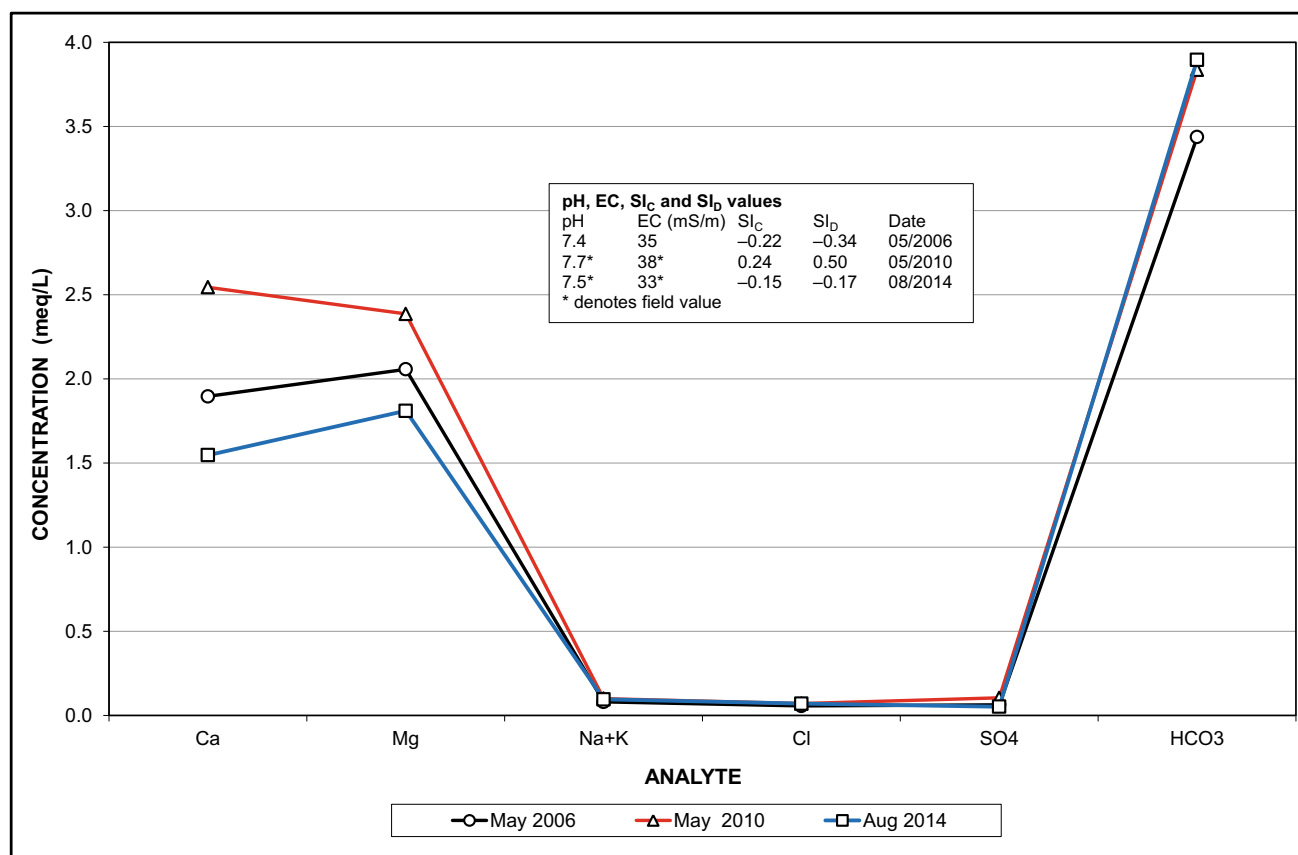


Fig. 26 Graphic comparison of Plover's Lake springs water chemistry between 2006 and 2014

(Sect. 7.7). The SI_c and SI_b values (text box in Fig. 31) indicate undersaturation of the water with respect to calcite and dolomite, respectively.

| Date | δ ² H (‰) | δ ¹⁸ O (‰) | ³ H |
|------------------------|----------------------|-----------------------|----------------|
| ca. 2009 ²¹ | -32.4 | -5.64 | 0.2 ± 0.2 TU |
| 19/05/2010 | -30.6 | -5.22 | 0.1 ± 0.2 TU |

The inorganic chemical composition reflected in Fig. 31 is virtually identical to that of the Danielsrust Spring water (Fig. 18) is not, however, matched by the respective ³H values (Table 5). These reveal a distinct difference in the relative age of the two springwaters. The smaller ³H concentration of the Nash Spring water suggests a comparatively older water that accords with a larger and almost certainly much deeper groundwater circulation pattern in the Uitkomst Basin compared to that of the Danielsrust Basin.

7.9 Uitkomst Spring

The Uitkomst Spring (JNNR4) water chemistry reflects an extremely fresh character with a field SEC of 1 mS/m. Together with the Mg–HCO₃ composition of this water, these characteristics help to distinguish groundwater draining the Pretoria Group sedimentary strata from that draining the Malmani Subgroup carbonate strata (Fig. 19). A further distinguishing hydrochemical characteristic of this groundwater is the elevated Fe and Mn concentrations (Table 5). The SI_c and SI_b values of -3.09 and -5.43 (Table 5) indicate significant undersaturation of the water with respect to calcite and dolomite, respectively. This is expected of groundwater draining from non-carbonate strata.

7.10 Cradle Spring

The Cradle Spring (CSp) drains the Motsetse Basin (Sect. 2.8 in Chapter “Physical Hydrogeology”). Its chemistry is characterized by the field variable values listed hereunder. The SEC value of 64 mS/m is indicative of a slightly impacted karst groundwater chemistry.

²¹ See Footnote 17.

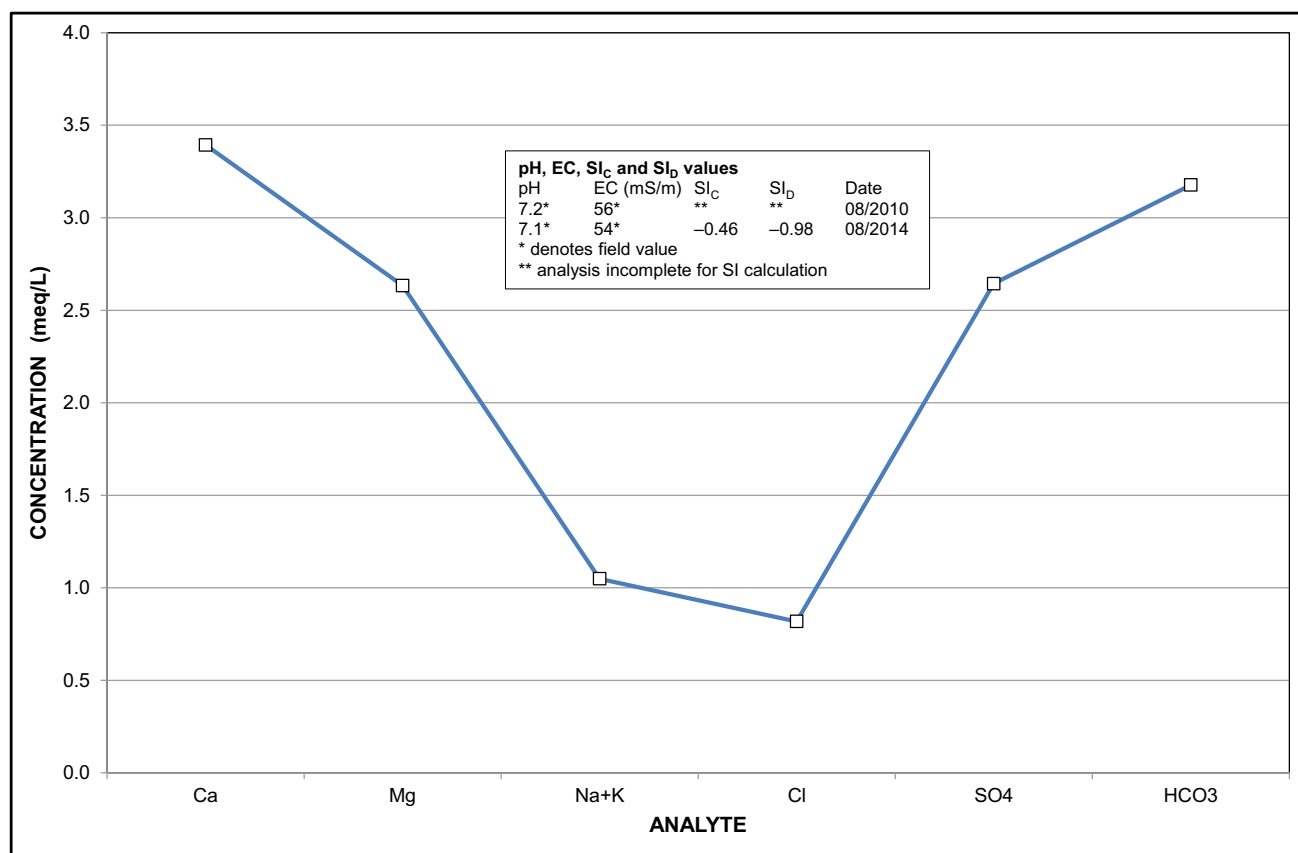


Fig. 27 Graphic of Kromdraai Spring water chemistry in 2014

| Date | pH | SEC | ORP | Temperature |
|------------|-----|---------|--------|-------------|
| 21/12/2010 | 7.7 | 64 mS/m | -35 mV | 21.0 °C |

| Date | pH | SEC | ORP | Temperature |
|------------|-----|---------|-------|-------------|
| 27/11/2014 | 7.3 | 40 mS/m | -6 mV | 20.0 °C |

7.11 Barlow Spring

The chemistry of the Barlow Spring (BaSp) water is characterized by the field values listed hereunder. Notably, the pH value is lower than that of the nearby Anderson Spring (Sect. 7.12).

| Date | pH | SEC | ORP | Temperature |
|------------|-----|---------|--------|-------------|
| 27/11/2014 | 7.0 | 42 mS/m | -16 mV | 20.4 °C |

7.12 Anderson Spring

The Anderson Spring (AnSp) water chemistry reflects a typical CaMg-HCO₃ composition.

7.13 Lesedi Spring

The chemistry of the Lesedi Spring (LeSp) water reflects a significantly higher SEC of 66 mS/m compared to that of the Anderson Spring measured on the same day. These springs are provisionally recognized as draining the same compartment. The more complete analysis of the LeSp springwater reveals further differences in significantly higher Ca, SO₄, and HCO₃ concentrations and a MgCa-HCO₃ composition.

| Date | pH | SEC | ORP | Temperature |
|------------|-----|---------|--------|-------------|
| 27/11/2014 | 6.9 | 66 mS/m | -13 mV | 19.7 °C |

The Lesedi property has 70 permanent residents who serve the cultural visitor center, restaurant, and overnight accommodation facilities. All of these are served by an

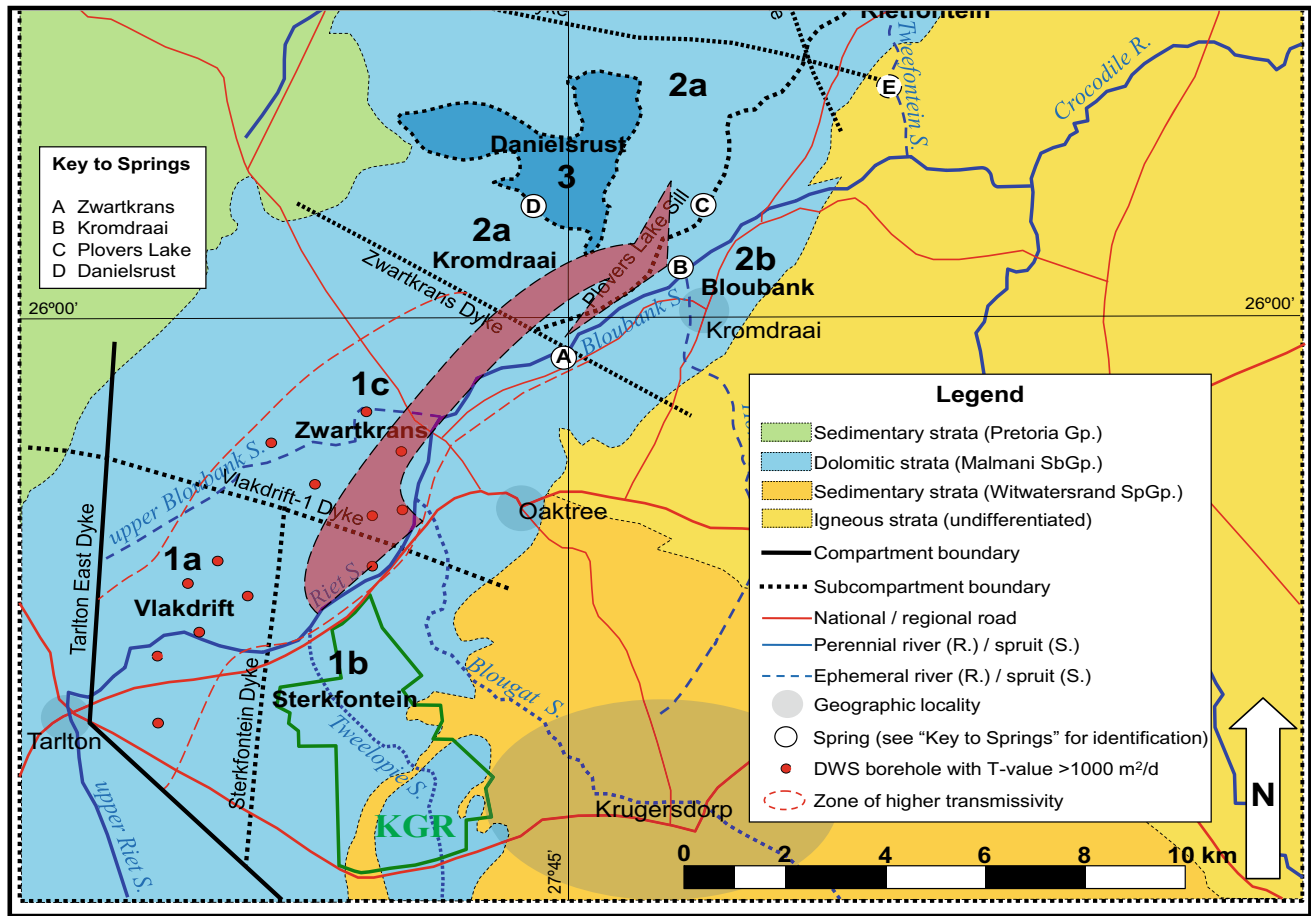


Fig. 28 Schematic illustration of the hypothetical flow path (arrowed) taken by groundwater bearing a mine water impact into the Kromdraai Subcompartment toward the Kromdraai Spring

on-site sanitation system comprising a septic tank/French drain located?

7.14 Broederstroom Spring

The Broederstroom Spring (BSp) water chemistry is characterized by the following field variable values.

| Date | pH | SEC | ORP | Temperature |
|------------|-----|---------|--------|-------------|
| 21/12/2010 | 7.3 | 49 mS/m | -13 mV | 22.8 °C |

Holland (2007) reports the following values for the listed isotope analytes. The tritium value of 5.2 TU is the highest of any springwater in the COH for which a ³H value is known. It indicates a relatively young groundwater that is probably associated with a shallow groundwater system. This observation finds support in the higher than normal ambient springwater temperature of ~23 °C as indicated above. The SI_C and SI_D values of 0.00 and 0.06 (Table 5)

indicate equilibrium conditions in regard to calcite and dolomite, respectively.

| Date | δ ² H | δ ¹⁸ O | ³ H |
|------------------------|------------------|-------------------|----------------|
| ca. 2006 ²² | -29.2‰ | -5.37‰ | 5.2 TU |

7.15 Krugersdorp Game Reserve Springs

A description of the springs enumerated in the KGR is given in Sect. 4.15 in Chapter “Physical Hydrogeology” and Table 15 in Chapter “Physical Hydrogeology” (see Fig. 5 for locations). Some of these springs are important for the reason that they reflect the chemistry of groundwater in the receiving groundwater environment located immediately downstream of the mine area. This was recognized as early as mid-2003 when the DWS commenced water quality

²² See Footnote 11.

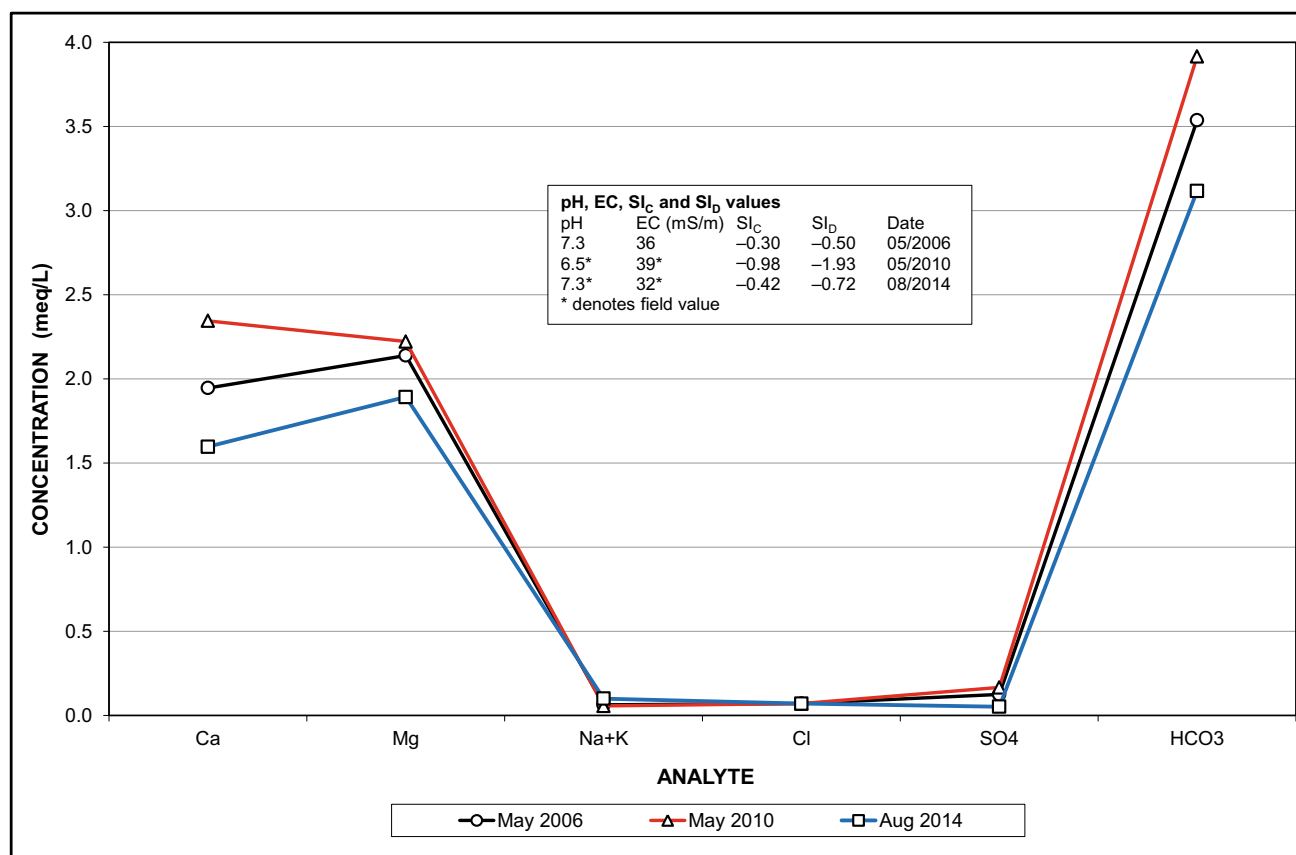


Fig. 29 Graphic comparison of Tweefontein Spring water chemistry between 2006 and 2014

monitoring at these sources. The results of field variable measurements are reported in Table 7.

It is evident that elevated SEC values distinguish the springs SP1, SP2, CSIR30, CSIR63, and AvSp that deliver a compromised groundwater quality indicative of an impacted resource, from the springs LSp, SP3, and BuSp that drain an unimpacted resource. The groundwater produced by the spring sources SP1 and SP2 is subject to routine chemical analysis by various parties. The last DWS directive issued to RU also includes the spring SP3 in this program. The results of the SG monitoring summarized in Table 8, are reflected in Fig. 32. This shows the median inorganic chemical composition of the groundwater produced by these sources in the 8-year period to September 2014.

A similar but more muted impact to that observed in regard to SP2 is reflected in the Ca–SO₄ composition of the SP1 springwater (Fig. 32). This, together with the median pH of 6.5 and comparatively low median total alkalinity of 34 mg CaCO₃/L (Table 8), is evidence of a mine water impact. Spring source SP3, on the other hand, produces typically fresh CaMg–HCO₃ karst groundwater draining from the area of smallholdings located to the west. The excellent quality of this water indicates that extensive modification of the natural landscape mainly by

agricultural land-use practices has not yet manifested a discernible impact on the ambient karst groundwater resource. It should be noted, however, that nitrate as an indicator analyte of agricultural impact has only been incorporated in the analytical suite since December 2012. The median value of 2.6 mg N/L for source SP3 is bracketed by those of the sources SP1 and SP2 (text box in Fig. 32). The SI_c and SI_b values for the springwaters (Table 8) reflect their typically undersaturated calcite and dolomite states, raising concern for the structural stability of the carbonate strata in the karst outlier, especially in the case of spring SP2.

The SEC and SO₄ trends associated with the water produced by the three monitored springs in the KGR are shown in Figs. 33 and 34, respectively. Whereas spring source SP1 shows a hardly discernible trend in these analytes, the source SP2 reflects an apparent rising trend until early-2011, followed by a falling trend until mid-2013 before again showing an increase at the end of the record. The SO₄ trend is more clearly evident than that of SEC.

The SEC and SO₄ trends are not readily explained because of the variability exhibited, with the SEC values bracketing an interval of ~100–450 mS/m (Fig. 33), and the SO₄ values an interval of 500–3200 mg/L (Fig. 34). The

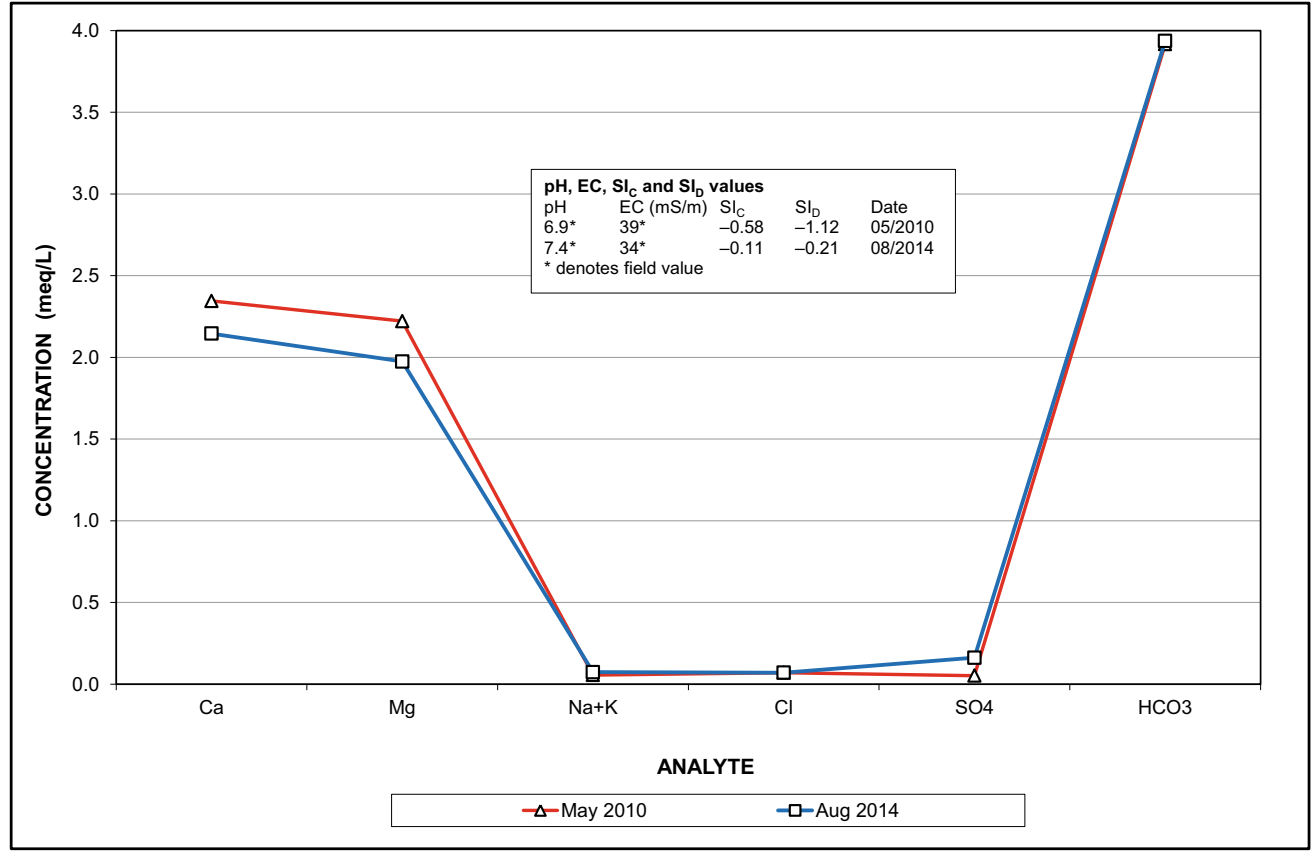


Fig. 30 Graphic comparison of Nouklip Spring water chemistry in 2010 and 2014

Plate 4 Massive hummock tufa deposit (under cascading water) on the downstream side of gauging weir A2H033 ~ 525 m downstream of the spring



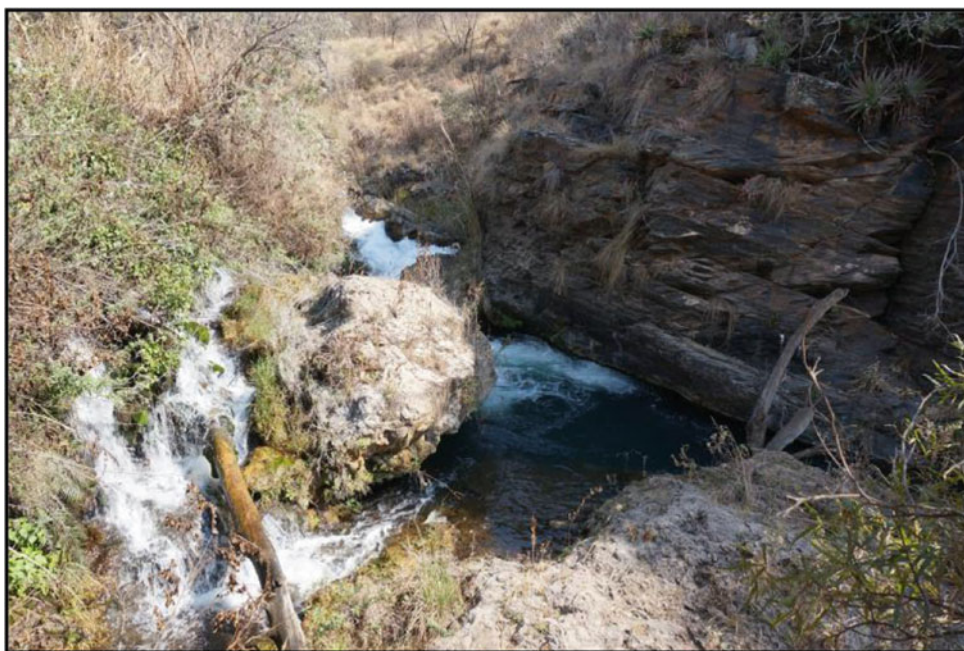
inclusion in Fig. 34 of the contemporary SO₄ values observed for the Hippo Dam explores the possibility of a correlation with the SP2 sulfate trend. The 3rd order

polynomial trendlines suggest that a correlation does exist. The excellent correlation of pH values in Fig. 35 dispels any doubts in this regard.

Plate 5 Uppermost tufa terrace (barrage) extending across the channel of the Grootvlei Spruit ~600 m downstream of the spring



Plate 6 Waterfall tufa deposit at left of picture where the Grootvlei Spruit cascades ~4 m into the Skeerpoort River gorge ~650 m downstream of the spring



It is evident from Fig. 35 that the pH of SP2 springwater exhibits a sharp drop from 6.5 in January 2010 to 3.3 in February 2010, after which a consistently declining trend to a value of ~3.0 in mid-2012 is demonstrated. The pH drop coincides with the substantial increase in raw mine water discharge from the mine area (Sect. 3.1 in Chapter “Physical Hydrology”). Similarly, the equally rapid increase to values >6 in the period mid-2012 to early-2014 coincides with the

commissioning of the immediate mine water control, management and treatment measures in June 2012 (Text Box 1 in Chapter “Physical Hydrology”). The subsequent period of lower pH values ending in mid-2014 again reflects the uncontrolled discharge of raw mine water from the mine area.

The hydrochemical character of the springwaters is compared with pristine karst groundwater in Fig. 36.

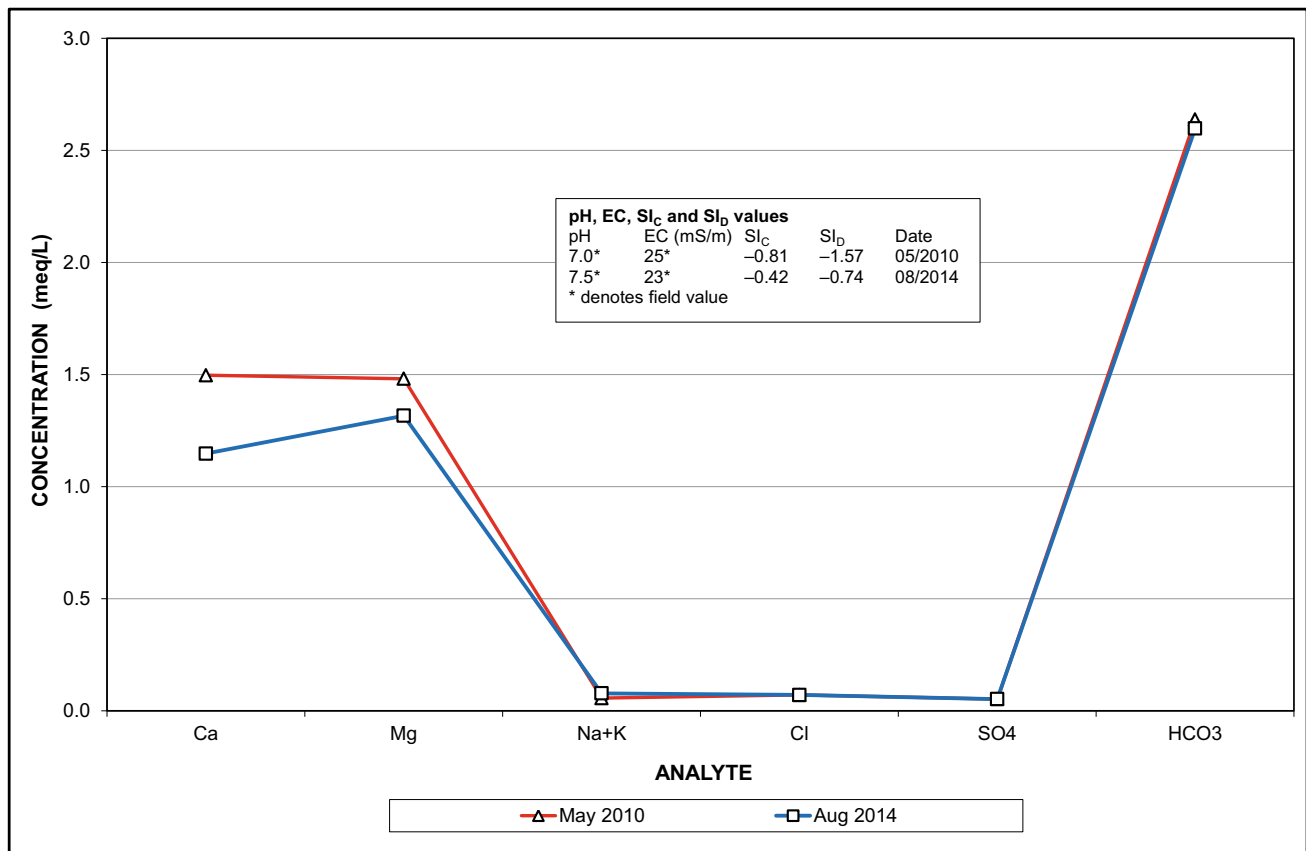


Fig. 31 Graphic comparison of Nash Spring water chemistry in 2010 and 2014

8 Selected Impacts

8.1 Agriculture

The impact of agriculture on the quality of groundwater resources is assessed on the basis of analytical results for pesticide residues in water. Groundwater samples collected from two boreholes (CSIR8 and CFM1) in the Oaktree area were subjected to multi-residue pesticide analysis by the South African Bureau of Standards (SABS) Chromatographic Services. The sources were selected for their position in proximity to and downgradient of intensive agricultural activity including the tunnel farming of flowers for export (Fig. 37). These show that no residues were detected in either of the samples. Similarly, Groenewald (2010b) reports that no knowledge of pesticide contamination is currently available. Although these circumstances suggest that no impact is present, future groundwater quality studies will further inform this aspect.

8.2 Historical Mining

The COH and surrounding area is witness to numerous forms of mining activity at various scales. These vary from

artisanal gold mine workings represented by stopes in the Black Reef Formation such as are seen in the KGR, to opencast workings for limestone, for example, the Aviary Quarry in the KGR, and dolomite, e.g., the large Sterkfontein Quarry at Bolt's Farm near Oaktree. The (often destructive) exploitation of numerous caves (including Sterkfontein) in the study area for limestone at the end of the nineteenth and beginning of the twentieth centuries is also well documented (e.g., McCarthy and Rubidge 2005).

The COH hosts the earliest proclaimed gold mine on the Witwatersrand. The Kromdraai Gold Mine is located on Ptn 43 (Ibis Ridge Farm) of the farm Kromdraai 520JQ commenced operations in 1881 and closed down in 1914 (G. Whatley, personal communication). In an article titled 'The Kromdraai Gold Field', The Star newspaper of 07 October 1893 reports on a substantial quantity of water encountered in the mine workings. As was common to many of the early Witwatersrand gold mines, the Kromdraai Gold Mine exploited gold-bearing horizons in the Black Reef Formation located at the base of the Malmani Subgroup dolomite succession. Only one of the original three adits to the Kromdraai Gold Mine still allows risk-free access to the underground workings, which comprise at least three levels linked by winzes. The water level in the mine fluctuates in the interval defined by the 3rd (deepest known) and the 2nd

Table 7 Field chemical variable values of springwater in the KGR

| Spring ^a | Date (dd/mm/yyyy) | SEC (mS/m) | pH (−log ₁₀ z _{H+}) | Eh (mV) | Temp (° C) | Source aquifer |
|-------------------------------|----------------------|--------------------------------------|---|------------|---------------|-------------------------|
| SP1/Spring 1/F6S7 | 24/11/2010 | 79.4 | 6.1 | 48.4 | 18.2 | Main karst outlier |
| | 14/08/2012 | 101.6 | 6.0 | 37.2 | 17.9 | |
| | 15/10/2013 | 96.0 | 6.0 | 23.4 | 18.3 | |
| CSIR30/Spring 2 | 24/11/2010 | 90.2 | 6.0 | 55.0 | 17.9 | Main karst outlier |
| | 14/08/2012 | 108.8 | 5.9 | 42.3 | 17.9 | |
| | 15/10/2013 | 101.5 | 6.0 | 23.1 | 17.8 | |
| CSIR63/Spring 3 | 24/11/2010 | 101.2 | 5.9 | 58.3 | 17.7 | Main karst outlier |
| | 14/08/2012 | 115.4 | 5.9 | 38.3 | 17.8 | |
| | 15/10/2013 | 113.7 | 5.9 | 26.8 | 17.5 | |
| SP2/CSIR37/Poplar Sp./F8S9 | 24/11/2010 | 90.9 | 5.4 | 85.2 | 17.6 | Main karst outlier |
| | 14/08/2012 | Spring inundated by Tweelopie Spruit | | | | |
| Lodge Sp. (LoSp) | 24/11/2010 | 12.6 | 5.3 | 92.2 | 19.2 | Wits quartzite |
| | 14/08/2012 | 21.1 | 5.3 | 77.0 | 19.1 | |
| | 15/10/2013 | 19.3 | 5.3 | 60.5 | 19.0 | |
| Aviary Sp. (AvSp) | 24/11/2010 | 201 | 7.3 | −16.5 | 17.2 | Zwartkrans Basin |
| | 14/08/2012 | 236 | 7.3 | −36.0 | 16.5 | |
| | 15/10/2013 | 209 | 7.1 | −42.9 | 16.6 | |
| SP3/Flip-se-Gat | 24/11/2010 | 21.5 | 8.2 | −61.3 | 19.1 | Zwartkrans Basin |
| | 14/08/2012 | 25.6 | 8.2 | −84.3 | 16.6 | |
| | 15/10/2013 | 23.6 | 8.0 | −84.0 | 18.3 | |
| Buffalo Sp. (BuSp) | 15/10/2013 | 7.7 | 5.7 | 37.8 | 18.3 | Toe of karst outlier |

^aCross-reference Table 15 in Chapter “Physical Hydrogeology”

Levels and reached a maximum elevation just above the 2nd Level (G. Whatley, personal communication) in the year 2000, notably an extremely wet year.

The current water level occupies an elevation of ~1420 m amsl, as inferred from the depth to groundwater rest level of ~12 m below surface measured in a water supply borehole (geosite KGM1) on the property in May 2010. The quality of the groundwater produced by this borehole (SEC = 18 mS/m, pH = 5.6) does not reflect an acidic mine water signature. The low SEC and pH values are characteristic of groundwater associated with quartzitic strata of the Witwatersrand Supergroup (Sect. 2.1.1). The absence of an acidic mine water signature is supported by ‘in-mine water’ EC, pH, and temperature measurements that reveal even lower SEC values (in the range 10–13 mS/m) but slightly higher pH values (in the range 6.1–6.4), at two localities within the partially flooded mine workings.

The differences with the borehole KGM1 groundwater might be attributed to the depth from which the latter is drawn; the pump has installed a depth of ~55 m below surface (G. Whatley, personal communication). This would indicate that the borehole penetrates some distance into the

underlying Witwatersrand Supergroup quartzites, which host a naturally acidic groundwater.

Figure 38 provides a comparison of the mine water and groundwater in the vicinity of the mine with that of surface water in the nearby Honingklip Spruit. Despite the ostensible similarity of Mg–HCO₃ chemical composition reflected in the graphs, a distinctive grouping of ‘mine’ water (samples KGM1 and KGM-MW) on the one hand, and groundwater (OB1) and surface water (HS1) on the other, is also apparent. Nevertheless, the absence of acid mine water development in the mine workings as well as the absence of visible decant after more than a century of ‘flooding’ is notable.

The groundwater elevation of ~1420 m amsl is slightly lower than the streambed elevation of the nearby Honingklip Spruit, which is interpolated at ~1423 m amsl. Circumstances, where the water level in the mine workings is partly influenced by discharge in the Honingklip Spruit, can therefore not be discounted. The mine water level would need to rise more than ~3 m above its current level before a reversal of the hydraulic gradient between the mine and the Honingklip Spruit is established.

Although two of the adits that provide access to the mine workings (one risk-free and the other hazardous) occupy a

Table 8 Statistical analysis of groundwater chemistry delivered by springs SP1, SP2, and SP3 in the KGR in the period September 2009–September 2014

| Spring | Chemical analyte | Statistical parameter | | | | | | | SANS (2011a) ^a |
|--------|-------------------------------------|-----------------------|-------------|--------------|--------------|--------------|-------|---------|---------------------------|
| | | <i>n</i> | 5%ile | Mean | Median | 95%ile | SD | CoV (%) | |
| SP1 | pH ^b @ 25 °C | 59 | 6.2 | – | 6.5 | 7.1 | 0.4 | 6 | 5.0–9.7 |
| | SEC (mS/m) | 59 | 91 | 99 | 99 | 106 | 4.9 | 5 | ≤ 170 |
| | TDS (mg/L) | 59 | 744 | 830 | 824 | 1010 | 123 | 15 | ≤ 1200 |
| | Ca (mg/L) | 59 | 58.6 | 109.2 | 113.0 | 143.1 | 25.7 | 24 | n.s. |
| | Mg (mg/L) | 59 | 44.8 | 57.8 | 55.0 | 79.6 | 11.0 | 19 | n.s. |
| | Na (mg/L) | 58 | 22.6 | 29.5 | 28.0 | 37.9 | 10.8 | 37 | ≤ 200 |
| | Cl (mg/L) | 59 | 16.0 | 26.0 | 21.0 | 58.8 | 13.9 | 53 | ≤ 300 |
| | SO ₄ (mg/L) | 59 | 413 | 470 | 469 | 528 | 37.5 | 8 | ≤ 500 |
| | HCO ₃ (mg/L) | 59 | 29.1 | 48.2 | 42.7 | 86.8 | 17.1 | 35 | n.s. |
| | Fe (mg/L) | 57 | 0.002 | 0.425 | 0.050 | 1.740 | 2.029 | 477 | ≤ 2.0 |
| | Mn (mg/L) | 58 | 0.008 | 0.091 | 0.050 | 0.415 | 0.148 | 163 | ≤ 0.5 |
| | Al (mg/L) ^c | 57 | 0.002 | 0.276 | 0.500 | 0.500 | 0.242 | 89 | ≤ 0.3 |
| | U (mg/L) | 50 | 0.003 | 0.106 | 0.003 | 0.017 | 0.721 | 678 | ≤ 0.015 |
| | SI _C | – | –2.24 | –1.50 | –1.55 | 0.56 | – | – | n.s. |
| | SI _D | – | –4.34 | –3.02 | –3.16 | –1.12 | – | – | n.s. |
| | EB (%) | 58 | –8.9 | 0.4 | 0.2 | 10.8 | 6.3 | 1475 | n.s. |
| SP2 | pH ^b @ 25 °C | 58 | 2.9 | – | 3.7 | 7.0 | 1.7 | 37 | 5.0–9.7 |
| | SEC (mS/m) | 58 | 139 | 252 | 260 | 351 | 68.3 | 27 | ≤ 170 |
| | TDS (mg/L) | 58 | 1094 | 2561 | 2500 | 3970 | 832 | 33 | ≤ 1200 |
| | Ca (mg/L) | 58 | 53.0 | 361.0 | 373.0 | 609.1 | 155.6 | 43 | n.s. |
| | Mg (mg/L) | 58 | 50.7 | 105.8 | 100.0 | 151.2 | 45.0 | 43 | n.s. |
| | Na (mg/L) | 58 | 38.4 | 70.2 | 70.0 | 104.9 | 21.0 | 30 | ≤ 200 |
| | Cl (mg/L) | 58 | 22.0 | 46.7 | 36.5 | 78.0 | 47.0 | 101 | ≤ 300 |
| | SO ₄ (mg/L) | 58 | 642 | 1589 | 1560 | 2508 | 543 | 34 | ≤ 500 |
| | HCO ₃ (mg/L) | 58 | 1.2 | 12.1 | 1.2 | 47.3 | 17.5 | 145 | n.s. |
| | Fe (mg/L) | 58 | 0.01 | 28.9 | 1.3 | 109.8 | 58.8 | 203 | ≤ 2.0 |
| | Mn (mg/L) | 58 | 0.99 | 22.2 | 17.0 | 57.2 | 20.4 | 92 | ≤ 0.5 |
| | Al (mg/L) ^c | 57 | 0.001 | 0.333 | 0.500 | 0.616 | 0.313 | 94 | ≤ 0.3 |
| | U (mg/L) | 58 | 0.003 | 0.021 | 0.011 | 0.074 | 0.033 | 157 | ≤ 0.015 |
| | SI _C | – | –5.07 | –4.13 | –4.28 | –0.66 | – | – | n.s. |
| | SI _D | – | –9.90 | –8.54 | –8.87 | –1.67 | – | – | n.s. |
| | EB (%) | 58 | –26.6 | –7.6 | –5.4 | 6.4 | 11.2 | –148 | n.s. |
| SP3 | pH ^b @ 25 °C | 60 | 6.5 | – | 7.8 | 8.2 | 0.5 | 7 | 5.0–9.7 |
| | SEC (mS/m) | 60 | 24.0 | 26.2 | 26.0 | 30.1 | 2.5 | 10 | ≤ 170 |
| | TDS (mg/L) | 60 | 127 | 180 | 162 | 210 | 127 | 70 | ≤ 1200 |
| | Ca (mg/L) | 60 | 19.0 | 26.0 | 24.0 | 35.2 | 10.0 | 39 | n.s. |
| | Mg (mg/L) | 60 | 11.0 | 14.4 | 14.0 | 18.1 | 3.7 | 26 | n.s. |
| | Na (mg/L) | 59 | 1.8 | 6.3 | 4.7 | 14.4 | 7.4 | 118 | ≤ 200 |
| | Cl (mg/L) | 59 | 2.5 | 10.0 | 7.0 | 25.1 | 10.0 | 100 | ≤ 300 |
| | SO ₄ (mg/L) ^d | 60 | 20.0 | 28.2 | 25.0 | 46.0 | 8.4 | 30 | 25.0 |
| | HCO ₃ (mg/L) | 60 | 81 | 95 | 96 | 115 | 14.6 | 15 | n.s. |
| | Fe (mg/L) | 58 | 0.001 | 0.143 | 0.050 | 0.815 | 0.244 | 170 | ≤ 2.0 |
| | Mn (mg/L) | 59 | 0.003 | 0.141 | 0.050 | 0.520 | 0.388 | 274 | ≤ 0.5 |
| | Al (mg/L) ^c | 59 | 0.010 | 0.332 | 0.500 | 0.500 | 0.228 | 69 | ≤ 0.3 |

(continued)

Table 8 (continued)

| Spring | Chemical analyte | Statistical parameter | | | | | | | SANS (2011a) ^a |
|--------|------------------|-----------------------|-------|-------|--------|--------|-----|---------|---------------------------|
| | | <i>n</i> | 5%ile | Mean | Median | 95%ile | SD | CoV (%) | |
| | U (mg/L) | | 0.003 | 0.005 | 0.003 | 0.012 | | 94 | ≤ 0.015 |
| | SI _C | – | –1.78 | –0.32 | –0.35 | 0.25 | – | – | n.s. |
| | SI _D | – | –3.53 | –0.63 | –0.67 | 0.47 | – | – | n.s. |
| | EB (%) | 59 | –8.2 | 6.6 | 6.3 | 17.4 | 9.8 | 150 | n.s. |

^aStandard health-related limit for consumption of 2 L/d over 70 years by a 60 kg person

^bLaboratory value ($-\log_{10}Z_{H+}$)

^cRange includes default values equal to 50% of a 1 mg Al/L detection limit

^dRange includes default values equal to 50% of a 50 mg SO₄/L detection limit

Bold text denotes value exceeding standard limit as described in note a

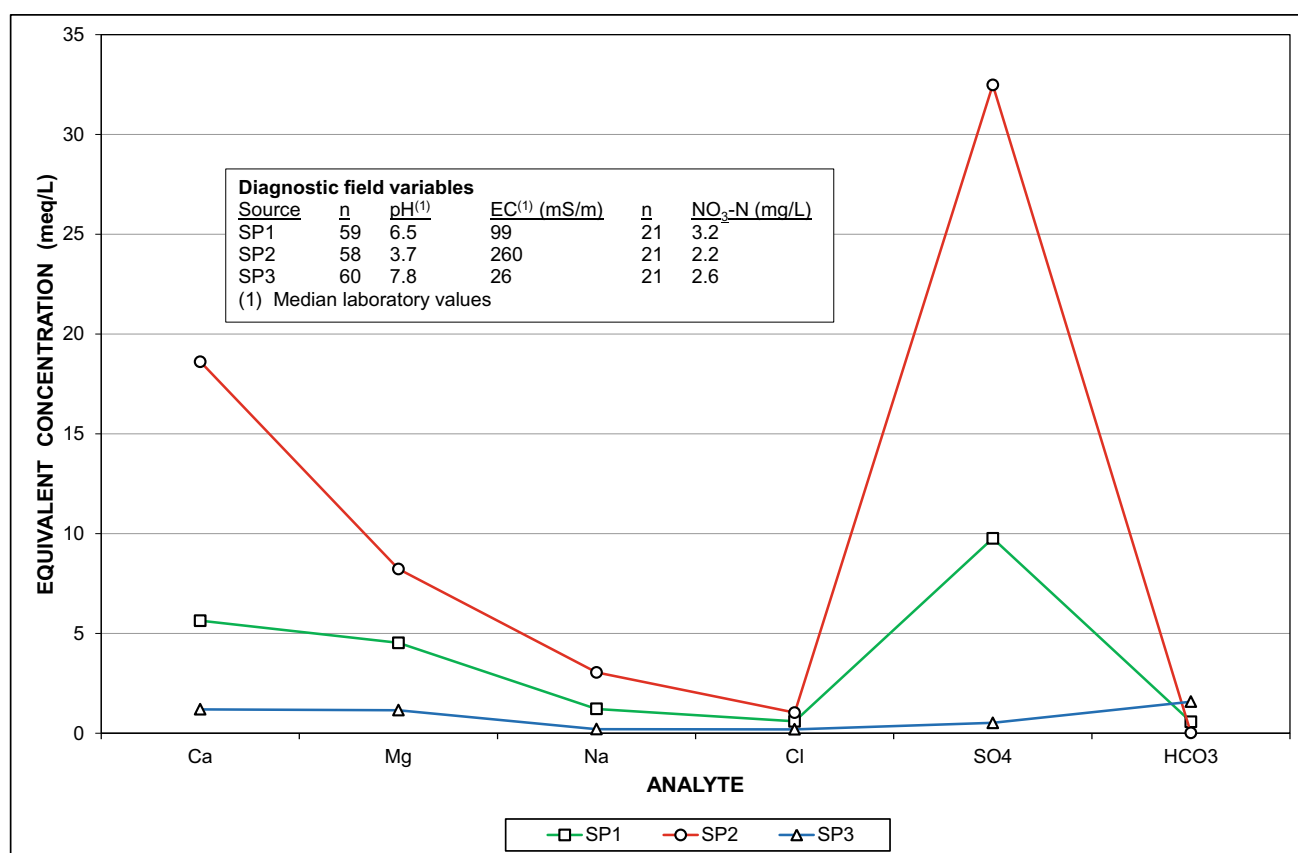


Fig. 32 Graphic comparison of median water chemistry associated with selected springs in the KGR in the period September 2009–September 2014 (data from Table 8)

similar elevation of ~1435 m amsl, the 3rd so-called ‘lost adit’ (G. Whatley, personal communication) was uncovered during earthworks along the regional road (R540) that passes the property. This adit occupies a lower surface elevation of ~1425 m amsl, which is only ~2 m above the level of the nearby Honingklip Spruit, and ~5 m above the mine water level elevation. It is probable that the highest recorded mine water level observed in 2000 (G. Whatley, personal communication) approached this elevation. If the Kromdraai

Gold Mine is therefore to decant, it will most likely be via this adit. Based on the present quality of the mine water, however, such decant is unlikely to contribute AMD into the receiving surface and groundwater environments.

It bears mention that the historical Kromdraai Gold Mine shares the ecological significance associated with many of the natural cave features in the study area, namely that of providing a habitat and breeding ground for bats (G. Whatley, personal communication).

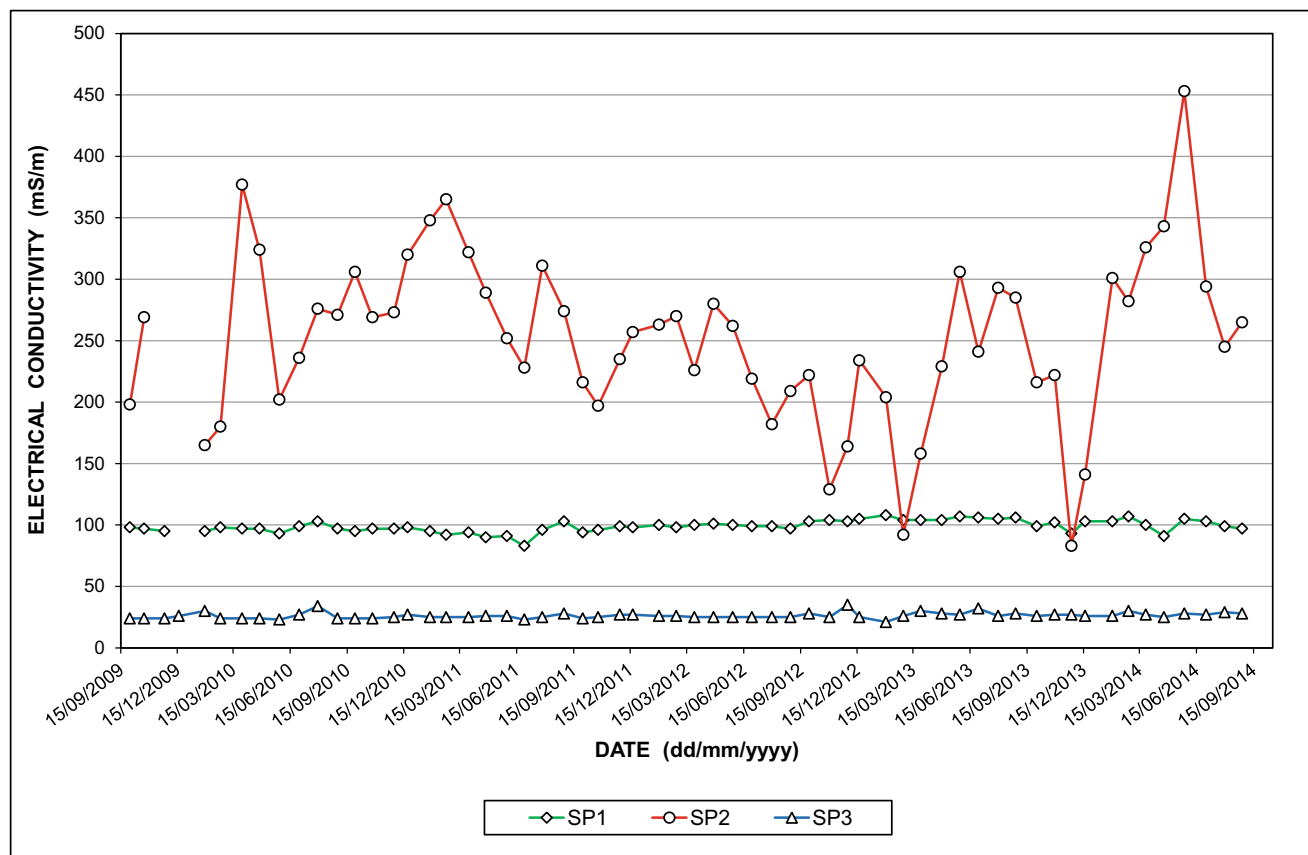


Fig. 33 Salinity trend for water produced by springs SP1, SP2, and SP3 in the KGR in the period September 2009–September 2014

8.3 Human Settlement

The issue of informal housing developments in the COH assumed disturbing proportions when such a community on Ptn 26 at Kromdraai resorted to civil unrest in order to air grievances they felt toward the West Rand District Municipality as responsible authority for the area (Damons 2010). The geo-environmental factors that inform the situation are summarized as follows:

- location of the settlement on ‘untested’²³ dolomitic ground;
- location of the settlement on undermined ground associated with the historical Kromdraai Gold Mine workings, the entrance to which is located on the adjoining property; and
- a comparatively shallow (<20 m) depth to groundwater rest level.

²³ The development of dolomitic terrain is subject to prior geotechnical investigation and assessment in accordance with guidelines put forward in the CGS/SAIEEG (2003) publication.

The combination of these factors creates understandably significant concern for a variety of reasons that include compromising human health and safety and water resource quality. It is therefore imperative that provincial government and district/local authorities are equally aware of the sensitivity and value of the COH environment.

A further concern associated with both informal and formal low-cost residential areas is the proliferation of refuse disposal sites associated with these areas. Examples are the refuse sites centered on the coordinates 26.07385° S–27.65700° E and 26.07073° S–27.65820° E to the north-east of the informal residential settlement located on Ptn 6 of Vlakplaats 160IQ in the south-eastern quadrant of the N14/R24 junction at Tarlton. Both sites are readily identifiable on the Google Earth® image of the area, which also reveals their location in the middle reaches of the Riet Spruit valley. This segment of the drainage only carries surface water into the Zwartkrans Basin during periods of excessive rainfall and runoff from the Randfontein area. This runoff is impounded in several dams, notably one located at 26.06515° S–27.66104° E. However, no surface water flow passes the downstream (eastern) boundary, located at 26.06436° S–27.66960° E, of the Jomajoco Farms property (J. van den Bosch, personal communication). Although the

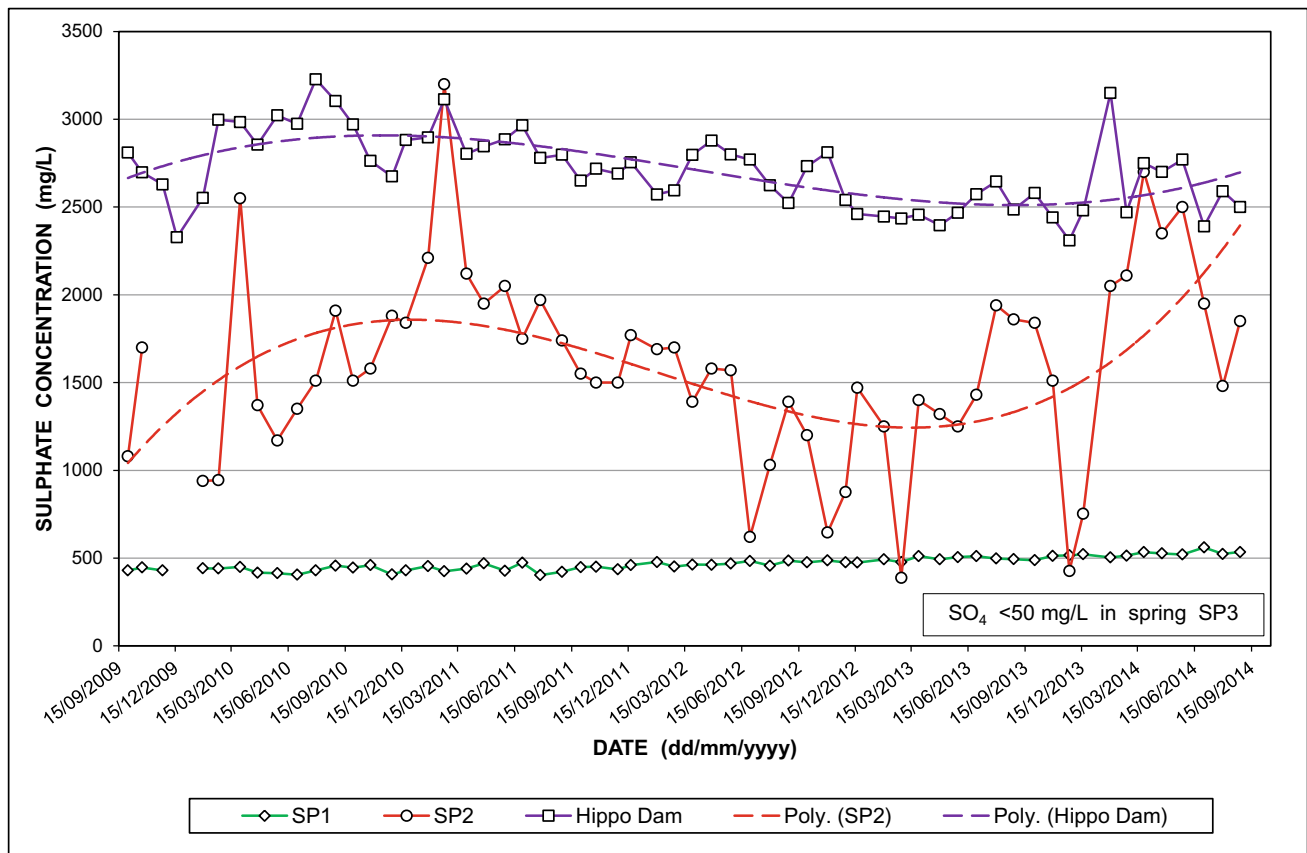


Fig. 34 Sulfate trend for water produced by springs SP1, SP2, and SP3 in the KGR in the period September 2009–September 2014; the Hippo Dam record provides a reference of contemporary surface water discharge quality

depth to groundwater rest level along this segment of the Riet Spruit channel is ~ 60 m bs (station A2N0598, Table 8 in Chapter “Physical Hydrogeology”), this otherwise substantial separation with the surface is short-circuited by swallow holes in the river bed that allow poorer quality surface water more rapid access to the aquifer. This might explain the total coliform and *E. coli* values of 36 and 5 c/100 mL, respectively, detected in a groundwater sample from station A2N0598 collected on 09/06/2010.

The provision of suitably adequate refuse/waste removal facilities for the low-cost and/or informal residential areas that have been developed on dolomitic ground in the study area is no less important than the provision of water and sanitation facilities to these communities. These represent opportunities for integrated land-use development between local (MCLM) and district (WRDM) municipal authorities. The illegal dumping of refuse in the COH is, however, not limited to areas of low-cost and/or informal housing. The image in Plate 7 shows an illegal dumpsite located immediately downstream of where the Malmani Road which serves the Sterkfontein Country Estates crosses the Riet Spruit. The refuse covered the entire drainage channel, including the active flow section. Exercising control over

such practices is extremely difficult, and must rely as much on pride in a ‘sense of place’ as it does on community ‘policing’. The situation has since been remedied through the intervention of local residents and landowners. The placement of a new cemetery in the upper reaches of the Zwartkrans Basin at 26.05667° S– 27.65645° E is considered a responsible development as it recognizes the ~ 70 m depth to groundwater level in this part of the karst environment.

8.4 Mine Water

The groundwater chemistry data generated by the DWS monitoring program in the Zwartkrans Basin provides an indication of the extent and magnitude of the mine water impact on the karst aquifer in this portion of the COH. The subsurface impact of mine water is defined by the pseudo-plume and principal flow path illustrated in Fig. 39. This path extends northwards from the Sterkfontein Subcompartment into the contiguous portion of the Zwartkrans Subcompartment and is characterized by SEC values of up to 300 mS/m and SO_4 concentrations of up to 1800 mg/L,

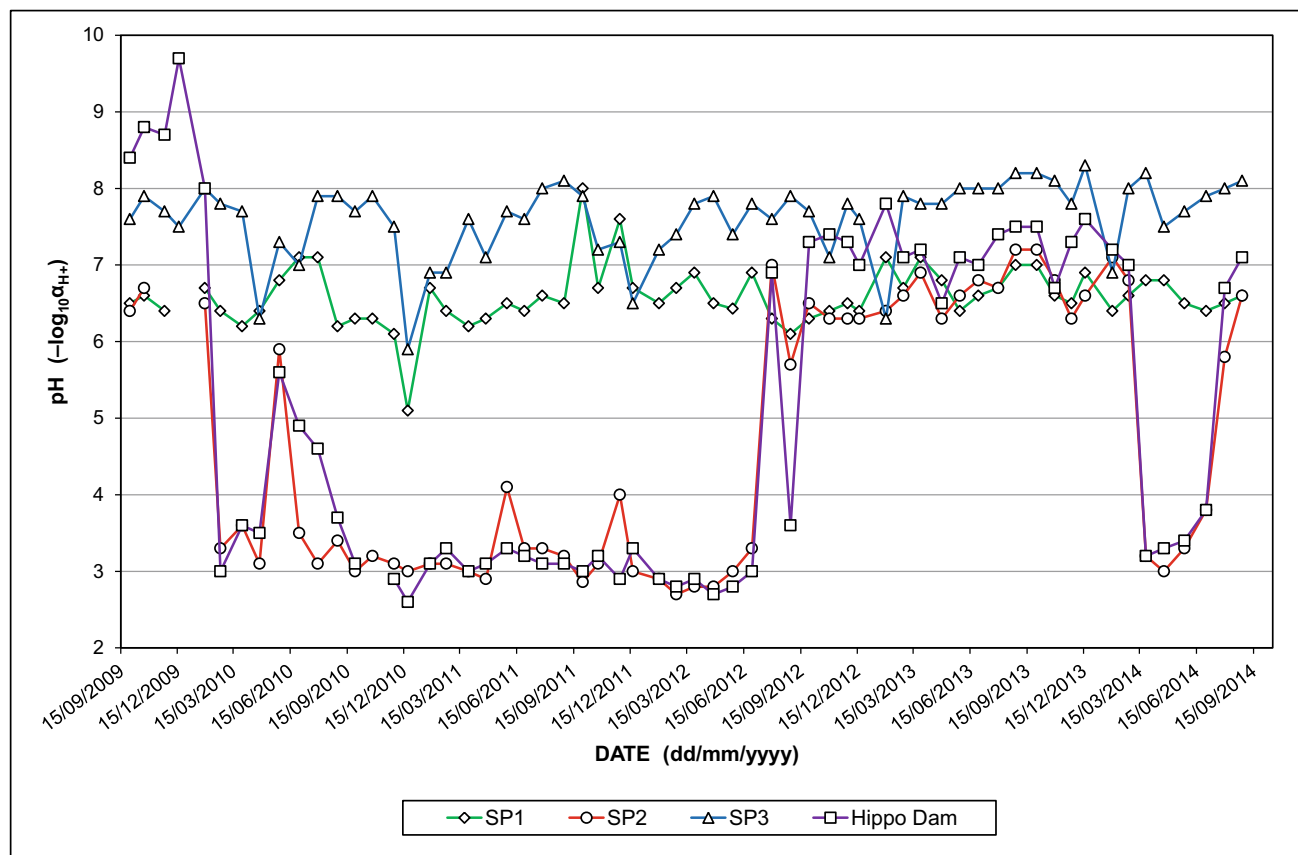


Fig. 35 Trend in pH for water produced by springs SP1, SP2, and SP3 in the KGR in the period September 2009–September 2014

although pH values >6.4 indicate that net alkaline conditions still prevail (see Sect. 13.2) as at late-2014. This is illustrated in Figs. 40, 41 and 42 with the aid of bar graphs for the chemical variables pH, EC, and SO_4 , respectively.

The SEC and pH values measured on the occasion of each SDM reported for stations F11S12 and MRd in Table 10 in Chapter “Chemical Hydrology”, are graphed in Fig. 43 (for SEC) and Fig. 44 (for pH). These data reflect the elevated SEC values (>350 mS/m) and depressed pH values (<3) that characterized the surface water lost to the karst aquifer in the period mid-2010 to mid-2012 (Sect. 5.2.1 in Chapter “Physical Hydrology”). It is this allogenic recharge that has manifested the mine water imprint on the karst groundwater of the Zwartkrans Basin observed in Figs. 40, 41 and 42.

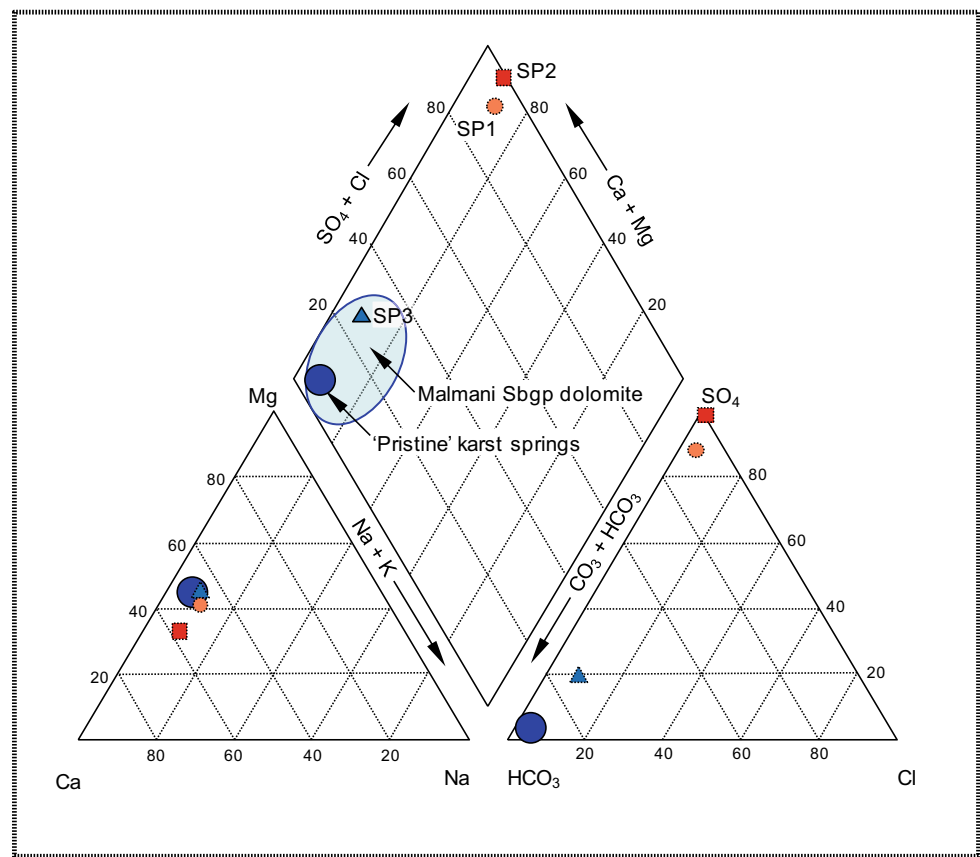
The footprint of the pseudoplume shown in Fig. 39 encompasses ~ 1030 ha. This represents $\sim 11\%$ of the Zwartkrans Basin, and only $\sim 4\%$ of the entire COH karst footprint. These observations provide context for the spatial extent of the mine water impact on the karst water resources of the COH.

The positive influence of the immediate mine water control and management intervention measures since

mid-2012, as evidenced by the lower SEC values (<300 mS/m as per Fig. 43) and higher pH values (>4 as per Fig. 44), signifies an improvement in the situation. This improvement is associated in part with the containment of uncontrolled raw mine water discharge into the environment in mid-2012, and except for a week or two in December 2012, was maintained until February 2014 (Hobbs 2014b). The subsequent ‘excursion’, described by Tancott (2014) as a “big problem”, was brought under control in July 2014. Hobbs (2013a, b, 2014a, b) has demonstrated that an observed improvement continues to manifest as decreasing SEC and SO_4 values in the monitoring boreholes located in each of the segments as of December 2014. Nevertheless, the undersaturated state of the karst groundwater in regard to calcite and dolomite reflects conditions of dissolution of these minerals, especially in proximity to the losing reach of the Riet Spruit. These circumstances are illustrated in Fig. 45, which also reveals the saturated state of the Sterkfontein Cave (SC) groundwater.

The magnitude of the mine water impact on the receiving karst groundwater resources is explored further in Sect. 13.2 in regard to the net alkalinity and net acidity of the groundwater. The demonstrated presence of karst

Fig. 36 Piper diagram of KGR median springwater chemistry (data from Table 8) compared to pristine karst springwater chemistry



groundwater exhibiting a net positive acidity, albeit marginal and generally associated with metal (mineral) acidity, is another concern.

The SI_C values of the more recent allogenic recharge from the Riet Spruit (Sect. 5.2.1 in Chapter “Physical Hydrology”) fall in the range -4.0 to -3.2 , reflecting undersaturation of the water in regard to this mineral. These circumstances equate to the conditions identified by Palmer (2003) and Worthington and Ford (2009) where water that is undersaturated with regard to calcite (typical of allogenic recharge) enters a karst aquifer via point recharge from a sinking stream carrying a high discharge. The information presented in Fig. 45 indicates that these circumstances extend to the karst groundwater, at least in proximity to the losing stream reach. Of concern in this regard is that Worthington and Ford (2009) indicate that these circumstances typically result in the concentrated dissolution of carbonate strata in the receiving karst aquifer. Together with the net acidity associated with this water (Sect. 13.2), the aggressive character of the allogenic recharge represents a concern that requires concerted assessment and evaluation.

The historical pattern and trend of groundwater SEC and SO_4 concentrations in proximity to the losing reach of the Riet Spruit between stations F11S12 and MRd is reflected in

the long-term monitoring data associated with the paired stations A2N0584–GP00302 and A2N0586–GP00300, and station A2N0600 (see Fig. 39 for station positions). These are presented in Fig. 46, and again reveal the comparatively recent increase in SEC and SO_4 concentration levels. The positions of these stations in relation to the principal direction of groundwater flow are shown in Figs. 39, 40 and 41.

As might be expected given their respective position along the principal flow path, the SO_4 concentration pattern shown in Fig. 46 indicates a later response at station A2N0600 than at station A2N0584. A concentration of ~ 300 mg SO_4/L was only manifested at the former ~ 600 days after this value was measured at station A2N0584. Given the distance of ~ 4500 m between these two stations, the travel time equates to a hydraulic conductivity (K) of 7.5 m/d. This value compares favorably with the range of K values (~ 1 –27 m/d) obtained by Holland (2007) from slug tests carried out on four boreholes in the area. It compares particularly well with the K values of ~ 4 –7 m/d obtained for borehole SCH2 (identified as SBH-2 in Fig. 4.21 and Table 4.9 of Holland 2007) located in the flow path (Fig. 19 in Chapter “Physical Hydrogeology”).

Accepting the transmissivity value of ~ 1000 m²/d previously assigned to this aquifer, a flow depth (d) of ~ 130 m is obtained from the relationship

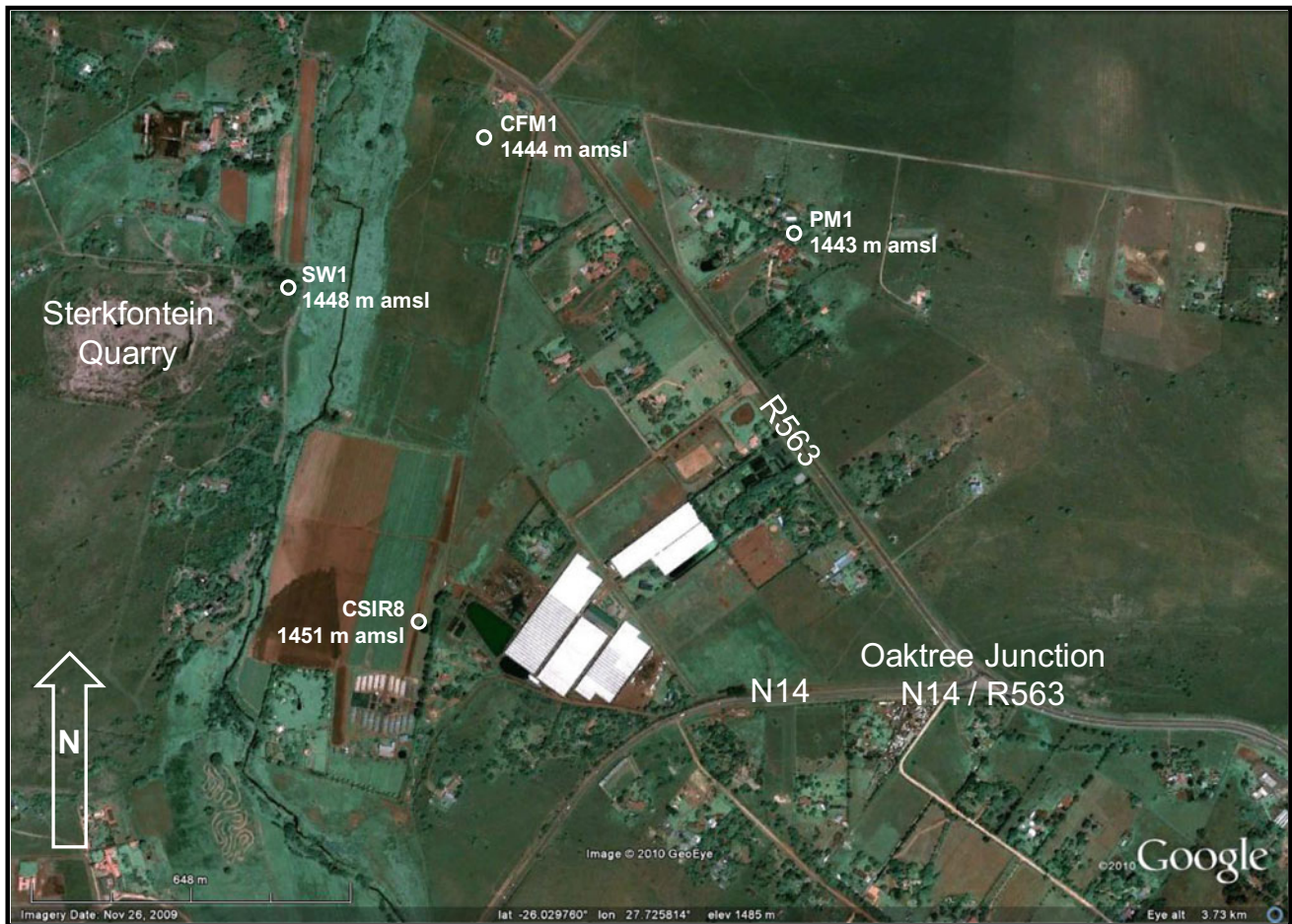


Fig. 37 Locality map of pesticide residue sample sources CSIR8 and CFM1

$$T = K \times d$$

The veracity of this value can be tested against the geological log (record) for station A2N0584 (originally assigned the number G36331) as reported by Bredenkamp et al. (1986). This record indicates that two horizons of leached and fractured chert-rich dolomite were intersected in the depth intervals of 20–40 m and 120–132 m below surface. The deeper aquifer produced an airlift yield of 50 L/s. It is the shallower karst aquifer at this location that has been targeted for monitoring by the recently established borehole GP00302, and which yields the slightly poorer quality groundwater evident in Fig. 41. The same drilling record, however, reports that a ~70-m thick chert-poor horizon separates the two aquifer horizons in borehole A2N0584. These circumstances illustrate the extremely heterogeneous and anisotropic nature that is typical of the so-called ‘Transvaal’ karst aquifers, and which favor the development of a pseudoplume (Ewers et al. 2012). This derives from the typically convergent nature of flow in the conduit system that militates against the hydrodynamic dispersion of contaminants in a karst aquifer.

Further chemical characterization of the groundwater associated with the mine water impact in the Zwartkrans Basin is shown in the Piper diagram in Fig. 47. The diagram represents all the stations sampled in late-2012, excluding the five stations enumerated on an ad hoc basis in December 2012.

It is evident from Fig. 39 that the pseudoplume of mine water contaminated groundwater discharges via the Zwartkrans Spring. The circumstances that describe this phenomenon are discussed in Sect. 7.1. Reference by Groenewald (2010) to the caves as occupying a low energy groundwater system, and by Martini et al. (2003) to the “... apparently static ...” pools in the cave system, support a distal location on the south-eastern margin of a postulated subsurface thalweg. This hypothesis finds support in the “flood induced pseudoplume” reported by Ewers et al. (2012), which describes the intrusion of contaminated groundwater from a flooded major conduit into peripheral porous karst strata during storm/flood events. Although the intruded water returns to the conduit as groundwater levels recede following passage of the flood, it leaves behind contaminants in various settings in the intruded portion of the karst aquifer. These circumstances are more likely to

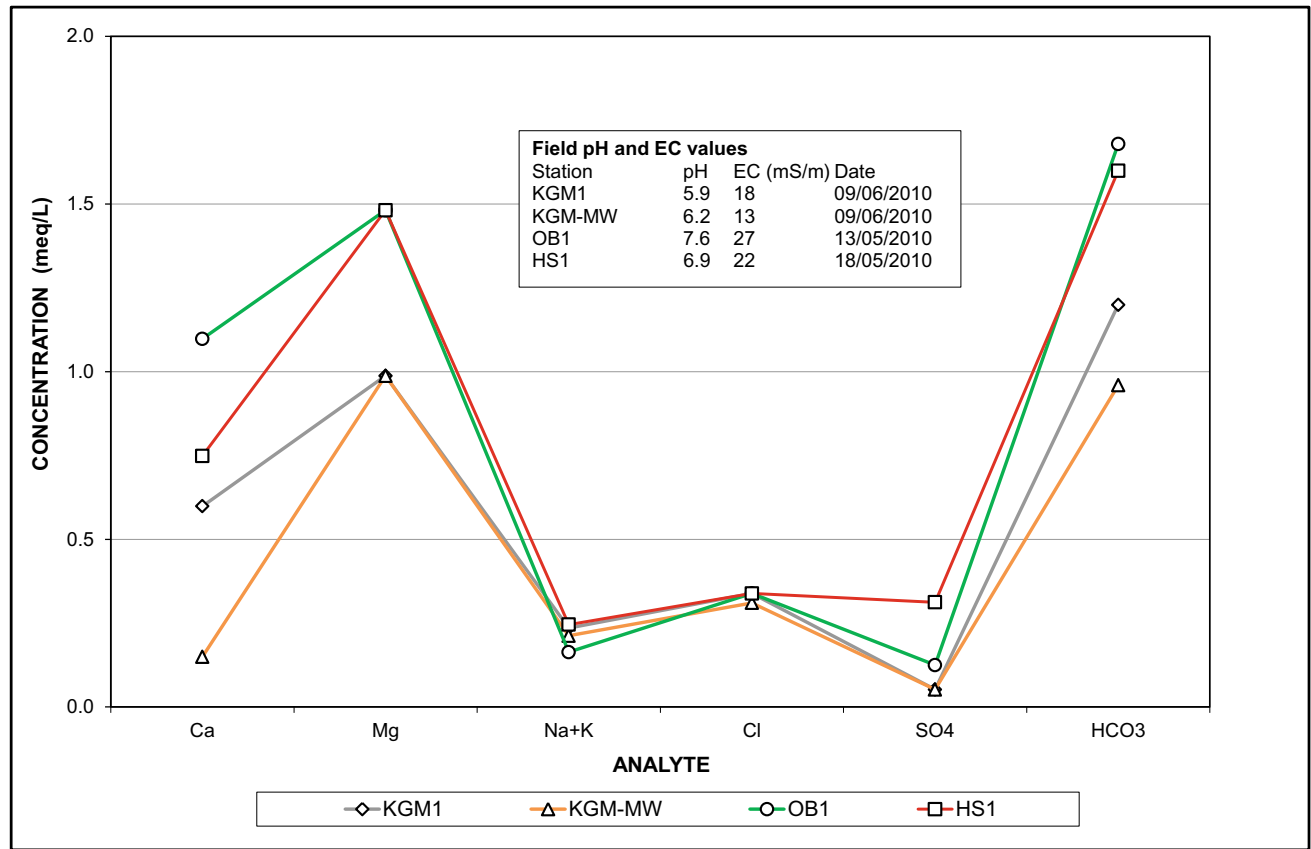


Fig. 38 Comparison of surface water and groundwater chemistry in the vicinity of the historic Kromdraai Gold Mine

Plate 7 View of an ‘illegal’ refuse disposal site in the channel of the Riet Spruit near its confluence with the Blougat Spruit



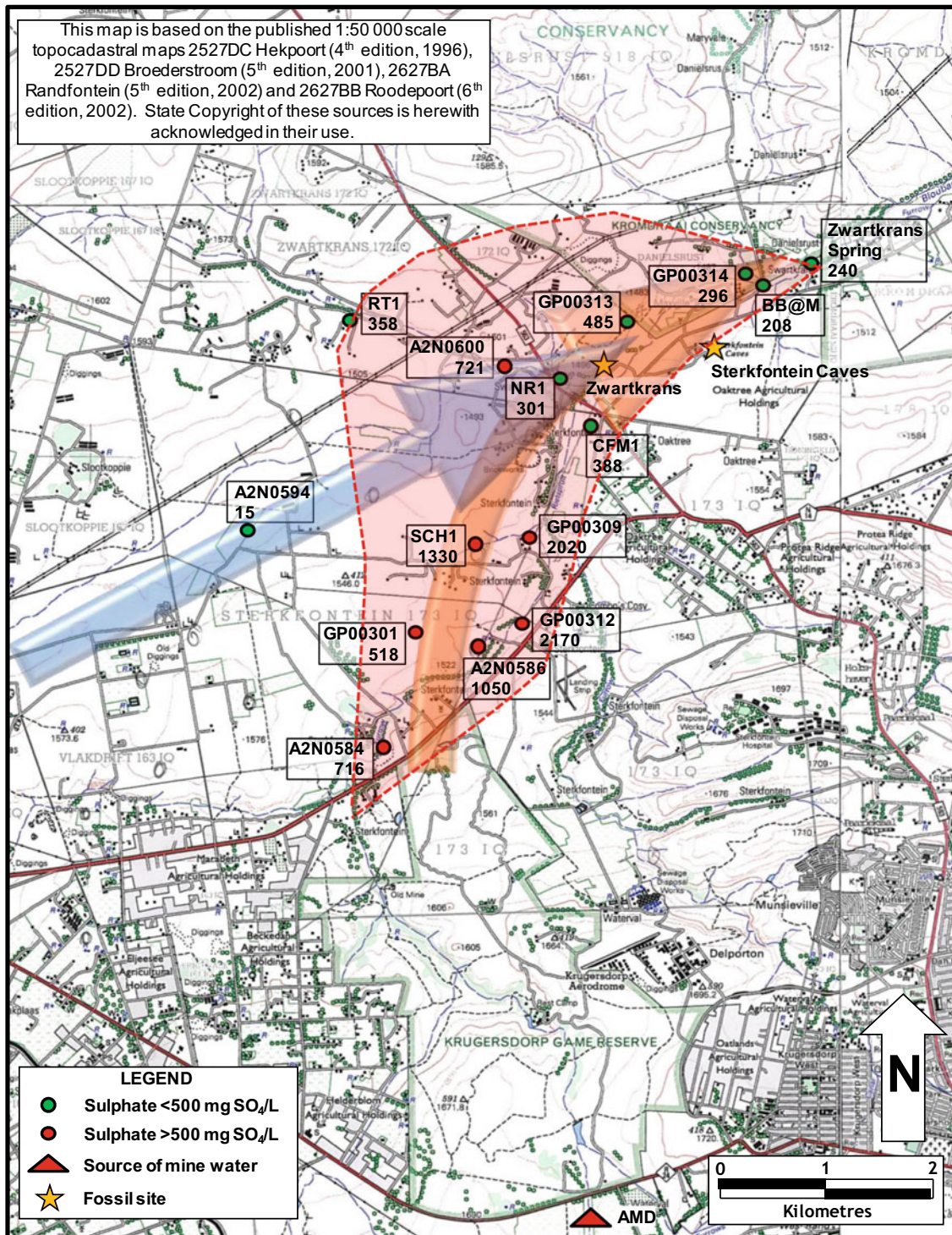


Fig. 39 Definition of the principal flow path describing the passage of allogenic recharge through the Zwartkrans Basin to the Zwartkrans Spring based on late-2014 sulfate concentrations in groundwater

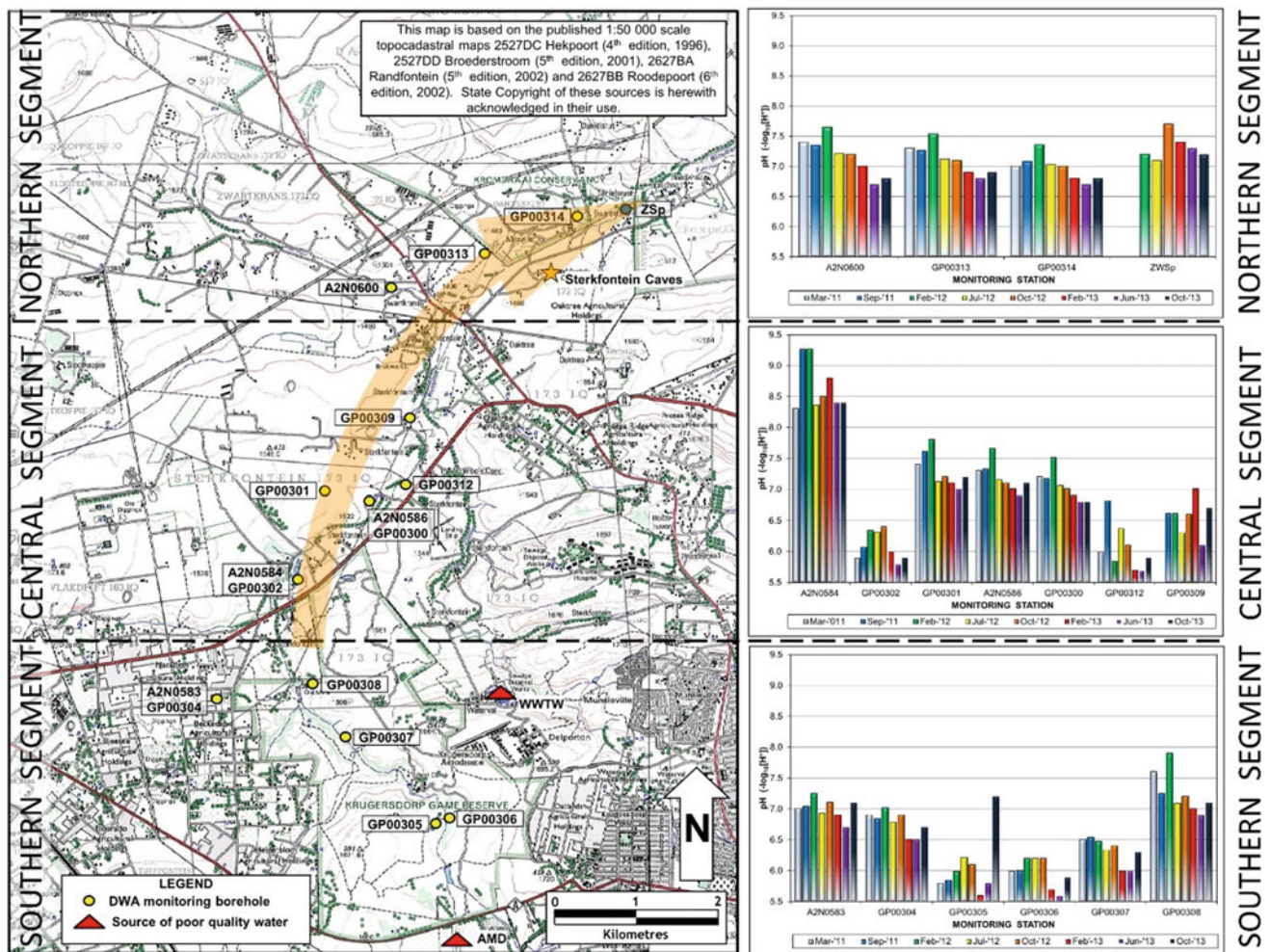


Fig. 40 Distribution of DWS monitoring boreholes with pH pattern and trend as bar graphs; arrow denotes principal direction of groundwater flow

prevail in the lower (downstream) reaches of a karst basin where conduits are convergent (Ewers et al. 2012), a hydrogeologic setting that suitably describes the location of the caves in the landscape. These circumstances underscore the distal location of the caves relative to a postulated subsurface thalweg as illustrated in Fig. 48. This reflects a combination of the hydrophysical and hydrochemical dynamics that describe the hydrogeology of the cave system within its broader hydro-environment along two transects.

The occurrence of mercury in mine and surface water sources in the study area has been discussed in Sect. 3.3.2 in Chapter “Chemical Hydrology”. Concern for its occurrence in groundwater sources precipitates the comparison made in Table 9, where the mine and surface water values derive from Table 40 in Chapter “Chemical Hydrology” (Sect. 3.3.2 in Chapter “Chemical Hydrology”). The comparison reveals the typically low concentrations of mercury in groundwater as evidenced by the singular exceedance of the various detection limits, under circumstances where

SANS (2011a) sets a standard chronic health limit of ≤ 0.006 mg/L for this metal in drinking water. The ‘poorest’ (highest) detection limit in Table 9 is $3 \times$ more stringent than this limit, which is exceeded in only two out of 66 groundwater samples.

9 Groundwater Fitness

9.1 Potable Use

The project has defined the quality of groundwater resources in far the greater portion of the study area as being suitable for human consumption in terms of the SANS 241 (2006) standard for drinking water quality. This does not, of course, provide solace to those groundwater users who have experienced a compromised quality of groundwater attributable to extraneous impacts associated with mine water and municipal wastewater effluent. The extent to which

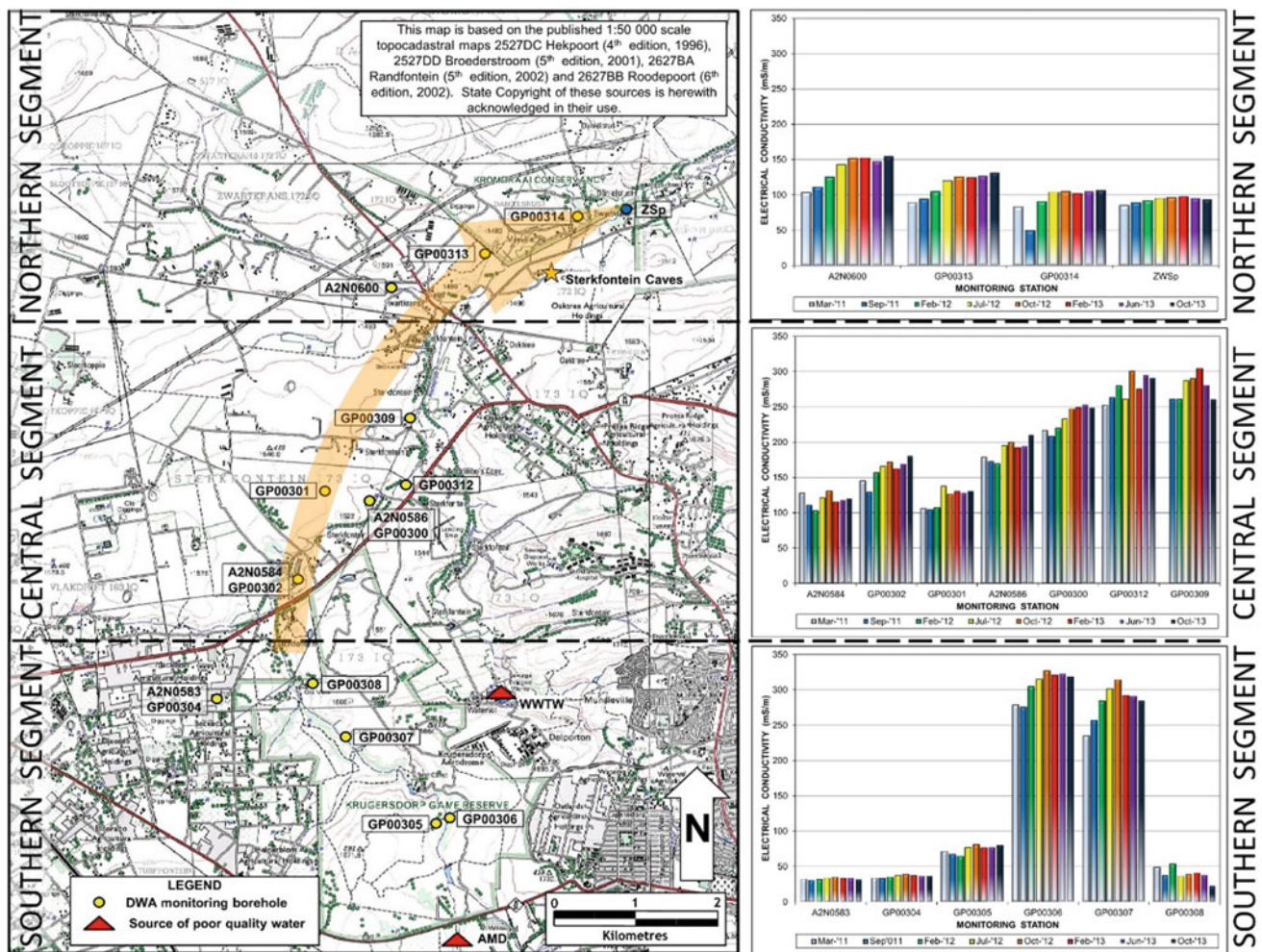


Fig. 41 Distribution of DWS monitoring boreholes with SEC pattern and trend as bar graphs; arrow denotes principal direction of groundwater flow

these impacts extend into the broader hydrogeologic environment is described by the water resources monitoring program implemented by the COH WHS MA and the DWS. The mine water impact has been discussed in Sect. 8.4.

The presence of heavy metals in both the mine wastewater and the municipal sewage wastewater also raises a concern for the potability of groundwater resources in the study area. As shown in Sect. 11, the presence of heavy metals such as Al, Co, Mn, Ni, and Zn could not be detected (for the detection limits reported in Sect. 9.3) in the groundwater from sources otherwise reflecting the most impacted quality in terms of SEC and SO_4 . The association of radionuclides with mine water raises a further concern. However, it is shown in Sect. 5.2.2 that none of the groundwater samples exhibited a U concentration greater than the detection limit of 0.001 mg/L (1 $\mu\text{g/L}$).

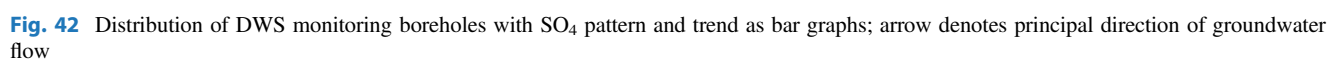
The above observations suggest that the fitness of groundwater in the study area for potable use is not unduly

compromised by inorganic elements, trace/heavy metals, or radionuclides. However, the observed presence of bacteriological contamination in some sources (refer to Sect. 6) cautions against the unqualified use of groundwater for drinking water purposes.

9.2 Agricultural Use

9.2.1 Livestock Watering

Guidelines in this regard are provided in the DWAF (1996b) publication. The target water quality range (TWQR) limits for the major inorganic analytes are typically less strict than for human consumption. For example, the TWQR for SO_4 (a variable that affects the palatability of water also for livestock) is 1000 mg/L compared to the 400 mg/L for humans. This is also true for trace/heavy metals, e.g., Mn and $\text{Fe} \leq 10 \text{ mg/L}$ for livestock compared to ≤ 0.1 and $\leq 0.2 \text{ mg/L}$, respectively, for humans.



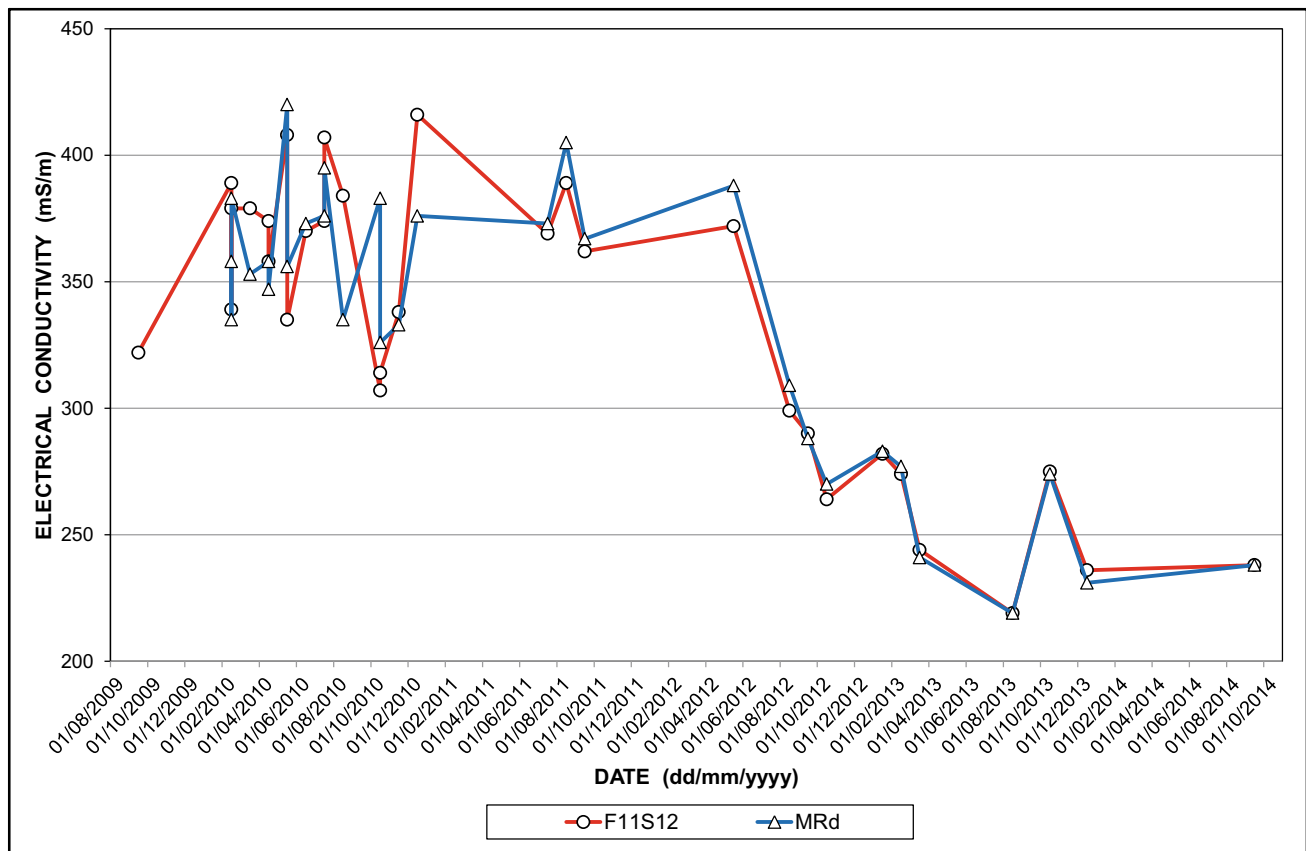


Fig. 43 Pattern and trend of SEC at flow gauging stations F11S12 and MRd on occasion of each synoptic discharge measurement (data from Table 10 in Chapter “Chemical Hydrology”)

Similarly, the observed presence of bacteriological contamination in some groundwater sources (refer to Sect. 6) is mitigated by the fecal coliforms TWQR of ≤ 1000 c/100 mL in 20% of samples, compared to the ≤ 10 c/100 mL in 1% of samples for humans. Under circumstances where the highest total coliform count (which includes fecal coliforms) recorded in this study for groundwater amounted to 500 c/100 mL, the fitness of groundwater in the study area for livestock watering is not unduly compromised by inorganic elements, trace/heavy metals, or bacteriological considerations.

9.2.2 Irrigation

An analysis of the 51 groundwater chemistry analyses generated by this study returned mean and median SAR values of 0.52 and 0.27, respectively. Grouped by compartment/subcompartment, this analysis yields the information in Table 10. Wilcox diagrams reflecting the SAR classification are presented in Figs. 49 and 50.

It is evident from Table 10 that the mean value is matched or exceeded in only three basins/subcompartments. Significantly, these are the compartments that receive allo-genic recharge from the poorest quality surface water

sources (Sects. 5.2 in Chapter “Physical Hydrology” and 1.2 in Chapter “Chemical Hydrology”). Nevertheless, the classification of the groundwater for irrigation use (refer to Sect. 4.2.2 in Chapter “Chemical Hydrology”) is no worse than a C3–S1 quality class rating as illustrated in Fig. 50. More typically, however, it exhibits a C2–S1 rating (Table 10), which allows its use for the irrigation of crops with a moderate salt tolerance on soils where a moderate amount of leaching occurs.

9.3 Cave Ecosystems

The fitness of groundwater quality in regard to cave ecosystems is important where the latter intersects the water table and provide refugia for stygobitic (groundwater) fauna (Tasaki 2006), also referred to as stygobionts or stygofauna (aquatic species) by Culver and Sket (2000, 2002). As far as could be established, such biota (typically blind amphipods) have been found in Sterkfontein Cave and two other caves (Koelenhof and Yom Tov) in the study area (Tasaki 2006). Durand and Peinke (2010) indicate that certain amphipod species (notably *Sternophylinx transvaalensis*) are also

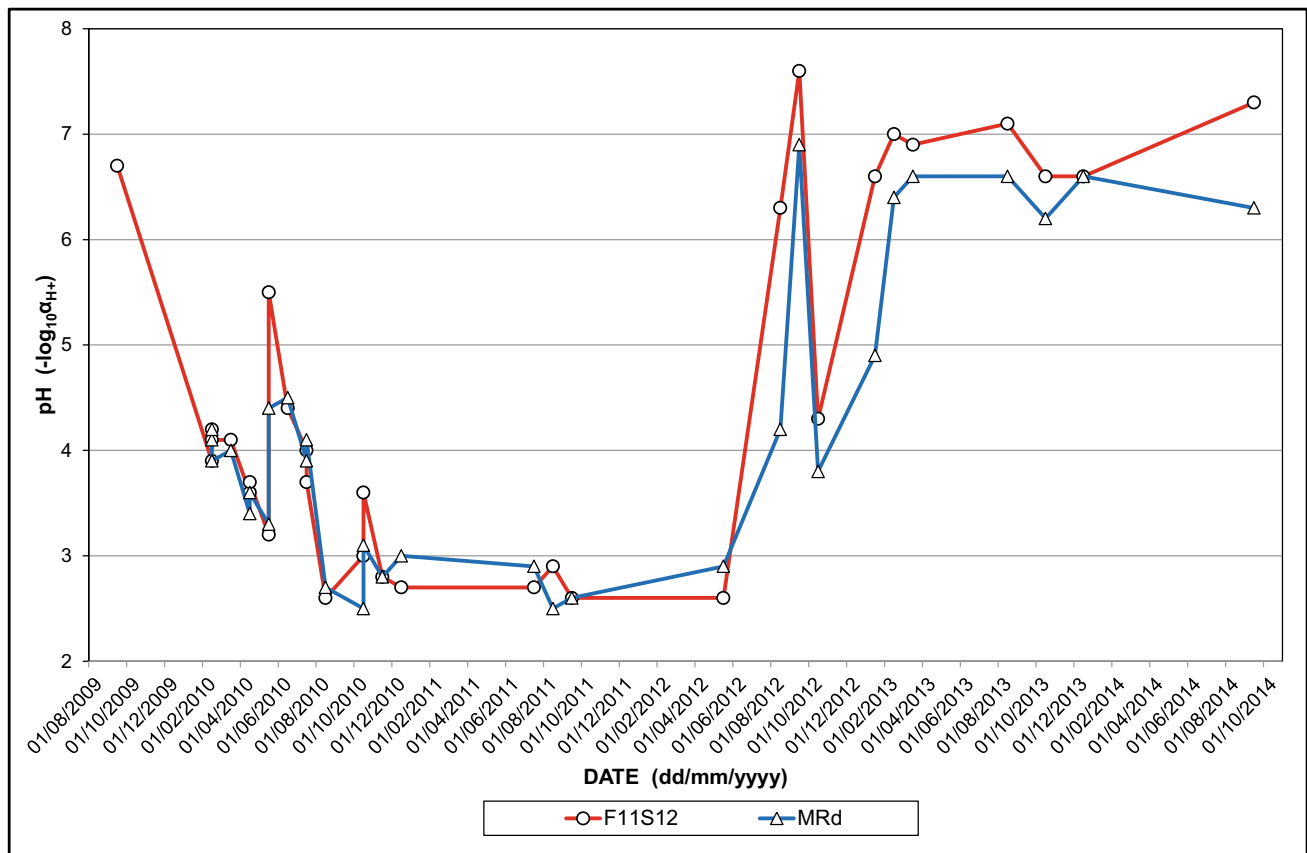


Fig. 44 Pattern and trend of pH at flow gauging stations F11S12 and MRd on occasion of each synoptic discharge measurement (data from Table 10 in Chapter “Chemical Hydrology”)

associated with springs in the John Nash Nature Reserve. As this report is concerned with water resources, the consideration of subterranean (cave-dwelling) terrestrial species (troglobitic fauna or troglobionts) is not considered. However, Durand and Peinke (2010) indicate that the humidity levels associated with ‘wet’ caves might be an important environmental factor for resident bat colonies.

The impact of pollution effects on cave systems is related to the same factors that inform the contamination of surface water and/or groundwater resources. These have previously been recognized as elevated nutrients (nitrate and phosphorus) associated with municipal wastewater effluent and agricultural return flows, and trace metals associated with wastewater effluent and mine water. The treated wastewater and/or agriculturally derived nutrients promote eutrophication in surface water systems through photosynthesis. However, the absence of sunlight in cave ecosystems precludes the excessive growth of aquatic vegetation in the subterranean environment (Graening and Brown 2000; Boulton et al. 2003). These authors recognize the negative impacts of organic pollution on cave ecosystems as being related to the following:

- alteration of the community assemblage;
- impoverishment of biodiversity; and
- increased risk of predation from surface fauna.

Culver and Sket (2002) identify the usual sequence of eutrophic impacts in caves as an initial increased population size of stygobites, followed by increased population sizes of non-specialized species usually accompanied by a decline in population sizes of stygobites, and culminating in the extirpation of the latter. As population increases in the food-poor environment of caves usually means an increase in available food (typically associated with eutrophication), observations of such a trend through routine biomonitoring activities offer an early warning of potentially catastrophic longer-term impacts on stygobitic fauna (Culver and Sket 2002).

Graening and Brown (2000) recognize that increased concentrations of Pb and Zn in cave water are manifested in the accumulation of these trace metals in cave sediments and the tissues of cave organisms rather than in their biomagnification in the food chain. This is identified as a concern under circumstances where heavy metals might be present in concentrations that are acutely toxic to aquatic organisms.

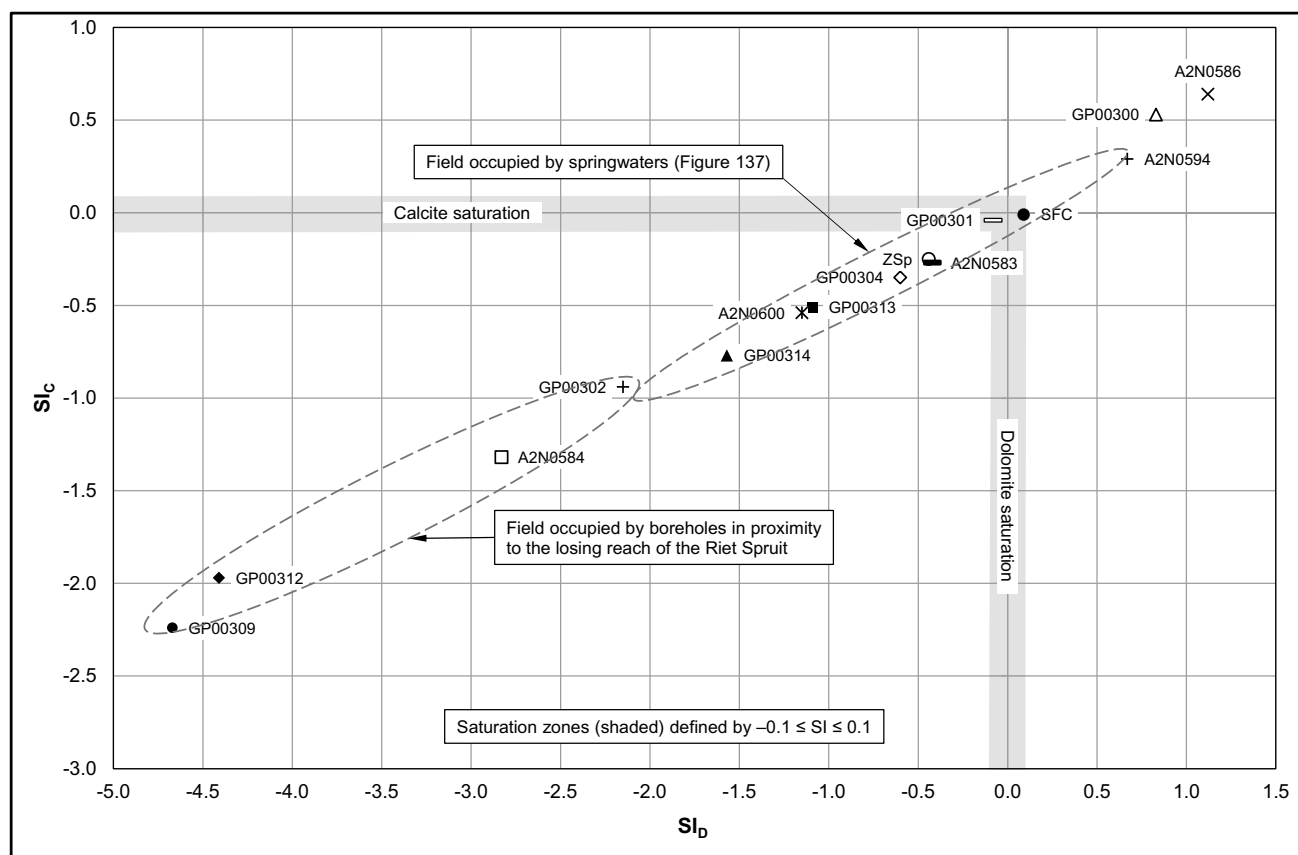


Fig. 45 Saturation state of karst groundwaters in the Zwartkrans Basin with respect to calcite (SI_C) and dolomite (SI_D)

The chemical analysis of a Sterkfontein Cave water sample collected on 13/05/2010 returned a NO_3-N concentration of 8.2 mg/L and a PO_4-P concentration of <0.2 mg/L but revealed no concentrations of the following trace metals above the specified detection limits (DLs).

| DL (mg/L) | Analyte |
|--------------|---|
| ≥ 0.100 | Al |
| ≥ 0.025 | Ag, B, Ba, Be, Bi, Co, Cr, Cu, Fe, Li, Mn, Mo, Ni, Sn, Sr, Ti, V, W, Zn, Zr |
| ≥ 0.020 | Pb, Se |
| ≥ 0.010 | As, Sb |
| ≥ 0.005 | Cd |

Whether the detection limits mask the possible presence of trace metals that at lower concentrations might still constitute a threat to the continued existence of stygobionts in the Sterkfontein Cave system (and other similar refugia in the study area) is beyond the scope of this study. Further, it is important to note that single measurements of inorganic nitrogen (NH_3 , NH_4 , NO_2 , and NO_3) are a poor basis for

assessment (DWAF 1996a). The likely biological consequences (at least in surface water systems) are best estimated from average summer inorganic nitrogen concentrations.

Nevertheless, the concurrently low PO_4 concentration and the absence of sunlight suggest that the trophic status of the Sterkfontein Cave water system is unlikely to change provided the current hydrochemical conditions prevail. Assurance in this regard can be obtained from regular biomonitoring programs (as described by Culver and Sket 2002) that target stygobitic fauna. Schneider and Culver (2004) have shown that focusing on the largest caves improves sampling efficiency for both terrestrial and aquatic underground species.

In support of Kenyon and Ellis (2010), it is also recommended that any cave biomonitoring program that is implemented in the COH includes the participation of recognized caving associations and their members. The contribution of such I&As, especially if these include knowledgeable and experienced local 'cavers', will extend the benefit of biomonitoring activities to less well-known and frequented caves.

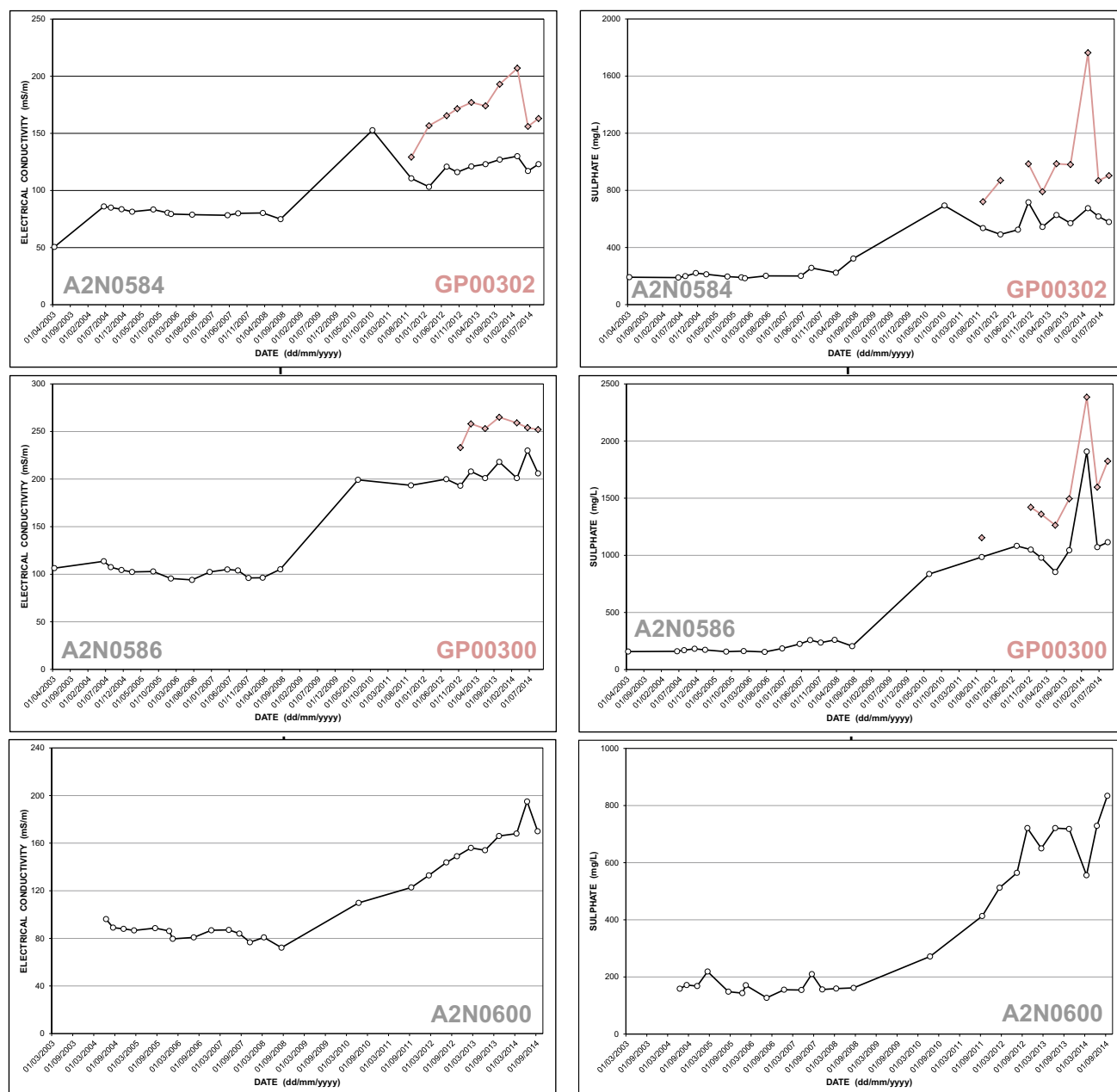


Fig. 46 Long-term pattern and trend of SEC (at left) and SO_4 (at right) in karst groundwater from DWS monitoring stations A2N0584/GP00302, A2N0586/GP00300, and A2N0600; note common time scales and postulated start of rise in concentrations (long vertical pecked line)

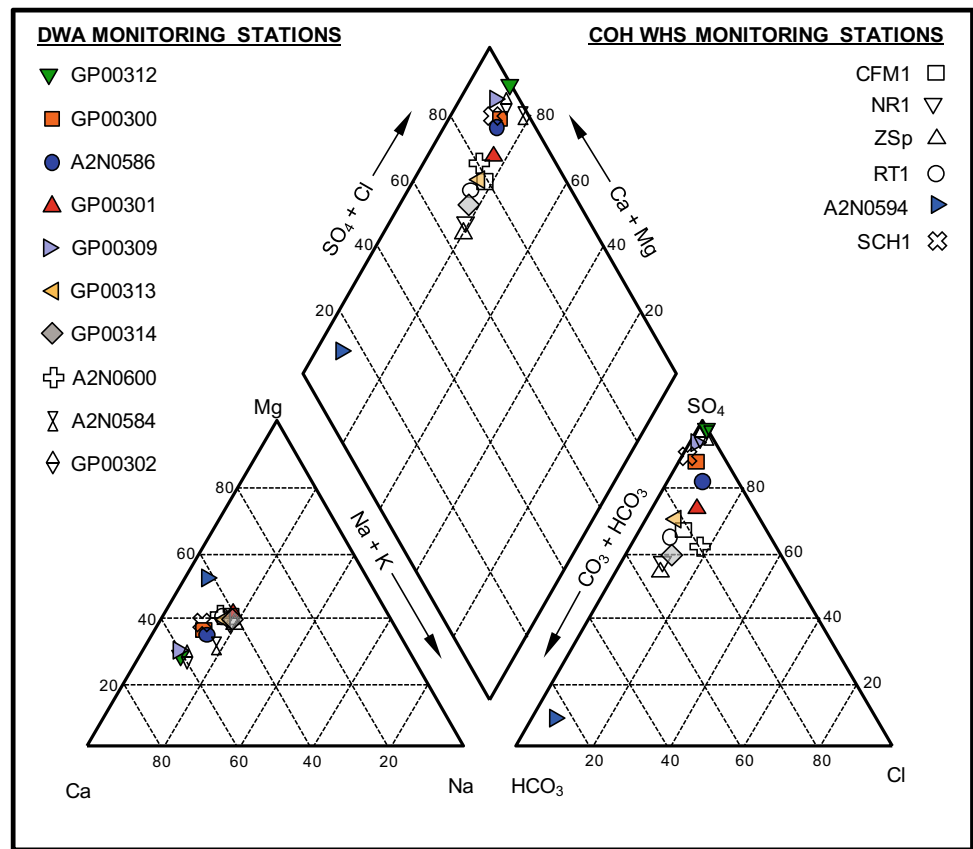
In conclusion, it is acknowledged that cave ecosystem monitoring extends well beyond the water resource environment alone. In the pursuit of ‘integrated monitoring’ across a broad spectrum of disciplines including geomicrobiology, geobiology, biogeochemistry, and biogeography (Engel et al. 2008), the author wholly supports the monitoring requirements put forward by Durand and Peinke (2010) in developing a holistic understanding of the karst ecology of the COH within the paradigm advanced by Williams (2008).

10 Vertical Hydrochemical Variation

10.1 Introduction

Although stratification is a common occurrence in many mines, the published literature seldom provides an explanation for this phenomenon. Wolkersdorfer (2008) discusses 13 case studies in which depth profiles for a range of variables (temperature, EC, TDS, pH, redox, resistivity, flow

Fig. 47 Piper diagram of recent groundwater chemistry defining the mine water impact on the karst groundwater of the Zwartkrans Basin



velocity, and density) are presented. The case studies represent three coal mines, five base metal mines, and five other mines (fluorspar, uranium, and salt). Their distribution ranges between North America (2 #), Europe (9 #), and the United Kingdom (2 #). The results indicate the association of various patterns with the following broad circumstances:

- ‘sharp’ changes in a profile are generally associated with the shaft interception of drives, tunnels, ore passes, etc. suggesting that these represent significant flow conduits (Erickson et al. 1982 cited in Wolkersdorfer 2008);
- ‘smoother’ profiles indicate a well-mixed flow regime or flow rates that are slow enough to allow chemical equilibrium;
- profiles exhibiting a gradually increasing (or decreasing) trend reflect diffusion-driven flow, whereas ‘constant-value’ profiles reflect convection-driven flow mechanisms; and
- in general, large-diameter shafts exhibit ‘smaller’ transition zones than ‘slim’ boreholes.

The manifestation of hydrochemical stratification in a flooded mine void is a particular aspect of mine water that attracts attention for the numerous implications it has for the management and treatment of AMD. These include the following:

- the presence of fresher and typically less acidic water at the top of the water column (Wolkersdorfer 2008 and references therein), suggesting a lesser impact on the receiving environment from uncontrolled and unmanaged decant;
- the association of less saline and circum-neutral pH water at shallower depth with younger recharge and shorter residence times than might be the case for ‘deeper’ mine water; and
- the abstraction of ‘better’ quality mine water from a shallow depth in a pump-and-treat management scenario to reduce the cost of treatment.

A fundamental question that arises from a consideration of stratification in a mine water body [Wolkersdorfer (2008) refers to mine water lakes], and especially under circumstances where hydrodynamic and hydrogeochemical factors inform the stratification, is whether or not a mine water lake exhibits a meromictic²⁴ character. Moreira et al. (2011) have shown that stratification models using electrical conductivity for density are not suited for simulating density created by

²⁴ See Glossary.

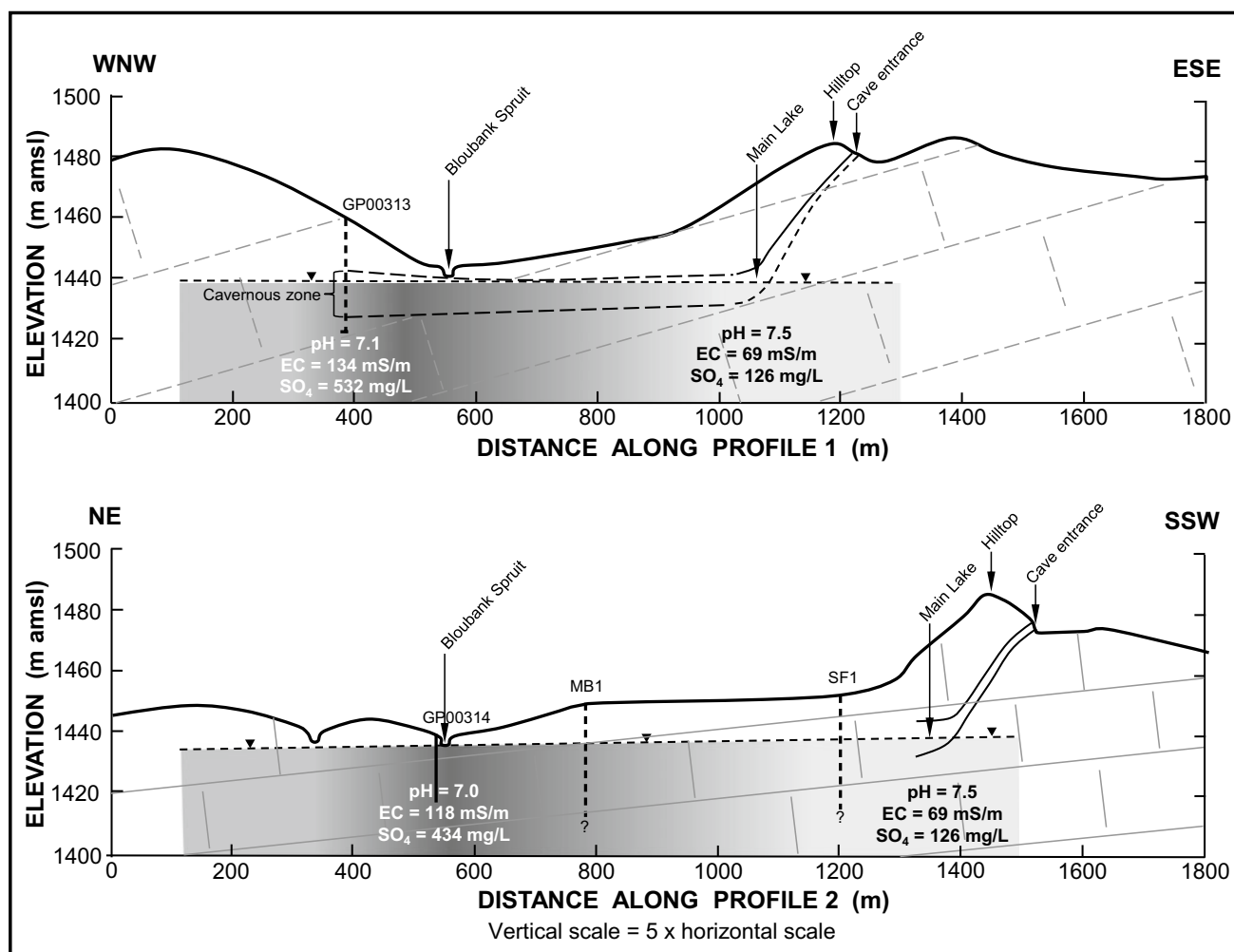


Fig. 48 Schematic profiles through the Bloubaank Spruit valley and Sterkfontein Cave illustrating the relationship between the water table and lake elevations and the stream channel; lateral gradational shading reflects relative intensity of mine water impact on karst groundwater as shown by recent pH, SEC, and SO_4 values; see Fig. 39 for location of the transects

Table 9 Summary of mercury values for various water sources in the study area

| Detection limit (DL) | Mine water ^a | | Surface water | | Groundwater | | Σn | Data source |
|----------------------|-------------------------|-----|---------------|-----|-------------|-----|------------|--------------------------|
| | <i>n</i> | >DL | <i>n</i> | >DL | <i>n</i> | >DL | | |
| 0.0001 mg/L | 1 | 0 | 1 | 0 | 23 | 1 | 25 | Hobbs and Cobbing (2007) |
| Value(s) >DL | – | – | – | – | 0.0056 mg/L | – | – | |
| 0.002 mg/L | 6 | 6 | 2 | 0 | 10 | 1 | 18 | Hobbs et al. (2010) |
| Value(s) >DL | 0.398– 3.61 mg/L | – | – | – | 0.008 mg/L | – | – | |
| 0.001 mg/L | 3 | 0 | 17 | 0 | 33 | 1 | 53 | This study |
| Value(s) >DL | – | – | – | – | 0.01 mg/L | – | – | |

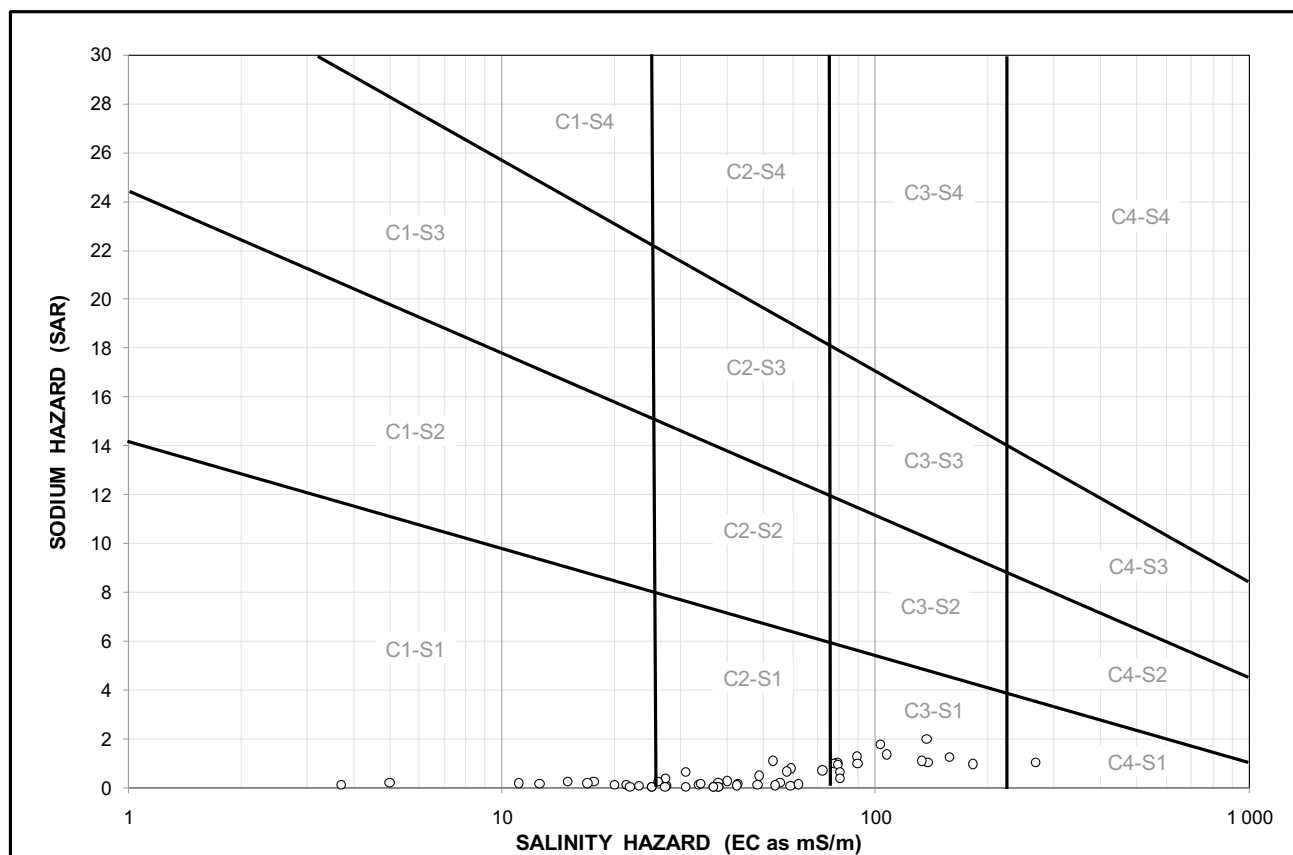
^aComprises both raw and treated/neutralized mine water

lake-internal geochemical transformation of solutes. The application of the UNESCO equation for deriving density from salinity and temperature data (Fofonoff and Millard 1983) as demonstrated by Wolkersdorfer (2008), assumes

non-reactive solutes and was shown by Moreira et al. (2011) to be inappropriate for modeling density-based stratification associated with reactive mineralized solutes, including iron and sulfate.

Table 10 Range of SAR values for basins/subcompartments

| Basin/subcompartment | Range of SAR values | | | | Classification per mean ^a |
|----------------------|---------------------|---------|------|---------|--------------------------------------|
| | <i>n</i> | Minimum | Mean | Maximum | |
| 1a | 6 | 0.07 | 0.27 | 0.65 | C2–S1 |
| 1b | 7 | 0.78 | 1.10 | 1.78 | C3–S1 |
| 1c | 11 | 0.40 | 0.99 | 1.99 | C3–S1 |
| 2a | 9 | 0.04 | 0.16 | 0.27 | C2–S1 |
| 2b | 7 | 0.11 | 0.50 | 0.91 | C2–S1 |
| 3 | 2 | 0.03 | 0.07 | 0.12 | C1–S1 |
| 4 | 2 | 0.03 | 0.03 | 0.04 | C2–S1 |
| 5 | 1 | | 0.03 | | C2–S1 |
| 6 | 2 | 0.09 | 0.10 | 0.12 | C2–S1 |
| 7 | 1 | | 0.03 | | C2–S1 |

^aWhere applicable**Fig. 49** Wilcox diagram illustrating the classification of groundwater chemistry in the study area for irrigation purposes

While the preceding discussion focuses on mine water lakes as intersected by shafts, the following discussion draws primarily on data generated from vertical physicochemical profiling carried out in monitoring boreholes. These facilities demonstrate varying degrees of mine water contamination as

manifested in natural aquifers, in particular the karst groundwater resource associated with the Malmani Sub-group dolomite that forms the Zwartkrans Basin in the downstream hydro-environment.

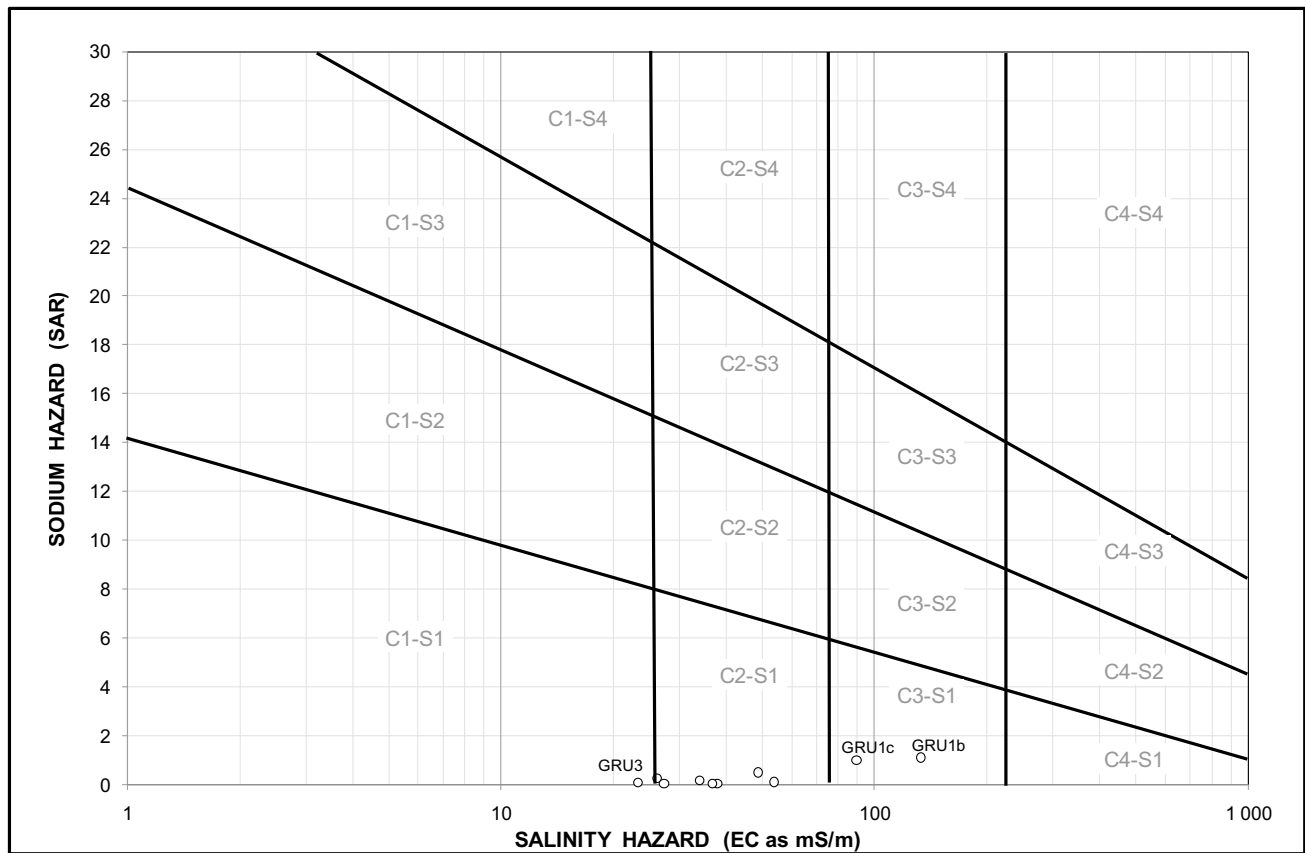


Fig. 50 Wilcox diagram illustrating the classification of groundwater chemistry per GRU for irrigation purposes

10.2 Methodology and Approach

The presence of vertical hydrochemical variation in a mine water or groundwater column was explored on the basis of profiles of the field variables EC, pH, ORP (oxidation–reduction potential or redox), and temperature measured on a number of occasions. The initial profiling was carried out by the DWS in late-2011 (October/November/December) in 22 monitoring boreholes (Table 11) using a YSI 6-series multiparameter sonde (model 600XLMD-BRC-DEEP, serial # 06K002D). The sonde was set to record a measurement every 5 s and lowered on a mechanically-driven winch running at ~ 0.05 m/s, giving a measurement every ~ 0.25 m. The instrument has a maximum operating head of 90 m. This was reached in only one borehole, namely GP00301 (Sect. 10.3.17).

The profiled boreholes are distributed in the southern part of the study area where stratification associated with poorer quality water ingress into the karst aquifer is more probable. The pattern and trend of mine water discharge into the karst environment since the start of gauged monitoring is shown in Fig. 51. The graph distinguishes between raw mine water (RMW) and treated/neutralised mine water (TMW), the aggregate of which represents the total mine water discharge.

The period during which the RMW contribution to total mine water discharge regularly exceeded 10 ML/d is clearly evident in Fig. 51. The DWS boreholes in the set (Table 11) had been sampled in early September 2011 following standard procedures that included purge pumping prior to sample capture only after stabilization of the field variables EC, pH, and temperature. Although these data provide a useful reference against which to evaluate the vertical profiling data as is discussed in the following sections, a different multiparameter sonde in the form of a CyberScan PC 10 pH/Conductivity meter was used (T. Moolman, personal communication). This limits a direct comparison of the respective results.

A second profiling run was carried out by the DWS in late-February 2013 with the same instrument used during the late-2011 profiling exercise. The 12 monitoring boreholes sampled on this occasion (Table 12) had been profiled following a routine sampling exercise carried out in mid-February 2013 during which the CyberScan PC10 multiparameter sonde was used for pH, conductivity, and temperature measurement.

Later profiling runs were carried out in June 2013 (Table 13), September and October 2013 (Table 14), and March 2014 (Table 15). The September and October 2013

Table 11 Summary of salient hydrophysical and hydrochemical data for monitoring boreholes subjected to vertical hydrochemical profiling in late-2011

| Station# | General location and station owner | Date profiled | Total depth ^a (m bs) | Rest water level depth (m bc) | Date sampled | Field variable value ^b | | |
|----------|------------------------------------|---------------|---------------------------------|-------------------------------|--------------|-----------------------------------|------------------|-------------------|
| | | | | | | SEC (mS/m) | pH | Temp (°C) |
| RG1 | Locus of decant; SG | 20/12/2011 | ~ 27 | 4.72 | Not sampled | Not available | | |
| RG2 | | | ~ 31 | 8.20 | | | | |
| RG3 | | | ~ 19 | 6.82 | | | | |
| MGP1 | Mine area; MG/MSA | | ~ 48 | 24.11 | | | | |
| MGP2 | | | ~ 59 | 34.66 | | | | |
| MGP3 | | | ~ 56 | 3.82 | | | | |
| GP00300 | Zwartkrans Basin; DWS | 19/10/2011 | ~ 36 | 21.70 | 05/09/2011 | 208 | 7.2 | 20.1 |
| GP00301 | | 21/10/2011 | ~ 148 | 58.77 | 05/09/2011 | 104 | 7.6 | 20.0 |
| GP00302 | | 01/11/2011 | ~ 33 | 21.98 | 06/09/2011 | 129 | 6.1 | 18.1 |
| GP00304 | | 04/11/2011 | ~ 53 | 44.74 | 06/09/2011 | 34 | 6.8 | 20.4 |
| GP00305 | KGR; DWS | 02/11/2011 | ~ 41 | 3.49 | 07/09/2011 | 67 | 5.9 | 18.7 |
| GP00306 | | 02/11/2011 | ~ 13 | 3.09 | 07/09/2011 | 276 | 6.0 | 17.5 |
| GP00307 | | 02/11/2011 | ~ 11 | 2.03 | 07/09/2011 | 257 | 6.5 | 15.8 |
| GP00308 | | 02/11/2011 | ~ 81 | 5.59 | 07/09/2011 | 38 | 7.3 | 19.6 |
| GP00309 | Zwartkrans Basin; DWS | 11/11/2011 | ~ 35 | 16.68 | 05/09/2011 | 261 ^c | 6.6 ^c | 18.8 ^c |
| GP00311 | | 21/10/2011 | ~ 119 | 68.38 | 05/09/2011 | 36 | 7.6 | 20.2 |
| GP00312 | | 21/10/2011 | ~ 23 | 7.14 | 05/09/2011 | 263 | 6.8 | 19.5 |
| GP00313 | | 11/11/2011 | ~ 36 | 20.34 | 07/09/2011 | 98 | 7.3 | 20.1 |
| GP00314 | | 01/11/2011 | ~ 13 | 3.46 | 06/09/2011 | 49 | 7.1 | 20.1 |
| A2N0583 | | 04/11/2011 | ~ 95 | 44.70 | 06/09/2011 | 32 | 7.0 | 20.6 |
| A2N0584 | | 01/11/2011 | ~ 55 | 21.87 | 06/09/2011 | 111 | 9.3 | 18.1 |
| A2N0586 | | 19/10/2011 | ~ 55 | 21.62 | 05/09/2011 | 172 | 7.3 | 20.5 |

^aDepth to which sonde was lowered on date profiled before encountering a terminating obstruction

^bAfter stabilization of variable value during purge pumping on date sampled

^cMeasured with a YSI 6-series model 600XLMD-BRC-DEEP multiparameter sonde

runs explored the influence of sampling activity on the post-sampling profile in the five DWS monitoring boreholes A2N0586, GP00300, GP00305, GP00309, and GP00313. The pre-sampling and post-sampling profiles carried out on 01/09/2013 and 22/10/2013, respectively, bracket the 01–03/10/2013 routine sampling exercise period. These results are discussed in the opening paragraphs of each of the relevant sections.

10.3 Results

The discussion of the individual profiling results follows the ‘south-to-north’ sequence described by the geographic location of the boreholes (Fig. 51).

The interrogation and discussion of the ORP measurements that form part of the profile data are subject to the caveat expressed in Text Box 1. The data are considered sufficiently valuable to present for their general interest and completeness rather than for their definitive substance. Such

a caution is also expressed by Montgomery et al. (2002) who state “... measurements of Eh in natural systems must be cautiously evaluated and not used strictly for calculations of chemical equilibria.”

Wolkersdorfer (2008) recognizes that the small diameter-to-length ratio of monitoring boreholes (compared to that of mine shafts) limits the influence of free convective flow on the water profile in such especially deep (>100 m) installations. The implication is that diffusion informs the hydrochemical profile in the standing water column in boreholes. It should be recognized, however, that the monitoring boreholes in this instance are mostly comparatively shallow (<50 m), and intersect natural aquifers rather than a mine void.

Finally, the evaluation of the profile data must also recognize the possible ‘disturbing’ influence on the water column by prior routine sampling. This is further complicated by the different ‘rest’ periods between sampling and profiling, viz. 6–8 weeks in late-2011 (Table 11), and ~2 weeks in February 2013 (Table 12). As already mentioned, the September and October 2013 runs explore this influence.

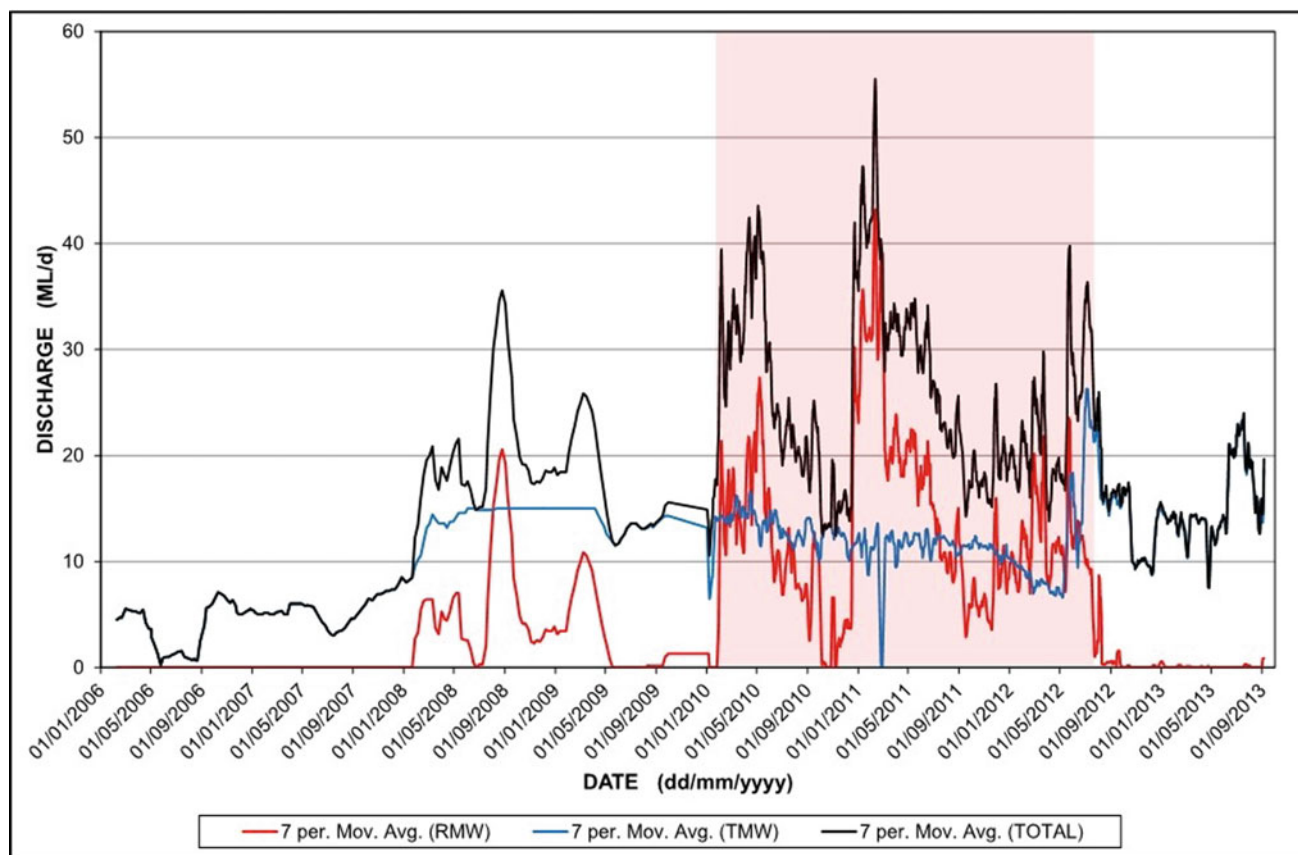


Fig. 51 Pattern and trend of mine water discharge into the karst environment (RMW = raw mine water; TMW = treated mine water)

Table 12 Summary of salient hydrophysical and hydrochemical data for monitoring boreholes subjected to vertical hydrochemical profiling in February 2013

| Station # | General location and station owner | Date profiled | Total depth ^a (m bs) | Rest water level depth (m bc) | Date sampled | Field variable value ^b | | |
|--------------|------------------------------------|---------------|---------------------------------|-------------------------------|--------------|-----------------------------------|-----|-----------|
| | | | | | | SEC (mS/m) | pH | Temp (°C) |
| CPS borehole | Mine area; SG | 26/02/2013 | ~ 60 | 49.56 | Not sampled | Not available | | |
| RG1 | | 26/02/2013 | ~ 27 | 4.52 | | | | |
| MGP1 | | 28/02/2013 | ~ 48 | 25.04 | | | | |
| MGP3 | | | ~ 56 | 4.10 | | | | |
| MGP4 | | | ~ 80 | 43.35 | | | | |
| GP00300 | Zwartkrans Basin; DWS | 28/02/2013 | ~ 36 | 21.41 | 21/02/2013 | 249 | 6.9 | 19.6 |
| GP00302 | | 26/02/2013 | ~ 33 | 22.00 | 19/02/2013 | 162 | 6.0 | 18.4 |
| GP00305 | KGR; DWS | 26/02/2013 | ~ 41 | 3.38 | 20/02/2013 | 76 | 5.6 | 19.3 |
| GP00309 | Zwartkrans Basin; DWS | 28/02/2013 | ~ 35 | 16.91 | 20/02/2013 | 304 | 7.0 | 17.3 |
| GP00313 | | 28/02/2013 | ~ 36 | 20.45 | 20/02/2013 | 125 | 6.9 | 20.2 |
| A2N0584 | | 26/02/2013 | ~ 55 | 21.94 | 19/02/2013 | 116 | 8.8 | 19.1 |
| A2N0586 | | 28/02/2013 | ~ 55 | 21.84 | 21/02/2013 | 192 | 6.9 | 19.9 |

^aDepth to which sonde was lowered on date profiled before encountering a terminating obstruction

^bAfter stabilization of variable value during purge pumping on date sampleable

Table 13 Summary of salient hydrophysical and hydrochemical data for monitoring boreholes subjected to vertical hydrochemical profiling in June 2013

| Station # | General location and station owner | Date profiled | Total depth ^a (m bs) | Rest water level depth (m bc) | Date sampled | Field variable value ^b | | |
|-----------|------------------------------------|---------------|---------------------------------|-------------------------------|--------------|-----------------------------------|-----|-----------|
| | | | | | | SEC (mS/m) | pH | Temp (°C) |
| GP00300 | Zwartkrans Basin; DWS | 06/06/2013 | ~ 36 | 21.74 | 27/06/2013 | 253 | 6.8 | 19.0 |
| GP00302 | | | ~ 33 | 22.20 | 25/06/2013 | 169 | 5.8 | 18.1 |
| GP00309 | | | ~ 36 | 16.86 | 25/06/2013 | 281 | 6.1 | 17.5 |
| GP00313 | | | ~ 37 | 20.60 | 26/06/2013 | 127 | 6.8 | 19.7 |
| A2N0584 | | | ~ 56 | 22.15 | 25/06/2013 | 118 | 8.4 | 18.4 |
| A2N0586 | | | ~ 77 | 22.19 | 27/06/2013 | 195 | 6.9 | 19.3 |

^aDepth to which sonde was lowered on date profiled before encountering a terminating obstruction

^bAfter stabilization of variable value during purge pumping on date sampled

Table 14 Summary of salient hydrophysical and hydrochemical data for monitoring boreholes subjected to vertical hydrochemical profiling in September and October 2013

| Station # | General location and station owner | Date profiled | Total depth ^a (m bs) | Rest water level depth (m bc) | Date sampled | Field variable value ^b | | |
|-----------|------------------------------------|---------------|---------------------------------|-------------------------------|--------------|-----------------------------------|-----|-----------|
| | | | | | | SEC (mS/m) | pH | Temp (°C) |
| GP00305 | KGR; DWS | 11/09/2013 | ~ 42 | 3.29 | 02/10/2013 | GP00305 | | |
| GP00300 | Zwartkrans Basin; DWS | | ~ 36 | 21.73 | | 80 | 7.2 | 18.3 |
| GP00309 | | | ~ 36 | 17.08 | 03/10/2013 | GP00300 | | |
| GP00313 | | | ~ 37 | 20.68 | | 249 | 6.8 | 19.2 |
| A2N0586 | | | ~ 90 | 22.16 | 02/10/2013 | GP00309 | | |
| GP00305 | KGR; DWS | 22/10/2013 | ~ 41 | 3.38 | | 261 | 6.7 | 20.4 |
| GP00300 | Zwartkrans Basin; DWS | | ~ 33 | 21.72 | 01/10/2013 | GP00313 | | |
| GP00309 | | | ~ 36 | 17.46 | | 131 | 6.9 | 19.6 |
| GP00313 | | | ~ 37 | 20.78 | 03/10/2013 | A2N0586 | | |
| A2N0586 | | | ~ 121 | 22.16 | | 210 | 7.1 | 19.5 |
| GP00302 | | | ~ 33 | 22.13 | 01/10/2013 | 249 | 6.8 | 19.2 |
| A2N0584 | | | ~ 55 | 22.09 | | 120 | 8.4 | 18.2 |

^aDepth to which sonde was lowered on date profiled before encountering a terminating obstruction

^bAfter stabilization of variable value during purge pumping on date sampled

Table 15 Summary of salient hydrophysical and hydrochemical data for monitoring boreholes subjected to vertical hydrochemical profiling in March 2014

| Station # | General location and station owner | Date profiled | Total depth ^a (m bs) | Rest water level depth (m bc) | Date sampled | Field variable value ^b | | |
|-----------|------------------------------------|---------------|---------------------------------|-------------------------------|--------------|-----------------------------------|-----|-----------|
| | | | | | | SEC (mS/m) | pH | Temp (°C) |
| GP00305 | KGR; DWS | 06/03/2014 | ~ 41 | 2.23 | 11/03/2014 | 76 | 6.1 | 18.6 |
| GP00300 | Zwartkrans Basin; DWS | | ~ 35 | 20.90 | 13/03/2014 | 249 | 7.2 | 19.6 |
| GP00302 | | | ~ 33 | 20.70 | 11/03/2014 | 194 | 6.5 | 18.1 |
| GP00309 | | | ~ 36 | 15.28 | 13/03/2014 | 301 | 7.8 | 19.5 |
| GP00313 | | | ~ 36 | 20.23 | 13/03/2014 | 132 | 7.2 | 20.1 |
| A2N0584 | | | ~ 55 | 21.24 | 11/03/2014 | 125 | 8.8 | 18.1 |
| A2N0586 | | | ~ 121 | 21.34 | 13/03/2014 | 183 | 7.3 | 20.1 |

^aDepth to which sonde was lowered on date profiled before encountering a terminating obstruction

^bAfter stabilization of variable value during purge pumping on date sampled

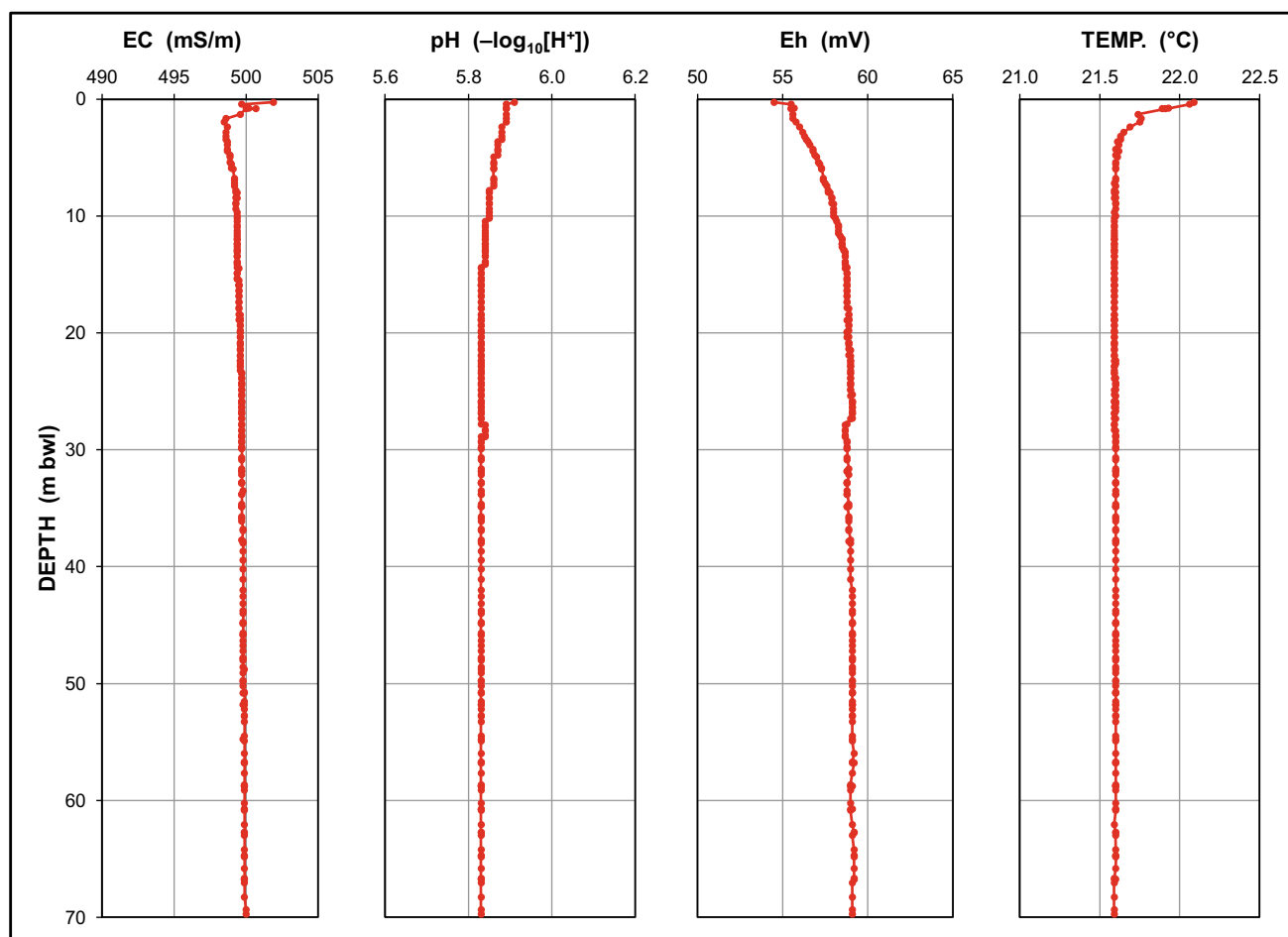


Fig. 52 Vertical profiles of field water chemistry variables in #18 Winze in October 2010

10.3.1 #18 Winze

Together with the BRI and #17 Winze, #18 Winze is one of three actively decanting shaft-like mine structures in the Western Basin (Plate 1). It is the most readily accessible of these structures for vertical profiling purposes. The results provide an example of the patterns associated with the profiled variables in this structure. It would be unreasonable, however, to view the profiling results as typical of all such structures in the Western Basin. It is also indefensible to extrapolate the profiling results to mine shafts in which the mine water rest level occurs tens of meters below surface, and which will never manifest active decant. The depth of ~70 m reached by the probe indicates that this structure extends at least this vertical distance into the subsurface. It is also reasonable to expect that the structure is lined with brickwork to at least this depth. The $\sim 2 \times 4$ m (~ 8 m²) rectangular shape of the structure decants at a rate of 10–25 ML/d (Plate 1), which equates to an upward flow velocity of ~ 0.01 – 0.04 m/s. These circumstances define the structure-specific hydrodynamic environment in which the profiling was carried out.

The profiles presented in Fig. 52 reflect a remarkably constant pattern over the entire water column profiled. The SEC value of 500 mS/m represents an unmistakable mine water signature which is accompanied by a pH value of little more than 5.8. The pH value is surprising under circumstances where raw mine water is typically characterized as highly acidic, i.e., pH < 5.0. It is reasonable to presume that the pH value of 5.8 characterizes that of the raw mine water rising from depth in the mine void. Its rapid drop to a pH of < 4.0 and even < 3.0 within tens of meters of the decant position exemplifies the rapidity of the hydrolysis reaction.

10.3.2 CPS Borehole

The CPS (Central Power Station) borehole is located ~250 m south of the overflow of the CPS pit and 1400 m south of #8 Shaft. The borehole is an old mine rescue facility, and would therefore have intersected underground mine workings at depth (B. van der Walt, personal communication). The interest in this borehole is its proximity to the CPS pit that is used as a settling facility for the

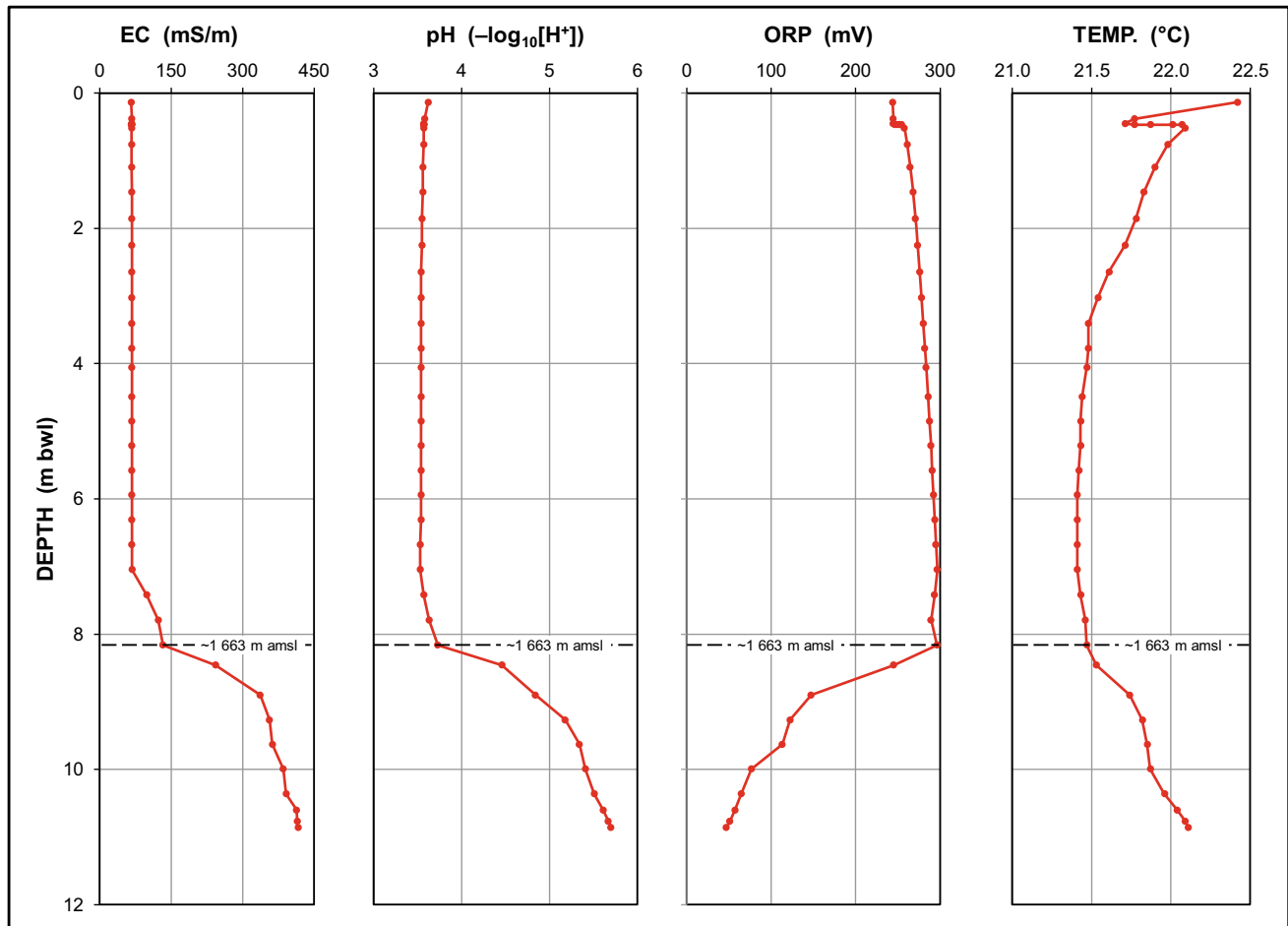


Fig. 53 Vertical profiles of field water chemistry variables in the CPS borehole in February 2013

sludge produced by the mine water treatment plant. A video log of the borehole revealed its construction to comprise plain steel casing to a depth of ~57 m bs (~1663 m amsl) (N. de Meillon, personal communication). The rest water level depth of 49.1 m bs equates to an elevation of ~1671 m amsl that correlates with the similar contemporary mine water elevation observed in the nearby #8 Shaft (Fig. 51).

The profiles presented in Fig. 53 indicate the borehole to be accessible to a depth of only ~60 m bs (~11 m bwl). Each profile also indicates a shift in trend at a depth of ~8 m bwl (~1663 m amsl). This shift is characterized by a dramatic increase in SEC (by ~350 mS/m) and pH (by ~2 pH units), and a substantial drop in ORP value (by ~250 mV). If the higher SEC and pH and lower ORP at depth is attributed to a mine water influence derived from the flooded mine workings, which observation finds support in the #18 Winze profile results for SEC, pH, and ORP (Fig. 52), then the overlying less saline, more acidic and more oxic conditions characterize the stagnant water column confined to the cased section of the borehole.

10.3.3 Borehole RG1

The December 2011 vertical profiles (Fig. 54) reflect a distinct change at a depth of ~17 m bwl (~22 m bs; ~1646 m amsl). This depth does not coincide with the top of the piezometer perforated interval, which extends from a depth of 22 m bwl (27 m bs; ~1641 m amsl) to the original end-of-hole at 31 m bs (36 m bs; ~1632 m amsl). The profile depth data indicate that the borehole is currently only accessible to a depth of ~23 m bwl (~28 m bs; ~1640 m amsl), having lost 8 m possibly due to caving or siltation. The SEC value increases from a constant ~45 to ~330 mS/m over a depth interval of only ~6 m. The temperature profile increases by ~1.0 °C in this interval. In the lower portion of this interval (21–23 m bwl; <1642 m amsl), the pH and ORP profiles reflect a sharp change characterized by a decrease in pH values by 3.5 pH units and an increase in ORP values by ~430 mV.

The February 2013 profiles for SEC, pH and ORP reveal a significant change from the December 2011 profiles. This change marks a migration of the fresh/saline water interface and the neutral/acidic water interface up the water column by

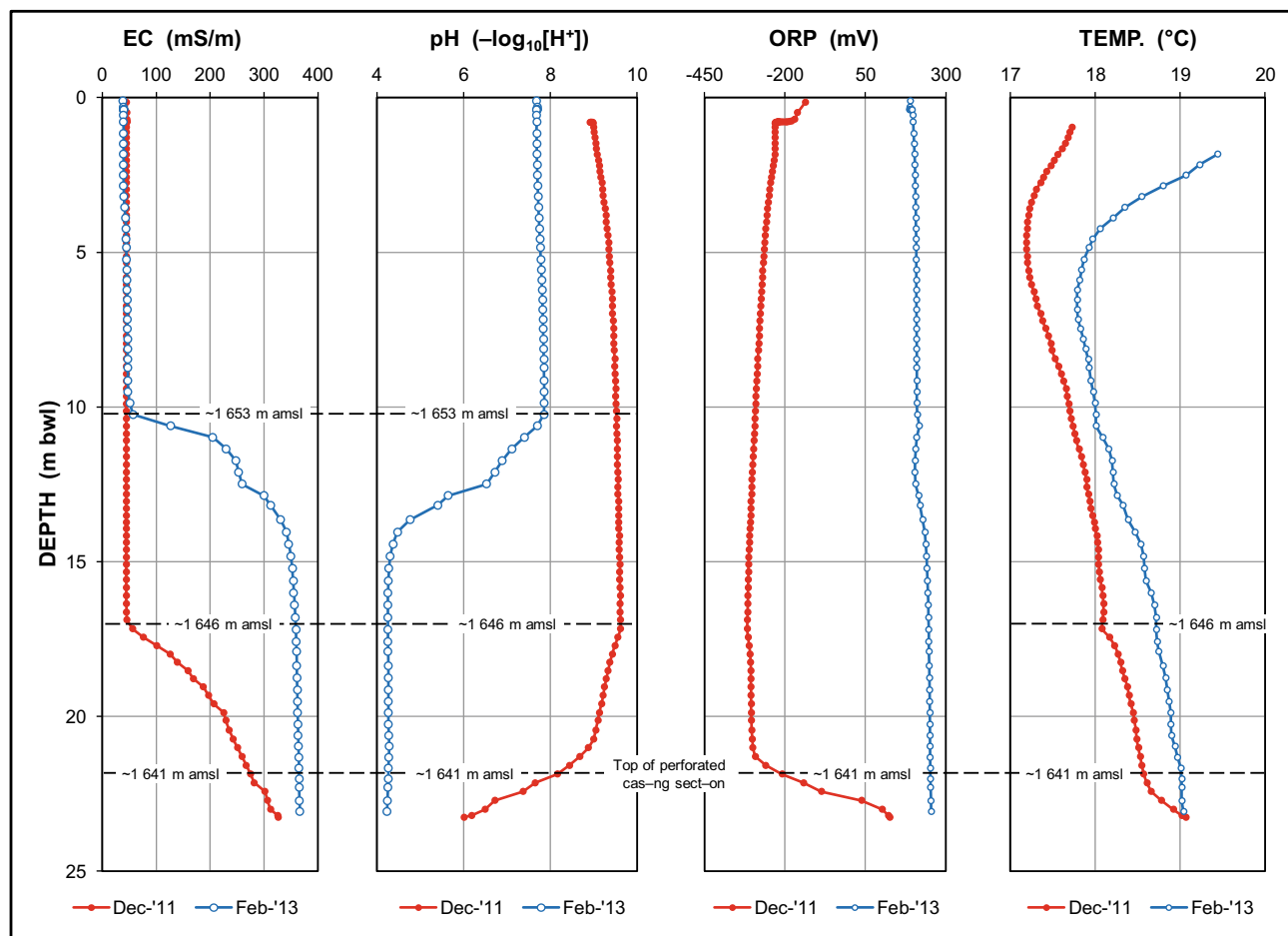


Fig. 54 Vertical profiles of field water chemistry variables in borehole RG1

~8 m. The change in ORP marks a shift toward a uniform more oxidizing condition across the entire water column. The temperature profile for the most part reflects a uniform positive shift of ~0.5 °C, suggestive of exothermic reactions driving a shift to oxidizing (aerobic) conditions generating a more acidic groundwater. The common mid-summer period of profiling negates a seasonal cause for the temperature shift.

The RG1 profiles unequivocally identify a zone (or at least the upper portion thereof) of impacted preferential groundwater flow at this location. The upward 'growth' in SEC and pH of this zone together with the ORP profile transition from strongly reducing (anoxic) to moderately oxidizing (oxic) conditions in a period of 14 months, seriously challenge an understanding of the geochemical (biogeochemical?) processes that occur in the subsurface of a karst environment impacted by acid mine water.

The constant and low SEC in the upper 10 m of the water column, compared to the steeply increasing SEC below this depth, highlights the potential misrepresentation of the

groundwater salinity (and probably also water chemistry) at this location based on a grab sample taken from <10 m bwl. This is exemplified by the results of routine chemical analyses reported by SG for the groundwater obtained from this borehole (Sect. 2.3.1).

10.3.4 Borehole RG2

The 'unremarkable' profiles (Fig. 55) are readily explained by the very weak yield (<0.2 L/s) as determined in 2007 when this borehole was subjected to purge pumping for water sample collection purposes. The borehole is therefore assessed as being in poor hydraulic connection with the contaminated karst aquifer of the dolomitic outlier. As a consequence, any water quality data obtained from this borehole must be viewed with caution because of its 'isolated and non-representative' nature. Nevertheless, the comparatively low pH of 4.8 is not readily explained under circumstances where the SEC of ~37 mS/m does not reflect a mine water influence at this location.

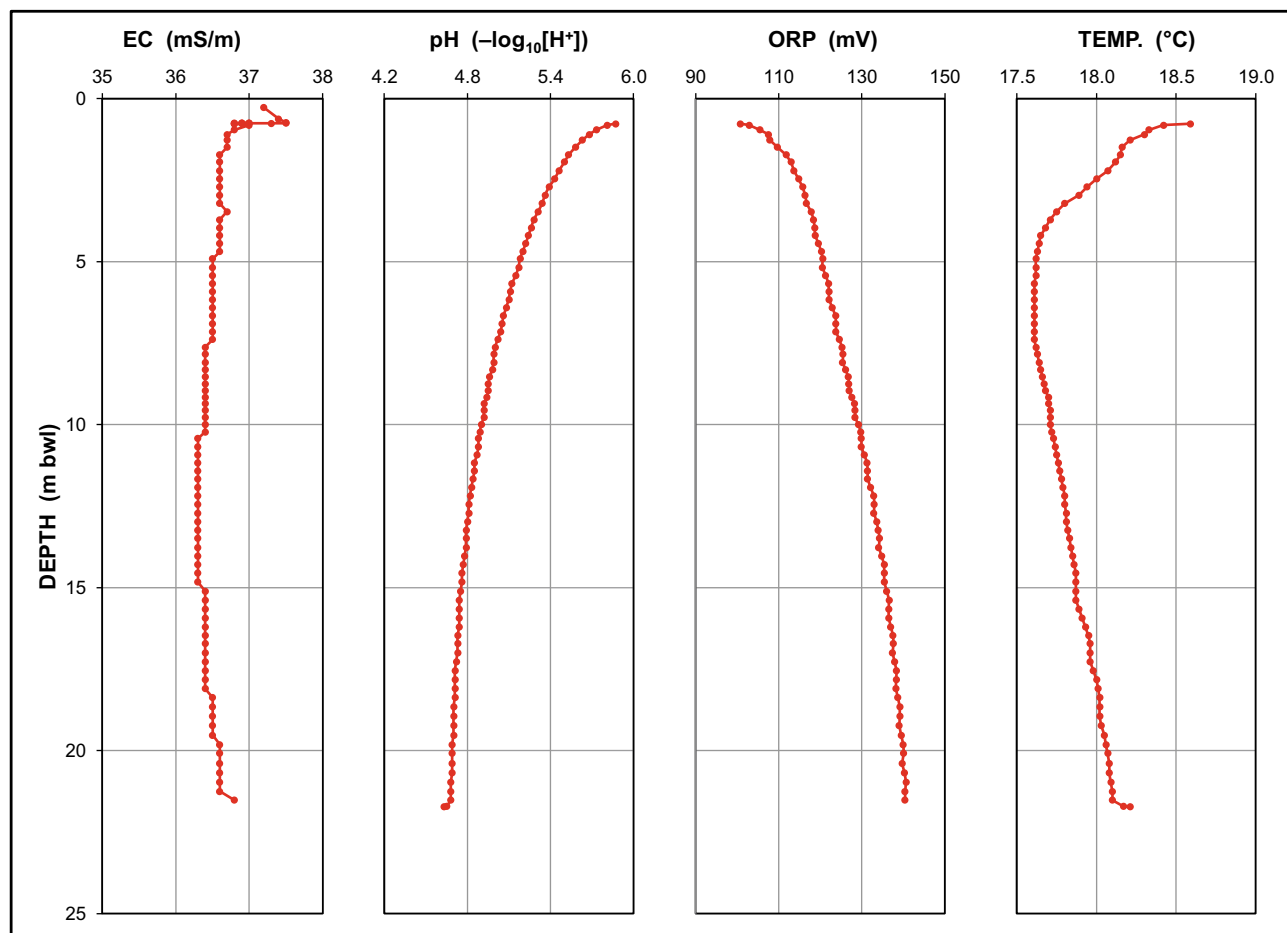


Fig. 55 Vertical profiles of field water chemistry variables in borehole RG2 in December 2011

10.3.5 Borehole RG3

The profiles obtained for this borehole are as ‘unremarkable’ as for borehole RG2, except for the very low (~ 9 mS/m) SEC values (Fig. 56). The latter suggests that there is no influence of mine water at this location ~ 150 m west of the Tweelopie Spruit, despite the groundwater level elevation of ~ 1657 m amsl in the borehole equaling the streambed elevation. Together with the slightly acidic pH values (~ 6.5), these results rather indicate an association with natural quartzitic groundwater most likely related to the West Rand Subgroup strata. The latter form the enclosing older strata along the western margin of the dolomite outlier. These strata are earmarked for future extraction, by the opencast mining method, of the gold and uranium reserves associated with the Government Reef in this area.

10.3.6 Borehole MGP1

The location of this borehole to the north of the West Wits Pit places it in the subsurface flow path of water that might drain from this opencast mining feature along the NE–SW striking (Fig. 6 in Chapter “Description of the Physical

Environment”) and steeply SSE-dipping (Fig. 7 in Chapter “Description of the Physical Environment”) Kimberley Reefs exploited by the West Wits Pit workings. The depth of ~ 49 m (Table 11) places the base of the borehole at an elevation of ~ 1651 m amsl, i.e., below the Tweelopie Spruit valley bottom of ~ 1657 m amsl to the west. With a groundwater level elevation at ~ 1676 m amsl, the profiles (Fig. 57) indicate changes in EC, pH, and ORP below an elevation of ~ 1666 m amsl. These changes are not evident in the temperature profile.

The profiles indicate a shift in EC and pH values between December 2011 and February 2013. The EC and pH shifts are again to more saline and more acidic conditions, respectively. Further, the step in EC values also reflect a vertical upward shift as was observed in boreholes RG1 (Fig. 54) and GP00305 (Fig. 62). The ORP shift is toward a more uniform vertical distribution of redox values that occupy a narrower range (240–280 mV) than that of the earlier December 2011 profile (220–320 mV). The temperature profiles are virtually identical over 80% of the water column.

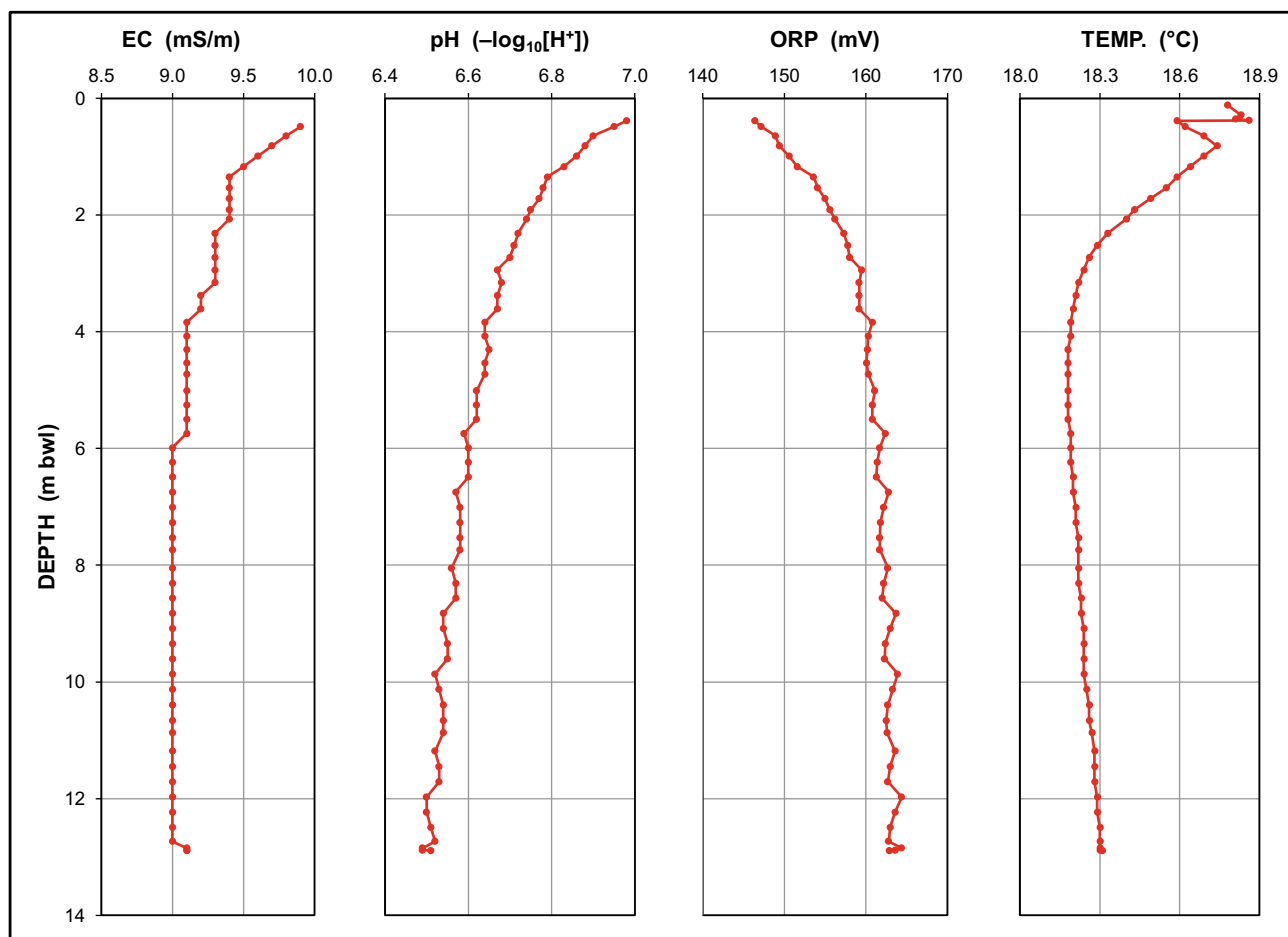


Fig. 56 Vertical profiles of field water chemistry variables in borehole RG3 in December 2011

The elevated SEC and low pH values associated with the deepest horizon suggest the influence of an acid mine water presence. The relatively constant SEC values of <50 mS/m in the upper 10 m of the profile, compared to the >100 mS/m in the lowest horizon, again highlights the potential misrepresentation of the groundwater salinity and chemistry at this location based on a grab sample taken from a shallow depth (<10 m) below the water level. It is shown in later sections (e.g., Sect. 10.3.16) that even a sample obtained after purge pumping might not provide a representative value for the variables EC, pH, ORP, and temperature (among others). The use of non-representative hydrochemical data presents another (and very basic) challenge to an understanding of the hydrogeochemical processes that occur in the subsurface.

10.3.7 Borehole MGP2

Located adjacent to the north-western rim of the West Wits Pit, this borehole also targets any possible mine water migration from the opencast facility. The profiling results (Fig. 58) show a hydrochemical profile characterized by an

acidic (pH ~ 4.5) fresh groundwater (SEC <15 mS/m) in a strongly oxidizing environment (ORP >400 mV). Except for the lower SEC, this is similar to that of borehole MGP1 (Fig. 57). The most plausible explanation for the low SEC and pH values is the possible association of this groundwater with the quartzitic strata of the Central Rand Group in the Witwatersrand Supergroup at this location. It should also be noted that the borehole is located on the north-western flank of the West Wits Pit workings, which places it in an unfavorable position relative to the hydrogeologic regime of the West Wits Pit as described for borehole MGP1 (Sect. 10.3.6). Together with the relatively shallow depth of 59 m (Table 11), these circumstances militate against the manifestation of an acid mine water presence at this location.

10.3.8 Borehole MGP3

The location of this borehole in the dolomite outlier provides a second opportunity (with borehole RG1) to evaluate the dynamic of the hydrogeochemical environment impacted by mine water. The profiles of this borehole (Fig. 59) indicate that SEC reaches and then maintains a maximum value of

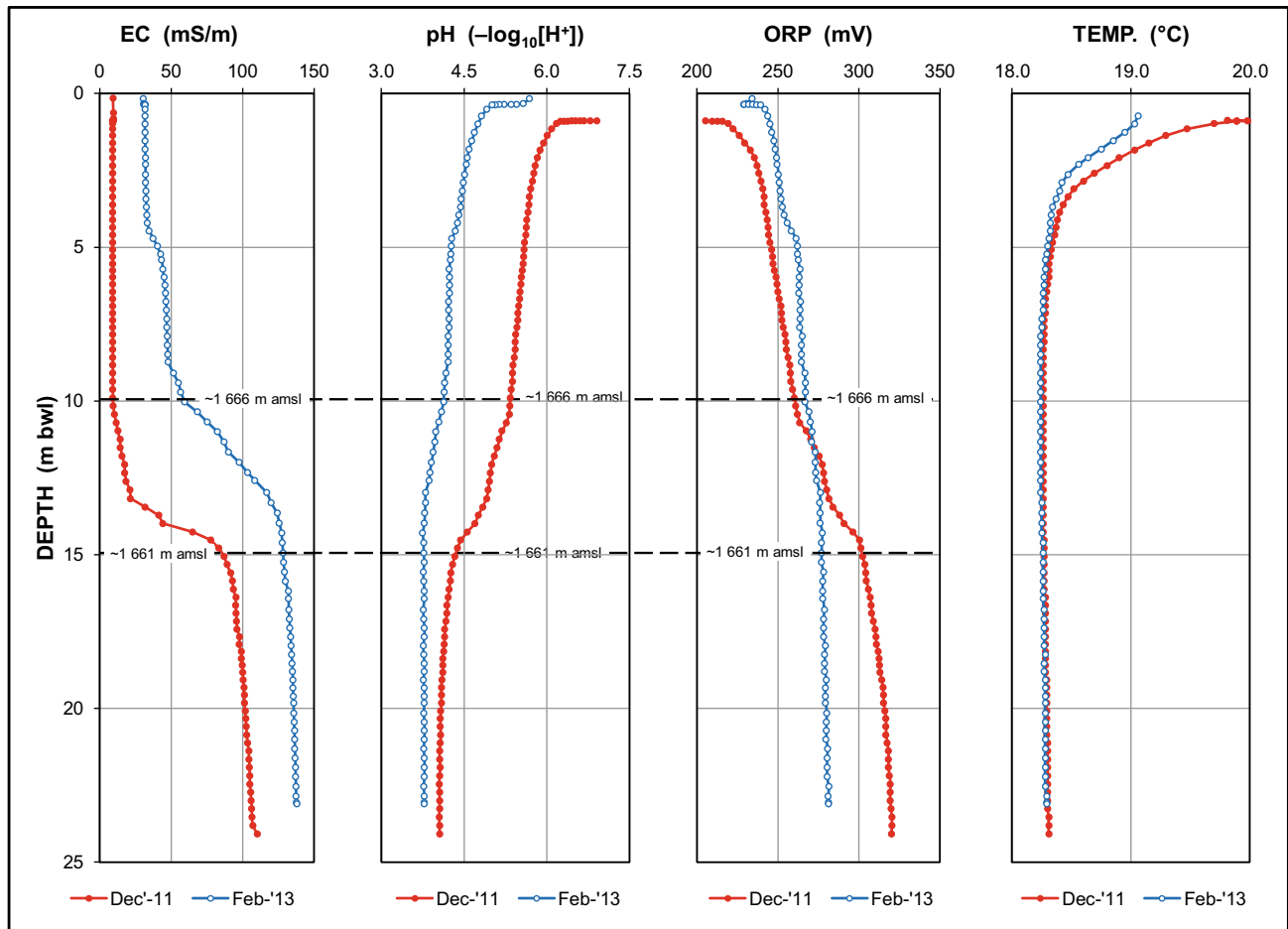


Fig. 57 Vertical profiles of field water chemistry variables in borehole MGP1

270–300 mS/m at a depth of ~20 m bwl (~24 m bs, ~1632 m amsl) which corresponds with the depth of the first water strike (Mothoa and Lombaard 2008).

The pH profiles on the two profiling occasions are similar, the February 2013 profile reflecting a shift to a slightly more acidic condition below ~1639 m amsl. This shift is accompanied by a prominent ORP shift to more oxic conditions. An anomaly in the February 2013 ORP profile at an elevation of ~1639 m amsl is identified, and a plausible adjustment is applied. The temperature profiles are practically identical over >80% of the water column.

The measure of congruence between the MGP3 and RG1 borehole profiles is explored in Fig. 60. The data sets have been normalized to absolute elevations on the vertical axis. The horizontal axes represent common scales. The groundwater rest level elevations of ~1662 and ~1651 m amsl in boreholes RG1 and MGP3, respectively, are evident in the profiles. The water table elevation in borehole MGP3 approximates the Tweelopie Spruit streambed elevation at this location. The difference of ~11 m between the water table elevations (the tops of each profile) in the two

boreholes reflects the hydraulic gradient of 0.022 that exists over the ~500 m distance between the two boreholes.

The congruence shown by the MGP3 profiles is discussed earlier in this section. Similarly, the geometry and interpretation of the RG1 profiles have been discussed in section. The purpose of Fig. 60 is to establish whether any congruence exists between boreholes RG1 and MGP3 given their locations within the dolomite outlier that hosts the locus of decant.

The assessment is somewhat constrained by the comparatively shallow depth (~25 m) of borehole RG1. Nevertheless, Fig. 60 suggests that the shallower profiles of RG1 represent an exaggerated form of the MGP3 profiles. For example, the step in SEC values from ~40 to ~350 mS/m at an elevation of ~1640 to ~1650 m amsl in RG1 is an exaggeration of the step from ~200 to ~300 mS/m at an elevation of ~1635 m amsl in MGP3. Similarly, the steps in pH and ORP are of greater magnitude in RG1 than in MGP3. Finally, the increase in temperature with depth is greater in RG1 than it is in MGP3. The similar pattern and trend shown by the profiled variables is therefore evident.

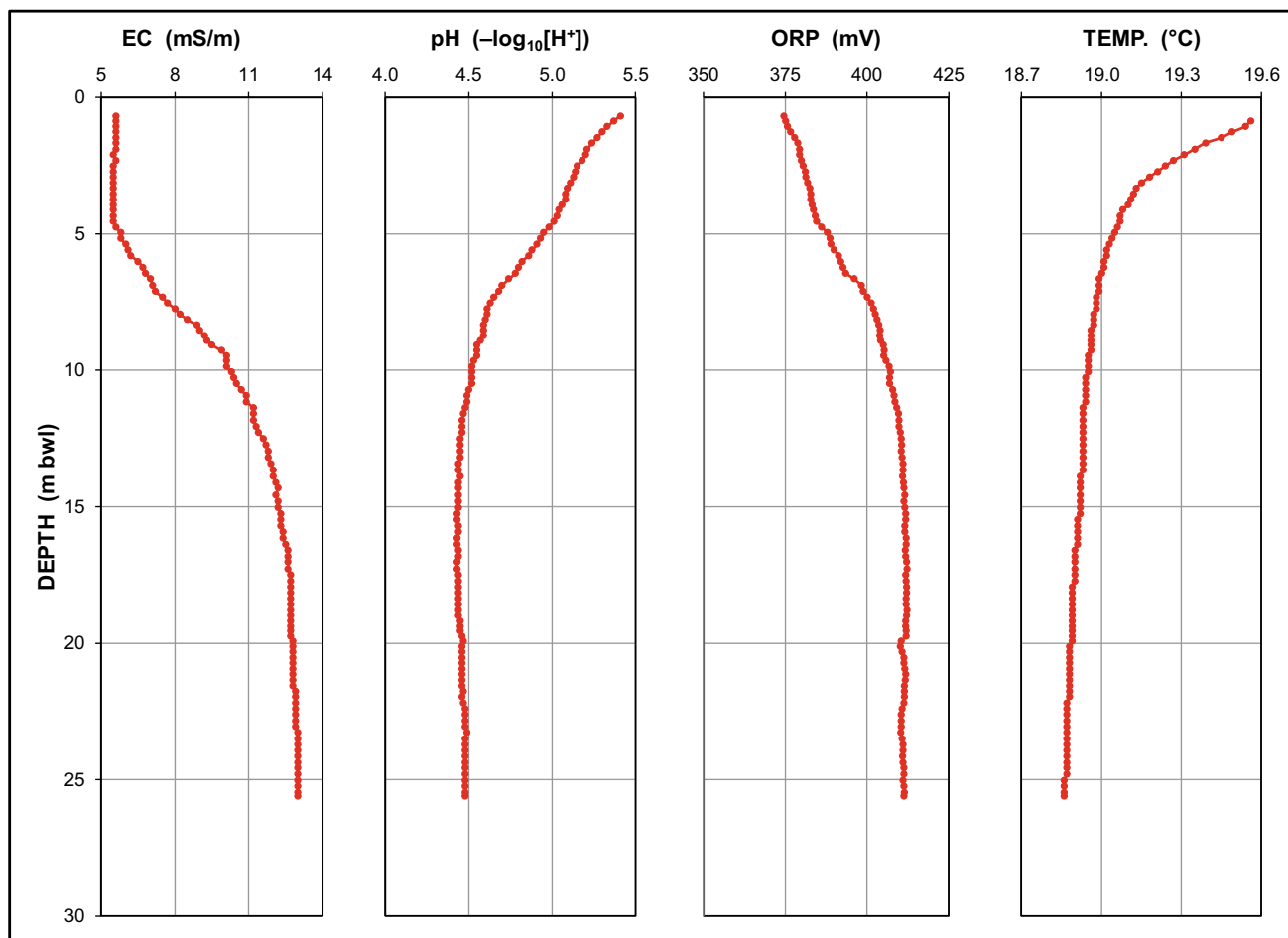


Fig. 58 Vertical profiles of field water chemistry variables in borehole MGP2 in December 2011

The profiles indicate that some measure of isotropy and homogeneity exists in the otherwise heterogeneous and anisotropic karst environment of the dolomitic outlier. The influence of factors such as borehole construction, e.g., depth, type, placement of casing, etc. on the profiles has not been investigated.

10.3.9 Borehole MGP4

This borehole is located on the south-eastern flank of the West Wits Pit and was established to meet the DWS directive that informs the disposal of high-density sludge generated by the refurbished and upgraded SG mine water treatment plant into this excavation. As in the case of borehole MGP2 (Sect. 10.3.7), its location places it in an unfavorable position relative to the hydrogeologic regime of the West Wits Pit as described for borehole MGP1 (Sect. 10.3.6). Despite its substantial depth of 80 m (Table 12), these circumstances militate against the manifestation of an acid mine water presence at this location, at least at the time of profiling in early-2013. This finds support in the fresh (SEC 15–21 mS/m) and slightly acidic (pH 4.5–

5.5) groundwater (Fig. 61) that is characteristic of the very weakly buffered quartzitic groundwater encountered in the West Rand Group strata of the Witwatersrand Supergroup (Sect. 2.1.1).

10.3.10 Borehole GP00305

Located in the southern portion of the KGR, this borehole penetrates the quartzite of the West Rand Group that forms the SW–NE striking ridge through the reserve. Water strikes at depths of ~25 and ~39 m bs (1608 and 1594 m amsl) inform a better understanding of the hydrochemical profiles.

The influence of purge pumping for routine sampling purposes on the pre- and post-sampling profile is explored in Fig. 62. The results suggest that purge pumping exerts little influence on the pH and temperature profiles, but causes significant shifts in SEC and ORP. The SEC profile reflects an upward migration by ~10 m of the SEC increase from ~40 mS/m in the upper section of the water column, to ~90 mS/m in the lower section of the water column.

The coincidence of the pH and ORP inflection points at ~22 m bwl (~1608 m amsl) with the first water strike is

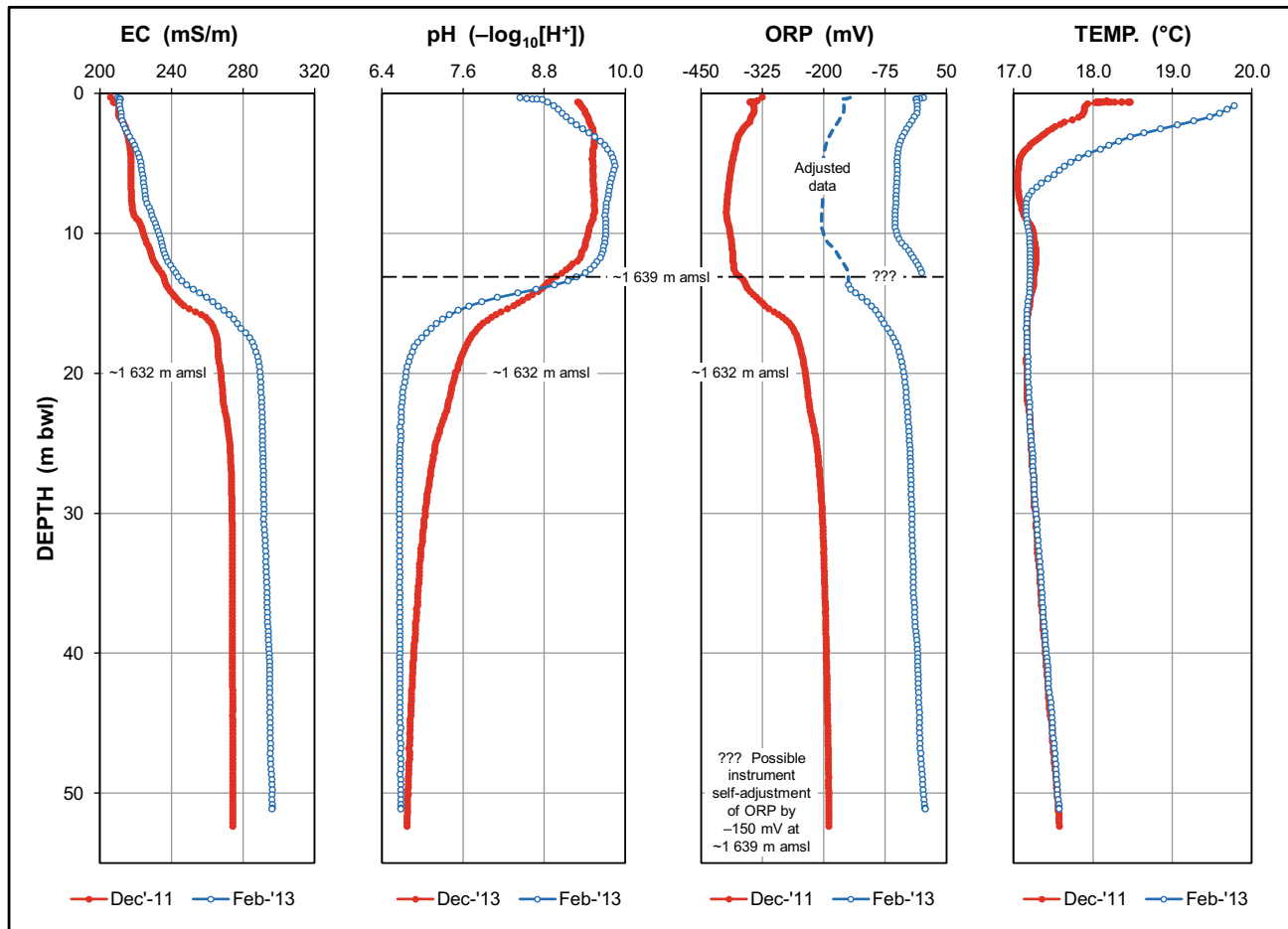


Fig. 59 Vertical profiles of field water chemistry variables in borehole MGP3

noteworthy. It is below this level in the borehole that the pH trend becomes negative and the ORP trend becomes positive. The association of these circumstances with an elevated SEC value of ~ 90 mS/m suggests a mine water influence rather than the naturally acidic but extremely fresh groundwater that characterizes the quartzitic strata in the study area (Sect. 2.1.1). The SO_4 concentrations of $\sim 300\text{--}350$ mg/L and Fe concentration of ~ 20 mg/L returned by recent chemical analyses of groundwater from this borehole provide substantiation in this regard.

The results of five profiling exercises are shown in Fig. 63. Only the temperature profiles below ~ 5 m bwl would appear to be consistent over time. The SEC, pH and ORP profiles exhibit a temporal variance that is difficult to explain. A noteworthy aspect of the SEC profile is the congruence exhibited by the earliest (November 2011) and the latest (March 2014) profiles, compared to the stepped nature of the other SEC profiles. The development and progression of the stepped character of the intermediate SEC profiles, however, is not readily explained, nor are the ostensibly random patterns that characterize the pH and ORP

profiles. For example, the negative ORP excursions at depths of ~ 5 , ~ 15 , and ~ 23 m bwl do not follow a temporal pattern, being manifested first at ~ 15 m bwl in February 2013, then at ~ 23 m bwl in September 2013, and most recently at ~ 5 m bwl in March 2014.

10.3.11 Borehole GP00306

Borehole GP00306 located on the east (right) bank of the Tweelopie Spruit in the southern portion of the KGR, targets the northern end of the dolomitic outlier. The very saline character (SEC ~ 328 mS/m) of the groundwater across the entire water column in this shallow (13 m) borehole indicates the well-mixed character of the groundwater in the saturated profile of the aquifer at this location. This is also true for the pH and the ORP profiles (Fig. 64), which reflect acidic and reducing conditions, respectively. The low pH value is of particular concern, as it indicates the lack of alkalinity in the karst system to maintain neutralization (buffering) of the acidic mine water entering this aquifer. This ‘deficiency’ might be attributed to the highly leached nature of the dolomite intersected in this profile.

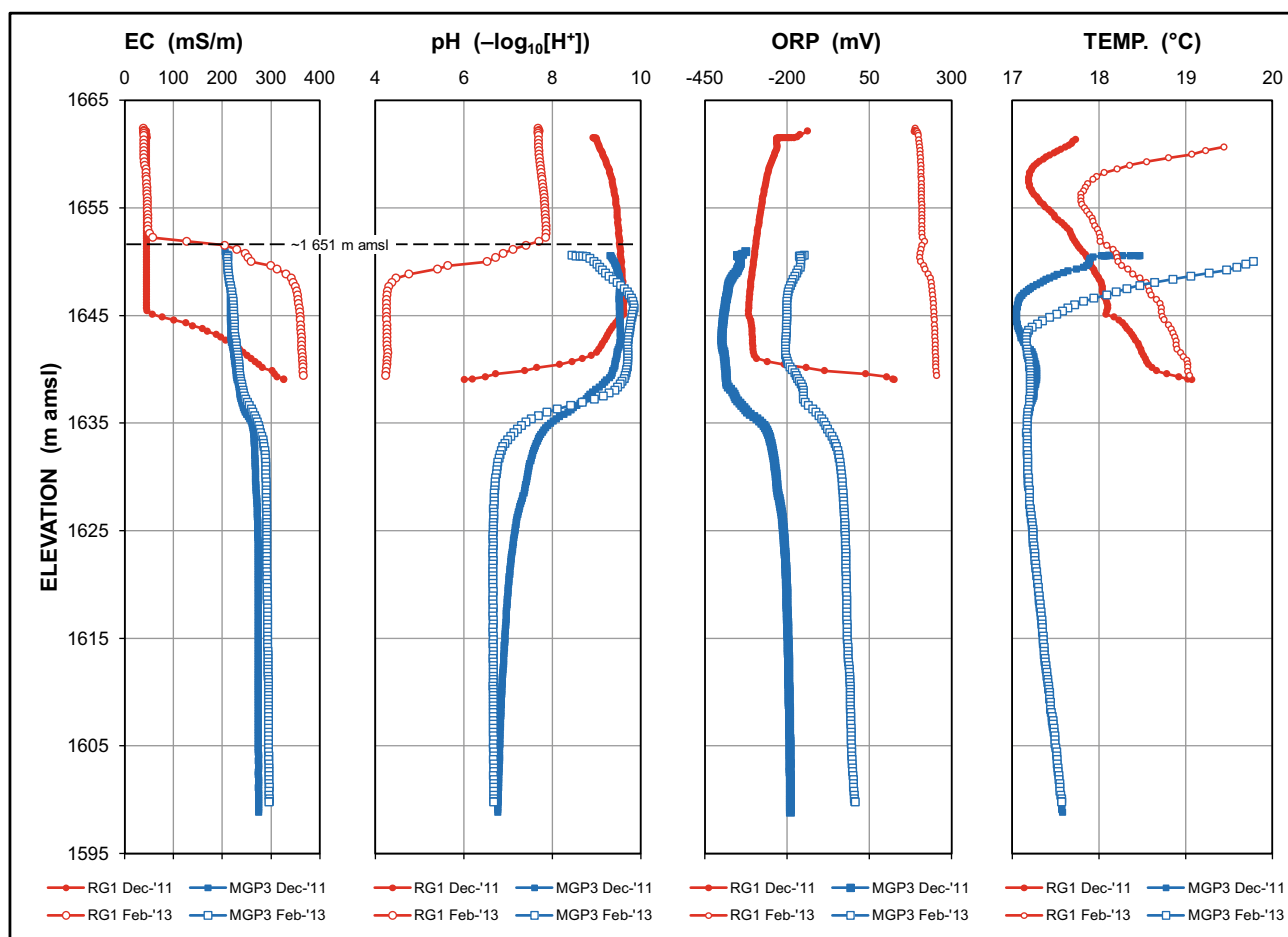


Fig. 60 Comparison of contemporary field water chemistry variable profiles in boreholes RG1 and MGP3 on two occasions

A comparison of the profile values with those of the September 2011 sampling exercise (Table 11) shows a slight discrepancy. In regard to SEC, this is represented by a profile value of 328 mS/m compared to 276 mS/m of the sample. A more pronounced difference in temperature of $<16.5^{\circ}\text{C}$ (profile) compared to 17.5°C (sample) is observed. The pH values, however, are similar at 6.1 (profile) and 6.0 (sample). An explanation of these differences is not readily apparent unless it is associated with the use of two different instruments as described in Sect. 10.2. This possibility, however, is not afforded much credence under circumstances where different instruments are more likely to return disparate pH values rather than either SEC or temperature values.

10.3.12 Borehole GP00307

Located on the west (left) bank of the Tweelopie Spruit in the KGR, this borehole explores the karst aquifer of the Zwartkrans Basin at the confluence of this stream with a

'blind' drainage that enters the KGR from the south-west. The SEC profile (Fig. 65) clearly reflects a mine water influence with values of ~ 335 mS/m. The pH of 6.7 at depth, however, suggests the presence of buffering that might be attributed to the better quality karst groundwater contributed by the 'blind' drainage.

The temperature profile shows a marked decrease from $\sim 17^{\circ}\text{C}$ near the water table to $\sim 14.5^{\circ}\text{C}$ at >6 m bwl, a rate of -0.4°C/m . Neither the pH nor ORP profiles indicate extraordinary trends that might suggest a subsurface environment favoring endothermic reactions that could drive a decrease in temperature of this magnitude.

10.3.13 Borehole GP00308

Borehole GP00308 is located at the northern end of the KGR on the right bank of the Tweelopie Spruit ~ 50 m from the stream. This borehole yielded little more than seepage water encountered at a depth of ~ 54 m bs (~ 49 m bwl;

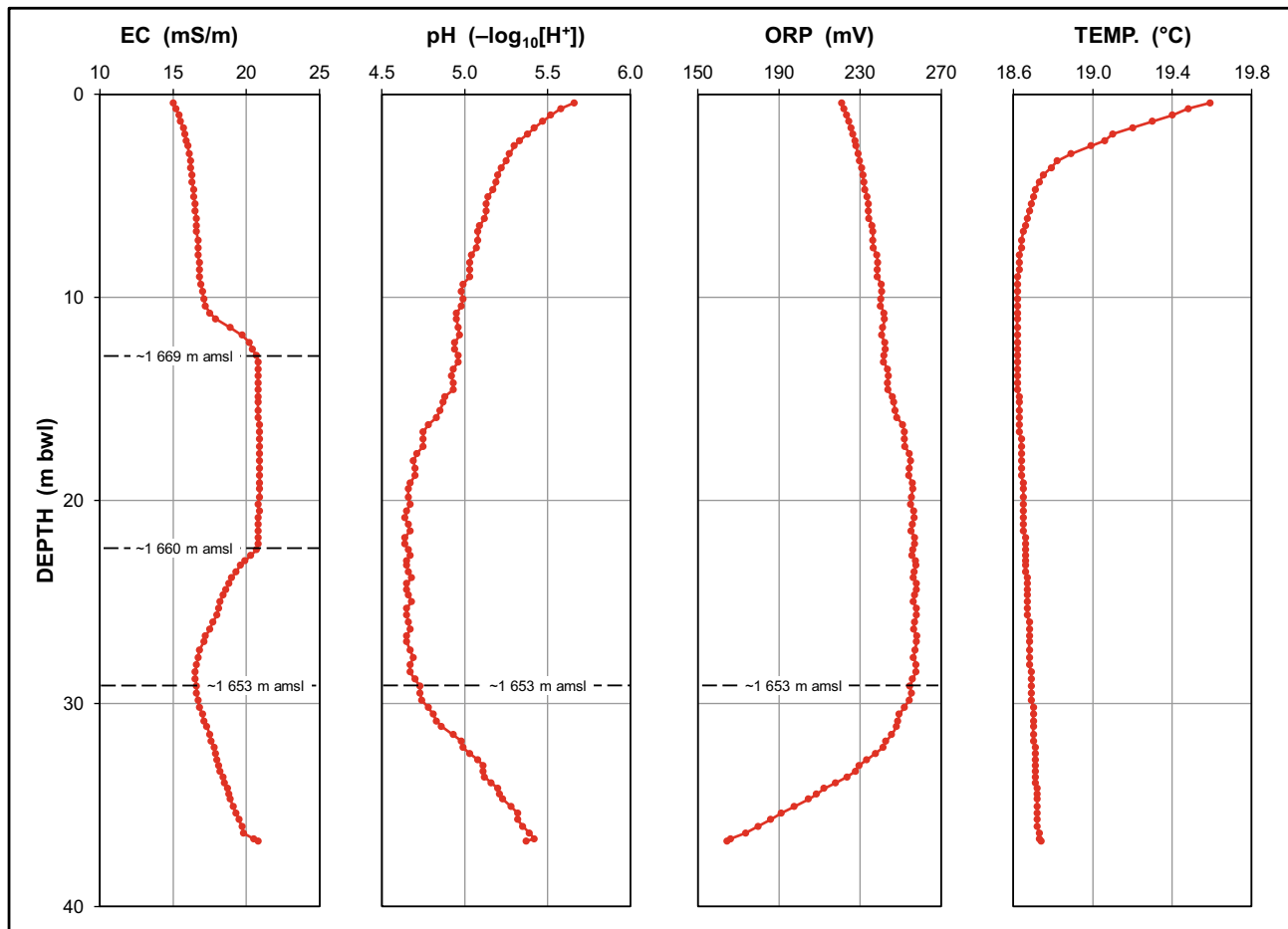


Fig. 61 Vertical profiles of field water chemistry variables in borehole MGP4 in February 2013

~1471 m amsl). These circumstances and the competence of the fresh chert-poor dolomitic strata informed the completion of the bore as an open hole except for 19 m of plain steel casing at the top.

The profiles, in particular those of SEC, pH, and ORP (Fig. 66) exhibit distinct ‘anomalies’ in the interval 50–57 m bwl (55–62 m bs, ~1470–1463 m amsl) located immediately below the seepage water strike zone. The pattern of the ORP anomaly in this interval is similar to that observed in two other boreholes, namely A2N0583 (Fig. 67) and GP00311 (Fig. 78). The increase in SEC from ~40 to ~65 mS/m at depth in this borehole is not considered to reflect a mine water influence on the basis of the mutual increase in pH. A further anomalous pattern is reflected in the pH and ORP profiles which are similar and, except at $\sim 1466 \pm 3$ m amsl, unlike the mirror-like images observed in most of the other profiles. This pattern might be associated with the static nature of the groundwater environment intersected by the borehole, the insignificant yield indicating a very low transmissivity and poor hydraulic connectivity.

10.3.14 Boreholes A2N0583 and GP00304

Located to the west of the KGR in the area of the Beckedan Smallholdings, this set of boreholes represents the hydrochemical profile where ostensibly no mine water impact²⁵ is manifested at the time (November 2011) of profiling. The similar surface elevations (~1594 m amsl) and depths to groundwater rest level (~44 m bc) of the boreholes again negate the need to normalize the data sets to a common datum.

The profiles (Fig. 67) reflect some measure of congruence and values that are indicative of a natural karst groundwater. This supports information generated for this portion of the study area that is exemplified in the chemistry of water discharged from the seeps that feed the Flip-se-Gat drainage in the KGR. These seeps deliver a combined perennial yield of 8–12 L/s characterized by an SEC of ~25 mS/m, a pH of ~8.0, and an Eh of –84 mV (Table 7). The deeper

²⁵ It is shown in Sect. 2.2 and Volume 2 that a gradual but persistent mine water impact is manifested at station A2N0583 as reflected in a doubling of the SO₄ concentration since 2004.

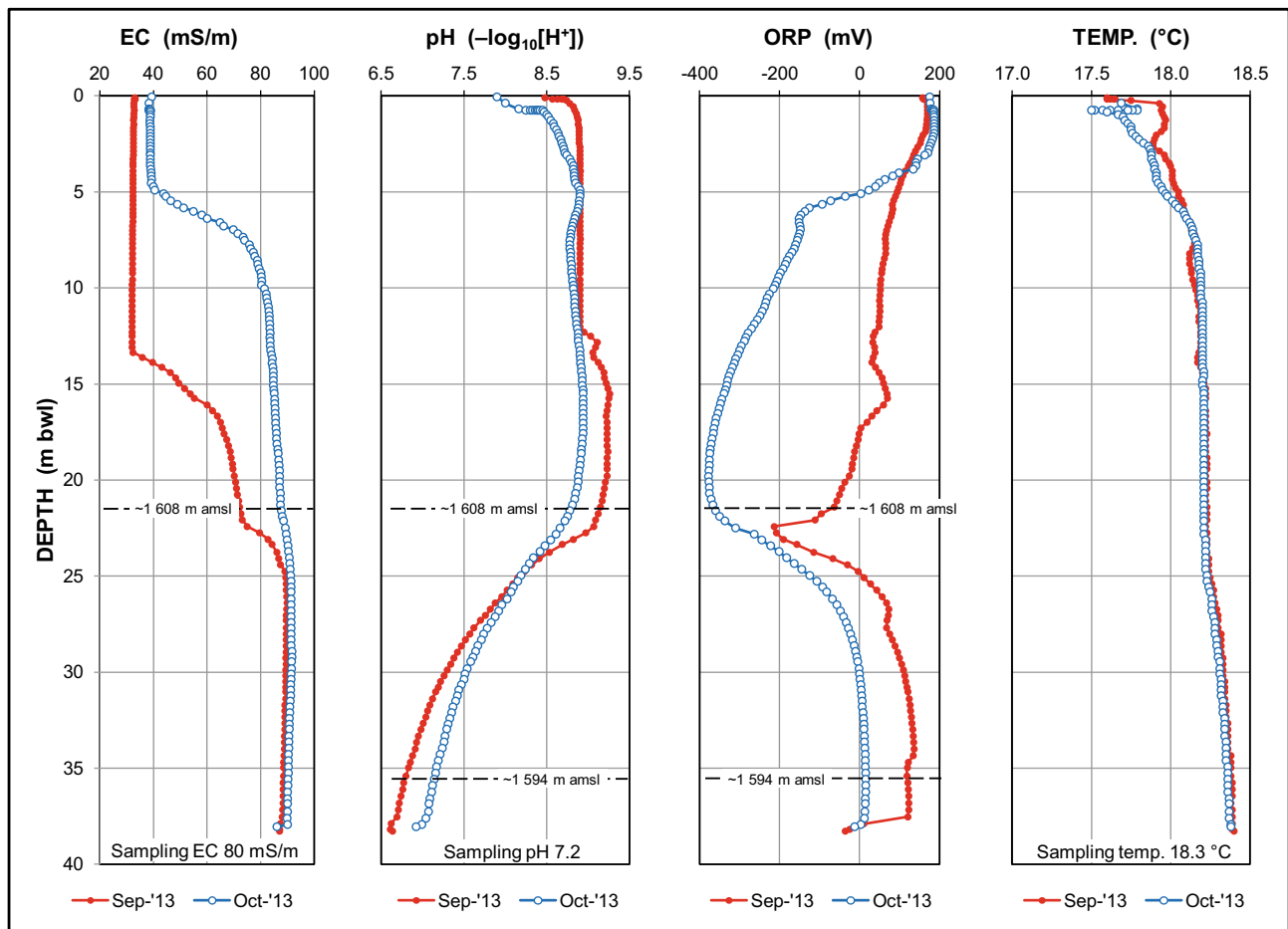


Fig. 62 Pre- and post-sampling vertical profiles of field water chemistry variables in borehole GP00305

A2N0583 profiles reveal an inflection point at a depth of ~ 12 m bwl (~ 1538 m amsl) that is evident for each profiled variable. A reason for this quite sharply defined horizon has not been established.

An anomalous aspect of the profiles is the sympathetic decrease in pH and ORP trend in the uppermost ~ 12 m of the water column. Only below this depth do these variables illustrate the typical mirror-like image that in most other instances in this study characterizes their relationship. Changes in the SEC and temperature profiles are also discernible below the inflection point in the water column.

10.3.15 Boreholes A2N0584 and GP00302

These boreholes are located within 20 m of each other at the confluence of the Tweelopie Spruit with its main stem, the Riet Spruit, on the farm Glen Almond. The ingress of surface water with a very strong mine water composition into the karst aquifer along this stream reach is documented in Sect. 5.2.1 in Chapter “Physical Hydrology”. The similar surface elevations (~ 1491 m amsl) and depths to groundwater rest level (~ 22 m bc) shared by the boreholes again

negate the need to normalize the data sets to a common datum. An assessment of the profile data must also recognize the fact that borehole A2N0584 extends to a depth of only ~ 57 m, and therefore intersects the same aquifer horizon as the shallower (~ 35 m) borehole GP00302. Onerous drilling conditions associated with highly leached and cavernous dolomite were encountered in GP00302 and contributed to the shallow final depth of this borehole. Unsurprisingly, Bredenkamp et al. (1986) reported an airlift yield of >40 L/s for the nearby borehole A2N0584.

The March 2014 profiles measured in these boreholes are compared in Fig. 68 and indicate largely congruent SEC and temperature results (similarly shaped profiles) but incongruent pH and ORP results. The SEC profile in borehole A2N0584 reveals a marked increase of ~ 70 mS/m over the ~ 2 m interval from elevation ~ 1461 m amsl to elevation ~ 1459 m amsl. Although both boreholes reveal a consistent elevated SEC at depth, the difference of ~ 60 mS/m is not readily explained. The higher SEC in the shallower borehole GP00302 is, however, consistent with the slightly higher temperature of this groundwater column. It is the difference

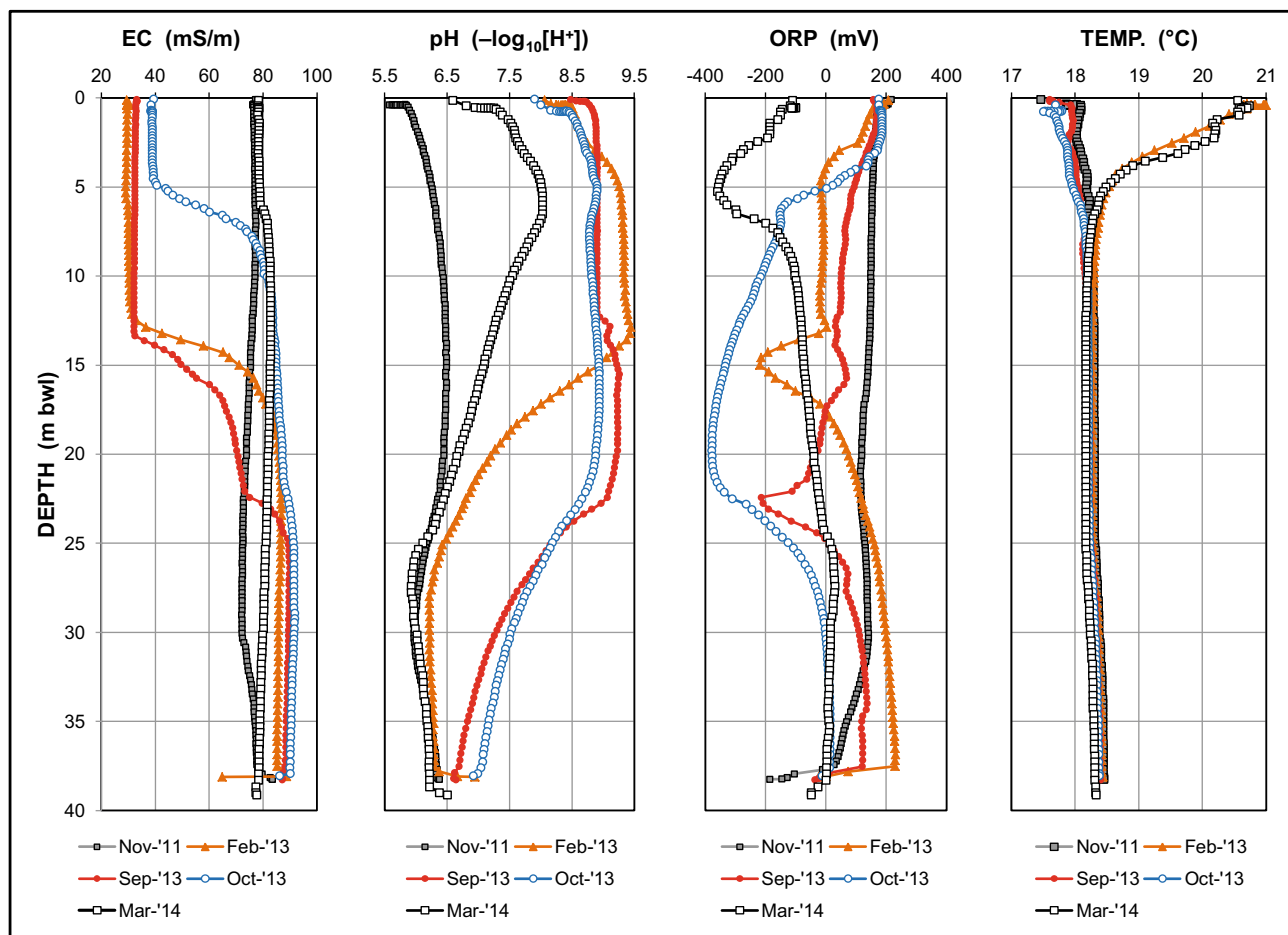


Fig. 63 Temporal variation in vertical profiles of field water chemistry variables in borehole GP00305

of ~ 0.4 °C between the two groundwater columns in the first ~ 12 m below the water table which is intriguing, especially if the difference is maintained at depth as logical extrapolation would suggest. Further, the increasing temperature gradient of ~ 0.4 °C per 5 m below an elevation of ~ 1451 m amsl in A2N0584 is also not readily explained, although its coincidence with the most reducing section of the groundwater column characterized by ORP values in the range -225 to -350 mV cannot go unnoticed. The most plausible explanation associates this trend with exothermic biogeochemical reactions in a strongly reducing (anoxic) environment at depth in the subsurface. The perforated casing in A2N0584 extends from ~ 5 m bwl to the end-of-hole at ~ 35 m bwl, and therefore extends to above the zone of maximum change in the SEC and pH profiles evident in Fig. 68.

Perhaps most surprising, however, is the considerable difference reflected in the pH profiles and, to a lesser extent, the ORP profiles. Not only are the pH profiles in the first ~ 12 m below the water table divergent, but the pH of ~ 9.2 at depth in borehole A2N0584 is three full pH units

(1000-fold) more alkaline than in borehole GP00302. The high pH is also in severe conflict with a mine water impact as is suggested by the SEC value of ~ 130 mS/m.

The ~ 3 m interval from elevation ~ 1464 m amsl to elevation ~ 1461 m amsl in borehole GP00302 brackets a step in each of the SEC ($\Delta = +45$ mS/m), pH ($\Delta = -1.1$) and ORP ($\Delta = +150$ mV) profiles. This horizon is not observed in borehole A2N0584.

It is apparent that the hydrochemical environment intersected in boreholes A2N0584 and GP00302 severely challenges an understanding of this environment at this location. The temporal change in profile variables in each borehole is illustrated in Fig. 69 (A2N0584) and Fig. 70 (GP00302), which provides an opportunity to determine the veracity of the profiling results and ascertain any site-specific differences.

Figure 69 indicates that the shape of the March 2014 profiles in borehole A2N0584 is replicated in each of the profiling events. The measure of temporal consistency is greater for SEC and temperature than for pH and ORP. The latter two variables reveal a greater variance over time in

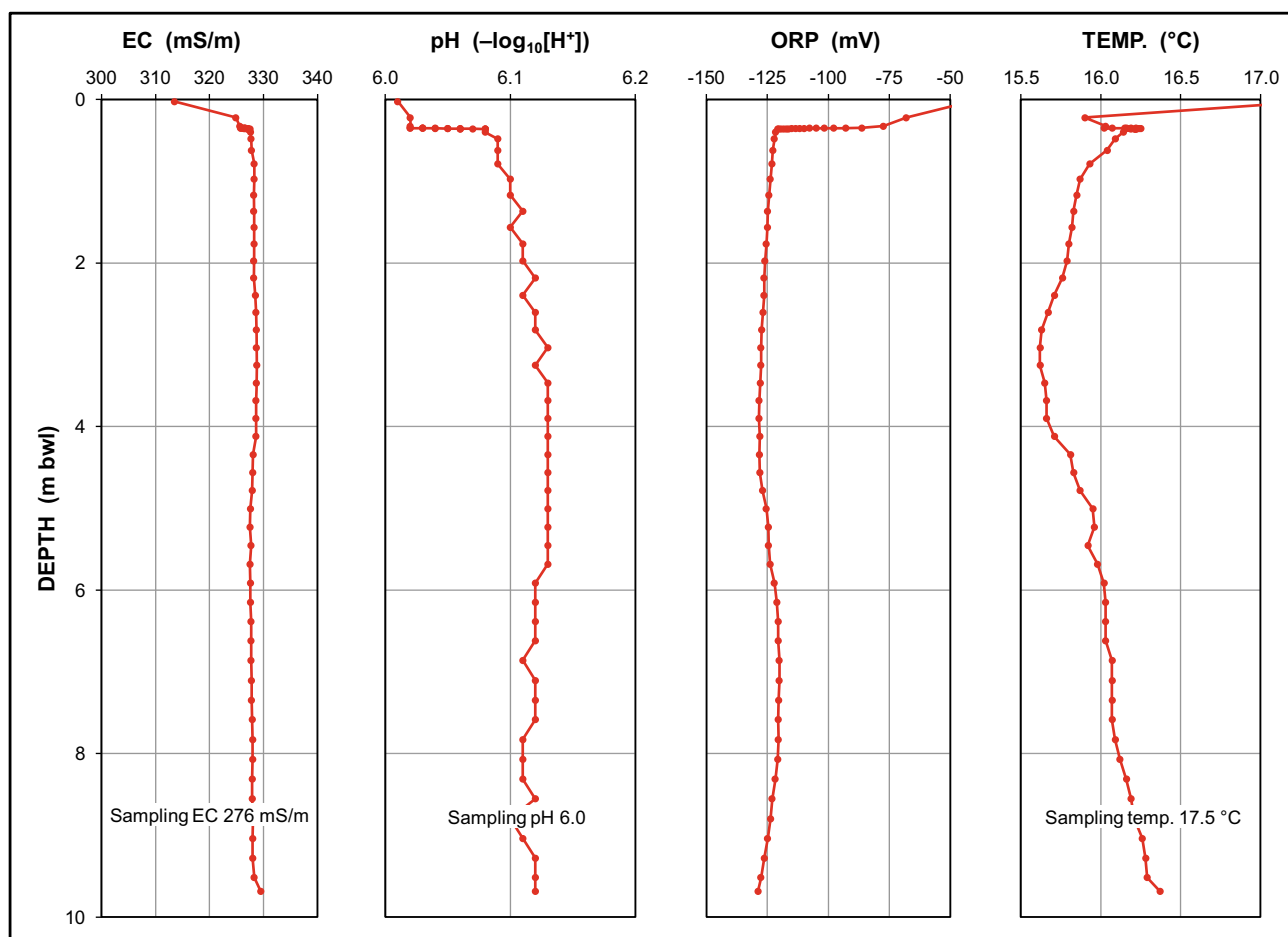


Fig. 64 Vertical profiles of field water chemistry variables in borehole GP00306 in November 2011

the upper 10 m of the groundwater column. The variance reduces considerably in the groundwater column below an elevation of ~ 1459 m amsl (>10 m bwl). The observed temporal consistency exhibited by each variable below ~ 1459 m amsl suggests that hydrochemical equilibrium exists in the deeper portion of the karst aquifer intersected by this borehole. The shallower portion of the karst aquifer experiences hydrochemical fluxes that are most likely driven by allogenic recharge associated with mine water discharges from the Western Basin. Nevertheless, it must be concluded that the profiling events present unequivocal results that do not reflect significant site-specific differences over time.

The groundwater column in borehole GP00302 represents the same hydrostratigraphic horizon that forms the upper 10 m of the karst aquifer intersected in borehole A2N0584. Figure 70 similarly indicates that the shape of the March 2014 profiles in this borehole is replicated in each of the profiling events. The measure of temporal consistency is again greater for SEC and temperature than for pH and ORP. It must again be concluded that the profiling events

present unequivocal results that do not reflect significant site-specific differences over time.

In light of the preceding discussion, the significantly different hydrochemical signatures that characterize the common hydrostratigraphic horizon in the groundwater columns of the two boreholes remain inexplicable. These circumstances are not readily explained on the basis of the current understanding of the hydrophysical and hydrochemical subsurface environments at this location.

It is possible that the observed profile patterns are informed by the 'as built' construction characteristics of the two boreholes. Borehole GP00302 was constructed with a single 140 mm diameter perforated uPVC casing 'string' installed to a depth of 33 m, and extending to surface with a perforated interval from ? to ? m bs. Borehole A2N0584 was constructed with two sets of perforated steel casing as follows (from Bredenkamp et al. 1986):

- an outer 330 mm diameter 'string' installed to a depth of ~ 40 m, extending to surface and perforated in the interval 27–40 m bs; and

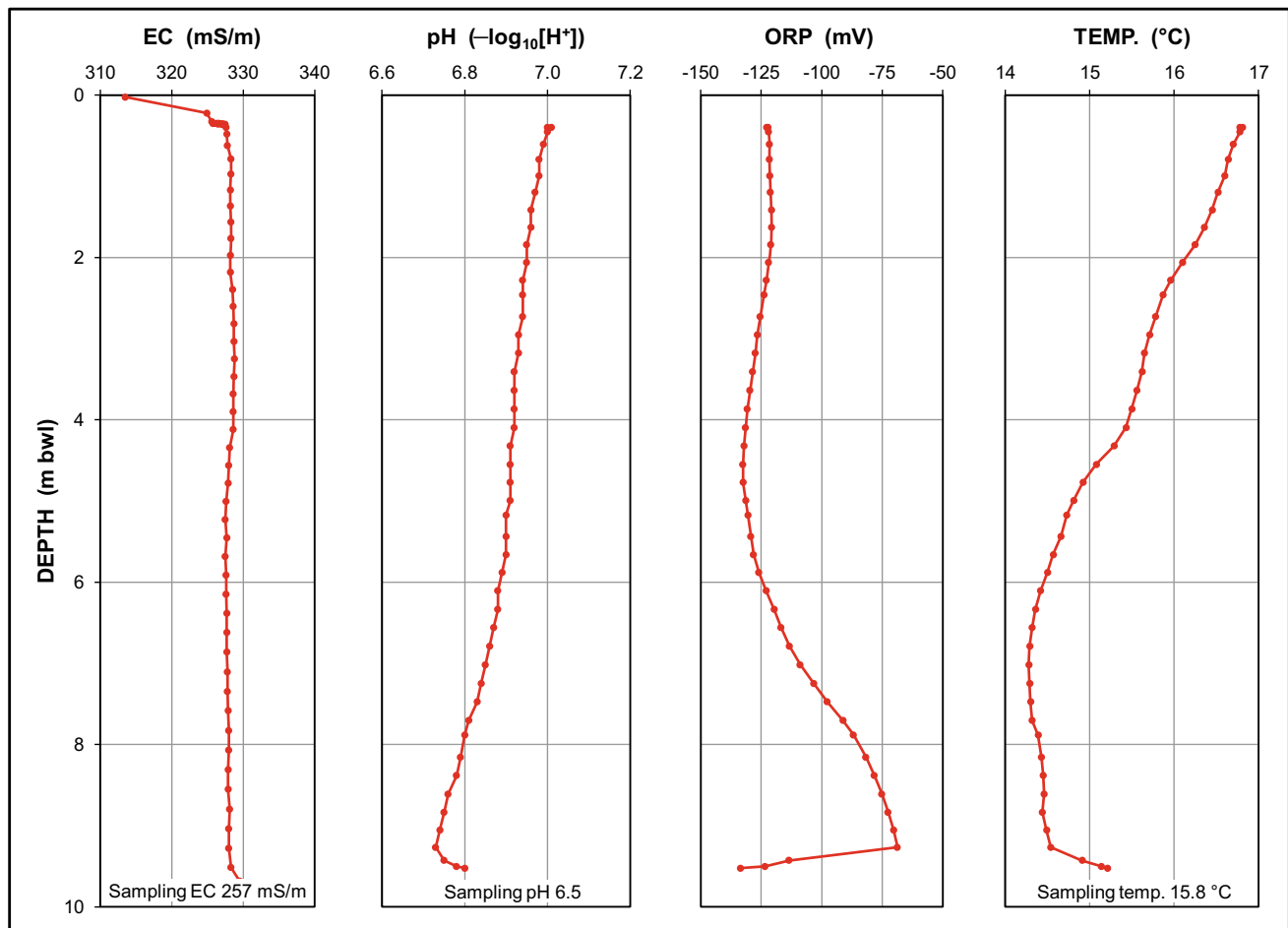


Fig. 65 Vertical profiles of field water chemistry variables in borehole GP00307 in November 2011

- an inner 250 mm diameter ‘string’ installed to a depth of ~57 m, extending to surface and perforated in the interval 26.5–57 m bs.

The greater complexity associated with the A2N0584 construction might account for the ‘anomalous’ pH and ORP profiles obtained for this borehole. It is not known to what extent the different casing materials used in the two constructions might account for the observed differences. A more likely cause for the differences must, however, be sought in the poorly understood hydro(geo)chemical domain and the complex interaction between mine water and dolomitic groundwater in a karst aquifer. Part of this complexity almost certainly relates to processes such as sulfidogenesis (sulfate reduction), Fe^{2+} oxidation, Fe^{3+} reduction, and production of carbonate alkalinity.

10.3.16 Boreholes A2N0586 and GP00300

This grouping of boreholes is located in the Sterkfontein Subcompartment ~270 m north-west of the Riet Spruit midway along the stream reach where surface water with a

very strong mine water composition enters the karst aquifer (Sect. 5.2.1 in Chapter “Physical Hydrology”). The rate of ingress varies from ~14 to >30 ML/d. The principal groundwater flow vector in this portion of the study area is shown in Fig. 19 in Chapter “Physical Hydrology”, indicating the boreholes to be located immediately down-gradient of the losing Riet Spruit. The impact of this ingress on ambient groundwater chemistry has been discussed at length in Sect. 2.3.3, especially in regard to borehole WBD5. An assessment of the profile data must recognize the fact that borehole A2N0586 (G36331 in Bredenkamp et al. 1986) intersects two horizons of leached and fractured chert-rich dolomite in the depth intervals 20–40 and 120–132 m bs, respectively. The deeper aquifer produced an airlift yield of 50 L/s (Bredenkamp et al. 1986). A ~80-m thick layer of chert-poor dolomite separates the two aquifer horizons. Borehole GP00300 intersects only the shallow aquifer.

The influence of purge pumping for routine sampling purposes on the pre- and post-sampling profiles in boreholes A2N0586 and GP00300 is explored in Figs. 71 and 72,

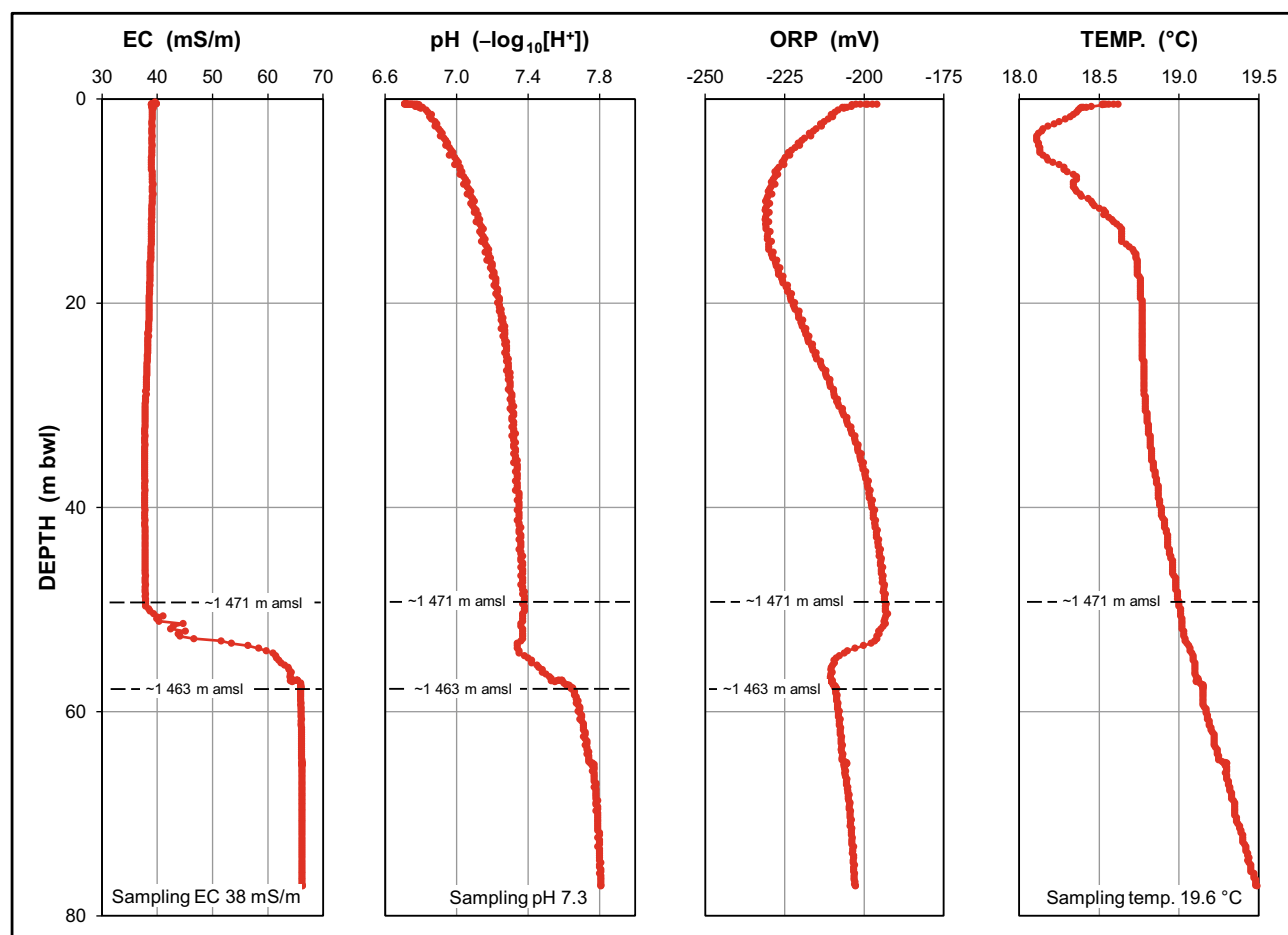


Fig. 66 Vertical profiles of field water chemistry variables in borehole GP00308 in November 2011

respectively. The A2N0586 results suggest that purge pumping exerts little influence on any of the variable profiles, causing only minor negative and positive lateral shifts in pH and ORP, respectively. A transition zone at ~10 m bwl is marked by an SEC, pH, and ORP anomaly that occurs in association with the center of the upper karst horizon. The reasonable measure of congruence²⁶ between the two sets of profiles is self-evident. The greatest difference between the older and more recent data sets is evident in the pH profile of borehole GP00300, the latest profile reflecting an accentuated replica of the earlier profile, but shifted by 3 full pH units (a factor of 1000) from an acidic to a basic character. The step in SEC and pH between elevations of ~1458 and ~1454 m amsl in borehole A2N0586 are similarly accentuated and is also manifested in the latest ORP profile. The

latter further indicates the development of a redox anomaly at an elevation of ~1440 m amsl (~26 m bwl) that is only hinted at in the earlier profile.

The influence of purge pumping for routine sampling purposes on the pre- and post-sampling profiles in borehole GP00300 (Fig. 72) is ostensibly more significant than in borehole A2N0586. The GP00300 results suggest that purge pumping exerts a 'normalizing' influence resulting in 'smoother' SEC, pH, and ORP profiles. Equally intriguing is the ~1 °C negative shift in temperature. These observations are not readily explained on the basis of current knowledge and understanding of the complex hydrophysical and hydrochemical interactions that characterize the hydrogeologic system. The established presence of a shallower and a deeper aquifer horizon at this location, however, suggests the delivery of different groundwater chemistries from the boreholes.

The deeper borehole A2N0586 which intersects both aquifers delivers a mixture of the shallow more saline and the deeper fresher groundwater. This is exemplified in the values obtained during the routine sampling of the boreholes

²⁶ The similar surface elevations (~1487 m amsl) and depths to groundwater rest level (~22 m bc) shared by the boreholes negate the need to normalise the data sets to a common vertical datum.

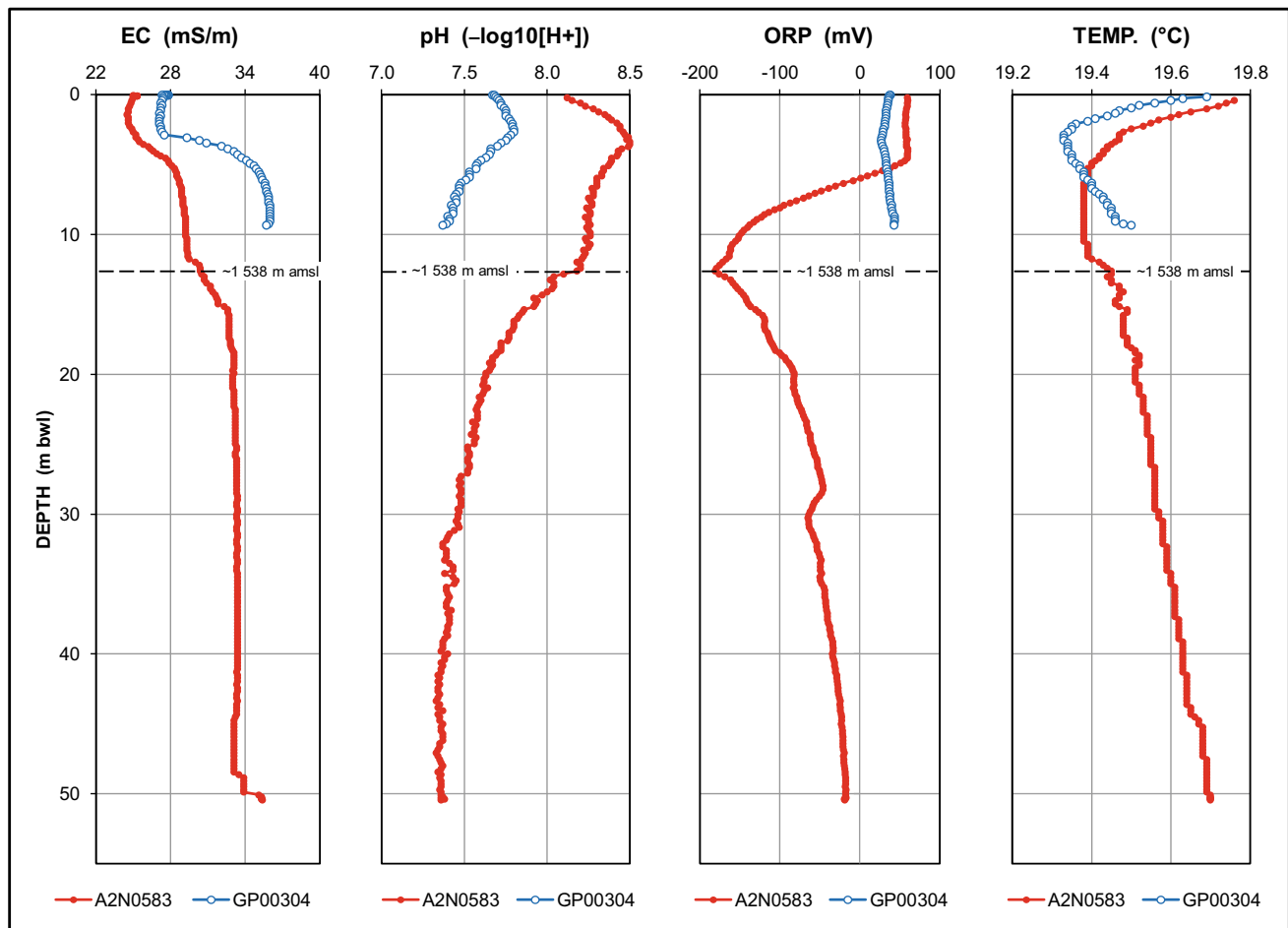


Fig. 67 Vertical profiles of field water chemistry variables in boreholes A2N0583 and GP00304 in November 2011

(e.g., Tables 11 and 12). The comparison, however, also indicates that none of the stabilized²⁷ SEC, pH, and temperature values is similar to that of any profile value. For example, the stabilized SEC values of 172 and 208 mS/m (for boreholes A2N0586 and GP00300, respectively) do not correlate with the ‘final’ values of ~210 and ~250 mS/m indicated by the SEC profiles for these boreholes (Figs. 73 and 74, respectively).

The above circumstances indicate that a different mixture of ‘shallow’ and ‘deep’ groundwater is produced by each borehole during pumping. This again poses the question of when might a ‘representative’ sample be considered ‘truly representative’. Of course, discrepancies introduced by factors such as the use of different instruments and the lapse of time between sampling and profiling also need to be included in an analysis of these circumstances.

²⁷ The field chemistry variables are monitored in a flow through cell during purge pumping of the borehole being sampled, and a sample collected only once the variable values have stabilised.

10.3.17 Borehole GP00301

Located ~600 m north-west of the Riet Spruit on the postulated western margin of the mine water impacted zone in the Sterkfontein Subcompartment, this borehole reports a depth to groundwater rest level of ~59 m bs. Notable changes in SEC, pH and ORP occur at an elevation of ~12 m bwl (~71 m bs, ~1453 m amsl), which coincides with the first water strike in the borehole.

The SEC value of ~125 mS/m in the lower portion of the profile (>35 m bwl; >94 m bs; <1430 m amsl) (Fig. 75) indicates the influence of poorer quality water on the typically much lower SEC associated with unimpacted natural karst groundwater. This influence is not yet evident in the pH values of ~7.4, possibly the result of effective neutralization (buffering) by abundant alkalinity in the karst hydro system. The moderately reducing conditions are characterized by ORP values in the range -200 to -150 mV. A slight freshening of the groundwater at the base of the water column (>80 m bwl, <1385 m amsl) is also evident.

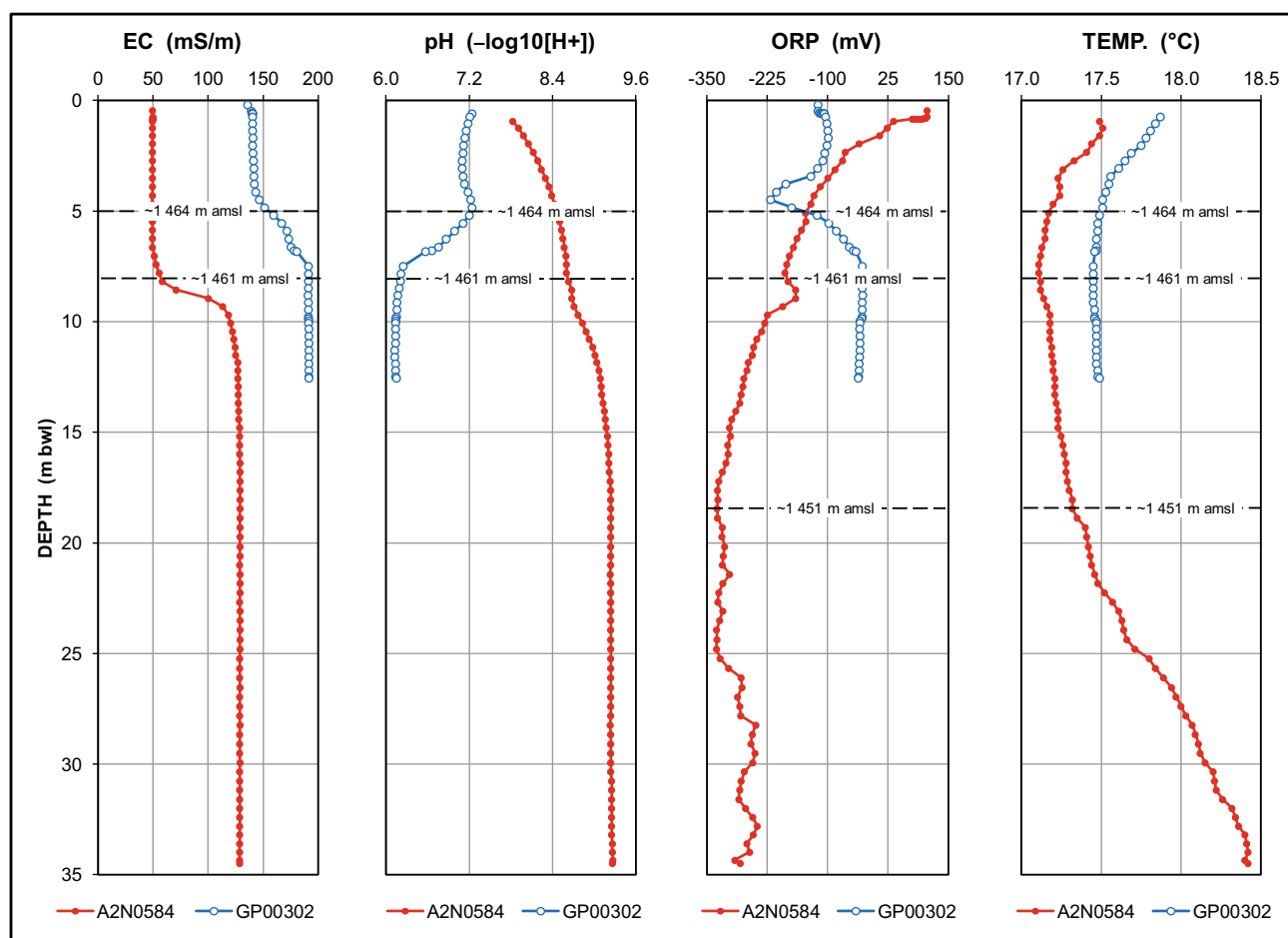


Fig. 68 Vertical profile of field water chemistry variables in boreholes A2N0584 and GP00302 in March 2014

10.3.18 Borehole GP00309

This borehole occupies a strategic position at the confluence of the Riet Spruit and the Blougat Spruit upstream of Oaktree. This location marks the subsurface confluence of infiltrated mine water (from the Riet Spruit) and infiltrated municipal wastewater (from the Blougat Spruit). The groundwater is drawn from the karst aquifer at this location, therefore, representing a mixture of these two allogenic sources of recharge.

The influence of purge pumping for routine sampling purposes on the pre- and post-sampling profile is explored in Fig. 76. The results suggest that purge pumping exerts little influence on the SEC profile, causes slight shifts in pH and ORP toward more alkaline and reducing conditions, respectively, and causes a significant negative shift in temperature. The pH and ORP changes are attributed to the drawing of a greater proportion of better quality karst groundwater into the radius of hydrogeochemical influence around the borehole.

The large measure of congruence between the respective SEC, pH, and ORP profiles generates confidence in the

veracity of the data sets. The significant difference between the sampled SEC and temperature values compared to the profiled values is attributed to the use of two different multiparameter probes as discussed in Sect. 10.2.

The results of six profiling exercises are shown in Fig. 77. The SEC increase from <200 to ~290 mS/m at ~4 m bwl is attributed to a fresher water horizon overlying the mine water impacted karst groundwater below this depth. The transition zone of ~3 m is also characterized by significant reversals in pH and ORP values. In all instances, the pH profiles trend toward more acidic conditions (by almost one full pH unit) with depth, and the ORP profiles toward more oxic conditions.

The low temperature of <14 °C that characterizes the bottom section of the November 2011 profile extends much further up the water column in the February 2013 profile. The four later profiles demonstrate first a positive migration to a value of almost 19 °C (through June–September 2013), followed by a reversal to a value of ~14.5 °C (through October 2013–March 2014). The latter is at least 4 °C lower than that which characterizes natural karst groundwater in

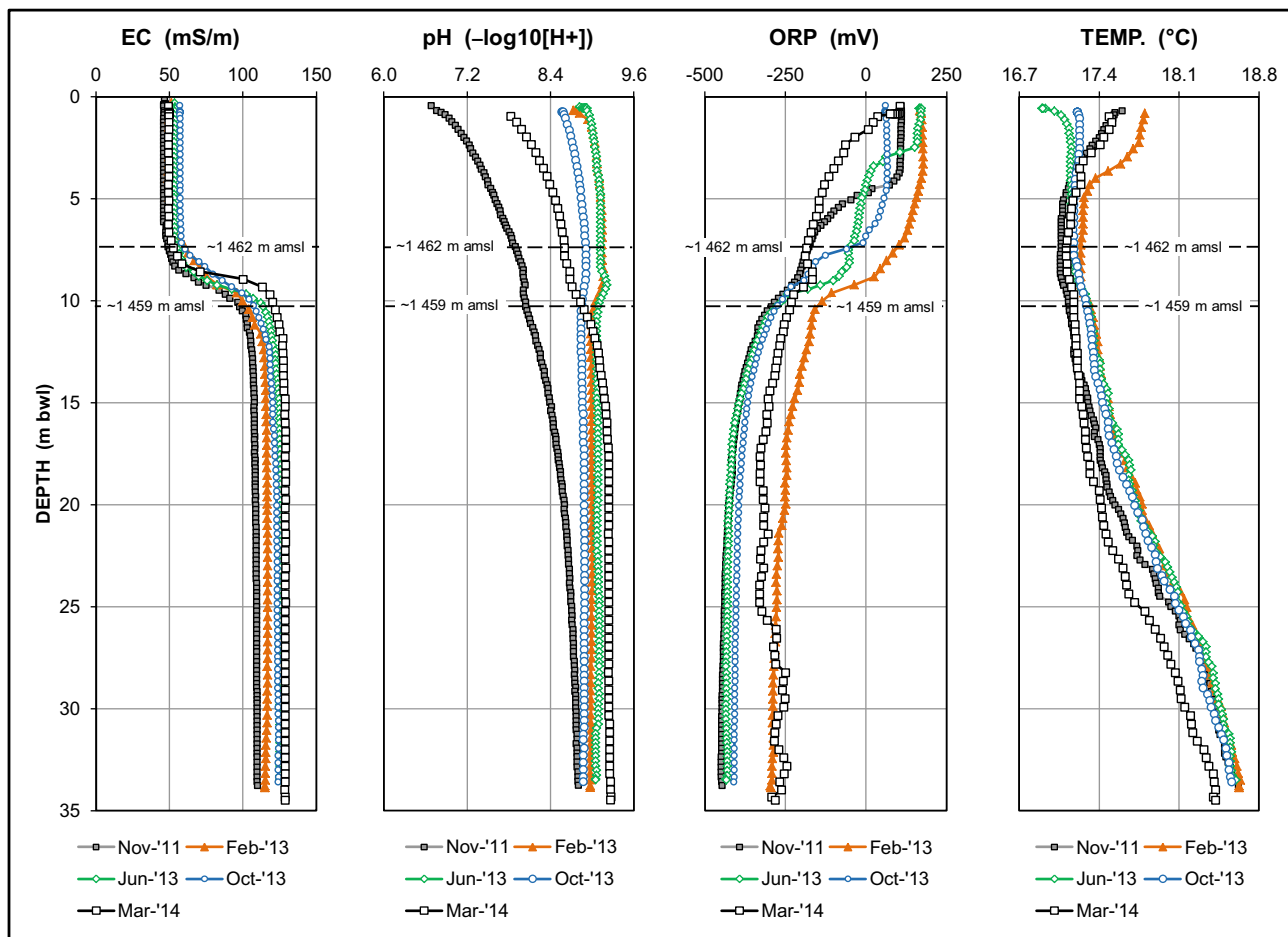


Fig. 69 Temporal variation in vertical profiles of field water chemistry variables in borehole A2N0584

the study area. An explanation for these circumstances has not yet been established, although endothermic redox reactions that accompany a shift from reducing (anaerobic) to oxic (aerobic) and more acidic conditions provide the most plausible cause. Support in this regard might be found in the thermodynamic complexity of redox processes that involve terminal electron-accepting processes (TEAPs) as discussed by Hoehler et al. (1998) and Jakobsen et al. (1998).

10.3.19 Borehole GP00311

The position of this borehole in the upper reaches of the Zwartkrans Basin characterizes the hydrochemistry of the dolomitic groundwater outside the influence of the mine water impact. This is supported by the SEC value of ~ 38 mS/m and the pH value of ~ 7.5 (Fig. 78). The step-wise increase in SEC at an elevation of ~ 1473 m amsl, and the synchronous but opposite pH and ORP patterns at this elevation, are not readily explained within the current knowledge framework. The redox profile indicates a step at a depth of ~ 39 m bwl (~ 107 m bs; ~ 1441 m amsl) that does not manifest as a change in any of the other three

variable profiles at this depth. The reason for a shift toward reducing conditions in a comparatively narrow horizon (<3 m in extent) at this depth is unclear. Nevertheless, the profile values compare favorably with the stabilized SEC value of 36 mS/m, pH of 7.6, and temperature of 20.2°C obtained during the sampling exercise in September 2011 (Table 11).

10.3.20 Borehole GP00312

The October 2011 profiles (Fig. 79) reveal the very strong presence of mine water in the karst aquifer at this location on the right bank of the Riet Spruit within 50 m of the stream channel. The SEC profile shows two step-wise increases, the first occurring within the upper 5 m of the profile, and the second below an elevation of ~ 1462 m amsl (>5 m bwl). As the water table occupies an elevation of ~ 1467 m amsl, which is ~ 4 m below the streambed elevation of ~ 1471 m amsl, the most saline horizon (~ 330 mS/m) is encountered >10 m below the streambed, in the lower section of the borehole. The pH profile indicates a uniform increase by ~ 0.3 units in this section. Nevertheless, of concern is the

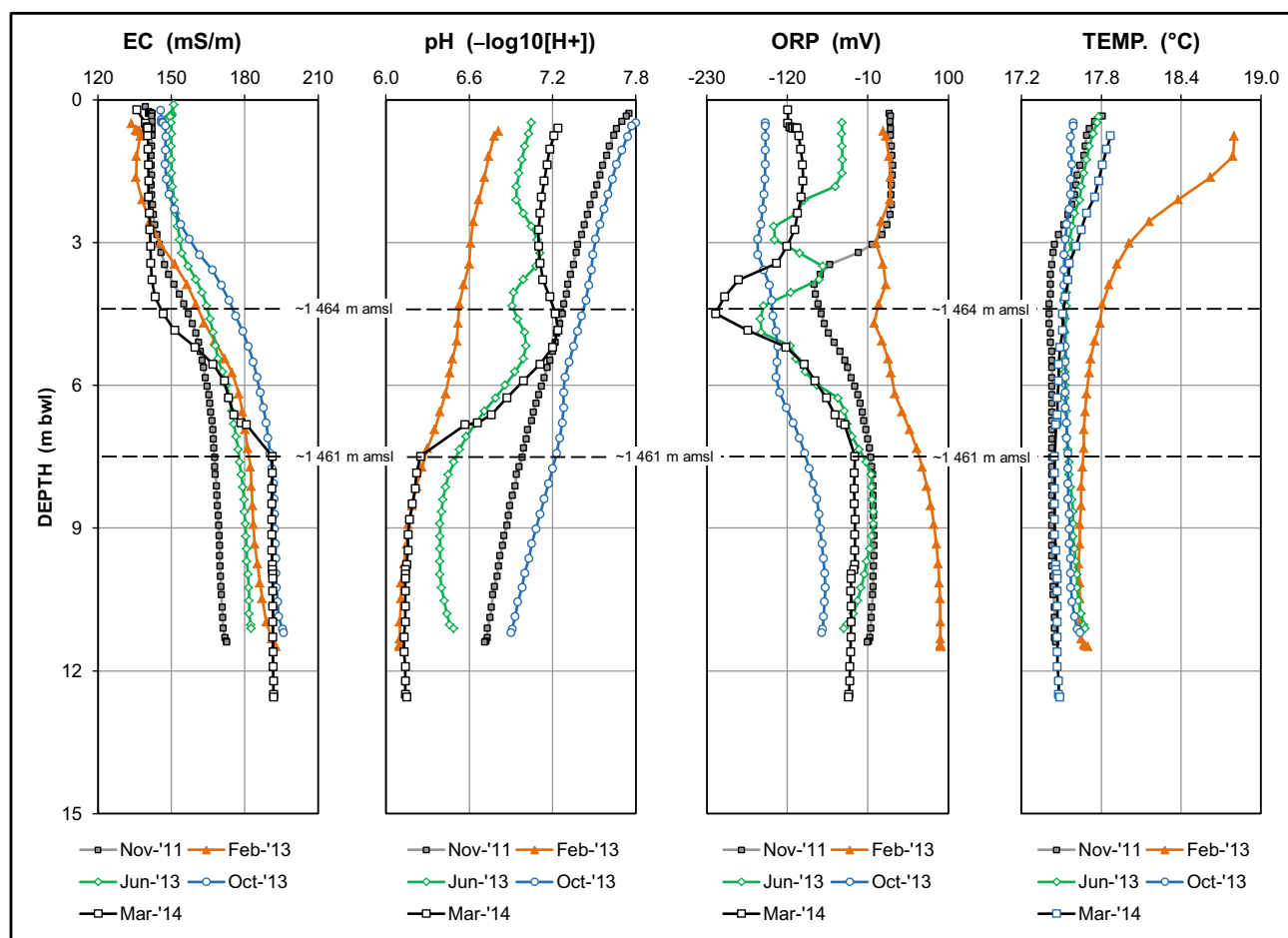


Fig. 70 Temporal variation in vertical profiles of field water chemistry variables in borehole GP00302

pH value of <6.0 , which is below the value of 6.4 that describes the limit at which net alkalinity is zero (Sect. 13.2). These circumstances suggest that the dolomite at this location no longer provides a neutralizing function. The ~ 0.5 °C decrease in temperature below ~ 1454 m amsl is not readily explained.

The stabilized values obtained during the September 2011 sampling exercise again show little correlation with the respective profile values. Neither the pH nor temperature values of 6.8 and 19.5 °C (Table 11), coincide with the profiles. Especially the pH value provides a false ‘positive’ indication in regard to this variable. Similarly, the SEC value of 263 mS/m (Table 11) under-reports the ‘final’ SEC profile values by ~ 70 mS/m.

10.3.21 Borehole GP00313

This borehole occupies an important position ~ 750 m to the northwest of Sterkfontein Cave, where it reflects the chemistry of karst groundwater draining from the Zwartkrans Basin toward the Zwartkrans Spring. The influence of purge

pumping for routine sampling purposes on the pre- and post-sampling profile is explored in Fig. 80.

The results suggest that purge pumping exerts little influence on the SEC and temperature profiles, and causes slight shifts in pH and ORP toward more alkaline and reducing conditions, respectively. The latter changes are attributed to the drawing in of a greater proportion of better quality karst groundwater into the radius of hydrogeochemical influence around the borehole. The significant difference between the sampled SEC, pH, and temperature values compared to the profiled values is attributed to the use of two different multiparameter probes as discussed in Sect. 10.2.

The results of six profiling exercises are shown in Fig. 81, together with the absolute elevation that brackets the Zwartkrans Spring. The ‘spikes’ on the November 2011 SEC profile coincide with the joint interval of 2.3 m between slotted screen sections. These are not evident in the other profiles. The SEC increase from ~ 105 mS/m in November 2011 to ~ 135 mS/m in the later profiles are attributed to the

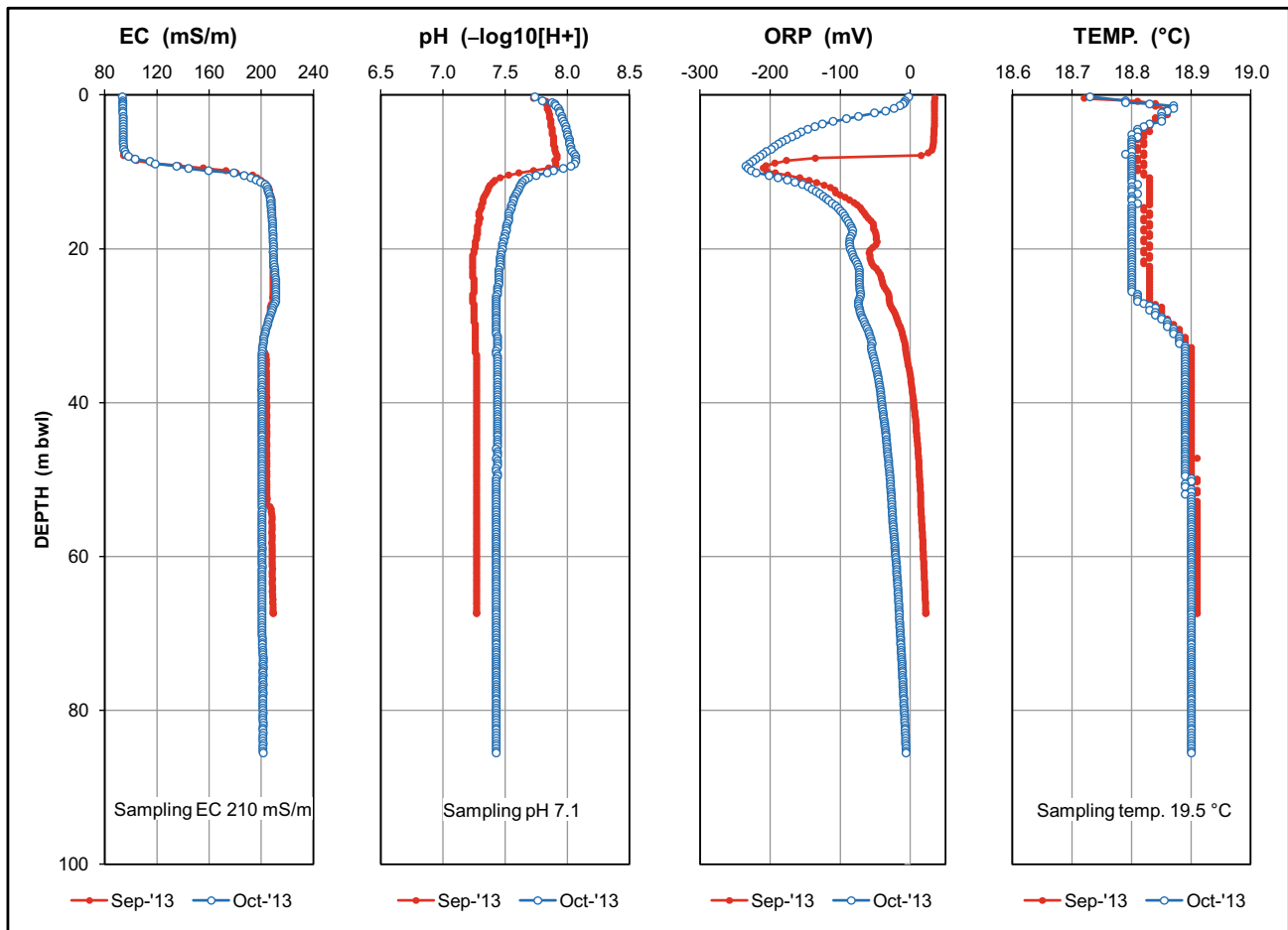


Fig. 71 Pre- and post-sampling vertical profiles of field water chemistry variables in borehole A2N0586

mine water influence on the karst water chemistry at this location. This surprisingly does not find support in the more alkaline pH reflected in the post-November 2011 profiles, all of which exhibit a remarkably similar trend. The initial significant shift from reducing to oxidizing conditions shown in the November 2011 and February 2013 ORP profiles is again attributed to a mine water influence. The subsequent incomplete return to reducing conditions in the three most recent profiles is attributed to a partial re-establishment of the natural karst hydrogeochemical system. The position of this borehole in the lower reaches of the Zwartkrans Basin imposes a complexity (including a municipal wastewater influence) that cautions against an unequivocal conclusion in this regard.

The relevance of the water-bearing horizon intersected by this borehole within the broader hydrogeologic framework has been discussed in Sect. 3.2.2 in Chapter “Physical Hydrogeology”. The base of the cavernous zone intersected by the borehole approximates the elevation of ~1429 m amsl (~11.5 m bwl; ~31 m bs) shown in Fig. 81. Both the pH and the ORP profiles show a slight

‘change’ (most noticeable in the November 2011 profiles) in pattern below this elevation, the change representing a trend reversal.

It is worth repeating that this borehole intersected a cavity between 17 and 32 m bs. The elevation of ~1429 m amsl is also located ~10 m below the current Lake water level of ~1439 m amsl in Sterkfontein Cave (Sect. 3.2.2 in Chapter “Physical Hydrogeology”). The temperature data >4 m bwl show little difference between the profiling events.

10.3.22 Borehole GP00314

This borehole is located between borehole GP00313 (Sect. 10.3.21) and the Zwartkrans Spring on the left (north) bank of the Bloubank Spruit within 10 m of the stream channel. Only 14 m deep, the borehole is in direct hydraulic continuity with the stream, an observation that finds support in the constancy of the profile values shown in Fig. 82. This constancy also indicates the well-mixed character of the groundwater in the near-surface saturated profile of the aquifer comprising highly leached to decomposed dolomite at this downstream location.

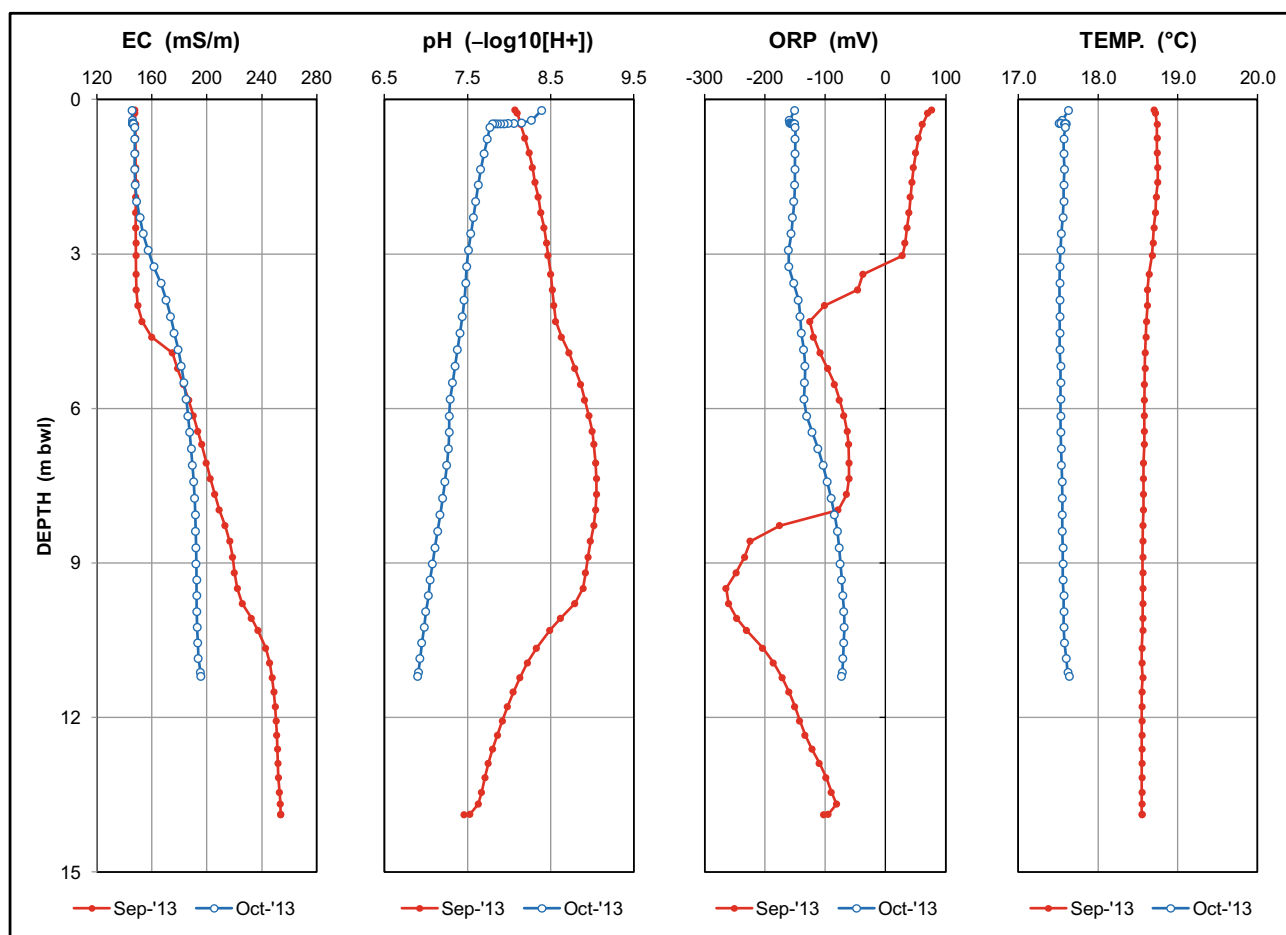


Fig. 72 Pre- and post-sampling vertical profiles of field water chemistry variables in borehole GP00300

The discrepancy between the profile SEC value of ~ 98 mS/m and the sampling SEC value of 49 mS/m is not readily explained. The profile value, however, is similar to the 84 mS/m of the Zwartkrans Spring water in May 2010, at which time the SEC of groundwater in the lower reaches of the Zwartkrans Basin had already started increasing (Fig. 24). The borehole is located ~ 700 m upstream of the spring, and its shallow depth suggests that it shares the shallow karst horizon draining toward the spring.

10.4 Discussion

The vertical hydrochemical profiling results reflect a substantially more complex subsurface hydrogeochemical environment than is apparent from the more mundane data and information collected in the course of routine hydrogeologic investigations. This complexity poses fundamental questions regarding the measure of understanding of the hydrogeochemical and biogeochemical environments and their interaction in the karst system of the study area.

The added complexity associated with the allogenic sources of recharge, primarily mine water and municipal wastewater effluent, challenge this understanding even further. Recognition of this complexity precipitates an admission of the inadequacy of the current understanding of the interaction between impacting water resources and the natural receiving karst groundwater environment. This limitation, however, must not stand in the way of the proactive implementation of water resource management measures required to mitigate any negative impacts within the framework of the current understanding of these inter-relationships.

Figure 83 shows that the Eh values that characterize the mine water and groundwater environments span a comparatively narrow range compared to that of pH. The limits are defined by values in the range ~ 200 mV at pH ~ 2.5 , to -150 mV at pH ~ 9.3 . These circumstances describe an Eh–pH condition which falls mainly in the stability field of ferrous iron at values more representative of mine water where Fe^{2+} is the dominant species, and in the amorphous Fe-oxyhydroxide $[\text{Fe}(\text{OH})_3]$ stability field at values most

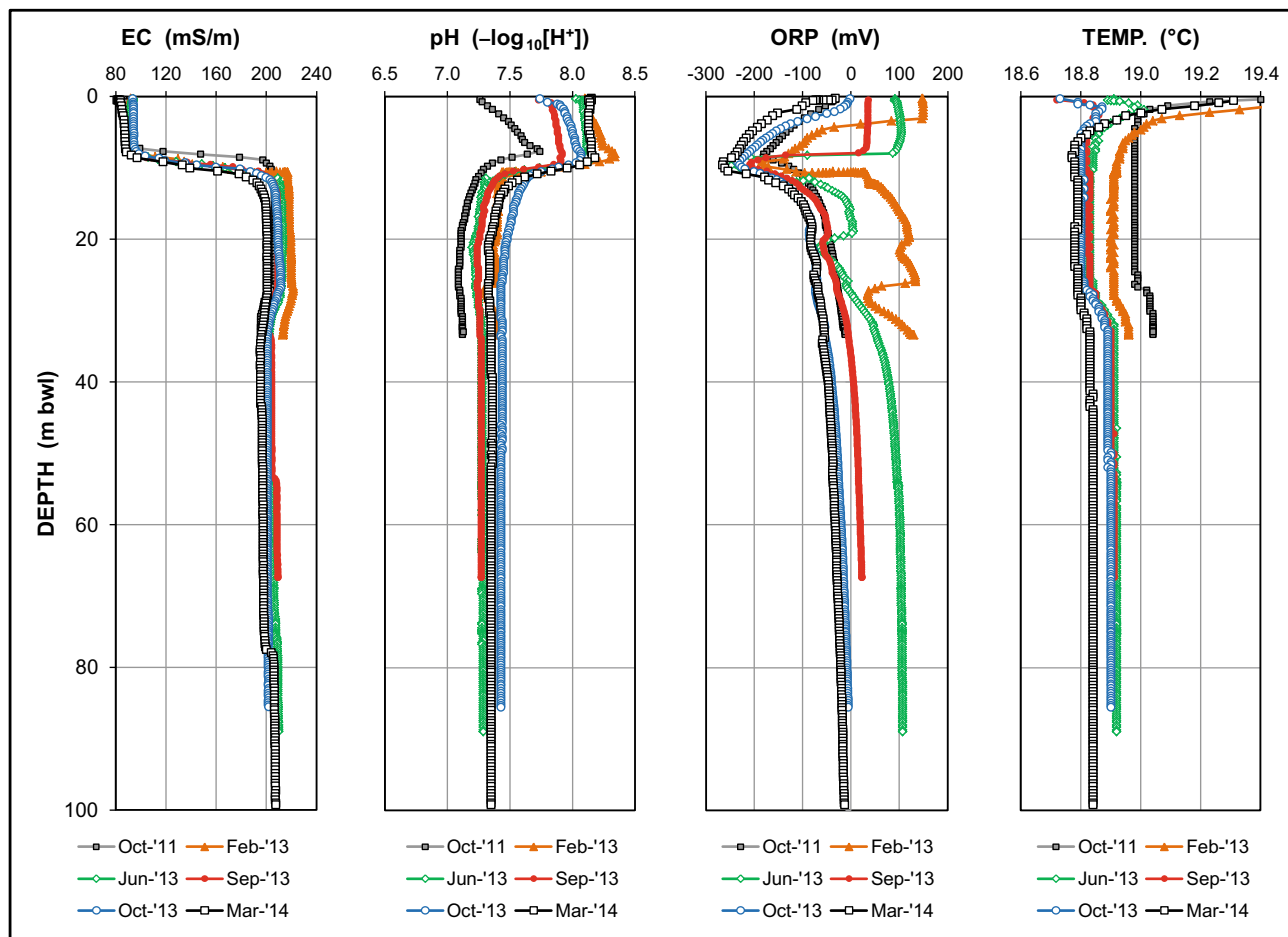


Fig. 73 Temporal variation in vertical profiles of field water chemistry variables in borehole A2N0586

representative of mine water impacted karst groundwater where ferric hydroxide is the dominant species.

The Eh–pH condition that characterizes the mine water and groundwater environments correlates well with that which defines environments that are isolated from the atmosphere. It is therefore surprising that the raw mine water (RMW) Eh–pH reference condition which forms the one end-member of the Eh–pH range, differs significantly from the condition that characterizes acidic mine drainage as defined by Baas-Becking et al. (1960) and Langmuir (1996) reported in USDA (2012). This is defined by the Eh–pH condition at A in Fig. 83 representing an acidic mine drainage environment in contact with the atmosphere, circumstances which closely describe the RMW sampling environment.

The other reference Eh–pH condition shown in Fig. 83 is that for the Zwartkrans Spring (ZSp). This source produces groundwater that exhibits a slight to moderate impact of contamination by mine water, as is reflected in the SEC value of ~ 98 mS/m and a pH of ~ 7.0 that is notably lower than that of pristine karst groundwater. The Eh–pH condition of the ZSp springwater is appropriate to these circumstances,

and points to the Eh–pH condition of those springs in the COH delivering pristine karst groundwater as defining the other end-member of the Eh–pH range opposite the RMW environment in Fig. 83.

The association of some of the impacted karst groundwater with the stability field of amorphous iron oxyhydroxide $[\text{Fe}(\text{OH})_3]$, the most unstable (soluble) but also ‘freshest’ mineral form of Fe (Plate 3 in Chapter “[Chemical Hydrology](#)”), supports the postulated presence of dolomite armoring by these precipitates (Sect. 12.2.3).

Text Box 1 The veracity of ORP measurements

Oxidation reduction potential (ORP or redox) measurements provide an indication of the electron activity $[e^-]$ that informs the potential for electron transfer in a medium (usually water) as sensed by an inert metal electrode immersed in the medium, the measurement being compared to a reference electrode of known potential immersed in the same medium, and corrected

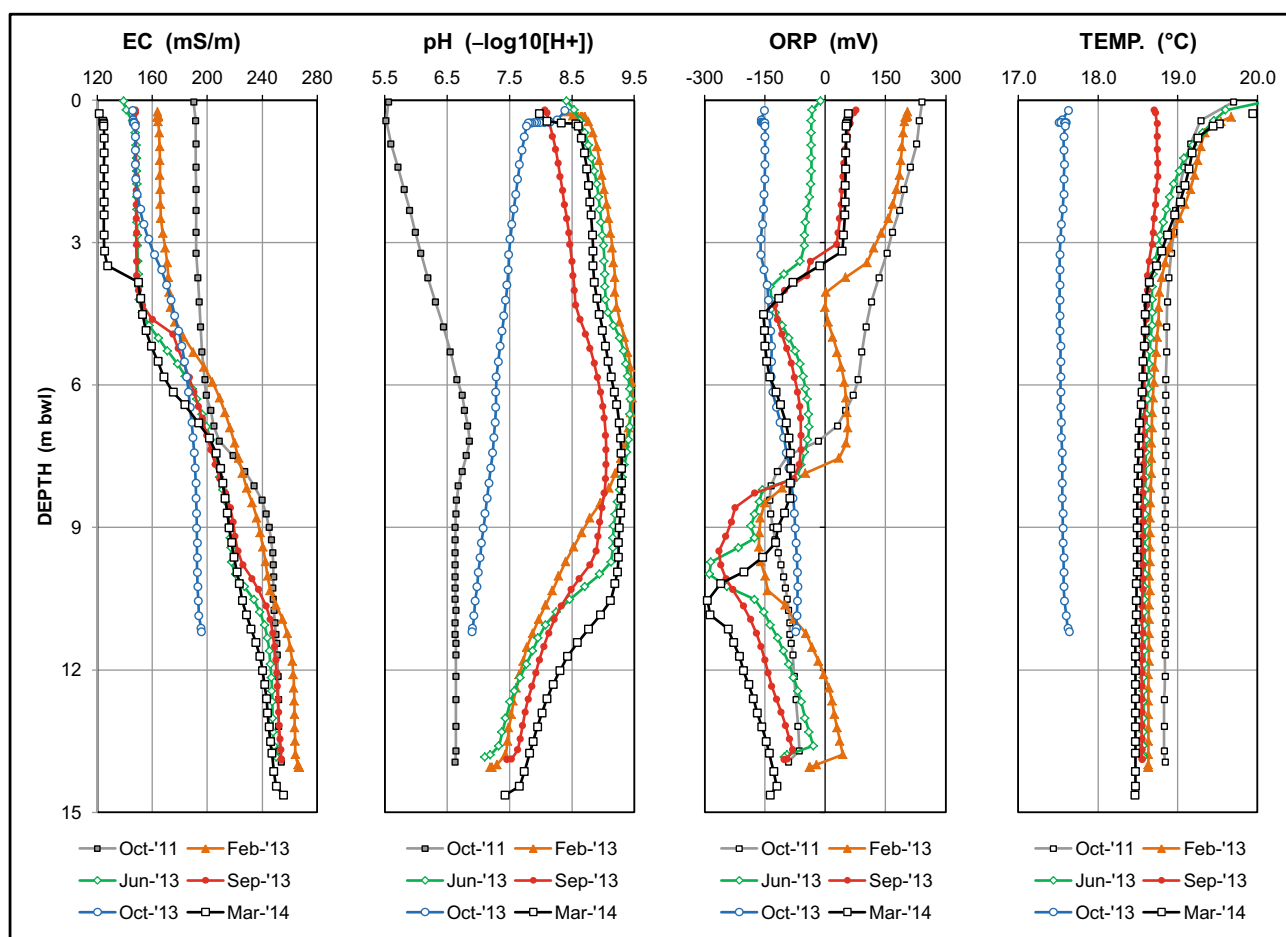


Fig. 74 Temporal variation in vertical profiles of field water chemistry variables in borehole GP00300

accordingly (Appelo and Postma 2009). Electron transfer potential is characterised as either the ability to accept electrons (indicating an oxidising environment recognised by positive ORP values) or to furnish electrons (indicating a reducing environment recognised by negative ORP values). ORP is a generic (less specific) term for E_h ($p\epsilon$) and defines measurements made relative to any reference electrode. E_h , however, defines the ORP value measured specifically against a standard hydrogen electrode (SHE) which has a reference point of 0 mV, and where $p\epsilon = -\log_{10}[e^-]$.

The inert metal electrode on the ORP sensor model 6032/6565 of the YSI 6-series multiparameter sonde is made of platinum (Pt). The reference electrode is that of the pH sensor, a Ag/AgCl (silver:silver chloride) electrode fitted to the sonde. The sensor reading reported is a voltage (accuracy ± 20 mV) relative to the reference electrode, e.g. +250 or -400 mV relative to Ag/AgCl. The difference in value between an E_h reading and an ORP reading reflects the voltage offset

between the different reference electrodes used. The ORP value can therefore be converted to an equivalent E_h value if the voltage offset is known, by adding/subtracting the offset value to/from the ORP value. This has not been determined for the ORP measurements reported in this document, which explains why the term E_h is not used in this context. A cursory review of the literature on redox measurements, in particular non-SHE reference electrode readings, reveals repeated cautions issued against the representativeness of these measurements (Stumm and Morgan 1981; Hem 1985; Appelo and Postma 2009; Weaver et al. 2007). The reasons for caution range from lack of equilibrium between different redox couples in the same medium, to “poisoning” of the Pt-electrode, e.g., the development of an iron oxyhydroxide (FeOOH) coating on the electrode when immersed in anoxic Fe^{2+} -rich water because of O_2 adsorbed on the electrode surface (Appelo and Postma 2009). Nevertheless, ORP measurements are

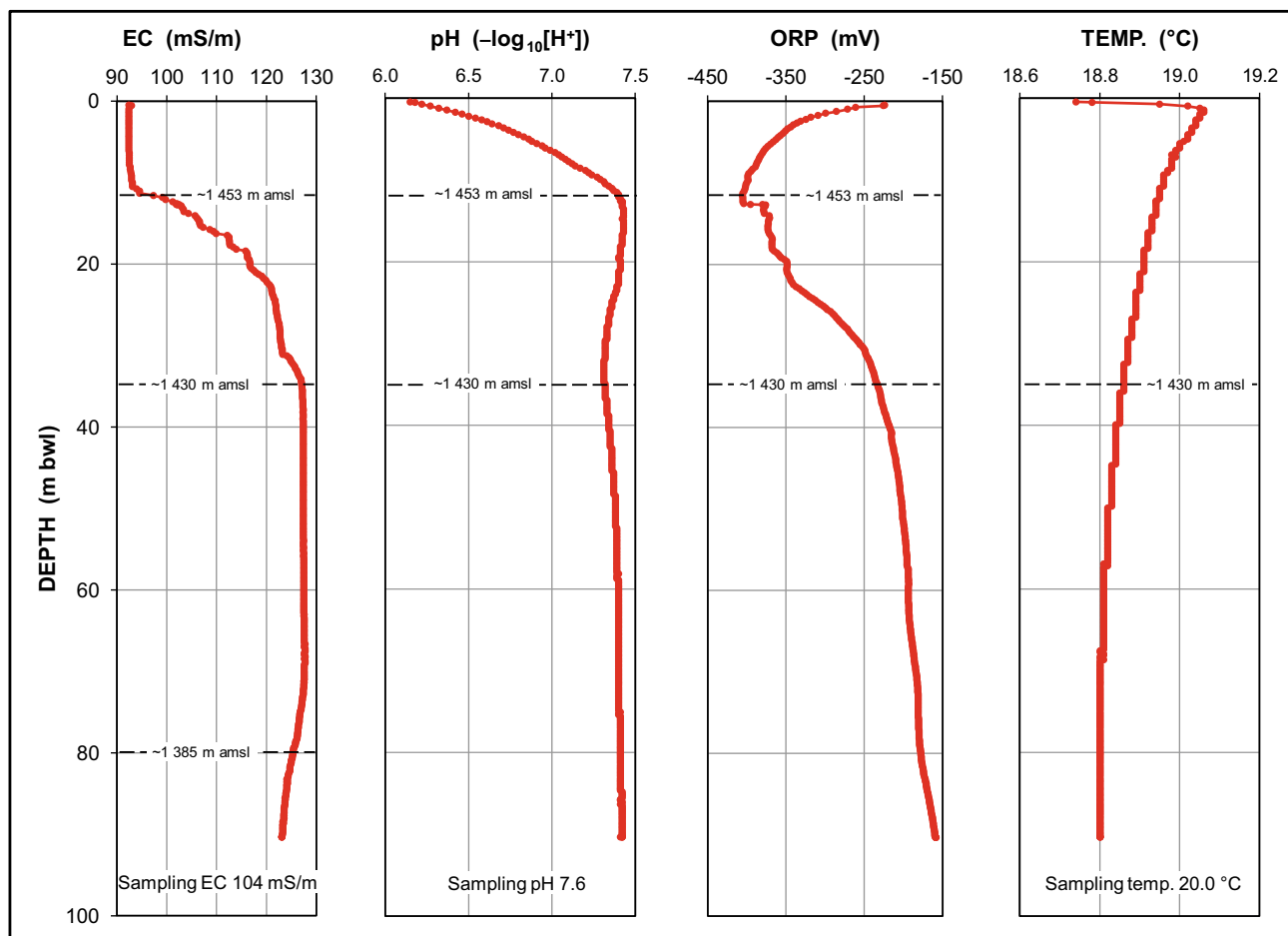


Fig. 75 Vertical profiles of field water chemistry variables in borehole GP00301 in October 2011

considered particularly useful in water containing a comparatively high concentration of a redox-active species, examples being acid mine water containing metals (Fe^{2+} , Fe^{3+}) and municipal wastewater containing strong oxidising (chlorine) and reducing (sulphite) agents. From this it is apparent that ORP measurements only gain usefulness for media where a predominant redox-active species is known to be present, or specific information about the host environment is known.

Recognition of the complexities that inform the determination of ORP values as described above, as well as lack of rigorous control over what is really being measured (Appelo and Postma 2009), militates against an over-interpretation of the ORP (and for that matter also the Eh) data presented in this study. Montgomery et al. (2002) express a similar caveat in regard to the use of Eh and ORP measurements. Hem (1985) reports that the numerical value of Eh is an indicator of redox **intensity** with little value as an

indicator of redox **capacity**. These limitations do not, however, detract from the value of qualitative inference provided by ORP (Eh) patterns and trends in regard to redox zones and conditions in the subsurface.

11 Bacterial Sulfate Reduction

The possibility that bacterial sulfate reduction (BSR) might be occurring in that portion of the karst aquifer where mine water entering the groundwater environment encounters infiltrating wastewater effluent must be considered. The organic matter associated with the latter might serve as the driving reductant, and positive indications in this regard are the comparatively low SO_4 and trace metal concentrations in groundwater in this portion of the Zwartkrans Basin. The process reduces SO_4 to H_2S (hydrogen sulfide), which in

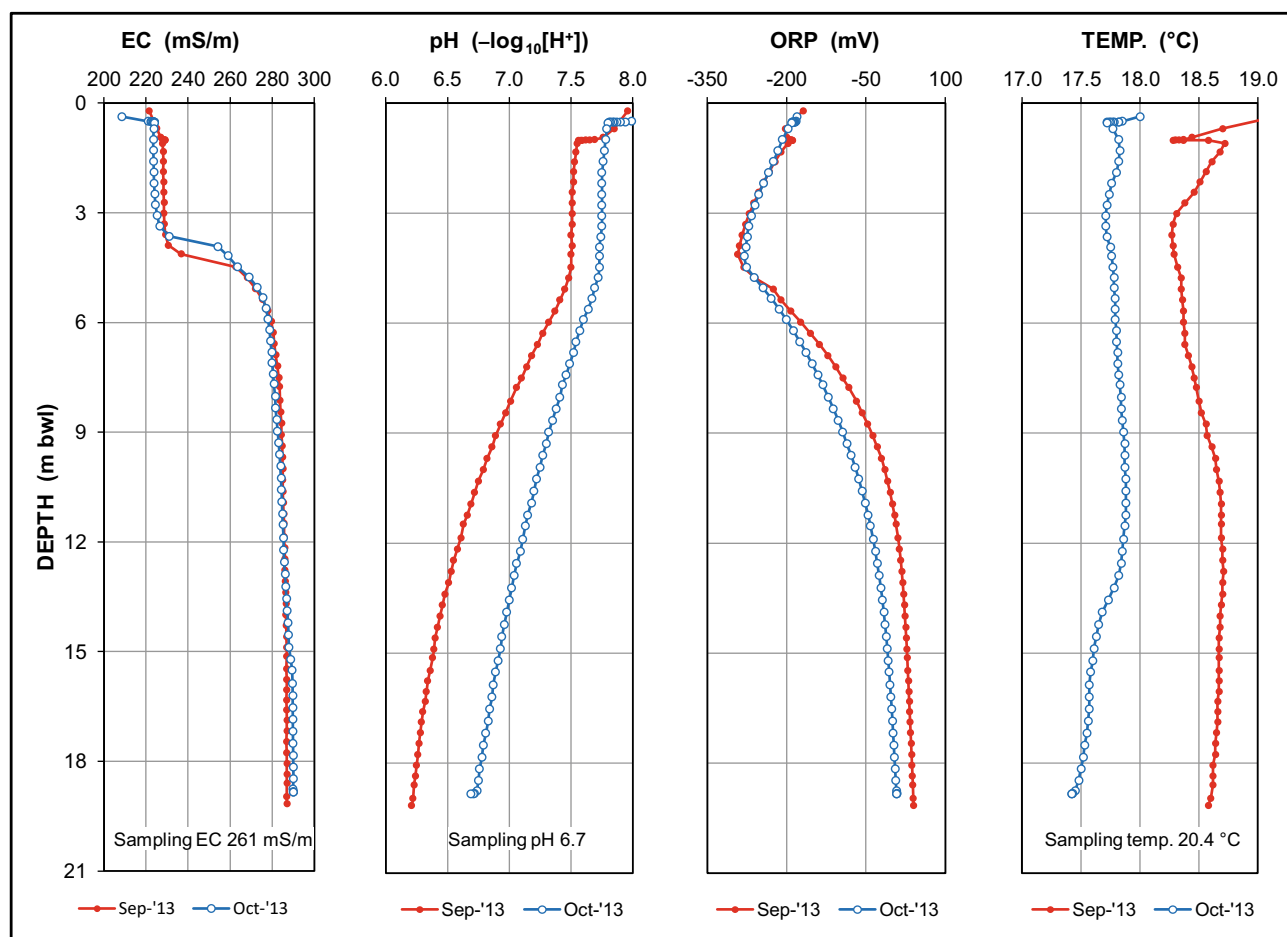


Fig. 76 Pre- and post-sampling vertical profiles of field water chemistry variables in borehole GP00309

turn reacts with metal ions such as Pb, Cu, Hg, and As to form metallic sulfides. The availability of excess Fe-oxide may consume all H_2S present in the groundwater (Appelo and Postma 2009), removing the characteristic ‘rotten egg’ odor from the water.

The precipitation of metal sulfides out of solution in a reducing (anaerobic) environment leads to a reduction in the concentrations of these metals in the groundwater. Further, Klaine et al. (2008) indicate that aquatic colloids comprise macromolecular organic materials that include the typical colloidal inorganic species of hydrous iron and manganese oxides. Their small nanoparticle size range (1 nm–1 μm) and large surface area per unit mass make them important binding phases for both organic and inorganic contaminants. Vesper et al. (2003) report the absorption of metals onto clays and other clastic particulates, onto organic material in the water, and onto iron or manganese oxides. Especially manganese oxides, recognized as a scavenger of radium (Sect. 5.2.2), are also recognized as extremely efficient scavengers of heavy metals. This possibility is demonstrated in Fig. 84.

Figure 84 shows the larger number of trace metals that exhibit elevated concentrations in the Riet Spruit surface water compared to those in the Blougat Spruit. Significant in the latter regard are Fe, Mn, and Ni. A further observation is the ubiquitous presence of Sr and, to a lesser extent Fe and V, in both surface water and groundwater sources.

Perhaps most significantly, however, is the undetectable presence (for the specified detection limits) of metals such as Al, Co, Mn, Ni, U, and Zn in the groundwater. This observation lends support for the possible occurrence of BSR in the karst aquifer. A study by Strosnider and Nairn (2010) demonstrated that concentrations of various trace metals including Al, As, Cd, Cr, Fe, Pb, V, and Zn reduced significantly when incubated in a mixture of acid mine water and municipal wastewater (see also Omoike and Vanloon 1999; Johnson and Younger 2006; McCullough 2008; McCullough et al. 2008; Strosnider et al. 2011; Hughes and Gray 2012). In essence, the mixing of these two environmental ‘liabilities’ is likely to generate beneficial reactions such as the following:

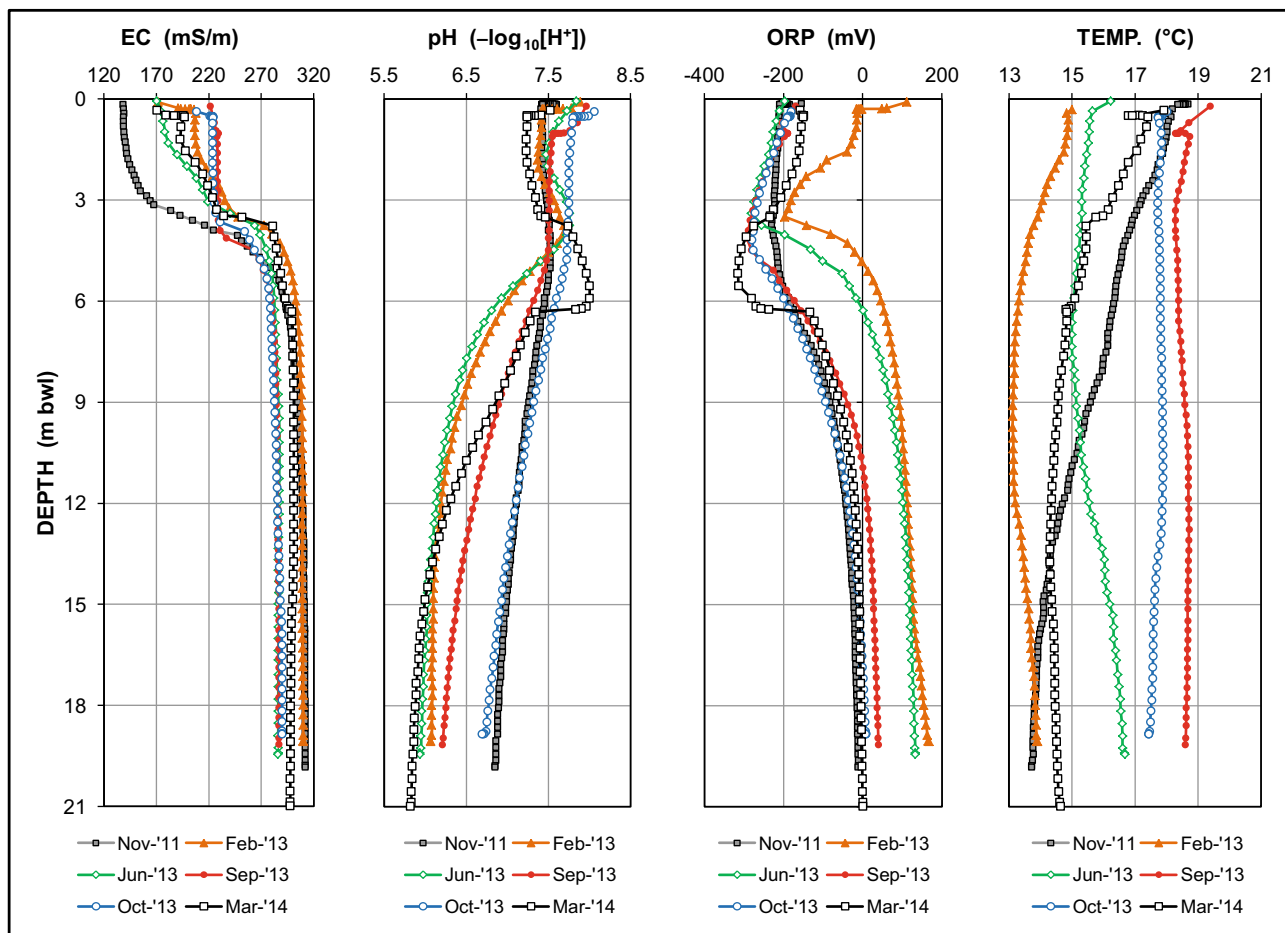


Fig. 77 Temporal variation in vertical profiles of field water chemistry variables in borehole GP00309

- dilution of hydrogen ion concentrations in mine water leading to reduced solubility of many metals at higher pH;
- reaction of phosphorus with dissolved Al and Fe in mine water resulting in precipitation;
- binding of many metals to organic ligands present in the municipal wastewater; and
- organic matter in the municipal wastewater provides a source of carbon that sulfate-reducing bacteria utilize to generate alkalinity and precipitate metals as sulfides.

It has similarly been demonstrated by Winfrey et al. (2010) that fecal indicator bacteria (FIB) counts reduced significantly when subjected to co-treatment with municipal wastewater and acid mine drainage in an engineered laboratory-scale passive system. Tutu et al. (2008) also attribute the observed increase in pH of AMD-related water in wetlands in the Central Rand Goldfield to desulfurization by bacteria.

Further evidence for sulfate reduction (sulfidogenesis) in the karst aquifer is provided by the metallic sulfide coating (Plate 8) on the data loggers in boreholes A2N0584, GP00302, and GP00305. The black deposit suggests the conversion of H_2S gas in the water, which might explain the absence of a 'rotten egg' odor (Cullimore 1999). The vertical hydrochemical profiles of these boreholes (Figs. 63, 69 and 70, respectively) do not reveal a common pattern or trend in the recorded variables, with only A2N0584 (Fig. 69) exhibiting strongly reducing conditions in the deeper section of the water column which favor the presence of sulfate-reducing bacteria (SRB). Similarly, an inspection of the groundwater chemistry associated with these boreholes indicates little congruence. It is postulated that anaerobic activities cause the increase in pH via (a) reduction of Fe^{3+} hydroxides as per Reaction ?, (b) conversion of strongly acidic sulfate to weakly acidic sulfide as per Reaction ?, and (c) production of carbonate alkalinity as per Reactions ? and ?.

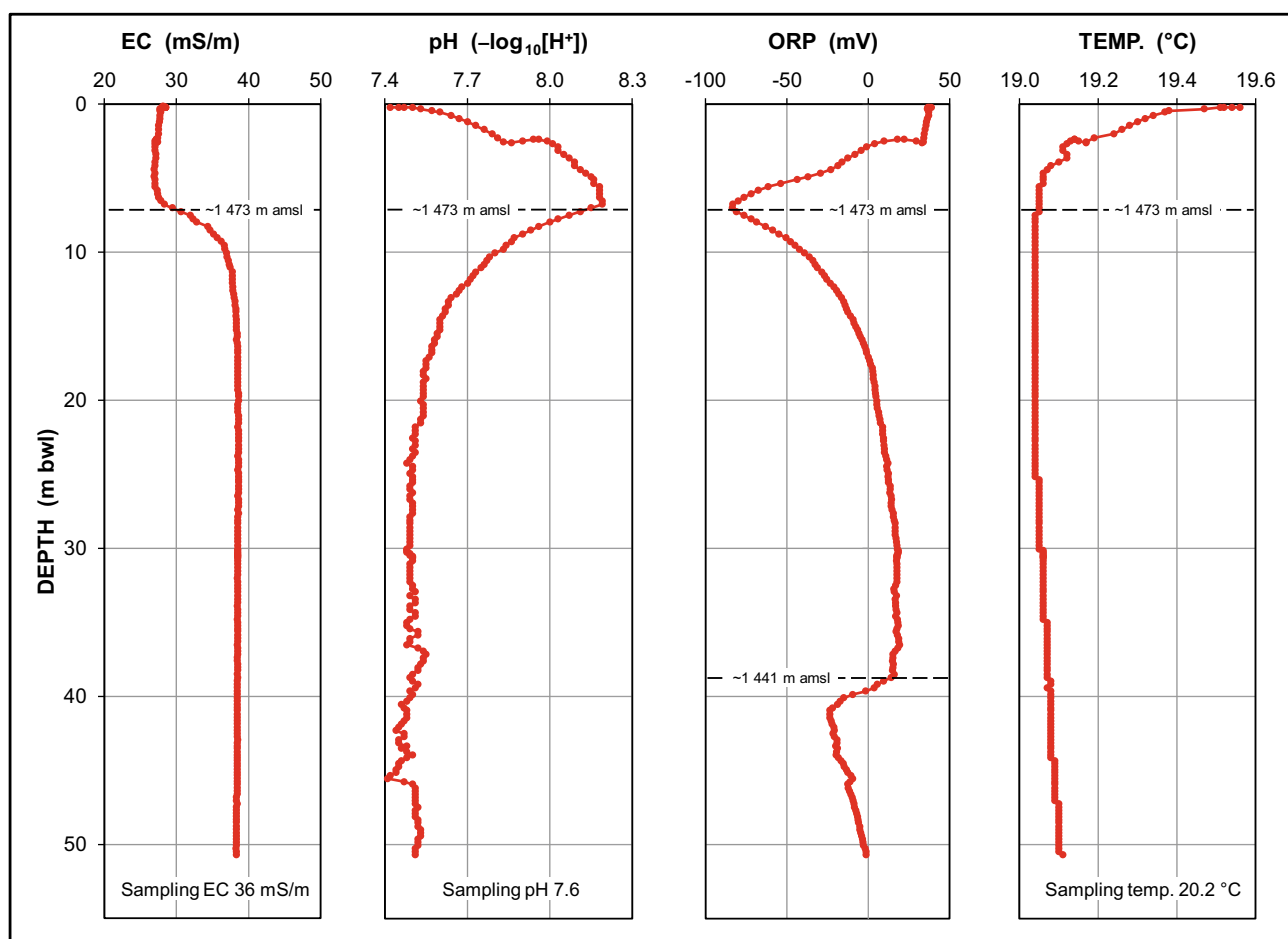


Fig. 78 Vertical profiles of field water chemistry variables in borehole GP00311 in October 2011

12 Dissolution of Carbonate Strata

The subject of karst denudation is afforded a 25-page chapter in the authoritative publication *Karst Hydrogeology and Geomorphology* by Ford and Williams (2007), and discussed extensively by Gabrovšek (2009). An earlier comprehensive review of carbonate rock dissolution by Morse and Arvidson (2002) reports the limited understanding of the kinetics of dolomite dissolution. In a study of the role of karstic dissolution in the global carbon cycle, Gombert (2002) mainly considered calcite (CaCO_3) in this role. Locally, Dirks et al. (2010) report long-term erosion rates of 3–5 m/Ma (3–5 mm/Ka), derived from cosmogenic ^{10}Be analysis of a quartz sample, for the plateau representing the African Erosion Surface south of the Malapa fossil site in the COH. More recently, Dirks and Berger (2013) describe the use of geologic and geomorphic evidence to explain landscape dynamics in the COH and propose an erosion rate of 5–6 m/Ma (5–6 mm/Ka) for dolomite along the plateau south of Malapa. The marginally greater erosion rate

accommodates differential erosion between more resistant chert and less resistant dolomite. Although centered on an iconic South African karst environment, these studies afford the process of solutional karst denudation little attention as an agent in the development of this landscape.

Morse and Arvidson (2002) point out the complexities revealed by two approaches to the study of karst denudation, namely solution-orientated studies (those that consider the chemical composition of solutions) and surface complexation studies (those that consider the effect of reaction processes on mineral surfaces). The first of these approaches is explored on the basis of newly acquired data and an improved understanding that informs the hydrophysical and hydrochemical environments in the COH. The results obtained from formula-derived, empirically-derived, and theoretically-derived approaches, are compared with observationally-derived values for this landscape sourced from the literature. The results are applied to various fossil sites on the property to demonstrate their relevance in reconstructing the probable prehistoric landscape at these localities.

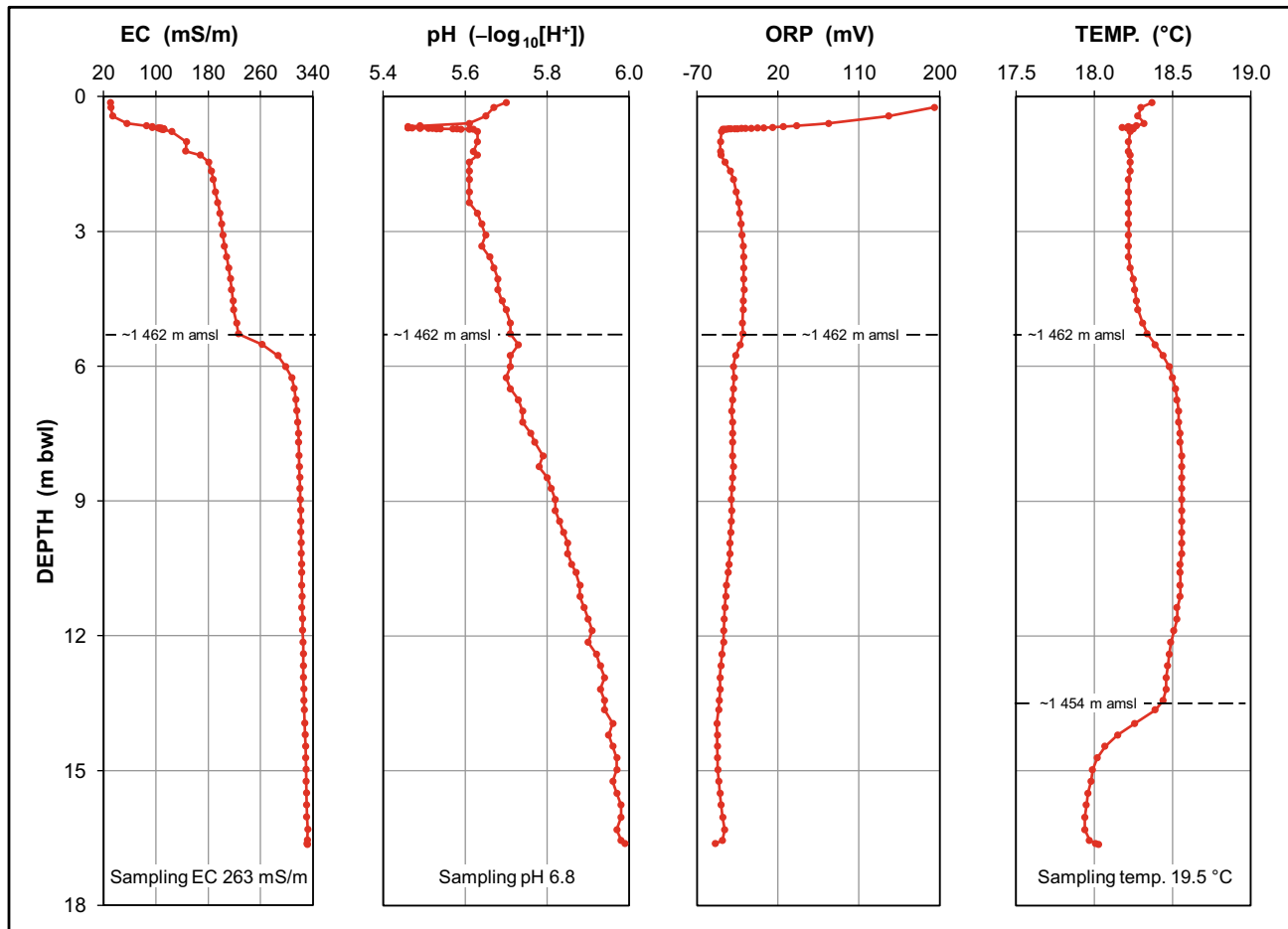
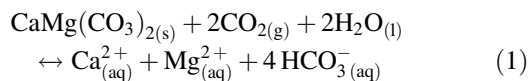


Fig. 79 Vertical profiles of field water chemistry variables in borehole GP00312 in October 2011

12.1 Natural Solutional Denudation

Kaufmann (2003) recognizes three principal agents in the evolution of karst landscapes as being those associated with hillslope, fluvial and chemical processes, respectively. Embedded in karst development, these processes act in tandem, the hillslope processes comprising weathering, slope wash, and soil creep representing short-range agents, and the fluvial (erosion and sedimentation) and chemical (karst denudation) processes representing long-range agents, i.e., controlling landscape evolution over long distances. Chemical dissolution of dolomite is a natural phenomenon described by the reaction



The rate of karst denudation by chemical dissolution is controlled mainly by the partial CO_2 pressure (P_{CO_2}) (White 1984; Kaufmann 2003), with temperature of lesser

importance. The denudation rate increases by $\sim 30\%$ with a decrease in water temperature from 25 to 5 °C (White 1984). Under circumstances where soil CO_2 is the primary driver of dissolution in karst environments, Brook et al. (1983) derived an empirical relationship between soil $\log[P_{\text{CO}_2}]$ values and mean annual actual evapotranspiration (AET) in mm described by the equation

$$\log[P_{\text{CO}_2}] = -3.47 + 2.09 \left(1 - e^{(-0.00172 \text{ AET})} \right) \quad (2)$$

Applying a study area AET value of 1540 mm (Sect. 2 in Chapter “Description of the Physical Environment”) in Eq. 2 gives a $\log[P_{\text{CO}_2}]$ value of -1.53 , i.e., $P_{\text{CO}_2} = 10^{-1.53}$ (0.03% or 300 mg CO_2/L air).

In addition to the dissolution of carbonate strata, Bakalowicz (2005) recognizes the transport and removal of the dissolved material as a necessary condition for karst development. This is typically provided by groundwater flow, a condition met in the COH by spring discharges.

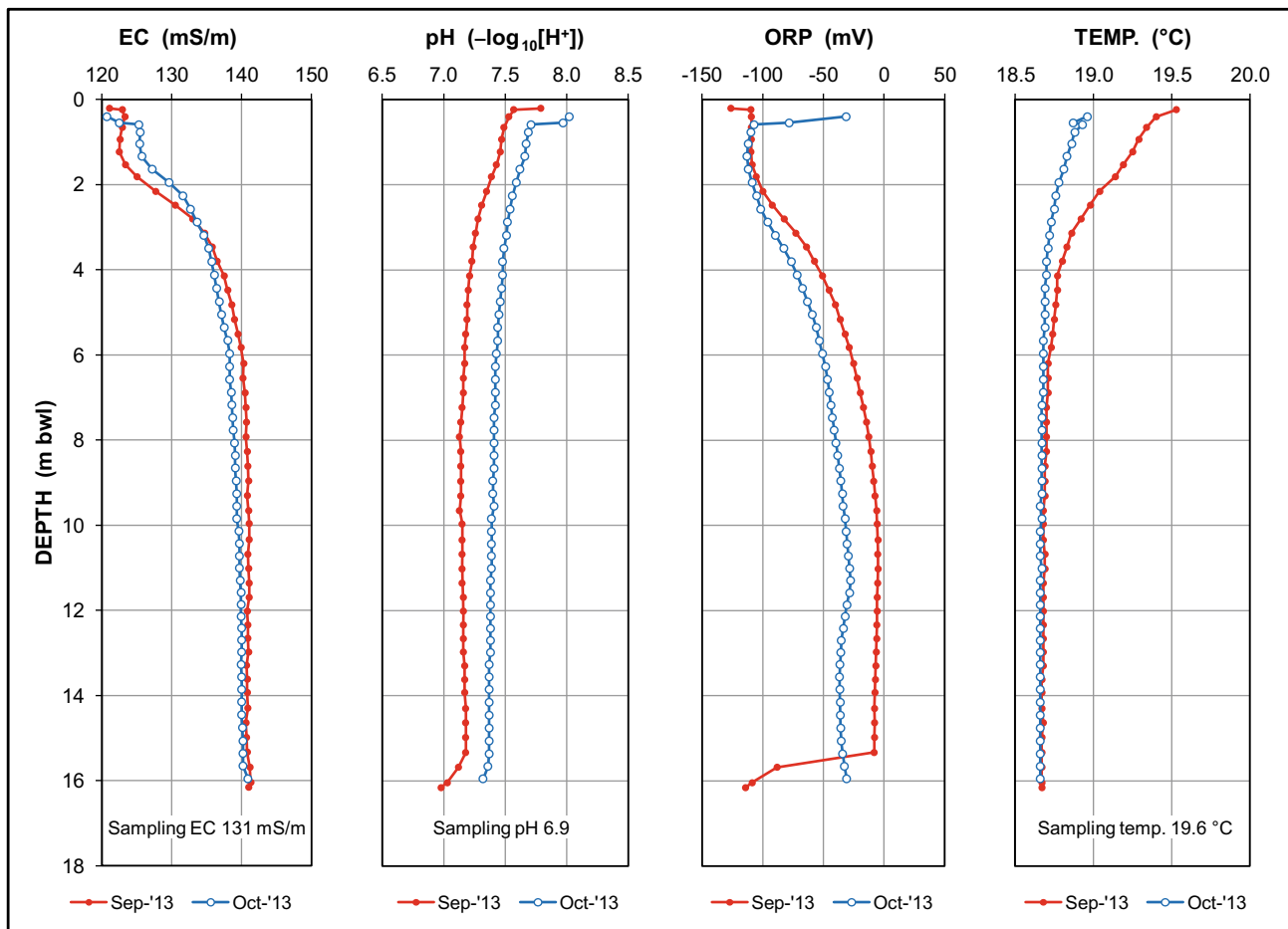


Fig. 80 Pre- and post-sampling vertical profiles of field water chemistry variables in borehole GP00313

12.1.1 Formula Approach

The Corbel (1959) formula is the simplest and most generic equation for calculating a first-order solutional denudation rate of a karst environment (Ford and Williams 2007; Gabrovšek 2009). It calculates limestone solution (D as mm/a) according to the relationship

$$D = 4 \cdot I \cdot T \div 100 \quad (3)$$

where I is runoff (dm) and T is the mean total alkalinity concentration (mg CaCO_3/L) of the water draining the karst environment, and the fraction $4/100$ ($\equiv 100/2500$) incorporates both the unit conversion factor of runoff to mm/a and the density of limestone (2500 kg/m^3). The application of the formula to the seven dolomitic compartments drained at rates $>20 \text{ L/s}$ returns the solutional denudation rates in the range $\sim 4\text{--}16 \text{ mm/Ka}$ reported in Table 16 for spring discharge and springwater chemistry ca. May 2010. The karst basins encompass 25,250 ha, which represents $\sim 94\%$ of the 26,860 ha footprint of dolomitic strata that underlie the COH.

A second set of spring discharge and springwater chemistry data for a smaller set of springs ca. August 2014, returns the solutional denudation rates reported in Table 17. Considering only those springs enumerated on both occasions, then the greater average runoff value of 1.62 dm/a (vs. 1.35 dm/a) and lower mean CaCO_3 value of 155 mg/L (vs. 169 mg/L) yield a denudation rate in the range $\sim 4\text{--}13 \text{ mm/Ka}$ for a mean of 10 mm/Ka compared to the 9.1 mm/Ka of the earlier data (Table 16).

The results might be questioned on the basis that the formula applies to limestone with a density of $\sim 2500 \text{ kg/m}^3$, whereas that of dolomite is $\sim 2850 \text{ kg/m}^3$ (Ford and Williams 2007). Although the formula also incorporates surface denudation, the results reflect primarily in situ dissolution as the T values represent the CaCO_3 concentration in the primarily autogenic springwater. Gabrovšek (2007) postulates that of the many assumptions that underpin estimation of the denudation rate, at least one of the following two, namely that (a) most of the dissolution occurs close to surface in the epikarst, or (b) dissolution in the

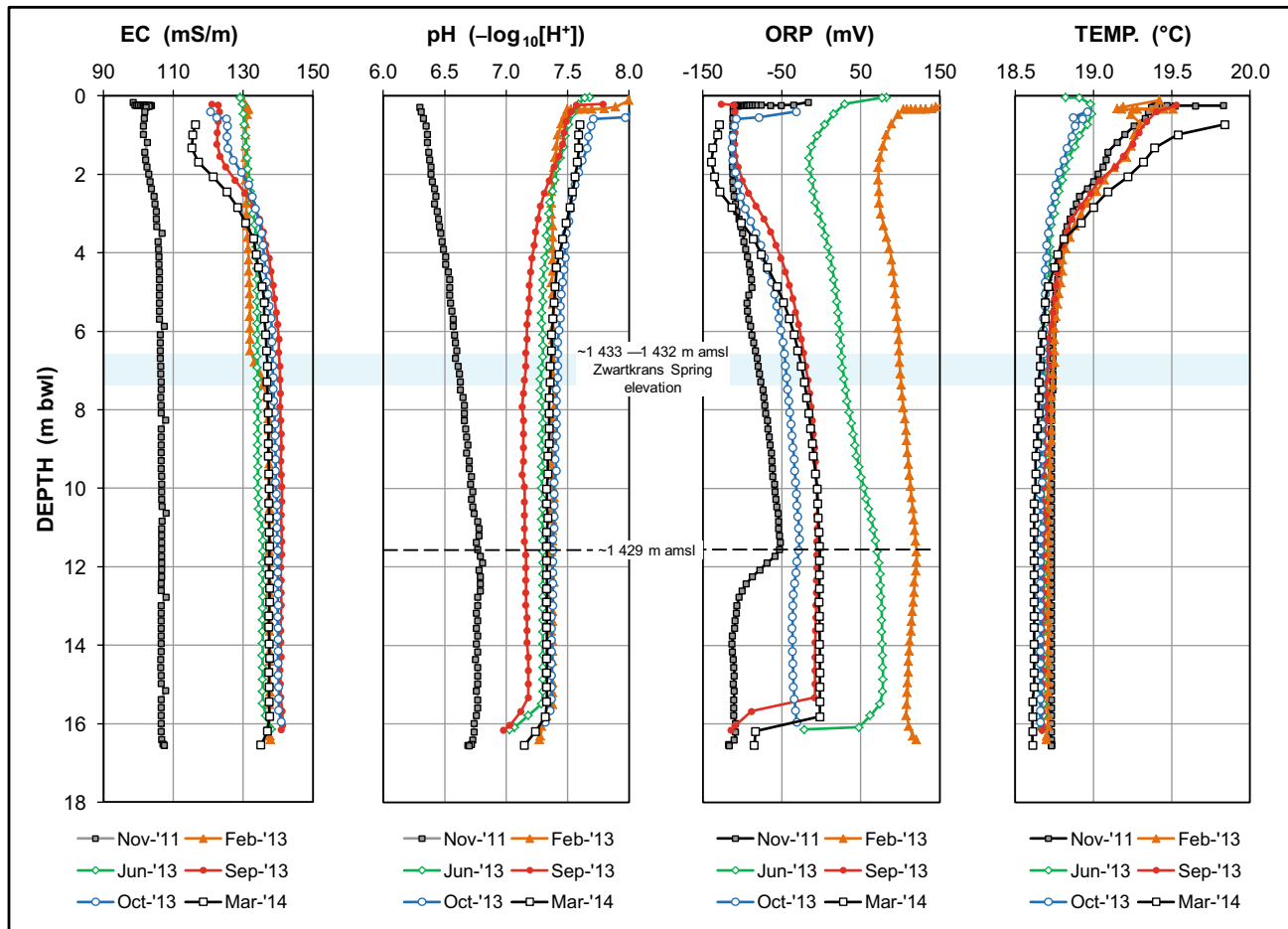


Fig. 81 Temporal variation in vertical profiles of field water chemistry variables in borehole GP00313

long-term at depth is integrated into a surface denudation, must be valid. The karst basins generate surface water runoff only intermittently following episodic rainfall events.

Gabrovšek (2009) reports the following formula that considers the density of rock

$$D = I \times c_{eq} \div \rho \quad (4)$$

where I is the difference between precipitation and evaporation (mm/a), c_{eq} is mineral solubility under given temperature and P_{CO_2} conditions, and ρ is the rock density (kg/m^3). The similarity to Eq. 3 is evident. Taking $P_{CO_2} = 1^{-1.53}$ (0.03% or 300 mg CO_2/L air) as per Eq. 2 at a temperature of 20 °C, and equating I to the groundwater recharge (Table 4 in Chapter “Physical Hydrogeology”), then Eq. 4 returns the dissolution rates presented in Table 18. Although generally slightly less than the values returned by Eq. 3 (Table 16), mainly attributable to the greater density of dolomite compared to limestone, the results returned by Eq. 4 are nevertheless in reasonable agreement.

Gabrovšek (2009) introduces a third equation for calculating the maximal solutional denudation as follows:

$$D = [M \times (P - E) \div 1000 \rho] \times c_{eq}(P_{CO_2}, T) \quad (5)$$

where M is the molar mass of calcite (100 g/mol), $P-E$ is infiltration I as in Eq. 4, c_{eq} is the equilibrium concentration of calcite (mol/m^3) in an open system for prevailing P_{CO_2} and temperature, and ρ is the rock density (g/cm^3). As might be expected, this equation returns the same results as Eq. 4 for $P_{CO_2} = 1^{-1.53}$ (0.03% or 300 mg CO_2/L air) and 20 °C.

12.1.2 Empirical Approach

AL du Toit (in Brink 1996) calculated that the Gerhardminnebron Eye draining the Gerhardminnebron Basin in the Lower Wonderfontein Spruit at a rate of 57 ML/d (~660 L/s), removed >10 tons of dolomite in solution daily. This equates to a dissolution-to-flow rate ratio of 0.2 t/ML. For dolomite, this translates into the creation of a void volume at a rate of ~3.5 m^3/d (~1280 m^3/a). Similarly, Swart et al. (2003) report analyses of springwater

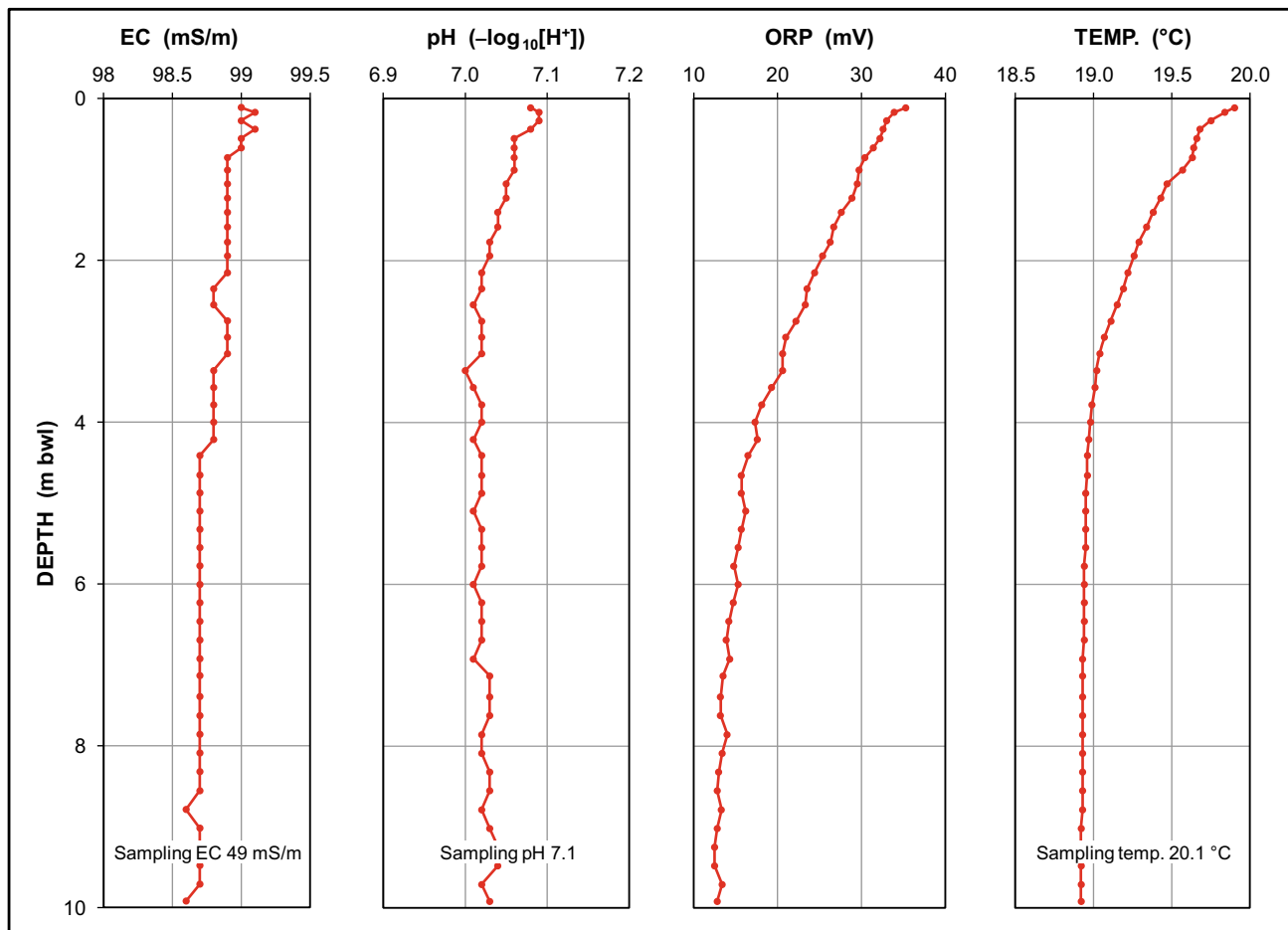


Fig. 82 Vertical profiles of field water chemistry variables in borehole GP00314 in November 2011

draining the Wonderfontein Valley as containing ~ 200 kg of dissolved limestone per million liters ($\equiv 200$ mg CaCO_3/L) in 1964. For a discharge of 200 ML/d, this implies the removal of >40 tons of limestone daily from this karst system. At a rate of ~ 14 m^3/d , this represents the development of a void volume of ~ 5110 m^3/a . A comparison with du Toit's ca. 1954 calculation reveals a similar dissolution-to-flow rate ratio of ~ 0.2 t/ML indicative of, among other factors, similar groundwater chemistry, and host groundwater-bearing strata.

Application of the dissolution-to-flow rate ratio of ~ 0.2 t/ML to the seven karst basins drained at rates >20 L/s, returns the dissolution rates reported in Table 19. The conversion from mass to volume is based on a rock density of 2850 kg/m^3 . The conversion of the dissolution rates to representative void development rates provides a simplistic volumetric (3-dimensional) perspective for comparison with the above-mentioned spatial (2-dimensional) denudation rate values.

The similar dissolution (denudation) rates returned by Eq. 3 (Tables 16 and 17) and Eq. 4 (Table 18), and the

empirically-derived values (Table 19) are evident in the respective mean values of 7.8, 7.2 and 7.9 mm/Ka. The correlation of the formula-derived values with the corresponding empirically-derived value is explored in Fig. 85. This suggests that the empirically-derived values exhibit a slightly better correlation with the Eq. 3 results ($R^2 = 0.79$) than with the Eq. 4 results ($R^2 = 0.73$). This observation is a little surprising seeing that Eq. 4 considers the density of dolomite rather than of limestone as in the case of Eq. 3 and should, therefore, return the better correlation.

12.1.3 Theoretical Approach

White (1984) and Kaufmann (2003) developed theoretical relationships between the solutional denudation rate and discharge/runoff (precipitation less evaporation) for different P_{CO_2} values and water temperatures. The equations incorporate terms that represent the strata and equilibria factors as well as rainfall, evapotranspiration, and temperature. Solutional denudation varies with the cube root of P_{CO_2} (Gabrovšek 2009) reflecting the dominance of the partial CO_2 pressure in the relation. This is illustrated in Fig. 86 for P_{CO_2}

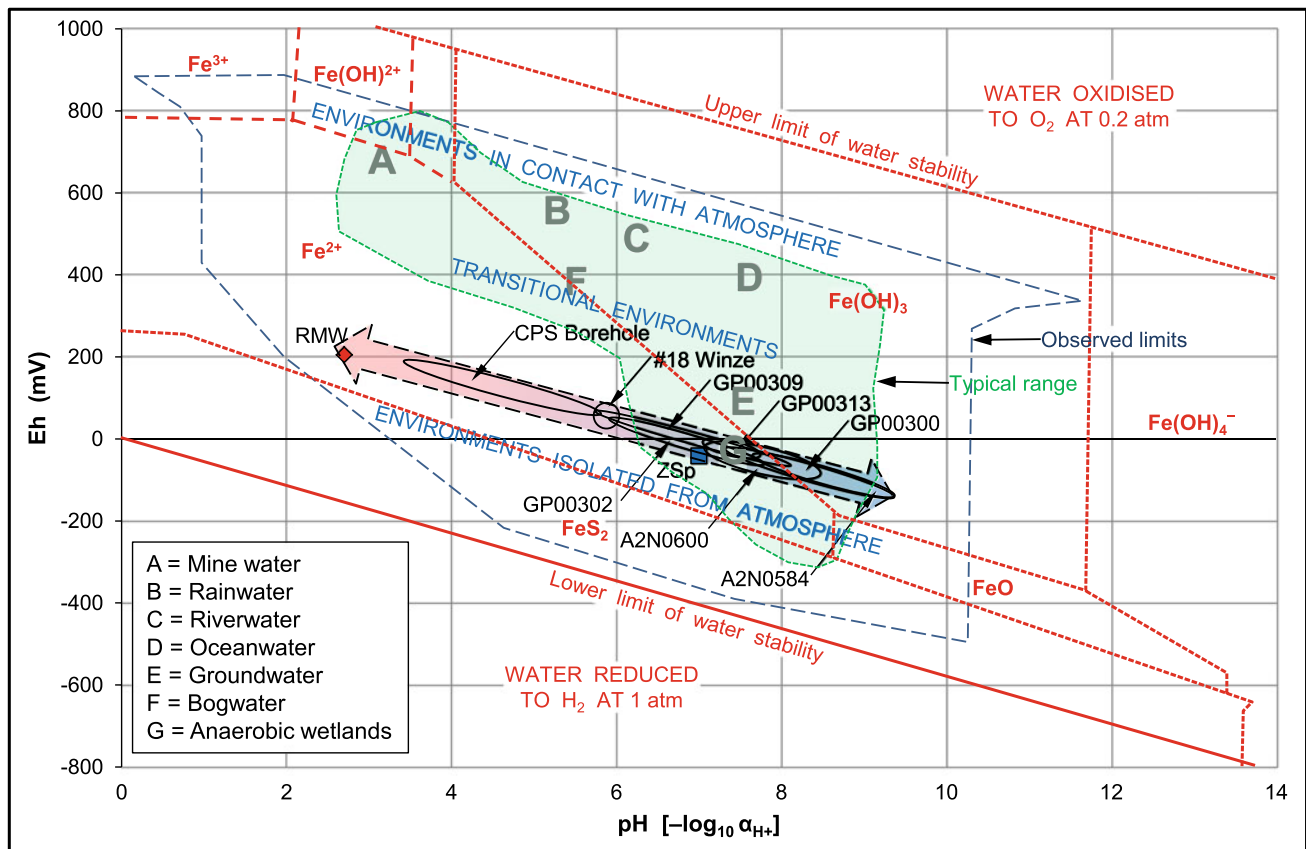


Fig. 83 Pourbaix diagram showing the distribution of Eh–pH values in mine water and groundwater environments in the subregion in relation to limits in the natural environment (redrawn in green and blue from USDA 2012) as defined by Baas-Becking et al. (1960), Garrels and Christ (1965) and Langmuir (1996), and stability fields for solid and dissolved forms of Fe at 25 °C and 1 atm (redrawn in red from Hem 1985)

values of $10^{-1.5}$, $10^{-2.5}$, and $10^{-3.5}$ atm at a water temperature of 25 °C.

Figure 86 also translates the range defined by the runoff rates listed in Tables 16, 18 and 19, to the equivalent denudation rate ranges of White (1984) and Kaufmann (2003). Reverse extrapolation of the mean value of 7.6 mm/Ka (from Table 19) to the Kaufmann (2003) graph (Fig. 86) suggests that an average (groundwater) discharge (runoff) value of ~118 mm/a (~1.2 dm/a) characterizes the karst environment in the COH. This equates to the discharge of 955 L/s from a karst area of 25,250 ha reported in Table 16.

12.1.4 Application

The observation by Martini et al. (2003) that the Sterkfontein Cave system hosted a water level 20–25 m above the present water level ~3.3 Ma ago, offers an opportunity to apply and test the karst dissolution rates reported above. Hobbs (2011) reports the association of this dewatering interval with elevations in the range 1456–1461 m amsl. In terms of the present landscape, the Blaauwbank Spruit valley to the

northwest of the caves would have been underwater to a depth of 15–20 m. It is more likely that the ~3.3 Ma BP landscape occupied a higher elevation, the prehistoric karst environment even then supporting a subterranean cave lake system as at present, with a water table located 20–25 m above the present water level.

Applying the Zwartkrans Basin denudation rate ‘extremes’ of 5.5 and 7.3 mm/Ka (Table 20) to the dewatering timeframe of ~3.3 Ma indicates a lowering of the land surface by ~18 m and ~24 m, respectively. Cognisant of the observation by White (2007b) that caves are the only features of the karst landscape for which “the age is locked in” and, as such, represent fixed elevation markers, then the values account quite reasonably for the magnitude of cave dewatering observed by Martini et al. (2003), lending support for the derived solutional denudation rates.

The above results also apply to the site of the Rising Star Expedition (Howley 2013) located in the Bolt’s Farm complex of fossil sites. Located at a depth of ~30 m below present surface, the fossil ‘deposit’ would have occupied a depth of 42–44 m below surface some 2 Ma ago.

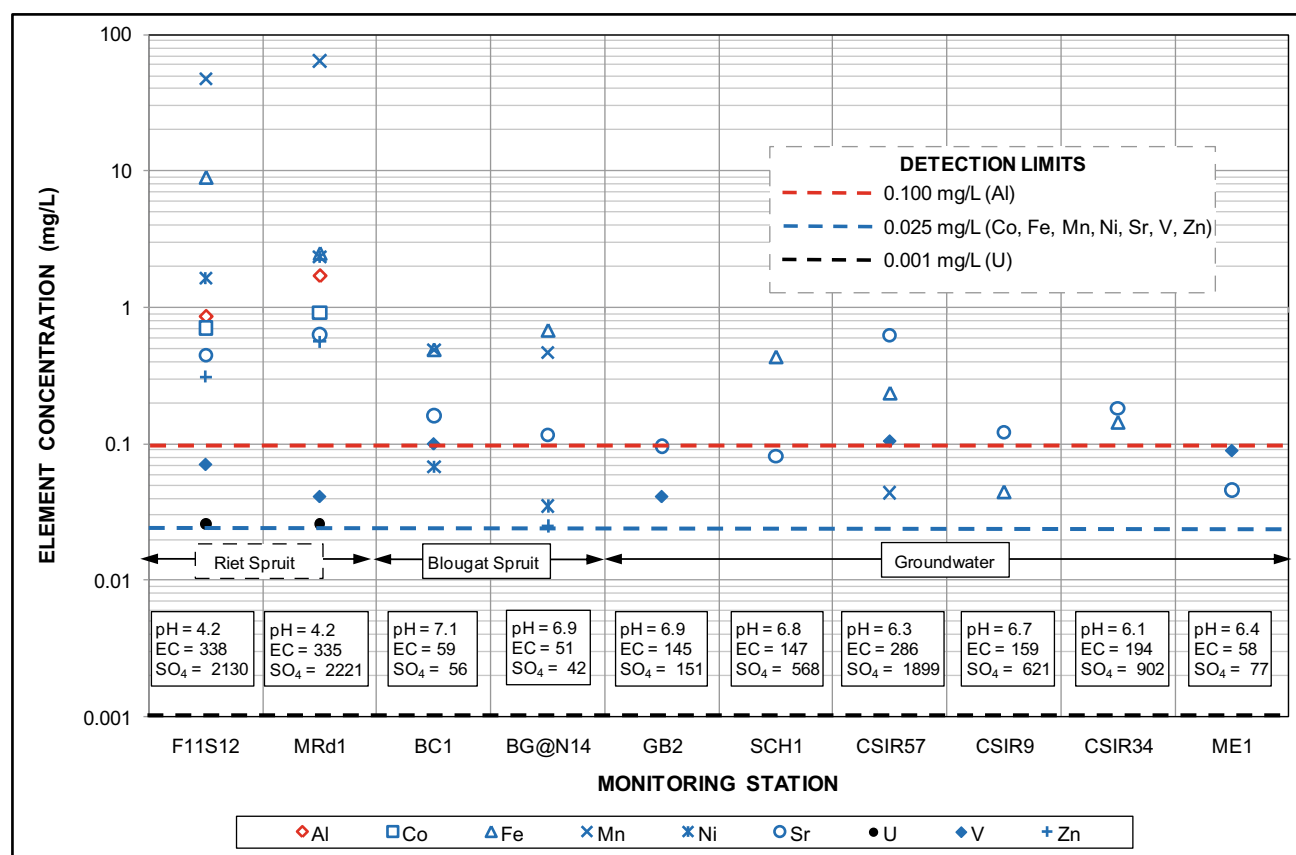


Fig. 84 Comparison of trace metal and other variable concentrations in surface water and proximate groundwater sources (SEC as mS/m; SO₄ as mg/L)

A similar analysis for the Malapa site, employing the denudation rates of 9.3 and 8.2 m/Ma, suggests that this site was located ~16–19 m below surface at ~2 Ma BP. This is considerably less than the ~50 m suggested by Dirks and Berger (2013) using a relational computation that gives estimated denudation rates of ~28 and ~24 m/Ma. The difference might be accounted for by exaggerated erosion rates associated with hillslope and fluvial processes (Kaufmann 2003) in the aptly-named more rugged Diepkloof Basin in which the Malapa site is located.

The relative constancy of spring discharge in the COH has been discussed in Sects. 2 and 4 in Chapter “Physical Hydrology”, and the similar constancy of springwater chemistry in Sects. 2.1 in Chapter “Chemical Hydrology” and 4 in Chapter “Physical Hydrogeology”.

12.1.5 Discussion

The average values of 8.0, 7.4 and 8.1 mm/Ka reported in Tables 16, 18 and 19, respectively, are bracketed by the theoretically-based White (1984) and Kaufmann (2003) values of ~9 and ~7.5 mm/Ka (Fig. 86, main diagram). The study area soil P_{CO_2} of $10^{-1.53}$ and mean water temperature of 20.9 °C (Table 16) approach the values of $P_{\text{CO}_2} = 10^{-1.5}$ atm

(0.032%) and 25 °C employed in the theoretical relationships described in Fig. 86. Under these circumstances, the theoretical denudation rate of Kaufmann (2003) is in better agreement with the average values than that of White (1984).

The formula-derived solutional denudation rate of the seven karst basins falls in the range of 4.7–16.2 mm/Ka, compared to the 3.4–14.8 mm/Ka range of the empirically-derived rate (Table 20). Both these ranges of denudation rate accommodate the 5–6 mm/Ka reported by Dirks and Berger (2013) for the dolomite plateau south of the Malapa fossil site. It must be recognized that the development of the karst landscape in the COH has also involved the hillslope and fluvial processes recognized by Kaufmann (2003) as completing the trilogy of principal agents in landscape evolution. The erosion associated with fluvial processes is given context by Dirks et al. (2010), who report a rate of vertical incision of the Skeerpoort River below the Gladysvale fossil site of 53 ± 9 mm/Ka based on a cosmogenic ^{10}Be study of valley bedrock strata. Dirks and Berger (2013) simplify this to ~55 mm/Ka.

Gladysvale cave is located in the Uitkomst Basin, which adjoins the Diepkloof Basin in which the Malapa site is located. These compartments occupy a similar



Plate 8 Data logger (length ~20 cm) from monitoring borehole GP00305 completely coated with black iron sulfide (FeS) precipitate on stainless steel instrument (photo N. de Meillon)

hydrostratigraphic position along the north-western margin of the COH and exhibit similar mean denudation rates of 8.6 and 8.1 mm/Ka, respectively (Table 20). Compared to the ~85% greater fluvial down-cutting rate, the difference demonstrates the greater efficacy of the latter as an agent in landscape development in the presence of conducive

physiographic conditions. These conditions also underpin the caution by Gabrovšek (2009) that methods that employ hydrochemistry (in this instance springwater chemistry) return a “batch result” of regional denudation that is subject to variation in climate and catchment over time.

The denudation rate values reported in Table 20 are similar to the range of 13.1–17.9 mm/Ka determined for the Cumberland Plateau, USA, from a geochemical mass balance (Florea 2015). Denudation rate values obtained by different methods in different environments listed by Gabrovšek (2009) and Florea (2015) as sourced from international literature provide for a more comprehensive comparison with the COH results reported in Table 20.

Values returned by the solute load method for four locations in Europe and one in New Zealand fall in the range of 48–95 mm/Ka. The order of magnitude greater results than are reported for the COH can mainly be attributed to much wetter climates. The local MAP of ~700 mm is >50% drier than the range 1450–3000 mm/a that characterizes the international locations. Much more comparable values in the range 6.0–14.6 mm/Ka are reported for limestone tablet exposure studies in tropical humid, temperate mountainous and Alpine environments with precipitation in the range 1300–3000 mm/a. Micro-erosion meter (MEM) and cosmogenic nuclide methods return higher values (15–150 mm/Ka) in similar MAP regimes. The lowest value of 1 mm/Ka was obtained by the cosmogenic nuclide method applied in an arid environment in Australia.

A further aspect of relevance to the historical landscape and cave water levels is the position of the ‘Little Foot’ fossil site in Sterkfontein Cave. The site is located ~25 m below surface and for a (maximum) present site surface elevation of 1487 m amsl places ‘Little Foot’ at an elevation of ~1462 m amsl (Bruxelles et al. 2014). This is at least ~22 m above the current maximum attainable cave water level of ~1440 m amsl. If the age of ‘Little Foot’ is now

Table 16 Estimate of solutional denudation rate based on the Corbel formula (Eq. 3) for spring discharges and springwater chemistry in May 2010

| Basin | Area (ha) | Spring | Discharge (L/s) | Runoff (dm/a) | CaCO ₃ (mg/L) | Temp (°C) | Denudation rate (m ³ /km ² /a ≡ mm/Ka) |
|---------------|-----------|---------------|-----------------|---------------|--------------------------|-----------|--|
| Zwartkrans | 9800 | Zwartkrans | 265 | 0.85 | 160 | 18.8 | 5.5 |
| Krombank | 5080 | Plover’s Lake | 60 | 2.10 | 192 | 19.8 | 16.2 |
| | | Kromdraai | 279 | | | | |
| Danielsrust | 740 | Danielsrust | 28 | 1.19 | 128 | 20.4 | 6.1 |
| Twefontein | 1160 | Twefontein | 30 | 0.82 | 196 | 20.6 | 6.4 |
| Diepkloof | 3800 | Nouklip | 143 | 1.19 | 196 | 22.6 | 9.3 |
| Uitkomst | 2860 | Nash | 130 | 1.43 | 132 | 21.4 | 7.6 |
| Broederstroom | 1810 | Broederstroom | 20 | 0.35 | 272 | 22.8 | 3.8 |
| Total average | 25,250 | | 955 | 1.13 | 182 | 20.9 | 7.8 |

Table 17 Estimate of solutional denudation rate based on the Corbel formula for spring discharges and springwater chemistry in August 2014

| Basin | Area (ha) | Spring | Discharge (L/s) | Runoff (dm/a) | CaCO ₃ (mg/L) | Temp (°C) | Denudation rate (m ³ /km ² /a ≡ mm/Ka) |
|---------------|-----------|---------------|-----------------|---------------|--------------------------|-----------|--|
| Krombank | 5080 | Plover's Lake | 65 | 2.14 | 159 | 20.1 | 13.6 |
| | | Kromdraai | 279 | | | 19.4 | |
| Danielsrust | 740 | Danielsrust | 28 | 1.19 | 131 | 19.6 | 6.3 |
| Tweefontein | 1160 | Tweefontein | 26 | 0.71 | 156 | 20.5 | 4.4 |
| Diepkloof | 3800 | Nouklip | 211 | 1.75 | 197 | 21.4 | 13.8 |
| Uitkomst | 2860 | Nash | 208 | 2.29 | 130 | 21.3 | 11.9 |
| Total average | 13,640 | | 817 | 1.62 | 155 | 20.4 | 10.0 |

Table 18 Estimate of solutional denudation rate based on Eq. 4

| Spring(s) | Recharge | | c_{eq} (mg CaCO ₃ /L) | Denudation rate (m ³ /km ² /a ≡ mm/Ka) |
|-----------------------------------|--------------------|------|------------------------------------|--|
| | % MAP ^a | mm/a | | |
| Zwartkrans | 18 | 130 | 160 | 7.3 |
| Plover's Lake + Kromdraai | 30 | 210 | 192 | 14.1 |
| Danielsrust | 17 | 119 | 128 | 5.3 |
| Tweefontein | 11 | 81 | 196 | 5.6 |
| Nouklip | 17 | 119 | 196 | 8.2 |
| Nash | 20 | 143 | 132 | 6.6 |
| Broederstroom + Anderson + Lesedi | 7 | 49 | 272 | 4.7 |
| Average | 17.1 | 122 | 182 | 7.4 |

^aFor an MAP of 710 mm**Table 19** Empirically-derived estimate of dissolution rate based on the mass of CaCO₃ removed

| Spring | Discharge (ML/a) | Runoff (mm/a) | Mass of CaCO ₃ removed (t/a) | Dissolution rate (mm/Ka) | Void development rate (m ³ /a) |
|---------------------------|------------------|---------------|---|--------------------------|---|
| Zwartkrans | 8357 | 85 | 1671 | 6.0 | 586 |
| Plover's Lake + Kromdraai | 10,691 | 210 | 2138 | 14.8 | 750 |
| Danielsrust | 883 | 119 | 177 | 8.4 | 62 |
| Tweefontein | 946 | 82 | 189 | 5.7 | 66 |
| Nouklip | 4510 | 119 | 902 | 8.3 | 316 |
| Nash | 4100 | 143 | 820 | 10.1 | 288 |
| Broederstroom | 883 | 49 | 132 | 3.4 | 62 |
| Total average | 30,369 | 115 | 6030 861 | 8.1 | 2131 |

thought to be ~ 3.7 Ma (Gardner 2015), then it is conceivable that this individual met its end close to the contemporary cave water level at an elevation in the range of ~ 20 – 27 m above the current water table. Further, it might well have fallen further (as much as ~ 50 m) than the ~ 20 m reported in the Balter (2014) article if this is what led to its demise.

12.1.6 Conclusion

An assessment of karst solutional denudation rates in the COH based on formula-derived, empirically-derived, and theoretically-derived approaches yields results that are in agreement with recently reported values and with the observed dewatering horizon developed over 3.3 Ma in Sterkfontein Cave. Cognisant of the variation in

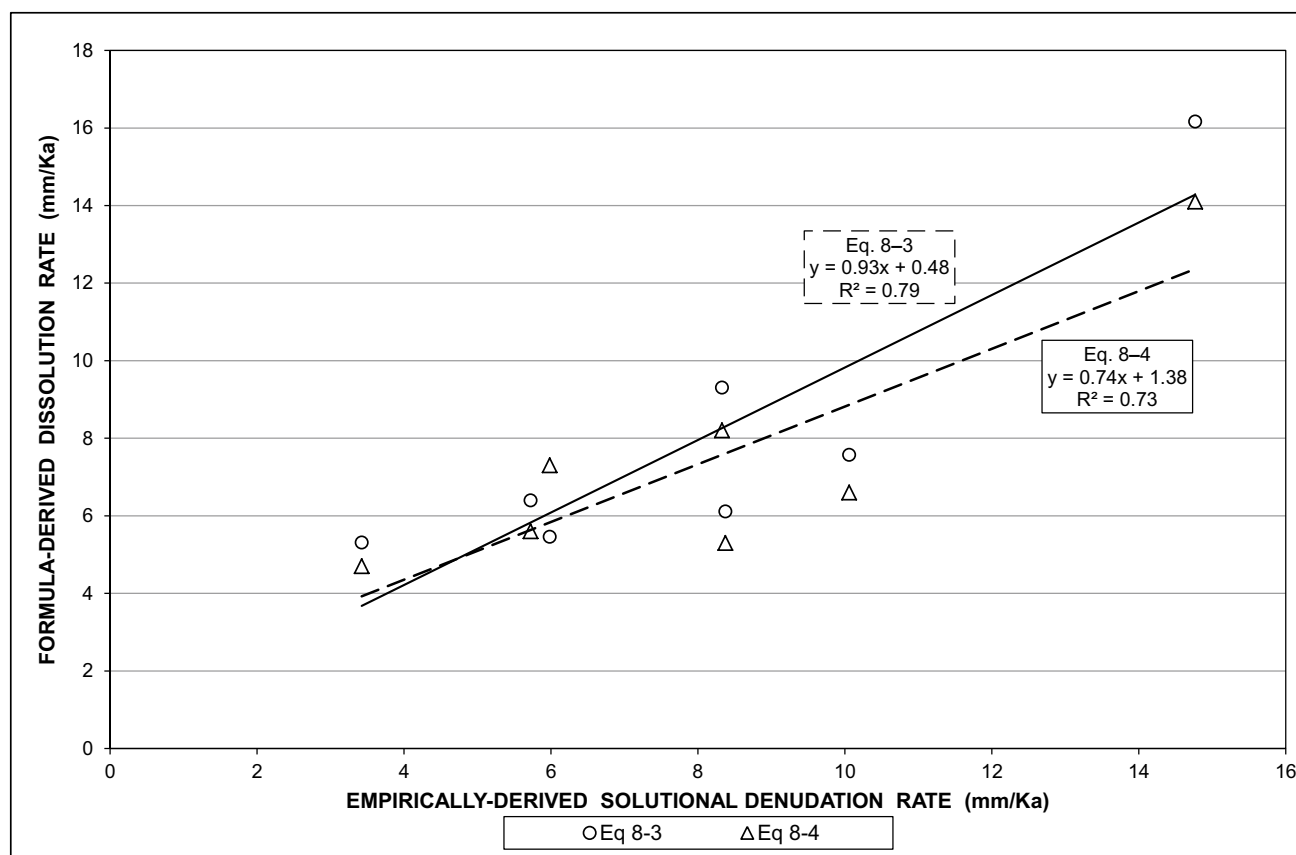


Fig. 85 Correlation of empirically-derived and formula-derived karst denudation/dissolution rates

climatological and physiographical factors that influence landscape evolution in the long-term (White 2007b), the mean solutional denudation rate in the COH is placed at 7.8 mm/Ka in the range 5–15 mm/Ka.

Studies that consider the effect of reaction processes on mineral surfaces (the surface complexation studies defined by Morse and Arvidson 2002) in the evaluation of karst denudation remain unexplored in a South African context. The manifestation of a combined mine water and municipal wastewater impact on a portion of the COH karst environment provides an opportunity to explore this aspect against a comparison with the pristine portions of this environment.

12.2 Interaction with Mine Water

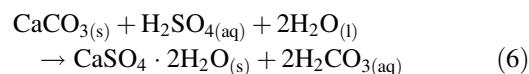
Sherlock et al. (1995) provide a synthesis of the neutralization of acid rock drainage (ARD) by carbonate and silicate minerals in the context of predicting and managing site-specific mining and processing wastes. Studies by Sasowsky and White (1993), Webb and Sasowsky (1994), and Sasowsky et al. (1995) provide valuable information on various aspects of the interaction between AMD and karst

aquifers in the Obey River Basin in north-central Tennessee (USA). These studies illuminate the conjecture that characterizes the geochemical interaction between acidic mine water and the karst aquifer in another location where such interaction occurs, namely the Zwartkrans Basin in the COH.

The two main hypotheses that inform this conjecture are summarized as either dissolution or armoring of dolomite (carbonate strata). It is apparent that these mechanisms relate to the two approaches discussed by Morse and Arvidson (2002), namely studies that consider the chemical composition of solutions, and those that consider the effect of reaction processes on mineral surfaces. These are explored in the following sections.

12.2.1 Carbonate Dissolution

Neutralization of SO_4 -rich AMD by calcite precipitates gypsum according to the reaction



and neutralization by dolomite precipitates epsomite according to the reaction (Lottermoser 2010)

Fig. 86 Denudation rate as a function of discharge for different P_{CO_2} values (insert diagram at a temperature of 25 °C [redrawn from Ford and Williams (2007) and Kaufmann (2003)]; the shaded areas (main diagram) define the identical runoff ranges listed in Tables 16, 18 and 19, and the pecked arrows the mean discharge/runoff rate (113 mm/a) and associated theoretical denudation rates for a P_{CO_2} of $10^{-1.5}$ atm; see text for discussion of reverse (anti-clockwise) arrow

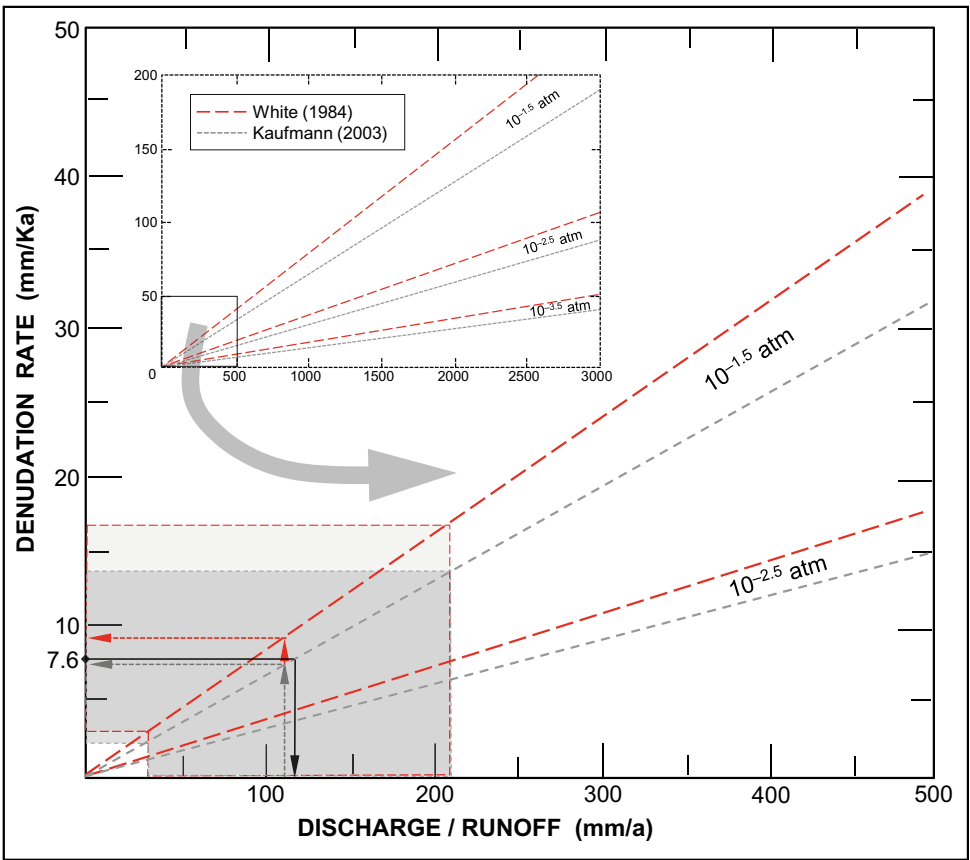
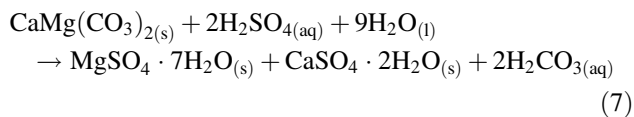


Table 20 Comparison of formula-derived and empirically-derived solutional denudation rates per karst basin and associated fossil site(s)

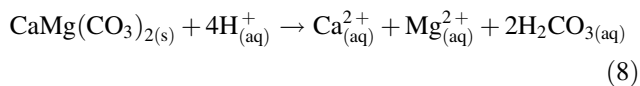
| Karst Basin | Solutional denudation rate (m ³ /km ² /a ≡ mm/Ka ≡ m/Ma) | | | | Fossil site |
|---------------|--|--------------------------|-----------------------------------|---------|---|
| | Formula-derived | | Empirically-derived (Table 19) | Average | |
| | Equation 3 (Table 16) | Equation 3 (Table 18) | | | |
| Zwartkrans | 5.5 | 7.3 | 6.0 | 6.3 | Sterkfontein Bolt’s Farm Swartkrans Minnaar’s Cave Cooper’s Cave Kromdraai |
| Krombank | 16.2 | 14.1 | 14.8 | 15.0 | Plover’s Lake Wonder Cave |
| Danielsrust | 6.1 | 5.3 | 8.4 | 6.6 | Drimolen |
| Tweefontein | 6.4 | 5.6 | 5.7 | 5.9 | – |
| Diepkloof | 9.3 | 8.2 | 8.3 | 8.6 | Malapa |
| Uitkomst | 7.6 | 6.6 | 10.1 | 8.1 | Gladysvale |
| Broederstroom | 5.3 | 4.7 | 3.4 | 4.5 | Gondolin |
| Average | 8.0 | 7.4 | 8.1 | 7.8 | |



Plate 9 Examples of **a** hard ferrihydrite crust effectively sealing the bottom of a stream channel, and **b, c** entombing/entombed in-stream vegetation. (Photo **b**, B Genthe)



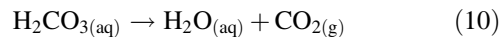
The dissolution of dolomite in the presence of free protons is also more simply described by the reaction



which consumes four moles of H^+ for each mole of Ca and Mg released into solution and produces carbonic acid (H_2CO_3) which adds alkalinity to the groundwater system through the release of bicarbonate (HCO_3^-) according to the reaction



Further dissociation of the H_2CO_3 results in the exsolution (degassing or release) of carbon dioxide (CO_2) according to the reaction



whereas Reaction 8 can proceed at a pH of up to slightly >8 where solid $\text{CaMg}(\text{CO}_3)_2$ is stable, i.e., the solution is in equilibrium with the atmosphere where $P_{\text{CO}_2} \approx 10^{-3.5}$ atm, Reactions 9 and 10 proceed only below a pH of ~ 6.4 (Barnes and Romberger 1968).

Scott (1995) reports the ‘consumption’ (dissolution) of dolomite in the East Rand Basin as ranging from ~ 0.9 t/d (321 t/a) to ~ 18 t/d (~ 6400 t/a) for ‘flow’ rates of 1 ML/d (most realistic) and 20 ML/d (worst case scenario), respectively, for ‘modeled’ ambient water chemistry. These values represent void volumes of ~ 115 to ~ 2250 m³ being created annually, i.e., at a rate of ~ 0.3 to ~ 6 m³/d. They also represent a dissolution-to-flow rate ratio of ~ 0.9 t/ML, which is nearly five times the value of ~ 0.2 t/ML associated with ‘pristine’ karst groundwater (Sect. 12.1.2).

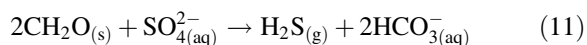
Apart from the dissolution of carbonate rocks, however, a second main source of positive alkalinity in mine drainage is SO_4 reduction (Kirby and Cravotta 2005a). This releases bicarbonate (HCO_3^-) to solution according to the reaction

Table 21 Net acidity and net alkalinity of various groundwaters in the COH environment

| Water source | Water type ^a | Acidity calculation analytes | | | | | | | |
|---------------------|-------------------------|--|-----------------|-----------|-----------|-----------|---|----------------|-------------|
| | | Total alkalinity (mg CaCO ₃ /L) | pH ^b | Fe (mg/L) | Mn (mg/L) | Al (mg/L) | Total acidity (mg CaCO ₃ /L) | Net alkalinity | Net acidity |
| | | | | | | | | | |
| CSIR57 ^c | 1 | 28 | 6.3 | 0.237 | 0.044 | <0.1 | 0.53 | 27 | -27 |
| CSIR57 ^d | | 108 | 6.8 | <0.025 | <0.025 | n.a. | 0.10 | 108 | -108 |
| CSIR57 ^e | | 4.1 | 5.7 | 0.003 | 14 | 0.2 | 27 | -23 | 23 |
| CSIR8 | 2 | 140 | 6.9 | 0.036 | n.a. | <0.1 | 0.63 | 139 | -139 |
| CSIR9 | 2 | 128 | 6.7 | 0.045 | n.a. | <0.1 | 0.65 | 127 | -127 |
| CSIR34 | 2 | 56 | 6.1 | 0.145 | 0.025 | <0.1 | 0.90 | 55 | -55 |
| NR1 | 2 | 224 | 7.1 | 1.62 | 0.061 | <0.1 | 3.6 | 220 | -220 |
| DC1 | 2 | 148 | 7.5 | 0.037 | n.a. | <0.1 | 0.62 | 147 | -147 |
| GB2 | 2 | 252 | 6.9 | 0.025 | 0.025 | <0.1 | 0.65 | 251 | -251 |
| SCH1 | 2 | 160 | 6.8 | 0.436 | 0.025 | <0.1 | 1.4 | 159 | -159 |
| ZSp ^e | 2 | 160 | 7.5 | <0.025 | <0.025 | 0.116 | 0.74 | 159 | -159 |
| ZSp ^f | | 169 | 7.1 | 0.040 | 0.005 | 0.20 | 1.20 | 168 | -168 |
| SFC ^f | 2 | 169 | 7.6 | 0.032 | 0.011 | 0.20 | 1.19 | 168 | -168 |
| SFC ^g | | 152 | 7.9 | <0.025 | <0.025 | 0.20 | 1.20 | 151 | -151 |
| SFC ^h | | 154 | 7.6 | <0.02 | <0.005 | 0.20 | 1.16 | 153 | -153 |

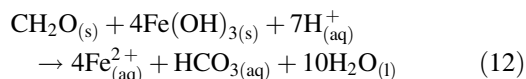
^a1 = impacted karst groundwater; 2 = slightly impacted karst groundwater^b-log₁₀2H⁺^cSample date 16/02/2010^dSample date 18/03/2007^eSample date 27/08/2014^fSample date 16/05/2014^gSample date 13/05/2010^hSample date 14/01/2011**Table 22** Free acidity and metal acidity associated with the results presented in Table 21

| Water source | Water type | Free acidity (mg CaCO ₃ /L) | Metal acidity (mg CaCO ₃ /L) | Total (calculated) acidity (mg CaCO ₃ /L) | Free: total acidity ratio (%) |
|--------------|------------|--|---|--|-------------------------------|
| CSIR57 | 1 | 0.01 | 0.09 | 0.10 | 10.0 |
| | | 0.03 | 1.06 | 1.09 | 2.75 |
| | | 0.1 | 12.6 | 26.7 | 0.37 |
| CSIR8 | 2 | 0.01 | 0.62 | 0.63 | 1.59 |
| CSIR9 | 2 | 0.01 | 0.64 | 0.65 | 1.54 |
| CSIR34 | 2 | 0.04 | 0.86 | 0.90 | 4.44 |
| NR1 | 2 | 0 | 3.57 | 3.57 | 0.1 |
| DC1 | 2 | 0 | 0.62 | 0.62 | 0.3 |
| GB2 | 2 | 0.01 | 0.65 | 0.66 | 1.52 |
| SCH1 | 2 | 0.01 | 1.38 | 1.39 | 0.72 |
| ZSp | 2 | 0 | 0.73 | 0.74 | 0.2 |
| | | 0 | 1.19 | 1.20 | 0.3 |
| SFC | 2 | 0.0006 | 1.2 | 1.2 | 0.05 |
| | | 0.0013 | 1.2 | 1.2 | 0.11 |
| | | 0.0013 | 1.2 | 1.2 | 0.11 |



where $2\text{CH}_2\text{O}$ represents organic matter.

Kirby and Cravotta (2005a) also report that reductive dissolution of metal hydroxides may contribute to alkalinity according to the reaction

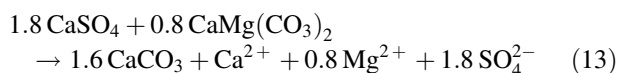


It has previously been reported (Sect. 1.2.4 in Chapter “[Chemical Hydrology](#)”) that the treated effluent discharged from the Percy Stewart WWTW carries an elevated bacteriological and nutrient (N, P, and COD) load (see Tables 11, 13 and 14 in Chapter “[Chemical Hydrology](#)”). Further, this water also enters the karst aquifer at a rate of ~ 7 ML/d (Table 19). This water mixes in the subsurface with the allogenic recharge of mine water (Sect. 5.2.1 in Chapter “[Physical Hydrology](#)”), the mixing nexus coinciding with the area around the confluence of the Riet and Blougat spruits targeted for monitoring by borehole GP00309. These circumstances reflect the addition of an organic matter component that potentially promotes in situ ‘natural’ bioremediation associated with the generation of alkalinity through bacteriological sulfate reduction (Knoeller et al. 2004; McCullough 2008; McCullough et al. 2008) in this portion of the karst aquifer.

Finally, it is worth noting the findings of Brown and Glynn (2003) that the in situ field dissolution rates of calcite and dolomite experimentally exposed to active acid mine drainage were 1000 times less than the rate calculated from laboratory-derived equations. Further, the dolomite in situ dissolution rate was typically an order of magnitude smaller than that of calcite. This is in keeping with the observation by Busenberg and Plummer (1982) that the CaCO_3 component of dolomite dissolves preferentially relative to MgCO_3 on exposure to acidic conditions. The import of these findings for the impact of AMD on the karst environment in the study area cannot be ignored.

12.2.2 Dedolomitization

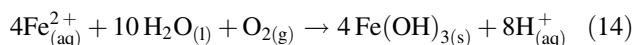
The possibility that the ingress of SO_4 -rich mine water into the dolomitic aquifer of the Zwartkrans Basin may cause dedolomitization similarly cannot be ignored. Although this phenomenon is comparatively rare in natural karst environments (Ford and Williams 2007), Plummer et al. (1990) describe its manifestation as calcite precipitation and dolomite dissolution driven by anhydrite (anhydrous CaSO_4) dissolution in the carbonate Madison aquifer, USA. The total mass transfer is given by the reaction (Appelo and Postma 2009)



where for each mole of dolomite that dissolves, two moles of calcite are precipitated and the Ca^{2+} , Mg^{2+} and SO_4^{2-} concentrations increase. The ingress of SO_4 -rich mine water as allogenic recharge into the dolomitic aquifer of the Zwartkrans Basin provides the driver for potential dedolomitization. This possibility adds another layer of complexity to the hydrogeochemical framework that informs the mine water impacted karst water resource.

12.2.3 Dolomite Armoring

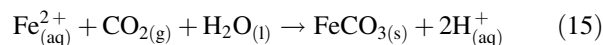
Armoring (or protection) of dolomite results from the precipitation of insoluble oxyhydroxides [mainly ferric hydroxide or ferrihydrite, $\text{Fe}(\text{OH})_3$] on the surface of the dolomite within fractures and karst features according to the reaction



Mineral surface passivation (Lindsay et al. 2015) by the efflorescent coating inhibits any further dissolution and reaction(s) that mediate neutralizing acidity in the water through dissolution of the dolomite. It is this coating/crust that also protects structures such as the concrete weir visible in Plate 3 in Chapter “[Chemical Hydrology](#)” from attack by the acidic surface water. Unfortunately, the precipitate is fatal to aquatic systems because the crust seals channel bottoms and entombs in-stream vegetation (Plate 9). It is also the armoring effect that inhibits the neutralizing capacity of crushed limestone when used for this purpose in passive AMD treatment systems such as open limestone channels (OLCs), limestone leach beds (LLBs), and anoxic limestone drains (ALDs). Ziemkiewicz et al. (1997), however, established from field studies that armored limestone in OLCs reduced acidity by between 10 and 60% of the rate of unarmored limestone. The greatest reductions were associated with steeper channel gradients (45–60%) and for mine water with a net acidity of 500–2600 mg CaCO_3/L .

Barnes and Romberger (1968) recognized >40 years ago the possible treatment option of introducing AMD via boreholes into carbonate strata. Clearly, environmental considerations at the time were considerably less emotive than today. The principal disadvantage is that neutralization occurs at the expense of added hardness. Further, dolomite as a source of carbonate produces undesirable quantities of magnesium salts (MgSO_4).

Sasowsky et al. (1995) posit the possibility that the availability of large amounts of CO_2 produced by Reaction 10 might also promote the precipitation of siderite (FeCO_3) according to the reaction



Webb and Sasowsky (1994) further report the experimental results of Bradley and Herman (1989) that indicate

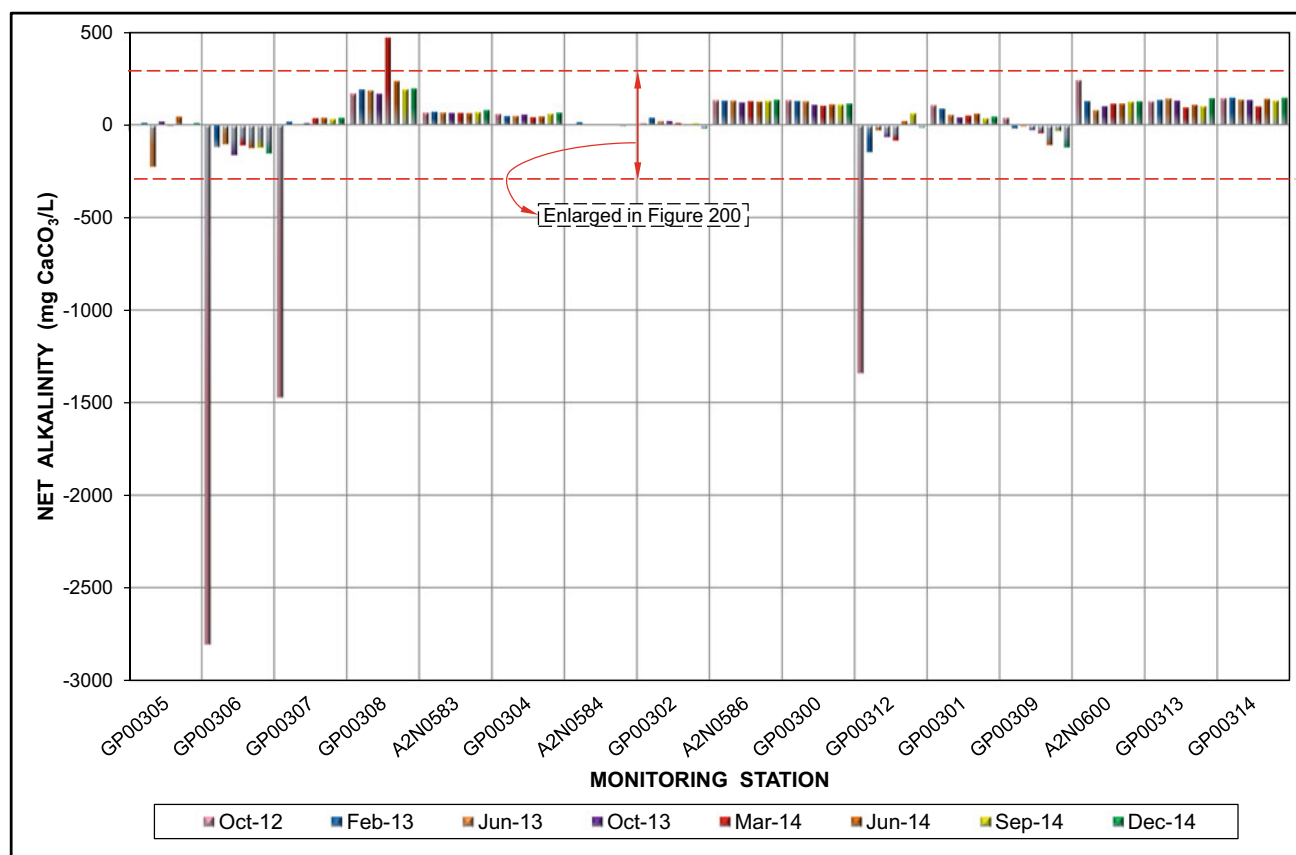


Fig. 87 Pattern and trend of net alkalinity in groundwater from monitoring boreholes

the adsorption of sulfate onto ferrihydrite at low pH values. Together with bacterial sulfate reduction (Sect. 11), this process might also account for the comparatively low SO_4 concentrations observed in the AMD pseudoplume in the Zwartkrans Basin (Sect. 8.4).

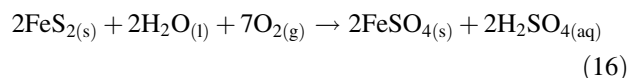
13 Hydrochemistry of Mine Water

The importance of acid mine drainage as a hydrologic agent in the study area warrants an understanding of salient aspects of the hydrochemistry associated with mine water. The analytes of primary interest in this regard are iron and alkalinity/acidity, and elements of their hydrochemistry are discussed in the following sections.

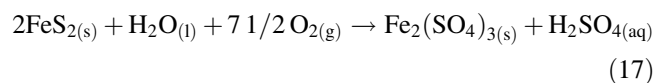
13.1 Iron Chemistry

Ferrous iron (Fe^{2+}) is present in much higher concentrations in raw mine water than other metals such as Mn, Cu, Pb, Zn, Co, Ni, and U. It is formed when iron sulfide (FeS_2) comes into contact with water, oxygen and, often catalyzed by

iron-oxidizing bacteria (e.g., *Gallionella* and *Sphaerotilus*) or sulfur-oxidizing bacteria (e.g., *Thiobacillus ferro-oxidans*, *Thiobacillus thio-oxidans* and *Ferrobacillus ferro-oxidans*), forms ferrous sulfate (FeSO_4) and sulfuric acid (H_2SO_4) resulting from oxidation by O_2 according to the reactions

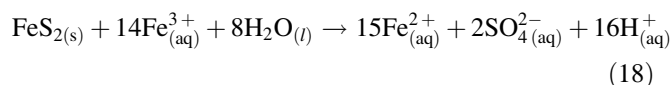


with limited available oxygen as in a closed system evidenced by reducing conditions (very low Eh), and



with excess available oxygen as in an open system evidenced by oxidizing conditions (very high Eh).

Oxidation by Fe^{3+} proceeds according to the reaction



The Fe^{2+} produced by Reaction 18 oxidizes to Fe^{3+} at pH <3 according to the reaction

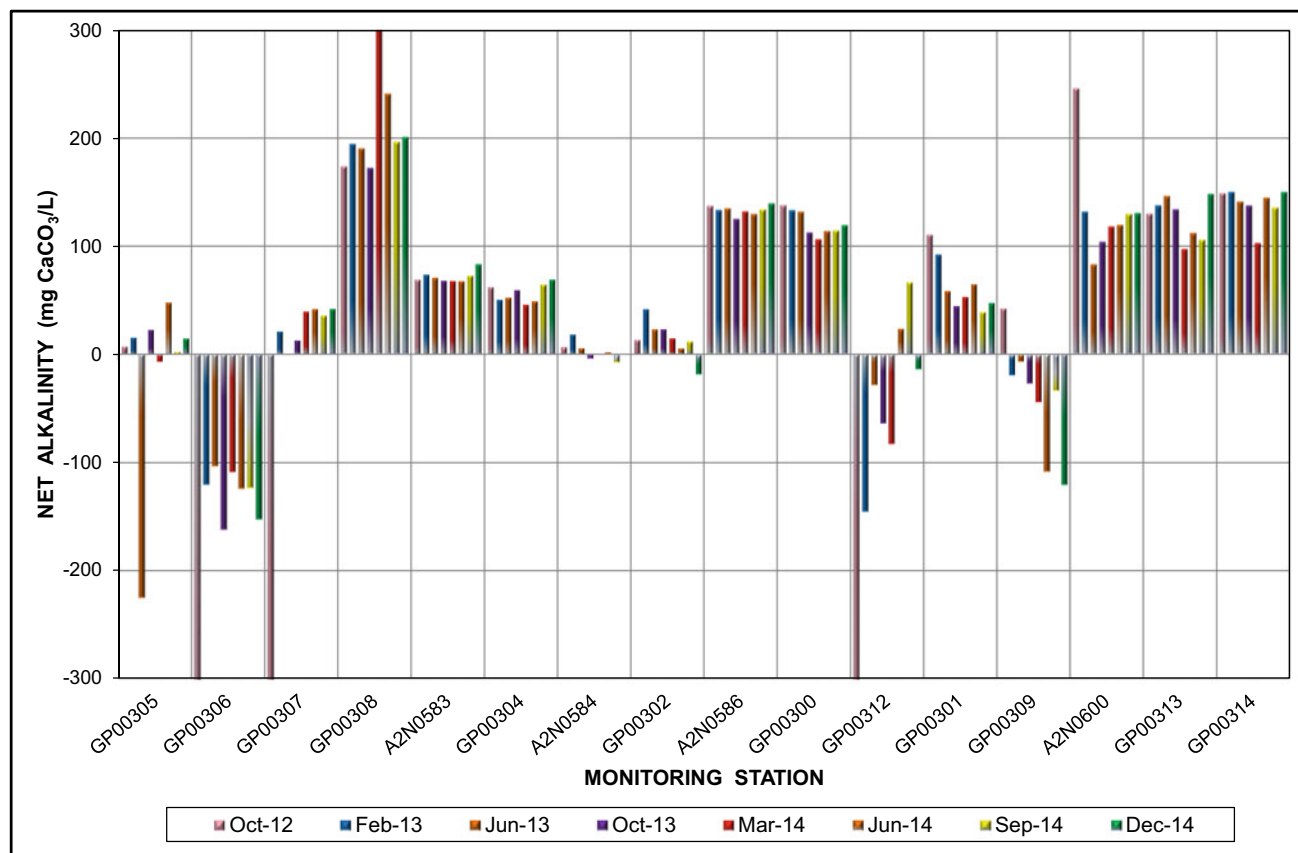
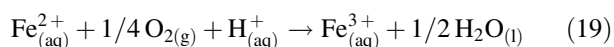
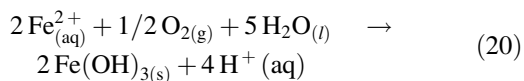


Fig. 88 Enlarged view of pattern and trend of net alkalinity shown in Fig. 87



and at pH >3 according to the reaction



which produces the ferric hydroxide precipitate known as ‘Yellow boy’.

13.2 Net Alkalinity and Net Acidity

A discussion of these characteristics in regard to mine and surface waters in the study area is presented in Sect. 3.5 in Chapter “[Chemical Hydrology](#)”. Their evaluation in regard to groundwaters further informs an assessment of water impacts on the karst water resource. Natural groundwater with a pH <6.4, such as the groundwater draining the quartzitic strata of the Witwatersrand Supergroup (Sect. 2.1.1), has no acid neutralizing (or buffering) capacity. This also applies to impacted karst groundwater that otherwise (and typically) would have a pH in the range of 7.5–8.0 and a total alkalinity of >150 mg CaCO₃/L in its unimpacted

state (Sect. 2.1.2). Calculations of the net alkalinity and acidity associated with various groundwater sources are presented in Table 21 and of the free and metal acidity components associated with these waters in Table 22. The results indicate that the karst groundwater, impacted to various degrees, maintains a positive net alkalinity, although instances of this reducing over time are observed adjacent to the losing reach of the Riet Spruit, e.g., station CSIR57 (aka WBD5). Further, free acidity contributes <5% to the total acidity in most instances, with >95% being contributed by metals. Gammons and Tucci (2013) similarly report that dissolved metals are a much greater source of acidity in the Berkely pit-lake, Butte, Montana, pit-lake waters than H⁺ or HSO₄⁻.

Calculation of the net alkalinity of groundwater sampled from the DWS monitoring boreholes downgradient of the mine area on eight occasions in the period October 2012 to December 2014 returns the results presented in Figs. 87 and 88. The results reflect the impact of the acid load contributed by influent surface water carrying a mine water signature as allogenic recharge to the karst hydro system traversed by the lower Riet Spruit in the Zwartkrans Basin. This load has been discussed in Sect. 3.5 in Chapter “[Chemical Hydrology](#)”.

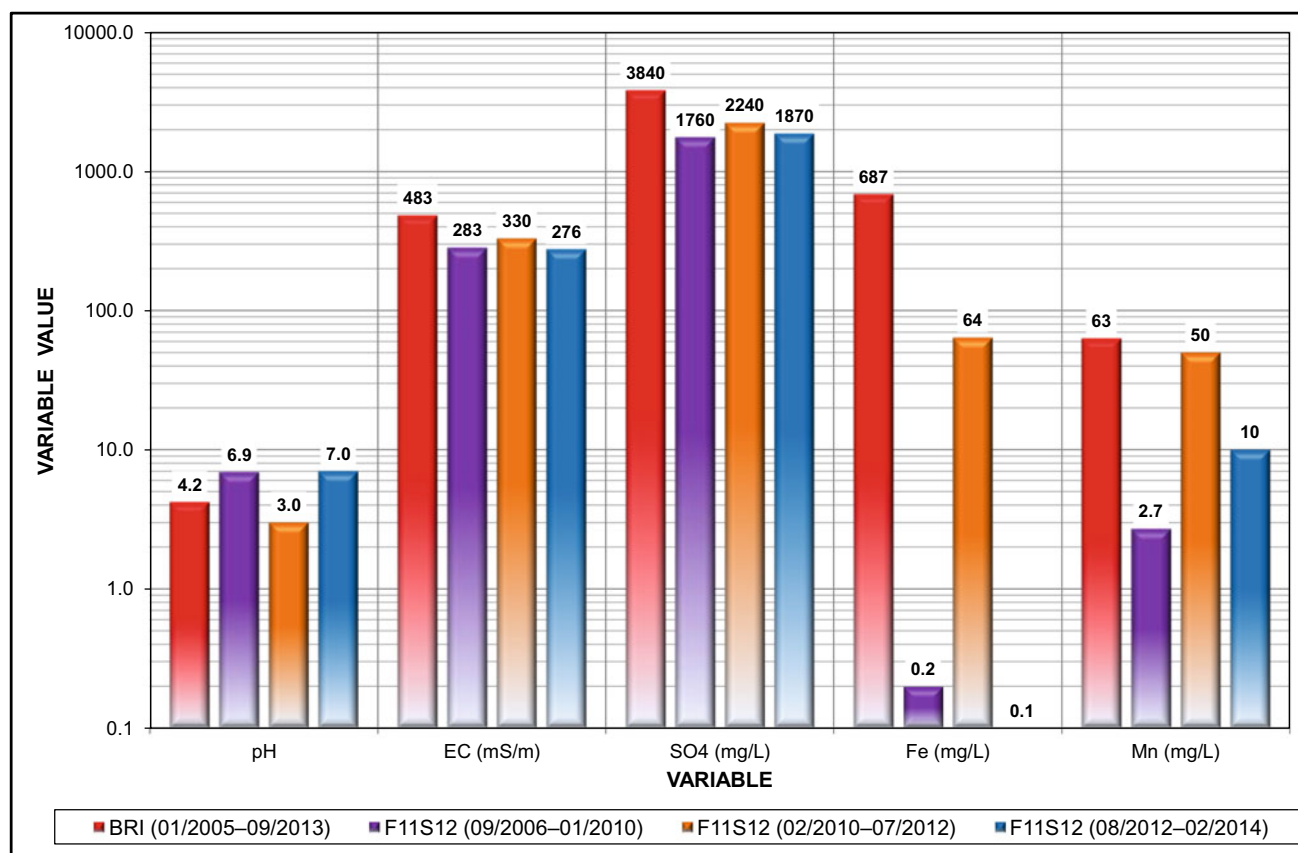


Fig. 89 Comparison of 'diagnostic' chemical variable values for raw mine water (BRI) and downstream surface water (F11S12) (data from Table 23)

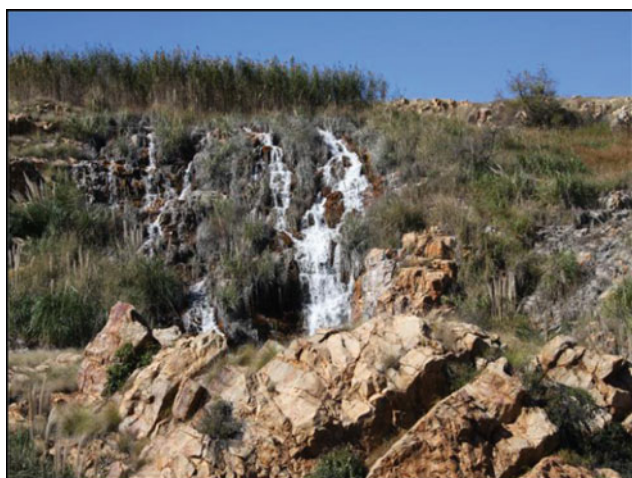


Plate 10 Waterfall over the quartzite ridge south of the Kruger Kloof Lodge in the KGR (photo H Weiss, date 13/05/2008)



Plate 11 Outlet of the Charles Fourie Dam in the KGR

The analysis reveals the generally positive net alkalinity of the groundwater, the exceptions being associated with boreholes located in very close proximity to the losing surface water drainages carrying mine water discharge. These boreholes are identified as GP00306 adjoining the

Tweelopie Spruit at the northern end of the karst outlier in the Krugersdorp Game Reserve, and GP00309 and GP00312 adjoining the Riet Spruit in the Zwartkrans Basin. The very low (and even negative) net alkalinity associated with borehole GP00305 is attributed mainly to the West Rand



Plate 12 Overflow of the Aviary Dam (impounded by the earth embankment at rear of photo) at the northern end of the KGR; compare condition of outlet pipe at left with that of same pipe in Plate 1 in Chapter “Chemical Hydrology”



Plate 13 Cascade and aeration of water over the causeway at station F11S12 (see Plate 8 in Chapter “Physical Hydrology” for scale of monitoring station)

Group quartzitic strata intersected by this borehole and that typically host a weakly mineralized and acidic groundwater (Sect. 1), although a more recent mine water impact must also be considered.

A closer inspection of the histograms suggests that in some instances the net alkalinity values indicate a declining trend, e.g., GP00300, GP00301, GP00302, and GP00309. This observation suggests a generally increasing mine water influence on the karst groundwater chemistry at these locations. Especially the persistent trend from a positive to an increasingly negative net alkalinity associated with the karst groundwater at station GP00309 is concerning and needs to be monitored closely. By comparison, the positive net alkalinity associated with the groundwater in Sterkfontein Cave (Table 22) is another encouraging sign of a limited impact from mine water on the karst groundwater in this environment. A similar observation in regard to the Zwartkrans springwater is testimony to the capacity of the karst hydro system to mitigate a mine water impact. However, the longevity and threshold of this capacity still need to be established.

13.3 Local Studies

Krige (2009) reports on studies carried out by DD Science Laboratory CC., using the acid–base titration method employed in standard acid–base accounting (ABA) determinations, to establish the neutralization potential of dolomite iro raw mine water from the decant area. The outcome suggested that 1 ML of mine water would dissolve 900 kg of CaCO_3 , creating a theoretical void of $\sim 0.32 \text{ m}^3$.

By extrapolation of the volume of mine water that had entered the karst aquifer since the commencement of decant in August 2002 up until the ‘capture-and-control’ of this discharge ca. February 2005, Krige (2009) reports a total void volume of $\sim 4500 \text{ m}^3$ that potentially had developed in

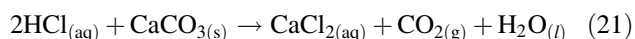
Table 23 Water chemistry data used in Fig. 89 to compare raw mine water from station BRI with Tweelopie Spruit surface water at station F11S12

| Station (period) | ‘Diagnostic’ chemical variable median value and count (<i>n</i>) | | | | |
|--------------------------------------|--|----------------|----------------------|----------------|----------------|
| | pH ($-\log_{10} a_{\text{H}^+}$) | SEC (mS/m) | SO_4 (mg/L) | Fe (mg/L) | Mn (mg/L) |
| Black Reef Incline (01/2005–09/2013) | 4.2 | 483 | 3840 | 687 | 63 |
| | <i>n</i> = 453 | <i>n</i> = 452 | <i>n</i> = 453 | <i>n</i> = 452 | <i>n</i> = 224 |
| F11S12 (09/2006–01/2010) | 6.9 | 283 | 1760 | 0.2 | 2.7 |
| | <i>n</i> = 173 | <i>n</i> = 172 | <i>n</i> = 171 | <i>n</i> = 33 | <i>n</i> = 33 |
| F11S12 (02/2010–07/2012) | 3.0 | 330 | 2240 | 64.0 | 50.0 |
| | <i>n</i> = 128 | <i>n</i> = 128 | <i>n</i> = 128 | <i>n</i> = 128 | <i>n</i> = 128 |
| F11S12 (08/2012–02/2014) | 7.0 | 276 | 1870 | 0.075 | 10.0 |
| | <i>n</i> = 83 | <i>n</i> = 83 | <i>n</i> = 83 | <i>n</i> = 82 | <i>n</i> = 83 |

the karst aquifer in this time. Further, it was suggested by Krige (2009) that this volume could be doubled (i.e., to $\sim 9000 \text{ m}^3$) on the basis of the additional carbonic acid (H_2CO_3) generated by the reaction between mine water and dolomite creating an equivalent volume of dissolution. These figures, and a value of $16,700 \text{ m}^3$ quoted by Liefferink (2010), have been placed in the public domain. Establishing the veracity of these figures is crucial to an informed assessment of this impact.

The procedure followed in the assessment described by Krige (2009) used raw mine water in the calculation. The karst aquifer that receives this water is, however, located north of the KGR a distance of $\sim 4.9 \text{ km}$ from where the mine water enters the environment (Tables 48 and 49 in Chapter “Chemical Hydrology”). In its path down the Tweelapie Spruit, this water cascades over a number of natural and man-made features, e.g., the waterfall over the quartzite ridge to the south of the Kruger Kloof Lodge (formerly the Ngonyama Lion Lodge) in the KGR (Plate 10), the spillway of the Charles Fourie Dam at the lodge itself (Plate 11), the outflow of the Aviary Dam (Plate 12) where this water leaves the KGR, and the causeway at station F11S12 (Plate 13). The cascading action serves to thoroughly aerate the water (Benedini and Tsakiris 2013; Nakasone 1987), the oxidization causing any ferrous iron (Fe^{2+}) in solution to precipitate out of solution as seen in the orange-brown staining and encrustation on surfaces at each of these locations. As a consequence, the chemical composition of the mine water has changed significantly by the time it reaches the Riet Spruit where it traverses the karst aquifer of the Zwartkrans Basin. The nature of this change is shown in the comparison of the long-term median concentration of elements monitored at the BRI (representative of raw mine water chemistry), with that of these elements monitored at station F11S12 for both the entire record and the early record. This is shown in Fig. 89 (see Table 23 for data), which reflects the very different SO_4 and Fe concentrations in the water at the two stations.

Another contentious aspect of the procedure described by Krige (2009) is the use of hydrochloric acid (HCl) to determine the mass of dolomite involved in a reaction between the mine void water and the acid according to the reaction



It is understood that HCl was used to speed up the reaction because of budget and time constraints (D. Dorling, personal communication). It is contended that the use of raw mine water and HCl in the acid–base titration exercise does not replicate the ‘real-world’ situation. This exercise would need to be repeated with H_2SO_4 and surface water having a composition similar to that passing station F11S12

(Table 23) in order to have greater relevance and application to the situation in the study area.

Studies carried out by the Council for Geoscience (CGS) to further inform the topic of dolomite dissolution in regard to the potential impact of AMD on the karst environment of the COH have entailed a comparative petrographic study (Roelofse 2010) as well as laboratory-based column leaching tests (Coetzee et al. 2010).

In the petrographic study, portions of two polished thin sections of a sample of dolomite were photographed under magnification before and after being exposed to acid mine water. Any changes associated with the exposure to the mine water were studied under a microscope using both plane and cross polarized light. A comparison of the ‘before’ and ‘after’ photomicrographs allowed for a qualitative assessment of observed changes/differences. Based on the following observations, it appears that partial dissolution of the dolomite occurred on exposure to acid mine water.

- A lower apparent birefringence after exposure compared to before exposure. This is most likely attributable to a loss of thin section thickness during exposure.
- Greater definition (under magnification) of carbonate grain boundaries after exposure.
- Preferential exploitation of cleavages within carbonate grains, resulting in greater definition of cleavage patterns in the post-exposure image.
- In some instances, a decrease in carbonate grain size following exposure.

The kinetic (column leaching) experiment was devised by the CGS using synthetic AMD prepared in the laboratory as a leachant to closely mimic the bulk composition of Western Basin AMD while maintaining the iron in a dissolved state. The pH of the leachant was adjusted to a value of 3.6 using H_2SO_4 . The leachant was passed through five columns each packed with dolomite of a different size fraction, i.e., <2 , 2–4, 4–8, 8–16, and $>16 \text{ mm}$, at a rate of 0.1 L/kg/d to simulate that of slow groundwater flow through a dolomitic aquifer. The kinetic tests revealed the following processes that occurred during the interaction between dolomite and synthetic AMD solutions:

- dissolution of the dolomite as indicated by the neutralization of the AMD at sufficiently high solid to liquid ratios; whether this will lead to the development of new cavities (or the enlargement of existing cavities) within the affected dolomitic areas cannot be determined, as this will be influenced by a combination of the flow rate, the surface area exposed and the rate at which mineral precipitation armors the reactive surface of the dolomite within the aquifer;

- precipitation of new minerals as identified at both macro- and micro-scales using optical and scanning electron microscopy, respectively; the minerals that precipitate will depend on the chemistry of the input solutions as well as the Eh–pH conditions under which precipitation occurs;
- armoring of the dolomite surface with reaction products, reducing the quantity of reactive material exposed;
- an increase in the pH of the solution, reducing the solubility of a number of its components; iron and aluminum are almost completely attenuated, manganese is partially attenuated with an apparent strong dependence on the available reactive surface area, while sodium and sulfate are not attenuated significantly; and
- increased concentrations of calcium and magnesium as a result of the dissolution of dolomite, with an apparent preferential dissolution of calcium over magnesium, in the final solutions produced by the tests.

13.4 Conclusions

The likely effects of AMD ingress into the karst aquifer(s) of the COH will be a rise in the pH of the influent mine water (as a result of the dissolution of dolomite and associated neutralization) to a value comparable to that of the ambient karst groundwater. This might lead to a structural weakening of the subsurface formation if the process continued over a long period of time without the dolomite surfaces becoming armored. The rise in pH would result in the reduction of the solubility of some of the contaminant species (e.g., the metals) in the mine water, significantly reducing Fe and Al in solution, partially removing Mn, and not having a significant effect on the Na or SO₄ concentration.

Influent mine water would therefore tend to react at the point of first contact with the dolomite resulting in neutralization and the precipitation of metals. The metal precipitates, which would include gypsum (CaSO₄), goethite [FeO(OH)], and crystalline and amorphous (botryoidal) aluminum oxyhydroxide [AlO(OH)] species, are likely to form on the reactive surfaces of the dolomite, preventing further neutralization from taking place. Influent mine water impacted surface water would therefore migrate further and further into the karst aquifer, most likely taking the form of a plume comprising a migrating reaction front ahead of various zones each representing a reaction subdomain controlled by factors such as oxidation–reduction state, microbial degradation, and mineral precipitation–dissolution reactions (e.g., Bjerg et al. 1995; Sherlock et al. 1995; Hunter et al. 1998; Elsner et al. 2004), and leaving behind an aquifer hosting an altered biogeochemical environment. How and to what extent the altered aquifer environment differs from the

original is unknown, as is the ability of this aquifer to regenerate its original hydrogeochemical character following a return to largely autogenic natural recharge.

In conclusion, natural attenuation of AMD by allowing it into dolomitic aquifer systems is not regarded as an appropriate or sustainable management strategy. However, a better understanding of the hydrochemical interaction between surface water of compromised quality and karst groundwater, and of the hydrogeochemical and biogeochemical processes that control the composition of groundwater, will assist authorities in making informed decisions for protection of the valuable water resources environment in the COH.

14 Carbon Flux in Springwater

14.1 Introduction

The role of karst aquifers in the transport and storage of carbon has recently received attention in publications by Veni (2013) and White (2013), among others. Veni (2013) estimates the global volume of organic carbon stored in karst aquifers at 200 km³. This does not include the amount of organic carbon stored in paleokarst, which is indicated to be substantially greater. Falkowski et al. (2000) indicate that sedimentary carbonate strata in the lithosphere represent a carbon reservoir of >60 petatons (1 Pt = 10¹⁵ t). This is ~800 times more than the reservoir represented by the oceans. Pokrovsky et al. (2009) demonstrated the efficiency of CO₂ sequestration in Mg-bearing carbonate strata.

Although karst environments undoubtedly represent a major sink for atmospheric carbon and CO₂ inputs from losing (effluent) streams and the epikarst, they also constitute a source of CO₂ from release by speleothem deposition, tufa or travertine deposition, and degassing from spring discharges and spring runs (White 2013). The data acquired in this study, together with the improved understanding of the hydrophysical and hydrochemical environments in the COH, provides material that facilitates a provisional and rudimentary assessment of CO₂ evasion via the karst springs on the property.

14.2 Approach

Given that the total inorganic carbon (TIC) in solution is the sum of all dissolved carbon species

$$[\text{TIC}] = [\text{CO}_2(\text{aq})] + [\text{H}_2\text{CO}_3] + [\text{HCO}_3^-] + [\text{CO}_3^{2-}] \quad (22)$$

all as mol/L concentrations, and that the combined [CO₂(aq)] and [H₂CO₃] can be calculated from alkalinity and pH as follows:

Table 24 Summary of carbon flux and export rates associated with COH spring discharges ca. May 2010

| Spring | Karst basin area (km ²) | Discharge (m ³ /s) | HCO ₃ (mmol/L) | γ_{HCO_3} | F_c (kg/d) | C (mg/L) | C-export rate (kg/km ² /a) |
|-------------------------|-------------------------------------|-------------------------------|---------------------------|-------------------------|--------------|----------|---------------------------------------|
| Zwartkrans | 98.0 | 0.136 | 3.20 | 0.89 | 451 | 38 | 1681 |
| Plover's Lake Kromdraai | 50.8 | 0.339 | 3.84 | 0.92 | 1350 | 46 | 9701 |
| Danielsrust | 7.4 | 0.028 | 2.56 | 0.93 | 74 | 31 | 3669 |
| Tweefontein | 11.6 | 0.030 | 3.92 | 0.92 | 122 | 47 | 3847 |
| Nouklip | 38.0 | 0.143 | 3.92 | 0.92 | 582 | 47 | 5590 |
| Nash | 28.6 | 0.130 | 2.64 | 0.93 | 356 | 32 | 4545 |
| Broederstroom | 18.1 | 0.028 | 5.44 | 0.91 | 158 | 65 | 2814 |
| Total average | 252.5 | 0.834 | 3.65 | 0.92 | 3094 442 | 44 | 4550 |

Table 25 Summary of carbon flux and export rates associated with COH spring discharges ca. August 2014

| Spring | Karst basin area (km ²) | Discharge (m ³ /s) | HCO ₃ (mmol/L) | γ_{HCO_3} | F_c (kg/d) | C (mg/L) | C-export rate (kg/km ² /a) |
|-------------------------|-------------------------------------|-------------------------------|---------------------------|-------------------------|--------------|----------|---------------------------------------|
| Plover's Lake Kromdraai | 50.8 | 0.343 | 3.18 | 0.91 | 1133 | 38 | 8138 |
| Danielsrust | 7.4 | 0.028 | 2.62 | 0.94 | 76 | 32 | 3760 |
| Tweefontein | 11.6 | 0.026 | 3.11 | 0.93 | 84 | 37 | 2645 |
| Nouklip | 38.0 | 0.185 | 3.93 | 0.92 | 756 | 47 | 7258 |
| Nash | 28.6 | 0.208 | 2.59 | 0.94 | 559 | 31 | 7136 |
| Total average | 252.5 | 0.790 | 3.09 | 0.93 | 2608 522 | 37 | 5787 |

$$[\text{H}_2\text{CO}_3] = \frac{[\text{HCO}_3]\gamma_{\text{HCO}_3}10^{-\text{pH}}}{K_1} \quad (23)$$

where $[\text{H}_2\text{CO}_3]$ is the carbonic acid concentration as mol/L, $[\text{HCO}_3^-]$ is the molar concentration of bicarbonate, γ_{HCO_3} is the activity coefficient of bicarbonate, and K_1 is the ionization constant of carbonic acid, then the carbon flux can be calculated from known spring discharge rate and springwater pH and bicarbonate concentration values as follows (White 2013):

$$F_C = 17.012 C_{\text{HCO}_3} \left\{ 1 + \frac{[\text{HCO}_3]\gamma_{\text{HCO}_3}10^{-\text{pH}}}{K_1} \right\} Q \quad (24)$$

where F_C is the total carbon flux as kg/d, C_{HCO_3} is the bicarbonate concentration as mg/L, Q_S is the spring discharge as m³/s, and all other terms are as for Eq. 23.

14.3 Results

Application of Eq. 25 to the seven karst basins (and eight springs) discussed in Sect. 12 returns the F_C values reported in Table 24.

The average total carbon loading in the karst spring waters is found to be 44 mg C/L in the range of 31–65 mg/L. The average total carbon flux carried is found to be ~442 kg/d (~161 t/a), with the eight springs delivering a combined total C-flux of 3094 kg/d (1129 t/a). The average C-export rate is calculated at 4550 kg/km²/a in the range 2814–9701 kg/km²/a for the seven karst basins.

A second set of SDMs and chemical analyses carried out on five of the springs listed in Table 24 in mid-August 2014, returned the results reported in Table 25. The average total carbon loading in the karst spring waters is found to be 37 mg C/L in the range 31–47 mg/L, compared to the 41 mg C/L and range 31–47 mg/L of the May 2010 data. The average total carbon flux carried is found to be ~522 kg/d (~190 t/a), with the five springs delivering a combined total C-flux of 2608 kg/d (952 t/a), compared to the ~497 kg/d and 2484 kg/d of the respective May 2010 results. The average C-export rate is calculated at 5787 kg/km²/a in the range 2645–8138 kg/km²/a for the six karst basins, compared to the 5470 kg/km²/a and range 3669–9701 kg/km²/a of the respective May 2010 results.

The results are not only in reasonable agreement with each other (Table 26), but also with values reported in the

Table 26 Comparison of carbon flux and export rates associated with COH spring discharges ca. May 2010 and ca. August 2014

| Spring | F_c (kg/d) | | C (mg/L) | | C-export rate (kg/km ² /a) | |
|-------------------------|--------------|-------------|----------|-------------|---------------------------------------|-------------|
| | May 2010 | August 2014 | May 2010 | August 2014 | May 2010 | August 2014 |
| Plover's Lake Kromdraai | 1350 | 1133 | 46 | 38 | 9701 | 8138 |
| Danielsrust | 74 | 76 | 31 | 32 | 3669 | 3760 |
| Tweefontein | 122 | 84 | 47 | 37 | 3847 | 2645 |
| Nouklip | 582 | 756 | 47 | 47 | 5590 | 7258 |
| Nash | 356 | 559 | 32 | 31 | 4545 | 7136 |
| Total average | 2484 497 | 2608 522 | 41 | 37 | 5470 | 5787 |

international literature. For example, Florea (2015) reports the conveyance of 25.8–62.4 Gg/a (~ 6900 – $16,700$ kg/km²/a) of CO₂ (equivalent to ~ 1900 – 4600 kg C/km²/a), based on dissolved inorganic carbon concentrations, from the atmosphere to the aqueous system through the dissolution of carbonate strata spanning an outcrop area of 3730 km² in the Cumberland River watershed of south-east Kentucky, USA.

14.4 Discussion

It is common cause that TIC dominates the total carbon (TC) concentration in springwater, the role is reversed in surface water where total organic carbon (TOC) dominates. The TIC derives from ‘dead’ carbon (weathering of carbonate strata), and the TOC from ‘live’ carbon (e.g., decaying plant and animal matter). It has been shown by White (2013) that whereas the carbon loading (mg/L) in

springwater responds only weakly to increased discharge, carbon fluxes (kg/d) reflect a much more prominent response. In other words, a significant (>tenfold) increase in spring discharge manifests only as a slight (<twofold) decrease in carbon loading attributable to dilution. Under similar circumstances, the carbon flux might well reflect a sympathetic response by increasing tenfold.

The total alkalinity (mg CaCO₃/L) concentrations associated with the bicarbonate (HCO₃) values listed in Table 5 allow an estimate of the total mass of calcium carbonate exported via the karst springs. This amounts to ~ 6000 t/a as shown in Table 19 (Sect. 12.1), and broadly represents a rate of total void development of ~ 2100 m³/a, or 8.2 m³/km²/a over a 25,490 ha extent of dolomite outcrop in the COH. This is equivalent to a denudation rate of 8.2 mm/Ka. A more detailed discussion in Sect. 12.1 provides greater elucidation of solutional denudation and void development rates in the COH.

Conclusions

Harrison Pienaar and Philip J. Hobbs

The understanding of the surface water and groundwater environments in the Cradle of humankind (COH), also in regard to their inter-relationship, is considerably expanded by this study. This understanding extends as much to the water chemistry aspect as it does to the water quantity aspect. Outcomes of the study that are considered especially significant are summarised as follows:

- the quantification of surface water flow losses in the lower Riet Spruit valley;
- the quantification of spring discharges;
- the definition of basins/subcompartments and corresponding groundwater resource units associated with the karst formations in the study area;
- the evaluation of the geochemical interaction between acidic mine water and the dolomitic strata that form the receiving karst aquifer in the study area;
- the development of semi-quantitative resource water quality objectives (RWQOs) to inform groundwater resource directed measures for the karst portions of the study area;
- the derivation of a fossil site risk assessment that informs the vulnerability of each declared fossil site and its associated cave system in the context of its hydrogeologic setting; and
- the development of a monitoring programme for the COH.

The platform built from historical data integrated with a wide range of rigorous and defensible newly generated and interpreted hydrologic and hydrogeologic data and information, underpins the situation assessment of the surface water and groundwater environments. This, in turn, has

provided the means to objectively gauge the impact of varied and numerous threats on the water resources in the study area. The salient conclusions drawn from the study are summarised in the following sections.

1 Surface Water Resources

1.1 Quantity

The Skeerpoort River system fed by dolomitic springs remains in a near pristine condition. The Bloubank Spruit system, on the other hand, has experienced above average discharges in its upper reaches via the Tweelopie Spruit and the Riet Spruit since the resumption of mine water decant in late-January 2010. Together with the treated sewage effluent discharged from the Percy Stewart WWTW via the Bloubank Spruit, these circumstances have resulted in an unprecedented volume and duration of surface water flow in the Bloubank Spruit system through the 2010 winter. Further, the combined discharge of raw and treated mine water witnessed surface water losses of between 20 and 32 ML/d to the dolomitic aquifer in the lower Riet Spruit, equating to an infiltration rate of as much as ~ 90 L/s/km.

1.2 Quality

The Skeerpoort River system continues to reflect a karst-dominated water composition of excellent quality. Up until mid-2010, the impact of the poor quality associated with the abnormal combined discharge of treated and raw mine water in the upper reaches of the Bloubank Spruit system was mitigated by (a) the contribution of treated wastewater effluent discharged by the Percy Stewart WWTW and (b) the above average surface water runoff associated with the extremely wet 2009–10 summer. Since mid-2010, the increase in SEC of Bloubank Spruit water from ~ 50 to > 100 mS/m, together with a decrease in pH

P. J. Hobbs: Deceased

H. Pienaar (✉) · P. J. Hobbs
Smart Places, Council for Scientific and Industrial Research,
Pretoria, South Africa
e-mail: hpienaar@csir.co.za

H. Pienaar
Hebei University of Engineering, Handan, China

from 7.2 to 6.9 at the downstream boundary of the Zwartkrans Basin, is considered to reflect an increasing contribution of mine water to the middle reaches of this drainage. This impact is less evident in the Zwartkrans Spring water, which in August 2010 still reflected a field SEC of ~ 77 mS/m. Similarly, the Lake water in Sterkfontein Cave continues to reflect an SEC of ~ 60 mS/m as it did in June 2006, a year after the start of monitoring of this variable by the DWS.

The quality of surface water resources in the Bloubank Spruit system is further compromised by bacterial contamination derived from wastewater effluent. These circumstances also make it difficult to assess agricultural impacts on the surface water resources, as these impacts are similarly associated with nutrient inputs.

2 Groundwater Resources

2.1 Quantity

The very wet 2010 and 2011 summers precipitated an exceptional recharge of groundwater resources in the study area. A rise in groundwater rest levels by at least ~ 1 m is testimony to these circumstances. Greater water level recoveries of as much as ~ 5 m are attributed to allogenic recharge associated with the infiltration of surface water contributed from extraneous sources including mining and municipal wastewater effluent. This infiltration has amounted to as much as 32 ML/d in the case of mine water, and a more modest 7 ML/d in the case of municipal wastewater effluent. It is concluded, therefore, that the aspect of groundwater quantity as represented by current 2014 groundwater rest levels compared to historical levels, reflects an extremely positive outlook.

2.2 Quality

As might be expected, the chemistry of groundwater in the study area reflects the greatest spatial variation depending on the position in the physical hydrogeologic environment. For instance, the subcompartments receiving water of compromised quality in terms of either trace/heavy metals and elevated salt loads associated with mine water, and/or elevated bacterial loads associated with municipal wastewater (both representing allogenic recharge), reflect the poorest groundwater chemical composition. In contrast, compartments (and subcompartments) receiving only autogenic recharge remain largely unaffected in terms of groundwater chemistry (and quality).

Despite the magnitude, severity and duration of allogenic recharge associated especially with the mine water, the

receiving karst environment continues to reflect a resilience to the negative impact from this source that is both surprising and comforting. This observation, however, raises the question as to whether the ostensible resilience has a threshold beyond which the biophysical condition of this resource degrades markedly to the detriment of karst ecosystem(s) hosted in this environment.

3 Mine Water Impact on Dolomite

A comparative petrographic study together with laboratory-based column leaching tests carried out by the CGS further elucidated the potential impact on the karst environment of the COH dolomite by infiltrating mine water.

The likely effects of AMD ingress into the karst aquifer(s) will be a rise in the pH of the influent mine water (as a result of the dissolution of dolomite) to a value comparable to that of the ambient karst groundwater. The rise in pH would result in the reduction of the solubility of some of the contaminant species in the mine water, significantly removing iron and aluminium from solution, partially removing manganese and not having a significant effect on the sodium or sulphate concentration. The metal precipitates, which would include gypsum, goethite and crystalline and amorphous (botryoidal) aluminium oxyhydroxide species, are likely to form on the reactive surfaces of the dolomite, preventing further neutralisation reactions from taking place. Influent mine water would therefore tend to react at the point of first contact with the dolomite, resulting in both neutralisation of the mine water and the prevention of further neutralisation from taking place. Over time the mine water would migrate further and further into the karst aquifer, and the buffering capacity of the aquifer would reduce progressively.

It is concluded, however, that natural attenuation of AMD by allowing it to enter dolomitic (carbonate) aquifer systems is not regarded as an appropriate or sustainable management strategy. This can only hasten the manifestation of a threshold to the observed resilience alluded to in Sect. 2.2, if such exists.

4 Resource Water Quality Objectives

The setting of resource water quality objectives (RWQOs) for groundwater quantity and quality in the COH expands the impact of the study.

4.1 Quantity

The statistical assessment of long-term groundwater rest level trends provides a means to quantify the setting of

RQOs for groundwater quantity in a part of the study area. The proposed RQOs recognise ‘permissible’ changes in groundwater rest level that vary across a compartment. Although the proposed RQOs do not find a priori support in the DWS library of existing RQOs in this regard, they are nevertheless put forward for consideration as advancing the knowledge base in regard to this GRDM component.

Long-term groundwater level monitoring data are only available for the Zwartkrans Basin. The proposed RQO for the upper reaches represented by the Vlakdrift Subcompartment, assigned a ‘*modified*’ class C SoE condition, is a change in groundwater rest level of ≤ 6.1 m. The middle reaches represented by the Sterkfontein Subcompartment, assigned a ‘*largely modified*’ class D SoE condition, is set a change in groundwater rest level of ≤ 3.6 m, and the Zwartkrans Subcompartment in the lower reaches, assigned a ‘*largely modified*’ class D SoE condition, is set a value of ≤ 2.3 m.

The remaining nine karst basins, which are either assigned a ‘*slightly modified*’ class B/BC or a ‘*natural*’ class AB SoE condition, represent a natural environment that remains largely unaffected by changes in land use activities and practices. For this reason, the setting of RQOs as above is not an imperative at this stage. Further, it would be required that a better understanding of groundwater rest level behaviour and trends in these groundwater resource units is developed before RQOs can be set with the necessary statistical support to generate confidence.

4.2 Quality

The setting of RQOs in regard to groundwater chemistry (quality) is a comparatively much simpler exercise given the relationship of analytical groundwater chemistry data with the discharge(s) of associated groundwater compartments, especially where these are coupled with springwater chemistries. The springs draining the largely pristine Danielstroom, Tweefontein, Uitkomst and Diepkloof basins do not reflect anthropogenic impacts on the chemistry (quality) of the groundwater produced by these hydrogeologic environments, compared to the chemistry of groundwater produced via the Zwartkrans Spring. The latter drains the most severely compromised hydrogeologic regime in terms of groundwater quality in the study area, with groundwater analyses typically exhibiting electrical conductivity values > 100 mS/m, SO_4 concentrations > 150 mg/L, and Cl concentrations > 50 mg/L. The geographic extent of this footprint in the host aquifer is still comparatively limited.

5 Karst Solutional Denudation

An assessment of karst solutional denudation rates in the COH based on formula-derived, empirically-derived, and theoretically-derived approaches yields results which are in agreement with recently reported values and with the observed dewatering horizon developed over 3.3 Ma in Sterkfontein Cave. Cognisant of the variation in climatological and physiographical factors that influence landscape development in the long term, the mean solutional denudation rate in the COH is placed at 7.6 mm/Ka in the range 3–15 mm/Ka.

Studies that consider the effect of reaction processes on mineral surfaces (the surface complexation studies defined by Morse and Arvidson, 2002) in the evaluation of karst denudation remain unexplored in a South African context. The manifestation of a combined mine water and municipal wastewater impact on a portion of the COH karst environment provides an opportunity to explore this aspect against a comparison with the pristine portions of this environment.

6 Fossil Site Hydro-vulnerability

It is concluded that nine of the 14 fossil sites in the COH exhibit a *very low* or *low vulnerability*. This is attributed to their location (a) in groundwater compartments that are hydrogeologically separate from those where the contaminated water impact is manifested, and (b) at substantial elevations above the ambient groundwater level. Only the Bolt’s Farm site exhibits a *very high vulnerability*. This is because of its position immediately down-gradient of the two main sources of poor quality surface water, namely mine water via the Riet Spruit and treated municipal wastewater via the Blougat Spruit. This is compounded by the fact that (a) both these drainages lose water to the karst aquifer, and (b) at least one cave system in this area, Alladin’s (aka Quarry) Cave, is known to intersect the water table (P Boshoff, personal communication). The Sterkfontein site is assigned a *high vulnerability*. The fact that this cave system intersects the water table is mitigated by the observed long-term cave water quality record and other hydrochemical data. These reflect circumstances where the cave water does not exhibit the measure of impact observed in the Zwartkrans Subcompartment as is recorded for the Zwartkrans Spring. The Swartkrans, Minnaar’s and Plover’s Lake sites exhibit a *moderate vulnerability*. This is mainly because of a relatively shallow (5–25 m bs) water table. In conclusion, therefore, it is apparent that the majority of the

fossil sites in the COH are not under threat from either changes in surface water or groundwater levels and/or changes in surface water or groundwater chemistry (quality), whether due to mine water or treated sewage effluent ingress,

or from agricultural land use practices. The sites that are the most vulnerable have been identified and are earmarked for specific monitoring activities.

Recommendations

Harrison Pienaar and Philip J. Hobbs

Recommendations that address aspects specific to the water resources and ancillary aspects such as fossil site hydrovulnerability and cave ecosystem integrity have been put forward in the body of the report. They are not repeated in this section. The following recommendations are of a more general nature, and are put forward for consideration by the Cradle of Humankind World Heritage Site Management Authority (COH WHS MA) and broader scientific community.

- *Hydrovulnerability assessment*: It is advisable to extend the hydrovulnerability assessment to other cave systems in the study area. These will comprise those non-inscribed sites that researchers and cavers are familiar with, and therefore can be subjected to such assessment in cooperation with the caving fraternity.
- *Gravimetric survey*: It is advisable to carry out gravimetric surveys in the lower Riet Spruit valley extending from the confluence of the Tweelopie Spruit and the Riet Spruit down to the confluence of the Blougat Spruit and the Riet Spruit, as well as along the southern boundary of the KGR across the footprint of the dolomite outlier. The results of these surveys will indicate the measure of karst dissolution present in these important corridors that host the N14 national and the R24 regional roads, respectively.
- *Mine water treatment*: The Inter-Ministerial Committee (IMC) on acid mine drainage (AMD), as per the Coetzee et al. (2010) report, recommends (amongst others) that the mine water treatment capacity in the headwaters of the Tweelopie Spruit be increased to accommodate a decant volume of at least 40 ML/d. This recommendation is

supported unequivocally. It is imperative that all raw mine water generated in the upper reaches of the Tweelopie Spruit be captured and prevented from entering the environment in an untreated state. It is recognised, however, that the implementation of this recommendation lies within the jurisdiction of national government in the form of the Department of Water and Sanitation.

It is further recommended that additional mine water treatment facilities be established in the headwaters of the Tweelopie Spruit to further ‘polish’ the treated mine water that is generated by the expanded mine water treatment capacity and released into the environment. This might include the construction of artificial wetlands in the lower gradient upper reaches, and the placement of limestone in the river channel at selected high-energy cascade features such as waterfalls and dam spillways.

- *Monitoring*: Empower the tourist guides at Sterkfontein Cave to generate hydrogeologic data through simple observations. For example, tape measurements of the cave water level and regular determination of field water quality parameters with a handheld multi-parameter probe can be recorded daily in a log book. The information can then be communicated to tourists as a demonstration of more ‘intimate’ knowledge of the host hydrogeologic environment, expanding on the historical focus placed on the palaeoanthropological significance of the site.
- *Monitoring committee*: It is recommended that a monitoring committee comprising a core of key stakeholder groupings (e.g. national, provincial and local government, environment and tourism, agriculture, and NGOs) be established. This committee, chaired by the Management Authority, should function in cooperation with the similar committee established within the Team of Experts that advises the IMC on AMD.
- *Research*: Investigate the possibility of bacterial sulphate reduction in the confluence of the Riet Spruit and the Blougat Spruit. This supports the key science question posed by Banner et al. (2007) (in Martin and White 2007)

P. J. Hobbs: Deceased

H. Pienaar (✉) · P. J. Hobbs
Smart Places, Council for Scientific and Industrial Research,
Pretoria, South Africa
e-mail: hpienaar@csir.co.za

H. Pienaar
Hebei University of Engineering, Handan, China

- regarding the fate and transport of redox-sensitive elements and their microbial consequences and feedbacks. Research in this regard will benefit from expertise in the field of biogeochemistry.
- *Communication strategy*: It is important that the COH WHS Management Authority communicates the outcome of the water resources situation assessment and on-going monitoring activities to as a wide an audience as possible. This represents the most powerful means to counter the common and popular misperceptions that prevail regarding the AMD risk to the World Heritage status of the site. The COH WHS MA should consider various avenues of communication including public information meetings in the area, the print media and awareness campaigns.
 - *International Recognition*: The COH WHS MA should avail itself of every opportunity to disseminate the results of its hydrologic and hydrogeologic studies to a peer audience using appropriate international platforms such as conferences, symposia and peer-reviewed academic journals.

Instead of fearing asteroids, we should fear ourselves.

Yuval Noah Harari

(on Homo sapiens and mass extinctions, in "Homo Deus: A Brief History of Tomorrow", Vintage, London, 2016)

Acknowledgements

The author is indebted to the many landowners who granted access to geosites (especially boreholes and springs) at and from which invaluable hydrogeologic data were sourced. The study would not have been possible without the cooperation of the following persons, listed in alphabetical order. The author offers his apologies to any individual inadvertently omitted from this list.

| Stakeholder/landowner/contact | Property and/or geosite description and/or organisation |
|-------------------------------|---|
| Bacchiere, C | Olera Farmers, Kromdraai 520JQ |
| Bailey, P | Owner, The Cradle/Motsetse Nature Reserve |
| Barnard, P | Danielsrust 518JQ |
| Brengosz, R | Ptn 38 (Moon Valley Ranch), Rietfontein 522JQ |
| Brooker, J | Owner, Glen Afric Country Lodge, Broederstroom |
| Carpenter, H | Facilities Supervisor, Nedbank Olwazini Estate LMDC |
| Carstens, M | Plot 3, Beckedan Agricultural Holdings |
| Coleman, D | Ptn 35, Zwartkrans 172IQ |
| Cox, D | Manager, Nedbank Olwazini Estate LMDC |
| de Klerk, P | Ptn 7, Kromdraai 520JQ |
| de Wit, L | Plateau Farm Estate, Kromdraai 520JQ |
| Deysel, J | Maintenance Supervisor, Sterkfontein Cave, Maropeng |
| Dispan, P | Ptn 143, Sterkfontein 173IQ |
| Dorling, D | Director, DD Science Laboratory cc |
| Doyle, G | Supervisor, Crab Farm Estate, Kromdraai 520JQ |

(continued)

| Stakeholder/landowner/contact | Property and/or geosite description and/or organisation |
|-------------------------------|---|
| du Plessis, K (Ms) | Data Manager, DD Science Laboratory cc |
| du Toit, S | Specialist: Environmental Protection, Mogale City LM |
| du Toit, S | Manager, Plover's Lake Estate, Kromdraai 520JQ |
| Erasmus, M (Mrs) | Plot 173, Oaktree Agricultural Holdings |
| French, G (Ms) | Kalkheuwel West Estate |
| Fouche, M | Maintenance Manager, Maropeng |
| Fourie, L | Plot 34, Waterval Agricultural Holdings |
| Gaylord, J | Greensleeves Medieval Restaurant, Zwartkrans 172IQ |
| Gomes, M | Chairman, Kromdraai Irrigation Board |
| Gomes, S | Long-term local resident |
| Grobler, H | Ptn 8, Kromdraai 520JQ |
| Hearne, E | Owner, Rhino and Lion Game Reserve, Rietfontein 522JQ |
| Hewitt, J | Owner, Kenjara Lodge, Kromdraai 520JQ |
| Jackson, B | Plot 15, Danielsrust 518JQ |
| Jardim, I | Ptn 66/25, Sterkfontein 173IQ |
| Joubert, W | Savannah Game Reserve, Danielsrust 518JQ |
| Keller, S | ex-Environmental Manager, SibanyeGold |
| Kok, J | Royal Thatch, Zwartkrans 172IQ |
| Kotze, J | Dwarsvlei 503JQ |
| Krige, G | Plot 129, Sterkfontein Farm Estate |
| Kruger, L | Ptn 78, Sterkfontein 173IQ |

(continued)

| Stakeholder/landowner/contact | Property and/or geosite description and/or organisation |
|-------------------------------|---|
| Lotz, R | Ptn 5, Lotz Kontrei, Kromdraai 520JQ |
| Lourens, W | Chief Ranger, Glen Afric Country Lodge, Broederstroom |
| Maidment, S | Kalkheuwel West Estate |
| Malherbe, C (Mrs) | Plot 72, Sterkfontein 173IQ |
| Malherbe, D | Plot 72, Sterkfontein 173IQ |
| Maré, E (Ms) | Plant Manager, Percy Stewart WWTW, MCLM |
| Marshall, L | Manager, Maropeng aAfrica |
| Mashitsho, D | Municipal Manager, Mogale City Local Municipality |
| McClauchlan, P | Oaktree Agricultural Holdings |
| McDonald, A | Plot 150, Sterkfontein Farm Estate |
| Mitchell, E | Plot 167, Sterkfontein Farm Estate |
| Mostert, J | Game Ranger (former), Krugersdorp Game Reserve |
| Nash, J | Owner, John Nash Nature Reserve |
| Norquoy, N | Wild Cave Adventures |
| Oosthuizen, T | Plot 9, Danielsrust 518JQ |
| Pera, K | Rhino and Lion Game Reserve, Rietfontein 522JQ |
| Potgieter, P | Exclusive Mineral Water, Plot 71, Sterkfontein 173IQ |
| Robeni, B | Chief Ranger, Motsetse Nature Reserve / The Cradle |
| Roodt, P | Plot 66, Oaktree Agricultural Holdings |
| Roos, G | Bergland Instant Lawn, Sterkfontein 173IQ |
| Roos, H (Mrs) | Ptn 5, Zwartkrans 172IQ |
| Roxmouth, C | Plot 56, Zwartkrans 172IQ |
| Rubin, A | ex-Manager, Maropeng aAfrica |
| Rykaart, J | General Manager (former), Krugersdorp Game Reserve |
| Saunders, E | Plot 160, Sterkfontein Farm Estate |
| Scheepers, J | Plot 137, Sterkfontein Farm Estate |
| Schilling, G | AquaMine, Rietfontein 522JQ |
| Schutte, P | Ptn 8/2, Chrisuél, Sterkfontein 173IQ |
| Smith, S | Manager, Ptn 35 (Ekutheni Estate), Kromdraai 520JQ |
| Steyn, C | Electrical Foreman, Sibanye-Stillwater |
| Steyn, D | Plot 119, Sterkfontein Farm Estate |

(continued)

| Stakeholder/landowner/contact | Property and/or geosite description and/or organisation |
|-------------------------------|---|
| Steyn, H | Plot 162, Sterkfontein Farm Estate |
| Tarr, R | Oak Tree Farm, Oaktree Agricultural Holdings |
| van den Bosch, J | Jomajoco Farms, Vlakdrift 163IQ |
| van der Merwe, P | Danielsrust Game Farm, Danielsrust 518JQ |
| van der Merwe, D | Danielsrust Game Farm, Danielsrust 518JQ |
| van der Merwe, P | Glen Almond, Sterkfontein 173IQ |
| van der Walt, B | ex-HDS Plant Manager, SibanyeGold |
| van Ekeren, K | Ptn 3, Dwarsvlei 503JQ |
| van Niekerk, J | Plot 37, Waterval Agricultural Holdings |
| van Rooy, F | Boland Farm, Danielsrust 518JQ |
| van Rooy, J | Boland Farm, Danielsrust 518JQ |
| van Wyk, P | Rietfontein 522JQ |
| Vieira, J (Mrs) | Proprietor, Cradle Food Market, Oaktree |
| Viljoen, W | Ptn 106, Sterkfontein 173IQ |
| Visser, H | Manager, John Nash Nature Reserve, Tweefontein 523JQ |
| Wessels, F | Rhino and Lion Game Reserve, Rietfontein 522JQ |
| Whatley, G | Kromdraai Gold Mine, Kromdraai 520JQ |
| Whillier, J | Plot 127, Sterkfontein Farm Estate |
| Zorab, R | ex-Director, SibanyeGold |

The author also extends a sincere word of thanks to the CSIR and DWS colleagues who participated in various aspects of the field work. These individuals are listed, in alphabetical order, as follows.

| Name | Position/Affiliation |
|---------------|---|
| Bugan, R | Research Scientist (CSIR Natural Resources & Environment) |
| de Meillon, N | Scientific Technician Production (Department of Water & Sanitation) |
| Leyland, R | Research Scientist (CSIR Built Environment) |
| Masinge, H | Technician (CSIR Natural Resources & Environment) |
| May, F | Research Scientist (ex CSIR Natural Resources & Environment) |
| McMillan, P | Technician (CSIR Natural Resources & Environment) |

(continued)

| Name | Position/Affiliation |
|------------------|--|
| Mmabatswa, S | Trainee (Department of Water & Sanitation) |
| Mokoena, M (Ms) | CSIR Intern (National Research Foundation) |
| Moolman, T | Auxilliary Services Officer (Department of Water & Sanitation) |
| Mukwevhu, L | CSIR Intern (National Research Foundation) |
| Musetsho, M | Trainee (Department of Water & Sanitation) |
| Mvandaba, V (Ms) | CSIR Intern (National Research Foundation) |
| Ngcobo, K (Ms) | Trainee (Department of Water & Sanitation) |
| Shadung, J | CSIR Student Intern (University of Johannesburg) |
| Socosa, L (Ms) | CSIR Student Intern (Tshwane University of Technology) |
| Zengeya, T | Research Scientist (ex CSIR Natural Resources & Environment) |
| Pienaar, H | Comptence Area Manager (CSIR Natural Resources & Environment) |

Especially the efforts and support of Mr T (Theo) Moolman in the field-sourcing of the vertical hydrochemical profiling data presented in Sect. 8.10, Chapter “Chemical Hydrogeology” are gratefully acknowledged.

The final and greatest appreciation must be expressed towards the staff of the Management Authority who have demonstrated absolute confidence in the service provided to this authority over the many years that the CSIR served as Professional Service Provider. The following individuals are listed, in alphabetical order, as follows:

| Name | Position |
|---------------|---------------------------|
| Mills, P | Deputy Director (retired) |
| Pienaar, H | Deputy Director |
| Pillay, M | Director |
| Sibanyoni, J | ex-Assistant Director |
| Smith, L (Ms) | Deputy Director |

Unnumbered plates



Discharge in the Riet Spruit at its intersection with the Malmani Road; note the red colouration of the water due to dissolved ferrous iron (Fe^{2+}) indicative of a strong acid mine water presence as revealed by the following field values: pH = 2.3, SEC = 410 mS/m, ORP = 254 mV (photo P Hobbs, date 12/01/2011)



The ~21 L/s Broederstroom Spring that rises under the concrete slab (at feet of seated figure) which forms part of the spring protection measures (photo P Hobbs, date 21/12/2010)



View of the first portion of the newly constructed and commissioned Train 4 (of 4) of the high density sludge (HDS) mine water treatment plant showing CaCO_3 -dosed raw mine water moving from stirred condition (left) to aerated condition (right); trains 3 to 1 extend to back of view (photo P Hobbs, date 11/05/2012)



Surface expression of the Moketsi Dyke giving rise to the ~ 2 L/s Moketsi Spring at left rear of picture (photo: P Hobbs)



View of the > 130 L/s Nash Spring (geosite JNNR3, also called the 'Bridge' or 'Rondawel' spring) in the John Nash Nature Reserve (photo P Hobbs, date 19/05/2010)

"If a man and his story are in conflict, it is the man who must change."

Adam Johnson

(from The Orphan Master's Son)



Resistant quartzite of the Witwatersrand Supergroup creating a ~15 m high waterfall (figure at bottom right for scale) on the Blougat Spruit downstream of the Percy Stewart Wastewater Treatment Works; the ameliorative effect of the aeration generated in the cascading water on its downstream quality is a fortuitous 'gratis' natural intervention (photo P Hobbs, date 26/09/2012)

*How many years can a mountain exist, before it is
washed to the sea? The answer, my friend,
is blowing in the wind.*

*Robert Allen Zimmerman aka Bob Dylan
(American folk-rock musician 1941–present)*

Glossary

Acid mine drainage The drainage emanating from mining operations or mine residue deposits as a result of the accelerated oxidation of sulphidic minerals, most commonly iron pyrite (FeS_2), due to exposure to water and oxygen, and which process is accelerated in the presence of iron- or sulphur-oxidising bacteria. Generally referred to by the acronym AMD.

Allogenic Describes a system that derives its water entirely from that running off a neighbouring non-karst catchment area (Ford and Williams 2007).

Analyte A chemical substance whose presence and/or concentration in a sample is determined (Lee 1989).

Anion An ion (atom or complex of atoms) that has gained one or more electrons to exhibit a negative electric charge, e.g. Cl^- , SO_4^{2-} .

Aquifer A stratum of water-bearing rock that has the ability to both store and transmit groundwater in quantities that are sufficient to sustain the long-term water-yielding properties of a borehole that intersects such stratum, for the water supply purposes required of the borehole. For example, a low-yielding aquifer that can sustain a sufficient groundwater yield to meet a comparatively low-demand domestic supply is as 'good' as a high-yielding aquifer that can sustain a groundwater yield capable of supplying water for large-scale irrigation or municipal water supply purposes.

Autogenic Describes a system composed entirely of *karst* strata, and which derives its water only from rainfall on such a system (Ford and Williams 2007). Andreo et al. (2008) recognise autogenic recharge over carbonate strata as including direct recharge, localised or concentrated recharge via swallow holes and indirect recharge from the bed of superficial water courses.

Aven A vertical or highly inclined shaft extending upward from a cave passage, generally to the surface. May equally be described as a shaft when seen from above.

Commonly related to enlarged vertical joints. (http://network.speleogenesis.info/directory/glossary/term.php?gloss_id=161)

Cation An ion (atom or complex of atoms) that has lost one or more electrons to be left with a positive electric charge, e.g. Na^+ , Mg^{2+} .

Confined aquifer An *aquifer* in which the *hydrostatic head* (pressure) is greater than that of atmospheric pressure, generally from the load exerted on the aquifer by overlying impervious (confining) strata, and therefore supports a *potentiometric surface* that is located above the 'roof' of the *aquifer*. This is typically represented by a groundwater level that stands at a shallower depth than that at which water was first encountered in a borehole penetrating the confined aquifer, and which phenomenon finds ultimate expression in the form of an artesian or free-flowing borehole.

Cutter Term used by North American karst scientists to describe a soil-covered *grike* that tapers with depth (Ford and Williams 2007).

Doline An enclosed topographic depression, basin or typically grassy hollow caused by direct solution and subsidence of the dolomite/limestone surface zone (solution doline), or formed by collapse over a cave (collapse doline) (Field, 2002); a collapse doline more readily conforms to the generally deeper funnel or shaft geometry with rocky cliff-bounded sides typical of a *sinkhole*.

Electrical balance Also referred to as the ionic or charge balance, it is a measure of the accuracy of a chemical analysis determined by the formula $(\sum \text{Cations} - \sum \text{Anions}) \div (\sum \text{Cations} + \sum \text{Anions}) \times 100$, which expresses the difference between the sum of the major positively charged *cations* and that of the major negatively charged *anions* as a percentage. Whereas a value of 0% denotes a perfect balance, an error margin of $\pm 5\%$ is generally considered acceptable for fresh water (Hem

1985; Appelo and Postma 2009). The calculation of this parameter in this study has considered only analyses which are complete for their reported sampling date, i.e. are not missing any major anion or cation. Where significant, the calculation has also included elements such as NO_3 , PO_4 , Fe and Mn which might materially influence the charge balance.

Epikarst The zone of highly weathered strata that occupies the top of the *vadose zone* and might or might not be covered with soil, and gradually grades downward into largely unweathered bedrock that forms the main body of the *vadose zone* (Ford and Williams 2007). Also referred to in some *karst* texts as the subcutaneous zone.

Gaining stream A river or stream that receives groundwater discharge; also referred to as an effluent drainage (stream).

Geosite The term used to describe any feature that represents a site of geological and/or hydrogeological interest in the environment, whether natural as in the case of a spring or artificial such as a borehole, dug well, mine shaft or tunnel. The DWA/NORAD (2004) recognises ten types of geosite described as the following: borehole, dug well, wellpoint, drain, tunnel, mine, seepage pond, spring, sinkhole and lateral collector.

Grike A vertical or sub-vertical cleft in a limestone pavement developed by solution along a joint or system of crisscrossing joints (UNESCO 1972). Ford and Williams (2007) identify these features (also called *kluftkarren*) as the 'master features' in a karst environment, serving as drains intersecting the *epikarst*.

Groundwater management unit An area of a catchment that requires consistent management actions to maintain the desired level of use or protection of groundwater; delineation is based on management considerations rather than geohydrological criteria (Parsons and Wentzel 2007).

Groundwater resource unit A groundwater body that has been delineated or grouped into a single significant water resource based on one or more characteristics that are similar across that unit (Parsons and Wentzel 2007).

Hydraulic conductivity The rate of flow (m^3/d) of water through a 1 m^2 cross section of *aquifer* under a *hydraulic gradient* of 1 (Driscoll 1986). Typically expressed as 'k' with the unit $\text{m}/\text{d} \equiv \text{m}^3/\text{d}/\text{m}^2$.

Hydraulic gradient The slope of the *potentiometric surface* that also describes the direction of groundwater movement in an *aquifer*.

Hydrological year A hydrological year (aka water year) is defined as the 12-month period October for any given year, through to September of the following year. By convention (see https://water.usgs.gov/nwc/explain_data.html), it is designated by the calendar year in which it ends, and which spans 75% of the composite 12 months.

Hydrophobic Lacking an affinity for water.

Hydrostatic head Describes the water table in a *phreatic aquifer*, or the potentiometric head in a *confined aquifer*, that represents the elevation of the groundwater rest level which, in turn, determines the direction of groundwater flow. For example, in a *phreatic aquifer*, groundwater drainage is from a higher elevation to a lower elevation, i.e. driven by gravity drainage. In a *confined aquifer*, groundwater drainage is from an area of a greater head (hydrostatic pressure) to an area of lower head, i.e. driven by differences in pressure (from higher to lower).

Inlier An area (usually of limited extent) of older strata completely surrounded by younger strata.

Juvenile acidity Describes the acidity (in mine water) that is associated with pyrite oxidation within the zone of mine water level fluctuation once complete rebound has been achieved (Younger 1997).

Karst The type of landscape that develops on carbonate rocks such as dolomite and limestone, and is formed principally by the dissolving of rock, giving rise to a landscape characterised by sinkholes and ground subsidence, losing surface water drainages, a well-developed subsurface drainage system, strong interaction between the circulation of surface water and groundwater, and caves (Ford and Williams 2007). Often also supports *aquifers* capable of storing and transmitting substantial quantities of groundwater typically draining to springs or 'eyes'.

Karst barré An isolated *karst* that is impounded by impermeable strata (Ford and Williams 2007), examples of which in the study area are represented by the Danielsrust Basin and the dolomitic *outlier* that hosts the *locus of* (mine water) *decant* (LoD). Note that the definition makes no reference to the age of the impounded strata relative to the impounding strata, as is the case in the distinction between *outlier* and *inlier*.

Locus of decant The area on the Sibanye-Stillwater property that hosts the various point and diffuse sources of acid mine drainage; includes the Black Reef Incline (BRI), #17 Winze and #18 Winze. Referred to in this manuscript by the acronym LoD.

Losing drainage A river or stream that loses some or all of its water into the subsurface, where it becomes ground-water; also referred to as an influent drainage (stream); in a karst environment, such loss typically occurs through a stream sink, swallet or swallow hole.

Median Statistical parameter that defines the value which is exceeded 50% of the time in a data set, the remaining 50% of values being below this value, and which means that this value is not unduly influenced (skewed) by anomalously high or low values in the data set.

Meromictic A water body (typically a lake) in which the layers of water do not mix or mix only partially/incompletely, leaving a non-mixing bottom layer (monimolimnion) of denser water that remains stagnant and is generally anaerobic. Meromictic surface lakes generally have large relative depths compared to their surface area, and are sheltered from the wind which is the primary driving agent for mixing. The density differences caused by the high dissolved solids concentration are greater than those due to temperature.

Nanoparticle Material with at least two dimensions between 1 and 100 nm. Nanoparticles have always existed in our environment, from both natural and anthropogenic sources. Nanoparticles in air were traditionally referred to as ultrafine particles, while in soil and water they were described as colloids (Klaine et al. 2008).

Occurrence survey The first phase of study of trace elements and *hydrophobic* organic contaminants in stream-bed sediment and tissues of aquatic organisms. The primary objective is to determine which target constituents are common and important to water quality conditions in each study unit (Shelton and Capel 1994).

Outlier An area (usually of limited extent) of younger strata completely surrounded by older strata.

Phreatic aquifer An *aquifer* in which the hydrostatic pressure is equal or similar to that of atmospheric pressure, and therefore supports a *potentiometric surface* that is equivalent to a *water table*. Also referred to as an unconfined *aquifer*.

Phreatic surface The surface defined by the *potentiometric surface* in a *phreatic aquifer*, and which is equivalent to the *water table*.

Potentiometric surface The theoretical surface fitted to the groundwater level elevation, in layman's terms often referred to as the *water table*, and which represents the spatial dimensions of the *hydrostatic* (pressure) *head* in a *confined aquifer* (Freeze and Cherry 1979; Domenico and Schwartz 1998; Ford and Williams 2007).

Raw mine water Mine water (typically acidic) that fills the mine void and decants into the environment either as subsurface flow or upon daylighting in the form of point or diffuse sources of discharge without having been treated in any manner other than that effected by natural factors such as oxygenation/aeration and in situ neutralisation by carbonate strata such as dolomite.

Resource water quality objective The measure(s) that must be imposed to ensure that the Class that has been assigned to a groundwater resource as part of a Groundwater Resource Directed Measures assessment is met. The measure(s) might for example consider the maximum allowable lowering and/or fluctuation of groundwater rest level, and the maximum allowable deterioration of groundwater quality. In the absence of data, the measure(s) generally take the form of qualitative descriptions, whereas semi-quantitative or even quantitative measures can be derived from long-term data records.

Salt load The mass of dissolved salts carried by a water body per unit time (typically expressed as t/d or t/a), calculated as the product of the flow volume (typically expressed as ML/d, where 1 ML/d \equiv 1000 m³/d) and the salt concentration (typically expressed as mg/L, where 1 mg/L \equiv 0.001 kg/m³).

Sinkhole An engineering/engineering geology term of North American origin (Ford and Williams 2007) for a collapse *doline* forming a hole on surface (WRC/IUCN/SAKWG 2010); synonymous terms are closed depression, *doline*, ponor, stream sink, sumidero, swallet and swallow hole (Field 2002).

Spruit Afrikaans word for stream or creek, essentially describing a surface water drainage feature (often ephemeral) of lesser magnitude than a river.

Stygobite A form of aquatic fauna that completes its entire life cycle in a cave environment.

Thalweg Hydrological term that describes the deepest part of a watercourse and, therefore, generally the path of fastest flow in a river or stream.

Total dissolved solids Evaporating a liquid and measuring the mass of residues left (drying and weighing), returns a 'total dissolved solids' (TDS) value under circumstances where certain salts decompose during drying, a subtle difference to 'total dissolved salts' as a measure of the combined content of inorganic and organic substances contained in a liquid.

Transmissivity The rate at which water is transmitted through a vertical section of an *aquifer* 1 m wide and extending the full saturated height (depth 'd') of the

aquifer under a *hydraulic gradient* of 1 (Driscoll, 1986). Typically expressed as 'T' with the unusual unit m^2/d [L^2/T], derived from its association with the product of *hydraulic conductivity* 'k' with units m/d [L/T] and 'd' (as previously defined) with units m [L], i.e. $T = kd$.

Treated mine water Mine water (typically acidic) that has been neutralised by means of the high density sludge (HDS) process prior to its release into the environment.

Troglobite A form of terrestrial fauna that completes its entire life cycle in a cave environment.

Vadose zone The unsaturated zone between the land surface and the **water table**.

Vestigial acidity Describes the acidity (in mine water) that is associated with the products of pyrite oxidation taken up in solution during the re-watering of mine workings, and is manifested in the 'first flush' when decant commences (Younger 1997).

Water table The surface represented by the groundwater level in a *phreatic aquifer*.

Winze A steep (not vertical) shaft which joins different levels in an underground mine. In the strictest sense, a winze has its entrance below surface within the mine, and not at surface as is the case with a shaft, and is excavated downwards, usually on a reef (Handley 2004).

References

- Abiye T (2010) Senior lecturer, hydrogeology. School of Geosciences. University of the Witwatersrand. Personal communication, 1 June 2010.
- Abiye TA (2014) Mine water footprint in the Johannesburg area, South Africa: Analysis based on existing and measured data. *S Afr J Geol* 117(1):87–96
- Acoccks JPH (1988) Veld types of South Africa, 3rd edn. Botanical Research Institute, South Africa, p 146
- Aller L, Bennett T, Lehr JH, Petty RJ (1985) DRASTIC—a standardized system for evaluating ground water pollution potential using hydrogeologic settings. US Environmental Protection Agency. Robert S. Kerr Environmental Research Laboratory. Office of Research and Development. EPA/600/2–85/018, 163 pp
- Allison C, Coetzee H, de Wit M (2011) Study of geo-contamination related to acid mine drainage in the West Rand, as a result of South Africa's gold mining industry. Inkaba yeAfrica poster presentation. GeoSynthesis 2011, 28 Aug–2 Sept 2011, Cape Town
- Andreo B, Vías J, Durán JJ, Jiménez P, López-Geta JA, Carrasco F (2008) Methodology for groundwater recharge assessment in carbonate aquifers: application to pilot sites in southern Spain. *Hydrogeol J* 16(5):911–925
- Appelo CAJ, Postma D (2009) Geochemistry, groundwater and pollution, 2nd edn. 4th corrected reprint. CRC Press, 649 pp
- Arimoro FO (2007) Macroinvertebrates functional feeding groups in River Orogo, a second order stream in southern Nigeria. *Niger J Sci Environ* 6
- ATSDR (2011) Toxic substances portal: Nickel. Agency for Toxic Substances and Disease Registry. Available at <http://www.atsdr.cdc.gov/substances/toxsubstance.asp?toxid=44>
- Awofolu OR, du Plessis R, Rampedi I (2007) Influence of discharged effluent on the quality of surface water utilized for agricultural purposes. *Afr J Biotechnol* 6(19):213–223
- Baas-Becking LGM, Kaplan IR, Moore D (1960) Limits of the natural environment in terms of pH and oxidation-reduction potentials. *J Geol* 68:243–284
- Bailly-Comte V, Jourde H, Pistre S (2009) Conceptualization and classification of groundwater–surface water hydrodynamic interactions in karst watersheds: case of the karst watershed of the Coulazou River (Southern France). *J Hydrol* 376:456–462. <https://doi.org/10.1016/j.jhydrol.2009.07.053>
- Bailey GN, King GCP (2011) Dynamic landscapes and human dispersal patterns: tectonics, coastlines, and the reconstruction of human habitats. *Quat Sci Rev* 30:1533–1553. <https://doi.org/10.1016/j.quascirev.2010.06.019>
- Bakalowicz M (2005) Karst groundwater: a challenge for new resources. *Hydrogeol J* 13:148–160. <https://doi.org/10.1007/s10040-004-0402-9>
- Bakalowicz M (2006) Importance of regional study site conditions in elaborating concepts and approaches in karst science, pp 15–22. In: Harmon RS, Wicks C (eds) Perspectives on karst geomorphology, hydrology and geochemistry—a tribute volume to Derek C. Ford and William B. White. Special Paper 404. Geological Society of America. 366 pp
- Balter M (2014) ‘Little Foot’ fossil could be human ancestor. Published 14/03/2014 on Science/AAAS. Accessed on 26/03/2014 at <http://news.sciencemag.org/africa/2014/03/little-foot-fossil-could-be-human-ancestor>
- Banks D (2004) Geochemical processes controlling minewater pollution. In: Groundwater management in mining areas proceedings of the 2nd IMAGE-TRAIN advanced study course. Pecs. Hungary, pp 17–44
- Banner J, Boston P, Colucci L, Cowan B, Frappier A, Gentry C, Harmon RS, Katz B, Long A, Martin JB, Musgrove M-L, Partin J, Rasmussen J, Wong C, White WB (2007) Geochemistry of modern karst systems. Focus group on geochemistry and climate, pp 82–89. In: Martin JB, White WB (eds) Frontiers of karst research. Special publication 13. Workshop proceedings and recommendations. 3–5/05/2007. San Antonio. Texas. Karst Waters Institute. Leesburg. Virginia, 118 pp
- Barnard HC (1996) Investigation into the deterioration of groundwater quality in a part of the Zwartkranz Compartment, District Krugersdorp. Report GH3886. Department of Water Affairs & Forestry. Pretoria, 6 pp
- Barnard HC (2000) An explanation of the 1:500 000 general hydrogeological map Johannesburg 2526. Department of Water Affairs & Forestry. Pretoria, 84 pp
- Barnes HL, Romberger SB (1968) Chemical aspects of acid mine drainage. *J (water Pollut Control Fed)* 30(3):371–384
- Bauer C, Kellerer-Pirklbauer A, Lieb GK (2008) Human impact on karst environments: a case study from central Styria, Austria. *Geophysical Research Abstracts*, vol 10. EGU2008-A-01339
- Beater M, Kilian D (2009) Environmental management framework and management plan for the Cradle of Humankind World Heritage Site, its proposed buffer zone, and the Muldersdrift area. Status Quo Report. 382,239. Prepared for the Management Authority, Department of Economic Development, Gauteng Province. SRK Consulting, Johannesburg, 138 pp
- Béga S (2008a) Pollution threatens Cradle of Humankind. Sourced on 06/01/2010 at http://www.environment.co.za/topic.asp?TOPIC_ID=2124
- Béga S (2008b) Cradle's heritage status in danger. Sourced on 06/01/2010 at http://www.iol.co.za/index.php?set_id=1&click_id=13&art_id=vn20081115091504526C425147
- Béga S (2010) Is river of acid threatening fossil treasures? Study targets mine water at Cradle of Humankind. *Saturday Star*, 17 Apr 2010

- Béga S (2012a) Study lightens toxic water gloom at Cradle fossil sites. *Saturday Star*, 14 Jan 2012
- Béga S (2012b) A toxic delay. *Saturday Star*, 28 Jan 2012
- Béga S (2012c) There's life in this dead river, say scientists. *Saturday Star*, 26 May 2012
- Béga S (2012d) AMD threat to heritage site – study. *Saturday Star*, 26 May 2012
- Béga S (2013) Water taints life in Cradle: toxic mine water chokes country estate. *Saturday Star*, 28 Sept 2013
- Beltrán R, de la Rosa JD, Santos JC, Beltrán M, Gómez-Ariza JL (2010) Heavy metal mobility assessment in sediments from the Odiel River (Iberian Pyritic Belt) using sequential extraction. *Environ Earth Sci* 61(7):1493–1503
- Benedini M, Tsakiris G (2013) Water quality modelling for rivers and streams. Springer, Dordrecht, p 288
- Berger LR (2001) Viewpoint: is it time to revise the system of scientific naming? *National Geographic News*. Sourced on 28/06/2010 at http://news.nationalgeographic.com/news/2001/12/1204_hominin_id.html
- Berger LR, Brink J (undated) An atlas of southern African mammalian fossil bearing sites—late Miocene to late Pleistocene. Chapter 6: The sites: dolomitic and other cave deposits. Sourced on 24/05/2010 at http://www.proflieberger.com/files/An_Atlas_of_southern_African_Fossil_Bearing_Sites.pdf
- Berger LR, de Ruiter DJ, Churchill SE, Schmid P, Carlson KJ, Dirks PHGM, Kibii JM (2010) *Australopithecus sediba*: A new species of Homo-like Australopithecus from South Africa. *Science* 328:195–204
- Berger LR, Hawks J, De Ruiter DJ, Churchill SE, Schmid P, Deleuzene LK, Kivell TL, Garvin HM, Williams SA, DeSilva JM, Skinner MM, Musiba CM, Cameron N, Holliday TW, Harcourt-Smith W, Ackermann RR, Bastir M, Bogin B, Bolter D, Brophy J, Cofran ZD, Congdon KA, Deane AS, Dembo M, Drapeau M, Elliott MC, Feuerriegel EM, Garcia-Martinez D, Green DJ, Gurtov A, Irish JD, Kruger A, Laird MF, Marchi D, Meyer MR, Nalla S, Negash EW, Orr CM, Radovic D, Schroeder L, Scott JE, Throckmorton Z, Tocheri MW, van Sickle C, Walker CS, Wei P, Zipfel B (2015) *Homo naledi*, a new species of the genus *Homo* from the Dinaledi Chamber, South Africa. *eLife* 4:e09560, 35 pp
- Bertram E (2008) Assistant director: Groundwater information. Directorate: Hydrological Services. Department of Water Affairs & Forestry. Email communication, 18 Mar 2008
- Bertram E (2010) Assistant director: Groundwater information. Directorate: Hydrological Services. Department of Water Affairs. Personal communication, 28 June 2010.
- Beukes NJ (1978) Die karbonaat gesteentes en ysterformasies van die Ghaap-groep van die Transvaal-supergroep in die Noord-Kaapland. (E. The carbonate rocks and iron formations of the Ghaap Group of the Transvaal Supergroup in the Northern Cape.) PhD thesis (unpublished). Rand Afrikaans University, Johannesburg, 580 pp
- Beukes NJ (1987) Facies relationships, depositional environments and diagenesis in a major early Proterozoic stromatolitic carbonate platform to basinal sequence, Campbell Rand Subgroup, Transvaal Supergroup, South Africa. *Sedimentary Geol* 54:1–56
- Bjerg PL, Rügge K, Pedersen JK, Christensen TH (1995) Distribution of redox-sensitive groundwater quality parameters downgradient of a landfill (Grindsted, Denmark). *Environ Sci Technol* 29(5):1387–1394
- BKS (2011) Witwatersrand gold fields acid mine drainage: Due diligence report. TCTA Contract 08-041, 154 pp
- Blackeagle C (2014) Is it a karst terrane, karst terrain, or both? Sourced on 19/12/2012 at <http://speleogenesis.info/community/blog/post/?id=Is-it-a-karst-terrane-karst-terrain-or-both>
- Bollmohr S, Thwala M, Jooste S, Havemann A (2008) An assessment of agricultural pesticides in the Upper Olifants River Catchment. Report N/0000/REQ0801. Resource Quality Services. Department of Water Affairs and Forestry. Pretoria, 45 pp
- Bonacci O, Pippin T, Culver DC (2009) A framework for karst ecohydrology. *Environ Geol* 56:891–900. <https://doi.org/10.1007/s00254-008-1189-0>
- Bonneville S, Behrends T, van Cappellen P (2009) Solubility and dissimilatory reduction kinetics of iron(III) oxyhydroxides: a linear free energy relationship. *Geochim Cosmochim* 73:5273–5282
- Boonzaier B (2010) Proprietor: geowater systems. Personal communication, 15 Dec 2010
- Boshoff P (2013) Caver. Personal communication, 26 Nov 2013
- Boudinet P (2012) A statistical model of karstic flow conduits. *Speleogenesis and Evolution of Karst Aquifers* (12):9–16. Sourced on 19/12/2012 at http://www.speleogenesis.info/directory/karstbase/pdf/seka_pdf11251.pdf
- Boulton AJ, Humphreys WF, Eberhard SM (2003) Imperilled subsurface waters in Australia: biodiversity, threatening processes and conservation. *Aquatic Ecosyst Health Manage* 6(1):41–54
- Bradley MJ, Herman JS (1989) Sulfate adsorption onto iron and aluminium hydroxides. *Eos, Trans Am Geophys Union* 70:326
- Brassington R (1998) *Field hydrogeology*, 2nd edn. Wiley, London, p 248
- Bredenkamp DB, van der Westhuizen C, Wiegman FE, Kuhn CM (1986) Ground-water supply potential of dolomite compartments west of Krugersdorp. Report GH3440, vols 1, 2. Department of Water Affairs & Forestry, Pretoria, 81 pp
- Bredenkamp DB, Vogel JC, Wiegman FE, Xu Y, Janse van Rensburg H (2007) Use of natural isotopes and groundwater quality for improved estimation of recharge and flow in dolomitic aquifers. Report KV 177/07. Water Research Commission, Pretoria, 68 pp
- Bredenkamp G, van Staden S (2009) Environmental management framework and management plan for the Cradle of Humankind World Heritage Site, its proposed buffer zone, and the Muldersdrift area. Terrestrial and aquatic ecology. Specialist report to SRK Consulting, Johannesburg, p 34
- Brink ABA (1996) Case History 18: Malmani subgroup—sequence of events relating to mining and the accelerated development of sinkholes and dolines in the Far West Rand. In: Brink ABA (ed) *Engineering geology of South Africa*, vol 1, pp 240–248
- Brink D (2008) Letter to the Chairperson: western basin technical task team titled crisis situation in the Krugersdorp Game Reserve. 01/09/2008. African Bush Adventures, Krugersdorp, 11 pp
- Brook GA, Folkoff ME, Box EO (1983) A world model of soil carbon dioxide. *Earth Surface Processes Landforms* 8(1):79–88. <https://doi.org/10.1002/esp.3290080108>
- Brooker J (2011) Owner. Glen Afric Country Lodge. Personal communication, 7 Jan 2011
- Brown L (2009) Environmental management framework and management plan for the Cradle of Humankind World Heritage Site, its proposed buffer zone, and the Muldersdrift area: Surface and groundwater. Specialist report. Prepared for the Management Authority, Department of Economic Development, Gauteng Province. SRK Consulting. Johannesburg, 80 pp
- Brown JG, Glynn PD (2003) Kinetic dissolution of carbonates and Mn oxides in acidic water: Measurement of in situ field rates and reactive transport modelling. *Appl Geochem* 18:1225–1239
- Bruxelles L, Clarke RJ, Maire R, Ortega R, Stratford D (2014) Stratigraphic analysis of the Sterkfontein StW 573 *Australopithecus* skeleton and implications for its age. *J Hum Evol*. Available online 31 Mar 2014 and accessed on 7 Apr 2014 at <http://www.sciencedirect.com/science/article/pii/S004724841400058X>
- Burke JJ, Moench MH (2000) *Groundwater and society: resources, tensions and opportunities*. ST/ESA/265. United Nations. New York. 170 pp

- Busenberg E, Plummer LN (1982) The kinetics of dissolution of dolomite in CO₂-water systems at 1.5° to 65 °C and 0.0 to 1.0 atmosphere P_{CO₂}. *Am J Sci* 282:45–78
- Carpenter H (2010) Facilities supervisor. Nedbank Leadership and Management Development Centre. Personal communication, 19 Nov 2010
- Carpenter H (2011) Facilities supervisor. Nedbank Leadership and Management Development Centre. Personal communication, 13 Jan 2011
- Carpenter H (2013) Energy and water manager. Group Property Services. Nedbank Group Ltd. Personal communication, 25 Feb 2013
- Cawthorn RG, Eales HV, Walraven F, Uken R, Watkeys MK (2006) The bushveld complex, pp 261–282. In: Johnson MR, Anhaeusser CR, Thomas RJ (eds) *The Geology of South Africa*. Geological Society of South Africa/Council for Geoscience, Johannesburg/Pretoria, p 691
- Cecil LD, Green JR (2000) Radon-222, pp 175–194. In: Cook PG, Herczeg AL (eds) *Environmental tracers in subsurface hydrology*. Kluwer Academic Publications, Boston/Dordrecht/London, p 529
- CGS (undated) Progress report, Western Mining Basin—15 October to 14 December 2004. Draft report. Witwatersrand Water Ingress Project. Council for Geoscience. Pretoria, 89 pp
- CGS/SAIEEG 2003. Guideline for engineering-geological characterisation and development of dolomitic land. Council for Geoscience/South African Institute of Engineering and Environmental Geologists Joint Document. Endorsed by the Geotechnical Division of the South African Institute of Civil Engineers. South Africa, 66 pp
- Chirenje E, Nyabeze PK, Coetzee H, Hobbs PJ (2010) Geophysical surveys, Sterkfontein Caves. Specialist report to the COH WHS Management Authority. Council for Geoscience/CSIR. Pretoria, 9 pp
- Choquette PW, Pray LC (1970) Geologic nomenclature and classification of porosity in sedimentary carbonates. *Am Assoc Petrol Geol* 54:207–250
- Cledenin CW (1989) Tectonic influence on the evolution of the early Proterozoic Transvaal Sea, southern Africa. PhD thesis (unpublished). University of the Witwatersrand, Johannesburg
- Coetzee H, Wade P, Ntsume G, Jordaan W (2002) Radioactivity study on sediments in a dam in the Wonderfontein Spruit catchment. DWAF-Report 2002, Pretoria
- Coetzee H, Winde F, Wade P (2006) An assessment of sources, pathways, mechanisms and risks of current and potential future pollution of water and sediments in gold-mining areas of the Wonderfontein spruit catchment. Report 1214/1/06. Water Research Commission, Pretoria, 202 pp
- Coetzee H, Chirenje E, Hobbs P, Cole J (2009) Ground and airborne geophysical surveys identify potential subsurface acid mine drainage pathways in the Krugersdorp Game Reserve, Gauteng Province, South Africa. Short paper. 10th SAGA Biennial Technical Meeting and Exhibition, 13–18 Sept 2009, Swaziland
- Coetzee H, Hobbs PJ, Burgess JE, Thomas A, Keet M (2010) Mine water management in the Witwatersrand gold fields with special emphasis on acid mine drainage. Report to the Inter-Ministerial Committee on Acid Mine Drainage, Pretoria, p 128
- Cole DI (1998) Uranium, pp 642–658. In: Wilson MGC, Anhaeusser CR (eds) *The Mineral Resources of South Africa*. Handbook 16. Council for Geoscience, 740 pp
- Cooke HBS (1969) Preservation of the Sterkfontein ape-man cave site, South Africa. Reprinted from *Studies in Speleology*, vol 2, Part 1, 34 pp
- Corbel J (1959) Erosion en terrain calcaire (vitesse d'érosion et morphologie). Reprinted in *Progress Phys Geogr* 32(6):684–690. <https://doi.org/10.1177/0309133308096756>
- Cornaton F, Goldscheider N, Jeannin PY, Perrochet P, Pochon A, Sinreich M, Zwahlen F (2003) The VULK analytical transport model and mapping method, pp 155–160. In: Zwahlen F (ed) *Vulnerability and risk mapping for the protection of carbonate (karst) aquifers*. Final report. COST Action 620. European Commission, Brussels, 297 pp
- Cullimore DR (1999) *Microbiology of well biofouling*. Lewis Publishers/CRC Press, Boca Raton, p 239
- Culver DC, Sket B (2000) Hotspots of subterranean biodiversity in caves and wells. *J Cave Karst Stud* 62(1):11–17
- Culver DC, Sket B (2002) Biological monitoring in caves. *Acta Carsologica* 31/1(4):55–64
- Cummins KW, Merritt RW, Andrade PCN (2005) The use of invertebrate functional groups to characterise ecosystem attributes in selected streams and rivers in south Brazil. *Stud Neotr Fauna Environ* 40(1):69–89
- Dallas HF (2007) River Health Programme: South African Scoring System (SASS) data interpretation guidelines (Draft report). Prepared for the Institute of Natural Resources and the Resource Quality Services River Health, Department of Water Affairs and Forestry, Pretoria/Cape Town
- Damons A (2010) Squatters claim Cradle of Humankind. Accessed on 08/06/2010 at <http://www.news24.com/SouthAfrica/News/Squatters-claim-Cradle-of-Humankind-20100418>
- Davidson B, Wei YP (2012) Assessing the 'wicked problems' associated with the quality of groundwater used in irrigation: a case study from the North China Plain. *Hydrogeol J*. Published online 05 January 2012. <https://doi.org/10.1007/s10040-011-0811-5>
- DEA (2014a) State of Conservation report for the fossil hominid sites of South Africa World Heritage Site (the Sterkfontein, Swartkrans, Kromdraai and environs component) (C 915 BIS). Report to the UNESCO World Heritage Committee. Department of Environmental Affairs, Management Authority and CSIR, Dec 2014, 12 pp
- DEA (2014b) Amendment of environmental authorisation: the immediate and short term interventions for the treatment of acid mine drainage in the Western, Central and Eastern basins of the Witwatersrand Gold Fields, Gauteng Province. Department of Environmental Affairs correspondence dated 05/03/2014 to the Department of Water Affairs, 3 pp
- DEA (2016) State of Conservation report for the fossil hominid sites of South Africa World Heritage Site (the Sterkfontein, Swartkrans, Kromdraai and environs component) (C 915 BIS). Report to the UNESCO World Heritage Committee. Department of Environmental Affairs, Management Authority and CSIR, Dec 2016, 10 pp
- De Jesus ASM (1985) On the behaviour of radium in tailings dams and environmental waters in the Witwatersrand (South Africa) gold/uranium mining area. In: *Proceedings of the 2nd international mine water congress*, Granada, Spain, pp 633–645
- De Villiers S, Mkwelo ST (2009) Has monitoring failed the Olifants River, Mpumalanga? *Water SA* 35(5):671–676
- Dickens CWS, Graham PM (2002) The South African scoring system (SASS) Version 5 rapid bioassessment method for rivers. *Afr J Aquatic Sci* 27(1):1–10
- Dirks PHGM, Berger LR (2013) Hominin-bearing caves and landscape dynamics in the Cradle of Humankind, South Africa. *J Afr Earth Sci* 78:109–131. <https://doi.org/10.1016/j.jafrearsci.2012.09.012>
- Dirks PHGM, Kibii JM, Kuhn BF, Steininger C, Churchill SE, Kramers JD, Pickering R, Farber DL, Mériaux A-M, Herries AIR, King GCP, Berger LR (2010) Geological setting and age of Australopithecus sediba from Southern Africa. *Science* 328:205–208. <https://doi.org/10.1126/science.1184950>
- Dirks PHGM, Berger LR, Roberts EM, Kramers JD, Hawks J, Randolph-Quinney PS, Elliott M, Musiba CM, Churchill SE, de Ruiter DJ, Schmid P, Backwell LR, Belyanin GA, Boshoff P,

- Hunter KL, Feuerriegel EM, Gurtov A, du Harrison GJ, Hunter R, Kruger A, Morris H, Makhubela TV, Peixotto B, Tucker S (2015) Geological and taphonomic evidence for deliberate body disposal by the primitive hominin species *Homo naledi* from the Dinaledi Chamber, South Africa. *Elife* 4:e09651
- Doerflinger N, Jeannin PY, Zwahlen F (1999) Water vulnerability assessment in karst environments: a new method of defining protection areas using a multi-attribute approach and GIS tools (EPIK method). *J Environ Geol* 39(2):165–176
- Dorling D (2010) Proprietor. DD Environmental Science cc. Communication to the Western Basin Void Sub-group Monitoring Committee Meeting. Mogale City Local Municipality offices, 17 Aug 2010
- Dorling D (2011) Proprietor. DD Environmental Science cc. Personal communication, 13 Oct 2011
- Doyle G (2010) Resident Manager. Crab Farm Estate. Personal communication, 13 May 2010
- Driscoll FG (1986) *Groundwater and Wells*, 2nd edn. Johnson Filtration Systems Inc. St. Paul. Minnesota, 1089 pp
- Duane MJ, Pigozzi G, Harris C (1997) Geochemistry of some deep gold mine waters from the western portion of the Witwatersrand Basin, South Africa. *J Afr Earth Sci* 24(1/2):105–123
- Dublyansky YV (2014) Hypogene speleogenesis—Discussion of definitions, pp 1–3. In: Klimchouk A, Sasowsky ID, Mylroie J, Engel SA, Engel AS (eds) *Hypogene cave morphologies*. Karst Waters Institute. Special publication 18, 103 pp. ISBN: 978-0-9.789.976-7-0
- Dunne S (2003) A Localised European Approach (LEA), pp 161–163. In: Zwahlen F (ed) *Vulnerability and risk mapping for the protection of carbonate (karst) aquifers*. Final report. COST Action 620. European Commission, Brussels, 297 pp
- Durand JF (2012) The impact of gold mining on the Witwatersrand on the rivers and karst system of Gauteng and North West province, South Africa. *J Afr Earth Sci* 68:24–43
- Durand JF, Peinke D (2010) Issue paper 4: The state of karst ecology research in the Cradle of Humankind World Heritage Site. pp 88–101. In: WRC/IUCN-SAKWG. The karst system of the Cradle of Humankind World Heritage Site. Report KV 241/10. Water Research Commission, Pretoria, 402 pp
- Durand JF, Meeuvis J, Fourie M (2010) The threat of mine effluent to the UNESCO status of the Cradle of Humankind World Heritage Site. *J Transdiscip Res S Afr* 6(1):73–92
- du Toit S (2010) Environmental Manager. Mogale City Local Municipality. Personal communication, 26 May 2010
- DWA/NORAD (2004) *Standard Descriptors for Geosites*. Version 1.1. Department of Water Affairs and Forestry/Norwegian Agency for Cooperation Development, Pretoria, 122 pp
- DWA (2006) *Groundwater resource assessment 2*. Department of Water Affairs, Pretoria
- DWA (2009) *Green Drop Report 2009*. Version 1. South African Waste Water Quality Management Performance. Department of Water Affairs, Pretoria, 124 pp
- DWA (2010a) Document WMA03 CROCODILE WEST MARICO RESERVOIR SITES.doc. Sourced on 18/06/2010 at http://www.dwaf.gov.za/hydrology/dwafapp2_wma/
- DWA (2010b) *West Rand Dolomite Compartments*. Final version 1.0. A1 map at scale 1:85 000 available from Directorate: Water Resources Planning Systems. Department of Water Affairs, Pretoria
- DWA (2011) *Green drop report 2011*. Waste Water Service Regulation. Department of Water Affairs, Pretoria, 450 pp
- DWA (2013a) *Feasibility study for a long-term solution to address the acid mine drainage associated with the East, Central and West Rand underground mining basins: assessment of the water quantity and quality of the Witwatersrand mine voids*. Report No. 5.2. Edition 1. Project No. P RSA 000/00/16512/2, Pretoria. South Africa, 270 pp
- DWA (2013b) *Newsletter: AMD FS LTS*. Ed. 2, 13 pp
- DWAF (1996a) *South African Water Quality Guidelines*. Volume 7: Aquatic Ecosystems, 2nd edn. Department of Water Affairs and Forestry, Pretoria, 159 pp
- DWAF (1996b) *South African Water Quality Guidelines*. Volume 5: Agricultural Use: Livestock Watering, 2nd edn. Department of Water Affairs and Forestry, Pretoria, 163 pp
- DWAF (1996c) *South African Water Quality Guidelines*, vol 4: Agricultural Use: Irrigation, 2nd edn. Department of Water Affairs and Forestry, Pretoria, 199 pp
- DWAF (1996d) *South African Water Quality Guidelines*. Volume 2: Recreational Water Use, 2nd edn. Department of Water Affairs and Forestry, Pretoria, 85 pp
- Ellis R, Grove A (2010) Issue paper 12: Legal aspects of karst and cave use in the Cradle of Humankind World Heritage Site, pp 286–352. In: WRC/IUCN-SAKWG. The karst system of the Cradle of Humankind World Heritage Site. Report KV 241/10. Water Research Commission, Pretoria, 402 pp
- Elsner M, Schwarzenbach RP, Haderlein SB (2004) Reactivity of Fe (II)-bearing minerals toward reductive transformation of organic contaminants. *Environ Sci Technol* 38(3):799–807
- Engel A, Northup D, Gary M, Gonzalez B, Gonzalez J, Hutchens E, Jones D, Macalady J, Spear J, Spilde M (2008) Focus group on caves and karst as model systems in geomicrobiology, pp 90–95. In: Martin JB, White WB (eds) *Frontiers of Karst Research*. Special publication 13. Karst Waters Institute, Leesburg, Virginia, 118 pp
- EPS (1994) *Guidance document on collection and preparation of sediments for physicochemical characterisation and biological testing*. Report EPS 1/RM/29. Environmental Protection Series. Environment Canada, 129 pp
- Erickson PM, Kleinmann RLP, Posluszny ET, Leonard-Mayer PJ (1982) Hydrogeochemistry of a large mine pool. In: *Proceedings of 1st international mine water congress*, Budapest, Hungary, A, pp 27–42
- Eriksson PG, Reczko BFF (1995) The sedimentary and tectonic setting of the Transvaal Supergroup floor rocks to the Bushveld Complex. *J Afr Earth Sci* 21:487–504
- Eriksson PG, Altermann W, Hartzer FJ (2006) The Transvaal Supergroup and its precursors. pp 237–260. In: Johnson MR, Anhaeusser CR, Thomas RJ (eds) *The Geology of South Africa*. Geological Society of South Africa/Council for Geoscience, Johannesburg/Pretoria, p 691
- Esterhuysen A (2009) *Environmental management framework and management plan for the Cradle of Humankind World Heritage Site, its proposed buffer zone, and the Muldersdrift area: Cultural-Heritage*. Specialist report to SRK Consulting, Johannesburg, p 26
- Ewers RO, White KA, Fuller JF (2012) Contaminant plumes and pseudoplumes in karst aquifers. *Carbonates Evaporites* 27(2):153–159. <https://doi.org/10.1007/s13146-012-0099-0>
- Falkowski P, Scholes RJ, Boyle E, Canadell J, Canfield D, Elser J, Gruber N, Hibbard K, Höglberg P, Linder S, Mackenzie FT, Moore B III, Pedersen T, Rosenthal Y, Seitzinger S, Smetacek V, Steffen W (2000) The global carbon cycle: a test of our knowledge of Earth as a system. *Science* 290:291–296
- Field MS (2002) *A lexicon of cave and karst terminology with special reference to environmental karst hydrology*. Report EPA/600/R-02/003. United States Environmental Protection Agency, Washington, DC, 214 pp
- Field MS (2006) *Tracer-test design for losing stream-aquifer systems*. *Int J Speleol* 35(1):25–36
- Fleisher JNE (1981) *The geohydrology of the dolomite aquifers of the Malmani Subgroup in the South-Western Transvaal*. Report Gh3169. Department of Water Affairs, Pretoria, 228 pp

- Florea LJ, Vacher HL (2006) Springflow hydrographs: Eogenetic vs. telogenetic karst. *Ground Water* 44(3):352–361
- Florea LJ (2015) Carbon flux and landscape evolution in epigenic karst aquifers modelled from geochemical mass balance. *Earth Syst Processes Landforms*. <https://doi.org/10.1002/esp.3709>
- Fofonoff NP, Millard RC, Jr (1983) Algorithms for computation of fundamental properties of seawater. UNESCO Technical Papers in Marine Science 44, Paris, 53 pp
- Foote RM (1967) Sinkhole formation by groundwater withdrawal: Far West Rand, South Africa. *Science* 157(3792):1045–1048
- Ford DC (2003) Perspectives in karst hydrogeology and cavern genesis. *Speleogenesis and Evolution of Karst Aquifers*. Issue 1. 12 pp. Sourced on 19/12/2012 at http://www.speleogenesis.info/directory/karstbase/pdf/seka_pdf4470.pdf
- Ford DC (2006) Karst geomorphology, caves and cave deposits: a review of North American contributions during the past half century, pp 1–14. In: Harmon RS, Wicks CW (eds) *Perspectives on karst geomorphology, hydrology and geochemistry*. Special Paper 404. Geological Society of America, 366 pp
- Ford TD, Pedley HM (1996) A review of tufa and travertine deposits of the world. *Earth-Sci Rev* 41:117–175
- Ford D, Williams P (2007) *Karst Hydrogeology and Geomorphology*. Wiley, Chichester, 562 pp. ISBN: 978-0-470-84.997-2
- Förstner U, Wittmann GTW (1976) Metal accumulations in acidic waters from gold mines in South Africa. *Geoforum* 7(1):9. [https://doi.org/10.1016/0016-7185\(76\)90.056-7](https://doi.org/10.1016/0016-7185(76)90.056-7)
- Fourie M (2005) A rising acid tide. *EarthYEAR J Sustain Dev* 1:36–41
- Fourie HE, Thirion C, Weldon CW (2014) Do SASS5 scores vary with season in the South African Highveld? A case study on the Skeerpoort River, North West Province, South Africa. *Afr J Aquat Sci* 39(4):369–376
- Fox LE (1988) The solubility of colloidal ferric hydroxide and its relevance to iron concentrations in water. *Geochim Cosmochim Acta* 52(3):771–777
- FSE (2014) Annual Report 2013. Federation for a Sustainable Environment. Available from <http://www.fse.org.za/>
- Gabrovšek F (2007) On denudation rates in karst. *Time in Karst*, Postojna, pp 7–13. Available at <http://www.carsologica.zrc-sazu.si/downloads/361/gabrovsek1.pdf>
- Gabrovšek F (2009) On concepts and methods for the estimation of dissolutional denudation rates in karst area. *Geomorphology* 106:9–14. <https://doi.org/10.1016/j.geomorph.2008.09.008>
- Gammons CH, Tucci NJ (2013) The Berkely Pit Lake, Butte, Montana, pp 362–376. In: Geller W, Schultze M, Kleinmann R, Wolkendorfer C (eds) *Acidic pit lakes: the legacy of coal and metal surface mines*. Springer, Heidelberg, 525 pp
- Gams I (1991) The origin of the term karst in the time of transition of karst (kras) from deforestation to forestation. In: *Proceedings of the international conference on environmental changes in Karst Areas (IGU/UIS)*. Quaderni del Dipartimento di Geografia 13. Università di Padova, pp 1–8
- Gardner EK (2015) New instrument dates old skeleton; ‘Little Foot’ 3.67 million years old. *Purdue University News*. Sourced on 04/04/2014 at <http://www.purdue.edu/newsroom/releases/2015/Q2/new-instrument-dates-old-skeleton-little-foot-3.67-million-years-old.html>
- Gauchon C, Ployon E, Delannoy J-J, Hacquard S, Hobléa F, Jailliet S, Perrette Y (2006) The concepts of heritage and heritage resource applied to karsts: protecting the Choranche Caves (Vercors, France). *Acta Carsologica* 35(2):37–46
- Gayer KH, Woontner L (1956) The solubility of ferrous hydroxide and ferric hydroxide in acidic and basic media at 25 °C. *J Phys Chem* 60(11):1569–1571
- Goldscheider N (2003) The PI method, pp 144–154. In: Zwahlen F (ed) *Vulnerability and risk mapping for the protection of carbonate (karst) aquifers*. Final report. COST Action 620. European Commission, Brussels, 297 pp
- Goldscheider N (2012) A holistic approach to groundwater protection and ecosystem services in karst terrains. *AQUA mundi*, pp 117–124. <https://doi.org/10.4409/Am-046-12-0047>
- Gombert P (2002) Role of karstic dissolution in global carbon cycle. *Glob Planet Change* 33:177–184
- Gomes M (2010) Chairman. Kromdraai Irrigation Board. Personal communication, 05 Oct 2010
- Gomes M (2011) Chairman. Kromdraai Irrigation Board. Personal communication, 11 Jan 2011
- Gondwe BRN (2010) Exploration, modelling and management of groundwater-dependent ecosystems in karst—the Sian Ka’an case study, Yucatan, Mexico. PhD thesis. Technical University of Denmark, Lyngby, 87 pp + Appendices
- Gordon AK, Muller WJ (2010) Developing sediment quality guidelines for South Africa. Phase 1: Identification of international best practice and applications for South Africa to develop a research and implementation framework. Report KV 242/10. Water Research Commission, Pretoria, 49 pp
- Govender B (2010) Assistant Director. DWS. Communication to the Western Basin Void Sub-group Monitoring Committee Meeting. Mogale City Local Municipality offices, 13 July 2010
- Graening GO, Brown AV (2000) Trophic dynamics and pollution effects in Cave Springs Cave, Arkansas. Publication MSC-285. Final report to the Arkansas Natural Heritage Commission. Department of Biological Sciences. Arkansas Water Resources Center, 44 pp
- Gray NF (1996) Field assessment of acid mine drainage contamination in surface and ground water. *Environ Geol* 27:358–361
- Groenewald Y (2010a) Acid mine water pollution a ‘ticking time bomb’. *Mail&Guardian*, 1–8 Apr 2010
- Groenewald J (2010b) Issue paper 11: the impacts of agriculture on the water resources and water-based ecosystems of the Cradle of Humankind World Heritage Site, pp 241–285. In: WRC/IUCN-SAKWG 2010. The karst system of the Cradle of Humankind World Heritage Site. Report KV 241/10. Water Research Commission, Pretoria, 402 pp. ISBN: 978-1-77.005–969-6
- Gunn J (ed) (2004) *Encyclopedia of caves and karst science*. Fitzroy Dearborn/Taylor and Francis, New York/London, p 902
- Hamilton-Smith E (2006) Thinking about Karst and World Heritage. *Helictite* 39(2):51–54
- Hammer Ø, Harper DAT, Ryan PD (2001) PAST: Paleontological statistics software package for education and data analysis. *Palaeontol Electron* 4(1):9. http://palaeo-electronica.org/2001_1/past/issue1_01.htm
- Handley JRF (2004) Historic overview of the Witwatersrand Goldfields, Howick, 224 pp.
- Hardin G (1968) The tragedy of the commons. *Science* 162:1243–1248
- Harding WR, Thornton JA, Steyn G, Panuska J, Morrison IR (2004) Hartbeespoort Dam remediation project (phase 1). Action plan (Volume 1) final report. DH Environmental Consulting, 166 pp
- Harlow GE, Orndorff RC, Nelms DL, Weary DJ, Moberg RM (2005) Hydrogeology and ground-water availability in the carbonate aquifer system of Frederick County, Virginia. Scientific investigations report 2005–5161. US Geological Survey, 30 pp
- Harril JR, Prudic DE (1998) Aquifer systems in the Great Basin Region of Nevada, Utah, and adjacent states—summary report. Professional paper 1409-A. US Geological Survey, 66 pp
- Heath RG, van Zyl HD, Schutte CF, Schoeman JJ (2009) First order assessment of the quantity and quality of non-point sources of pollution associated with industrial, mining and power generation. Report 1627/1/09. Water Research Commission, Pretoria, 167 pp

- Hem JD (1985) Study and interpretation of the chemical characteristics of natural water. Water Supply Paper 2254, 3rd edn. US Geological Survey, 263 pp
- Henry AG, Ungar PS, Passey BH, Sponheimer M, Rossouw L, Bamford M, Sandberg P, De Ruiter DJ, Berger L (2012) The diet of *Australopithecus sediba*. *Nature*. <https://doi.org/10.1038/nature11185>
- Hershey RL, Mizell SA, Earman S (2010) Chemical and physical characteristics of springs discharging from regional flow systems of the carbonate-rock province of the Great Basin, western United States. *Hydrogeol J* 18:1007–1026
- Herr C, Gray NF (1997) Sampling riverine sediments impacted by acid mine drainage: problems and solutions. *Environ Geol* 29(1/2):37–45
- Hill L, McMillan P, Cheng P (2014) An assessment of the biotic response in streams of the Western Basin that receive neutralised acid mine drainage. Report no. CSIR/NRE/WR/IR/2014/0021/B, Pretoria, 26 pp
- Hobbs PJ (1988a) Hydrogeology of the Verwoerdburg dolomite aquifer. Report GH3502. Department of Water Affairs and Forestry, Pretoria, 158 pp
- Hobbs PJ (1988b) Recent test pumping of the Malmani Subgroup dolomite aquifer in perspective, pp 35–42. In: GWD-GSSA. Workshop on dolomitic ground water of the PWV area, 28 Mar, Ground Water Division of the Geological Society of South Africa, Pretoria, 145 pp
- Hobbs PJ (2004) Intermediate groundwater Reserve determination for Quaternary catchments A21A and A21B. Project 2002–316. Department of Water Affairs & Forestry, Pretoria, 179 pp
- Hobbs PJ (2008a) Groundwater levels and dolomite—nuisance or necessity, pp 213–223. In: Proceedings of the “Problem Soils in South Africa” conference. SA Institute for Engineering and Environmental Geologists, 3–4 Nov 2008. ESCOM Conference Centre, Midrand, South Africa, 232 pp
- Hobbs PJ (2008b) Situation analysis of hydrologic and hydrogeologic factors informing the Royal Engineering groundwater supply on Sterkfontein 173IQ, Krugersdorp. Report CSIR/NRE/WR/ER/2008/0107/C. Council for Scientific & Industrial Research, Pretoria, 14 pp
- Hobbs PJ (ed) (2011a) Situation assessment of the surface water and groundwater resource environments in the Cradle of Humankind World Heritage Site. Report prepared for the COH WHS Management Authority. Department of Economic Development, Gauteng Provincial Government, South Africa, 424 pp. Available online at <http://www.dwaf.gov.za/ghreport/> as report 2.2(2657)
- Hobbs PJ (2011b) Assessment of the water level rise in Sterkfontein Caves, Cradle of Humankind World Heritage Site, Gauteng Province. Report CSIR/NRE/WR/ER/2011/0083/A. Council for Scientific & Industrial Research, Pretoria, 14 pp. Available online at <http://www.dwaf.gov.za/ghreport/> as report 2.2(?)
- Hobbs PJ (2011c) Gladysvale fossil site: opinion on the hydrosensitivity of the site. Letter report. Council for Scientific & Industrial Research, Pretoria, 4 pp
- Hobbs PJ (2012) Pilot implementation of a surface water and groundwater resources monitoring programme for the Cradle of Humankind World Heritage Site: situation assessment and status report for the period April to September 2012. Report CSIR/NRE/WR/ER/2012/0088/B. Prepared for the Management Authority, Gauteng Tourism Authority. Council for Scientific and Industrial Research, Pretoria, 39 pp. Available online at <http://www.dwaf.gov.za/ghreport/> as report 2.2(?)
- Hobbs PJ (2013a) Response to the AED interpretation of groundwater quality at Sterkfontein Country estate in December 2013. Letter report dated 04/04/2013. Prepared for the Department of Water Affairs. Council for Scientific and Industrial Research, Pretoria, 10 pp
- Hobbs PJ (2013b) Pilot implementation of a surface water and groundwater resources monitoring programme for the Cradle of Humankind World Heritage Site: situation assessment and status report for the period April 2012 to March 2013. Report CSIR/NRE/WR/ER/2013/0023/B. Prepared for the Management Authority, Gauteng Tourism Authority. Council for Scientific and Industrial Research, Pretoria, 48 pp. Available online at <http://www.dwaf.gov.za/ghreport/> as report 2.2(2866)
- Hobbs PJ (2013c) Surface water and groundwater resources monitoring, Cradle of Humankind World Heritage Site, Gauteng Province, South Africa: Water resources status report for the period April to September 2013. Report CSIR/NRE/WR/ER/2013/0083/A. Prepared for the Management Authority, Gauteng Tourism Authority. Council for Scientific and Industrial Research, Pretoria, 47 pp. Available online at <http://www.dwaf.gov.za/ghreport/> as report 2.2(2866)
- Hobbs PJ (2014a) Surface water and groundwater resources monitoring, Cradle of Humankind World Heritage Site, Gauteng Province, South Africa: Water resources status report for the period April 2013 to March 2014. Report CSIR/NRE/WR/IR/2014/0049/A. Prepared for the Management Authority, Gauteng Tourism Authority. Council for Scientific & Industrial Research, Pretoria, 34 pp. Available online at <http://www.dwaf.gov.za/ghreport/> as report 2.2(2957)
- Hobbs PJ (2014b) Surface water and groundwater resources monitoring, Cradle of Humankind World Heritage Site, Gauteng Province, South Africa: Water resources status report for the period April to September 2014. Report CSIR/NRE/WR/ER/2014/0063/A. Prepared for the Management Authority, Gauteng Tourism Authority. Council for Scientific & Industrial Research, Pretoria, 45 pp. Available online at <http://www.dwaf.gov.za/ghreport/> as report 2.2(3087)
- Hobbs PJ (2015a) Surface water and groundwater resources monitoring, Cradle of Humankind World Heritage Site, Gauteng Province, South Africa: Water resources status report for the period April 2014 to March 2015. Report CSIR/NRE/WR/ER/2015/0026/A. Prepared for the Management Authority, Gauteng Tourism Authority. Council for Scientific & Industrial Research, Pretoria, 43 pp. Available online at <http://www.dwaf.gov.za/ghreport/> as report 2.2(4702)
- Hobbs PJ (2015b) Surface water and groundwater resources monitoring, Cradle of Humankind World Heritage Site, Gauteng Province, South Africa: Water resources status report for the period April to September 2015. Report CSIR/NRE/WR/ER/2015/0067/A. Prepared for the Management Authority, Gauteng Tourism Authority. Council for Scientific & Industrial Research, Pretoria, 47 pp. Available online at <http://www.dwaf.gov.za/ghreport/> as report 2.2(3296)
- Hobbs PJ (2015c) Discussion of surface water and groundwater interaction in the upper Crocodile River basin, Johannesburg, South Africa: Environmental isotope approach by Abiye et al. *S Afr J Geol* 118(4):511–515
- Hobbs PJ (2016a) Surface water and groundwater resources monitoring, Cradle of Humankind World Heritage Site, Gauteng Province, South Africa: water resources status report for the period April 2015 to March 2016. Report CSIR/NRE/WR/ER/2016/0058/A. Prepared for the Management Authority, Gauteng Department of Economic Development. Council for Scientific & Industrial Research, Pretoria, 34 pp. Available online at <http://www.dwaf.gov.za/ghreport/> as report 2.2(4703)
- Hobbs PJ (2016b) Surface water and groundwater resources monitoring, Cradle of Humankind World Heritage Site, Gauteng Province, South Africa: Water resources status report for the period April to September 2016. Report CSIR/NRE/WR/ER/2016/0073/A. Prepared for the Management Authority, Gauteng Department of Economic Development. Council for Scientific & Industrial

- Research, Pretoria, 29 pp. Available online at <http://www.dwaf.gov.za/ghreport/> as report 2.2(4704)
- Hobbs PJ (2017a) Surface water and groundwater resources monitoring, Cradle of Humankind World Heritage Site, Gauteng Province, South Africa: Water resources status report for the period April 2016 to March 2017. Report CSIR/NRE/WR/ER/2017/0008/A. Prepared for the Management Authority, Gauteng Department of Economic Development. Council for Scientific & Industrial Research, Pretoria, 28 pp. Available online at <http://www.dwaf.gov.za/ghreport/> as report 2.2(4705)
- Hobbs PJ (2017b) Surface water and groundwater resources monitoring, Cradle of Humankind World Heritage Site, Gauteng Province, South Africa: Water resources status report for the period April to September 2017. Report CSIR/NRE/WR/ER/2017/0072/A. Prepared for the Management Authority, Gauteng Department of Economic Development. Council for Scientific & Industrial Research, Pretoria, 26 pp. Available online at <http://www.dwaf.gov.za/ghreport/> as report 2.2(4706)
- Hobbs PJ, Hill L, McMillan P (2018) Surface water and groundwater resources monitoring, Cradle of Humankind World Heritage Site, Gauteng Province, South Africa: Water resources status report for the period April 2017 to March 2018. Report CSIR/NRE/WR/ER/2018/0010/A. Prepared for the Management Authority, Gauteng Department of Economic Development. Council for Scientific & Industrial Research, Pretoria, 37 pp. Available online at <http://www.dwaf.gov.za/ghreport/> as report 2.2(4782)
- Hobbs PJ (2017c) TDS load contribution from acid mine drainage to Hartbeespoort Dam, South Africa. *Water SA* 43(4):12. <https://doi.org/10.4314/wsa.v43i4.10>. <http://www.wrc.org.za/Knowledge%20Hub%20Documents/Water%20SA%20Journals/Manuscripts/2017/04%20October%202017/3402.pdf>
- Hobbs PJ, Cobbing J (2007) A hydrogeological assessment of acid mine drainage impacts in the West Rand Basin, Gauteng Province. Report CSIR/NRE/WR/ER/2007/0097/C. Council for Scientific & Industrial Research, Pretoria, 100 pp
- Hobbs PJ, de Meillon N (2017) Hydrogeology of the sterksfontein cave system, cradle of humankind, South Africa. *S Afr J Geol* 120(3):403–420
- Hobbs PJ, Mills PJ (2011) The Koelenhof Farm fish mortality event of mid-January 2011. Report prepared for the Management Authority. Department of Economic Development, Gauteng Province, South Africa, 21 pp
- Hobbs PJ, Mills PJ (2012) Managing the threats to the Cradle of Humankind World Heritage Site, South Africa, pp 53–54. In: Yordanova M, Stefanova D, Mikhova AD (eds) Collection of Abstracts. International Scientific-Practical Conference on Protected Karst Territories—Monitoring and Management, 16–20 Sept 2012. Shumen. Bulgaria, 112 pp. Available at <http://www.prokarstterra.bas.bg/forum2012/conf-proceeding.html>
- Hobbs PJ, Venter J (2010) Situation assessment of the surface water and groundwater environments in the Cradle of Humankind World Heritage Site: Sediment chemistry assessment. Report prepared for the COH WHS Management Authority. Department of Economic Development, Gauteng Provincial Government, South Africa, 22 pp
- Hobbs P, Lindsay R, Maherry A, Matshaya M, Newman RT, Talha SA (2010) The use of ²²²Rn as a hydrological tracer in natural and polluted environments. Report 1685/1/10. Water Research Commission, Pretoria, 96 pp
- Hoehler TM, Alperin MJ, Albert DB, Martens CS (1998) Thermodynamic control on hydrogen concentrations in anoxic sediments. *Geochim Cosmochim Acta* 62(10):1745–1756
- Holland M (2007) Groundwater resource directed measures in karst terrain with emphasis on aquifer characterization in the Cradle of Humankind near Krugersdorp. MSc thesis (unpublished). University of Pretoria, Pretoria, 112 pp
- Holland M, Cobbing J (2008) Desktop geohydrological assessment of the Tarlton dolomites. Project 14/14/5/2. Activity 13. Water Geosciences Consulting for Department of Water Affairs, Pretoria, 61 pp
- Holland M, Witthüser KT (2009) Geochemical characterization of karst groundwater in the Cradle of Humankind World Heritage Site. *Environ Geol* 57:513–524
- Holland M, Wiegman F, Cobbing J, Witthüser KT (2009) Geohydrological assessment of the Steenkoppies dolomite compartment. Project 14/14/5/2. Activity 25. Water Geosciences Consulting for Department of Water Affairs, Pretoria, 70 pp
- Holland M, Witthüser KT, Jamison AA (2010) Issue paper 6: Hydrology of the Cradle of Humankind World Heritage Site; geology, surface and groundwater, pp 125–140. In WRC/IUCN-SAKWG. The karst system of the Cradle of Humankind World Heritage Site. Report KV 241/10. Water Research Commission, Pretoria, 402 pp
- Holmes P, James KAF, Levy LS (2009) Is low-level environmental mercury exposure of concern to human health? *Sci Total Environ* 408:171–182
- Howley A (2013) Final day of excavations. Sourced on 20/01/2014 at <http://newswatch.nationalgeographic.com/2013/11/27/final-day-of-excavations/>
- Hughes TA, Gray NF (2012) Acute and chronic toxicity of acid mine drainage to the activated sludge process. *Mine Water Environ* 31:40–52. <https://doi.org/10.1007/s10230-011-0168-y>
- Huizenga J-M (2004) Natural and anthropogenic influences on water quality: an example from rivers draining the Johannesburg Granite Dome. MSc thesis (unpublished). Rand Afrikaans University (now the University of Johannesburg), Johannesburg, 74 pp
- Hunter KS, Wang Y, van Cappellen P (1998) Kinetic modeling of microbially-driven redox chemistry of subsurface environments: Coupling transport, microbial metabolism and geochemistry. *J Hydrol* 29:53–80
- Jakobsen R, Albrechtsen H-J, Rasmussen M, Bay H, Bjerg PL, Christensen TH (1998) H₂ concentrations in a landfill leachate plume (Grindsted, Denmark): In situ energetics of terminal electron acceptor processes. *Environ Sci Technol* 32(14):2142–2148
- Jamison AA (In preparation) Structural and geological controls of geohydrology and dolomite cave systems in the Cradle of Humankind World Heritage Site. MSc thesis. University of the Witwatersrand
- JFA (2006) Environmental impact document—proposed discharge of treated mine water via the Tweelopies receiving water body into the Rietrivier, Mogale City, Gauteng Province. Final draft. Johan Fourie & Associates for Harmony Gold Mining Company Ltd., 145 pp
- Johnson KL, Younger PL (2006) The co-treatment of sewage and mine waters in aerobic wetlands. *Eng Geol* 35:53–61
- Jones WK (2013) Physical structure of the epikarst. *Acta Carsol* 42(2–3):311–314
- Jooste S (2011) Specialist Scientist. Department of Water Affairs. Personal communication, 25 Mar 2011
- Kafri U, Foster MJB, de Tremmerie F, Simonis J, Wiegman FE (1986) The hydrogeology of the dolomite aquifer in the Klip River—Natalspuit Basin. Report GH3408. Department of Water Affairs and Forestry, Pretoria, 96 pp
- Kasum J, Pilić M, Jovanović N, Pienaar H (2019) Model for forensic hydrography. *Trans Maritime Sci* 2:246–252
- Katz BG, Catches JS, Bullen TD, Michel RL (1998) Changes in the isotopic and chemical composition of ground water resulting from a recharge pulse from a sinking stream. *J Hydrol* 211:178–207

- Katz BG, Chelette AR, Pratt TR (2004) Use of chemical and isotopic tracers to assess nitrate contamination and ground-water age, Woodville Karst Plain, USA. *J Hydrol* 289:36–61
- Kaufmann G (2003) Karst landscape evolution. *Speleogenesis and Evolution of Karst Aquifers*. Issue 3, 10 pp. Sourced on 19/12/2012 at http://www.speleogenesis.info/directory/karstbase/pdf/seka_pdf4473.pdf
- Kaufmann JE (2013) Populations living on karst, p 60. In: NCKMS 2013. Program with abstracts. 20th National Cave and Karst Management Symposium—a changing climate. National Cave and Karst Research Institute, Carlsbad, 62 pp
- Kemmer FN (ed) (1988) The NALCO water handbook, 2nd edn. Nalco Chemical Company. McGraw-Hill, 1019 pp
- Kendall C, Caldwell EA (1998) Fundamentals of isotope geochemistry, pp 51–86. In: Kendall C, McDonnell JJ (eds) *Isotope tracers in catchment hydrology*. Elsevier, Amsterdam, p 839
- Kenyon P, Ellis R (2010) Issue paper 7: the uses of caves and karst in the Cradle of Humankind World Heritage Site. pp 141–162. In: WRC/IUCN-SAKWG. The karst system of the Cradle of Humankind World Heritage Site. Report KV 241/10. Water Research Commission, Pretoria, 402 pp
- King J, Pienaar H (eds) (2011) Sustainable use of South Africa's inland waters: a situation assessment of Resource Directed Measures 12 years after the 1998 National Water Act. Water Research Commission, Pretoria
- Kirby CS, Cravotta CA (2005) Net alkalinity and net acidity 1: theoretical considerations. *Appl Geochem* 20:1920–1940
- Kirby CS, Cravotta CA (2005) Net alkalinity and net acidity 2: practical considerations. *Appl Geochem* 20:1941–1964
- Kirkland DW (2014) Role of hydrogen sulfide in the formation of cave and karst phenomena in the Guadalupe Mountains and Western Delaware Basin, New Mexico and Texas. Special Paper 2. National Cave and Karst Research Institute, Carlsbad, New Mexico, USA, 87 pp
- Kiss M, Tanács E, Bárány-Kevei I (2011) Ecosystem services in Hungarian karst areas. *Acta Climatol Chorol Tomus* 44–45:41–49
- Klaine SJ, Alvarez PJJ, Batley GE, Fernandes TF, Handy RD, Lyon DY, Hahendra S, McLaughlin MJ, Lead JR (2008) Nanomaterials in the environment: behaviour, fate, bioavailability, and effects. *Environ Toxicol Chem* 27(9):1825–1851
- Klimchouk A (2004) Towards defining, delimiting and classifying epikarst: Its origin, processes and variants of geomorphic evolution. *Speleogenesis and Evolution of Karst Aquifers*. Issue 4. 13 pp. Sourced on 19/12/2012 at http://www.speleogenesis.info/directory/karstbase/pdf/seka_pdf4501.pdf
- Klimchouk AB (2006) Unconfined versus confined speleogenetic settings: variations of solution porosity. *Int J Speleol* 35(1):19–24
- Klimchouk AB (2011) Hypogene speleogenesis: hydrogeological and morphological perspective. Special paper 1, 2nd edn. National Cave and Karst Research Institute. Carlsbad, NM. 106 pp. ISBN-13: 978-0-9.795.422-0-6. Available at http://www.speleogenesis.info/directory/karstbase/pdf/seka_pdf9378.pdf
- Klimchouk A (2014) The methodological strength of the hydrogeological approach to distinguishing hypogene speleogenesis, pp 4–12. In: Klimchouk A, Sasowsky ID, Mylroie J, Engel SA, Engel AS (eds) *Hypogene cave morphologies*. Karst Waters Institute. Special publication 18. 103 pp. ISBN: 978-0-9.789.976-7-0
- Klimchouk AB, Ford D, Palmer A, Dreybrodt W (eds) (2000) *Speleogenesis: evolution of karst aquifers*. National Speleological Society, Huntsville, p 527
- Klimchouk AB, Ford DC (eds) (2009) Hypogene speleogenesis and karst hydrogeology of artesian basins. Special paper 1. Ukrainian Institute of Speleology and Karstology, Simferopol, 208 pp
- Knoeller K, Fauville A, Mayer B, Strauch G, Friese K, Veizer J (2004) Sulfur cycling in an acid mining lake and its vicinity in Lusatia, Germany. *Chem Geol* 204:303–323
- Kok TS, Wiegman FE, Fayazi M (1985) Results of exploration drilling in dolomite on Rietvallei 377, and at Erasmia and Valhalla, Pretoria. Report GH3379. Department of Water Affairs and Forestry, Pretoria, 91 pp
- Kok TS (1992) Recharge of springs in South Africa. Report GH3748. Department of Water Affairs, Pretoria, 9 pp
- Korom SF, Seaman JC (2012) When “conservative” anionic tracers aren't. *Ground Water* 50(6):820–824
- Kozuskanich J, Novakowski KS, Anderson BC (2010) Fecal indicator bacteria variability in samples pumped from monitoring wells. *Ground Water* 10. <https://doi.org/10.1111/j.1745-6584.2010.00713.x>
- Kralik M, Keimel T (2003) The time-input method, pp 172–180. In: Zwahlen F (ed) *Vulnerability and risk mapping for the protection of carbonate (karst) aquifers*. Final report. COST Action 620. European Commission, Brussels, 297 pp
- Krige G (2009) Hydrological/chemical aspects of the Tweelapie-/Riet-/Blaauwbankspruit, with specific reference to the impact water, decanting from the Western Basin mine void, has on this system. Revision 2. African Environmental Development, Sterkfontein, 66 pp
- Krige WG (2010) Issue paper 10: the impact of urbanisation on the water resources and water-based ecosystems of the Cradle of Humankind World Heritage Site, pp 211–240. In: WRC/IUCN-SAKWG. The karst system of the Cradle of Humankind World Heritage Site. Report KV 241/10. Water Research Commission, Pretoria, 402 pp
- Krige G (2011) Local resident and Environmental Consultant. Personal communication, 13 Jan 2011
- Krige G, du Toit S (2005) Report on aquatic biomonitoring and toxicological integrity of the Tweelopiespruit and the upper Wonderfonteinspruit in relation to the decant of mine water from the Western Basin mine void—winter cycle 2005. Revision 00. African Environmental Development, Sterkfontein, 32 pp
- Krige G, van Biljon M (2006) Hydrological/chemical aspects of the Tweelapie-/Riet-/Blaauwbankspruit, with specific reference to the impact water, decanting from the Western Basin mine void, has on this system. Revision 1. African Environmental Development, Sterkfontein, 66 pp
- Krige WG, van Biljon M (2010) Issue paper 9: the impacts of mining on the water resources and water-based ecosystems of the Cradle of Humankind World Heritage Site, pp 177–210. In: WRC/IUCN-SAKWG. The karst system of the Cradle of Humankind World Heritage Site. Report KV 241/10. Water Research Commission, Pretoria, 402 pp
- Kuhn CM (1989) Hydrogeology of the Midrand-Kempton Park dolomite. Report GH3501. Department of Water Affairs and Forestry, Pretoria, 125 pp
- Langmuir D (1971) The geochemistry of some carbonate ground waters in central Pennsylvania. *Geochim Cosmochim Acta* 35:1023–1045
- Langmuir D (1996) *Aqueous environmental geochemistry*: Upper Saddle River. Prentice-Hall, NJ, p 600
- Larson EB, Mylroie JE (2013) Quaternary glacial cycles: karst processes and the global CO₂ budget. *Acta Carsologica* 42(2–3):197–202
- Lee CC (1989) *Environmental engineering dictionary*. Government Institutes, Inc., 629 pp
- Leskiewicz AF (1986) Exploitable potential of ground water resources in storage in the dolomite of the Bapsfontein, Delmas and Springs area for emergency supplies. Report GH3463. Department of Water Affairs and Forestry, Pretoria, 40 pp
- Leyland R (2010) Groundwater risk and hazard maps. Report CSIR/BE/IE/IR/2010/0046/C. Council for Scientific & Industrial Research, Pretoria, 37 pp

- Leyland R (2013) Research Scientist. Built Environment. Council for Scientific & Industrial Research. Personal communication, 18 Feb 2013
- Leyland RC, Witthüser KT, van Rooy JL (2008) Vulnerability mapping in karst terrains, exemplified in the wider Cradle of Humankind World Heritage Site. Report KV 208/08. Water Research Commission, Pretoria, 97 pp
- Liefferink M (2011) Chief Executive Officer. Federation for a sustainable environment. Personal communication, 13 Jan 2011
- Lindsay MBJ, Moncur MC, Bain JG, Jambor JL, Ptacek CJ, Blowes DW (2015) Geochemical and mineralogical aspects of sulfide mine tailings. *Appl Geochem*. <https://doi.org/10.1016/j.apgeochem.2015.01.009>
- Liu X, Millero FJ (1999) The solubility of iron hydroxide in sodium chloride solutions. *Geochim Cosmochimica Acta* 63(19/20):3487–3497
- López-Chicano M, Bouamama M, Vallejos A, Pulido-Bosch A (2001) Factors which determine the hydrogeochemical behaviour of karstic springs: a case study from the Betic Cordilleras, Spain. *Appl Geochem* 16:1179–1192
- Lottermoser BG (2010) Mine wastes: characterization, treatment and environmental impacts, 3rd edn. Springer, Berlin, p 400
- Lotter L (2012) Water loss management in the City of Tshwane: updated up to end March 2012. Slide presentation. Sourced on 19/05/2013 at <http://www.dwa.gov.za/Projects/Vaal/April2012/6.2%20b%20WC%20WDM%20City%20of%20Tshwane.pdf>
- Louw L (2012) Mogale Gold: Making the most of AMD. *Mining Mirror*. October 2012, pp 10–15. Sourced on 11/03/2013 at http://www.myvirtualpaper.com/doc/brookepatrick/mining_mirror_october_2012_e-book/2012100301/12.html#18
- Malan JA (1990) The stratigraphy and sedimentology of the Bredasdorp Group, southern Cape Province. MSc thesis (unpublished). University of Cape Town, Rondebosch, 197 pp
- Mangole K (2010) Tour guide. Sterkfontein Cave. Personal communication, 13 May 2010
- Maré E (2010) Plant Manager. Percy Stewart WWTW. Personal communication, 26 May 2010
- Maropeng Staff (2012) Various Visitor Centre personnel. Personal communication, 19 Jan 2012
- Martin J (2006) The Kuruman Spring. *Soc Dyn* 32(2):218–227
- Martin JB, Brown A, Ezell J (2013) Do carbonate karst terrains affect the global carbon cycle? *Acta Carsologica* 42(2–3):187–196
- Martin JB, White WB (eds) (2007) Frontiers of karst research. Special publication 13. In: Proceedings and recommendations of the workshop held May 3 through 5, San Antonio, Texas. Karst Waters Institute. Leesburg, Virginia, 118 pp
- Martini JEJ (2006) Karsts and caves, pp 661–668. In: Johnson MR, Anhaeusser CR, Thomas RJ (eds) *The Geology of South Africa*. Geological Society of South Africa/Council for Geoscience. Johannesburg/Pretoria, 691 pp. ISBN: 978-1-919-908-77-9
- Martini J, Kavalieris I (1976) The karst of the Transvaal (South Africa). *Int J Speleol* 8(3):229–251. Available at <http://scholarcommons.usf.edu/cgi/viewcontent.cgi?article=1504&context=ijs>
- Martini JEJ, Wilson MGC (1998) Limestone and dolomite, pp 433–440. In: Wilson MGC, Anhaeusser CR (eds) *The mineral resources of South Africa*, Handbook 16. Council for Geoscience. Pretoria, 740 pp. ISBN: 1-875-061-52-5
- Martini J, Wipplinger PE, Moen HFG, Keyser A (2003) Contribution to the speleology of Sterkfontein Cave, Gauteng Province, South Africa. *Int J Speleol* 32(1/4):43–69. Available at <http://scholarcommons.usf.edu/cgi/viewcontent.cgi?article=1223&context=ijs>
- Masondo M (2010) R7m to clean up toxic water. *The Times*, Friday 19 Mar
- Maupin TP, Agouridis CT, Barton CD, Warner RC, Yu X (2013a) Specific conductivity sensor performance: I. Laboratory evaluation. *Int J Min Reclamat Environ* 27(5):329–344. <https://doi.org/10.1080/17480930.2013.764701>
- Maupin TP, Agouridis CT, Edwards DR, Barton CD, Warner RC, Sama MP (2013b) Specific conductivity sensor performance: II. Field evaluation. *Int J Min Reclamat Environ* 27(5):345–365. <https://doi.org/10.1080/17480930.2013.764702>
- McCarthy TS (2006) The Witwatersrand Supergroup, pp 155–186. In: Johnson MR, Anhaeusser CR, Thomas RJ (eds) *The Geology of South Africa*. Geological Society of South Africa/Council for Geoscience, Johannesburg/Pretoria, p 691
- McCarthy TS, Charlesworth EG, Stannistreet IG (1986) Post-Transvaal structural features of the northern portion of the Witwatersrand Basin. *Trans Geol Soc S Afr* 89:311–323
- McCarthy T, Rubidge B (2005) The story of earth & life: a southern African perspective on a 4.6-billion-year journey. Struik Publishers, Cape Town, 333 pp. ISBN: 1-77-007-148-2
- McCarthy TS, Venter JS (2006) Increasing pollution levels on the Witwatersrand recorded in the peat deposits of the Klip River wetland. *S Afr J Sci* 102:27–34
- McCullough CD (2008) Approaches to acid mine drainage water in pit lakes. *Int J Min Reclamat Environ* 22(2):105–119
- McCullough CD, Lund MA, May JM (2008) Field-scale demonstration of the potential for sewage to remediate acidic mine waters. *J Mine Water Environ* 27(2):31–39. <https://doi.org/10.1007/s10230-007-0028-y>
- McMillan PH (1998) An integrated habitat assessment system for the rapid biological assessment of rivers and streams. Internal STEP report no. ENV-P-I 98,088. CSIR, 37 pp
- Mellor ET (1917) The geology of the Witwatersrand. Explanation to the geological map. Special Publication 3. Geological Survey of South Africa, 46 pp
- Meyer R (2014) Hydrogeology of groundwater region 10: The karst belt. Report TT 553/14. Water Research Commission, Pretoria, 285 pp
- Middleton BJ, Bailey AK (2008a) Water Resources of South Africa, 2005 Study (WR 2005). Book of Maps. Vers. 1. Report TT 382/08. Water Research Commission, Pretoria, 85 pp
- Middleton BJ, Bailey AK (2008b) Water Resources of South Africa, 2005 Study (WR 2005). User's Guide. Vers. 1. Report TT 381/08. Water Research Commission, Pretoria, 179 pp
- Mills P (2010) Environmental Manager, COH WHS Management Authority. Personal communication, 18 June 2010
- Mogale Gold (2009) Ground-water monitoring program (OESH Department), 1 Mar 2009, 8 pp
- Montgomery DR, Zabowski D, Ugolini FC, Hallberg RO, Spaltenstein H (2002) Soils, watershed processes, and marine sediments, pp 159–194. In: Jacobson MC, Charlson RJ, Rodhe H, Orians GH (eds) *Earth system science: from biogeochemical cycles to global change*. International Geophysics Series, vol 72. Academic Press. London, 527 pp
- Moolman T (2012) Senior Geotechnician, Department of Water Affairs. Personal communication, 12 Jan 2012
- Moore WS, Reid DF (1973) Extraction of radium from natural waters using manganese-impregnated acrylic fibres. *J Geophys Res* 78(36):8880–8886
- Moreira S, Boehrer B, Schultze M, Dietz S, Samper J (2011) Modeling geochemically caused permanent stratification in Lake Waldsee (Germany). *Aquatic Geochem* 17:265–280
- Morse JW, Arvidson RS (2002) The dissolution kinetics of major sedimentary carbonate minerals. *Earth-Sci Rev* 58:51–84. [https://doi.org/10.1016/S0012-8252\(01\)00083-6](https://doi.org/10.1016/S0012-8252(01)00083-6)
- Mothoa TP, Lombaard AJ (2008) Drilling of three monitoring boreholes at mogale gold plant—randfontein. Draft report by

- AquaEarth Consultants for Mogale Gold/Mintails SA, Randburg, p 12
- Mucina L, Rutherford MC (eds) (2006) The vegetation of South Africa, Lesotho and Swaziland. Strelitzia 19. South African National Biodiversity Institute, Pretoria, 807 pp
- Mulder MP (1988) Dolomitic resource quantification, pp 54–60. In: GWD-GSSA. Workshop on dolomitic ground water of the PWV area, 28 March. Ground Water Division of the Geological Society of South Africa, Pretoria, 145 pp
- Nakasone H (1987) Study of aeration at weirs and cascades. *J Environ Eng* 113(1):64–81
- Nel A (2011) Whole effluent toxicity assessment. Report EUJ11-009. Department of Zoology, University of Johannesburg, 10 pp
- Nel A, van der Merwe-Botha M, du Toit S (2011) In-stream biological and chemical integrity of the surface streams at Nedbank Olwazini Conference Centre, Muldersdrift. Assessment of macro-invertebrate communities, aquatic toxicology and hydrochemistry—winter cycle 2011. Report 001/08/2011. Water Group, 32 pp
- Obbes AM (2001) The structure, stratigraphy and sedimentology of the Black Reef-Malmani-Rooihooft succession of the Transvaal Supergroup southwest of Pretoria. *Bulletin* 127. Council for Geoscience, Pretoria, 89 pp. ISBN: 1-875.061-80-0
- O'Bourke NC, Hartman GL, Fuglevand P (2008) In situ specific gravity vs grain size: a better method to estimate new work dredging production. Paper presented at the 39th Texas A&M dredging seminar, 9–11 June 2008. St Louis. Missouri, pp 215–224. Available at <https://www.westernredredging.org/index.php/information/proceedings-presentations/category/35-session-2b-dredging-studies-and-projects>
- Oelofse SHH, Roux S, De Lange W, Mahumani BK, Le Roux W, du Preez M, Greben HA, Steyn M (2012) A comparison of the cost associated with pollution prevention measures to that required to treat polluted water resources. Report 1845/1/11. Water Research Commission, Pretoria, 101 pp
- Olivier J, van Niekerk HJ, van der Walt IJ (2008) Physical and chemical characteristics of thermal springs in the Waterberg area in Limpopo Province, South Africa. *Water SA* 34(2):163–174
- Omoike AI, Vanloon GW (1999) Removal of phosphorus and organic matter removal by alum during wastewater treatment. *Water Res* 33(17):3617–3627
- Osborne RAL (2003) Partitions, compartments and portals: cave development in internally impounded karst masses. *Speleog Evol Karst Aquifers* 1(4):12
- Osmond JK, Cowart JB (2000) U-series nuclides as tracers in groundwater hydrology, pp 145–173. In: Cook PG, Herczeg AL (eds) *Environmental tracers in subsurface hydrology*. Kluwer Academic Publications, Boston/Dordrecht/London, p 529
- Palmer AN (2003) Dynamics of cave development by allogenic water. *Speleogenesis and Evolution of Karst Aquifers*. Issue 1. 11 pp. Sourced on 19/12/2012 at http://www.speleogenesis.info/directory/karstbase/pdf/seka_pdf4483.pdf
- Palmer AN (2007) Cave geology. Cave Books, Dayton, p 454
- Palmer AN (2011) Distinction between epigenic and hypogenic maze caves. *Geomorphology* 134:9–22
- Parrish JD, Braun DP, Unnasch RS (2003) Are we conserving what we say we are: measuring ecological integrity within protected areas. *BioSciences* 53(9):851–860
- Parshall RL (1950) Measuring water in irrigation channels with Parshall flumes and small weirs. US Soil Conservation Services. Circular 843. US Department of Agriculture, Washington, DC
- Parsons R, Wentzel J (2007) Groundwater resource directed measures manual. Report TT 299/07. Water Research Commission, Pretoria, 109 pp
- Partridge TC (1973) Geomorphological dating of cave openings at Makapansgat, Sterkfontein, Swartkrans and Taung. *Nature* 246:75–79
- Partridge TC, Maud RR (1987) Geomorphic evolution of southern Africa since the Mesozoic. *S Afr J Geol* 90(2):179–208
- Partridge TC, Granger DE, Caffee MW, Clarke RJ (2003) Lower Pliocene hominid remains from Sterkfontein. *Science* 300(5619):607–612
- Paykani ARM, Mardan HR (Undated) Methods of controlling ferric hydroxide precipitation results from corrosion in acidizing treatments. Sourced on 20/07/2012 at <http://www.pogc.ir/Portals/0/maghalat/890703-6.pdf>
- Payment P, Locus A (2010) Pathogens in water: value and limits of correlation with microbial indicators. Issue paper. Ground Water, 8 pp. <https://doi.org/10.1111/j.1745-6584.2010.00710.x>
- Pickering R (2010) Comparison between *Australopithecus Sediba* (MH1) and other hominin taxa, in the context of probabilities of conspecificity. *S Afr J Sci* 106(7/8):1–2. <https://doi.org/10.4102/sajs.v106i7/8.348>
- Pickering R, Kramers JD (2010) Re-appraisal of the stratigraphy and determination of new U-Pb dates for the Sterkfontein hominin site, South Africa. *J Hum Evol* 59:70–86
- Pickering R, Dirks PHG, Jinnah Z, De Ruiter DJ, Churchill SE, Herries AIR, Woodhead JD, Hellstrom JC, Berger LR (2011) *Australopithecus sediba* at 1.977 Ma and implications for the origins of the genus *Homo*. *Science* 333(6048):1421–1423. <https://doi.org/10.1126/science.1203697>
- Pienaar H, Xu Y, Braune E, Cao J, Dziki S, Jovanovic NZ (2021) Implementation of groundwater protection measures, particularly resource directed measures in South Africa. *Water Policy*
- Plummer LN, Busby JF, Lee RW, Hanshaw BB (1990) Geochemical modeling in the Madison aquifer in parts of Montana, Wyoming and South Dakota. *Water Resour Res* 26:1981–2014
- Pokrovsky OS, Golubev SV, Schott J, Castillo A (2009) Calcite, dolomite and magnesite dissolution kinetics in aqueous solutions at acid to circumneutral pH, 25 to 150 °C and 1 to 55 atm pCO₂: new constraints on CO₂ sequestration in sedimentary basins. *Chem Geol* 265:20–30. <https://doi.org/10.1016/j.chemgeo.2009.01.013>
- Pretorius DA (1986) The goldfields of the Witwatersrand Basin. In: Anhaeusser CR, Maske S (eds) *Mineral deposits of southern Africa*, vol I. Geological Society of South Africa, Johannesburg, pp 489–493
- Prudic DE, Harrill JR, Burbey TJ (1995) Conceptual evaluation of regional ground-water flow in the carbonate-rock province of the Great Basin, Nevada, Utah, and adjacent states. Professional paper 1409-D. US Geological Survey, 102 pp
- Quinlan JF, Ewers RO (1985) Ground water flow in limestone terrains: Strategy, rationale and procedure for reliable, efficient monitoring of ground water quality in karst areas. In: *Proceedings of the National symposium and exposition on aquifer restoration and ground water monitoring*. National Water Well Association, Worthington, Ohio, pp 197–234
- Quinlan JF, Ewers RO (1986) Reliable monitoring in karst terranes: it can be done, but not by an EPA-approved method. *Ground Water Monitoring & Remediation*. Winter 1986, pp 4–6
- RAIS (1995) Formal toxicity summary for Ni and Ni compounds. Risk Assessment Information System available at http://rais.ornl.gov/tox/profiles/nickel_and_nickel_compounds_f_V1.html
- RHP (2005) State-of-rivers report: monitoring and managing the ecological state of rivers in the Crocodile (West) Marico Water Management Area. River Health Programme. Department of Environmental Affairs and Tourism, Pretoria, 53 pp
- Reimold WU (2006) Impact structures in South Africa, pp 629–649. In: Johnson MR, Anhaeusser CR, Thomas RJ (eds) *The Geology of*

- South Africa. Geological Society of South Africa/Council for Geoscience, Johannesburg/Pretoria, p 691
- Reynders AG (1988) Production borehole drilling in the Middle and Lower Klip River Valley. Report GH3562. Department of Water Affairs and Forestry, Pretoria, 132 pp
- Rising Star Expedition Blog (2014) Sourced on 03/08/2014 at <http://newswatch.nationalgeographic.com/2014/04/01/wrapping-up-round-two/>
- Robb LJ, Robb VM (1998a) Gold in the Witwatersrand basin, pp 294–349. In: Wilson MGC, Anhaeusser CR (eds) The Mineral Resources of South Africa. Handbook 16. Council for Geoscience, 740 pp
- Robb LJ, Robb VM (1998b) Environmental impact of Witwatersrand gold mining, pp 14–16. In: Wilson MGC, Anhaeusser CR (eds) The Mineral Resources of South Africa. Handbook 16. Council for Geoscience, 740 pp
- Roberts CPR (1988) An overview of the proposed emergency ground water supply project in the Pretoria-Witwatersrand-Vereeniging (PWV) area, pp 1–4. In: Proceedings of the workshop on dolomitic ground water of the PWV area, 28 Mar 1988. Ground Water Division of the Geological Society of South Africa, Pretoria, 145 pp
- Roberts DL, Botha GA, Maud RR, Pether J (2006) Coastal Cenozoic deposits, pp 605–628. In: Johnson MR, Anhaeusser CR, Thomas RJ (eds) The Geology of South Africa. Geological Society of South Africa/Council for Geoscience, Johannesburg/Pretoria, p 691
- Roos H (2011) Landowner. Ptn 5 of Zwartkrans 172IQ. Personal communication, 10 Oct 2011
- Rösner T, Boer R, Reyneke R, Aucamp P, Vermaak J (2001) A preliminary assessment of pollution contained in the unsaturated and saturated zone beneath reclaimed gold-mine residue deposits. Report 797/1/01. Water Research Commission, Pretoria, 285 pp
- Roux S (2010) Water laundering. Water Sewage & Effluent, Nov 2010, pp 35–45
- RSA (1973a) 1:50 000 geological series 2527DC Hekpoort. The Government Printer, Pretoria
- RSA (1973b) 1:50 000 geological series 2527DD Broederstroom. The Government Printer, Pretoria
- RSA (1986) 1:250 000 geological series 2626 West Rand. The Government Printer, Pretoria
- RSA (1987) 1:10 000 orthophoto map 2627BA5 Sterkfontein, 2nd edn. The Government Printer, Pretoria
- RSA (1996) 1:50 000 topocadastral series 2527DC Hekpoort, 4th edn. The Government Printer, Pretoria
- RSA (1998) National Water Act: Act No 36, 1998. Government Gazette No 19182. Vol 398. 26 August 1998. Government Printer, Pretoria, 201 pp
- RSA (2001) 1:50 000 topocadastral series 2527DD Broederstroom, 5th edn. The Government Printer, Pretoria
- RSA (2002) 1:50 000 topocadastral series 2627BB Roodepoort, 6th edn. The Government Printer, Pretoria
- RSA (2008) Restrictions on taking water from Steenkoppies Dolomitic Compartment. National Gazette No 30863, vol 513, 14 Mar 2008. Government Printer, Pretoria, pp 152–167
- Rubin T (2012) Managing Director. Maropeng aAfrika. Personal communication, 09 Oct 2012
- Rutledge AT, Mesko TO (1996) Estimated hydrologic characteristics of shallow aquifer systems in the Valley and Ridge, the Blue Ridge, and the Piedmont Physiographic Provinces based on analysis of streamflow recession and base flow. Professional paper 1422-B. US Geological Survey, 58 pp
- Sahuquillo A, Rigol A, Rauret G (2002) Comparison of leaching tests for the study of trace metals remobilisation in soils and sediments. J Environ Monit 4:1003–1009
- Salvati R (2002) Natural hydrogeological laboratories: a new concept in regional hydrogeology studies. A case history from central Italy. Environ Geol 41:960–965
- SANS (2015a) South African National Standard (SANS) 241–1. Drinking water. Part 1: Microbiological, physical, aesthetic and chemical determinands. Edition 2. Standards South Africa, Pretoria, 14 pp
- SANS (2015b) South African National Standard (SANS) 241–2. Drinking water. Part 2: Application of SANS 241–1. Edition 2. Standards South Africa, Pretoria, 14 pp
- Sasowsky ID, White WB (1993) Geochemistry of the Obey River Basin, north-central Tennessee: a case of acid mine water in a karst drainage system. J Hydrol 146:29–48
- Sasowsky ID, White WB, Webb JA (1995) Acid mine drainage in karst terranes: geochemical considerations and field observations, pp 241–247. In: Beck BF, Pearson FM (eds) Karst GeoHazards: engineering and environmental problems in Karst Terrane. Proceedings of the fifth multidisciplinary conference on sinkholes and the engineering and environmental impacts of Karst, 2–5 Apr 1995. Gatlinburg, Tennessee, 581 pp
- Schaefer DH, Thiros SA, Rosen MR (2005) Ground-water quality in the carbonate-rock aquifer of the Great Basin, Nevada and Utah, 2003. Scientific investigations report 2005–5232. US Geological Survey, 32 pp
- Schneider K, Culver DC (2004) Estimating subterranean species richness using intensive sampling and rarefaction curves in a high density cave region in west Virginia. J Cave Karst Stud 66:39–45
- Schrader A, Erasmus E, Winde F (2014) Determining hydraulic parameters of a karst aquifer using unique historical data from large-scale dewatering by deep level mining—a case study from South Africa. Water SA 40(3):555–570
- Schulze RE, Maharaj M, Lynch SD, Howe BJ, Melvil-Thomson B (1997) South African atlas of agrohydrology and –climatology. Report TT82/96. Water Research Commission, Pretoria, 276 pp. ISBN: 1-86.845-271-9
- Scott R (1995) Flooding of Central and East Rand gold mines: an investigation into controls over the inflow rate, water quality and the predicted impacts of flooded mines. Report 486/1/95. Water Research Commission, Pretoria, 275 pp
- Secombe A (2008) Mine water calamity. Mining mx, 5 Nov 2008. Sourced on 04/01/2011 at http://www.miningmx.com/special_reports/green-book/2008/886408.htm
- Slabbert L (2007) Toxicity evaluation of selected surface and mine water from the West Rand mining basin, Krugersdorp. In: Hobbs P, Cobbing J (eds) A hydrogeological assessment of acid mine drainage impacts in the West Rand Basin, Gauteng Province. Report CSIR/NRE/WR/ER/2007/0097/C. Council for Scientific & Industrial Research, Pretoria, 100 pp
- Shelton LR, Capel PD (1994) Guidelines for collecting and processing samples of stream bed sediment for analysis of trace elements and organic contaminants for the National Water-Quality Assessment Program. Open-File Report 94–458. USGS. Sacramento, California, 31 pp
- Sherlock EJ, Lawrence RW, Poulin R (1995) On the neutralization of acid rock drainage by carbonate and silicate minerals. Environ Geol 25:43–54
- Slabbert L (2004) Methods for direct estimation of ecological effect potential (DEEEP). Report no.: 1313/1/04. Water Research Commission, Pretoria, 100 pp
- Strachan L, Ndengu S, Mafanya T, Coetzee H, Wade P, Msezane N, Kwata M, Mengistu H (2008) Regional gold mining closure strategy for the Central Rand Goldfield. (Draft). Report produced for Department of Minerals & Energy, Pretoria, 283 pp
- Strosnider WH, Nairn RW (2010) Effective passive treatment of high-strength acid mine drainage and raw municipal wastewater in

- Potosí, Bolivia using simple mutual incubations and limestone. *J Geochem Explor* 105:34–42
- Strosnider WH, Winfrey BK, Nairn RW (2011) Alkalinity generation in a novel multi-stage high-strength acid mine drainage and municipal wastewater passive co-treatment system. *J Mine Water Environ* 30:47–53. <https://doi.org/10.1007/s10230-010-0124-2>
- Strydom HA (2009) Chapter 26: Protected areas, pp 951–970. In: Strydom HA, King ND (eds) *Environmental management in South Africa*, 2nd edn. JUTA Law, Cape Town, p 1142
- Strydom HA, King ND (eds) (2009) *Environmental management in South Africa*, 2nd edn. JUTA Law, Cape Town, p 1142
- Strydom W, Funke N, Hobbs P (2016) The Witwatersrand acid mine drainage conundrum contextualised: mapping and understanding different coalitions, positions and interests in the AMD policy subsystem. Council for Scientific and Industrial Research, Pretoria, p 12
- Stumm W, Morgan JJ (1981) *Aquatic chemistry*, 2nd edn. Wiley Interscience, New York, p 583
- Stumpf S, Valentine-Darby P, Gwilliam E (2009) NPS inventory and monitoring program. *Aquatic Macroinvertebrates—Ecological role*. US National Park Service
- Supper R, Motschka K, Bauer-Gottwein P, Ahl A, Römer A, Neumann-Gondwe B, Merediz Alonso G, Kinzelbach W (2008) Spatial mapping of karstic cave structures by means of airborne electromagnetics: an emerging technology to support protection of endangered karst systems. *Geophys Res Abst* 10. EGU2008-A-01126
- Swain LA, Mesko TA, Hollyday EF (2004) Summary of the hydrogeology of the Valley and Ridge, Blue Ridge, and Piedmont Physiographic Provinces in the Eastern United States. Professional paper 1422-A. US Geological Survey, 31 pp
- Swart CJU, James AR, Kleywegt RJ, Stoch EJ (2003) The future of the dolomitic springs after mine closure on the Far West Rand, Gauteng, RSA. *Environ Geol* 44:751–770. <https://doi.org/10.1007/s00254-003-0820-3>
- Tancott G (2014) Excess AMD in West Rand a big problem. April 3 sourced on 18/06/2014 at <http://www.infrastructurenews/2014/04/03/excess-amd-in-west-rand-a-big-problem/>
- Tasaki S (2006) The presence of stygobitic macroinvertebrates in karstic aquifers: a case study in the Cradle of Humankind World Heritage Site. M.Sc. thesis (unpubl.). University of Johannesburg, Johannesburg, 144 pp
- Taylor CJ, Greene EA (2008) Chapter 3: Hydrogeologic characterization and methods used in the investigation of karst hydrology. In: Rosenberry DO, LaBaugh JA (eds) *Field techniques for estimating water fluxes between surface water and ground water*. Techniques and methods 4-D2. United States Geological Survey, 128 pp
- TCTA (2012) AMD Progress Report August 2012. Report to the Inter-Governmental Task Team meeting, Pretoria, 9 pp
- Thompson JG (1980) Acid mine waters in South Africa and their amelioration. *Water SA* 6(3):130–134
- Toens PD, Griffiths GH (1964) The geology of the West Rand, pp 283–321. In: Haughton SH (ed) *The geology of some ore deposits in Southern Africa*, vol I. Geological Society of South Africa, 625 pp
- Tucker RF, Viljoen RP (1986) The geology of the West Rand Goldfield, with special reference to the southern limb, pp 649–688. In: Anhaeusser CR, Maske S (eds) *Mineral deposits of Southern Africa*, vol I. Geological Society of South Africa, Johannesburg, p 1020
- Tutu H, McCarthy TS, Cukrowska E (2008) The chemical characteristics of acid mine drainage with particular reference to sources, distribution and remediation: the Witwatersrand Basin, South Africa as a case study. *Appl Geochem* 23:3666–3684
- UNESCO (1972) Glossary and multilingual equivalents of karst terms. United Nations Educational Scientific and Cultural Organization, Paris, p 72
- USDA (2012) *Groundwater-dependent ecosystems: level II inventory field guide*. Forest Service General Technical Report WO-86b, 124 pp
- USEPA (2002) *Methods for measuring the acute toxicity of effluents and receiving waters to freshwater and marine organisms*, 5th edn. Report no.: EPA-821-R-02-012. U.S. Environmental Protection Agency, USA
- van Biljon M (2006) Geohydrological review of the potential impact on the Sterkfontein dolomite during increased surface water runoff. Rison Groundwater Consulting for Johan Fourie & Associates on behalf of Harmony Gold Mining (Ltd.), 67 pp
- van den Bosch J (2010) Owner. Jomajoco Farms. Personal communication, 09 June 2010
- van der Merwe P (2009) Owner. Danielsrust Game Farm. Personal communication, 01 Dec 2009
- van der Walt B (2009) HDS Plant Manager. Rand Uranium. Personal communication, 11 Aug 2009
- van der Walt B (2011) HDS Plant Manager. Rand Uranium. Personal communication, 20 Jan 2011
- van der Walt B (2013) HDS Plant Manager. SibanyeGold. Personal communication, 26 Feb 2013
- van Dyk G, Esterhuyse CJ, Goussard F (2007) Groundwater observations and impact management in the mining, urban and industrial environment of the Sishen Kathu aquifer. In: *Proceedings of the groundwater 2007 conference*. Ground Water Division. Geological Society of South Africa, 5 – 7 Oct 2007, Bloemfontein
- van Schalkwyk A (1981) Ontwikkelpatroon en risiko-evaluasie in dolomietgebiede. In: *Proceedings of the seminar on the engineering geology of dolomite areas*. Department of Geology. University of Pretoria, 26 – 27 Nov 1981, Pretoria, pp 9–24
- van Schie K (2013) Finally some life back in mine water. *The Star*. Monday 18 Mar 2013
- van Wyk E (2010) Estimation of episodic groundwater recharge in semi-arid fractured hard rock aquifers. PhD thesis (unpublished). University of the Free State, Bloemfontein, 273 pp
- Vegter JR (1988) Dolomitic ground water for the metropolitan PWV-area: a resuscitation of ideas, pp 7–11. In: *Proceedings of the workshop on dolomitic ground water of the PWV area*, 28 Mar 1988. Ground Water Division of the Geological Society of South Africa, Pretoria, 145 pp
- Vegter JR (1995) An explanation of a set of national groundwater maps. Report TT 74/95. Water Research Commission, Pretoria, 81 pp
- Veni G (2013) A framework for assessing the role of karst conduit morphology, hydrology, and evolution in the transport and storage of carbon and associated sediments. *Acta Carsologica* 42(2–3):203–211
- Venter J, Motlakeng T, Kotoane M, Coetzee H, Hobbs P, Wade P (2010) Establishment of a monitoring system for surface water and groundwater in the Cradle of Humankind World Heritage Site: Sediment sampling and analysis results. Internal project report prepared by the CGS for the CSIR/CGS Joint Venture, Pretoria, 24 pp
- Vermeulen A (2013) Return of macroinvertebrates in West Rand stream a sign impact of AMD has lessened. *Mining Weekly*, Friday 26 Apr 2013. Sourced on 04/05/2013 at <http://www.miningweekly.com/page/environmental/>
- Vesper DJ, Loop CM, White WB (2003) Contaminant transport in karst aquifers. *Speleogenesis and Evolution of Karst Aquifers*. Issue 2. 11 pp. Sourced on 19/12/2012 at http://www.speleogenesis.info/directory/karstbase/pdf/seka_pdf4490.pdf
- Vesper D (2008) Karst resources and other applied issues, pp 65–73. In: Martin JB, White WB (eds) *Frontiers of Karst Research*. Special publication 13. Karst Waters Institute. Leesburg, Virginia, 118 pp

- Vías JM, Andreo B, Perles MJ, Carrasco F, Vadillo I, Jiménez P (2003) The COP method, pp 163–171. In: Zwahlen F (ed) Vulnerability and risk mapping for the protection of carbonate (karst) aquifers. Final report. COST Action 620. European Commission, Brussels, 297 pp
- Visser DJL (1989) The geology of the Republics of South Africa, Transkei, Bophuthatswana, Venda and Ciskei and the Kingdoms of Lesotho and Swaziland. Explanation: Geological map (1:1 000 000). Geological Survey and Department of Mineral and Energy Affairs, Pretoria, 491 pp
- Visser H (2018) Reserve Manager. John Nash Nature Reserve. Personal communication, 6 Dec 2017
- Wade PW, Woodbourne S, Morris WM, Vos P, Jarvis NV (2002) Tier 1 risk assessment of radionuclides in selected sediments of the Mooi River. Report 1095/1/02. Water Research Commission, Pretoria, 92 pp
- Walter GR, Necsoiu M, McGinnis R (2012) Estimating aquifer channel recharge using optical data interpretation. *Ground Water* 50(1):68–76. <https://doi.org/10.1111/j.1745-6584.2011.00815.x>
- Waltham T (2008) Fengcong, fenglin, cone karst and tower karst. *Cave Karst Sci* 35(3):77–88 (also available at www.speleogenesis.info 2011)
- Wanty RB, Nordstrom DK (1993) Natural radionuclides, pp 423–441. In: Alley WM (ed) Regional Ground-Water Quality. Van Nostrand Reinhold, New York, p 634
- Watson J, Hamilton-Smith E, Gillieson D, Kiernan K (eds) (1997) Guidelines for Cave and Karst Protection. IUCN Gland, Switzerland, p 63
- Weaver JMC, Cavé L, Talma AS (2007) Groundwater sampling, 2nd edn. Report TT 303/07. Water Research Commission, Pretoria, 168 pp
- Webb JA, Sasowsky ID (1994) The interaction of acid mine drainage with a carbonate terrane: evidence from the Obey River, north-central Tennessee. *J Hydrol* 161:327–346
- Wells JD, van Meurs LH, Rabie GF, Moir F, Russell J (2009) Chapter 15: Terrestrial minerals, pp 513–578. In: Strydom HA, King ND (eds) Environmental management in South Africa, 2nd edn. JUTA Law, Cape Town, p 1142
- WHC (2013) State of conservation of world heritage properties inscribed on the world heritage list. Document WHC-13/37.COM/7B.Add, pp 100–104, Paris, 17 May 2013. Available at <http://whc.unesco.org/en/documents/123027>
- Whatley G (2010) Owner. Kromdraai Gold Mine. Personal communication, 26 May 2010
- White WB (1984) Rate processes: chemical kinetics and karst landform development, pp 227–248. In: LaFleur RG (ed) Groundwater as a Geomorphic Agent. Allen & Unwin, London, 390 pp. ISBN-13: 978-0-045-510-696
- White WB (1993) Analysis of karst aquifers, pp 471–489. In: Alley WM (ed) Regional ground-water quality. Van Nostrand Reinhold, New York, 634 pp. ISBN: 0-442-00-937-2
- White WB (2002) Karst hydrology: recent developments and open questions. *Eng Geol* 65:85–105
- White WB (2007) A brief history of karst hydrogeology: contributions of the NSS. *J Cave Karst Stud* 69(1):13–26
- White WB (2007b) Evolution and age relations of karst landscapes. Time in Karst. Postojna, pp 45–52. Available at <http://www.carsologica.zrc-sazu.si/downloads/361/white5.pdf>
- White WB (2013) Carbon fluxes in karst aquifers: sources, sinks, and the effect of storm flow. *Acta Carsologica* 42(2–3):177–186
- White S, White N (2009) Bullita Cave, Gregory Karst, N.T. Australia: a maze cave in Proterozoic dolomite, pp 1010–1013. In: White WB (ed) Proceedings of the 15th international congress of speleology, vol 2. Symposia. Part 2, 19–26 July, Kerrville, Texas, 680 pp
- WHO (2009) Handbook on indoor radon: a public health perspective, 110 pp. Available at http://www.who.int/ionizing_radiation/env/radon/en/index1.html
- WHO (2011) Guidelines for drinking-water quality, 4th edn. 564 pp. Available at http://www.who.int/water_sanitation_health/publications/2011/dwq_guidelines/en/index.html
- Wiegman F (2009) Consultant. Golder Associates Africa. Personal communication, 31 July 2009
- Wilkinson MJ (1973) Sterkfontein Cave system: evolution of a karst form. MA thesis (unpubl.). University of the Witwatersrand, Johannesburg, 96 pp
- Williams PW (1983) The role of the subcutaneous zone in karst hydrology. *J Hydrol* 61:45–67
- Williams PW (2008) World heritage caves and karst: a thematic study. No 2 IUCN/WCPA, Switzerland, 57 pp
- Winde F, Wade P, van der Walt IJ (2004) Gold tailings as a source of water-borne uranium contamination of streams—the Koekemoerspruit (South Africa) as a case study Part III of III: fluctuations of stream chemistry and their impacts on uranium mobility. *Water SA* 30(2):233–239
- Winfrey BK, Strosnider WH, Nairn RW, Strevett KA (2010) Highly effective reduction of fecal indicator bacteria counts in an ecologically engineered municipal wastewater and acid mine drainage passive co-treatment system. *Ecol Eng.* <https://doi.org/10.1016/j.ecoleng.2010.06.025> (article in press)
- Wirries DL, McDonnell AJ (1983) Drainage quality at deep coal sites. *Water Resour Bull* 19:235–240
- Withüser KT, Leyland RC, Holland M (2010) Vulnerability of dolomite aquifers in South Africa, pp 119–131. In: Xu Y, Braune E (eds) Sustainable groundwater resources in Africa: Water supply and sanitation environment. UNESCO Paris and CRC Press/Balkema. Taylor & Francis Group, 282 pp
- Withüser K (2011) Consultant. Metago Water Geosciences (Pty) Ltd. Personal communication (in the capacity of COH WHS Project BIQ005/2008 Steering Committee Member), 27 Jan 2011
- Wolkersdorfer C (2008) Water management at abandoned flooded underground mines. Fundamentals, tracer tests, modelling, water treatment. International Mine Water Association. Springer, Berlin, 465 pp
- Worthington SRH (2001) Depth of conduit flow in unconfined carbonate aquifers. *Geology* 29(4):335–338
- Worthington SRH (2005) Hydraulic and geological factors influencing conduit flow depth. *Speleogenesis and Evolution of Karst Aquifers*. Issue 7, 19 pp. Sourced on 19/12/2012 at http://www.speleogenesis.info/directory/karstbase/pdf/seka_pdf4514.pdf
- Worthington SRH, Ford DC (2009) Self-organized permeability in carbonate aquifers. *Ground Water* 47(3):326–336
- Worthington SRH, Gunn J (2009) Hydrogeology of carbonate aquifers: a short history. *Ground Water* 47(3):462–467
- WRC/IUCN/SAKWG (2010) The karst system of the Cradle of Humankind World Heritage Site. Report KV 241/10. Water Research Commission, Pretoria, 402 pp
- Wright I (2012) Managing Director. Ozone Services Industry (Pty) Ltd. Personal communication, 09 Oct 2012
- WS&E (2012) Responsible use, pp 17–21. *Water Sewage & Effluent* 32(3):48
- Younger PL (1997) The longevity of minewater pollution: a basis for decision-making. *Sci Total Environ* 194(195):457–466
- Zartman RE, Frimmel HE (1999) Rn-generated ^{206}Pb in hydrothermal sulphide minerals and bitumen from the Ventersdorp Contact Reef, South Africa. *Mineral Petrol* 66:171–191
- Zhang M, Zhang C, Wang K, Yue Y, Qi X, Fan F (2011) Spatiotemporal variation of karst ecosystem service values and its correlation with environmental factors in Northwest Guangxi.

- Environmental Management, China. <https://doi.org/10.1007/s00267-011-9735-z>
- Ziemkiewicz PF, Skousen JG, Brant DL, Sterner PL, Lovett RJ (1997) Acid mine drainage treatment with armored limestone in open limestone channels. *J Environ Qual* 26(4):1017–1024. <https://doi.org/10.2134/jeq1997.00472425002600040013x>
- Zohary T, Jarvis AC, Chutter FM, Ashton PJ, Robarts RD (1988) The Hartbeespoort Dam ecosystem programme 1980–1988. CSIR, 12 pp
- Zwahlen F (ed) (2003) Vulnerability and risk mapping for the protection of carbonate (karst) aquifers. Final report. COST Action 620. European Commission, Brussels, 297 pp

Bibliography

- Andre BJ, Rajaram H (2005) Dissolution of limestone fractures by cooling waters: early development of hypogene karst systems. *Water Resour Res.* <https://doi.org/10.1029/2004WR003331>
- Bögli A (1964) Mischungskorrosion – ein Beitrag zur Verkarstungsproblem. *Erdkunde* 18:83–92. <https://doi.org/10.3112/erdkunde.1964.02.02>
- Botrell SH, Gunn J, Lowe DJ (2000) Calcite dissolution by sulfuric acid. In: Klimchouk A, Ford DC, Palmer AN, Dreybrodt W (eds) *Speleogenesis: evolution of karst aquifers*. National Speleological Society, Huntsville, pp 304–308
- Dubljansky JV (1990) Regularities of the formation and modelling of hydrothermal karst. *Nauka*. Novosibirsk, 151 pp (in Russian)
- Dubljansky JuV (2000) Dissolution of carbonates by geothermal waters. In: Klimchouk A, Ford DC, Palmer AN, Dreybrodt W (eds) *Speleogenesis: evolution of karst aquifers*. National Speleological Society, Huntsville, pp 158–159
- Dublyansky VN, Lomaev AA (1980) *Karst caves of Ukraine*. Naukova dumka, Kiev, 180 pp (in Russian)
- Ford DC, Williams PW (1989) *Karst geomorphology and hydrology*. Unwin Human, London, p 601
- Hill CA (1996) *Geology of the Delaware basin, Guadalupe, Apache and Glass Mountains, New Mexico and West Texas*. Permian Basin Section-SEPM Publication 96–39. 480 pp
- Hill CA (2000) Sulfuric acid hypogene karst in the Guadalupe Mountains of New Mexico and West Texas. In: Klimchouk A, Ford DC, Palmer AN, Dreybrodt W (eds) *Speleogenesis: evolution of karst aquifers*. National Speleological Society, Huntsville, pp 309–316
- Hill CA (2003a) Caves and karst in New Mexico. *New Mexico Earth Matters* 3(1). New Mexico Bureau of Geology and Mineral Resources, 1–4
- Kaveev MC (1963) About influence of carbon dioxide, originated during destruction of oil deposits, on development of karst processes. *Doklady. AN SSSR* 152(3). (in Russian)
- Laptev FF (1939) *Aggressive action of water on carbonate rocks, gypsum and concrete*. Moscow-Leningrad, 120 pp (in Russian)
- Lismonde B (2000) *Corrosion des cupoles de plafond par les fluctuations de pression de l'air emprisonné*. *Karstologica* 35:39–46
- Lowe DJ (1992) *The origin of limestone caverns: an inception horizon hypothesis*. PhD thesis (unpublished). Manchester Metropolitan Municipality
- Malinin SD (1979) *Physical chemistry of hydrothermal systems with carbon dioxide*. Nauka, Moscow, 111 pp (in Russian)
- Palmer AN (1991) Origin and morphology of limestone caves. *Geol Soc Am Bull* 103:1–21
- Slabe T (1995) *Cave rocky relief and its speleological significance*. Ljubljana, ZRC ZANU, 128 pp
- W&SA (2012) Cradle of Humankind water monitoring results. *Water Sanitation Africa* 7(3):41–47

Index

A

Acidic mine water, 321
Acid mine drainage, 1, 3, 33, 153
Acid mine drainage ingress, 298
Administrative responsibilities, 5, 7
Agricultural impacts, 49
Anthropogenic impacts, 24
Archaeology, 24

B

Bacterial sulfate reduction, 296, 313
Bacteriological quality, 106, 107, 110, 151, 159, 232, 233
Bacteriological variables, 93, 97, 99, 117
Bioreactor system, 223

C

Calcareous sandstone, 34
Carbonate strata, 31, 33–37, 40
Carbon flux, 318–320
Cave system, 321, 323, 325
Cave water chemistry, 220, 222, 223
Characteristics, 11, 17, 20
Chemical hydrogeology, 211
Chemical hydrology, 83
Climate, 11
Cradle of Humankind World Heritage Site, 1, 3

D

Discharge measurement, 44, 67, 68, 75, 79, 81
Discharge pattern, 46–48
Discharge regimes, 89, 121
Dolomitic aquifers, 167
Dolomitic groundwater, 213, 232, 238, 239, 286, 290
Dolomitic strata, 17, 20, 321
Drainage, 11, 13, 16, 19, 20, 27, 28

E

Ecology, 24
Ecosystem services, 31, 32
Effective governance, 7
Epikarst, 39–41
Evapotranspiration, 12, 16, 17

F

Flow gauging weir, 56, 57
Flow measurements, 54, 57, 60, 66, 67, 69, 71, 72, 74–77, 79, 81
Fossil site risk assessment, 321
Fossil sites, 1, 2, 4
Full supply capacity, 43

G

Geochemical interaction, 321
Geological structures, 170, 173
Geomorphologic settings, 24
Geophysics, 17
Geotechnical characteristics, 34
Global karst, 31
Groundwater abstraction, 174, 178, 180, 198
Groundwater chemistry analyses, 167
Groundwater data sources, 168
Groundwater discharge, 174, 176, 177, 180, 189, 192, 194, 199, 207
Groundwater drainage pattern, 168, 202, 204, 205
Groundwater management areas, 170
Groundwater management units, 170, 177
Groundwater recharge, 168, 179, 180
Groundwater resource directed measures, 168, 321
Groundwater resources, 1, 3, 43, 67
Groundwater rest levels, 174, 176, 178, 181, 182, 187, 202, 204
Groundwater supply potential, 167

H

Hydro-ecosystem, 31, 32
Hydrogeochemistry, 87
Hydrogeological monitoring programme, 7
Hydrogeologic features, 189
Hydrogeology, 3
Hydrological year, 44, 48, 51, 54, 59, 62, 63
Hydrology, 3
Hydrophysical data, 272
Hydrophysical framework, 7
Hydro-vulnerability assessment, 325

I

Implementation, 7
Integrated, 7, 8
Isotope results, 223, 229, 230, 241

K

Karst aquifers, 31–36, 39
 Karst denudation, 299, 300, 308
 Karst ecosystems, 7
 Karst formations, 18, 170, 321
 Karst hydrosystem, 8, 9, 33, 34, 38
 Karstic ground-water basins, 170
 Karst morphology, 36
 Karst terrane, 44, 74
 Karst water resources, 33
 Knowledge, 7

L

Legal, 5, 7
 Limestone, 31, 33–37
 Lithostratigraphic units, 211, 212

M

Management actions, 7
 Management Authority, 3
 Mean annual runoff, 43, 64
 Mine water discharge, 51–56, 67, 81, 83, 85, 87, 91, 92, 94, 96, 97, 109, 121, 127, 130, 133, 134, 144–147, 149, 156, 159, 165
 Mine water treatment, 325
 Mining geology, 21
 Monitoring boreholes, 214, 216–220, 254, 259–261, 268–272, 306, 313, 314
 Monitoring program, 1
 Monitoring programme, 321
 Monitoring station, 99, 112
 Morphology, 11, 18, 19, 21, 28
 Municipal wastewater discharge, 93, 117, 143, 147
 Municipal wastewater effluent, 223, 225, 233, 259, 263, 293

N

Normal flow conditions, 66

O

On-site treatment, 80

P

Palaeontology, 24
 Perennial sources, 49
 Permeable hydrogeologic boundaries, 170
 Physical environment, 11
 Physical hydrogeology, 167
 Physical hydrology, 43
 Plate, 329
 Point source mine water discharges, 216
 Protected area, 5, 7
 Pseudo-boundary, 173

Q

Quaternary catchments, 43, 60

R

Rainfall, 11–16
 Raw mine water, 85–88, 91, 92, 122, 130, 134, 141–150, 155, 156, 158, 159, 161
 Receiving karst aquifer, 321
 Regional groundwater chemistry, 211
 Resource water quality objectives, 321, 322
 Risk assessment, 35, 321

S

Soils, 17
 Source-specific temporal assessment, 215
 South African, 5, 7, 11, 12, 31, 33, 34, 36, 40, 168, 189, 197, 229, 299, 308, 323
 Speleogenesis, 35–40
 Spring discharges, 321
 Springwater chemistry, 226, 232–236, 255, 301, 305–307
 Statistical analysis, 84–86, 96–98, 102, 104, 105, 108, 110, 118, 119, 134, 138
 Subsurface environments, 43
 Surface water and groundwater environments, 321
 Surface water chemistry, 83, 94, 95, 112, 113, 117, 119, 120, 130, 148, 155, 156
 Surface water drainage, 43
 Surface water flow losses, 321
 Surface water losses, 106, 136, 151
 Surface water resources, 58, 102, 148, 211, 321, 322
 Sustainable functioning, 8
 Synoptic discharge measurement, 193–195

T

Threat status, 7
 Trace metals, 92, 93, 101, 103, 110, 116, 161
 Treated wastewater, 93, 116, 117
 Trends of change, 7

U

Unconsolidated sedimentary material, 174
 Undesirable constituents, 7
 United Nations Educational, Scientific and Cultural Organisation (UNESCO), 1
 Upstream impacts, 218

V

Vegetation, 16, 17
 Vulnerability aspects, 34

W

Wastewater convergence, 107
 Wastewater effluent, 56–58, 60, 80
 Water quality, 2, 3
 Water quality monitoring, 83, 87, 89, 91, 143, 146, 158
 Watershed, 11, 14–16
 Water supply, 33, 34
 Wetland sanitation system, 223